



14th International Symposium of Continuous Surface Mining



BOOK OF PROCEEDINGS

Roumpos Christos
Michalakopoulos Theodore
Galetakis Michael
Pavloudakis Francis *Editors*

Greece, Thessaloniki 23-26 September 2018

**Aristotle University
Research Dissemination Center**



ATHENS 2019

ISBN 978-618-84489-1-9



International Symposium of Continuous Surface Mining



*Public Power Corporation of Greece
Mines Business Unit*



*National Technical University of Athens
School of Mining and Metallurgical Engineering*



*Technical University of Crete
School of Mineral Resources Engineering*

The Technical Editing of the Book of Proceedings was carried out by:

*Daphne Sideri, Dr., Mining Engineer &
Nikolaos Paraskevis, MSc., Mining Engineer*

Table of contents

<i>Foreword</i>	6
<i>Symposium Committees</i>	10
<i>Session 1: Mine planning and design</i>	11
Simulating the BWE-Conveyor-Stacker System in Python using Salabim	12
A Holistic Approach for Highly Selective Mechanical Process Chains	24
Integrated Operation in Mining through Digitalization – from a Concept to a Solution.....	35
Current State and Development of Continuous Systems on EPS Opencast Coal Mines.....	43
<i>Session 2: Modeling and simulation</i>	58
Ultimate Pit Limit Determination for Fully Mobile In-Pit Crushing and Conveying Systems: A Case Study.....	59
Assessment of the Added-Value of Sentinel 1 & 2 for Mapping and Monitoring Surface Mining.....	73
Application of the Push-Relabel Algorithm to Lignite Surface Mine Optimization	88
Use of Mine Planning Software in Mineral Resources and Reserves Estimation of the Lava Lignite Deposit in Serbia – Greece.....	100
Carbon: A WebGIS Software to Evaluate and Model Open-Pit Lignite Mining Systems	110
Model-based Investigations of Hybrid Mining Systems Using Cutting, Crushing and Conveying Technology in Medium Hard Rock.....	123
Why One Dimension is Not Enough – A Comparative Study of Lignite Resources Estimation Using Drillhole Mineable Lignite Compositing of Uncorrelated Seams and Mineable Lignite Compositing of Correlated Lignite Seams	136
Unsupervised Machine Learning Applications on Greek Lignite Mining Industry.....	152
An Evolutionary Solution for Coal Reserves Modelling and Production Scheduling.....	168
Geostatistical Estimation of Coal Reserves in Kardia Mine using Kriging and Conditional Simulation Methods	184
<i>Session 3: Equipment and mining systems</i>	198
Experimental Investigation of the Activated Rock Cutting Process	199
Determination of Optimal Life Cycle of Bulldozer in Open Pits with Continual Systems in PE EPS	209
The Role of the Independent Expert in Material Handling and Mining Equipment Design and Approval.....	224

Development of a Real-Time Mine-Face Inspection System for the Early Detection of Hard Rock Formations during Mining by Bucket-Wheel Excavators.....	233
Simulating the Performance of Bucket Wheel Excavators by Means of Soft Computing Techniques	247
Analysis of Dislocation of Continual System at “Field D” in Function of Overburden and Coal Production at Eastern Part of Kolubara Coal Basin	258
A Real-Time Event-Driven Database System for Maintenance Planning and Productivity Analysis in Continuous Surface Mining Operations.....	265
Methods of Decreasing of Bucket Wheel Excavators Failures Working In Soils Including Unmineable Intrusions	273
Open Pit Mine Conveyor Belt shifting using modern surveying equipment – An overview	289
Overview of the Results of Researches Related to Adaptation of Bucket Wheel Excavators Operating in Romanian Lignite Open Pits for Excavation in Rocks with Increased Cutting Resistance.....	303
New Method of Residual Lifetime Assessment of Bucket Wheel Excavators Operating in Romanian Lignite Open Pits	310
<i>Session 4: Geotechnical engineering</i>	<i>319</i>
The Role of Geological Faults in Mine Stability: Amynteon mine, Western Macedonia (Greece) as a Case Study	320
A Cloud-Based Real-Time Slope Movement Monitoring System.....	336
The Impact of the Coal Clay in the Slope Geometry of the OCM Radljevo North Opening Cut .	351
Reliability Evaluation during Slopes Progressive Failure.....	356
Avoiding Instability Conditions in Sector 6 of the Southern Field Mine in Northern Greece	368
Investigation of the Stability of Deep Excavation Slopes in Continuous Surface Lignite Mines .	377
PPC Excavator Production improvement of 20% by iBelt 2D Radar Control.....	394
Gearless Drives for Medium Power Belt Conveyors	402
Mining 4.0 - Our Digital Journey.....	409
<i>Session 5: Health & Safety, Environment</i>	<i>412</i>
Control of Social and Environmental Risks During Opencast Lignite Mining	413
A Review of the Effectiveness of Health & Safety Management Systems according to OHSAS 18001 Standard at PPC’s Lignite Mines	428
Innovative Approaches to Coal Surface Mine Sites Rehabilitation: A Case Study of Megalopolis Lignite Fields.....	437
Impact of Environmental Policies on Lignite Plants Generation In the Greek Wholesale Electricity Market	453
Alkali Activating of Low-Alumina Mine Tailings for more Sustainable Raw Material Supply ...	471

Occupational Accidents in Turkish Energy Sector	480
Adaptation of Fruit Crops in Rehabilitated Old Mines Soils in West Macedonia Lignite Centre.	492
Evaluation of Honey Producing Potential of Robinia Pseudacacia in Reforested Old Lignite Mines in West Macedonia.....	498
Sustainable Development Analysis of Lignite Mining, by Coupling Environmental, Economic and Social Indicators.....	504
Technological and environmental upgrading of lignite from Amynteon and Ahlada deposits, in Northern Greece, via selective grinding.....	518
<i>Session 6: Land reclamation.....</i>	<i>525</i>
Moving from Energy Depletion to Energy Crops in Exhausted Continuous Surface Mines	526
Towards a New Deal for the Lignite Industry in Western Macedonia	537
Backfilling and Securing of abandoned Small Scale Coal Mines in Mongolia with Coal Combustion By-Products (CCB's) - the BASMIC Project.....	544
Environmental Reclamation Planning of Continuous Surface Lignite Mines in Closure Phase: A Risk-Based Investigation.....	551
A Multi-Criteria Methodology for Low-Risk Evaluation of Mine Closure Restoration in Continuous Surface Lignite Mining Projects	563
<i>Session 7: Water management - Environmental monitoring</i>	<i>579</i>
Planning of Mavropigi and Kardias Mines Depressurization Systems by Three Dimensional Groundwater Flow Numerical Modeling	580
Improvement Methods of Pumping Station Function in Coal Mines of Western Macedonia Lignite Centre	593
Alfeios River Sectional Diversion for the Expansion of the Continuous Surface Mining Operations of Megalopolis Mines in the Peloponnese Peninsula, Greece	602
Surface Mining in Western Macedonia, Greece: PM10 Emissions and Dispersion.....	619
Statistical Analysis and Spatial Distribution of Trace Elements Contained in Clays Excavated in Western Macedonia Continuous Surface Mining Complex.....	631
<i>Session 8: Geological exploration, quality control, homogenization.....</i>	<i>643</i>
Structural Geology of the Lignite Mines in the Ptolemais Basin, NW Greece.....	644
Structural Analysis of Greek and Bulgarian Coals by Solid-State ¹³ C Nuclear Magnetic Resonance (NMR) Spectroscopy	651
Energy Efficiency by Ecological Coal Quality Management in EPS and Its Benefits	667
Morphology, Mineralogy, and Chemistry of Fly Ash from the Ptolemais Power Stations, Northern Greece, and its potential as partial Portland cement substitute	675
Open Pit Mine 3D Geological face mapping perspectives obtained by a fully automated, terrain following, rotary-wing UAVs mission.....	689

Investments in Geological Exploration and Affection on Mining Operating Cash Costs at Lignite Open Pits Kolubara (Lazarevac), Serbia	704
Do Coal Combustion Products Affect the Groundwater Quality Around Power Plants Area of the Lignite Ptolemis Basin?.....	715

Foreword

The 14th International Symposium of Continuous Surface Mining (ISCSM) gave an opportunity to professionals from the mining industry and practitioners from consulting companies, equipment suppliers and software providers, individuals from research institutions and government agencies as well as academic scholars and researchers, to present their work and to share and discuss the latest developments on continuous surface mining.

Over 150 participants from 10 countries attended ISCSM and more than 60 papers were presented, covering the following broad topics and research areas: (i) Mine Planning and Design, (ii) Modelling and Simulation, (iii) Equipment and Mining Systems, (iv) Geotechnical Engineering, (v) Occupational Health & Safety, Environment, (vi) Geological Exploration, Quality Control, Homogenization.

The Symposium was organized by the Department of Mining Engineering, Public Power Corporation (PPC) of Greece, in collaboration with the School of Mining and Metallurgical Engineering of the National Technical University of Athens (NTUA) and the School of Mineral Resources Engineering of the Technical University of Crete (TUC).

The contribution of the members of both the Local and the International Organizing Committees is greatly appreciated. Furthermore, special thanks are extended to Professors V. Pavlovic and C. Drebenstedt, members of the Conference Board, for their continuous support. Our sincere gratitude is extended to Professor Z. Agioutantis for his active involvement and contribution.

Finally, we would like to thank the sponsors of the Symposium, ABB S.A., Epiroc Hellas, Hyetos S.A., Geosysta Ltd, Planetek Hellas, HELMA S.A. and WIRTGEN Group for their generosity.

Dr. Christos Roumpos, Former Assist. Professor, Public Power Corporation of Greece
Assoc. Professor, Theodore Michalakopoulos, National Technical University of Athens
Professor Michael Galetakis, Technical University of Crete
Dr. Francis Pavloudakis, Public Power Corporation of Greece



ABB in mining

We offer you over 50 years of experience in delivering electrical and automation equipment for open-pit mining and high-volume bulk material handling. We ensure that even the most challenging requirements are fulfilled. We enable customers to lead in safety, productivity and energy efficiency through digital, collaborative operations.

Large open-pit mining operations throughout the world use our control and drive systems to save energy, improve productivity, and enhance system value. We are a leading supplier of electrification, automation, and control and drive systems for a full range of mining equipment, including; bucket-wheel and bucket-chain excavators, spreaders, stackers, reclaimers, crushers, shovels, draglines, belt conveyor systems, and stockpiles.

With a centralized control room you can monitor and control existing equipment and auxiliary facilities in an open-pit mine. Data, verbal information, radio signals, video images, and satellite messages will be transmitted and centrally collected. This information can also be fed into the customer's operating network, or provided to other users. Mine operators have a complete overview of the mine at all times, and they can determine who else can receive the information.

As a strong partner, committed to your success we provide you with a wide range of services during and after final delivery: 24 hours a day, 365 day a year. We strive to ensure you have uninterrupted and reliable operations and the rapid delivery of any spare part. We develop and implement individually tailored solutions that work with highest reliability.

Whatever your business is handling - from coal to copper ore, from iron ore to overburden - to be successful in the fields of open-pit mining and bulk-material handling you need a strong partner - ABB.



Epiroc Hellas provides service and sales for our surface and underground drilling and tunneling equipment including loading and haulage, hydraulic attachment tools, rock drilling tools and geotechnical equipment. Our sales and service team responsible for mining and demolition equipment have transferred from Atlas Copco to become part of the newly created company, Epiroc Hellas. Our products and factories are the same, staff is the same but we have a new dynamic name and image.

Epiroc is a leading productivity partner for the mining, civil engineering, infrastructure and natural resources industries. With cutting-edge technology, Epiroc develops and produces innovative drill rigs, tunneling equipment, rock excavation, hydraulic attachment tools, and provides world-class service and consumables. The company was founded in Stockholm, Sweden, and has passionate people supporting and collaborating with customers in more than 150 countries.

The decision to split from Atlas Copco was to create two world-leading companies that were fully focused on their different end markets and demands. Epiroc customers are from the mining, civil engineering, infrastructure and natural resources industries, whilst Atlas Copco is more focused on manufacturing and process industries.



HYETOS S.A. is a private Consulting Engineers Company which provides Engineering, Consulting, Research and Expertise Services of high quality on various scientific fields, such as Hydraulics, Environment, Geology - Geotechnics, Structural Engineering etc with a strong presence in Central and Western Macedonia.



Geosysta Ltd provides engineering consultancy, scientific services and software systems directed towards the geotechnical and mining sector with great emphasis and experience in slope stability, landslides and geotechnical monitoring. Our core value is to sustain a strong connection with our clients while at the same time maintaining our technical and scientific independence.



Planetek Hellas is a Greek company, member of the Planetek Group that since 1994, operates in the field of Satellite Remote Sensing, Spatial Data Infrastructure and Software development for the “on board” and “ground” segment space applications. Founded in 2006, Planetek Hellas provides solution oriented services in the field of Geomatics, involving the use of EO data and systems for environmental & critical infrastructure monitoring, urban planning, civil protection and security.

Planetek has designed, built and commercializes Rheticus, the trademarked award winning Geospatial Analytics Platform, through which the company's solutions are offered in the market. Rheticus represents a disruptive approach of IaaS (Info as a Service) globally scalable, subscription based with low recurrent costs. Rheticus integrates and makes use of state of the art technologies of nowadays such as HPC, AI, Cloud and Internet. More info: www.rheticus.eu.

The company is also active in the field of promotion of Earth Observation and Cosmic Exploration data exploitation and pursues close relations with Education and Research Organizations inside and outside Greece.



HELMA S.A. and WIRTGEN GROUP cooperate for very long time in the field of road construction and mining technologies and machineries in Greek territory.

WIRTGEN GmbH has developed the methodology and technology of Selective Surface Mining, supplying Global Market with three different types of machines, 2200 SM, 2500 SM and 4200 SM and application in mines of iron, gypsum, bauxite, phosphate, limestone, granite, coal etc. In Greece the Selective Surface Mining technology is applied in PPC mines in Ptolemaida.

Symposium Committees

Organizers

*Public Power Corporation of Greece
Mines Business Unit*

*National Technical University of Athens School of
Mining and Metallurgical Engineering*

*Technical University of Crete
School of Mineral Resources Engineering*

Local Organizing Committee

Roumpos C., Dr., Former Assist. Professor

Michalakopoulos Th., Assoc. Professor

Galetakis M., Professor

Pavloudakis F., Dr.

Conference Board

Roumpos C., Dr., Former Assist. Professor

Pavlovic V., Professor

Drebenstedt C., Professor

International Organizing Committee

Agafonov J., Professor

Agioutantis Z., Professor

Bui N., Professor

Cehlár M., Professor

Galitis N., Dr.

Hardygora M., Professor

Hu Z., Professor

Ignjatović D., Professor

Karmis M., Professor

Kazanin O., Professor

Kecojevic V., Professor

Koukouzas N., Dr.

Kouridou O., Head of Mines Business Unit

Lazar M., Professor

Lilić N., Professor

Meechumna P., Professor

Nelson P., Professor

Panagiotou G., Professor

Rakishev B., Professor

Schafrik S., Assoc. Professor

Singh P., Professor

Totev L., Professor

Session 1: Mine planning and design

Simulating the BWE-Conveyor-Stacker System in Python using Salabim

George N. Panagiotou

Laboratory of Excavation Engineering, School of Mining Engineering & Metallurgy, National Technical University of Athens, Greece

ABSTRACT

The BWE-Conveyor-Stacker mining system has been simulated during the last 45 years using various IT tools including general purpose or simulation specific programming languages and commercial simulation software. The paper presents a simulator of the BWE-Conveyor-Stacker system developed using solely Open-Source Software tools that are freely available for downloading from the Internet. At present stage of development, the simulator can accommodate a mining system that consists of a BWE, any number of conveyor sections, and a Stacker or a Bunker Spreader. It runs on a single GUI window which is sectioned to include data input, simulation output and plots. A detailed output report for each project is generated, in pdf format, for printing and record keeping. The simulator has been developed in Python using Salabim, a discrete event simulation package recently available, and runs as Microsoft Windows application.

1. INTRODUCTION

The Bucket Wheel Excavator (BWE)-Conveyor-Stacker mining system is the dominant material handling system used in lignite opencast mining and it is characterized by high production rates due to its continuous operation, high owning and operating cost and limited flexibility to meet changes in mine layouts and operation plans. The stochastic nature of the events occurring during the operation of the system (different material types and flow rates, machinery failure frequency and repair times duration etc.) makes stochastic simulation the best method for studying such systems in order to achieve results that are close to real life mine production figures.

The BWE-Conveyor-Stacker system has been simulated during the last 45 years using various IT tools including general purpose programming languages like FORTRAN [1], simulation specific languages like GPSS/H® [2] or commercial simulation software like ARENA® [3] and numerous papers on the topic have been published.

Moving into the era of *Open-Source Software* (OSS) the paper presents *BWE-Conveyor-Stacker-Sim*, a simulator for BWE, conveyors and stacker mining system operations with a graphical user interface, developed using programming tools that are freely available for downloading from the Internet.

BWE-Conveyor-Stacker-Sim has been developed in Python, a mainstream OSS computing language using Salabim, a Python package for Discrete Event Simulation (DES) recently available and runs as Microsoft Windows application.

2. PYTHON

Python is an interpreted high-level programming language for general-purpose programming, created by Guido van Rossum, first released in 1991 and still under continuous development/maintenance. Python interpreters are available for many operating systems and have a large and comprehensive standard library, while third-party packages, with specific functionalities that facilitate programming, are widely available for free downloading and use by importing them

into the Python code. *CPython* is the reference implementation of the Python programming language. Written in C, CPython is the default and most widely used implementation of the language [4].

Python is developed under an OSI-approved open source license making it freely usable and distributable, even for commercial use. Python's license is administered by the Python Software Foundation [5].

Python exists in two versions: *Python 2.x* (current release 2.7.15) and *Python 3.x* (current release 3.7.0). Python 2.x is legacy, Python 3.x is the present and future of the language.

3. SALABIM

Salabim is a Python third-party package created by Ruud van der Ham, first released in 2017, still under continuous development, which is freely available under an MIT License, and it is imported into the Python code for creating simulation models [6]. The package (current release 2.3.2.4) comprises discrete event simulation, queue handling, resources, statistical sampling and monitoring, while real time animation is built-in. It runs both in Python 2.7 or 3.x for the implementations CPython, PyPy and Pythonista (iOS). Salabim itself is provided as a single Python script, called *salabim.py* and this file can be placed in any directory where the simulation models reside [7].

Running simulation models under PyPy is highly recommended for production runs, when run time is important, since it has been found that execution is faster 6 to 7 times compared to CPython. However, for development CPython or Pythonista is recommended.

To demonstrate the basic structure, process interaction, component definition and output of a Salabim-based simulation model, a simple self-explanatory example of a shovel-truck simulation model, developed by the author, is given below:

```
# A Simple Shovel-Truck Simulation Model in Salabim
__author__ = 'panagiotou'
import salabim as sim
# INPUT DATA SECTION
number_of_trucks = 3
truck_interarrival_time = 2    # min
number_of_shovels = 1
loading_time = 2.5             # min (includes spotting time)
travel_dump_return_time = 7    # min
simulation_time = 8            # hours
# SIMULATION MODEL
class Truck(sim.Component):
    """
    Inherits from the salabim class sim.Component and controls trucks
    into the wait-load-travel-dump-return cycle
    """
    def process(self):
        while True:
            self.enter(queue_for_loading)
            # Truck enters the 'Queue for Loading'
            yield self.request((shovels, 1))
            # One truck requests the 'Shovel' for loading
            self.leave(queue_for_loading)
            # Truck leaves the 'Queue for Loading'
            yield self.hold(loading_time)
            # Shovel is loading the Truck
            self.release((shovels, 1))
```



```

        # Truck departs from the 'Shovel'
        yield self.hold(travel_dump_return_time)
        # Truck travels, dumps and returns to the 'Queue for Loading'
# HOUSEKEEPING STATEMENTS
env = sim.Environment(trace=True)
queue_for_loading = sim.Queue('Queue for Loading')
shovels=sim.Resource("Shovel",capacity=number_of_shovels)
for i in range(number_of_trucks):
    Truck(at=i * truck_interarrival_time)
# At most 'number_of_trucks' trucks are generated, the
# 1st truck arrives at the 'Queue for Loading' at time=0, the rest
# in time intervals = trucks_interarrival_time
env.run(duration=(simulation_time * 60))
# Runs simulation for 'simulation_time * 60' min
queue_for_loading.print_statistics()
# Prints statistics for the 'Queue for Loading'
shovel_util = (shovels.claimed_quantity.mean() /
               shovels.capacity.mean())
# Calculates Shovel's Utilization and then prints it
# as % of the available time
print('Shovel is %0.2f %% busy' % float(shovel_util*100))

```

The output of the shovel-truck simulation model of the above example, for a simulation run with input data those of the INPUT DATA SECTION of the code, is shown below:

```

Statistics of Queue for Loading at      480
-----
Length of Queue for Loading
duration      480
mean          0.003
std.deviation 0.056
minimum       0
median        0
90% percentile 0
95% percentile 0
maximum       1

Length of stay in Queue for Loading
entries       152
mean          0.010
std.deviation 0.090
minimum       0
median        0
90% percentile 0
95% percentile 0
maximum       1

Shovel is 79.17 % busy

```

	all	excl.zero	zero
Length of Queue for Loading	480	1.500	478.500
mean	0.003	1	
std.deviation	0.056	0	
minimum	0	1	
median	0	1	
90% percentile	0	1	
95% percentile	0	1	
maximum	1	1	
Length of stay in Queue for Loading	152	2	150
mean	0.010	0.750	
std.deviation	0.090	0.250	
minimum	0	0.500	
median	0	1	
90% percentile	0	1	
95% percentile	0	1	
maximum	1	1	

4. BWE-CONVEYOR-STACKER-SIM: A QUICK TOUR

BWE-Conveyor-Stacker-Sim is a simulator that models the operation of a continuous mining system comprised of a BWE excavating waste or lignite in a mine bench and loading conveyor sections that follow pre-defined routes, between the BWE and a Stacker or a Bunker Spreader, depending on the type of the material being excavated.

The simulator has been developed in Python using Salabim as Microsoft Windows application and has a fully graphical user interface (GUI). All the action happens in the main window of the application (Fig. 1). The 'menu bar' on the top of the application's window has clickable buttons that

activate ‘drop-down’ menus, ‘cascaded’ sub-menus and ‘pop-up’ widows, when appropriate, through which the user makes selections or enters data for the model’s parameters (Fig. 2).

The *Options* button enables the user to select the *Rock Type* excavated by the BWE and to enter data for the *Simulation Parameters*.

In the *INPUT* section of the application’s window, which is sub-divided into four sub-sections, the user enters text regarding project related information and data regarding BWE, Conveyor Groups, Stacker and Bunker Spreader operational parameters, as well as time data for the equipment’s failures frequency and repairs duration.

The *Run* button enables the user to execute a *Simulation* run of the model. Upon clicking this button, the currently (final) selected options are displayed in the *Selected Options* window, the simulation output is displayed in the *Results* sub-section and conveyors overflow statistics, over the simulation time, is shown in the *Plots* sub-section of the *OUTPUT* section.

The *Report* button prepares a detailed simulation report in pdf format and opens it with a *pdf Reader* so that the user can ‘print’ and ‘save as’ it using standard *pdf Reader* procedures.

The *Help* button provides access to the *User Manual* and to information regarding *BWE-Conveyor-Stacker-Sim*.

Finally, the *Quit* button of the menu bar exits the application in a proper way.

Figure 3 shows a screenshot that displays the input values, the selected options and the simulation output for a specific project.

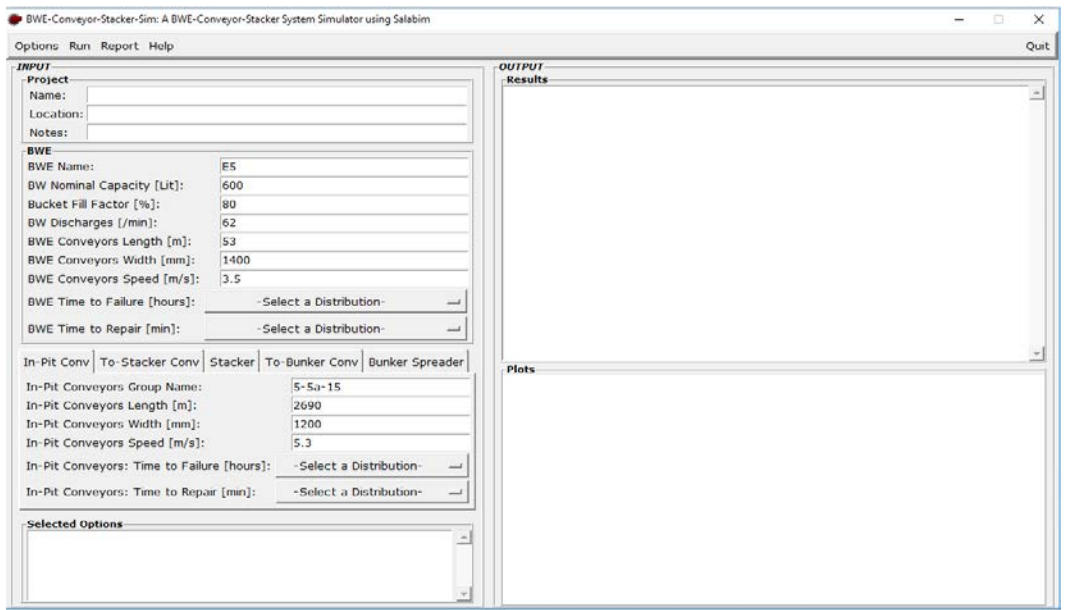


Figure 1. BWE-Conveyor-Stacker-Sim main window.

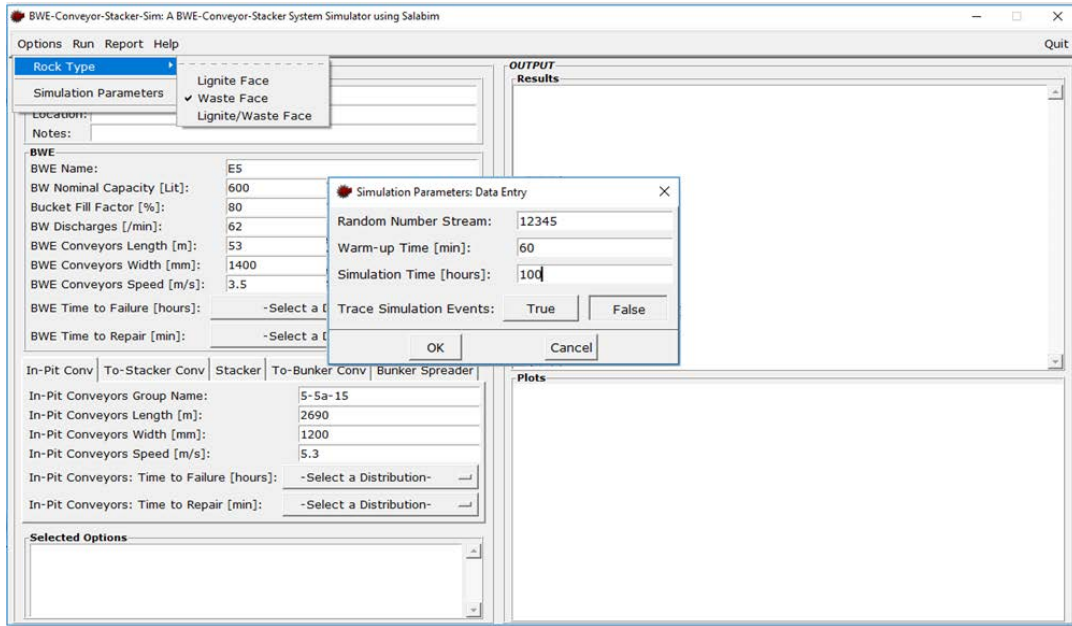


Figure 2. BWE-Conveyor-Stacker-Sim ‘drop-down’ menus, ‘cascaded’ sub-menus and ‘pop-up’ windows.

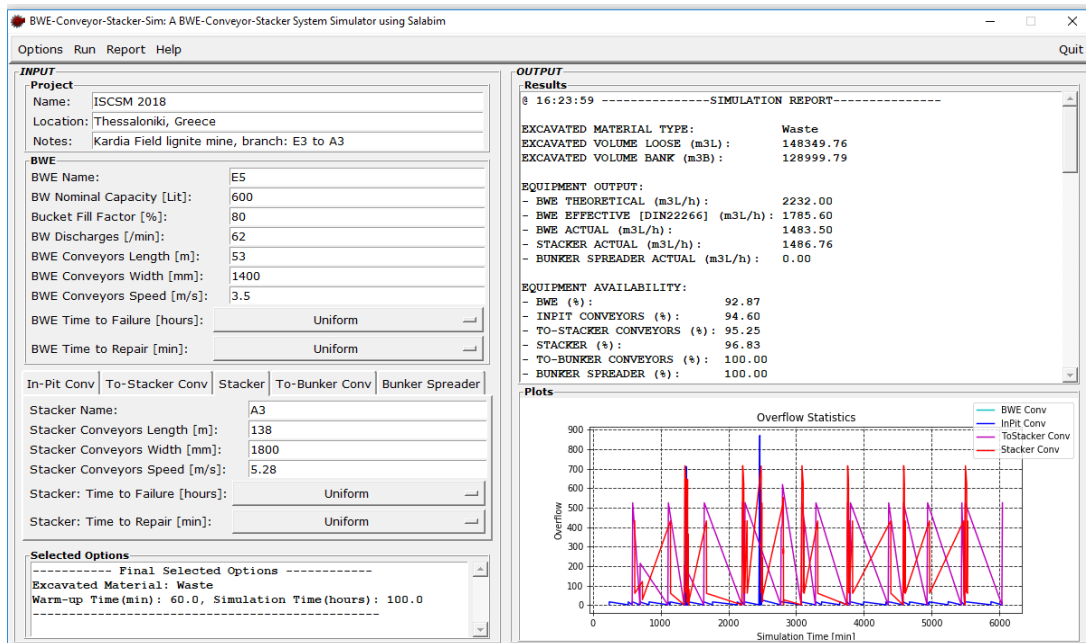


Figure 3. BWE-Conveyor-Stacker-Sim in action.

5. BWE-CONVEYOR-STACKER-SIM: BEHIND THE SCENES

BWE-Conveyor-Stacker-Sim, at present stage of development, is capable to simulate a continuous mining system configuration with a BWE, an in-pit conveyors group, an out-of-the-pit conveyors group feeding with waste material the stacker, a Stacker, an out-of-the-pit conveyors group feeding with lignite the bunker spreader, and a Bunker Spreader. A conveyors group may consist of one or more belts with different lengths but with the same belt width and running speed. Equipment breakdowns frequency and repairs time for all equipment are taken into account in the system's analysis.

Such materials handling systems, which operate in series and form a network of continuous material flow, require proper matching of the flow rate that each piece of equipment can achieve, in order to avoid overloading and material overflow (spillage), or underloading leading to high production costs. Furthermore, production rates are heavily affected by unplanned maintenance periods, due to equipment failures that force the stoppage of all up-stream equipment.

The simulation of a continuous material flow system using discrete event simulation technics can be performed by dividing the continuous stream of the material into discrete units of material of the same mass, as shown in Fig. 4 [8]. In *BWE-Conveyor-Stacker-Sim* the discrete material unit is the volume of the material excavated by one bucket of the BWE. This bucket-load (= bucket_nominal_capacity * bucket_fill_factor), being either waste or lignite, is transported along the mining system from the BWE to the waste dump or the lignite bunker during the simulation run.

The number of input parameters for a simulation run is rather minimal and include:

- Simulation time
- Warm-up time (for the simulation run)
- Bucket nominal capacity
- Bucket fill factor
- Number of bucket discharges per minute
- Materials unit weight and swell factor

and

- Conveyor length
- Conveyor width
- Conveyor speed

for each conveyors group.

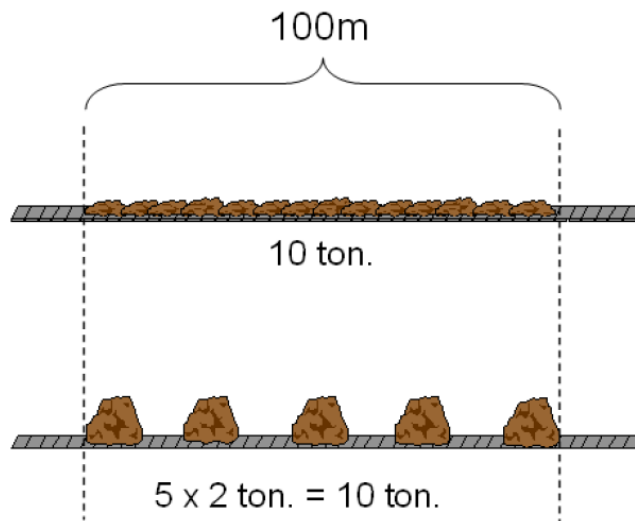


Figure 4. Transformation of continuous material flow into discrete material flow [8].

As in the real world, the time between equipment breakdowns and the time of the required repairs varies stochastically following some statistical distribution, which can be determined after a statistical analysis of the respective data collected from mine records. The *BWE-Conveyor-Stacker-Sim* user can select the appropriate statistical distribution, which fits better the particular breakdown and repair time data, from a list of nine distributions:

- Beta
- Constant
- Erlang
- Exponential

- Gamma
- Normal
- Triangular
- Uniform
- Weibull

and the input data required for the selected distribution are entered, for each unit of equipment, via a ‘pop-up’ window (Fig. 5).

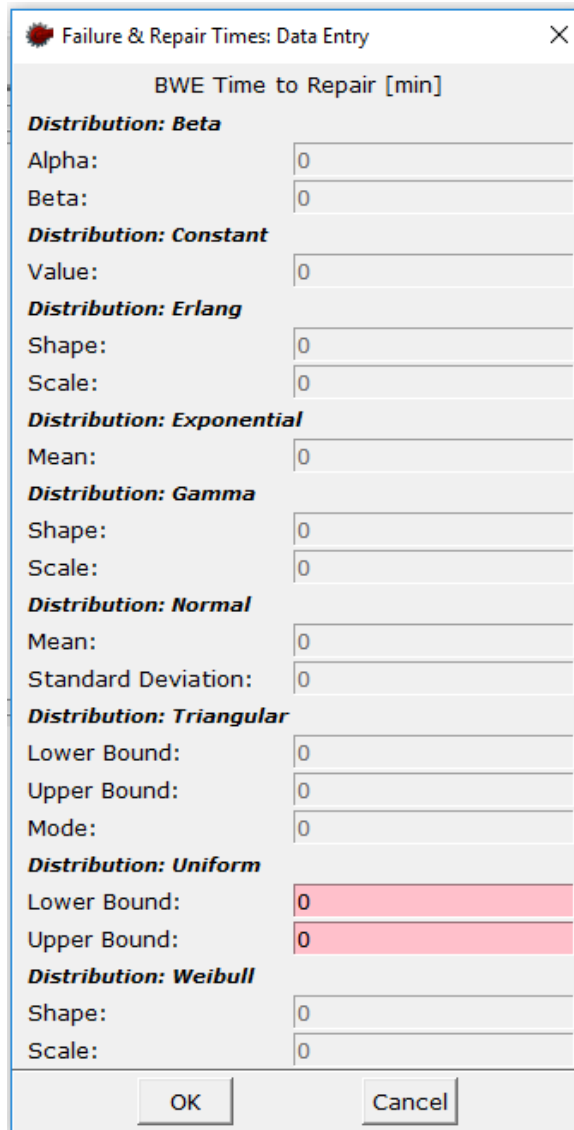


Figure 5. Available repair time distributions for BWE; data entry ‘pop-up’ window.

A simulation run may or may not include a user defined ‘warm-up’ period at the start of the simulation. The purpose of the ‘warm-up’ period is to allow for the system to get operationally ‘normalised’ (it may take more than 20 minutes for the first bucket-load to travel from the BWE to the Stacker, depending on the conveyors length and speed). During this period simulation statistics are not collected, and the actual simulation run and statistics collection start when the ‘warm-up’ period ends.

Hypothetical surge bins are assumed to exist at the head of each conveyor group, including the BWE, Stacker and Bunker Spreader conveyors, to control possible material overflows and the collected statistics are graphically displayed.

Following a simulation run, the user is provided with a customised simulation report which includes production estimates; utilisation, availability and breakdown/repair statistics for the equipment (Fig. 3). In addition, a detailed simulation report is provided as a pdf formatted document suitable for record keeping.

6. BWE-CONVEYOR-STACKER-SIM: PROGRAMMING TECHNICALITIES

BWE-Conveyor-Stacker-Sim has been developed in Python using the PyCharm Professional Integrated Development Environment (IDE), Ver. 2018.2.1 [9], for editing, debugging and running the code, and it is a Microsoft Windows application for Windows 10. It runs under both Python Versions 2.7.15 and 3.7.0 [4]

In addition to standard Python libraries, the following third-party packages have been imported into the code of *BWE-Conveyor-Stacker-Sim*:

- Salabim Ver. 2.3.2.4, for the discrete system simulation [7]
- Tkinter, the standard Python interface to the Tk Graphic User Interface toolkit [10]
- Pmw Ver. 2.0.1, a toolkit for building high-level compound widgets in Python using Tkinter [11]
- Matplotlib Ver. 2.2.2, for creating the plots [12]
- Fpdf Ver. 1.7.2, for generating the simulation report as pdf document [13]

7. BWE-CONVEYOR-STACKER-SIM: AN EXAMPLE

The Kardia Field lignite mine which is located in northwest Greece and is owned and operated by the Public Power Corporation of Greece SA (PPC), has been the test-bed for many simulation modelling studies during the last 40 years using various IT tools, including programming languages like FORTRAN and GPSS/H® and simulation software packages like ARENA®, in which the author has been involved [1], [2], [3].

A mining branch of the Kardia Field mine that consists of (Fig. 6):

- BWE: E5 (KRUPP SchRs 600/3.3 x 21)
- In-pit conveyors group: 5-5a-15 (length: 2690m, width: 1200mm, speed: 5.3m/s)
- Out-of-the-pit conveyors group feeding the stacker: 30-31-32-33 (length: 3668m, width: 1800mm, speed: 5.3m/s)
- Stacker: A3 (TAKRAF A2RS B 6700.60)
- Out-of-the-pit conveyors group feeding the bunker spreader: K1-K2 (length: 1680m, width: 1800mm, speed: 5.2m/s)
- Bunker Spreader: KB (SALTZITTER MASCHINEN A.G. U.B 1000-B1000/15)

has been used to test *BWE-Conveyor-Stacker-Sim* capabilities.

One of the tests carried out was to check the time it takes for a bucket-load discharged by the bucket wheel to travel from the BWE to the Stacker. The simulator estimated this time 20.71 min, while the actual time, measured by mine personnel, is 20.61 min, and this confirms the model's capability to accurately simulate the movement of the excavated mass along the conveyors network.

The customized simulation report of a simulation run for 100 hours and with one hour 'warm-up' period, for the Kardia Field mine branch E5 to A3, when excavating waste material, is shown in Fig. 7.

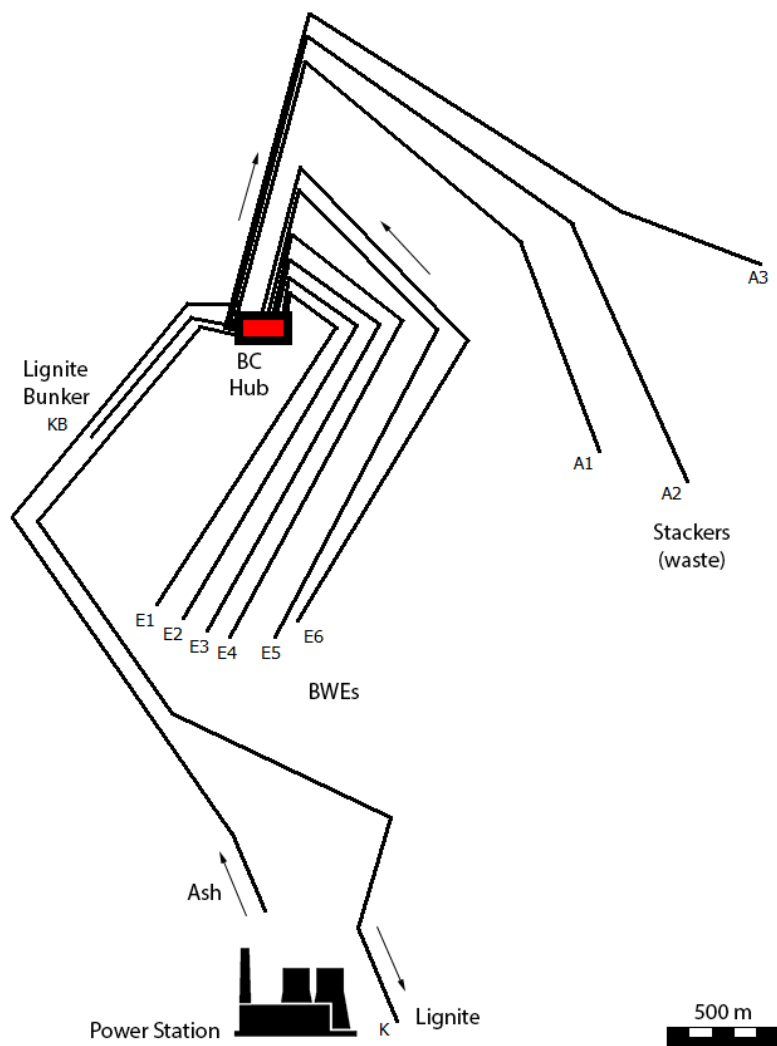


Figure 6. Kardia Field lignite mine. Equipment layout [14]

8. CONCLUSIONS

The application of simulation models for studying complex mining systems under real life conditions is well accepted by modern mine management, especially in the design and planning phases of new mining projects or when optimizing existed ones to meet certain conditions. The dynamic character of the processes, activities and entities within a mining system and the stochastic character of the events occurring during the operation of these systems, make simulation to be the only reliable method for manipulating such systems.

```

@ 17:38:09 -----SIMULATION REPORT-----
EXCAVATED MATERIAL TYPE:                Waste
EXCAVATED VOLUME LOOSE (m3L):           142687.68
EXCAVATED VOLUME BANK (m3B):            124076.24

EQUIPMENT OUTPUT:
- BWE THEORETICAL (m3L/h):               2232.00
- BWE EFFECTIVE [DIN22266] (m3L/h):     1785.60
- BWE ACTUAL (m3L/h):                   1426.88
- STACKER ACTUAL (m3L/h):                1426.88
- BUNKER SPREADER ACTUAL (m3L/h):       0.00

EQUIPMENT AVAILABILITY:
- BWE (%):                               92.90
- INPIT CONVEYORS (%):                   94.53
- TO-STACKER CONVEYORS (%):              95.64
- STACKER (%):                           96.96
- TO-BUNKER CONVEYORS (%):               100.00

EQUIPMENT UTILIZATION:
- BWE (%):                               86.15
- INPIT CONVEYORS (%):                   92.18
- TO-STACKER CONVEYORS (%):              96.83
- STACKER (%):                           100.00
- TO-BUNKER CONVEYORS (%):               100.00
- BUNKER SPREADER (%):                   100.00

TRANSPORTED MATERIAL BY:
- BWE CONVEYORS (m3L):                   142687.68
- INPIT CONVEYORS (m3L):                 142687.68
- TO-STACKER CONVEYORS (m3L):            142687.20
- TO-BUNKER CONVEYORS (m3L):             0.00

DISPOSED MATERIAL BY:
- STACKER (m3L):                         142687.68
- BUNKER SPREADER (m3L):                 0.00

MATERIAL TRAVEL TIME ON:
- BWE CONVEYORS (min):                   0.26
- INPIT CONVEYORS (min):                 8.47
- TO-STACKER CONVEYORS (min):            11.54
- STACKER CONVEYORS (min):               0.44
- FROM BWE TO WASTE DUMP (min):          20.71

NUMBER OF FAILURES:
- BWE:                                    17
- INPIT CONVEYORS:                       19
- TO-STACKER CONVEYORS:                  10
- STACKER:                                7
- TO-BUNKER CONVEYORS:                   0
- BUNKER SPREADER:                       0
    
```



```

DOWNTIME (OWN FAILURES):
- BWE: (min):                425.74
- INPIT CONVEYORS (min):     328.48
- TO-STACKER CONVEYORS (min): 261.36
- STACKER (min):             182.20
- TO-BUNKER CONVEYORS (min):  0.00
- BUNKER SPREADER (min):     0.00

DOWNTIME (OTHERS FAILURES):
- BWE: (min):                772.04
- INPIT CONVEYORS (min):     443.56
- TO-STACKER CONVEYORS (min): 182.20
- TO-BUNKER CONVEYORS (min):  0.00

TOTAL DOWNTIME (OWN & OTHERS FAILURES):
- BWE: (min):                1197.78
- INPIT CONVEYORS (min):     772.04
- TO-STACKER CONVEYORS (min): 443.56
- STACKER (min):             182.20
- TO-BUNKER CONVEYORS (min):  0.00
- BUNKER SPREADER (min):     0.00

```

Figure 7. Simulation report for the Kardia Field mine branch E5 to A3 example when excavating waste material

Discrete-event simulation modelling can be used to evaluate the design of a new mining system or the effect of changes to the performance of existing systems. Fine tuning changes of equipment operational parameters can be thoroughly studied, critically analyzed and justified in the office, based on economic or operational criteria, before deciding to apply in the field. To solve these problems, it will take a few minutes of computing time on a typical PC, while easy to use data input templates and customized simulation output, with meaningful diagrams, make simulators an engineering tool for everyday use.

BWE-Conveyor-Stacker-Sim is a simulator that simulates a continuous mining system using discrete event simulation techniques and can be used for the planning and analysis of BWE-Conveyor-Stacker operations in opencast lignite mines assisting engineers and mine management in optimal equipment selection, sizing, optimizing and scheduling.

BWE-Conveyor-Stacker-Sim is a paradigm of engineering software developed using solely Open-Source Software tools that are freely available for downloading from the Internet. It has been coded in Python using Salabim, a newly available and very promising package for creating discrete event simulation models in Python.

Future work should focus on extending the model's capabilities to simulate multi-bench operations and animate the simulated system in real time, exploring present and future developments of the Salabim package.

ACKNOWLEDGMENTS

The author thanks the Mining Engineering Unit, Mines Central Support Department of the Public Power Corporation of Greece SA for providing the Kardia Field mine equipment specification details and the time study data used in the simulation model.

REFERENCES

- [1] Panagiotou, G. N. (1979). Computer simulation of the mining operations in an opencast lignite mine. M.Sc. Thesis, University of Newcastle Upon Tyne, UK.
- [2] Michalakopoulos, T. N., Arvaniti, S. E. and Panagiotou, G.N. (2005). Simulation of a continuous lignite excavation system. In *Mine Planning and Equipment Selection 2005* (eds. RK Singhal et al.), Reading Matrix, Irvine, 1694-1706.
- [3] Michalakopoulos T. N., Roumpos C. P. and Panagiotou G. N. (2007). ARENA simulation of continuous lignite excavation systems. In *Mine Planning and Equipment Selection 2007* (eds. RK Singhal et al.), Reading Matrix, Irvine, 636-647.
- [4] www.python.org. Assessed on August 1, 2018.
- [5] www.python.org/psf. Assessed on August 1, 2018.
- [6] van der Ham, R. (2018). Salabim: discrete event simulation and animation in Python. *Journal of Open Source Software*, 3(27), 767, <https://doi.org/10.21105/joss.00767>
- [7] www.salabim.org. Assessed on August 07, 2018
- [8] Fiorini, M. M. and Furia, J. (2007). Simulation of continuous behavior using discrete tools: ore conveyor transport. *Proceedings of the 2007 Winter Simulation Conference*, IEEE, 1655-1662.
- [9] www.jetbrains.com/pycharm. Assessed on August 1, 2018.
- [10] <https://docs.python.org/2/library/tkinter.html>. Assessed on August 1, 2018.
- [11] <http://pmw.sourceforge.net>. Assessed on August 1, 2018.
- [12] <https://matplotlib.org>. Assessed on August 1, 2018.
- [13] <http://pydoc.net/fpdf/1.7.2>. Assessed on August 1, 2018.
- [14] Michalakopoulos T. N, Roumpos C. P., Galetakis M. J. and Panagiotou G. N. (2014). Discrete-event simulation of continuous mining systems in multi-layer lignite deposits. *Proc. of the 12th Int. Symposium Continuous Surface Mining - Aachen 2014*, 225-239.

A Holistic Approach for Highly Selective Mechanical Process Chains

Bruno Grafe, Carsten Drebenstedt, Taras Shepel, Vishal Vilas Yadav

TU Bergakademie Freiberg, Germany

ABSTRACT

The paper describes the holistic approach of the research project InnoCrush. The greater goal of the project is to prepare innovations in the field of mechanical driven and highly selective process chains in mineral extraction. The core features of such process chains lie in a) the use of mechanical excavation methods instead of drilling and blasting and b), the subsequent utilisation of a near-face mechanical, dry, selective comminution to create a pre-concentrate. With the synergetic use of both technologies, a major part of the waste material can be separated from the ore either during excavation as well as during subsequent comminution. Hence, the waste can directly be backfilled or dumped. The focus lies on vein like deposits that can profit most from such technological chains. The project itself focuses on Lead-Zinc and Fluorite-Barite Ores.

Such process chains can provide benefits in terms of great automation potential, minimization of emissions, increase of work and rock safety, as well as considerable financial savings during final comminution steps. The latter can be traced back to the fact that considerably less material must be milled during the final comminution steps. Limitations however, are present in the form of toughness and abrasivity of the rock as well as the potential of ore and waste for a selective comminution.

A summary of the present results within the project InnoCrush is given as well as discussing how a multilevel, holistic approach to synergy-dependent process chains is necessary in order to push the boundaries of mechanical excavation chains further.

1. BACKGROUND

Europe being on the consuming side of the world's primary mineral production is under necessity to create a secure and reliable supply situation. In that context, the European Commission coined the term "Critical Raw Material" (CRM). Currently 27 Materials, mainly mineral resources, but also coking coal and natural rubber fall under this category. Light and Heavy Rare Earth Elements as well as Platin Group Elements count as one material group each within this assessment (see Table 1). CRMs are materials of high economic importance to the Union's economy that at the same time are subject to a globally very concentrated production. Often, this concentrated production is accompanied by unstable political conditions, further increasing the potential supply risk should political situations change [1]. The recent geopolitical developments emphasize the necessity of a diverse supply market in order to minimize negative impacts on the global economy.

In order to a) diversify the global supply of CRMs to create a more resilient market in general and b) at the same time create a more favourable supply situation for the EU, it is obvious that diversified sources for the aforementioned minerals must arise.

To reach these two goals, the most direct solution would be to increase the mineral production within the Union. Whilst Europe is not rich in big, near to face, bulky deposits – also due to hundreds of years of mining activity. Many smaller and complex deposits can be found, especially in the area of south eastern Europe [2] but also in Saxony, Germany [3]. As part of these deposits, vein-like deposits are in the focus of the research project InnoCrush, a young research group of 11 scientists of 6 six chairs at TU Bergakademie Freiberg. Hydrothermal veins often consist of a multitude of mineralisations and often are accompanied by CRMs as in the example on Figure 1. Lead-Zinc ores

that are accompanied by Germanium and Indium also can be found in Freiberg. Since Saxony is rich in smaller complex vein-like deposits, they are in the focus of InnoCrush.

Table 1: List of Critical Raw Material as of 2017 [1]

2017 CRMs (27)			
Antimony	Fluorspar	LREEs	Phosphorus
Baryte	Gallium	Magnesium	Scandium
Beryllium	Germanium	Natural graphite	Silicon metal
Bismuth	Hafnium	Natural rubber	Tantalum
Borate	Helium	Niobium	Tungsten
Cobalt	HREEs	PGMs	Vanadium
Coking coal	Indium	Phosphate rock	

*HREEs=heavy rare earth elements, LREEs=light rare earth elements, PGMs=platinum group metals

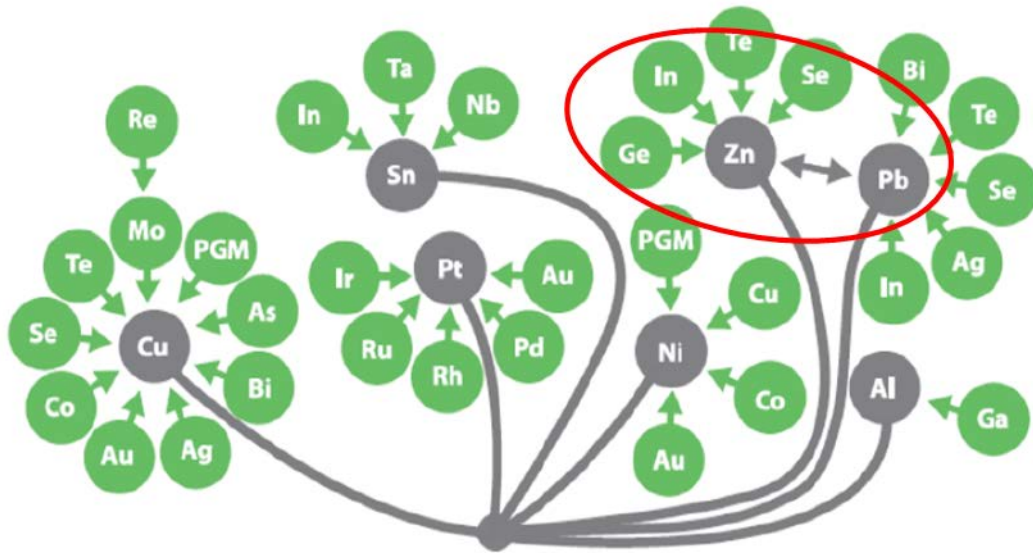


Figure 1: Sources of certain critical (and non-critical) raw materials (green) and their associated base metal (grey) [4]

Albeit a potential for the exploitation of such deposits does exist, this must be seen in the context of the industrial, social and ecological environment that defines the Union:

- rather high technology and industrialization level
- rather high level of education and educated workforce availability
- good infrastructure
- rather high work safety standards
- rather high environmental protection and recultivation standards
- rather high wages
- issues with the public acceptance of large scale projects, especially mining projects

In this environment, high tech solutions with a minimum possible environmental impact are of the essence. A successful transformation towards the well discussed Mining 4.0 has the potential to result in a comparative advantage of the mining manufacturing industry of Europe additionally. This is of global interest since even developing mining countries, e.g. South Africa, are facing a rise in wages, hence mining costs, and the necessity for higher automated low impact mining technologies [5].

As highly automated low impact mining is the focus, the whole technology chain must be tailored towards the following aims:

- minimisation of tailing material and waste
- minimisation of ground disturbance
- minimisation of emissions towards local communities
- minimisation of energy consumption during production of the final concentrate
- provision of highest work safety standards
- all this while...
- provision of acceptable mining cost, this is only possible by limiting the active workforce in a mine

Since, for the final answer of the question “mining, or no mining”, the whole process chain must be designed and evaluated as one piece - rather than solitarily optimizing individual work steps. As such the rather novel and synergetic combination of two emerging technologies in mining has been chosen: *cutting excavation* in combination to near face *dry selective comminution*.

2. DEPOSITS UNDER FOCUS

Two kinds of hydrothermal ores are under focus: Fluorite-Baryte-Ores (F-Ba) and Lead-Zinc-Ores (Pb-Zn). Currently there is one fluorite mine in operation in Saxony; the mine Niederschlag operated by Erzgebirgische Fluss- und Schwerspatwerke GmbH. For sampling, a nearby, similar, smaller deposit was chosen: the Gneiss quarry Dörfel that is operated by the Max Bögel Group.

Pb-Zn-Ores could be sampled from the Research-and-Teaching Mine of TU Freiberg, “Reiche Zeche” in Freiberg (Figure 2).

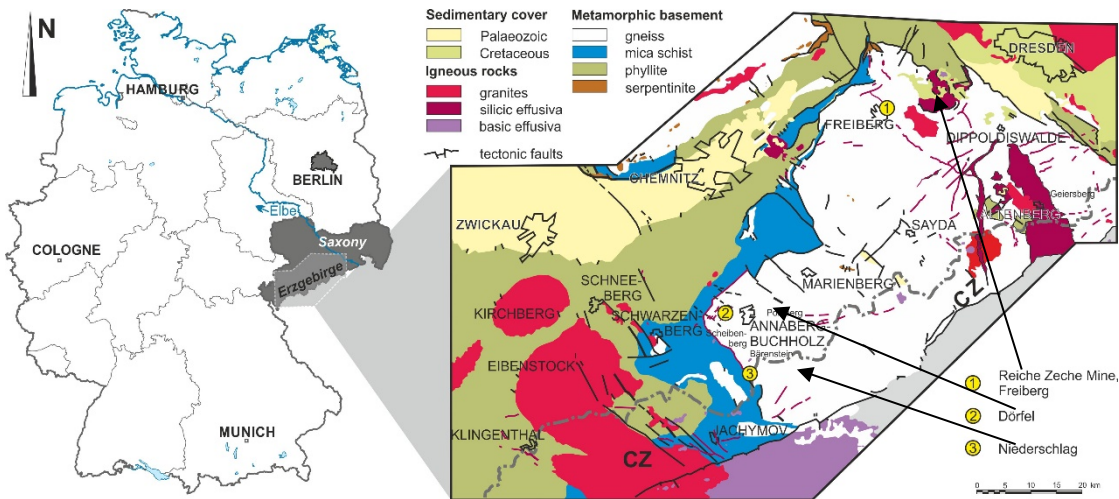


Figure 2: Location of the sampling areas within Germany and Saxony [6]

The vein deposits are mainly embedded in Gneiss as host rock in the form of metasediments (grey gneisses) and metamagmatites (red and grey gneisses). The Freiberg gneiss domain consists of a grey augengneiss formed by Variscan high metamorphism of Early Cambrian granodiorite [7]. The polymetallic mineralisations are of hydrothermal origin (lead, zinc, silver) that are mainly linked to Permian tectonic activity [8]. The veins are usually subdivided according to their orientation and mineral associations [9]. For the project, veins are of importance because they show a stark change

from host rock to vein material. As such, the most effect from highly selective mining technologies is expected.

3. PROCESS CHAIN

In its core, the process scheme introduces the innovative combination of selective cutting and selective comminution for high grade, smaller deposits such as vein-like deposits. As can be seen in Figure 3, the basic process chain consists of (a) an excavation by mechanical means which is followed by (b) a near to face mechanical, selective comminution that creates (c) a pre-concentrate which is hauled to the final milling and enrichment processes. The selective excavation ensures that only vein material is brought into the enrichment part of the process chain. The selective comminution creates a preconcentrate from the vein material. By such, the amount of material to handle in the enrichment part of the process chain is reduced at two stages. This reduces the effort necessary for haulage of ore as well as the amount of energy required for milling the ore. A reduction of the material to mill can have a tremendous impact on the total energy consumption of the total production chain as it can account for 80 – 90 % of the total energy consumption of a typical mine [10, 11, p. 141].

A separation of vein material and host rock takes place during excavation and another separation step of gangue material takes place during the selective comminution. As such the early removed waste (d) can be dumped/ backfilled very early in the process chain. Since the material will not be milled, it will not occur as a fine slurry. As such, the total material to be treated in tailing ponds can be reduced. This significantly decreases the environmental impact and can have a positive effect on public acceptance.

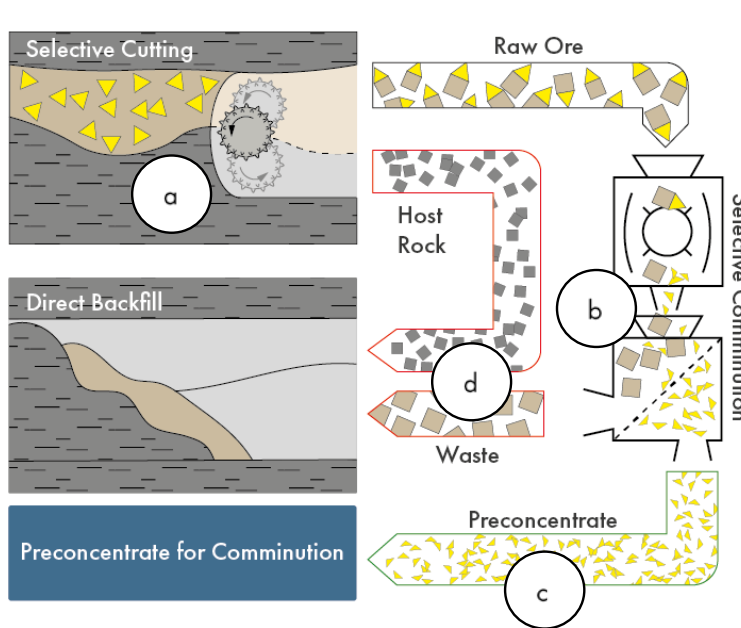


Figure 3: Scheme of highly selective mechanical production chain

Additionally, explosive gases do not occur. Hence, rising limits for NO_x-gases at working places are not critical. Furthermore, the influence to the surrounding rock and local communities is limited [12, 13]. As a result of this technological chain, the in Table 2 summarized results are to be expected:

Table 2: Advantages and disadvantages of the proposed production chain

Advantages cutting excavation	Advantages selective comminution
<p>Continuous, highly automatable operation</p> <p>No blasting → no blasting gases and limited damage to surrounding rock mass</p> <p>No sizing needed</p> <p>Homogeneous particle distribution</p> <p>Very high selectivity potential</p>	<p>Dry process</p> <p>Early ore enrichment</p>
Disadvantages cutting excavation	Disadvantages selective comminution
<p>Limited number of production units → higher breakdown influence, more blending effort needed</p> <p>Limited by rock strength and abrasivity</p>	<p>Differences in rock properties between ore and waste must allow for sel. comminution</p>
Synergetic Advantages	
<p>Possibility of direct backfill after early waste separation → minimization of environmental impact</p> <p>Reduction of the overall material to mill, haul → reduction of operating cost</p> <p>Reduction of energy consumption and tailing material → reduction of operating cost</p>	

To enable this process chain, several aspects must be addressed. Therefore, the InnoCrush project is comprised of six entwined work groups: Mineralogy, Mining, Processing, Automation, Modelling and Economics whose work will be described below.

3.1. Rock Cutting

To unlock smaller vein-like deposits, a cutting machine must be able to cut both ore and - if the necessity arises - the host rock. The mostly hard and tough host rock effects high forces during cutting. The major limitation of mechanical excavation machines is their limited ability to perform well in geotechnical conditions exceeding a certain abrasivity and rock strength. As such, the activated cutting technologies are under research within the project.

The testing rig for linear rock cutting HXS 1000-50 (Figure 4) is used for conventional and activated cutting to quantify the forces and dynamics during excavation.

It features a modular design for testing of different cutting tools. The maximum cutting forces are 75 kN. The forces are measured with a maximum frequency of up to 10 kHz. In order to evaluate the specific energy consumption during cutting, the volume of the outbroken material can be measured utilizing a laser scanner [14].

Within the project, continuous percussive activated cutting is researched. As Figure 5 exemplifies, the cutting forces at the tool are by the factor ~10 bigger than the forces that are transmitted to the cutting head.



Figure 4: Linear Cutting Test Rig HXS 1000-50 at Institute of Mining and Special Civil Construction of Freiberg University of Mining and Technology [15]

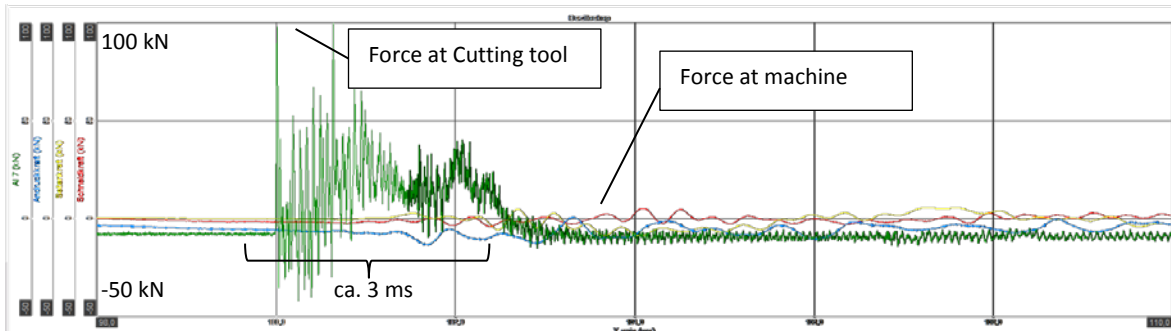


Figure 5: Impulse distribution during an impact test at the tool and at the machine

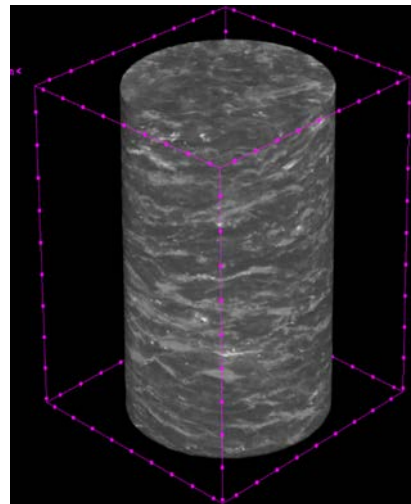
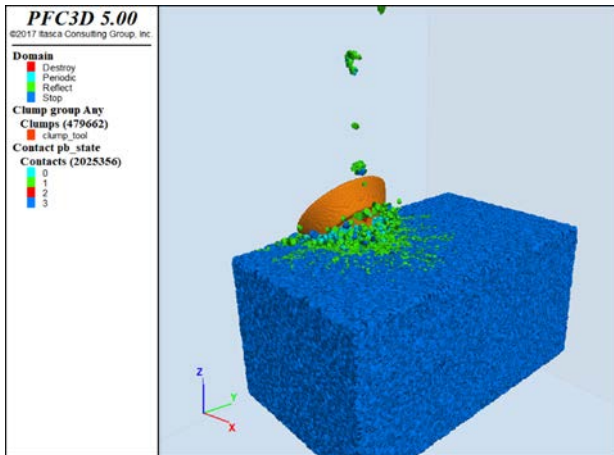


Figure 6: 3D- Simulation of the Rock-Cutting Process using PFC3D (left) and computer tomography of gneiss samples after compression tests (right)

Cutting of rock is a complex process between the rock, cutting tool and cutting machine. Simulation models are used in the project for a better understanding of the interaction of rock properties, cutting tool geometry and cutting parameters as well as extending the experimental results to a wider set of parameters. Two different DEM methods, 3DEC and PFC3D, are used to investigate

different issues (Figure 6, left). The simulations include scenarios of regular cutting, activated cutting as well the influences of thermal treatment.

Flanking the cutting and simulation experiments, a deep mineralogical analysis of foliated rocks on the example of gneiss is being done. In this regard, the mechanical properties, their explanation and deeper understanding in regard to the their foliation is being executed. A part of this is a CT-analysis of the cracking behaviour of gneiss depending under different foliation and loading scenarios is conducted at the St. Petersburg University of Mining in Cooperation with InnoCrush.

Test results and developed new technical solutions will be then implemented in a conceptual numerical model of a mining machine and then verified on the basis of real-time simulator for excavation equipment.

3.2. Ensuring Selectivity

To ensure selectivity, the cutting machine’s operator should be able to distinguish between either ore and host rock and/or different mineralization zones within the given deposit.

To allow for such, a twofold sensor concept is applied. First, the cutting forces are measured during excavation. By such, an estimation of the rock mass condition as well as the detection of boundary layers is possible (Figure 7). To apply such a system, a deep understanding on the evocation of cutting forces in relation to the rock mass is necessary.

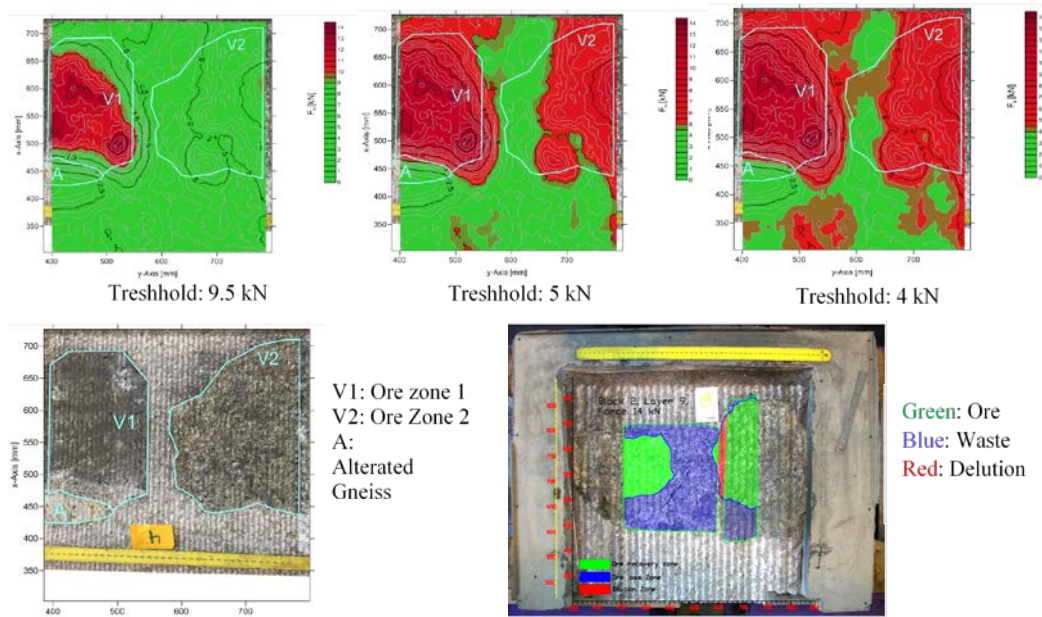


Figure 7: Exemplary results for cutting tests on a heterogeneous sample, top row shows the overlay of the spatial cutting force analysis using different force thresholds to identify lithological boundaries. Lower row shows the identification of different zones in the rock sample (left) and overlay of the identification process with the sample (right); after [9].

Second, a near-face belt based hyperspectral on-line analysis is carried out. This results again in twofold: a) the actual mineral content of the cut ore can be estimated and b) a crosscheck for plausibility of the previously conducted cutting force analysis is carried out. However, the belt analysis will be conducted with some delay to the excavation.

These information then can be used to remove the excavated host rock for direct backfill. Further applications of the data are quality measurements and near-time deposit model updating. This improves the prognosis quality in extraction planning [16].

3.3. Selective comminution

Selective cutting with the support of a sensor-based host rock rejection provides a product with low diluted vein material. The cut vein material consists of the valuable component and the gangue minerals of the vein. The comminution machine can exploit a large enough difference in the properties of the components in a selective way.

Comminution is a process in which the material resistance against crack propagation is overcome. Most ores consist of various components with different properties. A comminution machine, which is sensitive to the given differences of the components, favours or disadvantages the comminution differently for different components. As such, they will be comminuted to a different extent and the result will be different grain size distributions for the different mineral fractions. This behaviour is a property of the whole comminution system [17, 18]. Of course, a subsequent separation step is necessary. The application of selective comminution needs a system chain with a feed material, a comminution machine and a separation machine. As seen in see Figure 8, the feed material defines the potential, the comminution machine exploits this potential and the separation machine uses the exploited potential.

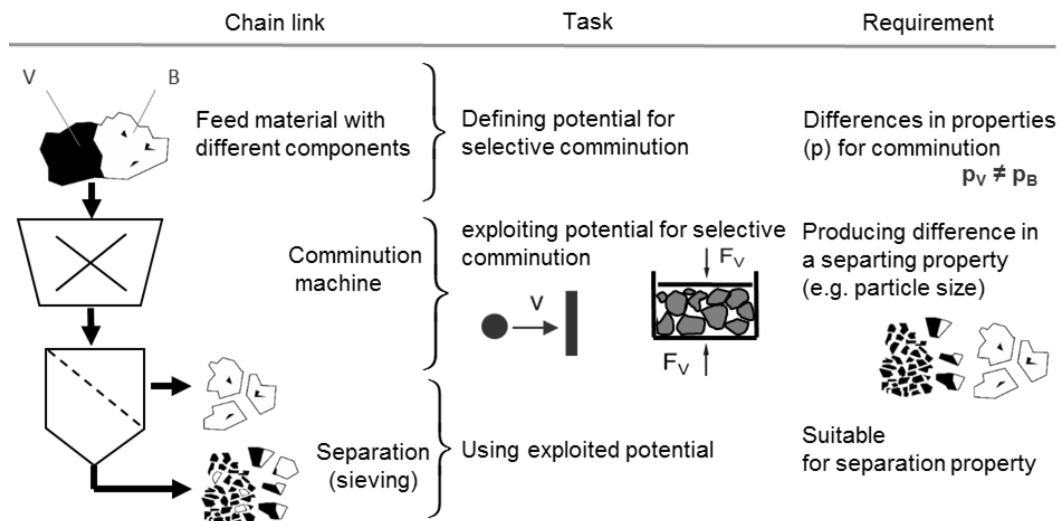


Figure 8: System chain of selective comminution by exploiting material properties for preferential breakage and subsequent sieving as pre-concentration step [9]

InnoCrush investigates the selective comminution to reject gangue components at an early stage in beneficiation. The combination of comminution and classification is particularly cost-effective. A beneficiation close to the excavation site advantages a fast backfilling with coarser gangue or tailings. The InnoCrush project focuses on impact load and confined bed comminution as two promising kinds of loadings for the investigated ores. An additional task is to find out if the form of the chips after cutting excavation influences the selective comminution behaviour.

3.4. Holistic Evaluation

To bring all the previous tasks together, a holistic evaluation is being conducted with the following aims:

- Identify the expected benefits of the innovative process chain in comparison to conventional drilling and blasting processes.

- Develop an integrated evaluation model to assess the innovative process chain regarding economic, ecological and social aspects in order to underpin the previously identified benefits.
- Provide a basis for decision-making on the adoption of innovative process chain with consideration of the needs of mine operators [9].

Based on previous research conducted at TU Freiberg [19, 20] an NPV based monetary model is created to assess the effects of this process chain in comparison to drill and blast based chains. Combined with this, emission factors like noise, dust, gaseous emissions and waste materials are integrated into the monetary model to provide ecological indicators. Work safety and public acceptance provide the social indicators. With the environmental, the social and the monetary model integrated into one, a decision model can be created with respect to the users' priorities.

To homogenize the model and the users and stakeholders' priorities the quality function development method (QFD) is applied [21]. This method enables the comparative assessment of needs and priorities of potential users (e.g. mine operators) and technical specifications of this new process. A survey with mining experts and mining companies was undertaken for the evaluation of the priorities of potential users. The results of the QFD should not only be used for the development of the integrated model (decision-making module), but also for the assessing future improvement potentials for the innovative process chain in order to meet the wishes of the customers even more precisely and finally facilitate the market entry.

4. CONCLUSION

In the highly interlinked research group InnoCrush, 11 scientists from 6 different chairs work towards highly selective low impact resource production chains. The background is introduced to shed light on the implications and necessity of such work. The final aim is to push the implementation of highly automative selective low impact mining methods towards a broader applicability. The research combines mineralogy, mining, modelling, rock mechanics, automation, comminution and economics into one concept. Such research projects are of major importance a) to ensure that well trained interdisciplinary researchers are available, able to support Europe as a hub for innovation and b) to bring forward the applicability of such novel technologies in general. This applies even more in relatively slow transformative sectors like the resource sector. Here the industry needs a strong and robust knowledge base as security to apply novel concepts. Universities with their freedom of research approach can provide exactly these tools for the resource industry.

ACKNOWLEDGEMENTS

The support of Max Bögel Baustoffe GmbH for the possibility of obtaining sample material at its site in Dörfel (Erzgebirge) is highly acknowledged.

The cooperation with Prof. Talovina, from the Saint Petersburg Mining University is also highly appreciated.

Furthermore, the project *InnoCrush - Dynamic methods of mechanical excavation and comminution for high selective production chains in Critical Raw Materials in Saxony* is financially supported by the European Union (European Social Fund) and the Saxonian Government (Grant No. 100270113).

REFERENCES

- [1] European Commission, Critical Raw Materials (2018). Available online: http://ec.europa.eu/growth/sectors/raw-materials/specific-interest/critical_de..
- [2] Melcher F. and Reichl, C. (2017). Economic geology of the Eastern and South-eastern European (ESEE) region. *Berg Huettenmaenn Monatsh*, vol. 162, no. 7, pp. 238–244.
- [3] Staatsministerium für Wirtschaft Arbeit und Verkehr (2017). Rohstoffstrategie für Sachsen: Rohstoffwirtschaft - eine Chance für den Freistaat Sachsen.
- [4] European Commission (2018). Report on critical raw materials and the circular economy.
- [5] Rupprecht, S. M. (2017). Innovation and modernization of the South African mining industry, in *Mine Planning and Equipment Selection*, pp. 15–19.
- [6] Schlothauer T. (2002). Einzelzirkon-Altersdatierungen und geochemische Untersuchungen am Teplice-Rhyolith und rhyolitischen gesteinen des Eibenstocker Massivs, Diplomarbeit, TU Bergakademie, Freiberg.
- [7] Tichimirowa M., Sergeev S., Berger H.-J. and Leonhardt D. (2012). Inferring protoliths of high-grade metamorphic gneisses of the Erzgebirge using zirconology, geochemistry and comparison with lower-grade rocks from Lusatia (Saxothuringia, Germany). *Contributions to Mineralogy and Petrology*, pp. 375–396.
- [8] Romer R., Schneider J. and Linnemann U. (2010). Post-Variscan deformation and hydrothermal mineralization in Saxo-Thuringia and beyond: a geochronologic review. *Pre-mesozoic Geology of Saxo-Thuringia – From the Cadomian Active Margin of the Variscan Orogen*, pp. 347–360.
- [9] Grafe B. et. al. (2018). Innocrush: new solutions for highly selective process chains. *Proceedings of the 11th German-Russian-Resource Forum: Alternative technologies for the development of non-economic deposits*.
- [10] Wang C., Nadolski S., Mejia O., Drozdiak J. and Klein B. (2013). Energy and cost comparisons of HPGR based circuits with the SABC circuit installed at the Huckleberry mine. *45th Annual Canadian Mineral Processors Operators Conference*, Ottawa, Ontario, pp. 121–135.
- [11] Jeswiet J. and Szekeres A. (2016). Energy consumption in mining comminution. *Procedia CIRP*, Vol. 48, pp. 140–145.
- [12] Ausschuss für Gefahrenstoffe (AGS) TRGS 900 (2018). Arbeitsplatzgrenzwerte. *Gemeinsames Ministerialblatt (BMBI): Bundesministerium für Arbeit und Soziales (BMAS)*.
- [13] Drebenstedt C. and Paessler S. (2008). Measuring the effects of blast-induced vibrations on buildings with fibre Bragg gratings. *International Journal of Mining, Reclamation and Environment*, Vol. 22, No. 2, pp. 90–104.
- [14] Vorona M., Gaßner W. and Drebenstedt C. (2010). Scientific reports on resource issues. *Bergbau und Spezialtiefbau*, TU Bergakademie Freiberg.

- [15] Vorona M., Drebenstedt C., Kholodnyakov G. and Kunze G. (2012). Optimierung des Schneidprozesses und Prognose der relevanten Arbeitsgrößen bei der Gesteinszerstörung unter Berücksichtigung des Meißelverschleißes. Dissertation, TU Bergakademie Freiberg, Freiberg.
- [16] Benndorf J. (2017). Turning Geo-data into Mining Intelligence – Nutzung von Online-daten zur Echtzeitmodellierung im Gold- und Kohlebergbau. Berg Huettenmaenn Monatsh, Vol. 162, No. 10, pp. 418–422.
- [17] Hesse M. (2017). Selektive Zerkleinerung von Erzen und Industriemineralen bei Prallbeanspruchung. Dissertation, TU Bergakademie Freiberg, Freiberg.
- [18] Truschko, W. L. et al. (2017) Проблемы Недропользования (RUS): Форум-Конкурс Молодых Ученых. St. Petersburg.
- [19] Inthavongsa I., Drebenstedt C., Bongaerts J. and Sontamino P. (2016). Real options decision framework: strategic operating policies for open pit mine planning. Resources Policy, Vol. 47, pp. 142–153.
- [20] Inthavongsa I., Sontamino P. and Drebenstedt C. (2015). A prototype of real options valuation framework for open pit mines planning: A road to build a dynamics decision making tools. Proceedings of the 24th International Mining Congress of Turkey, IMCET.
- [21] Rosin K., Liu J. and Bongaerts J. C. (2017). Economic, ecological and social assessment of a new "Smart Mining Technology". Conference of young scientists, Sankt- Petersburg.

Integrated Operation in Mining through Digitalization – from a Concept to a Solution

Darko Danicic¹, Nadica Drljevic¹, Franz Rietschel²

¹ Elektroprivreda Srbije, Balkanska 13, 11000 Beograd, Germany

²ABB, Haenchenstr. 14, 03050 Cottbus, Germany

ABSTRACT

The whole world is talking about Industry 4.0 or Digitalization. This trend also arrived in the Mining business a few years ago, but what does it mean for the Miner?

This joint presentation with Elektroprivreda Srbije (EPS) is about a system approach by ABB to reach the convergence of Information Technology (IT) and Operational Technology (OT) to harvest the huge benefits of integrated operation. An actual project will be presented, where ABB is developing on behalf of EPS a system for pro-active planning and production control with the involvement of all required stake and shareholders.

The Production Planning, developed by DMD Consulting and integrated with ABB Ability™ Stockyard Management System (SYMS), creates optimized plans for material homogenization on the belt conveyor systems from the source (mine excavators) to the destination (direct train loading or stockyard). To achieve a fully coordinated production all actions of the required machinery have to be performed in a strict sequence. Such coordination requires a lot of well aligned activities. To support the operator all production management, control and planning functionalities need to be integrated in a single system.

For instance the mine excavators have to be positioned at the right spot and need to perform in a defined way. Further, in order to control such a complex system a dedicated way of delegation to Process Control, a good Material Tracking, Downtime Management and Production Control with forecast functionality is required. And ABB's Stockyard Management System covers all those roles.

In this common presentation EPS and ABB will explain the geological and technological reasons for the implementation of such a system, present the concept of a continuous mining methodology with online quality control to create the desired quality already on the belt conveyor system and state the challenges of implementation of such a digitalization project.

1 SYSTEM FOR COAL QUALITY MANAGEMENT IN EPS

1.1 Reasons for the implementation

More than 60% of the electricity in the Republic of Serbia are produced from coal combustion in power plants which makes the coal to the most important raw material.

In order to maintain continuity in coal production for further use in power plant and stabile supply of electricity, any obstacles have to be overcome. These obstacles reflect in lower availability of deposits with equalized quality of observed parameters, such as caloric value, content of moisture, ash and sulphur etc., with increased stratification, higher depths and on other natural unfavourable characteristics.

To solve such complex situation and fulfil demands coming of the power plants, an integrated conceptual design was developed through a system for coal quality management.

The project which will be described in the following paper covers 5 coal excavators in 2 different fields which all are connected with a large belt conveyor system. At a certain point all

material is passing a distribution area at the crushing plant to be conveyed to the stockyard or train loading. Due to the more and more challenging geological conditions the variations of the coal quality per excavator are becoming bigger as it is shown at the left site of the Figure 1.

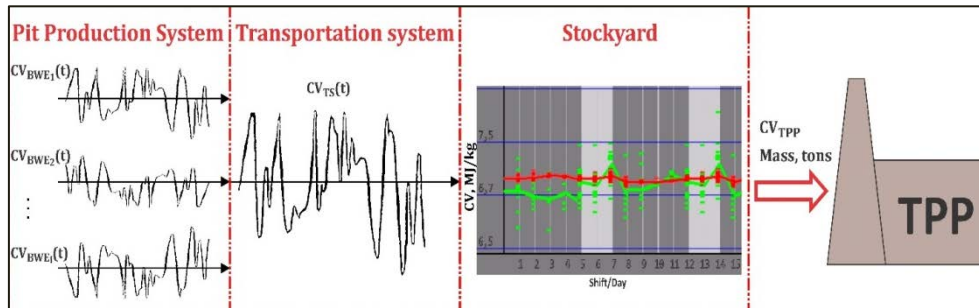


Figure 9. Graphic scheme of general concept for coal quality management

Every bucket wheel excavator (BWE) is digging coal with a deviating calorific value (CV) per tonne. Sometimes the quality is good and better than required, but also sometime the quality parameters does not meet the minimum requirements of the coal fired power plant. That's why in this conventional operation a stockyard is required in order to homogenize the coal production and provide the Thermal Power Plant (TPP) its required quality.

But now a new concept is ruling this way of operation. As there are more than only one excavator available for a parallel production this opens opportunities for an optimized process control. If all 5 excavators or even just a pair are performing in an aligned way they can prepare already online at the belt conveyor system the required material quality. By digging an expected quality at a certain point in a certain time it allows the system to forecast the material flow and predict if it is possible to meet the right material requirements.

1.2 Integrated concept of developed system

The aim, which has to be fulfilled with implementation of Coal Quality Management System, is to secure sufficient quantity and quality of coal in complex preconditions on available open cast mines in Kolubara coal basin for further use in power plant "Nikola Tesla".

This aim was fulfilled with an integrated system consists of a pro-active planning and production control for the all requests, accessibilities, limitations, possibilities, combinations, sources, and destinations of the coal production.

So the first step is to provide information coming from planning of work for each participant in electricity production derivate from coal. Different levels of planning give data for distribution of coal for the power plant "Nikola Tesla" with required quality parameters.

After that, necessary data are downloaded in system and solving of set tasks starts through planning and monitoring and control of the processes. The interaction of the complete process is shown in the following Figure 2.

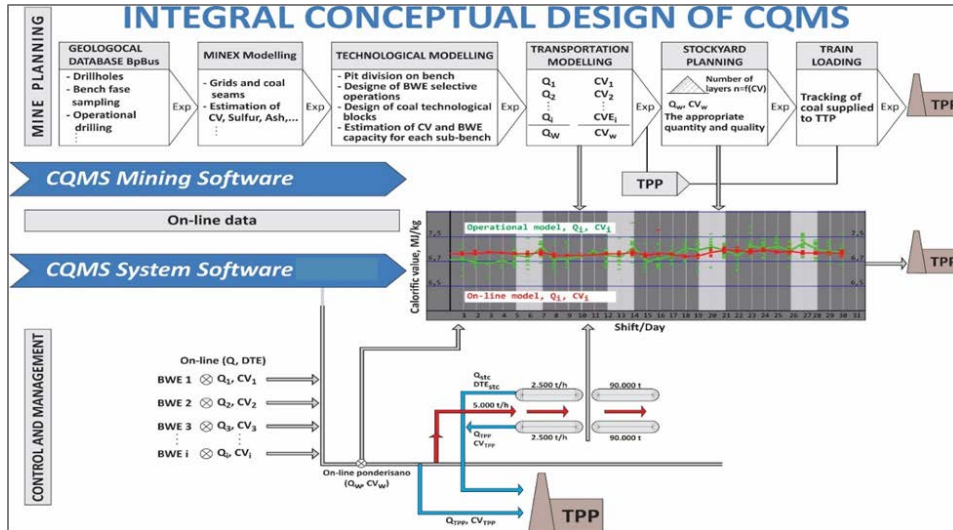


Figure 10. Adopted solution for coal quality management system

The Part of planning is resolved in CQMS mining planning software and fully integrated by ABB.

The part of monitoring and control is done in ABB Ability™ Stockyard Management System-CQMS.

In this project SYMS is the center of gravity for all data handling. By automated data interfaces the SYMS coordinates all required information starting from the Process Control System, over Planning & Downtime Management up to the integration of Laboratory Management.

Each of these software contains different and interconnected activities, which must be carried out in a defined order. The joint product is an optimized working plan for coal homogenization on belt conveyors from excavating point to the loading point, observed and controlled via its transport until destination.

CQMS mining planning software consists of a few models and related actions from geological modelling, bench modelling, technological modelling, transportation modelling, stockyard planning and train loading [1].

After the detailed mine exploration, sampling and laboratory analyses, *geological model* will be made in software package MINEX. This is the basis for the further work in planning. Geological blocks, defined in model, contain all necessary information regarding volume, quality etc. in assigned net 20x20 m.

Next step is creation of *bench model*, also in MINEX, with clear vertical division of coal deposit considering height for each coal system. *Technological modelling* of block is derived from previous activity based on the planned balance for coal excavation, technical characteristics of equipment and geological conditions inside the geological blocks for every coal bench.

Technological blocks, created and anticipated for excavation, will be defined for each coal system and belonging excavators, with assigned selective work, the number of sub-benches and quality and capacity for each of them along with necessary working capacity for excavators (bucket wheel and chain excavators). After the *model for material transport* is activated, next step in planning is simulation of excavators work and analysis for created technological blocks on all benches along with conveying of material to destination (loading into wagons or stockyard).

Stockyard planning depends from destination of excavated coal from the mine and it can be planned for disposal of coal (Strata method), or taking of coal with two reclaimers. For the old stockyard and the combined machine working there, plan for coal can be define for taking and disposing, too.

The last step of planning is **train loading** directly from open cast mine, combined loading from mine and from stockyard(s), or direct loading from the stockyard.

ABB Ability™ Stockyard Management System (SYMS) - system software for monitoring, control and management of processes integrates necessary data from planning software and the Process Control Systems. According to additional measurement devices positioned throughout the whole production system (GPS, online analyzers and belt scales) the SYMS provides all necessary information, audio and visual, about fulfilment of requested aim in system for coal quality management.

The SYMS provides material tracking and quality management for a dedicated coal quality management system. This digital application includes several functions that can minimize handling efforts and increase the efficiency of bulk material handling of mines and stockyards. It is a configurable system that can be used to digitalize the complete material handling chain. The material flow can be modelled across all belt conveyors and transportation equipment which can be used for tracking, inventory management and forecasting. Further, in order to control such a complex system a dedicated way of Delegation to Process Control with a Plan Handling Application, a Downtime Management and Production Control Module was delivered.

All Data which are coming from planning and additional data from measurement devices on site are processed, transferred and observed during processes of coal excavation, transportation and distribution on stockyard or loading into trains.

Then all available material properties and quality information are associated with the tracked material via automated data interfaces.

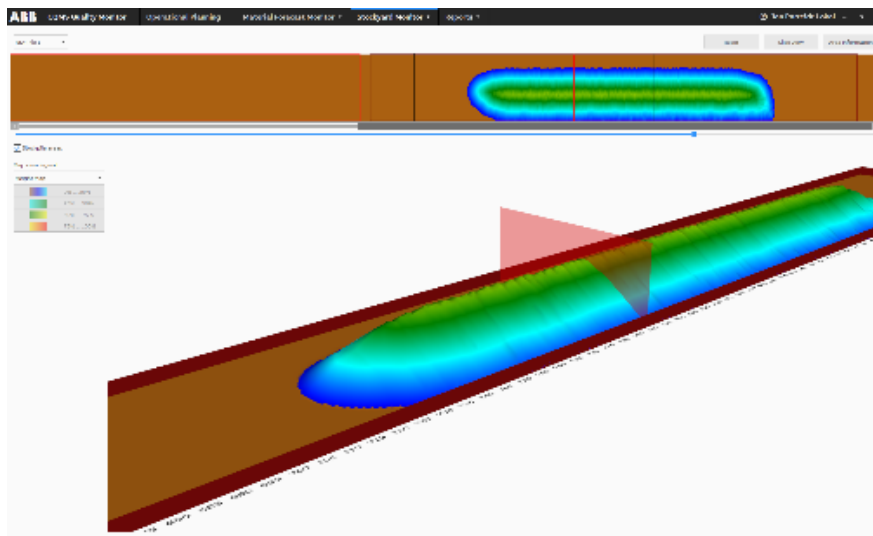


Figure 3. Virtual Stockpile Model in 3D Client

Finally the so called digital twin of the material flow provides the operator with a production forecast as well as an inventory overview at any time, without needing to do an extra survey.

These Data can be used for operational optimization and control. It provides possible solutions as well as opportunities for decision-maker in a system to react according to the potential problems during operation.

Furthermore the user management is integrated to the already existing plant infrastructure which enables a seamless synchronization of all users and their rights. As the whole Coal Quality Management System requires that each involved participant within the process has concrete, clear and unequivocal tasks to establish complete technological discipline and work organisation provided by the use of highest technical achievements which connect natural conditions in deposit and possibilities of mining's and thermo-energetic equipment.

2 CHALLENGES

The major challenges are caused by operational possibilities, their complexity and how strict they need to be executed.

For instance there are several operation possibilities in total can run 5 excavators in parallel from two different fields to one or two destinations. The main options are the following,

First of all, the preferred operation is direct train loading from the mine. If all excavators performed well and the material was mixed according to the production plan online at the belt conveyor system already the material can be delegated direct to the train loading station.

To ensure quality adequate operation at a certain point where all material comes together on the belt conveyor system a decision needs to be taken if everything works out or an alternative plan needs to be activated. Based on this review the decision can be taken to add some material from the stockyard or convey the complete material from the mine to the stockyard for dedicated mixing and blending like the conventional way. The option of direct train loading from mine and parallel feeding from Stockyard enables high production rates by keeping the coal quality in the optimal required range.

Highest performance production from the mine can be achieved with a material split for direct train loading and stacking to the stockyard. This includes additional challenges like switching surge bins to manage the material flow from the mine conveyors with 5.000t/h to belt conveyors in the crushing plant where each conveyor is limited to 1.250 t/h. The surge bin handling as well as the split and merge of the material flow is also covered by the SYMS.

At the end of the day this leads to several operational possibilities and even more route possibilities. Because every specific way of operation also leads to 28 possible routes in the mine, 24 possibilities in the transient bunker, 23 different lines through the crushing plant, additional 12 for train loading and even 13 to the stockyard and 7 from the stockyard.

In combination the operators are facing thousands of options, which need to be prefiltered in order to ensure an easy and manageable operation.

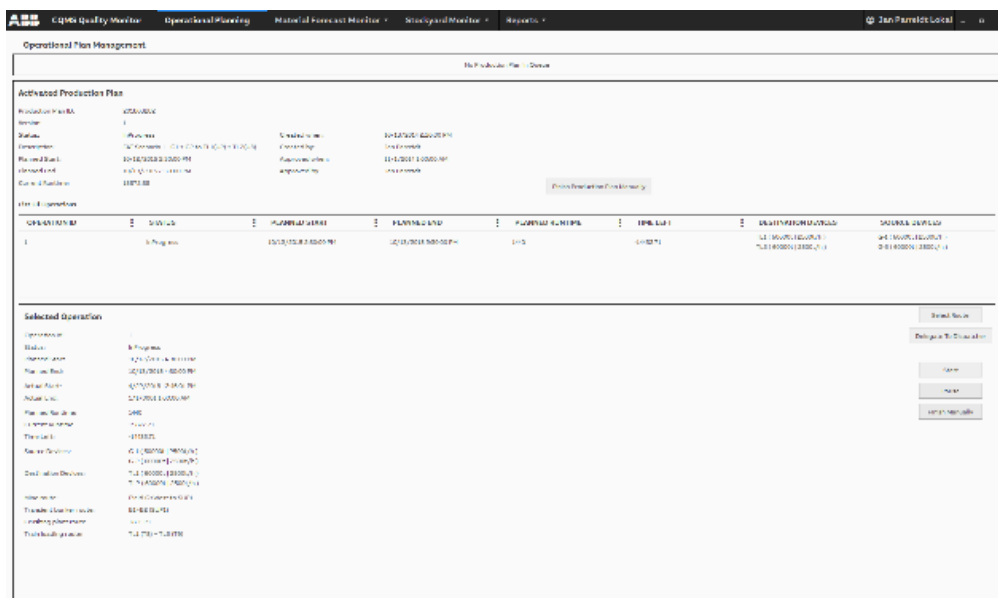


Figure 4. Plan Handling Tool

During the project several discussion happened about the routes and which should be the default one for each constellation. When all was said and done the filter were implemented according to the specific technological and operational constraints. And in order to enable the

operator still enough flexibility for his operation it is possible to choose another route which is not the default one. For sure again filtered according to availability and technological constraints of the equipment like maximum tonnage or operating direction to avoid any kind of failure.

And this is what was clear on operational side. During the engineering we were facing the challenges which are inherent with such a complex project.

In general there are 5 relevant phases for the implementation of such an interdisciplinary system set up with the involvement of different departments.

2.1 Phases from a concept to a solution

1. Concept phase

At the beginning there was an idea. Later on the idea needed to be worked off in order to develop a concept. Thanks to the good empowerment from the Management and the strong commitment of all involved co-workers the concept was well developed by EPS in collaboration with consulting teams and the university.

1.1. Phase of understanding for the supplier

In order to realize such a well-grown concept it was essential to fully understand it and develop a solution which can realize all points accordingly. Therefore it was necessary to review all operational possibilities, who will be involved in the execution and how it could be realized in a technical solution. During this phase the complexity became more clear and how strict it needs to be executed which led to a slightly scope creep from ABB point of view.

2. Basic engineering

During the basic engineering all required equipment have been specified, the general network integration concept was developed and how everything can be installed on site. But beside the normal tasks of the basic engineering a detailed processes for the execution were developed with all its user and their specific roles and actions were defined. In collaboration with the technological experts from customer side this engineering phase which is normally more related to technical clarification have gotten a more consultative engineering approach.

The hierarchy and structure of responsibilities which was valid over decades in separated working groups or departments now needs to be connected and an aligned in a single process. Therefore a process Modell was developed with all involved roles. And different roles mean different responsibilities, which lead to the requirement of an integral user management. All different roles can be managed in groups with specific rights and permissions. Also all views and rights can be modified according to the role or even location of an employer. This shall enable a process whereby all interactions between the different stake holders are clear and executable in a way that the system is able to ensure an automated failure avoidance. The challenge is here to ensure the quality of the operation vs. providing the operator still enough flexibility to manage all equipment according its reliability. During the complete project development this challenge was paid out most attention.

Anyway after the definition of all regulatory and general technical aspects the project proceeded with the normal engineering.

In such a complex System it is important to configure and maintain only one set of data for all Machine parameters, Material Quality and property configuration as well as a fully integrated user management in all system parts connected and automatically synchronized with the existing plant infrastructure.

At the same time it is important to ensure safety requirements for backup, redundancy and cyber security.

3. Detail engineering

Within this phase the complete integration was engineered in detail. The Hardware & Virtualization concept was really connected to the IP addresses on site, the equipment choices finalized, all installation and single line drawings were finished and the system engineering finalized for execution.

4. Additional Development & Software Enhancement

As the basic and detail engineering was more time consuming than expected, it was important for ABB to realize the development work contemporary in order to do not loose time. This leads in digitalization and automation projects normally to a further challenge. In regards to ongoing definitions during the engineering process it would be the best to implement the changes only after final decisions. On the other hand with the focus on the project execution time line it is necessary to get as much work finished as possible.

This challenge was overcome with a dedicated repository management which allowed smoothly ongoing changes. And as it was a quiet complex project all activities and tests have been tracked, which ensured a qualitative development.

5. Simulation and Testing

After the development was done, the system was connected to the final destination environment via VPN. The complete system has been set up with all Clients, the wireless communication infrastructure, the camera system and all cabinets etc. at the ABB Lab in Cottbus, Germany.

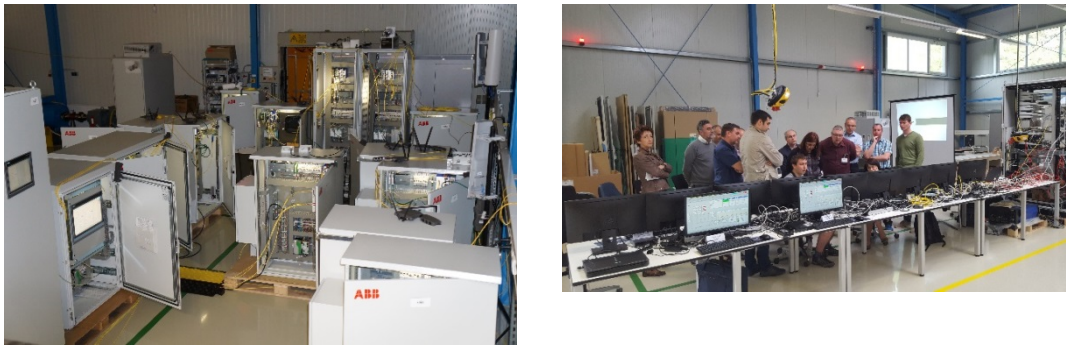


Figure 11. Pictures from FAT in Cottbus, Germany

Besides delivering all components for the production control, ABB moreover had to deliver further important equipment which simply belongs to such a system. For example ABB delivered and integrated also a fully automated camera-based fire detection system for early recognition and detection of possible fire origination. The thermal cameras swing continuously over the defined area and measure the temperature on each spot. In case of an alarm, the system provides an output signal which will be highlighted as alarm in the control system. In addition it generates a warning sound and show the camera picture in the central control room to the operators which has been tested too.

During the test already all services were running in the right domain like it will be on site later on. The planning system as well as the SYMS with all services, applications and web clients was hosted on the server which would be sent out to site later. In this way it was possible to realize issues before going out to site.

In accordance to this virtual commissioning some replay services have been developed in order to enable a realistic testing. It was possible to receive plans from the planning system and delegate them to the different control systems in the mine, the crushing plant and stockyard. And

according to simulated process signals in these control systems it was possible to simulate and review the material tracking functionality and forecast the production.

This integral test is an important step to figure out further issues which have not been occurred during system development.

6. Installation & Commissioning

Even if “virtual commissioning” was performed as best as possible, during real commissioning normally happen further non predictable situations which lead to further modifications on site.

7. Operator Support

After finishing the installation and commissioning a digitalization project is just partially finished. All parties have to use now the system and learn how everything got adopted by the operation. Normally it happens that some developed functionalities can be optimized in respect to real life requirements and slightly modifications need to be implemented. Also it is important to support the operators during the first time and overcome their worries about the use of such a complex and integrated system

3 SUMMARY

A Digitalization project is different to conventional automation and electrification business. Especially cross-divisional optimization and the development of new production processes require a more consultative engineering approach.

Where it was possible in the past to make the dimensioning of the components, prepare all drawings, review and test its functionality, deliver them and commission it according to the requirements, a digitalization project requires more focus on the roles, tasks and process itself. It is important to consider all specific requests and the systems.

This project was a great experience and the developed solution is of outstanding value. A single system covers all interactions from the borehole to the power plant supply. By an integration starting from the Geological Modell it is possible to dig an expected quality at a certain point which was planned by a pro-active planning system at a certain time.

The automated integration of all systems based on the ABB AbilityTM Stockyard Management System with its tracking, quality management and production forecast features enables the five excavators or even just a pair to perform in an aligned way and prepare the required material quality already online at the belt conveyor system. This enables a faster supply of the produced material to the coal-fired power plant. And by skipping the stockyard as much as probable it is possible to reduce the overall energy consumption of the production equipment as well as save the equipment against mechanical wear anyway.

REFERENCES

[1] Drljevic, N. (2010). Development of technological model of excavator’s work for operational planning and coal quality management at Tamnava mines, Master thesis, Belgrade, pp 36-45.

Current State and Development of Continuous Systems on EPS Opencast Coal Mines

Dragan Ignjatovic¹, Vladimir Pavlovic², Slobodan Mitrovic³, Branko Jevtic³

¹Faculty of Mining and Geology, Djusina 7, Belgrade, Serbia

²Opencast Mining Centre, Kraljice Marije 25, Belgrade, Serbia

³EPS, Balkanska 13, Belgrade, Serbia

ABSTRACT

Currently, opencast coal mines of Electric Power of Serbia (EPS) produce about 40 million tons of coal per year within two basins and five opencast mines. On that basis, 70% of electric power is being produced in Serbia. Since some opencast mines are undertaking closure procedure, it is necessary to open replacement capacities in order to continue coal production. This paper shows the current state, development perspectives, opening plans for new opencast mines and planned continuous mining systems which are foreseen to operate in the future time period.

1. INTRODUCTION

Along with Germany, Poland, Czech Republic, Turkey and Greece, the Republic of Serbia has one of the largest coal productions in Europe. The total annual production is about 40 million tons of coal and about 120 million cubic meters of overburden (Figure 1)[3]. Coal production is carried out from two large basins, Kolubara (about 30 million tons of lignite coal per year) and Kostolac (about 10 million tons of coal per year), across five opencast mines. The favorable deposit conditions (primarily the conditions of coal seams inclination, reserves, etc.) enable the use of highly-productive continuous mechanization within the Excavator-Conveyors-Spreader (ECS) system on the overburden and the Excavator-Conveyors-Crusher (ECC) system on coal.

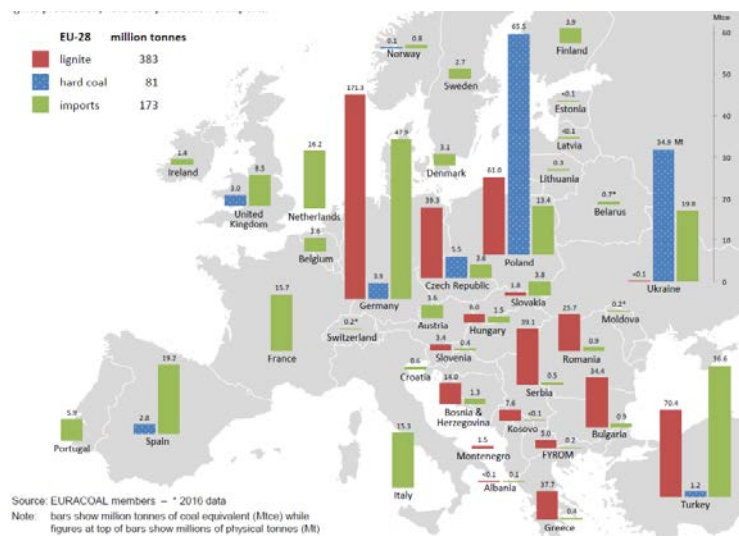


Figure 1. Production and import of coal in Europe.

Almost the entire amount of the produced coal is burnt in thermal power plants (TPP). There are 8,355 MW currently installed, out of which 5,171 MW are in coal fired power plants.

Additionally, a new TPP is in construction at the Drmno site, with 350 MW of power. The percentage of coal in the production of electricity ranges from 70–75%, and consequently Serbia is the leading country in Europe, after Poland (79%). Figure 2 shows the percentage of coal in electricity production in Europe [3].

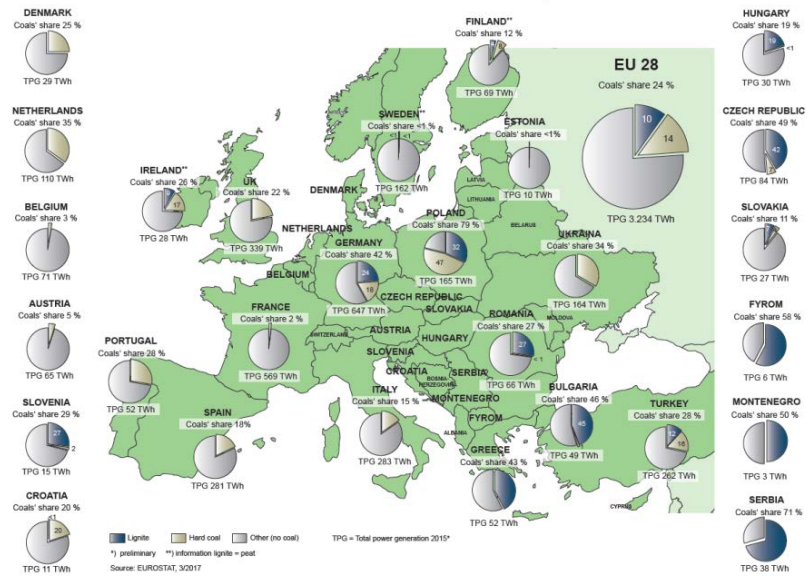


Figure 2. Percentage of coal in electricity production.

In the future, the role of coal in the production of electrical energy will remain a priority, and relatively large coal reserves are in favour of that (Figure 3)[3]. On the other hand, the percentage of renewable energy sources in Serbia is above the European average (around 22%), and a construction of about 500 MW of new renewable energy sources is planned.

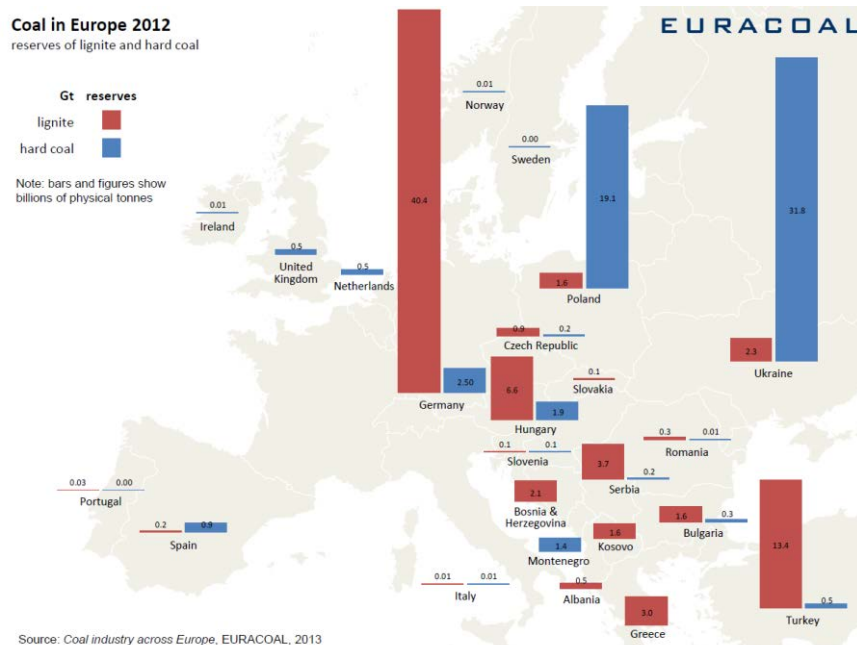


Figure 3. Coal reserves in Europe.

2. CURRENT PRODUCTION AND APPLIED CONTINUOUS EQUIPMENT

Coal mining under the Electric Power of Serbia takes place on a total of five opencast mines across two basins - Kolubara basin (Field C, Field D, Field G, Tamnava WestField), and Kostolac basin (Drmno). The total production in 2016 amounted to 37.65 Mt, and 39 Mt of coal in 2017. Figure 4 shows the production of coal and overburden from the beginning of opencast mining, as well as the production of coal and overburden in 2017 [4].

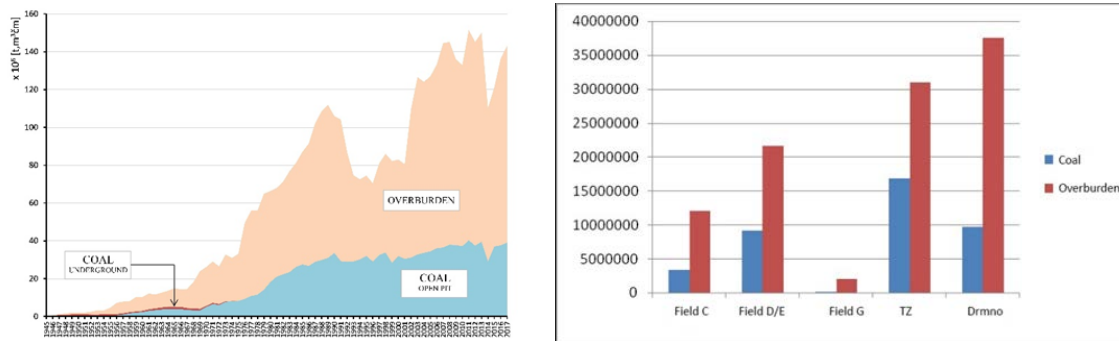


Figure 4. Production of coal and overburden until now and EPS production in 2017.

In 2018, the planned production in the Kolubara basin is 29 Mt of coal and about 70 Mm³ of overburden, while the planned production in the Kostolac basin is about 10 Mt of coal and about 37 Mm³ of overburden.

2.1. Current situation on the Kolubara basin opencast mines

The production of coal in the Kolubara basin began in 1896, by underground mining. There were fourteen mines in total, where coal was mined until 1974. The opencast mines of the Mining Basin (MB) Kolubara started by removing the overburden in 1950 and mining coal in 1952. The production of MB Kolubara in the 1946-2017 period was 1.098 Bt of coal and 2.363 Bm³ of overburden - ratio 1:2.15. The current state is very complex primarily due to the occurrence of instability in the inner dumps of Fields C and D, the instability of the excavation benches in the Vreoci village region, as well as lagging behind in the realization of investments, primarily related to the opening of the replacement mine Field E (relocation of the Pestan river, regional road, infrastructure facilities and drainage facilities), as well as the opening of opencast mine Field G.

Opencast mine Tamnava West Field

The opencast mine Tamnava West Field was opened in 1994, and to date about 210 Mt of coal and 440 Mm³ of overburden have been mined - a ratio of 1:2.06. The mining is currently performed with two ECS systems for overburden excavation and four ECC systems for coal and interlayer excavation. According to the Long-term Mining Development Strategy on EPS Coal Basins (LTMDs), a production of 12 million tons of coal is planned annually by 2032, after which in the last five years, a production of 7 million tons of coal is planned annually. However, due to delays in the realization of investments for the opencast mine Field G opening, the equipment from the Veliki Crljeni mine (Field G) was operating in the area of the Tamnava West Field mine in the previous period, so the production amounted to 16.85 Mt of coal in 2017. In this case, 30.95 Mm³ of overburden were excavated. All of this has affected the work on Tamnava West Field opencast mine due to extraordinary circumstances with altered technology. A special problem was the rehabilitation of the 2014 floods consequences, when the inner dump had to be partially reconstructed. The planned

production for 2018 is 12.5 Mt of coal and 26.5 Mm³ of overburden. During 2017, the construction of the 12,000 m³ spreader was completed, so the largest part of the planned investments in this mine will be completed with the finalization of the fine coal stockyard and the construction of the stationary conveyor SUP 2. In the following period, two bucket-wheel excavators (SRs 2000 and SchRs 1600 - Figure 5[4]), both with 6,600 m³/h capacities, conveyors with 2,000 mm belt width (eight conveyors about 11 km long) and two spreaders of 8,500 m³ class for the inner dump disposal.

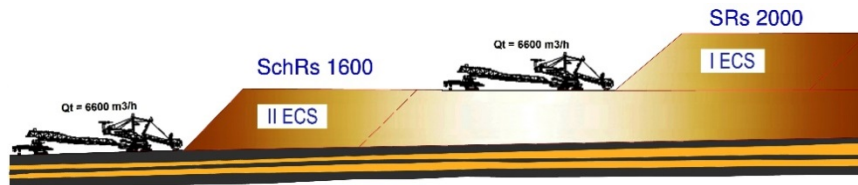


Figure 5. Continuous equipment on overburden excavation on opencast mine Tamnava West Field.

Three bucket-wheel excavators (SchRs 630 and SchRs 740) and a ERs 1000 bucket chain excavator are used for mining coal and interlayer (Figure 6)[4]. They're in conjunction with conveyors with a 1,600 mm belt width (a total of thirteen conveyors with a length of about 13 km), with distribution stations for coal and interlayer, with a new 12,000 m³ class spreader.

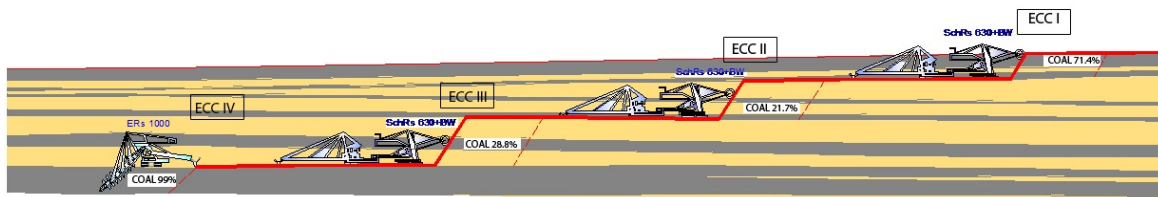


Figure 6. Continuous equipment on coal mining and interlayer removal on opencast mine Tamnava West Field.

After being transported with SU and SUP stationary conveyors to the crusher plant, coal is crushed to 30 mm and then directly loaded into trains or deposited at the stockyard. The completion of the fine coal stockyard is expected in 2018, when the coal quality management system should also start operating.

According to new observations, until the opening of the mine Radljevo, the opencast mine Tamnava West Field would have somewhat increased capacity (13 Mt of coal). Also, due to the instability of the excavation and opencast mine benches in the eastern part of the basin, a further trend of increased production from the western part of the basin can be expected.

Opencast coal mine Field G

The overburden excavation on the opencast mine Field G began mid-2017, while coal mining began at the end of the same year (about 150,000 tons excavated). The current problem is the completion of the planned investments in this mine, mainly the relocation of the main roadway. Due to delays in the realization of investments, the projected mining technology has somewhat changed. The main mining project foresaw annual production of up to 5 million tons of coal. According to the LTMDS, a lower production is planned (1 million tons of coal annually) after the opening of the Radljevo mine. After new consideration, the planned production is 6 million tons until the opening of the Radljevo mine, after which the annual production changes to 3 million tons of coal. The project predicts that the overburden should be mined with one ECS system (a system that previously worked on the Veliki Crljeni mine, 4,100 m³/h bucket-wheel excavator, a conveyor system with 1,600 mm

belt width, and due to the need to fill the corridor for the future rail line and roadway, as well as the regulation of the Kolubara river in Phase III, there will be a selective disposal of clay and gravel, so there will be two spreaders assigned). The coal will also be mined with one ECC system - a 4,100 m³/h bucket-wheel excavator, a conveyor system with 1,600 mm belt width and a crushing plant (Figure 7)[2]. The total planned length of the conveyor at the overburden is 6 km, and 8 km on coal.



Figure 7. Continuous equipment of opencast mine Field G.

Opencast coal mine Field B/C

Coal mining at opencast mine Field B/C started in 1952. So far, about 100 Mt of coal and 250 Mm³ of overburden have been excavated - a ratio of 1:2.5. At the moment, excavation is carried out with three ECS systems on the overburden, one system on the interlayer and one coal system (Figure 8) [4]. The upper bench system (IV ECS) has a new bucket-wheel 6,600 m³/h class excavator, a system of four conveyors with 2,000 mm belt width and an 800 m³/h class spreader. The excavated overburden is dumped in the area of the inner dump Field D. The other two overburden ECS systems are of smaller capacity, with 1,500 mm belt width conveyors (eleven conveyors, 5,000 m). The overburden is partially dumped in the space of the Field D and Field B inner dumps. The coal is mined with C 700 and SRs 1200 bucket-wheel excavators and is transported to the dry separation plant in Vreoci by conveyor system with 1,500 mm belt width (8 conveyors).

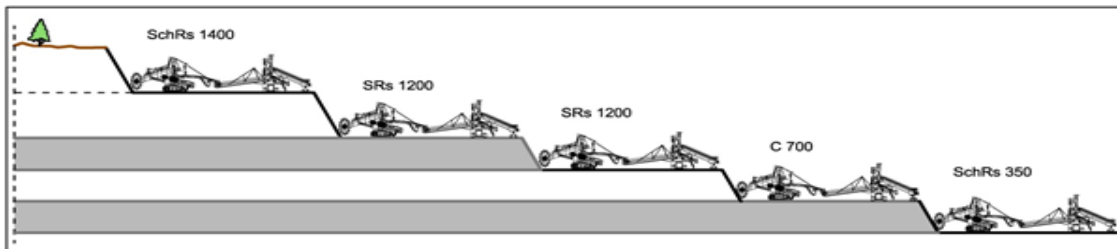


Figure 8. Continuous equipment of Field C.

The biggest current problem on this mine is the unstable inner dump, due to which the most part of the overburden is being deposited in the area of Field D. In addition, there are drainage problems as well as rather obsolete equipment (except the IV ECS system). According to the LTMDs, it is planned to increase production from the current 3.2 to 6.6 million tons of coal annually by 2025, and then to continue the mining on the replacement mine Field E. However, due to delays in the realization of investments and the instability of the inner dump, the production in 2017 amounted to 3.28 Mt of coal. 12 Mm³ of overburden were excavated. All of this has influenced the work in Field C to exceptional circumstances with changed technology. The planned production for 2018 is 3.2 Mt of coal and 15.5 Mm³ of overburden.

Opencast coal mine Field D

The excavation of the overburden on the opencast mine Field D started in 1961, and up to now about 540 Mt of coal and 1,45 billion m³ of overburden have been excavated - a ratio of 1:2.7. Due to the problems with the graveyard displacement in the Vreoci village, the planned technology of work on this mine was changed, so the mining is carried out on two separate locations - in the region of the Vreoci village and in the area of the future opencast mine, Field E, where the top coal seam is being mined. The overburden excavation in the Vreoci region is done with three ECS systems and one ECC system (bucket-wheel excavators, type SRs 1200), while disposal is done in the inner dump with A₂RsB 3500 type spreaders. The coal mining is carried out with one ECC system with an excavator of theoretical capacity of 4,100 m³/h (Figure 9)[4]. The transport of coal and overburden is done with 1,500 mm belt width conveyors with a 9.5 km route. The second mining site is located at Field E, where only the top seam is being excavated, as well as part of the inclined main coal seam. Two ECS systems and one ECC system are used for mining. The overburden excavation is done with SchRs 1760 and SRs 1200 excavators, while ARs 1800 and ARs 1600 spreaders are used for dumping. Excavator SRs 1300 is used for coal mining. The transport of overburden and coal is done with 1,800 mm and 1,500 mm belt width conveyors of 13 km length to the dry separation plant in Vreoci.

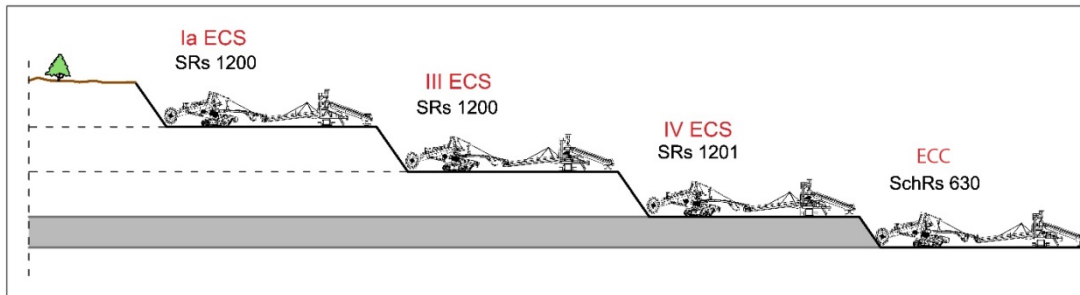


Figure 9. Continuous equipment of Field D - Vreoci.

The production in 2017 amounted to 9.1 Mt of coal, with 21.6 Mm³ of overburden. The plan is to mine about 9 Mt of coal and 22,5 m³ of overburden in 2018. There is still 15 Mt of coal left for mining until 2020 in the area of Field D. The top seam mining in the area of Field E continues with the annual production of 4 Mt of coal progressing to the south, then towards the west and the boundary of Field E with Field F. The biggest current problem is the occurrence of instability on the overburden benches towards the Vreoci village. Another major problem is the drainage of the south part of the mine, as well as the very old and unreliable equipment.

2.2. The current state on the Kostolac coal basin opencast mines

The production of coal began in 1870 in the Kostolac basin, by underground mining. There were three underground mines up until 1974. Mining in the Kostolac basin began by overburden excavation in 1942 and coal mining in 1943. The production of TPPs Kostolac since 1945 was about 250 Mt of coal and 900 Mm³ of overburden - a ratio of 1:3.6. Only opencast mine Drmno is an active coal mine currently in the Kostolac coal basin. Drmno was opened in 1984, and so far 170 Mt of coal and 630 Mm³ of overburden were excavated - a ratio of 1:3.7. In 2017, 9.7 Mt of coal and 37.5 Mm³ of overburden were excavated.

The continuous mining system used for overburden excavation has five ECS systems, with a total of six excavators (five bucket-wheel excavators and one bucket chain), while five spreaders are supposed to be used for the overburden deposit (Figures 10 and 11)[4]. The overburden transport is carried out on two sides: V ECS, IV ECS and III ECS systems on the east side, while the transport of

the overburden with the II ECS and I ECS systems is on the west side of the mine with a total length of over 30 km.

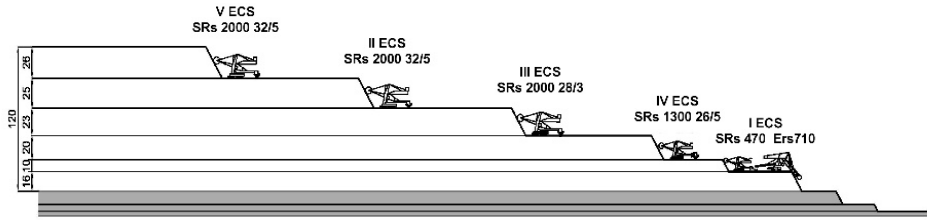


Figure 10. Layout of the ECS systems for the overburden.

The lengths, as well as the necessary number of conveyors in the systems, vary depending on the progress of mining operations and the expansion of the mining fronts. The number of conveyors is determined by the complex geometry of the final mine and dump contours in the analyzed period. The width of the conveyor belt ranges from 1,400 mm to 2,000 mm.

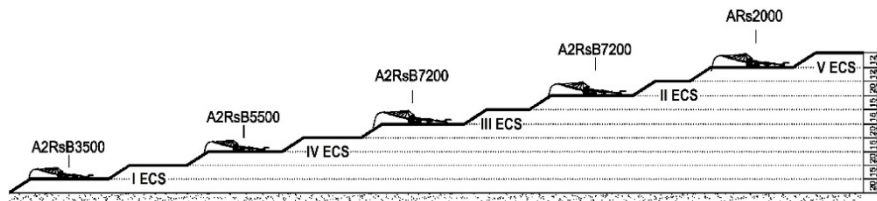


Figure 11. Continuous equipment on the Drmno inner dump in the Drmno opencast mine.

The upper three ECS systems are disposing throughout the entire length of the disposal front, while the IV ECS and I ECS systems only dispose in the western, deeper part of the mine.

A continuous ECC system is used for coal mining. The mine is divided into two main parts due to the transport, eastern and western. In the period from mid-2014 until the end of 2015, coal was mined only from the eastern part. During 2015, along the eastern part, bucket chain excavator ERs 710 was engaged on coal mining, and occasionally, according to the possibilities and needs, a SRs 470 bucket-wheel excavator joined in (Figure 12)[4]. The excavated coal is being transported by a conveyor system to a TPP stockyard. All conveyors have a 1,800 mm belt width.

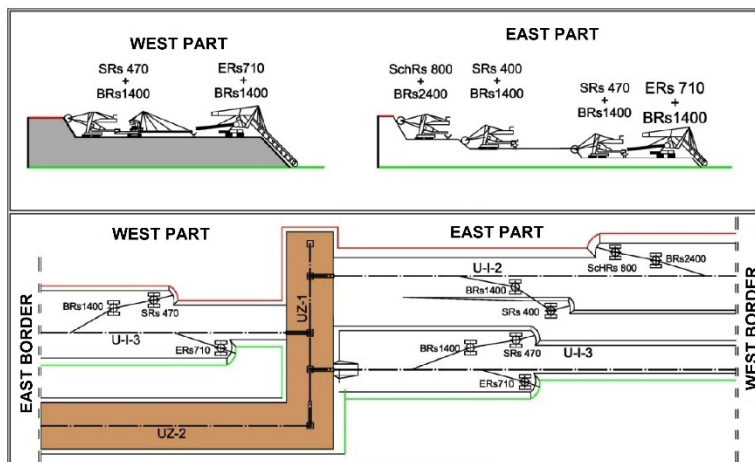


Figure 12. Basic conceptual scheme of two-front mining.

Along the eastern part, bucket-wheel excavators SchRs 800 and SRs 400 are used for mining on the top two benches, while bucket-wheel SRs 470 and bucket chain ERs 710 excavators are used for the lower two benches. The coal excavated by the bucket-wheel excavators is transported to a discharge bunker with a U-I-2 conveyor (belt width 1,800 mm) and a system of five conveyors (belt width 1,800 mm).

3. PLANNED DYNAMICS OF MINING DEVELOPMENT IN EPS

No increase in capacities is foreseen within the Kolubara coal basin according to the Energy Development Strategy of the Republic of Serbia for the next five years, i.e. production will remain at the level of about 30 Mt of coal per year. Due to the introduction of the new thermal power plant TPP Kostolac B, with a power of 350 MW, the production of coal is supposed to increase to 12 Mt of coal in 2020 in the Kostolac coal basin. There will be replacement capacities within the MB Kolubara (Field G, which started with coal production at the end of 2017, Field E, which will be the replacement capacity for Field D and Field C, and at the end Radljevo, which will be opened due to coal quality management in the first phase, and then as a replacement capacity for Field G).

3.1. Planned dynamics of mining development in the Kolubara coal basin

The planned dynamics of development were processed in several documents. The LTMDS clearly defines the conditions and measures for the realization of the required coal production level, in order to ensure the security of the Republic of Serbia's power system and the development and sustainable strategy of EPS[2]. Safe and stable production of coal from the Kolubara basin is key and a precondition for achieving balance of electricity production in the Republic of Serbia, because that lignite is supplying TPP Nikola Tesla A, Nikola Tesla B, Kolubara and Morava with total installed power of 3,285 MW. In order to achieve these objectives, the concept of uniform quality coal mining with the maximum annual production capacity in the eastern part of the basin must be verified up to 15Mt, and in the western part of the basin up to 25 Mt, with the inclusion of all available basin reserves in the function of existing and future thermal capacities, with set priorities and dynamics of the next activities.

In order to define a strategic framework and a real and reliable concept for the future development of the Kolubara basin, a situational analysis has been done with a comprehensive overview and assessment of the political, economic, ecological, sociological and technological environment, as well as internal and external factors that can have a key impact on the realization of the LTMDS[2]. The total coal proved reserves on mines currently in operation are:

- Field C: 32 Mt (life of mine until 2027)
- Field D: 19 Mt (life of mine until 2020)
- Field E: 279 M (life of mine until 2045)
- Field G: 36 Mt (life of mine until 2028)
- Tamnava West Field 260 Mt (life of mine until 2039)
- Radljevo: 362 Mt (life of mine 35 years)

The planned production according to the LTMDS has partially changed, primarily by more intensive mining at Tamnava West Field and Field D, so that the remaining reserves within Field D are now around 12 Mt of coal and will be mined during the following two to three years. Furthermore, the opening of Field G was also delayed, and coal mining on Radljevo mine will not start in 2019 as planned in this document, but more realistically in 2022. In addition, due to inner dump benches slide problems, the plan for the disposal of overburden has been modified.

The mining on Field D will be completed in the eastern part of the basin in the next five-year period, and part of that equipment will move to Field C, so these two mines will be working at the same time in 2020.

Opencast coal mine Field E (Eastern part of basin)

Coal mining on Field E was actually started by excavating the top bench with equipment from Field D. The LTMDs planned that the top bench will be excavated independently with two ECS and one ECC system, and that the main coal bench is excavated with part of equipment from Field C. Two more large ECS systems with a 6,600 m³/h capacity will be purchased for this purpose, with 2,000 mm belt width conveyors. On Figure 13[2], a technological cross section is shown in 2025 in the eastern part of the Kolubara basin. The planned capacity is 10-11 Mt of coal per year. The life of mine Field E is practically until 2045, when mining will be continued on Field F.

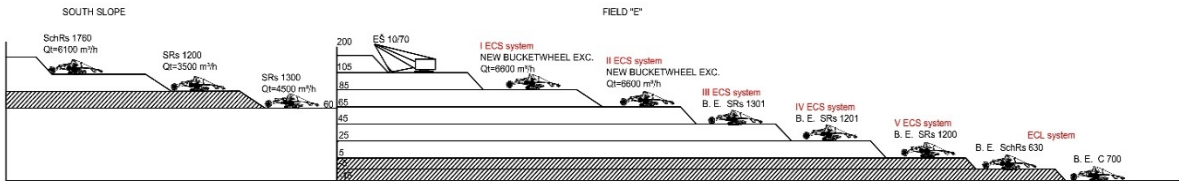


Figure 13. Continuous equipment in the eastern part of the basin in 2025.

Western part of the basin

In the western part of the basin, mining on Tamnava West Field will be carried out with the existing equipment and higher production than planned, in order to compensate for the lack of coal from the eastern part of the basin until production increase on Field G and Radljevo mine opening. Field G will also be working with a capacity that is considerably higher than planned in the LTMDs, and only when Radljevo is opened, the capacity on this mine can be reduced [2].

A Feasibility Study and a Main Mining Project were done for opencast mine Radljevo. However, due to problems with the equipment purchase for the planned start of operation (the used bucket-wheel excavator SchRs 630 and a spreader), the dynamics of the opening have been shifted, so realistic observations show that the overburden excavation can start in 2020 with one ECS system, and that the second system (capacity 6,600 m³/h) should start operating in 2022. Coal production should start then as well (2.3 Mt that year). The planned annual production is 7 Mt of coal and 22 Mm³ of overburden. The total proved reserves amount to about 450 Mt of average quality coal - 7,240 kJ/kg. For mining these coal quantities, it is necessary to excavate and dispose of about 1.6 Bm³ of overburden.

The excavation of overburden will be done with two ECS systems, first one with a bucket-wheel excavator with a 6,600 m³/h capacity, 2,000 mm belt width conveyors (9,800 m) and a 8,500 m³ class spreader. In the first phase, the disposal will be carried out at an outer dump with I ECS system, and then into the inner dump, with the second ECS system with a 4,100 m³/h capacity bucket-wheel excavator, coupled with a mobile conveyor, 1,600 mm belt width conveyors (8,000 m) and a 5,500 m³ class spreader (Figure 14)[2]. Coal and interlayer mining will be executed with two ECC systems; two 4,100 m³/h class bucket-wheel excavators, 1,600 mm belt width conveyors (8,000 m), SU 2,000 mm belt width conveyors (4,000 m) and an 8,500 m³ class spreader paired with 2,000 mm belt width conveyors (4,500 m).

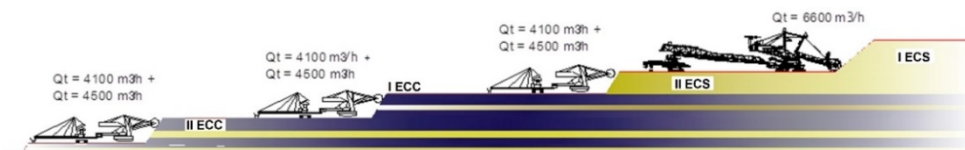


Figure 14. Continuous equipment on Radljevo.

During 2017, the possibility of supplying the new TPP Kolubara B block with coal from the Kolubara basin was analyzed. According to this, there are no plans for opening new mines, just a gradual increase in the capacity of Radljevo mine. Figure 15[4] shows the production capacities and coal reserves in the Kolubara basin in 2025.

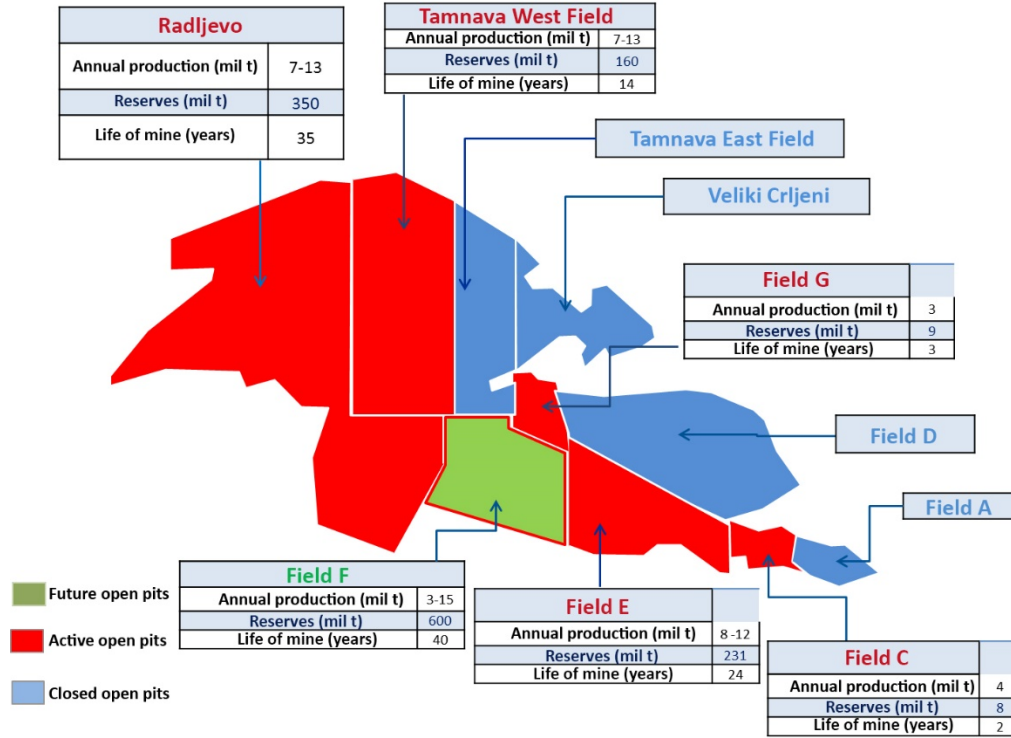


Figure 15. Overview of production capacities and proved coal reserves of MB Kolubara in 2025.

3.2. Planned dynamics of mining development in the Kostolac coal basin

The planned development dynamics of Kostolac basin mining are defined by LTMDs. According to this Strategy, it is planned to increase capacities in the function of supplying the new TPP Kostolac B3. In the limited area of opencast mine Drmno, there is a total of 1.387 Bm³ of overburden and 60.26 Mm³ of interlayer overburden. In the limited area of the mine there are a total of 290*10⁶ t of coal within two coal layers. When the previously excavated mass in the planned contour of the mine is calculated, there is still about 1.26 Bm³ of overburden and about 250 Mt of coal. The average overburden to coal ratio is about 4,8 m³/t.

The planned increase in overburden production in 2019 will be achieved by purchasing a new (VI) ECS system. A 6,600 m³/h bucket-wheel excavator is planned on the excavation, along with a system of eight 2,000 mm belt width conveyors and an 8,500 m³/h capacity spreader. Figure 16 [2] shows the technological profile of the overburden excavation, while Figure 17 [2] shows the technological profile on coal mining.

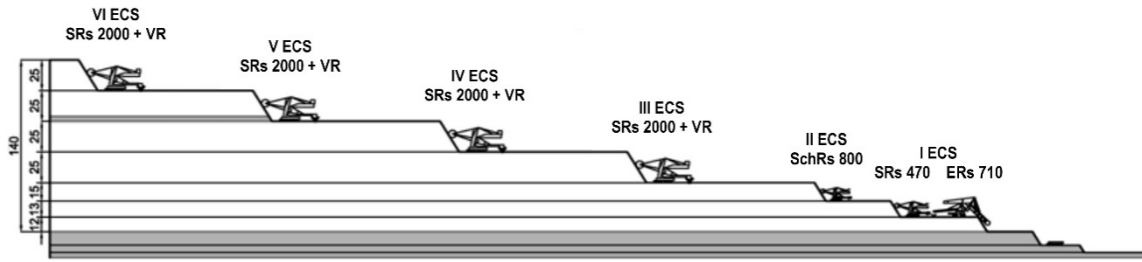


Figure 16.Continuous equipment of overburden excavation in 2019.

During 2018, the open pit slope coal conveyors will be reconstructed, and redirected towards the eastern border, and then through the crushing plant to the coal stockyard. Due to the more intense appearance of the second coal layer, it will be mined with the current V ECS system and directed to the slope conveyors. Also, the construction of a third dump line and the introduction of a coal quality management system are planned.

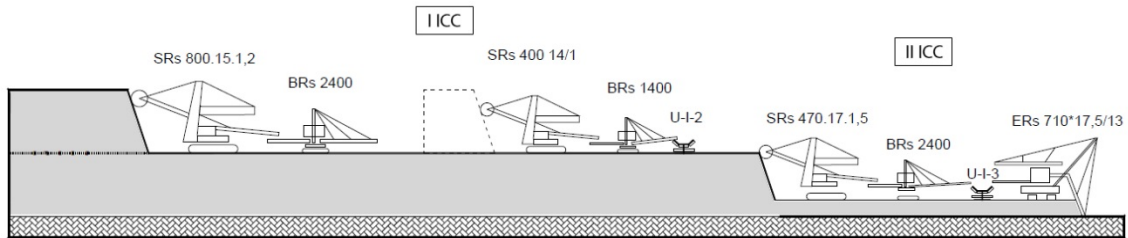


Figure 17.Continuous equipment on coal mining in 2019.

4. APPLIED CONTINUOUS SYSTEMS

Within the Electric Power of Serbia, ten ECS systems are currently working on overburden excavation and ten systems on coal mining and interlayers, i.e. a total of thirty seven bucket-wheel and bucket chain excavators and thirty spreaders and mobile conveyors (one hundred forty six conveyors with a total length around 350km).

Large lignite reserves in Serbia and the favorable location of the lignite basin from the aspect of energy and power transfer to large consumers, mining, geological and climatic conditions, geometries of deposits and physical and mechanical characteristics of the working environment, provide the possibility for opening large opencast mines with annual capacities up to $15 \cdot 10^6$ tons of coal annually, i.e. they enable the introduction of large continuous mining mechanization. High output continuous mining systems are used for overburden and coal mining on almost all opencast mines in Serbia.

The introduction of this mechanization on opencast coal mines in Serbia is associated with the opening of the first large opencast lignite mines. Along with the development of the opencast coal mining system, basic and auxiliary machinery has also improved, and increasingly adapted to the conditions of the working environment. On the other hand, working conditions on opencast mines are becoming more and more difficult, as the shallow and more reachable parts of the deposit are already excavated. Therefore, the problem of excavation in difficult geological conditions is increasingly present, where large production and economic effects will not be achieved without the use of modern mechanization.

Table 1 shows the existing continuous equipment on the Kolubara basin opencast mines and Table 2 shows their output characteristics [4].

Table 1. Existing continuous equipment on the Kolubara basin opencast mines

Excavators		Spreaders and mobile conveyors		Belt conveyors	
Type	Piece	Type	Piece	Type	Piece
SRs 1200.22/2+VR	1	A ₂ RsB 3500.60+BRs	4	1500	70
SRs 1200.24/4+VR	4	ARs 1600(37+33+60)*18	1	1600	10
SRs 1201.24/4+VR	1	ARs 1800(14+33+60)*20	1	1800	7
SchRs 1760.32/5	1	BRs 1600/(28+50)*9	1	2000	25
SRs 1301.24/2.5	1	ARs/BRs 1600(28+50)*15	2		
SRs 1300.26/5+VR	1	ARs/BRs1600/(28+50)*17	4		
SchRs 630.25/6	4	ARs 1400(22+60)*21	1		
SchRs 900.25/6	1	A ₂ RsB 8500.60	2		
SRs 2000.32/5+VR	1	ARs 1200/(18+30)*11	1		
SchRs 1600.25/3+VR	1	BRs 1200.29/32	1		
SchRs C-700s	1	BRs1600/(17.5+32.5)*15	1		
SchRs 350.12/5	1	BRs 1400/(37+50) *1	1		
LWK-102	1	PA 2000	2		
ERs 1000/20	1				
SchRs 740.25/6	1				
SchRs 1400	1				
SchRs 1600.25/3+VR	1				
Total	23	Total	22		

Table 2. Basic output characteristics of Kolubara excavators at the end of 2017

Excavator	Start year	Realized outputs (t and m ³)		Effective time (h)		Time usage (%)		Output usage (%)	
		Coal	Overburden	Coal	Overb.	Coal	Overb.	Coal	Overb.
SchRs 350.12/5	1972	42406948	6659240	97943	20564	31	35	43	35
SchRs C700.15/1.5	1987	20291064	45824813	23550	54463	28	39	28	33
SRs 1200.22/2	1967	115146278	79053161	105225	73286	36	54	35	34
SRs 1201.24/4	1968	479936	232072561	361	181193	42	50	45	46
SRs 1200.24/4	1968	3573149	258121754	5479	200951	44	49	31	47
SRs 1200.24/4	1975	/	246456469	/	190382	/	51	/	47
SRs 1200.24/4	1976	/	223143970	/	186179	/	51	/	44
SRs 1200.24/4	1976	/	223418567	/	182805	/	50	/	44
SchRs 630.25/6	1977	210497422	229940	144152	312	42	/	40	/
SRs 1300.26/5+VR	1987	167038567	657123	107218	561	42	/	38	/
SchRs 1760.32/5+VR	1990	/	162770370	/	87837	/	42	/	37
SRs 1301.24/2.5+VR	2011	7276066	12274720	7523	13712	31	40	31	33
SRs 2000.32/5+VR	1995	/	205017623	/	93008	/	47	/	41
SchRs 630.25/6	1994	121035352	4594498	79337	3663	43	40	41	24
SchRs 630.25/6	2000	12611937	62767397	9865	42011	17	46	38	47
ERs 1000/20	1977	83048298	816393	76303	894	23	/	54	/
SchRs 900.25/6	1978	789350	224446870	859	149054	/	44	/	45
SchRs 1600.25/3	2010	/	90466162	/	36584	/	53	/	48
SchRs 630.25/6	1980	189068639	/	118585	/	38	/	40	/
SchRs 740.25/6	2014	13625795	/	9555	/	39	/	32	/
SchRs 1400 25/3	2017	/	6328675	/	2808	/	35	/	44

Table 3 shows the existing continuous equipment on the Kostolac basin opencast mine Drmno, and Table 4 shows their output characteristics[4].

Table 3. Existing continuous equipment the Kostolac basin opencast mine Drmno

Excavators		Spreaders		Belt conveyors	
Type	Pieces	Type	Pieces	Type (mm)	Pieces
SRs 470.20/3	2	A ₂ RsB 3500.50	1	1400	7
SRs 470.17/1.5	1	A ₂ RsB-5500.55	1	1600	5
SRs 470 14/1	2	A ₂ RsB 7200.95	2	1800	13
SRs 400.14/1	1	ARs 2000/15/60/60.22	1	2000	9
SchRs 800.15/1.5	1	BRs 2400.59	3		
SH 630.15/1.5	1	BRs 1400/17.5+32.5	1		
SRs 2000.28/3+VR	1				
SRs 2000.32/5+VR	2				
SRs 1300.26/5+VR	1				
ERs 710.17.5/16	2				
Total	14	Total	9	Total	34

Table 4. Basic output characteristics of Kostolac excavators at the end of 2017

Excavator	Start year	Realized output (t and m ³)		Effective time (h)		Time usage (%)		Output usage (%)	
		Coal	Overburden	Coal	Overb.	Coal	Overb.	Coal	Overb.
SRs 470.17/1.5	1987	26219254	5014063	54988	20237	35	44	31	20
ERs 710.17.5/13/16	1983	634279	47785344	1841	106684	35	37	35	34
SRs 2000.28/3+VR	1985	/	208116168	/	102402	/	36	/	38
SRs 2000.32/5+VR	1997	/	163853604	/	75842	/	41	/	42
SRs 2000.32/5+VR	2009	/	99163453	/	30518	/	41	/	63
SRs 1300.26/5+VR	1988	/	92627621	/	84512	/	33	/	30
SchRs 800.15/1.5	1995	67183547	/	72885	/	39	/	34	/
ERs 710.17.5/13/16	1991	25249719	3338398	75043	11057	36	62	28	28
SRs 470.20/3 (12)	1975	/	45154279	/	134177	/	36	/	24
SRs 470.20/3 (11)	1975	/	40607468	/	98242	/	34	/	29
SRs 400.14/1 (14)	1985	28146781	13549899	37423	40699	22	33	27	15
SH 630.15/1.5	1978	22723153	16547543	33120	44485	25	40	29	19

4.1. Achieved results and condition of equipment

Until the beginning of the nineties, applied mining technology on opencast mines in Serbia followed the most modern world trends, as the realized capacities and the use of equipment could be measured with the results achieved in the most developed mining countries. In addition, a very strong supporting industry was built, which has been very successful in the production of spare parts, some auxiliary machines, belts, etc. However, after the economic sanctions against Serbia, there was a great delay in replacing worn out equipment and the acquisition of new mechanization, so Serbia became greatly behind in the application of modern solutions, in comparison with developed countries. Maintenance was maximally reduced, while coal mining was unadapted with the overburden excavation and the timely opening of new mines as replacement capacity. All of this has affected the decline of equipment utilization in time and capacity. Also, there have been several major damages on the bucket-wheel excavators and spreaders.

Over the past 15 years, a lot has been done to modernize and revitalize old equipment and acquire new. The most modern solutions in the field of power supply and control were applied on the

new modernly designed equipment that was subsequently procured. Also, a lot has been done on the unification of all parts of the equipment, and for the first time, it was insisted that the equipment provides the highest level of work and environmental protection (noise and dust)[1].

EPS strategically decided to increase the capacity of the overburden systems from the previous 3,500-4,000 m³/h to 6,600 m³/h, and the conveyor width from 1,500-1,600 mm to 2,000 mm with installed power up to 4*1,000 kW per station, which allowed the conveyors to be used up to 3,000 meters long. The capacity of the spreaders has been increased to 8,800 m³/h, while a 12,000 m³/h capacity spreader was set for overburden disposal.

Due to the need for selective work on coal mining, the concept of applying an up to 4,800 m³/h capacity excavator paired with mobile conveyors has been retained. After purchasing this equipment, opencast mines Tamnava West Field and Drmno are among the most modern mines in Europe. In the last few years, despite the catastrophic floods in 2014 and significantly reduced mining conditions, the indicators of time and capacity utilization of equipment are at a high level.

5. NEW AND REVITALIZED CONTINUOUS EQUIPMENT

In accordance with the LTMDs, new EPS opencast mines are going to be opened, for which new and revitalized equipment will be necessary[2]:

- In 2017, for opencast mine Field C, a new ECS system was installed, with a 6,600 m³/h capacity - SchRs 1400 bucket-wheel excavator (KRUPP manufacturer), four 2,000 mm belt width conveyors with installed power up to 4*1,000 kW (KOPEX manufacturer) and an 8,800 m³/h capacity spreader (SANDVIK manufacturer). In addition to this equipment, in the function of the dump dislocation, three more 2,000 mm belt width conveyors will be purchased with a total length of 2,500 m.
- At the beginning of 2018, a 12,000 m³/h interlayer overburden spreader started to operate on opencast mine Tamnava West Field.
- On opencast mine Drmno, the installation of a new ECS system is in the final phase, with a 6,600 m³/h capacity - SchRs 1400 bucket-wheel excavator (KRUPP manufacturer), eight 2,000 mm belt width conveyors with power up to 4*1,000 kW (GOSA FOM manufacturer) and an 8,800 m³/h capacity spreader (SANDVIK manufacturer).
- For mine Field E, a purchase of two systems with 6,600 m³/h capacity (one should start operating in 2025, the other in 2028) is planned. It is also planned to procure 1,600 and 2,000 mm belt width conveyors with five distribution devices, as well as to replace the existing 1,800 mm belt width conveyor a 2,000 mm belt width one and purchase a new spreader for the existing V ECS system.
- Currently used equipment from the MIBRAG Company (bucket-wheel excavator SchRs 630 27/10 and an ARs 1400 spreader) is being purchased.
- For opencast mine Radljevo, purchases of one 6,600 m³/h system and two 4,800 m³/h capacity systems for coal and overburden excavation are planned, with distribution stations and an interlayer overburden spreader.
- The majority of the old equipment was modernized by electrical part replacement, while a modernization of the mechanical equipment is also scheduled for the old equipment which will continue operating (for example, the SRs 2000 excavators will have their rotor drive modernized with the unification of the reduction drive).

5.1. Coal stockyards and coal quality management

Intensive works are currently underway on the expansion of the opencast mine Tamnava West Field stockyard and the introduction of a coal quality management system. In addition to the existing 200,000 tons stockyard, a new 400,000 tons stockyard with a 5,000 t/h capacity spreader and two

2,500 t/h capacity reclaimers will be set up. Two 2,500 t/h capacity crushers (FAM manufacturer) are going to be installed. The quality management of coal is in the implementation phase, and it consists from the original solution of EPS and the Faculty of Mining and Geology of integrating the geological and technological model with on-line monitoring of the coal quality and quantity. The system should be operational by the end of 2018[1].

A similar stockyard is planned in the eastern part of the basin, but its introduction is expected after 2025. The construction of a third stockyard line and the introduction of a coal quality management system are being prepared in the Kostolac basin[1].

6. CONCLUSION

Favorable deposit conditions enabled the use of continuous systems for coal and overburden mining. In the last ten years, EPS has decided to increase capacity when purchasing new systems, so four new systems with a 6,600 m³/h capacity and 2,000 mm belt width conveyors were purchased. This strategic decision significantly influenced on securing the required capacities despite the considerable difficult conditions of mining in the recent years. Since coal will remain the most important energy source in the following period, opening new opencast mines and purchasing new continuous systems for mining overburden and coal are planned. Subjective and objective changes in the dynamics of the opencast mines development in relation to the Long-term Mining Development Strategy on EPS Coal Basins point to the necessity of urgent innovation of this document.

REFERENCES

- [1] D. Ignjatovic, V. Pavlovic (2016). Continuous mining system in Serbia and contemporary tendencies in development on lignite opencast mines. ISCSM2016, Belgrade.
- [2] Long-term Mining Development Strategy on EPS Coal Basins, Opencast Mining Centre, 2015.
- [3] Coal industry across Europe, European Association for Coal and Lignite, 2017.
- [4] Technical documentation of Electric Power of Serbia.

Session 2: Modeling and simulation

Ultimate Pit Limit Determination for Fully Mobile In-Pit Crushing and Conveying Systems: A Case Study

Edward Hay, Micah Nehring, Peter Knights, Mehmet S. Kizil

The University of Queensland, School of Mechanical and Mining Engineering, Queensland 4072, Australia

ABSTRACT

Fully-mobile in-pit crushing and conveying systems have different pit shape requirements to traditional truck haulage systems due to linear bench and flat floor constraints imposed by conveyor systems. As the shape of a pit is largely based on the ultimate pit limit, it is desirable to have the additional shape requirements of fully mobile in-pit crushing and conveying systems included in the ultimate pit limit determination process. This paper discusses and highlights why there are different requirements for these systems, and what they are. A method of including these extra requirements during ultimate pit limit determination is presented. A case study has been included that shows the method working successfully, with scheduling of the pits to further highlight fully mobile in-pit crushing and conveying viability. This case study shows that through the reduced mining costs, a fully mobile in-pit crushing and conveying pit can return a higher Net Present Value, despite being smaller than the traditional truck and shovel pit for the same deposit. The development of this method provides the opportunity for the metalliferous industry to accurately determine ultimate pit limits for a mine considering the use of fully mobile in-pit crushing and conveying systems.

1. INTRODUCTION

Though In-Pit Crushing and Conveying (IPCC) mining systems have been utilised in the mining and quarrying industries for several decades, the use of the Fully Mobile IPCC (FMIPCC) variant remains largely underutilised. Interest in FMIPCC has grown significantly over the last 15 years due to their lower operating costs and ability to overcome several issues in the industry, such as: mines becoming larger and deeper, declining grades, shortages of labour and large off-highway tyres, higher diesel fuel costs, and concerns about greenhouse gas emissions. In addition, to reducing or negating the impact of these issues, they also have the potential to enhance resource recovery [1].

Despite the increased interest in FMIPCC systems, there is a lack of fundamental understanding regarding their operational constraints, and how these influence pit shape, as well as how planning/designing pits differs from Truck and Shovel (TS) systems. Both pit shape and pit design can be traced back to the Ultimate Pit Limit (UPL) determination process that is completed during various stages of feasibility studies.

This paper introduces the UPL problem, and highlights how the requirements for this differ between TS and FMIPCC systems. A potential solution that includes the additional requirements for calculating the UPL for FMIPCC systems is then presented, with a simple case study showing the application of the method.

2. ULTIMATE PIT LIMIT DETERMINATION

Ultimate pit limit determination is the process of calculating which material is economical to mine, and which is not, in order to extract the minimum volume of material for maximum financial

value. This process is generally completed using one of three common solution methods; these are: floating cone, Lerchs-Grossmann, and network flow.

Originally presented in 1966 [2], the heuristic floating cone algorithm was widely used across industry due to its ease of comprehension and fast running times. As the name implies, the algorithm calculates the ultimate pit through systematically imposing a cone (composed using safe wall angles) above each block (starting at the top). For each of these cones, if the sum of all blocks inside it is positive, the blocks are considered to be part of the ultimate pit. As each block is investigated independently, this method overlooks the possibility of two ore blocks located near each other sharing waste material. When investigated individually these blocks may not be worth mining, but as they share overlying waste, if investigated together, they would contribute positive value. This is known as the joint support problem, and is illustrated in Figure 1. Due to this, the algorithm is not able to reliably return the truly optimal solution.

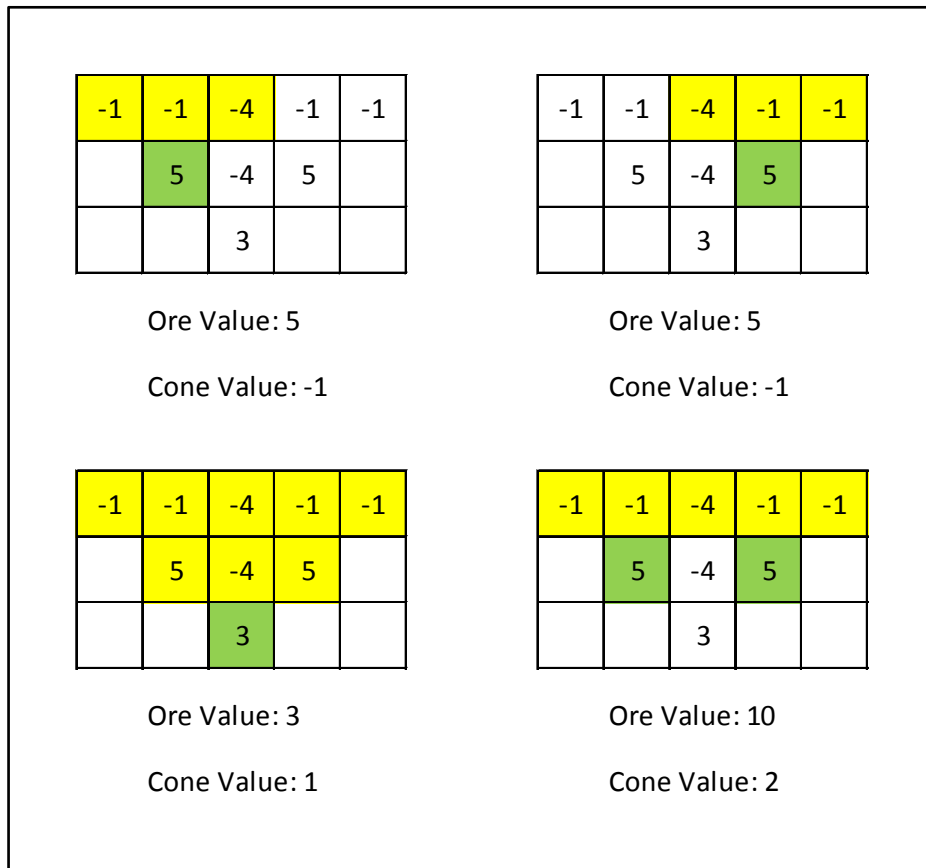


Figure 12. Joint support problem of floating cone algorithm.

The rigorous Lerchs-Grossmann algorithm [3] is based in graph theory, with each node in the graph representing a single block of the block model, and taking a value equal to the blocks economic value. The safe wall angles in this algorithm are implemented as directed arcs within the graph, linking blocks lower down to overlaying blocks above, as illustrated in Figure 2. Once the graph is set up, solving for the ultimate pit is analogous to solving for the maximum closure of a graph. This is completed through the use of a series of naming conventions that dictate graph transformations that in turn solve for the maximum closure. As this algorithm no longer investigates blocks as individuals, it is able to overcome the joint support problem experienced by the floating cone algorithm. Due to this algorithms ability to always return the mathematically provable optimal solution, it has become the standard in UPL optimisation across the industry.

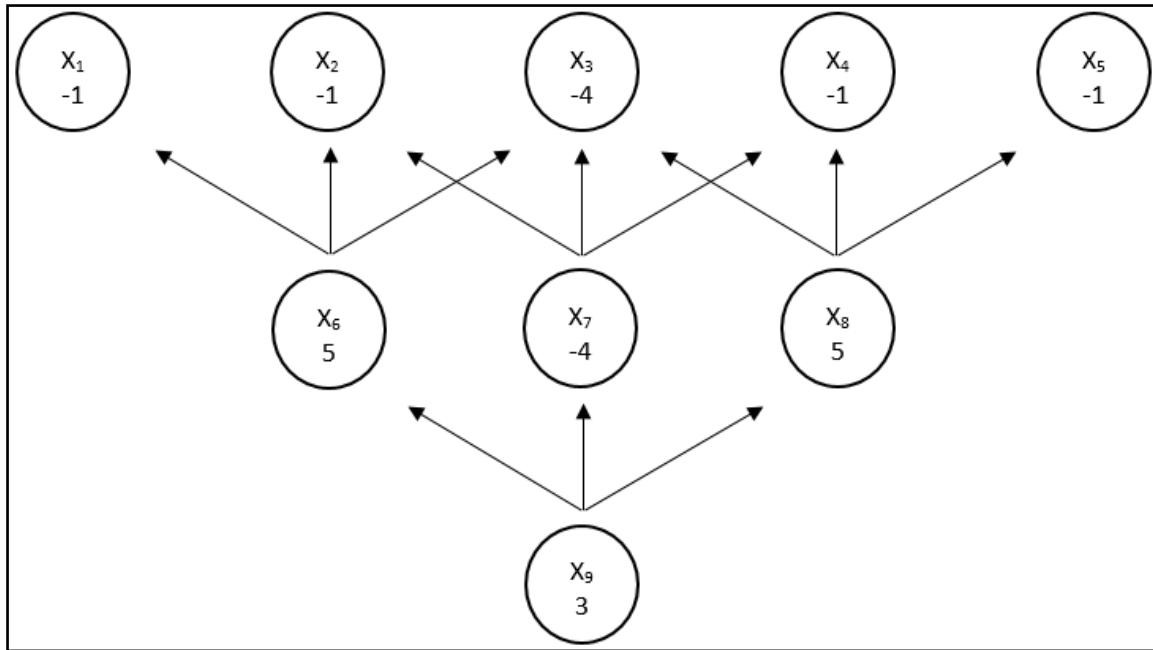


Figure 13. Graph set up of Lerchs-Grossmann algorithm.

The rigorous network flow solution was also presented by Lerchs and Grossmann [3], noting that the block model can be transformed into a bipartite network, with each block in the model being represented by a node in the network. Nodes representing positive value blocks are linked to the source of the network with an arc with capacity equal to their value, and nodes representing negative value blocks are linked to the sink of the network with an arc with capacity equal to their absolute value (i.e. their value but positive). Safe wall angles are implemented as infinite capacity arcs between the positive nodes and their respective overlying negative nodes. An example network is illustrated in Figure 3. Once the network is complete, the UPL is found by solving for the maximum flow/minimum cut dual solution of the network. Much like the Lerchs-Grossmann algorithm, this method overcomes the joint support problem. In addition to this, due to the importance of the solution of general network flow problems in operations research, there has been a great deal of resources used to develop efficient computer codes to solve for maximum flows [4]. This method is also able to compute mathematically provable optimal results, it is not however considered standard in industry, though it is implemented in industry specific software packages.

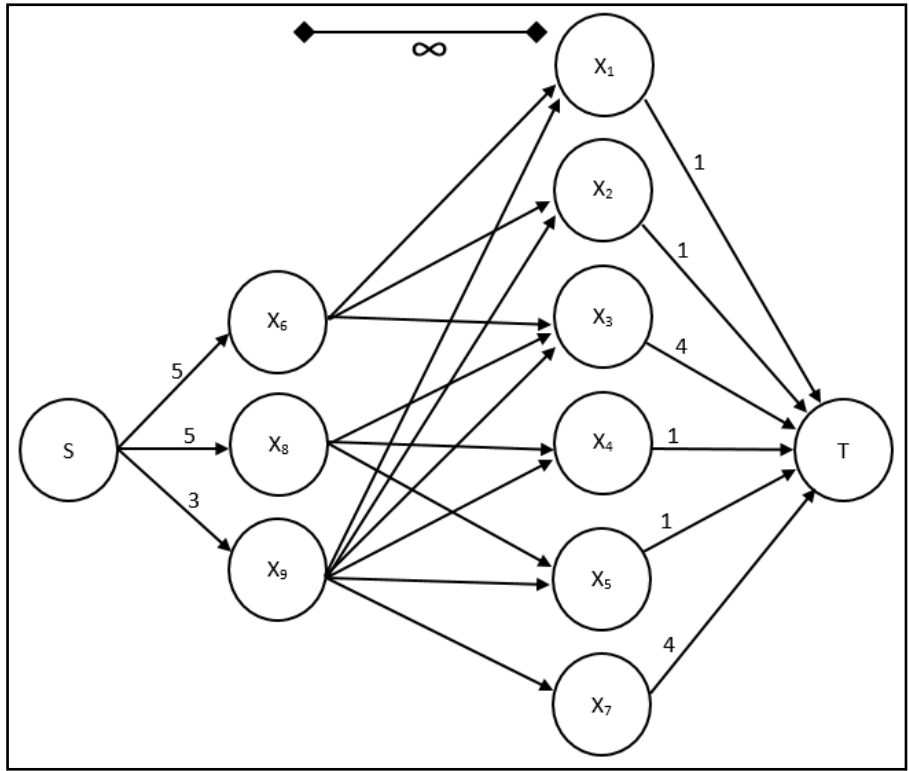


Figure 14. Bipartite network flow set up.

Fundamentally, these three methods all achieve the desired outcome, with varying complexity, solution time, and accuracy. This is completed with the only constraint imposed being the geometric constraint of safe wall angles, which is seen as inter-block dependencies denoting which blocks must be removed in order to access a deeper block.

3. DIFFERENCES IN UPL REQUIREMENTS

Due to the different operational natures of FMIPCC systems when compared to TS systems, there are fundamental differences in the requirements of pit design [5]. It is important to first note that all UPL determination and subsequent pit designs must adhere to the geotechnical constraints of mining, i.e. safe wall angles. For a TS system, the only requirements that must be met during pit design are that at least one access ramp is available for entry and exit from the pit, and that the minimum mining width for the mining equipment is met. As each of these requirements does not affect that UPL, UPL determination can be completed using existing methods, with pit design to follow. This traditional approach returns UPL outlines that resemble an inverted cone (Figure 4). This approach has been used for many decades, allowing mine planning engineers to take advantage of the flexibility of TS systems, fitting them into the pit as required.

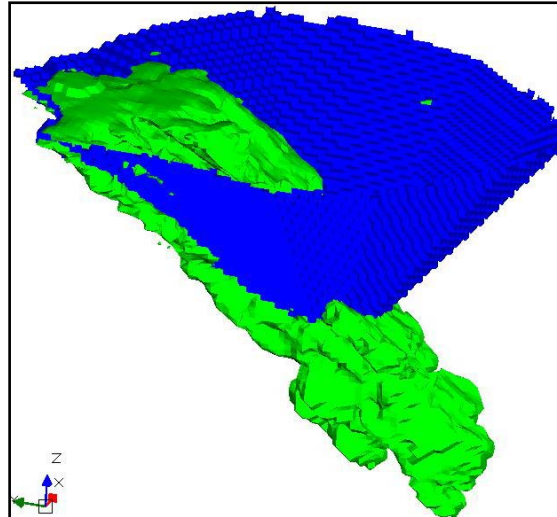


Figure 15. Example of traditional inverted cone UPL (blue) for an orebody (green).

For FMIPCC systems, these two requirements remain unchanged as access to the pit and fitting equipment is still required. However, there is also additional requirements that arise from the use of conveyors. The first of these is that in order for conveyors to work efficiently, they must be used in linear setups, similar to a strip mining operation. This imposes the requirement that mining benches must be mostly regular and horizontally extensive [6]. Due to this linear extensiveness, and the way in which conveyors are moved across the pit, this requirement is extended to include the pit floor being flat. The second requirement rises from the chosen pit exit strategy, which for an FMIPCC system, there are five categories to consider, these are:

- adapting conventional access ramps to house the conveyor;
- use of high angle conveyors to climb the pit walls;
- excavation of a slot to run the conveyor up;
- developing a decline to house the conveyor; and,
- the inclusion of a fixed straight conveyor wall in pit design.

Which of these strategies is appropriate for FMIPCC is dependent on two factors; what type of conveyors can operate in each scenario (and their rated capacities), and each options ability to directly access the pit floor at any stage during operation. Table 1 shows the broad groups of conveyors available, and their relevant parameters. It can be seen that while pouch or pipe conveyors have the flexibility (both in terms of incline and radius of curvature) to use existing access ramps, or climb the conveyor wall steeper than a belt conveyor, they do not have the capacity to satisfy the material movement requirements of mining systems. This means that in order to satisfy capacity constraints, belt conveyors must be used.

Table 3. Conveyor Details

Conveyor Type	Capacity	Maximum Incline	Radius of Curvature
Pouch [7]	Up to 450 tph	30°	> 8 m
Pipe [8]	Up to 3,000 tph	30°	> 45 m
Belt [9]	Up to 12,000 tph	18°	~3,000 m (for belt with capacity to meet mining demand)

With the type of conveyor limited to belt conveyors, only the latter three options for pit exit remain possible. However, each options ability to access the pit floor at any stage must be taken into account. Cutting a slot to run the conveyor in presents the opportunity to access the pit floor at any level, however, a complication arises when the pit floor progresses deeper. In order to deepen the slot to reach the new pit floor, the conveyor would have to be removed while excavation occurred, then reassembled before operation could continue; thus introducing an undesirable delay to production. The development of a decline allows the use of belt conveyors, however, access to the pit floor is limited. A dedicated decline would only access the pit floor at its greatest depth, making this option unsuitable for FMIPCC systems.

The only strategy that sufficiently meets the capacity and accessibility requirements is the use of a fixed straight conveyor wall in the pit design. The ideal situation for this conveyor wall is that it is long enough for the pit exit conveyor to reach from the pit floor to the crest with no transfer points. However, due to the 18° incline angle limitation of belt conveyors, this would make the straight wall impractically long in some situations. If this is the case, the number of transfer points should be minimised due to the inefficiencies of transfer points arising from material spillage and hang ups [10], and the reduction in reliability of a series connected system (which FMIPCC systems are) for each additional component introduced [11].

If an FMIPCC is to be investigated accurately, these two major differences in pit shape (a flat floor and a straight wall) must be designed for. As the shape of a pit is fundamentally developed from the UPL, it is necessary for these two requirements to be included during UPL determination.

4. FMIPCC UPL DETERMINATION

4.1. Previous Work

There has previously been one method developed for including the additional requirements of FMIPCC systems into the UPL determination process. Young [12] programmed the Lerchs-Grossmann algorithm into *Microsoft Excel*. It was implemented using a simple safe wall angle stating that the nine blocks above must be removed in order to access the block underneath, providing nine dependency arcs to blocks above. In addition to this, Young implemented an additional dependency arc towards the straight wall. This additional arcs then means that the block next to the ore block must also be mined in order to access it (Figure 5). If this additional arc is added to each block, and stops at the conveyor wall location, a UPL that includes a straight wall is returned. While this development provides a rigorous solution for UPL determination for FMIPCC, it is limited to the use of a predetermined conveyor wall location at 90°. In order for a FMIPCC UPL solution to be more accurate, the conveyor wall must be oriented such that value is available as early as possible. The implementation of an additional conveyor arc did show positive results as a proof of concept; however, it needs to be implementable at any orientation.

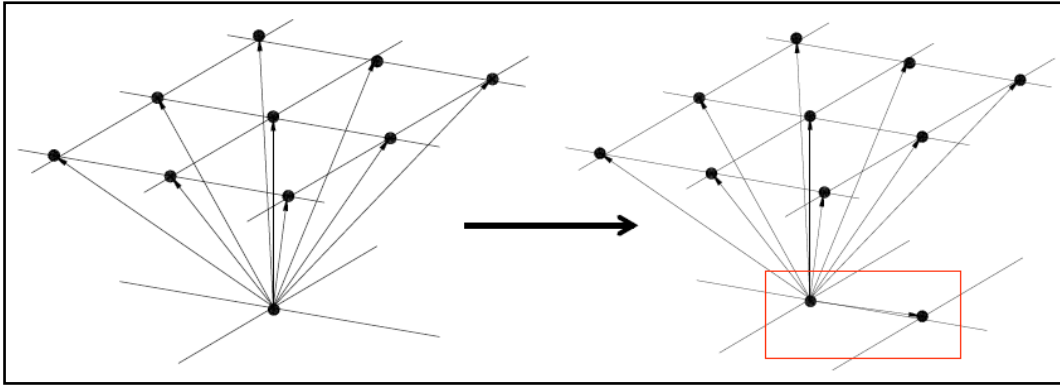


Figure 16. Additional dependency for modified Lerchs-Grossman algorithm [12].

4.2. Developed Algorithm

When developing a new method for FMIPCC UPL determination, there are several important points to note. Firstly, given that mathematically rigorous methods exist for traditional UPL determination, it is noted that reverting to a wholly heuristic method is undesirable. Secondly, due to the constraints of FMIPCC systems, the schedule of mining will resemble that of a strip mining operation. This means, due to the concept of the time value of money, that material closer to the surface, and closer to the fixed conveyor wall is potentially worth more than material that is deeper and further away. Thirdly, as the UPL changes due to an increase in depth, the optimal orientation for the conveyor wall may also change with depth. Due to this, the UPL must be calculated for each level of the block model acting as the floor. This is achieved by limiting the levels which are available for optimisation, and running the process for each floor level. With these concepts in mind, an algorithm that consists of three phases was developed, with examples highlighted on a small block model.

Phase one accepts a block model as its input, converting it to a bipartite network. It then calculates the traditional UPL for the limited model by finding the maximum flow of the bipartite network, which is the input into Phase two. This process is completed for each level of the block model being set as the pit floor.

Phase two uses the result of phase one to determine the orientations that have the potential to provide the highest value for each floor level. This is achieved through analysing the value of the blocks on each level, at each orientation, when a straight wall is imposed on the edge of the economic material. This is completed by forming a convex hull around the blocks that are part of the UPL from phase one, then fitting an arbitrarily oriented bounding box around the convex hull. Using one edge of this bounding box as the conveyor wall, discounting powers are attributed to blocks dependent on where they are in the pit. Figure 6 shows an example of this process for a case with the conveyor wall located at 180° , i.e. the bottom edge of the bounding box (red line). Not that blue blocks are part of the traditional UPL, and yellow blocks are not part of it. It can be seen that all blocks within the convex hull (purple line) are given a discounting power, and only additional blocks between the convex hull and the conveyor wall are included, with other blocks attributed a null discounting power (“-“ in Figure 6). Blocks that are within the convex hull, but not part of the UPL are included in this process, as they will be required to be mined in order to create a flat pit floor that extends out to the conveyor wall location. These discounting powers are attributed according to each block's location with relation to its depths and proximity to the conveyor wall, mirroring the basic scheduling concepts of FMIPCC systems. The sum of all blocks that are attributed a discounting power (with null blocks ignored) is calculated for each level at each orientation. The sum of all levels at each orientation is then taken to provide the weighted (by location) total value of the ultimate pit at each orientation.

Phases one and two are completed for each level of the block model acting as the pit floor level, providing a potential value for the deposit at every orientation, at each depth. The highest value orientation for each depth is then taken and provided to phase three as the input. Phase three takes the traditional UPL from phase one for each depth, and the maximum potential value orientation linked to each depth, and uses these to add additional dependencies to the bipartite network model that link each block to its neighbouring block in the direction of the conveyor wall. These dependencies are only added to the floor level to ensure a flat floor, as higher levels inherit the additional requirement due to being precedents of the floor blocks. An example of the additional dependencies for the same simple case can be seen in Figure 7. This model is then solved for the rigorous solution using the network flow method. Figure 8 shows the result of this process. It can be seen that there is now a straight conveyor wall at 180° (bottom of the figure), and a flat floor, with the waste blocks previously not included, now forming part of the pit. It can also be seen that due to the final solution being rigorous, the ore block (7,3) on the “Middle Level” that was part of the traditional UPL, is now no longer part of the FMIPCC UPL as there is too much additional waste between it and the conveyor wall. This rigorous solution is completed for each floor level, with all FMIPCC UPL options provided to the user for further scheduling to identify the highest value pit.

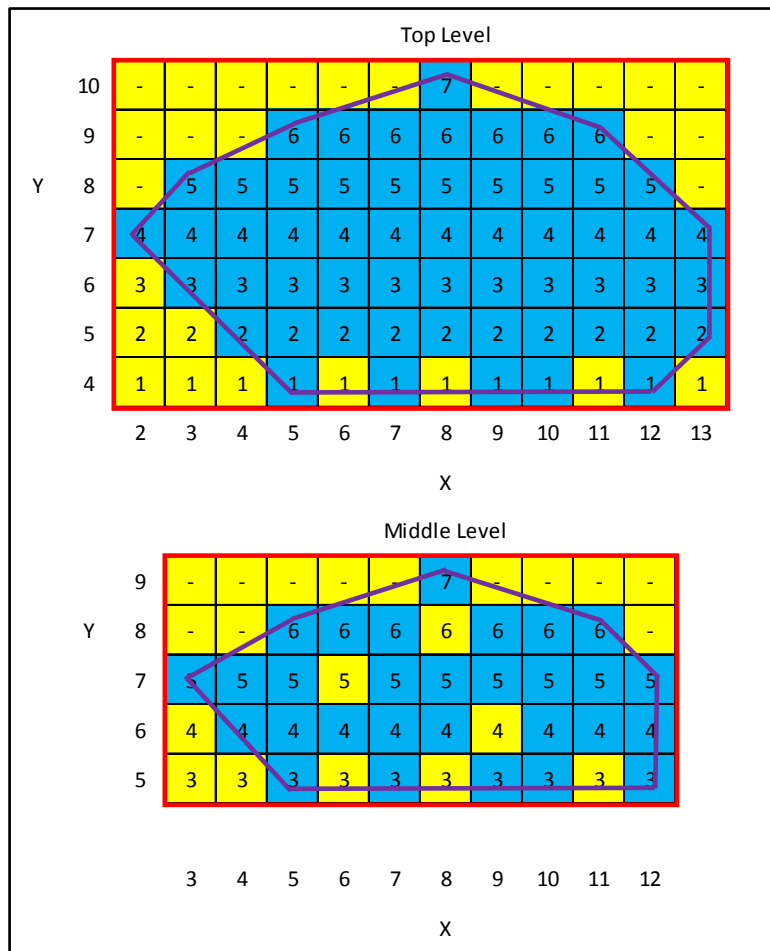


Figure 17. Example of discounting power for value calculation for conveyor wall at 180°.

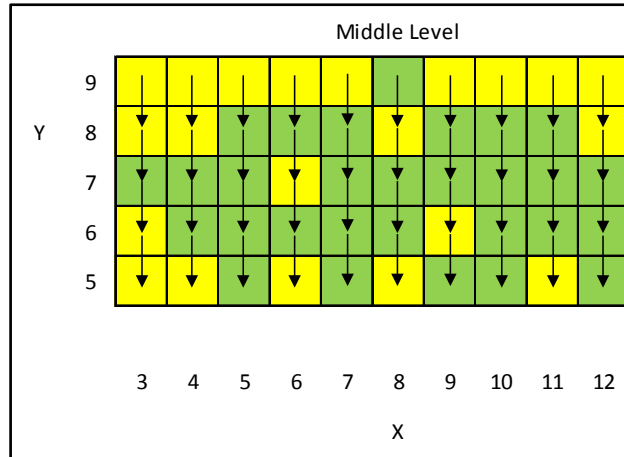


Figure 18. Additional dependencies for simple case at 180°.

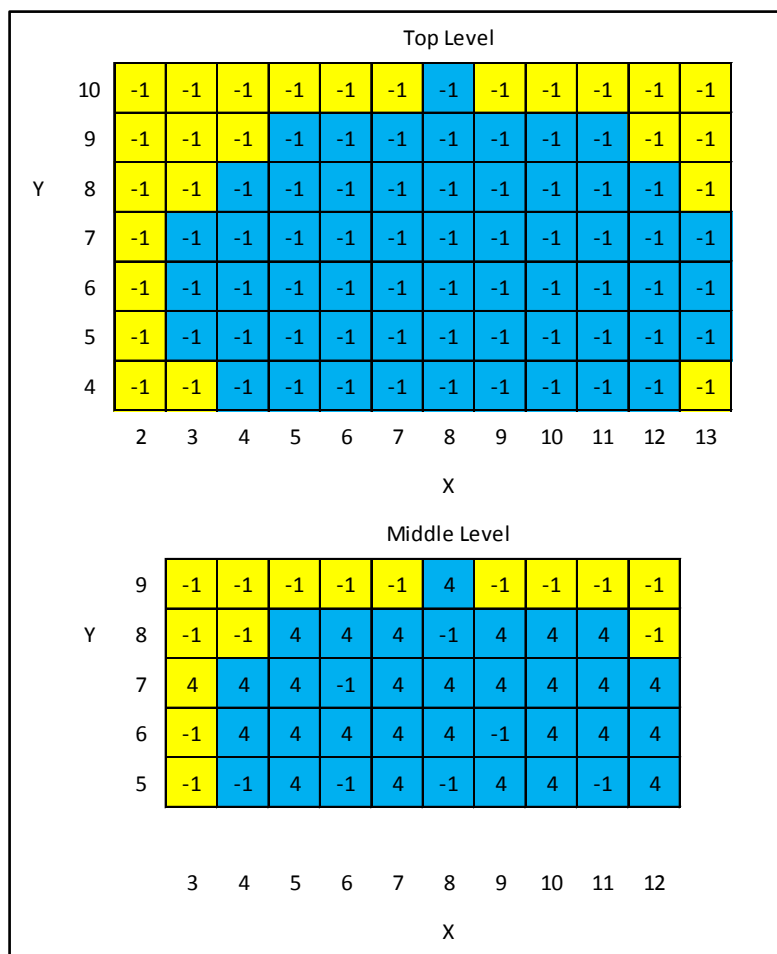


Figure 19. FMIPCC UPL with additional requirements included.

5. CASE STUDY

5.1. Introduction

To highlight the applicability of this method, a simple case study has been completed that compares the same deposit using both traditional UPL determination for use with a truck haulage system, and the presented FMIPCC UPL determination method. To further evaluate the viability of FMIPCC systems, each option was scheduled in order to compare the Net Present Values (NPV).

The case study was completed on a copper block model that was developed using real data from several real deposits, then scaled down to suit a simple case study. The model was 15 blocks in both the X and Y direction, and had five levels in the Z direction, with Z=5 being the surface level. Blocks are cubic, measuring 25 m in each direction, with a density of 2.7 t/m³. The grades of the 471 mineralised blocks range from 0.101% to 0.699%. The top level of the model is predominantly waste, with some low grade ore available, with the next three levels gradually increasing in grade as depth increases. The lowest level than shows a decrease in grade again. Figure 9 shows the grade tonnage distribution of the model.

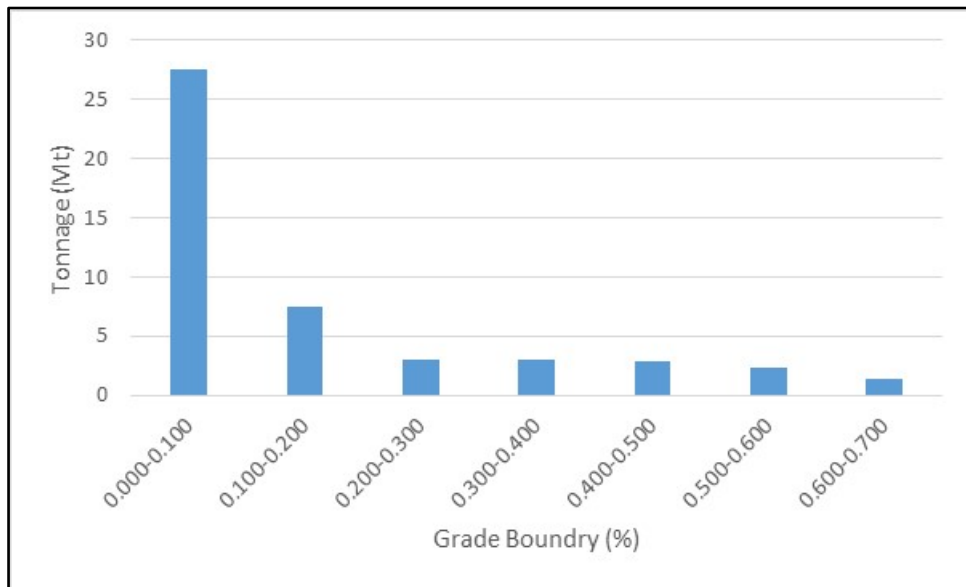


Figure 20. Grade tonnage distribution of case study block model.

5.2. Parameters and Inputs

Table 2 shows the parameters used in the case study. Note that the values associated to mining, processing, metallurgical recovery and copper price are not intended to be accurate of the industry at large, but values commensurate with the scaled block model. These values equate to an economic cut-off grade of 0.136%, providing 432 blocks above cut-off grade.

Table 4. Case study parameters.

Parameter	Value
Truck and shovel mining cost	\$5 + \$0.50/t for each level below the top level
FMIPCC mining cost	\$3.50 + \$0.35/t for each level below the top level
Processing cost	\$6/t ore
Metallurgical Recovery	85%
Copper price	\$5200/t product
Safe wall angle	45° all round
Discount rate	9%

5.3. Results

There are two parts to the results of this case study; the UPL comparison, and the scheduled pit comparison. There are five UPLs, one for the TS pit, and four options for FMIPCC pits (one for each floor level excluding the surface). The FMIPCC pits are distinguished as FM4 for the FMIPCC UPL that has its floor on level 4. Table 3 shows the numerical results for each UPL, with the pits shown in Figure 10. The conveyor locations for the FMIPCC UPLs are shown in black. It is important to note that a maximum incline of 18° for the conveyors equates to approximated travelling three blocks horizontally, to move up a level when using cubic blocks.

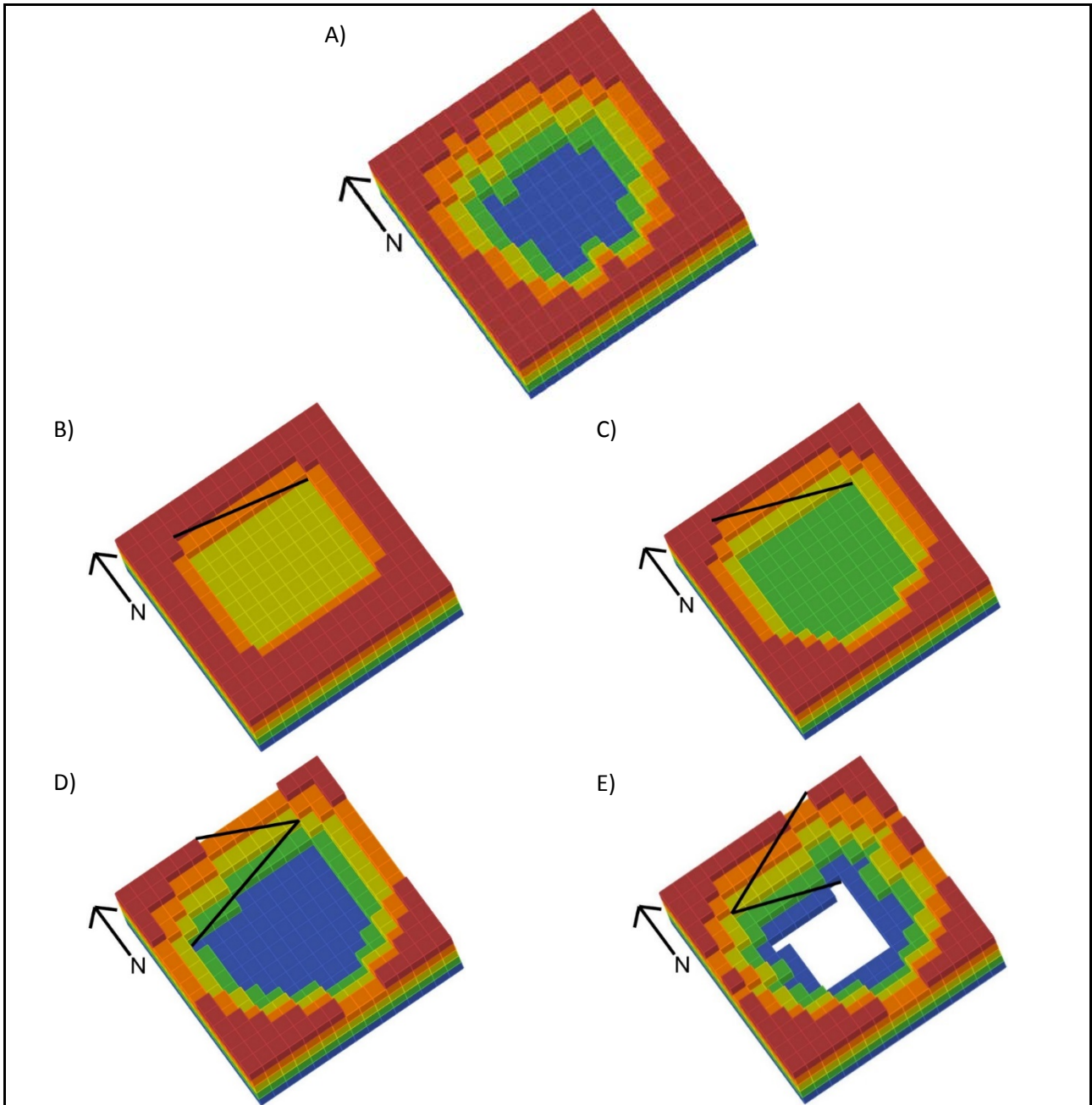


Figure 21. Case study UPLs. A) TS, B) FM4, C) FM3, D) FM2, E) FM1.

Table 5. Case study UPL numerical results.

Result	TS	FM4	FM3	FM2	FM1
Orientation of conveyor wall (°)	N/A	0	0	351	351
UPL value (\$M)	41.83	18.20	44.89	68.34	69.96
Total material (Mt)	14.30	7.51	13.96	20.38	19.87
Ore (Mt)	11.73	6.83	10.59	14.30	14.68
Waste (Mt)	2.57	0.68	3.37	6.08	5.19
Stripping ratio (t/t)	0.22	0.10	0.32	0.42	0.35
Average grade (%)	0.369	0.287	0.344	0.369	0.364
Product (kt Cu)	36.73	16.64	30.99	44.90	45.46
Resource recovery (%)	64.35	37.50	58.10	78.47	80.56

The UPL for the TS case resembles and inverted cone as expected, though it also shows a flat floor. This is a limitation of the block model having low grade ore on the lowest level. Any of the four block long straight wall segments are not appropriate for pit exit conveyors, and are purely coincidental. It can be seen that each of the FMIPCC UPLs has a flat pit floor that is appropriate for the use of conveyors. The UPLs for FM4 and FM3 have their straight conveyor walls located at 0° orientation; each of these is long enough for a pit exit conveyor to exit the pit with no switchbacks/transfer stations required. The UPLs for FM2 and FM1 have their straight conveyor walls located at 351°. This orientation equates to a change of approximately 6.3 blocks in the X direction for one block change in the Y direction. This makes the conveyor wall appear as a string of smaller straight sections. As these two UPLs are deeper than FM4 and FM3, but are no wider, the pit exit conveyors are required to switchback in order to exit the pit. Looking at each of the FMIPCC UPL pits, it can be seen that the additional requirements of a flat pit floor and a straight conveyor wall have been met using the presented method of FMIPCC UPL determination.

Comparing the results, it can be seen that as the FMIPCC UPLs get deeper, their resource recovery increases, which directly translates to progressively higher UPL values. However, when comparing them to the TS case, this relationship no longer remains true. Although FM3 has a lower resources recovery and a higher stripping ratio than the TS case, it is still able to produce a higher UPL value. This is due to the decrease in mining cost when using an FMIPCC system.

Scheduling of the TS pit was completed according to the existing convention of progressing down and the out across the deposit, targeting high grade material first. FMIPCC operations typically operate on a two or three bench basis; the scheduling for these is similar, the only difference being a third active level for a three bench scenario. An example for two bench operation scheduling follows these steps:

- Mining starts on the top level, at one end of the conveyor wall.
- Mining progresses along this row until all blocks have been removed; mining continues in this fashion row by row across the top level until all precedent blocks for mining the first row of level two are removed.
- Once the second level is uncovered, mining is split between the two levels, progressing across the pit until both levels are completely mined.
- This process is repeated for all remaining pairs of levels.

Each scenario had the same mining and processing rates, with the same restrictions applied to them, these were:

- Mining capacity of 20 blocks per year must be fully utilised (except final year when a shortfall is expected).

- Processing capacity of ten blocks per year, must be fully utilised once processing starts (except final year when a shortfall is expected).
- Blocks may be processed the same year that they are mined.
- Stockpiled blocks are kept independently, maintaining their original grade.
- Rehandling cost of stockpiled material is negligible.

One last consideration during scheduling was that pits with three or more available levels can be scheduled using either a two bench or three bench method. For example, FM3 has three available benches, and can be mined as either a two bench operation, followed by an individual bench, or all three benches at the same time. As a result of these options, there is a total of eight scheduled pits. Table 4 shows the numerical results of scheduled pits, with the bench sequences highlighted.

Table 6. Case study scheduled results.

Result	TS	FM4	FM3	FM2	FM1
Bench sequence	N/A	2	2-1 3	2-2 3-1	2-2-1 3-2
UPL value (\$M)	41.83	18.20	44.89	68.34	69.96
Life of mining	16.95	8.90	16.55	24.15	23.55
Life of processing (start year)	27.8 (1)	16.2 (1)	25.1 (2)	33.9 (2)	34.8 (2)
NPV (\$M)	13.87	9.11	10.55 15.60	7.18 12.61	1.32 3.53
Equivalent annual annuity (\$M)	1.37	1.10	1.07 1.59	0.68 1.20	0.12 0.33

The first result to observe is that for each of the FMIPCC pits that has two scheduling options (two bench or three bench operation), the cases where three benches are mined concurrently first consistently outperform the two bench sequence cases. This is due to them being able to access higher grade ore earlier on.

Secondly, for traditional TS cases, a higher UPL value (due to different mining equipment or higher capacities) translates to an accordingly higher NPV for the same deposit. It can be seen that this relationship does not remain true for FMIPCC cases. This is due to the scheduling constraints of FMIPCC systems having a larger detrimental effect of the value of scheduled pits. This highlights the importance of scheduling each UPL that is returned from the FMIPCC UPL determination algorithm, not just the once with the highest undiscounted value. The only FMIPCC pit with a higher NPV than the TS case is the FM3 pit, scheduled as a three bench operation. This FMIPCC adds an additional \$M1.73 to the deposits NPV through the use of an FMIPCC system, even though it has a higher stripping ratio, and a lower resource utilisation. Due to the uneven mine/processing lives of these two schedules, the Equivalent Annual Value (EAV) has been investigated. This shows that the FM3, three bench operation also has a higher EAV, showing that this option is a better investment. Of note between these two scenarios is that the TS case is able to start processing in year one, whereas the FM3 scenario is not able to start processing until year two due to a lack of available ore, yet still returns a higher NPV.

6. CONCLUSION

This paper aimed to identify and communicate how the additional requirements of FMIPCC systems alter the requirements of pit shape. As pit shape is based largely on the UPL, these additional requirements had to be included during UPL determination. The method of including these requirements discussed in this paper uses the mathematical principles of convex hulls, bounding boxes, and future value discounting to provide the orientation of a conveyor wall that has the best

potential for creating value. It runs as an extension to the existing network flow method for calculating UPLs, and as such, the final results from the algorithm are mathematically rigorous.

The case study completed highlights that the presented method does now include the additional requirements of FMIPCC in the UPL determination phase. In addition to this, it identifies that it is important to schedule each FMIPCC option for a deposit, as the more limited scheduling of FMIPCC options has a larger negative impact on NPVs than traditional scheduling.

The development of this method advances the ability for industry to optimise and design a mine that is to use an FMIPCC system.

REFERENCES

- [1] Nehring, M., Knights, P., Kizil, M. S., & Hay, E. (2018). A comparison of strategic mine planning approaches for in-pit crushing and conveying, and truck/shovel systems. *International Journal of Mining Science and Technology*, 28(2), 205-214.
- [2] Carlson, T. R., Erickson, J. D., O'Brian, D. T. & Pana, M. T. (1966). Computer techniques in mine planning, *Mining Engineering*, 18(5):53-56.
- [3] Lerchs, H., & Grossmann, I. F. (1965). Optimum Design of Open-Pit Mines, *CIM Bulletin*, 58:47-54.
- [4] Fox, B. L. (1978). Data structures and computer science techniques in operations research, *Operations Research*, 26(5):686-717.
- [5] Dean, M., Knights, P., Kizil, M. S., & Nehring, M. (2015). Selection and planning of fully mobile in-pit crusher and conveyor systems for deep open pit metalliferous applications. *Proceedings of Third International Future Mining Conference, Sydney, Australia, 4-6 November 2015*. Australian Institute of mining and Metallurgy, Sydney, 219-225.
- [6] Atchinson, T., & Morrison, D. (2011). In-Pit Crushing and Conveying Bench Operations, paper presented to Iron Ore Conference, Perth, Australia, 11-13 July 2011.
- [7] Enclosed Bulk Systems, n.d. EBS Conveyor [online]. Available from: <<http://www.enclosedbulk.com>> [Accessed: 19/08/2015].
- [8] Contitech (2014). Conti®Pipe High-Speed Closed-Trough Belt Conveyor System for especially tight curves and high productivity [online]. Available from: <<https://www.contitech.de>> [Accessed 9/10/2015].
- [9] Sandvik (2008). In-Pit Crushing and Conveying-IPCC [online]. Available from <<http://www.miningandconstruction.sandvik.com>> [Accessed: 10/10/2015].
- [10] Spilker, E. C., Albers, T. J., & Lordi, A. C. (1980). Technical aspects of overland belt conveyors, Society of Mining Engineers of AIME, Las Vegas, Nevada, preprint number 80-54.
- [11] Frankel, E. G. (1984). *Systems Reliability and Risk Analysis*, pp. 73-106 (Springer Netherlands: Dordrecht).
- [12] Young, J. (2015). Optimisation of in-pit crusher conveyor ultimate pit limits, Undergraduate honours thesis (unpublished), University of Queensland, Brisbane.

Assessment of the Added-Value of Sentinel 1 & 2 for Mapping and Monitoring Surface Mining

**Marianthi Stefouli¹, Antigoni Panagiotopoulou², Eleni Charou²,
Yiota Spastra⁴, Emmanuel Bratsolis², Nicholas Madamopoulos³ and Stavros Perantonis²**

¹Greek Institute of Geology and Mineral Exploration (I.G.M.E.), 13677 Acharne, Greece

²Institute of Informatics and Telecommunications, NCSR Demokritos, 15310 Ag. Paraskevi, Greece

³Hellenic Air Force Academy, Department of Aeronautical Sciences, TGA 1010 Dhekeleia, Greece

⁴Planetek Hellas, 44 Kifisias Avenue, 15125 Marousi, Athens, Greece

ABSTRACT

The Greek mining industry constitutes a major sector of the economic activity of the country and supplies essential raw materials for primary industries. Moreover, the industry provides a major source of employment in the country, and because, as a rule, the processing of these raw materials takes place in the region in which they are excavated, the industry also contributes considerably to coveted regional growth. Every mining activity impacts the nearby environment, causing the so-called mining hazards. Active mining operations are usually well monitored by the owners and by the mining authorities. In this framework, the issues of acceptance from local populations, corporate social responsibility, systems of quality control, and systems that allow collection and disclosure of full and accurate information (Databases, GIS, etc.) are all of particular importance. Within the EU Geocradle project a system is under development for monitoring legal / illegal quarries using satellite imagery in cooperation with the personnel of the Ministry of Environment / The Authority of the Ministry of Environment and Energy / Special Secretariat of Inspectors – Auditors / Body of Inspection for Southern Greece / Department of Mining Inspection. Surface mining also includes the activity of the coal mining. The methodology described in this work refers to the Monitoring of Lignite Mining Activities in Ptolemais basin in Greece.

1. INTRODUCTION

The Greek mining industry constitutes a major sector of the economic activity of the country (it constitutes 4-5% of the Gross Domestic Product (GDP), with the inclusion of interrelated enterprises such as quarrying, processing and production of intermediate and final products) and supplies essential raw materials for primary industries, such as cement, production of energy, non-ferrous metals (aluminum, nickel, etc), the industry of stainless steel etc. Considering the coal mining activity, Greece abounds in lignite resources of 5.8 billion tonnes, of which 3.1 billion tonnes are economically workable [1]. Moreover, the industry provides a major source of employment in the country, and because, as a rule, the processing of these raw materials takes place in the region in which they are excavated, the industry also contributes considerably to coveted regional growth.

Every mining activity impacts the nearby environment, causing the so-called mining hazards. Typical geohazards recorded by both active and inactive mines include: collapses migrating to the ground surface and sinkholes; slope instabilities; subsidence or uplift of the ground surface; pollution to air, soil and water by toxic waste, visual pollution etc. [2]. Active mining operations are usually well monitored by the owners and by the mining authorities. Quality, safety and environmental protection, constitute significant challenges but also the most pressing needs of this era – deeply influencing not only the development of the mining industry, but also its traditional character of many centuries and finally its very existence. In this framework, the issues of acceptance from local

populations, corporate social responsibility, systems of quality control, and systems that allow collection and disclosure of full and accurate information (Databases, GIS, etc.) are all of particular importance.

Within the EU Geocradle project a system is under development for monitoring legal / illegal quarries using satellite imagery in cooperation with the personnel of the Ministry of Environment / The Authority of the Ministry of Environment and Energy / Special Secretariat of Inspectors – Auditors / Body of Inspection for Southern Greece / Department of Mining Inspection. Information about Geocradle can be accessed on the following link: <http://geocradle.eu/en/regional-capacities/feasibility-studies/> . Surface mining also includes the activity of the coal mining. The methodology described in this work refers to the Monitoring of Lignite Mining Activities in Ptolemais basin in Greece.

1.1. Objective

The aim of the study is to evaluate the use of Earth Observation (EO) data and in particular of the multi-temporal Sentinel-1 & mainly Sentinel-2 data for the monitoring of the Amyntaio lignite mine and the assessment of quarrying and rehabilitation activities. The pilot project area is shown in Figure 1. The selected test site represents specific problems that accrue to lignite mining.

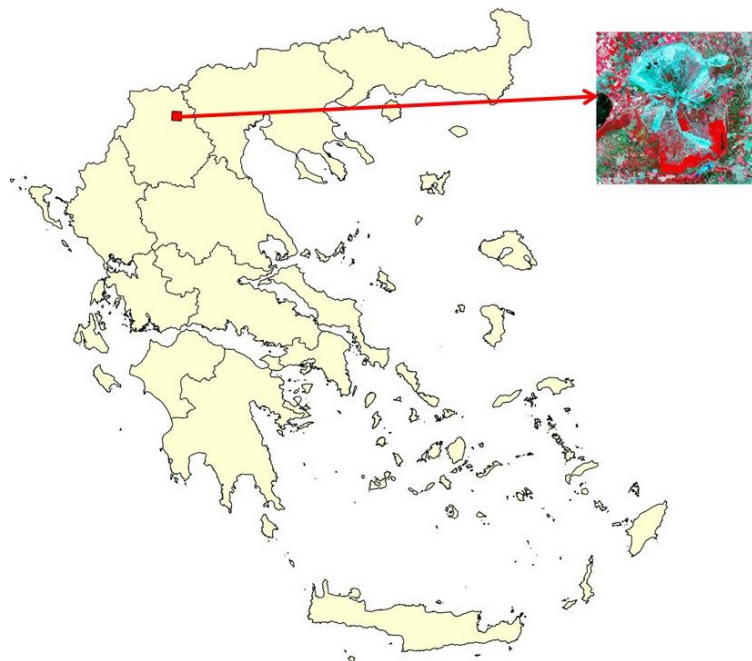


Figure 1. Pilot project area

The site under investigation is the area extending west—northwest of the Amyntaio opencast coal mine, located at the homonymous (Amyntaio) basin at Florina Prefecture, Northern Greece. The mine operates as a large-diameter well, draining most of the basin, Figure 2.

Regarding the geological conditions, 75% of the lignite deposits in Greece are of Neocene age. The wider Florina–Ptolemaida basin is a part of the Pelagonian geotectonic zone of Greece, consisting of crystalline-schist bedrock overlapped by Neogene and Quaternary sediments. The bedrock formations are either members of the Triassic–Jurassic carbonate cover or the upper cretaceous pelagic sediments, of the Pelagonian zone lithostratigraphic series. The Neogene deposits

are distinguished in three series (lower, lignite and upper). The lower and upper series (surrounding the lignite deposits) consist of fine grained deposits, sandy clays to marls, of fluvial-lacustrine origin, with lenticular intercalations of marly limestones, at the upper parts of the lower series. After the deposition of Neogene sediments, in the early Pleistocene, tectonic activity divided the initial basin in new sub-basins. Feathering processes supplied the sub-basins with Quaternary fluvial-stream deposits and alluvial fans.

The present paper is organized into 5 Sections. Section 2 describes data and methodology, while the processing techniques which are utilized are presented in Section 3. The Amyntaio mine landslide event is separately described in Section 4. Conclusions are drawn in Section 5.

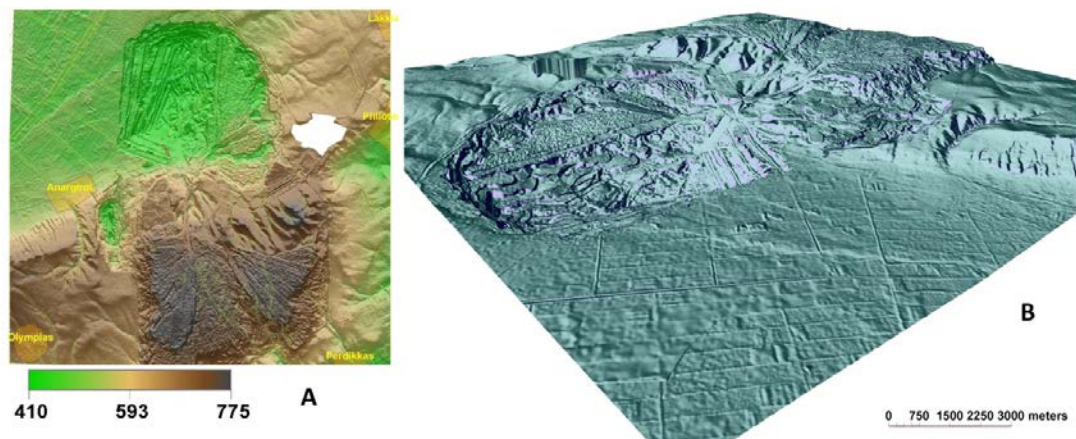


Figure 2. Geomorphology of the area of study as it is shown on the processed data of Digital Elevation Model (A) and 3D of Slopes (B) using the Hellenic Cadastre data.

2. DATA AND METHODOLOGY

Integrated identification, collection, assessment and use of available EO - Sentinel-1 & 2 data, along with available maps and relevant monitoring information are included during the analysis of the Amyntaio lignite mine. Multi-temporal Sentinel-1 & 2 data for the time interval of 2015 to 2017 have been selected to be evaluated for “the mapping and monitoring of the mine”. Synergistic use of the collected information along with the Sentinel-1 & 2 data with the variable acquisition dates have been used in the analysis as a base for future planning and rehabilitation of the area.

Main sources of information are:

- Geologic maps of IGME at 1:50,000 scale
- Topographic data of the Geographical Service of the Army at scales 1:50,000 published at 1970
- Ortho photographs of the Hellenic Cadastre at 1 meter resolution and a Digital Elevation Model at 5 meter resolution (Acquisitions during the 2009 to 2012 period)
- Data of the EU Copernicus service <http://land.copernicus.eu/pan-european>
- Sentinel-1 & 2 satellite system multi-temporal data as these have been mainly selected to be evaluated for “monitoring the lignite mine”.

Acquisition dates of the Sentinel 2 data are:

28/8/2015, 2/8/ & 15/8 of 2016, 19/5-1/6-21/6-27/8 of 2017, 8/6 & 13/7 of 2018.

Selection of data has been based on covering needs for yearly assessment of changes along with those occurred after the main landslide of the 10/6/2017 event. A large scale landslide occurred during mining extraction of lignite by the Public Electricity Cooperation on the 10th of June (21^o 37 22 E, 40^o 36 18 N).

2.1. The Sentinel-2 System

The Sentinel-2 satellite system has been financed and is part of the EU Copernicus Program:

1. It is a relatively new system with the data acquisition started in the beginning of 2015
2. Its specifications are comparable but with enhanced features in relation to other satellite systems like the Landsat series, Figure 3
3. The data are freely available to the scientific community

Sentinel-2 carries a super-spectral instrument with a sun-synchronous 786 km orbit that allows covering all the land surfaces and coastal waters between -56 and +84 degrees latitude with a 290 km swath width at a 10 days revisit time at the equator (5 days revisit time at the equator based on 2 satellites). Sentinel 2 data are freely available to the scientific community in <https://cophub.copernicus.eu/dhus/#/home>.

Landsat image of the 10th of June 2017 has been used for comparison with the Sentinel-2 images.

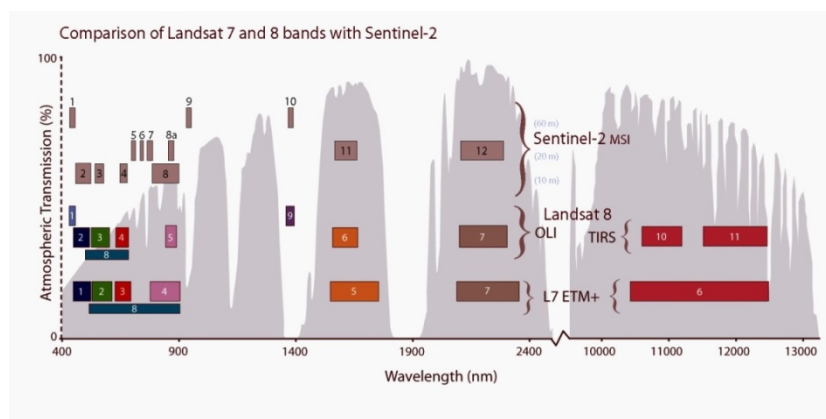


Figure 3. Sentinel 2 systems covers 13 different spectral bands with a resolution ranging from 10 to 60 meters.

2.2. The Sentinel-1 Satellite System

The Copernicus system also supports the Sentinel-1 satellite:

<https://sentinel.esa.int/web/sentinel/missions/sentinel-1/satellite-description>.

The Sentinel-1 provides an all-weather, day-and-night radar imaging capability for Copernicus land and ocean services. Interferometric Synthetic Aperture (SAR) data can detect surface movements with an accuracy of a few millimetres per year and can provide an accurate tool for monitoring of land subsidence, structural damage and underground construction to improve safety and reduce economic loss.

A small scale application for the pilot project area is also included using the Rheticus[®] of the Planetek cloud-based data and services hub. This system is able to process radar and optical data from multiple open-data satellite constellations designed to continuously deliver updated geoanalytics information through complex automatic processes and minimum interaction with human beings. Rheticus[®] Displacement represents a model concept (through subscription) in monitoring Critical Infrastructure (mines, dams, pipelines, bridges etc) with the use of SAR data and the Permanent Scatter technique (PS), designed for users with high expectations in the value of information and its user friendliness provision. Using European Copernicus Sentinel-1 (S1) open data images and Multi-Temporal SAR Interferometry (MTInSAR) techniques, the service is

complementary to traditional survey methods, providing a long-term solution to slope instability and geohazards monitoring.

The general Plan of the methodology applied for the Pilot Sites is shown in Figure 4.

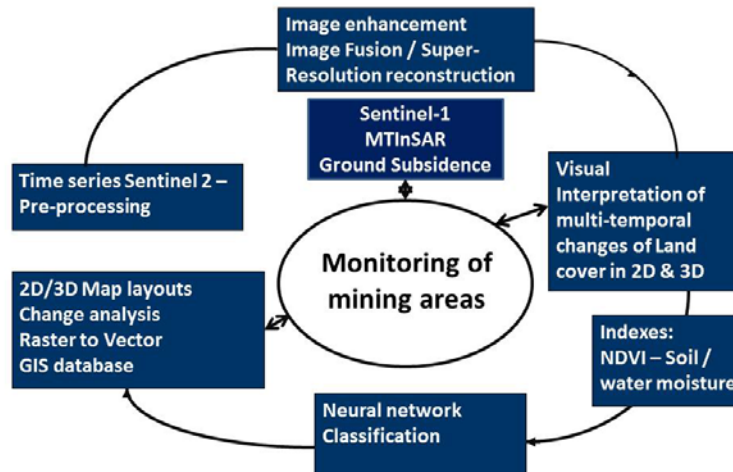


Figure 4. Techniques applied for the monitoring of the Amyntaio lignite mine.

3. PROCESSING TECHNIQUES

Various image processing and vector GIS techniques have been used for the analysis of both the satellite imagery and the collected map data and field information, which are the following:

- Georeferencing
- Resampling
- Colour Composites
- Intensity Hue Saturation (HIS) Images
- Identification of Areas of Interest (AOI)
- Automatic combination of the classification result of multi-temporal imagery
- Automatic conversion of raster to vector data
- Collection / Input / Coding, Storage / Management, Retrieval of various data
- Processing / Analysis
- Presentation / Display, & Map making.

The TNTgis has been used for processing of both raster and vector data: <http://www.microimages.com/products/>

3.1. Stochastic Regularized Super-Resolution Reconstruction of Sentinel-2 Images

Special emphasis has been given to the spatial enhancement of the Sentinel-2 images using Stochastic Regularized Super-Resolution (SRSR) Reconstruction techniques. The SRSR technique Lorentzian + BTV [3-6] is employed for the experiments of single image resolution increase with the Sentinel-2 images. In particular, resolution enhancement per factor 2 is performed on the images of bands B2, B3, B4, B8, B5, B6, B7, B8A, B11, B12 and per factor 4 is performed on the images B5, B6, B7, B8A, B11, B12. SR image reconstruction is applied to a synthesized sequence, which consists of 16 frames. The particular image sequence is created by sub-pixel shifting, employing various motion vectors, the original Sentinel-2 image. The above task takes place for each one of the

original images of the different bands B2 to B12. The Lorentzian estimator combined with the Bilateral Total Variation (BTV) regularization performs the task of SR reconstructing the sequence of frames coming from the original Sentinel-2 image. A bilinearly interpolated median frame from the above sequence of frames is utilized as initialization of the SR reconstruction procedure. A Gaussian kernel 3x3 is assumed so that to simulate the effect of sensor point spread function on the image during acquisition which has caused blurring effects. Single image resolution increase is performed and no information transfer among the different bands takes place. Thus, the resolution increase of each one of the images B2, B3, B4, B5, B6, B7, B8, B8A, B11 and B12 takes place individually.

The SR reconstruction problem is formulated by means of 2 terms, the data-fidelity term and the regularization term [3-4]. A gradient based method, the steepest descent, is employed to perform the minimization task and results in X , the solution to the SR problem under consideration (Eq. 1) [3] after n number of iterations. The step size in the direction of the gradient is determined by a scalar parameter β . The regularization term poses a penalty on the unknown matrix X in order to direct it to a better formed solution. The coefficient λ which is employed determines the strength with which the particular penalty is enforced and is called the regularization parameter. The constructed SR algorithm demonstrates reduced sensitivity to outliers.

$$X_{Lr_{n+1}} = X_{Lr_n} - \beta \left\{ \sum_i 2F_i^T H^T D^T \frac{(DHF_i X_{Lr_n} - Y_i)}{2lorpar^2 + (DHF_i X_{Lr_n} - Y_i)^2} + \lambda \sum_{l=-P}^P \sum_{m=0}^P a^{|m|+|l|} [I - S_y^{-m} S_x^{-l}] \text{sgn}(X_{Lr_n} - S_x^l S_y^m X_{Lr_n}) \right\} \quad (1)$$

The data-fidelity SR performance of the Lorentzian + BTV method can be explained in terms of the form of the employed error norm. The Lorentzian error norm is much resistant since it is a redescending estimator [3-4] and its influence curve returns to 0. Thus, this error norm gives diminishing weight to outliers whose magnitude is above a certain value which is determined by the scale parameter $lorpar$. Outliers have diminishing effects on this estimator since they are given weights of decreasing values according to their magnitude. The value of the parameter $lorpar$ denotes where the rejection of outliers begins.

Results show that the improved spatial resolution of the images obtained can assist at the enhancement of small scale features, Figure 5.

The SR performance of the Lorentzian + BTV method works well with the Sentinel-2 bands with the 10 meters resolution, Figure 5. Bands with 20 meters resolution are spatially enhanced but the resulting image shows signs of "blurring". The optimized images proved valuable for both visual interpretation of detailed features and the application of automatic classification techniques.

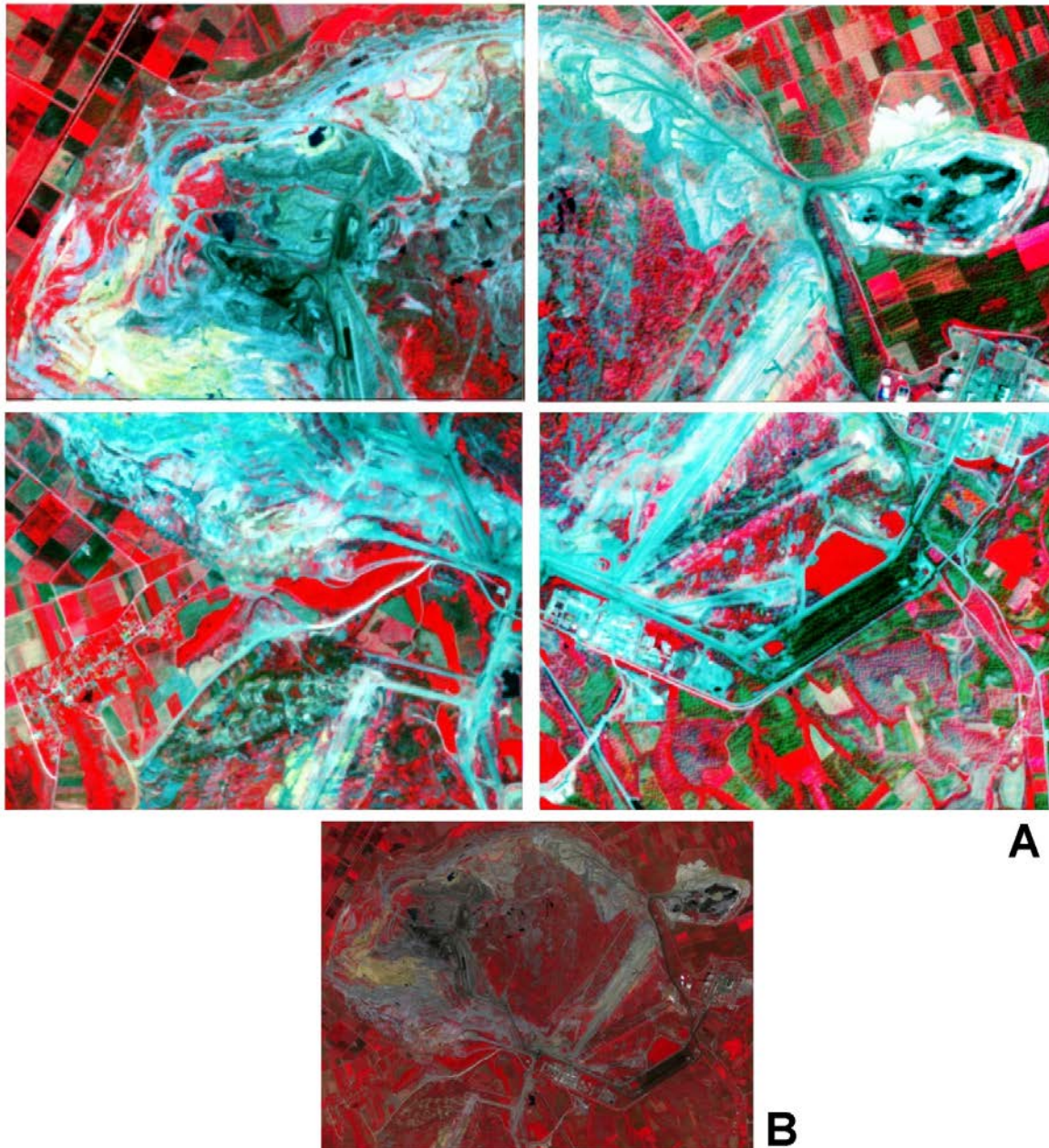


Figure 5. Evaluation of the Super-Resolution technique **A.** Enhanced image using stochastic regularized SR reconstruction technique - 5 m resolution **B.** Original RGB 8/4/3 image.

3.2. Classification

Image Classification - Unsupervised Classification techniques using neural networks: Artificial Neural Networks (ANNs) are generally quite effective for the classification of remotely sensed data [7]. For classification purposes, the Adaptive Resonance ANN method was used on the Sentinel 2 images in order to discriminate all inherent land cover classes of the satellite images using automated conversion of raster to vector data: the raster output of the classification and/or interpretation process was converted to vector data and these data were analysed with the corresponding map data and observation acquired on the Ortho-photos. Further processing and analysis was performed to derive information concerning changes identified in the pilot study area.

3.3. The Processing of Sentinel Satellite Data

3.3.1. Ground Deformation Using Multi-Temporal Sentinel-1

The following methodology has been used for the pilot project area so as to estimate ground motion: Rheticus browses and accesses (on a weekly basis) the products of the rolling archive of ESA S1 Scientific Data Hub; S1 data are then handled by a mature running processing chain, which is responsible of producing displacement maps immediately usable to measure with sub-centimetric precision movements of coherent points. The results of the processing are shown in Figure 6.

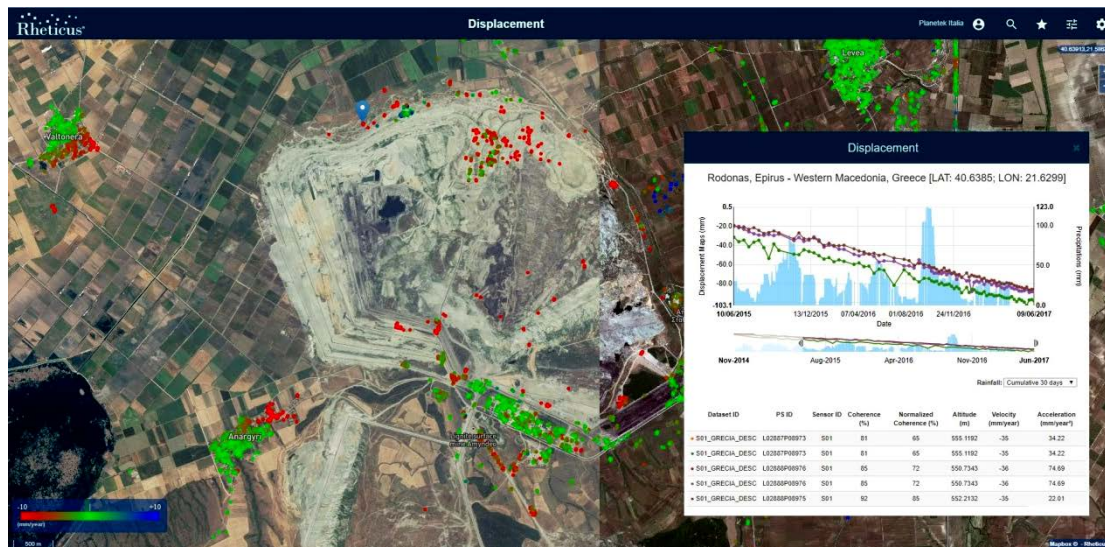


Figure 6. Results of MTInSAR techniques: Red dots show subsidence

Land subsidence due to over-exploitation of the local aquifers for agricultural reasons is causing damages to two villages so far: Anargiroi and Valtoneira [2] as shown in Figure 6 (red dots). Subsidence of the two villages cannot be attributed to dewatering of the mine, because subsidence (red dots in Figure 6) is limited in the area of the villages, and not in the area between the mine and the two villages. If subsidence was due to the dewatering of the mine, subsidence of the area between the mine and the villages would be larger than the subsidence of the villages (as the distance from the mine is smaller).

As shown in Figure 7, the Quaternary depositions cover most of the area:

(a) The Proastion formation, formed by fluvial-stream deposits of Low-Middle Pleistocene age [8] which overlie with unconformity the Neogene deposits.

(b) The Perdikas formation includes fluvial-lacustrine sediments of Low-Middle Pleistocene age [8]. Between Anargiri and Valtoneira Villages, Perdikas formation consists of alternating sandy clays and clayey sands, with a total thickness varying from 20 to 70 m. This relatively loose and compressible formation is responsible for the manifestation of land subsidence phenomena.

(c) The Anargiri formation includes fluvial-stream deposits of Middle Pleistocene age [8], consisting of clayey sands or thin sands which in places show clay layers or lenses with angular fragments.

The main tectonic line that dominates in the study area is Anargiri fault. It is a typical normal fault resenting a strike of NNE–SSW direction and 60_ dip angle to the North. This fault passes through Anargiri village and extends southwest bordering Lake Cheimaditida [9].

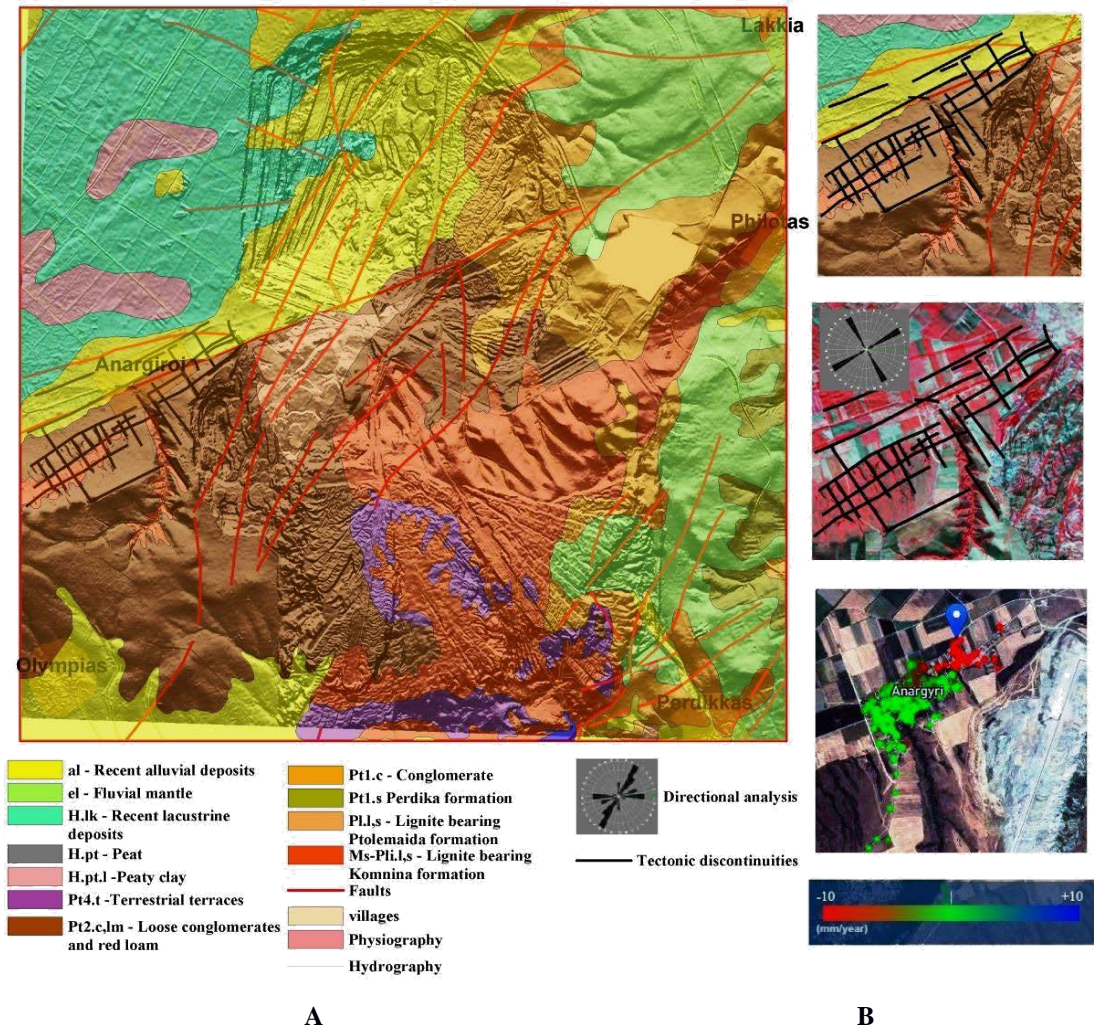


Figure 7 A. Geologic formations, faulting of the IGME geologic map **B.** Interpretation of tectonic discontinuities and InSar measurements of Anargyroi area.

Anargyroi village has been particularly affected by land subsidence. Regional and local tectonics must have played a role on the differential subsidence measured by InSar data. Tectonic discontinuities have been interpreted using the shading relief map and the Sentinel-2 images. The discontinuities have NE/SW & NW/SE directions - rose diagram. As it is shown subsidence (red dots) has been measured and these are related to the main NE fault lines of the IGME map and the interpreted tectonic discontinuities - surface ruptures of NW, SE directions, Figure 7.

Rheticus[®] Displacement provides accurate information to monitor over time, through MTInSAR analysis, movements occurring across landslide features or structural weaknesses that could affect buildings or infrastructures.

3.3.2. Land Monitoring / Change Analysis Using Sentinel-2

The lignite mining activities changed radically the geomorphological status of the study area. This is very well recorded on the long time series satellite data, Figure 8 [10].

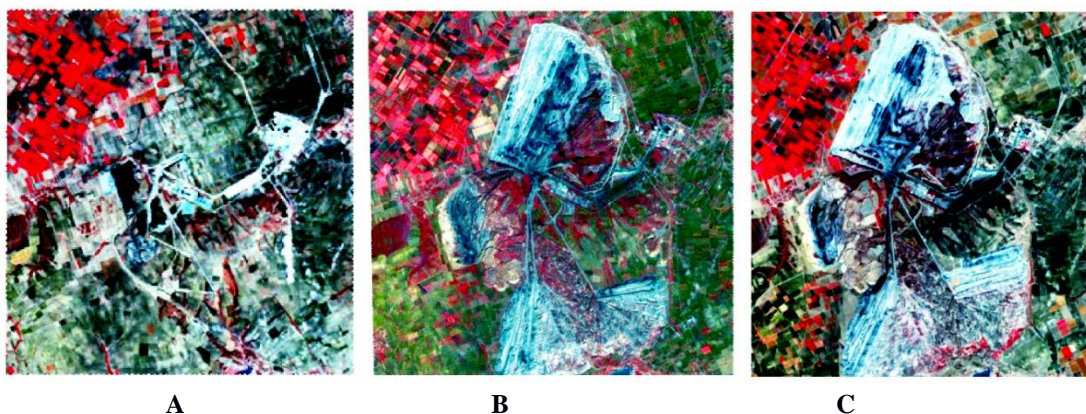


Figure 8. A. Landsat TM image dated summer 1986 B. Landsat ETM image dated summer 1999 C. Aster image dated summer 2001.

Monitoring of the mining activities on yearly intervals and map updating is supported and this has been evaluated for the pilot project area using multi-temporal Sentinel-2 satellite data, Figure 9.

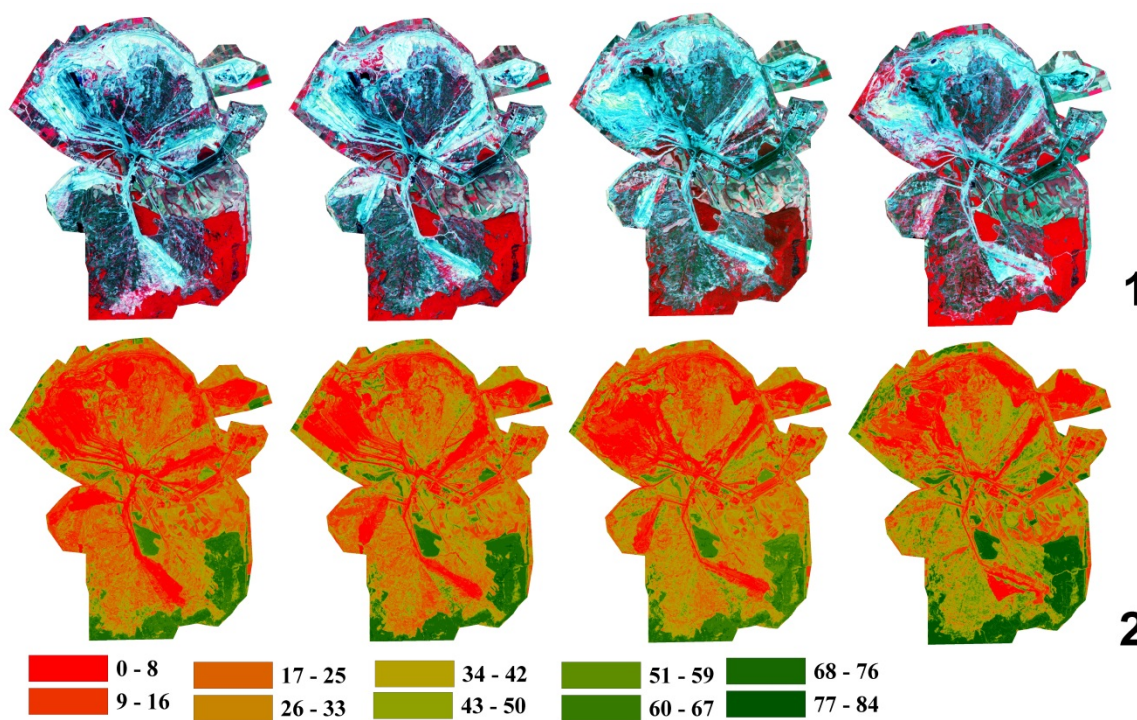


Figure 9. Multi-temporal analysis of Sentinel-2 images for the period of 2015 to 2018 (Acquisition dates of the Sentinel 2 data are: 28/8/ 2015, 15/8/ 2016, 27/8/ 2017, 13/7/ 2018): 1. False colour enhanced images 2. NDVI: Red colours show low vegetation quality 0 to 50 – green colours high vegetation quality 51 to 85.

In summary the following have been identified:

- Changes of surface area of the mine area
- Active / Inactive mine areas
- Changes of vegetation cover
- Changes due to the landslide event

4. AMYNTAIO MINE LANDSLIDE EVENT

The Landslide event has been recorded by two different satellite systems that of Landsat 8 and Sentinel-2, Figure 10.

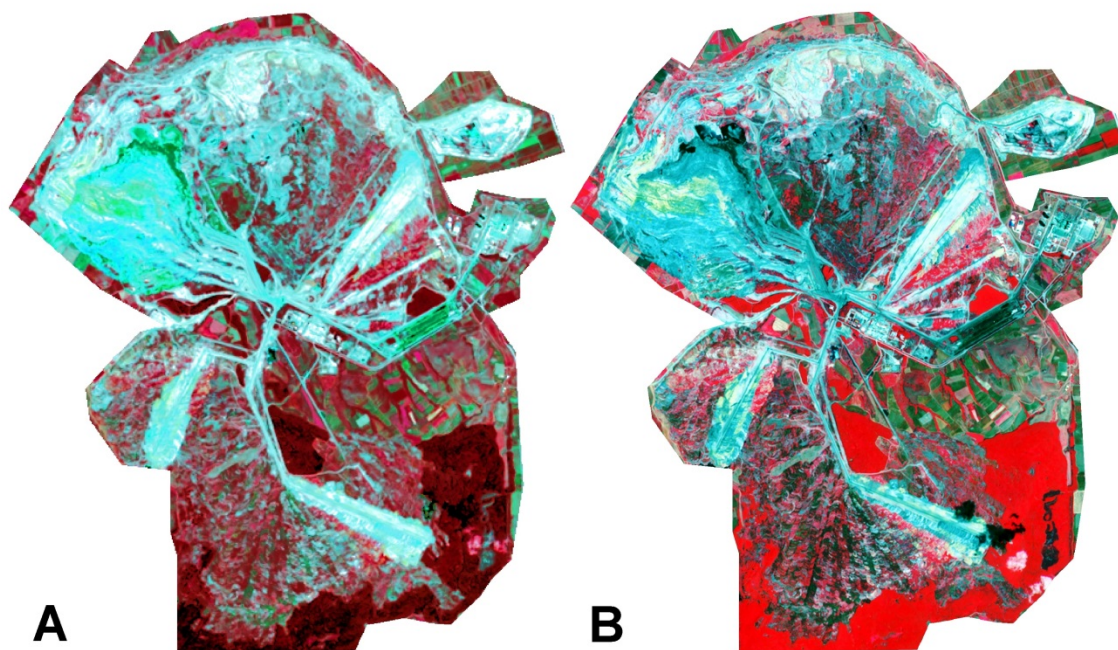


Figure 10. Landsat 8 image the of 10th June 2017 (A) versus Sentinel-2 of the 21st June 2017 (B)

Comparison of the spatial resolution of Landsat images with Sentinel-2 has been carried out. Sentinel-2 images are of higher resolution and of an improved temporal resolution of covering the area every 5 days. Areal extend of quarry areas can be accomplished more effectively on Sentinel-2 than Landsat data due to improved spatial resolution after the optimization with the application of SRSR reconstruction technique Lorentzian+BTV.

Monitoring & Mapping of the land surface changes due to the landslide of the 10th of June 2017 is supported.

The false colour composites of Sentinel-2 images managed to pick up the conditions of the mine activities (Figure 11). This enables the classification of the subset of mine area into different categories like: 1.Active mine works (generally covered by bare soil), 2. Formerly rehabilitated areas, 3. Mine tailings, 4. Deposition operations. Different land cover types have been mapped in the mining area and the surface extent for each cover type has been estimated.

Changes of activities / Works in the mining field can be easily interpreted on the multi-temporal imagery. Vegetation cover of restored areas that it is shown with bright red colours on false colour images can also be monitored and mapped quite effectively, Figure 12. The use of Sentinel-2 images holds a considerable promise for monitoring and developing effective environmental management, reclamation and rehabilitation strategies on a long-term basis for integrated environmental management. It is an effective tool for mapping large mining districts and land use cover and changes.

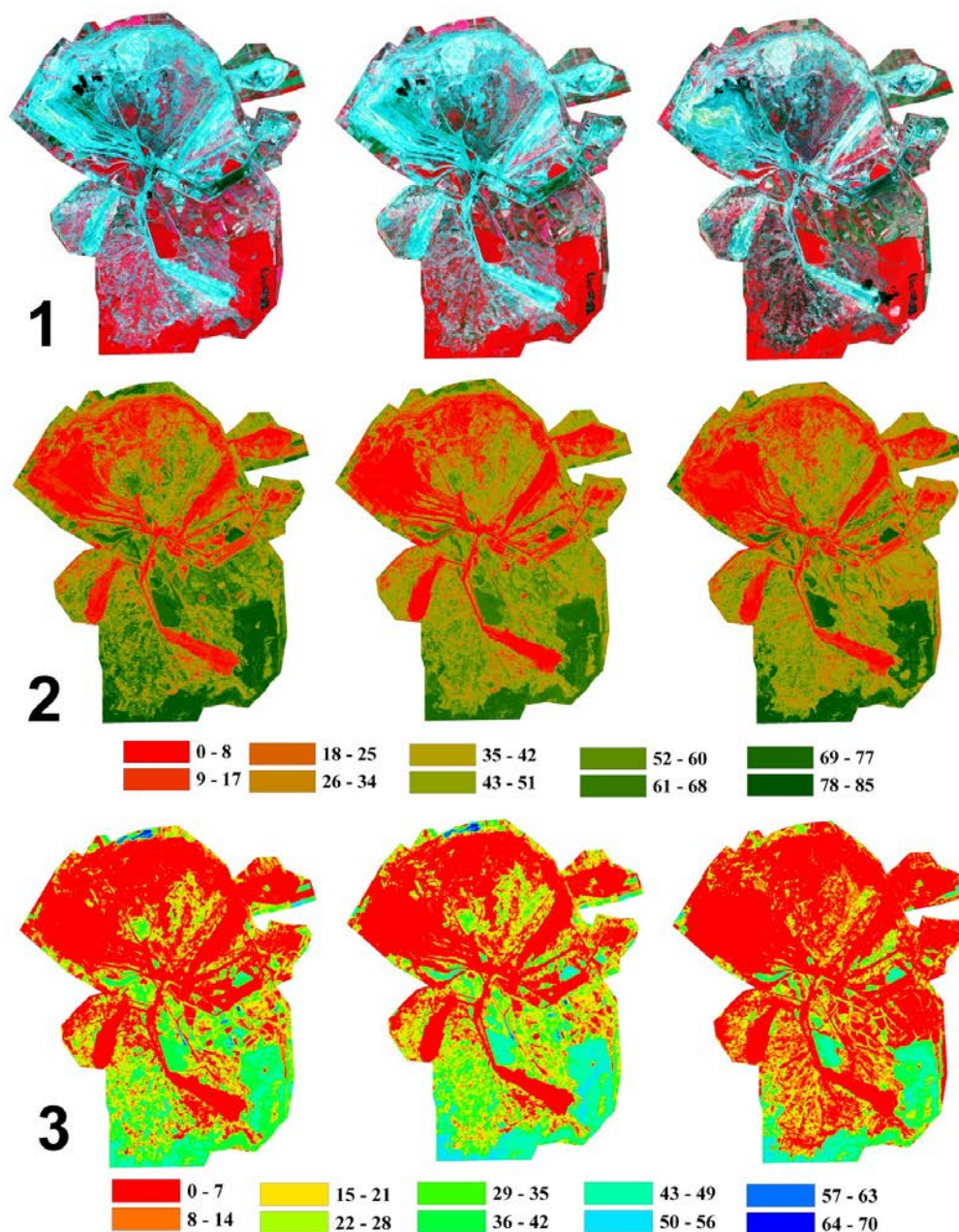


Figure 11. Multi-temporal analysis of Sentinel-2 images before and after the Landslide event (Acquisition dates of the Sentinel 2 data are: 19/5-1/6-21/6-27/8 of 2017): 1. False colour enhanced images: Visual interpretation of changes can be easily accomplished. 2. NDVI: Red colours show low vegetation quality 0 to 50 – green colours high vegetation quality 51 to 85 3. Soil moisture: Red colours show low soil moisture 0 to 40 – blue colours high soil moisture content 41 to 71.

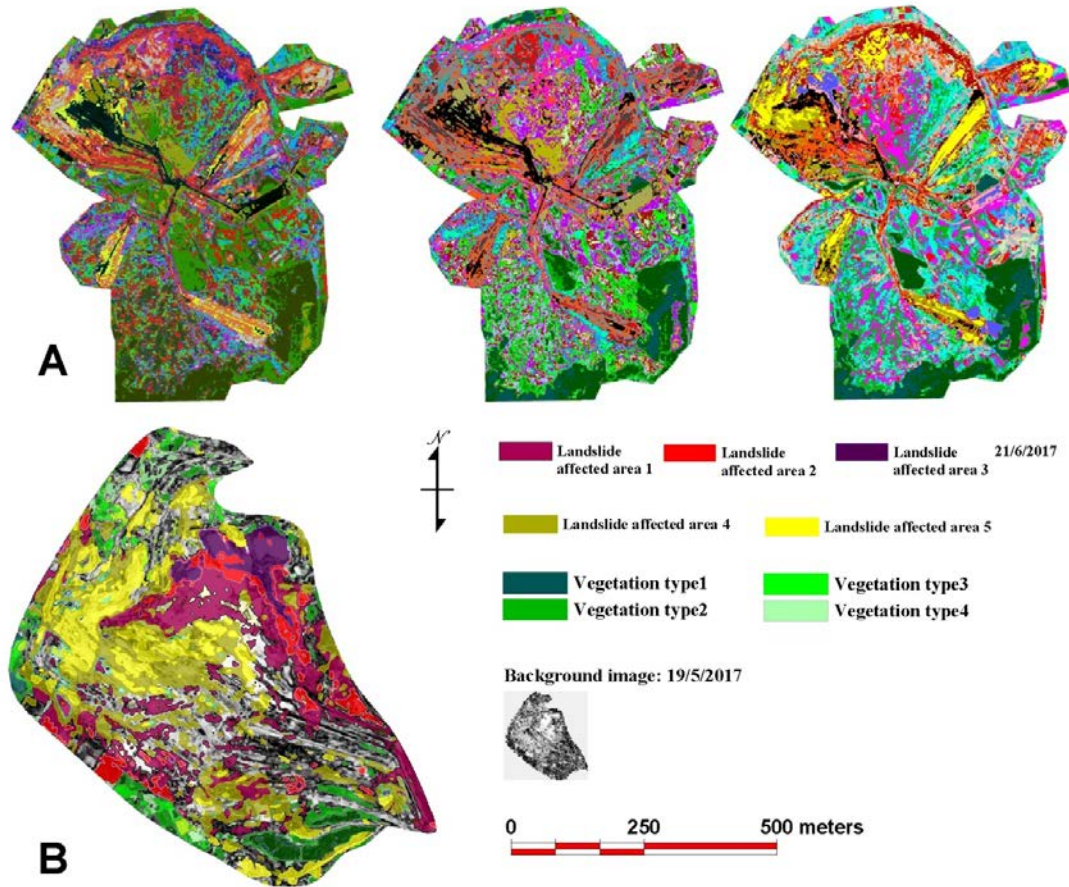


Figure 12 A. Adaptive Resonance classifier as applied to the lignite mine area for the acquisition dates of the Sentinel 2 data of 19/5-1/6-21/6 of 2017 B. Map & Legend for the “landslide affected area”.

5. CONCLUSIONS

Environmental monitoring is now an integral part of mining operations. Remote sensing data enables the identification, delineation, and monitoring of surface mining areas, including ground motion / subsidence, and changes in surface land use. The state of the art applied techniques and the developed methodology could be applied for the Monitoring of aspects of mining activities and eventually it could be used for the mitigation of the environmental, social and economic footprint. It targets policy and decision makers and generally the competent authorities at all levels, which are in charge of development and implementation of policies as well as the authorization and inspection of mining activities.

Remote sensing provides valuable information concerning different environmental parameters. In general the immediate benefits / application of the developed methodology, if it is coupled with high resolution images (up to 1-0.5 meters), to "End Users" and the mining industry in general are as following:

- Mapping and monitoring (Ground motion, Change analysis / track any detectable potential changes of surface morphology) based on satellite Sentinel-1&2 data due to the multi-temporal character of the data
- Validation of the status of mining activities
- Identification of mining activities which can be archived by developing a Monitoring System (Tool) with the use of EO data
- Evaluation of rehabilitation activities on mining areas

- Evaluation of the contribution of Earth Observation data on supporting studies for the identification of Mining Areas and supporting inspections by interested parties.
- Mine Site Mapping - Mapping Disturbed / Undisturbed Land - Land Use / Cover Changes - Delineation of areas where potential excavations activities are taking place.
- Identification and characterization of the nature of the changes observed - Compliance with permitting regulations.
- Documentation of the conditions of lands related to the mine.
- Reclamation monitoring.
- Discrimination of geologic setting - Geologic feature extraction to support interpretation of measured ground motion features / subsidence.
- Planning exploration activities - Managing mining activities.
- GIS database creation - Staff and Public relations / visualization.

Generally sufficient data required for environmental mapping are not available and therefore, satellite data can be analyzed to generate GIS database information required for environmental studies. Generated database can be used to assess changes that are taking place in the environment. The added advantage of the proposed approach is that it makes available to end-users a variety of the data and that it helps in efficient analysis and the support of the activities of "End Users".

New environmental policies require many agencies to provide public access to information gathered with public funds. By virtue of its geographically structured approach, an Atlas offers an intuitive, self-paced, and self-contained way to provide secure public viewing of data such as multi-temporal information provided by satellite systems, census data, land cover / use, and available environmental information.

REFERENCES

- [1] Kavouridis, K. (2008). Lignite industry in Greece within a world context: mining, energy supply and environment. *Energy Policy*, 36(4), 1257–1272.
- [2] Loupasakis, C., Angelitsa, V., Rozos, D. and Spanou, N. (2013). Mining geohazards—land subsidence caused by the dewatering of opencast coal mines: The case study of the Amyntaio coal mine, Florina, Greece. Springer Science & Business Media Dordrecht.
- [3] Panagiotopoulou, A., & Anastassopoulos, V. (2009). Regularized super-resolution image reconstruction employing robust error norms. *Optical Engineering*, 48(11), 1-14.
- [4] Panagiotopoulou, A., & Anastassopoulos, V. (2012). Super-resolution image reconstruction techniques: Trade-offs between the data-fidelity and regularization terms. *Information Fusion*, 13(2012), 185-195.
- [5] Panagiotopoulou, A., Bratsolis, E., Charou, E., & Perantonis, S. (2017). Building block extraction and classification by means of aerial images fused with super-resolution reconstructed elevation data. *Journal of Applied Remote Sensing*, 11(4), doi:10.1117/1.JRS.11.045004.
- [6] Bratsolis, E., Panagiotopoulou, A., Stefouli, M., Charou, E., Madamopoulos N. and Perantonis S. (2018). Comparison of Optimized Mathematical Methods in the Improvement of Raster Data and Map Display Resolution of Sentinel-2 Images. To be presented (accepted) in ICIP-2018.
- [7] Vassilas, N., & Charou, E., (1999). A new methodology for efficient classification of multispectral satellite images using neural network techniques. *Neural Processing Letters*, 9(1), 35 – 43.

[8] Institute of Geological and Mineralogical Exploration - I.G.M.E. (1997). Geological map of Greece, scale 1:50.000, Ptolemaida sheet, I.G.M.E., Athens.

[9] Loupasakis, C. (2006). Study of the geotechnical conditions of the Amintaio coalmine slopes close to the Anargiri village, Aetos Municipality, Florina Prefecture, Greece, Unpublished report. IGME - Institute of Geological and Mineralogical Exploration, Athens, p 48.

[10] Charou, E., Stefouli, M., Dimitrakopoulos, D., Vasiliou, E., & O. D. Mavrantza. (2010). Contribution of Remote Sensing in Impact Assessment of Mining Activities on land and water resources. Mine Water and the Environment, Springer, DOI 10.1007/s10230-010-0098-0.

Application of the Push-Relabel Algorithm to Lignite Surface Mine Optimization

Panagiotis Mpinos and Ioannis Kapageridis

Technological Educational Institute of Western Macedonia, Koila, Kozani, 52100, Greece

ABSTRACT

Open pit optimisation is a process aiming at the determination of the extents of the optimum pit such that the profit made in mining the pit is maximised. The choice of blocks to mine for the optimum pit is an example of the selection problem. A selection problem is based on a set of tasks, where each task has a value or a cost. In most cases, there are certain relationships between tasks, such that in order to perform one task a number of prerequisite tasks must be performed. The solution of the selection problem is the subset of tasks that the sum of their value is the maximum possible within the set when performed. In terms of mining, each block (a task in the selection problem) in a 3D block model is assigned either a profit or a loss based on the revenues and costs associated with mining the block. Geologic constraints are used to establish slope requirements for each block which are used to determine the blocks which must be removed prior to the removal of any given block. Traditional methods of solving the selection problem in open pit optimisation included the floating cone algorithm and the Lerchs-Grossman algorithm based on graph theory. The latter dominated open pit optimisation software products and solutions in the 80s and 90s and offered mining engineers a solid solution to the pit optimisation problem. A decade later from the first implementation of the Lerchs-Grossman algorithm, Picard proved that the pit optimisation problem could be solved with more efficient maximum flow algorithms. In 1988 Goldberg and Tarjan published the first paper describing the Push-Relabel algorithm for solving the maximum flow problem. Later in 1997, Cherkassky and Goldberg published a paper describing a very efficient implementation of the more general Push-Relabel algorithm. This algorithm is used in our case study of surface lignite mine optimisation. A lignite deposit from the region of Kozani as well as all associated technical and financial parameters are used as input to the Push-Relabel implementation provided by a mine planning software package, and the optimisation output is analysed in order to assess the benefits of applying the Push-Relabel algorithm to lignite deposits.

1. INTRODUCTION

Open pit optimisation is a process commonly applied in mine planning of surface mines to produce optimum pit limits to use as a guide for pit design. The optimisation step is also considered an efficient way to convert mineral resources to mineral reserves as it allows the enforcing of financial and technical constraints and parameters to the mine design process in an automated and mathematically robust way. It is commonly used even at the mineral resources estimation stage to limit the reported quantities inside a conceptual pit and raise the confidence in the mineral resources report.

Surface coal and lignite mines have been commonly modelled in the past using a more two-dimensional approach, based on grid or triangulation models that did not allow the application of open pit optimisation algorithms, normally requiring a three-dimensional blocks model of the deposit. The financial aspects of coal deposits are also considered stable along the Z axis, in most cases where the deposit consists of a small number of coal horizons with standard qualities, leading to the conception that pit optimisation is an unnecessary effort. The lignite deposits in Greece,

however, normally consist of multiple lignite layers with varying quality parameters in all three dimensions, making them ideal targets for computerised open pit optimisation.

The case study presented in this paper discusses the application of the Push-Relabel method, one of the more recent optimisation methods, and provides a comparison with the well-established Lerchs-Grossman method which is used by the mining industry the last three decades.

2. HISTORY OF OPEN PIT OPTIMISATION

2.1. Before Computers

Before computers found their way into mine planning, mining engineers relied on manual methods on hand-drawn cross-sections to produce a pit design. A simple optimisation of economic pit depth was usually performed with the aid of a calculator for regular shaped orebodies using incremental cross-sectional areas, for ore and waste, and an overall pit slope. Incremental stripping ratios were calculated and compared against the break-even stripping ratio. The final pit shell was then produced by drawing increasingly larger pit shells on cross section such that the last increment had a strip ratio equal to the design maximum. This was a very labour-intensive approach and could only ever approximate the optimal pit [1].

2.2. Floating Cone Method

The Floating Cone algorithm was introduced by Pana (1965) [2]. The method was developed at Kennecott Copper Corporation during the early 1960s and was the first computerised attempt at pit optimization, based on a three-dimensional block model of the mineral deposit. Final pit limits are developed by using a technique of a moving “cone” (or rather an inverted cone). The cone is moved around in the block model space from top to bottom generating a series of interlocking cone-shaped openings. The disadvantage of this approach is that it creates overlapping cones, and it is incapable of examining all combinations of adjacent blocks. For this reason, the algorithm fails to consistently give realistic results and tends to “mine” more tonnage for less value.

2.3. Lerchs-Grossman Method

The same year the floating cone algorithm was introduced (1965), Lerchs and Grossmann published a paper that introduced two modelling approaches to solving the open pit optimisation problem [3]. The Lerchs-Grossman (LG) algorithm is well documented in the technical literature [4, 5, 6, 7]. Lerchs and Grossmann presented two implementations of the pit optimisation algorithm, the first based on Graph Theory (heuristics) and the second on Dynamic Programming (operations research). They both produced optimum pit limits based on an undiscounted cash flow – an economic block model including both ore and waste. Essentially the methods determined which blocks should be mined to obtain the maximum value from the pit. LG requires a technical and a financial parameter:

1. **Pit slopes:** these define the blocks that need to be removed before each block considered in the block model. They are used to generate “arcs” between blocks.
2. **Block value:** refers to the economic value of each uncovered block. It will be negative for waste blocks and amount to all waste mining and hauling costs. Ore blocks will have values based on the mining, hauling, processing, selling and any other costs, and the revenue from the recovered ore.

Working from the lowest positive block(s) and using the block values and structure arcs, the method branches upwards between blocks forming a graph (Figure 1). Branches are flagged based on

their total value. Positive branches are worth mining once uncovered. Negative branches are also flagged, and the method looks for positive ones that lie below them. In this case, the two branches are combined in a way to produce a positive total branch. The scanning is repeated until no structure arc goes from a positive branch to a negative. Once this is complete, the complete graph defines the optimum pit. Any negative branches left on their own are not to be mined.

In mathematical terms, the LG algorithm finds the maximum closure of a weighted directed graph [1]. The blocks in the model represent the vertices of the graph, the block values represent the weights, and the mining constraints (i.e. the pit slopes) represent the arcs. The LG algorithm provides a mathematically optimum solution to the problem of pit optimisation. The algorithm itself has no “sense” of the nature of the optimisation problem – it works on a set of vertices and arcs. Whether these are defined in one, two or three dimensions and the number of arcs per block makes no difference to the algorithm. The LG algorithm has been used for over 30 years on many feasibility studies and for many producing mines.

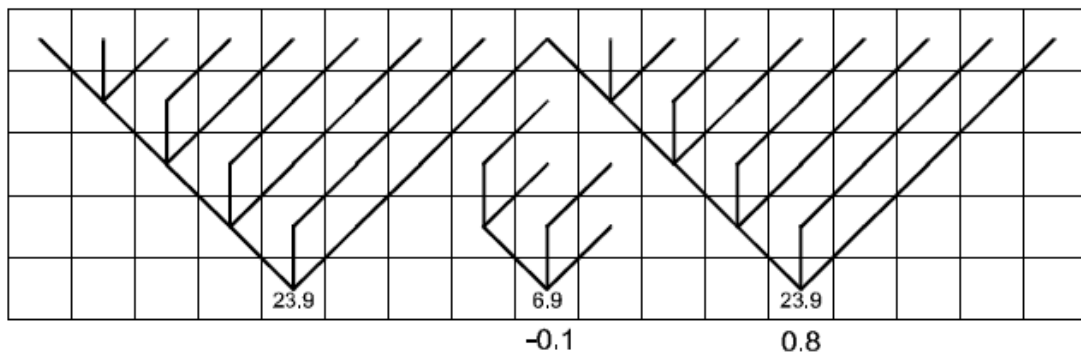


Figure 1. Example of LG optimisation showing three positive blocks surrounded by negative blocks (with a value of -1) linked with branches forming a final graph. The negative branch in the middle is not to be mined [8].

2.4. Network Flow Methods and the Push-Relabel Method

Lerchs and Grossmann suggested that the ultimate-pit problem could be expressed as a maximum closure network flow problem and presented their approach - a method of solving a special case of a network flow problem. Picard proved that a maximum closure network flow problem (like the open pit optimisation) could be reduced to a minimum cut network flow problem which could be solved by an efficient maximum flow algorithm [9]. This meant that network flow algorithms could be used instead of the LG algorithm, and they can calculate identical results in a fraction of the time.

The Push-Relabel algorithm considered in this paper is one of the first efficient maximum flow algorithms used in solving the open pit optimisation problem [10, 11, 12]. It has been shown that the Push-Relabel algorithm outperformed the LG algorithm in nearly all cases [13]. In cases where the number of vertices (blocks in the pit optimisation problem) is greater than a million, network flow algorithms perform orders of magnitude faster and compute precisely the same results [1]. The pit optimisation module of Maptek Vulcan mine planning software is based on implementations of both the LG and Push-Relabel algorithms.

3. THE PUSH-RELABEL METHOD

3.1. Historical Background

The maximum flow problem is a classical combinatorial problem that arises in a wide variety of applications. The basic methods for the maximum flow problem include the network simplex method of Dantzig [14], [15], the augmenting path method of Ford and Fulkerson [16], the blocking flow method of Dinitz [17], and the push-relabel method of Goldberg and Tarjan [10], [18]. Prior to the push-relabel method, several studies have shown that Dinitz’s algorithm [17] is in practice superior to other methods, including the network simplex method [14], [15], Ford-Fulkerson algorithm [16], Karazanov’s algorithm [19], and Tarjan’s algorithm [20]. Several recent studies ([21], [22], [23] and [24]) show that the push-relabel method is superior to Dinitz’s method in practice [25].

3.2. The Push-Relabel Method

The definition of a pit with valid slopes is termed a “closed set” or “closure”. It consists of a set of nodes V that have no arcs initially. Based on the required pit slopes, a set of arcs E is defined representing the dependencies between blocks. A closed set of blocks is free to be removed and does not depend on the removal of other blocks. Finding an optimal pit is the process of finding a closure with maximum total value [26]. This problem is called a maximum closure problem. It is easy to observe in Figure 2, that the optimal pit consists of block {b, c, f, g, h, i}, with a total value of 3.

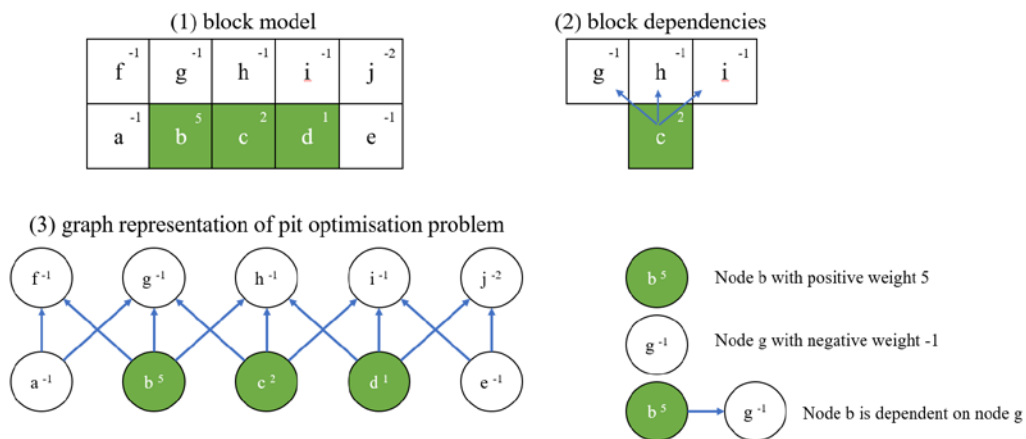


Figure 2. Simple example of block model (1), block dependencies (2) and graph representation (3) for a pit optimisation problem [26].

Two additional special nodes are required: the flow starts from the *source* node and finishes at the *sink* node. Each arc is like a pipe and has a nonnegative capacity function u allowing flow up to a limit passing through it. The flow and capacity along an arc must be positive. The nodes (blocks) represent a joining of pipes, so the amount of flow into a node must equal the total flow out of the node, which is called the *conservation constraint*. Each node (block) has a weight value equal to the economic value of the block. Defining a complete flow graph means that we need to make the following changes to the graph of the block model in Figure 2:

- Add two special (virtual) nodes: source s and sink node t .
- For all the existing arcs (blue), assign infinite capacities.
- Add links from source to all positive nodes, with the capacities equal to the weight of the nodes.

- Add links from negative nodes to sink, with the capacities equal to the absolute weight value of the nodes.
- Remove the weights on nodes.

Figure 3 shows the updated graph once all changes are made. The relation between the flow and mining concepts is not as straightforward as the relation between a closure and a pit [26]. One way to describe this is to consider the ore as the water stored in a source that as much as possible needs to be sent to a destination through a pipe network. The source node connects to all ore blocks, and the destination (sink) connects to all waste blocks. In the network, the economic value of a block is not reflected on a node but is measured by the capacity of the pipe (arc) that connects it with the source or the destination. Since the pipes representing block dependency have unlimited capacity, the bottlenecks of the networks are the pipes connected to the source or destination. Three types of pipes can be identified: “waste-to-destination”, “source-to-ore”, and “block-to-block”.

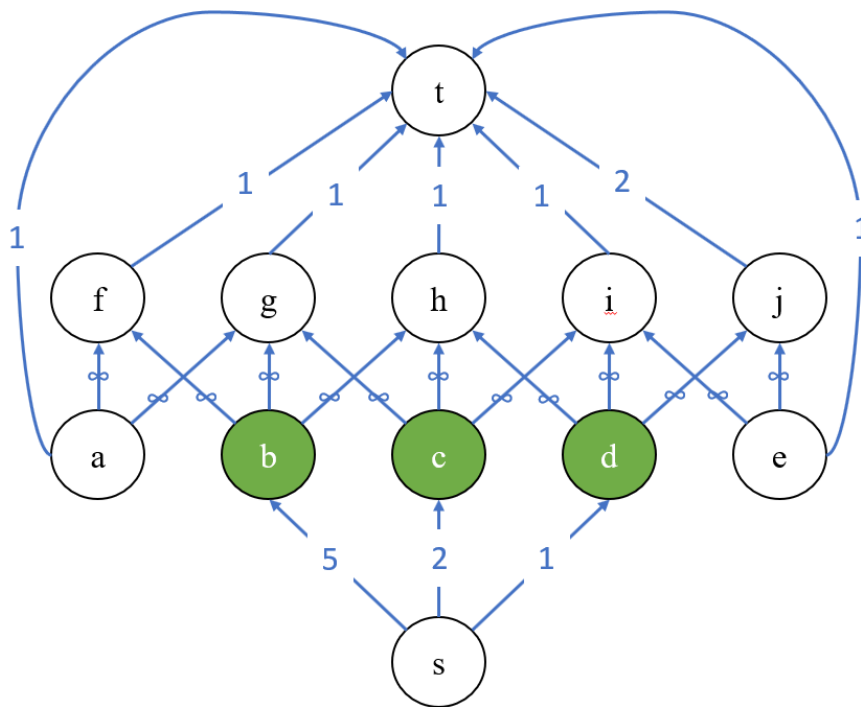


Figure 2. Flow graph representation of the pit optimisation problem.

The conservation constraint at a node v indicates that the excess $e_f(v)$, defined as the difference between the incoming and outgoing flows, is equal to zero. A *preflow* satisfies the capacity constraints and the conservation constraints that requires the excesses to be nonnegative. An arc is *residual* if the flow on it can be increased without exceeding its capacity and *saturated* once the capacity is reached. The residual capacity $u_f(v, w)$ of an arc between nodes v and w is the amount by which the arc flow can be increased. The *distance labelling* $d: V \rightarrow \mathbf{N}$ satisfies the follow conditions: $d(t) = 0$ and for every residual arc (v, w) , $d(v) \leq d(w) + 1$. A residual arc (v, w) is *admissible* if $d(v) = d(w) + 1$. A node v is *active* if v is not the source or the sink node, $d(v) < \text{number of nodes}$, and $e_f(v) > 0$.

The push-relabel method maintains a preflow f , initially set to zero on all arcs, and a distance labelling d . The $d(v)$ is initially set to the distance from v to t in the graph. In its first stage, the push-relabel method repeatedly performs the *update operations*, *push* and *relabel* until there are no active nodes left. The update operations modify the preflow f and the labelling d . A *push* from v to w increases $f(v, w)$ and $e_f(w)$ by $\delta = \min \{e_f(v), u_f(v, w)\}$, and decreases $f(w, v)$ and $e_f(v, w)$ by the

same amount. A *relabeling* of v sets the label of v equal to the largest value allowed by the valid labeling constraints. The second stage of the method converts f into a flow.

4. A COMPARATIVE CASE STUDY

4.1. Input Block Model

A lignite deposit from the area of West Macedonia in NW Greece was used in the study. It consists of a few lignite layers, and a simpler structure compared to other lignite deposits commonly found in the area. The roof and floor of the mineable lignite area of the deposit was modelled as grid surfaces using inverse distance interpolation. The composited qualities of lignite were also modelled as grids. These grid models were used to generate a stratigraphic block model in Maptrek Vulcan as shown in Figure 4. The vertical size of the blocks and their base and top side follows the roof and floor grid models of mineable lignite. The horizontal dimensions of the blocks were 10x10m.

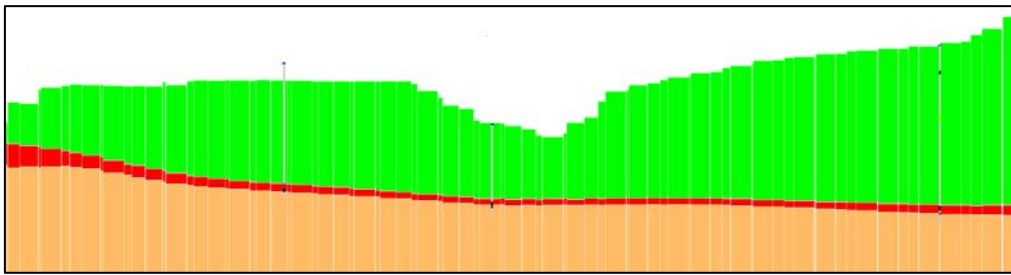


Figure 4. Section through the stratigraphic block model showing overburden (green), mineable lignite area (red), and underburden (orange).

A number of financial parameters were included as variables to the stratigraphic model. These included all mining and processing related costs, and revenue from selling of recovered lignite. The calculation of these parameters was based on the volume of each block, the thickness of mineable lignite and parting, the specific gravity for lignite and waste, and the type of each block (overburden, lignite deposit, underburden). A simple script was used to calculate the necessary parameters in the blocks, as shown in Table 1. The constant values of waste and lignite associated costs and lignite revenue were set using historical information. The script stored the calculated values to corresponding block model variables, including the final block value which represents the undiscounted cash flow of uncovered blocks. This value is necessary as input for the pit optimisation process. The value was positive for the lignite deposit blocks and negative for overburden and underburden blocks.

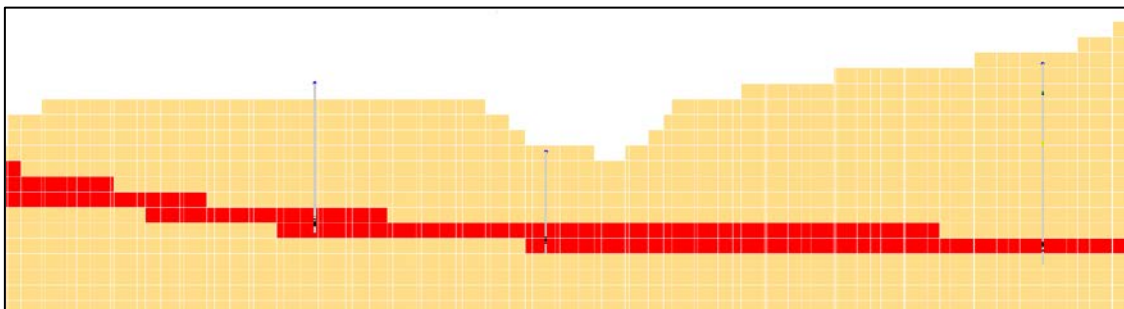
All current methods of pit optimisation require a regular block model, i.e. a model with equally sized (regular) blocks. This meant that the stratigraphic block model that contained the calculated block values had to be regularised to a standard block size. This size was set to 10x10x8m. Only the block value variable was transferred to the regularised block model as it was the only parameter necessary as input to pit optimisation. This variable was calculated for each block using a sum of the intersecting stratigraphic model blocks' values weighted by their volume inside the regular block. Figure 5 shows the same section shown in Figure 4 but through the regularised model and coloured by block value. Blocks shown in red contain both a lignite and waste component, but the weighted sum of their values results in a positive regular block. These blocks were used as input to the pit optimisation process.

Table 1. Block value calculation script based on mineable lignite thickness, block volume and specific gravities of lignite and waste.

```

if (seam eqs "cx") then
  coal_volume = thickness * 100
  parting_volume = volume - coal_volume
  coal_tonnage = coal_volume * 1.22
  parting_tonnage = parting_volume * 1.6
  revenue = coal_tonnage * 26
  mining_cost = (coal_tonnage * 1.535) + (parting_volume * 0.95)
  processing_cost = coal_tonnage * 1.184
  other_cost = coal_tonnage * 4.054
  block_value = revenue - mining_cost - processing_cost - other_cost
else
  coal_volume = 0
  coal_tonnage = 0
  parting_volume = 0
  parting_tonnage = 0
  waste_volume = volume
  waste_tonnage = volume * 1.6
  revenue = 0
  mining_cost = waste_volume * 0.95
  processing_cost = 0
  other_cost = 0
  block_value = revenue - mining_cost - processing_cost - other_cost
endif

```

**Figure 5.** Section through the regularised block model showing positive (red) and negative (orange) blocks passed to pit optimisation.

4.2. Pit Slopes

The second piece of information required by the pit optimisation process is the required pit slopes. In our example, these were based on a conceptual geological model of the deposit area and information related to the stability of different types of rock. The area to be optimised was split into three slope regions based on azimuth as shown in the following figure. A 10° slope interpolation area was used to transit between slope regions. The north-east and east region of the pit (between 0° and 135° azimuth) was considered more stable and was processed with a 45° slope, while the south region (between 135° and 210° azimuth) was considered less stable and was processed with a 33° slope. A 36° pit slope was used in the west and north-west region (between 210° and 360° azimuth).

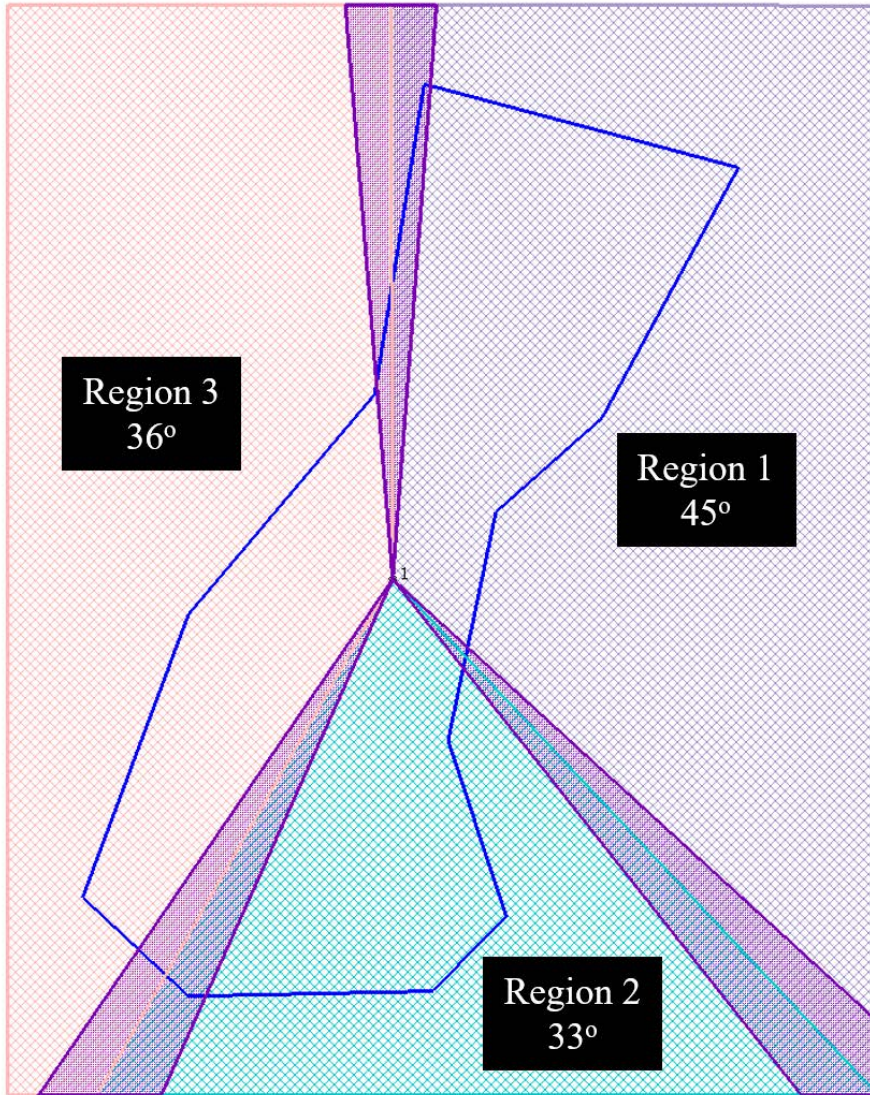


Figure 6. Slope regions and slope interpolation zones shown in plan view over the approximate pit limits and block model extents

4.3. Pit Optimisation

Two separate pit optimisation runs were set up using the same input information (block model and pit slope regions). Two separate block model variables were added to the block model to store the output coding from the two runs – one for the LG method and one for Push-Relabel. Each run produced a separate log file providing details on the input data, optimisation process and output. The following table shows sections from the two log files with information on the blocks used in the optimisation process (feasible blocks), blocks to be mined based on the optimisation (blocks to be mined), ore, waste and air blocks in both cases, the undiscounted economic value of the optimum pit (economic value from the optimum pit) and the time taken to run each optimisation (processing time and total run time respectively).

Once both runs were completed, the optimum pit limits produced by each method were displayed as contours surrounding the blocks to be mined on each bench (level of blocks). The pit limits were 100% identical between the two methods. Figure 7 shows the produced optimum pit limits in plan view. The effect of using different slope regions is clear. The fact that both runs produced identical results was further supported by the information in the log files – both runs produced the same optimum pit economic value based on the same number of blocks to be mined. In

other words, the two optimisation runs produced the same result numerically and geometrically to the last block. However, the time spent to produce this result was very different. LG required one hour and 45 minutes to complete the optimisation while Push-Relabel required one minute and 33 seconds!

Table 2. Parts of optimisation log files from the LG (top) and Push-Relabel (bottom) optimisation runs. The first three digits of the economic value of the optimum pit are hidden for confidentiality purposes.

```
- Number of feasible blocks for the optimiser: 856834 blocks.
  - 31916 Ore blocks (+),
  - 315848 Waste blocks (-),
  - 509070 Air blocks (0).
- Maximum arcs for each block.....: 87 arcs.
- Number of arcs evaluated.....: 378776250 arcs.
- Number of feasible arcs to the optimiser...: 58908200 arcs.
- Number connections/disconnections made.....: 5349553 connections.
- Processing time.....: 1:45:42 Hrs.
- Economic value from the optimum pit.....: xxx94524.69
- Number of blocks to be mined.....: 484838 blocks.
  - 14533 Ore blocks (+),
  - 104873 Waste blocks (-),
  - 365432 Air blocks (0).
```

```
- Number of blocks for the optimiser.....: 856834
  - 31916 Ore blocks (+),
  - 315848 Waste blocks (-),
  - 509070 Air blocks (0).
Initialization time.....: 0:00:01
- Economic value from the optimum pit.....: xxx94524.69
- Number of blocks to be mined.....: 484838
  - 14533 Ore blocks (+),
  - 104873 Waste blocks (-),
  - 365432 Air blocks (0).
Computation time.....: 0:00:51
Total time.....: 0:01:28
- Pit 0: Factor Index = 0 Value = 0.00000
Total run time.....: 0:01:33 Hrs.
```

5. CONCLUSIONS

Pit optimisation is a process that can automate the definition of pit limits and make open pit design more efficient and less time consuming. The LG algorithm has been well established and accepted by the mining industry as the method for pit optimisation of most mineral deposits. Coal and lignite deposits were not so often approached and designed using pit optimisation. The case study presented in this paper proves that there is value in using pit optimisation for lignite deposits and that the current methods can provide a consistent and efficient way to limit the extents of lignite mines both horizontally and vertically. Speed improvements of the Push-Relabel method open up the opportunity to solve problems consisting of millions of blocks (such as large lignite mines) that were previously too large for the traditional LG method.

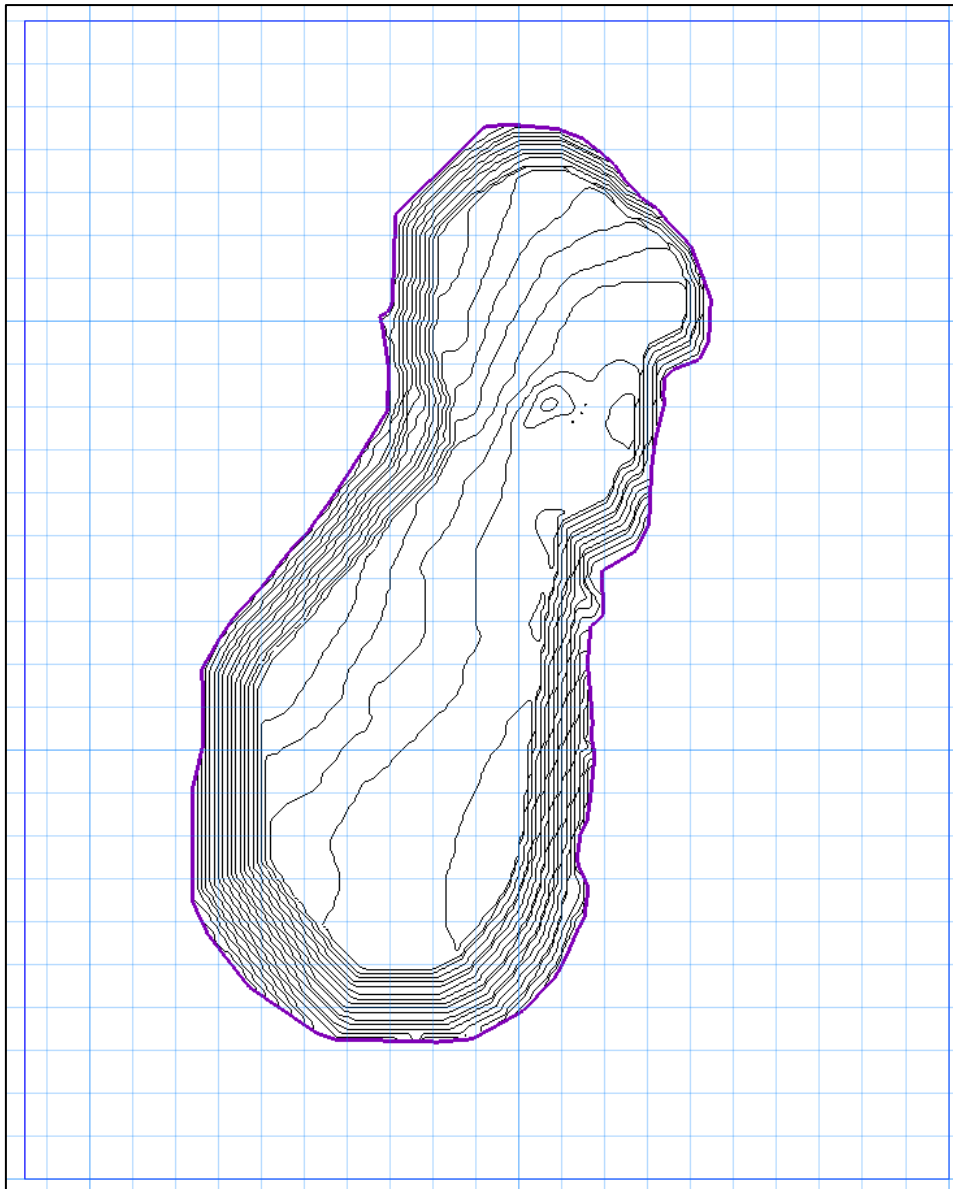


Figure 7. Optimum pit limits produced by both LG and Push-Relabel methods. The effect of applying different slopes in different regions is evident through the change in contour density of the pit walls.

REFERENCES

- [1] Poniewierski, J. (2000). Pseudoflow Explained - A discussion of Deswik Pseudoflow Pit Optimization in comparison to Whittle LG Pit Optimization. Deswik Mining Consultants Pty Ltd.
- [2] Pana, M. (1965). The simulation approach to open-pit design, In J. Dotson and W. Peters, editors, Short Course and Symposium on Computers and Computer Applications in Mining and Exploration, College of Mines, University of Arizona, Tuscon, Arizona. pp. ZZ-1 – ZZ-24.
- [3] Lerchs, H. and Grossmann, I. F. (1965). Optimum design of open pit mines, The Canadian Mining and Metallurgical Bulletin, Vol. 58, January, pp.47-54.
- [4] Kim, Y. C. (1978). Ultimate pit design methodologies using computer models the state of the art, Mining Engineering, Vol. 30, pp. 1454-1459.

- [5] Seymour, F. (1995). Pit Limit Parameterization from Modified 3D Lerchs-Grossmann Algorithm. SME, Preprint Number 95:96.
- [6] Alford, C.G., Whittle, J. (1986). Application of Lerchs–Grossmann pit optimization to the design of open pit mines, In Large Open Pit Mining Conference, AusIMM–IEAust Newman Combined Group, pp. 201–207.
- [7] Hustrulid, W.A., Kuchta, M. (2006). Open Pit Mine Planning & Design, 2nd Edition, Taylor & Francis.
- [8] Whittle Programming Pty Ltd (1998). Whittle Four-X Strategic Planning Software for Open Pit Mines, Reference Manual.
- [9] Picard, J. (1976). Maximal closure of a graph and applications to combinatorial problems, *Management Science*, Vol. 22, No. 11, pp. 1268–1272.
- [10] Goldberg, A.V., Tarjan, R.E. (1988). A new approach to the maximum-flow problem. *Journal of the Association for Computing Machinery*. 35 (4): 921-940.
- [11] King, V., Rao, S. (1992). A faster deterministic maximum flow algorithm. In *Proceedings of the Third Annual ACM-SIAM Symposium on Discrete Algorithms, SODA '92*, pp 157-164, Philadelphia, PA, USA, Society for Industrial and Applied Mathematics.
- [12] Goldfarb, D., Chen, W. (1997). On strongly polynomial dual simplex algorithms for the maximum flow problem, *Mathematical Programming* 77(2):159-168.
- [13] Hochbaum, D., Chen, A. (2000). Performance Analysis and Best Implementations of Old and New Algorithms for the Open-Pit Mining Problem, *Operations Research*, Volume 48, Issue 6, pp. 823-970
- [14] Dantzig, G.B. (1951). Application of the Simplex Method to a Transportation Problem. In T. C. Koopmans, editor, *Activity Analysis and Production and Allocation*, pages 359–373. Wiley, New York, 1951.
- [15] Dantzig, G.B. (1962). *Linear Programming and Extensions*. Princeton University Press, Princeton, NJ, 1962.
- [16] Ford, Jr., L.R., Fulkerson, D.R. (1962). *Flows in Networks*. Princeton University Press, Princeton, NJ.
- [17] Dinitz, E.A. (1970). Algorithm for Solution of a Problem of Maximum Flowing Networks with Power Estimation. *Soviet Math. Dokl.*, 11:1277–1280.
- [18] Goldberg, A.V. (1987). *Efficient Graph Algorithms for Sequential and Parallel Computers*. PhD thesis, M.I.T., Cambridge, MA.
- [19] Karzanov, A.V. (1974). Determining the Maximal Flow in a Network by the Method of Preflows. *Soviet Math. Dokl.*, 15:434–437.
- [20] Tarjan, R.E. (1984). A Simple Version of Karzanov’s Blocking Flow Algorithm. *Oper. Res. Lett.*, 2:265–268.
- [21] Anderson, R.J., Setubal, J.C. (1993). Goldberg’s Algorithm for the Maximum Flow in Perspective: a Computational Study. In D. S. Johnson and C. C. McGeoch, editors, *Network Flows and Matching: First DIMACS Implementation Challenge*, pages 1–18. AMS, Providence, RI.
- [22] Derigs, U., Meier, W. (1989). Implementing Goldberg’s Max-Flow Algorithm—A Computational Investigation. *ZOR—Methods and Models of Operations Research*, 33:383–403.

- [23] Derigs, U., Meier, W. (1992). An Evaluation of Algorithmic Refinements and Proper Data-Structures for the Preflow-Push Approach for Maximum Flow. NATO ASI Series on Computer and System Sciences, vol. 8, pp. 209–223. Nijhoff, The Hague.
- [24] Nguyen, Q.C., Venkateswaran, V. (1993). Implementations of Goldberg–Tarjan Maximum Flow Algorithm. In D. S. Johnson and C. C. McGeoch, editors, Network Flows and Matching: First DIMACS Implementation Challenge, pp. 19–42. AMS, Providence, RI.
- [25] Cherkassky, B.V., Goldberg, A.V. (1997). On Implementing Push-Relabel method for the maximum flow problem. *Algorithmica* 19: 390-410.
- [26] Bai, V.X., Turczynski, G., Baxter, N., Place, D., Sinclair-Ross, H., Ready, S. (2017). Pseudoflow method for pit optimization, Whitepaper, Geovia-Whittle, Dassault Systems.

Use of Mine Planning Software in Mineral Resources and Reserves Estimation of the Lava Lignite Deposit in Serbia – Greece

Ioannis Kapageridis¹, Athanasios Apostolikas² and Efstratios Koundourellis²

¹Technological Educational Institute of Western Macedonia, Koila, Kozani, 52100, Greece

²LARCO GMMSA, 27 Fragkokklisias Street, Maroussi 15125, Athens, Greece

ABSTRACT

The use of mine planning software in the evaluation and estimation of mineral resources and reserves is well established nowadays in the mining industry for the design and scheduling of surface mines and it is a requirement for the reporting of mineral resources and reserves according to international reporting codes. The fundamental principles of these codes are the transparency of the reported material, the relevance of the information included in the report and the competency of the persons involved in the estimation and reporting process. This paper describes the application of mine planning software in the estimation and modelling procedures of the operational lignite mine of LARCO GMMSA at the Lava deposit in Serbia, Kozani. All stages of exploration data analysis, geological modelling, grade estimation, resources reporting, mine design and optimisation, reserves calculation and scheduling of the mining operations are explained. Data integration, advanced 3D graphics and specialised modelling algorithms all within a user-friendly environment contribute to the successful implementation of mining industry accepted procedures to the effective planning and estimation of the surface lignite mine. The more than 10-year long user experience of LARCO GMMSA trained personnel (geologists and mining engineers) adds to the effectiveness of the mine planning software implementation.

1. INTRODUCTION

1.1. Background

The Lava lignite mine is located 12km from the town of Serbia and 30km from the town of Kozani in the Kozani Prefecture (Figure 1). Geologically the basin that the coal deposit belongs to, is considered part of the wider tectonic dip that starts from FYROM. That dip having a general direction NNW-SSE was created from the Alpic tectonic activity during Neogene and is consisted of several smaller tectonic dikes. Into these dikes the neogenic lignitic and other sediments were deposited and then unconformably the quaternary formations were overlaid. The area geologically belongs to the Pelagonic zone. The formations encountered from the bottom to the top are:

- Mesozoic crystallic and dolomitic limestones (Triassic – Middle Jurassic).
- Unconformably to the Mesozoic formations, lie the Neogene sediments (clay, silt, sandstone, marl), which contain the lignite horizons.
- Quaternary sediments consisting mainly of conglomerates with clayish or calcious connecting material.

Tectonically the area has faults of small displacement. All the lignite layers converge towards the centre of the basin with an inclination of 5°. Concerning the Lava deposit, there are two main lignite layers and a minor third that appears at the edges of the basin. The lowest layer has an age of 6.72 – 6.43 Million years and spreads across the central and the most part of the south part of the deposit. Its thickness varies between 1.5 to 25 metres. Its largest part consists of brown coal with

alternations with small layers of clay. On top of that layer lies a layer of marl, on top of which the second lignite layer, consisting of compacted coal with a thickness of 2 – 3 metres and has an age of 6.27 – 6.01 Million years. That second layer overlaps the lowest layer and expands furthermore to the north and the south of the deposit. Finally, the third layer that appears at the edges of the basin has an average thickness of 5 metres and lies above the second lignite layer.

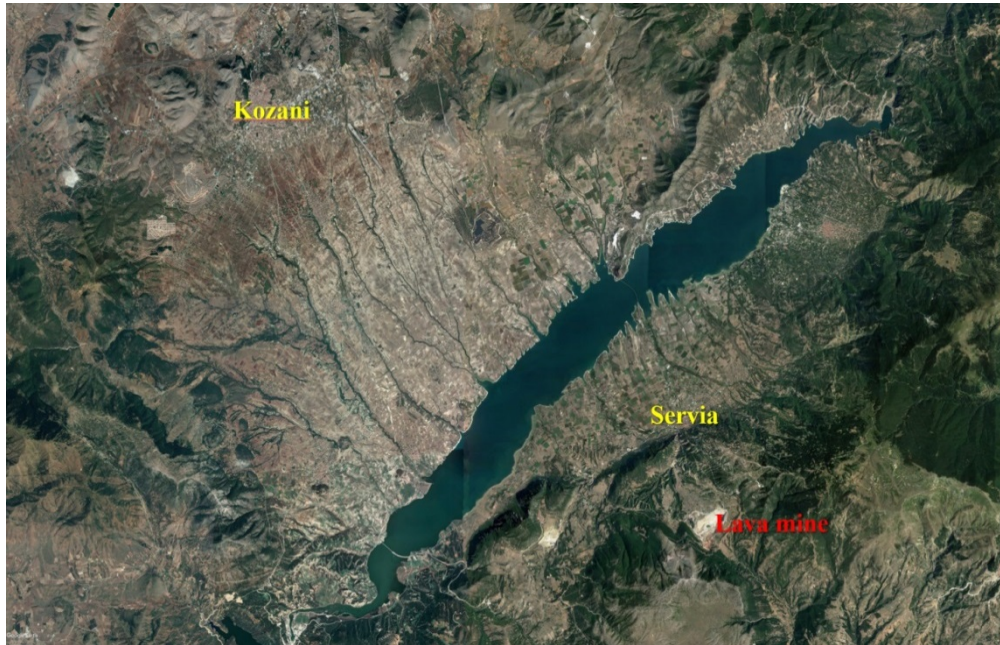


Figure 1. Location of the Lava lignite mine near the town of Servia in NW Greece (image from Google Earth Pro).

1.2. Available Data

The data used in modelling and estimation of lignite resources and reserves of the Lava deposit included 120 drillholes and survey data of the original and current topography. All data were imported into appropriate Maptek Vulcan databases and validated. Figure 2 shows the current topography triangulation model with draped imaged from Google Earth Pro and the location of the drillhole collars. It should be noted that the image data is older than the current topography model.

1.3. Software Implementation

Since 2007, LARCO GMMSA has been using Maptek Vulcan for mine planning in all of its mining operations including the nickel mines in Kastoria, Agios Ioannis and Evoia. The mineral resources and reserves estimation procedure for the nickel deposits has been presented in the past [1]. Maptek Vulcan is also used for mine planning of the lignite operation in Servia which is the subject of this paper. The application of Maptek Vulcan to lignite resource estimation, though for uncorrelated seams, has been presented in the past [2]. However, the steps involved in modelling the Lava lignite deposit and estimating resources and reserves have important differences to the procedure applied to the nickel mines and the other lignite mines in the region, as it will be discussed over the following sections.

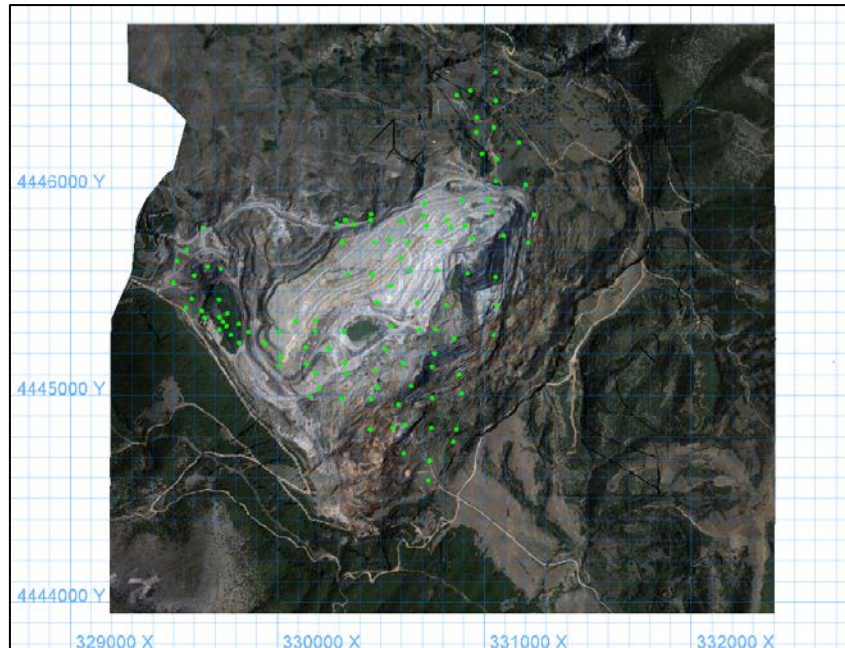


Figure 2. Current topography model with draped image from Google Earth Pro and drillholes collar location.

2. DATA PROCESSING

2.1. Current Topography

Current topography was surveyed by drone and modelled using Pix4Dmapper Pro (Pix4D SA). Figure 3 shows screenshots from the software and produced output using data acquired from the Lava mine. Pix4Dmapper Pro software uses images taken by hand, drone, or plane and creates precise, geo-referenced 3D maps and models used for data analysis. Some of the key outputs of the software include [3]:

- 3D Point Cloud: Accurate digital reconstruction and the geolocation of each point.
- Digital Surface & Terrain Model: the elevation value of each pixel, with or without above-ground objects.
- Orthomosaic: A geolocated high-resolution map with each pixel of the original images projected onto the digital surface model.
- Volume Calculation: Accurate volume calculations on a representation of stockpiles, with fully-adjustable base height.
- Contour Lines: A simplified representation of the topography with closed contours displaying the elevation.
- 3D Textured Model: Triangular mesh with photorealistic texture.
- Reflectance Maps: reflectance based on the pixel value in multispectral or thermal imagery.
- Index Maps: indices such as NDVI and NDRE or create of custom indices.

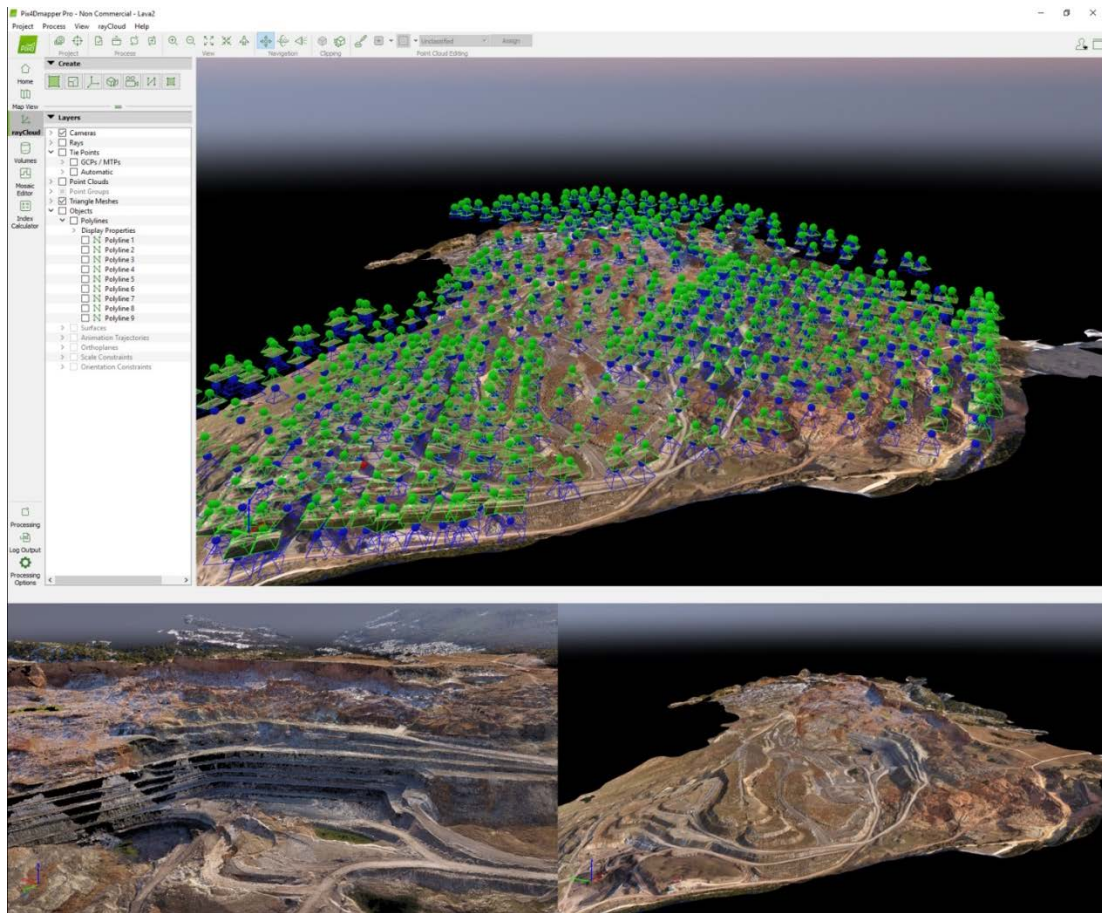


Figure 3. Screenshots from topography drone scan in Pix4Dmapper Pro (top: camera locations and triangulation model, bottom left: point cloud, bottom right: triangulation model).

The triangulation model produced by Pix4Dmapper Pro was imported in Maptek Vulcan to be used for lignite resources and reserves modelling.

2.2. Drillhole Database Development and Validation

Data from the 120 drillholes were imported to a drillhole database in Maptek Vulcan through CSV files containing collar information (hole ID, collar XYZ) and sample intervals (top and bottom depth, length, lithology, ash, etc.). The database was checked and validated both visually and through a number of tests related to collar coordinates and overlapping intervals. A separate database lithology table was generated by combining consecutive intervals of the same lithology. This table and lithology field were used to create drillhole sections in Vulcan and proceed with the correlation of lignite layers. The resulting correlation was stored in an extra field in order to have both the original lithology and the interpretation.

Sample intervals were composited to a standard length of 0.5m as they were originally of varying length, thus not suitable for block model estimation. The choice of composite length was based on the mining method used.

3. GEOLOGICAL MODELLING

The correlated lignite layers intervals were further processed and used to build grid models of the roof and floor of each layer (Figure 4). The grid models were cropped by the current topography surface and were checked against drillholes in sections. Minor layers of low lignite quality (waste) within the three main lignite layers were also modelled separately. Blocks inside these waste layers were to be excluded from estimation, as were the composites that came from these layers to minimise dilution.

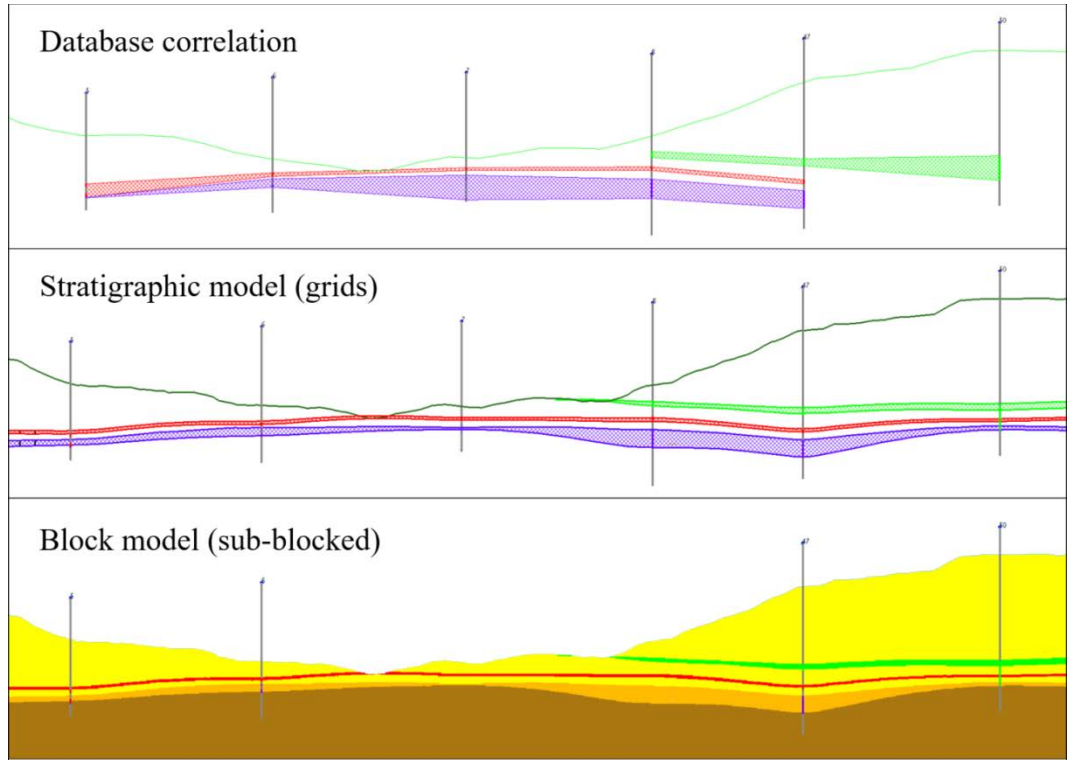


Figure 4. Example section showing database lignite layers correlation between drillholes (top), grid models representing stratigraphy (middle), and complete block model containing both structural and quality information of the lignite deposit. Drillholes missing in the bottom section are hidden behind the block model section.

4. LIGNITE RESOURCES ESTIMATION

The structural grid models of stratigraphy and the current topography triangulation model were used to create a sub-blocked block model. The main block size was set to 10x10x10m while the sub-block size ranged from 1x1x0.5m up to the main block size. The block model origin and extents were set in a way to cover all the area of interest in all three coordinate axes. Several block variables were defined allowing storage of quality estimations, lithology, resource classification and estimate validation parameters. The following table gives a summary of the main block model parameters.

Table 7. Block model parameters – all dimensions and coordinates are in meters.

Type	Sub-blocked - unrotated	Number of variables	
Origin X	330,000	Main block size X	10
Origin Y	4,444,000	Main block size Y	10
Origin Z	650	Main block size Z	10
Extent X	2,200	Minimum sub-block size X	1
Extent Y	3,200	Minimum sub-block size Y	1
Extent Z	550	Minimum sub-block size Z	0.5

Sub-blocking occurred only in cases where a main block intersected one of the surfaces included in the model, i.e. lignite and waste layers roof and floor surface, and the current topography surface. Maptek Vulcan initially breaks the main block to sub-blocks of the minimum size (1x1x0.5m in our case) and then joins together sub-blocks that no longer intersect the surface that caused the sub-blocking (a process called coalescing in Vulcan), thus leading to sub-blocks of sizes multiple of the minimum size (e.g. 2x2x2.5m). The aim of this process is to reduce the number of sub-blocks down to the absolutely necessary while still following the controlling surface to the greatest resolution possible.

All blocks were coded based on the controlling surfaces so that they belong to a particular zone of the deposit. The coding values were stored in a lithology variable that could be later used to select blocks for estimation, processing and reporting. The bottom section in Figure 2 shows the blocks coloured according to this variable.

Once the block model was constructed, multiple estimation runs were defined targeting the blocks of each lignite layer (block model zone). A single estimation run was used to estimate each layer with the resource classification of the produced estimates taking place afterwards through block model scripting. The main estimation parameters used in all lignite layers quality estimation are summarised in Table 2.

Table 2. Main lignite quality estimation parameters.

Search Ellipsoid		Other Parameters	
Bearing	0	Minimum samples	4
Plunge	0	Maximum samples	16
Dip	0	Maximum samples per octant	2
Major	200	Discretisation along X	4
Semi-major	200	Discretisation along Y	4
Minor	50	Discretisation along Z	1

The inverse distance squared weighting method was used to estimate ash and other quality variables in the block model. Ash and the other lignite quality parameters were considered to vary along all three axes (i.e. even along Z) within each layer, unlike the strictly stratigraphic approach of estimating qualities using grids.

Each block was split into 4x4x1 points (discretisation) which were estimated separately and then averaged to produce the final block value. This is a just a practical way to better approach the distribution of the estimated parameter within the block volume as inverse distance weighting is a point and not a volume estimator. As already mentioned, estimation was performed separately for each lignite layer, i.e. only blocks being inside the specific layer were estimated using sample composites only from that layer. Octant based search was used to ensure sample selection from surround drillholes to the block being estimated as shown in Figure 5. After estimation, it was possible to check how the sample selection strategy worked by using a special “Explain” function of Vulcan which allows the user to see graphically which samples were used in the estimation of a particular block and estimation related information about them (applied distance, applied weight, octant number, etc.) as shown in the detail window in Figure 5.

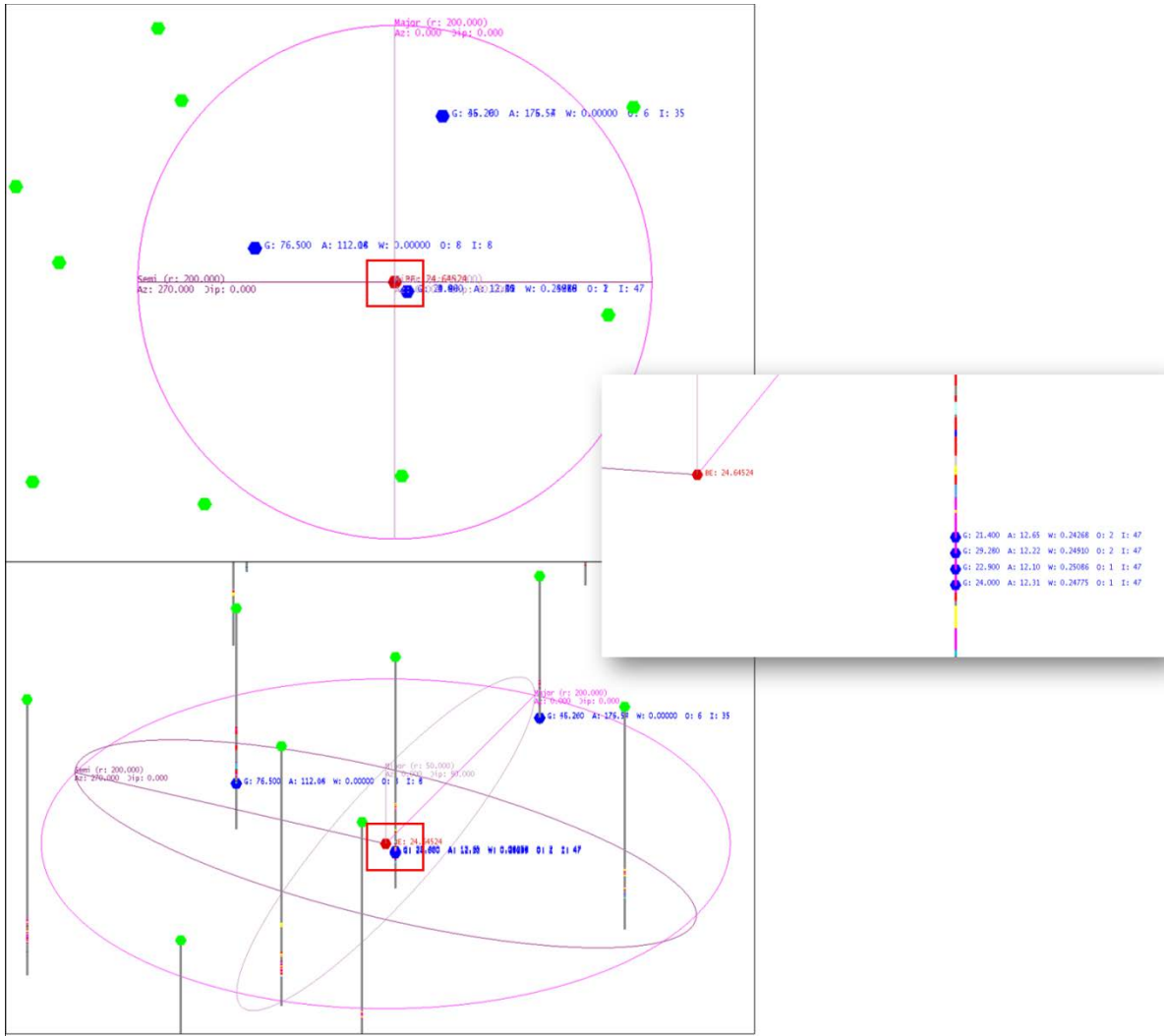


Figure 5. Plan and 3D view of search ellipsoid used to estimate ash in the lower lignite layer. The red box shows the area of the detail view on the right. The block in question is shown with a red dot while the selected samples are shown in blue.

Figure 6 shows a section through the block model coloured by ash content estimates. Estimates presented good agreement with the drillhole interval values. Generating a grade/tonnage curve for ash required some manipulation of the table produced by the corresponding function in Maptek Vulcan. The software expects a grade parameter and the tonnage calculated for each cutoff includes the blocks with an estimated grade value higher than the cutoff. In the case of ash, we need to report the material with an ash value lower than the cutoff so it was necessary to effectively reverse the tonnage table and reproduce the graph as shown in Figure 7. The curves show the sensitivity of lignite ash content and tonnage to the ash upper limit applied. It seems that after 60% there is little or no change on lignite ash and tonnage.

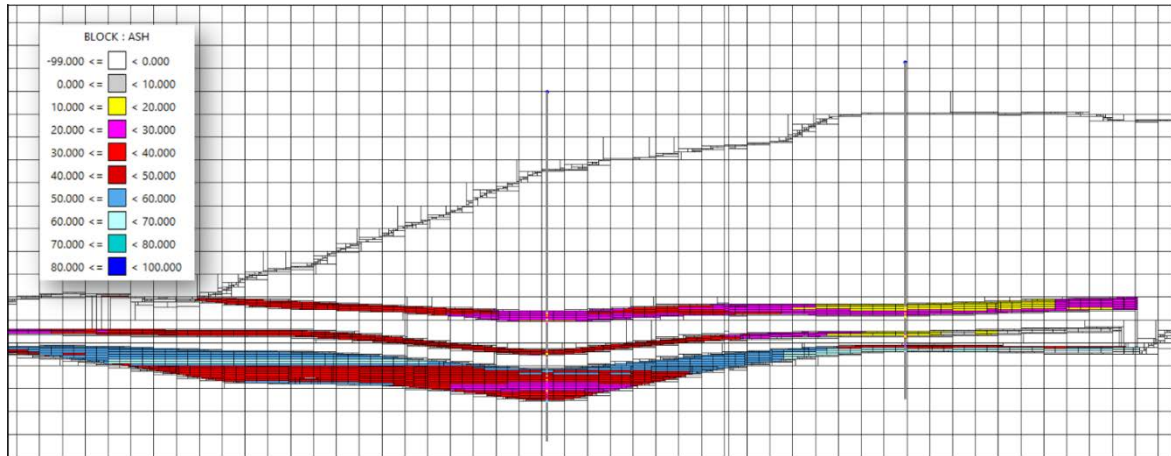


Figure 6. Block model section showing ash estimation inside each of the three lignite layers.

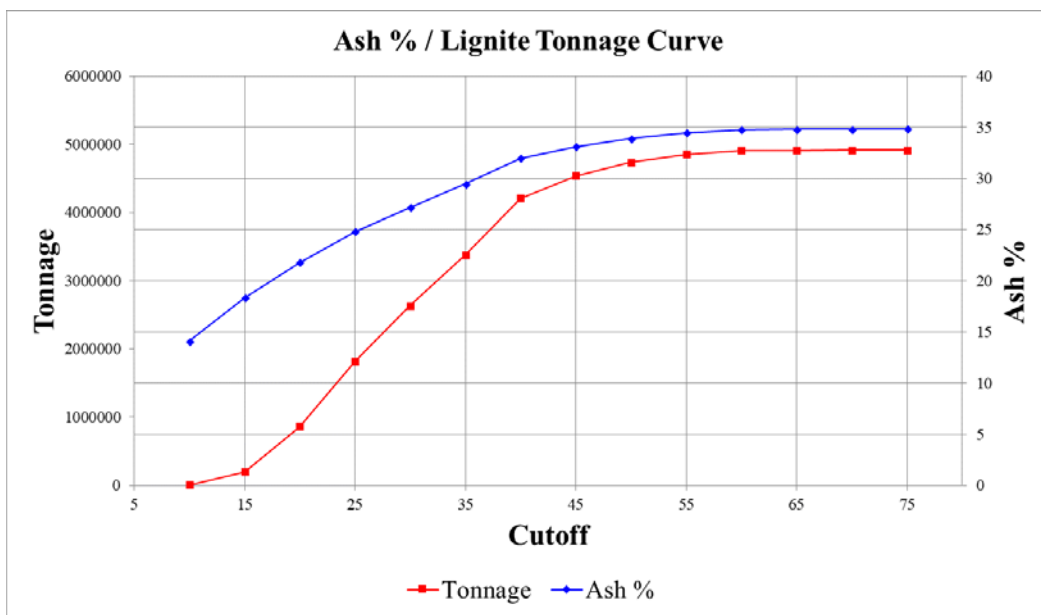


Figure 7. Grade/tonnage curve of lignite resources showing the effect of applying a different ash upper limit (cutoff).

Figure 8 below shows the results of drift analysis and comparison between the composited ash values used as input to resource estimation and the produced block estimates of ash. The smoothing effect of block model estimation with inverse distance is clear mainly along the X and Y axes. The histogram also shows that the block estimates distribution is narrower than the composites, which is normal (support effect). Generally, the estimates follow the main trends of the composites.

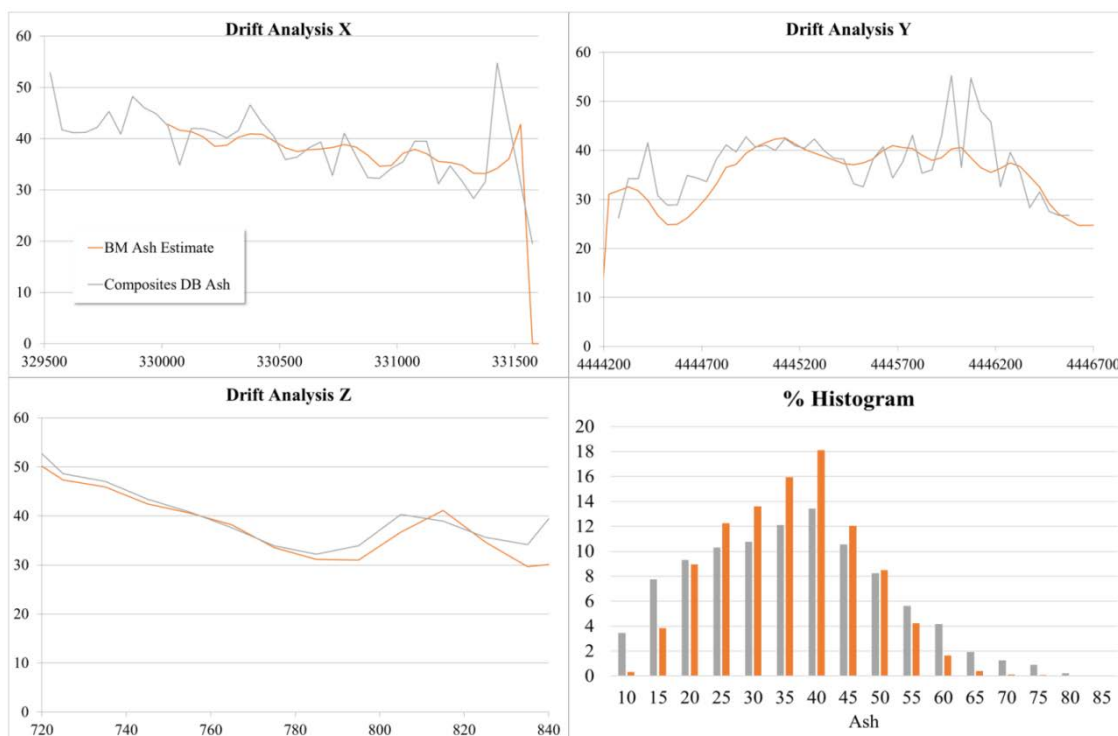


Figure 8. Drift analysis and histogram of composites database ash values and block model ash estimates.

5. LIGNITE RESERVES CALCULATION

For the lignite reserves calculation, a solid triangulation of the conceptual final pit was used to limit the considered volume. The final pit was derived using Lerchs-Grossman pit optimisation with some standard financial and pit slope parameters (Figure 9). Table 3 summarises the lignite reserves estimate for the Lava mine based on the mining operation at the start of 2018. Two scenarios are presented based on a different upper limit for ash (50 or 60%).

Table 3. Lava lignite mine reserves at the start of 2018

Ash 50%								
Lignite kTonnes	Ash %	Waste m ³ x1000	SR m ³ /t	Sector	Lignite kTonnes	Ash %	Waste m ³ x1000	SR m ³ /t
2,420	34.89	26,623	11.00	North	986	34.35	8,749	8.88
				Central	643	37.01	5,372	8.36
				South	792	33.84	12,503	15.79
Ash 60%								
Lignite kTonnes	Ash %	Waste m ³ x1000	SR m ³ /t	Sector	Lignite kTonnes	Ash %	Waste m ³ x1000	SR m ³ /t
3,040	38.85	26,107	8.59	North	1,056	35.59	8,690	8.23
				Central	962	42.67	5,105	5.30
				South	1,022	38.62	12,311	12.05

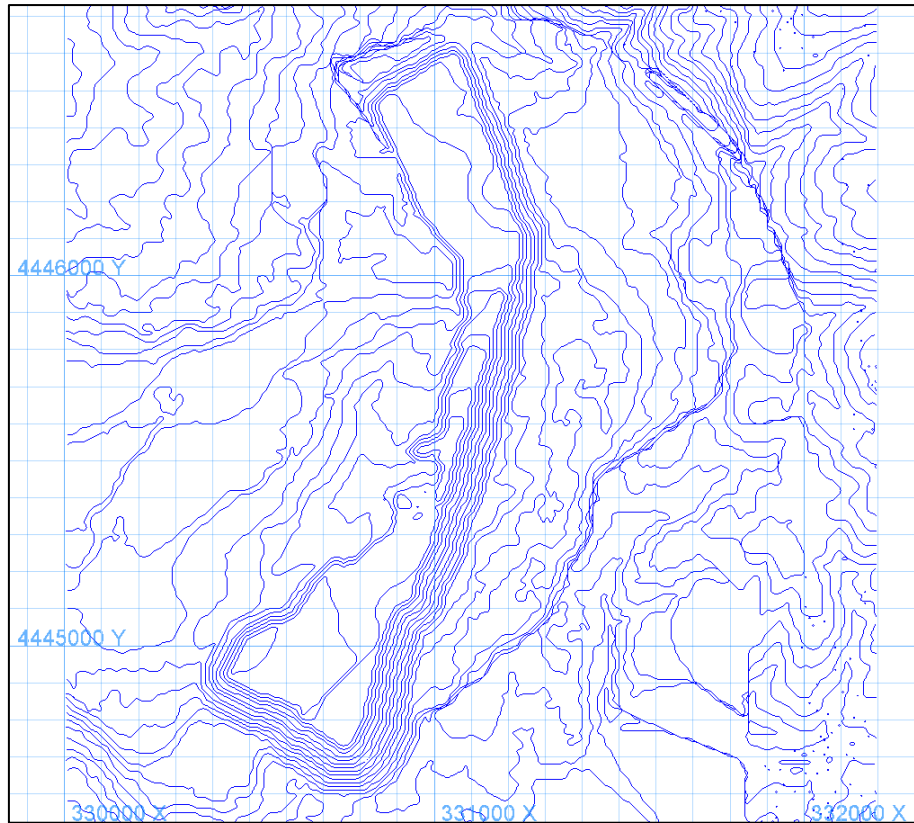


Figure 9. Optimised pit limits of the Lava lignite mine used to limit the material reported as reserves.

6. CONCLUSION

This paper discussed most aspects of the application of mine planning software to the evaluation of lignite resources and reserves of the Lava lignite deposit in NW Greece. The implementation of mine planning software produced results that increased confidence as to the available resources, formalised the mine planning procedure, aided the configuration of the mining methods applied, and helped in planning future mining operations by developing different mining scenarios with speed and clarity. Adopting the discussed approach increased confidence in the produced results and reduced the risks associated with the estimates, ensuring all important geological controls are considered. The use of a pit optimisation tool helped convert resources to reserves with more confidence and in a more standardised fashion that is widely accepted by the mining industry.

REFERENCES

- [1] Kapageridis, I., Apostolikas, A., Pappas, S., and Zevgolis, I. (2013). Use of Mine Planning Software for the Evaluation of Resources and Reserves of a Sedimentary Nickel Deposit, 13th International Congress of the Geological Society of Greece, Chania.
- [2] Kapageridis, I., Kolovos, C., Modelling and Resource Estimation of a Thin-Layered Lignite Deposit. In: 34th International Symposium on the Application of Computers and Operations Research in the Minerals Industries (APCOM 2009), Vancouver, 2009.
- [3] Pix4D SA (2018). Insights from Images: How Drones and Image-Based Mapping and Analytics are Transforming the Mining Industry, White Paper, Pix4D SA.

Carbon: A WebGIS Software to Evaluate and Model Open-Pit Lignite Mining Systems

Eleni Louvari and Andreas Pittas

Evmolpos, Earth Science Consulting Company

ABSTRACT

Carbon is a web-based open pit lignite mining management system to assist mining scientists and land managers in achieving “best practice” mining outcomes. The Carbon-WebGIS application gives the ability to the user to: 1) evaluate mining borehole data, based on specific user criteria, and calculate the upper and the bottom lignite surface, 2) print the original and the evaluated borehole with depth, 3) produce spatial model of Tonnage distribution and Lignite/Overburden thickness, taking into account faults and borehole distribution, 4) calculate volumes of overburden and lignite deposits over an area, 5) design open pit and calculate overburden and lignite volume in it, 6) produce cross sections over model and/or boreholes, 7) design and edit spatial data of model areas, open pit areas and fault structures, 8) export model data in .grd, .img, .asc format, vector gis data in .shp, .dxf format and parametric data in .csv format, and 9) create 2D and 3D maps showing lignite with depth, the boreholes, the faults and the open pits. Carbon is created based on Open Source architecture, using PostgreSQL/PostGIS, UMN MapServer, GeoExt and OpenLayers for GIS data manipulation and 2D map creation, and Three.js for 3D map creation. The Carbon WebGIS system can be a powerful tool in Mining Management mechanism.

1. INTRODUCTION

The modern way of management of the lignite deposits requires concise registration and monitoring of the resources at various stages of their exploration and extraction.

The current paper introduces Carbon, a Web Based open pit lignite mining management system to assist mining scientists and land managers in achieving “best practice” mining outcomes.

Considering the fact of the registered different needs of various geoscientists in an open pit system and the need of Map Services via Web Interface, the Carbon WebGIS System was designed to match different sets of different user needs. The geodatabase model has been developed using UML and the WebGIS system was developed using UMN MapServer [1], an open source tool, with integrated PostgreSQL/PostGIS Database System [2] and the possibility of generating and publishing WMS, WFS and KML services. PostgreSQL is a powerful, open source object-relational database system with over 30 years of active development, while PostGIS is a spatial database extender for PostgreSQL, which adds support for geographic objects and raster data allowing location queries to be run in SQL. The MapServer and an HTML viewer provide service to users who need GIS processing, advanced access to spatial database and also superior functionalities to a state of the art level. The Carbon WebGIS system is publicly available through a local network, encompasses all the available mining data supporting an active open pit lignite mining area.

The Carbon WebGIS system is considered as a versatile aspiration tool to manage a mining (RDBMS) system online, and make it easily accessible to a variety dedicated users via local network. As a matter of fact it provides a superior online tools for Spatial Editing, Mining and Geological analysis. The implementation uses open source tools to emphasize the value of the Web based GIS technology, its potential application as a valuable tool for resolving open pit mining problems and for exploring plans for further extension of a pit layout.

2. PROGRAM DESCRIPTION

Carbon is a server side application that is served through a web browser to the clients in a local network. Only certified users can access the application and there are three levels of users: the Administrator, the users with READ+WRITE+DELETE rights and the users with only READ rights.

Computerized deposit modelling provides a means of managing and mine plan creation. The basic strategy involves the creation of a borehole database that includes analytical results for various physical and chemical properties of the data to be modelled [3].

For this purpose, Carbon, includes two main modules:

- The first one provides the environment for entering borehole data, evaluate the boreholes based on specific user criteria, getting a scaled print out of the borehole section, create patterns for the geological formations, query the data, import and export ascii data, among others.
- The second module includes all the modelling algorithms using Raster GIS techniques, the model creation of the upper and the lower lignite surface, the creation of scaled model and borehole cross-sections, the design open-pit and calculate volumes.

2.1. Data Entry

The main environment of entering the basic borehole data (X,Y coordinates, Z altitude, Region, Responsible, Start Date, End Date) resembles a simple spreadsheet, as shown in Figure 1. Within this environment analytical tools of SQL can be applied to the data, in order to select only these that meet specific user criteria. Selected data can be exported in .csv format or printed. Ascii data can also be imported.

ID	Code	X (ECSM7(m))	Y (ECSM7(m))	Z (m)	Region	Drilling Rig	Responsible	Start Date	End Date	Area...	Type...	Moist...	App...	Type...	Sett...	C%...	N%	%-N%	Average...	Average...	Average...	Print...	Exp...
894	MAK-179	30381.298	4471431.222	409.61	Mesopotamya	Archer No3		30/08/2008	22/02/2016	4.96	115	73.3	8.1	454.76	378.19	78.2	8.87	10.22	32.88	36.28	402.81	1.2	8.77
895	PS-12	306891.159	4482976.666	461.3	wt			20/02/2017	20/02/2017	13.17	18.23	41.2	13.35	445.05	584.2	34.81	4.1	5.46	36.39	56.24	0	1.21	4.68
895	MAK-179	30381.298	4471431.222	409.61	wt			30/02/2017	20/02/2017	29.28	6.6	21	23.1	438.18	372.43	84.3	0.81	1.17	28.88	37.34	1943.81	1.2	0.97
895	MAK-183	307281.654	4482412.386	437.31	wt			30/02/2017	20/02/2017	40.32	6.4	47	35.4	430.93	348.23	82.6	1.32	1.3	24.4	37.34	1313.81	1.2	1.24
896	MAK-081	307198.548	4482788.139	434.81	wt			30/02/2017	20/02/2017	23.44	11.1	29.1	25.1	421.13	346.19	84.6	1.38	1.68	22.29	37.40	1962.12	1.2	1.4
899	MAK-024	307626.607	4482812.129	421.26	wt			30/02/2017	20/02/2017	28.92	14.4	14.8	24.1	430.66	373.26	89.5	0.4	1.18	28.36	35.23	1554.78	1.2	0.99
898	MAK-001	306484.71	4482184.827	462.1	wt			30/02/2017	20/02/2017	19.08	1.91	69.3	11	782	411.7	89.3	6.1	21.78	11.88	49.53	2042.4	1.2	18.14
897	MAK-002	306602.88	4482618.408	468.93	wt			30/02/2017	20/02/2017	18.2	1.95	46.9	10.1	473.03	416.73	37.2	4.55	23.49	21.33	56.83	1546.89	1.2	10.37
896	MAK-003	306681.908	4481931.908	474.41	wt			30/02/2017	20/02/2017	21.8	89.3	94.3	36.4	388.97	414.21	114.7	4.62	6.61	34.96	36.11	1891.12	1.2	7.11
891	MAK-001	306697.279	4481341.438	462.48	wt			30/02/2017	20/02/2017	13.34	181.3	24.6	5.4	351.18	471.18	30	4.56	38.13	27.82	45.24	1723.67	1.2	31.48
894	208394	306984.719	4481213.166	462.28	wt			30/02/2017	20/02/2017	11.81	184.4	39.69	27.13	473.83	398.23	86.6	1.42	3.78	25.14	37.2	0	1.32	2.34
891	208392	306884.812	4481224.79	461.8	wt			30/02/2017	20/02/2017	12.58	31.7	67.91	11.49	429.7	526.1	79.6	5.81	8.52	21.47	38.34	0	1.22	6.99
892	208390	306831.544	4482041.298	460.75	wt			30/02/2017	20/02/2017	12.84	32.25	76.04	11.34	428.2	310.49	87.33	6.39	6.42	23.29	37.76	0	1.24	7.61
891	207395	307081.181	4482412.439	461.18	wt			30/02/2017	20/02/2017	15.41	29.34	48.89	29.27	431.82	360.69	71.18	1.43	2.43	27.21	38.77	0	1.22	1.99
898	207399	306861.781	4481212.172	462.2	wt			30/02/2017	20/02/2017	16.11	21.26	41.35	36.1	431.15	342.1	71.81	1.36	2.28	26.26	36.21	0	1.29	1.66
879	207391	306861.497	4481282.149	433.91	wt			30/02/2017	20/02/2017	15.89	18.7	48.2	23.23	449.29	348.78	71.41	1.83	2.37	27.07	36.71	0	1.22	1.64
878	207389	306832.232	4481294.775	462.6	wt			30/02/2017	20/02/2017	14.81	36.13	41.08	4.71	426.45	378.4	47.81	4.07	11.43	24.13	38.02	0	1.28	8.13
877	206396	307081.152	4482412.474	434.79	wt			30/02/2017	20/02/2017	14.38	26.53	40.07	29.9	452.74	362.73	89.97	1.34	2.21	24	36.71	0	1.23	1.8
876	206394	307081.772	4482312.145	434.72	wt			30/02/2017	20/02/2017	19.81	23.7	41.85	36.89	436.02	347.27	84.71	1.36	2.44	26.46	37.01	0	1.22	1.86
875	206392	306861.809	4481282.182	431.26	wt			30/02/2017	20/02/2017	11.07	11.1	43.3	29.4	440.86	347.86	73.1	1.47	1.84	26.48	37.06	0	1.23	1.31
874	206390A	306819.395	4481240.274	437.8	wt			30/02/2017	20/02/2017	24.77	11.31	79.44	24.18	446.25	373.63	36.62	2.01	3.39	27.04	36.93	0	1.23	2.77
873	206388	306831.618	4481712.456	460.91	wt			30/02/2017	20/02/2017	13.33	22.2	49.32	13.38	437.82	384.13	35.3	3	4.86	24.43	37.03	0	1.21	3.85

Figure 22. A spreadsheet like window for entering borehole data.

Detailed cross-section data for each borehole (such as depth, analytical geological formations with depth, chemical measurements of ash, dry ash, humidity, etc.) can be entered in similar spreadsheet, giving the user useful tools for entering the geological data with depth quickly and easily.

The software includes a library with geological formation patterns, which can be easily applied to all borehole data for homogeneity (Figure 2).

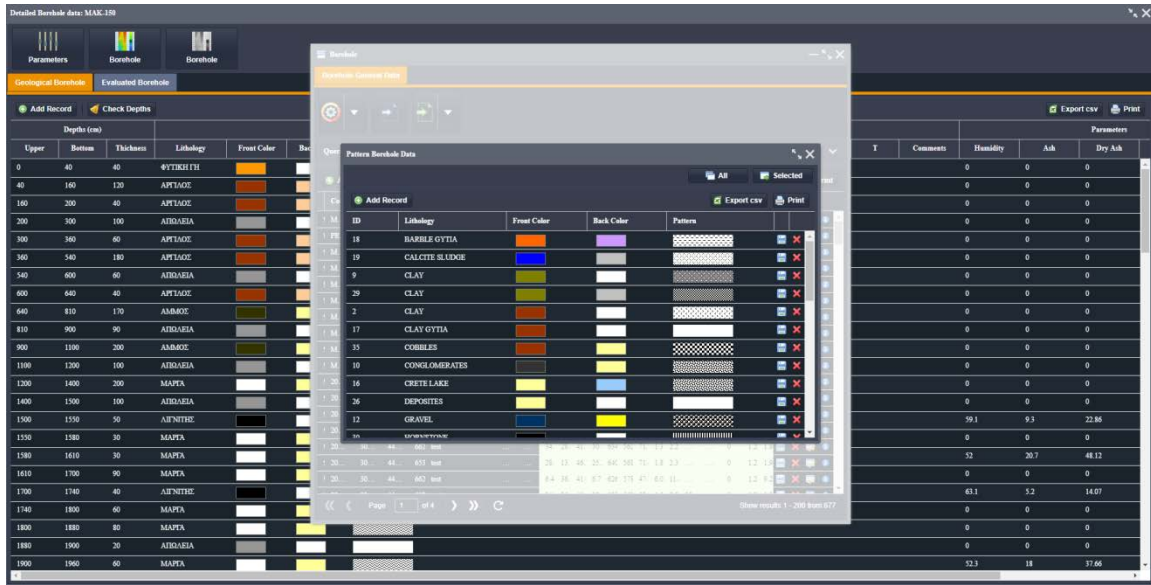


Figure 23. Library with geological formation patterns.

After the completion of the data entry the user can print out a scaled borehole section (Figure 3) in a graphical easily readable output of all the borehole data.

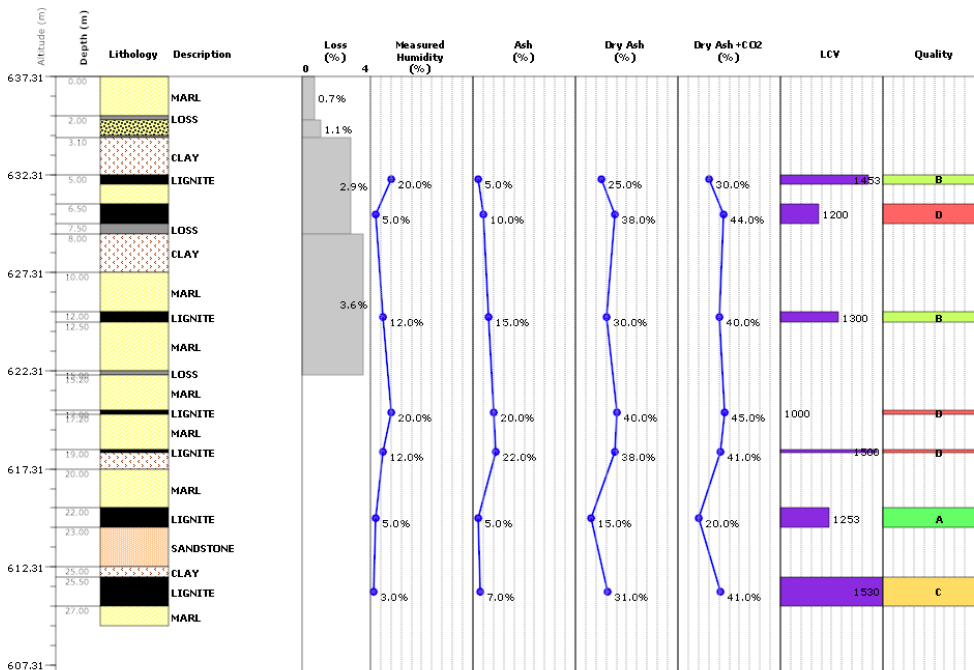


Figure 24. Detailed borehole section print out.

2.2. Borehole Evaluation

The geological reconnaissance of a lignite deposits can be materialized by models of various types. Thus, the initial problem relates to the evaluation of the boreholes, based on information gathered through geological exploration techniques, of which the boreholes (with their lithological, chemical and physical analyses) are the most common sources of information.

The evaluation of primary lignite borehole data is a process of integrating their layers in technically recoverable quantities of lignite and intermediate sterilized. The process is based on specific rules that have emerged as a result of the constraints set by the exploitation methods, the

technical properties of the machinery used, the exploitation requirements of the lignite deposits and the environmental constraints.

The parameters used by Carbon in order to evaluate the borehole data are shown in Figure 4 and is a result of thorough discussion with the geologist scientists of Lignite Center of Western Macedonia, Greek Public Power Corporation.

Figure 25. Criteria for the Evaluation process

The Evaluation process starts by characterizing the borehole layers as ‘Sterile’ based on the Ash Content and the layer thickness. If this ‘Sterile’ layer has thickness larger than a specific limit then this layer is characterized as ‘Interruption Sterile Layer’.

Afterwards, it temporarily iterates through the layers into extractable lignite portions and intermediate sterile. In order to achieve this, the software creates blocks of layers between the ‘Interruption Sterile Layers’ and after removing the corresponding thickness from the roof and floor layer of the block due to loss, proceeds to calculate the weighted average values of the moisture, ash and net calorific value (NCV) of the block, based on following equations:

$$\text{Average Block Ash} = \frac{\sum[\text{Ash}(i) \cdot \text{thickness}(i) \cdot \text{specific dry weight}(i)]}{\sum[\text{thickness}(i) \cdot \text{specific dry weight}(i)]} \quad (1)$$

$$\text{Average Block Humidity} = \frac{\sum[\text{Humidity}(i) \cdot \text{thickness}(i) \cdot \text{specific weight}(i)]}{\sum[\text{thickness}(i) \cdot \text{specific weight}(i)]} \quad (2)$$

$$\text{Average NCV} = \frac{\sum[\text{NCV}(i) \cdot \text{thickness}(i) \cdot \text{specific weight}(i)]}{\sum[\text{thickness}(i) \cdot \text{specific weight}(i)]} \quad (3)$$

$$\text{Average Specific weight} = \frac{\sum[\text{thickness}(i) \cdot \text{specific weight}(i)]}{\sum[\text{thickness}(i)]} \quad (4)$$

$$\text{Average Specific dry weight} = \frac{\sum[\text{thickness}(i) * \text{specific dry weight}(i)]}{\sum[\text{thickness}(i)]} \tag{5}$$

If the resulting values of Average Block Ash and Block Thickness satisfy the user constraints then the block is characterized as Lignite and proceeds to the calculation of final block ash, humidity and net calorific value (NCV). If the block does not meet the criteria then the bottom layer of the block is removed and the process is repeated until the block meets the criteria. If finally, the block results with one layer, which does not meet the criteria, then it is characterized as Sterile and the evaluation process continues with the next block.

An example of the print out of an evaluated borehole section is shown in Figure 5. In this figure, the quality of the blocks based on the dry ash content [4] is shown with different colors:

- Category A, with dry ash up to 20.7% (green).
- Category B, with dry ash between 20.7% and 30% (light green).
- Category C, with dry ash between 30% and 35% (orange).
- Category D, with dry ash between 35% and 45% (red).

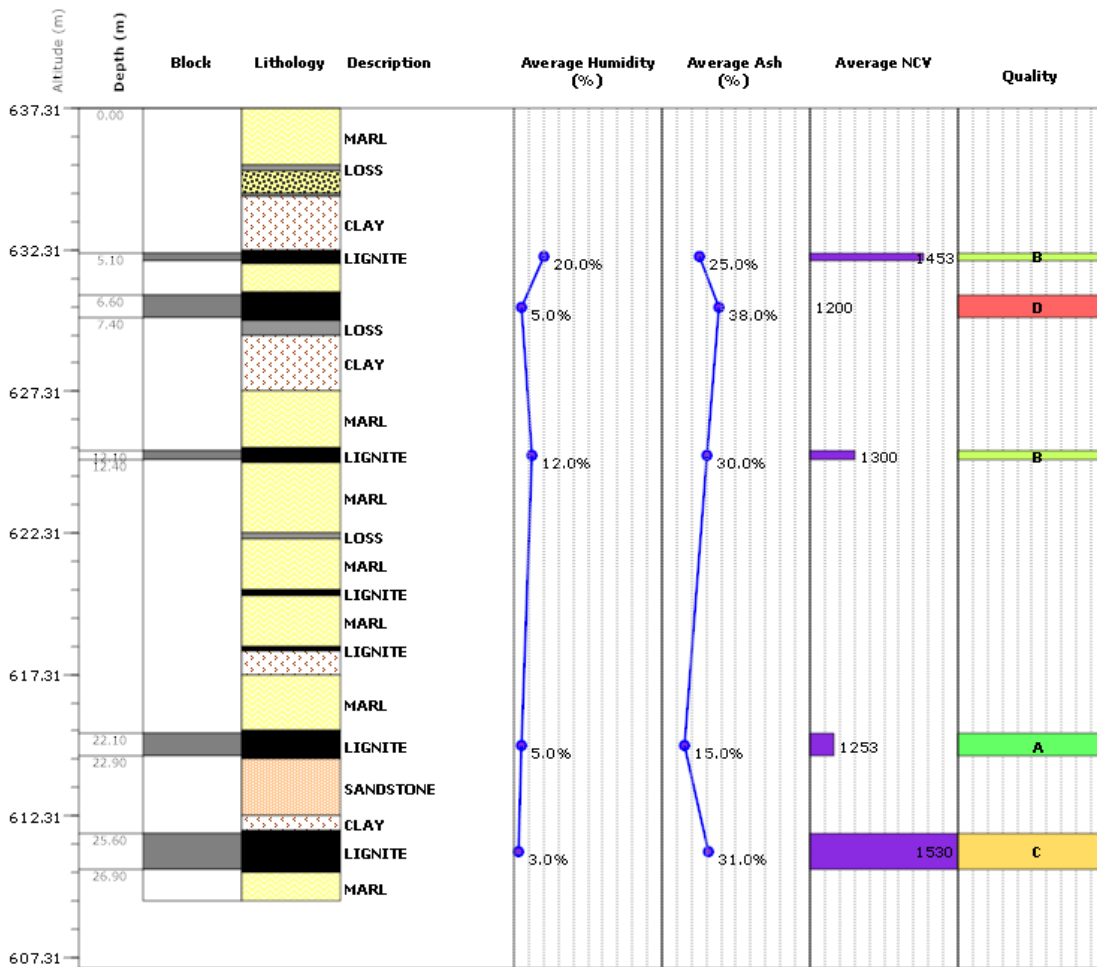


Figure 26. Evaluated borehole section.

When the whole evaluation process finishes, the software calculates, for each borehole, the lignite thickness, the upper sterile thickness, the middle sterile thickness, the upper and the bottom

lignite surface, the normalized average ash, the normalized average humidity, the normalized average NCV and the Exploitation Ratio. These data can be exported in ascii .csv format.

2.3. Map Creation

All spatial data, such as administrative borders, buildings, infrastructure, environmental protected areas, digital elevation models, orthophoto maps, etc., as well as borehole locations and faults are drawn on a 2D Map (Figure 6). Carbon includes various powerful tools for manipulation the spatial data:

- Parametric selection of spatial data based on SQL queries.
- Spatial selection of data on the map.
- Zoom to selected data.
- Export the selected spatial data in .shp or .dxf format.
- Import spatial data in .shp format and save them in geodatabase.
- Draw on the map points, lines and polygons, using cad like tools.
- Apply snapping tools while drawing.
- Modify spatial geometries, such as move, rotate, scale.
- Get information and modify the vertex coordinates of a geometry.
- Apply spatial geotools to polygons, such as split, merge, intersect, clip, buffer.

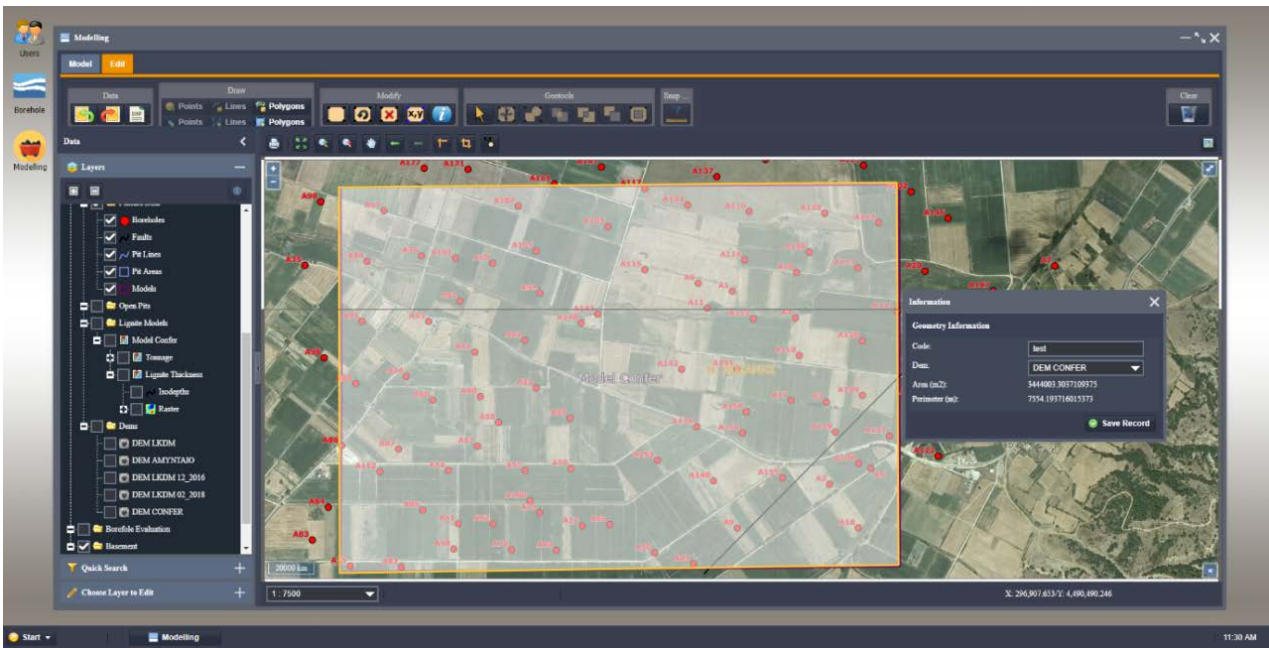


Figure 27. WebGIS Map environment of Carbon for drawing, editing and modelling spatial data, using advanced geospatial tools.

2.4. Modelling

‘Modelling’ refers to the process of creating 2D or 3D arrays of estimations. Various Geostatistical simulation algorithms have been used in geology and mining engineering to assess the uncertainty at un-sampled locations and to develop models of the continuity of variables. Carbon uses the evaluated borehole data in order to produce interpolated continuous surfaces of Lignite Upper Surface, Lignite Bottom Surface, Lignite, Sterile and Overburden Thickness, as well as Tonnage.

Powerful WebGIS tools (as discussed in the previous section) give the ability to the user to draw, edit on the 2D Map and finally save in the geodatabase a polygon (Model Polygon), including the evaluated borehole data to be modelled. This polygon is used as a border limit for creating the interpolated surfaces. In a similar way, faults can be drawn or imported on a map and saved in the geodatabase.

Each Model Polygon area is joined with a Digital Elevation Model, which can be imported as .img or created within the Carbon software using X, Y, Z point data.

The algorithm used for interpolation is the Inverse Distance Weighting (IDW) to a Power with a smoothing factor (Equation 6). IDW interpolation weights the data based on the assumption that values that are close to one another are more similar than those that are farther apart. The measured values closest to the prediction location will have more influence on the predicted value than those farther away based on the weighting power. The greater the weighting power, the less effect have points far from the prediction location during interpolation. IDW method produces a ‘bull’s-eye’ effect around the predicted values. In order to reduce this effect Carbon uses the Smoothing parameter. IDW method is an exact interpolator, when Smooth parameter equals zero, and needs good distribution of the original data. Carbon takes into account the existing faults during the Interpolation, as hard breaklines.

$$V_{ij} = \frac{\sum_{i=1}^n \frac{z_i}{\sqrt{d_{ij}^2 + \text{smooth}^2}^{\text{Power}}}}{\sum_{i=1}^n \frac{1}{\sqrt{d_{ij}^2 + \text{smooth}^2}^{\text{Power}}}} \quad (6)$$

where:

- d_{ij} is the distance of each cell of the interpolated surface from each borehole,
- z_i is the value of the borehole parameter to be evaluated and
- V_{ij} is the predicted value.

All the model parameters are specified by the user (Figure 7), such as the raster Columns, Rows, the Cellsize, the Power and the Smooth parameter of the IDW interpolation method and the maximum borehole data to use at each interpolation location. Carbon makes an original estimation of the raster properties (rows, columns, cellsize) based on the distribution of the borehole data that fall within the Model Polygon area.

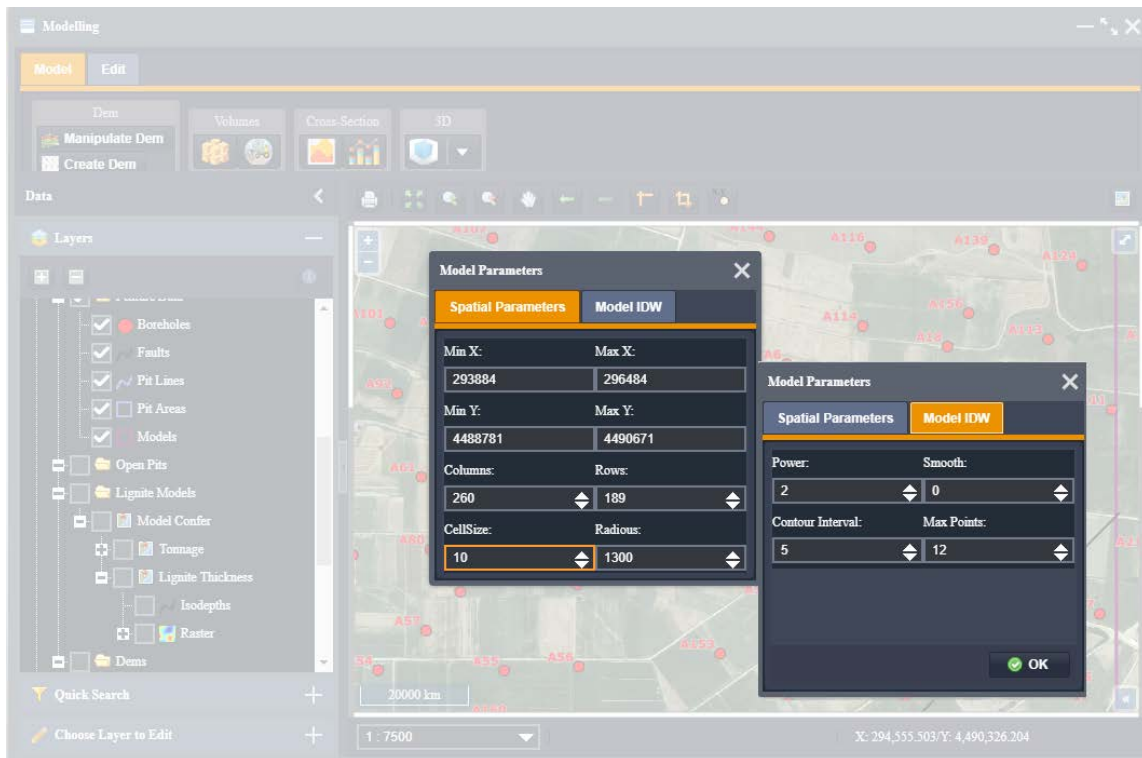


Figure 28. Specification of model parameters.

Carbon adds the produced interpolated surfaces on the map (Figure 8), giving the ability to the user either to print it or to export it, in various formats (.grd, .img, .asc), while the calculated volumes of overburden, lignite and middle sterile are saved in the geodatabase and joined with the Model Polygon (Figure 9).

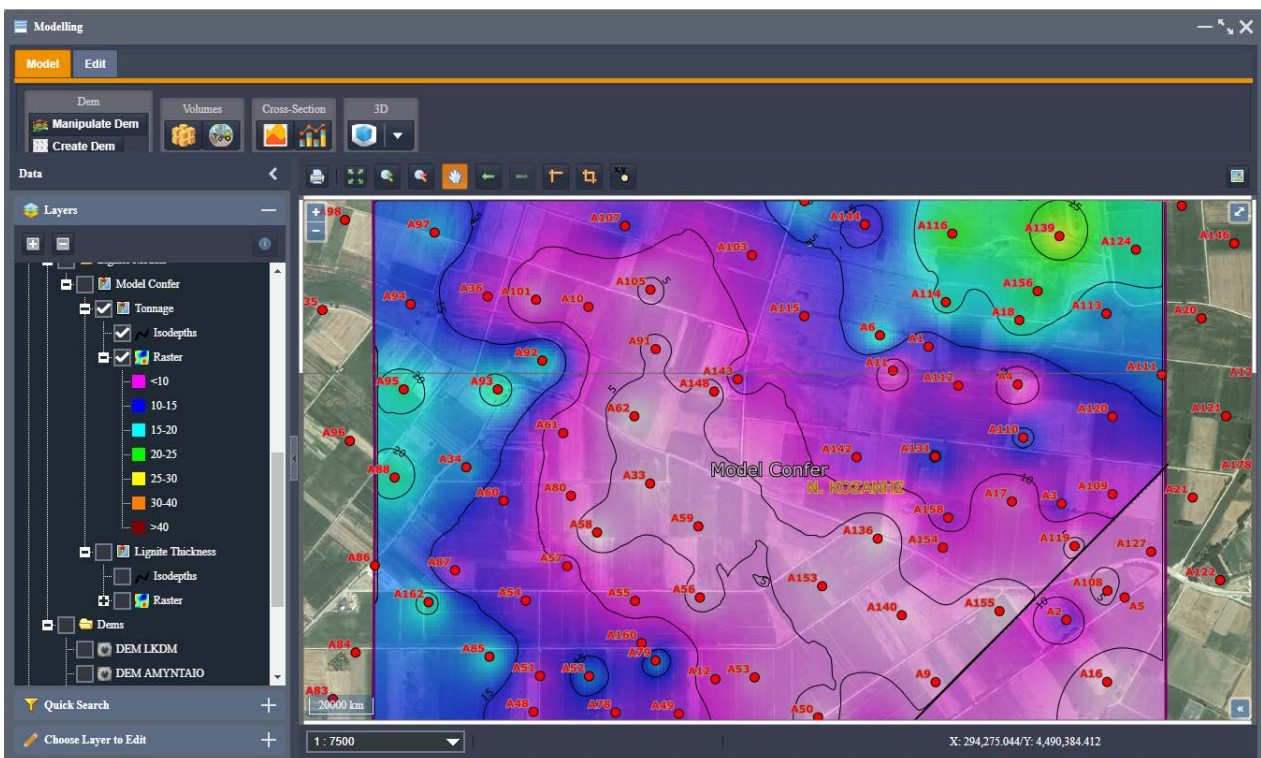


Figure 29. Interpolated surface of lignite tonnage drawn with transparency on the map.

Code	Perimeter GIS	Area GIS	Tonnage (tn)	Upper Orig. ...	Middle (m3)	Lignite (m3)	Upper No...	Depos+Li...	Exploitati...	DEM
17 Model Confer	7,554.04	3,437,834.15	39,098,644	165,492,758	77,118,584	35,405,916	223,246,590	112,260,509	5.71	DEM CO...

Figure 30. Volumes of Tonnage, Overburden, Middle Sterile and Lignite calculated for each Model.

2.5. Cross-sections

Geological cross-sections along a profile is widely used by geologists in order to interpret the horizontal and the vertical continuation of the geological formations and structures.

Scaled vertical cross-sections can be generated by Carbon, simply by drawing a line on the map. Cross-sections can be created by using either the model (Figure 10) or the boreholes (Figure 11).

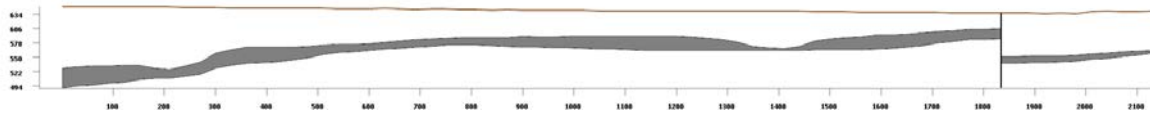


Figure 31. Model cross-section along a profile drawn on map.

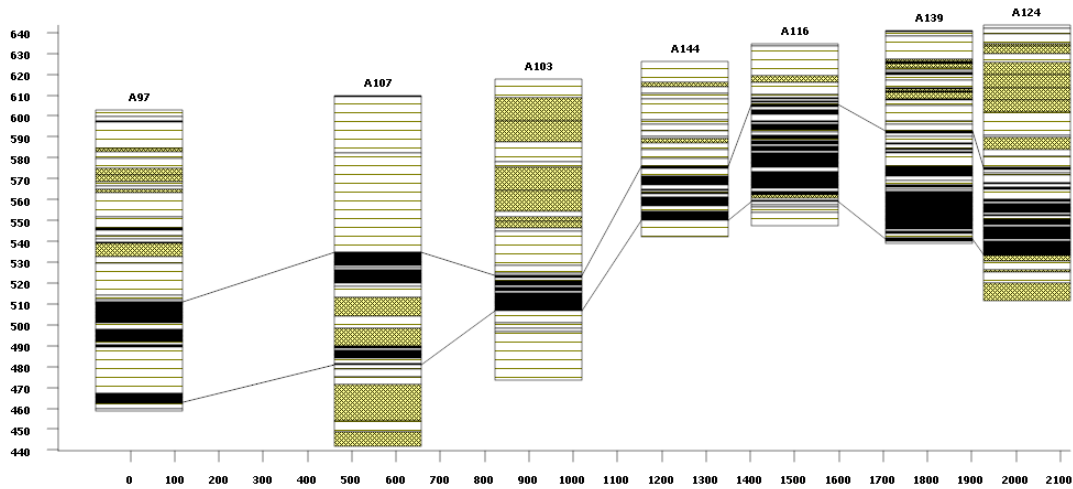


Figure 32. Borehole sections along a profile drawn on map.

2.6. Pit Design

Open-pit planning and design is a decision-making process that leads to a realistic and actionable plan to profitably harvest mineral resources. Planning can be carried out for a wide range of time periods, from the very short (e.g., the next shift of mining activities) to the very long (e.g., the profitable extraction over the complete life of the mine). Carbon focuses in pit design in order to calculate lignite volumes in it very easily and quickly for a step by step mining activity. The only user task is to draw a polygon on the map (Pit polygon) and define the digital elevation model that will be used for the pit creation. Dynamic editing allows for fast manipulation of pit design and reduces design time significantly. Parameters can be changed easily for fast configuration and

reconfiguration to consider various approaches. The geometry of the pit is defined by the following parameters:

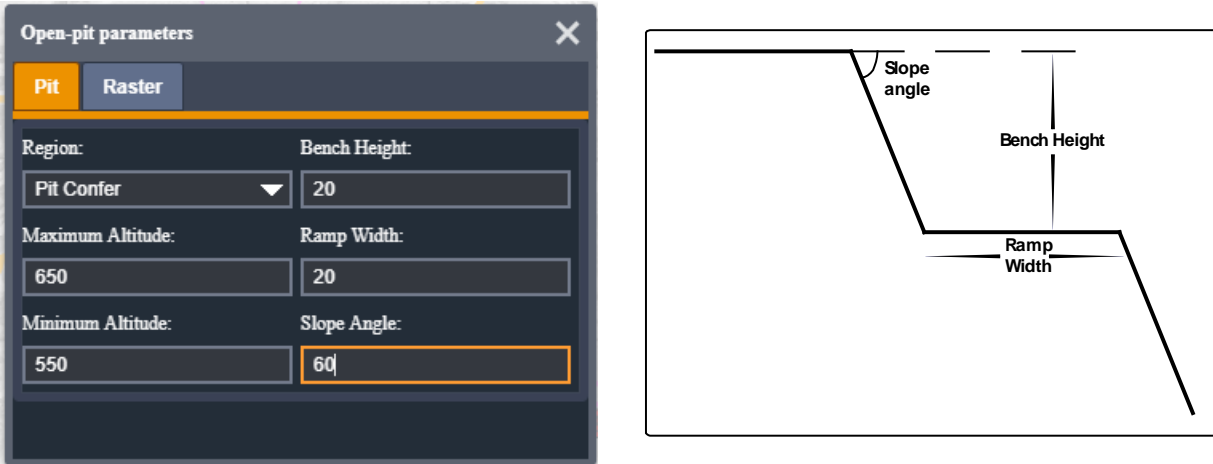


Figure 33. Parameters for open pit creation.

Carbon creates the open-pit taking into account the digital elevation model, creates the upper and the bottom lignite surface within the pit and calculates the volumes of overburden, middle sterile and lignite deposits, based on the pit geometry. The digital elevation of the pit is added on the map (Figure 13) and all the raster data can be exported as .img, .grd, .asc, while the design contour lines can be exported as .shp, .dxf.

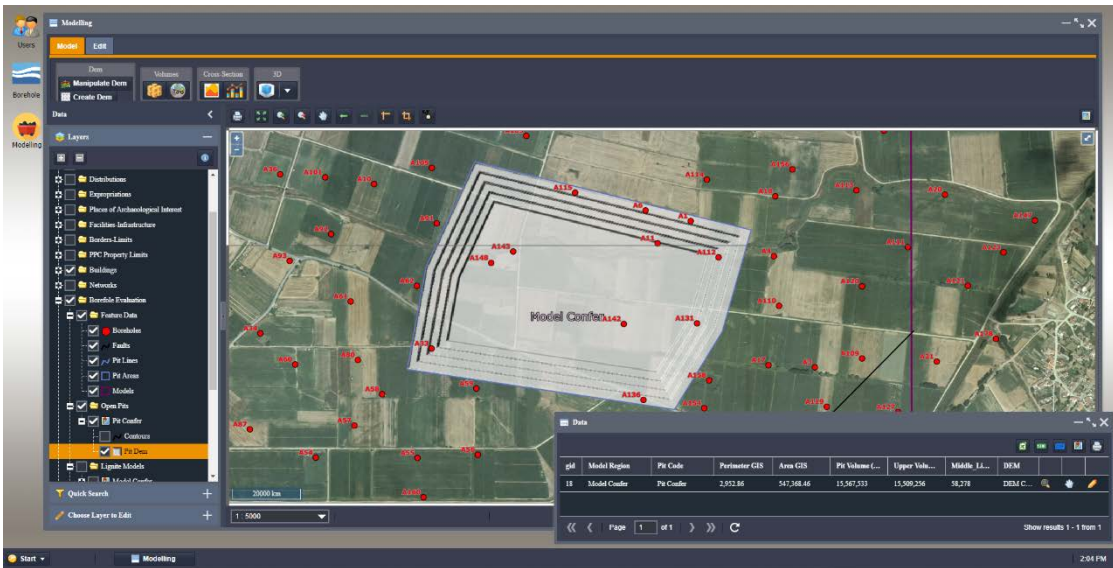


Figure 34. Digital elevation of the open-pit shown with transparency on the orthophoto map.

There is also an option to calculate the lignite volumes between the batches, where Carbon models the distribution of lignite and sterile thickness, as derived from the borehole data, taking into account the pit geometry.

2.7. 3D Models

Carbon uses the most advance technology in order to create and serve through web the 3D distribution of borehole data. More specifically, it uses the Three.js JavaScript library [5], based on

the WebGL technology. Three.js allows the creation of Graphical Processing Unit (GPU) without relying on proprietary browser plugins. This is possible thanks to the advent of WebGL.

The modelled data of upper and lower lignite surface are used in order to create the 3D surfaces as shown in Figure 14 and Figure 15. The user can move, rotate and zoom on the 3D plot. Additionally tools give user the ability to exaggerate the z value, make visible/invisible or transparent the surfaces and the faults and create 3D cross sections.

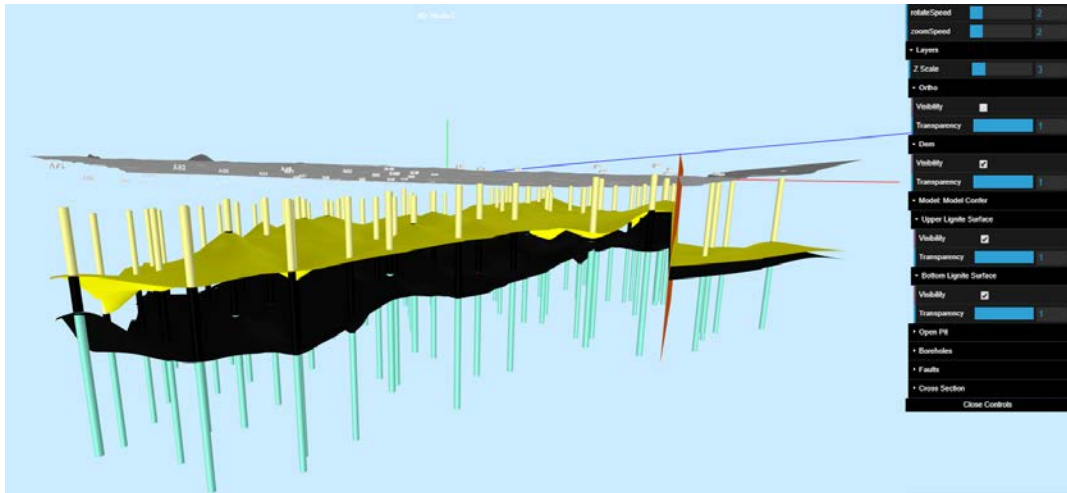


Figure 35. 3D plot of Digital elevation model (gray), upper lignite surface (yellow) and bottom lignite surface (black). Faults are drawn with orange color.

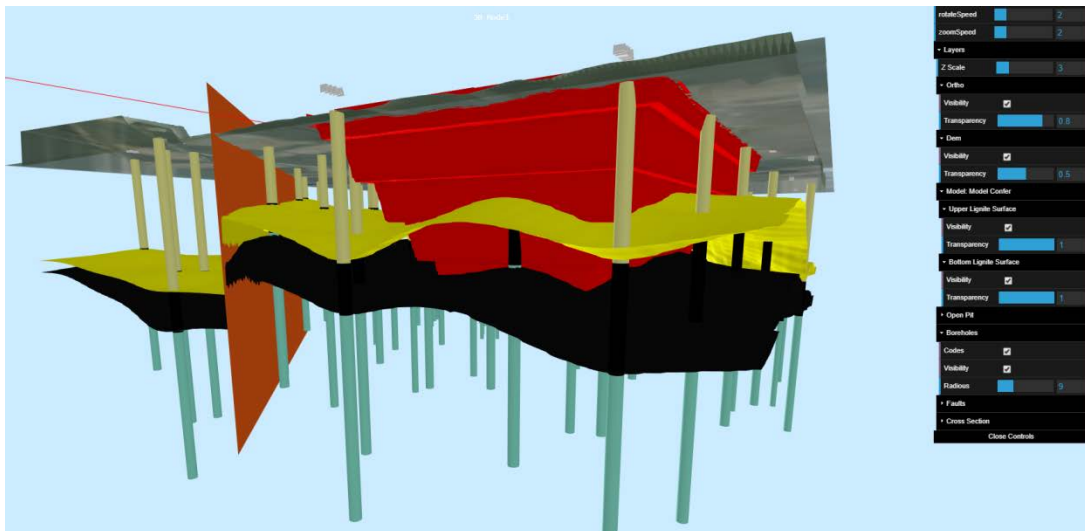


Figure 36. 3D Plot of the open-pit (red) with the upper and bottom lignite surfaces.

Carbon also creates 3D model of the Dry Ash and the Net Calorific Value using 3D IDW interpolation method. These data can be drawn on a 3D plot (Figure 16) and colored based on their values. Specific values can be isolated by the user, as shown in Figure 17, making it easier to interpret the borehole data.

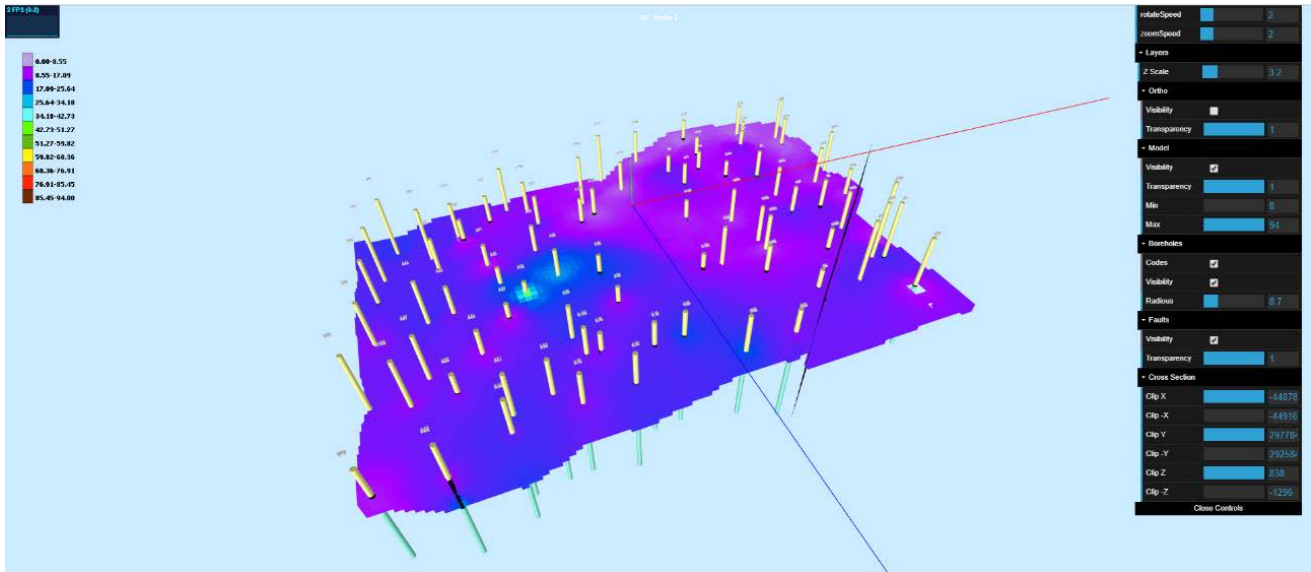


Figure 37. 3D Plot of Dry Ash distribution.

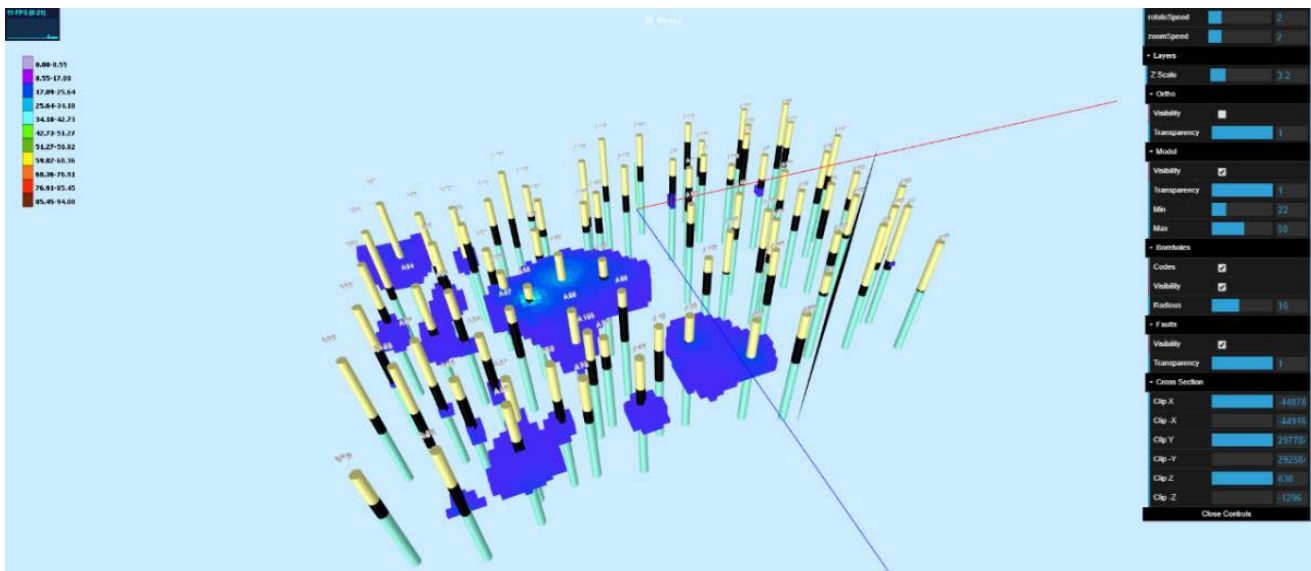


Figure 38. Isolation of specific Dry Ash values in the 3D Plot.

3. CONCLUSION

Operational mines have long used GIS, but in specific areas, such as environment monitoring and management, as well as geotechnical engineering. More recently, GIS’s functionalities has become much broader, leading to the mining industry to adopt GIS in operational studies and management.

More specifically, the exploitation of lignite deposits requires the interpretation of research boreholes, the creation of representative models, involving their lithological, structural, geometrical and chemical characteristics. Thus, the modelling of the geometry and extend of lignite deposits as well as its volume calculation are fundamental in managing lignite open-pits. This can only be achieved through a spatial decision support system. The construction of this spatial system demand the integration of the following [6]:

- A database management systems (RDBMS).
- A digital cartographical representation of data.

- A mathematical model to describe all relevant physical phenomena derived from choices taken during the planning process.

Carbon software provides advanced editing capabilities to store, manipulate and evaluate borehole data, model the upper and lower lignite surface, design open-pits, fast and easy and finally, generate multiple 2D and 3D outputs quickly for various options analysis. The user-friendly interface and simplified menus require minimal training.

Summarizing, the main functionalities of Carbon-WebGIS are:

- Store and manipulate mining borehole data.
- Evaluate mining data.
- Plot original and evaluated borehole data with depth in scaled sections.
- Model the tonnage distribution, upper surface and bottom lignite surface, lignite-sterile and overburden thickness, taking into account the faults.
- Calculate volumes over the model area.
- Design open pit structures and calculate volumes in it.
- Create cross section over a model area and along mining boreholes as well.
- Design and edit spatial data of model areas, open pit areas and fault structures.
- Create 3D plots with boreholes, digital elevation models, model areas and open pits with the ability to rotate, zoom, scale and create 3D cross-sections.
- Produce and print sophisticated 2D maps.

The more advanced capabilities can be integrated within a Holistic Decision Support System in order to produce a final Mining Declaration Management mechanism for the absolute, rational and more productive way of acting in open pit mining processes.

REFERENCES

- [1] UMN Mapserver. <http://mapserver.org>. Mapserver Engine for serving GIS data throw Web.
- [2] PostgreSQL/PostGIS. <https://www.postgresql.org>. PostgreSQL RDBMS system with additional GIS functionalities with PostGIS.
- [3] Luppens, J.A., Wilson E.S. and Stanton, W.R. Manual on Drilling, Sampling, and Analysis of Coal. Compiled by ASTM SUBCOMMITTEES D05.18 and D05.23
- [4] Koukouzas, K., Kotis, Th., Ploumidis, M. & Metaxas, A. (1979). Geological study of the lignite deposits Anargiron-Amyntaiou. Archives of the Greek Institute of Geology and Mineral Exploration, Volume No 9.
- [5] Three.js. <https://threejs.org>. JavaScript library for Web 3D Drawing.
- [6] Maidement, Z. Ye and McKinney, D. (1996). Map-based Surface and Subsurface Flow simulation models: An Object-Oriented and GIS Approach. CRWR Online report 96-5, Austin, Texas.

Model-based Investigations of Hybrid Mining Systems Using Cutting, Crushing and Conveying Technology in Medium Hard Rock

Markus Dammers and Christoph Deppe

thyssenkrupp Industrial Solutions AG, thyssenkrupp Allee. 1, 45143 Essen, Germany

ABSTRACT

One of the most important aspects in mine planning is the selection and dimensioning of equipment as it has a tremendous impact on the economics of the mining operation. At this stage, mine planners have to set up a philosophy how to mine, meaning either to use discontinuously or continuously operating equipment. In soft rock deposits the use of continuously operating equipment is already state-of-the-art, whereas it is not in medium hard rock. In the latter case truck and shovel operations are more common today, though the decision is not driven by economics but the degree of higher flexibility and lower initial investment. Another fact is the industry wide acceptance of this technology. But, there seems to be change in mindset as mining companies have to cope with stricter regulations concerning environmental factors. At this point, electrically driven and continuously operating equipment can make use of their inherent advantages.

This paper presents application potentials for continuous cutting, crushing and conveying systems. The evaluation methodology is a scenario-based comparison. Therefore, BARRACUDA[®]-type bucket wheel excavators, fully-mobile and semi-mobile In-Pit Crushing and Conveying systems, as well as discontinuous truck and shovel operations are compared against each other. A hypothetical mine cross-section is the basis of research and data is derived from literature, empirical values and project work. The results show application limits of abovementioned systems and outline potentials in cost effectiveness. In addition, it is the aim of the investigation to help mine planners in equipment selection and system process development.

1. INTRODUCTION

One of the most important aspects in mine planning is the selection and dimensioning of equipment as it has an enormous impact on the economics of the mining operation. A pre-requisite is that mine planning has already defined pit geometries, pushback sequences and production rates. An initial evaluation of operational requirements will narrow the amount of applicable systems. However, every trade-off feasibility study ends up in CAPEX, OPEX and total cost of ownership (TCO) evaluation by means of one of several discounted-cash-flow methods. CAPEX and OPEX are likely to be estimates and the sensitivity of the system to operational variables affects the accuracy of these estimates and hence the project feasibility [1,2]. This is especially relevant for tailor-made continuous mining systems.

Besides the conventional truck and shovel operation, the excavation process can be done by using bucket wheel excavators (BWE) connected to belt conveyors for material transportation, in soft rock mines. In hard rock mines, excavation can be realized by implementing an in-pit crushing and conveying system (IPCC) with a primary crushing stage located very close to the mining face inside the pit. A rather new type of technology is the BARRACUDA[®]-type bucket wheel excavator which is able to cut rock with a uniaxial compressive strength between to 50 and 80 MPa. In reality there is not always a strict separation of soft rock and hard rock deposits and different types of material have to be handled in most mines.

A holistic mine and equipment planning approach is necessary to enable a hybrid mining system using cutting, crushing and conveying technology in one mine. In principle, deposits can be exploited using a combination of various excavation technologies [3].

The following chapter introduces different continuous mining systems and highlights planning aspects when it comes to the combined application of discontinuous and continuous mining systems. In the following, a model-based investigation of hybrid mining systems based on different mining scenarios is carried out. The paper ends with a case study where all these systems are applied.

2. MINE PLANNING ASPECTS OF HYBRID CUTTING, CRUSHING AND CONVEYING SYSTEMS

Energy efficiency, environmental care and the minimization of operating costs are some of the top key figures for mining companies. The major differences with respect to energy efficiency of the existing mining technologies are in the energy requirement and the energy supply. Continuous mining equipment is electrically powered, while most discontinuous mining equipment is powered by diesel engines. The key to electrically powered mining machines is the belt conveying as transportation solution on every piece of equipment and from the mining face to the final location.

The degree of electrification in a mine decreases with the increase of discontinuously mining equipment. Fully electrically driven process chains inside the open pit can be realized by a BWE with self-propelled, electrically powered crawler undercarriages and subsequent transportation of loose material on conveyors.

The operation of fully mobile crushing plants, close to the mining face, only requires a shovel operation but no truck haulage. Big mining shovels are available in electrical versions which can be fed by the powering system coming from the mobile crushing plant.

A further decrease in mine electrification is the result of using an IPCC system with a semi mobile crushing plant (SMCP). Here, the material feeding requires a small truck fleet travelling from the shovel to the SMCP. Definitely, this system is one of the best choices in deep and narrow hard rock mines to guarantee selectivity and flexibility as well as minimizing huge energy (fuel) consumption caused by trucks in upward haulage and over long distances.

2.1. Cutting Solutions

BWEs can manage the sub-tasks loosening and loading in one step, resulting in the replacement of a separate shovel extraction by conventional BWE is applied in large size, soft rock deposits. They can range from small capacities of around 500 lm³/h in a compact size to giant excavators capable of handling huge overburden volumes of up to 19,000 lm³/h (mainly in European open pit lignite mines).

So far, most BWE applications worldwide have been in materials with a compressive strength of less than 6 MPa (see Figure 1). thyssenkrupp has designed a specific type of bucket wheel excavators for applications in materials of up to 50-80 MPa, the BARRACUDA[®] (Figure 2). The BARRACUDA[®] is a cutting machine for harder materials with high throughput rates which also incorporates the sub-tasks of loosening and crushing of the material. Due to the special cutting process, the material is broken into conveyable material size. It thus eliminates drilling and blasting which reduces a substantial cost factor in mining operations. [4, 5]

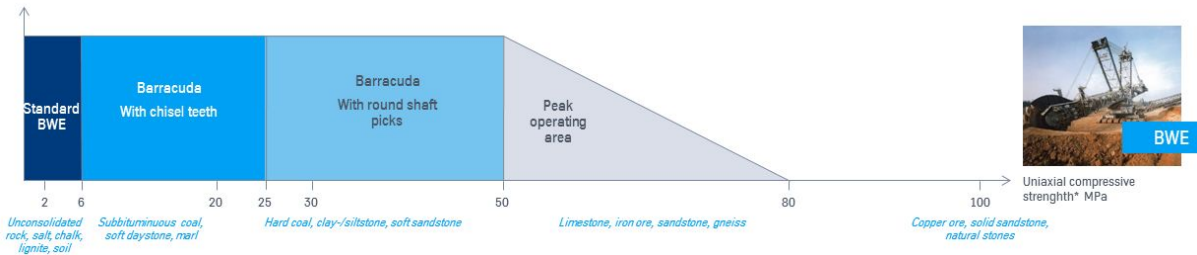


Figure 39. Application range of conventional bucket wheel excavators in comparison to the BARRACUDA[®]



Figure 40. BARRACUDA[®] bucket wheel excavator

2.2. Crushing Solutions

The essential parts of the crushing solutions are the crushing plants which basically crushes the material to a conveyable size. The plant design itself allows the installation of nearly all crusher types and sizes, thus soft and hard rock material can be handled (see Figure 3). High-capacity plants are in operation worldwide with hourly rates of more than 10,000 tons.

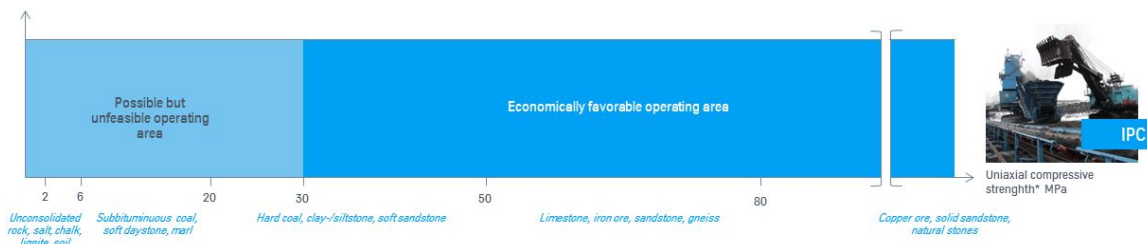


Figure 41. Material range of in-pit crushing and conveying systems

Fully-mobile Crushing Plants (FMCP). Crushing systems which totally eliminate the use of trucks are realized by electrically driven, crawler mounted mobile crushing plants. There, shovels directly load into the feed hopper of the crushing plant. The operational design of these systems allows multiple bench operations similar to the operational design of a BWE. The connection to the face conveyor is realized directly or by intermediate mobile transfer conveyors. The plants can be equipped with high capacity sizers and roll crushers in soft rock applications. In hard rock deposits, mobile plants equipped with grizzly plus jaw crusher, as currently realized in a Brazilian iron ore

mine (see Figure 4), or with the newly developed eccentric roll crusher (ERC) provide medium capacity ranges.



Figure 42. Mobile hard rock crushing plant

Semi-mobile Crushing Plants (SMCP). As the mining operation progresses and under consideration of an in-pit crushing and conveying system, semi-mobile crushing plants are recommended because they can be relocated by transport crawlers. The SMCPs can be applied in mine layouts with an irregular shape or in conical deep pits, where selective mining is quality-wise required and trucks are the technology of choice due to flexibility reasons. Huge overburden or waste masses from soft to hard materials from interwoven parts of the deposit are mostly handled by an IPCC system with semi-mobile crushing plants (see Figure 5) and final dumping by a spreader. [6]



Figure 43. Semi-mobile crushing plant at YiminHe coal mine

2.3. Combining Crushing, Cutting and Conveying Technologies

In most open pit mining applications, a combination of cutting, crushing and conveying technologies could and should be considered. The technology selection is influenced by the geology, the size of the mine, the waste ratio, shape and depth of the mineable deposit, the hardness and abrasiveness of the materials, the required annual production rates, initial investment, operating costs and mine life.

Design and planning of combined continuously working mining equipment that operates at the required production rates, and that meets the numerous site and geological constraints requires an integrated approach and solution. The basic requirements for successful implementation and design of a hybrid mining system are:

- Knowledge of mine requirements
- Experience in open pit mine planning of continuous mining systems
 - Initial locations and development of semi-mobile crushing plants
 - Connecting ramp configurations
 - Bench configurations for shiftable face conveyor
 - Incorporating of push-back planning (going deeper)
- Design and dimensioning of continuous mining equipment
- Close relationship and interfaces to the mine operators
- Flexibility in crusher type selection
- Expertise in designing in-pit and overland conveying systems as well as waste handling equipment

Mine development for an ore deposit extending into depth and width likewise with a hybrid continuous mining system could be realized with the following steps (exemplary):

- 1) Box cuts for initial installation of the semi-mobile crushing plants have to be prepared in a short time to open up the ore body as soon as possible
 - a) Opening up the mine by truck operation with horizontal haul distances to the waste area
 - b) Preparation of conveyor ramps and starting dam for spreader by truck haulage
 - c) Preparation of crusher pocket locationsThe first step ends with the installation of crushing plants, connecting conveyor and spreader equipment for waste handling
- 2) The mine is expanded in the overlying overburden and the intermediate waste to open and widen up the mine for fully mobile continuous mining systems
 - a) Benches will be prepared by using truck shuttle to the existing semi-mobile crushing plants
 - b) Face conveyor will be installed on the new benches and connected to the existing spreader-conveyor systemThe step ends with the start of operation in upper layers of either a mobile crushing plant or BWE cutting equipment connected to the shiftable face conveyor
- 3) Depth of mine has reached a reasonable level to install another semi-mobile crushing plant with separate conveyor routing to the processing plant for ore only
- 4) Harder waste layers, deeper in the mine and closer located to the ore body requires drilling and blasting but allows mobile crushing equipment connected to face conveyor as well
 - a) Similar to the upper layers, face conveyor will be installed and connected to the existing spreader

- b) Bench configurations can be planned in same dimensions as for the upper mining system
- c) Depending on material characteristics in overburden and waste, the operationally similar systems of BWE and mobile crushing plant are interchangeable on the different bench levels

In the end, the system can consist of semi-mobile crushing plants, BWEs and fully-mobile crushing plants in overburden and waste which are all connected to one single continuously working disposal system with conveyors and a spreader. A small flexible truck fleet can support, if required, the mining in narrow pit areas or assist in pre-stripping phases close to the topography to equalize yearly required stripping ratios.

3. TECHNO-ECONOMIC SIMULATION MODEL

A dynamic spreadsheet model has been developed for use in early project evaluation studies and decision making. The model simulates the abovementioned continuous mining systems including the necessary sub-processes drilling and blasting, as well as the discontinuous haulage by trucks. The following paragraphs give a detailed explanation of the model structure, outline results and conclude the KPI analysis.

3.1. Model Structure

The simulation structure is schematically shown in Figure 6. The model depends on input data and scenarios that have to be developed by establishing scenario-based production flow sheets. The accuracy of the details depends on the sub-process. Generally, sub-processes and costs are based on equipment cost databases [7], empirical values and project work. Relevant evaluation KPIs are generated by the model to allow for a scenario comparison with the respective base case. The truck and shovel scenario acts as the base case for this investigation.

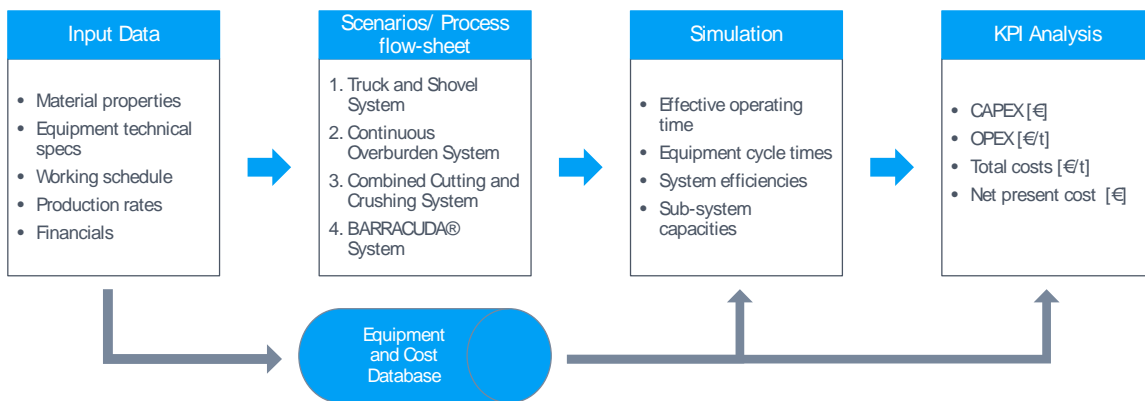


Figure 44: Model structure

To compare different mining systems, clearly defined system boundaries are necessary. The model uses an overall mine cross-section standard, which represents the mine bottleneck (Figure 7). That means a plant design for the assumed cross-section can be used for the overall mine life. A simplification of the mine is required for the model to be universally applicable. The developed scenarios for the mining cross-section are further described in the following section.

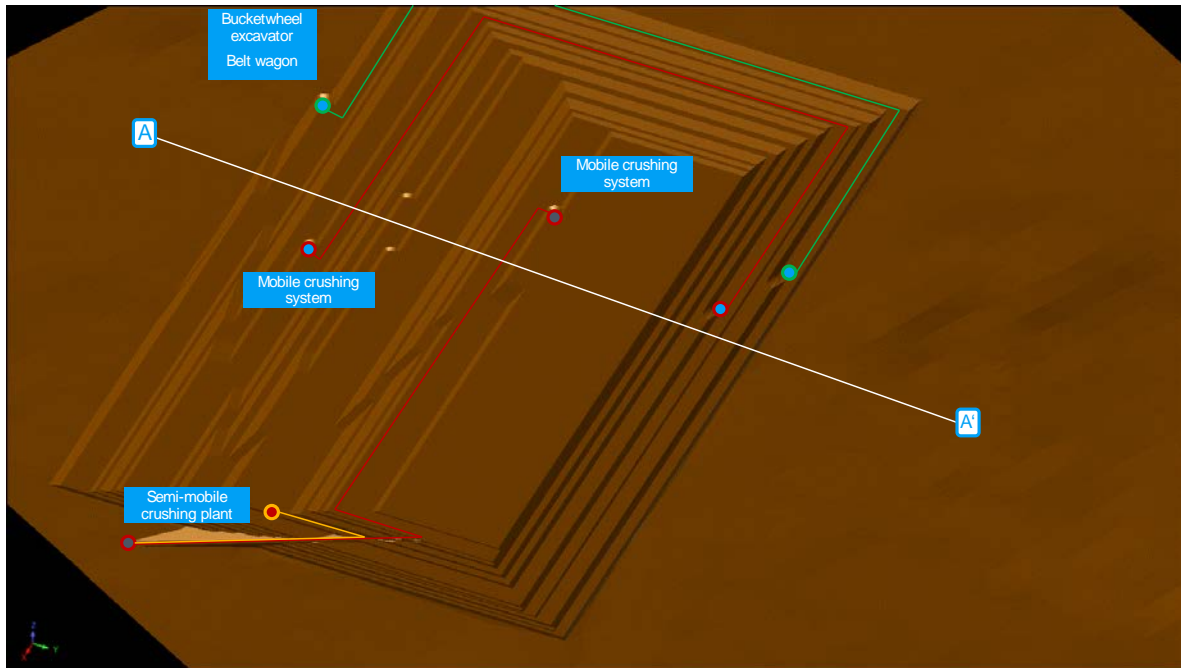


Figure 45. Schematic isometric view of model mine (it represents scenario 3)

3.2. Scenarios

This investigation compares in total four different scenarios:

1. Truck and Shovel System
2. Continuous Overburden System
3. Combined Cutting and Crushing System
4. BARRACUDA[®] System

The following conveyor map shall give an overview of the different scenarios and also about the amount of continuous mining equipment in use. The dark lines represent the coal conveyors and the blue lines are overburden and interburden conveyors.

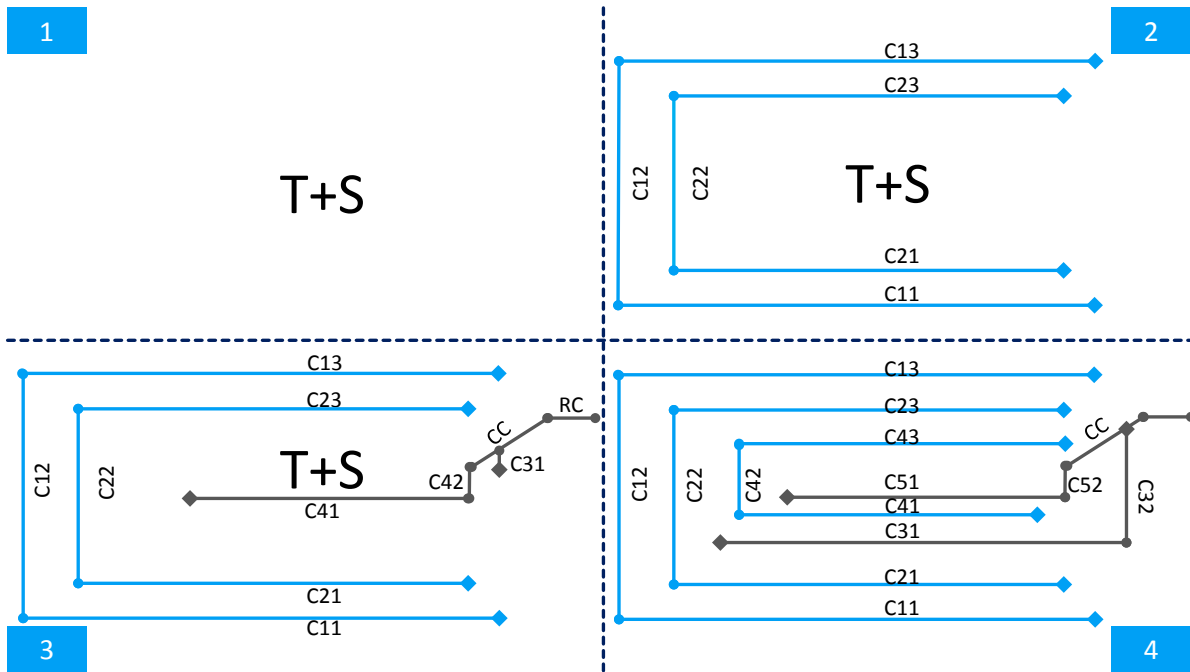


Figure 46. Conveyor map of different scenarios

The “truck and shovel” scenario simulates a coal mine which only operates trucks for overburden and interburden removal as well as coal production. The scenario also entails a coal crushing station to enable a valid comparison.

The second scenario “continuous overburden system” operates two parallel FMCPs connected to two spreader systems. The coal production and interburden removal is realized by trucks. This scenario is commonly applied in deposits with very irregular geology or where geology varies within very short distances. As for the previous scenario, a coal crushing station is implemented due to comparability.

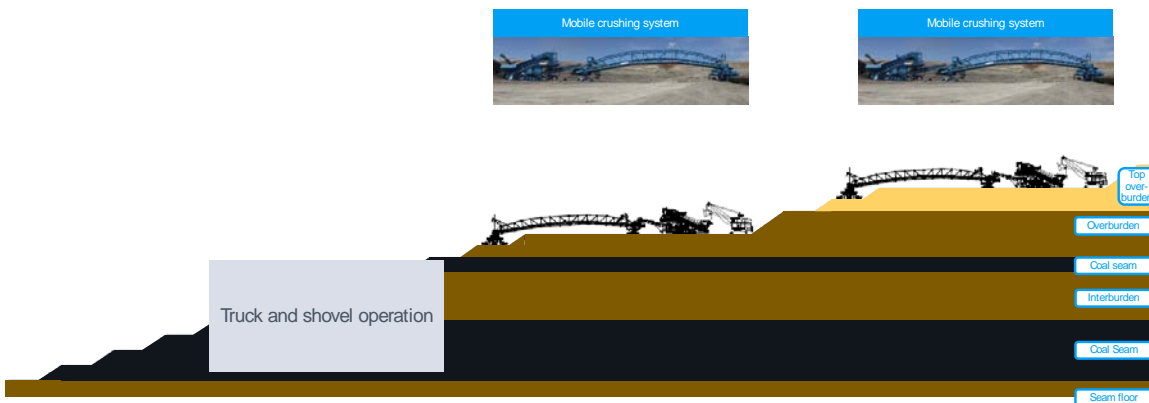


Figure 47. Cross-section of model mine (scenario 2)

The “combined cutting and crushing” scenario introduces a BARRACUDA[®] system for the first layer, a FMCP system for the second layer, a SMCP system which is fed by trucks for the first coal seam, for the interburden and partly the second coal seam, and a FMCP for the remaining part of the second coal seam. The truck and shovel system in the intermediate part enables the flexibility to

selectively mine coal and interburden at the same time, which would be more complicated with a FMCP system.

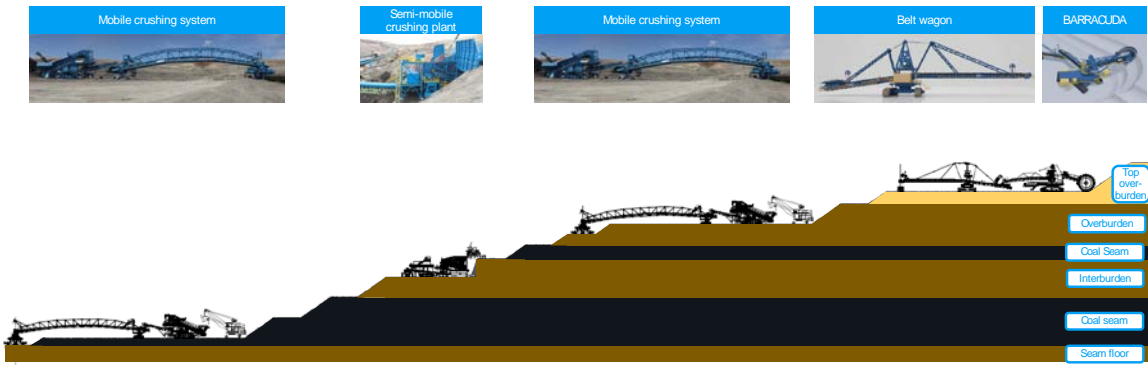


Figure 48. Cross-section of model mine (scenario 3)

The “*BARRACUDA*®” scenario only operates BWEs for overburden and interburden removal as well as coal production. BWEs are state of the art in multi-seam coal operations as they can selectively mine coal and waste on one bench.

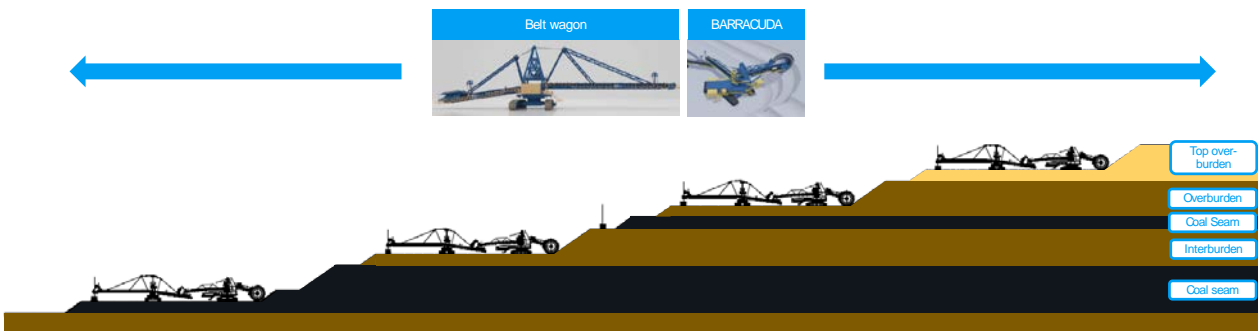


Figure 49. Cross-section of model mine (scenario 4)

3.3. Results and Conclusion

As mentioned in the previous section, the work includes a comprehensive literature review and the investigation of four case studies for the application of continuous mining systems in a hard coal operation. The approach of the work has been expanded to a more holistic evaluation of mining systems to ensure a better transferability to other mine sites. Due to confidentiality agreements with the project partners the used numbers are slightly altered. This has no effect on the evaluation as the comparisons or the relations are still the same.

The following input parameters are used for the simulation: [7, 8, 9, and 10].

Table 8. Input data

Input	Value	Unit
<i>Overall mine data</i>		
Yearly coal production	30.000.000	t/a
Depth	140	m
Width of cut	approx. 1,700	m
Length of cut	approx. 2,500	m
<i>Material properties</i>		
Coal density	1.2	t/m ³
Waste density	1.9	t/m ³
<i>Working time input</i>		
Hours per shift	8	h/shift
Shifts per day	3	shifts/d
Days per week	7	d/w
Days per year	354	d/a
Unproductive days (weather, etc.)	7	d/a
Holidays	30	d/a
Illness	7	d/a
<i>Financials</i>		
Labor costs (example. of low-wage country)	15,000	€a
Electricity costs	0.12	€/kWh

The selected KPIs for evaluation are CAPEX, OPEX, total costs and personnel requirements for each case study or mining system. Following simulation results are obtained (Figure 12):

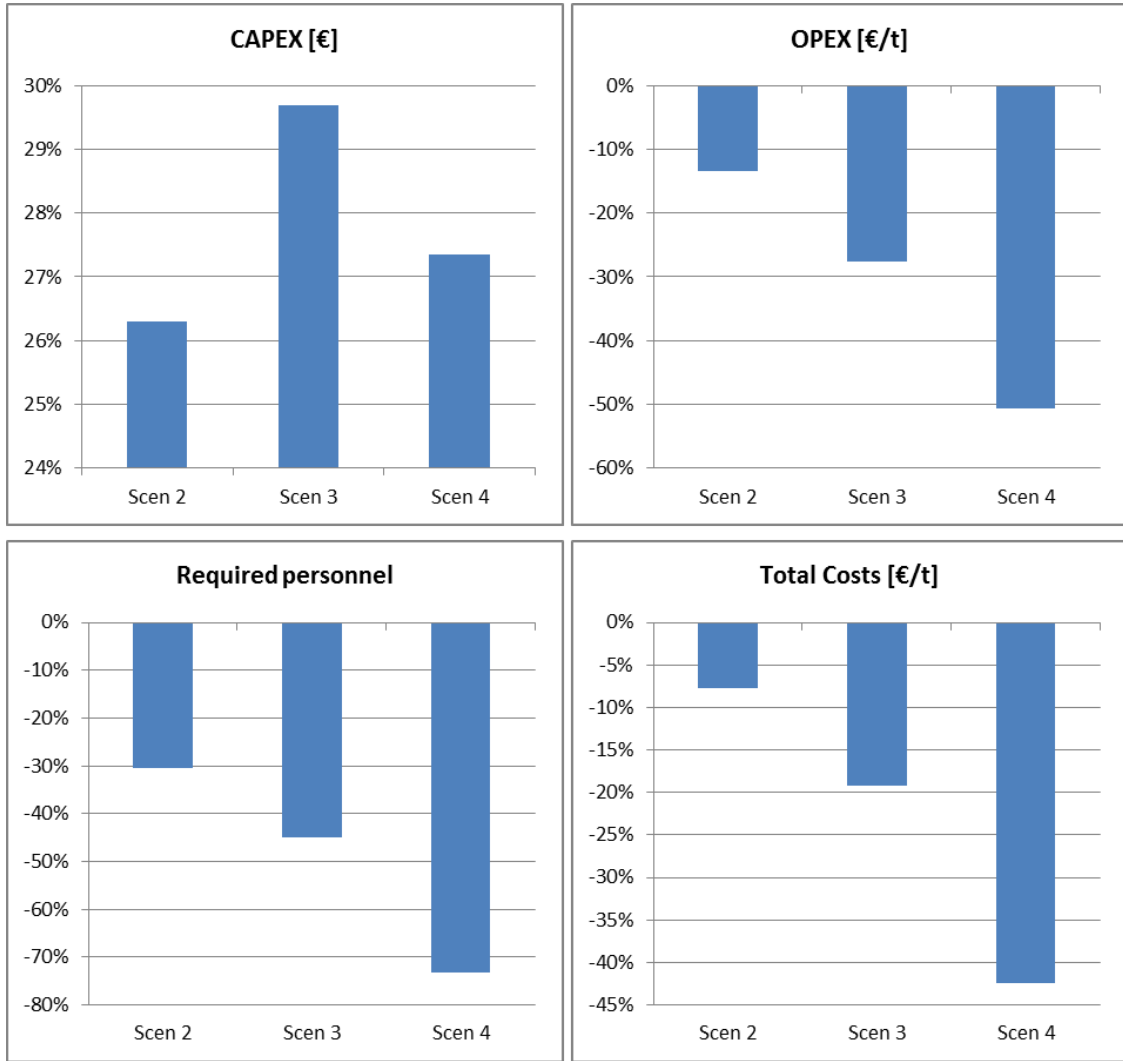


Figure 50. Simulation results

Usually continuous mining systems have higher CAPEX. Within this case study CAPEX increases of 25%-30% are obvious concerning the Truck and Shovel scenario. Interestingly, the BARRACUDA[®] system (scenario 4) has lower CAPEX than the scenario 3. Main reason is that this system only operates with 4 BARRACUDAs[®] which seems to be realistic since a BWE can selectively mine material in one block. OPEX savings of continuous systems are between 10%-50%. Total cost savings are between 8%-45% due to the higher capex share in the figure. Personnel savings are in the range of 30% and 75%.

Finally, one can conclude that all continuous mining systems have significantly higher initial CAPEX compared to the Truck and Shovel scenario. All other KPIs outline relevant savings. In addition, savings drastically increase from scenario 2 to scenario 4; hence with the application level of continuous mining systems.

4. CASE STUDY: YIMINHE COAL MINE IN CHINA

The hard coal open pit mine YiminHe, located in the Inner Mongolia of China, started its operation with crushing technology and continuously working conveyor equipment in 2007. A shovel-fed fully mobile crushing plant was put into operation connected to a shiftable conveyor system and prepared for multiple bench operation in the coal seam by use of two transfer conveyors.

The successful implementation of conveyor based equipment with a design capacity of up to 3,500 tons per hour led to a second in-pit crushing system for coal processing designed in the same capacity range but as a semi-mobile plant.

A further step towards a combined crushing, cutting and conveying approach was the decision by China Huaneng Group to order a BARRACUDA[®] system for overburden. The new system, which will start operation in 2019, implements a BWE, combined with a belt wagon, several mine conveyors and one large spreader for material disposal of up to 10,000 t/h. YiminHe coal mine is one of the large open pits where cutting, crushing and conveying is realized as the key to optimize operational costs and simultaneously minimizing the mine’s overall carbon footprint. Figure 13 and Figure 14 introduce the delivered and new systems.

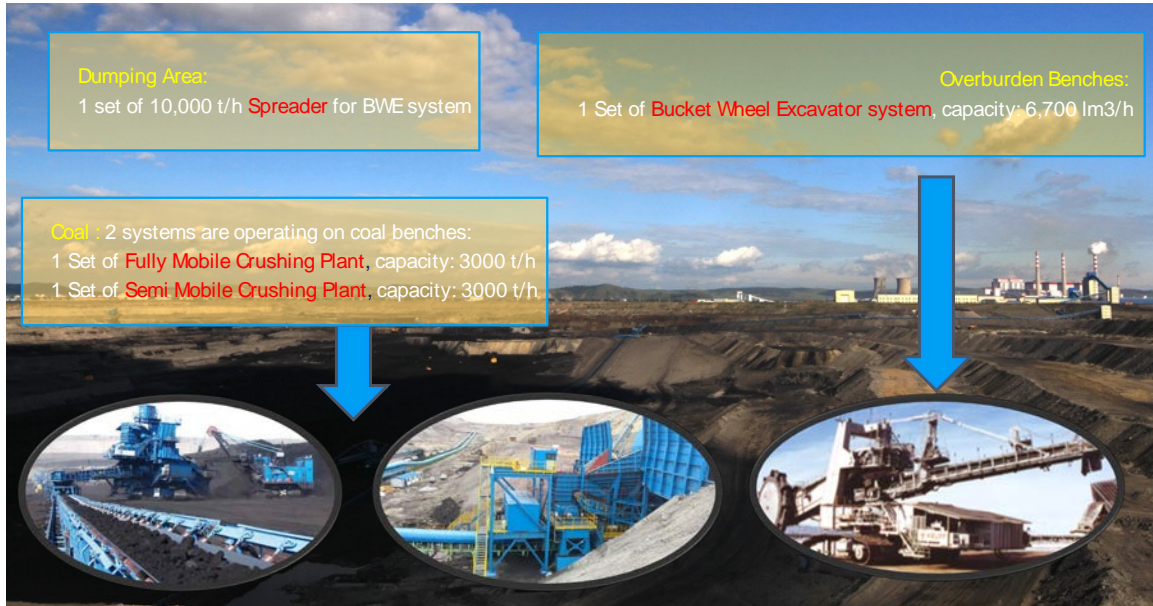


Figure 51: Overview continuous mining systems at YiminHe mine

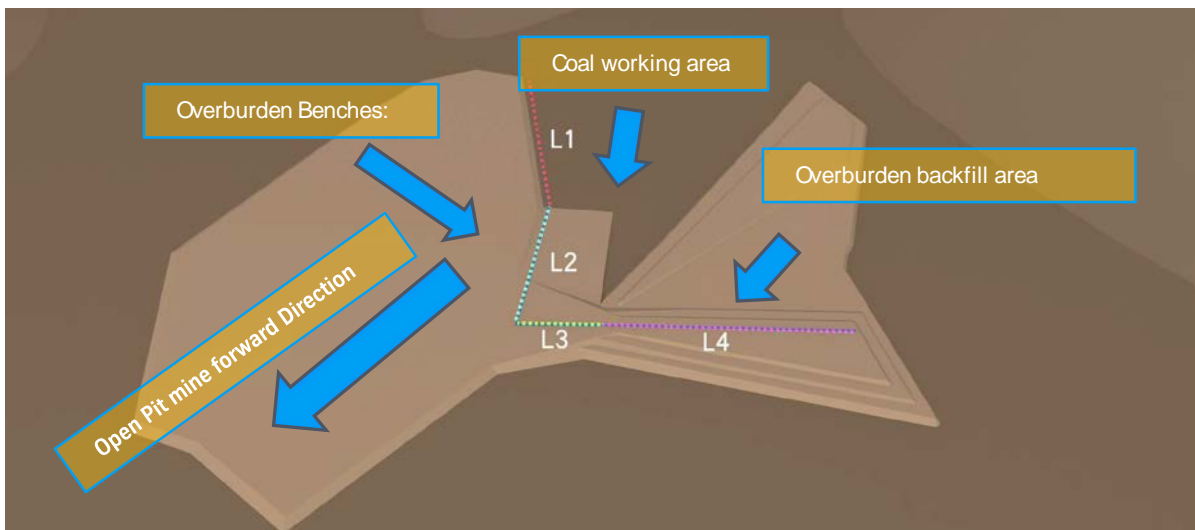


Figure 52: BARRACUDA[®] system overview

5. SUMMARY

Hybrid continuous mining systems are a real alternative for every mining project. A successful application requires a detailed mine planning experience and knowledge to handle both, ore and waste scheduling over a mine lifetime and on planned production quantities and qualities. Advanced mine techniques like using hard rock cutting with proven BWEs minimizes the requirements for drilling and blasting. Fully or semi-mobile in-pit crushing plants reduce the need of truck haulage significantly leading to cost savings for the mine operator.

This was valued by using a simplified simulation environment. The results show that while the CAPEX are 25-30% higher for continuous mining systems, savings in total costs are ranging between 8%-45%. This results from significant savings of 10-50% in OPEX due to the use of electrically powered equipment in general and reduced drilling and blasting costs for system incorporating the BARRACUDA[®].

REFERENCES

- [1] Berkheimer, E. (2011). Selection and Sizing of Excavating, Loading, and Hauling Equipment. SME Mining Engineering Handbook, 3, 931-939
- [2] Utey, W. (2011). In-Pit Crushing . SME Mining Engineering Handbook, 3, 941-956
- [3] Mentges, U. (2018). Delivering Results. World Coal, 03/18, 31-35.
- [4] Mentges, U., Walter J., Ebert S. (2017). Bucket Wheel Excavator Barracuda – A revolutionary new Mining Concept. GeoResources Journal, 03/17, 39-44.
- [5] Schröder, D., Raatz, V. (2016). Barracuda Concept. Presentation at AIMS International Mining Symposium, Aachen.
- [6] Raaz, V., Mentges, U. (2011). In-pit crushing and conveying with fully mobile crushing plants in regards to energy efficiency and CO2 reduction. Presentation at IPCC, Belo Horizonte.
- [7] InfoMine USA, Inc., Aventurine Engineering, Inc. (2016). Mine and Mill Equipment Cost guide, An Estimator's Guide 2016. InfoMine USA Inc. CostMine Division.
- [8] Winkler, S. (2016). Labor Market & Salary Report 2016 | 2017. German Chamber of Commerce in China.
- [9] GlobalPetrolPrices (2018). China Diesel prices, liter. Online, https://www.globalpetrolprices.com/China/diesel_prices/ , 18.07.2018
- [10] GlobalPetrolPrices (2018). China Gasoline prices, liter. Online, https://www.globalpetrolprices.com/China/gasoline_prices/ , 18.07.2018

Why One Dimension is Not Enough – A Comparative Study of Lignite Resources Estimation Using Drillhole Mineable Lignite Compositing of Uncorrelated Seams and Mineable Lignite Compositing of Correlated Lignite Seams

Ioannis Kapageridis and Andreas Iordanidis

Technological Educational Institute of Western Macedonia, Koila, Kozani, 52100, Greece

ABSTRACT

Lignite deposits in Greece of the type consisting of multiple thin lignite layers are traditionally estimated using a one-dimensional compositing approach that suffers from large error margins particularly in the presence of medium to large tectonism and uneven vertical distribution of lignite seams. Each drillhole is evaluated using mining and processing criteria leading to a number of mineable lignite “packages”, the sum of which is reported as the total mineable lignite at the drillhole horizontal location. The total minable lignite values from the various drillholes are interpolated horizontally leading to a two-dimensional model of the mineable lignite parameter. A more advanced version of this one-dimensional approach has been applied with improved results in the past. In this version, the one-dimensional approach was limited to a single mine bench and repeated separately for each bench, thus reducing the scale of potential errors and better approaching the vertical distribution of mineable lignite. In effect, each bench was approached as an isolated lignite “deposit”, reducing the effects of applying a one-dimensional approach to a 3D modelling problem but not making them completely disappear. Lignite deposits, such as the one examined in this paper, require the development of a thorough stratigraphic model to allow the reporting of accurate lignite resources and form the basis for solid mine planning and lignite reserves calculation. The evaluation of mineable lignite using mining and processing criteria can then be applied to modelled raw lignite seams leading to an overall three-dimensional model of the deposit that allows accurate lignite resources calculation even in the presence of tectonism. This paper presents all three modelling approaches through an extensive case study based on part of a real lignite deposit. The effects of using each of the approaches are analysed and the benefits of the three-dimensional approach are clearly demonstrated.

1. INTRODUCTION

1.1. The Modelling Problem and Solution Approaches

Thin layered lignite deposits (known as Zebra deposits) are commonly modelled using a one-dimensional compositing approach that suffers from large error margins particularly in the presence of medium to large tectonism and uneven vertical distribution of lignite seams. Each drillhole is composited using mining and quality criteria forming mineable lignite sections, the sum of which is reported as the total mineable lignite at the drillhole horizontal location. The total minable lignite values from the various drillholes are interpolated horizontally leading to a two-dimensional grid model of the mineable lignite parameter. This approach, even though capable of calculating global lignite resources with acceptable accuracy provided a high sample density, it is particularly prone to errors in calculating local lignite resources which are necessary for effectively planning and scheduling a continuous mining process. Another issue with this approach is the sensitivity of the results to potentially incomplete or incorrectly interpreted drillholes that due to the one-dimensional

nature of the modelling process can lead to significant errors in the local resource estimates. All this uncertainty has led to the use and experimentation with various interpolation algorithms like inverse distance and kriging and their parameters, in an effort to improve on the estimates produced by bringing the local estimate closer to the single value reported by the closest composited drillhole – but the real problem lies in what happens between drillholes.

Lignite deposits, such as the one examined in this paper, require the development of a thorough stratigraphic model to allow the reporting of accurate lignite resources and form the basis for solid mine planning and lignite reserves calculation. Such a stratigraphic model requires the painful but irreplaceable step of seam correlation in sections and plans before any compositing of mineable lignite takes place. The evaluation of mineable lignite using mining and processing criteria can then be applied to modelled raw lignite seams leading to an overall three-dimensional model of the deposit that allows accurate lignite resources calculation even in the presence of tectonism. This paper presents all three modelling approaches through an extensive case study based on part of a real lignite deposit. The effects of using each of the approaches are analysed and the benefits of the three-dimensional approach are clearly demonstrated.

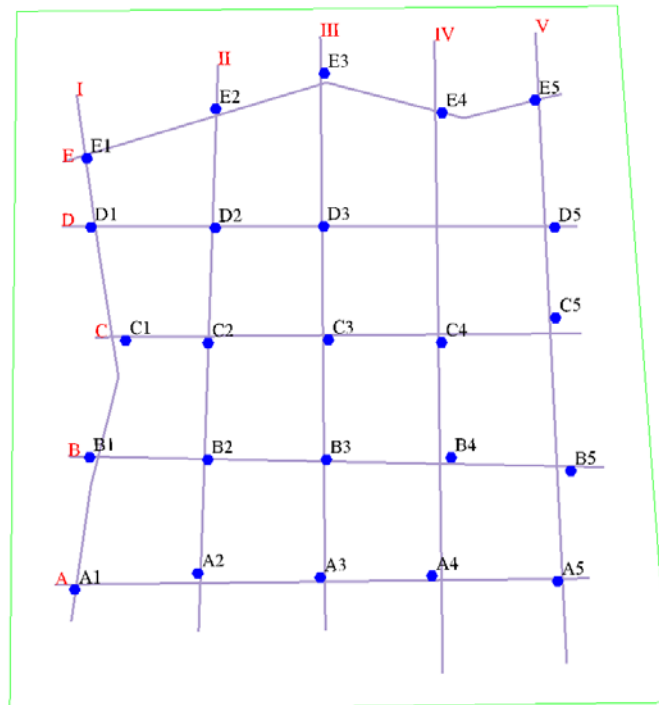


Figure 1. Location and naming of drillholes and sections used in the study.

1.2. Example Dataset

Data used to compare the lignite resource modelling approaches in this paper come from an exhausted lignite mine in NW Greece. A small area of the mine was selected and a total of 24 drillholes on a random grid of 5x5 (Figure 1). The model limits cover an area of 1.32km². The names and coordinates of the drillholes were changed for confidentiality purposes. The area topography was not used in the study for the same reason – the drillhole collar was taken as the top of overburden (excluding drillhole C5). Reported resources were limited only by the study area polygon – no pit surface was used in the study. Figure 1 shows the drillhole collar locations in plan view. Drillholes were named after their row and column number which correspond to the section names. For

example, drillhole A1 appears in Section A and Section I. The 24 drillholes contained a total of 2,950 original (raw) intervals. The dataset was imported and validated in Maptek Vulcan.

2. ONE-DIMENSIONAL COMPOSITING OF TOTAL DRILLHOLE MINEABLE LIGNITE INTERVALS

2.1. Method Analysis

The method to composite drillhole mineable intervals described in this section is very similar to the one applied in Greek lignite deposits [1]. The method used in this paper is using the corresponding mineable intervals option in Maptek Vulcan software plus some extra steps before and after applying this option to make it more suitable for lignite seams. A comparative study has been performed in the past to prove the similarity of the results produced by this approach and the software traditionally used for compositing of Greek lignite deposits [2]. The method is applied using the following steps:

- **Pass 1:** The program looks at samples down the hole and classifies each sample as lignite or waste based on the ash cutoff value specified.
- **Pass 2:** The program combines adjacent samples of lignite and waste to produce runs of pure lignite and pure waste.
- **Pass 3:** Working from the top of the hole down, the program checks if the waste interval between the first lignite run and the subsequent lignite run is shorter than the waste absorption maximum length. If the waste length is longer than this limit, then the lignite runs are left as separate composites and the waste length from the second lignite run to the third is checked. If the waste length is shorter than the limit, then the first lignite run, the waste run and the second lignite run are added together, and the resulting ash value is computed. If the ash value is higher than the lignite/waste cutoff value, then the lignite and waste runs are left as individual composites and the process moves onto the second and third lignite runs. If the resulting ash value is lower than the lignite/waste cutoff value, then the interval is accepted as a single lignite composite. The waste length between this new lignite composite and the subsequent lignite run is then checked, and the process described above is repeated.
- **Pass 4:** At this stage there are lignite runs that incorporate internal waste where possible and whose ash value is below the lignite/waste cutoff value. The procedure continues then to add upper and lower waste dilution to these lignite runs. It will add adjacent waste samples up to a dilution length specified. It should be noted that this step will not disqualify any lignite runs. Roof and floor losses area applied to lignite intervals and respective gains to waste intervals.
- **Pass 5:** The final pass checks all resulting lignite runs to see if they are longer than the minimum lignite run length. Lignite runs that are shorter than this limit, are reclassified as waste and absorbed into the surrounding waste runs. All quality calculations are length weighted.

Figure 2 shows a simplified example of the input (raw) and output (composited) version of a drillhole using the mineable intervals compositing method. Lignite and waste raw intervals are combined to form mineable lignite or waste composited intervals based on criteria such as minimum lignite thickness, maximum waste absorption thickness, mineable lignite ash upper limit (cutoff) and mineable lignite roof and floor losses and dilution.

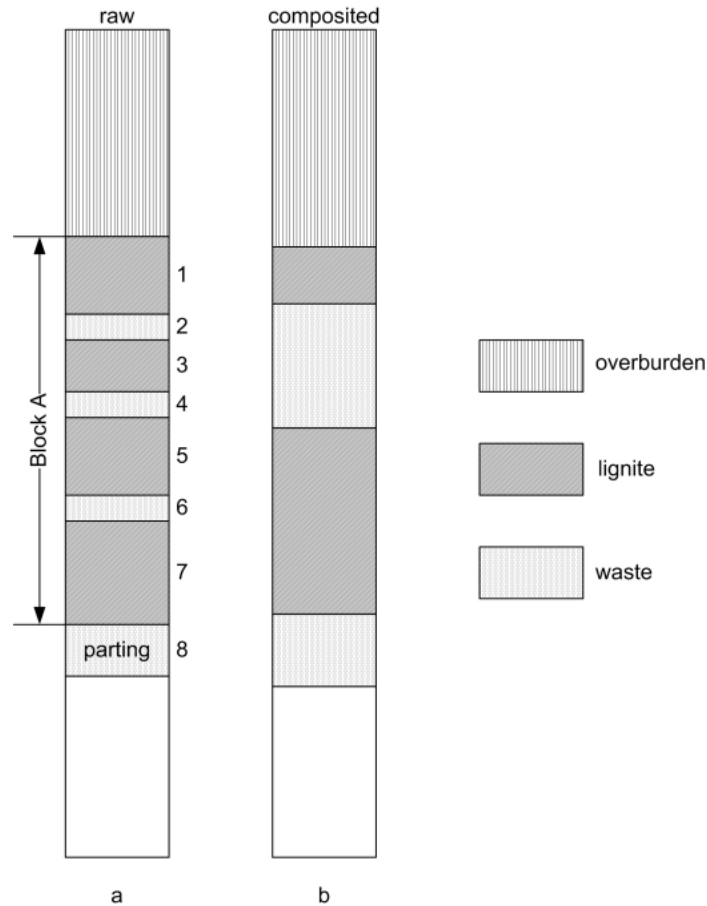


Figure 2. Simplified example of raw lignite and waste intervals (a) and composited mineable lignite and waste intervals (b).

2.2. Compositing

Applying this method to the 24 drillholes of the example dataset led to the generation of 1,016 composited mineable intervals of lignite and waste from the 2,950 raw intervals. The generated composites table was added to the original drillhole database. Figure 3 presents the output of each of the five passes of the mineable intervals compositing method on part of a drillhole from the dataset. Lignite intervals at each pass are coded as CO. Waste horizons are coded as WASTE after the first pass. Only part of the drillhole is shown due to space limitations. The total length (thickness) of mineable lignite per drillhole was calculated next. This was stored together with other information such as the top and bottom depth of mineable lignite in a formatted text file. The file contained information on the thickness and depths of overburden and midburden. These files were used to calculate and locate lignite resources within the study area limits. A 0.5m minimum mineable lignite thickness and 0.3m waste thickness was applied. The maximum ash content for lignite was set to 36% and the roof and floor losses for lignite were 0.1m.

2.3. Resource Modelling

Using the information contained in the formatted text files for the thickness, roof and floor of the mineable lignite and the corresponding values for overburden and midburden, grid models were generated using the inverse distance weighting method. The power of 1 for inverse distance was used for the roof and floor models, while the power of 2 was used to model thicknesses. Figure 4 shows section C – the overburden is clearly displayed as a single layer, while lignite and midburden are

shown together. The absence of seam correlation means that it is not possible to display (and model) lignite seams as separate layers in section.

Original			Pass 1			Pass 2			Pass 3			Pass 4			Pass 5		
Litho	Length	Ash	Litho	Length	Ash	Litho	Length	Ash	Litho	Length	Ash	Litho	Length	Ash	Litho	Length	Ash
AL	3.70	100.00	WASTE	3.70	100.00	WASTE	3.70	100.00	WASTE	12.60	100.00	WASTE	12.70	100.00	WASTE	12.70	100.00
CO	0.50	46.50	WASTE	0.50	46.50	WASTE	0.50	46.50	WASTE	0.60	100.00	WASTE	0.60	100.00	WASTE	0.60	100.00
MR	0.60	100.00	WASTE	0.60	100.00	WASTE	0.60	100.00	WASTE	0.60	100.00	WASTE	0.60	100.00	WASTE	0.60	100.00
AL	2.40	100.00	WASTE	2.40	100.00	WASTE	2.40	100.00	WASTE	2.40	100.00	WASTE	2.40	100.00	WASTE	2.40	100.00
AL	0.60	100.00	WASTE	0.60	100.00	WASTE	0.60	100.00	WASTE	0.60	100.00	WASTE	0.60	100.00	WASTE	0.60	100.00
CO	0.60	38.50	WASTE	0.60	38.50	WASTE	0.60	38.50	WASTE	0.60	100.00	WASTE	0.60	100.00	WASTE	0.60	100.00
MR	0.80	100.00	WASTE	0.80	100.00	WASTE	0.80	100.00	WASTE	0.80	100.00	WASTE	0.80	100.00	WASTE	0.80	100.00
CO	0.60	45.10	WASTE	0.60	45.10	WASTE	0.60	45.10	WASTE	0.60	100.00	WASTE	0.60	100.00	WASTE	0.60	100.00
AL	1.00	100.00	WASTE	1.00	100.00	WASTE	1.00	100.00	WASTE	1.00	100.00	WASTE	1.00	100.00	WASTE	1.00	100.00
MR	0.90	100.00	WASTE	0.90	100.00	WASTE	0.90	100.00	WASTE	0.90	100.00	WASTE	0.90	100.00	WASTE	0.90	100.00
CO	0.40	36.20	WASTE	0.40	36.20	WASTE	0.40	36.20	WASTE	0.40	100.00	WASTE	0.40	100.00	WASTE	0.40	100.00
MR	0.50	100.00	WASTE	0.50	100.00	WASTE	0.50	100.00	WASTE	0.50	100.00	WASTE	0.50	100.00	WASTE	0.50	100.00
CO	1.20	30.90	CO	1.20	30.90	CO	1.20	30.90	CO	1.20	30.90	CO	1.20	30.90	CO	1.00	30.90
MR	2.60	100.00	WASTE	2.60	100.00	WASTE	2.60	100.00	WASTE	2.60	100.00	WASTE	2.60	100.00	WASTE	2.80	100.00
CO	0.40	35.80	CO	0.40	35.80	CO	0.40	35.80	CO	0.40	27.22	CO	0.40	27.22	CO	0.40	27.22
MR	1.70	25.20	CO	1.70	25.20	CO	1.70	25.20	CO	1.70	25.20	CO	1.70	25.20	CO	1.90	27.22
MR	0.70	100.00	WASTE	0.70	100.00	WASTE	0.70	100.00	WASTE	0.70	100.00	WASTE	0.70	100.00	WASTE	0.90	100.00
CO	0.60	23.00	CO	0.60	23.00	CO	0.60	23.00	CO	0.60	9.90	CO	0.60	9.90	CO	0.60	9.90
MR	0.60	22.70	CO	0.60	22.70	CO	0.60	22.70	CO	0.60	9.90	CO	0.60	9.90	CO	0.60	9.90
MR	0.50	100.00	WASTE	0.50	100.00	WASTE	0.50	100.00	WASTE	0.50	100.00	WASTE	0.50	100.00	WASTE	0.50	100.00
CO	1.40	36.00	WASTE	1.40	36.00	WASTE	1.40	36.00	WASTE	1.40	100.00	WASTE	1.40	100.00	WASTE	1.40	100.00
MR	0.50	100.00	WASTE	0.50	100.00	WASTE	0.50	100.00	WASTE	0.50	100.00	WASTE	0.50	100.00	WASTE	0.50	100.00
CO	1.60	40.90	WASTE	1.60	40.90	WASTE	1.60	40.90	WASTE	1.60	100.00	WASTE	1.60	100.00	WASTE	1.60	100.00
MR	1.00	100.00	WASTE	1.00	100.00	WASTE	1.00	100.00	WASTE	1.00	100.00	WASTE	1.00	100.00	WASTE	1.00	100.00
CO	0.40	40.60	WASTE	0.40	40.60	WASTE	0.40	40.60	WASTE	0.40	100.00	WASTE	0.40	100.00	WASTE	0.40	100.00
AL	0.90	100.00	WASTE	0.90	100.00	WASTE	0.90	100.00	WASTE	0.90	100.00	WASTE	0.90	100.00	WASTE	0.90	100.00
CO	1.30	34.40	CO	1.30	34.40	CO	1.30	34.40	CO	1.30	34.40	CO	1.30	34.40	CO	1.10	34.40
MR	0.30	100.00	WASTE	0.30	100.00	WASTE	0.30	100.00	WASTE	0.30	100.00	WASTE	0.30	100.00	WASTE	0.50	100.00
CO	0.50	35.90	CO	0.50	35.90	CO	0.50	35.90	CO	0.50	28.83	CO	0.50	28.83	CO	0.50	28.83
MR	1.00	25.30	CO	1.00	25.30	CO	1.00	25.30	CO	1.00	25.30	CO	1.00	25.30	CO	1.30	28.83
MR	1.30	100.00	WASTE	1.30	100.00	WASTE	1.30	100.00	WASTE	1.30	100.00	WASTE	1.30	100.00	WASTE	1.30	100.00
MR	6.10	100.00	WASTE	6.10	100.00	WASTE	6.10	100.00	WASTE	6.10	100.00	WASTE	6.10	100.00	WASTE	6.10	100.00
CO	0.60	23.30	CO	0.60	23.30	CO	0.60	23.30	CO	0.60	23.30	CO	0.60	23.30	CO	0.40	23.30
MR	0.50	100.00	WASTE	0.50	100.00	WASTE	0.50	100.00	WASTE	0.50	100.00	WASTE	0.50	100.00	WASTE	0.70	100.00
CO	0.50	28.60	CO	0.50	28.60	CO	0.50	28.60	CO	0.50	27.98	CO	0.50	27.98	CO	0.50	27.98
MR	0.80	27.60	CO	0.80	27.60	CO	0.80	27.60	CO	0.80	27.98	CO	0.80	27.98	CO	0.80	27.98
CO	1.20	39.60	WASTE	1.20	39.60	WASTE	1.20	39.60	WASTE	1.20	39.60	WASTE	1.20	39.60	WASTE	1.40	39.60
MR	0.80	27.60	CO	0.80	27.60	CO	0.80	27.60	CO	0.80	27.98	CO	0.80	27.98	CO	0.80	27.98
CO	1.20	33.50	CO	1.20	33.50	CO	1.20	33.50	CO	1.20	33.50	CO	1.20	33.50	CO	1.00	33.50
MR	0.40	100.00	WASTE	0.40	100.00	WASTE	0.40	100.00	WASTE	0.40	100.00	WASTE	0.40	100.00	WASTE	0.60	100.00
CO	1.40	22.70	CO	1.40	22.70	CO	1.40	22.70	CO	1.40	22.09	CO	1.40	22.09	CO	1.40	22.09
MR	0.20	17.80	CO	0.20	17.80	CO	0.20	17.80	CO	0.20	29.19024	CO	0.20	29.19024	CO	0.20	29.19024
MR	0.20	100.00	WASTE	0.20	100.00	WASTE	0.20	100.00	WASTE	0.20	100.00	WASTE	0.20	100.00	WASTE	0.20	100.00
CO	0.25	18.00	CO	0.25	18.00	CO	0.25	18.00	CO	0.25	18.00	CO	0.25	18.00	CO	0.25	18.00
MR	0.75	100.00	WASTE	0.75	100.00	WASTE	0.75	100.00	WASTE	0.75	100.00	WASTE	0.75	100.00	WASTE	0.95	100.00
CO	0.80	21.20	CO	0.80	21.20	CO	0.80	21.20	CO	0.80	26.80	CO	0.80	26.80	CO	0.80	26.80
MR	0.80	32.90	CO	0.80	32.90	CO	0.80	32.90	CO	0.80	26.80	CO	0.80	26.80	CO	0.80	26.80
CO	0.40	25.80	CO	0.40	25.80	CO	0.40	25.80	CO	0.40	26.80	CO	0.40	26.80	CO	0.40	26.80
MR	0.20	100.00	WASTE	0.20	100.00	WASTE	0.20	100.00	WASTE	0.20	100.00	WASTE	0.20	100.00	WASTE	0.30	100.00

Figure 3. Example of drillhole composited with the 5-pass mineable interval compositing method – interval type changes from one pass to another are shown in light green and interval length changes in light blue.

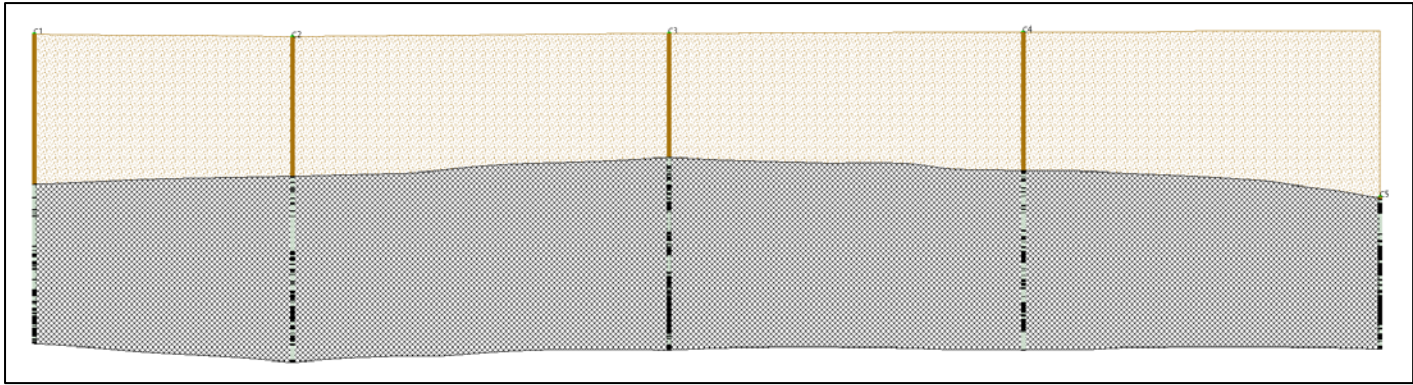


Figure 4. Section C showing composited drillholes and modelled overburden (brown), lignite roof and floor surfaces (black). Drillhole C5 is not used for the modelling of overburden roof and thickness.

As lignite seams are not correlated, we rely on the total mineable lignite thickness model for resource estimation. Stripping ratio is also calculated using the total overburden and midburden thickness models. Calculating lignite resources per bench is based on the total mineable midburden/lignite ratio and the thickness of their sum (lignite plus midburden) inside each bench. The same midburden/lignite ratio is effectively applied to all benches, with the only possibly varying parameter being the thickness of the mineable lignite plus midburden. For benches being totally enclosed in the area between the roof and floor of mineable lignite, this parameter is constant, leading to equal resources being reported in these benches.

3. ONE-DIMENSIONAL COMPOSITING OF DRILLHOLE MINEABLE LIGNITE INTERVALS PER BENCH

3.1. Method Analysis

The second approach considered is based on the 5-pass compositing method discussed in the previous section but adds an extra pass where the produced lignite and waste composite intervals are split and coded based on surfaces corresponding to mining benches (Figure 5). The height of the benches can be constant or different between benches, and essentially controls the vertical resolution of the calculation. As the interval splitting takes place after any quality and thickness-based classification to lignite or waste, the added sixth pass does not reduce the total mineable lignite of a drillhole produced by the previous method. It simply distributes the mineable lignite and waste to separate benches allowing the more accurate calculation of resources per bench. Mineable lignite or waste composite intervals vertically crossing the floor of a bench are split in two components, each coded according to the bench volume they belong to (e.g. CO560, CO570, etc.). This approach was used in the lignite resources estimation and mine planning study of the South Western Field (Public Power Corporation of Greece) in 2009 [3].

3.2. Compositing

The 1,016 mineable lignite and waste composite intervals from the previous method were intersected with bench surfaces every 10m vertically (pass 6). This led to the generation of 1,404 new composites that were stored in a separate table of the database. Figure 6 shows how this was done on the same part of the drillhole presented in Figure 3.

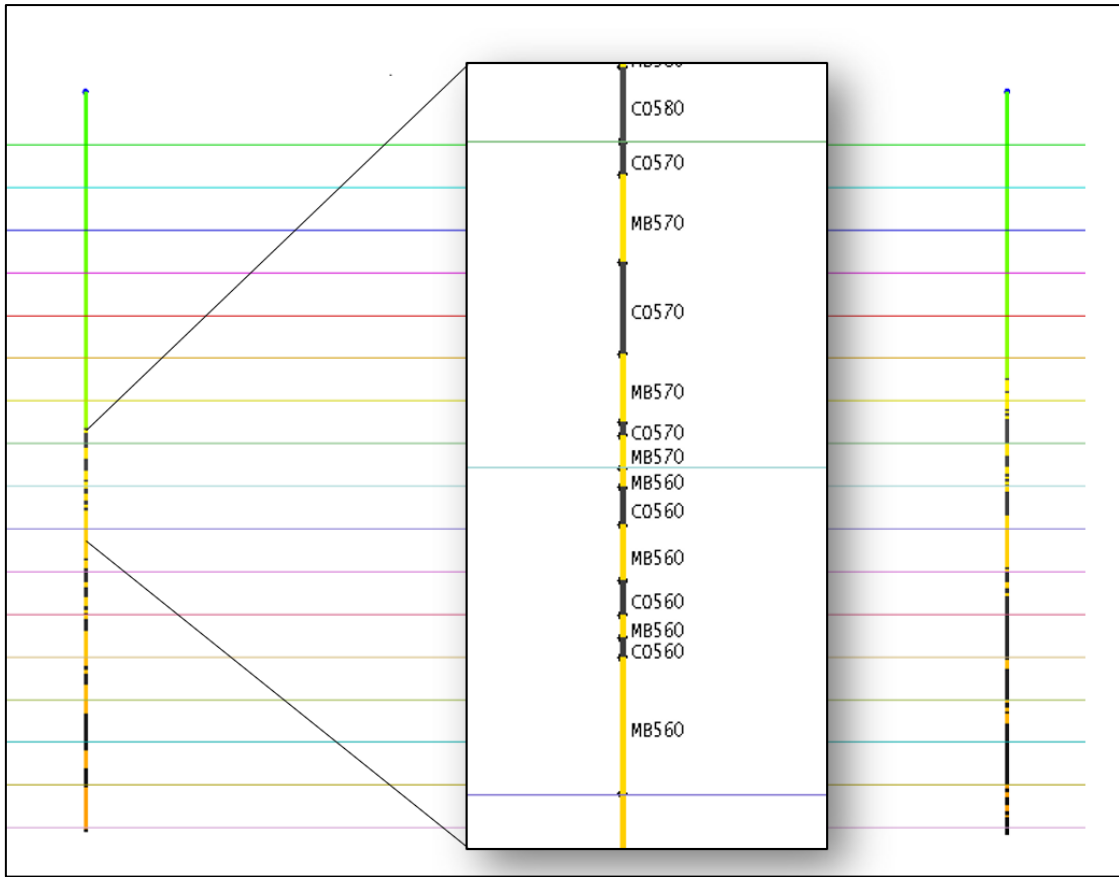


Figure 5. Splitting and coding of mineable lignite and waste intervals per bench.

The total length (thickness) of mineable lignite per drillhole and bench was calculated next. This was stored together with other information such as the top and bottom depth of mineable lignite inside each bench in separate formatted text files – one per bench. The files contained information on the thickness and depths of overburden and midburden in each bench. These files were used to calculate and locate lignite resources within the study area limits for each bench.

3.3. Resource Modelling

The same process followed in the previous method, was applied in the case of mineable lignite composites per bench. The formatted text files were used to generate grid models of the roof, floor and thickness of mineable lignite, overburden and midburden. This time, there were several models corresponding to the different benches, and resources were calculated per bench using the composited mineable thicknesses per bench. There was no need to use the waste to lignite ratio to calculate resources per bench, as the mineable overburden, midburden and lignite thicknesses were calculated directly for each bench using values related to each bench.

The horizontal extents of mineable lignite in each bench had to be considered during modelling. Vertical variations in lignite density meant that not all drillholes contained mineable lignite in each bench. This was addressed by applying polygonal masks to the grid models, limiting their horizontal extents as shown in Figure 7.

Original			Pass 5				Pass 6		
Litho	Length	Ash	Litho	Length	Ash		Litho	Length	Ash
AL	3.70	100.00	WASTE	12.70	100.00	BENCH 570	WASTE 570	10.00	100.00
CO	0.50	46.50							
MR	0.60	100.00							
AL	2.40	100.00	CO	1.00	30.90	BENCH 560	WASTE 560	2.70	100.00
AL	0.60	100.00							
CO	0.60	38.50							
MR	0.80	100.00							
CO	0.60	45.10							
AL	1.00	100.00							
MR	0.90	100.00							
CO	0.40	36.20							
MR	0.50	100.00							
CO	1.20	30.90	WASTE	6.50	100.00	BENCH 550	WASTE 550	6.50	100.00
MR	2.60	100.00							
CO	0.40	35.80							
CO	1.70	25.20							
MR	0.70	100.00							
CO	0.60	23.00							
CO	0.60	22.70							
MR	0.50	100.00							
CO	1.40	36.00							
MR	0.50	100.00	CO	1.10	34.40	BENCH 540	WASTE 540	8.40	100.00
CO	1.60	40.90							
MR	1.00	100.00							
CO	0.40	40.60							
AL	0.90	100.00							
CO	1.30	34.40							
MR	0.30	100.00	WASTE	8.70	100.00	BENCH 530	WASTE 530	0.90	39.60
CO	0.50	35.90							
CO	1.00	25.30							
MR	1.30	100.00							
MR	6.10	100.00							
CO	0.60	23.30							
MR	0.50	100.00	CO	1.85	29.19	CO 530	1.85	29.19	
CO	0.50	28.60							
CO	0.80	27.60							
CO	1.20	39.60							
CO	1.20	33.50							
MR	0.40	100.00							
CO	1.40	22.70	WASTE	0.95	100.00	WASTE 530	0.95	100.00	
CO	0.20	17.80							
MR	0.20	100.00							
CO	0.25	18.00							
MR	0.75	100.00							
CO	0.80	21.20							
CO	0.80	32.90	CO	2.00	26.80	CO 530	2.00	26.80	
CO	0.40	25.80							
MR	0.20	100.00	WASTE	0.30	100.00	WASTE 530	0.30	100.00	

Figure 6. Example of drillhole composited with the 6-pass mineable interval per bench composing method. In pass 6, the evaluated intervals are split and coded using bench surfaces.

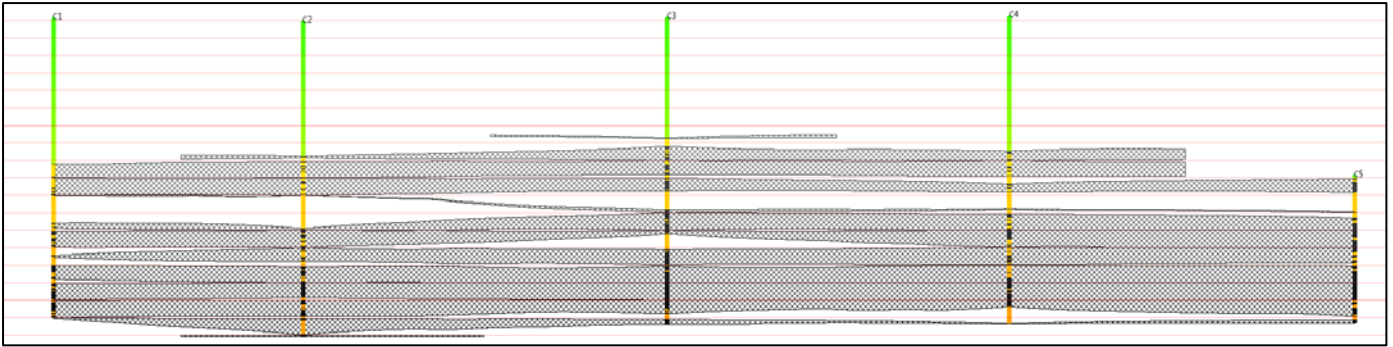


Figure 7. Section C showing composited drillhole intervals per bench and modelled mineable lignite roof and floor surfaces per bench (black).

4. THREE-DIMENSIONAL MINEABLE LIGNITE COMPOSITING OF CORRELATED LIGNITE SEAMS

4.1. Lignite Seam Correlation

The last method considered in our study was based on the geological analysis, correlation and modelling of the original (raw) lignite seams. The lignite seams were examined in cross sections and were manually correlated by selecting the drillhole intervals considered to belong to a particular seam and coding an appropriate seam field in the database. This was a fairly difficult and time-consuming process, the results of which were based to some degree on the geologist's interpretation. Figure 8 shows a drillhole section with the seam correlation stored in the database. This type of section helps to visualise the way correlation works before actual modelling of the seams. The software automatically links intervals with the same seam code between successive drillholes in a linear fashion aiding the user during correlation. A colour legend helps distinguish between seams as in our case there were so many that the section would become very confusing to the eye. Linking of correlated seams is not allowed through drillholes that don't contain them. Two characteristic marl horizons were used to group the lignite layers in upper and lower horizons. Upper horizons were numbered upwards (lowest one being U1) and lower horizons were named downwards (top one being L1). There was no particular reason for this convention other than the need to have a standard convention between drillholes. Horizon splits were named after the merging horizon e.g. splits U8A, U8B and U8C merge to U8 (Table 1).

All lignite seam codes and related splits were stored in a special database table and field to be used for structural modelling of the seams. A horizon list (table) was also stored for reference by other functions of the software. The horizon list should only contain stratigraphy that will be modelled. It is important to list the horizons in proper stratigraphic order with the first horizon being the uppermost deposit and the last horizon being the bottom of the modelling area of interest. The smallest split is defined in the Child Split column. Child splits are merged into larger horizons until the parent horizon is reached on the right side of the table. Horizons with no splitting are also listed in the Child Split column. Table 1 shows the horizon list and splits for our case study. The table is split in two parts – one for the upper horizons and one for the lower.

There were cases of very thin seams that existed in only one drillhole and a drillhole that was missing most of the upper lignite seams (C5). These and other stratigraphy issues were resolved using a special operation of Maptek Vulcan called FixDHD which we discuss in the following section. FixDHD is one of the first steps in the modelling procedure called Integrated Stratigraphic Modelling (ISM).

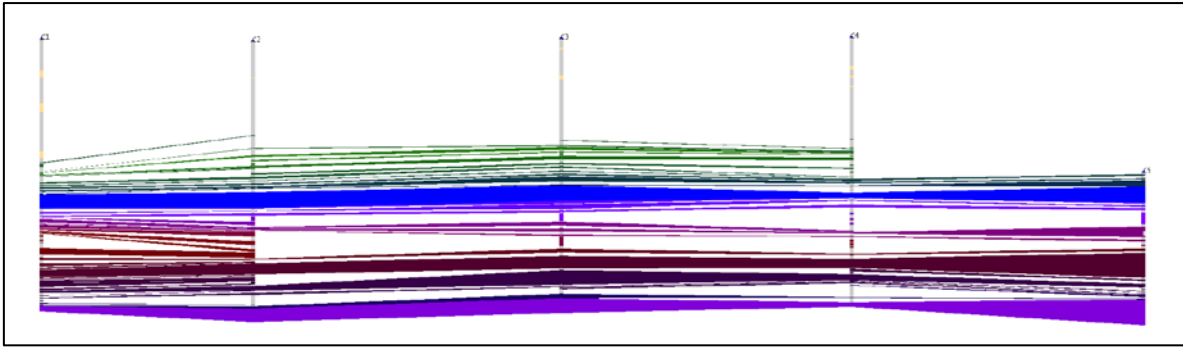


Figure 8. Section C showing drillhole database correlation – child splits are not shown linked to merge horizons.

4.2. Validating and Fixing Seam Correlation

Data for stratigraphic modelling, as in our case study, is provided from a drillhole database, with the horizons of interest noted. It is rarely possible to clearly identify all horizons in every hole. This may be due to:

- The geological nature of the deposit being drilled.
- Biases introduced when planning the drilling program.
- Poor logging practice.
- Lost data.

Our dataset, even though being limited to a small area of a much larger deposit and consisting of only 24 drillholes, presented the following data collection issues that need to be addressed:

- Short holes, which are not deep enough to include all horizons of interest or have a collar lower than the original topography surface.
- Difficulty determining the position of missing horizons that have thinned to zero thickness.
- Issues determining the position of daughter horizon boundaries within their merged parent horizon.

FixDHD was called to check the correlated lignite stratigraphy and fix possible problems. Several problems were initially identified that were stopping FixDHD from resolving the issues. These were problems related to the way correlation was coded (e.g. wrong seam sequence or seams existing in only one drillhole). In every trial run, FixDHD produced a detailed log file that explained the issues and suggested ways to resolve them. Once these problems were addressed, FixDHD produced a fixed version of the lignite stratigraphy table in the database. Table 2 shows how this table looks for drillhole C5.

The horizons are shown from top to bottom in the fixed table. As drillhole C5 was missing the top part of stratigraphy, several intervals were interpolated by FixDHD above its collar, shown with a negative *From* and *To* relative depth. Intervals interpolated or otherwise fixed by FixDHD are flagged with an F next to the column that was fixed (from, to, or thickness). Intervals unaltered by FixDHD are flagged DB. The final Flag column summarises the changes associated with an interval. For example, an interval with the original *From* value (column FF = DB) and a fixed *To* value (column TF = F) will have a final flag DBF (column Flag). Intervals with no changes are highlighted with light green colour in the table. FixDHD applies statistical modelling techniques to restore missing or unavailable data from the stored stratigraphy and manipulates the available data to meet required criteria for modelling. If the data is not enough to apply this techniques, less rigorous stacking methods are used. Similar changes to those shown for C5 took place in other drillholes, leading to a fixed correlation that could be effectively modelled.

Table 1. Finalised lignite horizon table showing how horizon splits are joined to form larger horizons based on the drillhole database correlation.

		Child	Merge Level 1	Merge Level 2
		Upper Horizons	U14	
U13				
U12				
U11				
U10				
U9C	U9			
U9B	U9AB		U9	
U9A				
U8C	U8			
U8B				
U8A				
U7				
U6				
U5H2	U5H			
U5H1				
U5				
U4				
U3				
U2				
U1				

		Child	Merge Level 1
		Lower Horizons	L1
L2			
L3			
L4A	L4		
L4B			
L4C			
L5			
L6			
L7			
L8A	L8		
L8B			
L8C			
L9			
L10A	L10		
L10B			
L11A	L11		
L11B			
L11C			
L12A	L12		
L12B			
L12C			
L13A	L13		
L13B			
L13C			
L14			
L15			
L16			

4.3. Structural Modelling

Once the fixed lignite stratigraphic table was produced, structural modelling of the lignite seams could be performed. Seam existence limits were generated to control the horizontal area of the seams of the fixed lignite intervals. The same interpolation method was used (inverse distance weighting with a power of one) as in the previous methods discussed in this paper for consistency. Grid models for the roof, floor and thickness of each seam were generated and masked with the corresponding seam limits. Figure 9 shows Section C with the modelled seams. It should be noted that no minimum seam thickness or quality criteria have been applied up to this stage. After roof and floor models for each horizon were created, thickness grids were automatically generated between adjacent pairs of surfaces. Every node in each thickness grid was forced to a value of zero or greater, which insured that no horizons cross each other. Should a horizon cross its neighbour, either the floor was forced to the roof position, or the roof was forced to the floor position.

4.4. Compositing and Quality Modelling

For each of the modelled seams, it was necessary to generate corresponding quality grids, one for each of the quality parameters (ash, moisture, calorific value). Inverse distance weighting to the power of two was used to interpolate composited quality values (single value per seam and drillhole) to the respective grid models. Figure 10 shows ash contour maps from some lignite seams. Estimating quality parameters separately for each seam leads to a much more detailed quality model than the previous two methods and allows the application of quality mineability criteria in three dimensions instead of one.

Table 2. Fixed lignite stratigraphy of drillhole C5 – fixed intervals are flagged F, while original are flagged DB.

Horizon	Merge	From	FF	To	TF	Thickness	TKF	Sthickness	Flag
CO_U14	CO_U14	-28.812	F	-28.444	F	0.368	F	0.368	FF
CO_U13	CO_U13	-25.098	F	-24.712	F	0.386	F	0.386	FF
CO_U12	CO_U12	-23.462	F	-22.913	F	0.548	F	0.548	FF
CO_U11	CO_U11	-21.004	F	-20.104	F	0.901	F	0.901	FF
CO_U10	CO_U10	-18.983	F	-18.61	F	0.372	F	0.372	FF
CO_U9C	CO_U9	-18.61	F	-18.489	F	0.121	F	0.121	FF
CO_U9B	CO_U9	-18.197	F	-17.676	F	0.521	F	0.521	FF
CO_U9A	CO_U9	-17.204	F	-16.629	F	0.575	F	0.575	FF
CO_U8C	CO_U8	-15.355	F	-14.961	F	0.393	F	0.393	FF
CO_U8B	CO_U8	-14.961	F	-14.765	F	0.197	F	0.197	FF
CO_U8A	CO_U8	-14.765	F	-13.388	F	1.376	F	1.376	FF
CO_U7	CO_U7	-12.563	F	-11.367	F	1.196	F	1.196	FF
CO_U6	CO_U6	-8.944	F	-7.807	F	1.137	F	1.137	FF
CO_U5H2	CO_U5H	-6.112	F	-4.753	F	1.358	F	1.358	FF
CO_U5H1	CO_U5H	-3.258	F	-2.392	F	0.866	F	0.866	FF
CO_U5	CO_U5	-1.86	F	-1.86	F	0	F	0	FF
CO_U4	CO_U4	-1.347	F	-0.523	F	0.823	F	0.823	FF
CO_U3	CO_U3	1	DB	2	DB	1	DB	1	DBDB
CO_U2	CO_U2	3.8	DB	4.4	DB	0.6	DB	0.6	DBDB
CO_U1	CO_U1	5	DB	9.3	DB	4.3	DB	4.3	DBDB
CO_L1	CO_L1	20.1	DB	20.8	DB	0.7	DB	0.7	DBDB
CO_L2	CO_L2	22.1	DB	23	DB	0.9	DB	0.9	DBDB
CO_L3	CO_L3	23.8	DB	25.4	DB	1.6	DB	1.6	DBDB
CO_L4A	CO_L4	26.8	DB	29.518	F	2.718	F	2.718	DBF
CO_L4B	CO_L4	29.518	F	30.963	F	1.445	F	1.445	FF
CO_L4C	CO_L4	30.963	F	35	DB	4.037	F	4.037	FDB
CO_L5	CO_L5	36.25	DB	39.5	DB	3.25	DB	3.25	DBDB
CO_L6	CO_L6	42.6	DB	43.5	DB	0.9	DB	0.9	DBDB
CO_L7	CO_L7	45	DB	46.5	DB	1.5	DB	1.5	DBDB
CO_L8A	CO_L8	48.4	DB	48.659	F	0.259	F	0.259	DBF
CO_L8B	CO_L8	48.659	F	49.351	F	0.692	F	0.692	FF
CO_L8C	CO_L8	49.351	F	49.5	DB	0.149	F	0.149	FDB
CO_L9	CO_L9	49.786	F	49.786	F	0	DB	0	FF
CO_L10A	CO_L10	51	DB	51	F	0	F	0	DBF
CO_L10B	CO_L10	51	F	53	DB	2	F	2	FDB
CO_L11A	CO_L11	54	DB	56.8	DB	2.8	DB	2.8	DBDB
CO_L11B	CO_L11	56.8	DB	59.6	DB	2.8	DB	2.8	DBDB
CO_L11C	CO_L11	59.6	F	59.6	F	0	DB	0	FF
CO_L12A	CO_L12	59.6	DB	67.909	F	8.309	F	8.309	DBF
CO_L12B	CO_L12	67.909	F	70.284	F	2.375	F	2.375	FF
CO_L12C	CO_L12	70.284	F	71	DB	0.716	F	0.716	FDB
CO_L13A	CO_L13	72	DB	73	DB	1	DB	1	DBDB
CO_L13B	CO_L13	73.76	F	73.76	F	0	DB	0	FF
CO_L13C	CO_L13	73.76	F	73.76	F	0	DB	0	FF
CO_L14	CO_L14	75	DB	77.5	DB	2.5	DB	2.5	DBDB
CO_L15	CO_L15	82.7	DB	84	DB	1.3	DB	1.3	DBDB
CO_L16	CO_L16	85	DB	85.4	DB	0.4	DB	0.4	DBDB

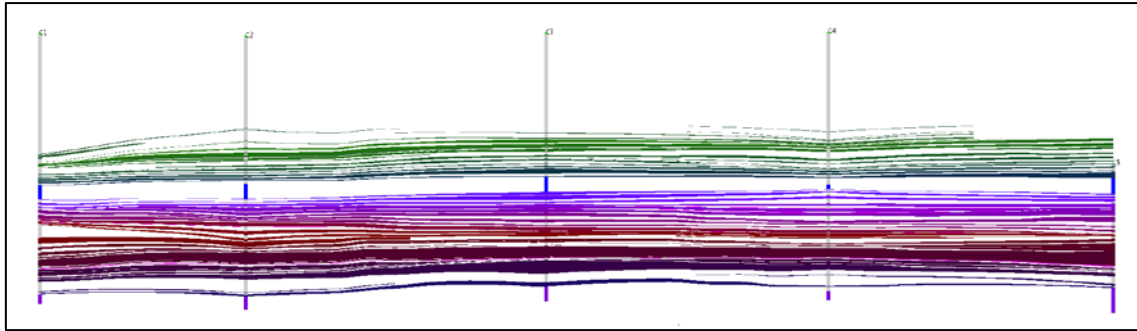


Figure 9. Section C showing modelled lignite seams – note the interpolated seams above C5 collar.

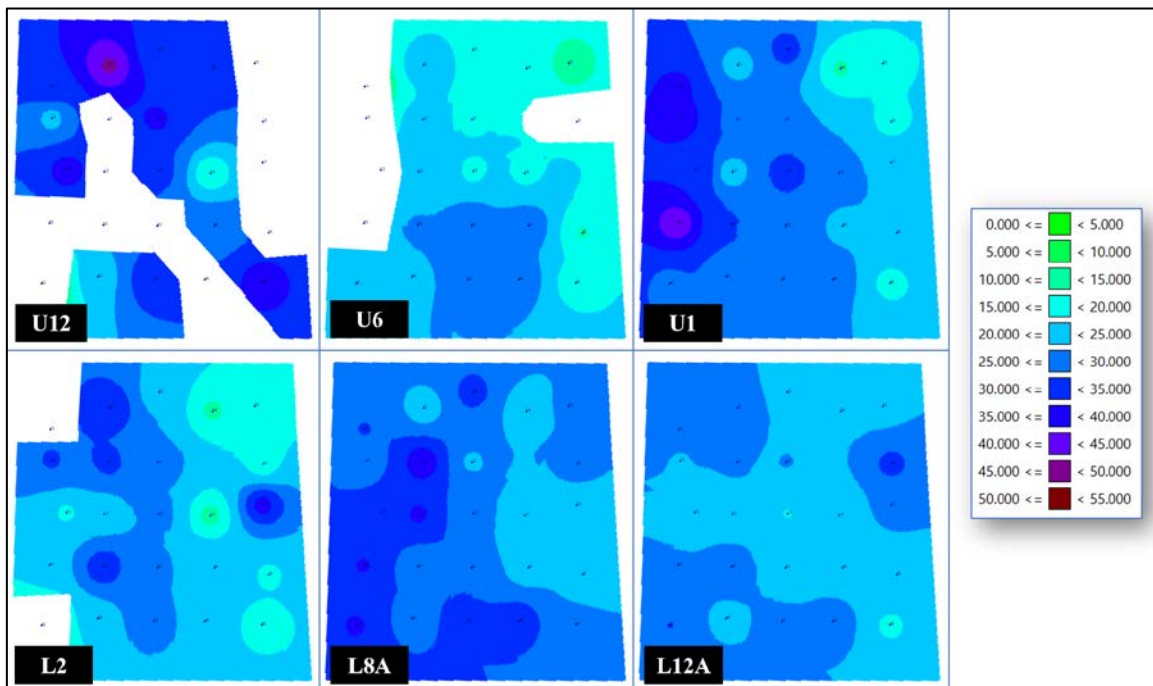


Figure 10. Estimated ash maps from some characteristic upper and lower lignite seams.

4.5. Resource Model Development

The resource model was based on the HARP (Horizon Adaptive Rectangular Prism) structure – a type of block model that represents an entire Integrated Stratigraphic Model. The HARP model is created directly from grids or faulted triangulations. All quality grids are automatically incorporated. A HARP model block contains 5 points in the roof of the block and 5 points in the block floor [4]. These points allow vertex angles to fluctuate, which allows the block to conform to structure roof and floor grids. HARP models accurately resolve horizons down to a few centimetres of thickness without the need to make huge models with extremely small Z sub-blocking.

All structural and quality grids generated for the modelled lignite seams of our study were used to construct a HARP model using the horizontal extents of the considered area. Each HARP block was initially coded as lignite or waste and received a seam code based on the formulated horizon list. Waste block seam codes had a prefix added to distinguish them from lignite (e.g. BD_L7 for burden block above L7). Figure 11 shows two sections through the produced HARP model coloured by ash estimates. It is quite clear that the HARP structure allows it to follow precisely the modelled stratigraphy.

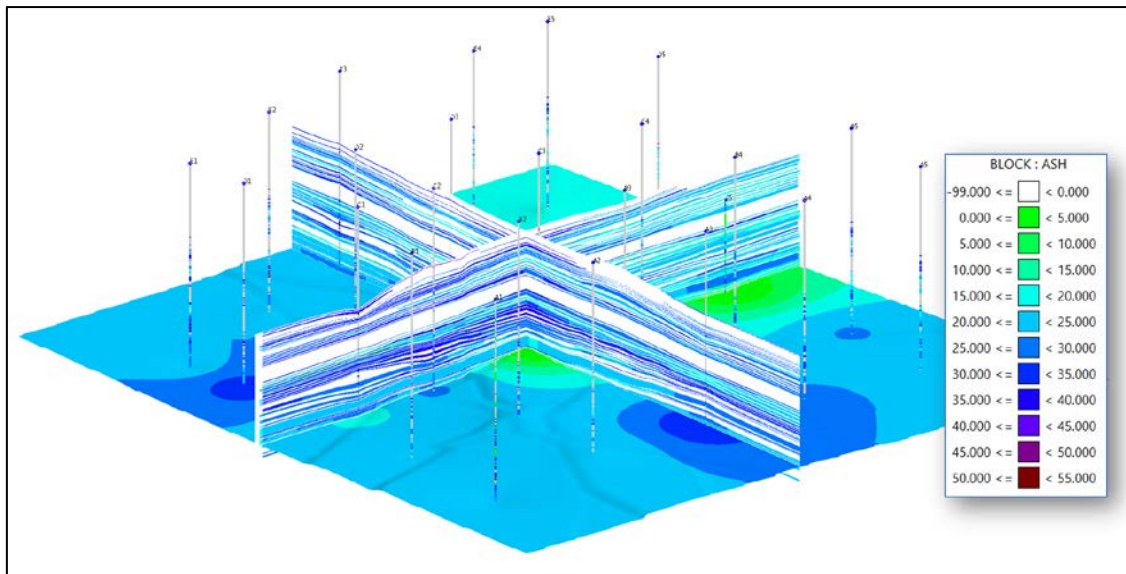


Figure 11. Vertical sections through lignite HARP model and floor of seam CO_13C coloured by ash – vertical scale was set to twice the horizontal to show more details.

4.6. Generation of Run-Of-Mine Model

Run of Mine (ROM) modelling in Maptrek Vulcan simulates the way in which material is extracted from a stratigraphic deposit. Basic parameters are defined for extraction. The ROM HARP model is constructed from the geologic HARP model using three rules, applied to the mine modelling process in the following order [5]:

1. **Minimum mining thickness:** Any horizon less than this thickness is not mined by itself.
2. **Minimum parting thickness:** Any waste material between seams less than this thickness is mined with the next seam, resulting in composited seams. Waste material becomes a parting in the composited seam. The assumption when using this option is that burden material less than this thickness cannot be separated in the pit, so it is mined with the product. However, compositing only takes place if the Minimum product to waste ratio is met.
3. **Minimum product to waste ratio:** The total product to total waste ratio in a working section must be greater than or equal to this ratio. Total waste is defined as all in-seam partings plus all between-seam parting.

In our study, the minimum mining thickness was set to 0.5m and the minimum parting thickness was set to 0.3m. A 0.1m roof and floor loss was also applied. The following figure compares two sections of the original (resource) and ROM HARP model showing the effect of applying mining criteria to lignite seams in three dimensions. Parts of seams disappear due to thickness and others get combined to form thicker mineable sections.

5. CONCLUSIONS - METHOD COMPARISON

The three methods compared in this paper were applied to the same dataset, using the same mine planning software package. Timewise, the first and simplest method of the three, the compositing of mineable of total drillhole mineable lignite intervals, was the fastest to implement (couple of hours). The number of drillholes used plays almost no role to the time required by this method. It was also very easy to setup and run. The produced models and information take the smallest amount of hard disk space.

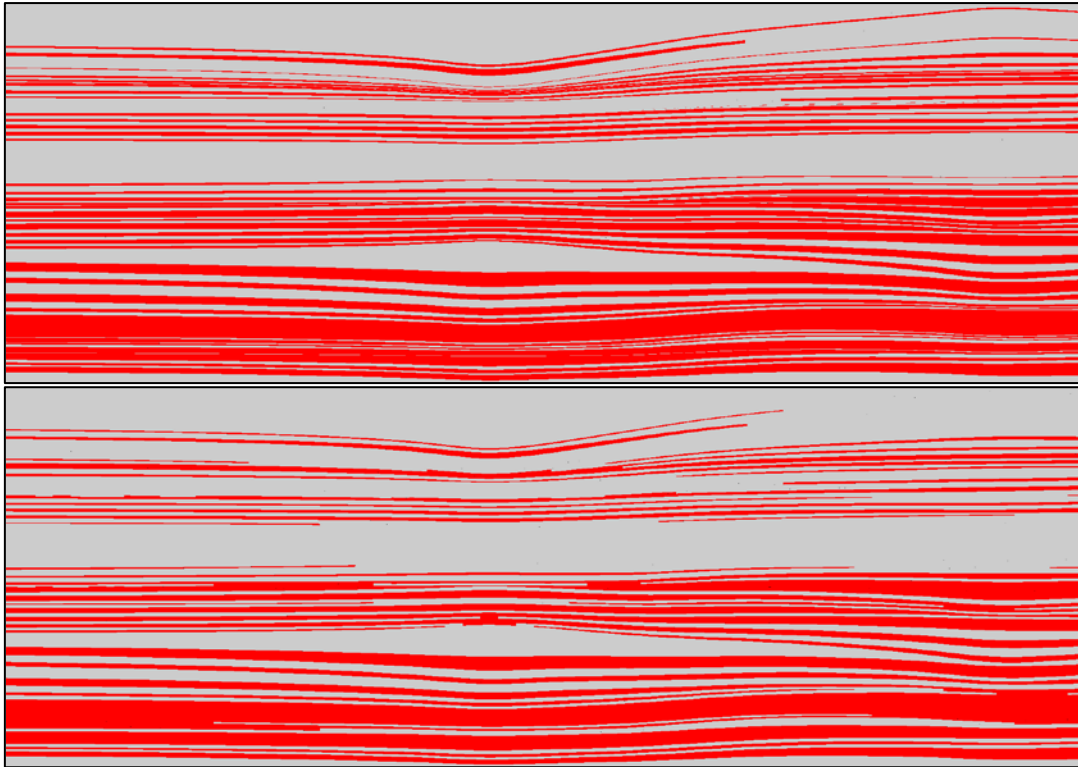


Figure 12. Original resource HARP model section (top) and ROM HARP model section (bottom) showing the changes in lignite seams after the application of mining criteria.

The second method, compositing of drillhole mineable lignite intervals per bench, required more time than the first method as the process was repeated for each bench considered (4-5 hours altogether). It required an extra compositing step to split the composites of the previous method by bench, and the development of a more complex reserve model based on sets of grids per bench. As all steps are fully automated, this method was still very easy to setup and run.

The third and most complex method, mineable lignite compositing of correlated seams, required correlation of lignite seams between drillholes – a step that took a couple of days to complete for the 24 drillholes of our case study dataset. It is quite impossible to estimate how much time it would take to correlate 100 drillholes or more as it would depend on other factors such as faulting which was not affecting the area considered in this study. Once correlation was complete, the other steps took little time to setup and run – a total of 4 hours to get the final ROM HARP model after correlation.

Table 3 below summarises the reserves calculated using each of the three methods. The reserves are split by bench, with the waste quantities given in m^3 while lignite is given in tonnes assuming a $1.2\text{t}/\text{m}^3$ specific gravity. Looking at the totals, it is clear that the higher the resolution of the calculation (going from method 1 to 3) the lower the reported total lignite. However, looking at the individual benches, the only real comparison can be made between method 2 and 3, as the first method has no real control of what is reported as bench quantities. Calculating bench reserves using method 1 is essentially applying the same stripping ratio on a different lignite plus midburden total to derive the individual values. Only overburden can be directly calculated from its modelled floor.

Both methods 2 and 3 report reasonably distributed quantities per bench, but we can still see differences between them. The effect of artificially grouping lignite intervals into bench mineable sections leads to a slight overestimation in the lower benches and some underestimation of the upper ones compared to the number reported by method 3. These differences would have been much larger in the presence of faulting. Comparison of quality parameters estimations gave similar differences.

Overall, it became quite clear during this exercise that the time spent in building a complete stratigraphic model based on lignite seam correlation is time well spent as it provides all the necessary quantity and quality information in three dimensions and to the highest resolution possible based on the available data. Any efforts to replace seam correlation and compositing with one-dimensional compositing of each drillhole separately, lead to over-simplification of geology and significant reduction of the effectiveness of mine planning.

Table 3. Summary of bench reserves produced by the three compositing methods.

Bench	1. Total Mineable Thickness Compositing			2. Mineable Thickness Compositing per Bench			3. Compositing of Correlated Lignite Seams		
	OB	CO	MB	OB	CO	MB	OB	CO	MB
650	14,577,846	-	-	14,577,846	-	-	14,577,846	-	-
640	13,185,074	-	-	13,185,074	-	-	13,185,074	-	-
630	13,185,074	-	-	13,185,074	-	-	13,185,074	-	-
620	13,185,074	-	-	13,185,074	-	-	13,185,074	-	-
610	13,185,074	-	-	13,185,074	-	-	13,185,074	-	-
600	13,175,050	5,675	5,295	13,055,385	61,243	78,653	13,102,556	31,679	56,119
590	11,289,779	1,073,032	1,001,102	9,812,684	708,640	2,781,857	9,668,205	764,268	2,879,979
580	5,184,748	4,529,428	4,225,803	5,001,697	4,646,698	4,311,129	5,129,774	4,260,537	4,504,853
570	1,325,006	6,714,642	6,264,533	1,592,875	4,864,147	7,538,743	1,508,645	5,063,741	7,456,645
560	69,358	7,425,533	6,927,771	504,643	4,623,182	8,827,779	498,204	4,839,959	8,653,571
550	-	7,464,801	6,964,407	-	2,092,204	11,441,571	-	2,162,843	11,382,705
540	-	7,464,801	6,964,407	-	7,802,640	6,682,874	-	7,884,321	6,614,807
530	-	7,464,801	6,964,407	-	8,664,512	5,964,648	-	9,472,897	5,290,994
520	-	7,464,801	6,964,407	-	7,465,063	6,964,188	-	7,836,396	6,654,744
510	-	7,464,801	6,964,407	-	9,209,149	5,510,783	-	9,691,051	5,109,199
500	-	7,464,801	6,964,407	-	12,940,138	2,401,625	-	12,230,637	2,221,503
490	-	6,726,605	6,275,695	-	6,531,122	2,979,474	-	4,900,503	2,928,823
480	-	1,425,875	1,330,293	-	1,393,525	1,013,852	-	731,332	993,575
470	-	161	150	-	106,621	29,975	-	53	11
Total	98,362,083	72,689,757	67,817,083	97,285,426	71,108,884	66,527,152	97,225,526	69,870,216	64,747,527

REFERENCES

- [1] Karamalakis, N. (1992). Computer software for the evaluation of lignite deposits. Mineral Wealth (Oryktos Ploutos – in Greek) 76M: p. 39-50.
- [2] Kapageridis, I. (2006). VULCAN 3D Software Application Study on Drillhole Evaluation. Maptek/KRJA Systems Ltd.
- [3] Kapageridis, I., Kolovos, C. (2009). Modelling and Resource Estimation of a Thin-Layered Lignite Deposit. In: 34th International Symposium on the Application of Computers and Operations Research in the Minerals Industries (APCOM 2009), Vancouver.
- [4] Maptek Pty Ltd. (2016). ISM Stratified Geologic Modelling, Maptek Vulcan Training Manual.
- [5] Maptek Pty Ltd. (2018). Integrated Stratigraphic Modelling, Maptek Vulcan 10.1 Online Help.

Unsupervised Machine Learning Applications on Greek Lignite Mining Industry

Louloudis G.¹, Louloudis E.² and Roumpos C.¹

¹ Public Power Corporation of Greece, Mines Division, 29 Chalkokondili Str., Athens, Greece

² Mathematician, Athens University of Economics and Business

ABSTRACT

In the new competitive environment, the surface lignite mining operations face many challenges which require the application of appropriate data mining techniques and analysis of all available data considering the whole mine life cycle. In this framework, statistical or machine learning algorithms can contribute to improve mining operations and increase efficiency and competitiveness.

In this paper, a proposal to implement two significant unsupervised machine learning methods and algorithms, the Principal Component Analysis (PCA) and Clustering, in all phases of surface lignite mining operations is presented.

In the first stage, it is suggested to apply PCA and Clustering in the phase of primary mineral deposit investigation. For that reason, data from borehole logs and geophysical exploration, satellite images, geological maps, etc. are used in order to determine the type, magnitude and location of the future mineral exploration, considering extensions to regions with lack of geological data.

Furthermore, applications of PCA and Clustering to mine planning phase can contribute to the improvement of mine planning efficiency. The segmentation of the whole mining area into characteristic operational sectors can be achieved based on PCA and Clustering results. Case studies in two surface lignite mines are presented with the use of the clustering method to geographically separate the mining regions according to their properties. An advantage of the method is the fast, accurate and friendly to user implementation in R code.

Another application of PCA and clustering refers to the analysis and improvement of the operational mining data. An example is provided concerning the actual monthly operational data of a continuous surface mining project as explanatory variables. The divergences between scheduled and real production indices and characteristic factors are revealed through PCA.

Finally the application of unsupervised learning techniques to the evaluation of environmental impacts of mining activities is also discussed. A case study regarding the lignite bearing fields mine water and regional waters relations is additionally presented.

1. INTRODUCTION

Machine learning is already in use by a variety of industries. Organizations are now forced to look deeper into their data to find new and innovative ways to increase efficiency and competitiveness. As part of the data mining task, statistical or machine learning algorithms can detect patterns in the data and make predictions about new data [1, 2]. Usually these techniques are broadly implemented in financial data frames considering different products or companies' income statement elements and balance sheet elements, stock exchanges as well as explanatory variables. The same can be done with mining industry companies or units. These applied techniques can potentially have a good insight of the market.

In this work, the application of two significant unsupervised machine learning methods and algorithms (PCA and Clustering) in all phases of the mining industry is proposed. In this framework, PCA and Clustering it is suggested to be applied in the phase of primary mineral deposit

investigation by using data acquisition of borehole logs. The above techniques have already been successfully applied in the fields of geophysics, satellite images, geological maps, etc., in order to determine many patterns and features. They can also be used to the determination of the type, magnitude and location of the geological survey's future extension to regions with lack of geological data. PCA and Clustering techniques are also suitable for the mineral deposit evaluation, geological structures recognition and especially precise tectonics detection.

Nowadays, the geospatial image processing, data analysis and modeling is an international trend [3]. It is friendly to user taking advantage of the wide variety of statistical tools to analyze raster image using R-code [4]. An example is the evaluation of multi-temporal Landsat-5 and Landsat-7 images, SPOT Panchromatic, and Aster data to map the natural environment on a local scale, and to assess the impact of mining activities by indicating the changes on land and water resources [5]. In this research work, the Self Organizing Map (SOM) Artificial Neural Network ANN method was used on the ASTER image in order to categorize all inherent land cover classes of the satellite images [5]. The above technique has also been applied for the assessment of vegetation changes in Natura 2000 sites in Greece, by using remote sensing data [6].

Downscaling by using Artificial Intelligence Neural Network on GRACE data, the estimation of the groundwater withdrawals at the aquifer scale has been accomplished [7]. This method can be applied for the estimation of the groundwater withdrawals for drainage and agriculture.

PCA and Clustering methods can also be applied to mine's exploitation planning phase. More analytically, the segmentation of the mine area into Sectors can be achieved based on PCA and Clustering results. The main task here is to use the method of clustering to separate geographically the regions of Lakkia and Klidi mines according to their properties. We also provide some tools in order to verify the fit that corresponds to clustering tending, number of clusters and accurate segmentation of the mine area, as well as to interpret the results. The reason that this method is very useful lies in the fact that it is applicable by using R code.

The PCA method could also be applied in the field of ground subsidence investigation, based on the geotechnical characteristics of the ground formations, as in the case of Thessaly plane [8].

Another application of PCA and clustering refers to the analysis and improvement of the operational mining data. An example is provided concerning the actual monthly operational data of Ptolemais South Field mine regarding the relevant indices as explanatory variables. The divergences between scheduled and real production indices and characteristic factors are revealed through PCA. The results can lead to appropriate actions and improvements.

Finally, unsupervised learning techniques have been applied to the assessment of environmental impacts related to mining activities. Examples of mine water and regional waters considering Megalopolis [9] and South Field lignite fields are presented.

2. METHODOLOGY – MATHEMATICAL BACKGROUND

2.1. Principal Component Analysis (PCA)

PCA is a mathematical transformation used for dimension reduction. Each principal component corresponds to a group of parameters that contribute strongly to the total variance of the data cloud. The big advantage that it carries is that it produces less uncorrelated variables, fact that is very useful for many cases e.g. use the components as explanatory variables in a linear regression. In fact, PCA rotates the axes so as to get maximum variation, corresponding to maximum meaningful information. In reality we could say that PCA is a "let's take a look from the point of view to comprehend better what we really see".

Principal component analysis is based on matrices eigenvalues and eigenvectors theory. In this framework, it is very useful to observe the loadings (the eigenvectors) of the components in order to understand how to interpret what each component denotes. After each individual principal

component (axis or factor) fingerprint is determined through its eigenvector, it is easy to distinguish, based on the great observations factor score value [10, 11], which of the observations have a certain relation with them, according to a specific generation mechanism (factor) that governs their origin [9]. The rest of the sampling cloud is considered as not related to this mechanism.

Assume that we have p explanatory variables X_1, \dots, X_p that form on k number of observations our data matrix \mathbf{X} . Let S the Covariance matrix of these variables, i.e.

$$S = \begin{bmatrix} s_{11} & \cdots & s_{1p} \\ \vdots & S_{i,j} & \vdots \\ s_{1p} & \cdots & s_{pp} \end{bmatrix} \text{ where } s_{i,j} = \text{Cov}(X_i, X_j) \quad (1)$$

This $p \times p$ matrix is symmetric and therefore the eigenvectors that correspond to the respective eigenvalues are orthogonal. This means that if U is the matrix containing the eigenvectors, then

$$U * U^T = \mathbf{I} \quad (2)$$

By spectral decomposition of a symmetric matrix, we get that:

$$S = U * \Lambda * U^T \quad (3)$$

where Λ is a diagonal matrix containing the eigenvalues: $\Lambda = \begin{bmatrix} \lambda_1 & \cdots & 0 \\ \vdots & \ddots & \vdots \\ 0 & \cdots & \lambda_p \end{bmatrix}$. The matrix Z

containing the principal components scores will be given by

$$Z = U * X \quad (4)$$

The variance explained by the PC's are the eigenvalues ordered. For each PC, we may get the proportion of variance explained by the formula

$$V_i = \frac{\lambda_i}{\sum_{j=1}^p \lambda_j}, \quad i=1, \dots, p \quad (5)$$

The first principal component $Z_{.1}$ absorbs the maximum variance. One safe way to determine how many of the Components we are going to keep is bootstrapping [12].

2.2. Cluster Analysis

Clustering is the task of partitioning the points into natural groups called clusters, such that points within a group are very similar, whereas points across clusters are as dissimilar as possible. Depending on the data and desired cluster characteristics, there are different types of clustering paradigms such as representative-based, hierarchical, density-based, graph-based, and spectral clustering [10]. Considering these different techniques, we used K-means for clustering observations and Hierarchical Single Linkage to cluster variables.

K-means Cluster analysis

In the observations clustering of cluster's applications K-means method was used. K-means is an iterative procedure till convergence.

Assume a data matrix \mathbf{X} with n observations and p explanatory variables. Analytically, we define: Let \underline{X}_{ki} be the i -th observation from the k -th group. We assume that there are n_k observations in the k -th group, $n = \sum_{i=1}^k n_i$ the number of the observations altogether and K the number of all groups. Let also

$$\underline{m}_k = \frac{1}{n_k} \sum_{i=1}^{n_k} \underline{X}_{ki} \quad (6)$$

the sample mean vector of the k -th group,

$$\underline{M} = \frac{1}{n} \sum_{k=1}^K \sum_{i=1}^{n_k} \underline{X}_{ki} \quad (7)$$

the overall mean vector of the observations.

Then,

Total Variation = Between Clusters Sum of Squares + Within Clusters Sum of Squares (TSS=BCSS+WCSS), where:

$$\text{TSS} = \sum_{k=1}^K \sum_{i=1}^{n_k} \|\underline{X}_{ki} - \underline{M}\|_2^2 \quad (8)$$

$$\text{BCSS} = \sum_{k=1}^K n_k \|\underline{m}_k - \underline{M}\|_2^2 \quad (9)$$

$$\text{WCSS} = \sum_{k=1}^K \sum_{i=1}^{n_k} \|\underline{X}_{ki} - \underline{m}_k\|_2^2 \quad (10)$$

By $\|\cdot\|_2$ we denote the Euclidean norm.

The method of K-means Clustering is described stepwise by the algorithm below.

- 1) K-means clustering starts with a number of n clusters.
Choose initial centroids randomly.
- 2) Assign each observation to the closest cluster (less distance from cluster center).
- 3) Calculate the mean vectors of each cluster and use them as new centroids.
- 4) Assign each observation to the closest cluster (center).
- 5) Repeat 3 and 4 until no further change occurs.

As the choice of the initial centroids affects the result, it is recommended to run the procedure some times for different initial centroids and take an overall result.

In order to determine the number of clusters, we want the BCSS to increase but with a lower rate such that it doesn't worth to create one more cluster. This can be represented by a plot with the number of clusters on the x-axis and BCSS on the y-axis (example of Fig. 4).

Hierarchical Cluster Analysis *Single Linkage Analysis*

The main step in the algorithm is to determine the closest pair of clusters. Several distance measures, such as single link, complete link, group average i.e., can be used to compute the distance between any two clusters. The between-cluster distances are ultimately based on the distance between two points, which is typically computed using the Euclidean distance or L_2 -norm. However, one may use other distance metrics, or, if available, a user-specified distance matrix.

In the explanatory variables clustering of cluster’s applications single linkage method was used, where given two clusters C_i and C_j , the distance between them, denoted $\delta(C_i, C_j)$ [20], is defined as the minimum distance δ between a point in C_i and a point in C_j .

$$\delta(C_i, C_j) = \min\{\delta(\mathbf{x}, \mathbf{y}) \mid \mathbf{x} \in C_i, \mathbf{y} \in C_j\} \tag{11}$$

The name *single link* comes from the observation that if we choose the minimum distance between points in the two clusters and connect those points, then (typically) only a single link would exist between those clusters because all other pairs of points would be farther away.

Clustering in the present examples is followed by Silhouette values method [13], a goodness of fit comparison. This method can be used to determine if each object is well assigned to its cluster compared to the other clusters. It can be used when the clustering is created by any technique (not necessary k-means).

3. RESULTS AND DISCUSSION

3.1. Unsupervised machine learning in mineral exploration and mine planning

The geometric basic elements of the lignite deposits and the corresponding physicochemical parameters of evaluated boreholes data are considered as parameters (explanatory variables).

Klidi mine planning - K-means clustering

The K-means Cluster Analysis of boreholes exploration data in Klidi mine revealed two clusters of drill holes.

The Cluster 1 (Fig. 1) corresponds to drills with lower topographic elevation of their head, lower lignite roof elevation, lower lignite bottom elevation, less overburden thickness, less lignite thickness, less intermediate waste formations, high ash content, high moisture and less specific gravity than average overall data cloud.

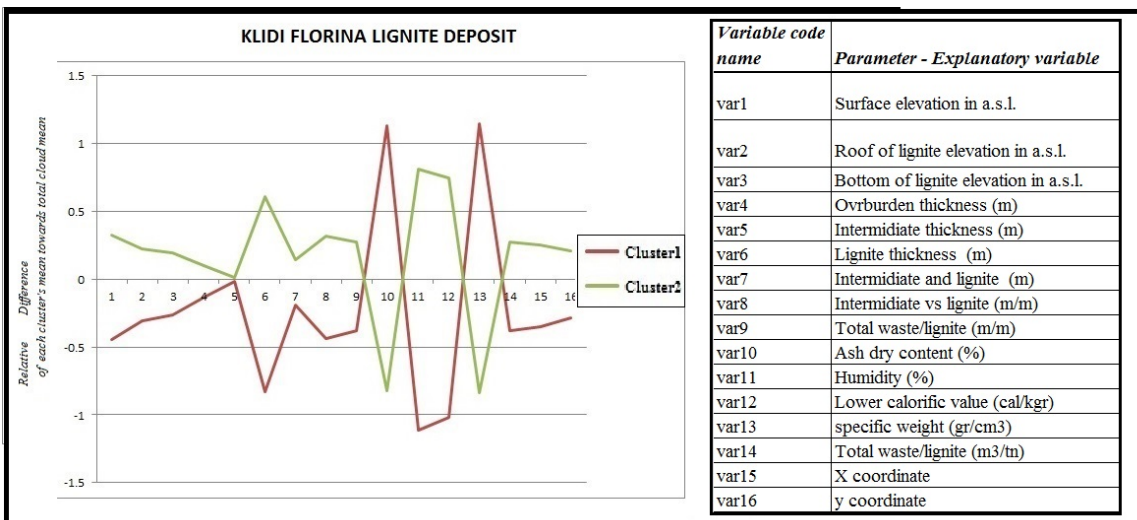


Figure 1. K-means Cluster Analysis of Klidi mine

The Cluster2 corresponds to drills with high topographic surface elevation of their head, increased lignite roof elevation, increase lignite bottom elevation, high overburden thickness, high lignite thickness, enough intermediate waste formations, less ash content, less moisture and higher specific gravity.

Cluster 1 depicts a region more suitable for mining activities but not clearly stated as financial efficient. In contrary, Cluster 2 depicts a more rich and financial efficient mineral deposit, but with difficulties regarding mining operation.

PCA of Klidi mine

After each individual principal component's (axis or factor) fingerprint is determined through its eigenvector, it is easy to distinguish, based on the great samples factor score value [5,9], which of the boreholes locations have a certain relation with them, according to a specific geological tectonic and geomorphological mechanism (factor) that governs their origin [9]. The rest of the sampling (evaluated borehole records [14, 15, 16]) cloud is considered as not affected by this mechanism.

Regarding Klidi boreholes data, 4 basic principal components were identified, PC1, PC2, PC3 and PC4 corresponding altogether to 88% of total cloud variance. The boreholes where PC1 mechanism dominate, define the northeast part of the deposit, oriented by the major faults. These boreholes are those having PC1 factor score (Z-score) greater than 1.0. This area of Sector PC1 is depicted in Fig 2 (Z-scores equipotential map colored scaled).

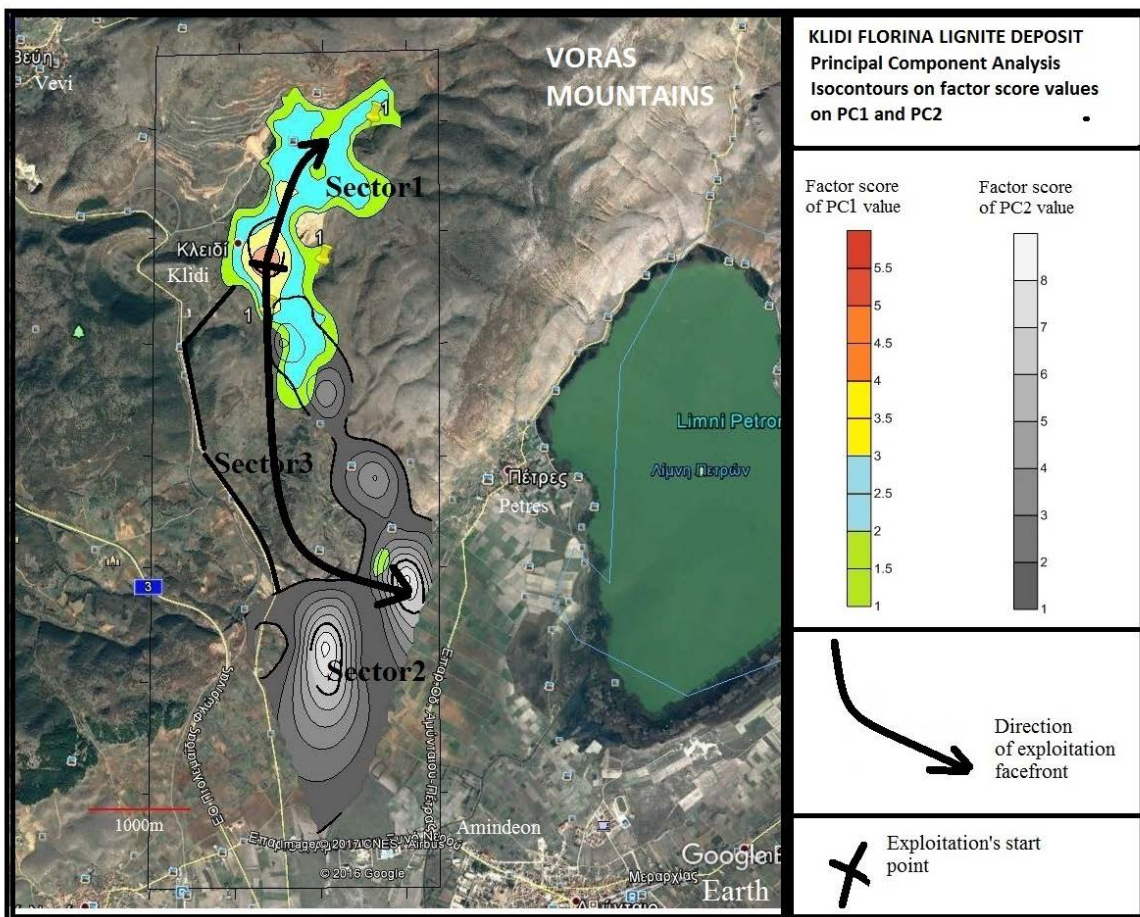


Figure 2: Equipotential lines of PC1 and PC2 factor scores (minimum curvature interpolation [17]). Proposed Mine planning course for future Klidi mine region.

All boreholes with PC1 factor score greater than one, are concentrated in north northeast survey, as depicted in Figure 2. The PC1 samples correspond to the Sector 1 of great financial significance while apparently this PC1 mechanism is direct connected, with higher lignite roof

elevation, higher lignite bottom elevation, higher total lignite thickness, higher Lower Calorific Value, but high moisture and high surface elevation. All these elements compose rich and easily exploitable deposit.

The second component PC2 involves increased overburden thickness, intermediate waste and increased waste to lignite ratio corresponding to a less financially efficient sector. The boreholes where the mechanism of PC2 dominates are those having factor score greater than 1.0 in PC2 (Fig.2). These are mainly located in the eastern part of the deposit, next to mountain Voras and in the east-southern part of the deposit next to Petron Lake (grayscale equipotential Z-scores lines on PC2). The rest principal components seem to have no significance, since each one has lower than 8% of total sampling clouds variance.

The third component PC3 involves large intermediate waste thickness, high intermediate waste to lignite ratio, lower lignite bottom elevation, as well as lower stripping ratio. The PC3 dominates to the rest of the deposit in Sector 3 and characterizes a medium financially efficient part of the deposit.

Lakkia mine planning and design - Hierarchical Clustering

From the dendrogram derived from the application of single linkage Hierarchical Cluster Analysis (Fig. 3), it is concluded that the basic parameters of exploitability, as waste to lignite ratio do have a large differential dissimilarity measure on the total set of explanatory variables. This is an indication of the sectors segmentation prospects during mine planning phase based exclusively on this ratio.

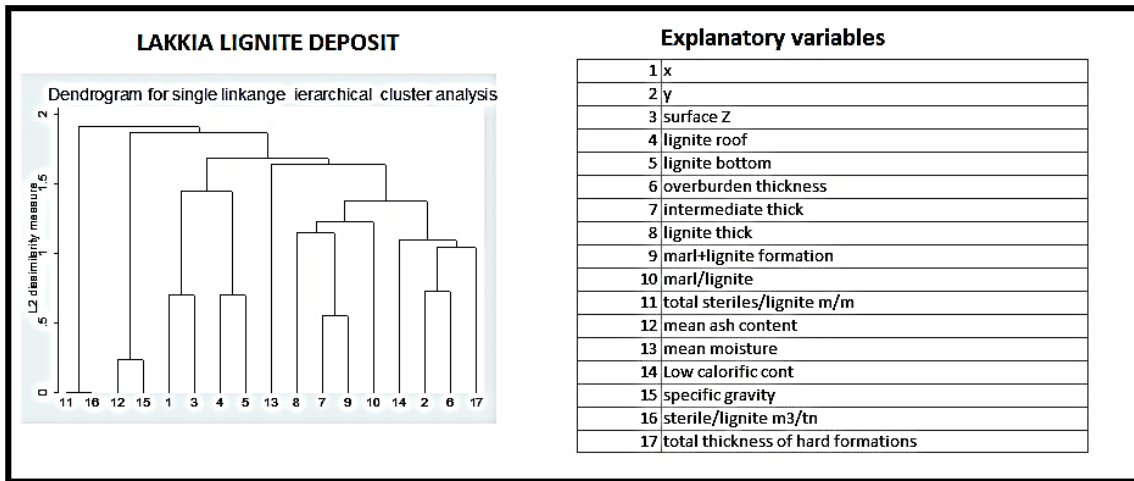


Figure 3. Dendrogram in Lakkia deposit data

Lakkia K-means clustering

As explained in Section 2.2, in order to determine the number of clusters, the BCSS needs to increase but with a lower rate such that it doesn't worth to create one more cluster. This can be represented by a plot with the number of clusters on the x-axis and BCSS on the y-axis (example of Fig. 4).

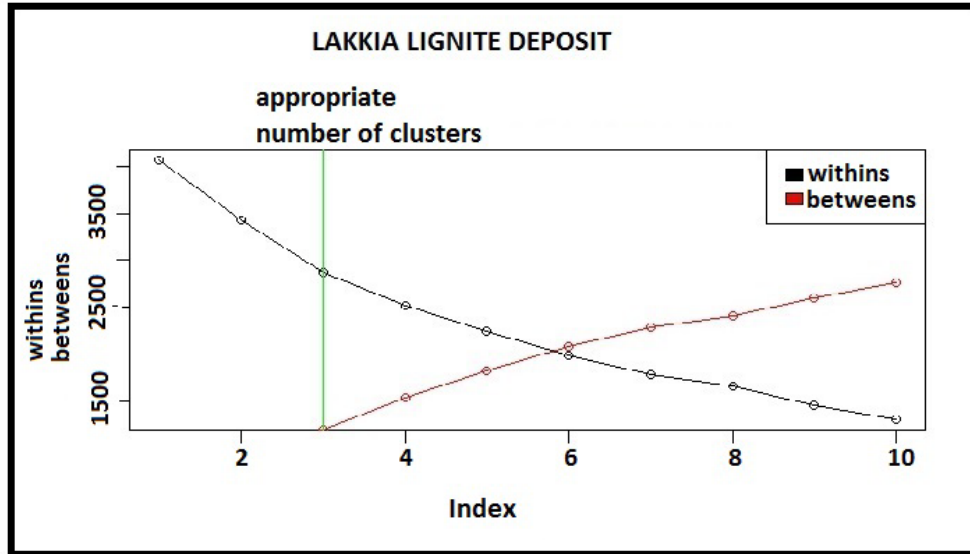


Figure 4: Optimum number of clusters identification in Lakkia exploration data

The K-means Cluster Analysis of drill holes exploration data in Lakkia mining area revealed two clusters of drill holes.

The Cluster1 (CL1 Fig. 6) corresponds to drill holes with lower topographic elevation of their head, lower roof lignite elevation, lower bottom lignite elevation, higher overburden thickness, higher intermediate lignite thickness, higher thickness marl plus lignite formations but containing revealing higher percentage of hard formations (Fig. 5).

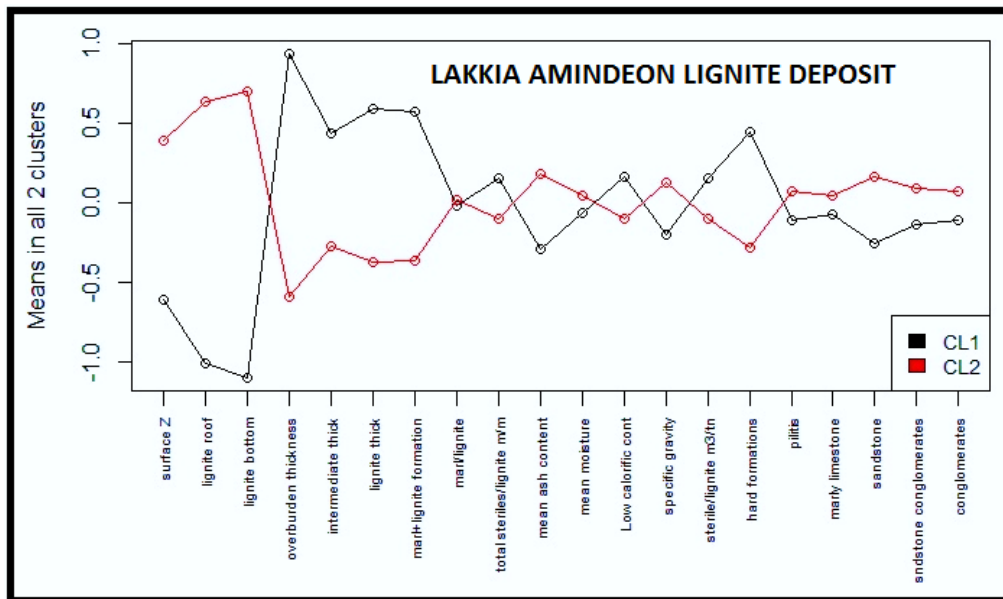


Figure 5. K-means Cluster Analysis of Lakkia mine

The Cluster 2 (CL2 Fig. 6) corresponds to drill holes with high topographic surface elevation of their head, increase of roof lignite elevation, increase bottom lignite elevation, less overburden thickness, but less lignite thickness containing and less thickness marl plus lignite formations with little hard formations (Fig. 5).

Cluster 2 depicts a more friendly to mining activities region, but not clearly stated financial efficient.

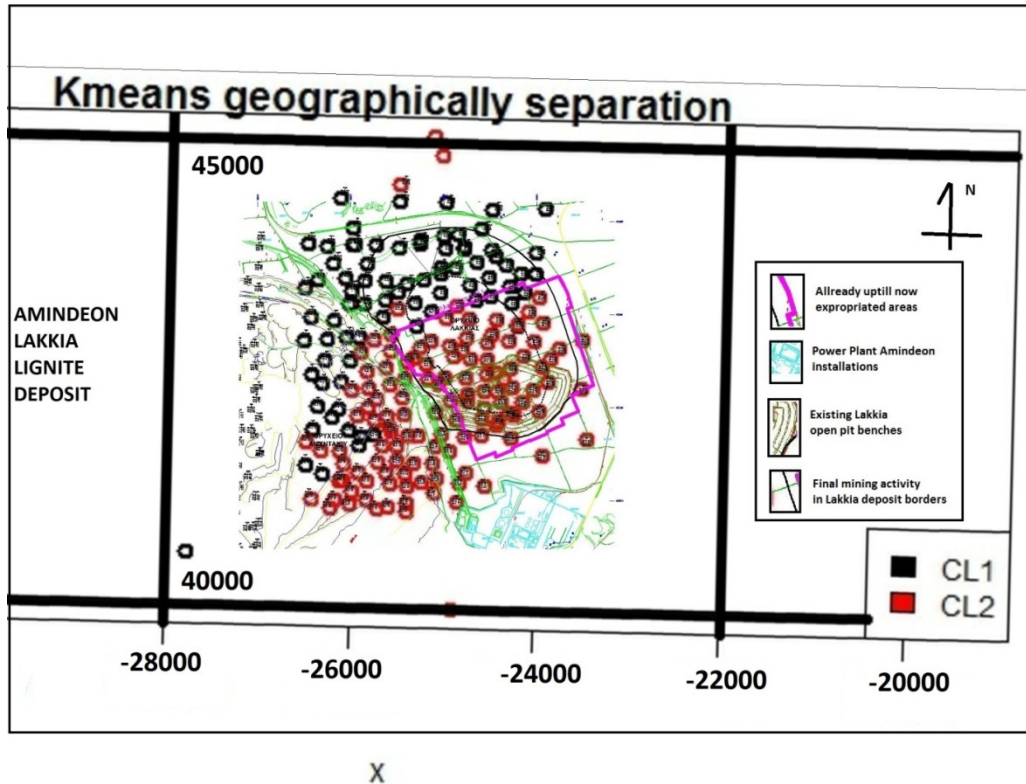


Figure 6. Segmentation of Lakkia deposit into Sectors by K-means Cluster Analysis

3.2. Unsupervised machine learning in an operational mine phase

Principal Component Analysis on 3 years monthly mining operating data of South Field mine in Ptolemais lignite bearing basin [18], considering 39 explanatory variables (Table 1), revealed 7 principal components, corresponding to 75% of total cloud's variance. The analysis refers to specific mining areas and mining conditions and summarizes that:

First Principal Component Comp1 describes intensive total overburden excavations and many waste excavations by Bucket Wheel Excavators (BWE) accompanied by the reduction of total overburden excavations by contractors, reduction of overburden excavations in Sector 7, reduction of lignite production by contractors in Sector 6, as well as reduction of total lignite production by contractors. This is followed by high operating availability factor, high average hourly output and increased utilization factor, revealing the advantage of continuous mining versus non-continuous mining in specific mining areas. As far as down times are concerned, tis component reveals a high number of maintenance hours, downtimes due to Power Plant as well as total downtimes.

Second Principal Component Comp2 describes increased excavations by non-continuous mining in specific areas of Sector 6, in parallel with an increase of deep bench intermediates and lignite production by contractors, accompanied with less lignite production by BWE and a decrease of waste removal with own non-continuous mining equipment.

Table 1. South lignite Field Operational efficiency PCA audit

Variable	Explanatory variable	Comp1	Comp2	Comp3	Comp4
-----		-----	-----	-----	-----
var1	Lignite production by Bucket Wheel Excavators	0.0481	-0.272	-0.0984	0.3237
var2	Excavations (only wastes) by BWE	0.2756	-0.0943	0.1492	0.029
var3	Own non continuous mining equipment (wastes)	0.1349	-0.2465	0.1967	-0.0147
var4	Total overburden excavations	0.2687	-0.1464	0.1801	0.0217
var5	Excavations by contractors in Sector 7 (overburden)	-0.193	0.0167	0.0841	-0.1072
var6	Excavations by contractors in Sector 6 (overburden)	-0.0138	0.3202	0.1045	-0.1042
var7	Sector 6 intermediates wastes in the lignite deposit (contractors)	-0.1669	0.2167	0.1279	0.2067
var8	Deep bench intermediates wastes (contractors)	-0.0972	0.1811	-0.1174	0.0336
var9	Total overburden excavations by contractors	-0.1627	0.306	0.1049	-0.0453
var10	Total overburden excavations	0.1478	0.1023	0.2738	-0.0157
var11	Lignite production in Sector 6 by contractors	-0.2121	0.0514	0.0672	0.0339
var12	lignite production in deep bench by contractors	0.0085	0.1687	-0.2121	-0.0163
var13	Total lignite production by contractors	-0.2028	0.2022	-0.1235	0.019
var14	Total lignite production	-0.1158	-0.105	-0.1961	0.3337
var15	Operating availability factor	0.2529	0.2312	-0.0237	0.0651
var16	Average hourly output	0.16	-0.2437	0.1364	0.072
var17	Utilization factor %	0.2904	0.1023	0.0633	0.0607
var18	Mining ratio	0.1574	0.1497	0.2065	-0.2919
var19	Ash content (%dry lignite)	-0.017	0.0627	-0.0226	-0.0265
var20	Lower Calorific Value	0.1427	0.0287	0.0722	0.049
var21	Productivity (FM3/(8hours*person))	0.3066	-0.0483	0.0248	0.0634
var22	Non active productivity %	0.0566	-0.0212	-0.1303	0.2188
var23	Overwork	-0.165	-0.0692	0.2663	-0.2479
var24	Illnesses 8h	-0.0581	0.1083	-0.1555	-0.0094
var25	Owing rest hours	0.1442	0.1581	0.0616	0.0194
var26	Maintenance hours in month	0.1593	0.2718	0.0419	-0.1536
var27	Planned downtimes for mine modifications (hours in month)	-0.0276	-0.1578	0.1446	-0.2055
var30	Downtimes in spreader	-0.0483	0.1832	0.3149	0.2586
var31	Downtimes due to Power Plant	0.234	0.1889	-0.2397	0.0132
var32	Mechanical failures (hours)	-0.0575	0.1607	0.3223	0.2746
var33	Downtimes due to belt melding	-0.1033	-0.0792	-0.1627	-0.0298
var34	Electrical failures (hours)	0.0397	0.104	0.0861	0.2937
var35	Downtimes due to mining causes (hours)	-0.1942	-0.0324	0.113	0.0646
var36	Downtimes due to personnel lack	0.0683	0.0115	0.0516	-0.1134
var37	Downtimes due to various causes	0.1088	0.1339	0.0142	0.3936
var38	Total downtimes	0.2023	0.04	-0.3167	-0.165
var39	Available operating hours	-0.2163	-0.1967	0.1965	0.047

This results to an increase of operating availability factor and available operating hours, increase of owing rest hours maintenance, downtimes in spreaders and mechanical failures, in combination to a decrease of average hourly output. Comp3 describes the consequences of extreme downtimes in spreaders and mechanical failures for a certain period and specific mining areas.

Comp4 describes maximization of total lignite production with the maximum contribution of BWE lignite production, in regions with minimum mining ratios. This results to the reduction of total downtimes.

3.3. Unsupervised machine learning in water environmental impact assessment

Factor analysis was implemented in order to determine principal components of water analysis acquisition data in the region of Ptolemais lignite bearing basin and its mountainous surroundings. By following the same methodology of a previous work regarding Megalopolis lignite bearing basin [9], an investigation was carried out on the impact of ash depositions to the surface and subsurface aquatic environment in the broader area of South Field, Ptolemais, lignite bearing basin.

The primary data frame loaded as input in Stata 1.1. The software platform was an initial matrix of 400 recent water samples that were collected, mainly during wet and dry season. 300 of these samples, covering an extended area from Florina to Aliakmon river [22], were collected and analyzed by I.G.M.E. [19] and NTUA [20] (Fig. 7). In addition, chemical analysis of 20 samples collected from the South lignite bearing basin was performed by Center of Standards and Tests of P.P.C. Chemical Laboratory and incorporated into the data set (Fig.8). The full data set is described by 15 hydro chemical parameters as explanatory variables.

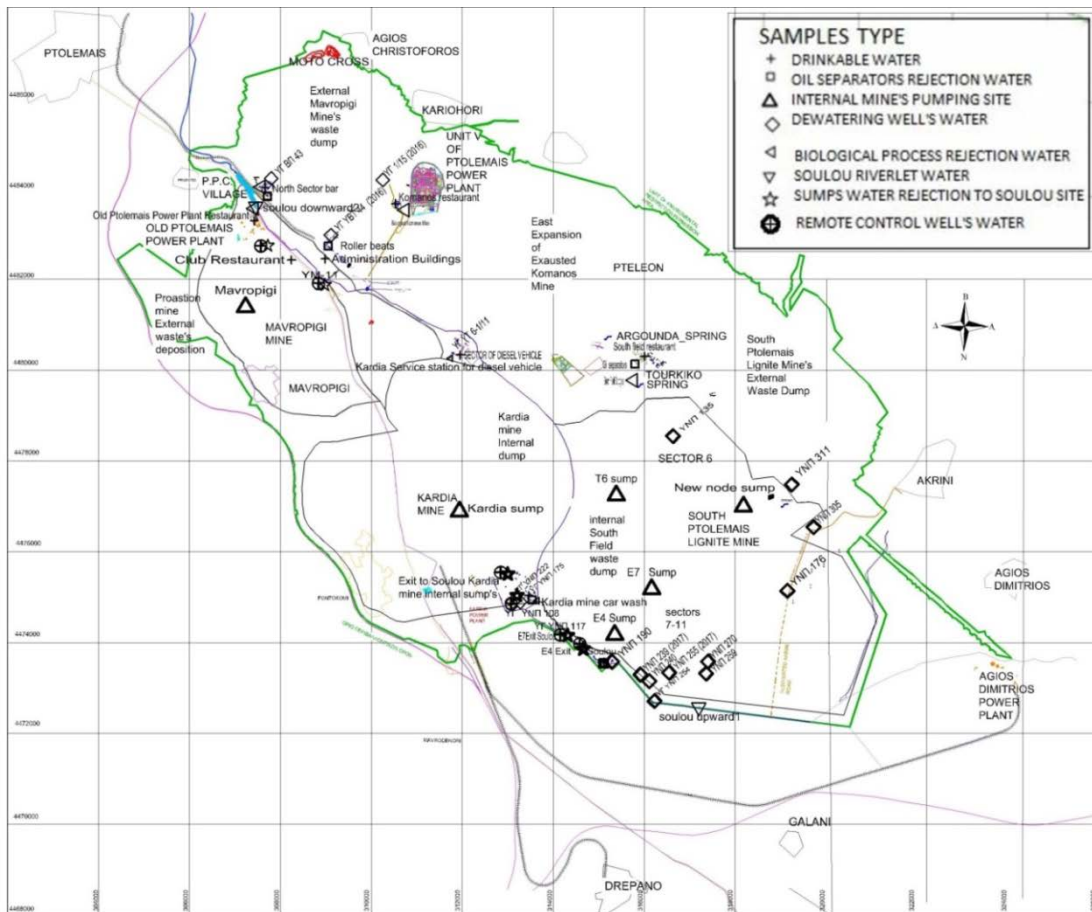


Figure 7. PPC water sampling sites location map in Ptolemais lignite bearing basin

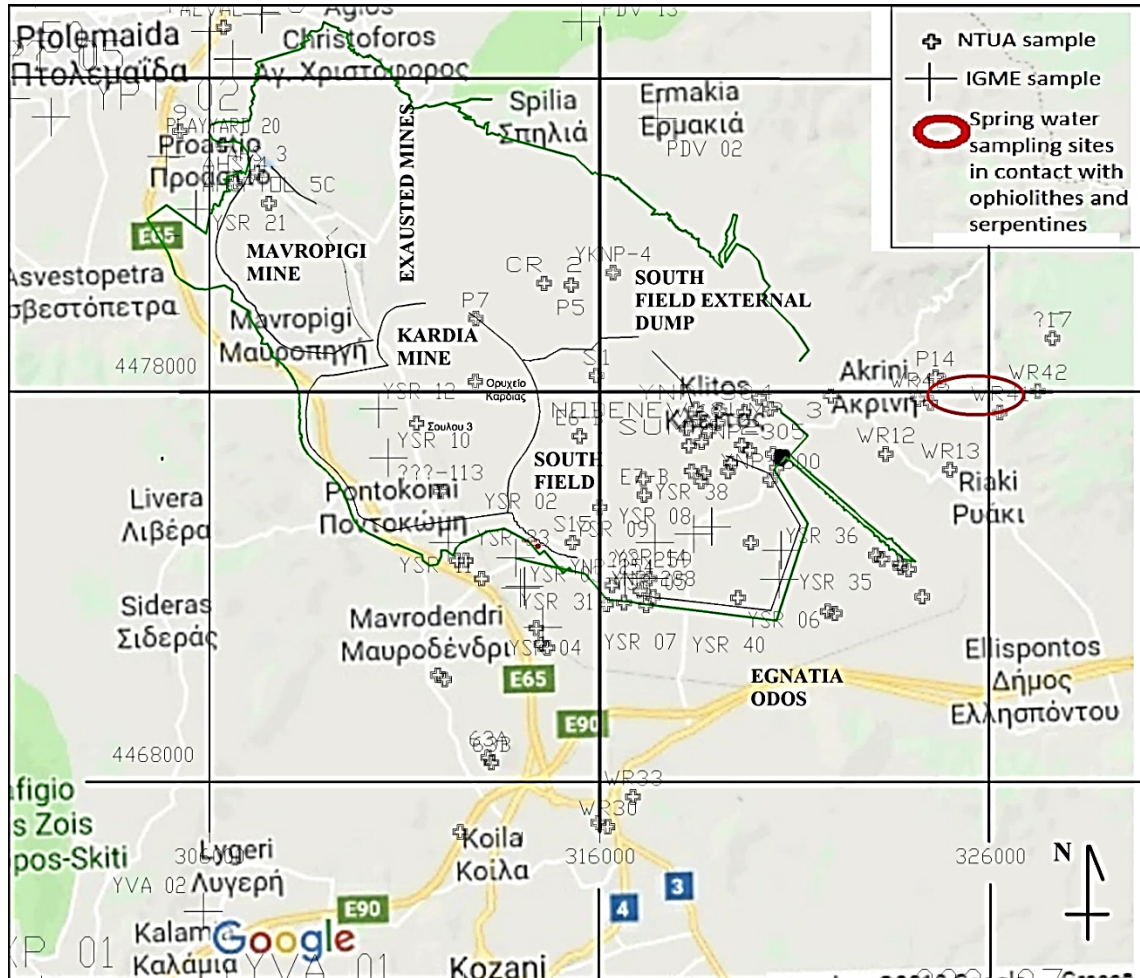


Figure 8. IGME and NTUA water sampling sites location map in Ptolemais lignite bearing basin

Cluster analysis of the 400 observations by K-means resulted to the classification of data cloud in 5 groups. Cluster 1 involves a mechanism that increases pH, E.C., Ca, K, Ni, Ba (Fig. 9, 10). This mechanism is the ash deposit leaching procedure, as in Cluster 1 four samples of are classified. No other sample of groundwater was classified in cluster1.

Principal Component Analysis results revealed 5 principal components (Fig. 11). In Fig. 11 the biplots diagram of first and second components are depicted.

First principal component corresponds to ash deposition leaching mechanism, as it reveals a combination of increased Ca, pH, SO₄, E.C., NO₃, Ba, B. None of the 390 surface and subsurface regional waters has a score more than 1.0 to PC1. Thus we come to the conclusion that this mechanism does not appear in sampling sites of regional waters.

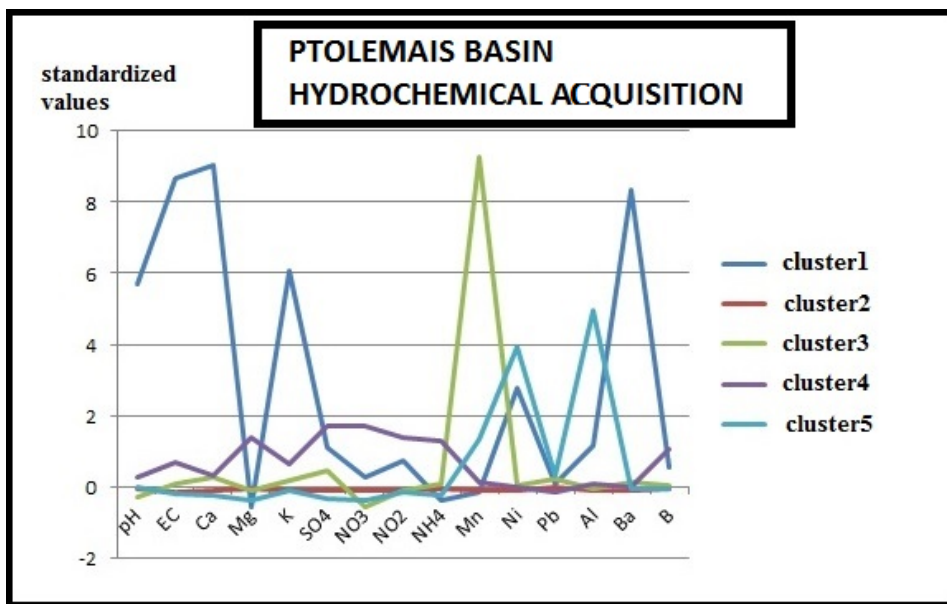


Figure 9. Clusters characteristics of Ptolemais basin hydro chemical acquisition

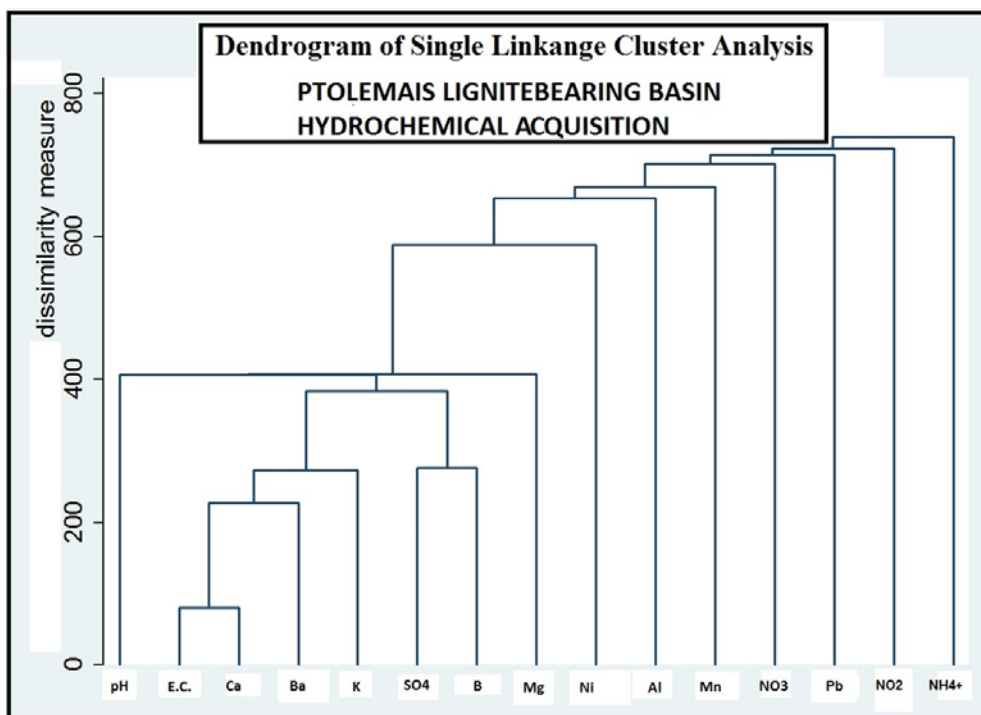
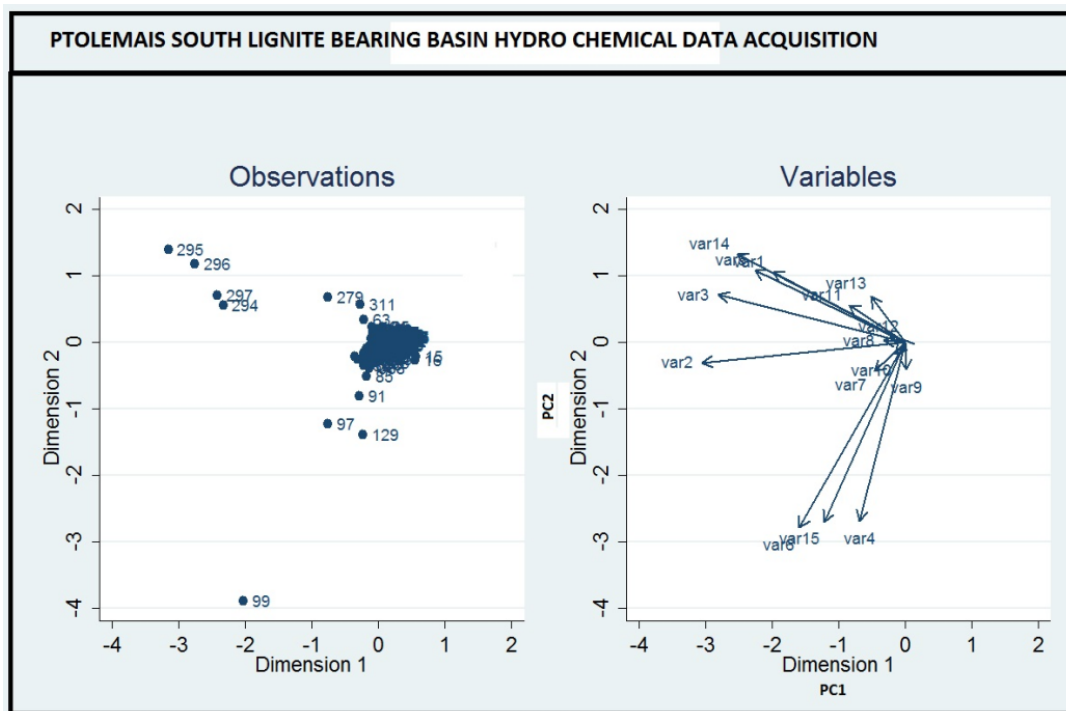


Figure 10. Ptolemais lignite bearing basin hydro chemical acquisition's single linkage dendrogram



Var1	pH
Var2	EC
Var3	Ca
Var4	Mg
Var5	K
Var6	SO ₄
Var7	O ₃
Var8	O ₂
Var9	NH ₄
Var10	Mn
Var11	Ni
Var12	Pb
Var13	Al
Var14	Ba
Var15	B

Figure 11. Biplots of PC1 and PC2 components in Ptolemais hydro geochemical acquisition

4. CONCLUSIONS

The application of PCA to the borehole data set could highlight the structure and the characteristics of the deposit. Furthermore, it can be used as a tool for mine planning and design purposes, and also for the optimization of strategic mine development. In addition, PCA can reveal useful indicators regarding the operation of mining equipment.

By applying PCA to hydro-chemical data, two goals could be achieved: First, PCA results can be used to generate an alarm system, which will warn of mine water leakage, before the logged parameter values reach a critical point. Second, PCA can be considered as an investigation technique of the environmental impact in an integrated mining and hydro-geological approach.

In addition, unsupervised machine learning could become a useful tool for hydro-chemical investigations, satellite image interpretation, deposit exploration, as well as for environmental impact assessment.

REFERENCES

- [1] Fijani E., Barzegar R., Deo R., Tziritis E., Skordas K. (2018). Design and implementation of a hybrid model based on two-layer decomposition method coupled with extreme learning machines to support real-time environment monitoring of water quality parameters, *Science of the Total Environment*.
- [2] Hall, P., Phan, W., Whitson K. (2016). “The evolution of Analytics and Challenges for Machine Learning in Business”, O’Reilly Media Inc., Boston-Tokyo.
- [3] Patra S, Bruzzone, L. (2011). A fast cluster-based active learning technique for classification of remote sensing images. *IEEE Trans Geosci Remote Sens* 49(5):1617–1626.[4] Introduction to remote sensing data analysis using R
- [5] Charou, E., Stefouli, M., Dimitrakopoulos, D., Vasiliou, E., Mavrantza, O.D. (2010). “Using Remote Sensing to Assess Impact of Mining Activities on Land and Water Resources”, *Mine Water Environment* 29, p.p. 45-52.
- [6] Gemitzi, A., Angelou, I. V. (2017). “Vegetation changes in Natura 2000 sites in Greece using remote sensing data”, 15th International Conference on Environmental Science and Technology, Rhodes, Greece.
- [7] Gemitzi, A., Lakshmi, V. (2017). “Downscaling GRACE data to estimate groundwater use at the aquifer scale”, 15th International Conference on Environmental Science and Technology, Rhodes, Greece.
- [8] Sideri, D. (2016). “Investigation of land subsidence in the west Thessaly basin by using geostatistical models based on the geotechnical behavior of the alluvial formations”, PhD Thesis on Geological Science Sector at School of Mines and Metallurgical Engineering, National Technical University of Athens, p.100-102.
- [9] Louloudis, G. (2017). “The worth of hydro geochemical data factor analysis (PCA) in interpretation of underground water origin. Megalopolis lignite bearing fields mine water and regional waters relations case study”, 15th International Conference on Environmental Science and Technology, Rhodes, Greece.
- [10] Zaiontz, C. (2013). Real Statistics using Excel, Principal Component Analysis, <http://www.real-statistics.com/multivariate-statistics/factor-analysis/principal-component-analysis/>.
- [11] Tesch, S., Otto, M. (1995). “Application of principal-component analysis to the interpretation of brown coal properties”, *Fuel* Vol 74 No.7 p.p. 978-982, Copyright © 1995 Elsevier Science Ltd. Printed in Great Britain.
- [12] Aaron, F., Caffo, B., Schwartz, B., Zipunnikov V. (2016). Fast, exact bootstrap Principal Component Analysis for $p > 1$ million. *Journal American Stat. Assoc.*
- [13] Karlis, D. (2018). Statistical Learning Notes for MSc in Statistics Athens University of Economics and Business, Department of Statistics, Athens, Greece.
- [14] Karamalakis, N. (1993). “Software package for evaluating lignite deposits”. *Scientific Bulletin* 42, Public Power Corporation, Greece, pp. 67–77.
- [15] Karamalakis, N. (2004). “Determination and quality test of lignite deposits”. Phd Thesis in School of mines, National Technical University of Athens.
- [16] Kolovos, N., Sotiropoulos, D., Georgakopoulos, A. (2005). Contribution on Lignite Recovery from Multi-Seam Deposits, *Energy sources*, pp 975-986.

- [17] Smith, W.H.F., Wessel, P. (1990). Gridding with continuous curvature splines in tension, *Geophysics*, Vol.55, No.3, p. 293-305.
- [18] Theodoridis, K. (2017). Monthly Activity Report of South Ptolemais lignite Field. Western Macedonian Lignite Center, Ptolemais, Greece.
- [19] Stamos, A. et al. (2010). Chemical analysis of ground water of Western Macedonian (09) Aquatic Department, IGME, Kozani, Greece.
- [20] Perraki, M. (2016). Mineralogy and petrographic geochemical relation between the occurrences of heavy metals in subsurface and surface waters of lignite mines fields Ptolemais region and in geological formations (hyper basic rocks, lignite, wastes) or bursting products of lignite (flying ash), Research Project, Final Report, NTUA, Athens.
- [21] Everitt B. S., Hothorn A. T. (2009). “A Handbook of Statistical Analyses Using R”, Paris.
- [22] Hamilton, Lawrence C. Thomson Books/Cole, (2006), *Statistics with STATA* (updated for version 9).
- [23] Ting-Nien Wu, Chiu-Sheng Su, (2008). “Application of Principal Component Analysis and Clustering to Spatial Allocation of Groundwater Contamination”, Fifth International Conference on Fuzzy systems and Knowledge Discovery, Water, Volume 4, p 236-240.
- [24] Roumpos, C., Pavloudakis, F., Galetakis, M. (2009). “Optimal production rate model for a surface lignite mine”. 3rd AMIREG International Conference Assessing the Footprint of 360 Resource Utilization and Hazardous Waste Management, Athens, Greece.
- [25] Chatzigiannis, G., Fanara, E., Xenaki, M. (2001). Lignite composition study in relation to electric power generation suitability investigation, Operational energy program, Subprogram 4, Energy raw materials, Ministry of Development, Athens p.p. 82-88.
- [26] Sungkyu Jung (2015). *Lecture Notes of University of Pittsburgh Department of Statistics*.
- [27] Mohammed J. Zaki, Wagner Meira JR. (2014). *Data mining and analysis. Fundamental Concepts and Algorithms*. Cambridge University Press.

An Evolutionary Solution for Coal Reserves Modelling and Production Scheduling

Ioannis Kapageridis¹, Allan Kerridge² and Eduardo Coloma³

¹Technological Educational Institute of Western Macedonia, Koila, Kozani, 52100, Greece

²Maptek Pty Ltd, Level 14, 10 Eagle Street, Brisbane QLD 4000, Brisbane, Australia

³Maptek Pty Ltd, Level 2, 190 Aberdeen Street, Northbridge WA 6003, Perth, Australia

ABSTRACT

Coal and other stratigraphic deposits consisting of multiple layers commonly require a lot of time and effort to produce a representative geological model that will allow accurate estimation of reserves and provide a solid basis for effective mine planning. The transition from such a 3D geological model of stratigraphy to an effective Run-Of-Mine model that can be used to calculate reserves is a critical part of this process. Approaches to achieve this transition range from one-dimensional mineable coal compositing of drillhole data to more effective three-dimensional aggregation of mineable coal seams based on an appropriate stratigraphic geological model. There are very few commercial software packages that integrate a complete stratigraphic modelling module, and even fewer that have the capability to take the process further into production scheduling. The solution presented in this paper is based on two commercial software packages part of the same family of products – Maptek Vulcan, a general mine planning package with advanced stratigraphic modelling capabilities, and Maptek Evolution, a mine scheduling package based on evolutionary algorithms. The examples presented in this paper show how the two packages together provide a complete solution for coal reserves modelling and production scheduling.

1. INTRODUCTION

Developing an effective coal resource model from drillhole data is a difficult and time-consuming process. In cases where the deposit consists of multiple coal layers, it becomes even harder as certain important steps like seam correlation require better understanding of the data in 2D (plans and sections) and 3D (complete derived model) and the overall process requires a lot more time. In such cases, proper geological software tools are essential in working with drillhole data to identify the correlation of seams in plans and sections and check the produced model in three dimensions. The visualisation and statistical analysis capabilities of the software become crucial. The amount of data and information is simply too large to handle with traditional methods of producing sections and plans.

Once seam correlation is complete, the drillhole database can be used to develop a complete structural and qualities model of stratigraphy. Seam extents, seam merging and splitting, faulting, and other aspects of geology need to be effectively addressed by the modeller and the software. The end result of this effort will be a stratigraphic model and a corresponding resource model commonly in the form of multiple grid models or an overall stratigraphic block model.

Prior to reporting coal reserves and moving to pit design and scheduling, it is necessary to convert the developed coal resource model to a coal reserve model by applying a number of parameters related to the mining method(s) applied and the coal quality targets. These parameters commonly include minimum mineable coal and waste thickness, maximum parting thickness when merging waste with coal to achieve minimum thickness, and maximum ash content for mineable coal. Roof and floor losses are also applied as well as mining dilution. The final coal reserves model

should be the result of sound geological interpretation and solid mining factors application with increased confidence.

The procedure discussed in this paper, covers all aspects of generating a coal reserves model starting with a correlated drillhole database. Two closely interacting software solutions are presented in the discussion that provide all necessary functionality to develop a coal reserves model and proceed with the scheduling of the produced reserves. Maptek Vulcan and particularly the Integrated Stratigraphic Modeller provides all the necessary functionality to produce a coal resource model using drillhole, topographical and tectonic data (Section 2). Maptek Vulcan also provides the tools to output the resource model in a format readable by Maptek Evolution – the second software package discussed in this paper, responsible for the development of the coal reserve model (Section 3) and production scheduling (Section 4).

2. STRATIGRAPHIC MODEL DEVELOPMENT

2.1. Overview of Integrated Stratigraphic Modelling

Maptek Vulcan integrates one of the most complete Integrated Stratigraphic Modelling modules (ISM) providing a variety of modelling methods to develop stratigraphic, structural and grade/quality grid models using an automated modelling process. A unique stratigraphic block model structure, the HARP (Horizon Adaptive Rectangular Prism) model, gives further flexibility and capabilities in stratigraphic reserves modelling. HARP's non-rectangular block models easily handle reverse faults and very thin horizons, that can be reserved against complex 3D solid shapes such as pit cutbacks and mining blocks (Fig. 1) [1]. A single file contains all the structural, quality, faulting and associated data. Geological resolution and stratigraphic fidelity are preserved. The steps included in the development of a stratigraphic model using ISM are as follows [2]:

1. **Database Validation:** the first step in the process is to validate the drillhole database in Vulcan and ensure all data entries are legitimate. This step allows *field-by-field validation* to check the contents of a specified field against a variety of possible entries for that field, for example, check if the logging codes are valid, if the data lies in certain ranges, and that data has been entered into a mandatory entry field. It also allows *global validation*, i.e. the contents of a field are checked against the contents of all other occurrences of that field in the database, for example, the hole name and/or Eastings and Northings for a hole will be checked against every other hole in the database.
2. **Drillhole Data Interpolation (FixDHD):** FixDHD is an option of ISM used to interpolate missing stratigraphic horizons in drillhole data to improve stratigraphic modelling. It 'recognises' that most drillhole data sets contain a number of problems and provides a range of interpolation options to best address these. If a horizon is missing in a drillhole, roof and floor positions are calculated using actual, logged, horizon intervals in drillholes surrounding the drillhole with the missing horizon. An inverse distance weighting method is applied to determine which intervals to use. Intervals which are both stratigraphically and geographically closest to the missing horizon receive the highest weight. Some typical data problems and the way FixDHD addresses these are outlined in the following paragraph (2.2).
3. **Stratigraphy Structural Modelling:** at this stage, the fixed stratigraphic information of the database is used to model structurally the roof and floor (upper and lower boundaries) of all horizons of interest as well as structural thickness, cropping and horizontal extents (masking). Faulting can be defined in four different ways:
 - **Zones and Crest and Toe** methods are all purely grid-based methods, and as such are not suited to modelling reverse or thrust faults. In the Zones method of fault definition, a series of mutually-exclusive, polygonal limits are applied. The faults are typically applied to an individual surface.

- **Blocks** and **Throw** methods are suited to more complex faulting scenarios, including reverse and thrust faults.

Grid models are commonly used for structural modelling as they allow quick and straightforward application of mathematical equations and relationships between them. Paragraph 2.3 covers this step.

4. **Compositing and Modelling of Qualities:** at this step ISM produces a composite for any specific interval down a hole. The composite interval (the structure) can be defined by geology, height, surfaces, or a combination of these. Analytical data can be extracted from multiple databases using depths or samples. This step is covered in Paragraph 2.4.
5. **HARP Model Generation:** a HARP model represents an entire Integrated Stratigraphic Model in a single block model file. The HARP model is created directly from grids or faulted triangulations. All quality grids are automatically incorporated. The development of the HARP model is covered in Paragraph 2.5.
6. **Run-Of-Mine (ROM) Model Generation:** ISM simulates the manner in which material is extracted from a stratigraphic deposit. Basic parameters are defined for extraction. The ROM model is constructed from the geological model using three rules. These rules are applied to the mine modelling process in the following order:
 - Minimum parting thickness
 - Minimum mining thickness
 - Minimum product to waste ratio

The output of this process is a new ROM HARP model.

7. **Strip Ratios Calculation:** at this final step, it is possible to calculate a ratio from a Stratigraphic Block model or HARP model. The stripping ratio is defined as the volume of waste material divided by the tonnage of product material.

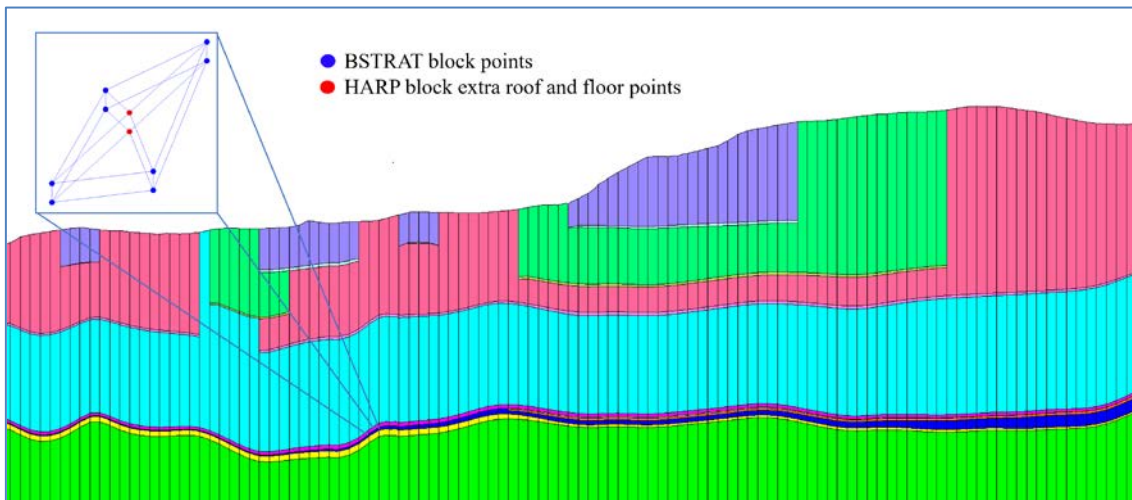


Figure 1. Example section through a Horizon Adaptive Rectangular Prism (HARP) model and detail of a HARP block showing the use of 5 points on the top and bottom side (see section 2.5).

Steps 6 and 7, i.e. the generation of the ROM model and calculation of strip ratios can now take place in Maptek Evolution. This leads to the development of a reserve ROM model, ready for scheduling, as opposed to the resource-based ROM model generated by ISM. However, the coal aggregation facilities in Maptek Evolution should not be considered as a direct replacement of the corresponding functionality of ISM, as the ROM model produced by ISM can be used in Maptek Vulcan to help design the mine and calculate resources before moving to the reserve model and scheduling in Maptek Evolution.

The purpose of stratigraphic modelling is to create an idealised representation of the stratigraphy in an area of interest. Such models allow comprehension of many useful characteristics. These include the geological processes affecting the stratigraphy, their three-dimensional inter-relationships and the accurate calculation of measurements (depth to horizons, fault locations, reserves etc). The following sections discuss the most important steps of the ISM modelling process in more detail.

2.2. Drillhole Stratigraphic Data Validation and Interpolation

Typically, data for coal resource modelling is collected in the form of drillholes in which the positions of horizons of interest are logged. Rarely, however, are the data so perfectly collected so as to provide information about all of the horizons to be modelled in every hole. As shown in Fig. 2, almost all drillhole data sets will contain holes where some of the horizons are not represented. The reasons for this are various; some inherent in the nature of the deposit being drilled, some introduced by the methods of the drilling program and some by poor logging practice or lost data. The reasons for the missing information fall into two main categories [1]:

1. Data that was not collected by the drilling program.
2. Data that was not available for collection because of pre and post-depositional geological processes.

The problems that can be caused by the first of these categories are:

- Short holes which are not deep enough to include all horizons of interest.
- Problems determining the position of missing horizons that have thinned to zero thickness.
- Problems determining the position of the boundary of daughter horizons in their merged parent horizon.
- Lost core, lost data or poor logging.

The problems that can be caused by the second category are:

- Removal of horizons from the top of the sequence by erosion.
- Weathering of horizons blurring upper boundaries.
- Sub-cropping of horizons against other geological features.
- Washout by erosion processes at the time of deposition.

In addition to the above, drillholes may not be vertical, which compromises the modelling requirement that we know the vertical thicknesses and position at a given location.

These problems are resolved using various techniques provided by the FixDHD option of the ISM. FixDHD will attempt to fill in these gaps using statistical modelling techniques to determine the missing or unavailable data from the known data, and to manipulate the available data to meet the required criteria for modelling. An example of the FixDHD operation is shown conceptually in Fig. 3. Where there is insufficient data for the statistical techniques to be employed, less rigorous stacking methodologies are employed, full details of which are supplied to a process log for auditing purposes. Generally, where horizons pinch-out, zero thicknesses are applied, where horizons have been removed via post-depositional processes, they are restored, where data has not been sampled, it is interpolated and where merged seams are identified, the merged seam is re-identified as the relative component splits.

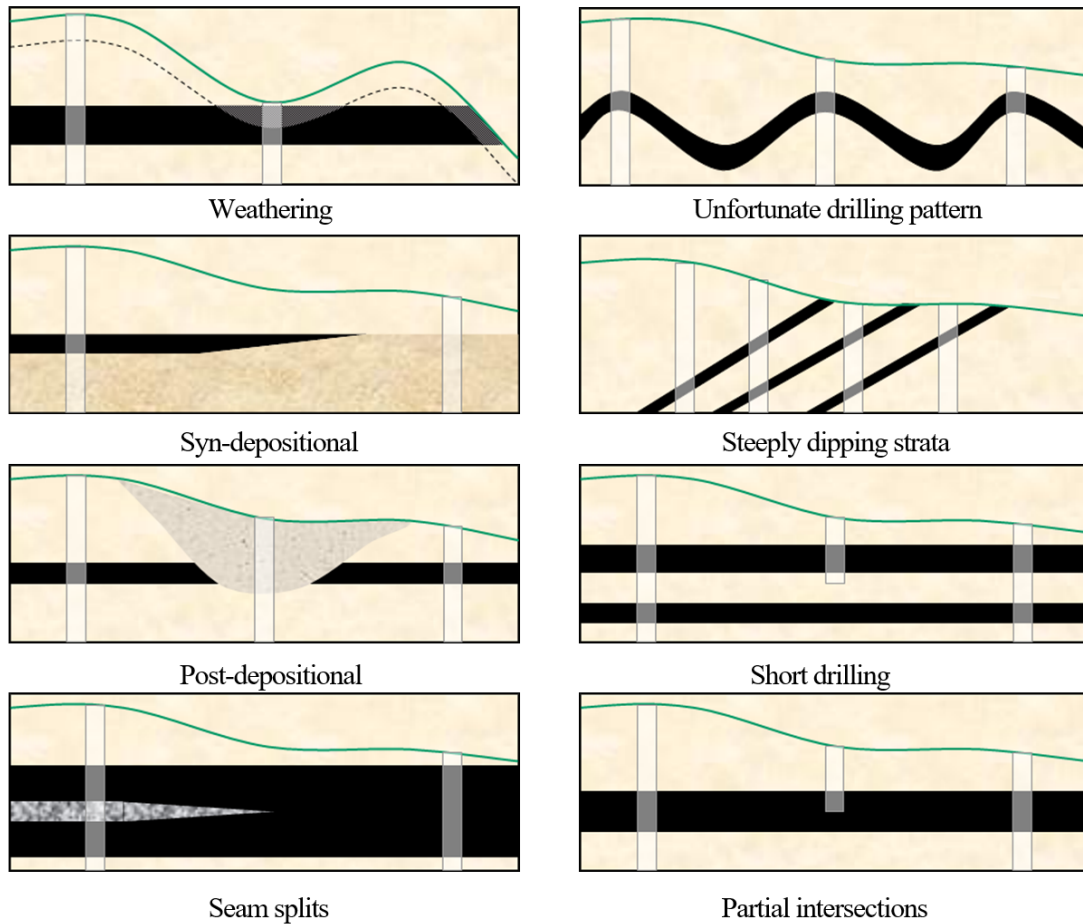


Figure 2. Potential issues with drillhole stratigraphic data that need to be addressed before structural modelling [3].

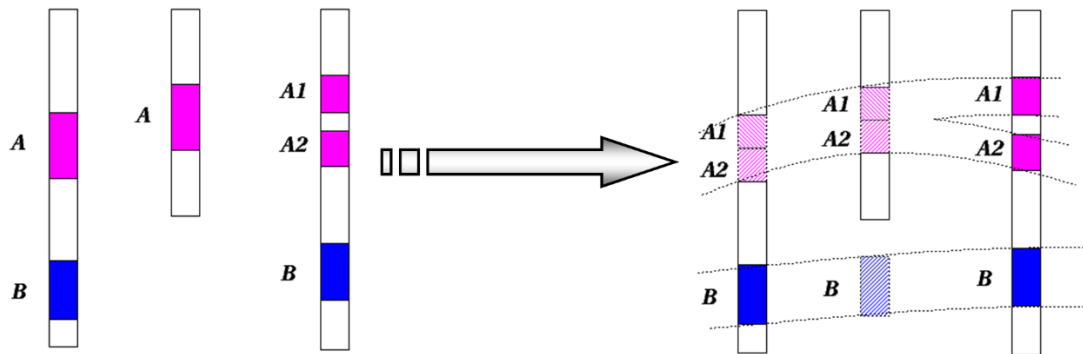


Figure 3. Concept of interpolating/fixing incomplete drillhole stratigraphic data (left) with FixDHD (right) [3].

If a drillhole is collared in a horizon, FixDHD does not consider the collar location as a reliable roof position for that horizon as it could be considerably higher in elevation. Therefore, the roof position for that horizon may be interpolated above the collar location using the surrounding, reliable intervals for the horizon in question. Similarly, a drillhole that terminates in a horizon does not reflect reliable floor positions for the horizon in which they terminate. This is because the horizon may extend deeper than what drilling indicates. Therefore, the floor position for that horizon may be interpolated below the drillhole terminus using the surrounding, reliable intervals for the horizon in question.

A major advantage of the FixDHD process over previous interpolation tools is that it works directly from the drillhole database. The fixed version of the stratigraphic data is kept together with the original, clearly marked to allow validation before modelling. After generating a consistent stratigraphic sequence in each drillhole, we can begin our structural modelling procedure.

2.3. Structural Modelling

There are three main methods of creating a structural model in ISM:

1. **Stacking**: creates all horizon models based upon one selected structural surface. A selected surface becomes a reference for creating the rest of the grids in the model. The remaining surfaces are created by adding and subtracting thicknesses and midburdens from the reference surface. The reference surface is the horizon in which there is the most confidence. This is generally the horizon with the most, or most reliable, data. It is modelled using one of the available modelling algorithms: *triangulation*, *inverse distance weighting*, *kriging*, *spline*, *least squares*, and *trend surface*.
2. **Structural Surfaces**: models individual roof and floor surfaces for each horizon using the available modelling algorithms mentioned above. As roof and floor surfaces represent the same type of data, a height above sea level, a single modelling method is used for both. After roof and floor models for each horizon are created, thickness grids are automatically generated between adjacent pairs of surfaces. Every node in each thickness grid is forced to a value of zero or greater, which insures that no horizons cross each other. Should a horizon cross its neighbour, either the floor is forced to the roof position, or the roof is forced to the floor position.
3. **Hybrid**: is an enhanced Stacking method. The ability to include additional design CAD data for any roof, floor or thickness interval for any horizon adds extra control. It is possible to control the horizontal and vertical influence of defined design data. A Hybrid method offers many of the advantages of either the Stacking or Structural Surfaces method with few of the drawbacks.

Each method has advantages and drawbacks. Regardless of the method, the produced structural model needs to be visually checked and compared against the correlated drillhole intervals in sections and in three dimensions. Figure 4 shows the comparison of database and grid (model) correlation in a drillhole section view window. Figure 5 shows multiple coal grid models in three dimensions constituting part of the structural model of a coal deposit. Faulting and seam limits are evident.

2.4. Compositing and Quality Modelling

In addition to the structural models of the seams, it is necessary to model various coal quality parameters such as ash content, sulfur, insitu moisture, calorific value and density. As the original analyses on the drillholes do not necessarily follow the correlated and fixed stratigraphy after the application of FixDHD, it is necessary to composite these values to receive a single value for each parameter per correlated seam before modelling the parameter in two dimensions as a grid model. A special compositing function of ISM is used to generate formatted text files with all the composite values - one file per seam. The information contained in these files is then used to model quality parameters per seam, commonly using the inverse distance weighting method.

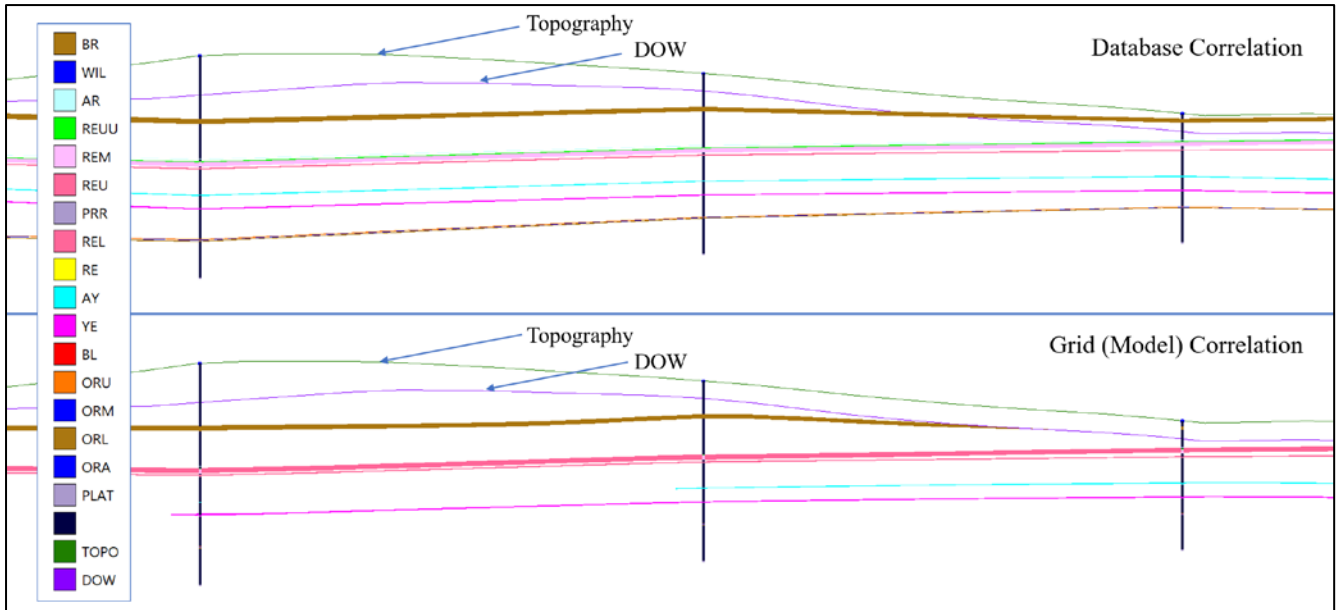


Figure 4. Comparison of database and grid model correlation in section view showing the effects of structural modelling and cropping of seams using topography and depth of weathering (DOW) surfaces.

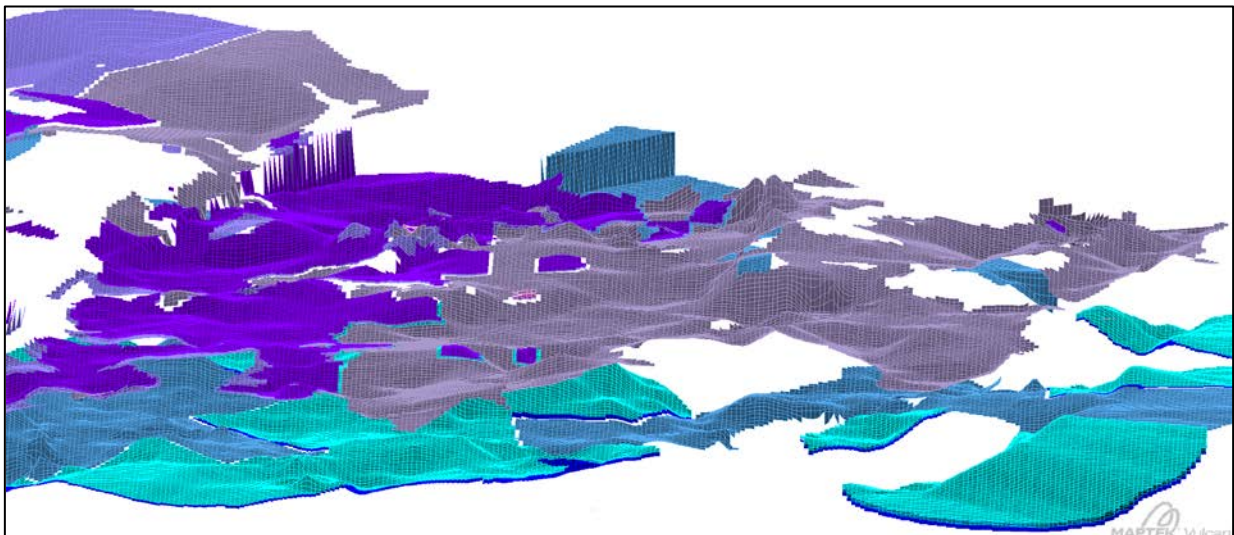


Figure 5. Grid models of coal seams floor developed with ISM showing the effect of seam limits and faulting.

In the situation where the deposit contains split horizons, one must consider how to treat qualities. There are a few strategies to consider:

- a. Quality information for the parent seam and any child horizons is considered and modelled entirely separately. Grid masks are used when reserving to ensure that only the parent qualities are used for the extent of the parent, and child qualities for the extent of the child horizon.
- b. The entire envelope of a split horizon is considered when compositing qualities. This means that the region from the top of the uppermost split to the base of the lowermost split is used across the extent of the parents and children. This involves compositing in partings between splits.
- c. Only child horizons are composited. A weighting method is used where parent seams exist to artificially split them into child quality values. If there is no breakdown of quality sampling within a parent horizon, then each child is given the full quality value of the parent seam.

- d. The methodology in part c is combined with a Run of Mine (ROM) horizon compositing exercise to produce ROM grids. These grids combine and split on mining rules, not geological logging.

2.5. HARP Model Development

Traditional stratigraphic block models (known as BSTRAT models) were used prior to Maptek Vulcan version 8.0 to represent stratigraphic deposits. Like all traditional block models, each block was formed by a cuboid. As each vertex of the cuboid is formed with right angles, the blocks could not adequately represent roof and floor structures. A HARP model block contains 5 points in the roof of the block and 5 points in the block floor. These points allow vertex angles to fluctuate, which allows the block to conform to structure roof and floor grids (Fig. 1). HARP models accurately resolve horizons down to a few centimetres of thickness without the need to make huge models with extremely small Z sub-blocking. HARP non-rectangular block models easily handle reverse faults and very thin horizons and can be reserved against complex 3D solid shapes such as pit cutbacks and mining blocks. The benefits of using HARP models for coal resource and reserve modelling have been presented in various case studies in the past ([4], [5]).

Development of the HARP model is basically a single step in the ISM process. All structural and quality grid models are combined to form a single stratigraphic block model using the 10-point block geometry of the HARP model that allows it to match exactly the shape of the structural grids. All quality grid models become block model variables and their node values are transferred to the corresponding blocks. As grids are named with the standard naming convention during the ISM process, the appropriate quality grid value is automatically associated with the relevant block in the HARP model based on the horizon variable. The grid value is populated into the HARP block vertically above the grid cell. The produced HARP model becomes a complete database of coal resources for the project. As HARP block sizes vary along the Z axis, it would be necessary to run a regularisation step to a standard block size to allow running a pit optimisation algorithm and derive optimum pit limits from such coal resource model.

3. RUN-OF-MINE MODELLING WITH MAPTEK EVOLUTION

3.1. Overview

With the latest version, Maptek Evolution can work with a reserve model based on solid triangulations – this allowed the development and integration of a new coal seam aggregation module that takes an in-situ model and produces practical run-of-mine reserves within a flexible, yet automated, step-based workflow system [6]. Getting seam aggregation right is critical for accurate estimation of tonnages, and easy and efficient scheduling for stratigraphic mines.

The coal transformation module in Maptek Evolution is designed to take the reserved insitu solids from a mine planning package and calculate step by step coal qualities and quantities for each stage of the mining and beneficiation process. The result of these calculations is the construction of a Coal Reserves Model. It uses a ‘pipeline’ calculation process that applies a series of pre-built or custom scripted transforms in order to perform these calculations. The module has been designed to be labour saving, while still offering flexibility.

3.2. Basic Concepts

An Evolution coal model consists of a collection of 3D solids with associated variables. For example, a solid may represent a coal seam in a mining block, with variables for volume, density, thickness and various coal qualities. Each solid or block model cell is referred to by Evolution as a

row, while the variables associated with that row are called *columns*. When dealing with coal models specifically, a row can also be called a horizon. A horizon is represented by a three dimensional solid and is the smallest user selectable unit within the model.

In Evolution, a *material* is a way to classify a horizon as product or waste. Each horizon has a material, which indicates whether that horizon should be considered worth mining or not. For example, there might be a material named coal that signifies this is the material we wish to mine for profit. Additionally, there might be a material called waste that informs Evolution that the material is waste and generates no profit. There might be several product material types – for example thermal, PCC, and coking coal. There might also be several waste types such as spoil, free dig and fresh. Most of the time, we are only interested in whether it is product or waste but defining multiple product or waste types can be useful for filtering, calculations for product washes, or equipment allocations.

While a given horizon may have only one material type – either waste or product – it may consist of some product material and some waste material. These form the product component and waste components respectively. However, when considered as a whole, these two components are aggregated into a total that when considered against product specifications, will dictate the material type of the total as either product or waste. This concept is particularly important during aggregation or loss and dilution. Even if the original imported horizons were completely waste or completely product, there will eventually be some mixing during the mining process.

When two horizons are aggregated into one larger horizon, the original horizons are not forgotten – they are stored as ancestors of the final horizon. The coal module considers these original ancestors and their location within the final aggregated horizon when calculating loss and dilution. This ensures that the qualities associated with any loss material is representative of the ancestors that were present in the region of the loss.

In our example, Maptek Evolution received the stratigraphic model of a coal deposit through a number of solid triangulations - each solid having a unique ‘address’ in the pit. This was achieved by defining a series of address ‘levels’ that identify its unique position within the mine. No two solids should share the same value for all address levels. For a typical coal mine, the levels might be:

- Pit – individual pit code
- Strip – strip number or code
- Block – block number or code in a strip
- Seam – seam code the block belongs to
- Material – type of material (e.g. coal, overburden, midburden)

These solid models were created in Maptek Vulcan and assigned a number of attributes related to structural and quality resource parameters. During the process of coal reserves model development in Maptek Evolution, the user can formulate a procedure of coal aggregation to convert the coal resources associated with the imported solids to coal reserves using the available coal database transformation options shown in Fig. 6. In other words, the user can create a customised aggregation procedure that suits the targeted coal deposit and the mining method(s) used to extract it.

A transform is a self-contained calculation that transforms incoming data, and then passes the result to the next transform. For example, a transform might import attributed Vulcan triangulation files into the program as horizons, while the next might calculate the effects of Loss and Dilution on that horizon. A later transform might account for moisture changes on the ROM stockpile by recalculating new tonnages and qualities at ROM moisture. Pre-built transforms can perform many standard calculations such as aggregation, seam wasting, and loss and dilution. Custom scripted transforms can also be created. The following paragraphs discuss the main coal database transformation options available. An example of a complete procedure is also provided at the end of this section.

3.3. Wasting Options

Wasting transforms (quality or thickness based) can be used to turn the material type of a coal reserve solid from what it is originally prior to importing to either overburden or midburden. In the case of quality-based wasting, the criteria are, as expected, based on quality variables. It can be used, for example, to turn solids of coal material type to waste if ash is greater than an applied limit.

Thickness based wasting allows the application of minimum mining thicknesses to the coal reserve solids. A different thickness can be applied to different seams reflecting the possible use of different mining methods to extract them. Solids with a thickness smaller than the applied minimum have their material type changed to either overburden or midburden.

Coal forced wasting can be used to change the material type of any solid to overburden or midburden and at the same time assign new values to its variables. This allows wasted seams to have variable values overridden with new values in case those quality values (density, moisture, ash, etc.) need to be changed to typical waste values. Variable value switching is also possible allowing wasted seams to have the values of variables swapped with other variables. Typical usage might be to transfer the values for product quantities (coal thickness, coal tonnage, etc.) to waste quantities.

3.4. Aggregation

This is the main step in the development of the coal reserves model in Maptek Evolution. The aggregation transform is designed to merge horizons too thin to practically mine into larger horizons. Aggregation can be limited so that it does not cross in pit benches. Aggregation occurs within groups of seams called *passes*. A horizon table is provided that allows for the definition of passes and their member horizons. Selecting a pass, or a horizon in the table will allow the following aggregation logic to be set for each pass:

- **Pass name** – all solids will have a new variable/column added that includes this pass name.
- **Minimum product thickness** – any product horizons less than this thickness will be aggregated to a neighbouring horizon.
- **Minimum waste thickness** – any waste horizons less than this thickness will be aggregated to a neighbouring horizon.
- **Set all product as** – if after aggregation a horizon still qualifies as product (based on the rules set), then its material will be set to this value.
- **Set all waste as** – if after aggregation a horizon does not qualify as product (based on the rules set), then its material will be set to this value.

The variables (or columns in Evolution terminology) that will be available for further transforms after the aggregation step need to be specified in this step. The columns are grouped in four categories: *Standard, Quantity, Quality and Other columns*. Standard columns include the total, product and waste component columns that relate to volume, density, moisture, tonnage and thickness that must be selected. Quantity columns (qualities) represent amounts that are proportional to the thickness of the solid, such as volume or tonnage. When solids are merged, the columns listed in this table will be summed to determine the value for the new aggregated solid. Quality columns (qualities) represent values that are homogeneous throughout the solid, such as density or ash. The following aggregation methods are available:

- **Minimum** – the value for the aggregated solid will be equal to the least value held by any of the solids being merged.
- **Maximum** - the value for the aggregated solid will be equal to the highest value held by any of the solids being merged.
- **Average** – the value for the aggregated solid will be the numerical average of the solids being merged.

- **Average (Non Zero)** - the value for the aggregated solid will be the numerical average of the solids being merged, excluding any solids with zero values.
- **Copy Top-most** - the value for the aggregated solid will be the same as the top most solid in the group being merged.
- **Copy Bottom-most** - the value for the aggregated solid will be the same as the bottom most solid in the group being merged.
- **Weighted Average** - the value for the aggregated solid will be the weighted average of the solids being merged. The weighting is given by the column specified in the Weight field of the table.

Other columns can also be defined that represent values that don't fit into the quantities or qualities categories. These values would categorise solid, such as a name, ID, or strip number. When solids are merged, the aggregated solid will have its value set equal to the top most solid in the aggregation group (Copy Top-most) or bottom most solid (Copy Bottom-most), depending on the aggregation method selected in the table.

The product definition of the aggregation step allows for setting rules to define whether a solid should be considered coal or waste. During aggregation, rows (blocks) that were initially coal may be diluted with waste to an extent that they are no longer suitable for sending to a wash plant. Every time solids are aggregated by this transform operation, the resultant merged solid will be checked against the conditions in this table. If all conditions are met, the solid will be turned to the product defined in settings for that pass. If any of the conditions fail, then the merged solid will be set to the waste defined in pass settings. Solids that have not been aggregated will not be changed.

3.5. Loss and Dilution

The Loss and Dilution transform can optionally add the effects of roof, floor and edge loss and dilution. If this transform runs after an aggregation transform, the loss and dilution will still reflect the qualities of the original pre-aggregated horizons in the regions of the loss (when specifying loss by thickness only). Roof and Floor loss and dilution can be specified in the following ways:

- **Thickness** – the specified thicknesses are lost from the roof and floor and report to the horizons above and below respectively as dilution. The basal seam will experience dilution from the seam below (underburden) as specified by the underburden dilution thickness and the area column selected.
- **Percent** – the volume of roof and floor loss is specified as a percentage of the original horizon's volume. The roof and floor loss become the roof and floor dilution for the horizons above and below respectively. The basal seam will experience dilution from the seam below (underburden) equal to the volume of material lost.

Edge loss and dilution can be specified similarly.

3.6. An Example of an Aggregation Procedure and Coal Reserves Model

The example presented in this paper consists of multiple coal layers that have been modelled from drillhole data and converted to solid triangulations with associated resource attributes. A typical section through the deposit is shown in Fig. 7 (top). Over 5000 solids were imported into a Maptek Evolution coal database and aggregated using a straightforward procedure based on the following criteria:

- Minimum product thickness: 0.3 m
- Minimum waste thickness: 0.3 m

- Maximum product ash content: 0.6 (fraction)
- Roof and floor loss and dilution: 0.1 m

An aggregated version of the imported coal database was created. The effect of aggregation is shown in Fig. 6. The aggregated coal database, representing the coal reserves, was then used to produce a coal production schedule in Maptek Evolution.

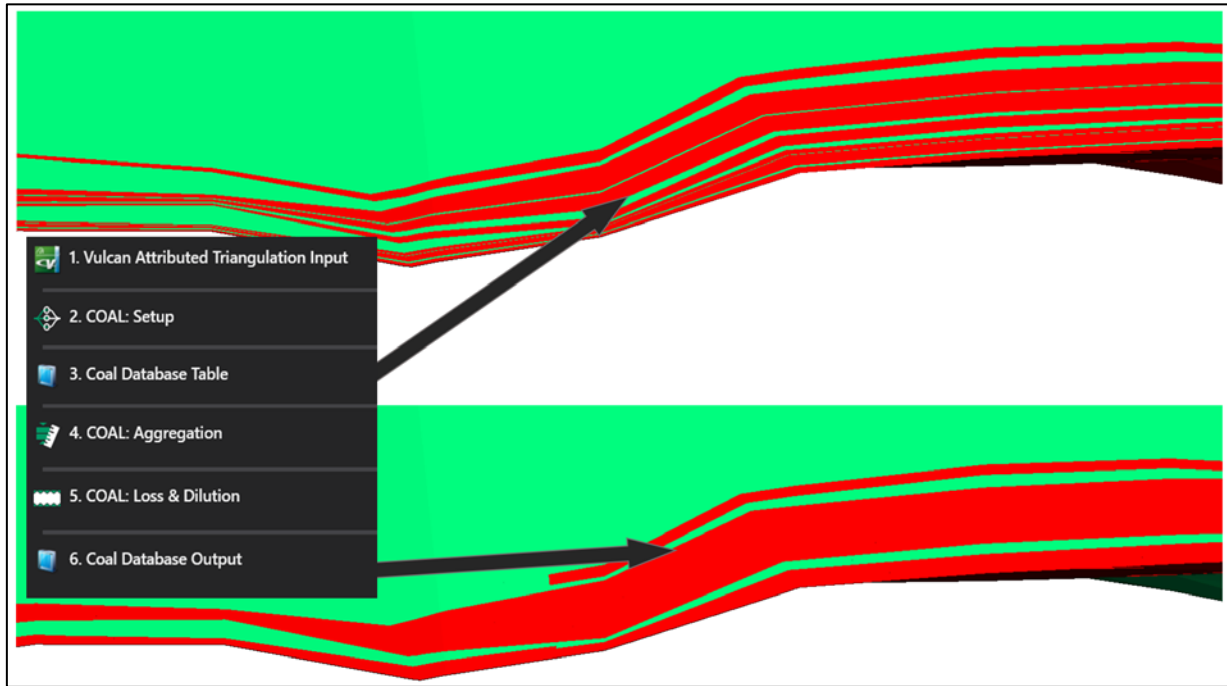


Figure 6. Example of imported coal seams (top) and aggregated coal seams (bottom) and associated steps in Maptek Evolution. Coal seams are shown in red while midburden is shown in green.

4. COAL PRODUCTION SCHEDULING WITH MAPTEK EVOLUTION

4.1. Overview of Evolution

Maptek Evolution is one of the most advanced scheduling systems commercially available and probably the only one based on evolutionary algorithms. The scheduling and optimisation functionality of Evolution is cloud-based – the reserve model and schedule setup are transmitted to a cloud facility for processing. The scheduling solutions found are transmitted back to the user for further analysis and approval.

Evolution consists of two main modules, *Strategy* and *Origin*. *Strategy* is a high-level scheduling solution focusing on value maximisation through the use of cutoff grade optimisation but allows for detailed constraint modelling as well (including blending). *Origin* is a tactical level scheduling system which allows the user to develop detailed mining schedules ready for medium term planning.

Optimisation in *Strategy* is based on a hybrid system consisting of a *core evolutionary algorithm*, a *local search evolutionary algorithm* and a *linear programming algorithm*, each with different responsibilities (Fig. 7). The main steps of scheduling operation are as follows [7]:

1. Creation of the initial population including a geometrically correct extraction sequence. (Graph Theory)

2. Calculation of the fitness of each individual and ranking of the population based on fitness. (Master and Local Search Evolutionary Algorithms)
3. Iteration through successive generations by generating an offspring population where each child competes with the parents for the privilege to progress to the next generation. (Master Evolutionary Algorithm)
4. The master algorithm calls on the secondary local search algorithm to boost the best individual found so far, by manipulating the threads through cut-off grade space whilst keeping the extraction sequence static. The improved individual is then sent back to the master where it replaces or upgrades its old self (analogue to exploring the local neighbourhood). (Local Search Evolutionary Algorithm)
5. Steps 2 to 4 are repeated until no improvement is registered, in other words when the population loses diversity and converges on a single high fitness value.

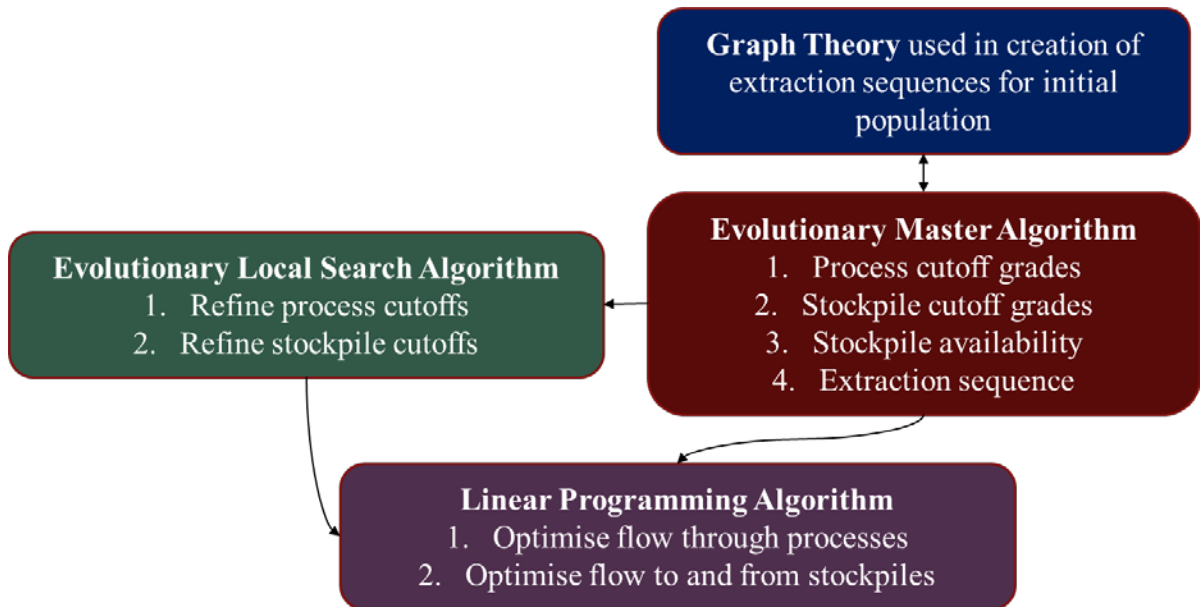


Figure 7. Maptek Evolution Strategy scheduling engine components.

4.2. Coal Production Schedule Setup

Setting up a schedule in Maptek Evolution involves a number of steps including the definition of the *flowchart*, *dependencies*, *calendar*, *objectives*, and *constraints*. The flowchart is used to select and define the reserve source models, number of mills, stockpiles and waste dumps to be used in the schedule. It highlights the relationship between the reserve models (block or solid models) and the mills, stockpiles and dumps, by indicating the direction of material flow (Fig. 8). All individual elements of the flowchart have parameters that need setting up.



Figure 8. A simple schedule flowchart in Maptek Evolution.

In the case where the reserve model is based on solids, as in our example, Evolution allows the definition of dependencies – mining sequence controls that define the feasible sequence of extraction. Dependencies also provide the ability to allocate specific equipment for each sequence. There are three types of dependencies: *geometric* (vertical dependencies) automatically generated to prevent under-cutting in an open pit environment, *generated* dependencies based on certain rules defined by Stage, Bench, Block ID, or any other attribute, and *manual* dependencies defined interactively by the user. Dependencies can be displayed graphically in the Viewer tab (Fig. 9).

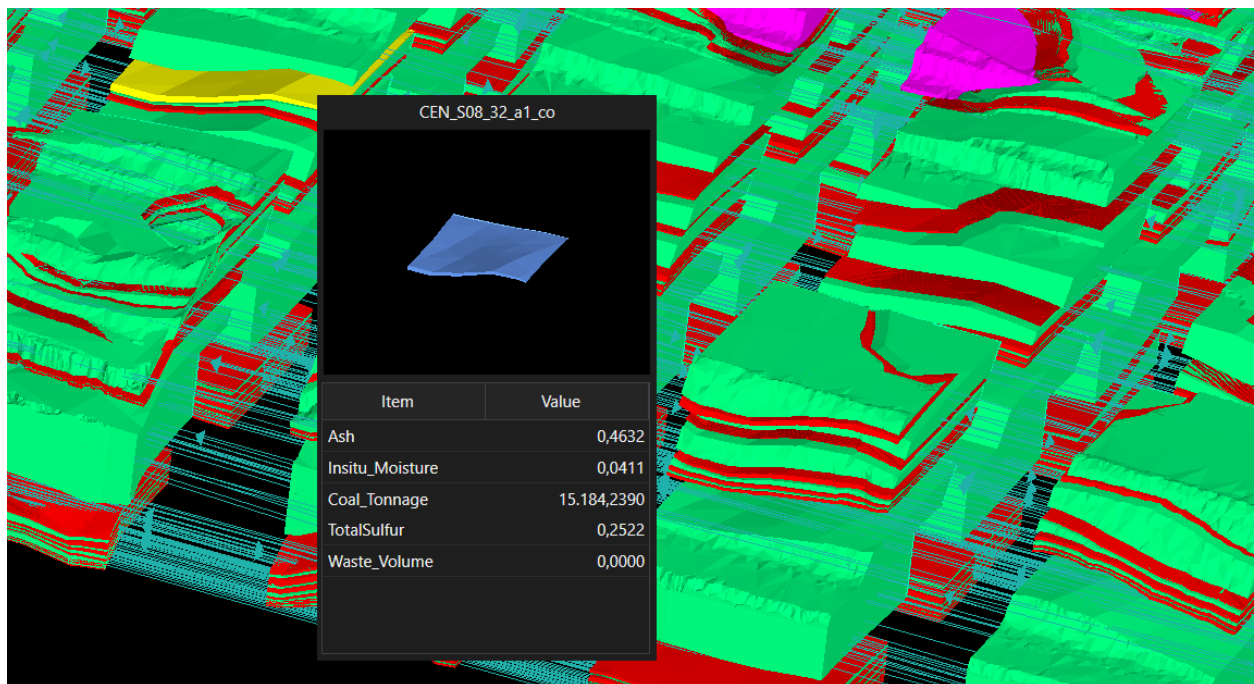


Figure 9. Graphical display of block dependencies (arrows) and popup block details window.

The calendar is used to define the number and length of periods in the schedule. Periods can be of different lengths, capacities, and utilisation. Setting up the calendar includes defining the number of periods and their length, defining the equipment resources and target and defining the end of period flag. Figure 10 shows an example of a calendar.

Depending on the type of schedule (material movement or equipment based) the user can define how much material will be moved in each period or fix equipment production rates and hours. Material objectives are used to control the waste variance tolerance for each period of the schedule. Evolution utilises the waste tolerance to control how hard the scheduler must work on each period to

achieve the movement target. A higher percentage number will generate a lower fitness, whereas a lower percentage variance will result in the scheduler refining the result based on a higher fitness value. Equipment productivity for the different parcels (e.g. coal and waste) included in each block can also be defined here.

Evolution provides a number of ways to constrain the produced schedule, including constraints such as sink rate and stage sink rate, stage availability, stage bench turnover, waste area and stockpile availability, waste area dependency and required tonnage, accumulations (stage, model, global, global process and process), and global and process blend. In our example, the stage availability constraint was applied to control the strips available in each period.

	Period 1	Period 2	Period 3	Period 4	Period 5	Period 6	Period 7	Period 8	Period 9	Period 10
Calendar										
Start Date	17-10-2018	17-10-2019	17-10-2020	17-10-2021	17-10-2022	17-10-2023	17-10-2024	17-10-2025	17-10-2026	17-10-2027
End Date	16-10-2019	16-10-2020	16-10-2021	16-10-2022	16-10-2023	16-10-2024	16-10-2025	16-10-2026	16-10-2027	16-10-2028
Days	365	366	365	365	365	366	365	365	365	366
Hours	8,760	8,784	8,760	8,760	8,760	8,784	8,760	8,760	8,760	8,784
Targets										
End of Period Target	Accumulation	Accumulation	Accumulation	Accumulation	Accumulation	Accumulation	Accumulation	Accumulation	Accumulation	Accumulation
Parcel Item Target	Tonnage	Tonnage	Tonnage	Tonnage	Tonnage	Tonnage	Tonnage	Tonnage	Tonnage	Tonnage
Target Value	5,000,000	5,000,000	5,000,000	5,000,000	5,000,000	5,000,000	5,000,000	5,000,000	5,000,000	5,000,000
Total Mill Capacity (tonnes)	2,000,000	2,000,000	2,000,000	2,000,000	2,000,000	2,000,000	2,000,000	2,000,000	2,000,000	2,000,000
Total Digger Available Hours	5,606.40	5,621.76	5,606.40	5,606.40	5,606.40	5,621.76	5,606.40	5,606.40	5,606.40	5,621.76
Total Max Digger Production (tonnes)	10,091,520	10,119,168	10,091,520	10,091,520	10,091,520	10,119,168	10,091,520	10,091,520	10,091,520	10,119,168
Total Min Digger Production (tonnes)	10,091,520	10,119,168	10,091,520	10,091,520	10,091,520	10,119,168	10,091,520	10,091,520	10,091,520	10,119,168
Digger 1										
Delay Hours	0	0	0	0	0	0	0	0	0	0
Utilisation (%)	80.00%	80.00%	80.00%	80.00%	80.00%	80.00%	80.00%	80.00%	80.00%	80.00%
Availability (%)	80.00%	80.00%	80.00%	80.00%	80.00%	80.00%	80.00%	80.00%	80.00%	80.00%
Unit Count	1	1	1	1	1	1	1	1	1	1
Available Hours	5,606	5,622	5,606	5,606	5,606	5,622	5,606	5,606	5,606	5,622
Max Production (tonnes)	10,091,520	10,119,168	10,091,520	10,091,520	10,091,520	10,119,168	10,091,520	10,091,520	10,091,520	10,119,168
Min Production (tonnes)	10,091,520	10,119,168	10,091,520	10,091,520	10,091,520	10,119,168	10,091,520	10,091,520	10,091,520	10,119,168
Mill 1										
Capacity (tonne)	2,000,000	2,000,000	2,000,000	2,000,000	2,000,000	2,000,000	2,000,000	2,000,000	2,000,000	2,000,000
Ore Definition	parcelName="Coa	parcelName="Coa	parcelName="Coa	parcelName="Coa	parcelName="Coa	parcelName="Coa	parcelName="Coa	parcelName="Coa	parcelName="Coa	parcelName="Coa

Figure 10. Schedule calendar showing period setup, targets, mining and processing capacities.

4.3. Coal Production Scheduling and Reporting

Once the schedule setup is complete and validated, Evolution goes online with the cloud servers to submit the schedule setup and reserves information for processing. Once scheduling is complete, the schedule solution(s) found is returned for further analysis and reporting. The user can decide which solution to choose depending on scheduling targets. Once the schedule sequence has been chosen, the fitness values of the scheduling targets can be viewed. Special charts are available that help identify in which periods the violations have occurred and assist the scheduler in making corrections and assessments before further processing is required. A violation within Evolution refers to the percentage difference between the target object and the schedule sequence results. These violation differences indicate to the user, the periods of the schedule requiring modification where the objectives are not being met.

A selected schedule can be viewed as a table and graphically as an animated sequence in Evolution or exported in CSV format (Fig. 11). Special reporting tools are available for quickly generated pivot tables and any other reports based on reserves and schedule information.

5. CONCLUSIONS

Coal reserves modelling and production scheduling is a procedure full of challenges. Effective use of available geological and mining data and information requires advanced software solutions

with the right tools to build realistic models of coal geology and produce solid mining scenarios. Development of a sound coal resource model should be based on maximum usage of available sampling data, while converting the resource model to a reserve should be based on proper application of mining factors. Maptek Vulcan and its Integrated Stratigraphic Modelling module provide all necessary functionality to build an in-situ model of coal resources from drillhole data. Maptek Evolution takes the in-situ model and produces practical run-of-mine reserves in a flexible, yet automated, step-based workflow system which allows users to define relevant parameters. The use of evolutionary algorithms to optimise the produced schedules adds extra value and flexibility. As explained in this paper, the solution based on Maptek Vulcan and Evolution provides a complete environment for coal reserves modelling and production scheduling.

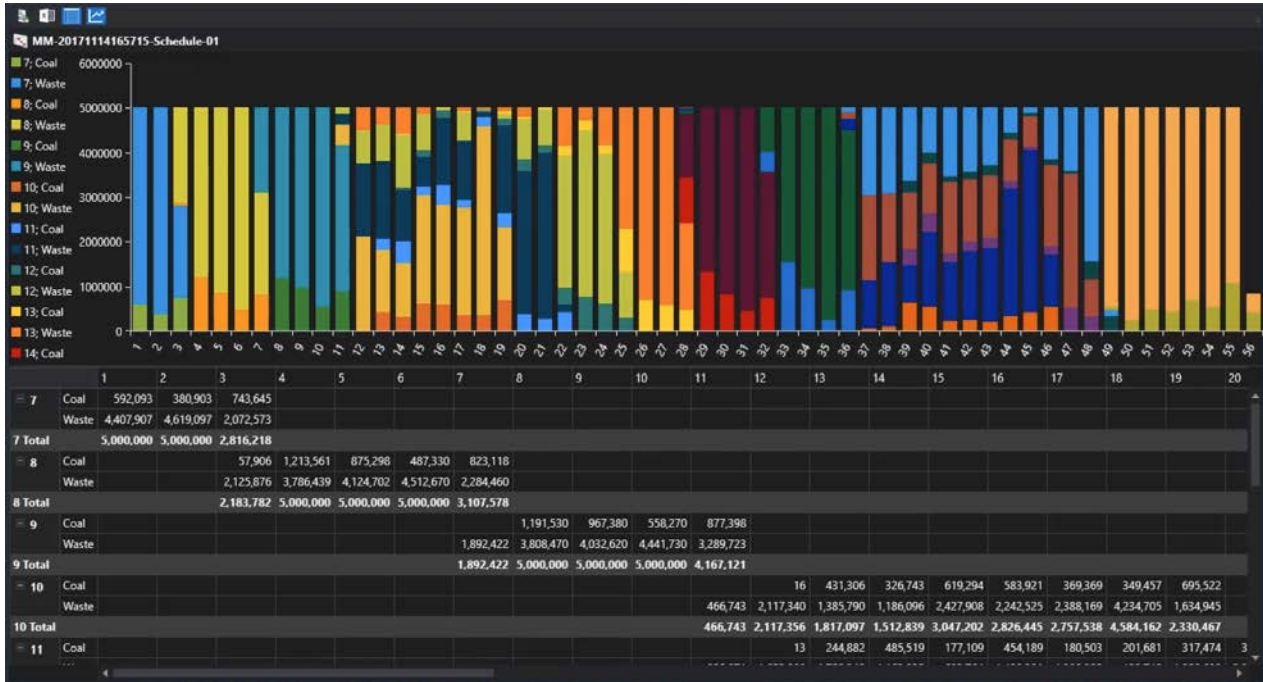


Figure 11. Schedule graph and table showing coal and waste tonnages per period and strip.

REFERENCES

- [1] Maptek Pty Ltd. (2016). ISM Stratified Geologic Modelling, Maptek Vulcan Training Manual.
- [2] Maptek Pty Ltd. (2018). Integrated Stratigraphic Modelling, Maptek Vulcan 10.1 Online Help.
- [3] Rens, D. (2002). Stratigraphic Modelling Manual – FixMap, Maptek Pty Ltd.
- [4] Saunders, D. (2015). Ongoing Improvements to Mine Planning, Forge Newsletter, September 2015, Maptek Pty Ltd.
- [5] Walker, J., Wilson, P. (2009). Bringing Out the Best Models, Forge Newsletter, June 2009, Maptek Pty Ltd.
- [6] Maptek Pty Ltd. (2018). Evolutionary Scheduler Milestone, Forge Newsletter, March 2018.
- [7] Myburgh, C., Deb, K., and Craig, S. (2014). Applying Modern Heuristics to Maximising NPV through Cut-off Grade Optimisation, Orebody Modelling and Strategic Planning Conference, Perth, Western Australia, November 2014.
- [8] Maptek Pty Ltd. (2015). Reserving the Maptek Way, Forge Newsletter, September 2015.

Geostatistical Estimation of Coal Reserves in Kardia Mine using Kriging and Conditional Simulation Methods

Panagiota Gkafa¹, Andreas Pavlides¹, Christos Roumpos² and Dionissios Hristopoulos¹

¹School of Mineral Resources Engineering, Chania, Greece

²Mines Business Unit of Public Power Corporation, Athens, Greece

ABSTRACT

Representative estimates of the total tonnage of coal deposit and its spatial distribution are key factors for mine planning and the design of the affiliated power plant. Accurate knowledge of such estimates is crucial for long-term mine planning as well as to determine economically feasible energy production needed to meet demands. Geostatistical methods have been extensively used in reserves estimation and mine planning in order to address such problems. The family of kriging methods provides tonnage accurate estimates as well as confidence levels that give an approximate estimate of uncertainty. Furthermore, conditional simulation methods can represent in more detail the uncertainty and spatial variability of the reserves.

In this study, both kriging interpolation and conditional simulation are applied to drill-hole data from the Kardia lignite mine, which is located in Northern Greece. After investigating the statistics of 608 drill-hole data from the area, multilinear regression was used to estimate a deterministic trend function. Different variogram models were fitted to the residuals that represent the spatial fluctuations. Based on the weighted square error, the best variogram model was selected. The optimal variogram model was then used for the application of Ordinary Kriging to the residuals, and the kriging predictions were combined with the deterministic trend to estimate the spatial distribution of coal. The resulting kriging maps were utilized to evaluate the reserves over the area of interest. Finally, to more accurately estimate the confidence levels of the reserves, 1000 conditional simulations were generated using the method of kriging-based polarization of unconditional realizations. The latter were generated by means of (i) the covariance matrix decomposition and (ii) the turning bands method.

1. INTRODUCTION

An important ratio (30%) of energy in Europe is generated from lignite which is a form of coal [1]. Lignite deposits exist all over the world, and many countries use them as an energy source. The low cost of lignite exploitation is the primary motivator for its use in energy generation.

However, lignite exploitation causes environmental problems such as carbon dioxide (CO₂) and hydrogen sulfide (H₂S) emissions, as well as deposition of ash and sludge [2]. There are solutions for these problems, for example, the use of filters for retention of fly ash and gas emissions, or the creation of specific areas for the deposition of solid waste.

Despite the environmental problems, lignite is currently an important energy source for developing economies, and the estimation of lignite reserves is of interest. Geostatistical methods are used for this type of analysis to capture the spatial distribution of lignite characteristics [3], [4]. Geostatistics provides useful tools to investigate spatial variations of the lignite distribution. Such analysis helps to optimize exploitation plans and to accurately predict reserves.

Geostatistics is a collection of stochastic methods for modeling and characterization of spatial attributes [3], [5]. Specifically, geostatistics is used to model the uncertainty of the unknown values

of the targeted attribute by means of mathematical tools. The final product involves maps for the attribute of interest generated by estimated values at the nodes of a specified prediction grid [6].

The objectives of this research are to map the spatial distribution of lignite thickness in Kardias mine, to predict the reserves contained the West Field South Sector, and to evaluate the uncertainty of the reserves estimation by means of geostatistical simulation.

1.1. Kardias Mine

In this research, we use data from Kardias mining field which is located in the central part of the western boundary of Ptolemais mining area (Figure 1). The area of the mine covers approximately 20 km². Faults striking from WNW-ESE to NW-SE dissect the mining field into several fault blocks. The western rim of the mining field is located near the mountain front. The thickness of the lignite-bearing layers, including intercalations, mainly ranges between 80 and 140 m. In a narrow part of the south-western boundary of the mining field, the thickness of the lignite-bearing layers increases in excess of 210 m. In the central and north-western parts of the mining field the thickness of the individual seams, which are partly replaced by intercalations, varies within wide limits. The overlying strata thicknesses vary between approximately 20 and 60 m. In the above mentioned south-western boundary zone, they amount to approximately 150 m [7].

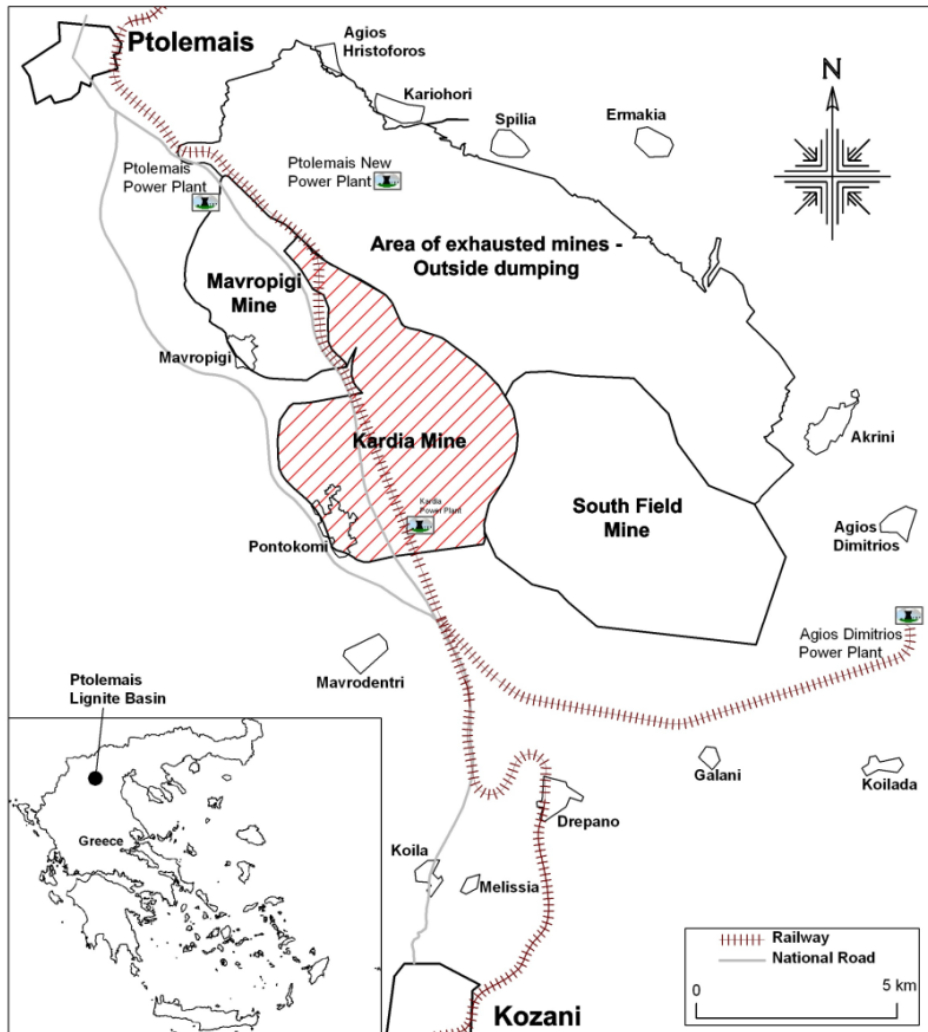


Figure 53. Ptolemais lignite basin and Kardias mine.

2. SPATIAL ANALYSIS

The following sections present the spatial model that will be used in this study to explore the spatial correlations of the data, predict lignite seam thickness over the field, estimate lignite reserves in West Field South Sector of Kardia mine, and investigate the uncertainty of the predictions.

2.1. Trend Analysis

It will be assumed that the lignite seam thickness varies over space as random field. A random field is determined by a joint probability density function based on which various statistical moments can be evaluated. The typical hypothesis is that the probability distribution is Gaussian, or that it can be transformed into a Gaussian by means of a suitable nonlinear transformation. Random fields analyzed as follows:

$$X(\mathbf{s}) = m_X(\mathbf{s}) + X'(\mathbf{s}). \quad (1)$$

The function $m_X(\mathbf{s})$ is the trend, which represents the deterministic spatial variation of the field $X(\mathbf{s})$ across the domain of interest. Hence, the trend represents the slow variations of the field in space. The trend is usually modelled by means of low order polynomials.

The function $X'(\mathbf{s})$ is a random field that contains the stochastic component of the random field $X(\mathbf{s})$ and represents the residuals, obtained after removing the trend from $X(\mathbf{s})$. Statistical homogeneity assumptions can usually be better justified for the residual field than for the original random field.

2.2. Variogram Analysis

The spatial correlations between the values of the spatial random fields $X(\mathbf{s})$ at two different locations are described by means of the variogram function, which is defined as

$$\gamma(\mathbf{r}) = \frac{1}{2} E \left[(X'(\mathbf{s}) - X'(\mathbf{s} + \mathbf{r}))^2 \right]. \quad (2)$$

In the above, \mathbf{r} is the distance (lag) vector between two points, and $E[\]$ is the expectation over the ensemble of the random field [8], [5].

If the random field is statistically homogeneous (stationary), then the variogram is directly connected to the covariance function $c(\mathbf{r})$ by means of the following Equation

$$\gamma(\mathbf{r}) = c(0) - c(\mathbf{r}). \quad (3)$$

The variogram that is obtained from the data Equation (3) is then fitted by means of a theoretical model. In this study, five variogram models are tested, Spherical, Exponential, Powerlaw, Gaussian and Cubic. The exponential variogram model is selected as the most suitable. The exponential model is given by the following function

$$c(\mathbf{r}) = \sigma^2 e^{-\frac{\|\mathbf{r}\|}{\xi}}, \quad (4)$$

where σ^2 is the variance of the random field, \mathbf{r} is the lag, and ξ is the correlation length under the assumption of statistical isotropy (i.e., lack of directional preference).

2.3. Kriging

Kriging refers to a family of stochastic spatial interpolation methods. These methods are based on linear combinations of the data values and the minimization of the mean squared error [9]. Kriging methods are used to estimate the value of a random field $X(\mathbf{u})$ at a point \mathbf{u} where data are missing in terms of the available measurements at $n(\mathbf{u})$ nearby points $\mathbf{s}_1, \dots, \mathbf{s}_{n(\mathbf{u})}$. The respective kriging estimator in the presence of a trend is defined by Equation (5).

$$\hat{X}(\mathbf{u}) = m_X(\mathbf{u}) + \sum_{i=1}^{n(\mathbf{u})} \lambda_i X'(\mathbf{s}_i), \quad (5)$$

where $m_X(\mathbf{u})$ is the trend at the target point, $X'(\mathbf{s}_i)$ represents the field residuals at the measurement locations, and λ_i are the linear kriging weights. The weights are calculated by the minimization of the mean square estimation error [10], [9]. The estimation error is defined by means of

$$\varepsilon(\mathbf{u}) = \hat{X}(\mathbf{u}) - X(\mathbf{u}) \quad (6)$$

where the estimate $\hat{X}(\mathbf{u})$ is given by means of Equation (5). Minimizing the expectation of the squared error leads to the following system of equations that involves the covariance function of the random field

$$\mathbf{C}_X \boldsymbol{\Lambda} = \mathbf{C}_u. \quad (7)$$

In the above, \mathbf{C}_x is the covariance matrix of the random field X at the measurement sites, $\boldsymbol{\Lambda} = (\lambda_1, \dots, \lambda_{n(\mathbf{u})})^T$ is the vector of the linear kriging weights, and \mathbf{C}_u is the vector of the covariance between the unknown point \mathbf{u} and the $n(\mathbf{u})$ neighbor points that contribute to the estimate.

2.4. Simulation

The uncertainty of reserves estimation significantly contributes to the financial risk of mineral resources exploitation. Uncertainty is introduced by sampling limitations, experimental errors, cost and price fluctuations, and geological factors such as the tectonic movements and the weathering of an area which disrupts the structure and quality features of the deposit. All these factors impact the estimation of total reserves [11]. The best available mathematical tools for exploring uncertainty and the probability of different exploitation scenarios are based on geostatistical Monte Carlo simulation methods [3], [5], [12], [13]. Conditional simulations, in particular, can generate different scenarios (realizations) that reproduce the statistical behavior of the spatial variability and also locally respect the available data [14], [15].

In this study two methods of conditional simulation are used. Both methods generate a set of unconditional realizations, which are then conditioned to the data by means of a kriging-based polarization method. The first method for the generation of unconditional realizations is based on the covariance matrix decomposition. The second method is based on the computationally efficient Turning Bands Method [16], [17]. Both methods are applied to the simulation of the residuals, and the entire field is reconstructed by adding the trend to the realizations of the residuals.

2.5. Conditional Simulation Based on Covariance Decomposition

Conditional simulation methods assume a given set D of data locations and a set of grid locations G where the values of the random field X are simulated. The simulation set is denoted by

$S=D \cup G$. This method is combined with kriging conditioning, and simulates the values of the random field X at the locations of the simulation set $S=D \cup G$ using the following steps:

1. The covariance model $c(\mathbf{r})$ is estimated from the data. In practice, first a variogram model is determined and then the covariance is obtained from Equation (3).
2. A vector $\hat{X}(S) = \{X(D) \cup \hat{X}(G)\}$ is derived by combining the data $X(D)$ with the kriging-based estimates $\hat{X}(G)$ at the points in G .
3. The covariance matrix \mathbf{C}_X is constructed for the points in S , and then a suitable factorization of the covariance matrix is evaluated, e.g., $\mathbf{C}_X = \mathbf{A}^T \mathbf{A}$.
4. A random vector \mathbf{u} is generated from the standard (zero mean, unit variance) normal distribution $N(0, 1)$. The length of \mathbf{u} is equal to the number of points in S .
5. The unconstrained simulation $X^u = \mathbf{A}\mathbf{u}$ is generated.
6. Using the unconstrained simulation values $X^u(D)$ as data, a second application of kriging generates the interpolated vector $\hat{X}^u(G)$.
7. The polarization vector $\hat{X}^u(S) = \{X^u(D) \cup \hat{X}^u(G)\}$ is then constructed.
8. Finally, the constrained realization on S is generated by means of $X^c = X^u + \hat{X} - \hat{X}^u$.

2.6. Turning Bands Method

In the second approach, the turning bands method is used to generate the unconditional realizations. Hence, steps 3-5 in the above flowchart are replaced by the following:

3. A number of lines with various azimuths that correspond to different spatial directions (bands) are generated.
4. In each band, a one-dimensional, unconditional simulation is performed. The one-dimensional realizations can be generated very fast.
5. The one-dimensional realizations along the different directions are back-transformed using a suitable transformation function to obtain a two-dimensional realization.

3. CASE STUDY

In this case study, we used 608 drill-holes from the Kardias mine in northern Greece to map the total lignite seam thickness over the area, in order to estimate the reserves of West Field South Sector of Kardias Mine. Two simulation methods were tested and compared, in order to assess the prediction uncertainty. The calculations are performed in the R programming environment using the RGeostats package [18].

3.1. Exploratory Data Analysis

The data, provided by the Mines Business Unit of the Public Power Corporation (PPC), corresponds to the total seam thickness of lignite for 608 drill-holes taken from the area of the mine. The seams are classified as lignite or waste by PPC, based on quality (ash content, lower calorific value, etc.) and technical (thickness, dilution by waste, etc.) criteria. The detailed analysis of these criteria is beyond the scope of this study.

The locations of the data are shown in Figure 2, and the summary statistics are given in Table 1.

Table 9. Data statistics for the total lignite seam thickness for the 608 drill holes from Kardia mine.

St. deviation (m)	Mean (m)	Median (m)	Min (m)	Max (m)
18.1	20.48	13.46	0.36	90.18

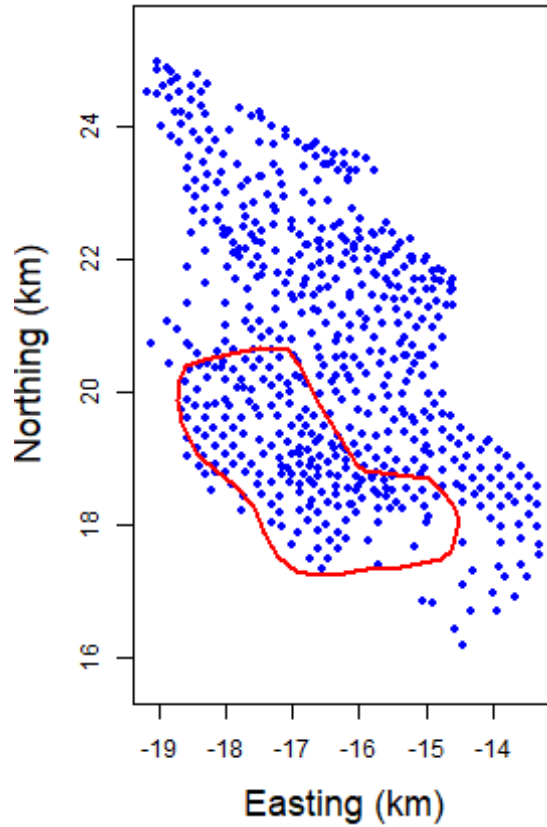


Figure 54. Locations of drill-holes (blue dots), and a contour line that highlights the targeted sector (red line).

3.2. Trend Analysis

There is no unique trend model that characterizes all lignite mines. In this study, we fit a linear polynomial trend model to the data. The model is defined by Equation (8)

$$m_X(\mathbf{s}_i) = a_0 + a_1x_i + a_2y_i. \tag{8}$$

In Equation (8) $m_X(\mathbf{s}_i)$ is the trend model, x_i and y_i are the coordinates of the drill-holes at locations \mathbf{s}_i , and a_0, a_1, a_2 are the coefficients of the trend model. The coefficients were estimated using linear regression, and their optimal values are presented in Table 2. Figure 3 represents the spatial distribution of the trend model.

Table 10. Coefficients of the linear trend model, (8) based on the data over the entire mine area and linear regression.

a_0	a_1	a_2
127.067	3.733	-2.192

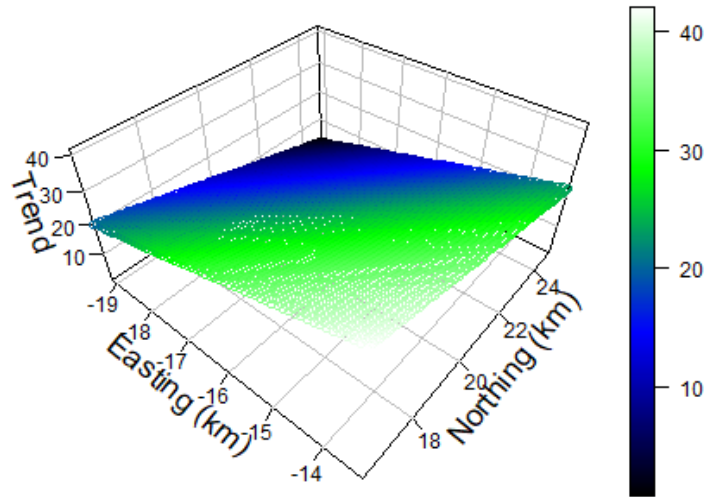


Figure 55. The spatial distribution of the linear trend model (8). The x axis represents the Easting Coordinates, the y axis represents the Northing Coordinates and the z axis represents the trend. The linear trend model is defined by means of the equation $m_x = 127.067 + 3.733x_i - 2.192y_i$.

The data residuals are obtained by removing the trend from the data. The histogram of the residuals is closer to the normal distribution compared to that of the original data as shown in Figure 4.

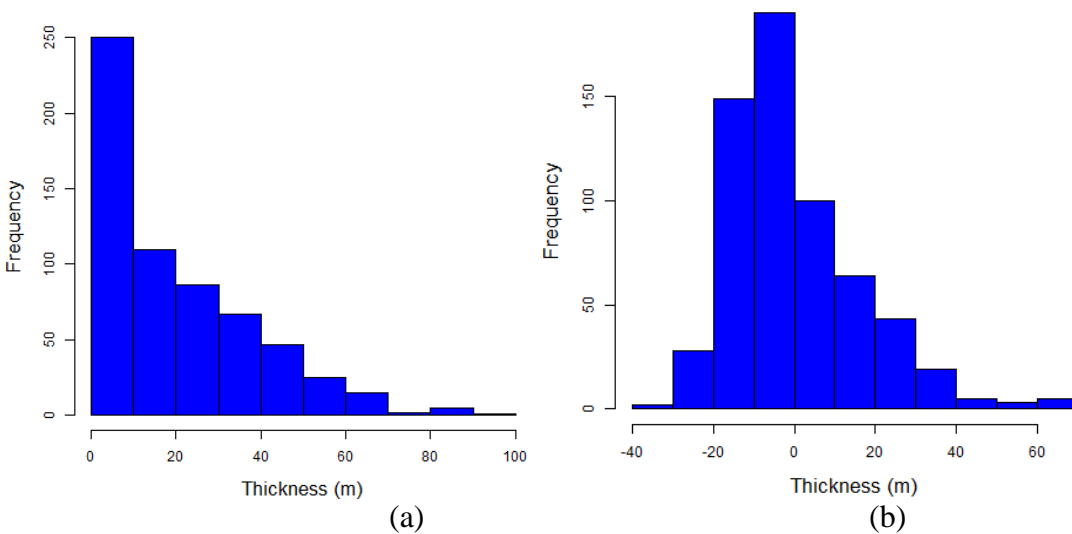


Figure 56. Histogram of (a) the original data (b) the residuals (detrended data).

3.3. Variogram Analysis

The spatial correlations of the fluctuation field $X'(s)$ in Equation (1) are modeled by means of the variogram function (2). The expectation in (2) cannot be directly evaluated, because the probability model is not a priori known. Instead, an experimental (empirical) variogram is estimated by replacing the expectation with the spatial average. Since it is impossible to have an adequate number of pairs for all possible distances, usually a theoretical variogram model is fitted with the experimental variogram (see [8] for details).

We tested five different theoretical variogram models (Spherical, Cubic, Gaussian, Power, and Exponential) in combination with nugget terms, which are presented in Figure 5. The best fit was

chosen based on the minimum sum of weighted squared errors. The sum of weighted squared errors is given by the following Equation

$$\varepsilon = \sum_{i=1}^L (\gamma(\mathbf{r}_i) - \hat{\gamma}(\mathbf{r}_i))^2 w_i \tag{9a}$$

$$w_i = \frac{P_i}{|\mathbf{r}_i|} \tag{9b}$$

In Equation (9a), L is the number of lags of the experimental variogram w_i is the weight for lag $i=1 \dots L$, \mathbf{r}_i is the lag vector, $|\mathbf{r}_i|$ is the Euclidean distance, and P_i is the number of pairs that are included in lag i . We selected the exponential model with nugget effect which gives the optimal fit. The fitting errors are shown in Table 3. In Table 4 the model parameters are shown. These parameters were estimated by minimizing the error function given in Equation (9a).

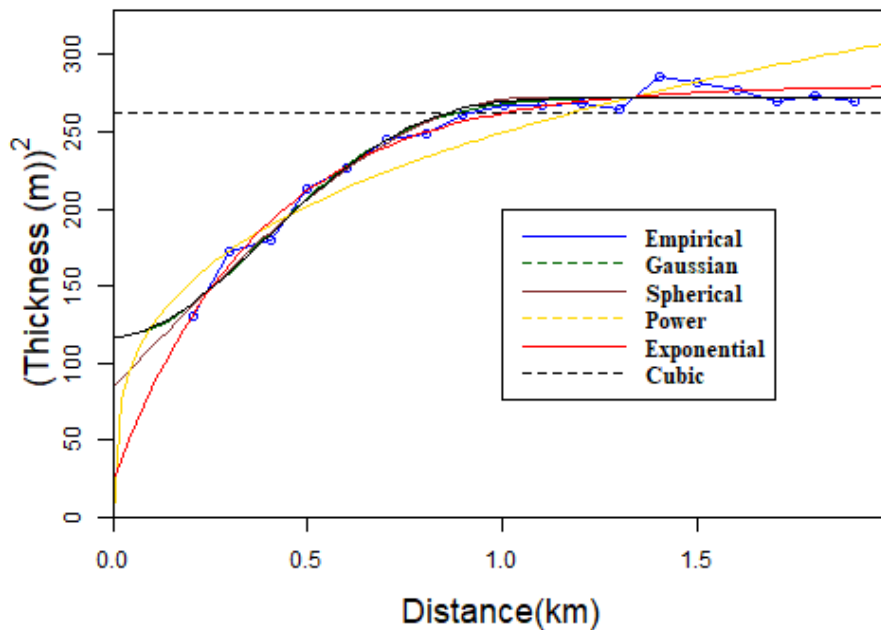


Figure 5. Empirical variogram and theoretical model fits (Gaussian, Spherical, Power, Exponential, and Cubic). The horizontal axis is the lag distance r . The vertical axis represents the lignite thickness variogram values for n each lag.

Table 11. Sum of squared weighted errors between the empirical and the theoretical variogram models. The total error for each model is equal to the sum of the weighted squared differences between the values of empirical and the respective theoretical variogram model.

Variogram Model	Squared Error
Cubic	798.42
Exponential	570.29
Gaussian	3360.97
Power	3836.48
Spherical	738.91

Table 12. Parameters of the optimal exponential variogram model for the lignite thickness residuals. σ^2 is the variance, ξ is the correlation length, and c_0 is the nugget. The parameters are estimated by minimizing the error function given in Equation (9).

$\sigma^2 (m^2)$	$\xi (m)$	$c_0 (m^2)$
256.14	0.38	24.13

3.4. Distribution of Lignite Reserves

For the visualization of the spatial distribution of lignite reserves, we used the ordinary kriging (OK) on the residuals, to interpolate the total lignite seam thickness. The interpolation grid consists of 118×176 cells, with the dimensions of each cell equal to 50 x 50 m. A kriging neighbourhood of 1.05 Km was selected based on the correlation length ξ of the chosen exponential model as shown in Section 3.3.

The maps of the predicted thickness and kriging standard deviation are shown in Figure 6 and Figure 7 respectively. The thickness map shows that higher values of thickness are concentrated in the eastern section of the mine. Regardless of this general trend, the highest values of the thickness are located in the south-west area of the map, mostly inside West Field South Sector of Kardia Mine. According to the map of kriging standard deviations, the lower uncertainty is found in the eastern areas of the mine, due to the high concentration of data within the kriging neighborhood.

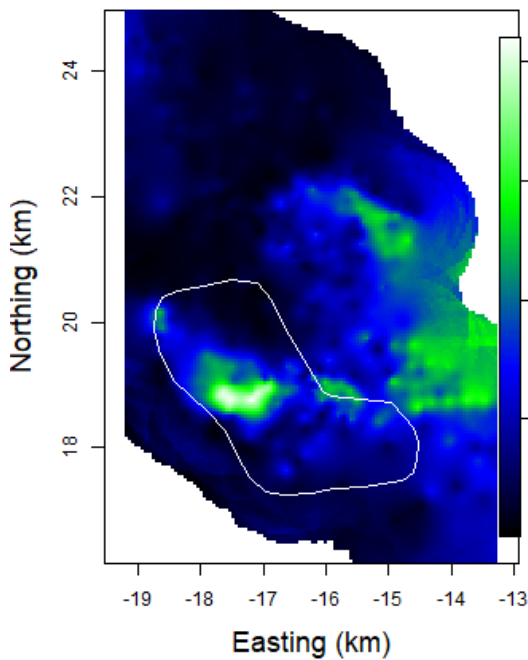


Figure 6. Map of kriging prediction of lignite thickness in Kardia mine.

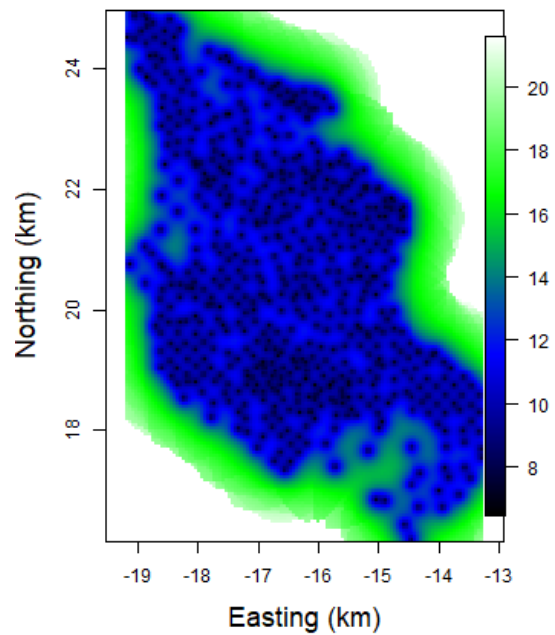


Figure 7. Map of kriging standard deviation of lignite thickness in Kardia mine.

3.5. Cross Validation

Leave-One-Out cross-validation (LOO CV) is used to validate the performance of the spatial model used. In this method, each drill-hole is removed from the data set, one at a time. The missing value is predicted using OK to estimate the residuals and calculating the linear trend based on the coefficients of Table 2. This process is repeated for all the sample points, and the estimates obtained are compared with the respective data values at the removed sites. Several LOO validation measures are listed in Table 5.

Table 13. Leave-One-Out cross-validation measures for the spatial model of lignite thickness. ρ is the Pearson’s correlation coefficient, RMSE is the root mean square error (m), MAE is the mean absolute error (m), MaxAE is the maximum absolute error (m), and ME is the mean error (m).

Measure	Model
RMSE (m)	12.15
MAE (m)	8.33
Max.AE(m)	57.96
ME (m)	0.08
ρ %	74.63

The cross-validation measures show that the overall performance of the model is good with a correlation coefficient between the LOO estimates and the data around 75%. In addition, the MAE is about 41% of the mean lignite thickness of the deposit.

3.6. Estimation of Lignite Reserves

The reserves were estimated for the specific sector (West Field South Sector) of Kardia Mine shown in Figure 8. To estimate the reserves we used the predicted thickness values for the grid cells that are located inside the boundaries of the target sector. These values are estimated by OK on a 59×88 grid using the parameters of the exponential variogram (range, nugget effect, and the sill) shown in Table 4, and a kriging neighbourhood equal to 1.05 km. The estimation of the reserves is based on the following equation

$$Reserves = \rho_l A \sum_{i=1}^{N_{cells}} X(s_i), \tag{10}$$

where, A is the area of each cell (10^4 m^2), $X(s_i)$ is the estimated thickness at the location, $N_{cells}=766$ is the numbers of cells within the boundaries of the sector, and $\rho_l=1.21 \text{ t/m}^3$ is the average density of lignite. The total lignite reserves are thus estimated at 206 Mt.

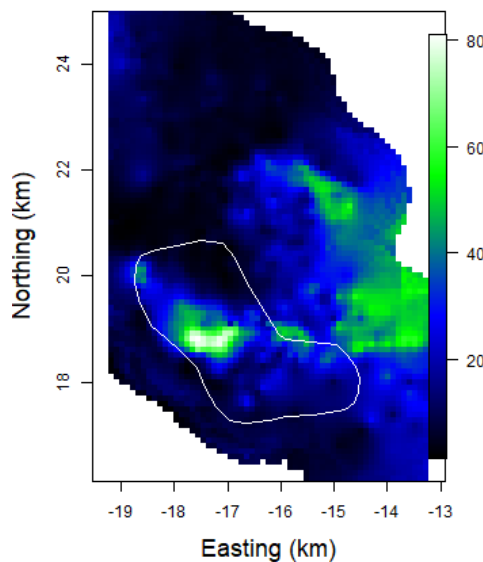


Figure 8. Map of estimated lignite thickness obtained by means of ordinary kriging of the residuals and a linear trend model. The sector outlined by the continuous curve (white line) denotes the area targeted by PPC for exploitation.

3.7. Investigation of Estimated Reserves Uncertainty

To consider the uncertainty of the lignite reserves, we used two conditional simulation methods. These involve (i) the unconditional realization polarization method, based on the covariance matrix decomposition (for the unconditional realizations) and kriging (for conditioning) and (ii) the Turning Bands Method. For each method 1000 scenarios were realized, using the same 59 x 88 grid as for the reserves estimates and the same exponential variogram parameters. In the Turning Bands Method, 1000 bands were used to generate the realizations. In Figure 9 we present a single realization for each conditional simulation method.

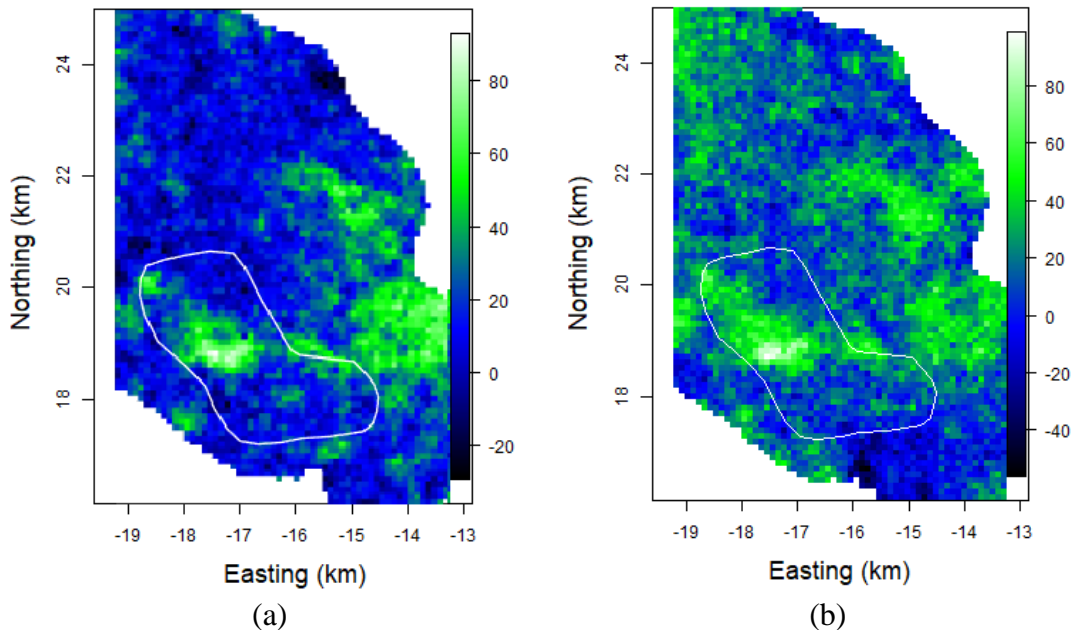


Figure 9. Typical samples of the ensemble of 1000 simulation for (a) covariance matrix decomposition and (b) turning bands. The sector outlined by the continuous curve (white line) denotes the area targeted by PPC for exploitation

The simulations include a small number of negative lignite thickness. Such negative values are located in areas where the data are sparse, giving large variance. While such values have no physical meaning, setting them to 0 thickness artificially would create a positive bias. Since the number of negative values is small, we decided against setting them to 0 to avoid the bias. It should be noted that as shown in Figure 8 there are no negative values in the kriging prediction. Such negatives appear only in some of the simulations.

The histograms for the simulated reserves within the West Field South Sector for both methods are shown in Figure 10. We adopted the percentiles at 5% and 95%, in order to estimate the reserves 90% confidence intervals. The results are presented in Table 6.

Based on the Turning Bands Simulation method, the lignite reserves for the West Field South Sector are estimated to be in the range from 193.0 to 216.6 Mt with 90% confidence, while the reserves based on the Polarization method are estimated to be in the range from 194.4 to 216.8 Mt. Hence, both methods produce similar results regarding the confidence intervals.

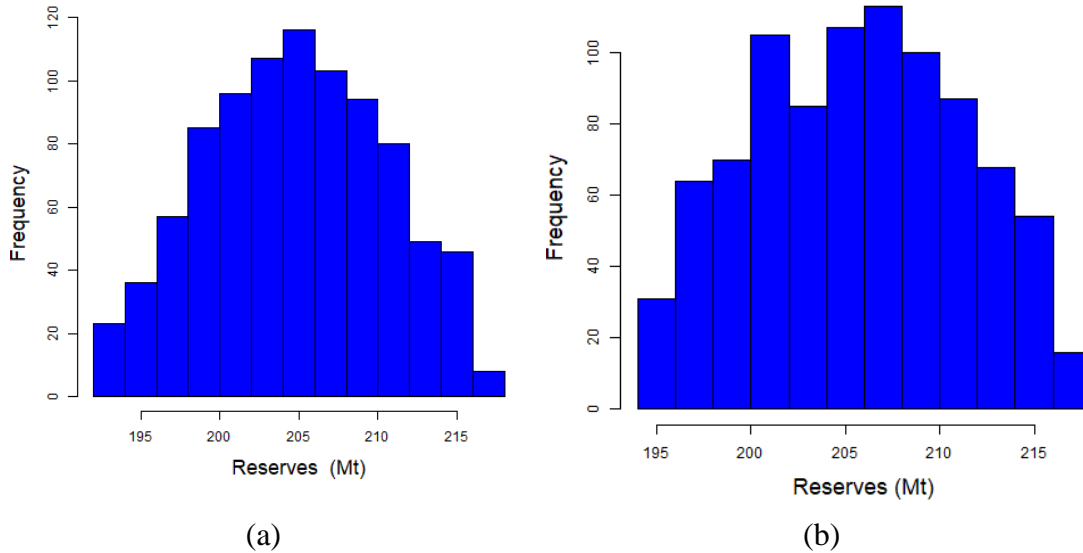


Figure 10. The histogram for the reserves estimated by 1000 conditional simulations for (a) Covariance matrix decomposition and (b) Turning bands.

Table 14. Bottom 5% and top 95% percentiles, and median of the estimated reserves based on the conditional Monte Carlo simulations using (i) covariance matrix decomposition and (ii) turning bands for the unconditional realizations.

Simulation method	X _{5%} (Mt)	X _{95%} (Mt)	Median
Covariance matrix decomposition	194.4	216.8	205.9
Turning bands	193.0	216.6	204.8

Both methods perform reliably based on the results. As shown in Table 6 the median for both methods is close to the predicted reserves (206 Mt, see Section 3.4.2). Both methods give similar percentile values for the reserves and histograms (Table 6 and Figure 8). As expected for conditional simulation, in both methods grid cells that are located close to drill-hole data have similar values with the data. The polarization method based on kriging conditioning gives smoother realizations than the turning bands method which relies on a finite number of bands. For the 59 x 88 grid used in this study both methods perform fast. However, the Turning bands method performs faster than the polarization method [17]. As seen in Figure 10, the use of 1000 bands is sufficient to simulate the field adequately without leaving artifacts from the linear interpolation.

4. CONCLUSION

This study presents an application of geostatistical analysis in the estimation of lignite reserves in Kardia mine. We used a spatial random field model to map the distribution of lignite seam thickness and to estimate the reserves for a specific sector of the mine targeted by PPC for exploitation. The spatial model involves a linear trend model that was removed from the original lignite thickness data to obtain the fluctuations (residuals). The exponential variogram function was selected to model the spatial correlation of the residuals, after testing different variogram models. For the estimation of the lignite reserves contained in the West Field South Sector of Kardia Mine, we used ordinary kriging of the residuals in combination with the linear trend.

In order to better estimate the uncertainty of the estimated reserves, two conditional simulation methods were used. The first one uses the covariance matrix decomposition method for generating

the unconditional realizations, while the second uses the Turning Bands method. Both approaches use the method of kriging polarization for conditioning. The approach based on covariance matrix decomposition is more accurate, leading to smoother spatial variation, while the second is computationally faster. For both methods, 1000 simulations were generated in order to estimate the confidence intervals of lignite thickness with 90% confidence. The reserves are estimated to lie in the range between 194.4 and 216.8 Mt by means of the polarization method. Both methods gave similar results for the statistical distribution of the estimated reserves.

Further study could focus on exploring different transformations of the data to approach the normal distribution. In addition it would be beneficial to use geostatistics to investigate lignite quality characteristics (lower calorific value, ash content, etc.) for the mine.

REFERENCES

- [1] Anonymous. EUROCOAL, "European association for coal and Lignite," 2014. [Online]. Available: <http://www.euracoal.org>.
- [2] Younger. PL, "Environmental impacts of coal mining and associated wastes: a geochemical perspective.," *Geological Society*, pp. p.169-209, 2004.
- [3] Chiles J.P., and Delfiner P., *Geostatistics :Modeling Spatial Uncertainty*. Wiley series in probability and statistics., 2nd Edition ed., New York, 2012.
- [4] Srivastava R.M., "Geostatistics: a toolkit for data analysis, spatial prediction and risk management in the coal industry.," *International Journal of Coal Geology*, no. 112, pp. p.2-13, 2013.
- [5] Christakos G., *Random field models in earth sciences.*, San Diego: Academic Press, 1992.
- [6] Goovaerts. P., *Geostatistics for natural resources evaluation*, New York: Oxford University Press, 1997.
- [7] Rheinbraun Engineering and Public Power Corporation, "Technical Mine Master Plan, unpublished report, 600p," 1996.
- [8] Olea R., "A six-step practical approach to semivariogram modeling," *Stochastic Environmental Research and Risk Assessment*, no. 20, pp. 307- 318, 01 July 2006.
- [9] Krige D.G., "A statistical approach to some basic mine valuation problems on the Witwatersrand.," no. 52, pp. 119-139, 1951.
- [10] Cressie N., *Spatial Statistics*, New York: John Willey and Sons, 1993.
- [11] Pardo-Iguzquiza E., Dowd P.A., Baltuille J.M., and Chica-Olmo M., "Geostatistical modelling of a coal seam for resource risk assessment," *International Journal of Coal Geology*, June 2013.
- [12] Luppens J., and Olea R., "Sequential simulation approach to modeling of multi-seam coal deposits with an application to assessment of a Louisiana lignite.," *Natural Resources Research*, December 2012.
- [13] Pavlides A., Hristopoulos D., Roumpos C., and Agioutantis Z., "Spatial modeling of lignite energy reserves for exploitation planning and quality control.," *Energy*, no. 92, pp. 1906-1917, 2015.
- [14] Journel A., and Huijbregts C. *Mining Geostatistics*, New York: The Blackburn Press, 2003.
- [15] Hohn M., and Britton J. A., "A geostatistical case study in West Virginia: All coals are not the same.," *International Journal of Coal Geology*, no. 112, pp. 125-133, 2013.

[16] Mantoglou A., and Wilson J.L., "The Turning Bands Method for Simulation of Random Fields Using Line Generation by a Spectral Method.," *Water Resources Research*, no. 18, pp. 1379-1394, 1982.

[17] Matheron G., "The Intrinsic Random Functions and Their Applications.," *Advances in Applied Probability*, vol. 5, pp. 439-468, 1973.

[18] Renard D., Bez N., Desassis N., Beucher H., Ors F., and Freulon X., *RGeostats: The Geostatistical R package, version[11.0.2]. MINES ParisTech / ARMINES.*

Session 3: Equipment and mining systems

Experimental Investigation of the Activated Rock Cutting Process

Taras Shepel and Carsten Drebenstedt

Freiberg University of Mining and Technology, Institute of Mining and Special Civil Engineering
09599 Freiberg, Gustav-Zeuner Street 1a, Germany

ABSTRACT

The development of hard rock cutting technologies represents a great interest in a number of mining and construction applications. Results of multiple researches demonstrate the potential of the activated rock cutting to significantly expand the application limits of the excavation equipment to harder rocks.

Basing on laboratory test results, the current study is focused on the investigation of the process of cutting granodiorite and dolomite samples with an activated cutting tool utilizing the impact rock fragmentation principle. The tests were carried out with the use of the Design of Experiments method. The obtained data enable characterisation of the influence of cutting parameters on the specific energy consumption and the advancing of the cutting tool into rock. Considerations on the applicability of the activated cutting technology to the continuous excavation of hard rocks are given in the paper.

1. INTRODUCTION

The development of sustainable technological solutions for the non-blasting excavation of hard rocks remains at the forefront of efforts of many researchers and engineers worldwide. Because of extensive research and development works, a number of hard rock excavation machines have entered the mining and construction markets. Among them are machines for underground applications as follows: Caterpillar Hard Rock Miner HRM 220 (utilizing the “Activated Undercutting Technology”), Atlas Copco Mobile Miner product line 22H, 40V and 55V (equipped with disc cutters), Wirth Mobile Tunnel Miner and Sandvik MN220 (equipped with undercutting discs), roadheaders Anderson Strathclyde RH22 and Dosco Mk.IIB (utilizing the water-jet-assisted rock cutting technology), and others [1, 2, 3].

Of particular interest are mechanical rock excavation machines equipped with activated cutting tools. The “activation” here assumes the application to the cutting tools of dynamic loads generated by oscillatory or impact actuators. It enables the considerable increase in cutting forces while just a portion of reactive forces is transmitted to the machine. For example, Caterpillar D11N Impact Ripper is reported to add almost 9 times (at a frequency of 510 blows per minute) the force of conventional ripper, which enables the ripping of normally unrippable rocks [4]. The D9L Impact Ripper has demonstrated the performance of up to 250% over the standard D9L ripper. It allows the impact rippers to compete in many cases with the drill and blast method. A power shovel EKG-5V equipped with an active bucket having built-in pneumatic percussion teeth is capable of the blast-free excavation of rocks with the Uniaxial Compressive Strength (UCS) of 60-80 MPa [5]. Some excavation tests were carried out in rocks with UCS of up to 160 MPa (see [6]).

The possibility to generate high cutting forces without considerable increase in weight of a base mining machine makes the activated rock cutting methods attractive for continuous excavation of hard rocks in both surface and underground mining applications. This paper presents results of experimental investigations aimed at the determination of parameters of working tools equipped with percussion conical cutters.

2. MATERIAL AND METHODS

2.1. Equipment

The activated rock cutting tests were carried out with the use of a linear cutting test rig HXS-1000-50 designed by ASW GmbH company specifically for the Freiberg University of Mining and Technology [7-9]. A modular design of the rig enables the installation of a pneumatic hammering device of special design instead of a cutter head. The movement of the hammering device is realized in 2 dimensions (axes Y and Z). A rock sample is placed on a worktable of the cutting rig, which moves along the X-axis.

The hammering device consists of a pneumatic hammer, two pneumatic cylinders for pressing a conical cutter into the rock prior to the impact, a cutter holder, a bush transmitting the force from the pneumatic cylinders to a cutting tool, and a housing defining the relative positioning of parts in space. Thanks to an adjustable swivel joint between the rig HXS-1000-50 and the hammering device, the inclination of the hammer in relation to the rock sample might be set.

As a cutting tool, the point attack pick BETEK BSR283 was used. The shank of the pick was cut off to and including the clamping groove in order to provide a constant diameter of the shank and prevent its possible plastic deformation during its striking with the hammer (Fig. 1).



Figure 1. The point attack pick BETEK BSR283 adapted for the hammering device.

Two foil strain gauges were placed at the pick's steel body. They were connected with two resistors following the Wheatstone bridge circuit principle to prevent the influence of the temperature of the pick on the measurement results. A wire of a draw wire sensor was attached to the hammer's piston in order to measure its displacement and then determine its speed and acceleration during striking the pick. Four piezoelectric sensors of the rig HXS-1000-50 enabled the measurement of 3 components of forces transmitted from the hammering device to the machine. Signals from the piezoelectric sensors, strain gauges and the wire sensor were recorded with a sampling frequency of 1 MHz with the use of the improved DEWE-5000 data acquisition system.

2.2. Rock samples

Two stone blocks of 500 x 850 x 200 mm in size (granodiorite and dolomite with UCS values of 205 MPa and 79 MPa, respectively) were used for the tests. The blocks were obtained by the sawing of boulders, so the blocks' surfaces were planar and smooth. A number of grooves were cut from the top of each block with an angle grinder in order to provide a pre-defined initial penetration of the pick into rock.

2.3. Test procedure

In order to determine the relationship between factors affecting the activated rock cutting process and output parameters of interest, the Design of Experiments (DoE) method was used. For unrelieved cuts, a 3-level factorial design for two variable parameters (3^2), which were the depth of cut (h) and the single impact energy (E), was applied. For relieved cuts, the Box-Behnken design for 3 factors (the influence of the spacing between cuts s was considered in addition to parameters h and E) varied at 3 levels was applied. For both designs, 3 centerpoints (with no replicates at the rest points) were provided. Constant and variable parameters and their values are listed in Table 1.

Table 1. Values of constant and variable parameters for unrelieved and relieved cuts

Parameter	Unit	Value(s)
Attack angle (γ)	deg.	50
Initial static axial loading of the pick (P)	N	3,000
Depth of cut (h)	mm	6; 10; 14
Spacing between cuts for relieved cuts (s)	mm	20; 30; 40
Single impact energy (E)	J	200; 250; 300

The tests were run in a sequence as follows (see Fig. 2):

- Positioning of the pick at the depth h beneath the rock surface at the point X_1 (static axial loading P is applied to the pick);
- Hammering the pick with a pre-defined single impact energy E ;
- Stepwise movement (with a step of 0.1 mm) of the rock along the X-axis until the pick's tip is placed at the point X_2 (additional sensors for positioning the pick in relation to the housing of the hammering device were used); recording X-coordinates of the points X_1 and X_2 .

Steps 2 and 3 were repeated until the length of a cut of approx. 300 mm was achieved. While hammering the pick, the indications of the strain gauges and piezoelectric sensors were recorded automatically due to set triggers.

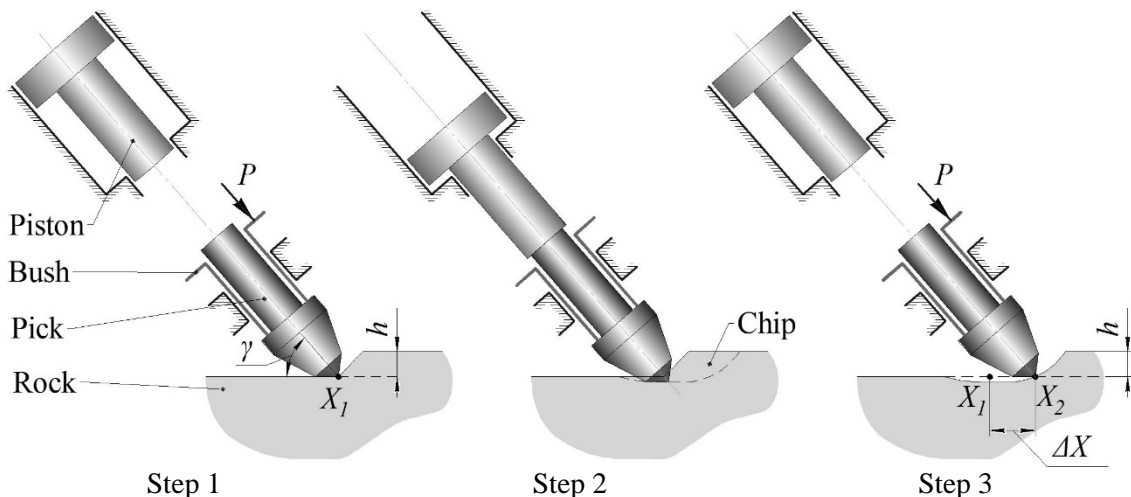


Figure 2. Test procedure (schematic).

After the completion of cutting the unrelieved cuts, the block's surface was scanned with a laser scanner of the rig HXS-1000-50. Then relieved cuts were cut, following the test procedure described above.

3. RESULTS

The activated cutting test enabled the obtaining of data as follows:

- A number of blows per meter of cut groove / the average advancing of the pick into rocks per blow (it allows the determination of an impact frequency required for the activated cutting of considered rocks with linear or rotary motion working tools);
- Energy consumption for cutting of 1 m³ of rock;
- Parameters of the impact impulse (force-time diagrams) for the estimation of the efficiency of transmitting the energy from the hammer to the rock, which effects thoroughly the efficiency of the rock fragmentation process;
- Forces transmitted to the machine during the activated cutting.

The DoE approach allows the establishment of regression models defining the relationship between input and response variables, taking into account validity, reliability, and replicability concerns. The regression models, as well as analysis of forces in the impact system, however, are not considered in this paper in order to avoid information overload.

3.1. Advancing of the pick into rock

The number of blows spent for the cutting of approx. 300 mm (along the X-axis) of the stone blocks are presented in Fig. 3 (for the unrelieved cutting mode) and Fig. 4 (for the relieved one).

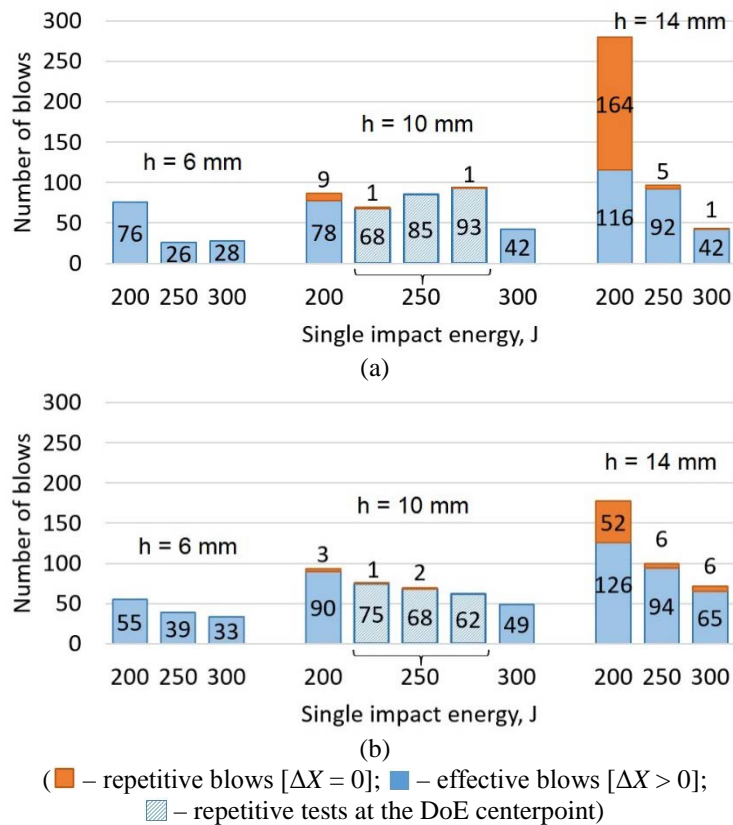


Figure 3. Number of blows per 300 mm of cut dolomite (a) and granodiorite (b) for the unrelieved cutting tests.

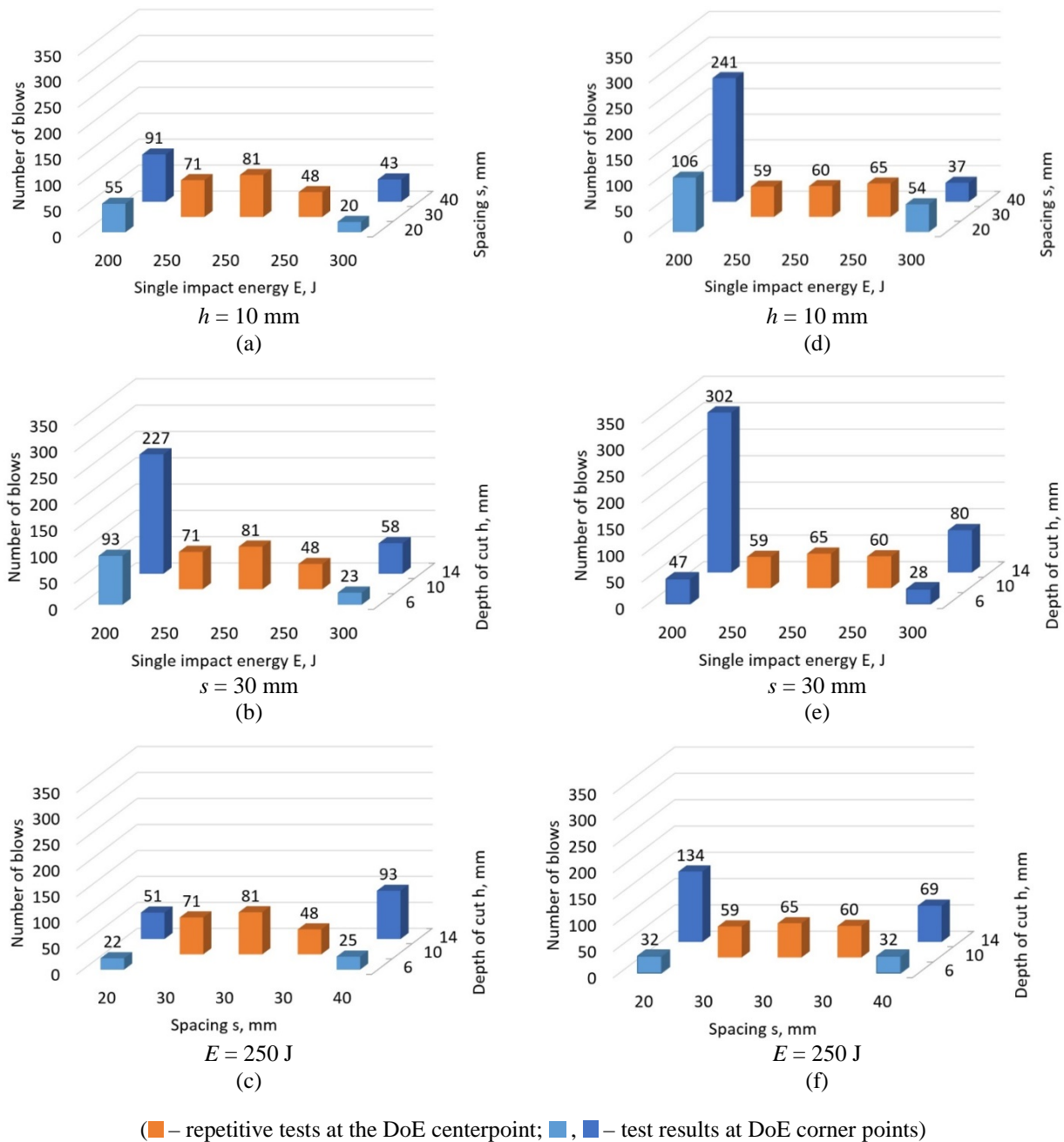


Figure 4. Number of blows per 300 mm of cut dolomite (a-c) and granodiorite (d-f) for the relieved cutting tests.

Under an effective blow here we understand such a blow, realisation of which resulted in the separation of chips from the rock, so the advancing of the pick along the X-axis would be possible ($\Delta X > 0$). Otherwise, the hammering of the pick has to be repeated until the chip separation.

The advancing of the pick into rock (ΔX) for different values h and E are shown in a view of box plots in Fig. 5 (for unrelieved cutting tests). Repetitive blows, for which $\Delta X = 0$, are not taken into account.

Each column in the box plots shows the data as follows (from bottom to top): the minimum value (2.5% of data points are below the lower mark), the first quartile (25%), the median (50%), the third quartile (75%), and the maximum (97.5%). The mean values are marked with a cross.

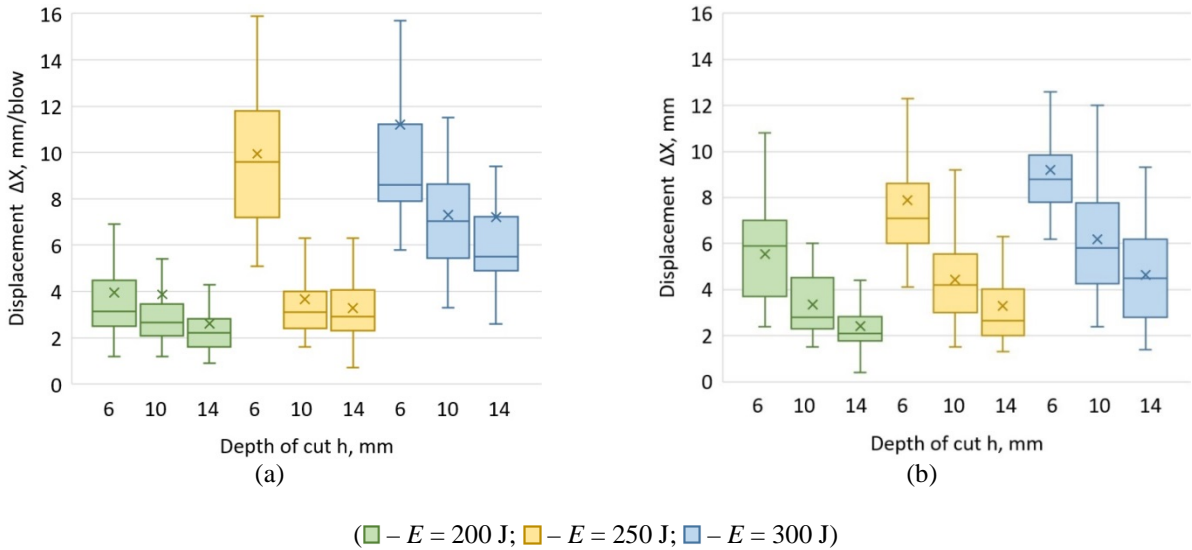


Figure 5. Advancing of the pick into dolomite (a) and granodiorite (b) for the unrelieved cutting tests.

Results of statistical analysis of the total number of blows per 300 mm of cut groove for the DoE centerpoints are given in Table 2.

Table 2. Results of statistical analysis of the total number of blows per 300 mm of cut groove for the DoE centerpoints

Parameter	Dolomite		Granodiorite	
	Unrelieved	Relieved	Unrelieved	Relieved
Count	3	3	3	3
Average	83	67	69	61
Coefficient of variation, %	15.3	25.4	10.1	5.2
95.0% confidence interval for the mean value	± 32	± 42	± 18	± 8

The obtained results show that the advancing of the pick into granodiorite/dolomite per one blow increases with increasing the single impact energy and decreasing the depth of cut.

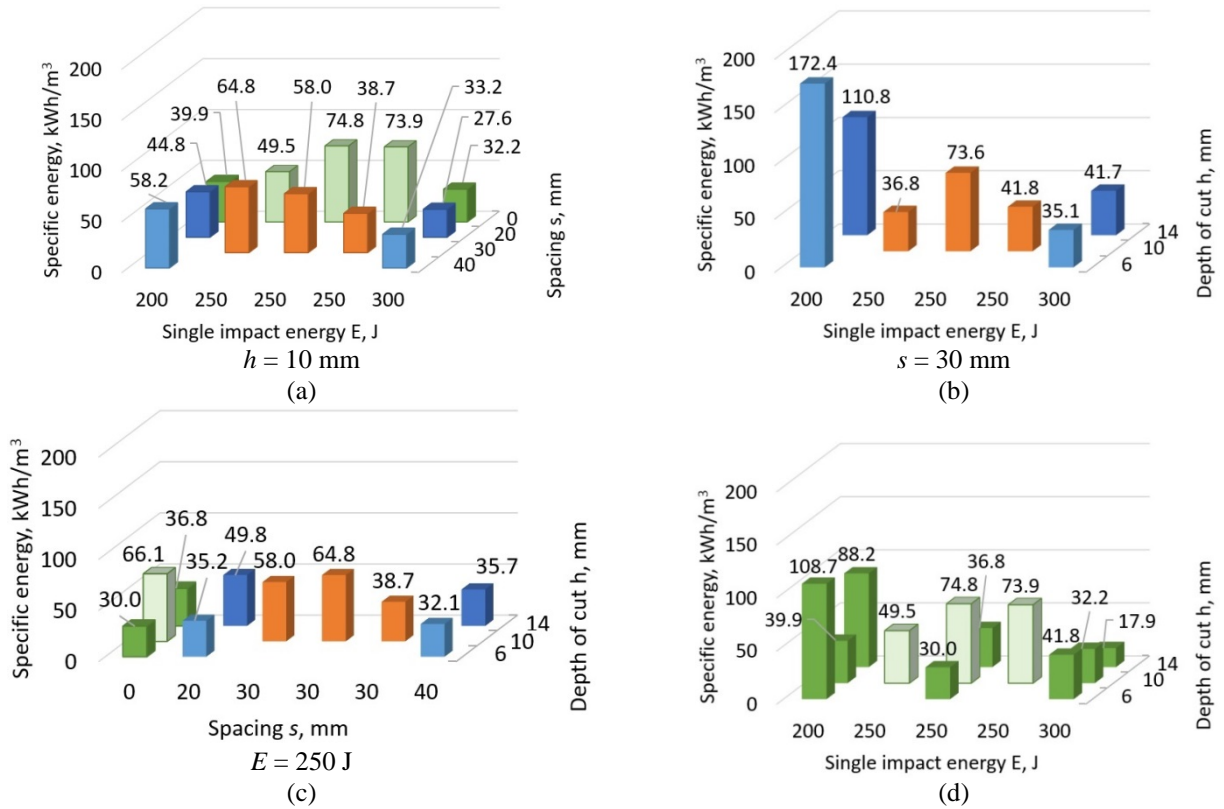
3.2. Specific energy consumption

The specific energy consumption was calculated as a ratio between the energy spent for hammering the rock and the cut volume as follows:

$$E_s = \frac{n \cdot E}{V}, \tag{1}$$

where n is the number of blows spent for the cutting of a groove; E is the single impact energy; V is the volume of the groove.

The calculation results are presented in Fig. 6, 7. The energy spent for the initial axial loading of the pick is not taken into account due to its negligible contribution (about 3%). The application of the initial axial loading of 3 kN to the pick was aimed at providing a tight contact between the pick and rock prior to the impact.



(■, ■ – repetitive tests at DoE centerpoints for relieved and unrelieved cuts, respectively; ■, ■ – test results for relieved cuts at DoE corner points; ■ – test results for unrelieved cuts at DoE corner points)

Figure 6. Specific energy consumption for the activated cutting of dolomite under relieved (a-c) and unrelieved (d) cutting conditions.

Results of statistical analysis of the specific energy consumption for DoE centerpoints are given in Table 2.

Table 2. Results of statistical analysis of the specific energy consumption for DoE centerpoints

Parameter	Dolomite		Granodiorite	
	Unrelieved	Relieved	Unrelieved	Relieved
Count	3	3	3	3
Average, kWh	66.1	53.8	52.4	48.6
Standard deviation, kWh	14.4	13.5	6.4	9.51
Coefficient of variation, %	21.7	25.1	12.1	19.6
95.0% confidence interval for the mean value, kWh	±35.7	±33.6	±15.8	±23.6

The obtained results show that the specific energy consumption generally decreases with increasing the single impact energy. For the unrelieved cutting tests, the minimum specific energy consumption was obtained for the maximum values of both depth of cut and single impact energy. The dependency of E_s on s/h ratio is of a mixed character, which differs from the one typical for the conventional cutting of rocks (see Fig. 8).

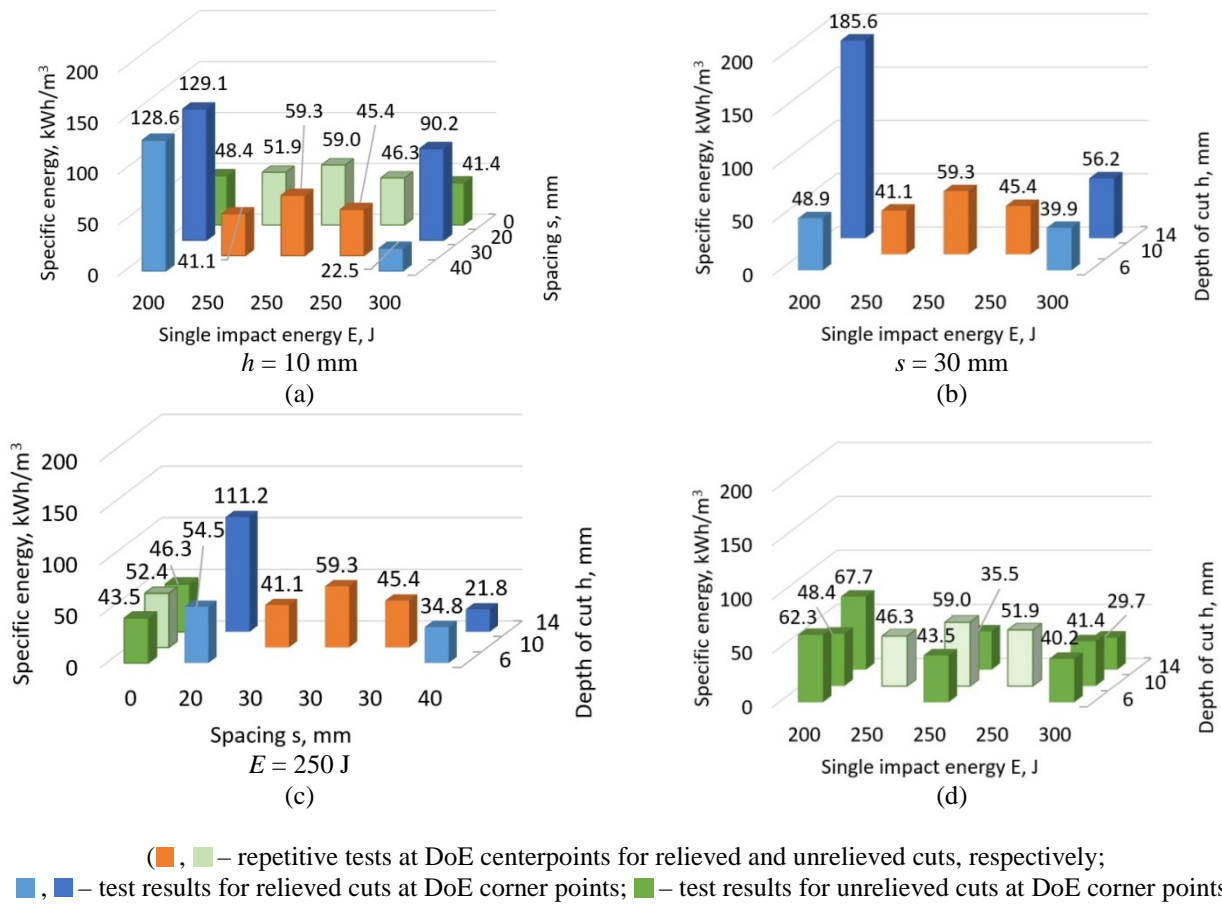


Figure 7. Specific energy consumption for the activated cutting of granodiorite under relieved (a-c) and unrelieved (d) cutting conditions.

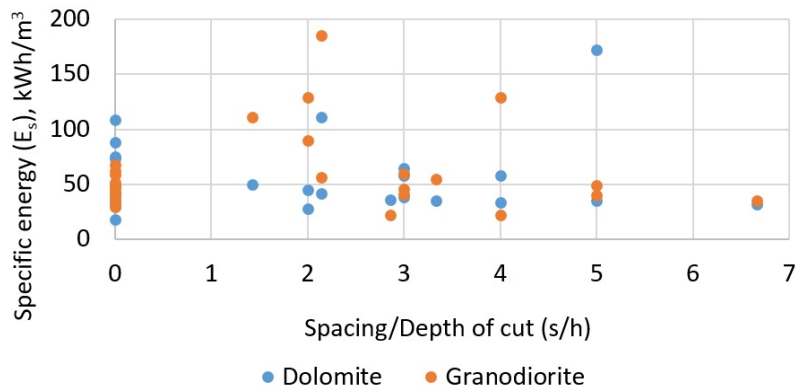


Figure 8. Effect of s/h ratio on the specific energy consumption.

4. DISCUSSION

The obtained results demonstrate a considerable potential of the activated cutting technology for hard rock excavation applications. The specific energy consumption values for the activated cutting are more or less of the same range as that for the conventional cutting (for comparison, the specific energy spent for cutting of granite with UCS of 210 MPa with $h = 4$ and $s = 8$ and 12 mm is in range from 35 to 61 kWh/m³ for relieved cutting conditions, see [9]).

An advantage of the activated cutting technology utilizing the impact rock fragmentation method is that the force of a high magnitude is applied to the cutting tool periodically over a short period of time (for a fraction of a millisecond), which should result in decreased wear of the cutting

tool due to the lower friction force while movement of the tool along the work face. Only a portion of forces is transmitted to the machine (the upper force limit of the rig HXS-1000-50 is 50 kN, while the force generated in the cutting tool during the activated cutting tests reached 120 kN).

The cutting tests demonstrated that insufficient single impact energy necessitates repetitive blows, which results in the separation of a powdered material (from crushed zone) stacking between the pick and rock. As a result, the contact area increases in size, reducing stresses in rock during its hammering. It decreases the efficiency of the fragmentation process and might result in the termination of the cutting process at all (it was observed during preliminary tests while cutting granodiorite with $h = 14$ mm and $E = 150$ J).

The subsequent rock cutting scheme (the single spiral cutting pattern) seems to be not optimal for the activated cutting due to the non-symmetrical interaction between the pick and rock. Because of random chipping, during relieved cutting the pick could contact the rock not with its tip, but with side area, which resulted in non-effective blows (with no chips) due to insufficient stresses induced in rock. It also caused high side forces, which led to a certain distortion of the pick. In case of the distortion (taking into account relatively small length of the pick's shank comparing to the one of picks for demolition works), the contact area between the hammer's piston and the pick is decreased, reducing the efficiency of transmitting the energy from the piston to the pick. This might serve as an explanation of the fact that for some relieved cuts the number of blows exceeds the one for unrelieved cuts. The double spiral cutting pattern (the cutting of two grooves with a big spacing and then a groove in between) seems therefore to be more preferable due to symmetrical pick-rock interaction conditions.

The impact frequency required for the continuous activated cutting might be calculated on the basis of diagrams presented in Fig. 3, 4. For the cutting speed ranging from 1.4 m/s to 3.0 m/s, which covers conventional range of cutting speeds for surface miners and roadheaders [10, 11], the cutting of dolomite with $E = 300$ J and $h = 14$ mm under unrelieved cutting mode would require the impact frequency in range from approx. 190 blows/s to 420 blows/s for dolomite and from approx. 300 blows/s to 650 blows/s for granodiorite. Taking into account the fact that serially produced (hydraulic) impact hammers have the single impact energy ranging primarily from 0.5 kJ to 20 kJ and the impact frequency in range from 1 blow/s to 40 blows/s, the speed of the activated cutting under considered cutting conditions has to be reduced to approx. 0.29 m/s for dolomite and 0.19 m/s for granodiorite (for the impact frequency of 40 blows/s).

5. CONCLUSIONS

The activated rock cutting technology has a considerable potential for extending the applicability of the blast-free mechanical excavation to harder rocks. The conducted cutting tests demonstrated that the specific energy consumption for the cutting of dolomite with UCS of 79 MPa with the depth of cut of 6-14 mm and the single impact energy of 200-300 J is in range 17.9-108.7 kWh/m³ for the unrelieved cutting mode and 32.1-172.4 kWh/m³ for the relieved one (with the spacing ranging from 20 to 40 mm). Appropriate ranges for granodiorite with UCS of 205 MPa are 29.7-67.7 kWh/m³ and 21.8-185.6 kWh/m³ for the unrelieved and relieved cutting modes, respectively. The specific energy consumption decreases with increasing both the single impact energy and the depth of cut. The activated cutting in accordance with the single spiral pattern is not optimal due to non-symmetrical cutting conditions decreasing the efficiency of transmitting the impact energy to the rock.

The impact frequency of commercially available impact hammers limits greatly the maximum cutting speed. For the considered cutting conditions, the maximum cutting speed required for the continuous cutting of dolomite under the impact frequency of 40 blows/s is approx. 0.29 m/s. An appropriate value for the granodiorite used in tests is approx. 0.19 m/s. Increasing the impact energy

and the efficiency of its transmission to the rock has a considerable potential for increasing the cutting speed and, as a result, the performance of a mining machine.

Acknowledgement

The work was financially supported by the European Union (European Social Fund) and the Saxonian Government [grant number 100270113]; it is a part of the Project InnoCrush – Dynamic methods of mechanical excavation and comminution for high selective production chains in Critical Raw Materials in Saxony.



REFERENCES

- [1] Caterpillar performance handbook. Caterpillar, Illinois, USA (2017).
- [2] Ramezanzadeh, A., & Hood, M. (2010). A state-of-the-art review of mechanical rock excavation technologies. *International Journal of Mining and Environmental Issues*, 1, 29–39.
- [3] Timko, R.J., Johnson, B.V., & Thimons, E.D. (1986). Water-jet-assisted roadheaders. Bureau of mines, Pittsburgh, USA.
- [4] Jensen, B.D. (1989). The Caterpillar D11n Impact Ripper. SAE Technical Paper Series, 1–8.
- [5] Mattis, A.R., & Zaitsev, G.D. (2003). Problems in the development of excavators for non-blasting mining and ways of their solution (in Russian). *Mining Informational and Analytical Bulletin (Scientific and Technical Journal)*, 12, 132–135.
- [6] Mattis, A.R., Labutin, V.N., Cheskidov, V.I., Zaitsev, G.D., & Kudryavtsev, V.G. (2005). Substantiation of the capacity of percussion devices and estimation of the performance capabilities for the active bucket excavator EKG-5V. *Journal of Mining Science*, 41 (5), 467–474.
- [7] Drebenstedt, C. (2009). State of the art and new concepts for prediction of cutting resistance on example of continuous mining equipment. *Innovations in Non Blasting Rock Destructuring*, TU Bergakademie Freiberg, 6–26.
- [8] Grafe, B., Shepel, T., Drebenstedt, C., & Hartlieb, P. (2017). Studies on the effect of high power microwave irradiation as a means of inducing damage to very hard rock to reduce the cutting resistance during mechanical excavation. *Proceedings to MPES – Mine Planning and Equipment Selection*, Lulea, 161–166.
- [9] Hartlieb, P., Grafe, B., Shepel, T., Malovyk, A., & Akbari, B. (2017). Experimental study on artificially induced crack patterns and their consequences on mechanical excavation processes. *International Journal of Rock Mechanics and Mining Sciences*, 100, 160–169.
- [10] Wirtgen surface mining manual. Wirtgen Group Company (2017).
- [11] Bilgin, N., Copur, H., & Balci, C. (2013). *Mechanical Excavation in Mining and Civil Industries*. CRC Press.

Determination of Optimal Life Cycle of Bulldozer in Open Pits with Continual Systems in PE EPS

Dragan Ignjatović¹, Predrag Jovančić² and Ivan Janković³

¹University of Belgrade – Faculty of Mining and Geology, Djušina 7, Belgrade, Serbia

²University of Belgrade – Faculty of Mining and Geology, Djušina 7, Belgrade, Serbia

³Ministry of Mining and Energy of the Republic of Serbia, Nemanjina 22-26, Belgrade, Serbia

ABSTRACT

Satisfactory time and capacity utilization of continual systems on open pits is possible just under the assumption of providing optimal conditions for their operation. One of the most significant preconditions is in-time and quality execution of all auxiliary works, which brings us to the fact that open pit has certain auxiliary mechanization (type, number, capacity, power, etc.). Currently, more than 330 heavy machines are hired in PE EPS's open pits. One third of that number are bulldozers. Cost for procurement and operation of auxiliary machines are relatively high. In total cost it varies from 13% to 18%. Particular problem which distinguishes from others is that low availability of dozers and high costs of exploitation is present in the last years in PE EPS's open pits. One of the reasons is untimely replacement of dozers which leads to additional costs for maintenance, higher fuel and grease consumption and low availability. This paper shows an overview on optimal dozer time period for replacement.

1. INTRODUCTION

Operational efficiency of capital mining equipment is in direct correlation with efficiency of auxiliary machines. Operation of auxiliary machines is reflected through in-time completion of planned auxiliary activities, meaning that appropriate number of various auxiliary machines (by type, capacity, power, etc.) must be available during production at the open pit mines. Lack or insufficient number of appropriate mechanization implies inappropriate execution auxiliary works, thus hindering operation of capital equipment by reduced time and capacity utilization, and it could have impact on safety of both workers and mechanization.

Dozers are most common auxiliary machines at coal open pit mines, both by type and the scope of tasks these machines can be used for. Some 50 dozers are daily operated on PE EPS's open pits out of 300 heavy duty auxiliary machines, while 113 are available. Average age of dozers is around 10 years and achieved 25,000 moto-hours (operating hours). Such structure of age and achieved operating hours is the reason for having more than twice as much available dozers in relation to operating ones.

Dozers can be used for numerous auxiliary tasks, however, most important ones are: development of routs for moving excavators and stackers, levelling of benches for shifting belt conveyors, piling of loose rocks within the range of bucket wheel, breaking up and levelling of "crescent" piles on waste dumps, development of communication routes and ramps, shaping of slopes, cleaning of benches and roads, moving of drive stations and return ends of belt conveyors, etc.

It should be noted that dozers are generating 45 – 50% of all auxiliary equipment costs (Figure 1). This implies the necessity for detailed analysis of all parameters of these machines, including current and historic trends, as well as some technical capabilities. Such analysis would enable better forecasting of their operation.

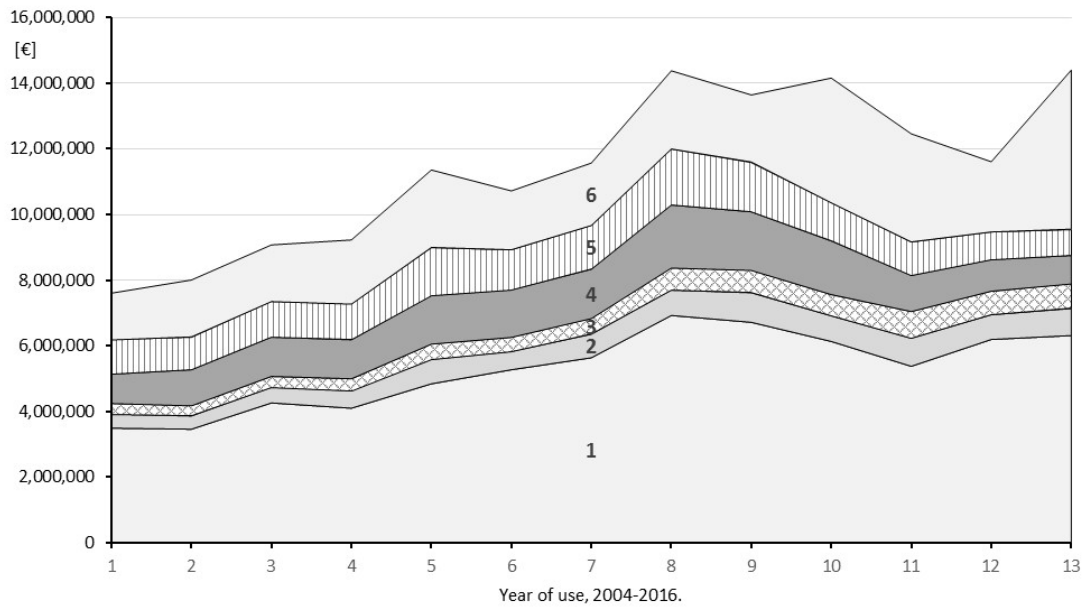


Figure 57. Operating costs of auxiliary machines in RB Kolubara for period 2004-2016 (costs for fuel, lubricants, spare parts and consumables); 1. dozers – 46.4%; 2. pipe layers – 5.9%; 3. hydraulic excavators – 4.7%; 4. passenger – off road vehicles – 11.5%; 5. trucks – 10.3%; 6. other – 21.2%.

Dozer's life on the open pit is related to numerous factors, where most important ones are machine's quality, operating conditions, maintenance quality, operating quality and others. Empirical data shows that dozer's life on open pits is 25-30,000 hours, i.e. around 10 years of operation. However, same data also shows that dozers after 6th year of operation are having lesser efficiency which is indicated by reduced number of effective hours which these machines can achieve, higher consumption of fuel and spare parts and more stoppages (failures) (Figure 2).

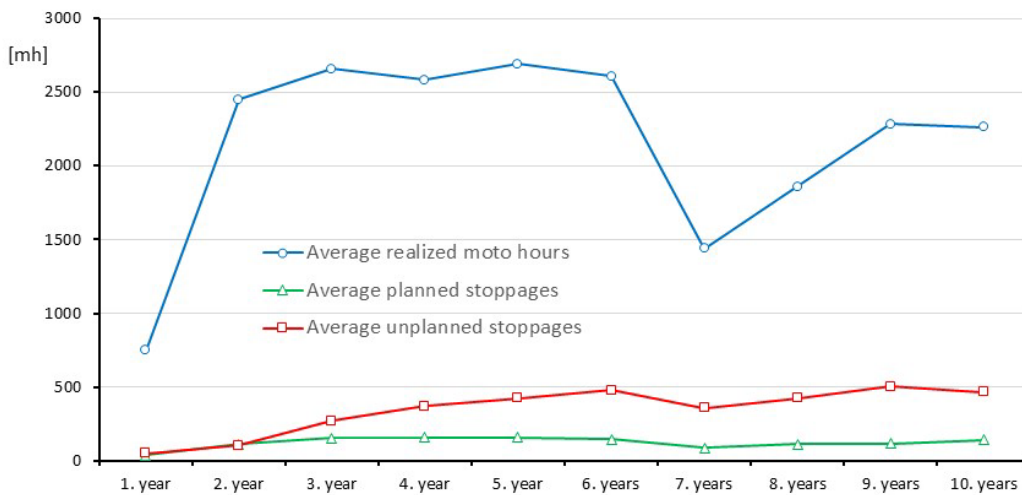


Figure 2. Average number of achieved moto hours in operation and stoppages of dozers for first 10 years of operation

Also, operating costs are increased more rapidly after 6th year of operation, in relation to achieved number of moto hours of dozer (Figure 3).

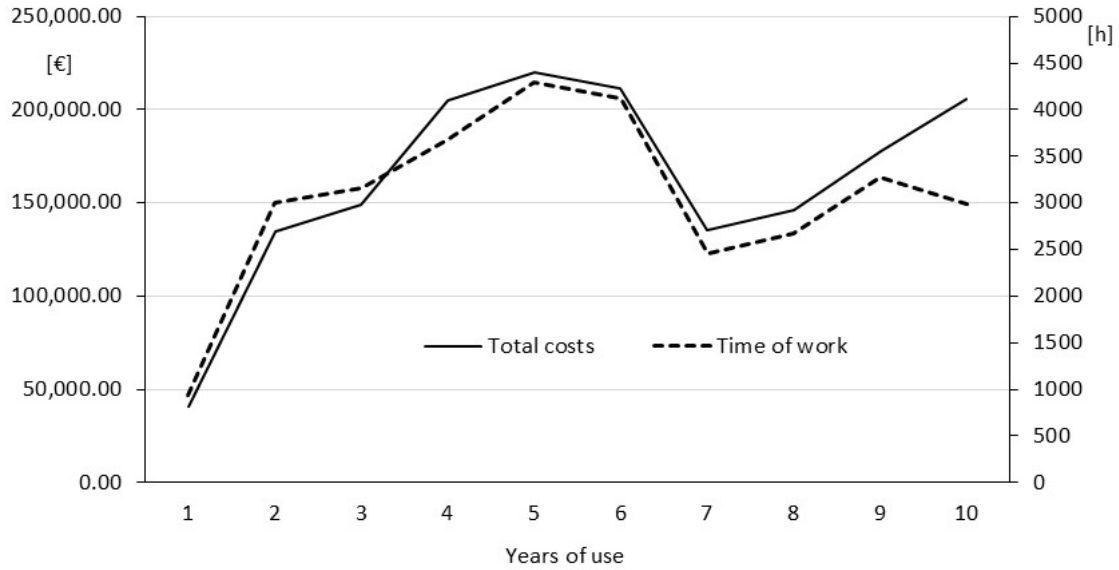


Figure 3. Relation between effective work time and total operating costs

2. LIFE CYCLE OF DOZER

Life cycle of mechanization refers to its duration, i.e. it starts just after the designing stage and production stage. Hence, it is the period during which the mechanization is in functional condition, meaning it is used [2, 5].

Life cycle of a machine, facility or any other technical system has complex structure, and it encompasses several distinctive but interrelated and timely adjusted groups of activities. Technical system is used only during one part of own life cycle, therefore, time it is used is shorter than time of its duration. Life cycle is defined by several stages:

- Concept / project requirements;
- Project concept;
- Main project – designing;
- Manufacturing;
- Application / operation and
- Decommissioning.

Also, operational life can be defined as:

- Technical operational life – period during which machine meets designed criteria and guaranteed capacities;
- Economical operational life – period defined by depreciation of investment, i.e. by comparison of net present value, future costs and future incomes. Economical life is usually shorter than technical life or prior to need for revitalization of machine.
- Licenced operational life – as specified by permit or by legislation changes related to permit.
- Technological operational life – defined by technology obsolescence. It is extended by reconstruction or modernization through investment maintenance.

Operational life can be also defined as [3]:

- Physical life (operational life of machine while it operates);
- Profit life (period of operational life while machine generates profit) and
- Economic life (period of operational life with highest profit).

As shown on Figure 4, operation of the machine with highest profit is just a short interval within the operational life. In this period profit is the highest due to low maintenance costs. Subsequent period has larger operational costs, but machine still generates profit, while finally, there is a period during which machine still can operate, but with large maintenance cost and declined reliability, meaning that we are not sure when machine will be available. At this time machine should be replaced [2].

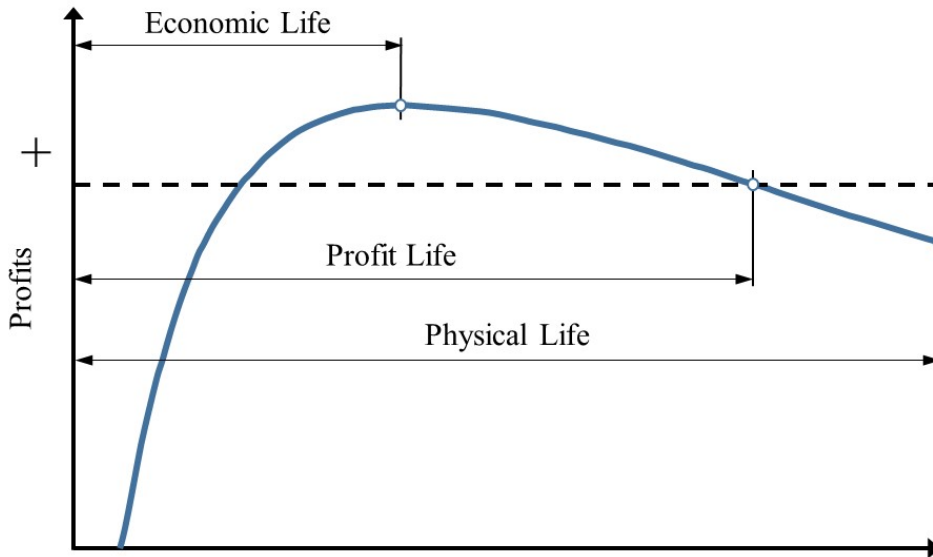


Figure 4. Relation between effective working time and total operating costs

Therefore, it can be said that economic life of the machine is defined by overall costs. However, it should be noted that any activity and each segment of life cycle requires investment of some kind. Life cycle costs can be classified as follows (Eq. 1):

- Ownership costs:
 - o Acquisition cost, including transport, supply, insurance,
 - o Administrative cost, including management, informatics.
- Operational costs, which are including labour, auxiliary facilities, installations required for work;
- Maintenance costs, which are including maintenance labour, spare parts, tools, devices and facilities for maintenance.

$$C_u = C_v + \int_0^T f(t)dt + C_k T, \tag{1}$$

where:

- C_u – total life cycle costs,
- C_v – ownership costs,
- C_k – specific operational costs per time,
- $f(t)$ – function of mean time between failures,
- T – time of machine application.

Optimal replacement time is at the moment with minimal cost (Figure 5). [2]

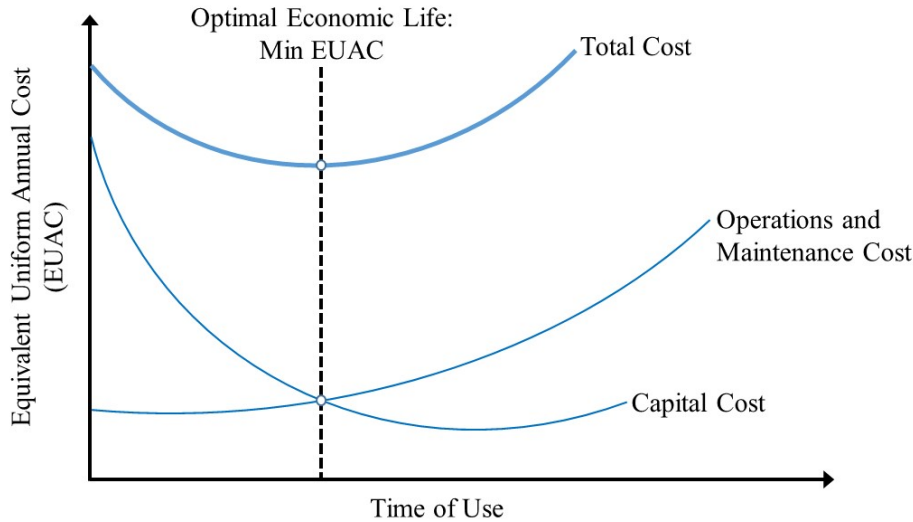


Figure 5. Economic life of the machine, based on the minimal cost method

Hourly ownership costs and operational costs for dozer could vary significantly. Parameters impacting these costs are: type of job performed, costs of fuel and lubricants, transportation cost from manufacturer, interest rates, etc. Analysis was performed according to recommended method for evaluation of hourly ownership and operational costs, including data on auxiliary machines (*Caterpillar* and *Komatsu* methods). Integration of these information with operational conditions will enable reliable evaluation.

Total costs, i.e. specific cost per moto hour is the sum of following costs:

$$TOTAL COSTS = OWNERSHIP COSTS + OPERATIONAL COSTS + COSTS OF OPERATOR$$

Table 15. Total costs for dozers in Kolubara basin (for period 2004-2016)

No.	Type	Manufacturer	Internal mark	Tot. no. of moto hours	Ownership costs	Operational costs	Costs for operator	Total costs
				[mh]	[€/mh]	[€/mh]	[€/mh]	[€/mh]
1.	D 8 R	Caterpillar	C-3	27,942	16.55	43.14	11.79	71.49
2.	D 8 R	Caterpillar	C-4	28,286	16.35	41.53	11.79	69.67
3.	D 8 R	Caterpillar	C-5	32,097	14.41	37.44	11.79	63.64
4.	D 8 R	Caterpillar	C-6	21,964	18.95	46.17	11.79	76.92
5.	D 8 R	Caterpillar	C-7	25,117	16.57	35.37	11.79	63.74
6.	D 8 R	Caterpillar	C-8	26,681	15.60	37.01	11.79	64.41
7.	D 8 R	Caterpillar	C-9	25,354	16.30	38.38	11.79	66.47
8.	D 8 R	Caterpillar	C-10	22,683	14.28	34.81	11.79	60.88
9.	D 8 R	Caterpillar	C-11	18,487	17.52	35.24	11.79	64.55
10.	D 8 R	Caterpillar	C-12	20,152	16.07	43.91	11.79	71.77
11.	D 8 R	Caterpillar	C-13	18,552	17.46	40.37	11.79	69.61
12.	D 8 R	Caterpillar	C-14	7,723	12.88	26.85	11.79	51.52
13.	D 8 R	Caterpillar	C-15	8,013	11.16	23.77	11.79	46.73
14.	D 8 R	Caterpillar	C-16	6,844	7.42	18.86	11.79	38.07
15.	D 8 R	Caterpillar	C-17	7,767	7.71	21.74	11.79	41.24
Average cost for CAT D8R:								61.38
1.	PR-752	Liebherr	L2	31,977	13.21	40.93	11.79	65.93
2.	PR-754	Liebherr	L-5	27,225	15.51	34.84	11.79	62.14
3.	PR-754	Liebherr	L-6	16,627	25.40	33.00	11.79	70.18
Average cost for Liebherr PR-752 and PR-754:								66.08
1.	PD 320Y-1	Pengpui	122	21,478	6.83	26.56	11.79	45.17
Average cost for Shanghai PD 320Y-1:								45.17

1.	SD32W	Shantui	140	7,434	12.19	33.31	11.79	57.29
2.	SD32W	Shantui	141	11,213	8.08	33.39	11.79	53.26
3.	SD32W	Shantui	142	9,011	10.05	33.01	11.79	54.86
4.	SD32W	Shantui	143	5,247	11.52	32.23	11.79	55.55
5.	SD32W	Shantui	144	7,415	12.22	27.89	11.79	51.90
6.	SD32 5	Shantui	145	25	/	/	/	/
7.	SD32 5	Shantui	146	23	/	/	/	/
Average cost for Shantui SD 32W, SD 32 5:								54.57
1.	TD 25 H	Dressta	32	34,749	9.27	39.94	11.79	61.00
2.	TD 25 H	Dressta	33	38,175	8.44	39.85	11.79	60.08
3.	TD 25 H	Dressta	34	26,119	12.33	38.77	11.79	62.89
4.	TD 25 H	Dressta	35	40,149	8.03	41.37	11.79	61.18
5.	TD 25 H	Dressta	36	41,681	7.73	46.52	11.79	66.04
6.	TD 25 H	Dressta	37	38,223	8.43	46.94	11.79	67.16
Average cost for Dressta TD25H:								63.06
1.	TD 25 M	Dressta	40	18,526	11.08	52.36	11.79	75.23
2.	TD 25 M	Dressta	42	8,499	16.74	92.66	11.79	121.19
3.	TD 25 M	Dressta	43	17,636	11.63	46.20	11.79	69.63
4.	TD 25 M	Dressta	44	13,953	14.71	48.23	11.79	74.72
5.	TD 25 M	Dressta	45	7,694	26.67	43.13	11.79	81.59
6.	TD 25 M	Dressta	46	10,755	9.55	39.71	11.79	91.05
7.	TD 25 M	Dressta	47	9,360	10.97	41.20	11.79	63.96
8.	TD 25 M	Dressta	48	10,478	9.80	38.50	11.79	60.09
9.	TD 25 M	Dressta	49	7,652	13.42	37.62	11.79	62.82
10.	TD 25 M	Dressta	50	7,653	8.95	38.77	11.79	59.51
11.	TD 25 M	Dressta	51	216	/	/	/	/
12.	TD 25 M	Dressta	52	247	/	/	/	/
13.	TD 25 M	Dressta	53	365	/	/	/	/
Average cost for Dressta TD25M:								72.98
1.	TD 25 E	StalowaWola	64	28,987	8.68	46.90	11.79	67.37
2.	TD 25 E	StalowaWola	65	20,991	11.98	41.65	11.79	65.43
Average cost for Stalowa Wola TD25E:								66.40
1.	TD 25 G	StalowaWola	70	34,046	7.39	38.75	11.79	57.94
2.	TD 25 G	StalowaWola	71	30,526	8.24	38.43	11.79	58.46
3.	TD 25 G	StalowaWola	73	33,282	7.56	41.75	11.79	61.11
4.	TD 25 G	StalowaWola	76	29,442	8.55	39.21	11.79	59.54
5.	TD 25 G	StalowaWola	90	39,374	6.39	45.09	11.79	63.28
6.	TD 25 G	StalowaWola	94	31,424	8.00	34.27	11.79	54.06
7.	TD 25 G	StalowaWola	95	23,440	10.73	43.65	11.79	66.17
8.	TD 25 G	StalowaWola	96	36,640	6.87	40.22	11.79	58.88
Average cost for Stalowa Wola TD25G:								59.93
1.	TD 40 B	Dressta	03	29,610	17.00	63.68	11.79	92.46
2.	TD 40 C	Dressta	04	36,881	13.65	58.16	11.79	83.60
3.	TD 40 C	Dressta	05	44,293	11.37	56.22	11.79	79.37
4.	TD 40 E	Dressta	06	15,122	29.87	64.20	11.79	105.86
5.	TD 40 E Extra	Dressta	07	23,686	19.10	71.60	11.79	102.49
6.	TD 40 E Extra	Dressta	08	5,680	17.74	71.22	11.79	100.75
7.	TD 40 E Extra	Dressta	09	19,176	15.74	75.60	11.79	103.12
8.	TD 40 E Extra	Dressta	10	6,645	22.72	58.77	11.79	93.28
Average cost for Dressta TD40:								95.12

Following conclusions can be made on average costs for powerful and very powerful dozers operating on open pits, based on data from table 1:

- Average costs for powerful dozers are: 63.75 €/mh;
- Average costs for very powerful dozers are: 95.12 €/mh.

Limiting costs based on these values are defined for powerful dozers at 70 €/mh and for very powerful dozers at 100 €/mh.

Operating costs by years for CAT D8R and Dressta TD25M dozers in PE EPS are shown on Figure 6. Costs increasing trend is evident in this interpretation. In case of applying profit life criterion CAT D8R dozer should be replaced after 7 years of operation, or in this case after 22,000 working hours on average. On the other hand, Dressta TD25M dozer should be replaced after 3 years and 8,500 working hours. Limiting cost for all dozers is 70 €/mh [1].

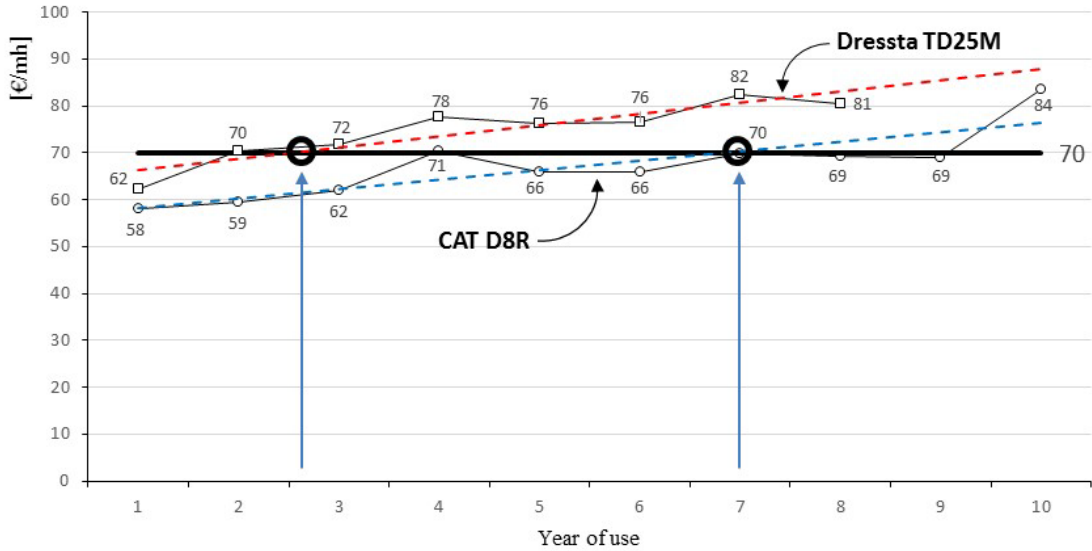


Figure 6. Diagram for determination of limiting costs value for CAT D8R and Dressta TD25M dozers

Same principle is used for analysis of other dozers operating at RB Kolubara open pits. Results are given in Table 2. Limiting cost for very powerful dozers (TD40) is at value of 100 €/mh [1].

Table 2. Year of operation on which operating costs are reaching optimal value of 70 €/mh (excluding dozer TD40)

	D8R	PR752&PR754	TD25M	TD25H	TD25E	TD25G	TD40
Optimal year for replacement	1 st year	1 st year	1 st year	1 st year	1 st year	1 st year	1 st year
	2 nd year	2 nd year	2 nd year	2 nd year	2 nd year	2 nd year	2 nd year
	3 rd year	3 rd year	3rd year	3 rd year	3 rd year	3 rd year	3 rd year
	4 th year	4 th year	4 th year	4 th year	4 th year	4 th year	4 th year
	5 th year	5 th year	5 th year	5 th year	5 th year	5 th year	5 th year
	6 th year	6 th year	6 th year	6 th year	6 th year	6 th year	6 th year
	7th year	7th year	7 th year	7 th year	7 th year	7 th year	7 th year
	8 th year	8 th year	8 th year	8th year	8th year	8 th year	8th year
	9 th year	9 th year	9 th year	9 th year	9 th year	9 th year	9 th year
	10 th year	10 th year	10 th year	10 th year	10 th year	10th year	10 th year

3. AVAILABILITY

Typical curve of failures, known as "bath tub" curve, is evident regarding dozers operating on open pit mines. Failure is a condition when the machine completely or partially loses operating capability and it is unable to meet the task requirements and function, as established by the machine design and specifications. One of the most important reliability indicators is failure frequency, i.e. expected number of failures in certain time interval. Failure frequency distribution curve is aforementioned "bath tub" curve, shown on Figure 7. Interpretation of this curve indicates that usually large number of failures occurs at the beginning of machine's service life, followed by the decline after this initial period. As machine approaches to the end of its life, curve enters the worn-out period with increasing rate of failures. First period is a period of early failures, caused by design flaws and

commissioning and control errors. These are usually repaired very fast. Second period is period of normal operation, with fairly constant failure rate frequency. Machine finished runing-in period and performs required function. Third period is the aging period, when number of failure rises, and decision should be made whether to replace the machine or overhaul it. Life cycle curve of mining mechanization is not the same for capital equipment and auxiliary machines, also curve differs for various types of these machines [2].

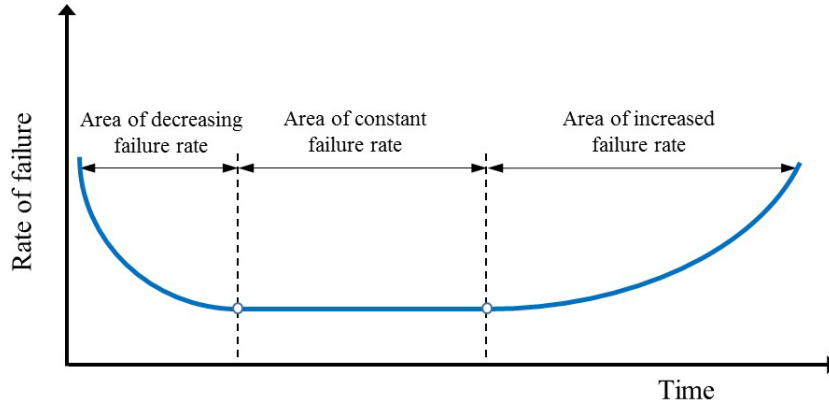


Figure 7. "Bath tub" curve, relationship of time and failure rate

Life cycle analysis of auxiliary machines operating on open pit mines brings the question related to term which can be used to describe certain properties of this technical system most completely, in relation to performing their functions. In this context following terms are defined: Reliability, Maintainability, Efficiency, Maintenance support, Availability, Dependability, etc. All of these are used to describe behaviour of technical system during specific time of system's life.

Effectivity function is a comprehensive indicator, expressed as probability that specific system will start operation in required time and that it will successfully complete criteria function during designed interval and at given environmental conditions. It should be noted that operation of auxiliary machines are exposed to unexpected impacts, i.e. failures and other events during the life of technical system which are of stochastic nature. Definition of efectivity function is given by Eq 2.

$$E(t, \tau) = R(t) \times A(\tau) \times FP \tag{2}$$

$R(t)$ – Reliability or probability to operate without failure during time t ,

$A(\tau)$ – Availability or probability that system will be available at any given moment of calendar time τ , i.e. system will be capable to operate,

FP – Functional suitability or level for meeting functional demands, meaning adaptability to the environment or operating conditions.

Research presented in this paper implemented technical availability, i.e. term Coefficient of technical utilization of machine. This coefficient is a variation of preparedness. Coefficient of technical utilization of machine is calculated as given in Eq. 3.

$$k_T = \frac{\sum_{i=1}^{i=n} t_{ri}}{\sum_{i=1}^{i=n} t_{ri} + \sum_{i=1}^{i=n} t_{oi} + \sum_{i=1}^{i=m} \theta_i} \tag{3}$$

where:

- k_T – coefficient of technical utilization;
- t_r – time in operation (at annual level),
- t_o – time in failure (non-planned stoppages at annual level - repairs),
- θ – time of planned stoppages caused by maintenance (preventive maintenance – services).

Availability, as preparedness, represents probability that system/machine will be capable to respond at any given moment and to perform its function. Difference between availability and preparedness is that availability function includes possibility that system/machine is in the storage facility. All the mentioned terms, reliability, preparedness and availability are of stochastic nature. In this case availability is in direct correlation to the scale of machine utilization, in technical aspect. Availability of auxiliary machines does not necessarily imply that machine is in operation or it is capable to operate.

Accurate indicators on coefficient of technical availability of all types of dozers are obtained based on relevant data, median range and least square method. It should be mentioned that the least square method is one of the most important method for processing experimental data, which involves components of numerical mathematics and statistics. This method is used to acquire functional relationship of experimental data arrays. Procedure for establishing annual trend of coefficient of technical availability in first 10 years is described in example of technical availability of CAT D8R dozers. Required data are given in Table 3.

Table 3. Achieved moto hours, planned and non-planned stoppages of dozers CAT D8R at RB Kolubara

	Int. mark	Y1	Y2	Y3	Y4	Y5	Y6	Y7	Y8	Y9	Y10
Achieved moto hours	C1	506	2799	2672	811	876	240	1196	702	1896	3429
Planned stoppages		24	80	96	95	64	16	68	22	54	198
Non-planned stoppages		0	0	184	224	196	0	140	956	394	160
Achieved moto hours	C2	898	1488	1592	970	2197	1968	1415	2352	915	2216
Planned stoppages		48	48	56	40	120	94	98	123	70	126
Non-planned stoppages		0	0	192	360	120	136	230	182	16	1096
Achieved moto hours	C3	1229	2258	4169	4811	3418	4827	3735	152	3343	
Planned stoppages		32	72	232	310	232	302	172		116	
Non-planned stoppages		0	0	272	104	518	218	174		666	
Achieved moto hours	C4	1045	2561	2883	4054	4960	3743	1438	3412	2124	2066
Planned stoppages		24	82	186	244	322	196	48	228	58	132
Non-planned stoppages		16	0	280	128	138	282	26	200	284	712
Achieved moto hours	C5	1183	2329	2862	3924	4747	4151	2266	2956	4144	3535
Planned stoppages		32	64	150	244	342	270	126	140	202	140
Non-planned stoppages		0	56	76	56	136	252	180	266	489	898
Achieved moto hours	C6	236	2972	5038	3218	2476	4441	1910	1673		
Planned stoppages		8	114	226	230	138	226	88	96		
Non-planned stoppages		0	4	52	128	136	180	122	264		
Achieved moto hours	C7	236	2128	3459	1732	3560	2382	4000	3507	4113	
Planned stoppages		8	64	114	106	202	114	224	184	148	
Non-planned stoppages		0	50	56	18	250	140	134	454	1004	
Achieved moto hours	C8	164	1813	1939	4458	4319	4335	1080	4315	4258,8	
Planned stoppages		0	72	76	208	204	188	52	184	208	
Non-planned stoppages		0	0	8	188	242	326	468	144	538	

Achieved moto hours	C9	169	1542	2694	3214	3681	3590	2766	2683	5015	
Planned stoppages		0	48	108	140	140	120	94	532	296	
Non-planned stoppages		0	0	16	40	220	92	330	484	272	
Achieved moto hours	C10	606	3056	4595	4621	5492	4313				
Planned stoppages		16	48	164	208	182	164				
Non-planned stoppages		8	48	72	190	184	88				
Achieved moto hours	C11	383	3845	676	3476	4832	5275				
Planned stoppages		8	80	16	124	190	238				
Non-planned stoppages		0	44	16	152	424	310				

Achieved moto hours	C12	650	5047	2677	2952	4893	3933				
Planned stoppages		16	138	102	176	200	262				
Non-planned stoppages		0	92	234	426	330	530				
Achieved moto hours	C13	286	1733	3296	3947	4881	4409				
Planned stoppages		0	40	104	226	228	170				
Non-planned stoppages		0	20	118	192	478	220				
Achieved moto hours	C14	1988	3174	2561							
Planned stoppages		52	100	100							
Non-planned stoppages		0	32	102							
Achieved moto hours	C15	996	2828	4189							
Planned stoppages		34	88	216							
Non-planned stoppages		0	94	192							
Achieved moto hours	C16	2072	4772								
Planned stoppages		40	250								
Non-planned stoppages		58	52								
Achieved moto hours	C17	2761	5006								
Planned stoppages		28	166								
Non-planned stoppages		0	0								

Coefficient of technical availability provides descending sequence of this coefficient, from minimal to maximal value, for dozers with similar performances (from C3 to C17). These values are given in Table 4.

Table 4. Coefficient of technical availability for dozers CAT D8R in Kolubara basin

Year 1	Year 2	Year 3	Year 4	Year 5	Year 6	Year 7	Year 8	Year 9	Year 10
0.954839	0.939535	0.860854	0.830613	0.820058	0.832381	0.675	0.725331	0.781197	0.7099656
0.961905	0.940481	0.888483	0.899888	0.873635	0.8867567	0.867085	0.822922	0.810424	0.7730155
0.963134	0.949153	0.892146	0.904238	0.887257	0.8882945	0.881026	0.84608	0.850943	
0.96699	0.951	0.911246	0.915951	0.887338	0.8939988	0.900943	0.879239	0.857084	
0.967213	0.956415	0.926813	0.918418	0.900364	0.9027492	0.915217	0.888542	0.861314	
0.967213	0.960073	0.926891	0.920701	0.902268	0.9036419	0.917852	0.929356	0.898263	
0.973663	0.961804	0.936896	0.920766	0.906401	0.9058904	0.951058	1		
0.97451	0.961812	0.947705	0.926439	0.908517	0.9162368				
0.974623	0.966537	0.951149	0.928977	0.910913	0.9187331				
0.975976	0.967904	0.953155	0.93319	0.915129	0.9442399				
0.97954	0.968758	0.954802	0.946965	0.937521	0.9447974				
0.989961	0.968975	0.955997							
1	0.969099	0.958478							
1	0.969543								
1	0.969811								

This data is used to calculate parameters for establishment real and mathematical distribution of technical availability by medial rank Q and least square method. These are given in Table 5 and Table 6 for first year of operation.

Table 5

	Ktr	Q	lnt	$lnln$
1	0.954839	4.545	-0.04621	-3.06787
2	0.961905	11.039	-0.03884	-2.14582
3	0.963134	17.532	-0.03756	-1.64628
4	0.96699	24.026	-0.03357	-1.29179
5	0.967213	30.519	-0.03334	-1.01026
6	0.967213	37.013	-0.03334	-0.77167
7	0.973663	43.506	-0.02669	-0.56029
8	0.97451	50.000	-0.02582	-0.36651

Table 6

	x	y	x^2	xy
1	-0.04621	-3.06787	0.002136	0.141775
2	-0.03884	-2.14582	0.001509	0.083343
3	-0.03756	-1.64628	0.001411	0.061839
4	-0.03357	-1.29179	0.001127	0.043361
5	-0.03334	-1.01026	0.001111	0.033679
6	-0.03334	-0.77167	0.001111	0.025725
7	-0.02669	-0.56029	0.000712	0.014954
8	-0.02582	-0.36651	0.000667	0.009464

9	0.974623	56.494	-0.02570	-0.18361
10	0.975976	62.987	-0.02432	-0.00612
11	0.97954	69.481	-0.02067	0.17126
12	0.989961	75.974	-0.01009	0.35490
13	1	82.468	0.00000	0.55453
14	1	88.961	0.00000	0.79016
15	1	95.455	0.00000	1.12851

9	-0.02570	-0.18361	0.000661	0.00472
10	-0.02432	-0.00612	0.000591	0.000149
11	-0.02067	0.17126	0.000427	-0.00354
12	-0.01009	0.35490	0.000102	-0.00358
13	0.00000	0.55453	0	0
14	0.00000	0.79016	0	0
15	0.00000	1.12851	0	0
Σ	-0.35615	-8.05087	0.01156	0.41189

Least square method (Eq. 4):

$$a\Sigma x^2 + b\Sigma x = \Sigma xy \tag{4}$$

$$a\Sigma x + nb = \Sigma y$$

$$0,01156a - 0,35615b = 0,41189$$

$$- 0,35615a + 15b = -8,05087$$

$$\Rightarrow a = 71,00748 ; b = 1,149234$$

$$y = 71,00748x + 1,149234$$

$$\beta = 71,00748$$

$$b = -\beta \ln \eta \Rightarrow \eta = 0,983946$$

Real distribution of technical availability of bulldozer CAT D8R in Kolubara basin, for first year of operation, is given in Table 7.

Table 7.Real distribution

K	f(t)	K	f(t)	K	f(t)
0.954839	1.04581E-29	0.967213	1.05467E-29	0.97954	1.05151E-29
0.961905	1.05235E-29	0.973663	1.05449E-29	0.989961	1.03981E-29
0.963134	1.05309E-29	0.97451	1.05423E-29	1	1.02114E-29
0.96699	1.05461E-29	0.974623	1.05419E-29	1	1.02114E-29
0.967213	1.05467E-29	0.975976	1.05364E-29	1	1.02114E-29

Mathematical distribution of technical availability of bulldozer CAT D8R in Kolubara basin, for first year of operation, is given in Table 8. Information given in this table is used to create diagram presented on Figure 8.

Table 8. Mathematical distribution

K	f(t)	K	f(t)	K	f(t)
0.96	1.05098E-29	0.966	1.05433E-29	0.972	1.05485E-29
0.961	1.05173E-29	0.967	1.05462E-29	0.973	1.05466E-29
0.962	1.05241E-29	0.968	1.05482E-29	0.974	1.05439E-29
0.963	1.05301E-29	0.969	1.05494E-29	0.975	1.05405E-29
0.964	1.05353E-29	0.97	1.05499E-29	0.976	1.05363E-29
0.965	1.05397E-29	0.971	1.05496E-29		

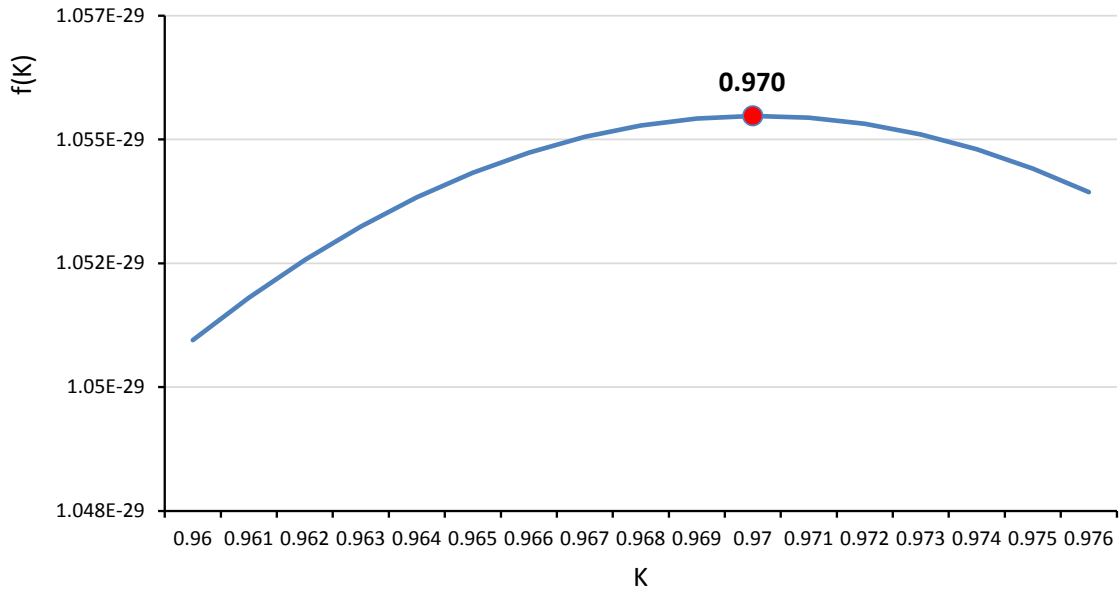


Figure 8. Coefficient of technical availability of bulldozer CAT D8R in Kolubara basin for 1st year of operation

Described procedure was performed for all ten years. Decreasing trend of technical availability coefficient for dozers CAT D8R in Kolubara basin for ten years of operation, only relating to dozers of similar performances (internal marks C3 to C17) is presented on Figure 9.

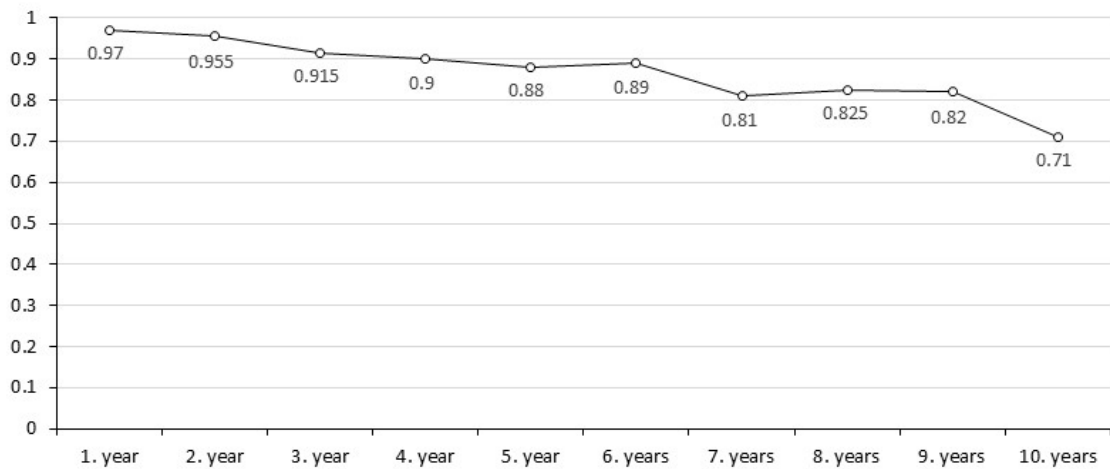


Figure 9. Declining trend of technical availability coefficient of bulldozer CAT D8R in Kolubara basin during first ten years of operation

This diagram (Figure 9) is used for further analysis related to optimal replacement time.

Lower limit of availability for dozer replacement is 0.80. This is limit value for linear correlation of time categories – time in operation, time of planned and non-planned stoppages. If the availability is lower than this value, then there should be more of the machines in the fleet of the open cast mine, thus increasing the costs. On the other hand, insufficient number of machines (dozers) will result in reduced execution of auxiliary operations, with influence on efficiency of continuous systems. Below is an example with CAT D8R and Shangai PD320Y-1. Optimal replacement time is established, based on diagrams of availability of these dozers (declining trend of technical availability coefficient of bulldozers in Kolubara basin for first ten years of operation) and limiting availability of 0.80. This diagram is shown on Figure 8 [1].

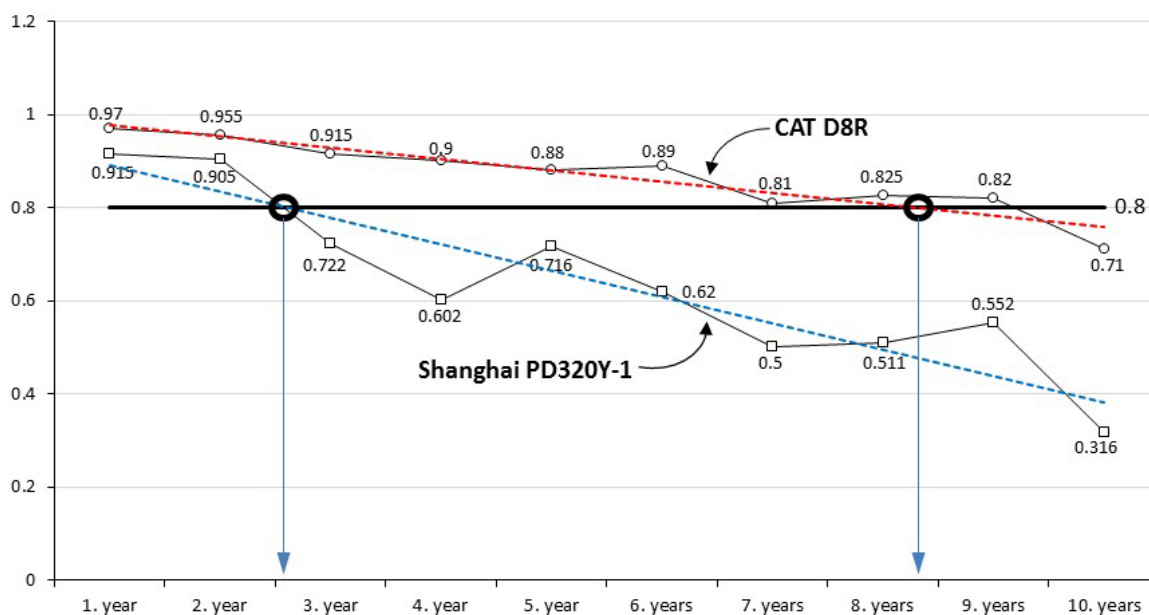


Figure 8. Optimal replacement of dozers CAT D8R and Shanghai PD320Y-1 according to availability

Therefore, CAT D8R dozer, in conditions of Kolubara open pit mines, should be planned for replacement after 8th year of operation, while Shanghai PD320Y-1 dozer after 3rd year of operation. Same procedure was applied to remaining types of dozers operating at open pit mines of Kolubara, and the results are given in Table 9 [1].

Table 9. Year of operation when the availability is reduced to 80%

	D8R	PR752&PR754	TD25M	TD25H	TD25E	TD25G	PD320Y-1	TD40
Optimal year for replacement	1 st year	1 st year	1 st year	1 st year	1 st year	1 st year	1 st year	1 st year
	2 nd year	2 nd year	2 nd year	2 nd year	2 nd year	2 nd year	2 nd year	2 nd year
	3 rd year	3 rd year	3 rd year	3 rd year	3 rd year	3 rd year	3 rd year	3 rd year
	4 th year	4 th year	4 th year	4 th year	4 th year	4 th year	4 th year	4 th year
	5 th year	5 th year	5 th year	5 th year	5 th year	5 th year	5 th year	5 th year
	6 th year	6 th year	6 th year	6 th year	6 th year	6 th year	6 th year	6 th year
	7 th year	7 th year	7 th year	7 th year	7 th year	7 th year	7 th year	7 th year
	8 th year	8 th year	8 th year	8 th year	8 th year	8 th year	8 th year	8 th year
	9 th year	9 th year	9 th year	9 th year	9 th year	9 th year	9 th year	9 th year
	10 th year	10 th year	10 th year	10 th year	10 th year	10 th year	10 th year	10 th year

4. CONCLUSION

Analysis showed that profit life (economical life) of dozer CAT D8R operating on open pit mines of EPS is around 7 years, while optimal operating time from the aspect of availability is 8 years. Considering other types of bulldozers operating on open pit mines of EPS (TD25M, TD25H, Liebherr 752 and 754, PD320Y-1, SD32W) operational life is around 8 years, excluding model TD 25 M, which exceeded the costs of 70 €/mh during 3rd year of operation [1].

Regarding availability, dozer CAT D8R reaches 80% on 8th year, while availability of remaining dozers is reduced to this value between 3rd and 5th year.

Fact that open pit mines are having sufficient number auxiliary machines (namely dozers) should be included into determination of their life cycle. These machines will complete all planned

tasks and create optimal conditions for operation of main mining machines (bucket wheel excavators, belt conveyors and stackers). It also should be noted that one hour of bucket wheel excavator – belt conveyor – stacker system operation is valued at several thousands of euros, and that value on one hour of dozer operation is below 100 €. Hence, it is more important that open pit mine has sufficient number of available dozers [1, 4].

Therefore, benefits emerging from this attitude on auxiliary machines selection, including savings and improvements, can be achieved by these activities:

- In-time replacement of auxiliary machines and vehicles:
 - Replace all machines with availability lesser than 0.8 and monitor declining trend of availability in order to properly plan the replacement;
 - Replace all the machines with increased operational costs (higher than those accepted by internal pricing or leasing) and in this case monitor increasing trend of costs to properly plan the replacement;
 - Replace all machines with long operational life and high operational costs, which are obsolete (difficult acquisition of spare parts and services);
- Usage of proven and quality machines with implemented unification as much as possible:
 - Implement unification to the fleet as much as possible, avoiding monopoly of the supplier of the equipment;
 - Use the machine with proven record and best results concerning their technical and operational specifications regarding availability, average working time and operational costs;
- Improvement of maintenance system:
 - Replace the machine using "old for new" in accordance to availability;
 - Implement aggregate replacement of the machine's components, with benefits in availability, longer life and guarantees for performed repairs;
 - Introduce "Quick Serve" for shorter services and better availability of the machine;
 - Optimize maintenance and operation procedures in terms of costs and machine safety;
- Implement modern and improved technologies in machine operation:
 - Using GPRS for machine monitoring in order to eliminate long transport of the machine and associated costs for tracks replacement.

Execution of these activities or just part of them will reduce the operational and maintenance costs, increase the volume of auxiliary works and create conditions for maximal utilization of Excavator – Conveyor – Stacker and Excavator – Conveyor – Crusher systems. In another words, these activities will increase time utilization and production rate utilization coefficients, at reduced costs.

REFERENCES

- [1] Optimizing organization, resources and costs of auxiliary mechanization to increase utilization of overburden and coal systems on open pit mines of EPS (in Serbian) (2018) Study, Faculty of Mining and Geology, Belgrade
- [2] Jovančić, P. (2014) Maintenance of mining machines (in Serbian), University of Belgrade – Faculty of Mining and Geology, Belgrade

[3] Gransberg, D.D. (2016) Major Equipment Life-cycle Cost Analysis, Principal Investigator Institute for Transportation Iowa State University

[4] Nurock, D., Porteous, C. (2008) Methodology to determine the optimal replacement age of mobile mining machines. Third International Platinum Conference 'Platinum in Transformation', The Southern African Institute of Mining and Metallurgy, 297-305

[5] Life Cycle Asset Management, Life Cycle Engineering, Inc., www.LCE.com

The Role of the Independent Expert in Material Handling and Mining Equipment Design and Approval

Przemysław Moczko, Damian Pietrusiak and Eugeniusz Rusiński

Department of Machine Design and Research
Faculty of Mechanical Engineering
Wrocław University of Science and Technology
Łukasiewicza 7, 50-370 Wrocław, POLAND

ABSTRACT

Design and delivery of material handling and mining equipment such as bucket wheel excavators, spreaders, reclaimers etc. is a complex process, which is prone to many faults made by designers and manufacturers.

Independent Expert institution is the recently common procedure of calling the external institution for the design crosscheck. Only recommended by standards, however very common, almost mandatory in all new industrial projects.

Described procedure is introduced in purpose to improve the quality of the entire deliverable of the project. Independent Expert responsibilities are design assessment, manufacturing control, erection control as well as performance tests supervision on the delivered structure. Described procedure increase the initial costs of the project, however limits the future investments and downtime of the machine. In case of the objects, which desirable durability time is of about 30 years, this brings savings difficult to estimate. In the paper, authors present their experiences gained as the Independent Expert during many projects completed in the field of material handling and mining equipment.

1. INTRODUCTION

The industry of mining, rock/minerals processing and continuous material handling characterizes with similar technique of the transportation system [1], [3]. That led to the similarity of machines and equipment which are used in all of the listed industry types. The most recognized are excavators (bucket wheel excavators), spreaders, stackers and stacker-reclaimers. There are also other commonly used machines such as ship loaders, chain scrappers and reclaimers, portal reclaimers, blending systems, mobile transfer conveyors, conveyor drive stations, transport crawlers and many more [2]. Also crushing systems such as semi mobile or mobile crushing stations are included in the same group of machines. All of peripheral machines and elements are usually connected with belt conveyors with different lengths from dozen of meters up to kilometres. In such a cases such system is called continues one. When instead of conveyors, large trucks and loading/discharging stations are used, then we call it intermittent transport system.



Figure 58. Bucket wheel excavator, stacker-reclaimer

Operational conditions are harsh, plenty of unexpected events and the machines, due to the high costs of erection, are expected to operate for decades [4],[5]. Combination of those facts, rises standard design challenge, to really complex projects. As a help, one can find standards and recommendations which were developed in decades. However, user without big experience may face with the problem which recommendation use and how to apply knowledge stated in the document. Moreover, the standards and recommendation development is always a step behind the actual market need. Most recently developed topic is the residual life estimation and operational time extension [8].

To assure that all necessary requirements will be fulfilled, Independent Expert audit becomes almost standards procedure in last years. However, it is worth to underline, that Expert very often is supporting the design process, playing not only checkout role but also a consultant help.

2. DESIGN STANDARDS, REGULATIONS, REQUIREMENTS

2.1. Leading documents

As mentioned in the first section, the described group of machines is exposed to multi-component loads, often of stochastic character, overloads which are not singular events [6],[7], [9]. Material handling and stacking/reclaiming machines and equipment are in favour position on comparison to the excavators which operates in the worst conditions.

That resulted in development of design recommendations dedicated to specific group of machines preferred in specific geographical areas. The most commonly used in the field of surface mining machines design is the German Standard DIN 22261 [10]. The next widely applied all around the world is the ISO 5049.1 [12] standard. However, this one is dedicated to materials handling machines and equipment. The third standard joins both areas and is suitable for mining and material handling machines and equipment design. It is the Australian standard AS 4324.1 [11]. There are also other applicable specialised standards but not as popular as the mentioned above [13][14]. There is also more general and popular EUROCODE 3 standard available[15].

Nevertheless, those three mentioned standards has a lot in common, especially when comparing the “main loads” load cases group. When going into details in the following groups of “main additional loads” as well “main additional and special loads” or “main additional and extraordinary loads” one will find more and more differences. Those differences can be found in some general assumptions i.e. in safety factor as well as well as in definition of very specific, extraordinary combination of loads. In general it can be stated that that the most comprehensive standard for material handling and also opencast mining machines is AS 4324 standard. DIN 22261 is considered as well detailed and safe standard for opencast mining machines. ISO 5049 standard provides enough

guidelines for experienced designers only. The very detailed comparison of the mentioned standards is presented in the article [27].

The important thing is the fact that AS standard recommends the design checkout to be done by external Independent Expert. Despite the fact that other standards do not states this recommendation, most modern design are proven by the Independent Expert anyway.

2.2. Independent Expert – design validation process

The scope of service of the Independent Expert in the design and approval process is not clearly defined by standards. As already mentioned AS standard recommends design checkout but does not define the scope. Therefore the role of Independent Expert may vary, depending on Purchaser requirements, experience or IE recommendations.

The complete scope of IE's service in material handling and mining equipment delivery is presented below. There are few steps in which the IE plays important role:

- a) Tender specification – at this stage it is necessary to clearly define technological conditions and requirements, which must be fulfilled by the new equipment. Based on that, detailed technological and technical conditions are defined, that enable to form tender documents. Independent Expert ma support and advice Purchaser at this stage to ensure the most optimal equipment choice and further delivery.
- b) Design of the equipment – Supplier of the equipment is responsible to design it in accordance to applicable standards to assure its safe and proper operation. The role of IE at this stage is to ensure, that design is made in accordance to technical conditions and that the applicable standards requirements are met as well. Therefore IE performs detailed checks of Purchaser design in the following steps:
 - Analysis and approval of supplier's load assumptions and preliminary stability calculations as well as GA or draft drawings with respect to applicable standards.
 - Check and verification of structural calculations. Special attention is paid to confirm if reasonable modelling of structures is applied, completeness and correct implementation of loading cases required by the specification is considered and if the fatigue resistant design is properly made. Supplier is requested to provide complete set of calculations, which enables IE to check the entire structural calculations of each component of machine. There are standards (eg. DIN 22261) in which such requirement is clearly defined.
 - IE's check calculations – as an optional and recommended by authors of this paper action is independent analysis of structural calculations in the area of static, dynamic and fatigue strength with the use of Finite Element Method (FEM), based on the shell model preferably. Such independent check usually consists of structural calculations for the most unfavourable loads combinations, which should provide confirmation that Supplier calculations are properly made.
 - The machine stability analysis for all load combinations (proof of machine stability for assumed loads) – this is very important step of check, that ensures safety of machine against overturning. IE checks stability calculations correctness in respect to standards requirements and considered dead and live loads and tipping axes as well.
 - Review of structural drawings – this activity ensures that proper manufacturing technology will be used for the equipment (welds types, dimensioning etc.) and also enables to identify poor design areas. Review of structural drawing shall be carried out with consideration of structural calculations results to pay special attention to highly stressed or responsible areas review.

- Providing by Independent Expert the certificate regarding the structural calculation and stability, based on the submitted documentation. This certificate confirms that no objections exist against commencement of erection.
- c) Fabrication and erection process – Independent Expert conducts periodical inspections to ensure that fabrication and erection process is made in accordance to design.
- d) Weighing and balancing of the equipment – if the equipment requires weighing and balancing, the IE supervise this stage of project too. A review of instructions for weighing and ballasting measurement for the equipment shall be carried out and approved by IE. After that the IE assists on site the Supplier during the weighing and ballasting measurements and checks/approves measurement results.
- e) Commissioning and performance tests – IE may be involved in the final commissioning stage of the project connected with performance tests. There are two types of tests usually scheduled: short and long one, where the short one refers to few hours up to few days, while the long one may last 1 or more months.
- f) Final certification – based on the entire review and process, IE provide the final certificate for operation, confirming that all project goals have been achieved and the equipment can be safely operated.

The above scope of work covers the most typical consultancy role of Independent Expert in the complete design and delivery process of material handling and mining equipment. This is long lasting process of check and approval, due to amount of work required and also due to long delivery time of such specialising equipment, which may last up to 36 months for more complex machines. Sometimes this scope may be limited or modified with the reference of individual project type or Purchaser wish and IE may be involved in design, manufacturing or final check.

3. MOST COMMON/FREQUENT FAULTS

Every step of check and approval process, which is listed above, involves various types of faults with different importance. Below there are typical of them listed for design and manufacturing stages. Examples of faults are given as well. The information presented below base on authors of this paper experience gathered during IE's projects completed for the last 20 years. More than 60 different mining and material handling machines were covered by such service.

3.1. Design faults

There are three following major types of faults, which occur at this stage of project.

- a) The first one reeferes to loads assumption, where not all loads are considered or loads are not properly calculated e.g: underestimation of material loads on conveyors and in transfer points, neglecting dynamic factor in material load calculations. It is also common issue that dead loads weights and locations are not precisely defined at the early stage of project.
- b) The second type of designing faults refers to strength calculations. As a standard the finite element method (FEM) is used for such purpose. However it is still common practice to conduct design calculation with the use of beam modelling approach, which is not detailed enough in the welded structures especially. The use of beam modelling limits significantly efficiency of such calculations in finding highly stressed locally limited areas, which are usually present in structural joints where beam modelling approach is limited in consideration of such geometry details (shape of gusset plates, radius details etc.). Independent Expert recommends to use plate modelling approach, which enables to consider most of such "hot spot" locations (see figure 2 as example). In case of checking of Supplier's structural calculations made with the beam modelling approach, the IE usually performs his own check calculations with the use of plate modelling approach. There were many cases in authors of

this paper IE’s experience, that significant “hot spots” were identified with the use of the plate approach, while beam mode didn’t show any issues [25].

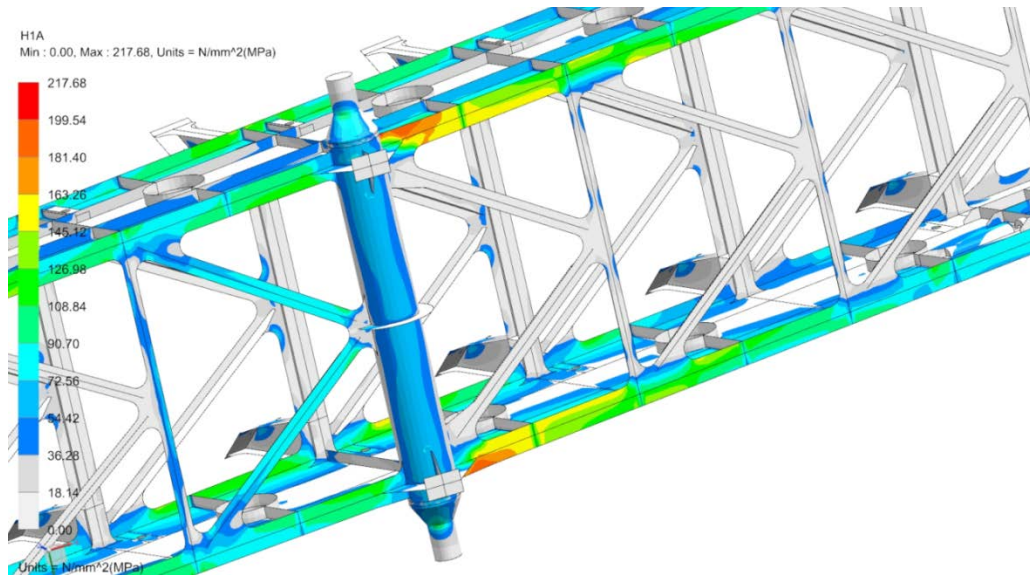


Figure 59. Example of “hot spot” identification with the use of shell modelling approach in the receiving boom structure

c) The third type of designing faults refers to acceptance of high, above permissible values stress, if the “hot spot” area is relatively small [16], [17]. Special attention must be paid when such case occurs[18]. Always both strength and fatigue assessment must be checked to assess if modification is required [24], [26]. In general, when low fatigue stress is observed in the area concerned, it is possible to accept static overstress. However no fatigue “hot spots” can be accepted if the stress amount exceeds permissible value. This fault is the reason of many cracks, which are observed during operations of mining and material handling equipment, which operates in heavy conditions, causing significant stress fluctuations in the structure [19]. Most of excavators (bucket and chain type) are examples of such machines. Also reclaimers or crushers may suffer significant dynamic loads if used for hard material reclaiming. In addition, crawler mounted machines indicate quite significant stress changes during movement (transport), on the contrary of rail mounted machines [22], [23]. Example of identified with the use of FEM calculations, small fatigue “hot spot”, which led to crack in the load carrying structure of semi mobile crusher, is presented in figure below.

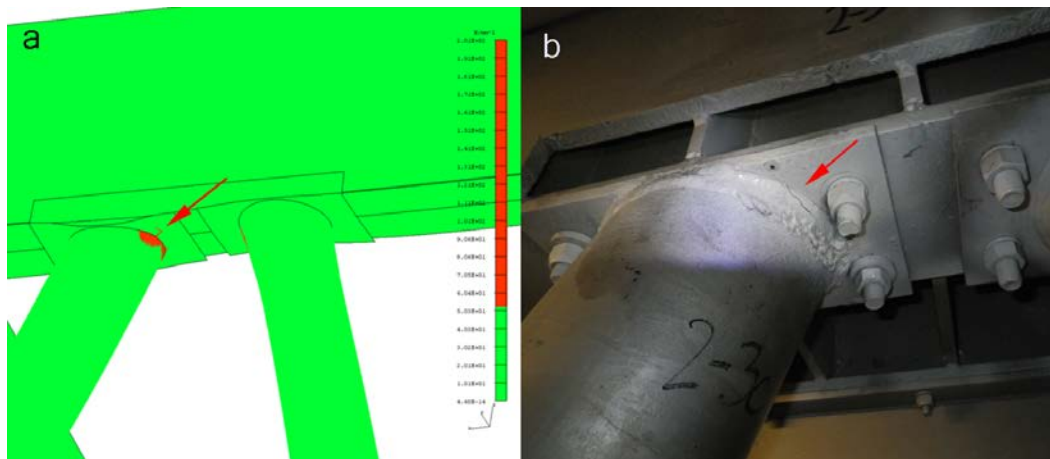


Figure 3. Improper DBS0 weld execution before a. and after b. rectification

3.2. Fabrication and erection faults

The most common types of faults, which occur at this stage of project are as follows:

- a) Execution of welded connections not as per design is frequently observed in the load carrying structures of material handling and mining equipment. Since welding quality plays very important role in fatigue resistance, this kind of fault has a great importance in structural safety of machines. When higher than typical welding class is required, many faults occur usually. Example of such case is presented in figure 3, where DBS0 butt weld shall be executed as flat grinded, notch free one.

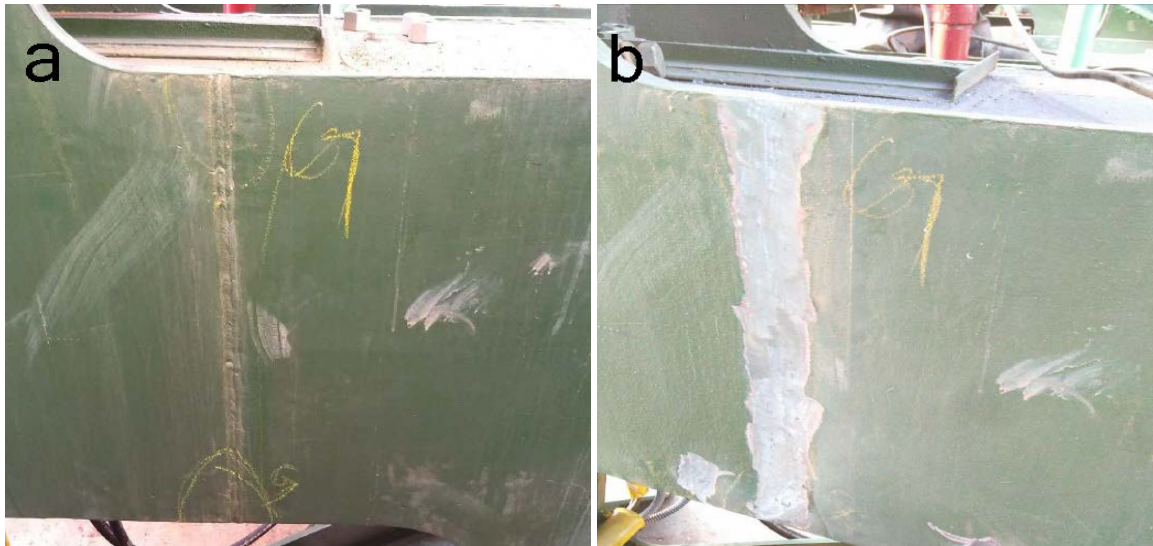


Figure 4. Improper DBS0 weld execution before a. and after b. rectification

- b) Geometry faults, missing elements faults. Misalignments, deviations from designed geometry are also common and frequently observed faults, which create stress peaks areas prone to fatigue cracks if stress fluctuations are present. Example of such faults are shown in figures below. It is the role of the Independent Expert to check the tested equipment for such problems and request rectification works. Such check usually requires many hours of investigations. However if IE has a detailed structural calculations, the check will be limited to highly stressed areas and these which have an impact on structural safety of the equipment. Therefore it is recommended to use plate or solid based structural calculations for such purpose instead of beam based calculations.



Figure 5. Geometry faults observed during inspections



Figure 6. Geometry faults observed during inspections

4. CONCLUSION

The role of the Independent Expert in material handling and mining equipment design and approval has the great importance and reflects the entire operational life of tested machine. Elimination of faults at the designing and manufacturing stage improves safety of operation. It also impacts operational costs since failures number can be reduced by IE's preventive actions [20]. Costs of repairs and down times of core equipment can be huge, however they can be reduced if faults are identified and corrected at the designing/manufacturing stage [21].

What is worth to mention that the scope of Independent Expert service in the design and approval process is not clearly defined by standards. In the paper authors presented recommendation for complete scope of work, which can be used for typical check of complex mining or material handling equipment. By completing of such scope, Independent Expert has the right to provide certificate confirming correctness of design and manufacturing of the equipment. In case of bigger deliveries of mining or material handling equipment it is common practice, that such certificate is requested by Purchaser to accept machines for operation.

As per authors experience, which is confirmed by completed more than 60 complex equipment check and approval projects, it can be concluded that there are always faults present at both design and manufacturing stages. If they are found and corrected early enough, problems during further operation are usually reduced significantly.

In authors of this paper opinion, legal regulations should be introduced to ensure check and verification of complex mining and material handling equipment by and Independent Expert.

REFERENCES

- [1] Kasztelewicz Z. (2012) *Koparki wielonaczyniowe i zwałowarki taśmowe*. Technologia pracy. ART-TEKST Publishing House.
- [2] Zamiralowa E., Lodewijks G. Shape Stability of Pipe Belt Conveyors: From Throughability to Pipe-Ability, *FME Transactions* (2016) 44, 263-271.
- [3] Morgan, R. C. (2011) *Design of Materials Handling Machines to AS4324.1-1995*, Australasian Structural Engineering Conference, Perth 2012.

- [4] Bosnjak S M, Oguamanam D C D, Zrnic N D. The influence of constructive parameter on response of bucket wheel excavator superstructure. Archives of Civil and Mechanical Engineering 2015; 15: 977-985.
- [5] Bosnjak S M, Gnjatović N, The Influence of Geometric Configuration on Response of the Bucket Wheel Excavator Superstructure, FME Transactions (2016) 44, 313-323.
- [6] Brkić A Đ, Maneski T, Ignjatović D, Jovančić P, Spasojević Brkić V K. Diagnostics of bucket wheel excavator discharge boom dynamic performance and its reconstruction. Eksploatacja i Niezawodność – Maintenance and Reliability 2014; 16 (2): 188–197.
- [7] Rusinski E, Dragan S, Moczko P, Pietrusiak, D. Implementation of experimental method of determining modal characteristics of surface mining machinery in the modernization of the excavating unit. Archives of Civil and Mechanical Engineering, 2012; 12(4):, 471–476, [tps://doi.org/10.1016/j.acme.2012.07.002](https://doi.org/10.1016/j.acme.2012.07.002).
- [8] Rusinski E., Czmochowski J., Moczko, P., Pietrusiak, D., Surface mining machines : problems of maintenance and modernization. Cham : Springer, cop. 2017.
- [9] Pietrusiak D., Evaluation of large-scale load-carrying structures of machines with the application of the dynamic effects factor, Maintenance and reliability 2017; 19 (4): 542–551.
- [10] DIN 22261-2 Excavators, Stackers and Auxillary Equipment in Brown Coal Open Cut Mines Part 2 Calculation Principals, German Institute for Standardization, 2016.
- [11] AS4324.1: Mobile equipment for continuous handling of bulk materials Part 1 - General requirements for the design of steel structures, Standards Australia, 1995.
- [12] International Organization for Standardization, ISO5049.1: Mobile Equipment for the Continuous Handling of Bulk Materials Part 1 Rules for the Design of Steel Structures, 1994.
- [13] DNV GL, RP-203: Fatigue design of offshore steel structures, 2014.
- [14] Norsork Standard 004, Design of steel structures, 2004.
- [15] EN 1993-1-9 (2005) (English): Eurocode 3: Design of steel structures - Part 1-9: Fatigue
- [16] Hobbacher A.F., Recommendations for Fatigue Design of Welded Joints and Components, Springer International Publishing Switzerland 2016.
- [17] Niemi E; Fricke W, Maddox SJ, (2006). Fatigue Analysis of Welded Components - Designer's Guide to the Structural Hot-Spot Stress Approach, Woodhead Publ., Cambridge.
- [18] Arsić, M., Bošnjak, S., Zrnić, N., Sedmak, A., Gnjatović, N.: Bucket wheel failure caused by residual stresses in welded joints, Engineering Failure Analysis, Volume 18, Issue 2, March 2011, Pages 700–712.
- [19] Rusiński E., Moczko P., Pietrusiak D., Low frequency vibrations of the surface mining machines caused by operational loads and its impact on durability, Proceedings of ISMA2014 International Conference on Noise and Vibration Engineering : USD2014 International Conference on Uncertainty in Structural Dynamics, Leuven, 15 to 17 September, 2014 / eds. P. Sas, D. Moens,

H. Denayer. Haverlee : Katholieke Universitet Leuven. Department Werktuigkunde, [2014]. s. 683-694.

[20] Stamboliska Z., Rusiński E., Moczko P.: Proactive Condition Monitoring of Low-Speed Machines, Springer International Publishing Switzerland 2015. ISBN 978-3-319-10493-5, 2015.

[21] Pietrusiak D., Moczko P., Rusiński E., Recent achievements in investigations of dynamics of surface mining heavy machines, 24th World Mining Congress Proceedings , October 18-21, 2016, Rio de Janeiro, Brazil. Rio de Janeiro : IBRAM,. s. 295-308, 2016.

[22] Pietrusiak D., Moczko P., Rusiński E., World's largest movable mining machine vibration testing - numerical and experimental approach. Proceedings of ISMA2016 International Conference on Noise and Vibration Engineering, 19 to 21 September, 2016 / eds. P. Sas, D. Moens, A. van de Walle. Leuven : Katholieke Universitet Leuven, s. 2287-2299, 2016.

[23] Pietrusiak D., Smolnicki T., Stańco M. The influence of superstructure vibrations on operational loads in the undercarriage of bulk material handling machine, Archives of Civil and Mechanical Engineering. 2017, vol. 17, nr 4, s. 855-862.

[24] Rusiński Eugeniusz, Moczko Przemysław, Derlukiewicz Damian: Use of finite element method in designing and operation of basic machines of open-cast mining, Zbornik na Trudovi - Masinski Fakultet Skopje. 2004, G. 23, br. 2, s. 49-57.

[25] Rusiński Eugeniusz, Moczko Przemysław: Evaluation of durability of elements of load-bearing structures, Design and selection of bulk material handling equipment and systems: mining, mineral processing, port, plant and excavation engineering. Vol. 2 / ed. by Jayanta Bhattacharya. Kolkata : Wide Publishing, 2012. s. 285-306.

[26] Bosnjak S, Petkovic Z, Simonovic A, Zrnic N, Gnjatovic N. Designing-in failures and redesign of bucket wheel excavator undercarriage. Engineering Failure Analysis 2013; 35: 95–103.

[27] Moczko P., Pietrusiak D., Rusiński E, Material Handling and Mining Equipment - International Standards Recommendations for Design and Testing, FME Transactions (2018) 46, 291-298.

Development of a Real-Time Mine-Face Inspection System for the Early Detection of Hard Rock Formations during Mining by Bucket-Wheel Excavators

M. Galetakis¹, A. Vafidis¹, T. Michalakopoulos², G. Apostolopoulos², C. Roumpos³, F. Pavloudakis³, A. Vasileiou¹, V. Deligiorgis¹ and A. Soutana¹

¹Technical University of Crete, Greece,

²National Technical University of Athens, Greece,

³Public Power Corporation of Greece

ABSTRACT

The existence of hard rock formation with high cutting resistance, during mining with bucket wheel excavator (BWE), causes frequent stoppages, increased equipment wear, or even severe damage of the BWE. These result to increased idle and break-down time, to high energy consumption, to low production rate and finally to increased mining cost. A proactive solution that was examined during the research project BEWEXMIN included the development of a real-time mine face inspection system. The system uses geophysical sensors for the early detection of hard rock formations during the excavation by BWE. More specifically an Electromagnetic (EM) sensor was employed for continuously measuring the electrical resistivity of the material in the mine face. The resistivity data were processed and evaluated in real time by specially developed software to estimate the diggability of the excavated material ahead of the excavation face. At the same time the risk of collision, between excavating buckets and hard rock formation, was also estimated. When the BWE approaches hard inclusions, visual and audio alarms were generated by the system. The above system was tested and evaluated in South Field Mine. Results indicated that the developed system can succeed high percentage of true alarms keeping at the same time the percentage of false alarms low.

1. INTRODUCTION

The machinery predominantly used for overburden removal, as well as, for lignite and inter-bedded waste layers extraction in surface mining operations in Europe, is the Bucket Wheel Excavator (BWE). First BWEs constructed in Germany were mainly used for the removal of the overburden in the large surface lignite mines. Overburden in these mines consisted of geological formations with low cutting resistance. Thus, the experience gained from the mining of these types of overburden formed the knowledge basis for the design and construction of the bucket wheel excavators [1, 2].

The continuous surface mining was later adopted in several European mines where the geological and mining conditions (especially in overburden formations), were different from those encountered in German opencast coal mines. This fact and the necessity to extract coal from deep deposits have resulted in increased occurrence of formations with excessive cutting resistance or even non-diggable requiring blasting (Figure 1). These cases have been increased in many European surface lignite mines recently, while in the past such cases were relatively seldom [3, 4].



Figure 1. Typical hard rock formations (consolidated conglomerates) occurring during overburden removal in South Field mine in Ptolemais, Greece. (Left): Thin hard rock layers within clay beds which can be difficultly excavated by BWE. (Right): Thick hard rock formations requiring blasting and removal by shovels and dumpers (Provided by PPC).

The existence of hard rock formation with high cutting resistance results in stoppage, increased equipment wear, or even severe damage of the bucket wheel excavator (BWE), resulting to increased idle and break-down time, to high energy consumption, to low production rate and finally to increased mining cost. In the recently completed research project BEWEXMIN different solutions to reduce failure rates of bucket wheel excavators working in such conditions were proposed and evaluated. The examined solutions included:

- the adaptation of the already working BWEs to those conditions and the requirements for newly built,
- the development of a system of continuous surveillance of machinery superstructure effort, and
- the development of a real-time mine face inspection system, based on geophysical sensors for the early detection of hard rock formations during the excavation by BWE.

The ultimate scope of the real-time mine face inspection system, that was mounted on a BWE boom, was to continuously monitor the subsurface ahead of the excavation face and to provide in real-time a clearly comprehensible warning to the BWE operator when hard (non-diggable) formations are identified. To develop such a system first an extensive program of field tests was carried out to determine the most promising geophysical method in detecting the hard rock formations. Based on results of the field tests a system (hardware and software) was developed and installed on a BWE operating at South Field Mine at Ptolemais area (Western Macedonia, Greece). The developed system was capable to monitor in real time the diggability of the excavated material and to predict the risk of collision of the bucket wheel with the hard rock formations.

This paper summarizes the phases of the development of the real time monitoring system as well as the obtained results during the field tests. First we describe the field tests which were carried out in order to determine the most suitable geophysical method for detecting hard rock formations in real time. Then we present the developed real-time mine-face inspection system (hardware and software) for the early detection of hard rock formations. Finally, the application of this system for the on-line monitoring of the excavation process by BWE in South Field lignite mine in Ptolemais (Greece) is presented and the obtained results are discussed.

2. FIELD TESTS AND GEOPHYSICAL METHODS SELECTION

Geophysical methods have been initially evaluated through literature review in terms of their ability to detect geological formations of high cutting resistance and hard rock inclusions during the excavation by BWEs. An extensive literature review identified that in the typical geologic

environment of lignite mines the electrical or electromagnetic methods are the most promising in detecting local features such as boulders. The Slingram (EM) Electromagnetic Method, the Ground Penetrating Radar (GPR) and Electrical Tomography (ET) were selected as the most appropriate [5].

To assess the capability of these selected geophysical methods in different opencast lignite mines facing the problem of the hard rock formations, numerous field tests were conducted. These field tests were carried out at the South Field mine Kozani Greece (PPC), at the Szczercow Field, Belchatow mine, Poland (PGE) and at Husnicioara Field and Rociuta mines, Romania (OLTENIA). The most extensive and detailed field test program was carried out Power Public Corporation (PPC) coal mine (Figure 2). In addition, for the assessment of GPR several simulations were performed in 2D and 3D (Figure 3).

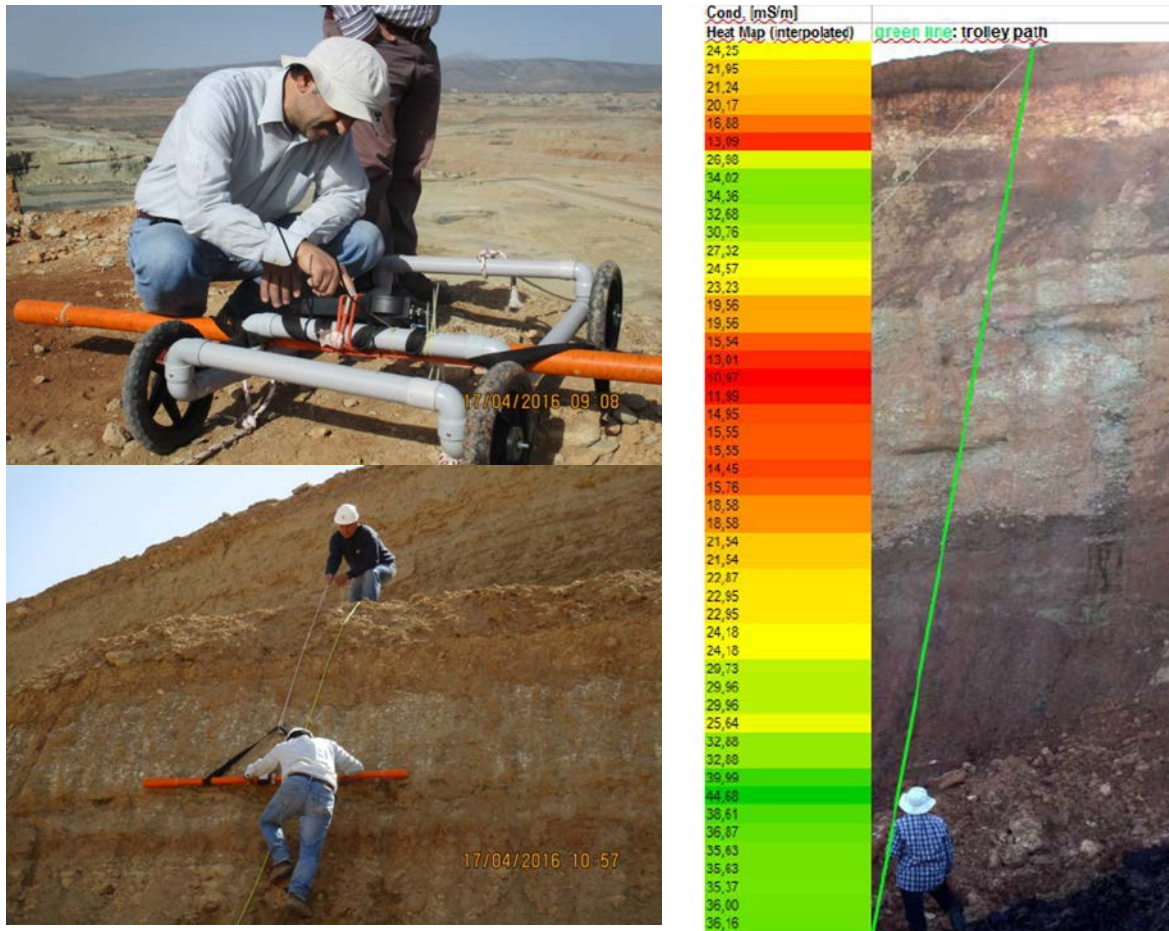


Figure 2. (Left) Electromagnetic (EM) equipment and measurements on the slope at South Field open pit mine. (Right) Apparent conductivity values deduced from the EM survey on the slope next to a photo of the mine front.

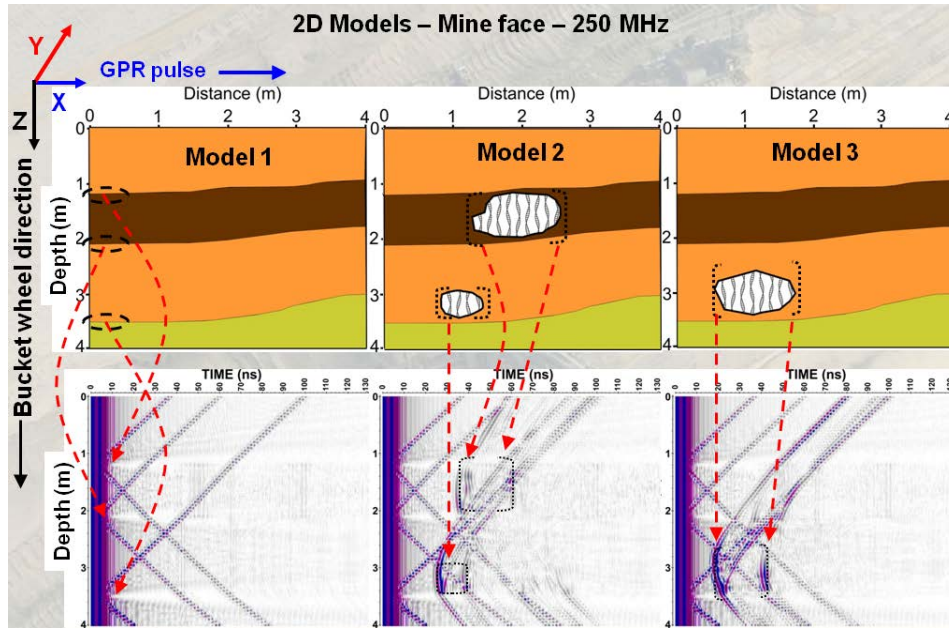


Figure 3. Radargrams from the simulations at the face mine using the GPR 250MHz antenna.

The selection of the most suitable geophysical method for the detection of hard formations via real-time mine face mapping was based on Analytic Hierarchy Process (AHP) multi-criteria decision method. The criteria used involved performance of the specific geophysical method in detecting boulders and hard layers, required geophysical and electronic equipment, data processing and evaluation, ability to work in harsh environment and ease of installation of the equipment on the boom of the bucket wheel excavator. The investigated geophysical methods were ranked according to AHP methodology and finally the Slingram (EM) was selected as the most promising method for real-time detection of hard rock during mining by BWE.

3. REAL-TIME MINE-FACE INSPECTION SYSTEM BASED ON GEOPHYSICAL METHODS

The developed system, as shown in Figure 4, consists of three subsystems. The first subsystem includes the measuring devices (EM sensor, differential GPS and CCD camera) installed on the bucket wheel and the boom of BWE.

The second subsystem is the EM control unit which collects, stores, transmits data and controls the operation of the EM sensor. GPS is connected and synchronized with EM sensor. Thus, the positioning and resistivity data from EM are transmitted simultaneously to control unit. The data, recorded in continuous mode at predefined sampling intervals (1s), were: time (UTC, coordinated Universal Time), coordinates (Latitude, Longitude, Altitude) and conductivity of the surveyed part of the mine face by the EM instrument.

The third subsystem is the developed software, installed on a fully rugged laptop hosted in the control cabin of the BWE, consisting of four modules. The first module receives data from EM control unit, performs the required pre-processing, and sends the corrected data to automated algorithm module. Automated algorithm module predicts the probability of occurrence of a hard rock formation at a specific position, and sends this information to expert system module. Expert system estimates the probability of collision (between excavating buckets and hard rock formation) and if necessary, generates alarms. The last module of the third subsystem is the visualization unit, which provides the machine operator with all required information as well as with real-time video for the visual inspection of the mine-face.

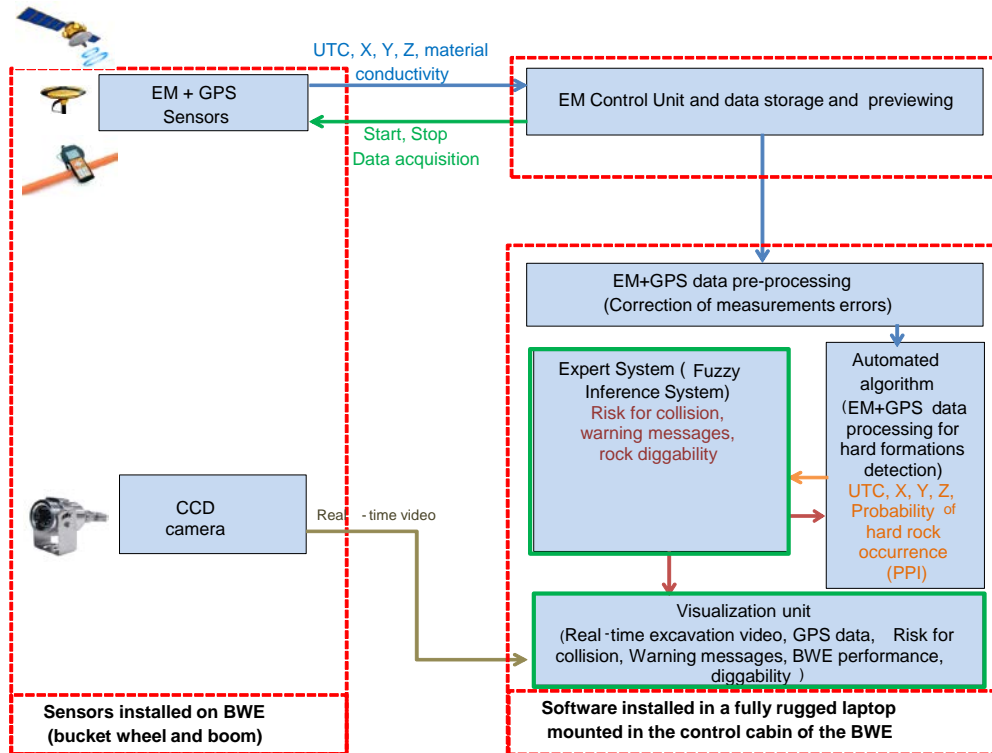


Figure 4. Overall system for real-time monitoring of the excavation process of the BWE.

Automated algorithm uses two different data-driven techniques. The first is called “simple mode” and is based on statistical process control. The second one called “advanced mode” is based on neural networks. Automated algorithm, either in simple or advanced mode, estimates the probability of occurrence of a hard rock formation based on the changes in resistivity values (Figure 5). Then a Fuzzy Inference System (FIS) estimates the risk of collision, between BWE and hard rock. More specifically, a Mamdani type FIS was created and trained [6]. The structural and operational characteristics of the used BWEs and the applied mining practices were used to modify the structure and the inference rules of the FIS and to maximize the exploitation of the existing factual and experiential knowledge about mining with BWEs. Moreover, we have also designed the graphical user-interface and the explanation-guidance facility (visualization unit) of the FIS in order to be comprehensible by the operator of the BWE.

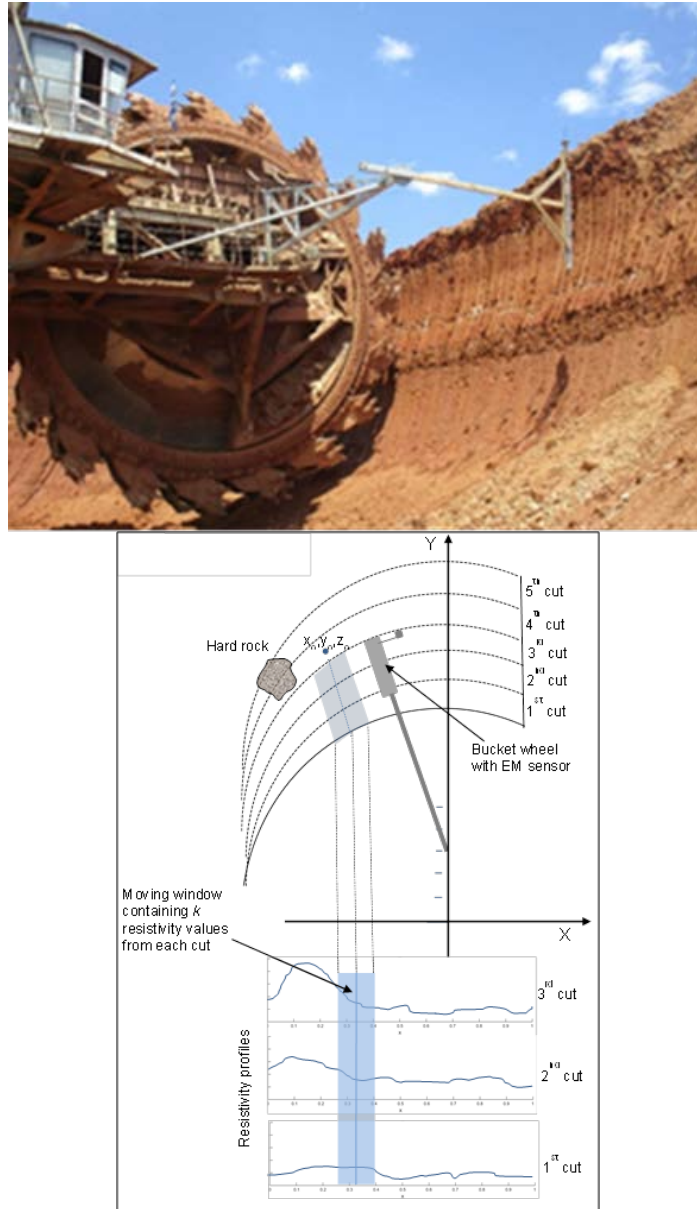


Figure 5. (Above) Mine face surveying during terrace cutting by a BWE equipped with the EM geophysical sensor. (Below) Schematic diagram showing successive resistivity profiles obtained during terrace cutting (3 cuts). Developed automated algorithm uses a moving window to examine local changes in resistivity profiles as bucket wheel approaches the hard rock.

The above developed software modules were integrated and transformed to a standalone application (HAROR, HARdROckReconnaisance) that was installed on a fully rugged laptop. The geophysical instrument (EM sensor, type CMD2) and the optical camera were connected to HAROR via the USB ports of the rugged computer. HAROR receives and records real time measurements from EM instrument and from a camera, processes-evaluates them and provides information in real time about the diggability of the excavated material, the probability of hard rock occurrence and the risk of collision. It also generates warning alarms for the BWE operator when risk of collision is increased.

As shown in Figure 6 HAROR main screen is divided into four panels. The first panel (top left) displays the excavation process as it is shown by the connected camera. The second panel (bottom left) provides information about the probability of hard rock occurrence, the effort of BWE (or the diggability of the excavated material) and the risk of collision (hitting a hard rock). These parameters are displayed in a five-level color scale in order to be easily observable by the operator. The third

panel (on the right) shows buttons which are controlling acquisition, storage and display (plot) of measurements and evaluated parameters during the excavation process. Typical generated plots of the measured resistivity, estimated probability of hard rock occurrence, BWE effort (or diggability) and risk for hard rock hitting are shown in Figure 7. The computational time (comp. time) in seconds is also shown to ensure that the required calculations can be executed in less than 1 second which is the selected sampling time. Higher computational time could result in delays of the real-time procedure. The same panel also includes the button for activation/deactivation of the audio alarm as well as the HAROR info button. The audio alarm is triggered when risk of collision exceeds a certain level. The fourth panel (bottom right) displays several useful information regarding, time location and the current measurements of the connected sensors. Depending on the mode of real-time operation (simple or advanced) this panel can also provide information regarding the BW position and the slewing speed of the boom.



Figure 6. HAROR main screen and menus during real time operation.

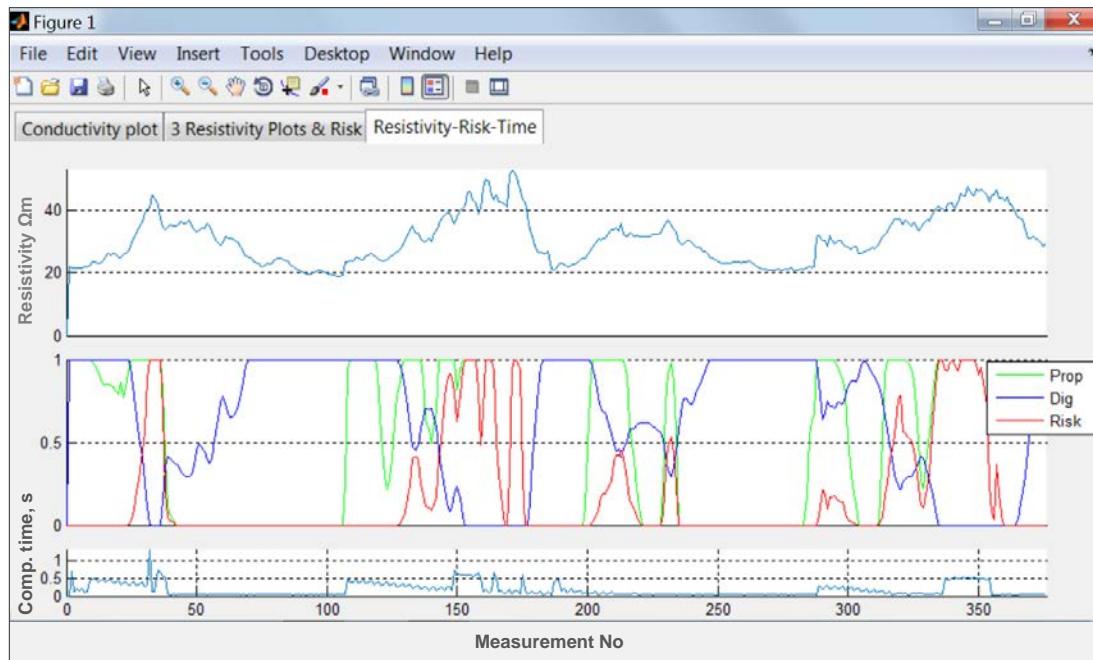


Figure 7. Available plots during HAROR operation.

4. FINAL TESTING AND EVALUATION

4.1. Final field test

The final test included the operation of BWE equipped with the real-time inspection system in the especially prepared site, where hard rocks were buried at certain distance in front of the working face. The BWE was excavating the material in successive slices by slewing operation (terrace cutting). The mean height of the excavated slices was 6m and the working width of the face was ~35m. Taking into account that the distance of the buried boulders from bench crest was 10m approximately, 35 successive slices were required to approach the boulders. The slewing speed of BWE boom was up to 20m/s. The last excavated slice was 0.5 m away from the location where the boulders were buried.

During the excavation, the distance of EM sensor from the mine face was increasing from 0.5m (at the starting point of the slewing operation) to 1.0m (at the end of the slewing operation). Several stoppages of the BWE occurred during this test. In addition to real time monitoring, the obtained data were also stored and sorted in accordance to excavated slices. More than 8000 measurements were sorted, coded and stored for later evaluation.

Figure 8 shows the bucket wheel trajectories, the angular location of the buried boulders, the slewing angles and the mine face at the beginning of the test. The thin layers within the reddish clay are hard or semi hard formations exhibiting relatively high resistivity. These hard formations, which due to their small thickness can be excavated by the BWE, were detected by the real time inspection system. However, by increasing the threshold limit of HAROR software (upper control limit of the used statistical process control) the generated unnecessary warning alarms were reduced significantly.



Figure 8. (Left) Trajectories of the BW, slewing angles and angular location of buried boulders at 50° from the advance direction axis. (Right) Mine face at the start of the field test. Within the reddish clay formation thin hard and semi hard layers are interbedded.

Figure 9 shows snapshots of the excavation and the gradual approach of the bucket wheel to the location where the boulders were buried. Figure 10 shows screenshots of the results obtained after processing and evaluation of the resistivity measurements by HAROR application. In the screen of the rugged laptop installed in the BWE operator’s cabin the probability of hard rock occurrence, the BWE effort (based on the diggability of the excavated material) and the risk of collision were displayed in real time. Moreover via the connected camera the excavated area was visually inspected.

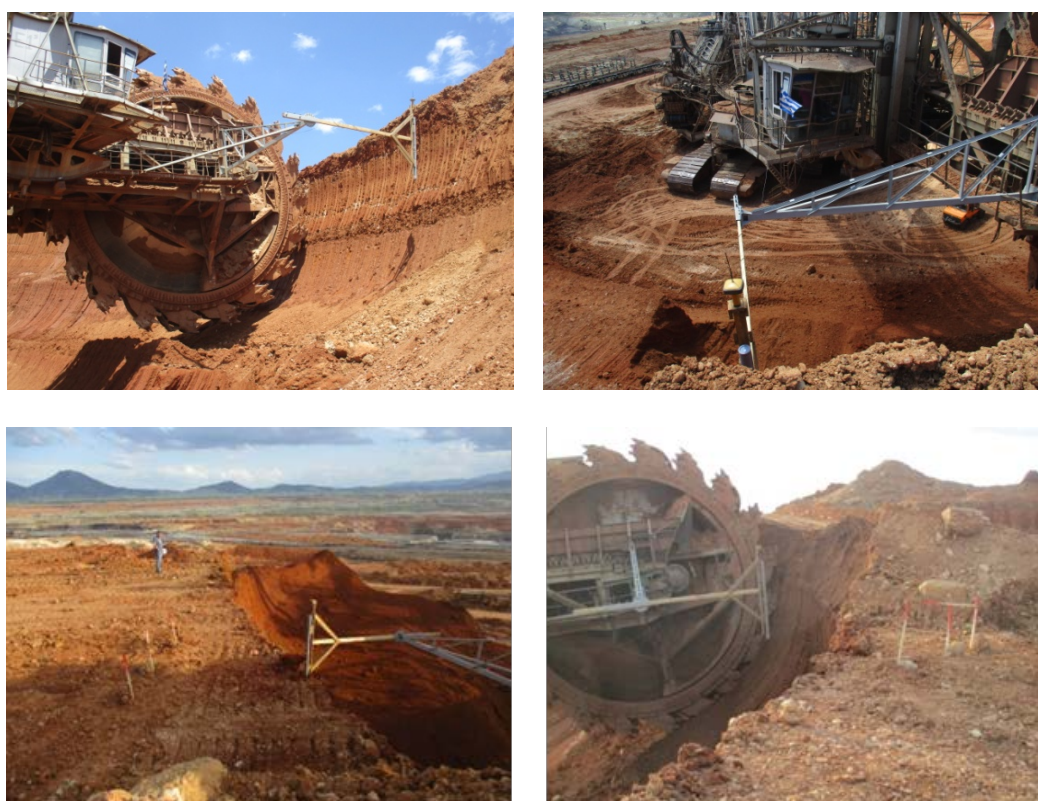


Figure 9. Snapshots of the excavation process during the field test. The location of the buried boulders is indicated by the wooden rods.



Figure 10. Visualization of the results of the real time inspection system on laptop screen in the operator cabin. In the left photo the camera was installed outside the cabin focusing on the excavation area. In the right photo camera was installed inside the cabin providing a more general view. In both photos the probability of hard rock occurrence, the BWE effort and the risk of collision are displayed using a five level color scale.

Figure 11 shows the resistivity data and the estimated parameters (probability of hard rock occurrence, diggability and the risk of collision) during the excavation of a slice. The trend in resistivity values, due to the slewing operation of the BWE, is clear. During slewing operation the cutting depth is changing progressively resulting to varying distance of EM instrument from the mine face. This affects the measurement of apparent resistivity since the air gap between the instrument and the mine face changes. As the slewing angle is increased the air gap also increases and the resistivity measurements indicate a growing trend. This change is systematic and its effect on resistivity measurements of the excavated material is compensated by de-trending the obtained values during the pre-processing stage. High resistivity values (measurements No 68, 92, 245 and 250) resulted from the occurred hard and semi hard lenticular formations within the reddish clay layers. At these values the estimated risk of collision is also high. These formations are shown in Figure 12.

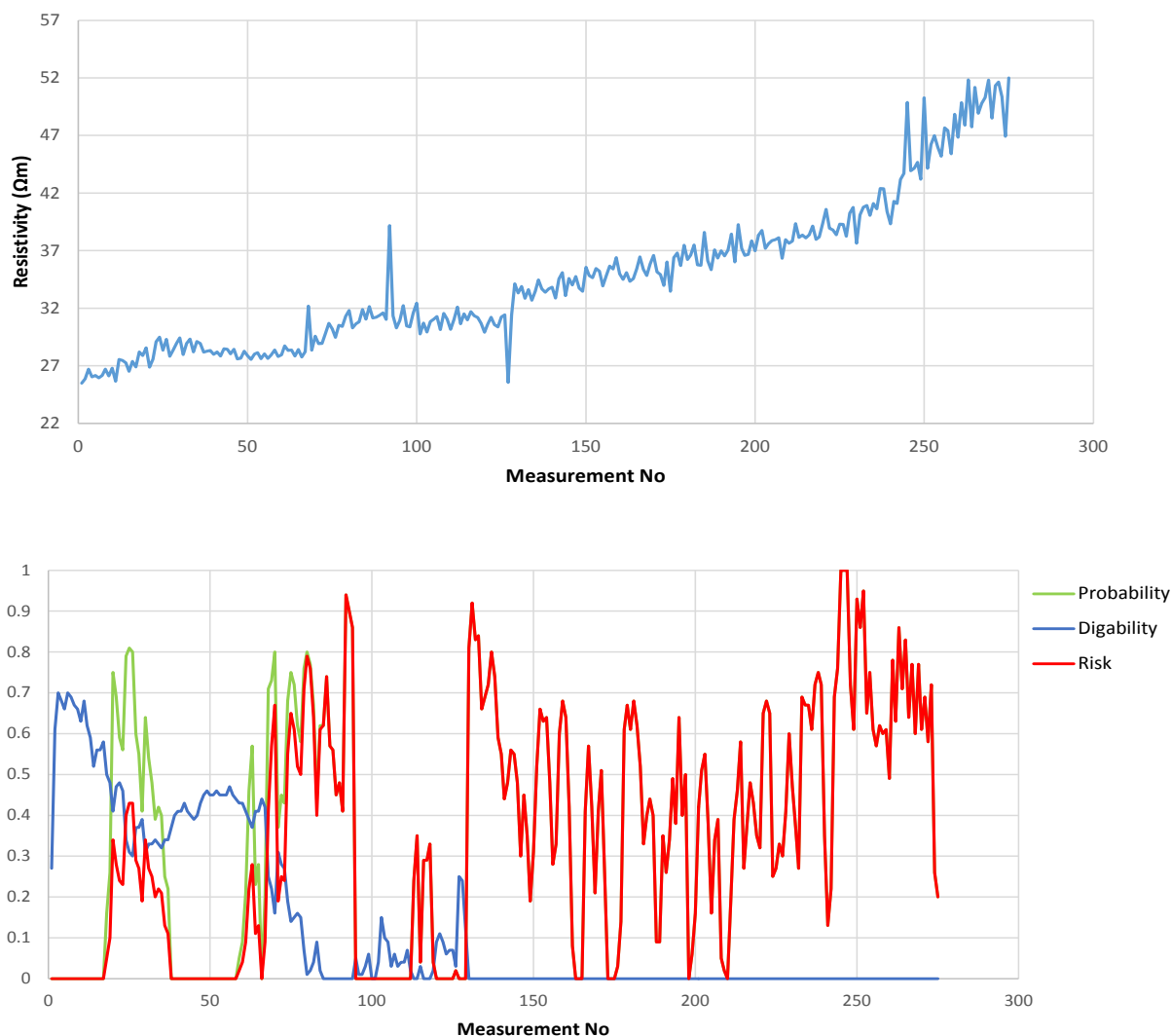


Figure 11. (Top) Variation of the resistivity during the excavation of the 12th slice. Measurements were taken every second. (Bottom) Variation of the estimated parameters: Probability of a hard rock occurrence, diggability and risk of collision.



Figure 12. Photograph of the mine face during the excavation. Thin hard and semi hard layers are interbedded within the reddish clays.

The last excavated slice was ~0.5m away from the place where the hard rock boulders were buried (Figure 13). During the excavation of the last two slices the resistivity values measured at the

angular location corresponding to boulders site were increasing progressively as well as the values of risk of collision. Figure 14 exhibits the resistivity profile during the excavation of the semifinal cut (~0.8m away from the buried hard rock). Measurements 38-45 show the change in resistivity due to the buried hard rocks, while measurements 46-53 due to the semi-hard formation.



Figure 13. Photograph of the mine face during the excavation of the cut slice. The distance of buried boulders (marked with the red circle) to bench crest was approximately 0.5m. Also the occurred semi hard formation (marked with the green oval) is shown.

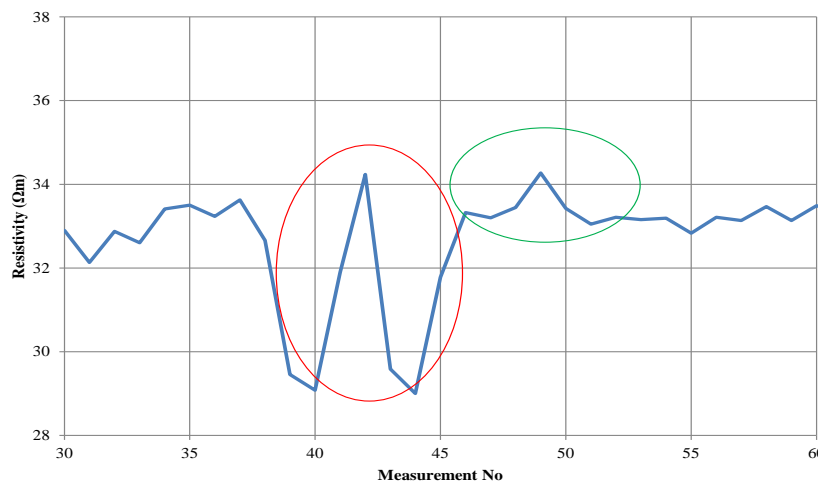


Figure 14. Resistivity profile during the excavation of the semifinal slice. The variation in resistivity due to buried hard rocks and to semi hard formation is shown.

4.2. Problems encountered and corrective actions

The problems encountered during the final test were mostly related to the harsh mining conditions. The main observed problems were:

- Frequent interruptions of the excavator operation resulting in measurement gaps. Measurements continuity is essential for data evaluation employing the Advanced Mode of the automated algorithm. Tackling this problem requires the intervention of the operator in order to stop the measurement collection by selecting the pause button from HAROR main menu and to restart it

when the excavator is again operating. Because this is not convenient for the excavator operator, the use of Simple Mode of HARROR application was finally adopted.

- Unnecessary warnings due to the presence of thin hard or semi hard layers or small lenticular hard rock formations that could be mined without creating problems to BWE. Preventing such warnings, requires proper selection of the relevant HAROR parameters which is driven by the application of optimization techniques and the verification from visual inspection. However these adjustments in HAROR are not frequent, provided that the geological conditions in the excavation area do not change radically.

- Random variations of EM sensor distance from the mine face and changes due to maneuvering of BWE during mining and/or to undulated surface of mine face. In the final test such variations were limited due to especially selected site for conducting the test. However in normal mining conditions these variations can be quite often and the monitoring system must be improved to tolerate them. Non-systematic change of the EM sensor distance from the mine face cannot be mitigated by the de-trending technique used by HAROR.

- Height change of the excavated slice. This change requires resetting the angle of the wooden arm that holds the EM sensor. In the developed system this is done manually by using a basket truck. This adjustment even though not frequent, is time consuming and requires halting of the excavator and the system. In order to keep the distance of EM sensor from the mine face constant and to adjust the arm angle automatically, it is proposed the construction of a robotic arm equipped with a distance measurement sensor and an angle adjustment mechanism. This arm could be designed and built at the stage of developing an industrial grade prototype.

- The effect of vibrations, dust and weather conditions. The vibrations generated in the arm holding the sensor during the excavation of soft formations were negligible, while those during the excavation of thin hard layers were more intense. EM sensor measurements have shown that they are not affected by vibration, dust and weather. However the effect of these factors on the sensor electronics could not be estimated during these tests, since a considerably longer operating time is required. In an industrial-type system the sensor and the electronic parts should be resistant to vibrations, dust and adverse weather conditions. The existing commercial EM sensors are not designed and built for continuous operation in mining conditions.

- Material falls from the mine face during the excavation. A PVC tube with foamy interior was used to protect the used sensor from material falls. In an industrial-type system, the sensor should be designed and built to withstand falls and strokes.

5. CONCLUSION

A real-time mine face inspection system based on geophysical sensors was developed for the early detection of hard rock formations during the excavation by BWE. More specifically, an Electromagnetic (EM) sensor was employed for the continuous measuring of the electrical resistivity of the material in the mine face. The resistivity data were processed and evaluated in real time by specially developed software to estimate the diggability of the excavated material ahead of the excavation face and the risk of collision.

Final field tests and results indicated that the developed real time mine face inspection system was able detect the presence of hard rock inclusions in the excavating area and to generate early warning alarms for the operator of the BWE. The integration of the automated algorithm based on statistical process control, the fuzzy expert system and the visualization unit in a standalone application (HAROR) proved successful and convenient for real-time monitoring. HAROR is fully parameterized and can be adjusted to operate in different geological and mining conditions.

The reliability of the system was mainly affected by the changing harsh mining conditions and the geological settings. Random changes in the distance of the EM sensor to face and in the height of cut can affect the performance of the system. Moreover the presence, within the reddish clay, of

several thin hard and semi hard layers which are diggable by BWE, creates unwanted warnings which should be eliminated by adjusting HAROR parameters.

The knowledge gained from the development of this full-scale system and from the conducted field tests is considered valuable for the next potential step of this research project, which is the development of an industrial grade real time system. An industrial grade system should include the following:

- A robotic arm (for holding the EM sensor) equipped with a distance measurement sensor and an angle adjustment mechanism.
- Especially manufactured electronics and EM sensor resistant to vibrations, dust, falls and adverse weather conditions.
- Use of EM sensors with capability to change to T-R layout and/or frequency for simultaneous measurements at different depths.
- Software code in a lower level programming language (e.g. C++) to reduce the computing time during real time operation. This will allow the use of higher measuring frequency and is anticipated to improve the system accuracy.

ACKNOWLEDGEMENTS

The research leading to these results has received funding from the European Commission - Research Fund for Coal and Steel under grant agreement No RFCR-CT-2015-00003. The presented results reflect only the authors' view and the European Commission is not liable for any use that may be made of the information contained therein.

REFERENCES

- [1] Durst W. and Vogt W. (1988). *Bucket Wheel Excavator*. Trans. Tech. Publications, Clausthal.
- [2] Rasper L. (1975). *The Bucket Wheel Excavator*. Clausthal.
- [3] Kavouridis K., Roumpos C., Galetakis M. and Pavloudakis F. (2008). 'Methods and Technological Improvements for the Efficient Removal of the Overburden Hard Rock Formations at South Field Lignite Mine, Ptolemais, Greece', *Proced. of 9th International Symposium 'Continuous Surface Mining'*, October 8-11, Petrosani – Romania, 91-100.
- [4] Huss W. (2014). 'Problems of Bucket-Wheel Excavators Body in Hardly-Workable Grounds in Polish Open Pit Mines' C. Niemann-Delius. (ed.), *Proc. of the 12th Int. Symp Continuous Surface Mining - Aachen, Lecture Notes in Production Engineering*, 59-71.
- [5] Overmeyer L., Kesting M. and Jansen K. (2007). 'SMT Technology – Sensory identification of material type and detection of the interfaces', *Bulk Solids Handling*, 27(2), 112-118.
- [6] Tripathi K. (2011). 'Review on Knowledge-based Expert System: Concept and Architecture', *IJCA Special Issue on Artificial Intelligence Techniques - Novel Approaches & Practical Applications*, 19-23.

Simulating the Performance of Bucket Wheel Excavators by Means of Soft Computing Techniques

Maria Menegaki¹, Theodoros Michalakopoulos¹ and Christos Roumpos²,

¹National Technical University of Athens, 9 Iroon Polytechniou Str., Zografou Campus, Greece

²Public Power Corporation of Greece

ABSTRACT

Fuzzy Cognitive Maps (FCMs) are signed digraphs, which consist of nodes representing the factors that describe the behaviour of a system, and edges, which are weighted arcs connecting the concepts and representing the causal relationships among them. FCMs offer certain advantages, e.g. they can incorporate uncertainty, show high ability to demonstrate complexity, are not demanding in terms of funds and time. Thus, as a soft computing technique, they have been used in various and completely different applications from various areas. In this paper, the FCM approach is used as a means for qualitatively modelling and analysing the efficiency of bucket wheel excavators, a crucial component of continuous surface mining systems. Using both an extensive review of scientific literature and expert judgment as the basis of the analysis, a simulation framework is developed to perform qualitative simulations with respect to the efficiency factors of the bucket wheel excavator. To this end, several parameters, e.g. characteristics of the excavated material, number and thickness of lignite layers, bucket wheel capacity and fill rate, maintenance of the system, experience of the operator, etc., are employed to reveal cause/effect relationships, explore the dynamics of the system and carry out what-if and sensitivity analyses. The model is a first step towards simulations intended to help mining practitioners. The main goal is to propose a different simulation approach for complex mining systems that can interconnect the factors affecting system's behaviour by providing a transparent and flexible model. In future research, the model can be combined with or tested against Learning Algorithms, which are used for automatic construction of FCMs from historical data, so as to develop a more advanced and accurate representation of the system under investigation.

1. INTRODUCTION

Lignite is Greece's most important indigenous energy resource, accounting in 2015 for 23.4% of the country's primary energy supply [2]. Given the security of supply, the low extraction costs and the stable prices, it is estimated that lignite will continue to hold a strong position in the Greek energy mix in the near future.

Most of the Greek lignite deposits have a multiple-layer structure characterized by the extreme splitting of lignite seams separated by non-lignite layers. The alternated waste layers, mainly marls and clays, are of varying thickness and cohesion and also exhibit intense spatial fluctuation. The most important deposits are located in the Ptolemais - Amynteon basin, in the area of Western Macedonia in northern Greece. Other deposits lie at Drama and Elassona, as well as in the south, at Megalopolis. There is also a large peat deposit of about 4 billion m³ at Philippi in the northern part of Greece (Eastern Macedonia). Only 30% of the total lignite reserves have been extracted to date and the remaining reserves are sufficient for over 40 years at current production rates.

For the exploitation of most of these deposits, the continuous surface mining method is used. High capacity bucket wheel excavators (BWEs), conveyor belts and spreaders, operating in series and forming a network of continuous excavated material flow, are used to achieve high output rate with low cost of mined lignite per ton [4], [13], [20], [21]. This serial operation makes the production

levels that can be achieved very sensitive to the reliability of the various equipment units. Bucket wheel excavators are the first link in the chain that can affect significantly the output of the mining system, since their efficiency plays a crucial role in the appropriate long and short-term mine planning and design activities.

There are a lot of parameters affecting the efficiency of BWEs including, in general, the properties of the material to be excavated and conveyed, the mechanical and operational parameters of the BWE, as well as the operational parameters of other components of the continuous mining system. So far previous research efforts have explored particular sets of parameters that influence BWE's productivity. For example, Wade et al. [26], Panagiotou [16], O'Regan et al. [14] investigated the parameters affecting BWE diggability. Ural [25] investigated the effects of operational parameters, such as slewing speed, bench height, terrace height, block width, etc., on output efficiency of a specific BWE type and defined their optimum value. Tanasijević and Ivezić [24] proposed a procedure for the dependability efficiency analysis of BWEs based upon fuzzy sets theory, as a tool for fast estimation of the quality of service and the in depth analysis regarding the design, the constructive, the maintenance and the logistic characteristics of BWEs. Galetakis et al. [4] developed an expert system for the estimation of the effect of material diggability and excavated blocks thickness on the efficiency of BWE used for the selective mining of multiple-layered lignite deposits.

This paper introduces the analysis of BWE efficiency making use of Fuzzy Cognitive Maps (FCMs), as a means for soft computing modeling. On this ground, the BWE's efficiency model is developed to reveal the efficiency factors of the BWE and explore the dynamics of the system. In total, 10 factors were incorporated in the model, the selection of which was based on an extensive literature review and the authors' expertise. The rest of the paper is structured as follows: Section 2 introduces the FCM approach. Section 3 discusses the development of the BWE's efficiency FCM and presents the analysis of the model towards revealing the interlinkages and interdependencies of the factors. Finally, Section 4 concludes with the main findings of this study.

2. METHODOLOGICAL BACKGROUND

2.1. Introduction to Fuzzy Cognitive Mapping

Cognitive maps represent social scientific knowledge and model decision making in social and political systems. Cognitive maps are interconnected, directed, logic graphs consisting of nodes and edges/arrows, which are mainly used to analyse a system's behaviour by investigating causal links among relevant concepts, and have their roots in Graph Theory [10]. Each variable is linked to one another by positive or negative signs. A positive value between concepts C_i and C_j means that an increase in concept C_i causally increases concept C_j , whereas a negative value between concepts C_i and C_j means that an increase in concept C_i causally decreases concept C_j . In this way, a binary comparison matrix of the cognitive map can be developed, where each variable is compared with one another according to causal relationships.

Figure 1 contains an example adopted from [8]. Here e_1 affects e_3 and e_4 in a positive way and e_2 and e_5 in a negative way. Moreover, e_2 affects e_1 , and there are no variables by which e_3 is affected. Furthermore, e_4 affects e_5 in a positive way. Finally, e_5 affects e_4 and e_2 (negative and positive, respectively).

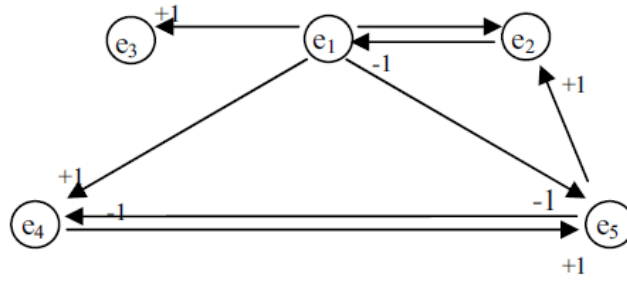


Figure 60. Example of causal cognitive map (adopted from (Hasiloglu & Cinar, 2008)).

Based on the causal cognitive map of Fig. 1, the following 5x5 adjacency matrix E is constructed:

$$E = \begin{bmatrix} 0 & -1 & 1 & 1 & -1 \\ -1 & 0 & 0 & 0 & 0 \\ 0 & 0 & 0 & 0 & 0 \\ 0 & 0 & 0 & 0 & 1 \\ 1 & 1 & 0 & -1 & 0 \end{bmatrix}$$

Real life problems, however, rarely have crisp boundaries. Thus, conventional cognitive maps were extended by the use of Fuzzy Logic creating Fuzzy Cognitive Maps (FCMs), which were introduced by Kosko [10] and can be regarded as a combination of Fuzzy Logic, “efficient in representing heuristic, commonsense rules” and Neural Networks, “efficient in learning heuristics” [11], [22]. A fuzzy set is characterized by a membership-degree function, which maps the members of the universe U into the unit interval [0,1]. The value 0 means that the member is not included in the given set, 1 describes a fully included member. Hence, for the universe U a fuzzy set A is defined by Eq. 1 as:

$$A = \{x, \mu_A(x) \mid x \in A, \mu_A(x) \in [0,1]\} \tag{1}$$

where $\mu_A(x)$ is the membership-degree function $\mu : x \rightarrow [0;1]$

FCMs, like simple cognitive maps, consist of nodes and weighted arcs. Nevertheless, in the case of FCMs the weights of the arcs are fuzzy and take any value lying in the interval [-1, 1]. The components of the system may come from existing research in the field, i.e. from literature review, from field experts, or both [3], [7], [9]. More explicitly, a FCM consists of nodes or concepts, $C_i, i = 1 \dots N$, where N is the total number of concepts. Each interconnection between two concepts C_i and C_j has a weight, a directed edge W_{ij} , which is similar to the strength of the causal links between C_i and C_j . W_{ij} from concept C_i to concept C_j measures how much C_i causes C_j . The direction of causality indicates whether the concept C_i causes the concept C_j or vice versa. Thus, there are three types of weights [19]:

- $W_{ij} > 0$ indicates a positive causality between concepts C_i and C_j . That is, the increase (decrease) in the value of C_i leads to the increase (decrease) on the value of C_j .
- $W_{ij} < 0$ indicates an inverse (negative) causality between concepts C_i and C_j . That is, the increase (decrease) in the value of C_i leads to the decrease (increase) on the value of C_j .
- $W_{ij} = 0$ indicates no causality between C_i and C_j .

It is important to note that $W_{ij} \neq W_{ji}$ in that causal relationship are not necessarily reversible. The weighting matrix is also known as adjacency matrix.

The method has been used in political and social sciences, computer sciences, engineering, medicine, decision support systems, time series forecasting, environmental management, energy planning, mathematics, and many others (e.g. [3], [5], [15], [18], [19]).

2.2. FCM Structural Analysis

The structural properties of a FCM can be analysed on the basis of Graph Theory and social networks analysis [15], [19]. The most commonly used indices, besides the number of concepts are: the number of connections, the number of transmitter concepts, the number of receiver concepts, the number of ordinary concepts, density, indegree, outdegree, C/N ratio, centrality, complexity and hierarchy index.

More specifically, transmitter concepts only affect other system components, whereas receiver concepts are only affected by other system components. Ordinary variables are those with both transmitting and receiving functions [1]. The *complexity* index of a map is the ratio of receiver to transmitter variables [15].

The *density* (D) is an index of connectivity and expresses how connected or sparse the maps are and is calculated by the number of available connections (C) divided by the maximum number of connections possible between N variables, according to Eq. 2:

$$D = \frac{C}{N(N-1)} \text{ or } D = \frac{C}{N^2} \quad (2)$$

Outdegree [od(v_i)] shows the cumulative strengths of connections exiting the variable and is calculated by the row sum of absolute values of a variable in the adjacency matrix E (Eq. 3), whereas *indegree* [id(v_i)] is the column sum of absolute values of a variable in the adjacency matrix E and shows the cumulative strengths of connections entering the variable (Eq. 4) [11]:

$$od(v_i) = \sum_{k=1}^N \overline{a_{ik}} \quad (3)$$

$$id(v_i) = \sum_{k=1}^N \overline{a_{ki}} \quad (4)$$

Centrality is the most important measure for map complexity, borrowed from social networks analysis, and represents the degree of relative importance of a concept to the operation of the system [10]. It is estimated by the summation of variable's indegree and outdegree according to Eq. 5 [1], [19]:

$$c_i = od(v_i) + id(v_i) \quad (5)$$

Finally, the *hierarchy index* (h) is a function of the outdegrees and number of variables in a given map and represents the type of system as fully 'hierarchical' (i.e. when $h=1$), or 'democratic'. (i.e. when $h = 0$). Democratic maps are much more adaptable to changes because of their high level of integration and dependence [15]. The *hierarchy index* (h) is estimated by Eqs. 6, 7 and 8 [15]:

$$h = \frac{12\sigma_{od}^2}{n^2 - 1} \quad (6)$$

where:

$$\sigma_{od}^2 = \frac{\sum_{i=1}^n (od_i - \mu_{od})^2}{n} \quad (7)$$

and

$$\mu_{od} = \frac{\sum_{i=1}^n od_i}{n} \quad (8)$$

2.3. Dynamic exploration and simulation of FCM

The mathematical representation of FCMs provides a snapshot of how the variables and linkages of the system, given its configuration, would resolve themselves, in the absence of change or intervention, with all feedback loops played out. This dynamic analysis is embedded in FCMs as a kind of inferential procedure and can either focus on the equilibrium end states or the transient behaviour during the iteration steps with reference to either all concepts or a subset of concepts of interest [6], [19]. Through this type of analysis, “what-if” scenarios are investigated, examining what state the system would go to if certain conditions are present.

In order to explore the dynamic interactions between the concepts involved in the collective map, key variables are increased or decreased continually, a process known as “clamping” by [10]. Although the values of the final vector are not that important, the relative changes to the conceptual system indicate trends that can serve as guidance for decision makers, and for better appraisal of the system dynamics [13].

The initial stimulus is an input vector, i.e. the ‘activation level’, that takes values in the unit interval 0 to 1 and excites the FCM adjacency matrix E by applying a multiplication of the input vector with the adjacency matrix. For n number of concepts, the input vector is 1 by n , the FCM adjacency matrix is $n \times n$, and the output is 1 by n . FCMs can handle different types of input data, that is, quantitative or qualitative or both. In case of quantitative data the input values should be normalised in the range 0 to 1. Zero values are attributed to concepts not present in the system, while value(s) of 1 indicate that the concept is present to its maximum extent.

In every step (k), the value A_i of each concept C_i is affected by the other nodes attached to it and is updated based on the following activation Eq. 9 [23]:

$$A_i^{(k+1)} = f(A_i^{(k)} + \sum_{\substack{j=1 \\ j \neq i}}^N A_j^{(k)} * W_{ji}) \quad (9)$$

where $A_i^{(k+1)}$ is the value of concept C_i at simulation step $k+1$, $A_i^{(k)}$ is the value of concept C_j at step k , W_{ji} is the weight of the interconnection between concept C_j and concept C_i and f is a transformation function (e.g. logistic or sigmoidal function) that limits the result of the product to the predefined activation interval $\{0, 1\}$ [3], [15], [18]. In this study, the sigmoid threshold function is used (Eq. 10), which hinders quantitative analysis but allows for qualitative comparisons between different concepts and/or scenarios:

$$f(x) = \frac{1}{1 + e^{-\lambda x}} \quad (10)$$

where λ is a real positive number (usually $\lambda=1$) and x is the value $A_i^{(k)}$ on the equilibrium point.

The simulation does not produce exact quantitative values but helps to identify the general pattern of system's behaviour via the achieved values of the concepts.

The simulation process used in this study consists of five steps described by the following algorithmic procedure [19]:

Step 1. Definition of the initial vector A that corresponds to the concepts identified by suggestions and available knowledge.

Step 2. Multiply the initial vector A and the matrix W .

Step 3. The resultant vector A at time step k is updating using the previous equations.

Step 4. This new vector A^k is considered as an initial vector in the next iteration.

Step 5. Steps 2–4 are repeated until $A^k - A^{k-1} \leq e$ (where e is a residual describing the minimum error difference among the subsequent concepts and in most applications is equal to 0.001) or $A^k = A^{k-1}$.

For the interpretation of the results, an average value for the concept under investigation is computed according to the following Eq. 11 [18]:

$$R(x) = \begin{cases} 0, & x \leq 0.5 \\ \frac{x - 0.5}{0.5} * 100\%, & x > 0.5 \end{cases} \quad (11)$$

where 0 corresponds to very low BWE efficiency and 1 corresponds to highest BWE efficiency.

3. DEVELOPMENT AND ANALYSIS OF THE BWE EFFICIENCY SYSTEM

3.1. Development of the FCM

The FCM model for studying the efficiency of bucket wheel excavators (BWE) was based on an extensive literature review and the authors' expertise. In total, the model includes 10 concepts, which are briefly discussed hereinafter:

- BWE efficiency (C1): The main metric providing a quantitative measure of the degree to which a BWE is achieving its maximum nominal excavation rate.
- Operator's skill (C2): The degree of training and experience an operator has accumulated over time, combined with her physical and mental capacity to continuously monitor the operation of the BWE, identify suboptimal operation and perform corrective actions.
- Diggability (C3): A measure of how easily a specific soil type is excavated by a BWE.
- Dimensions of excavated slice (C4): The physical dimensions of the slice cut by the BWE during slewing. Of particular interest is the actual cut of height, which can be much smaller than optimal in cases where the thickness of the excavated layer is less than the bucket-wheel radius.
- Mechanical reliability (C5): BWE downtime due to structural and component failures reduces the time available for productive operation.
- Auxiliary works (C6): The frequency, duration, and complexity of auxiliary works necessary for the operation of a BWE, e.g. cable shifts, conveyor shifts, ground clearing and levelling, reduce accordingly the BWE utilisation.
- Downstream processes (C7): Given that the system is linear, the BWE is dependent on the reliability of all downstream material handling processes. All units of a branch have to be up and running for the BWE to be able to excavate.

- Selective mining (C8): It is dictated by geological factors, mainly the thickness of the layers to be excavated. Especially in multi-layer deposits, in order to avoid losses or dilution of lignite, the cut height can be as small as 15 cm, thus adding to the complexity of the operation and reducing the utilised capacity of the BWE.
- Bad weather conditions (C9): They can affect both the condition of the excavated soil altering its diggability and the operator’s awareness of the existing conditions.
- Bucket fill factor (C10): The main metric providing a quantitative measure of the degree to which the capacity of each bucket is actually utilised. It is dependent on many of the above-mentioned concepts.

The cause-and-effect relationships among concepts were determined by the authors through discussion. The BWE efficiency FCM model is presented in Fig. 2 and was created using a computer-based FCM tool called Mental Modeler (freely available at: <http://www.mentalmodeler.org>) [6]. The adjacency matrix is given in Table 1.

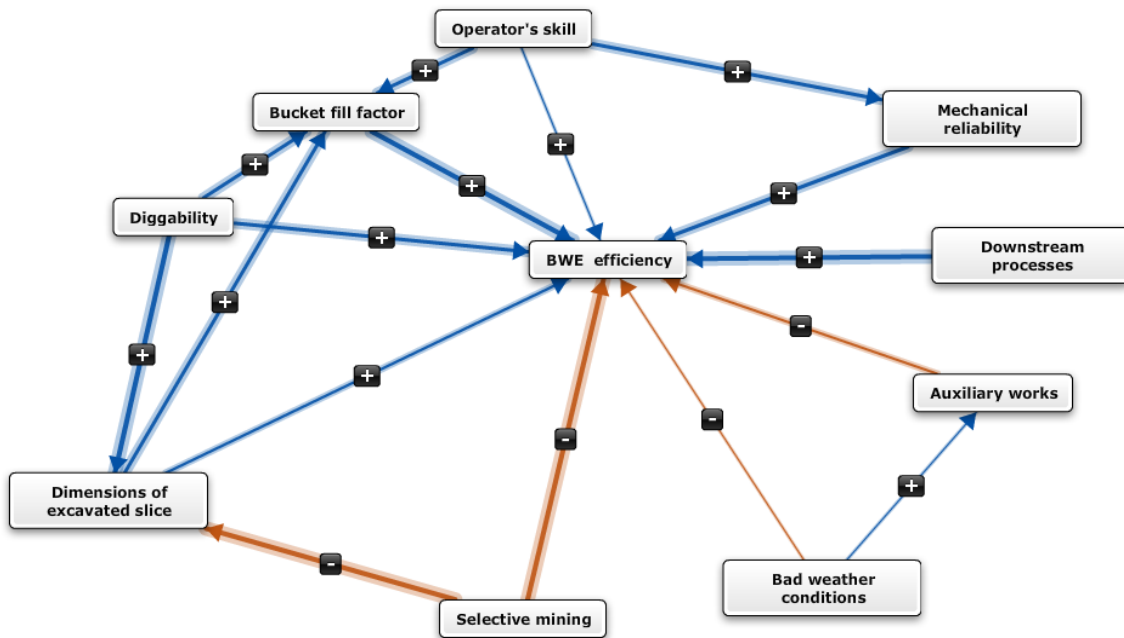


Figure 61. The BWE efficiency FCM model.

Table 16. The adjacency matrix of the BWE efficiency FCM model.

	C1	C2	C3	C4	C5	C6	C7	C8	C9	C10
C1	0	0	0	0	0	0	0	0	0	0
C2	0.15	0	0	0	0.5	0	0	0	0	0.5
C3	0.6	0	0	0.85	0	0	0	0	0	0.8
C4	0.3	0	0	0	0	0	0	0	0	0.66
C5	0.75	0	0	0	0	0	0	0	0	0
C6	-0.25	0	0	0	0	0	0	0	0	0
C7	1	0	0	0	0	0	0	0	0	0
C8	-1	0	0	-1	0	0	0	0	0	0
C9	-0.1	0	0	0	0	0.1	0	0	0	0
C10	1	0	0	0	0	0	0	0	0	0

3.2. Analysis of the BWE efficiency FCM

As shown by the causal relationships among the concepts of the FCM (Fig. 2), the efficiency of BWE increases with an increase in “Operator’s skills”, “Bucket fill factor”, “Diggability”, “Dimensions of excavated slice”, “Downstream processes”, and “Mechanical reliability” and decreases with an increase in “Selective mining”, “Bad weather conditions”, and “Auxiliary works”. The graph theory indices for the collective FCM are given in Table 2.

Table 2. Graph theory indices for the collective FCM.

0.028	10	16	5	1	4	1.6
-------	----	----	---	---	---	-----

There is only one receiver variable, namely the “BWE efficiency” and five transmitter variables, i.e. “Operator’s skills”, “Diggability”, “Selective mining”, “Bad weather conditions” and “Downstream processes”. The map has in total 16 connections and the ratio between connections and factors is 1.6. The density is equal to 0.16 and the hierarchy index is calculated at 0.028, indicating a ‘democratic’ map, i.e. a system that is open to change. Further, Table 3 presents the outdegree, indegree and centrality of the concepts of the collective map.

Table 3. The most central factors in the collective FCM.

BWE efficiency	0.00	5.15	5.15
Operator's skill	1.15	0.00	1.15
Diggability	2.25	0.00	2.25
Dimensions of excavated slice	0.96	1.85	2.81
Mechanical reliability	0.75	0.50	1.25
Auxiliary works	0.25	0.10	0.35
Downstream processes	1.00	0.00	1.00
Selective mining	2.00	0.00	2.00
Bad weather conditions	0.20	0.00	0.20
Bucket fill factor	1.00	1.96	2.96

The most influencing concept in the map is the “Diggability”, followed by the “Selective mining” and the “Operator’s skills”. The most central concepts, apart from the “BWE efficiency”, are (in order of significance) the “Bucket fill factor”, the “Dimensions of excavated slice”, the “Diggability”, and the “Selective mining”.

A number of simulations were conducted using the “clamping” process towards exploring the dynamic interactions between the concepts. The simulations were carried out using the FCM Tool 2nd edition (available at: http://www.cs.ucy.ac.cy/fcmdss/index.php?option=com_content&view=article&id=61&Itemid=68), which works in the Matlab environment. In particular, the transmitter variables were set to specific activation levels and were increased or decreased continually, and the output values of the “BWE efficiency” was computed. For conciseness reasons, however, only the results of selected simulations are presented hereinafter for illustrative purposes.

Simulation 1 – Worst-case conditions: In this simulation, the transmitter variables that increase the “BWE efficiency” (i.e. “Operator’s skills”, “Diggability”, and “Downstream processes”) are set to 0.1, whereas the transmitter variables that decrease the “BWE efficiency” (i.e. “Selective mining”

and “Bad weather conditions”) are set to 1. The system converges after 29 iterations and the efficiency of the BWE, based on Eq. 11, is estimated to 46.4%.

Simulation 2 – Best-case conditions: In this case, the transmitter variables that increase the “BWE efficiency” are set to 1, and the transmitter variables that decrease the “BWE efficiency” are set to 0.1. The system converges after 28 iterations and the efficiency of the BWE, based on Eq. 11, is estimated to 97.2%.

Simulation 3 – Sensitivity analysis for “Diggability”: In order to conduct the sensitivity analysis a series of simulations were performed holding constant the initial values of “Operator’s skills” (value: 1), “Downstream processes” (value: 1), “Selective mining” (value: 1), and “Bad weather conditions” (value: 0.5). The initial values used for “Diggability” were sequentially set to 0.10, 0.25, 0.5, 0.75 and 1, representing a wide range of possible situations. The results are given in Table 4.

Table 4. Results of Simulation 3 – “Diggability” sensitivity analysis

0.10	84.0%
0.25	85.9%
0.50	88.5%
0.75	90.5%
1.00	92.1%

As shown from Table 4, the efficiency of the BWE between the worst and best diggability conditions has a relative difference of approximately 10%.

4. DISCUSSION AND CONCLUSIONS

The efficiency of BWEs is a critical issue for continuous mining systems, especially in multi-layer lignite deposits. So far, several studies have been conducted aiming at analysing the parameters involved. Nevertheless, these studies are usually focused on a limited set of factors. This paper attempts to provide a more holistic discussion by determining the most decisive factors affecting the efficiency of BWEs, and the ways these factors interact with one another using the FCM technique. To the authors’ best knowledge this is the first attempt to model the efficiency of BWEs using FCM, towards examining the dynamics of the system.

Based on literature review and experts’ opinion the BWE efficiency FCM model was developed. In total, the model includes ten different factors, namely: “BWE efficiency”, “Operator’s skills”, “Bucket fill factor”, “Diggability”, “Dimensions of excavated slice”, “Downstream processes”, “Mechanical reliability”, “Selective mining”, “Bad weather conditions”, and “Auxiliary works”. The cause-and-effect relationships among concepts show that the efficiency of BWE increases with an increase in “Operator’s skills”, “Bucket fill factor”, “Diggability”, “Dimensions of excavated slice”, “Downstream processes”, and “Mechanical reliability” and decreases with an increase in “Selective mining”, “Bad weather conditions”, and “Auxiliary works”. Furthermore, a number of simulations were conducted, the results of which indicate significant differences in BWEs’ efficiency under favourable and hostile conditions, i.e. the efficiency ranges between 46% and 97%. Although simulations are not substitutes for quantitative predictions, nor do they provide real-value parameter estimations, they provide the means for theory testing and bridge the gap between ‘pure’ qualitative and quantitative approaches. Yet, this is a first step to this particular scientific field and, thus, further work remains to be done.

REFERENCES

- [1] Eden, C., Ackermann, F., & Cropper, S. (1992). The analysis of cause maps. *Journal of Management Studies*, 29(3), 309–324.
- [2] Euracoal (2018). Country profiles: Greece. Available at: <https://euracoal.eu/info/country-profiles/greece> (Accessed July 25th, 2018)
- [3] Felix, G., Nápoles, G., Falcon, R., Froelich, W., Vanhoof, K., & Bello, R. (2017, August 17). A review on methods and software for fuzzy cognitive maps. *Artificial Intelligence Review*, 1–31.
- [4] Galetakis, M. J., Papadopoulos, S., Vasiliou, A., Roumpos, C. P., & Michalakopoulos, T. (2015). Development of an Expert System for the Prediction of the Performance of Bucket-Wheel Excavators Used for the Selective Mining of Multiple-layered Lignite Deposits. In C. Niemann-Delius (Ed.), *Proceedings of the 12th International Symposium Continuous Surface Mining - Aachen 2014*, Cham: Springer International Publishing, 47–58.
- [5] Giordano, R., Passarella, G., Uricchio, V. F., & Vurro, M. (2005). Fuzzy cognitive maps for issue identification in a water resources conflict resolution system. *Physics and Chemistry of the Earth*, 30(6–7 SPEC. ISS.), 463–46.
- [6] Gray, S. A., Gray, S., de Kok, J. L., Helfgott, A. E. R., O’Dwyer, B., Jordan, R., & Nyaki, A. (2015). Using fuzzy cognitive mapping as a participatory approach to analyze change, preferred states, and perceived resilience of social-ecological systems. *Ecology and Society*, 20(2):11.
- [7] Gray, S.R.J., Gagnon, A.S., Gray, S.A., O’Dwyer, B., O’Mahony, C., Muir, D., Devoy, R.J.N., Falaleeva, M., Gault, J. (2014). Are coastal managers detecting the problem? Assessing stakeholder perception of climate vulnerability using Fuzzy Cognitive Mapping. *Ocean and Coastal Management*, 94, 74–89.
- [8] Hasiloglu, S., & Cinar, R. (2008). Evaluating direct marketing practices on the internet via the fuzzy cognitive mapping method. *International Journal of Business and Management*, 3(12), 31–38.
- [9] Jetter, A. J., & Kok, K. (2014). Fuzzy Cognitive Maps for futures studies-A methodological assessment of concepts and methods. *Futures*, 61, 45–57.
- [10] Kosko, B. (1986). Fuzzy cognitive maps. *International Journal of Man-Machine Studies*, 24(1), 65–75.
- [11] Kosko, B. (1992). *Neural Networks and Fuzzy Systems: A Dynamical Systems Approach to Machine Intelligence/Book and Disk*. Prentice Hall.
- [12] Michalakopoulos, T. N., Roumpos, C. P., Galetakis, M. J., & Panagiotou, G. N. (2015). Discrete-Event Simulation of Continuous Mining Systems in Multi-layer Lignite Deposits. In: C. Niemann-Delius (Ed.), *Proceedings of the 12th International Symposium Continuous Surface Mining*. Cham: Springer International Publishing, 225–239.
- [13] Neocleous, C., & Schizas, C. N. (2012). Modeling socio-politico-economic systems with time-dependent fuzzy cognitive maps. In *IEEE International Conference on Fuzzy Systems*. <http://doi.org/10.1109/FUZZ-IEEE.2012.6250798>.

- [14] O' Regan, G., Davies, A.L., Ellery, B.I. (1987). Correlation of bucket wheel performance with geotechnical properties of overburden at Goonyella Mine. In: Trans. Tech. Publications, Australia, 381–396.
- [15] Özesmi, U., & Özesmi, S. L. (2004). Ecological models based on people's knowledge: A multi-step fuzzy cognitive mapping approach. *Ecological Modelling*, 176(1–2), 43–64.
- [16] Panagiotou, G. N. (1990). Assessment of open pit excavators' diggability. In: Proceedings of the 2nd Mine Planning and Equipment Selection Conference, Singhal, R and Vavra, M. (eds.), 305–314.
- [17] Papageorgiou, E. I., & Salmeron, J. L. (2013). A review of fuzzy cognitive maps research during the last decade. *IEEE Transactions on Fuzzy Systems*, 21(1), 66–79.
- [18] Papageorgiou, E. I., Papandrianos, N. I., Karagianni, G., Kyriazopoulos, G. C., & Sfyas, D. (2009). A Fuzzy Cognitive Map based tool for prediction of infectious diseases. In *IEEE International Conference on Fuzzy Systems*, 2094–2099.
- [19] Papageorgiou, E.I. and Kontogianni, A. (2012). Using Fuzzy Cognitive Mapping in Environmental Decision Making and Management: A Methodological Primer and an Application, In: *International Perspectives on Global Environmental Change*, Stephen S. Young and Steven E. Silvern (eds.), InTech, 427-450. Available at: <http://www.intechopen.com/books/international-perspectives-on-global-environmental-change/using-fuzzy-cognitive-mapping-in-environmental-decision-making-and-management-a-methodological-prime>.
- [20] Papanicolaou, C., Galetakis, M., & Foscolos, A. E. (2005). Quality characteristics of Greek brown coals and their relation to the applied exploitation and utilization methods. *Energy and Fuels*, 19(1), 230–239.
- [21] Roumpos C., Partsinevelos P., Agioutantis Z., Makantasis K., Vlachou A. (2014). The optimal location of the distribution point of the belt conveyor system in continuous surface mining operations, *Simulation Modelling Practice and Theory* 47, 19-27.
- [22] Stylios, C. D., & Groumpos, P. P. (1998). The challenge of modelling supervisory systems using fuzzy cognitive maps. *Journal of Intelligent Manufacturing*, 9(4), 339–345.
- [23] Stylios, C. D., & Groumpos, P. P. (2004). Modeling Complex Systems Using Fuzzy Cognitive Maps. *IEEE Transactions on Systems, Man, and Cybernetics - Part A: Systems and Humans*, 34(1), 155–162.
- [24] Tanasijević, M. and Ivezić, D. (2007). Quality of service evaluation for bucket wheel excavator. *FME Transactions* 35, 141-148.
- [25] Ural, S. (2001). The Effects of Operational Parameters on the Output Efficiency of the Bucket Wheel Excavator. *Proceedings of the 17th International Mining Congress and Exhibition of Turkey-IMCET 2001*, 663-669.
- [26] Wade, N.H., Ogilvie, G.M., Krzanowski, R.M. (1987). Assessment of BWE diggability from geotechnical geological and geophysical parameters. In: *Continuous Surface Mining*, Trans. Tech. Publications, 375–380.

Analysis of Dislocation of Continual System at “Field D” in Function of Overburden and Coal Production at Eastern Part of Kolubara Coal Basin

M. Petrovic, M. Miskovic, S. Alimpijevic, G. Tomic and B. Simic

EPS/RB Kolubara, Svetog Save no.1, Serbia

ABSTRACT

Large reserves of lignite and suitable locations of basin, mountain-geological and climate conditions, geometry of deposit and physic-mechanical characteristics of working area enables use of high productive continual mechanization for excavation of overburden and coal throughout open cast mines within Kolubara coal basin.

For excavation, transport and disposal of overburden in use are co called ECS systems (excavator-bucket wheel or chain, conveyer belts with rubber, spreaders), and for coal exploitation ECC or ECL (excavators, conveyer belts, crushing plant or loading place) systems.

Use of this kind of systems has a lot of advantages comparing to discontinuous systems, but far more less flexibilities during occurrences of incidental cases, such as big land sliding or changes of technology and dislocation to new site caused by different circumstances. At Field D, which work continually for 58 years and with total production, for that time, of more than 500 mill.tons of coal, complex configuration of coal seams demanded special technology for work with often reconstructions and movement of systems. During 2007.almost all of production was stopped due to unsolved legal ownership, particularly problems about local cemetery. To ensure continuity in production it was necessary to relocate several systems to new location (former outside dump yard) and in a very short period and for that strict demanding and complex organization of works was conducted. This kind of work, at open cast mines, is always difficult and multiplex and with long time preparation period with no production which, in this particular case, had to be established in short time period.

This paper work shows activities taken during dislocation of system, starting from planning, and engagement of all other mechanization until re-establishment of production at this mine.

1. KOLUBARA COAL BASIN

Kolubara coal basin is situated 60 km south-west from Belgrade and stretches at area of 600 square kilometres.

Surface lignite mines in Kolubara coal basin covers area of municipalities Lazarevac, Lajkovac and Ub. Mining is done with high-efficient continual equipment. For excavation, transport and disposal of overburden in use are technological systems so called ECS (excavators (bucket wheel or chain), conveyors-with rubber and spreaders), and for coal exploitation ECC or ECL (excavators, conveyer belts, crushing plant or loading place) systems. Average annual production of coal in Kolubara coal basin is 30mill. tons, from which 90% is combusted in power plant “Nikola Tesla”, and 10% is processed and in use for other purposes. From coal in Kolubara coal basin more than 50% of total electric energy in Republic of Serbia is produced.

With river Kolubara coal basin is divided in two parts Western and Eastern, which is situated between rivers Turija, Pestan and Kolubara. Eastern part is, according to exploration degree and preparedness for surfes mining of coal, divided in nine geological deposits: A, B, C, D, E, F, G, and Sopic-Lazarevac. Curently, coal exploitation is proceed in fields C and D [1].

Western part of basin is spatially settled between river Kolubara on east and rivers Tamnava and Ub on south-west. This area is divided in 6 geological deposits: Veliki Crljeni, Tamnava-West, Tamnava East, Zvizdar, Radljevo and Trlic. Currently in use are fields Tamnava West and Field G.

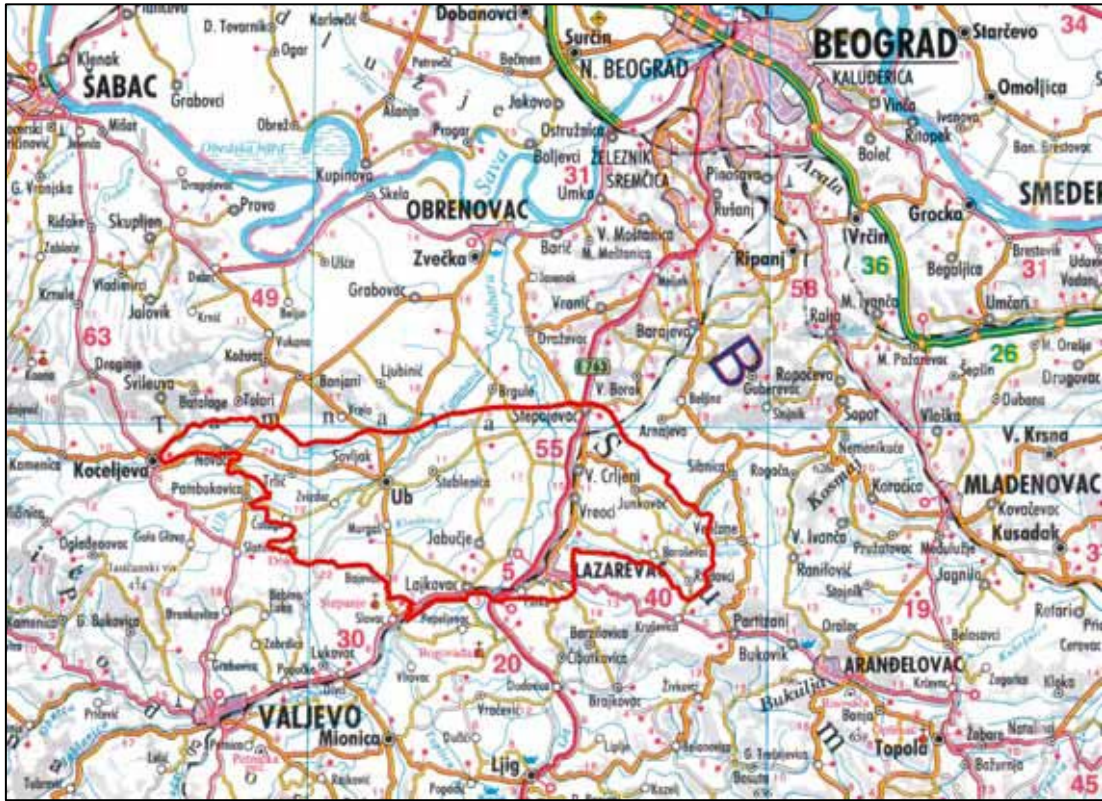


Figure 62. Spatial position of Kolubara coal basin

2. OPEN CAST MINE “FIELD D” 2007-2009

Open cast mine “Field D” currently employs 2500 workers. It spreads on 20 square kilometres and is most productive mine due to more than 60 years of production. Average annual production for the period from 2007-2009 is 13,5 mill. tons, and 40 mill. cubic meters of overburden. On this mine there is six overburden continual systems and two continual coal systems which have total length of 36 kilometres. Here are 10 bucket wheel excavators with capacity of 20.000-50.000 m³/t per day, 7 spreaders and 8 ES-s working on cleaning the roof of coal layer and preparation works [1].

3. SYSTEMS DISLOCATION

Settlement Vreoci with 3.300 settlers and more than 1000 households, as well as local cemetery with more than 6000 grave yards come up in front of mining activities from Field D in 2007. Unsolved problems with land purchase, household expropriation and no agreement with representative of local settlers about relocation of local cemetery led to almost stopping at this open cast mine, and for that suspension in coal production relevant for electro energy balance in Republic of Serbia. [1]. In mentioned year production of coal from this mine was very important.

This was a problem that nobody expected.

No plan or technical documentation anticipate or treated this sort of a problem. Management of Mining Basin Kolubara had to find solution which could overcome this problem for the purposes of continuance in production at this field. The only possible solution was to dislocate systems to 6-7 km remote location where needed amount of coal could be excavated after some overburden removal.

Dislocation of continual systems at open cast mine was always complex and hard work with long time preparation period with no production which, in this particular case, had to be established in short time period because there was no substitution mine which could overcome less coal from Field D.

In front of Kolubara's management were a several problems which has to be solved quickly: problem of security and safety of dislocation for heavy equipment in total weight of 40.000 tons; problem to dislocate systems without disturbance on working coal production; not possible engagement of extra employees who can do heavy and complex jobs during dislocation; problem in additional engagement of auxiliary machines (bulldozers etc) because Kolubara's auxiliary machinery were not enough for enormous work ahead; and the problem of finding the best solution, and how and where remove the systems to fulfil continuance in coal production.

1.	SRs 1200x 22/2	G-I	1.10.1967
2.	SRs 1201x 24/4+VR	G-II	15.12.1968; 9.2004
3.	SRs 1200x 24/4+VR	G-III	5.10.1969
4.	SRs 1200x 24/4+VR	G-IV	15.09.1975
5.	SRs 1200x 24/4+VR	G-V	23.12.1975
6.	SRs 1200x 24/4+VR	G-VI	22.10.1976
7.	SchRs 630x25/6	G-VII	5.08.1977
8.	SRs 1300x 26/5+VR	G-VIII	07.1987
9.	SchRs 1760x32/5	G-IX	15.06.1990; 21.10.2010
10.	SRs 1301x 24/2.5+VR	G-X	12.3.2008
11.	A ₂ RsB 3500x60+BRs	O-I	1.10.1967
12.	A ₂ RsB 3500x60+BRs	O-II	20.1.1969
13.	A ₂ RsB 3500x60+BRs	O-III	15.9.1975
14.	A ₂ RsB 3500x60+BRs	O-IV	23.12.1975
15.	ARs1600x(37+33+60)x18	O-V	11.6.1981
16.	ARs1800/(14+33+60)x20	O-VI	1991
17.	BRs(Ars)1600/(28+50)x 15BW)	BW -1	10.1987
18.	BRs(Ars)1600/(28+50)x 15 нови	BW-2	05.2010
19.	EŠ-5/45	21	1965
20.	EŠ-5/45	22	1966
21.	EŠ-5/45	23	1969
22.	EŠ-6/45	27	1961/1981
23.	EŠ-6/45	29	1986
24.	EŠ-6/45	31	1981/1992
25.	EŠ-10/70	10	1982/1985
26.	EŠ-10/70	11	1966/1988

osnovna oprema pk polje D

Figure 2. Basic equipment at Field D

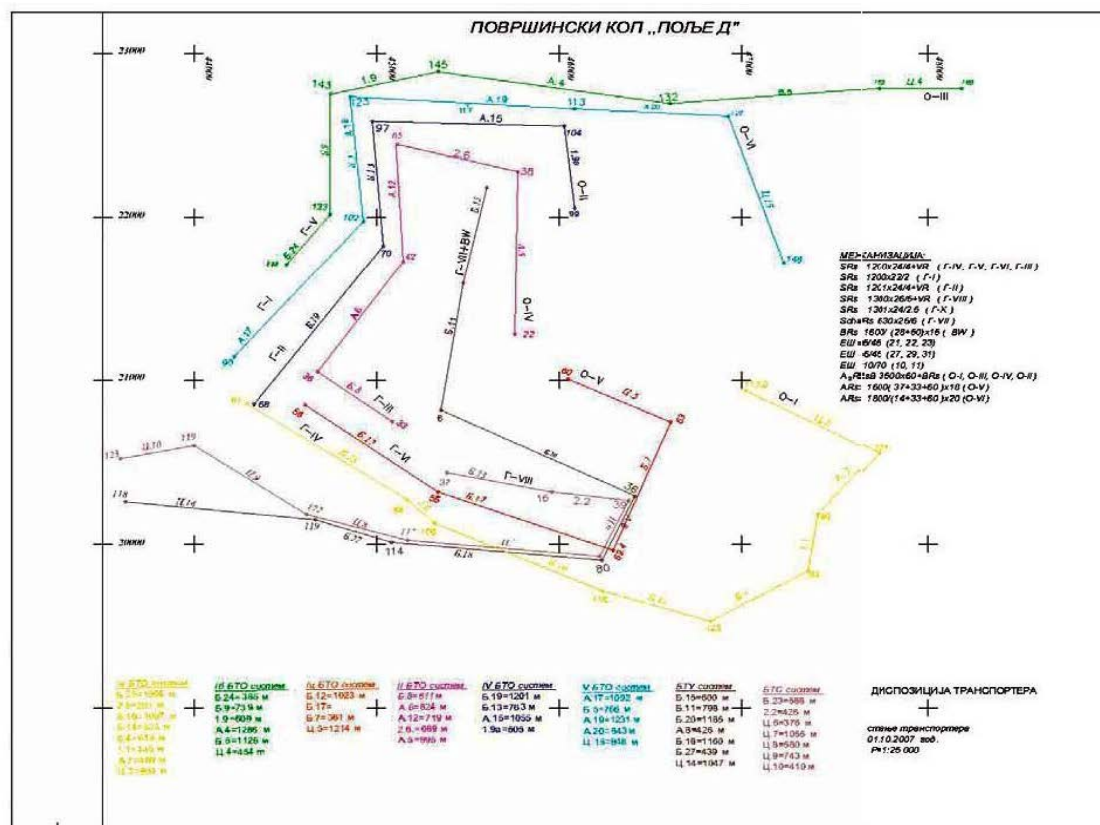


Figure 3. Overview of systems position at Field D prior to dislocation

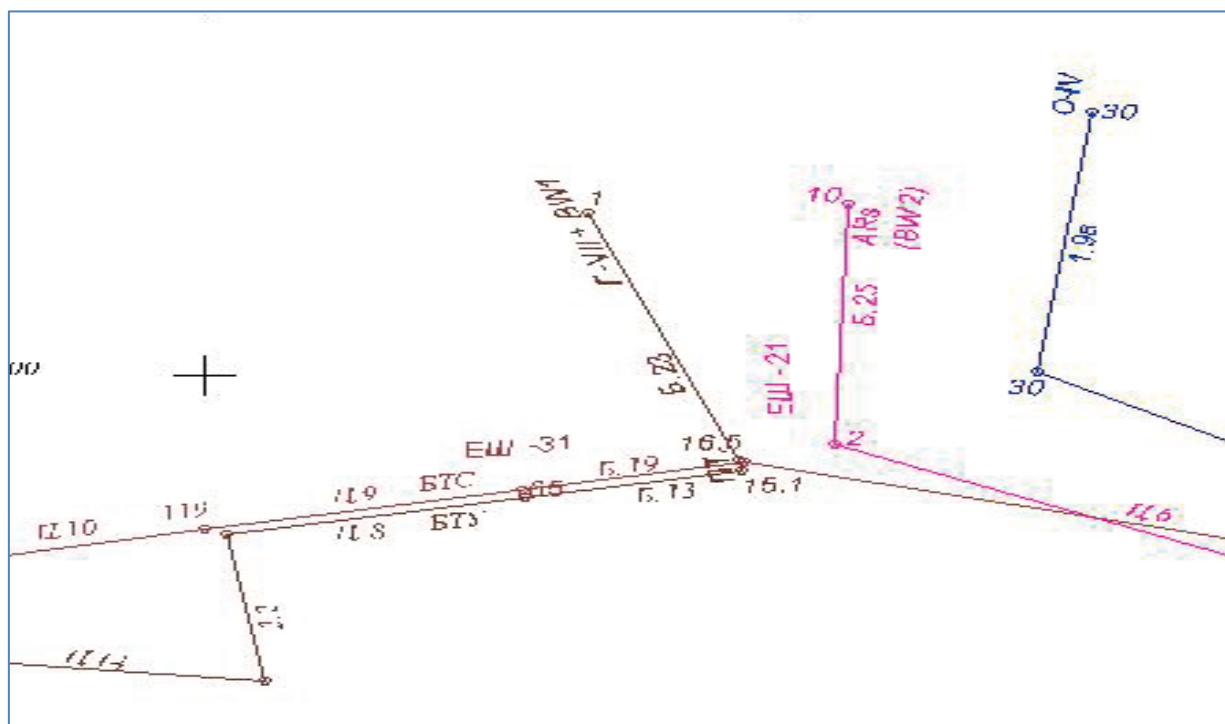


Figure 4. Conceptual solution of dislocation for coal systems at new ramp

4. DINAMIC OF CONTINUAL SYSTEMS DISLOCATION

In 2007-th at “Field D” Ia ECS system was stopped and relocated within 14 days on southern part (South Wing) where he started to work on area planned for further extension of “Field D”. System starts to work on 29-th November 2007, and instead bucket wheel excavator G-4, other buckler wheel excavator G-1 was engaged. Along with G-1 worked spreader O-1, and G-4 remained at position of V-th system for overburden.

During 2008, due to completing of works in contour of “Field D”, Ib ECS system also stopped. Reconstruction and total relocation of this system lasted 12 days, and on 2-nd of April works begun on outer dumping area, formed in previous times during opening of “Field D” in 1961. on so called “Eastern dump”, with the work of bucket wheel excavator G-6 and spreader O-5.

In 2009, after of 19 days for relocation and transportation of mechanisation, Ic ECS system starts to work on Eastern Dump on 9-th August, with bucket wheel excavator G-5 and spreader O-3.

Second ECS system was also relocated in 2009 within 11 days. This system started to work on 2-nd April on position of ex dump area from IV ECS system, eg. Inner dumping area of “Field D”.

Forth ECS system was relocated and mechanisation was transported for 12 days, and on 2-nd November it started to work extending “Field D” toward south.

After 14 days of transportation of mechanisation on 25-th May started to work relocated V ECS system with bucket wheel excavator G-4 and spreader O-6 in position of eastern Dump.

Coal systems ECL and ECC were relocated during annual repairment and without additional delay in coal production.

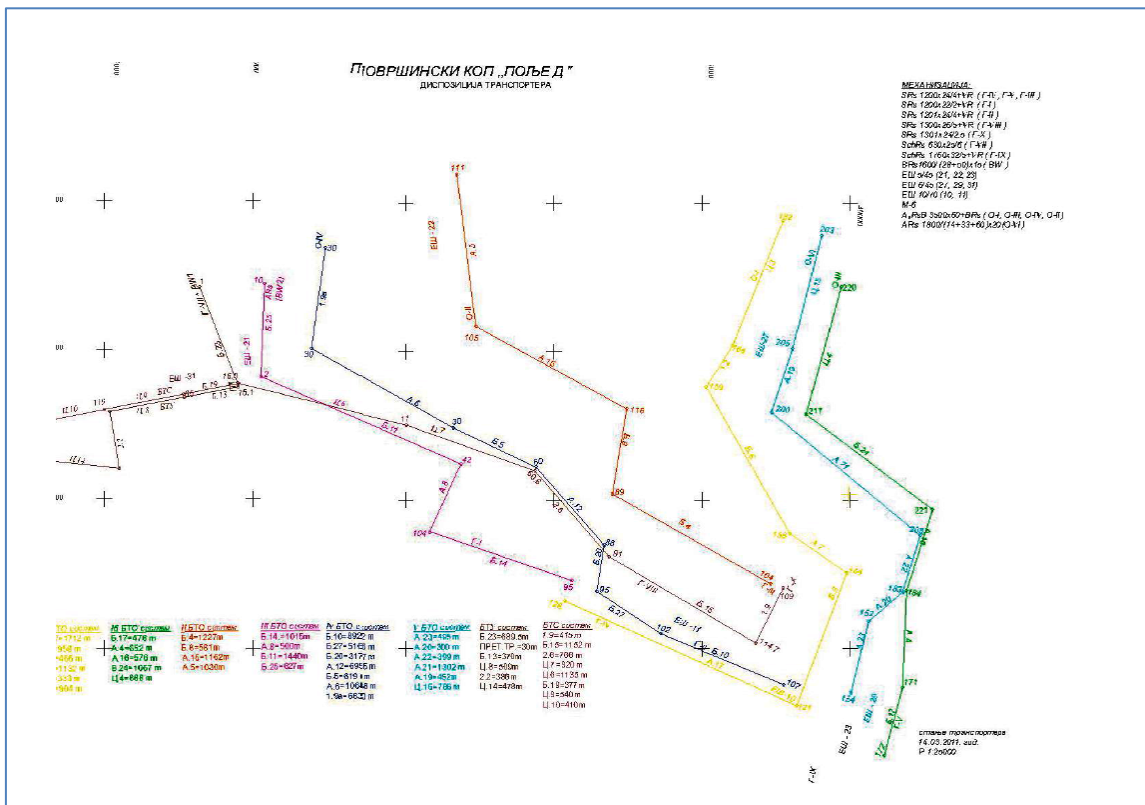


Figure 5. Position of continual systems at “Field D” after dislocations

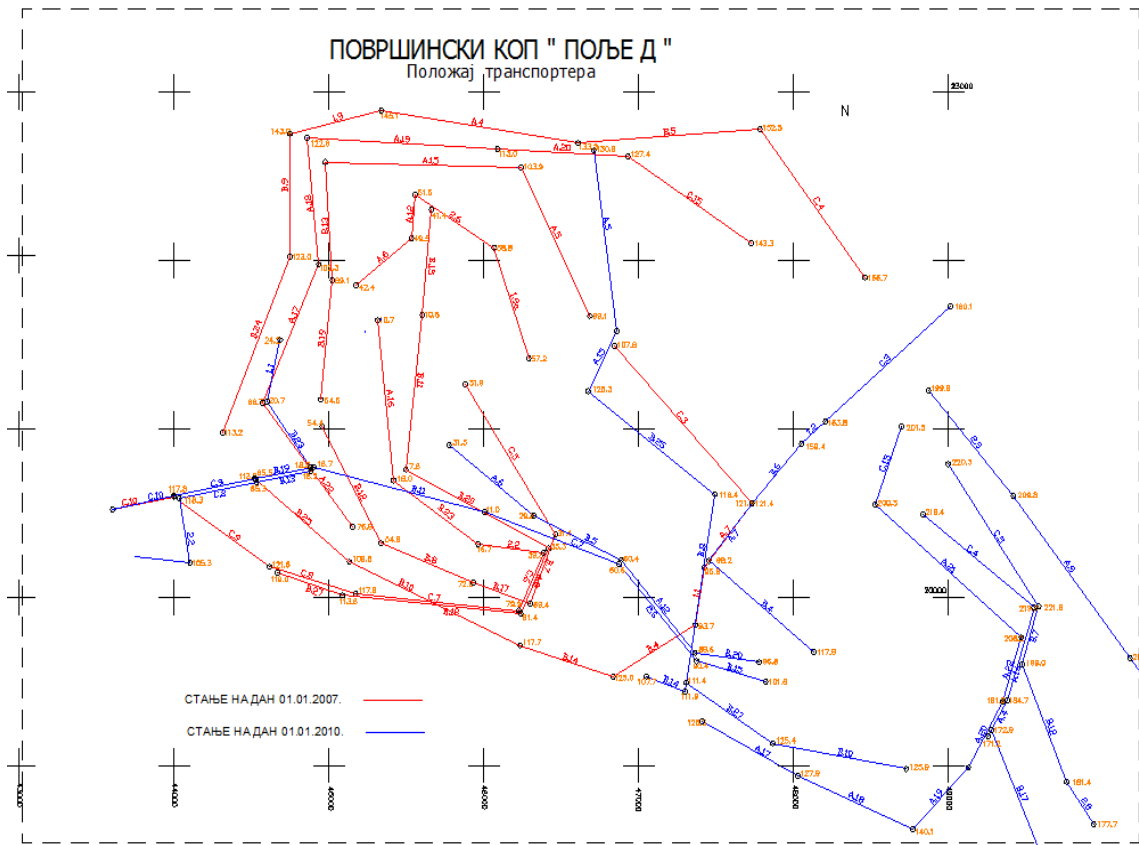


Figure 6. Position of continual systems at “Field D” prior and after dislocation

During preparation works for dislocation of systems between December 2007 and June 2009 surveying department at “Field D” executed 4411 recordings and marking of the routes for belt conveyers positioning and routes for mechanisation transportation. More than one million cubic meters of material was moved for earthy works on ramps and for the 35 kilometres of routes for mechanisation transportation and new conveyers positions.

Five bucket wheel excavators and four spreaders were transported over 60 kilometres, and overcome difference in height of 1100 meters. As for the routes of belt conveyers, 25 kilometres were dismantled and put in new position. Also, 46 power stations were disconnected and pulled and carried more than 200 kilometres to the new working positions.

50 kilometres of rails were dismantled and resets, 11 thousand pontoons, 4 thousand frames, 60 kilometres of rubber belts was shifted and more than 600 vulcanisations was done, 100 kilometres of high and low voltage were moved for systems relocation. Around 25 kilometres of new access roads were made with more than 100 000 m³ of stone aggregates.

In period from December 2007 to June 2009 in total 939 technological operations were conducted.

CONCLUSION

Economic-finance result of system’s dislocation at “Field D” is basic measure of justification and success. All works were done based to the conceptual solution of management in Kolubara and without expenses for outer services for development of technical documentation.

Planning and organisation of works for system’s dislocation was done by management of Mines Kolubara, and all work were carried with permanent employees from “Field D”. Coal production on this open cast mine wasn’t stopped, and production ratio, in last year of dislocation, was 99,32%, and plan for overburden systems, beside a delay of 82 days, was achieved with

111,48%. Minimal number of auxiliary machinery was engaged from extern public companies and private ownerships for dislocation's work.

Consequences from dislocation of systems and mining activities after are possibility for excavation of 8 million tons of coal on southern part of "Field D" and connection of belt conveyers transporting systems from "Field D" and "Field B". All of this was meaningfully for stabilisation of coal production and achievement of electro-energy balance in Republic of Serbia and long-time economic-finance benefit.

Calculation:

$$\begin{aligned} 1,5 \text{ kg of coal} &= 1 \text{ kWh electric energy} \\ 8 \text{ million tons of coal} &= 8 \text{ billion kg} / 1,5 = 5,33 \text{ billion kWh} \end{aligned}$$

$$\begin{aligned} 1 \text{ kWh} &= 0,05 \text{ euro} \\ 5,33 \times 10^9 \text{ kWh} \times 0,05 \text{ euro} &= 266,6 \text{ million euro} \end{aligned}$$

Dislocation of systems at "Field D" enabled gross finance-economy benefit of **266,6** million euro.

REFERENCES

[1] Technical documentation Kolubara Coal Basin, Lazarevac, (2007-2009)

A Real-Time Event-Driven Database System for Maintenance Planning and Productivity Analysis in Continuous Surface Mining Operations

Zach Agioutantis¹, Stamatini Delmadorou², Nikos Steiakakis², Chrysanthos Steiakakis² and Stergios Papaterpos³

¹Dept. of Mining Engineering, Univ. of Kentucky, 230 Mining & Minerals Resources Bldg., 504 Rose St., Lexington KY 40506-0107, USA

²Geosysta Ltd, Kountouriotou 7, Melissa, 15127 Athens, Greece

³Public Power Corporation, Athens, Greece

ABSTRACT

This paper presents a real-time event driven data management tool, which was developed as a Productivity and Maintenance Planning Tool for the surface lignite mines in northern Greece. The mines operate using a continuous mining system, utilizing bucket wheel excavators, conveyor belts, spreaders and stackers. Each mine features its own control center installation comprising of PLCs, Aspect Servers, OPC servers and a SCADA system. The data management system is installed on the network backbone and draws data from the OPC servers. Data are automatically populated by events and data polls and can be subsequently modified by control tower personnel. Reports are typically generated on a daily basis for production monitoring, productivity, equipment performance and utilization as well as maintenance tasks. The system has been operational since 2011.

1. INTRODUCTION

Currently, about 20-30% of the electric power generated in Greece is from lignite-fired thermal power plants. The Public Power Corporation (PPC) of Greece currently mines lignite in two different mining areas. The most extensive center is located in northern Greece and comprises of four separate mines, while the other is established in southern Greece consisting of one single mine. Both mining centers mine lignite predominantly using the continuous surface mining method which utilizes bucket wheel excavators (BWEs), an extensive belt conveyor network to transport the excavated material, and spreaders for dumping the waste material. In addition, the mines operate coal bunkers using stackers and reclaimers. Mines may be interconnected so that they can share resources.

In terms of maintenance planning and productivity analysis of the mining operation, industrial automation and control systems have been installed in certain lignite mines of the northern mining center. The South Field Mine operates two complete Supervisory Control and Data Acquisition (SCADA) systems, and each of the Kardia Mine and the Mavropigi Mine operate a separate SCADA system.

Similar remote-control systems have been utilized at several mines throughout the world in order to keep a track of and evaluate the entire mining execution process. The De Beers Finsch underground kimberlite mine, located in South Africa, serves as an excellent example of mine planning and automation system integration. By implementing a series of management and control systems related to the automation of load-haul-dump (LHD) units, the shift production schedule, the access control as well as the SCADA system, the De Beers Finsch mine personnel have succeeded to ensure the sustainability of the underground mine in the most profitable and cost-effective manner [2].

The international literature also includes examples of the implementation of such control systems that apply to auxiliary mine operations. For instance, the Suvodol Coal Mine, part of the

Mine Power Complex 'Bitola' in Skopje, has installed an automation system to manage and control the drainage system of the area in order to ensure the capability to sufficiently extract the coal ore. Thus, a control and monitoring system has been implemented to each of the drainage well stations consisting of a custom-made SCADA system, frequency inverters, programmable logic controllers, wireless communication devices and process instrumentation [3].

The widespread implementation of such automation systems into the mining industry confirms the importance and the necessity of their existence in order for the mining operations to be developed in terms of safety and profitability. Up to now due to the high installation and maintenance costs of industrial automation systems, their application was limited to large operations. Open systems are slowly entering the industrial automation arena aiming to provide lower cost solutions to small size industries [4, 5].

2. OVERVIEW OF THE INSTALLED INDUSTRIAL AUTOMATION AND CONTROL SYSTEM AT PPC

The PPC lignite mines in northern Greece employ an industrial automation and control system being hosted by a control tower in each mine. The fundamental function of that system is to allow equipment control and monitoring through a SCADA system. More specifically, Programmable Logic Controllers (PLCs) are installed on mining equipment, which serve both to control the equipment and at the same time generate data related to equipment operation as well as potential equipment failure. Such data are transferred to a central connectivity server and then made available to other systems. Each PLC system is typically driven by a single controller, while controllers are managed by multiple control networks in order to optimize information throughput. The central connectivity server (OPC), receives the event data generated by PLCs and produces user accessible data which can be used for visualization or stored for further processing. Due to the large number of PLCs in these systems there are two OPC servers installed in each system to balance the load. For redundancy each OPC server is duplicated so there are four OPC servers installed at each mine [1].

3. DEVELOPMENT OF A PRODUCTIVITY AND MAINTENANCE PLANNING TOOL

An event-driven data management tool was developed to manage the data received from the PLCs through the OPC servers and utilize them for productivity reports and maintenance management and reporting at the PPC mines. This Productivity and Maintenance Planning Tool application (named PET) was built around a database server. The database is populated by data and events received from the OPC servers through a dedicated utility program (dxserver). The database and database server sit on the network backbone. The data collected by the PET system is managed through a Windows application. Multiple windows clients can access the database server using client/server technology [1]. A brief overview of the entire network topology is schematically depicted in Figure 1. Figure 2 shows the SCADA system for one of the PPC mines, while Figure 3 presents the visual interface of the PET system. The visual interface is a Windows based application, which tracks data flow, allows data management and generates numerous reports either print-formatted or as excel spreadsheets. The application is fully parametric and allows mine personnel to customize the parameters tracked for each mine as well as several reporting features.

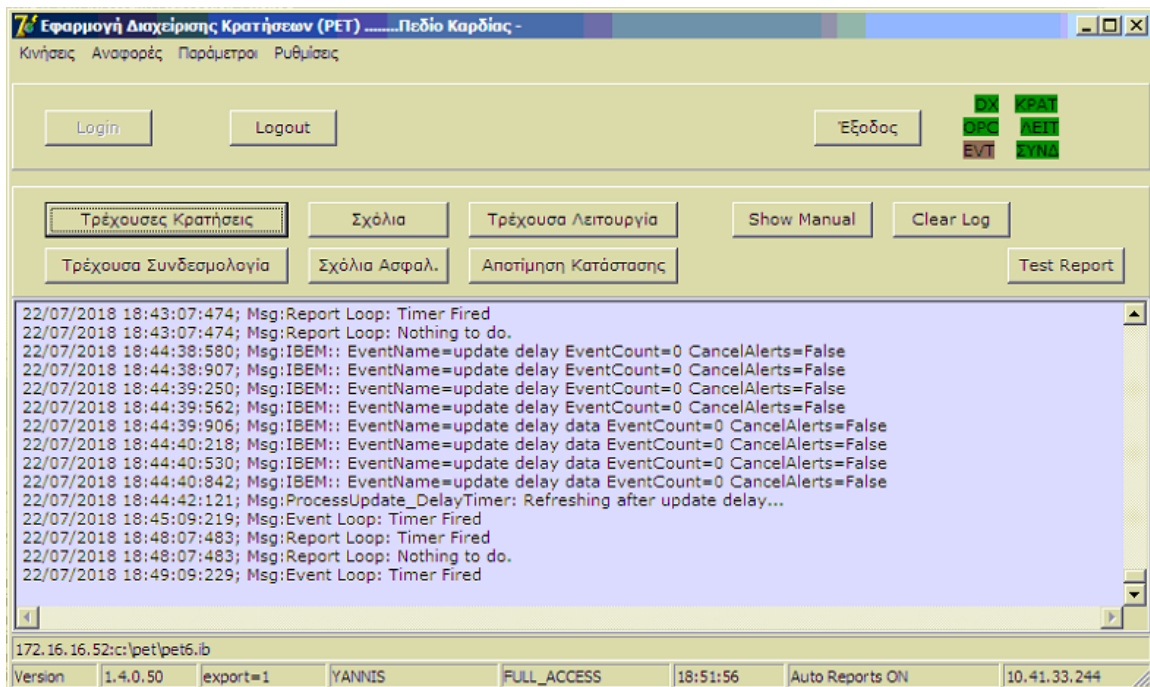


Figure 65. The user interface for the front-end windows application.

4. ENHANCING PRODUCTIVITY AND MAINTENANCE PLANNING AT THE PPC MINES

The program features a number of windows forms, through which the control tower operators can modify the data, enter comments, and/or delete records, which have been erroneously recorded. All forms are color coded (Fig. 4) to ensure easy access to the data by the control tower operators. The windows forms also provide different views such as a summary view, a detailed view, access to historical records per equipment unit, access to historical records per group of equipment (branch) as well as other grouping and sorting options.

Using these tools, it is very easy to identify repeated equipment failures or patterns within equipment or branch downtimes with respect to location, connectivity between branches, and even excavated / transported material. In addition, control tower operators can identify problems with PLC operation (erroneous timestamp after extreme weather events and other issues). They can also identify the distribution of failures in specific equipment parts (i.e., electrical motors, conveyor belts, etc.).

The application features a number of reporting options as shown in Figures 5 and 6. Figure 5 presents a grid of one of the main productivity and maintenance reports, where downtime conditions for each equipment unit are reported in detail (start and stop times, cause of delays or failures, etc.). This report can be generated on a per shift basis, on a daily basis, as well as for any period spanning a number of days (typically on a monthly basis) so that the mine personnel can get an overview of typical delays and causes for delays for the different equipment units. Figure 6 is one of the reports which details comments for every recorded failure. These comments are entered by the tower operators and give specific details on what caused the downtime or failure, on what actions have been taken on that particular shift to restore the unit, and potential instructions to the maintenance crew on additional maintenance needed. This report can also be generated on a per shift basis, on a daily basis as well as for any number of days. The program can also generate a number of charts that show production per bucket wheel excavator as a function of time, as well as production rates (tonnes per hour) for the BWEs (Figures 7 and 8). Production rates can be calculated using different

techniques (i.e., moving average, instantaneous production rates, etc.). The data can be used to track production from a specific bench as well as the productivity of equipment set up.

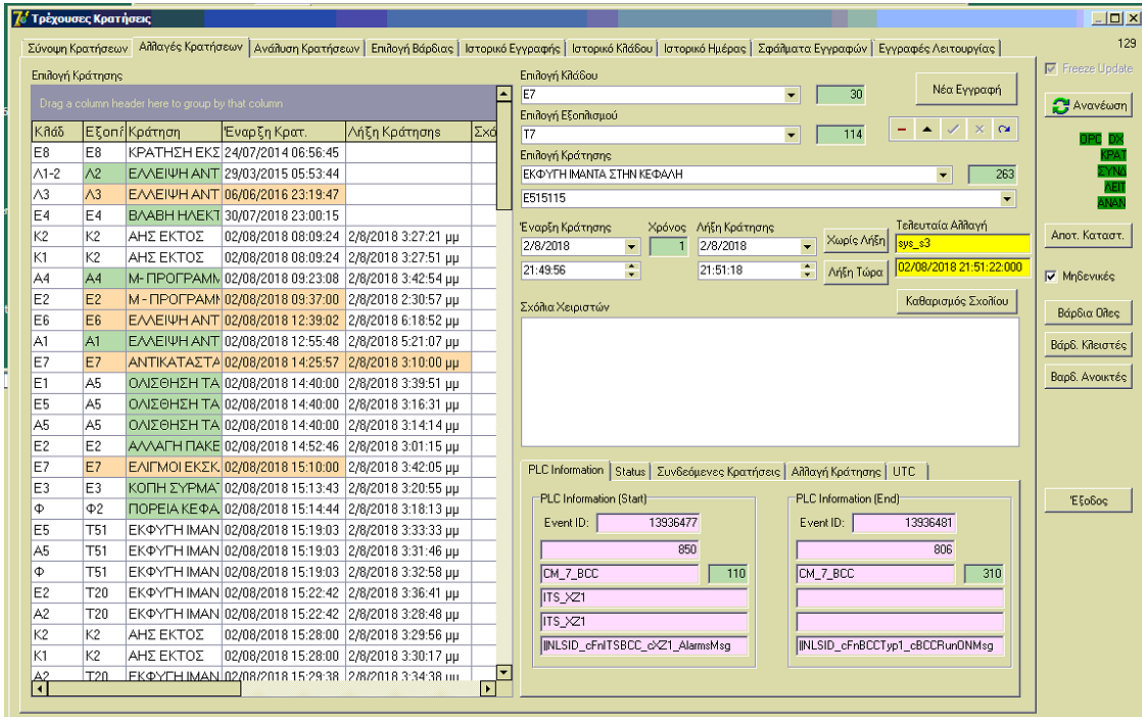


Figure 66. Main interface form where tower operators manage records of equipment failures.

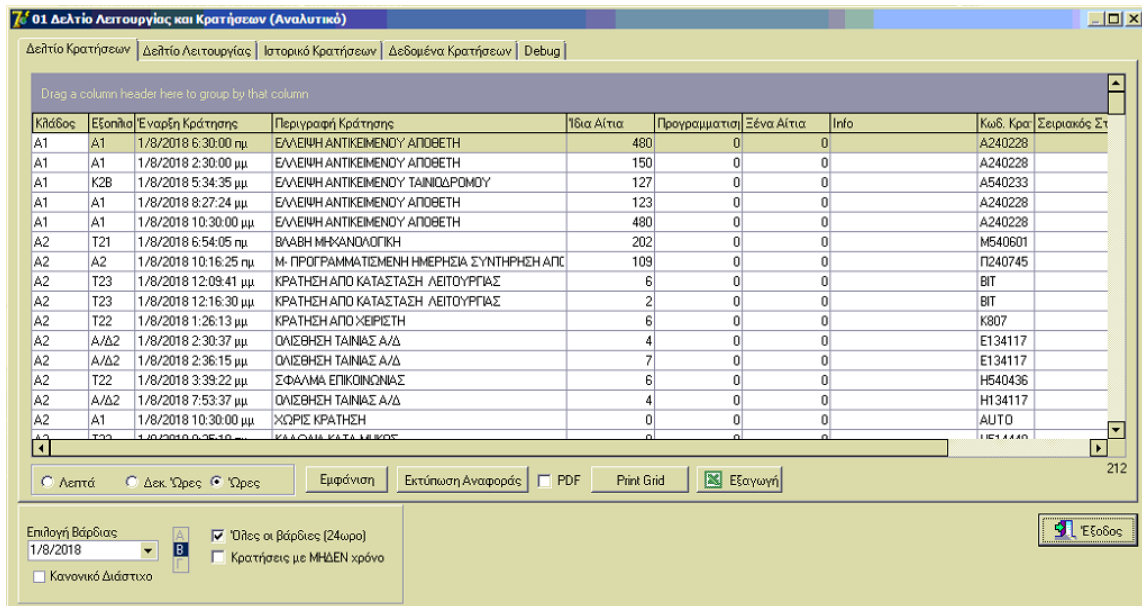


Figure 67. Grid view of the one of the main productivity and maintenance reports.

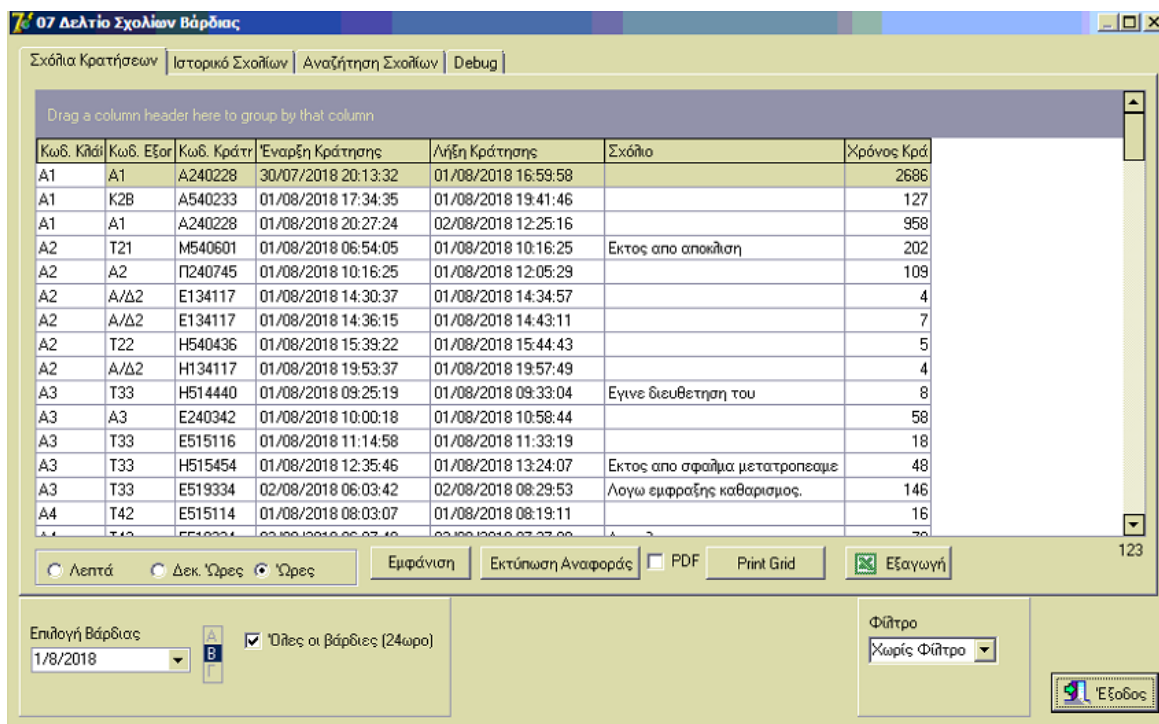


Figure 68. Grid view of one of the reports used to schedule maintenance operations.

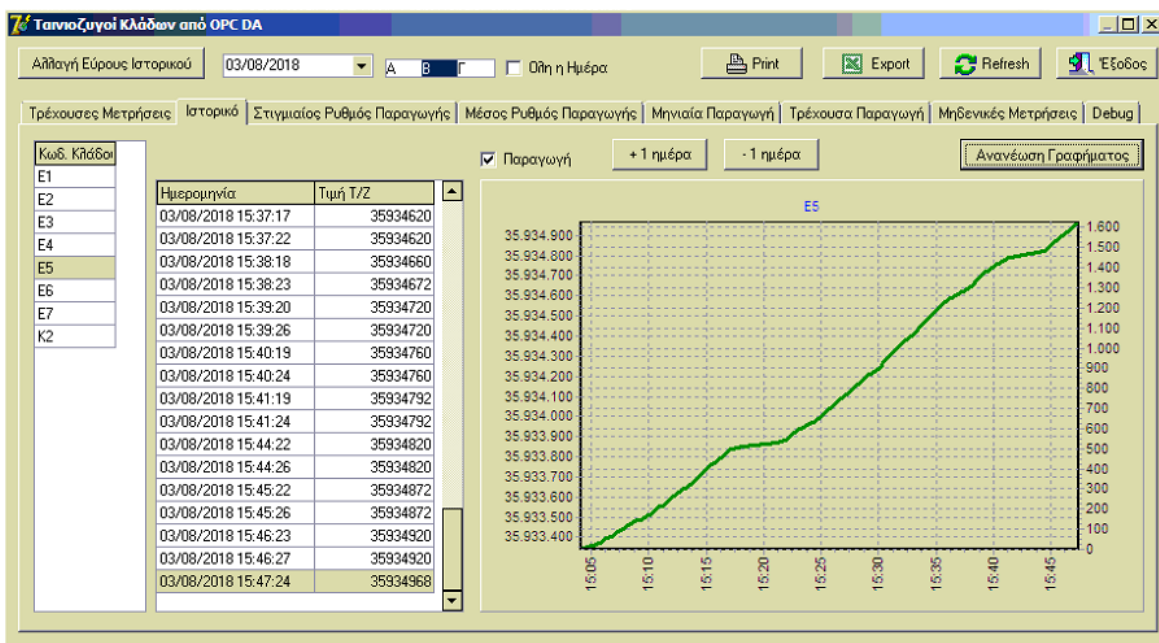


Figure 69. Total production in tonnes (left column on chart) and shift production (right column) for one BWE.

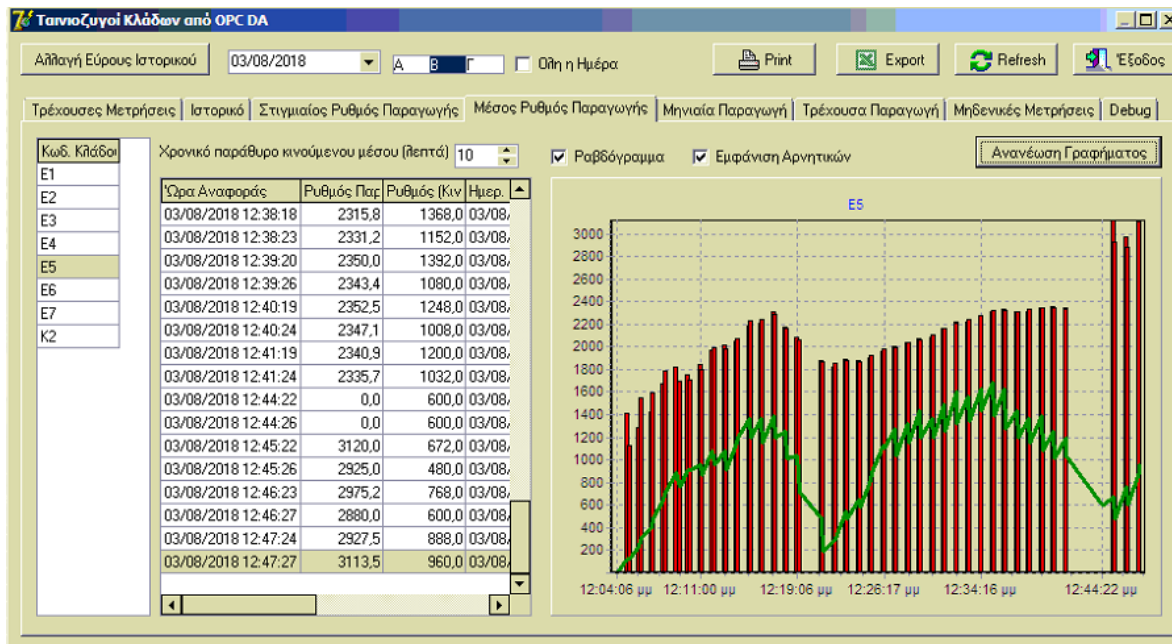


Figure 70. Average and instantaneous production rates per shift per BWE

A number of printable reports is automatically e-mailed to key mine personnel on a daily basis. E-mailed reports are fully customizable, including report type, report generation time, list of e-mail recipients, etc. Electronic reports are typically dispatched at the beginning of the first shift so that maintenance crews can be optimally utilized.

5. CONCLUSIONS

The data acquired and managed by this Productivity and Maintenance Planning Tool provide the mine personnel with a powerful decision support system. Some of the benefits realized by the development, installation and improvement of this tool is the accurate representation of production time and downtimes (delays due to equipment failure, or other reasons) as these times are automatically recorded through events and data generated by the OPC servers. In previous systems which were installed at PPC mines, such data were manually recorded by the control tower operators and in many cases there were considerable discrepancies between recorded times and actual times. In addition, mine personnel have instantaneous access to historical data for all types of failures (electrical, conveyor belts, mechanical, mining related, etc.). In the coming months this tool will be enhanced by providing additional capabilities to manage maintenance of specific equipment such as motors, electrical transformers, etc. This additional module (MMS) will interface directly with the existing system and it will reside on a separate server that will provide access to a different group of personnel dealing exclusively with maintenance issues. It is anticipated that this added capability will streamline maintenance operations and considerably reduce maintenance costs.

This Productivity and Maintenance Planning Tool can easily be adapted for other continuous and interlocked systems related to the mining industry such as thermal power stations, mineral processing facilities, cement processing plants, etc.

REFERENCES

- [1] Agioutantis, Z. & Papaterpos, S. (2015). A real-time event driven data management application for equipment monitoring in continuous surface mining operations. AIMS Conference, May 27-28, 2015, Aachen, Germany, pp. 19-30.

- [2] Burger, D.J. (2006). Integration of the mining plan in a mining automation system using state-of-the-art technology at De Beers Finsch Mine. *The Journal of The South African Institute of Mining and Metallurgy*, August 2006, 106.
- [3] Blazeski, G. & Dilevski, V. (2013). Automation System for the well drainage system at Coal Mine “Underlying Seam Suvodol”, Mining Power Complex Bitola. 5th Jubilee Balkanmine Congress & Commercial Exhibition, Ohrid.
- [4] Merchan, D.F., Peralta, J.A., Vazquez-Rodas, A., Minchala, L.I. & Astudillo-Salinas, D. (2017). Open source SCADA system for advanced monitoring of industrial processes. 2017 International Conference on Information Systems and Computer Science, Quito, Ecuador.
- [5] Lakshmi, A., Sangeetha, B., Naveenkumar, A., Ganesh, B. & Bharathi, N. (2012). Experimental Validation of PID Based Cascade Control System through SCADA-PLC-OPC Interface. 2012 International Conference on Computer Communication and Informatics (ICCCI–2012), Jan. 10-12, 2012, Coimbatore, INDIA.

Methods of Decreasing of Bucket Wheel Excavators Failures Working In Soils Including Unmineable Intrusions

Adam Bajcar, Marek Onichimiuk, Anna Nowak – Szpak and Marian Wygoda

“Poltegor – Instytut” Instytut Górnictwa Odkrywkowego, ul. Parkowa 25, 51-616 Wrocław, Poland

ABSTRACT

The article presents the work carried out in the Poltegor Institute, which aims to reduce the number of failures of bucket wheel excavators operating in soils including unmineable intrusions. This will be achieved by adaptation of bucket wheel excavators already in service and newly built to for exploitation in such conditions, monitoring of the load bearing capacity of a bucket wheel excavator, developing a diagnostic signal analysis method for current superstructure damage hazard assessment and continuous endurance monitoring.

1. INTRODUCTION

In existing as well as newly opened lignite mines there are more difficult mining conditions, mainly caused by the occurrence of unmineable inclusions and structures with excessive digging resistances in the overburden. In such conditions high dynamic loads as well as impulse ones occur during exploitation.

As a result of the unfavourable phenomena mentioned above, in the "Poltegor-Institute" works aimed at a comprehensive solution to the problem of increased failure of excavators exploited in hard-mineable soils were undertaken. One of them is project financed by the Research Fund of Coal and Steel and the Ministry of Science and Higher Education entitled “Bucket wheel excavators operating under difficult mining conditions including unmineable inclusions and geological structures with excessive mining resistance - BEWEXMIN”. The project is being carried out jointly with three industrial partners: PGE Górnictwo i Energetyka Konwencjonalna SA, Oltenia Energy Complex from Romania and Public Power Corporation from Greece, who in their respective countries are the largest producers of electricity from lignite. In addition, the following universities and research institutes participate in the project: VUHU Výzkumný ústav pro hnědé uhlí from Czech Republic, Technical University of Crete, National Technical University of Athens, University of Petrosani and KOMAG Mining Technology Institute.

The BEWEXMIN project is divided into three work packages that are interrelated and form a complete set of activities pursuing the same goal, which is to reduce the failure of bucket wheel excavators in difficult mining conditions [1]. These work packages are described below:

1. Optimal adaptation of currently exploited and new bucket-wheel excavators for mining of overburden including interlayers with excessive mining resistance and unmineable inclusions.
2. Monitoring system of bucket wheel excavator load carrying structure efforts and method of diagnostic signals analysis for current assessment of threats of load carrying structure damages as well as constant control of residual strength of the structure
3. Real-time mine-face inspection system, based on geophysical methods, capable to detect hard rock inclusions and geological formations which are difficult to be excavated by bucket-wheel excavators

2. OPTIMAL ADAPTATION OF CURRENTLY EXPLOITED AND NEW BUCKET-WHEEL EXCAVATORS FOR MINING OF OVERBURDEN INCLUDING INTERLAYERS WITH EXCESSIVE MINING RESISTANCE AND UNMINEABLE INCLUSIONS

2.1. Impulse load

The aim of the first working package is to determine the requirements for the construction of bucket wheel excavators working in soils containing unmineable intrusions and interlayers with excessive mining resistances to obtain as low dynamic loads as possible and proper resistance of the excavators' superstructures to these loads [2].

As part of the above task, a number of theoretical and practical works are carried out, which include, among others:

- development of a mathematical model of a bucket wheel excavator mining system with special consideration of the impulse load model,
- determining, on the basis of tests on real machines, the maximum values of stresses in the load-bearing structure from impulse loads during mining the soils with unmineable inclusions and the stress coefficient of mass vibrations as a function of excavated soils properties,
- development of a method for determining the design replacement force, allowing proper inclusion of impulse loads in the strength calculations of the load-bearing structure.

In work package 1, a theoretical analysis of the dynamic load of the bucket wheel boom resulting from the impact of the bucket into unmineable obstacle was also carried out. In the considerations, the quasi-static Hertz theory was adopted, taking into account local plastic deformations and the scattering of excited elastic vibrations during the impact. For the simulation tests describing the collision of the bucket wheel with a unmineable obstacle, the impulse load model was proposed (Fig. 1), in which the magnitude of the load increase in time and depends on the rotational speed of the bucket wheel, which during the first phase of the collision decreases from the nominal value to zero. The moment of immobilization of the wheel, resulting from the course of the simulation, marks the end of the first phase of the collision, when all the pulse energy is used for elastic and plastic deformation. In order to prevent a sudden change of the contact force, which may cause occurrence of vibration in the simulations resulting from the equation integration procedure, the variation of the contact force in the second phase of the collision according to the dependence (1) was assumed in the model of the impulse load.

$$P_I(t) = \begin{cases} 0 & \text{for } t > t_0 \\ K \left[\sin \left(\frac{\pi}{2} \frac{\varphi_{kn} - \varphi_k}{\varphi_{kn}} \right) \right]^{10-p} (t - t_0) & \text{for } t_0 \leq t \leq t_I \Rightarrow \varphi_k = 0 \end{cases}$$

$$P_{II}(t) = \begin{cases} P_I(t)_{\max} - K(t - t_I) & \text{dla } t_I < t \leq t_{II} \Rightarrow P_{II}(t) = 0 \\ 0 & \text{dla } t > t_{II} \end{cases} \quad (1)$$

where:

φ_k - angular speed of the bucket wheel,

φ_{kn} - nominal angular speed of the bucket wheel,

$P_I(t)_{\max}$ - maximum value of the contact force resulting from the simulation run for the first value $\varphi_k = 0$ after time t_0 ,

K - initial speed of value load increase,

t_I - end time of the first phase of the collision, from the simulation run, for the first value $\varphi_k = 0$ after the time t_0 ,

t_{II} - end time of the second phase of the collision, from the simulation run for the first value of $P_{II}(t) = 0$.

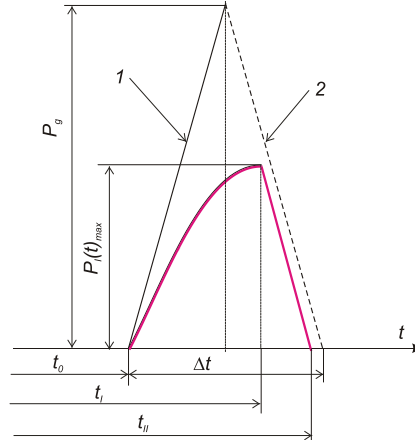


Figure 71 Schematic model of the bucket wheel's impulse load proposed for simulation tests

Where: 1.2 - straight line with a directional coefficient, K and $-K$ respectively

The rate of load increase is largely dependent on the size of the digging mechanism. As a measure of this size, one can use the power of bucket wheel drive. Therefore:

$$K = K_N N_s \quad (2)$$

Where: K_N - normalized value of the initial rate of the load increase, N_s - power of the bucket wheel drive motor.

Starting from the above-mentioned data taken from [3] and taking into account different nature of the variation of contact force a value of normalized initial increase rate of contact force equal to 68 kN/(s·kW) can be assumed. Verification of this value requires further experimental testing.

In order to achieve the objective of the WP-1 work package, i.e. to reduce the failure of bucket wheel excavators working in hard workable soils or in soils containing non-mineable inclusions, it is necessary to determine the maximum design loads of the excavator load structure from pulse loads.

During the impact of bucket into unmineable obstacle the actual load may exceed what was assumed in the machine design process. As part of the first work package, a method was proposed for determining the dynamic surpluses in the excavator's load-bearing structure elements during impact on such structures. The maximum size of the impulse occurs when the bucket and associated rotating elements of the mining mechanism are completely stopped after collision with obstacle. Then this impulse gives to the end of the bucket wheel kinetic energy equal to:

$$E_k = \frac{m_g}{2} \left(\frac{J_u \cdot v_0}{J_u + m_g \cdot R^2} \right)^2 \quad (3)$$

Where: E_k - bucket wheel kinetic energy before impact, J_u - the mass moment of inertia of rotating masses reduced to the bucket wheel axis, v_0 - circumferential cutting speed, R - bucket wheel radius.

It can be assumed that when the maximum deformation occurs, it is transformed in its entirety and the deformations caused by this in the individual members of the structure are equal to the stresses caused by the static force applied at the point of the impulse's operation. This force can be determined from the condition of obtaining the same value of the energy of the elastic deflection of

the boom as given kinetic energy during the impulse loading. The value of this static force is then expressed by the dependence:

$$F_s = \frac{J_u \cdot v_0}{J_u + m_g \cdot R^2} \sqrt{\frac{m_g}{\Delta_w}} \quad (4)$$

Where: F_s – The value of force in the place of the impulse, Δ_w - deflection of the boom in the bucket wheel axis.

It can be assumed that inaccuracies of the simplifications made will be compensated by an experimentally determined correction factor. Hence, the generalized force in the i -th bar of the structure caused by the impact will is:

$$S_{ui} = S_{1i} \cdot F_s \cdot k_{ui} \quad (5)$$

Where: S_{ui} – generalized force in the i -th bar, S_{1i} - generalized force induced by unitary force with the direction of the impulse, k_{ui} – correction factor.

2.2. Determination of the Bucket Wheel Suspension Stiffness

Determination of the bucket wheel suspension stiffness aims to determination the value of the coefficient of elasticity of this boom. This coefficient is one of the parameters necessary to determine the impact impulse from hitting a not workable obstacle by a bucket. The theoretical maximum value of this impulse results from the kinetic energy of the rotating components of the bucket wheel drive and the energy of elastic deflection of the bucket wheel boom.

The stiffness of the bucket wheel suspension can be determined on the basis of the bucket wheel boom deflection under the influence of the force acting vertically on the boom. For a real machine, this deflection can be determined experimentally or calculated theoretically.

This article describes the methods adopted for determining the stiffness of the bucket wheel boom of the K45 bucket-wheel excavator. Then, the obtained values of deflection of the bucket wheel boom are presented in an experimental and theoretical manner. At the end, the results obtained with both methods are compared.

Experimental Methods

One of the methods of experimental determination of the value of the bucket wheel coefficient of elasticity is the measurement of the boom deflection under the influence of force of a known value, which loads the bucket wheel. For this purpose, one of the following two methods can be used:

Method 1 is a method of direct measurement of deflection (f) of the bucket wheel boom under the influence of vertical force (F) from the known weight (see Fig.2). The deflection (f) is in this case the difference (Δy) between the distance (y_0) between the unloaded bucket wheel boom and the ground and the distance (y) between the boom and the ground after loading the boom with force (F).

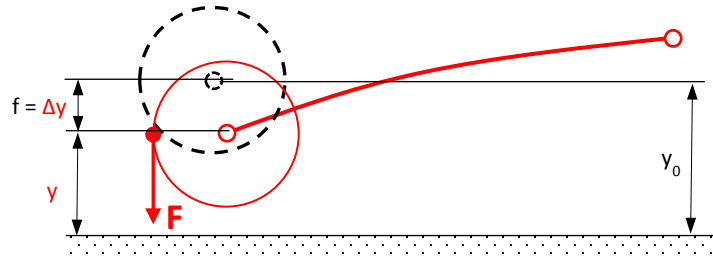


Figure 72 Diagram of boom deflection under the influence of vertical force

Technically, the first method involves installing a displacement sensor on the bucket wheel boom to enable the measurement of the bucket wheel axis distance to the ground and to attaching the weight to the bucket positioned in the horizontal axis of the bucket wheel, via a set of ropes and dynamometer, to enable the measurement of the force of weight loading the bucket wheel boom. Then, the load on the bucket should be lifted and lowered several times by means of a crane. When lifting and lowering the weight with a crane, the force value in the dynamometer and the distance between the bucket wheel axis and the ground are to be recorded simultaneously

Method 2 is an indirect method. It consists in measuring the angles of inclination of tangents to the boom deflection line under the influence of the force (**F**) of the bucket wheel attachment (see Fig. 3). The tangent values of the measured angles are the values of the derivative of the deflection line of the bucket wheel boom at the measuring points. After integrating the derivative thus obtained, we obtain a boom deflection line. Knowing the deflection line of the bucket wheel boom, we determine the value of the deflection (**f**). In this case, the force (**F**) can be invoked as in the first method or by means of the rope system by forcing force (**S**)

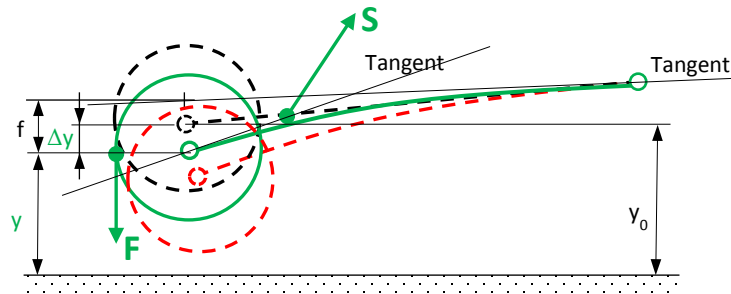


Figure 73 Diagram of deflection of the attached bucket wheel boom with winch force

Technically, the second method consists in installing tilt sensors on the bucket wheel boom. One of the sensors should be installed as close as possible to the axis of vertical movement of this boom, and the other possibly close to the axis of the bucket wheel. The remaining sensors should be placed on the bucket boom, between the two extreme ones. This is to enable measurement of the difference in the boom inclination between successive sensor locations. Then, the weight should be attached to the bucket positioned in the horizontal axis of the bucket wheel boom by means of a set of ropes and dynamometer. Then the set of ropes with the dynamometer should be tensioned and loosened several times through the movement of the hoisting winch of the machine vertical movement system. The inclinometer and dynamometer readings should be recorded simultaneously during tensioning and loosening of ropes with the dynamometer.

Method of Measurement

Method 1 directly gives the value of the boom deflection from the force of the load acting on the bucket. This is a big advantage of this method. However, it also requires the use of heavy equipment in the form of a crane. Moreover, it is necessary to freely hang the weight on the bucket.

Method 2 is an indirect method. It requires the possibility of measuring a small angle increment and performing integral calculations. This causes the method to be less accurate and requiring the use of fairly accurate tilt sensors. In comparison with the first method, however, it has such an advantage that it does not require the use of additional equipment in the form of a crane and does not require the weight hanging on the bucket. Thanks to this, the method is cheaper and easier technically and safer to implement.

Due to simpler technical implementation and greater safety, the second method has been selected (by us) to measure the deflection of the bucket wheel boom.

Inclinometers or acceleration sensors were considered as inclination sensors. We have inclinometers type B1N360V from Hans TURCK GmbH and type IS2A60P from GEMAC Chemnitz GmbH. In accordance with the data sheet, these sensors allow measuring the angle of inclination with a resolution not higher (not worse) than: 0.72" for the B1N360V sensor and 0.50" for the IS2A60 sensor.

Whereas, the B12/200 acceleration sensors allow measuring the acceleration with a resolution of 0.01m/s^2 , which allows you to measure the angle of inclination up to 30° : for vertical positioning of the sensor, with a resolution not higher (not worse) than 0.12° and for horizontal positioning of the sensor, with a resolution not greater (not worse) than 0.07° .

Measurement

Acceleration sensors have been selected for the measurement of the angle of inclination of the bucket wheel structure components. They enable the measurement of the angle of inclination with greater precision than the tilt sensors. The sensors have been set to work in a horizontal position using a special steel block.

Fig. 4 below shows the sensor installed at the measuring point 1a, on the upper surface of the lower flange. A tilt sensor was attached to the side of this flange, which served as a control. Sensors were attached to the structure via neodymium magnets.



Figure 74 View of the measuring point

All measuring sensors were located on the upper surface on the lower flange of the bucket wheel boom structure, at distances from the vertical movement axis of the boom, as shown in Fig. 4 below.

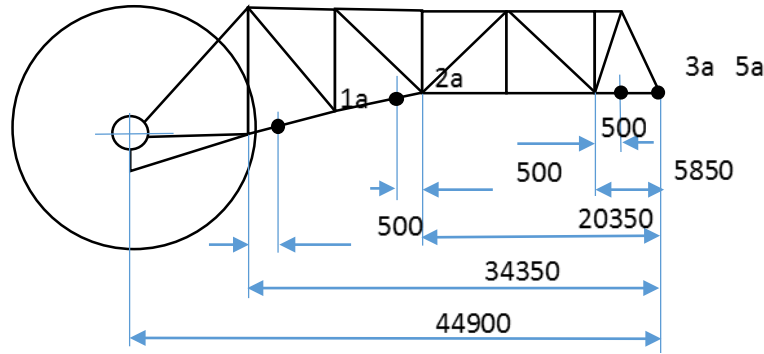


Figure 75 Diagram of distribution of measuring points

A load (bulldozer) was attached to the bucket via a U2A 20t force gauge, using sets of ropes (see Fig. 6). At the same time, it was tried to make the rope between the bucket and the bulldozer loading it vertically to the ground (ground).



Figure 76 Attachment of the auxiliary machine to the bucket

Using the winch of the excavator's bucket wheel boom rope system, the tension in the rope was induced. The force gauge readings for the measurement of the rope tension and the values of the acceleration sensor readings for the measurement of the boom deflection angles were read after stabilization of the load. Then, the loads were released, lowering the bucket wheel boom. After loosening the ropes connecting the bulldozer with the bucket, the readings of the measuring sensors were read. This operation was repeated 3 times.

During these operations, the readings of the acceleration sensors and dynamometer were recorded. The acceleration values were converted into the value of the structure angle of inclination at the measuring points. For the obtained values of angles of inclination, see Table 1 below. The increments of angles of inclination and their values in relation to the boom vertical movement axis were calculated on the basis of the difference between the values of the angles of inclination with the load and without the load (see Table 2). For the obtained increments, the corresponding tangent value (see Table 3) was determined, which was the value of the derivative of the deflection line at a given measuring point.

Table 1. Absolute readouts

a) Without load						b) Under load					
Point	1a	2a	3a	5a	F	Point	1a	2a	3a	5a	F
Item	degrees	degrees	degrees	degrees	kN	Item	degrees	degrees	degrees	degrees	kN
1	23.667	26.427	13.127	3.284	2.21	1	23.025	25.841	12.582	2.758	204.85
2	23.763	26.518	13.205	3.360	0.49	2	23.038	25.835	12.594	2.764	210.35
3	23.750	26.525	13.211	3.366	0.45	3	22.866	25.699	12.468	2.641	243.68

Table 2. Relative readouts

a) Increments						b) Relative values*					
Point	1a	2a	3a	5a	F	Point	1a	2a	3a	5a	F
Item	degrees	degrees	degrees	degrees	kN	Item	degrees	degrees	degrees	degrees	kN
1	0.642	0.586	0.545	0.526	202.64	1	0.116	0.060	0.019	0.000	202.64
2	0.725	0.683	0.611	0.596	209.86	2	0.129	0.087	0.015	0.000	209.86
3	0.884	0.826	0.743	0.725	243.23	3	0.159	0.101	0.018	0.000	243.23

* Angle values relative to reference point 5a (boom vertical movement axis)

Table 3. Derivative of the bucket wheel boom deflection

a) Angle of deflection						b) Tangent of the deflection angle					
x	3850	0850	850	0	m	x	3850	0850	850	0	m
Point	1a	2a	3a	5a	F	Point	1a	2a	3a	5a	F
Item	10 ⁻³ rad	10 ⁻³ rad	10 ⁻³ rad	10 ⁻³ rad	kN	Item	10 ⁻³	10 ⁻³	10 ⁻³	10 ⁻³	kN
1	2.025	1.047	0.332	0.000	202.64	1	2.025	1.047	0.332	0.000	202.64
2	2.251	1.518	0.262	0.000	209.86	2	2.251	1.518	0.262	0.000	209.86
3	2.775	1.763	0.314	0.000	243.23	3	2.775	1.763	0.314	0.000	243.23

The derivative of the line of the bucket wheel boom deflection was approximated by a linear function on the basis of the tangent values obtained at the measuring points (see Fig. 7). The X coordinate indicates the distance between the point and the axis of the bucket wheel boom vertical movement. The Y coordinate is the derivative value (tangent of the tangent) of the bucket wheel boom deflection line.

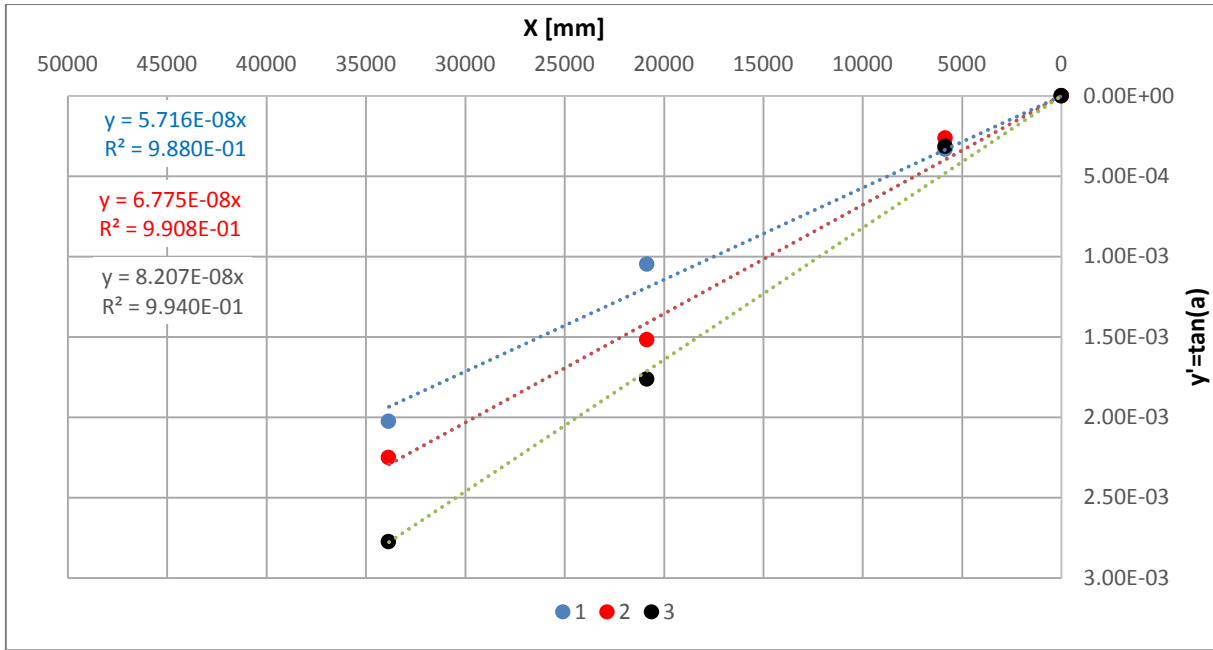


Figure 77 The derivative of the K45 excavator bucket wheel boom deflection line determined experimentally

By adding up the deflection increments (derived values) in the next coordinates of the boom, counting from the axis of its vertical movement, the deflection values of the bucket wheel boom were obtained. For the obtained results of deflection at the selected points for given loads ($j = 1,2,3$), see Table 4 below.

Table 4. Experimental values of the K45 excavator bucket wheel boom deflections

j	i	1	2	3	F_j	K_j
	X_i [mm]	44900	33350	20850	kN	kN/mm
1	Y_{ij} [mm]	58	33	12	203	3.500
2		68	39	15	210	3.088
3		83	47	18	243	2.928

Theoretical Method

The theoretical value of deflection of the bucket wheel axis can be determined by the analytical method, either by treating the bucket wheel structure as a beam with variable cross-section, supported in a pivot bearing on one side and suspended on a rope sling or numerically, using the finite element method.

The analytical method consists in solving, for a given load, the second order differential equation describing the curvature of the deflection of the analysed structure and determining the displacement of the bucket wheel axis on the basis of this deflection curve.

The finite element method (FEM) is based on the creation of a discrete model based on the geometry of the boom structure, determination of boundary conditions by enforcing forces and determination of restraints, automatic generation of the discrete model finite element stiffness matrix, which allows determination of displacements of all finite element nodes and approximation of the bucket wheel axis displacement.

The FEM allows, using computer aided support, obtaining relatively fast and accurate results, obtaining of which by analytical method is difficult. The FEM, in comparison to the analytical method, describes the behaviour of the structure in a more approximate way. However, due to much simpler use of it, and the possibility of computer-aided computations, it is now widely used in

engineering strength calculations of the structures and was therefore chosen as a theoretical method to determine the deflection of the bucket wheel boom.

The numerical model used to determine the bucket wheel boom deflection mapped all the structural elements of the body assembly, i.e.: the bucket wheel boom, the counterweight boom, the fixed mast, the movable mast, the middle part and the platform of the body. All these elements were modelled with two-dimensional coating elements, which ensured a very accurate reproduction of stiffness of each of them. The shroud cables were modelled with beam elements with stiffness corresponding to the ropes mounted on the facility. The rope system rigging is designed to maintain the position of the mining boom required by the operator (hence, its flexibility is compensated by the winch) and therefore, it has been mapped with rigid elements, while maintaining full kinematics. The whole body was supported by flexible elements that represented the stiffness of the chassis assembly. The model was supplemented with mass elements representing the installed elements of the machine/electrical sections (e.g. gear, switchgear, etc.). The whole was consistent with the location of the mass centres (individual elements and the entire body) in accordance with the proof of stability.

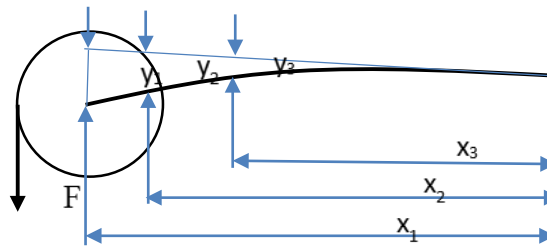


Figure 78 Diagram of boom deflection under the load (F)

For the theoretical values of the K45 excavator bucket wheel boom deflection for selected coordinates, counting from the bucket wheel boom vertical movement axis and for selected loads with vertical force (F) (see Fig. 8), applied vertically to the edge of the bucket blade, obtained by the finite element method, see Table 5 below.

Table 5. Theoretical values of the SchRs4000 excavator bucket wheel boom deflections (Bucket wheel boom vertical deflection under specific force)

j	i	1	2	3	F _j	K _j
	X _i [mm]	44900	33350	20850	kN	kN/mm
1	Y _j [mm]	61	45	27	200	3.279
2		76	56	34	250	3.289

Comparison of boom stiffness measurements

Figure 9 below shows the K45 excavator bucket wheel boom deflection lines, obtained by experimental method (the red line) and the same obtained theoretically (the blue line). The obtained deflection lines result from the vertical force acting on the cutting edge of the bucket with the value of 250kN.

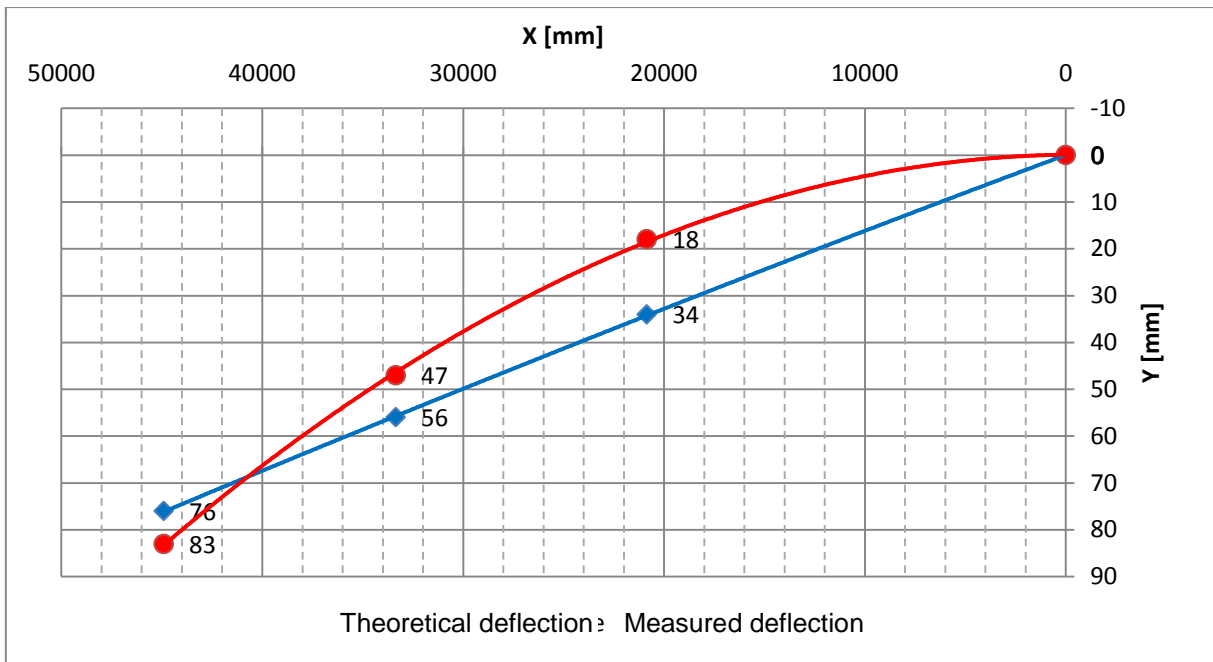


Figure 79 K45 excavator bucket wheel boom deflection lines

The theoretical deflection line of the bucket wheel boom shown in Fig. 9 is approximately a straight line, while the deflection line obtained experimentally is parabolic. The difference between the shape of both determined boom deflection lines results from the adopted simplification in the theoretical FEM model. In the FEM model, the shroud cables were modelled as beam elements. Despite the difference in the course of the deflection line, the value of the deflection in the bucket wheel axis obtained with both methods shows high consistency. The value of the deflection in the bucket wheel axis (coordinate $x = 44900\text{mm}$, measured from the boom vertical movement axis) is, respectively: the theoretical, $f = 76\text{mm}$ and the experimental, $f = 83\text{mm}$.

Due to the obtained experimental and theoretical consistency of the bucket wheel axis deflections, the method and adopted simplifications can be used in engineering calculations for theoretical determination of deflection and stiffness of the bucket wheel boom.

3. MONITORING SYSTEM OF BUCKET WHEEL EXCAVATOR LOAD CARRYING STRUCTURE EFFORTS AND METHOD OF DIAGNOSTIC SIGNALS ANALYSIS FOR CURRENT ASSESSMENT OF THREATS OF LOAD CARRYING STRUCTURE DAMAGES AS WELL AS CONSTANT CONTROL OF RESIDUAL STRENGTH OF THE STRUCTURE

Method of monitoring condition of the load-carrying structure components is based on stress measurement at diagnostic (reference) points. These points should be selected so, that on their basis, effort of the load-carrying structure in its critical points (monitoring points) due to the threat of depleting the load capacity of the entire structure could be determined. A method of selecting the reference points was developed to achieve this goal. Selection of critical structures and the transfer (interpolation) procedure of the measured stress values to the critical locations are based on strength calculations of a FEM model of an excavator unit. An appropriate measuring system needs to be designed or selected for the measurement of stresses. The measuring system should be able to collect data from all measuring systems (sensors) with the appropriate sampling frequency. It should be resistant to ambient operating conditions including electrical and power interference and should allow calibration and troubleshooting of measuring systems.

Signal from the measuring systems, after appropriate preparation (i.e. amplification, calibration, taring, etc.), after conversion to digital form, is introduced to the computing unit. The task of the computing unit is transferring the measured values from the reference points to the critical points, checking exceeding of critical stress values, counting fatigue cycles, monitoring the size of the external forces and the size of the load of the main electric drives.

Counted variables cycles will be collected in a variable load spectrum array. Before entering into the spectrum array, variable loads will be adjusted for the value of the pre-compression stresses of the structure (internal stresses). The pre-compression stresses will be measured by drilled pinhole method or by relieving the structure assemblies. The occurrence of stresses exceeding the critical ones will be checked on a regular basis, without collecting them in the monitoring system database. Exceeding of the critical stresses will be derived from the system as a signal used to indicate an overload. The load recovery time will be determined as the mean value of the appearance of the variable cycles and stored in a variable cycle recovery array.

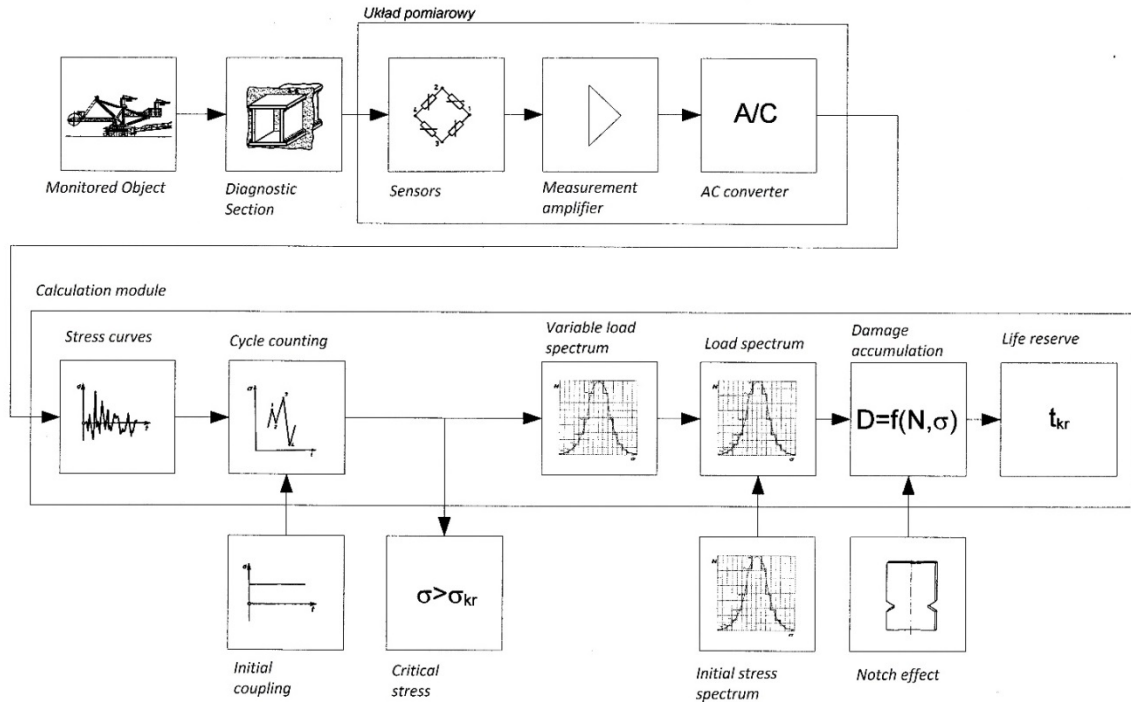


Figure 80 The ideogram of the load bearing structure monitoring system

When estimating durability of machines already in operation, the initial load spectrum array must be entered into the system. The initial spectrum can be obtained by determining the time of the machine operation so far and it is referred to the expected load recovery time on an ongoing basis. On this basis, the system builds a dynamic initial spectrum array.

After summing up the variable load spectrum and initial load spectrum, on the basis of the damage accumulation hypothesis, and after taking into account the type of notch and material properties (Wöhler curve), degree of wear of the structure is determined. On the basis of this durability and load recovery time spectrum, the structure life reserve (residual life) is estimated.

The task of the load-carrying structure is to transfer loads to the support points. Loss of ability to perform the task is equivalent to the depletion of its life reserve and entering into a condition preventing its normal operation. Depleting the structure reserve is associated with its operation. In general cases, depleting the structure reserve may be due to its excessive strain or load capacity depletion. Excessive strains are associated with the occurrence of unacceptable deflections, horizontal deflections and vibration of structural components. Load capacity depletion is associated with reaching the critical effort or fatigue of structural components or loss of stability or transformation of the structure into a geometrically variable system. For a correctly designed structure with components in normal condition, there should be no depletion of its reserve as a result of excessive strains. This can happen as a result of the loss of load capacity by its components. The load-carrying structure is protected at the design stage by suitable selection of the structure design, the profiles used and the selection of material prior to the occurrence of excessive deflection and deformation. Therefore, the occurrence of such phenomena during the operation will be associated with the degradation of structural components or combinations thereof, or occurrence of oversize loads (despite the activation of means of overload protection). The situation is similar in the case of vibration of the structure. Vibration is the result of the structural resonance due to cyclically variable loads. Therefore, adequate analysis of proper vibration is carried out at the design stage. Variation of the proper vibration of the structure is the result of changes in its stiffness or weight of its assemblies or components. Therefore, the occurrence of this type of phenomenon is also related to the degradation of structural components or combinations thereof. This does not include the upgrading changes that may interfere with the existing structure or its rigidity and require repeating the strength

calculations. When designing the structure, its designers use the available calculation methods specified in the standards and studies as well as calculation supporting tools. Although these methods are improved, aiming to make the most accurate reflection of reality, they do not specify precisely the impact of loads on structural components and the possibility of mutual excitation of the structural assemblies. This is due to the current state of knowledge, computational tools available and various kinds of simplifications and approximations applied. Moreover, there is no precise information on the presence of abnormal loads during operation and the intensity of mining process available at the design stage. For this reason, it is impossible to estimate the effort and fatigue life of the structure accurately at the design stage.

For the load-bearing structure, loss of stability is associated with the loss of ability to transfer external loads through the support. Such an event could take place in case of occurrence of loads abnormal to the work of the structure (in specific types of support through the exiting of the centre of gravity beyond the tipping edge). Such an event may also take place in case of degradation of structural components or connections at the points of support or in their vicinity or the occurrence of abnormal external loads.

Transformation of the structure into the geometrically variable system is the result of changes in its structure. This may occur in case of destruction of certain structural components from the degradation of components or combinations thereof.

As discussed above, the structure reserve depletion is largely the result of degradation of the structural components or combinations thereof. It can result from deterioration of the technical condition of individual components, fatigue processes occurring in them or exceeding the critical stress. These processes will result in changes in load capacity of the components. Therefore, monitoring of stresses seems to be the most appropriate.

Monitoring the stress of all components of the structure would be ideal. Due to the complexity of the structure (many components), installation of a very large number of measuring and processing modules would be required. Such an extended system would be expensive and interpretation and analysis of the collected data would be difficult. It might be inefficient, energy-intensive, complex and prone to failures. Therefore, it seems advisable to limit the amount of measuring and processing modules to the optimal amount. Therefore, we propose the concept of monitoring points, on the basis of which, condition of the entire structure would be determined. This approach forces to develop a method of selection of monitoring points. This method will be a procedure to identify locations of particular importance for the structure strength stability and on the basis of which, the life of the entire structure will be possible to be evaluated in the monitoring process.

It can easily assumed that monitoring locations can be selected in areas with difficult access, exposed to sensor damage or places with e.g. notch effect, where installation of the measuring system sensors will be impossible. Therefore, we proposed installation of the sensors in diagnostic locations, in which their installation is easier, and the sensors are less susceptible to damage and it is possible to interpolate their indications to the monitoring points.

The purpose of the measuring system is to collect information about stress changes occurring at the diagnostics points, their preliminary preparation and conversion into digital form allowing their further processing. The measuring system consists of the sensors, amplifier devices and transmitting measurement signals and systems for digitization of these signals. Due to the harsh working environment, it is required that sensors and other components of the measuring system were resistant to or protected against mechanical damage. Due to the strong electromagnetic fields coming from the high-power electric drives, the system should be resistant to electrical/power interference. Another factor affecting the operation of the system is the possibility of interruptions in operation. They can be caused by interruptions in the power supply or shutdowns. Due to this, the measuring system should be immune to power failure and be able to perform self-calibration when power is restored. During the system use, damage to or failure of its components (such as sensors, measuring amplifiers, transducers etc.) may occur, and in this regard, a method of replacement and repair of the

measuring system components should also be developed. In order to select the measuring instruments, the ranges of the measured signals, and the required accuracy of the measured stresses must be known. In addition, the operating frequency range that the measuring system should operate within is also important. It depends on the suppression by the structure any transmitted stress changes and their significance for fatigue of the monitored structure. The number of measuring points is important as well. It depends on the number of diagnostic points accepted and configuration of sensors at the diagnostic points. A signal transmission system and measuring amplifier system should be selected on the basis of the number of measuring points and their arrangement on the structure. The measuring amplifiers should ensure adjustment of the analogue signal to digital converters, by means of which, the measured values will be transmitted to the computing unit. Selection of a/d converters should be based on the computing unit solution accepted and the required computing accuracy.

The task of the computing unit is to process the measurement signals from the measuring system, the collection of measurement data (in the pass tables), and the preparation of output. A module development system (OS) is provided within the basic software. Launching the start-up procedure and restart after power restoration as well as the start-up of calculation and other software necessary to manage the monitoring system are the purposes of this system.

The load-bearing structure is, after assembling, subjected to forces from the complete structure kerb weight consisting of the weight of its components and the equipment installed on it. In addition, stresses resulting from the structure assembly process occur in the structural components. These are constantly acting static stresses, and these are pre-compression stresses of the structure. They are also the average value of stresses in the structural components. During the design process, it is only possible to estimate the stresses caused by weight of the structure own components and devices. Assembly stresses are unknown, since the magnitude of their occurrence is virtually impossible to estimate and depends on the accuracy of performance and installation. We can assume that they are much smaller than the loads caused by the complete structure kerb weight. In contrast, the stresses from the complete structure kerb weight may be the main value of stress. To determine the value of these stresses, we can use one of three methods of determining the constant stress. The first of these is a method for complete structure relieving, a second one is the relaxation of the surface layer (drilled pinhole method), and the third one is a theoretical calculation or the use of design calculations.

When installing a monitoring system on machines already in operation, there is a lack of knowledge about the previous processes of loading. Therefore, there is a need for using the method of initial load estimation. To estimate the initial condition, we propose to use one of two methods. The first one involves a one-time initial measurement of service loads and estimation of initial load spectrum for the previous lifetime basing on them. A static spectrum is the result. The second method, instead of the initial measurement, uses the data collected in the variable load spectrum, and determines the dynamic spectrum of initial loads as a result.

The cumulative fatigue damage hypothesis is used for the calculation of fatigue life. It consists determination of the number of cycles to the fatigue failure. This is done based on the load spectrum, the notch size and the material fatigue strength. This requires the implementation of an appropriate calculation method. To achieve the task, one of the three fatigue damage accumulation hypotheses can be used: Palmgren-Miner, Serensen or Haibach hypotheses.

Changes in stresses in the structural components caused by service loads are complex random waveforms. Their rating is based on the static theory of random processes and their analysis is based on the determination of the stress spectrum. Operational stresses are usually loads of wide spectrum of random processes. In this case, the stress distribution is obtained by counting the transitions between the minimum and maximum peak values. One such a passage is one cycle of changes. For simplicity, the stress range is divided into class intervals. By counting cycles of changes in individual class compartments, we can determine histogram of the frequency of occurrence of their values. The

variable load spectrum can be determined on the basis of this histogram. There are several ways to develop variable stress waveforms. These include the envelope, span pairs, complete cycles, counting of local extremes and level intersection methods. A suitable method of cycle counting and the method of determining the variable load spectrum were selected for the obtained measured values and algorithms for the computing unit.

4. SUMMARY

The issues described above are part of a comprehensive approach to the issue of the work of bucket wheel excavators in soils containing non-mineable inclusions. The BEWEXMIN project aims to develop tools to protect the excavator design against impacts resulting from contact of the bucket wheel with an obstacle by detecting these inclusions, reducing impact energy by optimization of bucket wheel drive and developing methods that take into account extraordinary loads in strength calculations, monitoring of superstructure and evaluation of its durability in real time.

Work financed from resources for science in 2015-2018 granted for the implementation of an international co-financed project.

REFERENCES

- [1] M. Galetakis, T. Michalakopoulos, A. Bajcar, C. Roumpos, M. Lazar i P. Svoboda, "Project BEWEXMIN: Bucket wheel excavators operating under difficult mining conditions including unmineable inclusions and geological structures with excessive mining resistance," 13th International Symposium Continuous Surface Mining, Belgrade, 2016.
- [2] J. Alenowicz i R. Rosik, "Wymagania stawiane ustrojom nośnym koparek wielonaczyniowych kołowych eksploatowanych w utworach trudno urabialnych," *Górnictwo Odkrywkowe*, nr 6, 2016.
- [3] S. Szepietowski, "Theoretical model of impulse load," "Poltegor-Institut" Instytut Górnictwa Odkrywkowego, unpublished, 2015.
- [4] A. Bajcar i J. Alenowicz, "Metody ograniczenia awaryjności koparek wielonaczyniowych kołowych eksploatowanych w gruntach trudno urabialnych," IX Międzynarodowy Kongres Górnictwa Węgla Brunatnego, Bełchatów, 2016.
- [5] J. Alenowicz, M. Onichimiuk i M. Wygoda, "Obciążenia ekstremalne w procesie projektowania i eksploatacji koparek kołowych przeznaczonych do pracy w gruntach trudno urabialnych kopalń odkrywkowych węgla brunatnego," *Górnictwo i Geoinżynieria*, tom 2, nr 33, 2009.
- [6] M. Řehoř i V. Moni, "Hodnocení vyskytu obtížně těžitelnych struktur na lomu Libouš v rámci řešení projektu BEWEXMIN," *Problemy provozu, údržby a oprav strojního zařízení, používaného při povrchovém dobytí*, 2016.

Open Pit Mine Conveyor Belt shifting using modern surveying equipment – An overview

Ioannis Karnaris

Public Power Corporation, Western Macedonian Lignite Center, Greece

ABSTRACT

One of the basic but most important procedures of an open pit mine is shifting of the conveyor belt and its relevant drive station and tail station. The cm-high accurate shifting of the conveyor belt and respective positioning of the drive stations and tail stations pontoons is of crucial importance as it secures -surveying wise- that the belt will operate flawlessly which will result in reduced belt maintenance. This paper presents a detailed analysis of the surveying method, equipment and computations needed -regarding both fieldwork and office work- for conveyor belts' and drive station / tail station on pontoons' shifting.

INTRODUCTION

Coal is an organic sediment consisting of a complex mixture of substances. It has a lot of commercial and industrial applications. It is an energy giving non-renewable source of energy while coal mining is one of the oldest industrial operations. The mining method selected for exploitation is determined mainly by the characteristics of the coal deposit and the limits imposed by safety, technology, environmental concerns, and economics. [1]

Lignite, formed from peat compressed at shallow depths at temperatures below 100 degrees Celsius, it's Greece's main electricity generator. [2] Greece ranked in the 5th position in EU-28 – behind Germany, Poland, Czech Republic and Serbia- in lignite production with 37.7mt, followed by Romania. [3]

Greece's Public Power Corporation (PPC)_[4] lignite mines follow the open-pit mining method in which several benches with their corresponding conveyor belts are established in both the overburden strata and the coal seam. Western Macedonia Lignite Center of PPC consists of 4 mines which cumulative in 2017 had nearly 200km of conveyor belts in varying sizes mostly being 1200 mm, 1600 mm, 1800 mm and 2400 mm. In a typical PPC mine the continuous method is mostly applied; one machine—the Bucket Wheel Excavator _[5]—rips coal from the face and loads it directly into a hauling unit. [1]

One of the basic but most important procedures of an open pit mine is the shifting of the conveyor belt and its relevant drive station and tail station. A conveyor belt shifting occurs usually every 30 days and its frequency is dependent on ground morphology (existence of hard formations or not), availability of the specific BWE and overall planning of the mine amongst other things. In Mine II the tailstation is being shifted 60-90m towards the bench in order for the BWE to be able to reach again the bench in its entire length (Figure 1).

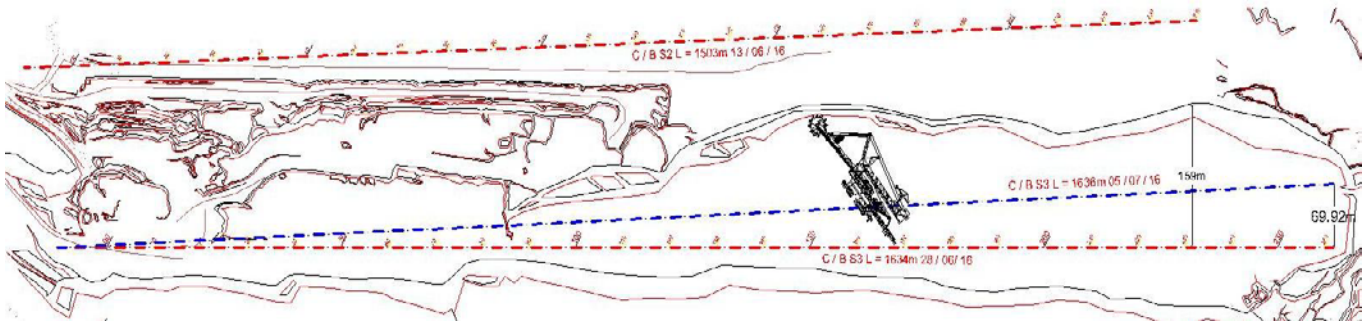


Figure 1. The new position (blue dash dotted line) of a conveyor belt in WMLC’s Mine II and the previous one (red line) in an AutoCAD drawing of the Planning Department of the Mine. The conveyor belt’s tail station is being shifted 70m towards the bench which the BWE is excavating

The cm-high accurate shifting of the conveyor belt and respective positioning of the drive stations and tail stations pontoons is of crucial importance as it secures -surveyingwise- that the belt will operate flawlessly which will result in reduced belt Mine Itenance.

For many years, surveying teams in WMLC were applying empirical methods for conveyor belt shifting. Moreover, the methodology involved climbing up to the drivestations disposal drum which was dangerous. Finally, they didn’t have the high precision surveying equipment of modern days. In the beginning of 2016 a study began –which lasted 6 months- in WMLC’s Mine II in which each drivestation, tailstation and their corresponding conveyor belts (in 50 m intervals) were surveyed with modern surveying equipment (dual frequency GNSS Receivers_[6] and robotic high precision Total Stations) from scratch (Figure 2), in order to discover and point out potential misalignments of the conveyor belts and the XYZ coordinates of every drivestation and tailstation for further analysis. Final step of the study was the creation of a shifting methodology in which only modern surveying equipment is being used during the entire procedure including an afterwards verification.

This paper presents a detailed analysis of the surveying method applied, equipment used and computations needed -regarding both fieldwork and office work- for conveyor belts’ and drive station / tail station on pontoons’ shifting. Finally, a comparison is being made over the vulcanizations made, over conveyor belts’ side tear segments, which are a clear indication of potential misalignments.



Figure 2. Each conveyor belt in WMLC’s Mine II was surveyed with dual frequency GNSS receivers in 120 epochs for optimum Real Time Kinematic accuracy, in 50m intervals of the belts

1. Materials and Methods

1.1. Defining parameters of the new methodology

WMLC's Mine II has over 90 km of conveyor belts (Figure 3) so conveyor belt vulcanization or / and replacing costs constitute a significant part of the annual running costs of the mine. Besides economical figures and cutting costs, trained personnel can be used elsewhere and at the same time health and safety can be increased within the mine due to lesser vulcanization work on slippery conveyor belts. First step of the entire process was to study the scanned drawings from drivestations and tailstations in PPC's archive; from the drawings used it was obvious that the easiest and safest way for the axis of the conveyor belt to be defined, the closest pontoon of the drivestation to the disposal drum should be used and therefore surveyed along with the tailstations' drum.

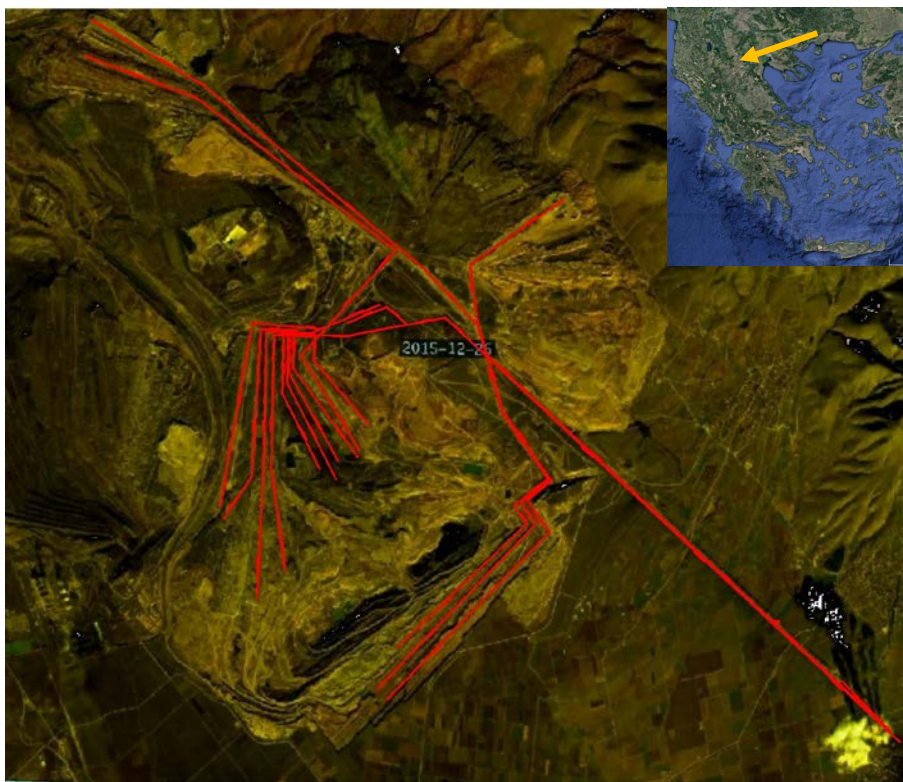


Figure 3. WMLC's Mine II conveyor belts (Images; Sentinel-2, 26-12-2015 & Google Earth)_{[7][8]}

In Figure 4, in a 2400 mm conveyor belt;

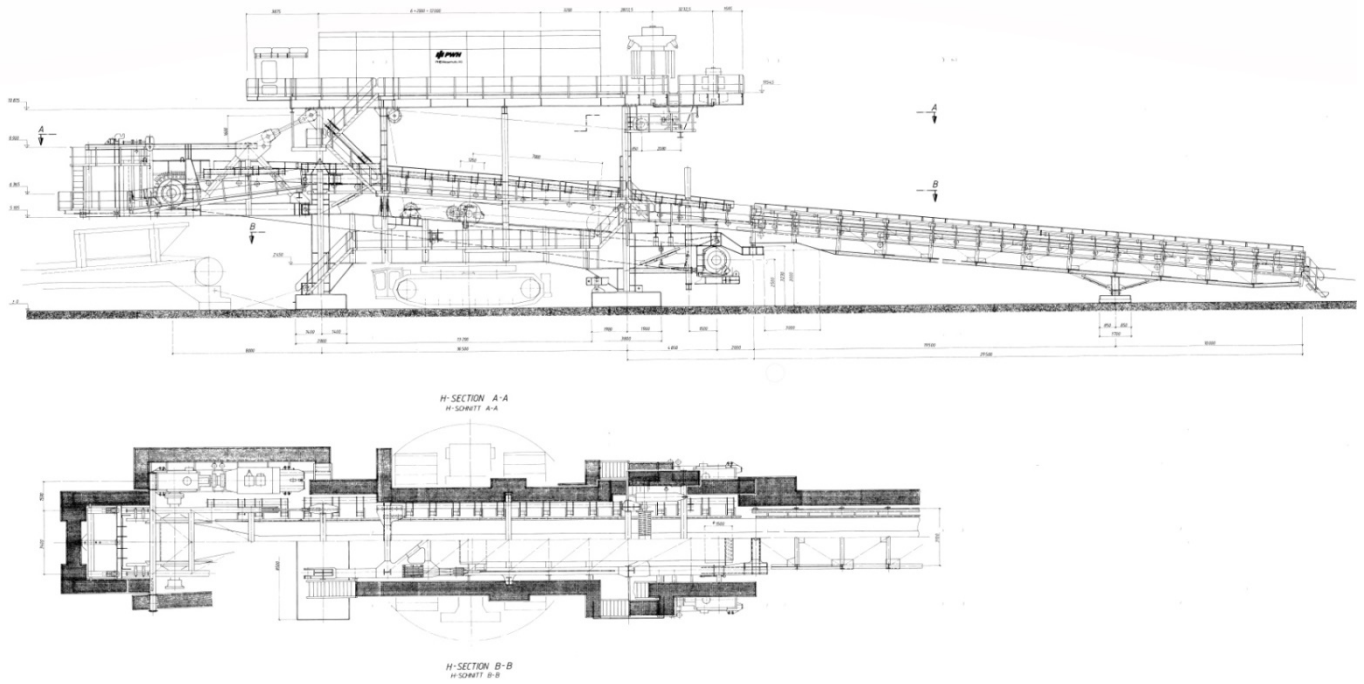


Figure 4. PWH PHB Weserhütte 2400mm Drivestation dimensions drawing (PPC S.A. Archive)^[9]

1. The drivestation's pontoon is 8500mm wide, so each pontoon's short side has an equal distance of 4250mm from the axis.
2. The center of the disposal drum is at 6600mm from the first pontoons first long edge (from left to right), at 6365mm above exiting ground
3. Disposal drum has $\Phi 1530$ mm diameter and
4. The drivestation's pivot point is at 16000mm from the longitudinal axis of the disposal drum. The pivot point is the point where the drivestation is anchored from the transport crawler in order to be shifted.



Figure 5. Damaged and covered in dried mud Drivestation's Pontoon



Figure 6. Tailstation drum not fully clear due to conveyor belt misalignment

By surveying and defining the pontoons' exact coordinates, all information needed is obtained. Surveying teams, however, encountered serious problems during the surveying campaign; most of the drivestation's pontoons were either damaged or / and covered in dried mud (Figure 5). Surveying teams overcame this difficult situation by firstly choosing the best Mine Itained side of the cleaned up (with the help from machinery supplied by fellow coworkers) pontoon and then surveying -using 10cc accuracy robotic total stations- 3 different points (in I & II telescopic thesis in order to minimize vertical axis errors of the total station) on the same (small) side of the pontoon; 2 on the edges and one in the middle. Implementing Autodesk's Civil 3D® [10] "*Create Best Fit Line*" command, made the creation of the optimal side of the pontoon possible and then by offset of 4250mm the axis of the drivestation is obtained.

Surveying teams overcame this difficult situation by firstly choosing the best Mine Itained side of the cleaned up (with the help from machinery supplied by fellow coworkers) pontoon and then surveying -using 10cc accuracy robotic total stations- 3 different points (in I & II telescopic thesis in order to minimize vertical axis errors of the total station) on the same (small) side of the pontoon; 2 on the edges and one in the middle. The mid-point isn't necessary to be at the middle of the small side of the pontoon but it is obligatory to be on a clean and intact spot. Base station and backsight coordinates of the total station are surveyed with a dual frequency GNSS receiver in 120 epochs. Implementing Autodesk's Civil 3D® [10] "*Create Best Fit Line*" command, made the creation of the optimal side of the pontoon possible and then by offset of 4250mm the axis of the drivestation is obtained.

Regarding the tailstation, each edge of the drum is surveyed (in I & II telescopic thesis) by using the reflectorless, with laser beam, function of the total station –with a constant vertical axis of the instrument-, so as to obtain the drum's axis; it will result from the center of the line created by the 2+2 points surveyed. The total station is set up not far from the drum itself but at a suitable position so as both drum's edges can be visible and surveyed. The accurate XYZ coordinates of the drum's axis will emerge after the point has been offset by the drums radius towards the drivestation. The final axis of the existing conveyor belt is finalized from –once more- implementing the "*Create Best Fit Line*" command between the line created from the 3 points of the small side of the drivestation's first pontoon offset by 4.25m and the tailstation's drum point.

1.2. New Drivestation & tailstation position calculations

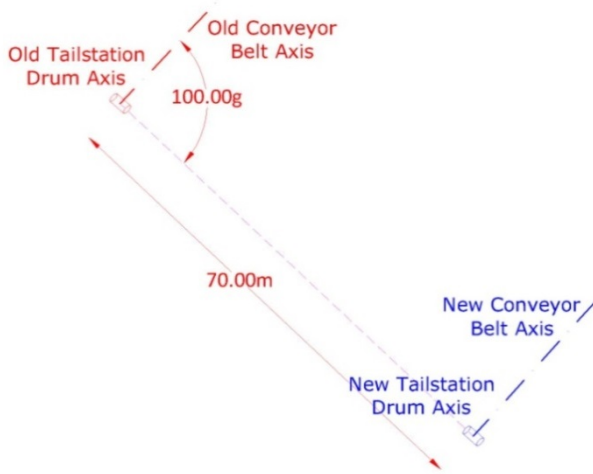


Figure 7. Tailstations' drum new position, office calculated

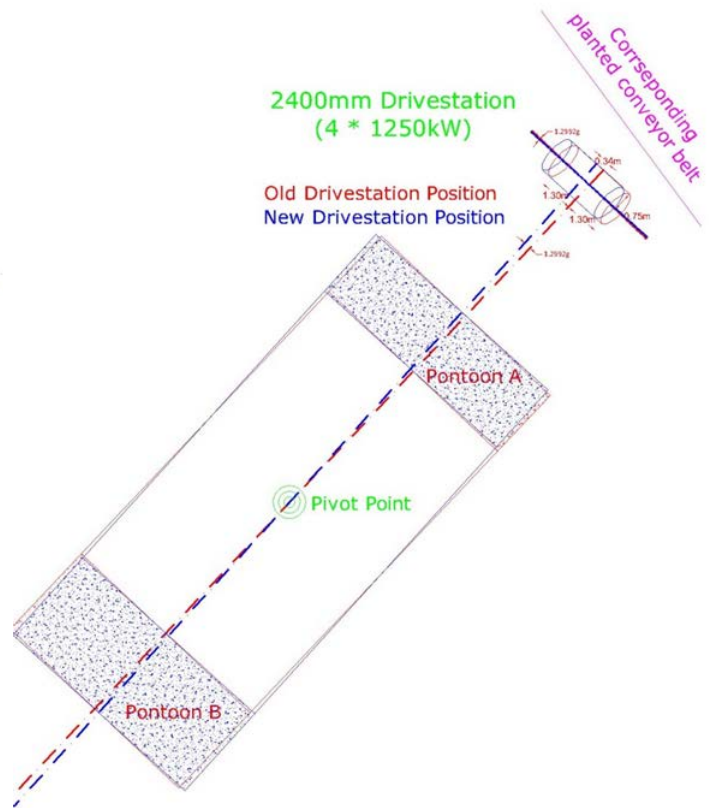


Figure 8. Drivestations' new position, office calculated

Once the axial points of the drivestation and tailstation have been surveyed, the calculation for the shifting of the conveyor is feasible; if a 70m shifting of a 3446.25m long conveyor belt is needed, then the new position of the tailstation's drum is calculated by creating the new point 70m perpendicularly from the previous position (Figure 7)

In Figure 8, the calculations for the new positioning of a 2400mm drivestation's pontoons are presented. In this scenario, the pivot point is kept in the exact same position and the rest of the coordinates needed for the stakeout of the new drivestation's pontoons can be easily extracted in a *.csv or *.txt file from Autodesk's Civil 3D® and imported into the total stations software. The drivestation cannot be staked out with a dual frequency GNSS receiver due to lack of open sky.

However, the new disposal point has been shifted by 34cm and as the corresponding next conveyor belt isn't shiftable the old and new disposal points must be identical. This is achieved by matching the 2 disposal points whilst creating a block and rotating it in reference with the disposal point.

The block will contain;

- the new drivestation's pontoons & disposal drum
- the new tailstation's drum
- the new pivot point

The end result is a drawing with everything setup for stake out in the field (Figure 9);

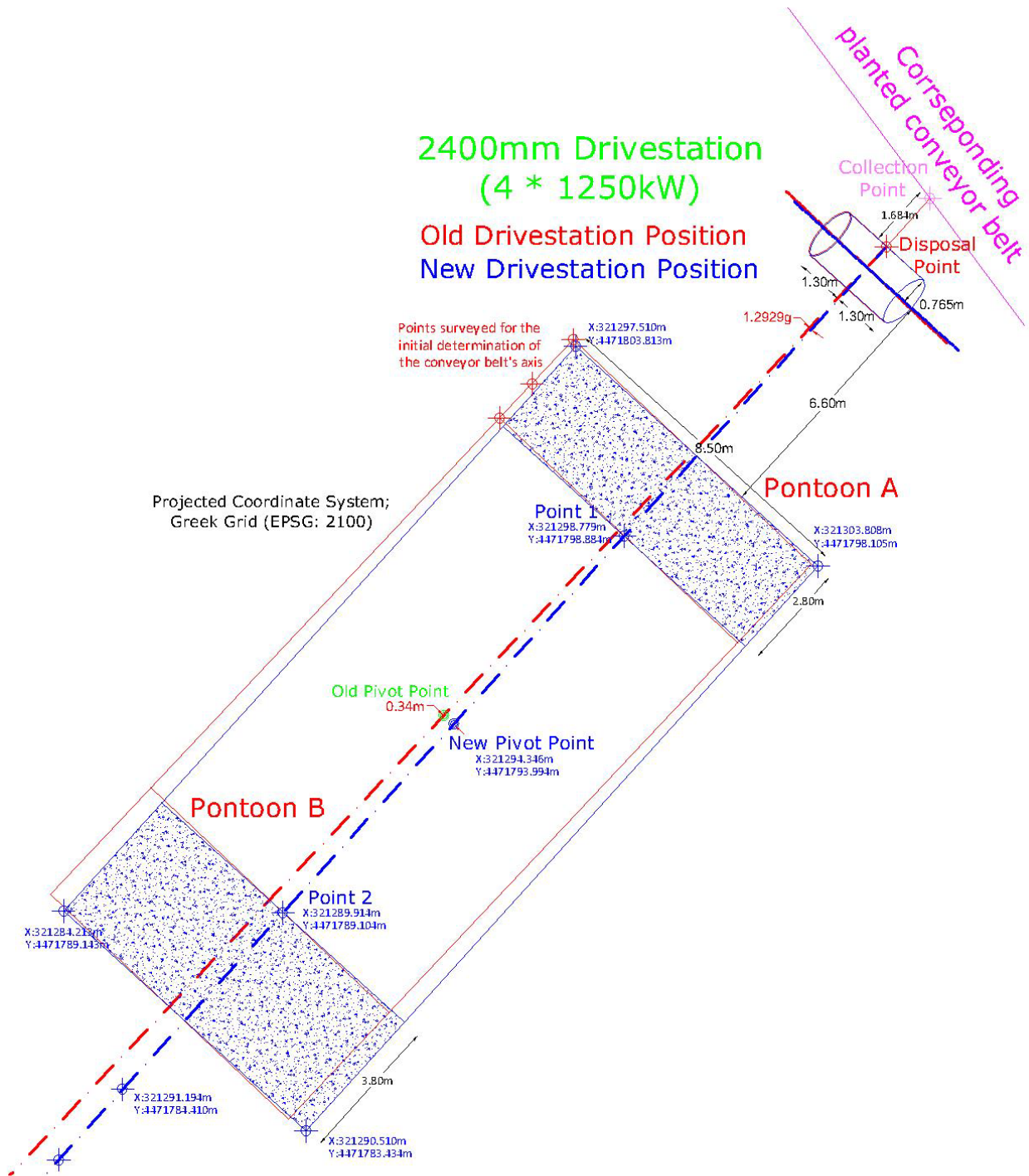


Figure 9. Drivestations' new final position, office calculated, ready for staking out

1.3. Fieldwork

The conveyor belt shifting begins with a sparse staking out –with the use GNSS receivers- of the new position of the entire belt, approximately every 50-100m in order for the appropriate machinery to lay a thick layer of gravel. Then the exact position of the tailstation's drum is being staked out along with a dense stake out of the new axis and finally the new positions of the drivestation's pontoons and tail are staked out, using total station. While the transport crawler shifts

the drivestation, the laser beam from the total station (which points out the exact position of the axis of one out of two pontoons, POINT 1 or 2 in Figure 9) guides the shifting team as well as the crawlers' operator. Additionally, wooden sticks with painted heads in red are being placed, for error avoidance and additional guidance (Figures 10 & 11). It must be noticed that modern surveying equipment have COGO_[11] functions, so if the drawing basis exists within the accompanying software, everything can be modified according to the specific needs in the field in real time.



Figures 10, 11. Final staking out of the drivetrain's pontoons new positioning with laser beam guidance

Regarding the tailstation's positioning, two points (one out of each pontoon) of the structure should be staked out (with a GNSS receiver for ease of use), in order to be fully aligned with conveyor belts' new axis;

- the pontoon's axis underneath the tailstation's drum (*point C*) and
- the outer part of the widened beam over the second pontoon, offset by 2.85m from the conveyor belts' axis (1300mm+400mm+350mm+800mm, *point D*) and at 13.4m (10000mm+2*1700mm) away from point C



Figure 12. PWH PHB Weserhütte 2400 mm Tailstation dimensions drawing (PPC S.A. Archive)^[9]

2. Results and Discussion

Whilst the first half of 2016 contained an enormous surveying campaign of Mine II's every drivestation's pontoons and tailstation's pontoons and drums, the second half was about instructing all surveying team members in Mine II the new methodology, implementing and enhancing it. So by 2017, the mine should start pinpointing tangible results.

According to the WMLC's Conveyor Belt Sector, on a daily basis, vulcanization teams -both from PPC and subcontractors- are being sent to the 4 mines. Their core duties involve mainly the following vulcanization work categories;

- Conveyor belts' worn parts
- Torn apart conveyor belt
- Traumatized conveyor belt part
- New Project
- Conveyor belt shortening
- Conveyor belt extension
- Conveyor belt side rips and tears
- Conversion

Throughout the years, the category "*Conveyor belt side rips & tears*" has been considered to be of surveying interest; side tears are being created when the conveyor belt continuously brushes up against the crates. Responsibility for conveyor belts misalignment isn't solely laid upon surveying teams, as there many more factors affecting the initial alignment;

- Telescopic Boom machinery keep hitting and therefore misaligning the cranes while cleaning the mud underneath
- many cranes missing crossplates and support struts
- inaccurately placed cranes lengthwise and/or inclination on the vertical axis
- over tightening of the conveyor belt

- old, worn and over-sloped conveyor belts
- rough and unevenly inclined berms

Though, misalignment still remains one of the basic reasons for “*Conveyor belt side rips & tears*” vulcanization works maintenance costs. Unfortunately, WMLC’s Conveyor Belt Sector keeps record of the categorized vulcanization teams’ everyday work, from 2017 on. So instead of comparing the before and after of the new conveyor belt shifting methodology implementation within Mine II, we will try to compare this specific category within the 3 mines that constitute Western Macedonia Lignite Center; it must be mentioned that Aminteon Mine due to the catastrophic landslide on early June 2017, doesn’t follow the continuous method (exclusively subcontractors excavation with conventional machinery) thus cannot be compared.

From the Tables 1 & 2, derived from the WMLC mines annual reports, it is obvious that Mine II achieved a significant improvement over the rest 2 mines in sides

- Mine II has double the total length in km (red column) than that of Mine III and almost triple the length of Mine I
- Mine II managed to achieve less than one quarter (20) vulcanization works for side tears of conveyor belts in 2017 than those of Mine III (90) and Mine I (81), which will remain the same for the 2018 comparison of Mine II and Mine I mines. Mine III will have achieved better results in 2018 but still had 50% more vulcanization works than Mine II while it had 62% less shiftings, shortenings and extensions and operated at a half total conveyor belts length.
- In 2017, 66.7% of side narrow parts vulcanization works in Mine I was referring to non shiftable conveyor belts. At the same period the corresponding percentage in Mine III and Mine II were 44.4% and 85% respectively. In 2018, percentages practically remained the same (60%, 47.6% and 85.7% respectively).
- In 2017, Mine III and Mine II completed the same amount of shiftings (49 and 47 respectively) while Mine I completed 60 shiftings -same as it will in 2018-. Regarding conveyor belt’s extensions and shortenings, Mine III completed 65 and Mine II 49.



Table 1. Narrow side tear vulcanization works carried out in 2017 in each mine of Western Macedonia Lignite Center, corresponding Conveyor Belts total length (in km) and vulcanizations per type of Conveyor Belt in each Mine

- In 2018 (raised in an annual basis, actual data until 01/08/2018), Mine III and Mine II will have completed the same amount of shiftings (66 and 64 respectively). Regarding conveyor belt’s extensions and shortenings, Mine III will have completed 27 and Mine II 82, while Mine I’s will increase to 41.
- In both 2017 & 2018, the shifting’s quantity is identical between the 2 major mines; however Mine II has achieved cutting costs in side narrow parts vulcanization. This also stands for combined extensions and shortenings as well; even though in 2018 Mine II’s extensions and shortenings number has surged from 49 to 72, the mine managed to keep the vulcanization works cost really low, unlike Mine III did in 2017.

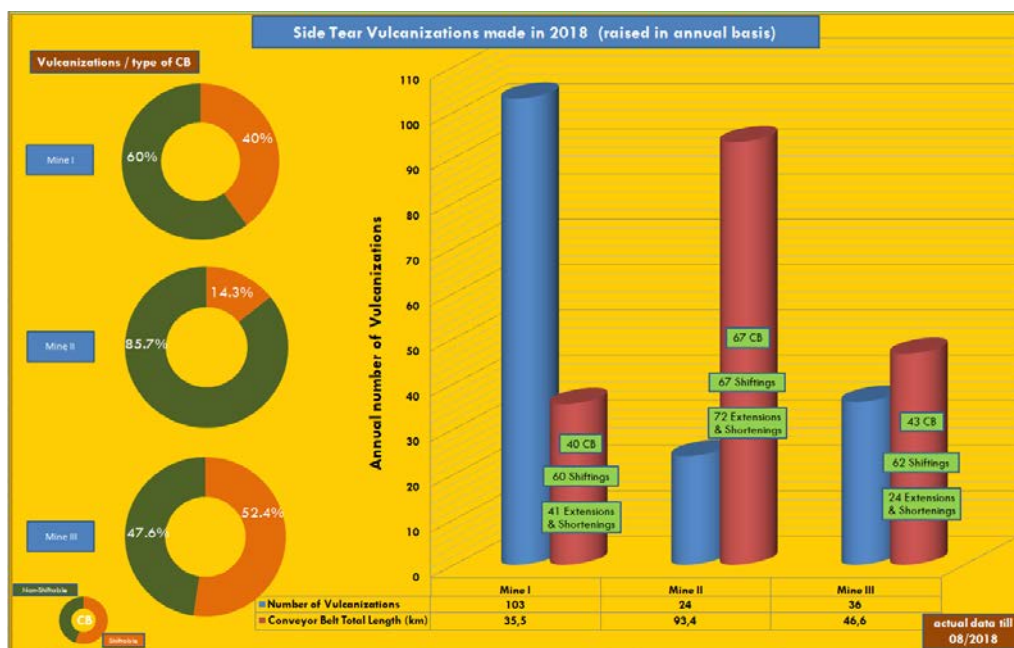


Table 2. Narrow side tear vulcanization works carried out in 2018 –raised in annual basis, actual data till 07/2018- in each mine of WMLC, corresponding Conveyor Belts total length (in km) and vulcanizations per type of Conveyor Belt in each Mine

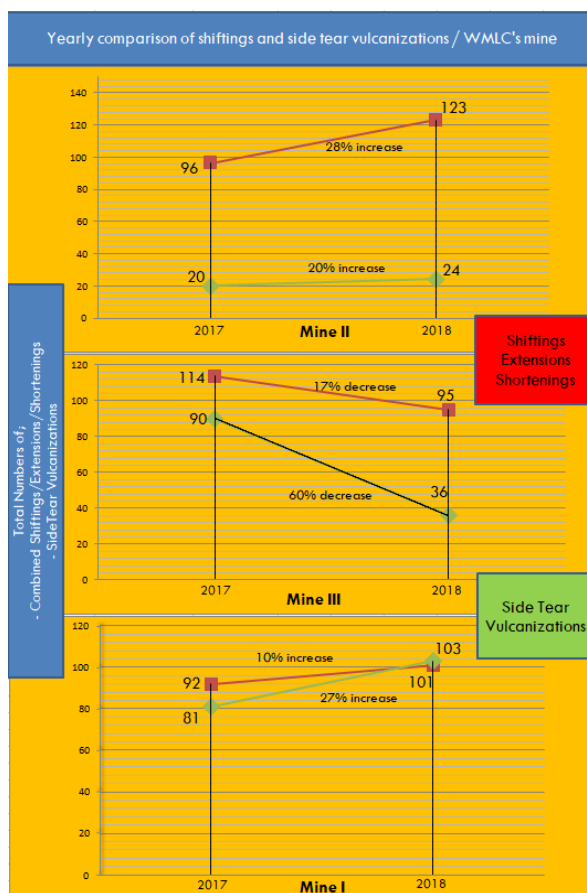


Table 3. Yearly comparison of shiftings and side tear vulcanizations per WMLC's mine

In Table 3, a yearly comparison of the increase or decrease of the (combined) number of shiftings / shortenings / extensions of each mine in regards to the corresponding number of side tear vulcanization works.

- Mine II's total number of shiftings / shortenings / extensions is clearly the lowest one in both 2017 and 2018.
- Vulcanization works number in both Mine III and Mine I follows the increase (Mine I) and decrease (Mine III) of the shiftings made, an indication of correlation between the vulcanization works and number of shiftings.
- Mine III seems to have improved results, as a 25% decrease in shiftings led to a 60% decrease in vulcanizations. However, Mine I saw a 10% increase in shiftings followed by a 27% increase in vulcanizations.
- Mine II has the biggest change in total number of shiftings made, an increase of 45%. Simultaneously, it has achieved the smallest change in vulcanizations made, only a 20% increase.

3. CONCLUSIONS

- The proposed shifting methodology does not require any additional software or hardware in order to be implemented
- While it does not require additional time in either office work or fieldwork, it is significantly more accurate than the previous empirical method because it relies upon drawings and measurements with modern surveying equipment. Additionally, there is control over the entire procedure; When the shifting procedure is finished, surveying teams survey the definite points of the drivestation and tailstation for next shiftings and as-built drawings
- It is significantly safer because surveying –and the rest shifting- team members as well as shifting team members don't have to climb up the drivestation
- It has increased the level of self-confidence of the surveying team members
- It increased the level of cooperation between surveying teams and the rest shifting teams of the mine
- Conveyor belt repairs can take operations offline for a significant amount of time, so less side tear vulcanizations means more efficiency
- The correlation between the disposal point and the collection point of the corresponding conveyor belt will be examined in the forthcoming year even though it is difficult to simulate it due to the nature of the materials in the conveyor belts and the unstable weather in the area
- More statistical data over side tear vulcanization works must be obtained for overall conclusions as there are many factors affecting the constant alignment of a conveyor belt. However, while implementation of the proposed methodology cannot take the credit for lesser side tear vulcanization works and thus costs, there is a strong indication within the existing analysis that it has an important role in this achievement. Conveyor belts and their satellite costs are a significant part of the annual operating cost of WMLC and a high one to be neglected.

POTENTIAL CONFLICTS OF INTEREST

The author declares no conflict of interest.

ACKNOWLEDGMENTS

The author would like to thank every surveying and shifting team member for their amazing work and collaboration, as well as all the anonymous reviewers for their advices and suggestions.

REFERENCES

Webpages;

[1] https://www.researchgate.net/publication/314502864_COAL_MINING_METHODS [accessed Aug 2018]

[2] <https://investingnews.com/daily/resource-investing/industrial-metals-investing/coal-investing/coal-101-a-look-at-lignite/> [accessed Aug 2018]

[3] <https://euracoal.eu/library/annual-reports/> [accessed Aug 2018]

[4] <https://www.dei.gr/en> [accessed Aug 2018]

[5] https://en.wikipedia.org/wiki/Bucket-wheel_excavator (last access 05/2018)

[6] https://en.wikipedia.org/wiki/GNSS_applications (last access 06/2018)

[7] <http://playground.getopendata.eu> (last access 07/2018)

[8] <https://www.google.com/intl/el/earth/> (last access 08/2018)

[9] http://en.grupotsk.com/proyectos/lineas_negocio/manejo-de-materiales (last access 08/2018)

[10] <https://www.autodesk.com> (last access 05/2018)

[11] <https://en.wikipedia.org/wiki/COGO> (last access 08/2018)

Overview of the Results of Researches Related to Adaptation of Bucket Wheel Excavators Operating in Romanian Lignite Open Pits for Excavation in Rocks with Increased Cutting Resistance

Maria Lazar¹, Iosif Andras¹, Andrei Andras¹, Florin D. Popescu¹, Sorin-Mihai Radu¹, Mircea Rîsteiu²

¹University of Petrosani, 20 Universitatii str., 332008 Petrosani, Romania

² "1 Decembrie 1918" University of Alba Iulia, 5 Gabriel Bethlen str 510009 Alba Iulia, Romania

ABSTRACT

The paper deals with the results obtained in the field of lignite and overburden rock cutting process using BWE-s in the conditions of Romanian lignite open pits, focused mainly on the newly arisen problem of occurrence in the working faces of structures with increased resistance. Due to changing geological environment, in Romanian lignite open pits endowed with BWE-s, the occurrence of structures with increased resistance – continuous layers, boulders - and a general decreasing trend of cuttability parameters of all overburden rocks is more and more present. Based on results of previously performed researches, and the new ones facilitated by the activity in the frame of BEWEXMIN project, the team of professionals from the University of Petrosani, CEO and University of Alba Iulia has extended the researches from cuttability assessment and teeth – bucket improvement towards the analysis of the operation in these conditions and its impact on the mining system of BWE. The main results of the performed theoretical, laboratory and field research is presented in the paper.

1. INTRODUCTION

In the open pit mines, both for coal harvesting and overburden rock removal, the use of Bucket Wheel Excavators (BWEs) is a traditional technology, mainly in Europe.

In the past years, in many European open pits the geological and rock environment become continuously harsher.

The occurrence of hard to excavate intrusions is more frequent, which lead to increase of downtimes due to failures, increased energy consumption, reduced productivity and overall increased production cost. The existing BWEs are not suitable to operate in such conditions.

The main cause of this situation is that the actual BWEs were designed initially for loading bulk material.

Their conversion and adaptation to coal and overburden rock harvesting from mine face dates back to early 50's of past century, when the design, manufacturing and operation norms were established in Germany and later in other countries [1], [2].

These machines were used at the beginning in easy mineable rocks, mainly lignite and brown coal and the corresponding -generally easy to be excavated – overburden rock.

Later, on the basis of gained experience, the BWE's widespread in other countries, such as Poland, Czech Republic and Romania.

There they were used in various - different from the original one - rock environment.

The main problems were the increase of the values of cutting forces and specific energy consumption, their important variability, and lower seam thickness, which are a cumulative effect on excavator's structural part overloading.

The design norms, transferred from earliest ones, became inadequate mainly related to the dynamic loads specific to the new operating environment, in terms of equivalence coefficients of dynamic load based on amplifying corresponding static loads [3]. These different assumptions do not consider the real character of overloads which lead to sudden failures or failures due to fatigue.

Even the newest Europe-wide used norm (DIN 22261), [7] uses the former dynamic coefficients, while the experience demonstrated that the real value of dynamic loads is much higher.

That is the reason for which the main goal of the mentioned BEWEXMIN project is to propose and develop proposals able to handle with the above-mentioned unwanted effects in terms of prediction and effect avoidance.

This goal can be fulfilled by the adaptation of existing BWEs to new conditions and to extend the results toward the design of new ones [4], [5], [6]. The constructive changes required must be based on deep knowledge of the phenomena occurring in the mentioned operating conditions, on which the project intend to contribute.

On the other hand, it is desirable to develop such a continuous monitoring system which can predict the possible failure caused by the occurrence of dangerous loads in critical parts of the load bearing structural elements in accordance with the current operating conditions.

The research has been foreseen in three directions, as follows: establishment of the requirements set to the load bearing structure of BWE, having in mind the minimization of dynamic loads; based on this, the next directions will be the development of the monitoring system, and a proactive approach based on continuous survey of the face, involving different geophysical methods and devices, in order to detect in real time the possibility of occurrence of hard inclusions.

2. SHORT OVERVIEW OF PERFORMED RESEARCH

In recent years, on working faces of open pit mines in many European countries it is clearly visible the increased amount of hard to be excavated structures and interlayers with excessive mining resistance.

These occurrences cause continuously serious problems during the operation of BWEs.

These kinds of occurrences were seldom before and only observed in some open pit mines, in different countries.

This is the reason for the low accent on studying this phenomenon, and if done, it was focused mainly on specific problem of involved mine and the results rarely were published.

When searching the literature we can find many references regarding the dynamic overload of the driving system of the bucket wheel and its avoidance. It is a general lack of mining environment description and it is difficult to correlate it with the failures occurred.

Some former researches were focused on bucket design and drive's overload protection using hydraulic safety clutches [7]. It is true, that interrupting the kinematic chain between the bucket wheel and the drive contributes to limit the transmission of extreme loads towards the structure, but this must be considered as an emergency act.

Another specific research was related to size the size of sparse boulders related to the bucket's dimension. It has an important influence on the extension and severity of damages, because in case of large bucket volume, greater than 4 m³, the boulder can be extracted from the face, and it produces damages on the on board conveyor flows.

If the boulder size exceeds the bucket's one, then the impact with teeth and bucket cutting edge produces high dynamic load on the mining system and load bearing structure.

Because the BWEs used in Germany are mainly with high volume buckets, the German specialists focused their attention mainly on preventing belt conveyor protection.

Even if the available sensors are well known and well developed, the results were in this case also weak related to the investment, mainly from point of view of data processing software. A detailed report on these issues we can be find in [5].

The results of the above-mentioned countermeasures were not very encouraging ones, the main finding was the conclusion that it is not possible to design and set-up a BWE in such way to be universal for any kind of mining environment in terms of safety, reliability and productivity.

The common weakness of previous researches is the lack of any correlation between damages and mining environment, between cause and effect.

Another difficulty encountered is the optimal location and number of sensors to be implanted in such a way that the acquired data provide maximum of information about the stress-strain state of the boom's elements and their processing itself, given the large spatial extent of the load carrying structure.

Apart from these experimental approaches, we may consider also theoretical ones, i.e. such theoretical models development which describe the effect of an external variable or impulse load on the load carrying structure and the bucket wheel.

Such a model of the time variation of an impulse load has been developed based on the collision between two elastic-plastic bodies. [6]

Searching answers to the mentioned open problems, the team of Petrosani University, has developed a bucket wheel 3D CAD model (Figure 1) on which by simulation we obtained its influence on the torque on wheel's axle. (Figure 2)

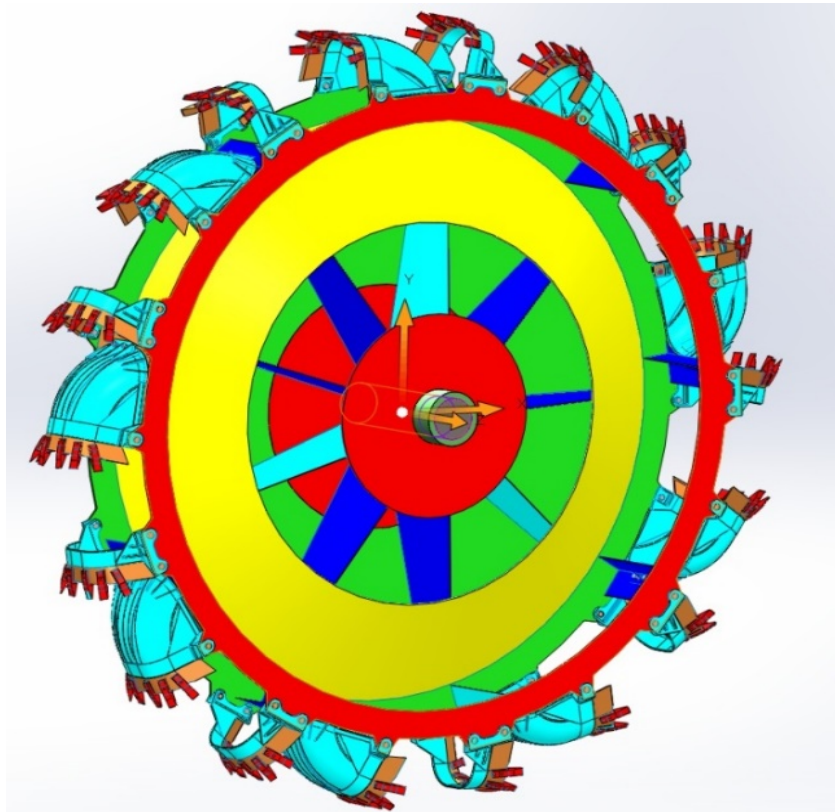


Figure 81. 3D model of the bucket wheel

In the same time, we mounted strain gauges on different parts of the boom structure at different bucket wheels which continuously measured data were transmitted by wireless system and recorded. (Figure 3).

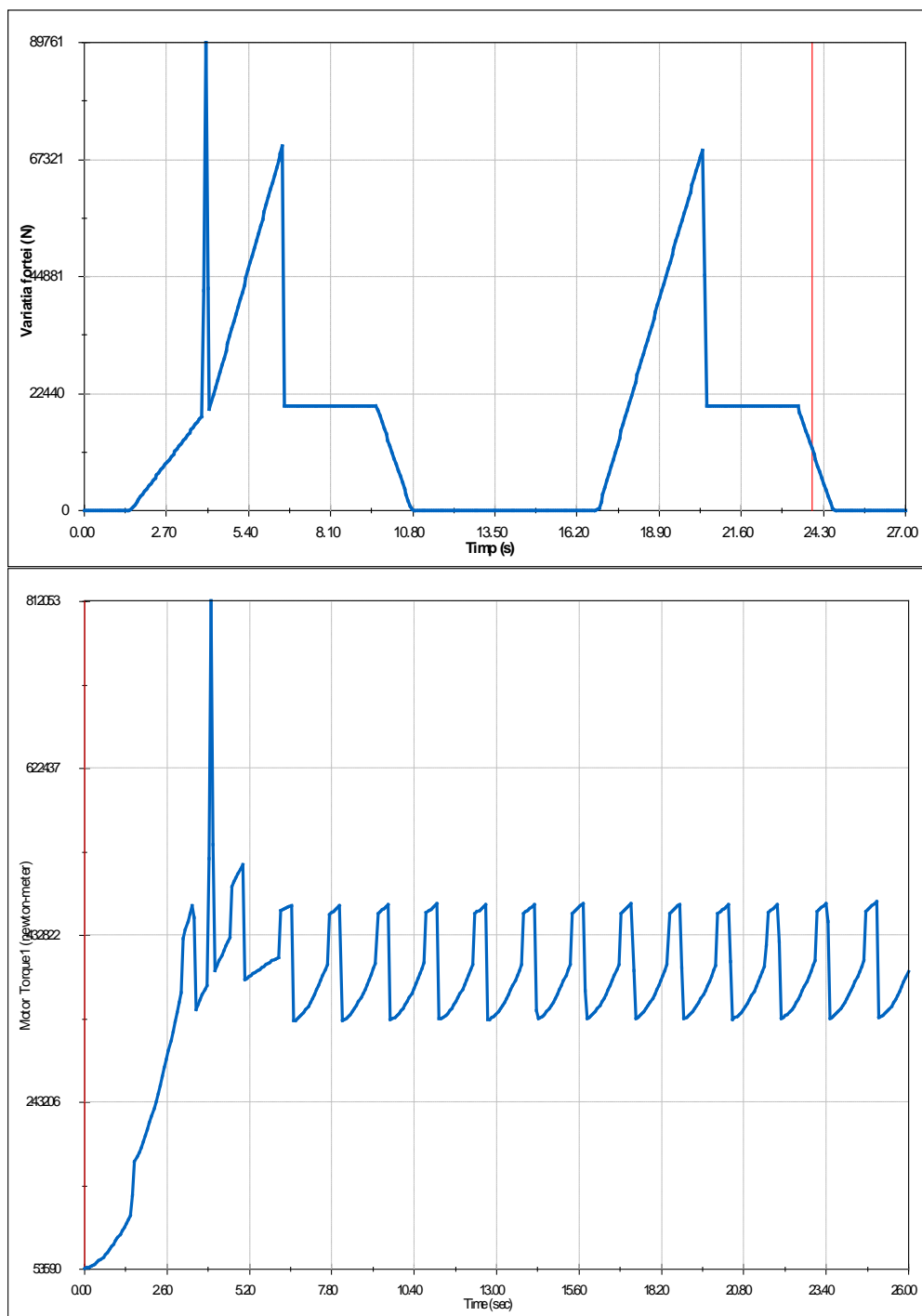


Figure 2. The impulse load time variation (top) and the effect on the wheel's axle torque (bottom)

The spectral analysis results (periodogram) of the measurement node with the largest values of strain are presented in Fig. 4.

Because the strain gauges use is very difficult and unreliable, we continued to use also accelerometers.

Additionally, we developed a model of the boom and we studied the spectra of its vibrations, excited by the mentioned resultant variable load. (Fig. 5)

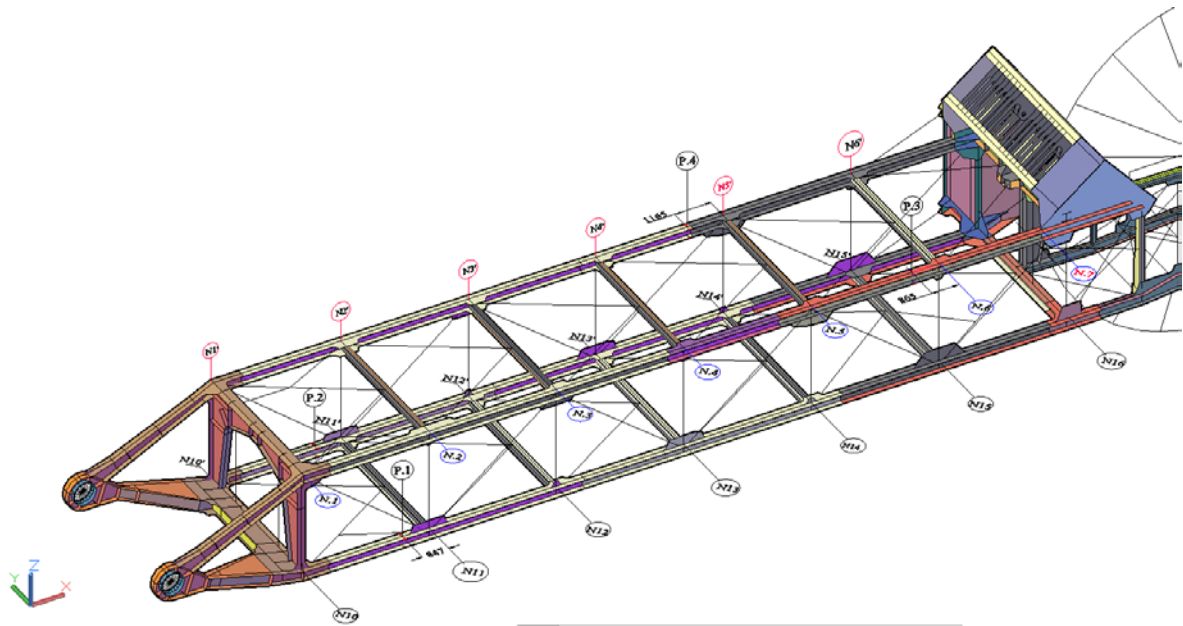


Figure 3. Location of electro-resistive transducers (ERT) on the bucketwheel boom

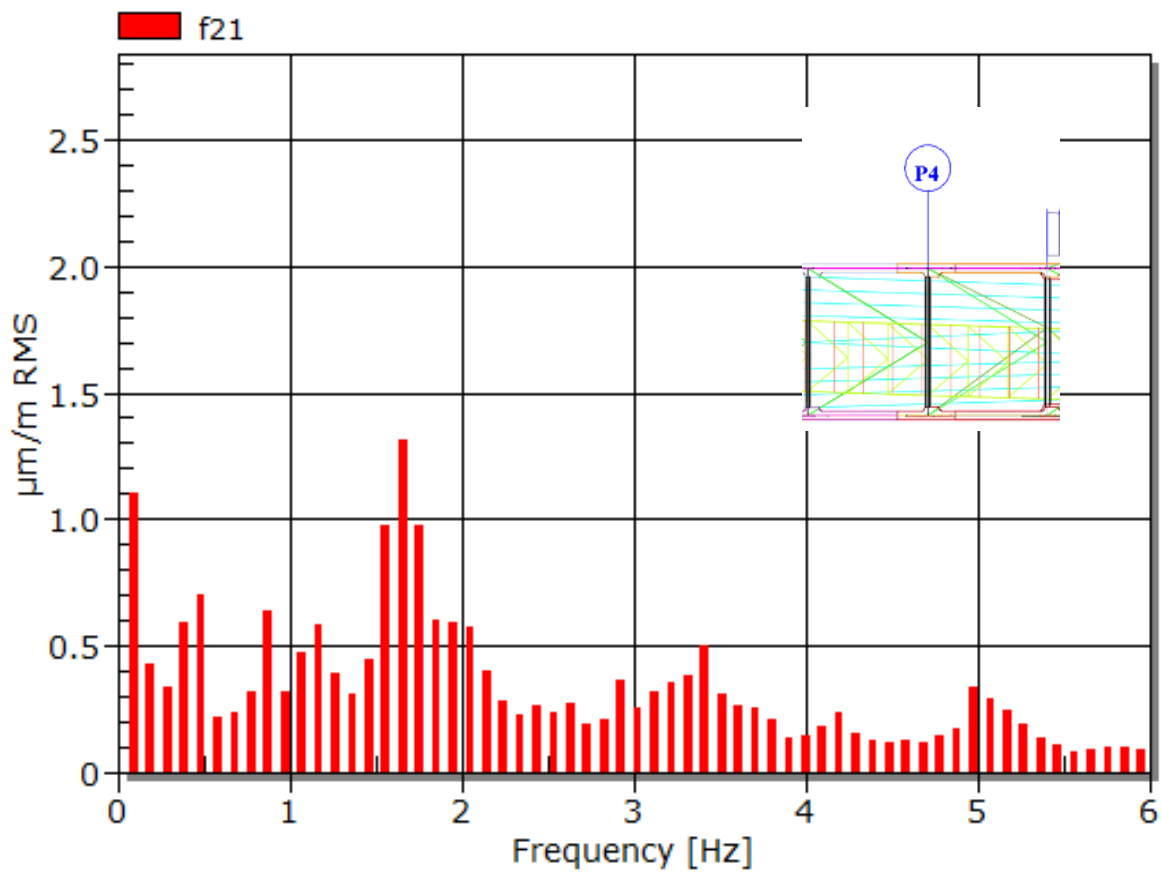


Figure 4. Periodogram of the measured stress using ERTs for node P4

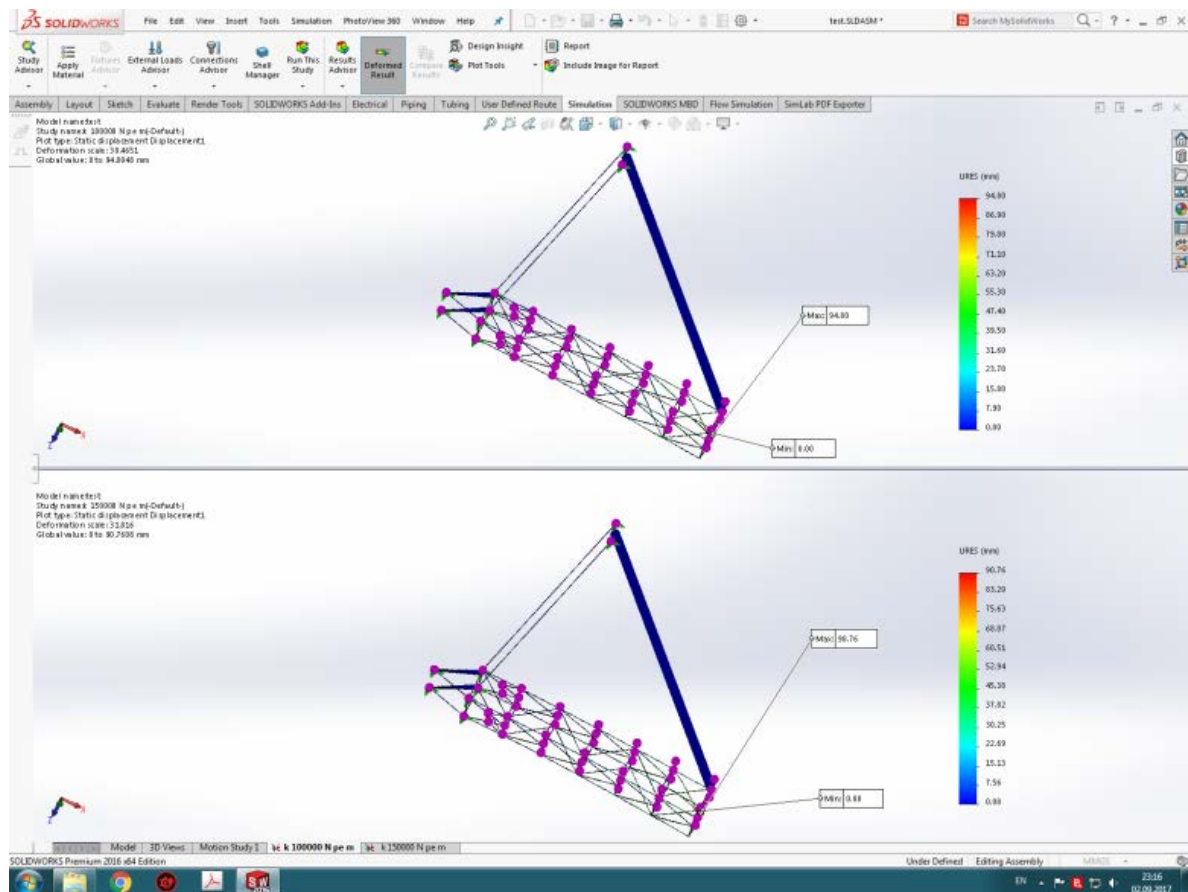


Figure 5. Strain simulation of boom under dynamic load

The correlated data processing is under way, but preliminary results show an acceptable concordance with theoretical ones.

3. RESULTS

The measurements performed until now have demonstrated that the load's signature has a vibration shape and is variable and it consist on the superposition of two components.

One is the proper vibration of the BWE's structure masses including the bucket wheel, the other is the vibration due to the influence of the excavating forces and other dynamical excitations.

The two components have close frequency spectra, and it is difficult to be discriminated from the general spectral picture the spectrum of vibration produced by the cutting force variability. The solution of this problem is the second main goal. The third research direction is to make connection between BWE operating parameters, the structure dynamic characteristics and the properties of the excavated rock environment in order to assess the real stress-strength state in critical points.

As result of this issue it will be possible to realize an adaptation of the existing BWE-s to operation in rocks with hard to excavate intrusions, and on the other hand to provide norms and design methods towards the development of a new generation of BWE-s.

The envisaged monitoring system will be useful not only to predict and avoid failure due to sudden excessive load, and for assess the degree of fatigue and on this basis to establish the remaining lifetime of the load bearing structural elements.

4. CONCLUSION

The research performed until now in the mentioned above three directions revealed the followings: in the direction related to the real time recognition of the occurrence of a boulder in order to allow the avoidance of its collision with the bucket wheel, the partners used many geophysical tools in real faces with hard intrusions or in “implanted” ones to find the deviation of different physical properties of intrusions from the basic rock’s one. In some cases, as in Husnicioara open pit sandstone inclusions the results were not satisfactory.

Referring to the second research direction which is focused on establishing the effect of a sudden increase of cutting force on the structural elements of the BWE (tooth, bucket, bucket wheel, on board belt conveyor, boom, drive system etc.) and to propose on this basis structural and constructive modifications or operating procedures in order to prevent or avoid the possible failure.

Such solution could be a monitoring system which uses filtering software able to detect the unwanted change, and an expert system to assist the decision taken by the operator or the automatic steering system.

REFERENCES

- [1] DIN 22261-2 Excavators, Stackers and Auxiliary Equipment in Brown Coal Open Cut Mines Part 2 Calculation Principals (2015). German Institute for Standardization.
- [2] Raaz, V. (1999). Grabkraftermittlung und Optimierung der maschinenverfahrenstechnischen Parameter von Schaufelradbaggern für einen energieund verschleißgünstigen Abbau von Abraum, Kohle und Zwischenmitteln im Tagebau, Braunkohle-Surface Mining 51 Nr. 5.
- [3] Sümegi, J. (2002). Kűlfejtűsi marótűrcsűs kotrűgepek jűvesztű szerkezetűnek elműleti vizsgűlata ęs fejlesztűse, Doktori ertekezűs, Miskolci Egyetem.
- [4] Durst, W., Vogt, V. (1988). Bucket Wheel Excavator. Trans Tech Publications, Clausthal-Zellerfeld, Vol. 7, FRG.
- [5] Rodenberg, J.F. (1987). Contribution to the Assessment of the Specific Cutting Force for Bucket Wheel Excavators, Continuous Surface Mining. Trans Tech Publications, Vol. 1, No.1-3/87, Clausthal, Germany.
- [6] Lu Zhong Lin (1983). Beitrag zur Festlegung der Auslegungs- und Betriebsparameter von Schaufelradbaggern durch Untersuchung ihrer Einflűsse auf das effektive Fűdervolumen und den Energieverbrauch sowie durch Untersuchung des Entleerungsvorganges des Fűdergutes, Dissertation, TH Aachen.
- [7] Srđan, B., Nenad, Z., Donatus, O. (2006) On the dynamic modelling of bucket wheel excavators, FME Transactions 34, 221–226.

Acknowledgment

The actual paper is supported by the European Union Research Found for Coal and steel by the research project RFCR-CT-2015-00003-BEWEXMIN „Bucket wheel excavators operating under difficult mining conditions including unmineable inclusions and geological structures with excessive mining resistance”. Conclusions should state concisely the most important propositions of the paper as well as the author’s views of the practical implications of the results.

New Method of Residual Lifetime Assessment of Bucket Wheel Excavators Operating in Romanian Lignite Open Pits

Iosif Andras, Maria Lazar, Andrei Andras, Sorin-Mihai Radu, Florin Vilceanu and Stela Dinescu

University of Petrosani, 20 Universitatii str., 332008 Petrosani, Romania

ABSTRACT

The paper deals with a method of residual lifetime assessment of the BWE-s operating in Romanian lignite open pits which is based on the correlation between the failure history of a fleet of BWE-s with different age and different working hours in working environment with different degree of difficulty with a laboratory- field fatigue assessment method based on hardness increase with the number of loading cycles of the elements of the boom structure. The results allow estimating the residual lifetime of the existing excavators and also to the forecast of overall system reliability of new or refurbished excavators to be implemented.

1. INTRODUCTION

Using surface hardness measurements on structural elements with a long history of cyclical loading as an indicator of the fatigue state is relatively new in the analysis of structures, subject of this kind of loading.

The representative structures subject of this approach are mainly the metallic bridges, cranes, buildings, mainly submitted to seismic loads, offshore and subsea structures, pipelines, and other mechanical parts, as gears. In the past time the load carrying structures of huge earth-moving machines, such as Bucket Wheel Excavators (BWE) became subject of this approach.

It was determined that the fatigue resistance coefficient decrease can be correlated with Brinell Hardness (HB) increase in the case of steel. Despite the different opinions of the specialists regarding the so called cyclic softening-hardening of steels, the hardening process in the vicinity of zones suffering plastic strain has been confirmed.

There are many theoretical approaches, not all showing the direct correlation of hardening and number of cycles. Such a correlation between the fatigue resistance coefficient (fatigue ratio) and Brinell Hardness has been statistically determined as in fig. 1. [7]

Another reference regarding a new interpretation of the Bauschinger effect is [8], where the hardening / softening of steel plates submitted to repeat bending loads.

The hardness increase with the number of variable load cycles – determined from the overall working hours -was determined on samples collected from critical parts of BWE boom elements and compared with hardness increase of genuine steel samples of same brand, submitted to tensile stress until failure, on which the hardness has been measured in the vicinity of breakage.

The hardness relative increase is significant leading to the conclusion that the hardness can be considered as an indicator of fatigue resistance, i.e. for the assessment of remaining lifetime of the structure in cause.

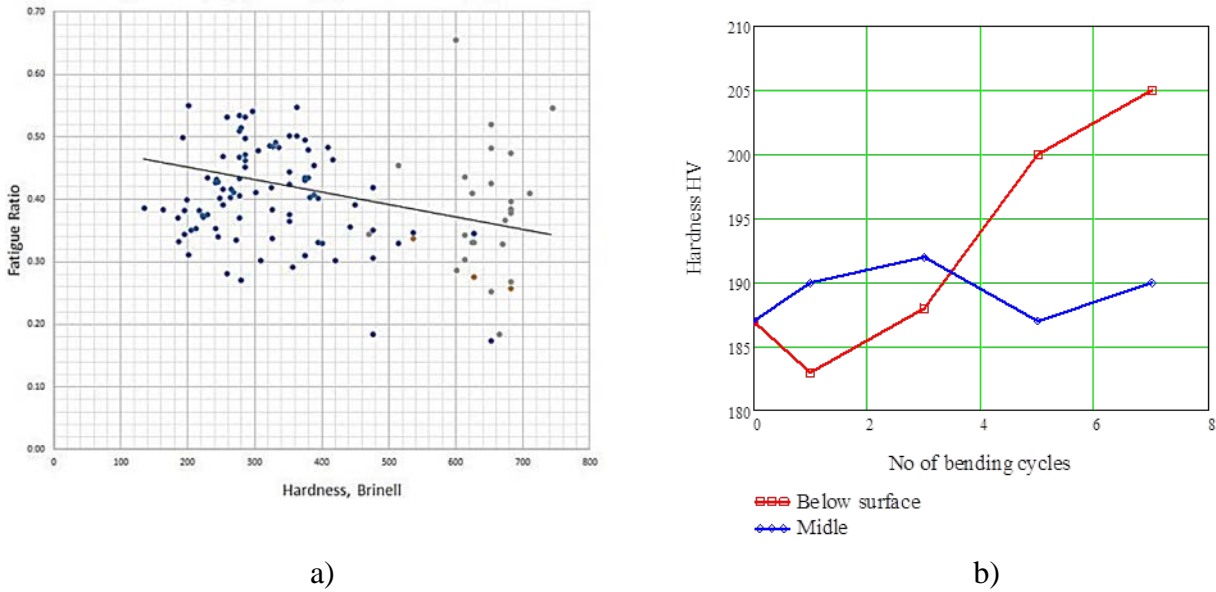


Figure 1. a) Brinell Hardness increase with fatigue resistance coefficient decrease , according to <https://barfatigueblog.org/2017/08/08/hardness-versus-fatigue-strength/>, b)Hardening-softening of steel plate submitted to bent load according to [8]

2. MATERIAL AND METHOD

In our approach, three types of measurements were considered, as follows:

Joint hardness and tensile strength measurements on samples made by the same kind of steel as the BWE boom elements, revealing an increase of surface hardness increase in the proximity of breakage relative to the hardness in the body of the sample;

Hardness and strength measurements on samples obtained from the BWE boom members, which were replaced during renewal of the respective structural element after failure;

In situ hardness measurements on selected points of constitutive elements of boom, using portable non-destructive hardness measurement devices, the points being selected on the basis of FEM analyses and fault history of the given BWE.

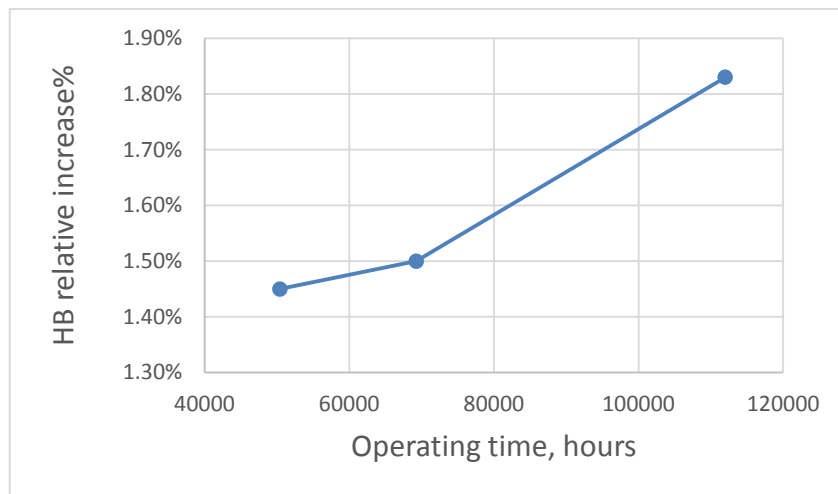


Figure 2 Brinell Hardness relative increase as a function of operating hours

Hardness based mechanical properties decay analysis is a less-used method of investigating structural features in mining machinery, but it can provide some properties that evolve over time in materials in the load-carrying structure of the machine.

The average Brinell Hardness variation of samples collected from BWE boom elements related to samples made from the same kind of steel, in original state, has been plotted, according to Fig. 2

We extended the hardness measurement on a batch of 7 machines type ERc1400-30/7 from different open pits from Oltenia coal basin, on the same subassembly, respectively, the bucketwheel boom, and the data being synthetized in table 1.

In the Fig. 3, the average hardness has been plotted in correlation with the age of service of different BWE -s from which the samples were collected. It can be observed that the general trend of HB is increasing; the last point value is due to the fact that the steel is other kind than the rest of BWE-s, and other deviations are due to the averaging and different load history (less operating hours at same age).

Table 1. Results of hardness measurements on the bucketwheel boom of E1400-30/7 excavators

No	Equipment/mine	Operating hours[hr]	Year of start	Average hardness [HB]
1	E14-07 -Rosiuta-Motru	50400	2000	120.66
2	E14-04-Pinoasa-Rovinari	51313	1991	155.28
3	E14-03-Pinoasa-Rovinari	64220	1989	124.44
4	E14-08-Rosiuta-Motru	69264	1993	116.99
5	E14-04 Tismana-Rovinari	72815	1986	158.99
6	E14-02-Rovinari Garla	95925	1983	151.65
7	<i>E14-02-Tismana - Rovinari</i>	<i>115684</i>	1971	<i>137.95</i>

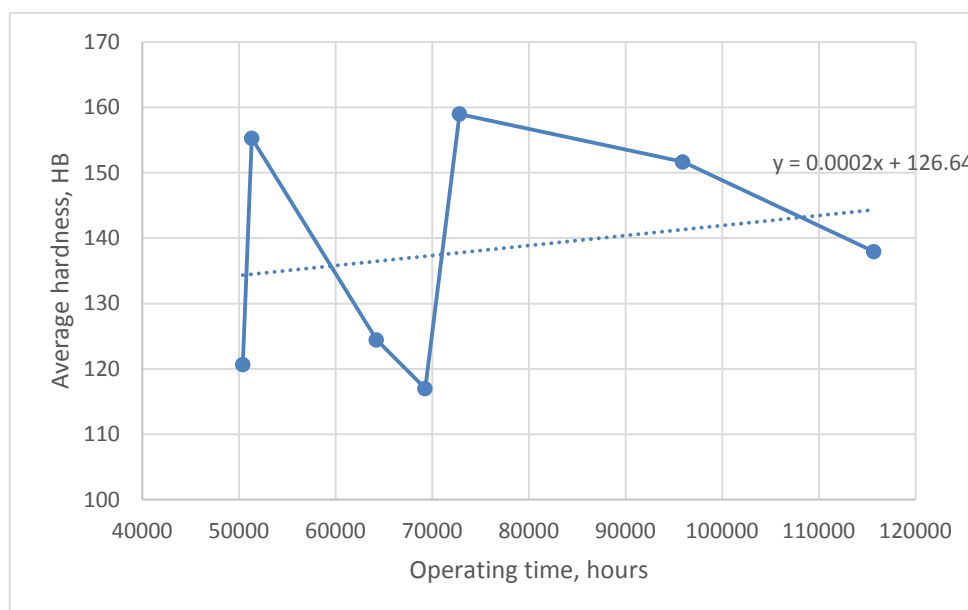


Figure 3. Evolution of average hardness measured on boom elements of excavators according to the operating time

Nevertheless, the differences of hardness between different elements of the boom structure can provide useful information about the fatigue level of different structural parts, for the identification of those in which the probability of expected failures is greater. This is very useful for sensors placement location for state monitoring.

To measure the hardness we used a portable device in the MIC 20 range to perform measurements on both sides of the boom, right/left wall, according to figure 4. The hardness measurement was performed after a mechanical pre-cleaning of the sampling area, at the lower/upper part of the diagonal strut, as in figure 5.

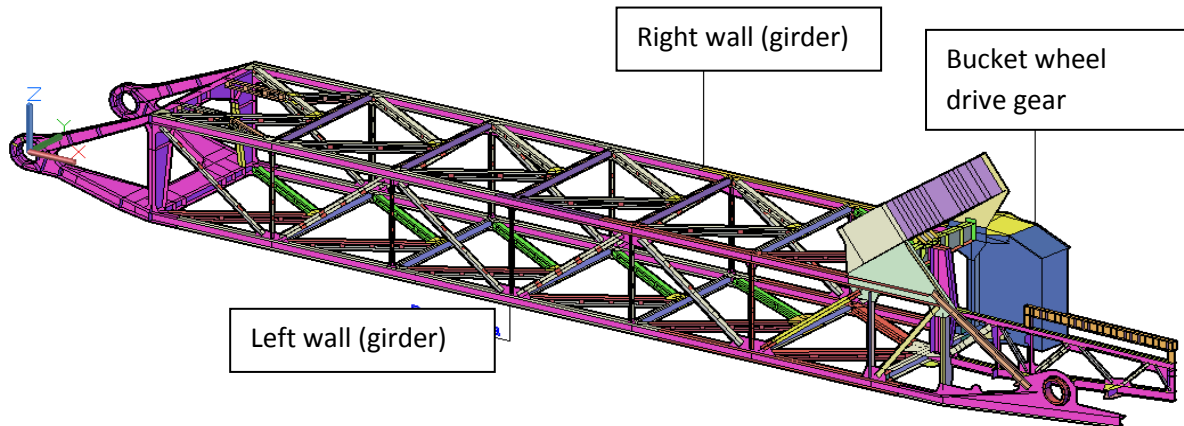


Figure 4. Constructive elements of a bucketwheel boom



Figure 5 . Hardness measuring points

We performed the hardness measurement on two machines type E 1400-307, 07 and 08, from the same open pit, under approximate temperature and excavation conditions to assess the hardness for which the structural properties of the materials are close. After processing the data, we have compiled and illustrated in figures 6 and 7.

From the figures we can find that in average the decay of properties is not affected by the operating time between excavators, but it is a clear difference between left and right wall (girder).

Also, the graphs indicate a difference between the joints (nodes) which shows an asymmetry between left and right and a concentration of hardening at the extremities of the boom relative to middle segment.

This fact, with correlation with other analyses can be useful for deriving a complex, multifactorial discrimination method of detecting the most vulnerable parts of the boom.

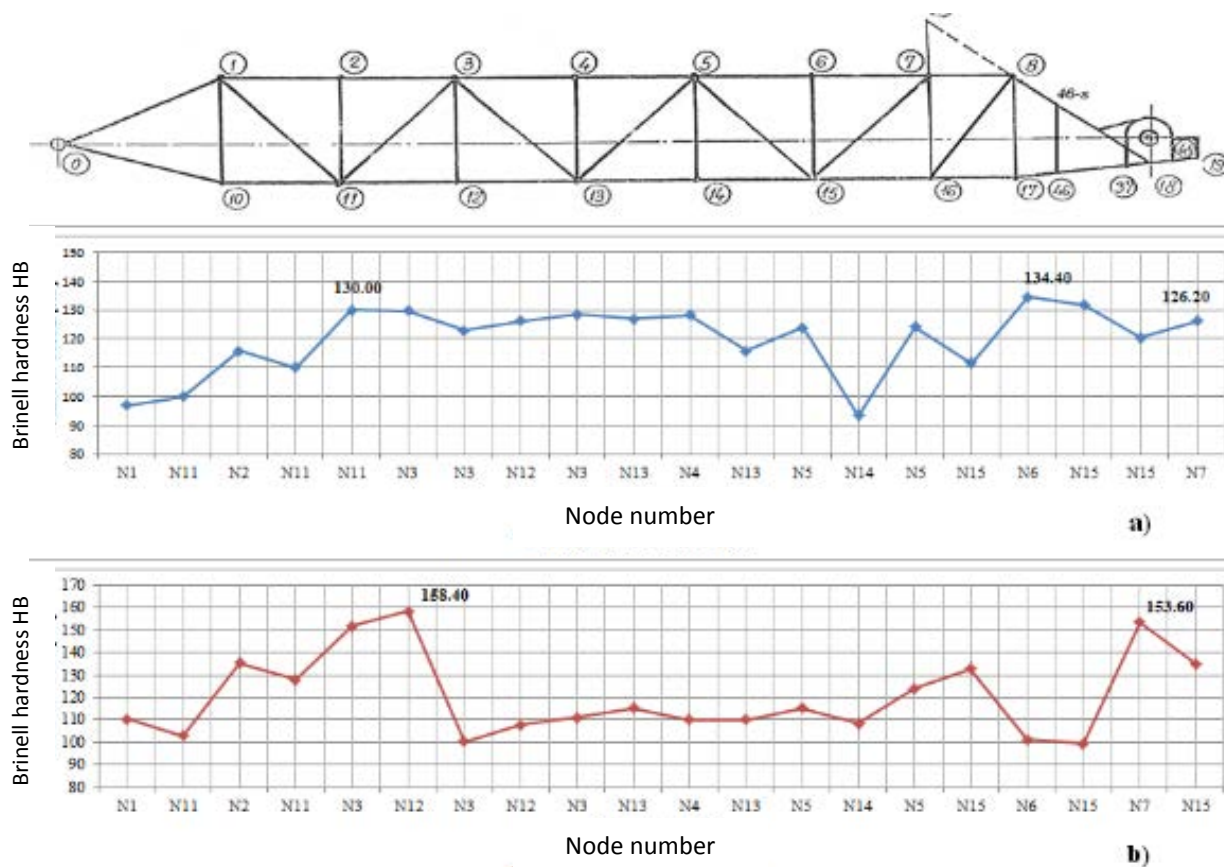


Figure 6. Distribution of hardness on the boom's right wall members of excavators: a) E14-07, b) E14-08 according to table No. 1

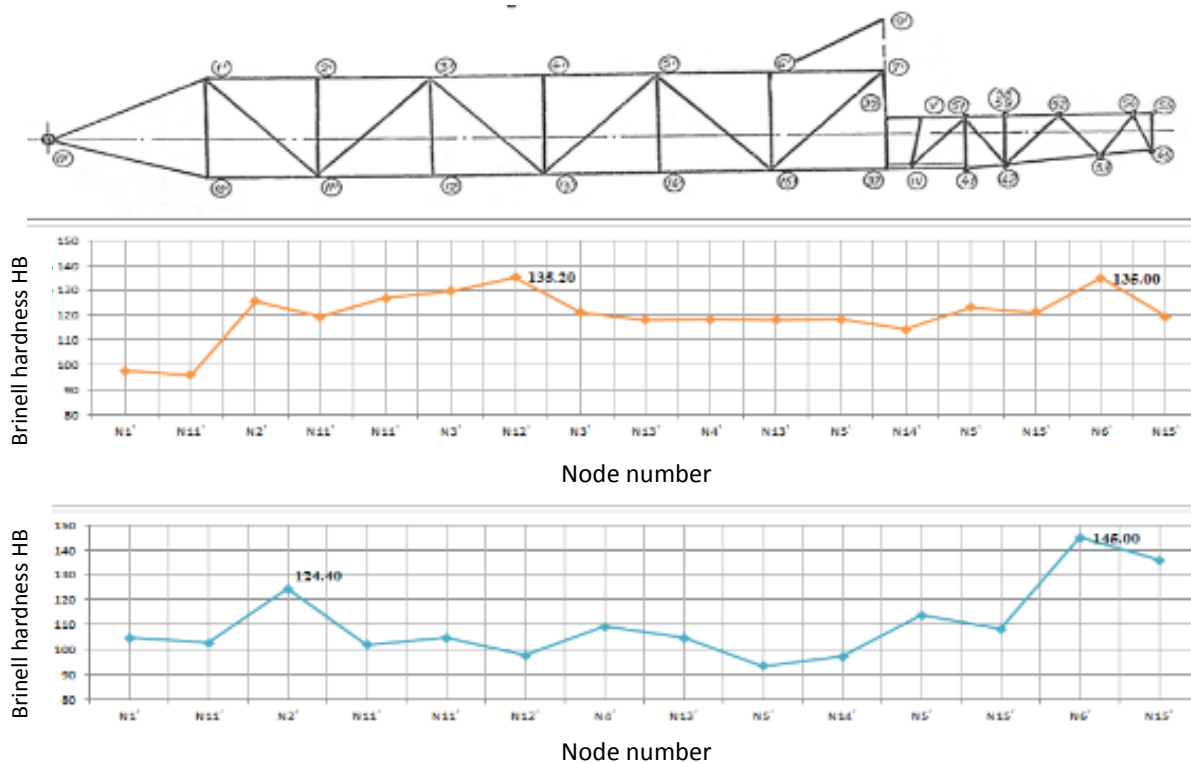


Figure 7. Distribution of hardness on the boom's left wall of excavators E14-07, E14-08 according to table No. 1

Table 2. Faults occurred at some representative BWE s relative to age, throughput and operating hours

Machine	Age of the machine [years]	@Type faults	Faults No.	Throughput 1000*[m ³ overburden +tons lignite]	Operating time [hours]
04 Pinoasa	25 years	9	13	44,129.884	51313
03 Pinoasa	28 years	9	12	52,518.749	64220
04 Tismana	31 years	10	13	56,622.949	72815
02 Rovinari-Garla	34 years	10	12	82,433.395	95925
02 Tismana	45 years	19	27	96,506.447	115684

@ load carrying system involved faults

3. INFLUENCE OF THE AGE OF BWE ON FAULTS FREQUENCY

The carrying structure of BWE suffers in time degradation by fatigue that affects the functionality of these machines, degradations that can be generated jointly by corrosion, due to the environment of working area, by the remaining deformations of the elements, generally caused by accidental crashes or by the fall of material blocks on the structure, cracks in structural elements which may occur due to overloading to non-conforming welds, decrease of fatigue resistance of materials.

The degradations that may occur over time on mobile heavy-duty machinery may be disposed of in the form of punctual charts of type defects for these machines. These charts have been drawn up after conducting the technical expertise of 25 machines used in lignite open pits or coal deposits.

The evolution of faults in the load carrying structure of some of these ERC1400-30/7 type machines operating in the open pits from CEO, resulted from an in-situ analysis carried out in 2016, is presented in table 2. The data from Table 2 shows that the number of faults was almost constant for a period of about 30 years, after which they grow.

In figures 8 to 12 different correlations between operating hours, failures occurred, throughput, rate of failure, production rate are presented.

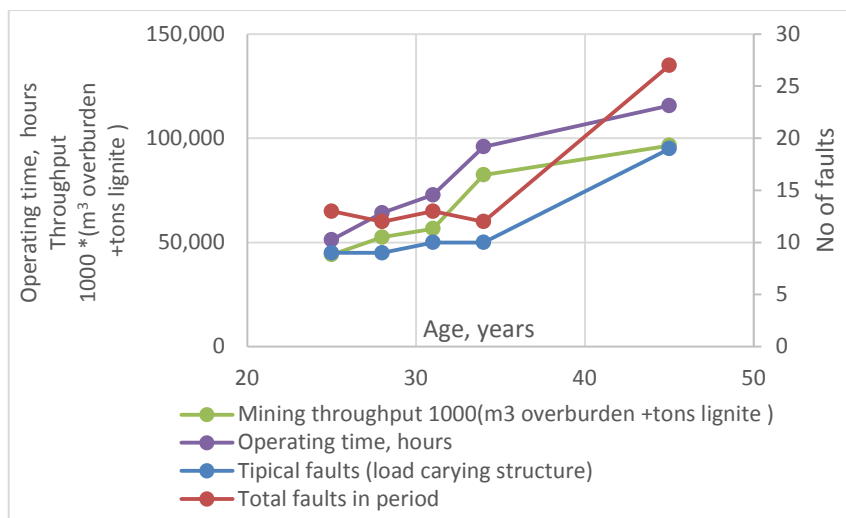


Figure 8. Main Correlation chart

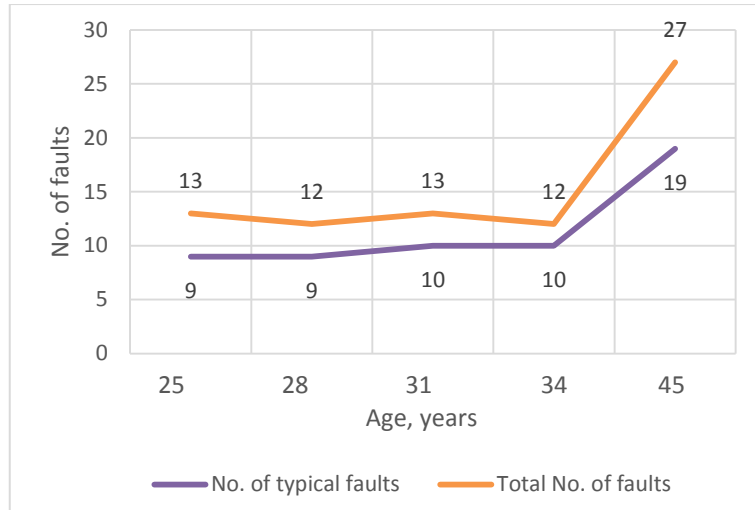


Figure 9. The number of failures according to the age of the machine

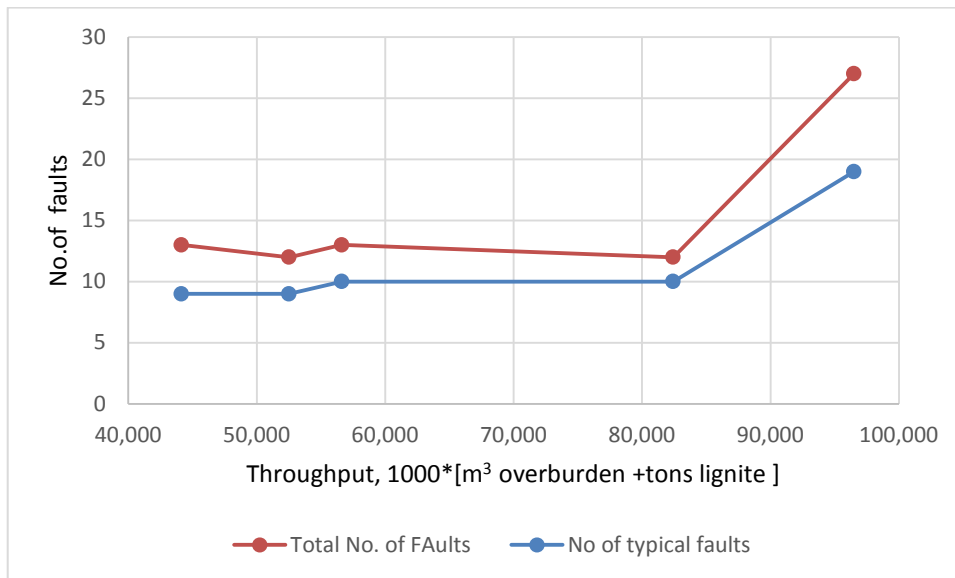


Figure 10. The number of failures according to the throughput

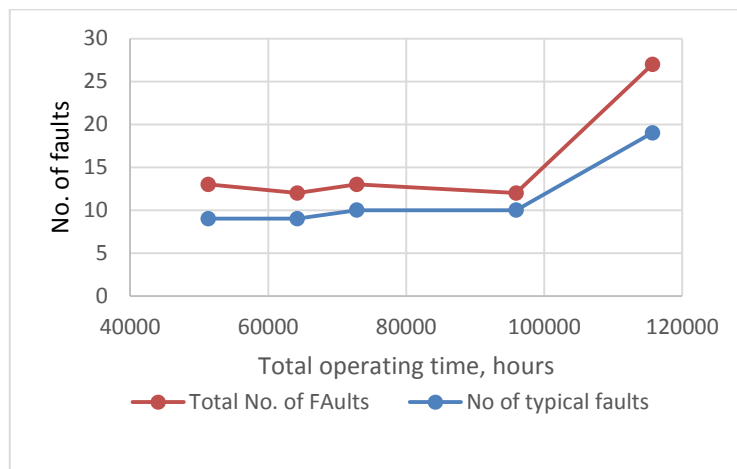


Figure 11. The number of failures according to the operating hours

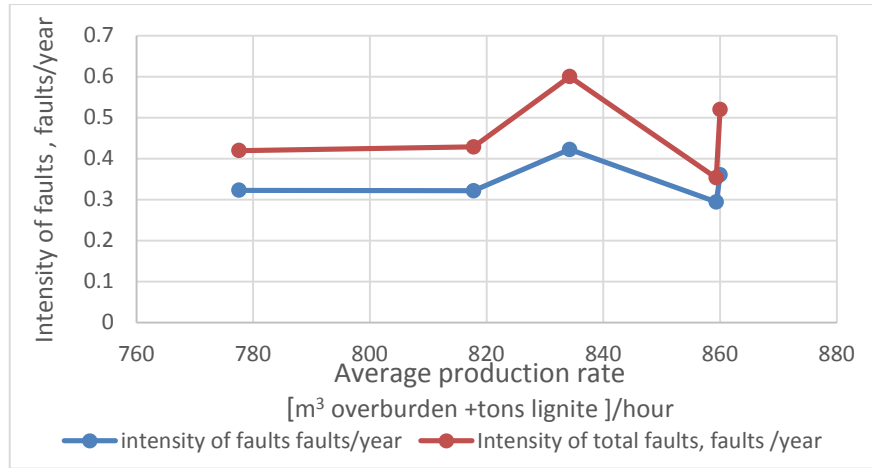


Figure 12. Correlation between the intensity of faults and production rate

By correlating the fault intensity with hardness growth, we can forecast the expected faults number dependence on the average hardness , as in figure 13.

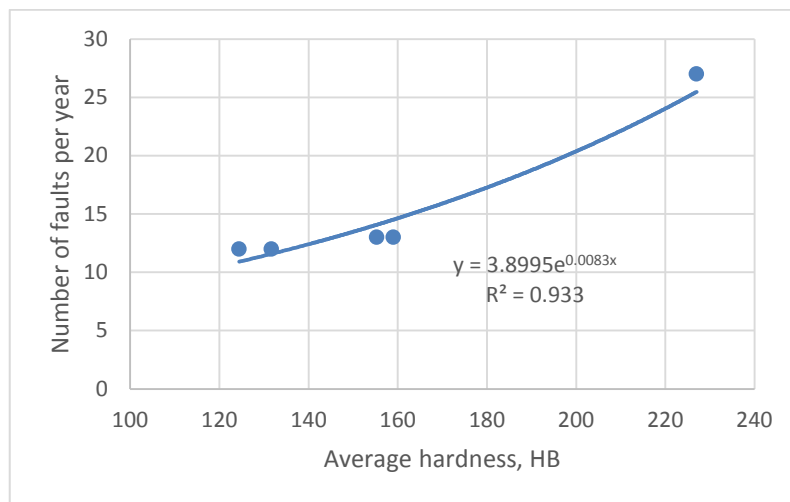


Figure 13. Correlation between fault intensity with hardness growth

4. CONCLUSIONS

Hardness based mechanical properties decay analysis is a useful method of investigating structural features change in mining machinery, and it can provide some information on the properties that evolve over time in the components of the load-carrying structure of the machine.

The hardness relative increase with the duration of service is significant, leading to the conclusion that the hardness can be considered as an indicator of fatigue resistance, i.e. for the assessment of remaining lifetime of the structure in cause.

Different correlations between operating hours, failures occurred, throughput, rate of failure, production rate were derived, which are useful for state monitoring of the BWE carrying structure.

By correlating the fault intensity with hardness growth, it is possible to forecast the expected faults number dependence on the average hardness.

The differences of hardness between different elements of the boom structure can provide useful information about the fatigue level of different structural parts, for the identification of those

in which the probability of expected failures is greater, which is useful for deciding the sensors placement location for state monitoring.

The results, in correlation with other analyses can be useful for deriving a complex, multifactorial discrimination method of detecting the most vulnerable parts of the boom.

The method presented itself is a new way to expertise and assess the state of the BWE-s and to forecast the remaining lifetime reserve.

REFERENCES

[1] Roessle, M. L., Fatemi, F., (2000). Strain-controlled fatigue properties of steels and some simple approximations. *Int. J. Fatigue* 22, 495–511

[2] Stephens, R.I., Fatemi, A., Stephens, R.R., Fuchs, H.O., *Metal Fatigue in Engineering* - ISBN: 978-0-471-51059-8.

[3] Lassen, T., Récho, N., (2006). *Fatigue Life Analyses of Welded Structures*, ISBN: 978-1-905209-54-5, Wiley-ISTE.

[4] ISO 14345/2004 *Fatigue -- Fatigue testing of welded components – Guidance*.

[5] DIN 22261-2 /1997 *Excavators, spreaders and auxiliary equipment in opencast lignite mines - Part 2: Calculation principles*.

[6] Vîlceanu, F., Radu, S.M., (2014). Methodology of establishing residual lifetime of lifting installation by non-destructive methods, 6th International Multidisciplinary Scientific Symposium, Universitaria Simpro 2014, Petroșani.

[7] <https://barfatigueblog.org/2017/08/08/hardness-versus-fatigue-strength/>

[8] Chandra, I.Y., Korda, A.A, (2016). Bauschinger effect on API 5L B and X56 steel plates under repeating bending load, *Proceedings of the 1st International Process Metallurgy Conference, AIP Conf. Proc.* 1805, 070006-1–070006-6 <https://doi.org/10.1063/1.4974447>

[9] Drumond, G., Roudet, F., Pasqualino, I., Pinheiro, B., Chicot, D., Decoopman, X., (2017). High cycle fatigue damage evaluation of steel pipelines based on microhardness changes during cyclic loads, 23 Congrès Français de Mécanique Lille.

Acknowledgment

The actual paper is supported by the European Union Research Found for Coal and steel by the research project **RFCR-CT-2015-00003-BEWEXMIN** „Bucket wheel excavators operating under difficult mining conditions including unmineable inclusions and geological structures with excessive mining resistance”

Session 4: Geotechnical engineering

The Role of Geological Faults in Mine Stability: Amynteon mine, Western Macedonia (Greece) as a Case Study

Spyros Pavlides, Alexandros Chatzipetros and Ilias Lazos

¹Department of Geology, Aristotle University of Thessaloniki, 54124, Greece

ABSTRACT

Landslides are destructive phenomena, related to negative environmental and economic effects. In many cases, geological faults hold a key-role, as they are responsible for the triggering of landslides. In the present paper, we examine the geological setting of the wider Amynteon lignite mine region (Western Macedonia, Greece), where a complicated landslide phenomenon occurred on June 10th 2017, leading to the cancellation of mining activities and the partial evacuation of the adjacent Anargyri village. The mine is located in a lignite-bearing Neogene lacustrine sequence, while six major fault zones are documented in the broader area, two of them affecting the mine itself. They are the NE-SW trending normal fault zones (Anargyri and Vegora faults) and the mine is located at the transfer zone between the overlapping tips of these two zones. Anargyri and Vegora faults are dipping to the NW and SE, respectively, forming a graben, as well a multitude of internal secondary faults. The presence of the geological faults is decisive for the mine stability, as they cause fragmentation of the lithological formation and cohesion degradation, while the hydrological conditions and mining activity further affect the mine stability. The combination of those factors led to the Amynteon lignite mine landslide phenomenon, proving the great importance of geological faults study during excavation activities.

1. INTRODUCTION

This paper focuses on the importance of faulting in mining activities, especially the surface continuous mining ones and is examining a large-scale landslide that took place on June 10, 2017 at the lignite mine of Amynteon, Western Macedonia, Greece. This major and complex landslide caused the collapse of a large part of the mine, destruction of machinery, cancelation of mining activities, partial destruction and evacuation of the adjacent Anargyri village and multiple socio-economic impacts. The study area is in the region of Western Macedonia, at an altitude of *ca.* 600 m and it is located between lakes Vegoritis and Chimaditis, close to the town of Amynteon. The smaller village of Anargyri is located on the southwest side of the mine (Figure 1).

2. GEOTECTONIC SETTING

2.1. Geological setting

The bedrock of the broader Western Macedonia area is comprised mainly of Pelagonian units. Palaeozoic metamorphic rocks are overlain either stratigraphically or tectonically by younger Mesozoic and Tertiary rocks [1]. Palaeozoic granite intrusions, as well as ophiolites and associated sediments are also present. The main part of the bedrock in the study area comprises of Triassic-Jurassic carbonates and the Middle-Late Cretaceous transgressive sediments. The bedrock is unconformably covered in places by post-alpine sedimentary formations, mainly lacustrine Middle Pliocene – Lower Pleistocene sediments, while Upper Quaternary deposits (mainly conglomerates, red beds, alluvium and scree) cover locally both. The Pliocene formation comprises of three main

horizons: the lower one is dominated by conglomerate, containing ophiolitic clasts, red clay and marls. A middle horizon comprises of fine-grained sediments, mainly white marl, with thin lignite-bearing layers. The uppermost horizon contains alternations of white marl and marly limestone with occasional sandy layers. The total thickness of the Pliocene deposits is more than 700 m at the central part of the basin. The Lower Pleistocene sequence is rather cohesive and consists of red clays with gravel parts at its lower part and red clay and breccia at its upper one [2].



Figure 82. Location of the mine in relation to Amynteon town and the adjacent lakes.

Three major horizons of Pliocene sediments outcrop in the broader Anargyri – Amynteon area. The lowermost horizon consists of conglomerate and red clay formations, changing gradually to sand and marl formations. The medium horizon consists of fine-grained sediments, clays and marls, including lignite beds. At the upper horizon alternations of marls and marly limestone, while locally sand layers and lenses are intercalated with the lignite bodies.

2.2. Structural setting

The area of NW Greece has been subjected to several deformations, which caused the formation of a variety of tectonic structures. Successive deformation phases affected the geotectonic evolution of the area, forming its current structure [3]. The overthrust the Pelagonian carbonates is imprinted on the schistosity and folding and is characterized by abundant ophiolitic *mélange*. The Late Cretaceous – Late Eocene compression formed NW – SE trending folds and thrusts. The major folding resulted in the formation of NW – SE trending anticline and syncline structures. During the Middle – late Miocene, an E – W compressional phase caused the strike-slip faults trending WNW – ESE. Some of them were reactivated as normal faults during the subsequent extensional neotectonic

events. The compressional deformation was completed during the late Miocene. This phase formed E-W reverse faults in the ophiolitic masses and reactivated of the inherited strike-slip faults.

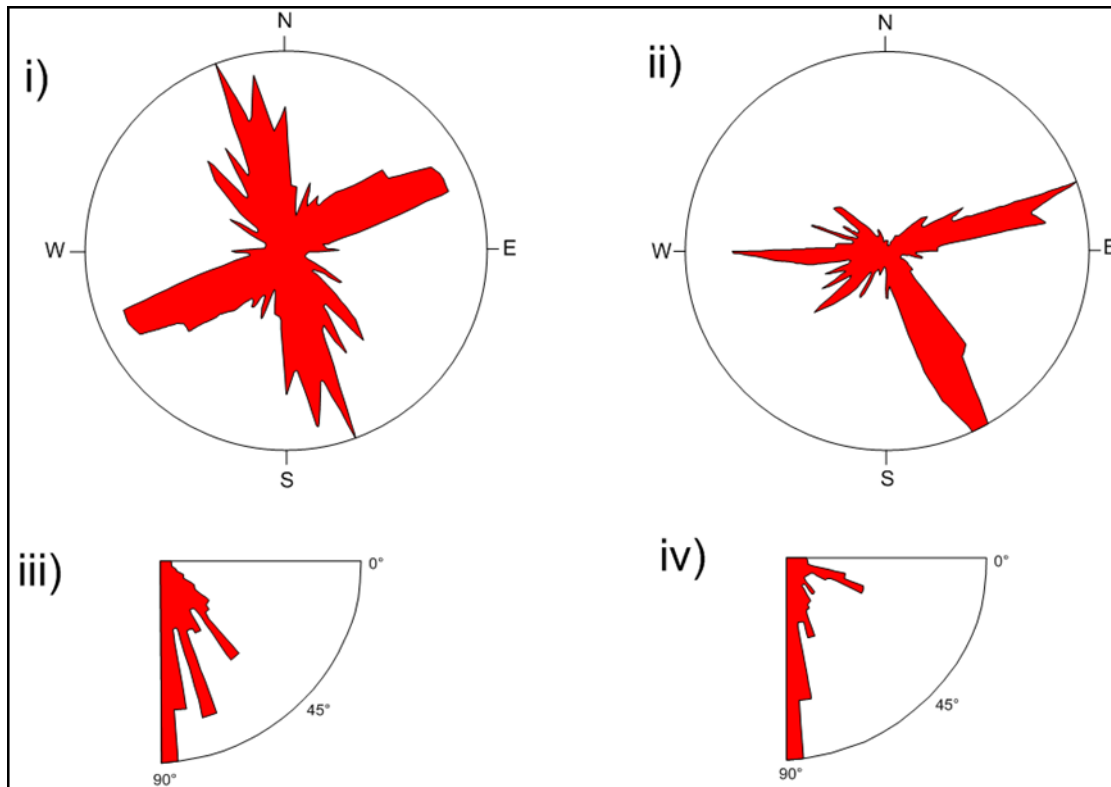


Figure 83. Fault distribution diagrams of the broader area, showing (i) the major NW – SE and ENE – WSW directions, (ii) dip directions, the majority of which is dipping to SSE and ENE, (iii) dip values ranging between 45° and 90°, the majority of which shows very high dip values (85° – 90° dip slip faults) and (iv) the pitch angle values ranging between 85° and 90°, confirming the extensional regime (dip slip typical normal faults) (modified from [4]).

The most recent and relevant to the current research deformation stages are the neotectonic ones. Two main neotectonic extensional periods are traced in the broader NW Greece region [2,4]. The Late Miocene – Pliocene one created or reactivated NW – SE trending normal faults, forming large depressions of the same direction, following mainly the NNW-SSE trending pre-existing syncline. The subsequent Middle-Late Quaternary tectonism is still active. This NNW – SSE trending extension caused the formation or reactivation of NE-SW to E-W striking normal faults (Figure 2). They caused further fragmentation and subsidence, forming smaller transverse sub-basins. The faults created or reactivated during this stage played the most important role in the neotectonic evolution of the area. One of the most important faults in the area is the Aliakmon - Servia one, which delineates the southern boundary of the Kozani - Ptolemais basin. A segment of this fault was activated during the May 13th, 1995 Kozani - Grevena M_w 6.6 earthquake [5–8].

2.3. Active faulting and seismicity

Amynteon lignite mine is located near the northern border of Ptolemais basin. Six main fault zones have been mapped in the broader area (Figure 3). They are Komnini - Asvestopetra (possibly extended to Pyrgi village), Emporion - Perdika, Anargyri (or Chimaditida - Anargyri), Perea - Maniakion, Vegora (or Vegoritida - Agios Panteleimon) and Nymfeon - Xinon Neron - Petres Lake [4]. The Amynteon mine is located between Anargyri and Vegora faults. A multitude of secondary faults also affect the area of the mine and might have contributed to the weakening of the rock/soil mass in combination with hydrogeological factors (see [9–13] and references therein).

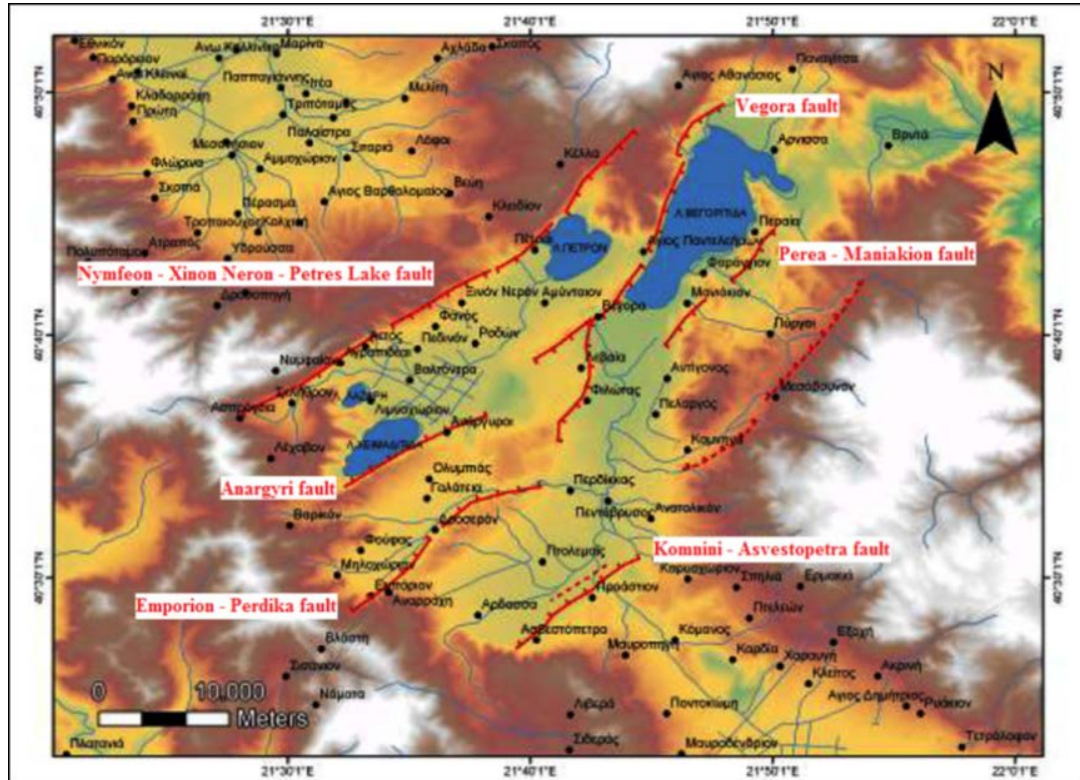


Figure 84. Simplified structural map of the study area (modified from [14], after [4]).

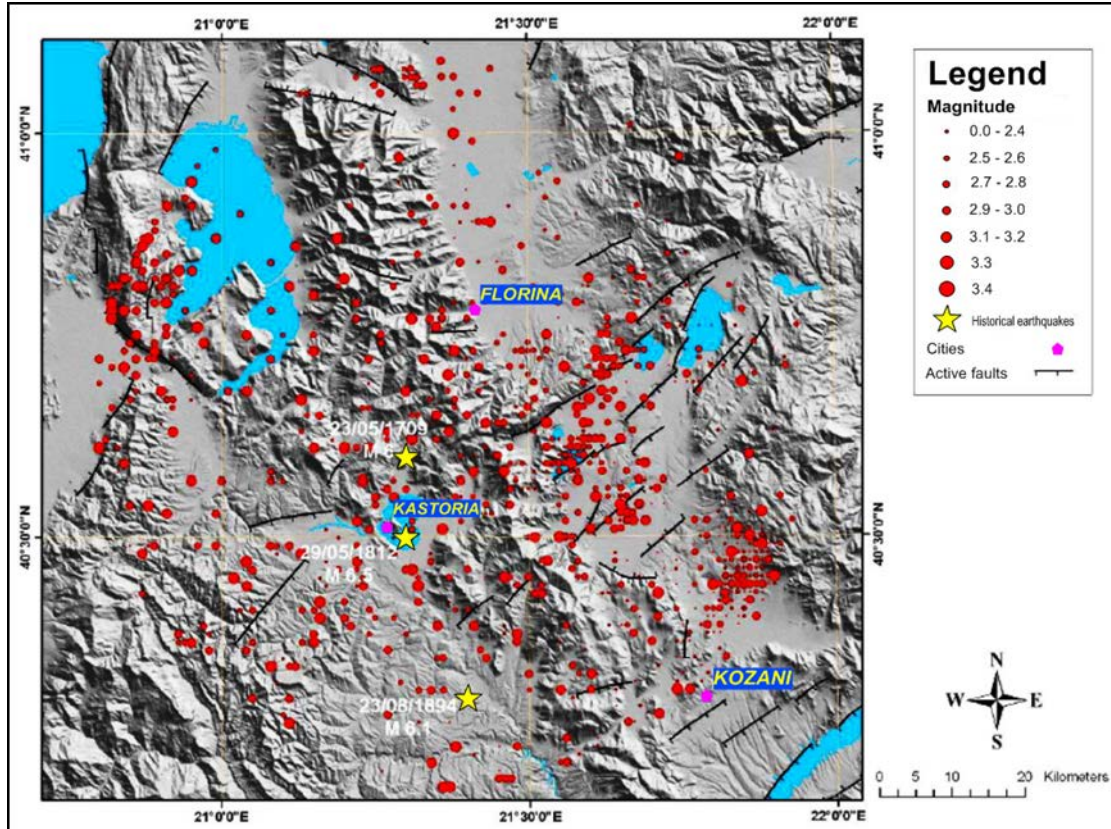


Figure 85. Map of the most important neotectonic faults of the broader area and the epicenter locations of the known seismic events of the study area for the time period between 1800 and 2007. Concentrations of microseismic events are observed at Nymfeon – Petres Lake, Anargyri and Emporion - Perdika faults [15].

Figure 4 shows the most important neotectonic faults of the wider area and the epicenter distribution of the known seismic events of the study area for the time period between 1800 and 2007 (historical earthquakes and instrumentally recorded of the last years). The epicentral locations of the seismic events are shown in different symbols, based on the magnitude. No strong earthquakes have been recorded within the Ptolemais basin area.

The broader area is characterized by low seismicity. The background seismicity, i.e. the instrumentally recorded earthquakes up to 2015, shows that magnitudes are ranging between 2.0 and 4.8. The majority of the magnitudes are up to 3.9 (Figure 5), while the mean value of the epicentral depth is 9 – 10 km. Seismic events of M_s 4.0 or higher are shown in Figure 6. No earthquake-induced surface ruptures have been observed.

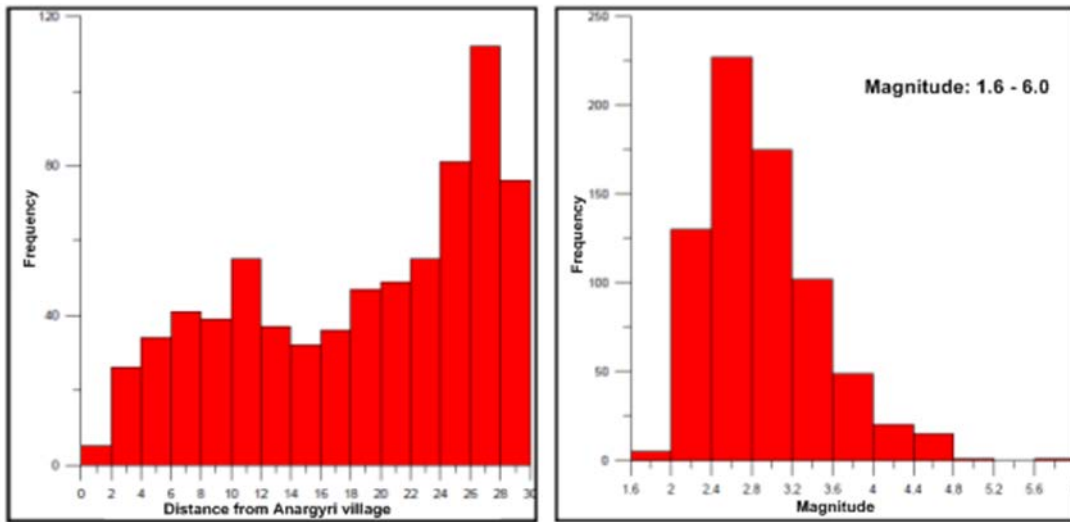


Figure 86. Left: Frequency of the earthquake seismic events distance from the Anargyri village. Right: Frequency of seismic events magnitude in the study area. The magnitude values range between 2.0 and 4.8 [12].



Figure 87. Epicentral locations of seismic events of magnitude larger than M 4.0 in the Amynteon lignite mine area.

On October 25th 1982, an earthquake (M_s 4.8) occurred (National Observatory of Athens, 40.58°N, 21.58°E, Laboratory of Geophysics AUTH, 40.5428°N, 21.6291°E) at the southern boundary of Chimaditida Lake, close to Anargyri fault, approximately 3.7 km SW of Anargyri village. In the broader study area, an earthquake of M_s 5.2 occurred in Vegoritida Lake (Arnissa, Maniaki and Pyrgi villages) in 1984. However, no strong seismic events have been recorded since. In 2015, no significant seismic events have been recorded in the close area of mine and Chimaditida, while in 2016 the microearthquakes of Table 1 were recorded.

Table 17. Seismic events in the study area during 2016 (National Observatory of Athens catalogues, Kolovos, <http://www.gein.noa.gr/el/seismikotita/katalogoi-seismwn>)

Date			Time (GMT)			Latitude (N)	Longitude (E)	Depth (km)	Magnitude (Local)
2016	JAN	16	20	52	1.2	40.57	21.59	23	2.3
2016	JAN	27	10	7	12.6	40.62	21.62	11	1.7
2016	FEB	6	18	21	40.8	40.6	21.59	17	2.1
2016	AUG	5	23	35	27.6	40.64	21.62	10	1.4
2016	SEP	9	11	31	29.8	40.6	21.64	15	1.6
2016	SEP	25	13	44	54.4	40.6	21.64	16	1.8
2016	OCT	11	5	11	50.9	40.57	21.6	10	2.3
2016	NOV	27	5	47	49.7	40.61	21.57	12	2.2
2016	NOV	27	8	36	28.2	40.59	21.6	10	2.1
2016	NOV	27	8	37	45.1	40.6	21.6	11	2.5
2016	DEC	3	13	35	17.3	40.59	21.61	12	1.9

Table 18. Empirical relationships, estimating moment magnitude, surface wave magnitude, maximum displacement and

Faults	Length km	Empirical relationships									Maximum displ.(m)		Average displ.(m)
		WC94			AJ98			PC04			WC94	PC04	WC94
		lower M_w	M_w	upper M_w	lower M_s	M_s	upper M_s	lower M_s	M_s	upper M_s			
Nymfeon-Petres fault	28	6.1	6.8	7.5	6.6	6.8	6.9	6.4	6.8	7.2	1.34	1.13	0.65
Nymfeon segment	18	5.9	6.5	7.2	6.4	6.6	6.7	6.2	6.6	7.0	0.81	0.60	0.46
Petres segment	7	5.4	6.0	6.6	6.0	6.1	6.3	5.6	6.3	6.5	0.28	0.15	0.22
Chimaditida-Anargyri segment	11	5.6	6.2	6.9	6.2	6.3	6.5	5.9	6.4	6.8	0.46	0.28	0.31
Vegora-Vegoritida segment	18	5.9	6.5	7.2	6.4	6.6	6.7	6.1	6.6	7.0	0.79	0.58	0.45
Vegora segment	6	5.4	5.9	6.5	5.9	6.0	6.2	5.5	6.2	6.5	0.23	0.12	0.19
Levea-Filotas segment	12	5.6	6.3	6.9	6.2	6.3	6.5	5.9	6.4	6.8	0.47	0.29	0.31
(WC94): [16]							$M_w = 4.86 + 1.32\log(SRL)$						
(AJ98): [17]							$M_s = 5.13 + 1.14\log(L)$						
(PC04): [18]							$M_s = 0.9\log(SRL) + 5.14$						
M_w : Moment magnitude M_s : Surface wave magnitude SRL : Surface rupture length (km) L : Fault length (km)													

average displacement.

Some of the faults in the area have been characterized as active [2,4,7,14], based primarily on geological and secondarily on seismotectonic criteria, i.e. association with deformation of recent sediments and seismicity respectively. They are the Vegora, the Nymfeon – Petres Lake and the Anargyri fault zones. The average and maximum expected earthquake magnitude (M_s) of the three major faults of the study area is associated with the geometry of these faults [16–18]. The estimated surface wave magnitudes for the Vegora – Vegoritida fault and the Nymfeon – Petres fault are M_s 6.5 – 6.6 and M_s 6.8, respectively, while the estimated surface wave magnitude of the Chimaditida – Anargyri fault is M_s 6.2 – 6.4 (Table 2).

2.4. Active faulting in the area of Amynteon mine

Of the faults that have been mentioned in the previous paragraphs, Vegora and Anargyri faults are directly associated with the Amynteon mine, as it is located in the transfer zone between the tips of those two faults.

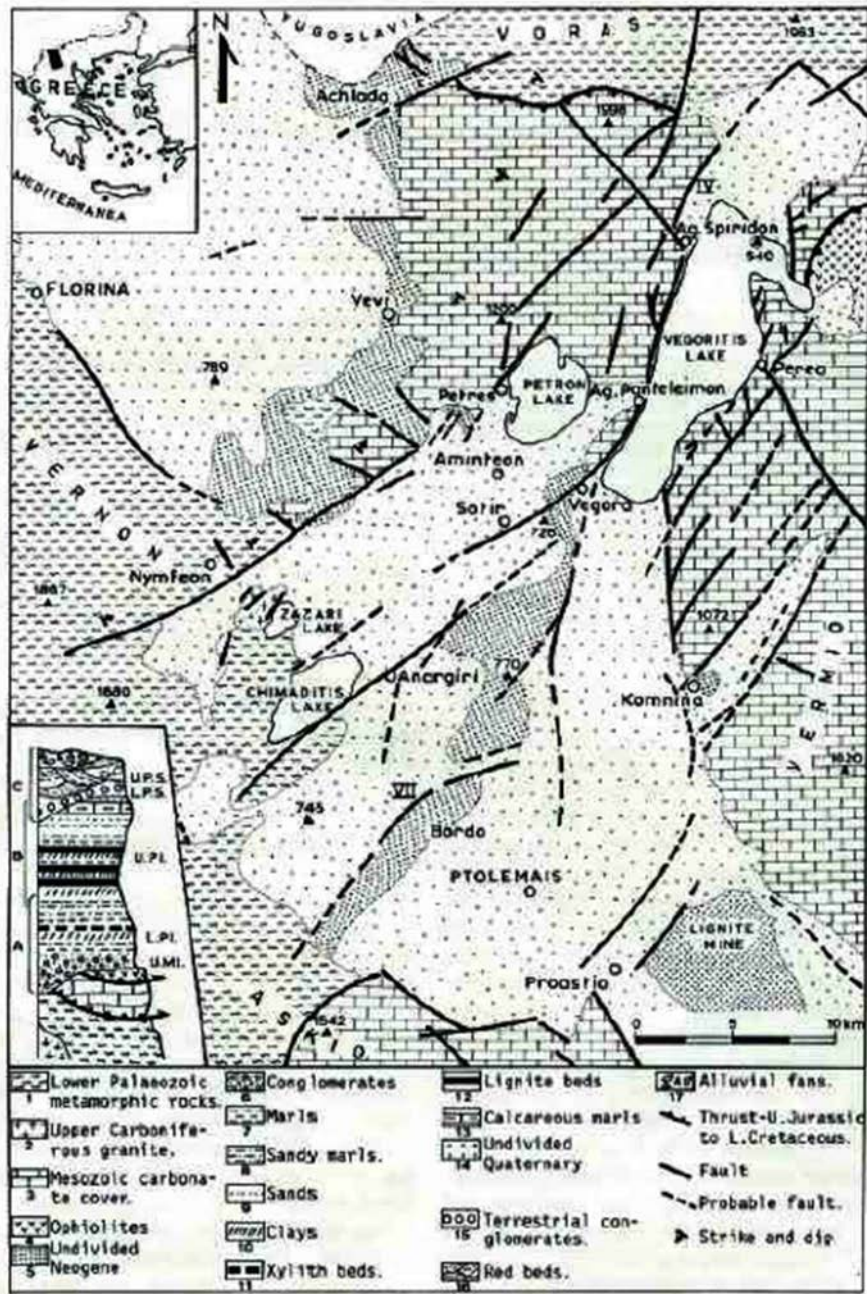


Figure 88. Simplified geological map of the Ptolemais – Amynteon region [2]. The dashed lines in the areas N and NE of Anargyri show the probable extensions of the Vegora and Anargyri faults, delimiting the northern and southern parts of the Amynteon mine area.

2.4.1. Anargyri fault

Anargyri fault is one of the major faults of Amynteon-Ptolemais basin and defines the southern shore of Chimaditida Lake, as well as the southern marginal lignite mine [4]. It strikes N60°E and dips to the NW. It forms the Chimaditida Lake, which is the most recent (Quaternary) structure of the basin. Based on drilling data from the lignite-bearing sediments, the estimated fault throw is 130 m. The Anargyri fault affects the entire Pliocene-Quaternary sequence (Figure 7). This fault has a very well defined morphological expression, forming a well-developed quasilinear scarp that fades away towards the NE (Figure 8 and Figure 9).

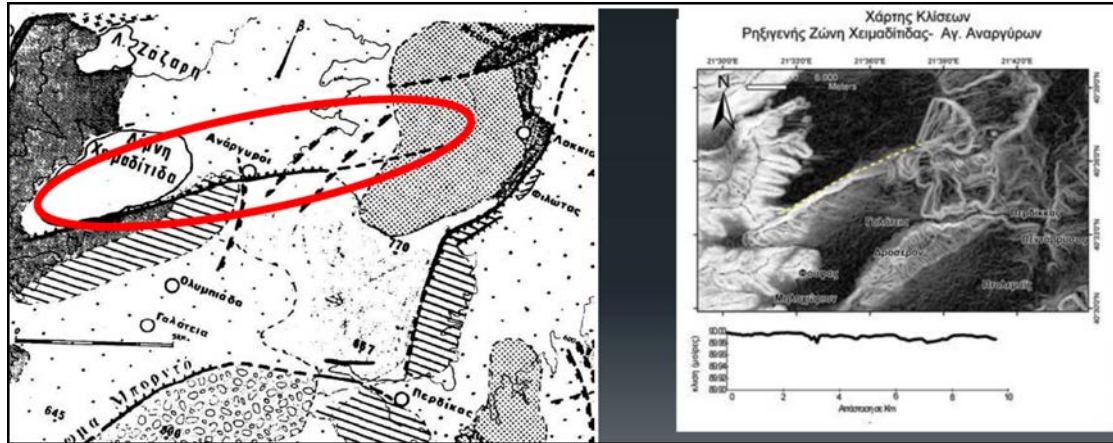


Figure 89. Left: the Anargyri fault (red ellipse) defines the southern Chimaditida Lake shore and its extension towards Anargyri village enters the mine area (shaded area) at its south-central part. Right: Slope angle map in relation to the Anargyri fault (yellow dashed line) [14].

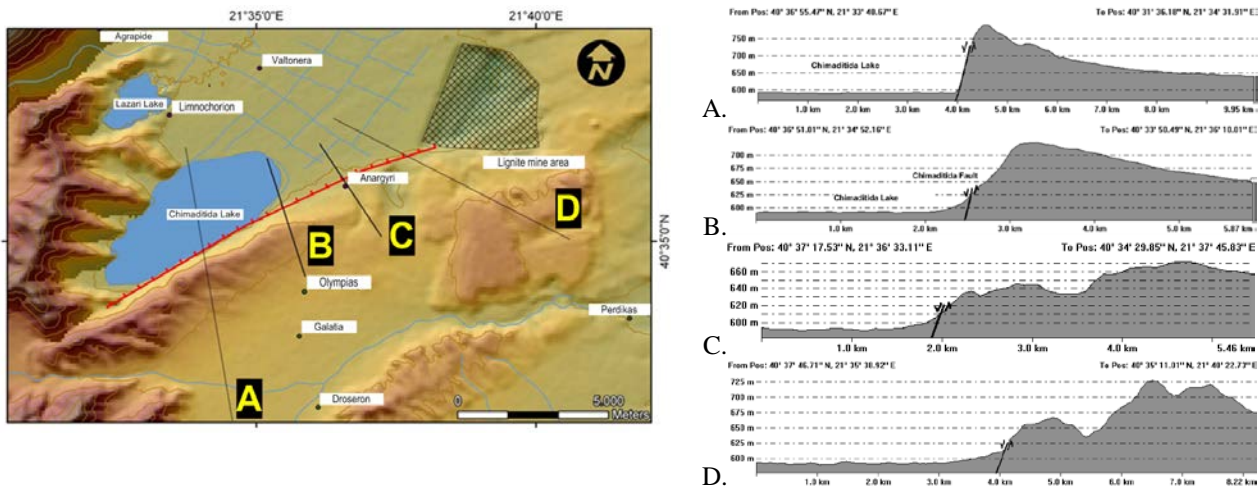


Figure 90. The surface trace of the Anargyri fault, dipping to the NW (red line) and morphological sections across its scarp.

2.4.2. Vegora fault

Vegora fault is a major normal fault along the western shore of Vegoritida Lake, with a NE – SW strike (between 30° and 40°), while the estimated dip angle is 60° SE (Pavlidis, 1985). The total length of Vegora fault is 20 km and it deforms the Mesozoic Pelagonian carbonates, forming the Vegoritida Lake. This fault zone is extended to WSW into the Pliocene and Quaternary sediments of Ptolemais basin, affecting the recent sediments. The fault throw is estimated between 200 and 500 m. It is also considered as an active structure, as it deforms Holocene scree that overlies the fault slickenside. The northern part of Amynteon mine is considered to be delimited by the extension of this fault to the SW. In published geological maps, this extension is considered as a probable and antithetic fault at the northern part of Chimaditida Lake (Figure 7), which together with Anargyri fault define the mining area Figure 10). In the agriculturally cultivated area, the fault is covered by very recent sediments (historical, lacustrine sediments) with no typical topographic expression. However, at the northeastern part of the mine area, a tectonic scarp has been developed in recent years (Figure 11), also known as “Kyrkos fault” to mine engineers, showing aseismic creep on the fault surface trace. These scarps (Figure 12) extend up to a landslide zone that was triggered on May 2016. The traces of this fault are associated with the extension of the Vegora fault. The evolution of

the scarps, as well as the area affected by the massive landslide of June 2017 are easily traceable by comparing series of satellite images [19]. Although it is clear that the northern scarps of the mine are delimited by this fault, additional geophysical data as well as morphotectonic analysis is needed to identify its detailed characteristics.



Figure 91. Mine area as of September 2014. The dashed yellow lines define the Anargyri and Vegoritida faults.



Figure 92. The northern part of the mine area. The yellow line shows the tectonic scarp (surface fault trace), also known as “Kyrkos fault”.



Figure 93. View of the “Kyrkos fault” scarp at the northern margin of the mine, as of July 2017.

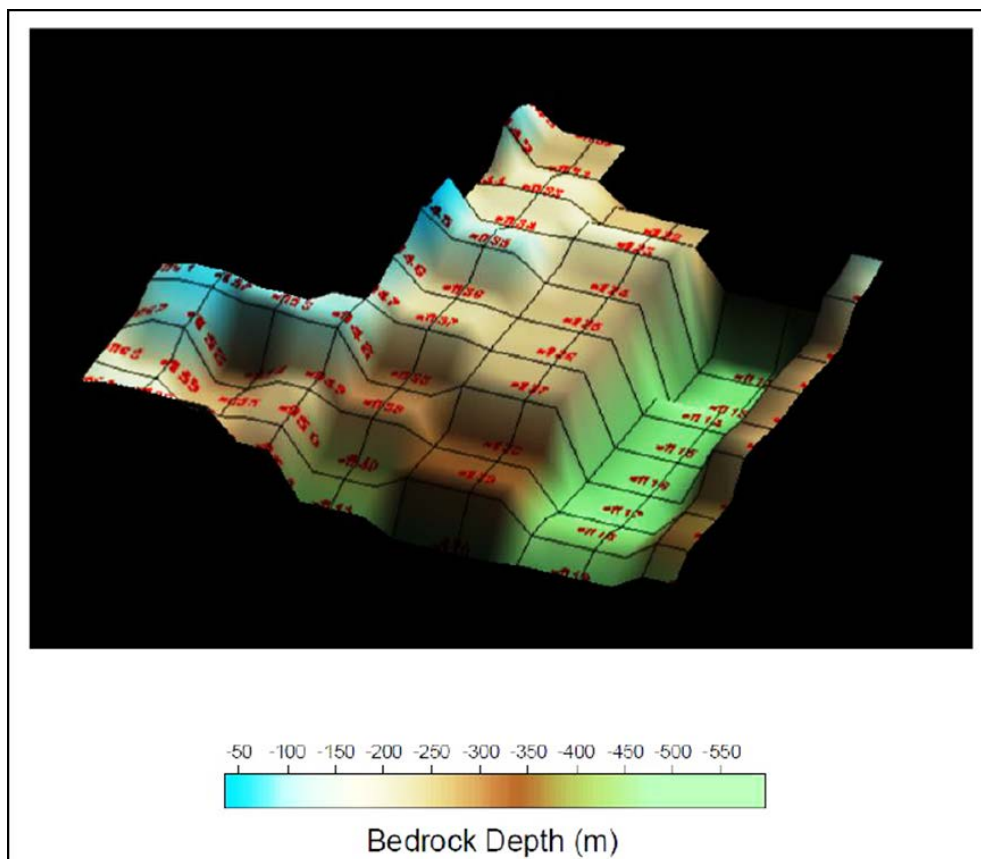


Figure 94. Three-dimensional bedrock determination of the Valtosero-Aetos area, based on the vertical electrical sounding results [20].

An electrical sounding geophysical survey carried out close to the northern mine margin, between Aetos and Valtonera village [20], confirms the existence in the area of the major NE – SW faults, as well as the transverse NW – SE faults (Figure 13). There are therefore adequate information showing increased structural complexity in the area in and near the mine.

3. DISCUSSION

In addition to the aforementioned two main fault zones, the lignite-bearing deposits of Amynteon mine show a very complex deformation pattern, as many smaller faults of shorter lengths and displacement affect the sedimentary sequence (Figure 14). This complex deformation is caused by the interaction of the two main Anargyri and Vegora fault zones, which form a local transitional transfer zone between them. The June 2017 massive landslide completely disrupted the internal structure of the sequence (Figure 15) and this highly fractured nature of the material may have contributed to the landslide itself [21].



Figure 95. Amynteon lignite sequence is characterized by a highly complex deformation pattern, caused by the interaction of cumulative displacement in the transfer zone between the two main Anargyri and Vegora fault zones. The photo was taken in 2010.



Figure 96. General overview of the June 2017 landslide. The internal structure of the sediments has been completely disrupted.

The faults in the interior of the mine show shorter length and displacement values and form complicated tectonic structures. A variety of deformation structures can be observed, such as layer displacement, grabens with complicated internal structure, bending, bed-parallel slip, pseudo-reverse phenomena such as reverse faults, anticlines, folds etc. This kind of phenomena are quite common throughout the area (e.g. Figure 16 and Figure 17), as well as in coal mines worldwide, forming

tectonic structures by combining normal (extensional) faults with compressional features. Regional compressional phenomena may also be associated with local “pincée” type compression (Figure 18).

Surface ruptures attributed mainly to mining activity have been formed in other sites in the broader area, most notably at Mavropigi, a village that was forced to be evacuated due to severe damages caused by gradually evolving surface rupturing [22,23].



Figure 97. Reverse faulting at Notio Pedio, in Ptolemais basin.

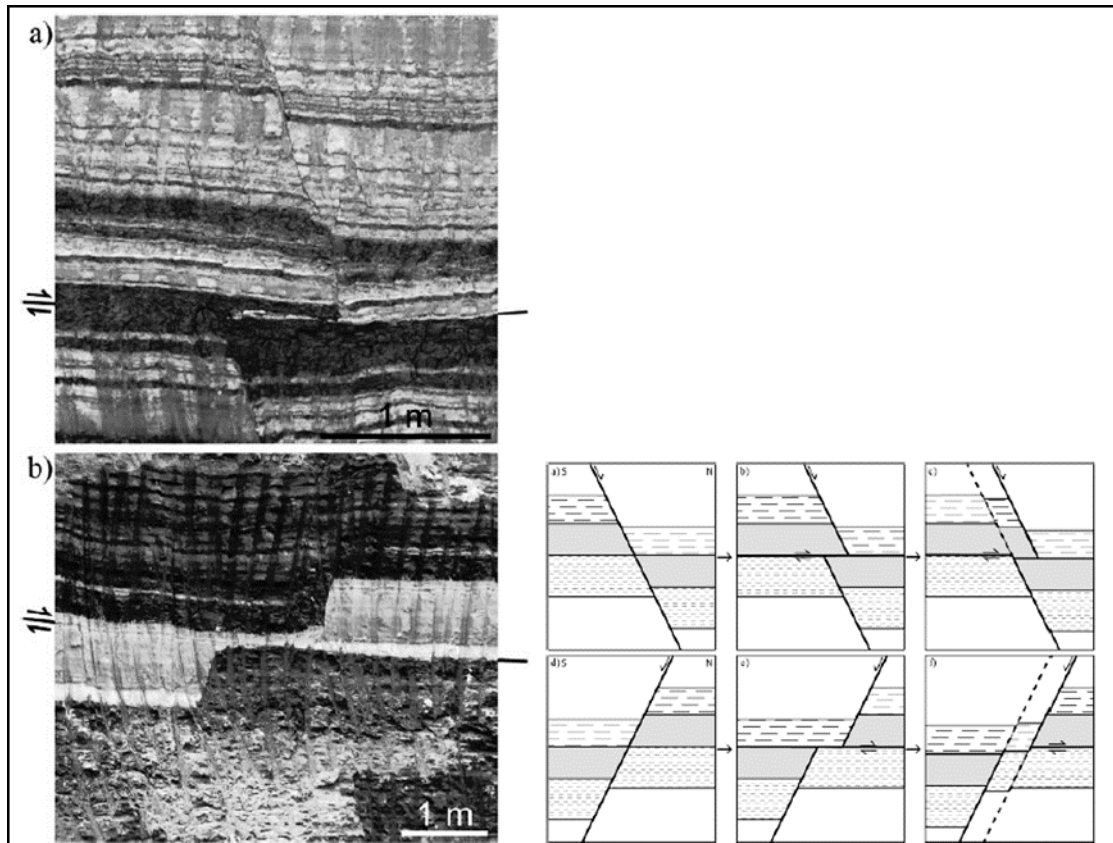


Figure 98. Left: Parallel to the bedding, lignite formations slip, due to the normal faults displacements (Kardia Mine). The estimated displacement step for each bed is 0.25 m. Right: Theoretical interpretation of the mine area [24].

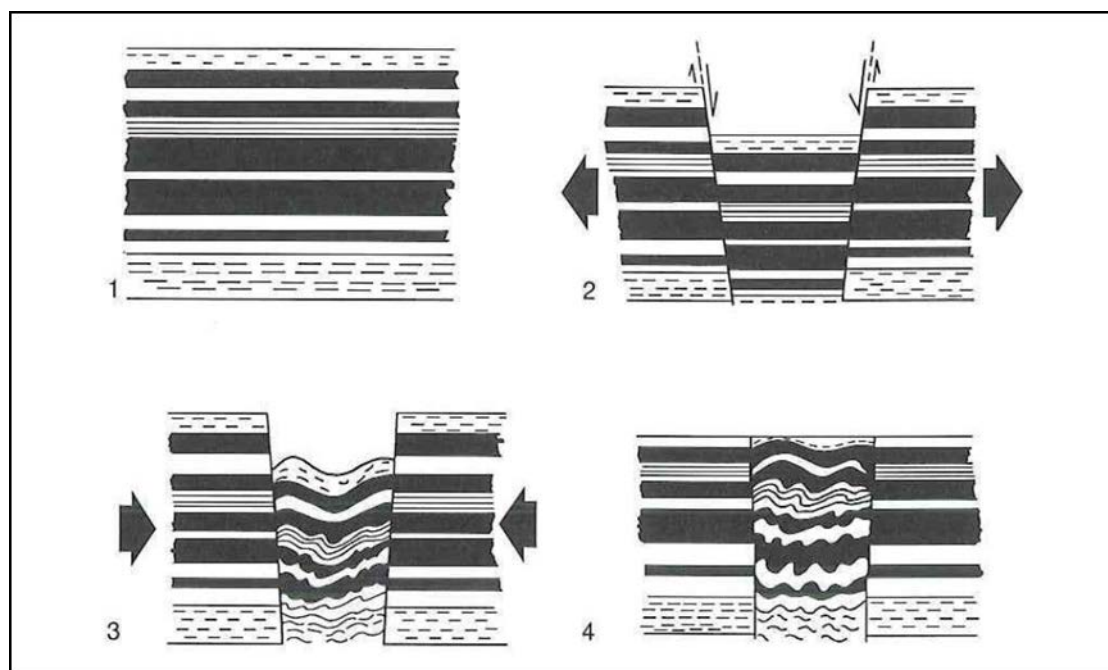


Figure 99. Evolutionary stages of a pincée structure: 1) Initial deposition of horizontal beds, 2) Formation of a small graben due to extension, 3) Bed “folding” into the graben due to weak compression, or simply due to gravitational reorganization of the downthrown material in a smaller space, 4) Final stage after the erosion [4].

In conclusion, the Anargyri lignite mine is delimited by two normal, extensional fault zones, striking E – W to ENE – WSW. The Anargyri fault is located at the southern part of the study area, dipping to the north, while the extension of Vegora fault is located at the northern part of the lignite mine, dipping to the south. Although the seismicity of the study area is low, these faults are considered active, based on geological criteria. There are no historically recorded surface ruptures attributed to seismic events. Inside the mine area there are several secondary normal faults, parallel to sub-parallel to the main normal fault zones, as well as transversely to them, creating a complex tectonic structure. The plasticity of the beds (mainly marls), the dipping angles of the formations and the combination of different faults lead to slip events and “compressional structures”, caused by extensional regime. The faults of the area, as discontinuities of the formations, act as detachment planes, expediting landslide phenomena, as the shear stress is reduced on the fault plane.

In general, the internal structural deformation of a mining area is tended to be neglected as a factor of stability and is only considered in the frame of mining potential. The Amynteon mine massive landslide shows that a complex deformation pattern can cause significant fragmentation, hence lowering cohesion and act as an additional factor that may expedite an imminent failure. Taking also into account the possibility of a fault zone being active, the need for detailed structural analysis in similar cases is imperative.

REFERENCES

- [1] Mountrakis DM. The Pelagonian Zone in Greece: A Polyphase-Deformed Fragment of the Cimmerian Continent and Its Role in the Geotectonic Evolution of the Eastern Mediterranean. *J Geol* 1986;94:335–47.
- [2] Pavlides SB, Mountrakis DM. Extensional tectonics of northwestern Macedonia, Greece, since the late Miocene. *J Struct Geol* 1987;9:385–92.
- [3] Kiliyas A, Mountrakis D. The Pelagonian nappe: tectonics, metamorphism and magmatism. *Bull Geol Soc Greece* 1989;23:29–46.
- [4] Pavlides S. Neotectonic evolution of the Florina-Vegoritiss-Ptolemais basin (W. Macedonia, Greece). Aristotle University of Thessaloniki, 1985.

- [5] Chatzipetros AA, Pavlides SB, Mountrakis DM. Understanding the 13 May 1995 western Macedonia earthquake: A paleoseismological approach. *J Geodyn* 1998;26:327–39. doi:10.1016/S0264-3707(97)00069-0.
- [6] Pavlides SB, Zouros NC, Chatzipetros AA, Kostopoulos DS, Mountrakis DM. The 13 May 1995 western Macedonia, Greece (Kozani Grevena) earthquake; preliminary results. *Terra Nov* 1995;7:544–9.
- [7] Mountrakis DM, Pavlides S, Zouros N, Astaras T, Chatzipetros A. Seismic fault geometry and kinematics of the 13 May 1995 Western Macedonia (Greece) earthquake. *J Geodyn* 1998;26:175–96.
- [8] Chatzipetros AA. Paleoseismological and morphotectonic study of Mygdonia, Eastern Halkidiki and Kozani-Grevena active fault systems. Aristotle University of Thessaloniki, 1998.
- [9] Loupasakis C, Angelitsa V, Rozos D, Spanou N. Mining geohazards—land subsidence caused by the dewatering of opencast coal mines: The case study of the Amyntaio coal mine, Florina, Greece. *Nat Hazards* 2014;70:675–91. doi:10.1007/s11069-013-0837-1.
- [10] Tzampoglou P, Loupasakis C. New data regarding the ground water level changes at the Amyntaio basin - Florina Prefecture, Greece. *Bull Geol Soc Greece* 2017;50:1006. doi:10.12681/bgsg.11805.
- [11] Tzampoglou P, Loupasakis C. Mining geohazards susceptibility and risk mapping: The case of the Amyntaio open-pit coal mine, West Macedonia, Greece. *Environ Earth Sci* 2017;76:542. doi:10.1007/s12665-017-6866-4.
- [12] Soulios G, Tsapanos T, Voudouris K, Kaklis T, Mattas C, Sotiriadis M. Investigation of the causes of ruptures on surface and buildings in Anargyri area, Prefecture of Florina. Thessaloniki: 2010.
- [13] Soulios G, Tsapanos T, Voudouris K, Kaklis T, Mattas C, Sotiriadis M. Ruptures on surface and buildings due to land subsidence in Anargyri village (Florina Prefecture, Macedonia). *Adv. Res. Aquat. Environ.*, Berlin, Heidelberg: Springer Berlin Heidelberg; 2011, p. 505–12. doi:10.1007/978-3-642-24076-8_59.
- [14] Xanthopoulou K. Contribution of geological data in seismic hazard assessment in western Macedonia. Aristotle University of Thessaloniki, 2006.
- [15] Tsapanos T. Seismicity and seismic hazard in western Macedonia. *Bull Geol Soc Greece* 2005;37:232–44.
- [16] Wells DL, Coppersmith KJ. New empirical relationships among magnitude, rupture length, rupture width, rupture area, and surface displacement. *Bull Seismol Soc Am* 1994;84:974–1002.
- [17] Ambraseys NN, Jackson JA. Faulting associated with historical and recent earthquakes in the Eastern Mediterranean region. *Geophys J Int* 1998;133:390–406. doi:10.1046/j.1365-246X.1998.00508.x.
- [18] Pavlides S, Caputo R. Magnitude versus faults' surface parameters: quantitative relationships from the Aegean Region. *Tectonophysics* 2004;380:159–88. doi:10.1016/j.tecto.2003.09.019.
- [19] Karagianni A, Lazos I, Chatzipetros A. Remote sensing techniques in disaster management: Amynteon mine landslides, Greece. *Int. Arch. Photogramm. Remote Sens. Spat. Inf. Sci. - ISPRS Arch.*, vol. 42, 2018. doi:10.5194/isprs-archives-XLII-3-W4-269-2018.
- [20] Atzemoglou A, Tsourlos P, Pavlides S. Investigation of the tectonic structure of the NW part of the Amynteon Basin (NW Greece) by means of a vertical electrical sounding (VES) survey. *J Balk Geophys Soc* 2003;6:188–201.
- [21] Karagianni A, Lazos I, Chatzipetros A. Remote sensing techniques in disaster management: Amynteon mine landslides, Greece. *Int. Arch. Photogramm. Remote Sens. Spat. Inf. Sci.*, 2018, p. 269–76. doi:10.5194/isprs-archives-XLII-3-W4-269-2018.
- [22] Kalogirou EE, Tsapanos TM, Karakostas VG, Marinos VP, Chatzipetros A. Ground fissures

- in the area of Mavropigi Village (N. Greece): Seismotectonics or mining activity? *Acta Geophys* 2014;62. doi:10.2478/s11600-014-0241-6.
- [23] Marinos V, Tsapanos T, Pavlides S, Tsourlos P, Chatzipetros A, Voudouris K. Large Induced Displacements and Slides Around an Open Pit Lignite Mine, Ptolemais Basin, Northern Greece. *Eng Geol Soc Territ - Vol 2* 2015. doi:10.1007/978-3-319-09057-3_47.
- [24] Delogkos E, Manzocchi T, Childs C, Sachanidis C, Barbas T, Schöpfer MPJ, et al. Throw partitioning across normal fault zones in the Ptolemais Basin, Greece. vol. 439. 2017. doi:10.1144/SP439.19.

A Cloud-Based Real-Time Slope Movement Monitoring System

**Chrysanthos Steiakakis¹, Georgia Papavgeri¹, Nick Steiakakis¹,
Zach Agioutantis² and Paul Schilizzi³**

¹Geosysta Ltd, Kountouriotou 7 & Karaoli Dimitriou 151 27 Melissia, Athens, Greece

²University of Kentucky, Lexington, Kentucky 40506, USA

³Public Power Corporation, Mines Business Unit, 29 Chalkokondyli str, 10432, Athens, Greece

ABSTRACT

Excavations and slopes in mines all over the world get deeper and steeper. This has been possible because of the significant technological achievements in mining technology and the increased efficiency of the excavating and hauling equipment. As mines become deeper, stability problems become more important and need to be evaluated and assessed even on a daily or hourly basis. Mining personnel must have access to accurate information on excessive slope movements and/or imminent failures. To assess slope conditions requires installing and maintaining a substantial monitoring system. Most such systems can generate significant data per hour or per day depending on the specific monitoring application. This vast amount of data needs to be efficiently processed and transformed to information that can be stored and evaluated quickly and efficiently in order to make operational decisions.

This paper presents a cloud based database software monitoring system that can efficiently record, transfer, store, analyze and evaluate monitoring data and generate easy to view and easy to use information. Data can be manually uploaded by mine personnel or automatically retrieved from monitoring devices. The data are stored in a firebird cloud database where they are automatically analyzed to generate appropriate displacement, velocity and other time series data. The results can be easily compared with other data, such as precipitation values, deep inclinometer readings, etc. The system can reliably and quickly generate information about excessive movements, alarm levels etc. and alert authorized personnel. Utilizing this system in every day mine operations in high and difficult slopes enhances safety and increases productivity.

1. INTRODUCTION

In major projects, such as mining operations, the need of a centralized data management system is crucial, for day to day decision making and long term planning. The database system needs to manage a considerable amount of data for more than one project, usually with many users involved from data uploading or preparation of reports and diagrams to evaluation of results. Many users from top management to local engineers need to have immediate access using mobile phones, tablets, laptops, etc.

Taking into account this need, an integrated data management system was developed over the last few years. The graphical user interface, that is used to control the data management system, consists of a Windows based application designed to communicate with the database using client/server protocols. The first version of this system was primarily designed to store, analyze and evaluate tunnel monitoring data [1]. An important update in 2012 allowed the users to import their own data structures, including data from different types of instruments, such as total stations, inclinometers, piezometers, stress cells, etc. Some of the new features include: instrument grouping and data correlation, even between different types of instruments, variable calculations with custom equations, display of monitoring points and instruments in multiple map environments such as Google maps and AutoCAD layouts, generation of reports, tables and graphs, as well as warning and

alarm levels. This database application system was also successfully used to import, analyze and evaluate monitoring data from an active mine in Greece [2].

The latest significant update in the database occurred in early 2018 where a web interface was added to the system. The new user-friendly web interface allows remote uploading of raw data, automatic calculations of the imported data and immediate visualization of results on a web browser.

All the aforementioned functionalities are described in this paper, highlighting some of the most important issues raised during the development of the system. Some of the upcoming features are also discussed in order to demonstrate the continuous development of the database according to the users' needs.

2. DATABASE STRUCTURE AND FUNCTIONALITIES

The data management system was developed as a client/server database system using Firebird 2.5 (an open source relational database system). The design of the database structure was based on the necessity to import measurements from different types of devices (instruments, sensors, total stations, etc.) in a central data management system. This feature facilitates the storage and management of a large volume of data from any type of device (total stations, GPS, inclinometers, piezometers, etc) without having to embed the characteristics of each sensor or measuring device into the system. In addition, a centralized management system allows comparison of the results from all these different types of monitoring devices, such as the movement rate of a mine slope (velocity) in relation to the precipitation data for the same area [3].

The initial design of the database included this feature by grouping the data into multiple hierarchical levels [4]. However, in order to optimize the grouping and management of devices as well as the evaluation of measurements, a new feature was developed that allows a device to belong in one or more tags (or named groups). Figure 1 shows a schematic representation of the updated database structure.

Output files from any device can be uploaded into the web-based front end of this system. The import function supports multiple data formatting options, such as .xls, .csv, .txt, etc. File import can be completed either manually, using files from the user's device (tablet, laptop, PC, etc.) or automatically via an ftp server. Every device type, such as inclinometers, tiltmeters, total stations, etc., includes its own calculated variables, such as cumulative displacement, tilt, vector displacement, etc. These variables can be defined by the user with custom fully parametric equations, which are similar to Excel spreadsheet formulas and are setup only once for each type of device. As soon as a file is imported, the system invokes the necessary routines to compute all calculated records. In a few seconds, raw measurements and calculated data are available for each device. Data can be exported into excel files and/or presented in charts and reports.

During data processing the system identifies missing information or multiple entries and the user is prompted by a pop-up message either to continue or cancel the import process. It is possible, however, that some of the imported values may have been derived from incorrect measurements. In this case the user has two options: either to mark the corresponding measurements as rejected, in order to exclude the calculated variables from the calculation procedure, or to suppress output of the measurements (in order to allow calculation continuity without displaying the results in the diagrams and/or tables). Additionally, it is possible that the location of a monitoring point, for example a survey target, may change slightly due to mining or other operations and the first measurement at the new location may appear as a peak value in the diagram. In this case the value should not be marked as rejected because it is a valid measurement; however, it can be marked as a new reference value. Calculations will then be adjusted accordingly to allow for continuity in the measurements.

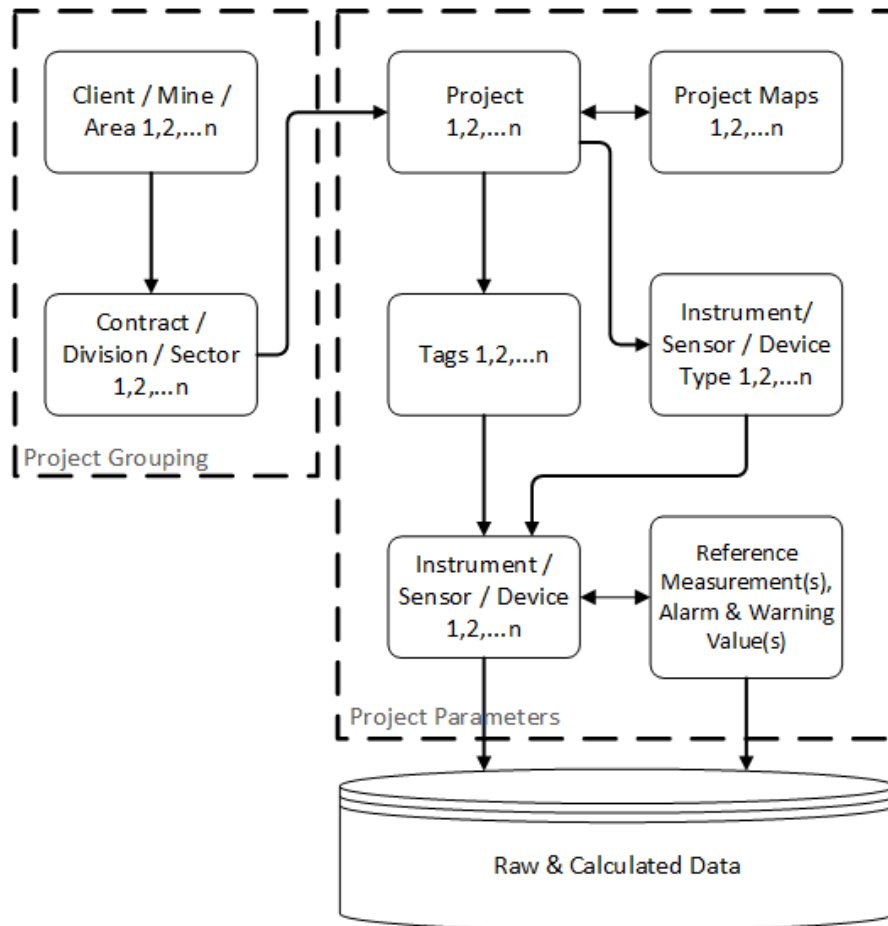


Figure 1. Schematic representation of the updated database structure

Furthermore, predefined warning and alarm levels can be set for the raw or the calculated variables of any device. When drastic changes occur (values above or below predefined limits) in the measured or calculated values then users can be notified via email.

Device or instrument locations projected on maps, together with predefined charts and value limits can also be displayed when belonging to the same tag (group), as shown in Figure 2. With the option of “tags”, devices of the same project can be grouped so that they can be viewed together regardless of their location or type. For the same type of devices, selected monitoring information such as velocity and vertical movement, can be viewed in the same time series as seen at the bottom of Figure 2. Other chart types can be generated such as rainfall, or different correlations between variables.

Users can also locate the monitoring points in multiple map environments such as Google maps, AutoCAD layouts or images based on their coordinates. Different coordinate systems, used in different parts of the world are also supported by this system, as well as conversion codes to convert these coordinates to standard latitude and longitude values.



Figure 2. Tags and related diagrams

3. RESOLVED ISSUES

A number of complexities of data storage, validation and calculations that emerged during the system development process and operation and how they were addressed are presented next. More specifically, the issues discussed, include options that have been developed in this data management system, concerning (a) data evaluation that need to be correlated and displayed for a specific time period as selected by the user (b) development of charts with common reference points for survey targets or other measured data (c) data reduction and display options for inclinometers, (d) record handling for tiltmeters and data error correction, and (e) parametric configuration for importing data files. The result of this effort was to develop a number of management tools in order to facilitate data evaluation.

3.1. Data evaluation for a specific time period

During the implementation of a project many devices (or sensors) are installed on different dates and collect measurements at different time intervals or frequencies. For proper data evaluation there is a need to compare measured data from different devices for a specific time range, irrespective of when they were installed and the number of measurements per device. A user friendly data management system, allows an easy correlation of measurements from different sensors and varying timestamps. This becomes extremely important when managing a large number of sensors with a wide variability on installation dates and measurement frequencies.

This functionality is implemented by defining a specific time period (by using a calendar) in the data visualization system. The default date range is 30 days but the user can define any other date/time range. In addition, only the devices that have actual data during the selected time period appear on the charts and the map (Google Earth or other type), for easy comparison and evaluation (Figure 3). Thus, the user can easily select different time periods, check which instruments have data, and evaluate the data for the selected time period.

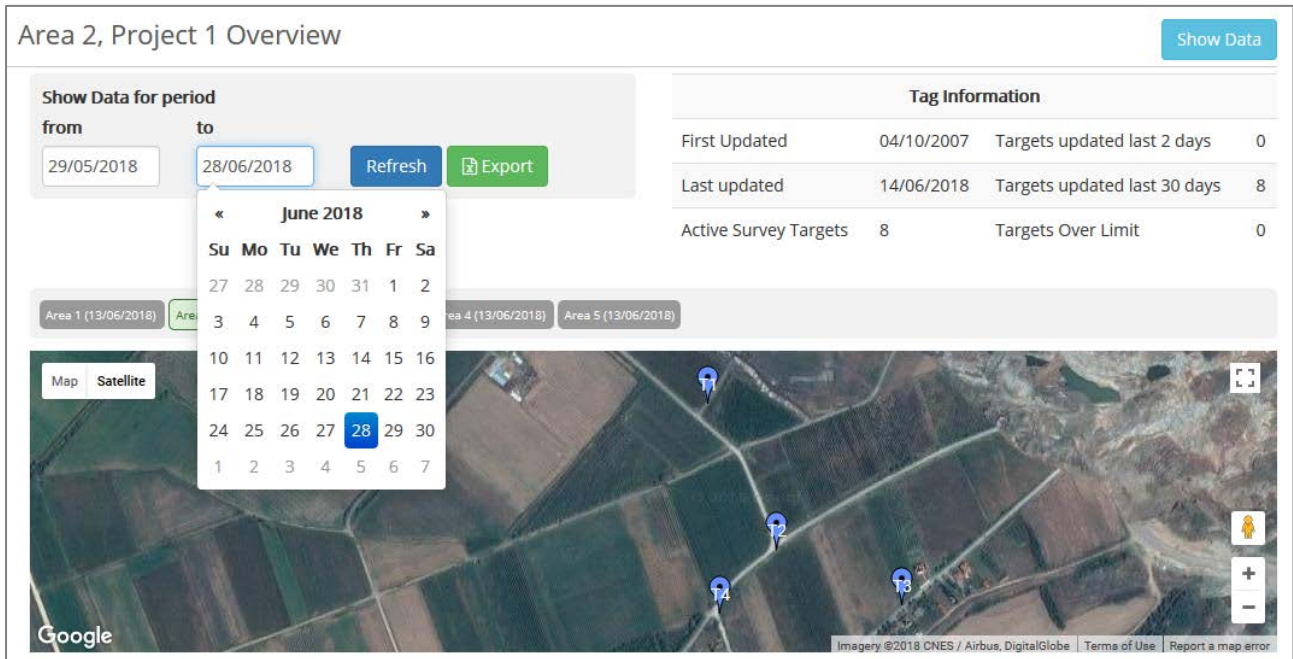


Figure 3. Date range through calendar selection and instruments display on the map

3.2. Survey Targets: Charts with a common reference point for many targets

In projects such as mining operations, it is necessary to evaluate the cumulative displacement or the vector displacement of specific survey targets installed at a particular area of interest, such as regions where high rates of movement have been observed. In order to evaluate and compare the movement of these targets in a single chart they should be presented with a common reference date. In most cases, however, the selected targets are not installed all at the same time, making the comparison of cumulative or vector movements more difficult. Additionally, the user should compare measurements for different time periods and intervals which would be very time consuming with a typical excel spreadsheet.

This functionality was added to the data management system, by allowing the user to specify whether the value of the variable shown in the chart becomes zero at the beginning of the selected time period and is considered as a temporary reference point for all subsequent measurements. For example, Figure 4 shows the cumulative displacement of 3 targets (S1, S2, and S3) that have been installed at different dates without forcing the initial values to zero. The installation dates of the targets depicted in Figure 4 are shown in Table 1.

Table 19. Installation dates for targets in Figure 4

Survey Target	Installation date	Common initial date for evaluation
S1	01/02/2018	05/06/2018
S2	12/04/2018	05/06/2018
S3	17/05/2018	05/06/2018

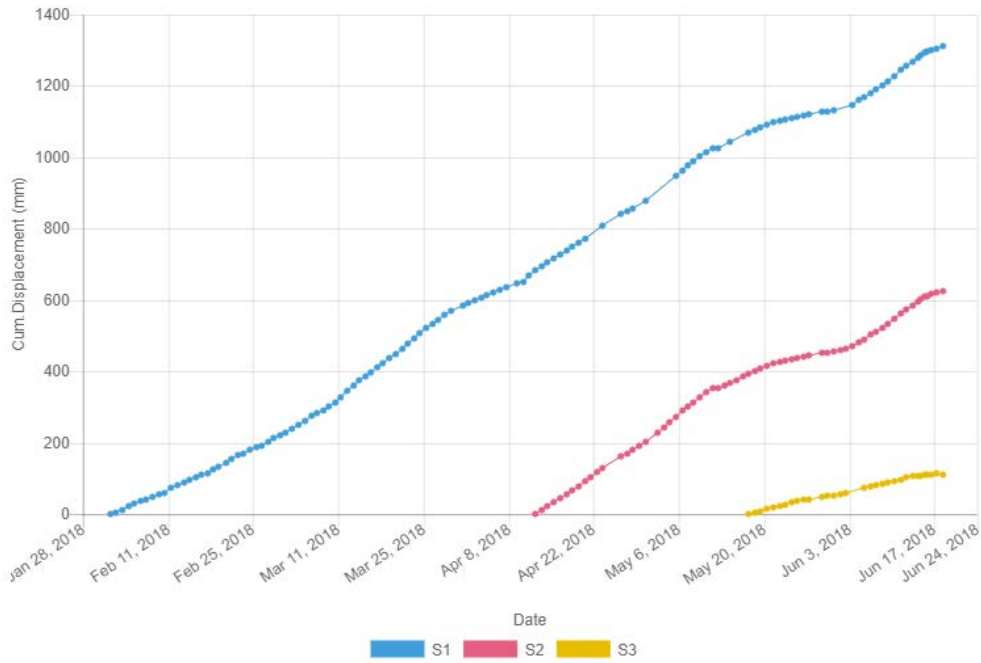


Figure 4. Time series graph showing targets with different installation dates

According to Table 1, target S1 was installed in February, S2 in April and S3 in May of 2018. If movements need to be evaluated for a time period in June, e.g., June 5th to June 18th, this period should be selected through the calendar form (Figure 3). When the “force to zero” option is selected for the selected variable (cumulative displacement) the graph in Figure 5 is generated, which allows an easy comparison of the movements of the three survey targets for the requested time period. As shown in Figure 5, for the selected time period, targets S1 and S2 have almost identical cumulative displacement, while target S3 presents lower cumulative displacements. This feature allows the user to easily understand that movements monitored by targets S1 and S2 are similar but different than these monitored by target S3.

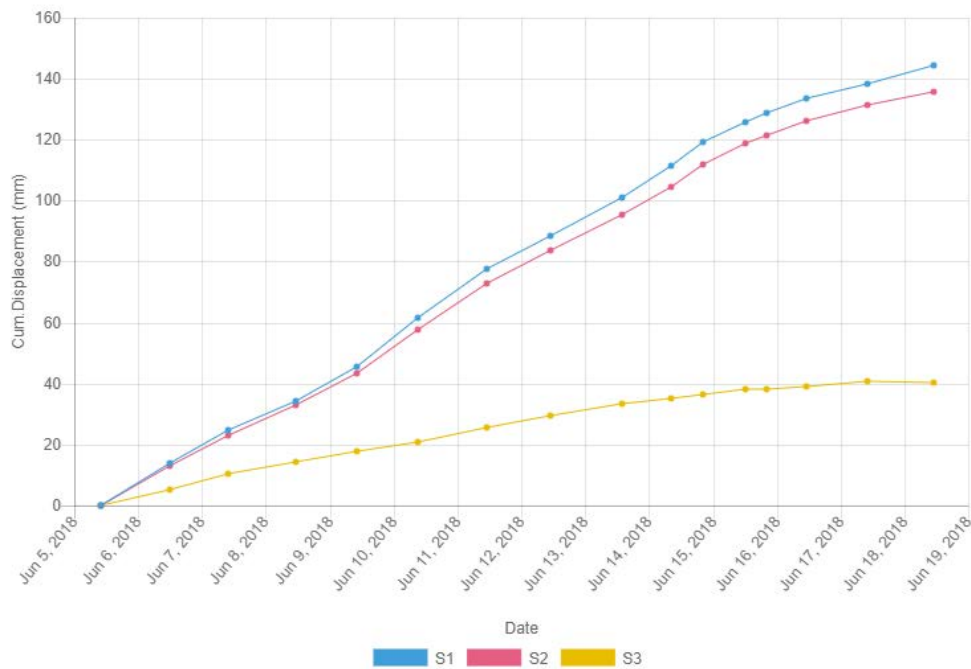


Figure 5. Time series graph showing targets with common initial date for evaluation

3.3. Inclinometers: Data reduction and display options

Inclinometer surveys can generate a huge amount of data points, especially when it is necessary to continuously monitor a moving slope (e.g. on a daily basis). Therefore, the process of storing, archiving and reducing all the raw data, by calculating the necessary variables, and visualizing the results should be immediate.

This process is efficiently carried out by the data management system and is concluded in a few seconds after importing all the inclinometer readings. Based on recent inclinometer readout units consisting of wireless tablets with mobile data transmission capabilities, the collected data can be transferred from the field to the data management system immediately after measurements are completed. The system then immediately performs data reduction and the users can see and evaluate the data through the web interface, regardless of their location. The incremental and the cumulative displacements are calculated using the inclinometer constant and the increments of depth in the respective equations, which makes this system capable of handling different probe outputs as provided by different manufacturers. It is even possible to manage the data collected from measurements in the same hole using different inclinometer probes. The data are calculated and presented in the same graph regardless the inclinometer model used. Figure 6 shows all the variables calculated for each measurement depth for each measurement date/time.

Rej	Print	Variable Description	Units	Date	Value	Diff from Ref	Diff from Prev	Reference Date
<input type="checkbox"/>	<input checked="" type="checkbox"/>	A0		2013-01-07	-33,0000	-32,0000	5,0000	2012-12-27
<input type="checkbox"/>	<input checked="" type="checkbox"/>	B0		2013-01-07	-18,0000	6,0000	6,0000	2012-12-27
<input type="checkbox"/>	<input checked="" type="checkbox"/>	A180		2013-01-07	15,0000	-16,0000	1,0000	2012-12-27
<input type="checkbox"/>	<input checked="" type="checkbox"/>	B180		2013-01-07	-19,0000	8,0000	3,0000	2012-12-27
<input type="checkbox"/>	<input checked="" type="checkbox"/>	Check Sum A		2013-01-07	-18,0000	-48,0000	6,0000	2012-12-27
<input type="checkbox"/>	<input checked="" type="checkbox"/>	Check Sum B		2013-01-07	-37,0000	14,0000	9,0000	2012-12-27
<input type="checkbox"/>	<input checked="" type="checkbox"/>	ADi		2013-01-07	-4,8000	-1,6000	0,4000	2012-12-27
<input type="checkbox"/>	<input checked="" type="checkbox"/>	BDi		2013-01-07	0,1000	-0,2000	0,3000	2012-12-27
<input type="checkbox"/>	<input checked="" type="checkbox"/>	CumADi		2013-01-07	-1258,9000	-1,6000	0,4000	2012-12-27
<input type="checkbox"/>	<input checked="" type="checkbox"/>	CumBDi		2013-01-07	-903,9000	-0,2000	0,3000	2012-12-27
<input type="checkbox"/>	<input checked="" type="checkbox"/>	AINCR	mm	2013-01-07	-1,6000	-1,6000	0,4000	2012-12-27
<input type="checkbox"/>	<input checked="" type="checkbox"/>	BINCR	mm	2013-01-07	-0,2000	-0,2000	0,3000	2012-12-27
<input type="checkbox"/>	<input checked="" type="checkbox"/>	ACUM	mm	2013-01-07	19,5000	-1,6000	0,4000	2012-12-27
<input type="checkbox"/>	<input checked="" type="checkbox"/>	BCUM	mm	2013-01-07	-25,6000	-0,2000	0,3000	2012-12-27

Figure 6. Raw and calculated data for each inclinometer reading

Furthermore, the need to evaluate the results of inclinometer readings at different time periods as well as change the reference date in the presented results, has led to the development of additional options in the data management system to facilitate this process.

More specifically, when an inclinometer chart is displayed, such as the cumulative displacement graph, the selected time period by default corresponds to the entire range of measurements. The initial (reference) date corresponds to the first inclinometer survey and the last date refers to the last survey. Figure 7(a) presents an initial and six subsequent surveys between

04/04/18 to 13/06/18. By default the user sees all seven surveys in the cumulative displacement graph and the location of the inclinometer on the map above the chart. However, the user may decide to visualize and evaluate data for a narrower time period. Figure 7(b) presents charts which include only the last three surveys, i.e. from 15/05/18 until the final survey of 13/06/18. The inclinometer curves are automatically generated from the collected data by suppressing data not in range. The user, however, may also select to use a different reference date, as can be seen in Figure 7(c) where the reference date is selected as 15/05/18 and only the subsequent surveys are presented. The different displacement values when using different reference curves is easily seen by comparing the graphs in Figure 7(b) and 7(c).

Based on these features, the inclinometer survey data can be evaluated immediately after data are collected in the field, even from different inclinometer probes (which is not recommended for accuracy reasons) and for different survey reference dates providing a robust data evaluation option.

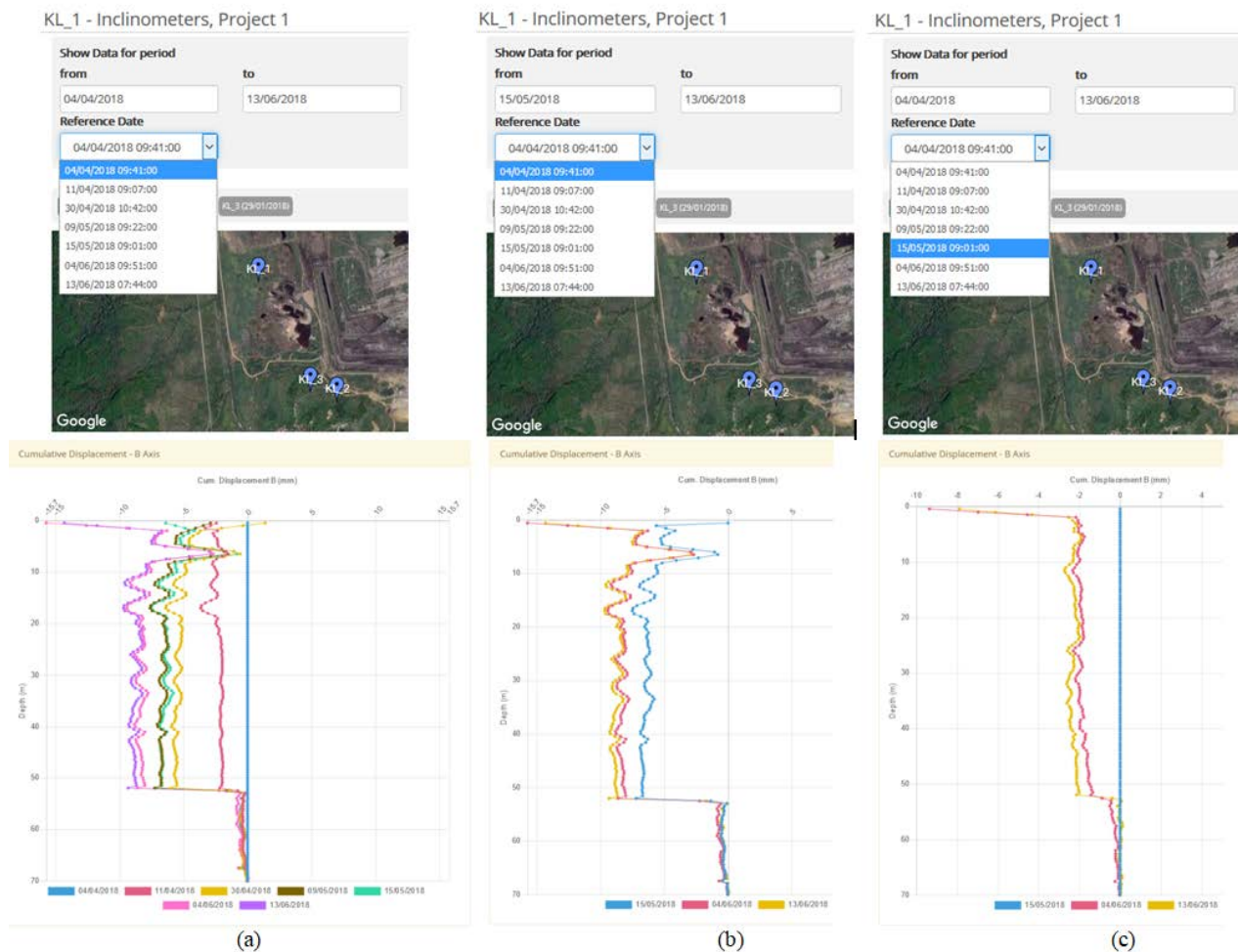


Figure 7. Time period and reference date options for inclinometer graphs

3.4. Datastream isolation

Some monitoring devices are equipped with multiple sensors which operate and collect data simultaneously. One such device is the bidirectional tiltmeter, which collects tilt measurements in two directions (i.e., North – South and West – East) as well as temperature measurements. The measured data are logged and exported in the same file and many data reduction software store the data from different sensors as a single multiple value record for different dates. Occasionally, however, it is necessary to treat either the raw or the calculated values corresponding to a single

device as separate entities. For example, if a malfunction occurs in one of the tiltmeter sensors, e.g. a cable is cut, then an entire datastream corresponding to that entity needs to be isolated. At a later time when the sensor is repaired and the device is fully functional, all datastreams should be restored. Thus there is a need to isolate and reject certain measurements within a single measurement record.

To satisfy this need, an option has been added to the database management system that allows datastream isolation by rejecting selected values within a single measurement record. Figure 8 shows an example where the records corresponding to sensor with W-E direction are marked as rejected in the top right window. Tools are available to select a range of measurements where the specific datastream rejection will be applied. With this feature, the data management system can easily be used to evaluate data even during periods with problematic or malfunctioning sensors. All collected data, from functioning and malfunctioning sensors are stored in the database, but only the non-rejected records are used for tilt calculation and visualization.

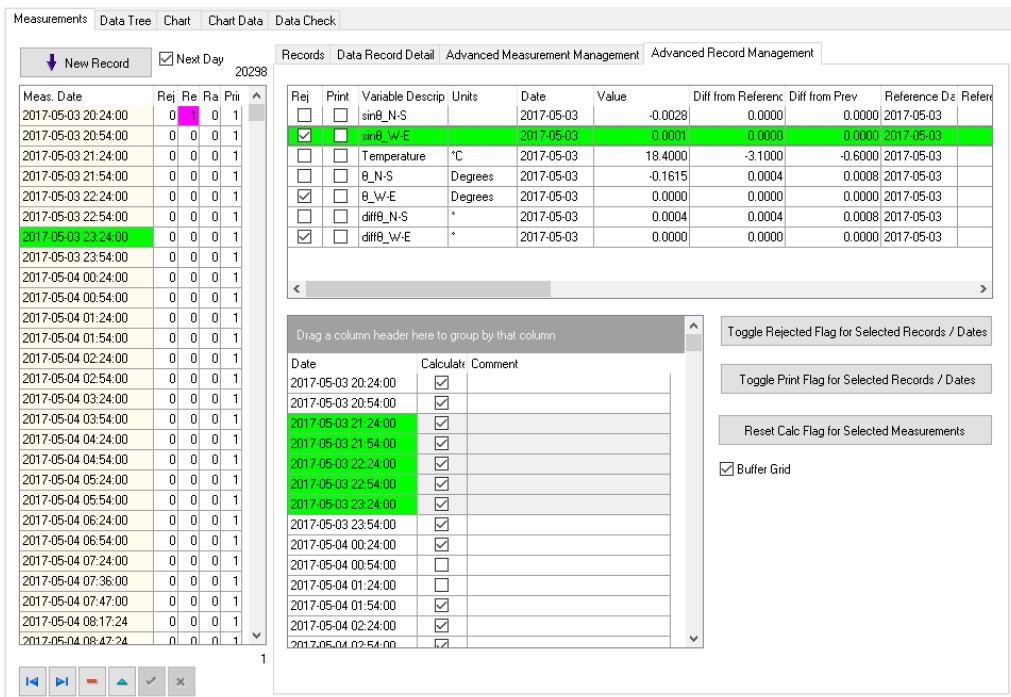


Figure 8. Datastream isolation options

3.5. Data error correction after a period of rejected values

It is well known that monitoring data collected from field campaigns often include to some extent erroneous or inaccurate records. These errors are either small enough so that they do not affect the results or can be corrected through appropriate calculations using calibration tables, etc. Sometimes, the calculated data are based on average values derived by processing a large amount of raw data, thus eliminating or significantly reducing possible errors. As a result, such measurements remain reliable within the accuracy limits of an instrument and can be safely evaluated.

However, in some cases larger systematic errors can occur, which may affect monitoring reliability. As a result the actual behavior of the monitored location is not well represented by the monitoring results. These errors may relate to malfunctions of the measuring or datalogging device.

Another case is related to shifting or re-positioning of survey targets and/or adjusting the coordinates of the base station. Calculations after adjustments are performed setting the first good measurement as a new reference point. Figure 9 shows the time series for vector displacement of a survey target with initial measurement date at 29/10/13 and a time period of rejected values between 25/01/14 and 14/03/14. The first correct measurement after the rejected period is set at 15/03/14.

Four data management options are available in order to help the user interpret and evaluate movements monitored by this survey target. These options are detailed below:

(1) *One Reference Record: The initial measurement date*

In this case the initial measurement date is set as the only reference point for all measurements. After the period of rejected measurements a sudden increase in the vector displacement is observed, which may be due to the new location of the survey target being monitored or due to the correction of the positional error of the measuring device (e.g. robotic total station, GPS receiver).

(2) *Two Reference Records: The initial and the first correct measurement after the rejected period – Reset new reference*

The first correct measurement after the period of rejected values is set as a new (second) reference point (15/03/14) and the calculated variable (vector displacement) at this point is reset as zero value. Every measurement after this date is calculated without having as reference date the initial measurement as in the previous case but the new reference point at 15/03/14.

(3) *Two Reference Records: The initial and the first correct measurement after the rejected period – Copy previous value to new reference*

The calculated displacement of the previous date of the new reference, which is the last correct measurement before the period of rejected values (at 24/01/14) is copied to the displacement value of the new (second) reference point (at 15/03/14), to consider the already measured displacement until the date of the target's repositioning or the correction of positional errors. The displacement value of the new (second) reference date is also added to the calculated value of every measurement after this date (15/03/14).

(4) *Two Reference Records: The initial and the first correct measurement after the rejected period – Copy previous value to new reference and add the expected value for the missing period*

In this case the displacement value calculated by linear interpolation for the period of rejected values is added to the value of the new (second) reference point (at 15/03/14). The previous correct displacement value is also added to the new reference date, as in the previous case. The new value of the second reference date is also added to the calculated values of every measurement after this date (15/03/14).

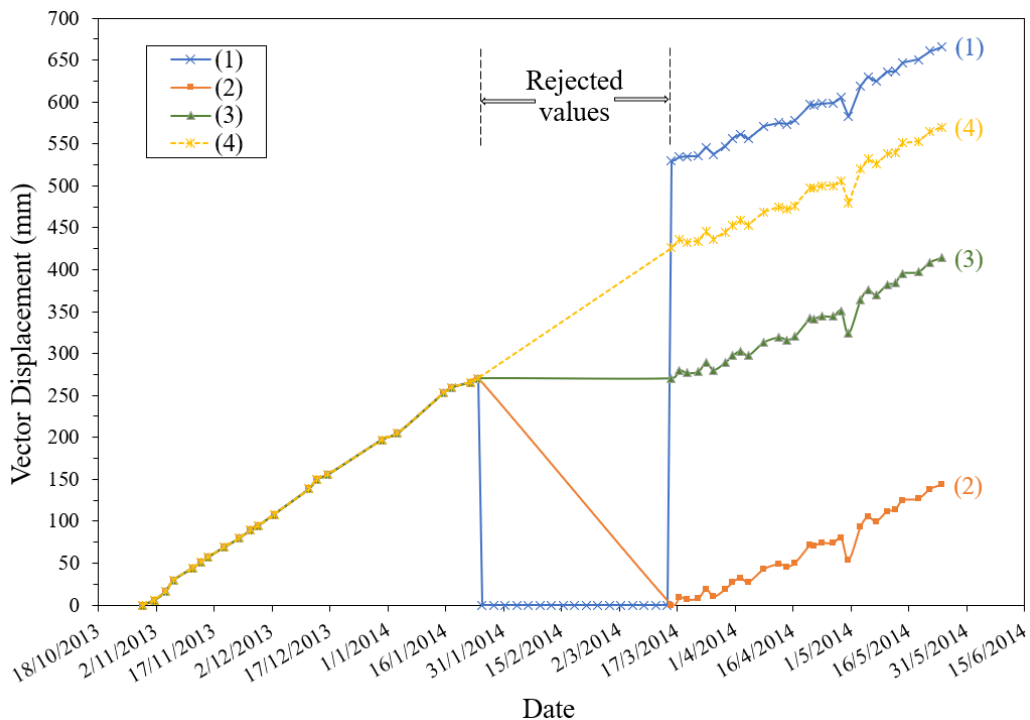


Figure 9. Different data evaluation options for measurements following a period with rejected values

Figure 10 shows a similar example for tiltmeter measurements, where due to a problem in the cable of the W-E sensor there was a period of rejected values between 13/1/18 02:44 and 17/1/18 12:30. The chart shows the time series for the tilt of W-E sensor for the first and the third option as was previously described.

Line (1) has only one reference record, the initial measurement date. It is observed that the calculated values of tilt after the period of rejected values do not correspond to the actual tilt, because the reference point from which the difference of the measured angle is calculated has changed. Line (3) has two reference records, defining as a new reference point the date of the first correct measurement after the rejected measurements. It is observed that the tilt line after the period of rejected values is smoothed as the systematic error that was previously added to the measurements has been removed.

With these functionalities, the user can easily manipulate the data and easily generate charts for reporting or further evaluation. Data reduction and presentation options are controlled by the user.

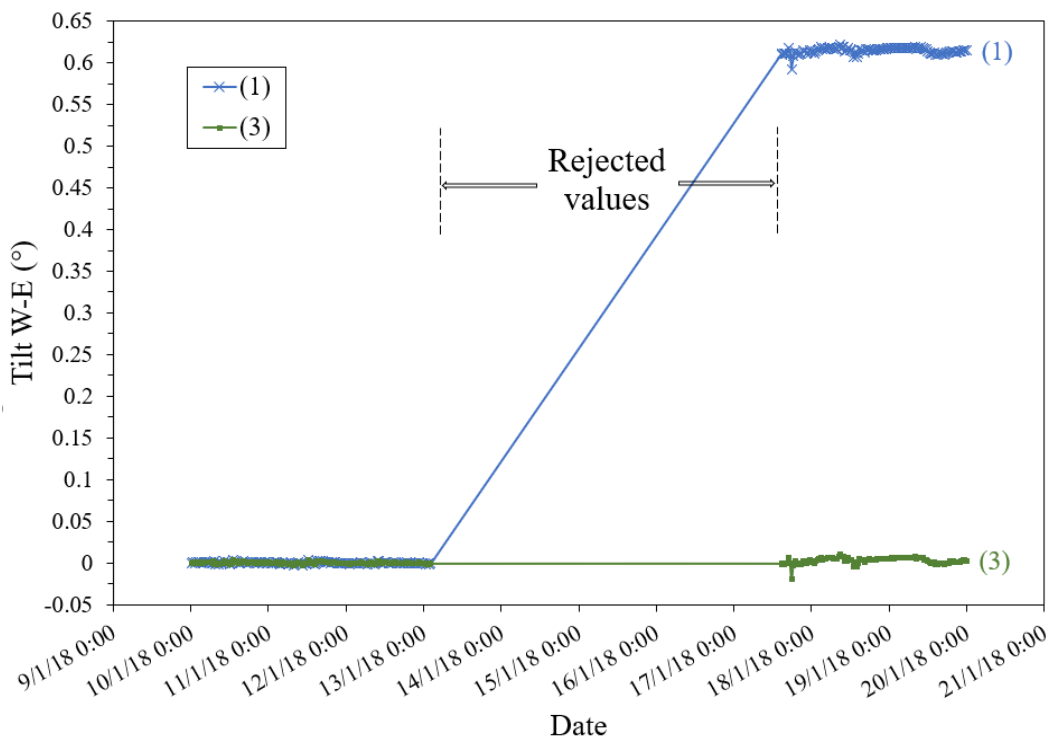


Figure 10. Tilt - Date chart with one (1) or two (3) reference measurements

3.6. Import file configuration: Format issues while importing raw data

The web interface of the data management system allows the user to import data in different file formats depending on the type of monitoring device. A number of different format types are supported, and the user can select the appropriate one in order to easily upload the measured data. Examples include, coordinate output from a robotic total station, data from a 12 channel datalogger, or hand collected measurements from standpipe piezometers, etc. However, even if these files follow a well-established data format, problems may occur when importing measurements due to intentional or unintentional changes of the file format of a specific measuring device. Some of the issues encountered are described below.

Different file format due to user's preferences

The same measuring device may allow different settings for different users, including but not limited to language, date formats, numbers of rows and columns, etc. This will result in different data file formats that may or may not be supported by the data import filters. Figure 11 shows an example where recorded data are displayed in Italian (a) or in English (b, c). But even for cases (b) and (c) the file format is different because the user has added some notes in the first rows of the file so the number of rows of the import file has also changed. The variability in data file formats, even from the same measuring instrument, can significantly complicate the semiautomatic import of measurements in the data management system. This issue has been encountered many times and has been addressed by building robust import algorithms that can accommodate such differences. This issue needs to be addressed in large projects with multiple devices (i.e. total stations) and many users while it is less of a problem for smaller projects.

File Edit Format View Help										

Calcolo Strati - Stazione bash10										
Angoli Orizzontali										
Misure del : 26/02/2018 04:11:10 Strati:3 Punti:3										
PtNr	Posiz. I	Posiz. II	Err	Med. I+II	M.Ridotta	Media	r=d-b	v=r+q	v ²	
	cc	(a)	(b)	(d)	cc	cc	cc"			
dy0	360.11683	160.12062	-37.9	360.11873	0.00000	0.00000	0	3	9	
P13	312.47425	112.47897	-47.2	312.47661	352.35789	352.35741	-5	-2	4	
P5	337.68628	137.68940	-31.2	337.68784	377.56912	377.56878	-3	0	0	
q = 3										

(a)

File Edit Format View Help										

Station: tx1d of 05/07/2018 10:12:19										
Horizontal angle Sets										
PtNr	Posit. I	Posit. II	Err	Mean I+II	M.Reduced	Mean	r=d-b	v=r+q	v ²	
	gon	gon	cc	gon	gon	gon	cc	cc		
tlofos	399.99913	199.99895	1.8	399.99904	0.00000	0.00000	0.0	0.0	0.0	
TN59	375.10220	175.10053	16.7	375.10137	375.10233	375.10233	0.0	0.0	0.0	
TN44N	379.30920	179.30845	7.5	379.30883	379.30979	379.30979	0.0	0.0	0.0	

(b)

File Edit Format View Help										
NOTE:										
Horizontal angle Point:TN46 Set:1 Position:II not Valid! The value was recomputed										
Vertical angle Point:TN46 Set:1 Position:II not Valid! The value was recomputed										
Distance Point:TN46 Set:1 Position:II not Valid! The value was recomputed										

Station: tx1d of 05/21/2018 11:55:00										
Horizontal angle Sets										
PtNr	Posit. I	Posit. II	Err	Mean I+II	M.Reduced	Mean	r=d-b	v=r+q	v ²	
	gon	gon	cc	gon	gon	gon	cc	cc		
tlofos	399.99923	199.99940	-1.7	399.99932	0.00000	0.00000	0.0	0.0	0.0	
TN59	375.09882	175.09778	10.4	375.09830	375.09898	375.09898	0.0	0.0	0.0	
TN44N	379.30539	179.30494	4.5	379.30517	379.30585	379.30585	0.0	0.0	0.0	

(c)

Figure 11. Different file format for the same instrument

Different file format due to the regional settings of the user's (uploader's) device

The output file format of an instrument may be affected by the regional settings of the platform (laptop, pc, tablet, etc.) used to download the data from the instrument. For example, depending on

the user preferences on the laptop, the decimal separator may be "." or ",". Figure 12 shows two output files using (a) a decimal point and (b) a comma as the decimal separator.

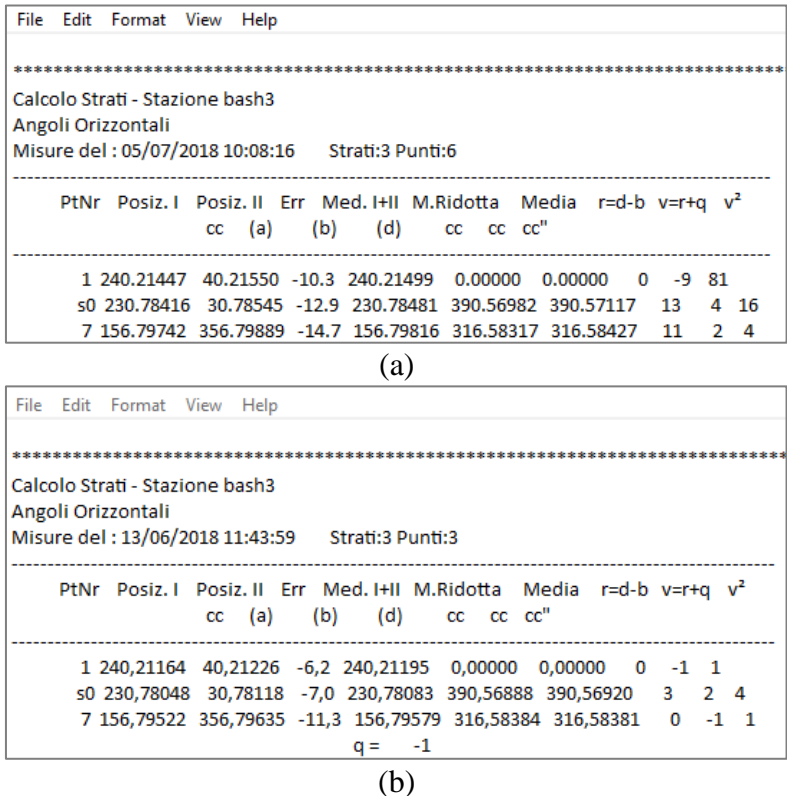


Figure 12. Different file format due to regional settings of the user's device

Additional issues have been encountered with the date format. In Europe the date is usually represented as DD/MM/YY, where in US it is MM/DD/YY. For example the first day of June 2018 can be represented as 01/06/18 (Europe) or 06/01/18 (US). Furthermore, users can adjust the regional settings of the laptop to any of these formats. In order to overcome problem when importing data from different sources, the data management system uses robust algorithms when reading the different files and compares results with previous recordings so in this way such errors are significantly reduced.

Inconsistent file format due to user setup

File formats and sensor setup should be consistent so as to minimize customization and manual interventions when importing data to a data management system. Sometimes, however, users may setup sensors and/or data files in an inconsistent format. Figure 13 shows an example of an output file from a tiltmeter, in which sensor measurements are primarily logged in the N-S and W-E directions. Sensor 3, however, follows a different pattern and data are logged in the following sequence: W-E, N-S. This is an inconsistency during sensor setup (probably due to a change in the cable connection sequence in the datalogger) that can create issues when importing data.

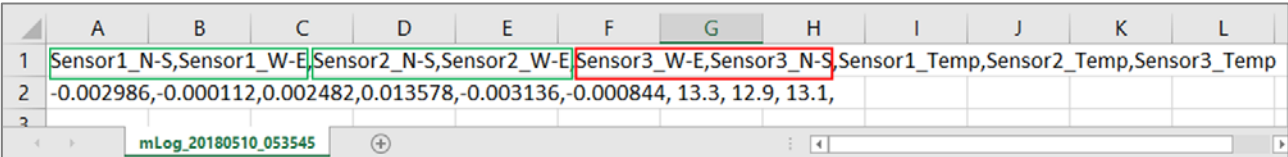


Figure 13. Different sensor sequence in the output file of a tiltmeter

It is easily understood that developing import procedures to a data management system is not a trivial matter. In addition, deviations from specified file formats are expected in large projects. This means that monitoring systems and/or data management systems should always be supported with a quality control/assurance functionality in order to ensure that data are reliable and accurate. This requires a robust software package with multiple options that serve individual user needs. Nevertheless, fully automated procedures for data import and data reduction and visualization are still not the norm in geotechnical monitoring.

4. UPCOMING FEATURES

The data management system is constantly being improved and new options are developed to make the interface more user-friendly and functional according to the user needs.

An important feature that will be developed in the near future is a well-organized alarm notification system. An alarm can be activated when a single measurement value exceeds the default limit set for a monitoring device. Therefore, an alarm can be displayed for a single sensor or a single topographic monitoring target. This does not mean, however, that there is a critical event such as a downward movement of an entire slope. In order to evaluate a situation and generate a warning or an alarm, data from different sources should be combinedly evaluated. Such combinations could include alarms and measurements from more than one similar or different devices located in the same area. A combination of increased precipitation, together with increased piezometer values as well as large displacement vectors could be used to indicate potential slope movements. Such a system should be well organized to combine the alarm values from different regions and/or instrument types and to correctly interpret the severity of the incoming alarms. The email notification to predefined users with respect to alarm levels would also contribute to increase the safety of operations.

Additional features will be related to data import, so that the user responsible for uploading measurements will be able not only to insert a comment but also to edit the measurement records according to this comment. Comments can be used to document changes in device layout (e.g. re-positioning of a survey target), erroneous measurements, heavy rainfall at a specific date, or even an observed crack. It is expected that the data management system will provide options for logging these comments so as to contribute to a more reliable evaluation of measurements.

Finally, the web interface will be updated to allow users to customize the output. Although there may be multiple monitoring campaigns active at a given time, there may be an area of particular interest that needs to be evaluated on a daily basis. The update will allow users to select the area and the devices (charts and tables) that will be initially presented. These changes will be possible through a web-drive dashboard.

5. CONCLUSION

In this paper a robust cloud-based data management software application is presented. The database is cloud-based while the user interface is available both as a Windows application and as a browser based application. This geotechnical monitoring system has evolved over many years and has been successfully used for slope monitoring in large surface mines.

During the initial development of this system, special consideration was given to (a) the routines that pertain to data import from various input files, (b) numerous features that allow users to customize output in ways that help them visualize and evaluate measurements for different monitoring scenarios, (c) features that allow seamless integration of the front end (windows and web) to the back-end data management system, etc.

The data management system is constantly updated to include new features, such as additional options for warning and alarm notifications, logging of field information correlated to the measurements and many others. All improvements are based on the experience of the developing

team as well as interaction with the industry and aim to produce a top-of-the-line user-friendly geotechnical monitoring package.

REFERENCES

- [1] Agioutantis, Z., Kaplanidis, G., & Steiakakis, C. (2014). Development of a database for geotechnical monitoring applications. 7th Hellenic Conference on Soil Mechanics and Geotechnical Engineering.
- [2] Kavvadas M., Agioutantis Z., Schilizzi P., & Steiakakis C. (2013). Stability and movements of open-pit lignite mines in Northern Greece, Proceedings of the 18th ICSMGE, 2193-2196
- [3] Steiakakis, C., Agioutantis, Z., Apostolou E., Papavgeri, G., & Tripolitsiotis A. (2016). Integrating weather and geotechnical monitoring data for assessing the stability of large scale surface mining operations. *Open Geoscience*, 2016, 8, 694–699.
- [4] Agioutantis, Z., Steiakakis, C., Papavgeri, G., & Schilizzi, P. (2015). Development of a geotechnical data management system for mining operations. Proceedings of 26th Annual General Meeting & Conference – SOMP 2015, Session VI, Latest Innovations in Mining Education & Research, 141–147.

The Impact of the Coal Clay in the Slope Geometry of the OCM Radljevo North Opening Cut

Branko Petrović¹, Tomislav Šubaranović² and Ivica Ristović²

¹PE EPS Belgrade, Branch MB Kolubara, Organizational unit Project, Lazarevac, Serbia

²University of Belgrade, Faculty of Mining and Geology, Belgrade, Serbia

ABSTRACT

Opening a new surface coal mine is a very complex process depending on a large number of factors that directly or indirectly define the conditions and dynamics of mining operations. The investigation of the future excavation area should be at such a level that available data should show the state of the terrain as realistic as possible on that occasion. It happens often that the influence of certain parameters is ignored or for some other reason is being eliminated, which later creates great complications, which often lead to human and equipment vulnerability.

In this paper, influence of interlayers coal clay particles was analysed, slope geometry of the opening cut of the OCM RADLJEVO NORTH, as well as on its position in relation to the OCM TAMNAVA WEST FIELD internal dump site.

1. INTRODUCTION

Surface mine OCM RADLJEVO NORTH is located about 50 km from Belgrade, west of OCM TAMNAVA WEST FIELD (Figure 1.).



Figure 1. Location of the OCM RADLJEVO NORTH within the Kolubara coal basin, (contour of the basin marked with a red line).

The thickness of the carbon series in the RADLJEVO NORTH seam ranges up to 90 m. The layers of xylitol coal with the interlayers of spent, amorphous and ground coal, as well as, coal clay of wetlands are covered with aleuritic clays, sandy sediments of flowing wetlands, rarely clean well sorted sands of river sediments. The total geological resources of coal were determined in the quantity of 532.316.714 t, with the average quality of the lower heat value of LHV = 7249 KJ / kg.

After the May 2014 floods, at the OCM TAMNAVA WEST FIELD, there was an awareness regarding the problem of forming a safe use opening cut of the new RADLJEVO NORTH mine. Due to the change in the overburden dump technique in the OCM TAMNAVA WEST FIELD (Figure 2),

there was a breakdown of the internal dump site, which deviated from the designed level of the internal dump site.

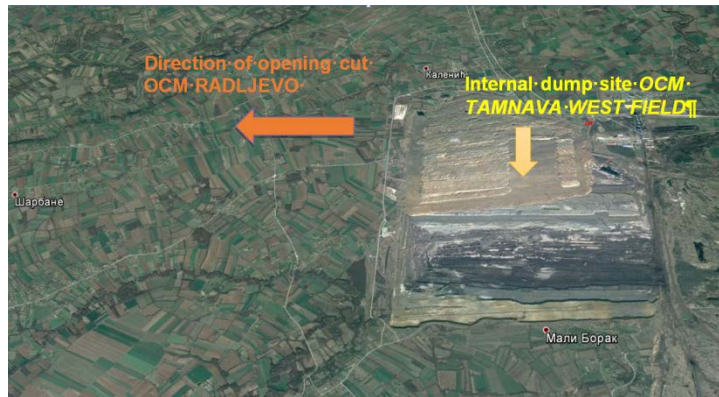


Figure 2. Internal dump site OCM TAMNAVA WEST FIELD with the direction of the OCM RADLJEVO NORTH opening cut.

By analysing the previously designed partial and general slopes of the OCM TAMNAVA WEST FIELD internal dump site, there was a knowledge of the necessity of their correction, i.e. their mitigation and leaving the block of coal and roof sediments in the zone towards the future opening cut. This block will have the role of a safety causey that the final slope of the OCM TAMNAVA WEST FIELD internal dump site will rely on (Figure 3).

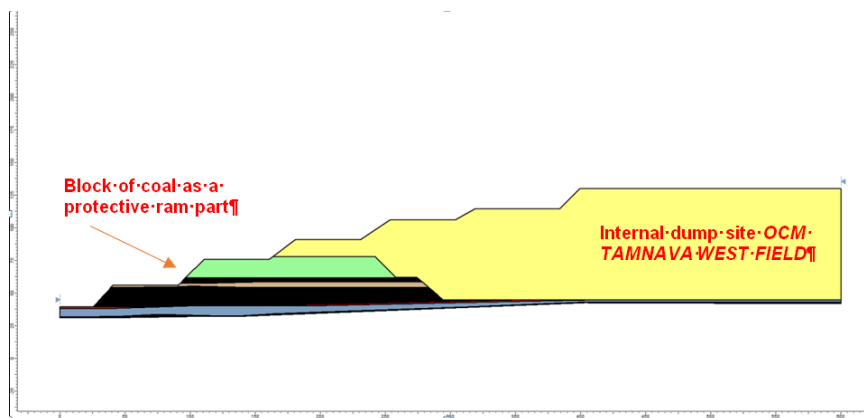


Figure 3. Cross section of internal dump site OCM TAMNAVA WEST FIELD.

2. ESTIMATE OF SLOPES STABILITY FACTORS ON THE INTERNAL DUMP SITE OF THE OCM TAMNAVA WEST FIELD

The analysis of the stability of slopes of the OCM TAMNAVA WEST FIELD internal dump site was done by application of the Morgnsterm-Price method, along with the Mohr-Coulomb criterion of fracture, for the degree of sedimentation where the pore pressure coefficient is $ru = 0.2$. For different heights and their different slopes, have been made calculations (results shown in Figure 4) to define the slope geometry that provides the required safety factor values (Fs).

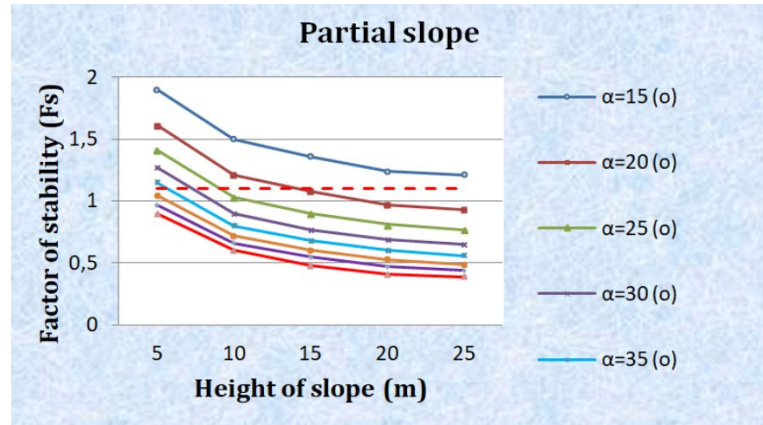


Figure 4. Safety factors for partial slopes of the OCM TAMNAVA WEST FIELD internal dump site.

Based on the data from the above diagram, the height of the partial slope of the internal dump site $H = 15$ m can be adopted, as well as its inclination $\alpha = 20^\circ$.

Figure 5 shows the results of the stability analysis of the general slope of the internal dump site, for its different heights and slopes. On the basis of these obtained data, and in accordance with the legislation, the height of the general slope $H_g = 54$ m and the inclination $\alpha = 11^\circ$ can be adopted.

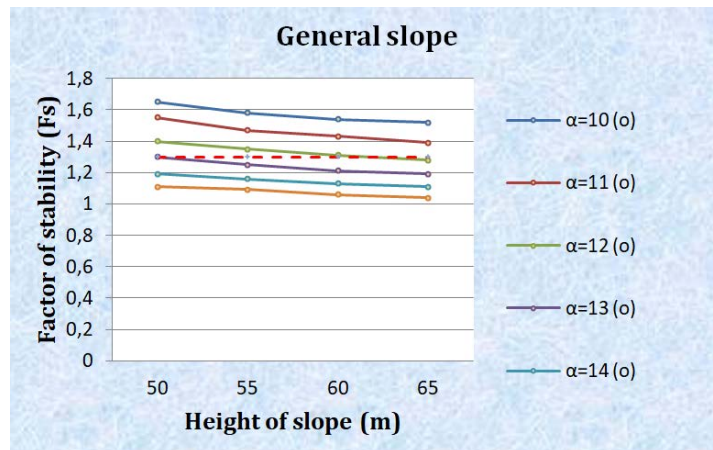


Figure 5. Safety factors for the general slope of the OCM TAMNAVA WEST FIELD internal dump site.

3. POSITION OF OPENING CUT IN RELATION TO THE INTERNAL DUMP SITE OF THE OCM TAMNAVA WEST FIELD

The opening cut must be so done that it does not risk the existing mining works with its geometry and position, while at the same time guaranteeing the safety of future planned works. According to the originally planned positioning and geometry of the OCM TAMNAVA WEST FIELD internal dump site, the safety factor (F_s) of the slope is made consisting of the internal dump site inclination and a block of coal that remains in the zone between the internal dump site and the opening cut. The length of coal measured at its bottom side is 269 m. Because of its poor physical and mechanical parameters, interlayers coal clay deposits in the coal represent the plane at which the total masses move. Figure 6 shows the analysis of the stability of the observed slope (safety factor $F_s=1.01$).

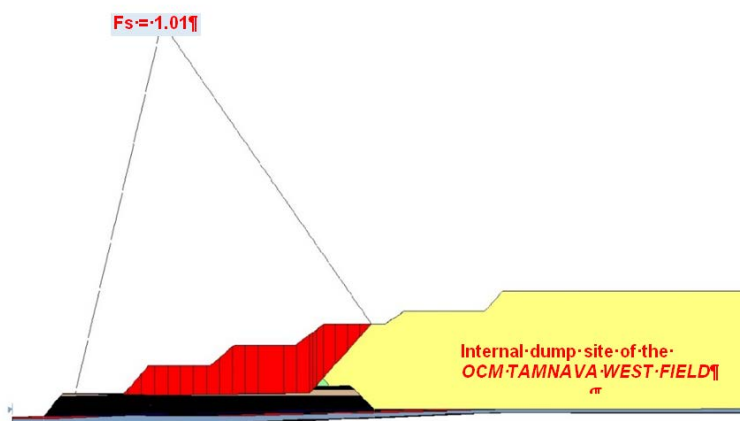


Figure 6. The originally planned general slope of the internal dump site and coal block ($F_s = 1.01$).

For reasons of increasing the stability of this slope, it is necessary to move the seal of the opening cut to the west in order to increase the width of the safety zone around the internal dump site and the opening cut. This shift should be about 100 m, so the length of the left coal will then be about 370 m, with the safety factor $F_s = 1.33$ (Figure 7).

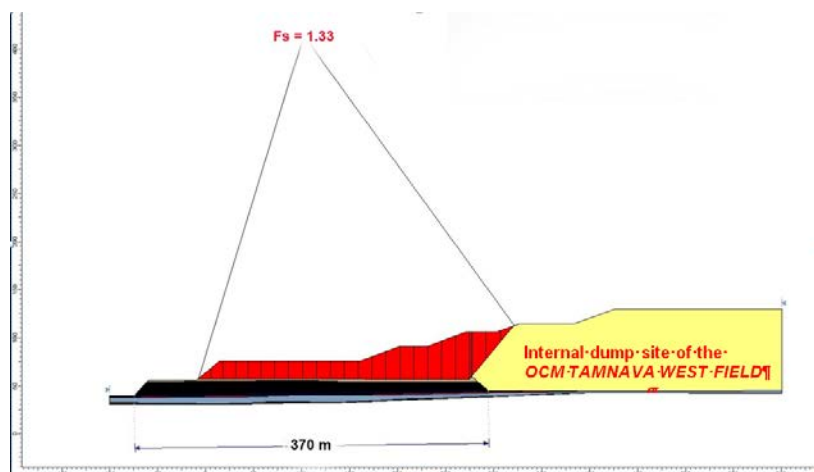


Figure 7. Corrected general slope of internal dump site and coal block ($F_s = 1.33$).

4. CONCLUSION

From the previously stated, the reason for the correction of the opening cut of the OCM RADLJEVO NORTH position was corrected and the necessity of its shifting towards the west in the length of about 100 m, leaving one block of coal and roof aleurite sediments at an average length of about 370 m as a safety block to the OCM TAMNAVA WEST FIELD internal dump site.

The reason for the correction of the opening cut position was due to the change in the post-storage technology after the floods of May 2014, that is, the reduction of the accommodation space.



Figure 8. Correction of the opening cut position.

By moving the initial position of the opening cut of the OCM RADLJEVO NORTH for about 100 m towards the west (Figure 8), conditions for its safer work and its uninterrupted development towards the west in the width of about 2 km (north-south direction) will be met.

REFERENCES

- [1] Technical mining project of surface protection of the OCM RADLJEVO NORTH from ground water, University of Belgrade - Faculty of Mining and Geology, Belgrade (2016).
- [2] Preliminary project for exploitation of coal on OCM RADLJEVO NORTH, Vattenfall Europe Mining Consulting and University of Belgrade - Faculty of Mining and Geology, Belgrade (2010).
- [3] Technical documentation by Kolubara coal basin company.

Reliability Evaluation during Slopes Progressive Failure

Alexandros V. Deliveris¹, Ioannis E. Zevgolis² and Nikolaos C. Koukoulas¹

¹Chemical Process & Energy Resources Institute / Centre for Research & Technology Hellas,
Egialias 52, Maroussi, Greece

²Department of Civil Engineering / Democritus University of Thrace, Kimmeria Campus, Xanthi,
Greece

ABSTRACT

Progressive failure of slopes is a relatively common problem in surface lignite mines. In the present work, a probabilistic methodology that takes into account the inherent geotechnical uncertainty is suggested for the evaluation of a homogeneous slopes' reliability during progressive failure phenomena. The proposed methodology is built upon the reliability index based Point Estimate Method combined with finite elements computations. Shear strength parameters are considered non-correlated random variables following normal distribution. Stability for various safety states, up to the ultimate failure state, is expressed and evaluated in terms of global reliability indices and global probabilities of failure. For illustrative purposes, a typical case example is solved following the suggested methodology. It is anticipated that the established reliability model may be further extended in order to take into consideration slopes' transition failure probabilities during progressive failure.

1. INTRODUCTION

Progressive failure of slopes is a relatively common problem encountered in surface lignite mines [1, 2]. In many instances, working pit slopes experience great deformation levels before approaching ultimate limit states. The non-uniform stress-strain distributions developing along slip surfaces, in combination with the presence of brittle – prone to strain-softening – soils, are the main causes for progressive failure occurrence [3]. Since the progressive failure of slopes is primarily attributed to the non-uniform stress-strain levels upon potential shearing surfaces, limit equilibrium methods are not capable of credibly simulating this complicated process. Instead, finite element models are more applicable for this purpose, due to their ability of capturing the stress-strain behavior of soil. The capability of finite element models to simulate soil strain-softening behavior, by the reduction of shear strength parameters with the accumulated shear strains, has been used by various researchers [4, 5, 6]. In an attempt to incorporate geotechnical uncertainty, other researchers approached the problem from a reliability point of view, examining the probability of progressive failure propagation along certain slope slip surfaces [7, 8, 9]. However, in these works, probabilistic simulation of slopes' progressive failure was formulated within the framework of limit equilibrium. In this study, the probabilistic modeling of slopes' progressive failure was conducted via the finite element method. In particular, the evaluation of an excavated slope's reliability during the development of progressive failure conditions, is performed using a finite element model (developed on program Plaxis 2D [10]), combined with the probabilistic point estimate method. A detailed description of the proposed reliability model, accompanied by the essential assumptions and simplifications made, are given in the next sections, followed by an illustrative case example.

2. SLOPES PROGRESSIVE FAILURE RELIABILITY MODEL

In this work, a reliability model able to probabilistically simulate slopes' progressive failure is proposed. For this purpose, a finite element slope model is merged with the point estimate method

[11, 12]. For the individual slope's progressive failure states, stability is evaluated in terms of global slope failure probability or in terms of the complementary event of global slope reliability.

2.1. Deterministic approach

Figure 1 illustrates the alteration of principal stresses due to the unloading process taking place during excavation of a typical cut. As a result of the developing shear strains due to the produced gravity forces, soil shear strength is unevenly mobilized along potential slip surfaces [13].

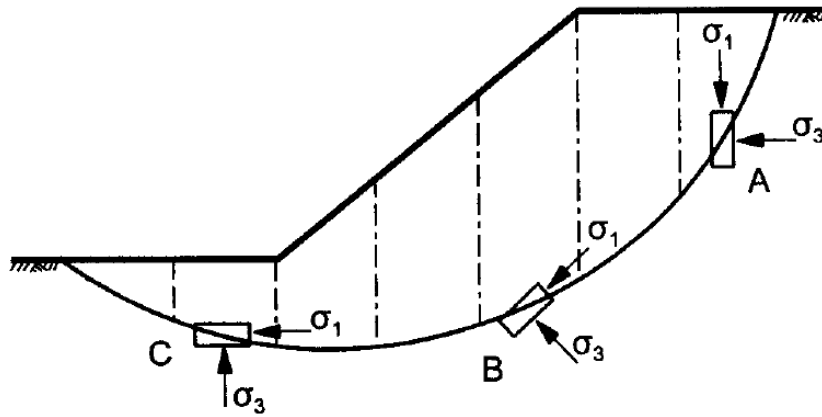


Figure 100. Principal stresses alteration due to slope excavation [13].

This unloading process during slope excavation may be simulated by finite elements, through the successive removal of soil element clusters, modeling the actual staged construction procedure of the slope. The major and minor principal stresses, $\sigma_{1,i}$ and $\sigma_{3,i}$, along a potential slope slip surface, at i locations upon it, may be employed for the evaluation of normal and shear stresses, σ_i and τ_i , respectively, according to Eq. (1) and Eq. (2).

$$\sigma_i = \frac{\sigma_{1,i} + \sigma_{3,i}}{2} + \frac{\sigma_{1,i} - \sigma_{3,i}}{2} \cos(2\theta) \tag{1}$$

$$\tau_i = \frac{\sigma_{1,i} - \sigma_{3,i}}{2} \sin(2\theta) \tag{2}$$

Angle θ represents the angle between the direction of the minor principal stress and the orientation of soil element plane failure, where in most unfavorable conditions, corresponding to the maximum developing shear stress, it is determined by the soil friction angle φ through Eq. (3).

$$\theta = 45 + \frac{\varphi}{2} \tag{3}$$

The available shear strength s_i , at slope working conditions, is calculated by the Mohr-Coulomb failure criterion, and the soil shear strength parameters c and φ , according to Eq. (4).

$$s_i = \sigma_i \cdot \tan\varphi + c \tag{4}$$

In this manner, for a slope under working stress conditions, local safety factors $SF_{L,i}$ along potential slip surfaces, are computed as ratios of available to mobilized shear strengths by Eq. (5).

$$SF_{L,i} = \frac{S_i}{\tau_i} \tag{5}$$

In addition, global safety factors SF_G may also be established through the averaging of the available and mobilized shear strengths at n locations along potential slip surfaces, by Eq. (6).

$$SF_G = \frac{\sum_{i=1}^n \frac{S_i}{n}}{\sum_{i=1}^n \frac{\tau_i}{n}} = \frac{\frac{S_1 + S_2 + \dots + S_n}{n}}{\frac{\tau_1 + \tau_2 + \dots + \tau_n}{n}} \tag{6}$$

For the direct simulation of slope progressive failure, the capability of finite element models to yield areas of local overstress is utilized. In particular, in the portions of the slip surface where the shear stress becomes equal to the shear strength and the local safety factor approaches the value of 1, residual strength parameters are assigned. As a result, stress relaxation produced in the failed portions of the slip surface, induces overstress in the remaining sections (that do not fail) upon the shear surface. Assigning, in turn, residual shear strength values in the adjacent portions of the slope’s slip surface that sequentially fail, the process of progressive failure is simulated throughout consecutive calculation stages, as shown in Figure 2.

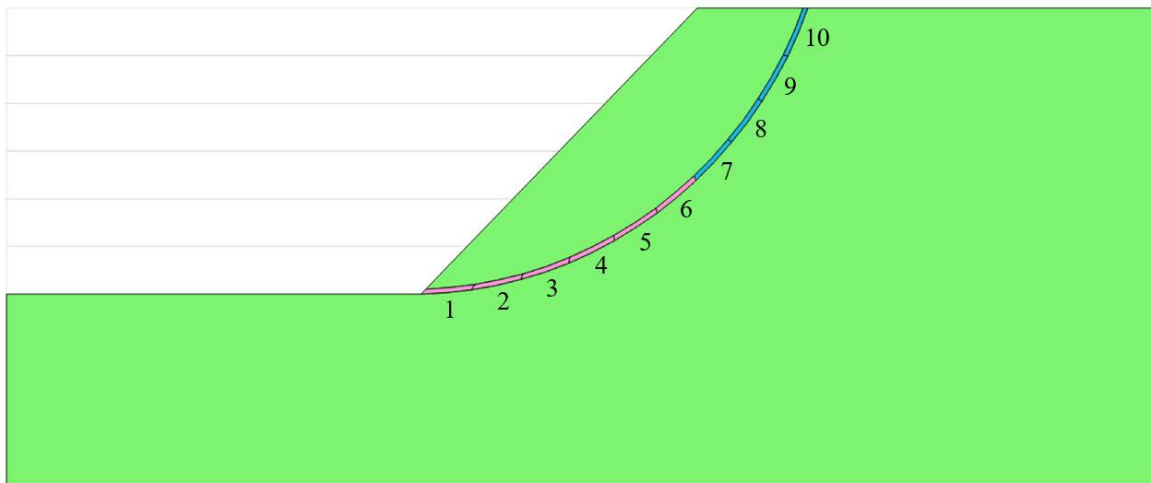


Figure 101. Progressive failure simulation along slope’s slip surface failed portions.

2.2. Probabilistic treatment

In this work, local and global safety factors, as were defined and formulated in the previous section, shall be used as critical indicators for the evaluation of slope’s stability. Through their probabilistic treatment as performance functions of variable nature, statistics associated with computation of their values will be determined. For this purpose, the probabilistic point estimate method is merged with the finite element model. For a performance function Y , indicating either a local or global safety factor, evaluation of Y is performed at certain distances of one standard

deviation σ above and below the mean μ of the random variables. In case that Y depends on two random variables X_1 and X_2 , its evaluation is performed at locations determined by Eq. (7), Eq. (8), Eq. (9) and Eq. (10). Then, evaluation of Y is realized by Eq. (11), Eq. (12), Eq. (13) and Eq. (14).

$$X_1^+ = \mu[X_1] + \sigma[X_1] \quad (7)$$

$$X_1^- = \mu[X_1] - \sigma[X_1] \quad (8)$$

$$X_2^+ = \mu[X_2] + \sigma[X_2] \quad (9)$$

$$X_2^- = \mu[X_2] - \sigma[X_2] \quad (10)$$

$$Y_{++} = Y(X_1^+, X_2^+) \quad (11)$$

$$Y_{+-} = Y(X_1^+, X_2^-) \quad (12)$$

$$Y_{-+} = Y(X_1^-, X_2^+) \quad (13)$$

$$Y_{--} = Y(X_1^-, X_2^-) \quad (14)$$

Weighting factors P , may be determined by the correlation coefficient between the involved random variables ρ_{X_1, X_2} , according to Eq. (14) and Eq. (15).

$$P_{++} = P_{--} = \frac{1}{4} \cdot (1 + \rho_{X_1, X_2}) \quad (14)$$

$$P_{+-} = P_{-+} = \frac{1}{4} \cdot (1 - \rho_{X_1, X_2}) \quad (15)$$

The lower order statistics of Y , and in particular, the mean, variation and standard deviation are determined by Eq. (16), Eq. (17) and Eq. (18).

$$\mu[Y] = P_{++} \cdot Y_{++} + P_{+-} \cdot Y_{+-} + P_{-+} \cdot Y_{-+} + P_{--} \cdot Y_{--} \quad (16)$$

$$Var[Y] = P_{++} \cdot Y_{++}^2 + P_{+-} \cdot Y_{+-}^2 + P_{-+} \cdot Y_{-+}^2 + P_{--} \cdot Y_{--}^2 - (\mu[Y])^2 \quad (17)$$

$$\sigma[Y] = \sqrt{Var[Y]} \quad (18)$$

Assuming that Y follows a normal distribution, the reliability index β is determined by Eq. (19). Through the integral of the cumulative standard normal distribution function $\Phi[\beta]$, as this is evaluated by Eq. (20), the probability of failure P_F is calculated by Eq. (21).

$$\beta = \frac{\mu[Y] - I}{\sigma[Y]} \quad (19)$$

$$\Phi[\beta] = \frac{1}{\sqrt{2\pi}} \int_{-\infty}^{\beta} e^{-\frac{z^2}{2}} dz \tag{20}$$

$$P_F = 1 - \Phi[\beta] \tag{21}$$

2.3. Case example

In order to examine the risk of a progressive failure from a probabilistic point of view, the established computational scheme is applied on a typical slope example. The finite element model representing the construction of an excavated slope of 6 m height and 45° inclination is displayed in Figure 3.

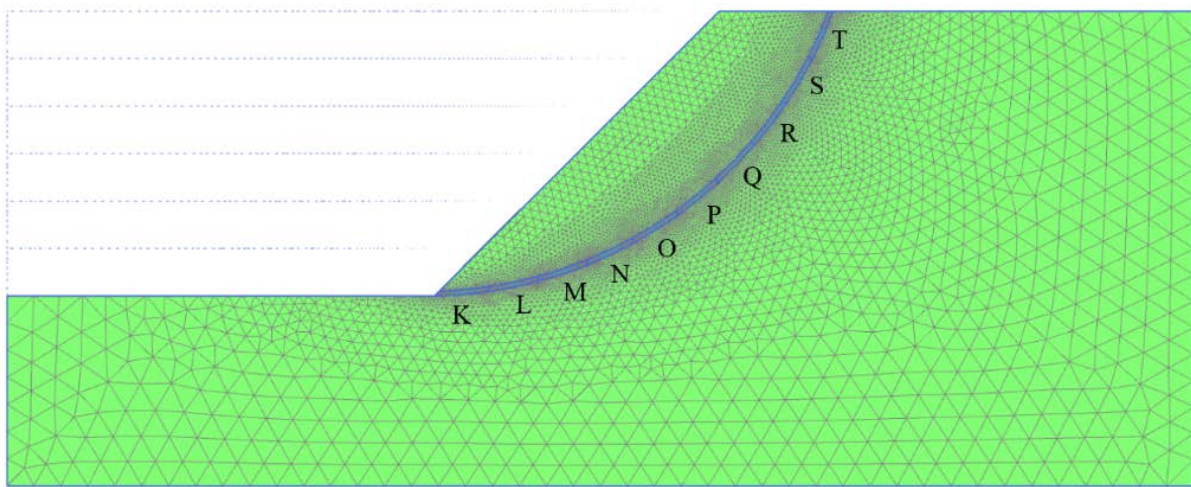


Figure 102. Finite element model simulating the construction of an excavated slope.

The slope’s potential slip surface is simulated by an elastic-perfectly plastic Mohr-Coulomb soil model. Shear strength parameters are simulated as random variables following normal distributions. Statistical parameters of the random variables are shown in Table 1. Cross-correlation between random variables was neglected ($\rho_{\phi,c}=0$).

Table 20. Soil material parameters’ statistics assigned to the assumed shear band.

Material parameter	Mean value μ	Coefficient Of Variation COV (%)	Standard deviation σ
Friction angle ϕ ($^{\circ}$)	20	10	2
Cohesion c (KPa)	25	20	5

The rest of the soil outside the shear band is simulated by a linear elastic material model. The assigned deterministic properties for the elastic soil material are displayed in Table 2.

Table 21. Deterministic material properties of the linear elastic soil outside the slope shear band.

Parameter	Value
Young's modulus E (KPa)	25000
Poisson's ratio ν (-)	0.3
Unit weight γ (KN/m ³)	18

The residual soil properties assigned to the portions of the slope's shear band that have failed are shown in Table 3. In this study, it is noted that the residual properties that represent soil strain-softening behaviour during the simulation of slope progressive failure are treated as deterministic quantities.

Table 22. Residual material properties assigned to the failed portions of the shear band.

Parameter	Value
Residual friction angle ϕ_r (°)	10
Residual cohesion c_r (KPa)	5
Young's modulus E_r (KPa)	5000

3. RESULTS

The non-uniform shear stress distribution along the slope's slip surface, after the excavation is completed, is depicted in Figure 4. The Figure clearly shows the continuous decrease of the applied shear stresses from the toe to crest. In addition, as may be seen from Figure 5, a respective constant reduction of the shear strain along the slip surface is also observed. The non-uniform stress-strain distribution is leading to the uneven distribution of local safety factors, as displayed in Figure 6. The local safety factor value of 1 in the first portion of the slip surface near the slope's toe, as shown in Figure 6, evidences a local slope failure. Through the probabilistic treatment of the slope stability model, distribution of the respective local failure probabilities along the slope's slip surface is shown in Figure 7. Local failure probability at the first portion of the slip surface raises to 28%.

The continuous decrease of the local probability of failure from the toe to the crest indicates a potential mode of slope progressive failure. The high local failure probability at the second portion of the slip surface is rather attributed to the quite large coefficient of variation of the respective local safety factor, as this is depicted in Figure 8. The mean global slope safety factor reduction, for the various safety states during progressive failure is displayed in Figure 9. For the initial state 0, where all portions of slip surface are operating under peak shear strength conditions, the global safety factor mean raises to 2.10, whereas for the final state 6, where six portions of the slip surface have been failed, the mean global safety factor is equal to 1.07.

The uncertainty associated with the evaluation of the global slope safety factor, for the various states of progressive failure, expressed in terms of the coefficient of variation is shown in Figure 10. A slight fluctuation of the variability (between 12% and 14%) corresponding to the evaluation of the global safety factor is observed. On the other hand, Figure 11 illustrates a significant decrease of the global slope reliability index, which is rather dominated by the large drop of the global mean safety factor during the development of slope progressive failure. The significant increase of global slope probability of failure, for the various states of slope progressive failure is exhibited in Figure 12. Very close to the slope's ultimate limit states, in particular at state 6, global slope probability of failure raises to 18%.

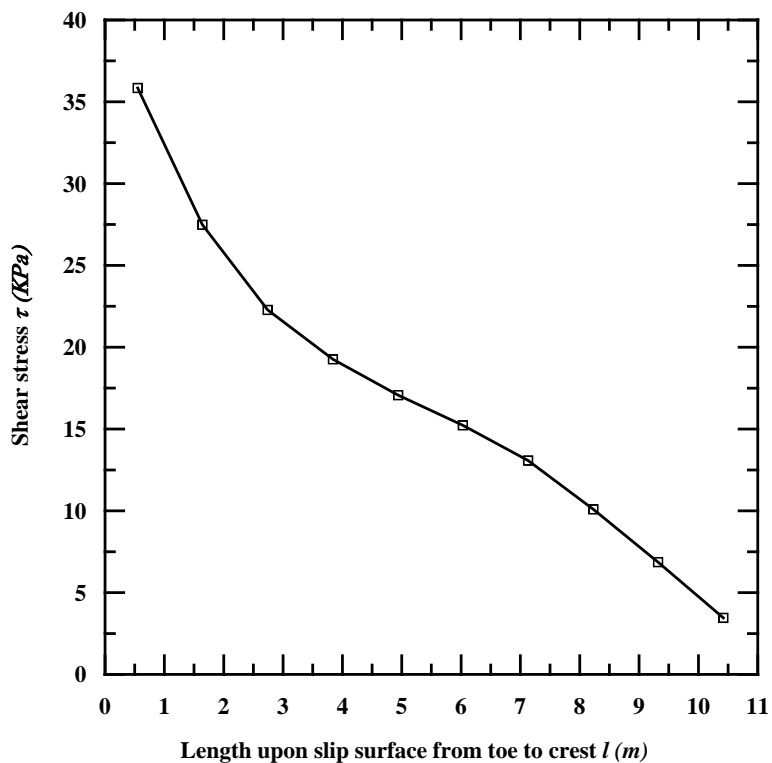


Figure 103. Shear stress distribution along slope's slip surface.

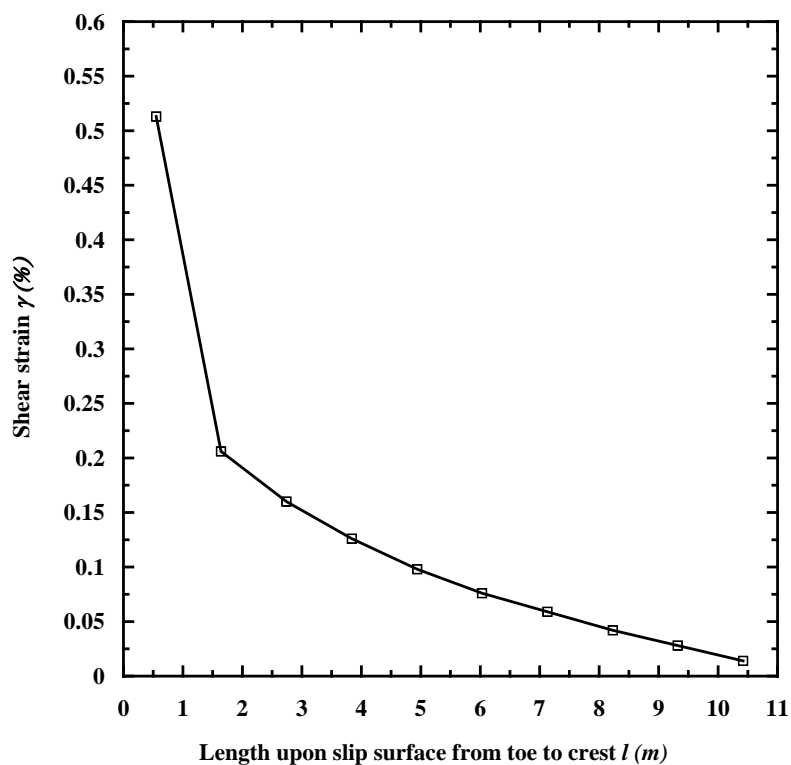


Figure 104. Shear strain distribution along slope's slip surface.

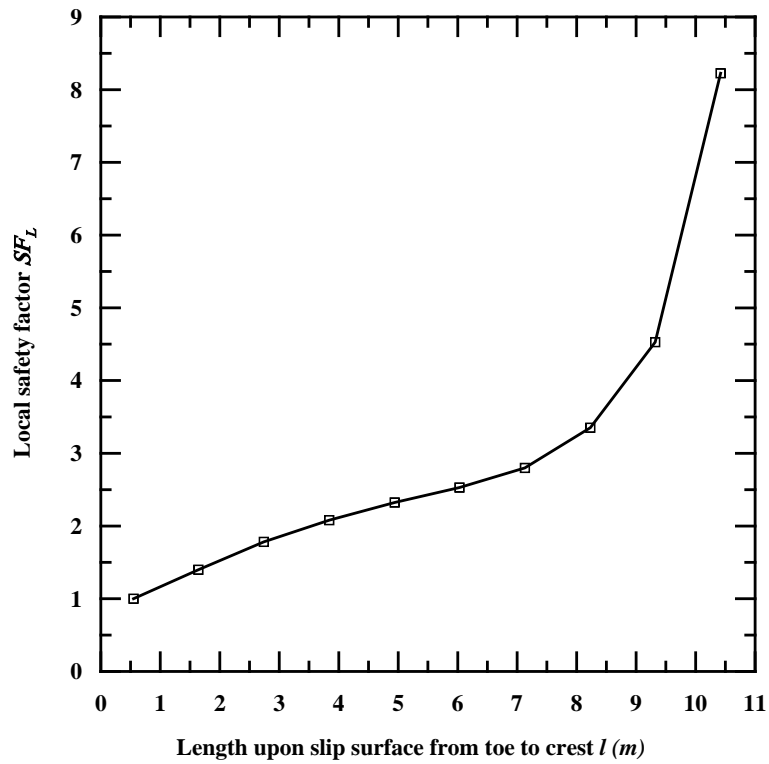


Figure 105. Local safety factor distribution along slope's slip surface.

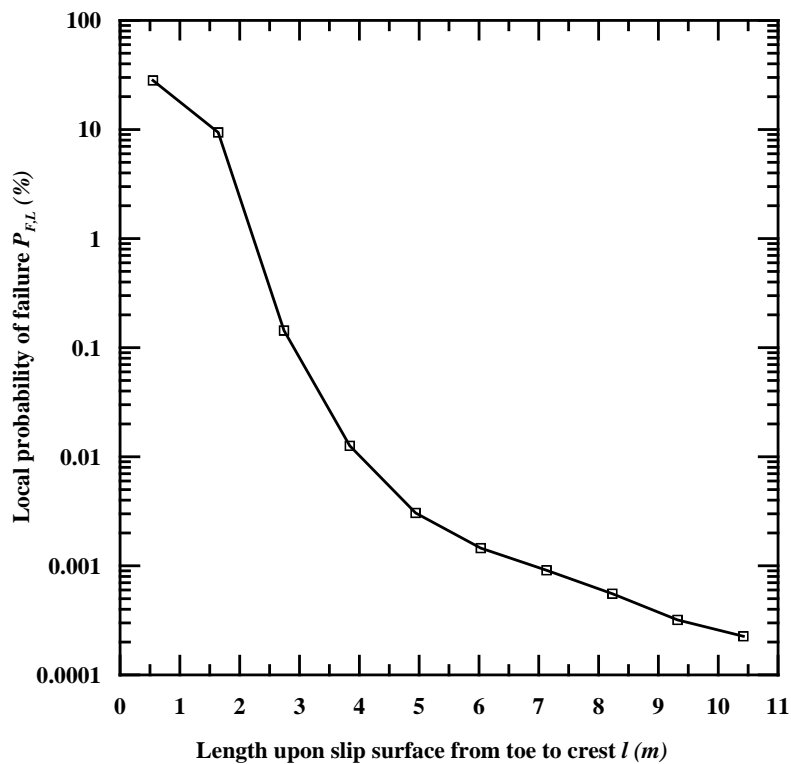


Figure 106. Local failure probability distribution along slope's slip surface.

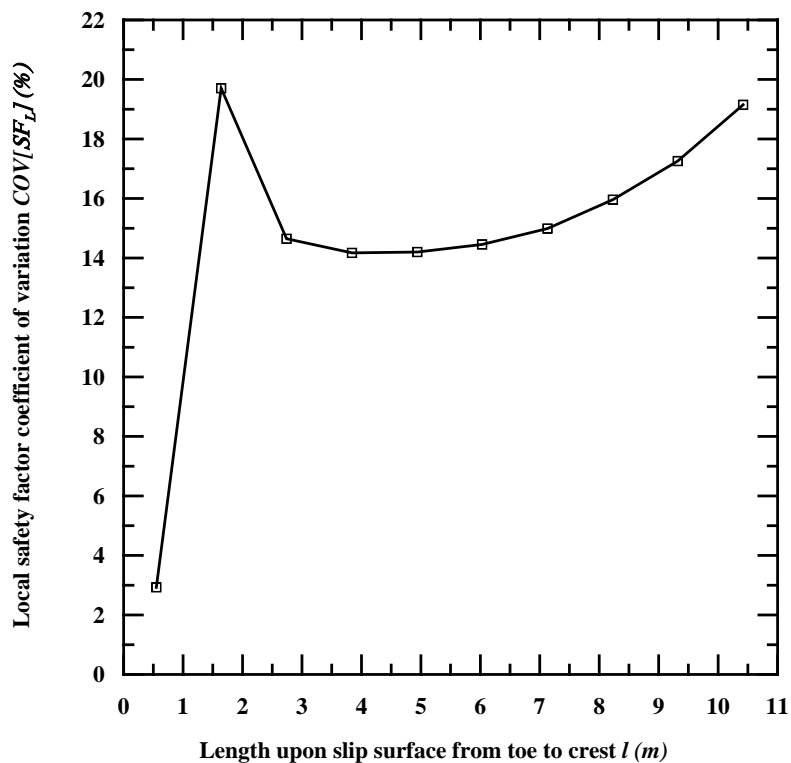


Figure 107. Local coefficient of variation distribution along slope's slip surface.

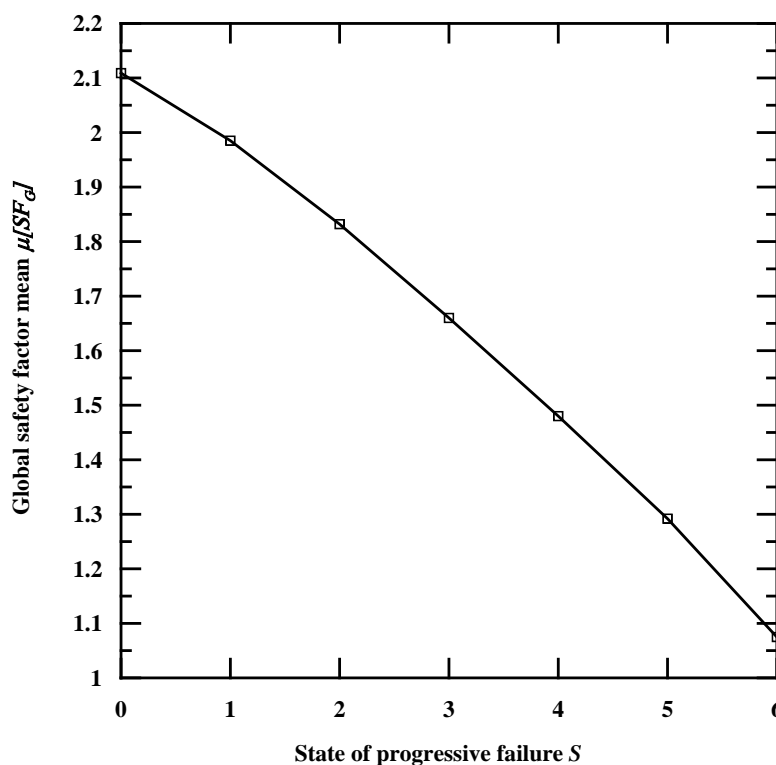


Figure 108. Global mean safety factor at the states of progressive failure.

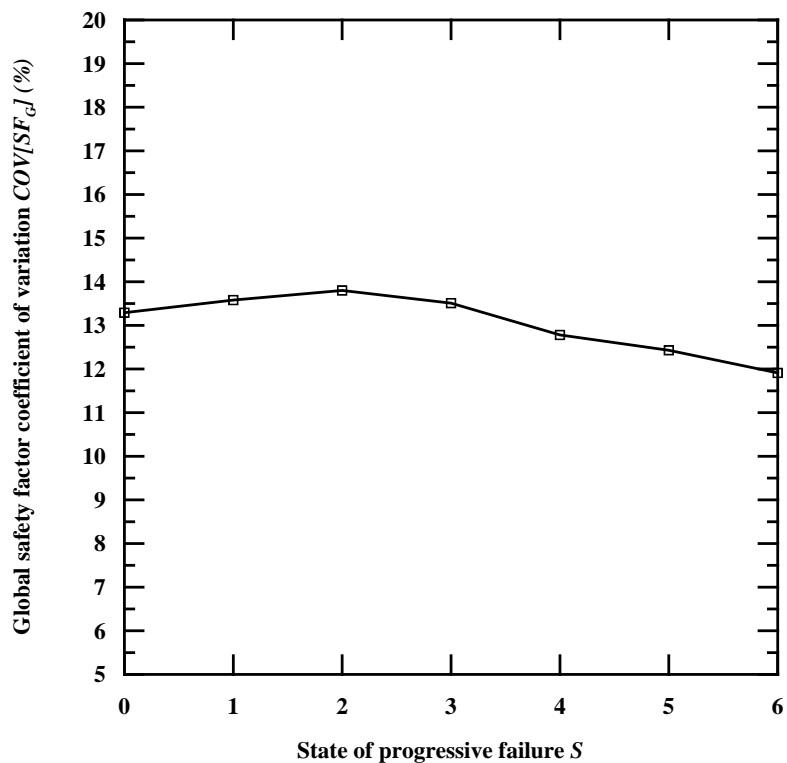


Figure 109. Global coefficient of variation safety factor at the states of progressive failure.

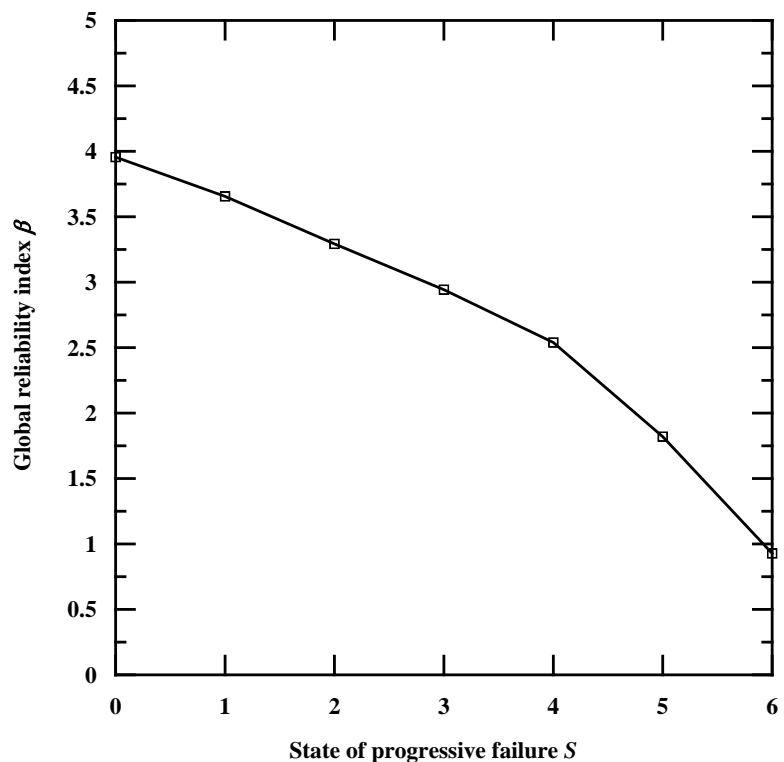


Figure 110. Global reliability index at the states of progressive failure.

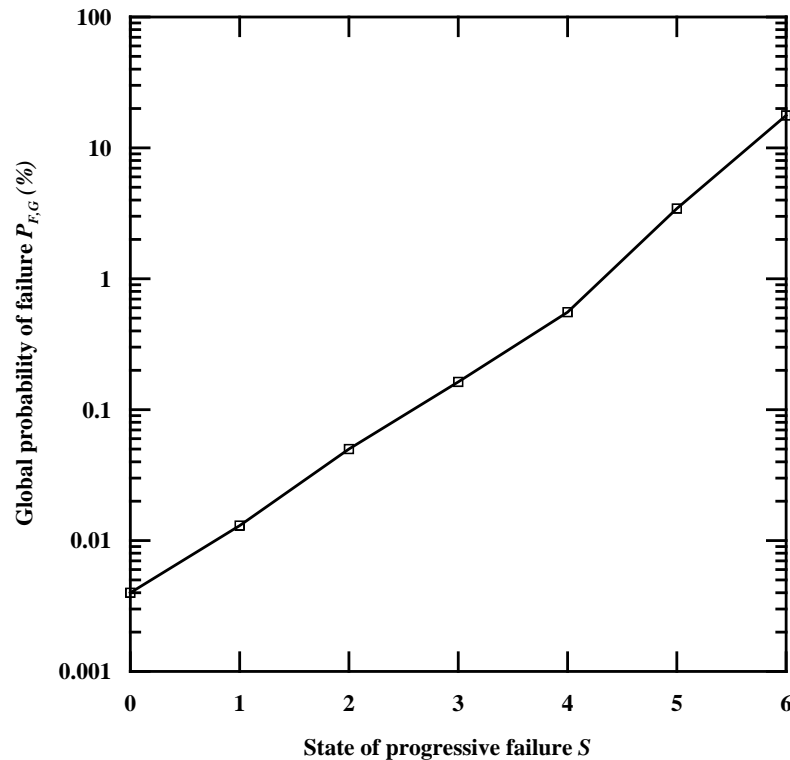


Figure 111. Global reliability index at the states of progressive failure.

4. CONCLUSIONS

In this work, a practical reliability model for the probabilistic simulation of slopes' progressive failure was developed. A finite element slope stability model was combined with the probabilistic point estimate method. The risk associated with the global stability of slopes, during development of progressive failure was investigated. The significant increase of global slope failure probability at the various states of progressive failure was evidenced, and it was principally attributed to the remarkable reduction of the mean value of the global safety factor. Regarding the uncertainty associated with the calculated global safety factors at the states of progressive failure, only slight changes were observed. Even if the stability of brittle soil slopes seems to be assured by large global safety factors and respective probabilities of failure, the probability for progressive failure initiation is noteworthy and should not be ignored. The proposed methodology for the assessment of slope stability risk may be proved useful to surface mine owners, in the case where slopes undergo progressive failure problems.

REFERENCES

- [1] Leonardos, M. (2004). Methods and procedures for monitoring, assessment and improvement of slope stability in deep excavated Greek lignite exploitations. PhD dissertation, National Technical University of Athens, Greece.
- [2] Kavvadas, M., Agioutantis, Z., Schilizzi, P., & Steiakakis, C. (2013). Stability and movements of open-pit lignite mines in Northern Greece. Proceedings of the 18th International Conference on Soil Mechanics and Geotechnical Engineering, Paris.
- [3] Lo, K. Y. (1972). An approach to the problem of progressive failure. Canadian Geotechnical Journal, 9(4), 407-429.

- [4] Lo, K. Y., & Lee, C. F. (1973). Stress analysis and slope stability in strain-softening materials. *Geotechnique*, 23(1), 1-11.
- [5] Dounias, G. T., Potts, D. M., & Vaughan, P. R. (1996). Analysis of progressive failure and cracking in old British dams. *Geotechnique*, 46(4), 621-640.
- [6] Potts, D. M., Kovacevic, N., & Vaughan, P. R. (1997). Delayed collapse of cut slopes in stiff clay. *Geotechnique*, 47(5), 953-982.
- [7] Chowdhury, R. N., & A-Grivas, D. (1982). Probabilistic model of progressive failure of slopes. *Journal of the Geotechnical Engineering Division*, 108(6), 803-819.
- [8] Bourdeau, P. L. (2004). Probabilistic modelling of landslide reactivation by embankment load. 9th ASCE Specialty Conference on Probabilistic Mechanics and Structural Reliability, New Mexico.
- [9] Metya, S., Bhattacharya, G., & Chowdhury, R. N. (2016). Reliability analysis of slopes in strain-softening soils considering critical slip surfaces. *Innovative Infrastructure Solutions*, 1(1).
- [10] Plaxis, B.V. (2018). *Plaxis 2D AE. 2D finite element geotechnical analysis software*, Delft, Netherlands.
- [11] Rosenblueth, E. (1975). Point estimates for probability moments. *Proceedings of the National Academy of Sciences*, 72(10), 3812-3814.
- [12] Rosenblueth, E. (1981). Two-point estimates in probabilities. *Applied Mathematical Modeling*, 5, 329-335.
- [13] Abramson, L. W., Lee, T. S., Sharma, S., & Boyce, G. M. (2002). *Slope stability and stabilization methods*, 2nd Edition, John Wiley & Sons, New York.

Avoiding Instability Conditions in Sector 6 of the Southern Field Mine in Northern Greece

Nestor Kolovos

Public Power Corporation S.A – Hellas/Western Macedonian Lignite Center/Greece

ABSTRACT

Tectonic structure system crossing the mine benches of Southern Field Mine in Ptolemais basin could activate tension forces towards the open slopes, creating thus possible instability conditions. Detailed study of the geological conditions contributes to detect any instability factors and explain the mechanism of possible failure. Continuous observing, measuring and mapping of tension cracks and deformation movements is of major importance in order safety measures to be taken to avoid any mining failure.

1. INTRODUCTION

Greece is the fifth largest lignite producer within the European Community. The exploitable lignite reserves in the Florina-Ptolemais-Kozani tectonic basin come up to 1,7 billion tons, representing 2/3 of the total lignite reserves of Greece. During last years the Western Macedonian Lignite Center produces about 30-40 million tons of lignite annually to feed 4 thermal power plants, with a total installed capacity of 3775MW (Figure 1).

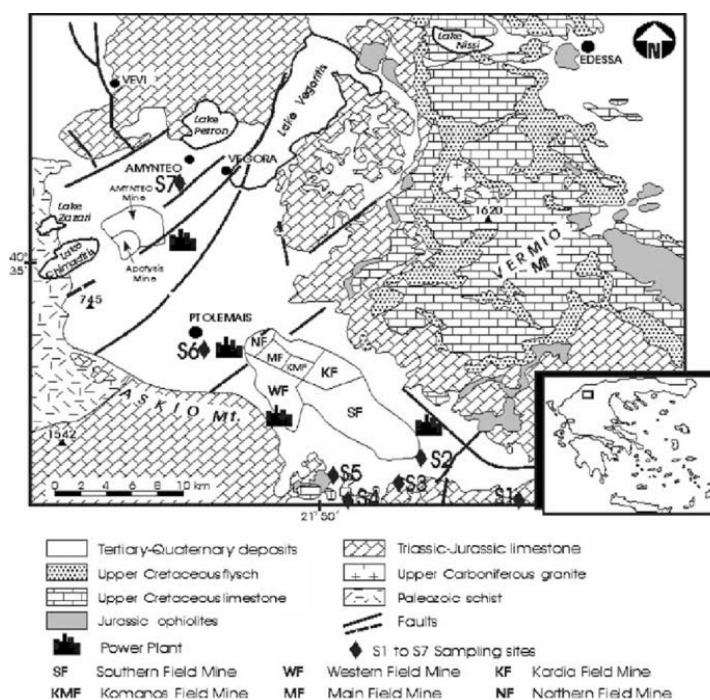


Figure 1. Simplified geological map of the Ptolemais Kozani area

This lignite is produced in 4 big mines, with the Southern Field Mine being the biggest lignite mine in the Balkan peninsula, feeding the Agios Dimitrios Power Plant since 1983. During the last years the mining activities in Southern Field Mine are conducted at the Sector 6 which is extended to the eastern part of the South Field Mine (area of the old settlement of Haravgi-Klitos) (Figure 2).



Figure 2. View of Sector 6 of Southern Field Mine

Its annual lignite production ranges between 13-15 million tons and total excavations range between $60 \times 10^6 - 80 \times 10^6 \text{ m}^3$ (bulk). Big bucket wheel excavators connected to long conveyor belts run in continuous operation digging the mine benches (Figure 4). [1]

The sediments of the Ptolemais basin, where the main lignite deposits are located, belong to Neogene (Pliocene) and are covered by those of Quaternary (Pleistocene and Recent). [2]

The overburden is defined by three coloured sediment series consisting of clays, gravels, sands, sandstones and conglomerates, named by their colour as red, yellow and green series (Figure 3 and 4). [2]

The Southern Field Mine deposit is characterized as a "zebra" type or multiseam lignite deposit dominated by the multiple interchanges of lignite and thin sterile intercalations consisting mainly of clays, marls and sands (Figure 3 and 4). [2]

A typical stratigraphic column is given in Fig. 3 [3].

Major and minor faults crossing NE-SE and E-W the lignite layers, acting as structural discontinuities upon which local failure of a bench or an overall slope can occur, may be considered as possible instability factors which have to be studied in order to eliminate or avoid any mining slope failures (Figure 5).

The knowledge of the geometry, the geological structure and the quality characteristics of both the lignite and the sterile intercalated layers is of utmost importance in designing the optimum lignite recovery. [1]

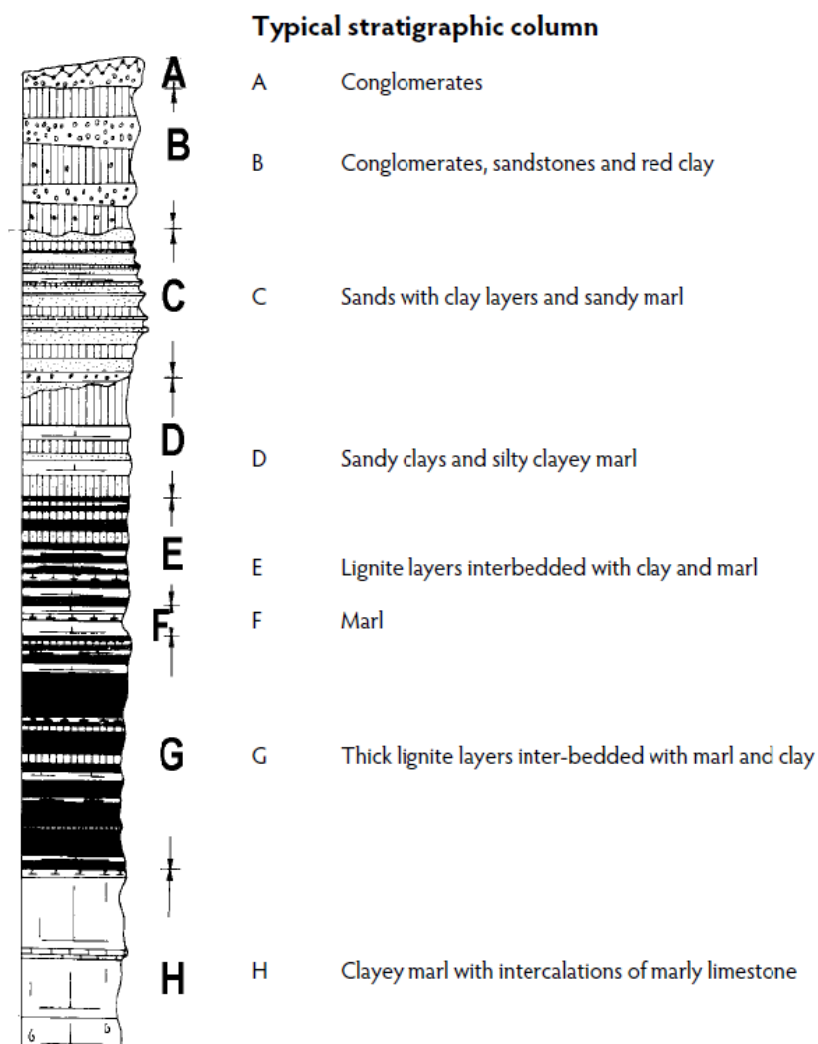


Figure 3. Typical stratigraphic column [3]

On March 2016 tension cracks on the floor of the second mine bench were observed, giving alert for possible activation of instability conditions. Although this is not unusual in large and deep open pit mines, it had to be studied since they are combined with faulted zones which dominate and characterize the area.

2. MATERIALS AND METHODS

In order to avoid any instability problems and apply slope stability principles properly, the geometry, the geological structure, the groundwater conditions and the mechanism of possible sliding must be understood well. Next, site conditions must be applied precisely to the model for analysis. [4]

To assess the instability conditions, mine photo (Figure 4), mine plan (Figure 5), borehole records, geological and geotechnical mapping and geological cross section AA' (Figure 6) of the area were studied. Special attention was paid on stratigraphy (Figure 3 and 4), the nature of

geological layers, the tectonic structure, the direction and dipping of mining benches, the inclination of lignite layers and the water works crossing the fault zones.



Figure 4. Face view of Sector 6 of Southern Field Mine

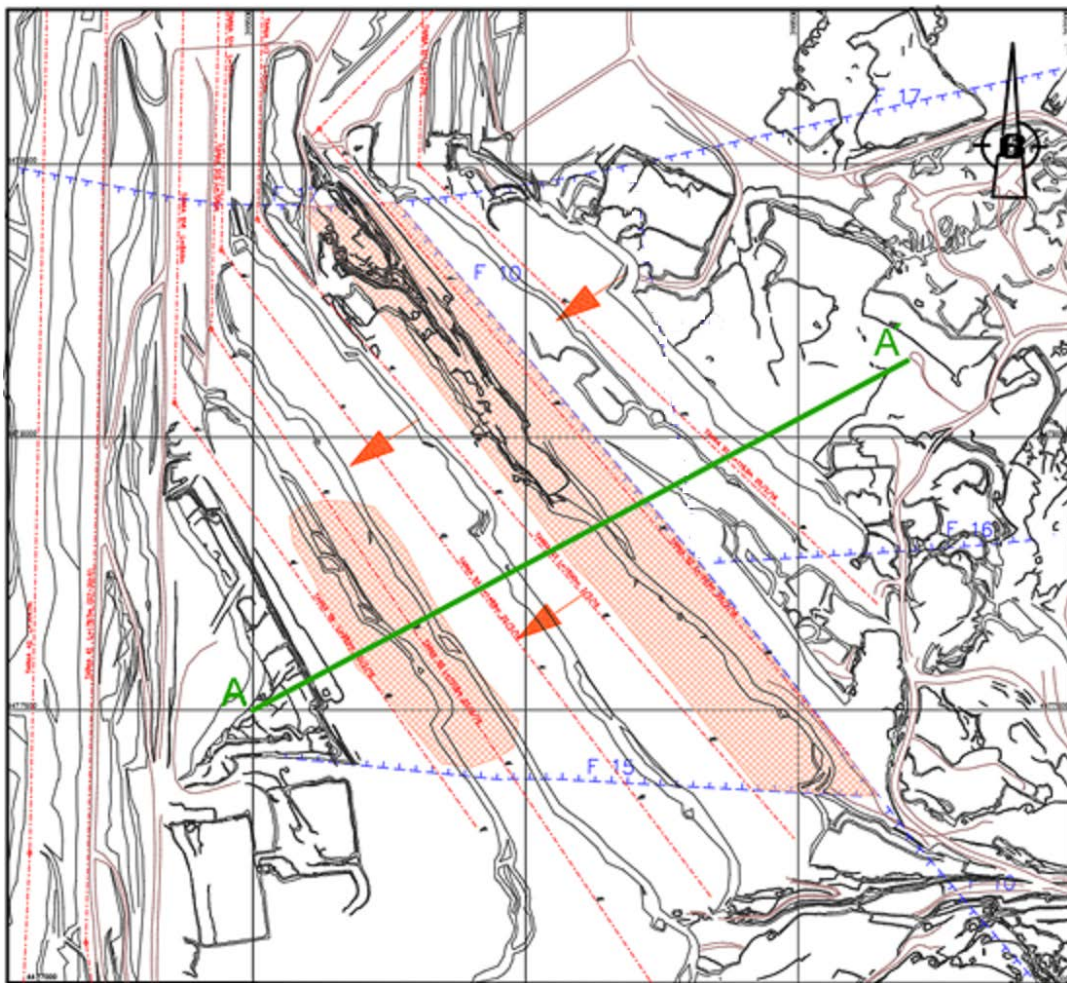


Figure 5. Geotechnical map of Sector 6 of Southern Field Mine

3. RESULTS AND DISCUSSION

The operation of Southern Field Mine is very important for the power supply of Greece and its uninterrupted operation is often critical.

Mining operations may take place even in moving slopes, as long as safety of personnel and equipment is satisfied. [5]

Mining operations can proceed safely with minimum interruption if failure mechanisms are understood and slopes are properly monitored even in moving slopes. [6]

Geotechnical planning and design in surface mining operations is a very important issue and should be considered in all phases of mine operation, from the exploration phase to the postclosure stage. [7]

In fact, it is challenging to determine the failure mechanism. Experience and knowledge when combined with good observation lead to successful predictions on failure mechanisms on failed slopes or slopes to be excavated. It is essential to estimate probable failure mechanism in order to use proper and adequate method during slope stability estimation or slope stability analysis.

When the stability of a bench, which is important in a particular mining operation, is suspect, its stability must be assessed on the basis of the geological structures, groundwater conditions and other controlling factors which occur in that specific slope.

While the overall slopes are clearly important in terms of the economics of the entire mining operation, the stability of individual benches is usually a matter of more immediate concern to the engineering responsible for the day-to-day mining operations. [8]

Slope failure in a bench, which carries a main haul road or huge bucket wheel excavator connected to long conveyor belts, can cause severe disruption to the mining programme. It is also in these relatively small failures, which can occur with very little warning, that lives can be lost and equipment damaged. [9]

The stability of an individual bench is controlled by local geological conditions, the shape of the overall slope in that area, local groundwater conditions and also by excavation technique used in creating a slope. These controlling factors will obviously vary so widely for different mining situations that it is impossible to give general rules on how steep a bench should be to ensure that it will be stable. [8]

Sector 6 is developing towards the eastern part of the South Field Mine, leaving open slopes westwards (Figure 4 and 6).

The geological structure is dominated by a system of normal faults F17, F10, F16 and F15, striking in NW-SE, NE-SW and E-W directions and dipping at 72° – 78° . Thrusts of faults range between 30m – 70m.

Faults F17, F10 and F15 form the boundaries of a block which is dipping towards the open slopes and occupies the main part of Sector 6 of the Southern Field Mine (Figure 5).

These faults reaching the top surface of lignite act as structural discontinuities upon which local failure of a bench or an overall slope can occur.

The surface of the mine is located at 700m – 720m and the lignite bottom is at 535m.

The thickness of the overburden ranges between 60m and 80m while the thickness of the coal deposit ranges between 30m and 60m.

The lignite bottom in the central part of Sector 6 is at 620m while towards the open slopes dipping to 535m. Arrows in figure 5 show this direction towards the short shaded area.

The mining activities are developed in 7 benches, 6 of them named as S, having a mean thickness of 20m (Figure 6).

The general inclination of lignite layers is $3,4^{\circ}$. However locally it gets steeper reaching $4,5^{\circ}$.

Although this angle is not too steep, the presence of faults, especially the F10 which strikes parallel to the mine benches and the dipping of lignite layers towards the open excavations cause possible instability conditions. This is deteriorated by the reduced cohesion in fault zones and the

earth forces developed due to the dipping of coal layers towards the open slopes. The whole situation becomes worse due to the presence of thin clay layers between the coal ones which could be possible sliding surfaces. [10]

There are not serious water problems inside the coal layers. Water comes from the overburden sand and gravel layers and is collected by channels at the toe of slopes and driven towards pump stations. However problems arise when these channels run through faulted zones and water enters inside the weak zones.

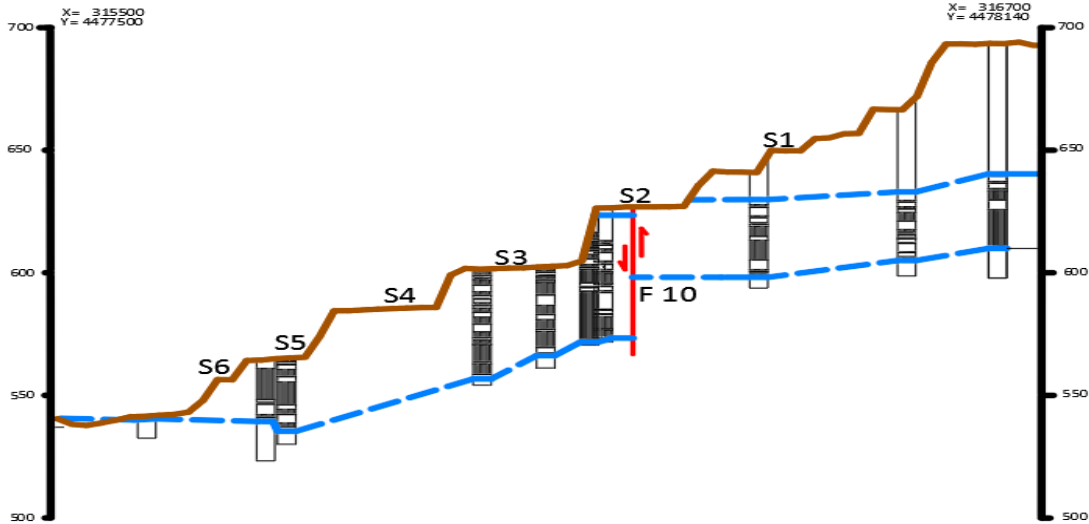


Figure 6. Cross section AA' of Sector 6 of Southern Field Mine (distorted scale)

As it has been referred the first indications of instability appeared in the floor of the upper bench S2 as tension cracks running parallel to the fault F10. This area is indicated with the long shaded area in Figure 5.

Impending slope failures can be detected and analyzed long before any crack formation at the slope crest becomes visible. [10]

The answer to the question of the failure type is not only of scientific significance but it has practical implications concerning the suitability and the effectiveness of the stabilizing measures to be taken and also the proper interpretation of the slope monitoring data. [10]

In this case it is assumed that if a failure is to occur this is going to be a plane failure (Figure 7) along clay layers which are present inside the coal deposit.

The thin clay layers are often present in the marl-lignite intercalations of the Ptolemais mines, they are characterized by a significantly low residual strength (5° - 10°) [5] and they often serve as part of the compound sliding mechanisms of the local mines.

This is assumed because

- a) the plane on which sliding will occur strikes parallel or nearly parallel to the slope face.
- b) The failure plane “daylights” in the slope face and its dip is smaller than the dip of the slope face.

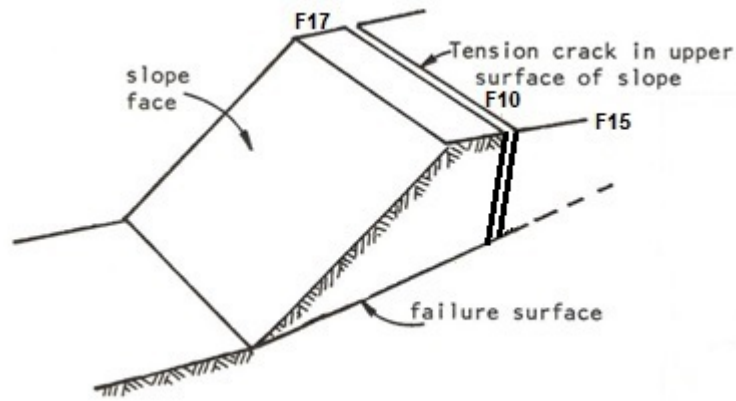


Figure 7. Assumed slope failure model

The most important factor for the stability is the shear strength available in the planar part of the failure surface, which shows that a progressive failure is taking place.

The sliding will occur if the dip of the failure plane is greater than the angle of friction of this plane. The main driving force acting on the slope is the gravitational force which is directly proportional to the slope inclination.

Since no water in lignite layers exists it is assumed that the slope is completely drained. In practical terms, this means that there is no water pressure in the tension cracks or along the sliding surface due to earth forces developed due to the geometry of the slope. There may be moisture in the slope but as long as no pressure is generated, it will not influence the stability of the slope. However, if water enters through heavy rain or from drainage channels inside the tension cracks, this will build up water pressure in the tension crack and will cause instability conditions.

Because of the current mining activities and the urgent demand for coal production remedial measures had to be taken in order the mining works to be continued and any danger for mining failure to be avoided.

The remedial measures which decided were:

1. Filling of any cracks with clay.
2. Continuous observing, monitoring and mapping of tension cracks on primary and secondary faulting zones.
3. Collecting of waters running on the floor of the benches.
4. Sealing up of any trenches at the faulted zones with clay or rubber pieces from old conveyor belts or making passages with plastic or metallic pipes
5. Giving priority to the excavations on the upper benches
6. Flattening of slopes
7. Strictly following the mining planning
8. Avoiding any excavations in the toe of slopes
9. Avoiding any excavations in the lower benches

After two years of operation no serious slope failure has occurred. The mine continuously its operation succeeding all its production targets satisfying the lignite demand in the Power Plant Station. Minor local failures occurred in cases when water entered inside faults (Figure 8) and when detachment and sliding of lignite layers from marls occurred in the faulted zone. (Figure 9).



Figure 8. Water intrusion from a channel in a fault zone



Figure 9. Local slope failure due to detachment of lignite from marl in the fault zone

4. CONCLUSION

In surface mining crack formation is recognized as a precursor of impending slope failure and collapse.

The first benefit from the early failure detection and the slope monitoring is an improved safety environment. The second is the deeper understanding and better control of the slope stability in the mine.

Mining operations may take place even in moving slopes, as long as safety of personnel and equipment is satisfied.

Major and minor faults crossing the lignite layers and acting as structural discontinuities may be considered as possible instability factors which have to be studied in order to eliminate or to avoid any mining slope failures.

The stability of an individual bench is controlled by local geological conditions, the shape of the overall slope in that area, local groundwater conditions and also the excavation technique used in creating a slope.

Apart from the overall slope special attention must be paid to the individual slopes since local failures may affect the progress of mine works.

Any cracks striking parallel to faulted zones should be considered as possible tension cracks initializing possible slope failure.

Any water flow must be collected in order to avoid flooding of cracks and faulted zones.

Thin clay layers should be considered as sliding planes activating slope failure.

The designed geometry of slopes must be strictly followed in order to avoid any instability problems.

REFERENCES

- [1] Karnaris I. and Kolovos N., (2018). Geological face mapping in Open Pit Mines using fully automated terrain following rotary-wing UAVs. Proceedings of Geomapplica International Conference on Geomatics, 25-29 June 2018, Syros - Myconos Islands, Greece, (In print).
- [2] Kolovos N. Georgakopoulos A., Fillipidis A., and Kavouridis C. (2002). Environmental effects of lignite and intermediate steriles coexcavation in the Southern Lignite Field Mine of Ptolemais, Northern Greece. *Energy Sources* 24, 6, 561-573.
- [3] Anastopoulos, J.C., Koukouzas, C.N.: Economic Geology of the Southern part Ptolemais lignite basin (Macedonia - Greece). Institute of Geology and Mineral Exploration, Athens, pp.101–136 (1972)
- [4] Abramson, L.W., Lee, T.S., Sharma, S. and Boyce, G.M. (2001). *Slope Stability and Stabilization Methods*. 2nd edition, John Wiley & Sons, 712 p.
- [5] Kavvadas M., Agioutantis Z., Schilizzi P., and Steiakakis C. (2013). Stability and movements of open-pit lignite mines in Northern Greece. In: Proceedings, 18th International Conference on Soil Mechanics and Geotechnical Engineering (XVIII ICSMGE), Paris, 2-6 September 2013, pp. 2193-2196.
- [6] Zavodni, Z. M., 2000. Time-Dependent Movement of Open-Pit Slopes. Chapter 8, Slope stability in surface mining, Hustrulid, McCarter, VanZyl (eds), Society for Mining, Metallurgy and Exploration
- [7] Steiakakis C., Agioutantis Z., Schilizzi P., Papakosta E., Tsalidis A. and Pagonis G. (2013). 6th International Conference on Sustainable Development in the Minerals Industry, 30 June–3 July 2013, Milos island, Greece.
- [8] Hoek E. and Bray J., (1981). *Rock Slope Engineering*. Revised Third Edition, The Institution of Mining and Metallurgy, London, 358 p.
- [9] Kolovos C.J., (2004). *Coal Mining Technology* (in Greek). ION, Athens, 342 p.
- [10] Leonardos M., (2014). Rim slopes failure mechanism and kinematics in the Greek deep lignite mines. 12th International Symposium Continuous Surface Mining, Aachen, Germany, 21-24/9/2014.

Investigation of the Stability of Deep Excavation Slopes in Continuous Surface Lignite Mines

Michael Kavvadas¹, Christos Roumpos² and Paul Schilizzi²

¹ School of Civil Engineering, National Technical University of Athens, Greece

² Public Power Corporation, Greece

ABSTRACT

The paper investigates the stability of slopes in PPC lignite mines in Greece, where continuous surface mining is applied with excavation depths up to 200m. Experience with the behaviour of such excavations shows that slope instabilities are usually governed by sliding along a sub-horizontal, unfavourably sloping, interface between coal and an underlying stiff, high plasticity clay or marl layer, very close to the bottom of the slope, where shear stresses are largest.

The typical mechanism of such instabilities is triggered by the sharp contrast in stiffness between adjacent lignite and clay/marl layers causing different elastic rebound upon removal of the horizontal confinement during excavation. The resulting differential horizontal strain causes shearing along the lignite-clay interfaces and the development of significant negative excess pore water pressures in the stiff clay. Shearing is larger in deeper interfaces (close to the base of the slope) and increases drastically in cases of unfavourably sloping interfaces (towards the mine). If the shear stresses approach the peak strength of the interface, creep movements become appreciable, gradually reducing the available strength of the interface towards a low residual value. This strength reduction is accelerated by dissipation of the negative excess pore water pressures in the clay, as pore water can drain towards the adjacent lignite (through tension cracks caused by the elastic rebound).

The paper investigates the effect of these parameters on slope stability by a set of parametric analyses. The results are plotted in dimensionless graphs which can be used in preliminary stability analyses of lignite slopes. It is shown that (in addition to height and inclination) the most important parameter is the inclination of the sub-horizontal lignite-clay interface at the base of the slope.

The paper also reviews several slopes in the PPC lignite mines which remained stable despite movements with relatively constant velocities reaching up to 100 mm/day, while others have failed when velocities accelerated abruptly although much smaller. These cases show that the absolute magnitude of slope velocity is not always relevant in predicting slope instability, while slope acceleration (plotted as the inverse of velocity versus time) is a better indicator.

1. INTRODUCTION

Lignite (brown coal) exploitation is of primary interest in Greece because lignite is a local resource that currently contributes in the production of more than 30% of domestic electricity demand [1]. While its contribution in power generation gradually reduces with time, mainly due to international carbon tax policies and subsidies of competing renewable energy technologies, lignite exploitation for power generation is expected to remain commercially profitable in Greece, provided that mining operations are optimized and managed efficiently.

The Hellenic Public Power Corporation (PPC) operates several lignite mines in Greece for electricity production in coal-firing power plants. Most of the major mines are in Western Macedonia (Amyntaion-Ptolemais Field) with smaller mines in central Peloponese (Megalopolis Field). In all mines, continuous surface mining techniques are employed, with large bucket excavators and a

network of conveyor belts to transport the ore to the power stations and the sterile overburden for disposal by spreaders (usually by backfilling already exploited mines).

The Amyntaion-Ptolemais Lignite Field is developed in a ca. 150 km long and ca. 15-20 km wide tectonic graben (basin), up to 200 m deep, which extends in the NNW-SSE direction from Prilep (FYROM) in the north up to Servia (Greece) in the south. The graben was created in the Middle to Upper Miocene, during a paroxysm of post-alpine tectonism, by normal faulting of the basal formations which include late Cretaceous limestones and Paleocene-Eocene flysch, and was gradually filled with lacustrine sediments [2]. The Lower Horizon of these sediments, hosting most of the lignite seams, is about 50-80 m thick, consists of very stiff to hard clays and marls, and was deposited between the upper Miocene and lower Pleistocene. The deposition of marls was associated with clay sedimentation and simultaneous precipitation of carbonates (mostly due to changes of the pH and temperature of the water), resulting in clay deposits with an appreciable content in calcium carbonate (marls). As these deposits have undergone gravitational consolidation with overburden pressures corresponding to 150-200 m of fill, and cementation by carbonate bonding, their present strength is high (UCS = 0.5 - 1 MPa). A characteristic hard Basal Marl is encountered at the bottom of the lignite sequence and is used to mark the bottom of the exploitable deposits. The lower Horizon of the sediments is covered by a thick (70-120 m) Upper Horizon of Pleistocene steriles including bluish marls, brownish stiff clays and occasional weak conglomerates and water bearing sandy layers [3], [4]. A relatively thin (5-10m) cover of fluvial Holocene deposits completes the sequence near the present ground surface.

The Megalopolis Lignite Field is smaller in extent (ca. 40 by 10 km) and thinner (up to 100 m deep), has similar geologic history but developed at a later geologic era; thus its lignite seams have higher moisture and lower energy content while the steriles have lower strength compared to the Amyntaion-Ptolemais deposits (due to smaller gravitational consolidation and weaker cementation by carbonates). Although shallower, the mining slopes of the Megalopolis Field present analogous stability problems with the deeper Amyntaion-Ptolemais Field, due to their lower shear strength.

The PPC mines are exploited by removal and disposal of the Upper Horizon steriles and excavation and exploitation of the lignite seams in the Lower Horizon. Excavation is usually performed by large bucket-wheel excavators operating on benches of the slope; the ore and the steriles are transported by a network of conveyor belts to distances of several kilometers. After exploitation, the mines are backfilled by steriles of the same or another mine. The above exploitation method creates excavation slopes with a sequence of benches (60-150 m wide) and drops (15-25 m high) having an overall inclination (v:h) between 1:4 and 1:7 (Figure 1).

2. GEOTECHNICS OF LIGNITE SLOPE STABILITY

A typical ground profile in the PPC lignite mines includes a thick zone of sterile overburden (50-120 m deep) covering the exploitable deposits (30-80 m thick) giving a total excavation depth 100-200 m. The exploitable deposits include packets of lignite seams separated by sterile interlayers consisting of hard clays, usually with medium (15-35%) to high (35-50%) carbonate content (marls). The sterile interlayers in the lignite packet have thickness varying between a few millimeters and several tens of centimeters (or even more). Steriles with lower carbonate content (less than 15%) are more common in the upper steriles, usually have high plasticity (PI>30-40%) and low friction angle (18-22 degrees); deeper steriles usually have medium to high carbonate content, lower plasticity (PI=10-30%) and higher friction angle (22-26 degrees).



Figure 112. Typical exploitation of mine slopes using large bucket-wheel excavators and conveyor belts. Continuous advance of the slope requires a sequence of benches (60-120 m wide) and drops (15-25 m high), having an overall inclination (v:h) between 1:4 and 1:7. The figure shows five, 25 m high benches in the upper steriles of the Mavropigi mine in the Ptolemais Field.

Sterile materials are very stiff to hard due to heavy gravitational consolidation in conjunction with appreciable cementation by carbonate bonding. Steriles with low to medium carbonate content have low to medium cementation but are heavily compacted by gravitational consolidation having low porosity (void ratio 0.60-0.80), low moisture content (20-30%) and relatively high unit weight (19-20 kN/m³). Due to low porosity, they tend to strongly dilate with shearing, developing significant negative excess pore water pressures under undrained conditions. The negative excess water pressures increase the effective stresses in the short term, temporarily increasing strength (and improving stability conditions) until drainage reduces the excess pore water pressures back to zero. On the contrary, deeper, medium to high carbonate content steriles (marls) were usually cemented by strong carbonate bonds early in their depositional history, when their porosity was still large. The high strength of the carbonate cementation bonds has prevented subsequent compaction (consolidation) under additional overburden, maintaining their initial high porosity up to the present day. Thus, typical deep marly steriles have very high porosity (void ratio 1.0-2.2), very high moisture content (35-80%) and very low unit weight (15-18 kN/m³), despite their high initial cementation-induced strength which often reaches 1 MPa. In these high-porosity materials, structure tends to collapse with shearing; thus, the material loses its cementation strength and tends to reduce its volume, developing significant positive excess pore water pressures under undrained conditions. The positive excess water pressures decrease the effective stresses, decreasing strength and occasionally lead to stability failure.

Lignite layers have very low unit weight (13-14 kN/m³), very high moisture content¹ (80-120%), very high porosity (void ratio² 2 – 3), relatively high compressive strength (UCS = 0.4-0.8 MPa), relatively high friction angle (30-35 degrees) but are brittle and crack easily when the in-situ

¹ Defined in geotechnics as the weight ratio of water to dry matter (=wet matter minus water)

² Defined in geotechnics as the volume ratio of voids to matter (=total volume minus solids)

confinement is reduced (due to very low tensile strength) [5]. Thus, in deep excavations, where the in-situ horizontal stress is reduced significantly by the excavation, the lignite beds in the slope develop vertical cracks and thus deform more than the overlying and underlying sterile layers (which deform plastically without cracking). Lignite cracking increases mass permeability and thus enhances and accelerates drainage of the neighbouring sterile layers, affecting their shear strength (see discussion above). The deepest lignite packet is usually underlain by a hard, strongly cemented, very high porosity basal marl which forms the bottom of the exploitable deposits in the basin.

As filling of the basin occurred relatively late in the tectonic history of the area, and thus post-depositional tectonic faulting is rather low, lignite and sterile layers are usually sub-horizontal (maximum inclination of a few degrees) and relatively continuous with few dislocations (jumps) by some tens of centimeters up to a few meters. Most dislocations breaking the sequence of the lignite beds in the horizontal plane are co-depositional faults, caused by underwater slope instabilities during deposition of the loose and weak lacustrine deposits containing the organic materials which eventually produced lignite. Despite that, lignite strata are occasionally crossed by tectonic faults (with jumps of several meters), especially close to the boundaries of the graben where tectonic activity was more intense.

Experience with the PPC mines shows that slope instabilities are usually associated with sliding along a sub-horizontal lignite-to-clay/marl interface, located either slightly above or (more often) slightly below the base of the slope. The sliding surface usually reaches the ground surface along a near-vertical tension crack at some distance behind the crest of the slope.

Sub-horizontal lignite-to-clay/marl interfaces are critical in slope stability for the following reasons:

1. An interface close to the bottom of the slope is more critical than similar interfaces at higher elevations (because the mass of the sliding body increases with depth) and similar interfaces much deeper than the bottom of the slope (for kinematic reasons).
2. These interfaces have lower shear strength compared to the overlying lignite and even the underlying clay/marl for the following reasons:
 - a. The significant reduction of the in-situ horizontal stress in the slope due to the deep excavation, causes significant horizontal tensile strains in the slope. As the E-moduli (in unloading) of the brittle coal layers and the more ductile clay/marl interlayers are different³, their corresponding tensile strains are different, causing shearing along the coal-clay interfaces. The resulting shear stresses can often exceed the peak strength of the interface leading to a post-peak (or even residual) shear strength, which is much lower than the peak strength of stiff clays and carbonate-cemented clays (marls). Shearing along these interfaces causes the development of appreciable negative (in low porosity clays) or positive (in high porosity bonded marls) excess pore water pressures which temporarily increase (or decrease) the effective stress normal to the interface, increasing (or decreasing) its corresponding frictional shear strength. Unfortunately, the beneficial for stability strength increase is short-lived, because groundwater reaching the interface (mainly through cracks in the lignite – see below) dissipates quickly the negative excess pore water pressures, drastically reducing the effective stresses and the corresponding frictional shear strength.
 - b. Due to the high tensile strains, the brittle lignite seams develop vertical cracks, thus providing free access of groundwater to the lignite-clay interfaces, which reduce (dissipate) any negative excess pore water pressures caused by the shearing. This effect is more pronounced at the interfaces, as it will take longer times to dissipate the excess pore pressures in the interior of a thick layer of intermediate sterile.

³ The E-modulus of the lignite in unloading is much smaller, mainly because the lignite is brittle and develops vertical cracks which open freely, while the clay is more ductile and deforms plastically without cracking.

3. Usually, a lignite-to-marl interface is more critical than a geometrically similar lignite-to-clay interface. The reason is that marls usually have high initial porosity because cementation by carbonate bonds usually develops early in the sedimentation history, when the freshly deposited material still has high porosity, and prevents further densification (consolidation) under the weight of subsequent overburden sediments. Upon shearing, the carbonate cementation bonds break and the material tends to collapse (reduce its volume significantly) because it can no longer support the overburden pressure with its current (high) porosity. Under undrained conditions, the tendency for structure collapse causes the development of significant positive excess pore water pressures which reduce the effective stresses, reducing the shear strength of the material. On the contrary, low porosity clays are dilatant and thus their strength increases with shearing (even temporarily).
4. Such interfaces are relatively flat and continuous, as discontinuities are rather rare. Thus, the potential failure surface at the base of the slope can follow such an interface along great lengths.

When the combination of strength and geometry of a lignite-to-marl interface close to the bottom of the slope gives a low safety factor for stability ($SF = 1.1$ to 1.2), the slope moves by sliding along the critical (and other neighbouring) interfaces. The rate of movement of a slope can range between a few mm/day to a few tens of mm/day and, depending on the conditions (e.g. rainfall), can be steady, accelerating or decelerating with time. In a specific slope, the rate of movement is larger when the safety factor is lower; however, reaching conclusions about the safety factor of a slope from the rates of movements of other slopes is not safe, because the correlation between safety factor and rate of movement depends on other factors which can vary significantly among even similar slopes (e.g. the inclination and strength characteristics of the critical interface).

These movements are usually manifested via “overhanging coal” conditions, where a coal layer close to the bottom of the slope moves more than the underlying sterile (marl), creating an overhanging coal layer (Figure 2). As slope movements evolve, the protrusion of the overhanging coal increases and when the bending capacity of the protruding coal is exceeded, the overhang fails and crumbles to the base of the slope.

The typical mechanism triggering slope instability along a critical lignite-to-marl interface starts with relative movement (sliding) of the interface, caused by elastic rebound of the upper coal (due to the removal of the horizontal confinement by the deep excavation) which creates large shear stresses along the interface. In some cases, such movements are aggravated by a static (i.e., non-seismic) frictional activation (sliding) of neighbouring major sub-vertical tectonic faults marking the edges of the graben, due to the reduction of the normal stresses on the fault by the excavation of the mine.

If the marl below the critical interface has low porosity, the shear stresses cause significant negative excess pore water pressures which temporarily increase the shear strength of the interface and can maintain the stability of the slope in the short-term. Unfortunately, these negative excess pore water pressures tend to dissipate relatively quickly with time, due to cracking of the brittle overlying coal (which increases its mass permeability) and the occasional presence of some high permeability deep sandy horizons, which facilitate access of groundwater to the interface, increasing the pore water pressure back to the ambient hydrostatic value, which gradually reduces the shear strength to a lower long-term (drained) value. In this case, long-term failure of the slope is more critical.



Figure 113. Critical lignite-to-marl interface close to the base of the slope. The coal expands horizontally more than the underlying marl (due to tension cracking) and overhangs the underlying marl. When the overhang exceeds the bending capacity of the lignite cantilever, the coal breaks and falls at the toe of the slope (left part of Figure).

Alternatively, if the marl below the critical interface has high porosity, conditions become more adverse for stability in the short-term, because the shear stresses break the carbonate bonds causing structure collapse (i.e., strong tendency for volume reduction) which reduces the shear strength of the interface in two ways: (1) by eliminating cohesion due to breaking of the bonds, and (2) by developing appreciable positive excess pore water pressures (due to the tendency of the marl to reduce its volume) which reduce the frictional component of shear strength. The combined effect of these two factors is a sharp drop of strength along the critical interface which can cause slope instability in the short-term. Although the positive excess pore water pressures tend to dissipate relatively quickly with time, by drainage through tension cracks of the brittle coal, the loss of cohesion of the marl is never recovered and thus its long-term strength, although higher than the short-term strength, is always much lower than the initial one. In this case, short-term failure of the slope is much more critical, but even long-term conditions are adverse for stability.

It is pointed out that the usual peripheral dewatering of the mines via pumped wells is not effective in improving the stability of the slope because such dewatering is usually limited in the upper higher permeability horizons (sandy sterile strata above the lignite zones) but cannot influence the pore water pressures along the critical coal-to-marl interface since: (1) the depth of dewatering does not reach the depth of the critical interface and (2) even if it did, the average horizontal distance of the peripheral dewatering wells from locations along the critical interface is too large to achieve drainage (over 300-600 m in typical slopes).

Following the above logic, if the shear stresses along the critical lignite-to-clay/marl interface are well below the short- and long-term peak strength of the interface, the slope remains stable, possibly moving with some acceptable velocity (caused by the advancing production fronts), provided that these additional movements do not cause appreciable strength reduction along the critical interface (by creep). On the contrary, if the shear stresses along the critical lignite-to-clay/marl interface exceed or even approach the short- or long-term peak strength of the interface, then continued movement of the slope will reduce the available strength of the interface below the peak value, eventually leading to slope instability in the short- or long-term, depending on the initial

porosity of the critical clay/marl layer (see discussion above). In all cases, the long-term (drained⁴) shear strength at large strains (residual⁵ value) is a safe value of the shear strength to be used in stability analyses of lignite mining slopes.

Laboratory measurements of the drained strength along such interfaces show that, while the peak drained strength can be appreciable (cohesion 15-30 kPa, friction angle 22-26 degrees), the corresponding residual strength is much lower, corresponding to practically zero cohesion (about 5 kPa) and friction angle about 20-24 degrees. Thus, with prolonged movement of the slope, the shear strength along the critical interface can drop, causing instability.

In addition to the geometry of the slope, groundwater conditions and the shear strength along the critical interface at the base of the slope, the inclination of this interface with respect to the horizontal is very important in controlling slope stability. Experience shows that even very mild, but adverse, inclinations of the critical interface (dipping towards the excavation by only a few degrees) can drastically reduce the safety factor of the slope. Such unfavourably sloping interfaces (by 2-6 degrees) are very common in the PPC lignite mines, due to slight tilting of the lignite-bearing deposits by neo-tectonism and the gradual rise of the bedding planes close to the edges of the graben. Most of the observed slope instabilities in PPC lignite mines are associated with such unfavourably sloping interfaces.

3. MONITORING OF MINING SLOPES

Realistic design of slopes in lignite mines has to account in detail the above critical factors: geometry of the slope, groundwater pressures, mechanical characteristics and inclination of the critical interface. Thus, geotechnical investigations are a very important issue of the mine planning process in relation to the sustainability of surface mining projects [6], while geotechnical modelling, with due attention to groundwater conditions, is one of the critical issues related to optimizing mine production and performance [7]. Despite the density and elaboration of ground investigations, most of the above factors are largely unknown, uncertain or variable.

Due to the above, and independently of the elaboration of the engineering design, monitoring the actual response is of paramount importance in ensuring safety of the slopes and adapting excavation speeds during the advancement of the production fronts and after final excavation of the permanent slopes. Thus, continuous slope monitoring is integrated in the PPC surface mining standard procedures. Slope monitoring is usually performed by geodetic measurement of rates of movement in three-dimensions (in mm/day) using a set of reflector targets on the slope and high precision geodetic instruments (total stations) placed in stable positions across the slope. In most cases, 3D coordinates of the targets are recorded and daily movements are calculated by subtraction. In slopes considered stable and having practically constant rates of movement, monitoring is often performed by measuring only the distance of each target from the total station. In critical slopes with large and/or accelerating rates of movement, inclinometers and standpipe piezometers are also installed to determine the geometry of the sliding surface and the corresponding pore water pressure regime.

Experience shows that a wide range of velocities (rates of movement), between a few mm/day and a few tens of mm/day, can occur in stable slopes, with the slope behaving satisfactorily as long as these speeds do not accelerate appreciably with time. Our experience indicates that the absolute velocity of movement in a slope cannot be used as a criterion to distinguish between safety and incipient slope instability. Safety threshold velocities up to about 20-30 mm/day, often used empirically in mining industry, can be irrelevant in many cases; there are examples of mining slopes

⁴ Even in cases where the short-term (undrained) strength is smaller, i.e., in collapsible high porosity marls, experience shows that the short-term (fully undrained) conditions do not control the stability of the whole slope due to relatively rapid drainage via the cracked lignite.

⁵ To account for loss of cohesion and elimination of any tendency for dilation, by prolonged shearing

moving with higher (but relatively constant) velocities over long periods of time without failing catastrophically, while other slopes have failed abruptly when slope velocities as low as 10-15mm/day started to accelerate.

Figure 3 shows the rates of movement (mm/day) measured at several locations of the south slope of the Mavropigi mine (Ptolemais-Amytraion field), in an area very close to the edge of the basin, approaching the final permanent slope. The objective is to exploit all the lignite in the area, reaching up to the end wall of the basin, because the coal has very good quality and includes very little sterile interlayers. As the deposits have good mechanical characteristics and the bedding planes are favourable for stability (their inclination dips away from the mine) the average inclination of the ca. 85m deep mine is about 1:2.5. The end wall of the basin is a schist covered with a tectonically transported mass of crystalline limestone with base inclined unfavourably towards the mine. As the limestone has much higher permeability than the underlying schist, rainwater seeping through the limestone, reaches the limestone-schist interface reducing its shear strength and accelerating the rates of movement of the slope. The high speeds of movement in March and especially in early July 2018 are clearly associated with high rainfall intensities in the area and are reduced a few days after the end of the rains. However, the slope has remained stable, despite rates of movement well exceeding 40 mm/day over several days, and extensive cracking at the crest of the slope.

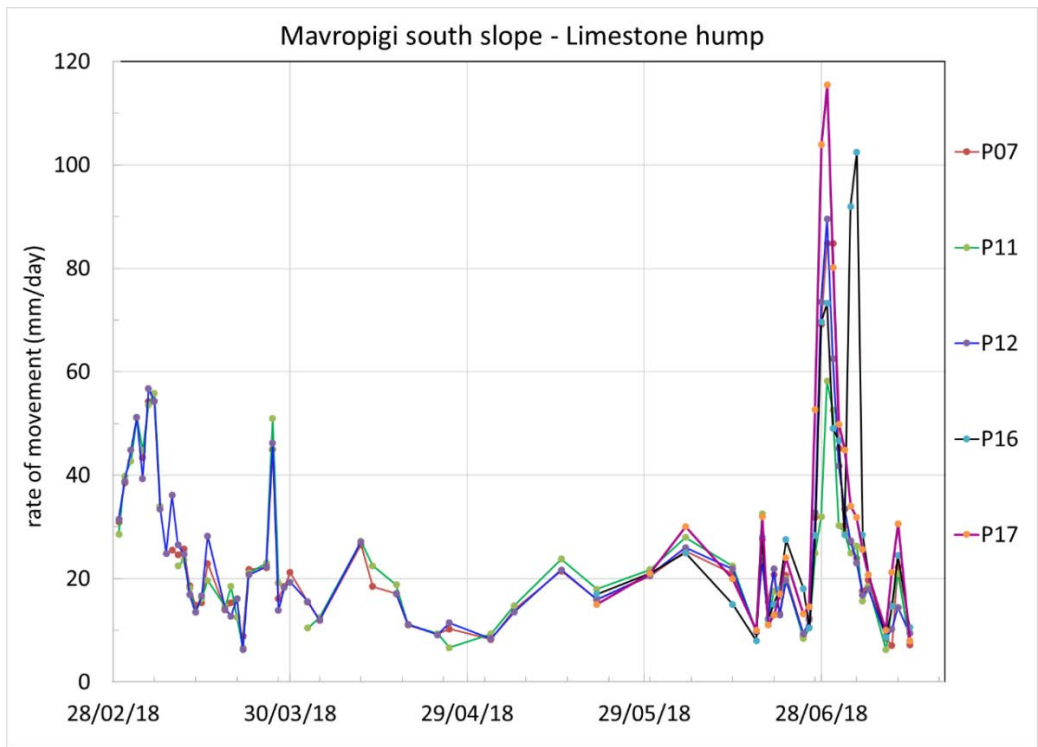


Figure 114. Measured rates of movement at the limestone area of the Mavropigi south slope over a period of five months. The high rates of movement in March and in early July 2018 are associated with high rainfall intensities in the area. The slope remains stable despite rates of movement well exceeding 40 mm/day over several days.

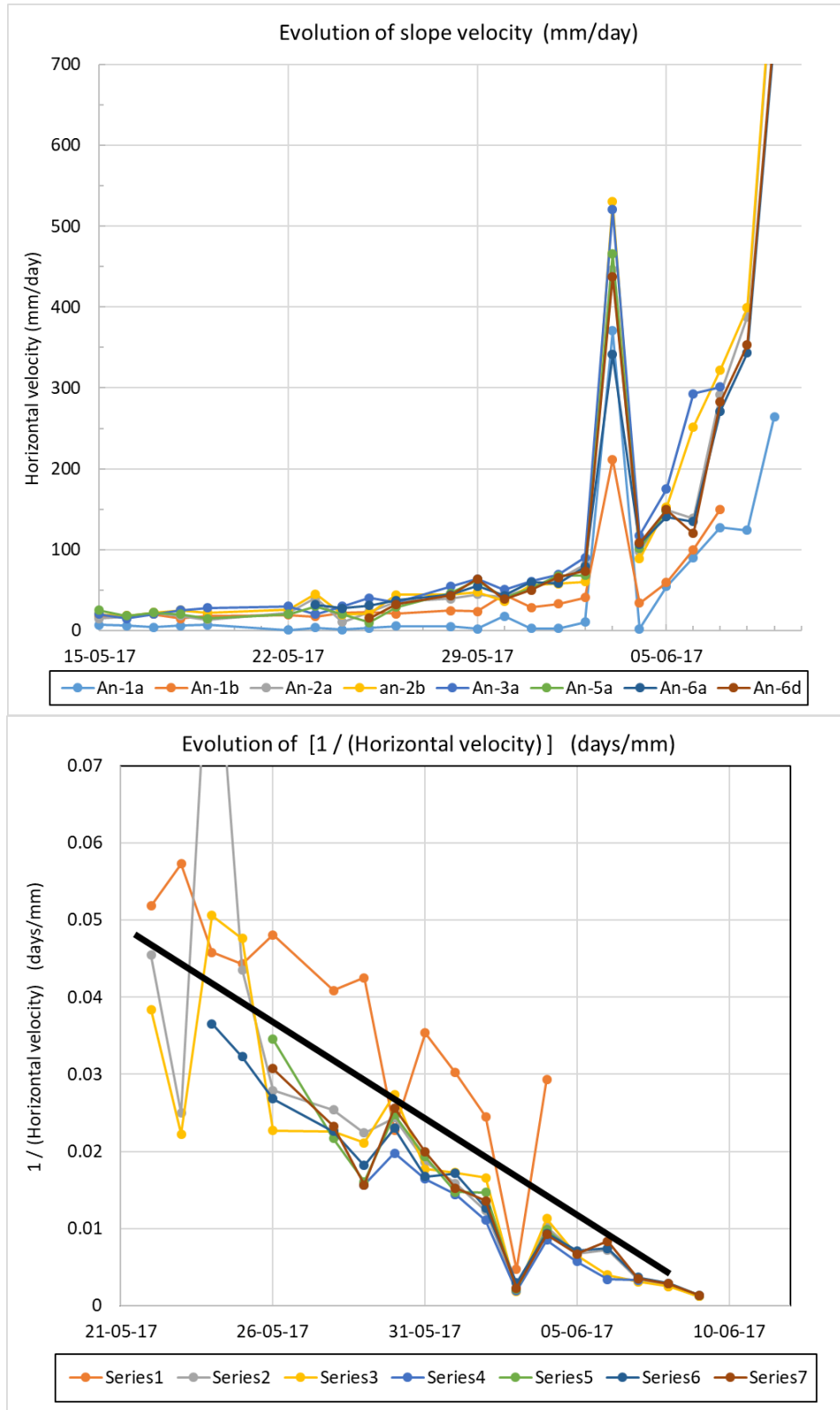


Figure 115. Evolution of the horizontal rate of movement (in mm/day) at characteristic targets on the south-west slope of the Amyntaion mine over a two-month period prior to the great slide of 10/6/2017. Top part: temporal evolution of velocity. Bottom part: temporal evolution of inverse velocity (1/v).

Figure 4 (top part) shows the evolution of the horizontal rate of movement (in mm/day) at characteristic targets on the south-west slope of the Amyntaion mine over a two-month period prior to the great slide of 10/6/2017. The figure shows that until 21/5/2017, slope displacement velocities

were practically constant (20-40 mm/day). After 21/5/2017, velocities started to accelerate and the slide was triggered after 31/5/2017, and especially on 3/6/2017 when heavy rainfall filled the open tension cracks with rainwater. After that date, rates of movement accelerated abruptly with values over 200 mm/day in most targets, reaching 700 mm/day on the day before the catastrophic failure of the slope which occurred on 10/6/2017.

Figure 4 (bottom part) shows the evolution of the inverse displacement velocity (1/v) after 21/5/2017 (1/v data before that date are not shown because they show extreme scatter and are inconclusive). The inverse velocity method for predicting time to failure in slopes was proposed by Fukuzomo [8] and its effectiveness has been proven in many types of slopes, including open pit mines [9]. The dataset shown in the bottom part of Figure 4 confirms that slope failure should occur on 10/6/2017 (see the thick black line, averaging the trends of all targets). However, if one considers only the dataset between 22/5/2017 and 30/5/2017 the trend is not clear, which means that in the present case, the inverse velocity method could provide a definite prediction of time to failure starting from about ten days before failure; after that date, slope velocities increased so much that even the simple velocity – time plot (top part of Figure 4) would provide definite predictions about the upcoming catastrophic slide.

4. ANALYSIS OF STABILITY IN LIGNITE MINING SLOPES

This section investigates the parameters which control the stability of lignite mining slopes. Based on experience, the analysis assumes that failure of such slopes occurs along a sub-horizontal interface between an overlying lignite zone and an underlying stiff plastic clay-marl layer at the base of the slope. Figure 5 shows a typical sliding surface, having a relatively small inclination to the horizontal plane (angle β' , $\tan \beta' = 1/h'$). The sliding surface is assumed to reach the crest of the slope, at distance (S) from the crest, with a planar transition sloping at 30 degrees to the vertical plane. As the length of the sub-horizontal sliding surface is much longer than that of the inclined transition, the assumed geometry of the transition has negligible effect on the calculations.

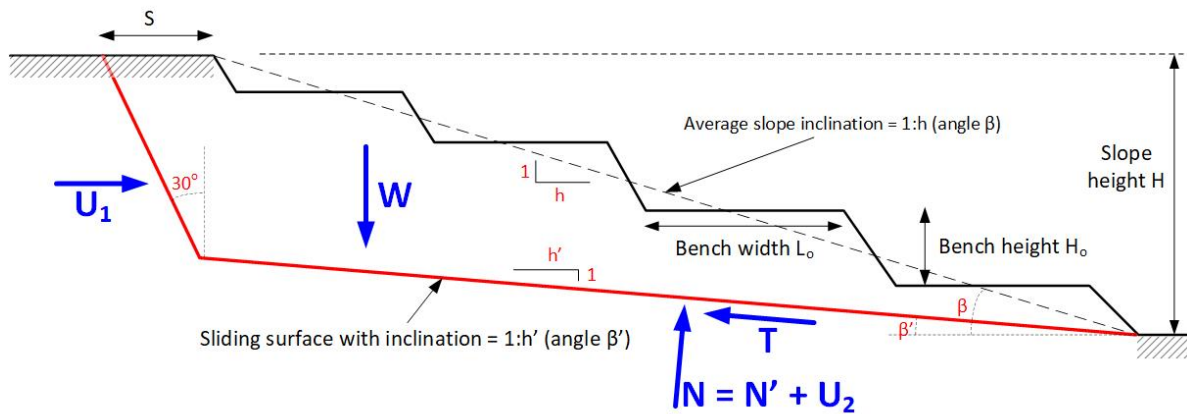


Figure 116. Geometry and forces on a typical sliding mass of a lignite mining slope.

The investigated lignite slope has an overall height (H), average inclination β ($\tan \beta = 1/h$) and consists of a series of benches, each having width (L_o), height (H_o) and individual slope about 45 degrees (controlled by the characteristics of mining equipment). To achieve a specific average inclination ($1:h$) the required bench width (L_o) is equal to:

$$L_o = \frac{h-1}{(H/H_o)-1} H \tag{1}$$

The forces acting on the sliding mass are: The weight (W) of the sliding mass, where γ is the average unit weight of the ground (in the range 15-17 kN/m³) and (S) is the distance from the crest of the slope where the sliding surface emerges:

$$W = \frac{1}{2} \gamma H^2 \left\{ \frac{2S}{H} + h - \frac{1}{h'} \left(h + \frac{S}{H} \right)^2 \right\} \quad (2)$$

The water force (U_1) in the tension crack at the high side of the sliding mass:

$$U_1 = \lambda_1 \left(\frac{1}{2} \gamma_w Y^2 \right), \quad Y = \left(1 - \frac{h}{h'} \right) H - \frac{1}{h'} S \quad (3)$$

where (λ_1) is the fraction of the water force with respect to being completely water-filled ($\lambda_1 = 1$) and completely dry ($\lambda_1 = 0$), and (Y) is the depth of the sliding surface at the kink point (Figure 5).

In Figure 5, (N) is normal force and (T) is the shear force acting at the base of the sliding surface. In effective stress analysis, the normal force (N) has two components: the effective normal force (N') and the water pressure (U_2): $N = N' + U_2$ and:

$$U_2 = \lambda_2 \left(\frac{2}{3} \gamma_w Y L' \right), \quad L' = H \left(h + \frac{S}{H} \right) \sqrt{1 + \left(\frac{1}{h'} \right)^2} \quad (4)$$

where (L') is the length of the base of the sliding surface and (λ_2) is the fraction of the steady-state groundwater force acting at the base of the sliding mass, with respect to steady-state flow in the slope with piezometric surface at ground surface ($\lambda_2 = 1$) and no water pressure ($\lambda_2 = 0$). The steady-state groundwater pressure (p) along the base of the sliding mass is assumed to be parabolic with maximum value ($p = \lambda_2 \gamma_w Y$) at the deepest point and zero at the toe of the slope.

Force equilibrium on the sliding mass gives:

$$N = W \cos \beta' - U_1 \sin \beta' \quad (5)$$

$$T = W \sin \beta' + U_1 \cos \beta' \quad (6)$$

The limiting shearing resistance (T_u) along the base of the sliding mass is the sum of the cohesive and frictional components:

$$T_u = c' L' + (N - U_2) \tan \phi' \quad (7)$$

where (ϕ' , c') are the effective friction angle and effective cohesion along the base of the sliding mass (interface between an overlying lignite zone and an underlying stiff plastic clay-marl layer). Experience with the stiff interface clays/marls of the PPC mines in Greece shows that for peak strength conditions (at small shear strains): $\phi'_p = 22-26$ degrees, $c'_p = 15-30$ kPa, while for residual strength conditions (at large shear strains): $\phi'_r = 20-24$ degrees, $c'_r = 0-5$ kPa.

Using equations (2) to (7), the overall safety factor of the slope is calculated by the formula: $SF = T_u / T$, in terms of the following input: *geometry parameters*: H , S , $1:h$, $1:h'$, *action parameters*: γ , γ_w , λ_1 , λ_2 , *effective strength parameters*: ϕ' , c' .

The above analysis was applied in lignite slopes with the following constant parameters: bench height $H_o = 25$ m, average unit weight of ground $\gamma = 17$ kN/m³, unit weight of water $\gamma_w = 10$ kN/m³, $\lambda_2 = 1$ (steady-state hydraulic flow conditions at the base of the sliding surface), effective ground cohesion $c' = 5$ kPa, effective friction angle $\phi' = 22$ degrees. The following parameters were varied in the analyses: total slope height $H = 50 \div 200$ m, average slope inclination (1:h) in the range $1:4 \div 1:6$, inclination of the base of the sliding surface $\beta' = 0 \div 6$ degrees, and $\lambda_1 = 0 \div 1$ (fraction of the

water force in the tension crack, with respect to complete filling). The results of the analyses are summarised in Figure 6 to Figure 9. These graphs can be used in preliminary assessments of slope stability and in sensitivity analyses to investigate the relative effect of the various parameters on the calculated safety factor of the slope.

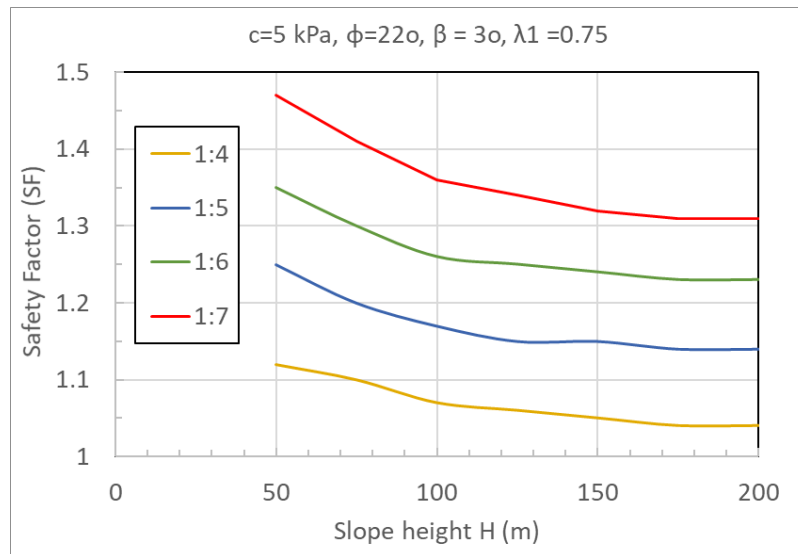


Figure 117. Correlation of the slope safety factor (SF) with the total slope height (H), for four average slope inclinations (1:h = 1:4, 1:5, 1:6, 1:7) and the following values of the remaining parameters: $c' = 5$ kPa, $\phi' = 22$ deg, $\beta = 3$ deg, $\lambda_1 = 0.75$.

Figure 6 plots the correlation of the slope safety factor (SF) with the total slope height (H), for four average slope inclinations (1:h = 1:4, 1:5, 1:6, 1:7) and the following values of the remaining parameters: $c' = 5$ kPa, $\phi' = 22$ deg, $\beta = 3$ deg, $\lambda_1 = 0.75$. The safety factor reduces with increasing slope height by approximately the same magnitude for all investigated slope inclinations (the plotted lines are practically parallel). The effect of reducing the average slope inclination is significant: in a 150m deep mine, the safety factor reduces from 1.32 to 1.05 when the average slope inclination increases from 1:7 to 1:4.

Figure 7 plots the correlation of the slope safety factor (SF) with the inclination (β) of the critical lignite-marl interface at the base of the slope, for four average slope inclinations (1:h = 1:4, 1:5, 1:6, 1:7) and the following values of the remaining parameters: $c' = 5$ kPa, $\phi' = 22$ deg, $H = 150$ m, $\lambda_1 = 0.75$. The safety factor reduces drastically with increasing inclination of the critical lignite-marl interface towards the excavation (unfavourable inclination). Varying the inclination of the critical lignite-marl interface between zero (horizontal surface) and 6 degrees (dip towards the excavation), reduces the safety factor from 2.09 to 1.01 (for slope inclination 1:7) and from 1.47 to 0.82 (for slope inclination 1:4). This effect is very important, much more important than the effect of the average slope inclination (Figure 6), considering that the inclination of the critical lignite-marl interface was varied only slightly (between 0 and 6 degrees) and that this parameter cannot be measured or assessed with accuracy, because the inclination of the base of the sliding surface can vary due to random tilting of the bedding planes and the presence of faulting.

These conclusions are accentuated in Figure 8, which is similar to Figure 7 with the difference that the inclination (β) of the critical lignite-marl interface at the base of the slope is now favourable for stability (dip away from the excavation). The safety factor now increases drastically with increasing inclination of the critical lignite-marl interface. Varying the inclination of the critical lignite-marl interface between zero (horizontal surface) and 4 degrees (dip away from the excavation), increases the safety factor from 2.09 to 5.17 (for slope inclination 1:7) and from 1.47 to 3.13 (for slope inclination 1:4). Based on these results, it is concluded, that the inclination of the

critical lignite-marl interface at the base of the slope (along which the failure surface develops) is the most important, but quite uncertain, parameter in stability analyses of lignite mine slopes. Favourable inclination can drastically improve slope stability, while even the slightest unfavourable inclination decreases the safety factor very significantly.

Figure 9 plots the correlation of the slope safety factor (SF) with the water pressure factor (λ_1) in the tension crack, for four average slope inclinations (1:h = 1:4, 1:5, 1:6, 1:7) and the following values of the remaining parameters: $c' = 5$ kPa, $\phi' = 22$ deg, $H = 150$ m, $\beta = 3$ deg. The lowest value ($\lambda_1 = 0$) corresponds to a dry crack (no water filling of the tension crack) and the largest value ($\lambda_1 = 1$) corresponds to a full crack (full water filling of the tension crack). Although the effect of the (λ_1) factor on the safety factor of the slope is very important, in most practical cases the tension crack is almost filled ($\lambda_1 = 0.65 - 0.90$) and thus the variability of the calculated safety factor is reduced significantly.

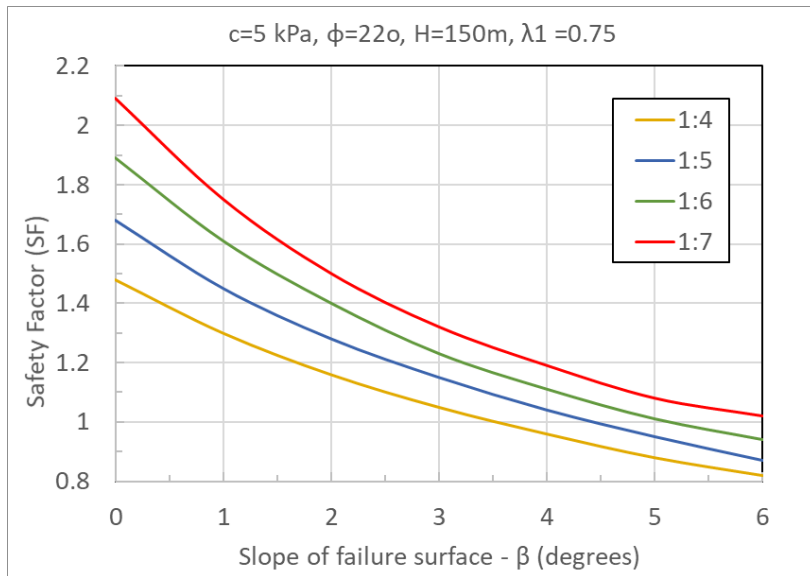


Figure 118. Correlation of the slope safety factor (SF) with the inclination (β) of the critical base interface, for four average slope inclinations (1:h = 1:4, 1:5, 1:6, 1:7) and the following values of the remaining parameters: $c' = 5$ kPa, $\phi' = 22$ deg, $H = 150$ m, $\lambda_1 = 0.75$. The base of the failure surface dips towards the excavation (unfavourably).

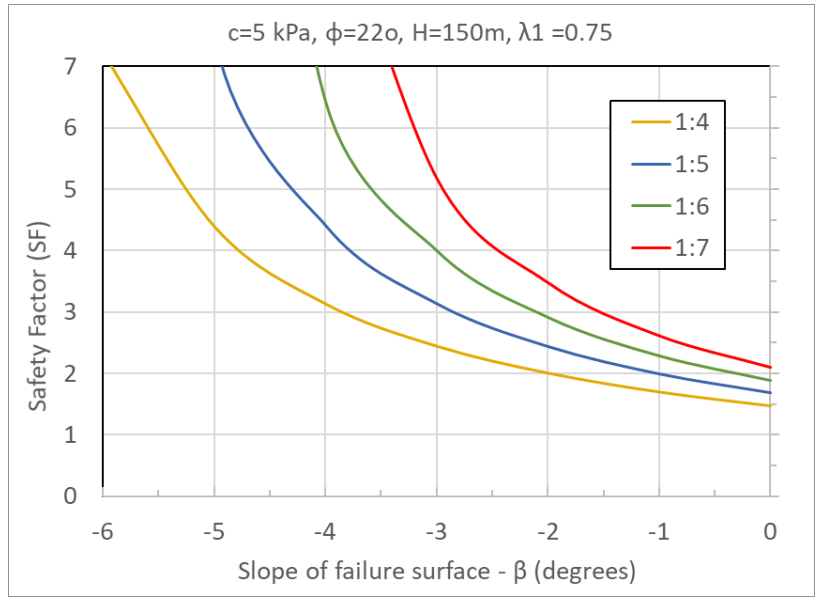


Figure 119. Correlation of the slope safety factor (SF) with the inclination (β) of the critical base interface, for four average slope inclinations (1:h = 1:4, 1:5, 1:6, 1:7) and the following values of the remaining parameters: $c' = 5$ kPa, $\phi' = 22$ deg, $H = 150$ m, $\lambda_1 = 0.75$. The base of the failure surface dips away from the excavation (favourably).

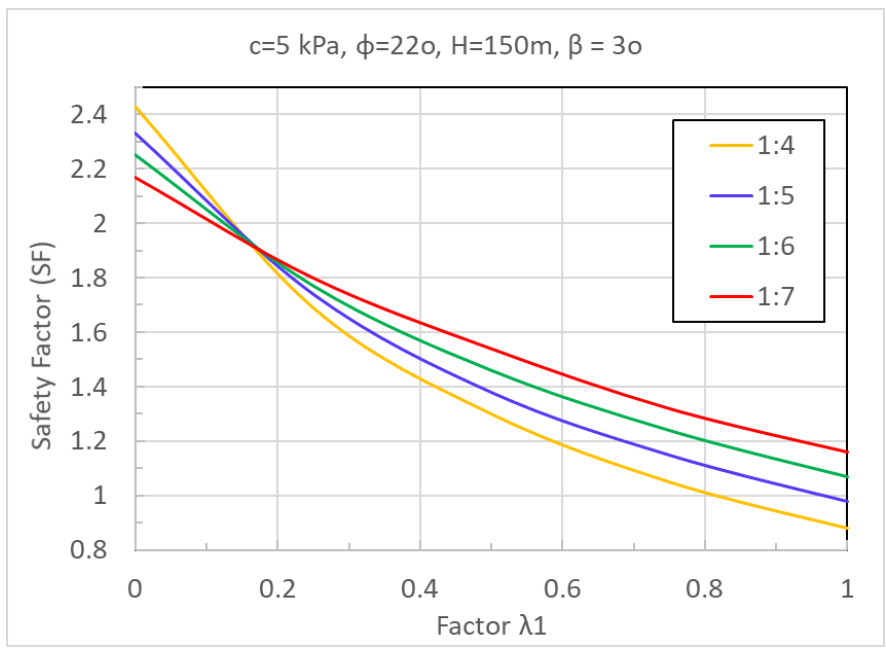


Figure 120. Correlation of the slope safety factor (SF) with the water pressure factor (λ_1) in the tension crack, for four average slope inclinations (1:h = 1:4, 1:5, 1:6, 1:7) and the following values of the remaining parameters: $c' = 5$ kPa, $\phi' = 22$ deg, $H = 150$ m, $\beta = 3$ deg.

5. CONCLUSIONS

Experience with PPC mines shows that slope instabilities are usually associated with sliding along a sub-horizontal lignite-to-clay/marl interface, located either slightly above or (more often) slightly below the base of the slope. The sliding surface usually reaches the ground surface along a near-vertical tension crack at some distance behind the crest of the slope. The sterile interlayers are very stiff to hard due to heavy gravitational consolidation in conjunction with appreciable cementation by carbonate bonding. Medium to high carbonate content steriles (marls) were usually cemented by strong carbonate bonds early in their depositional history, when their porosity was still

large. The high strength of the carbonate cementation bonds has prevented subsequent compaction (consolidation) under additional overburden, maintaining their initial high porosity up to the present day. Thus, typical deep marly steriles have very high porosity and very low unit weight despite their high initial cementation-induced strength which often reaches 1 MPa. In these high-porosity materials, structure tends to collapse with shearing (cementation bonds break); thus, the material loses its cementation strength and, furthermore, tends to contract (reduce its volume), developing significant positive excess pore water pressures under undrained conditions. The positive excess water pressures decrease the effective stresses, decreasing strength (in addition to strength reduction caused by the broken cementation bonds) and occasionally lead to stability failure. The typical mechanism triggering slope instability along a critical lignite-to-marl interface starts with relative movement (sliding) of the interface, caused by elastic rebound of the upper coal (due to the removal of the horizontal confinement by the deep excavation) which creates large shear stresses along the interface. In some cases, such movements are aggravated by a static (i.e., non-seismic) frictional activation (sliding) of neighbouring major sub-vertical tectonic faults marking the edges of the graben, due to the reduction of the normal stresses on the fault by the excavation of the mine.

If the marl below the critical interface has low porosity, the shear stresses cause significant negative excess pore water pressures which temporarily increase the shear strength of the interface and can maintain the stability of the slope in the short-term. Unfortunately, these negative excess pore water pressures tend to dissipate relatively quickly with time, due to cracking of the brittle overlying coal (which increases its mass permeability) and the occasional presence of some high permeability deep sandy horizons, which facilitate access of groundwater to the interface, increasing the pore water pressure back to the ambient hydrostatic value, which gradually reduces the shear strength to a lower long-term (drained) value. In this case, long-term failure of the slope is more critical.

Alternatively, if the marl below the critical interface has high porosity, conditions become more adverse for stability in the short-term, because the shear stresses break the carbonate bonds causing structure collapse (i.e., strong tendency for volume reduction) which reduces the shear strength of the interface in two ways: (1) by eliminating cohesion due to breaking of the bonds, and (2) by developing appreciable positive excess pore water pressures (due to the tendency of the marl to reduce its volume) which reduce the frictional component of shear strength. The combined effect of these two factors is a sharp drop of strength along the critical interface which can cause slope instability in the short-term. Although the positive excess pore water pressures tend to dissipate relatively quickly with time, by drainage through tension cracks of the brittle coal, the loss of cohesion of the marl is never recovered and thus its long-term strength, although higher than the short-term strength, is always much lower than the initial one. In this case, short-term failure of the slope is much more critical, but even long-term conditions are adverse for stability.

In addition to the geometry of the slope, groundwater conditions and the shear strength along the critical interface at the base of the slope, the inclination of this interface with respect to the horizontal is very important in controlling slope stability. Experience shows that even very mild, but adverse, inclinations of the critical interface (dipping towards the excavation by only a few degrees) can drastically reduce the safety factor of the slope. Such unfavourably sloping interfaces (by 2-6 degrees) are very common in the PPC lignite mines, due to slight tilting of the lignite-bearing deposits by neo-tectonism and the gradual rise of the bedding planes close to the edges of the graben. Most of the observed slope instabilities in PPC lignite mines are associated with such unfavourably sloping interfaces.

In order to investigate the relative effect of various parameters on the calculated safety factor of typical lignite mining slopes, a method is developed to analytically calculate the safety factor of a lignite slope in terms of the following input:

1. Geometrical parameters: H (total slope height), S (distance of tension crack from the crest of the slope), $I: h$ (average slope inclination), $I:h'$ (inclination of the critical interface at the base of the slope)
2. Action parameters: γ (average unit weight of the ground), γ_w (unit weight of water), λ_1 (water pressure factor in the tension crack), λ_2 (fraction of the steady-state groundwater force acting on the critical interface at the base of the sliding mass).
3. Effective strength parameters of the critical interface: ϕ' (friction angle), c' (cohesion)

The results of the parametric analyses show that the inclination of the critical lignite-marl interface at the base of the slope (along which the failure surface develops) is the most important, but quite uncertain, parameter in stability analyses of lignite mine slopes. Favourable inclination can drastically improve slope stability, while even the slightest unfavourable inclination decreases the safety factor very significantly.

Slope monitoring is integrated in the PPC surface mining standard procedures to supplement design adapting it to local conditions. Experience shows that a wide range of velocities (rates of movement), between a few mm/day and a few tens of mm/day, can occur in stable slopes, with the slope behaving satisfactorily as long as these speeds do not accelerate appreciably with time. Local experience indicates that the absolute movement velocity in a slope cannot be not used as a criterion to distinguish between safety and incipient slope instability. Safety threshold velocities often used empirically in mining industry, can be irrelevant in many cases; there are examples of mining slopes moving with higher (but relatively constant) velocities over long periods of time without failing catastrophically, while other slopes have failed abruptly when slope velocities as low as 10-15mm/day started to accelerate. The inverse velocity method for predicting time to failure has been proven in open pit mines and is used in PPC mines for the assessment of monitoring data.

REFERENCES

- [1] Roumpos C., Pavloudakis F., Liakoura A., Nalmpanti D., Arampatzis K. (2018). Utilisation of lignite resources within the context of a changing electricity generation mix, 10th Jubilee International Brown Coal Mining Congress" Belchatów ", Belchatów, Poland; 04/2018, 355-365
- [2] Pavlides S. & Moutrakis D. (1987). Extensional tectonics of northwestern Macedonia, Greece, since the late Miocene. *J. Struct. Geol.*, 9, 385-392.
- [3] Anastopoulos G.C. & Koukouzas C.N. (1972). Economic geology of the Southern part of Ptolemais lignite Basin (Macedonia-Greece). *Geol. Geoph. Res.*, XVI (1), 189p (in Greek).
- [4] Steenbrick J. (2001). Orbital signatures in lacustrine sediments. The Late Neogene intramontane Florina-Ptolemais-Servia Basin, Northwestern Greece. *Mededelingen van de Faculteit Aarwetenschappen. Univ. Utrecht*, No 205, 167p.
- [5] Kavvadas M., Agioutantis Z., Schilizzi P. & Steiakakis C. (2013). Stability and movements of open-pit lignite mines in Northern Greece, Proc. 18th International Conference on Soil Mechanics and Geotechnical Engineering (ICSMGE), Paris, France.
- [6] Roumpos C., Papacosta E (2013). Strategic mine planning of surface mining projects incorporating sustainability concepts, *Proceedings, 6th International Conference on Sustainable Development in the Minerals Industry (SDIMI 2013)*, 30 June – 3 July 2013, Milos Island, Greece: 645–651.
- [7] Dimitrakopoulos, R. (Ed.), (2018). *Advances in Applied Strategic Mine Planning*. Springer Nature (800 p).

[8] Fukuzono, T., (1985). A new method for predicting the failure time of a slope. In Proceedings of the Fourth International Conference and Field Workshop on Landslides, Tokyo 1985. Tokyo University Press. pp 145–150.

[9] Carlà, T., Farina, P., Intrieri, E., Botsialas, K., Casagli, N., (2017). On the monitoring and early-warning of brittle slope failures in hard rock masses: Examples from an open-pit mine. *Engineering Geology* 228 (2017) 71-81. DOI: <https://doi.org/10.1016/j.enggeo.2017.08.007>

PPC Excavator Production improvement of 20% by iBelt 2D Radar Control

Matthias Schönhofer¹, Dimitri Kasapidis², Dimitrios Spanidis³ and Emmanuil Dougalis⁴

^{1 2}indurad GmbH, Aachen, Germany

^{3 4} Public Power Corporation, Athens, Greece

ABSTRACT

This paper describes the installation, functions and benefits of the indurad iBelt volumetric conveyor belt measurement solution developed for a Bucket Wheel Excavator at PPC, Greece. The indurad iBelt is a modular conveyor belt control solution based on original indurad radar sensors designed and built for harsh environments. For PPC, iBelt was installed on the E3 excavator boom conveyor belt in the South Field coal mine. iBelt measures the excavated material volume in real time and displays all information in the operators cabin HMI to feed it into the industrial network of the mine. PPC engineers now have the ability to control the productivity of the excavator from a remote engineer station, which has resulted in a 20% increase in average hourly production of the excavator. iBelt is therefore a reliable and highly robust step towards the digitalization of mines and advanced process control.

1. INTRODUCTION

iBelt is the world's first conveyor belt volumetric measurement solution that combines high accuracy and stability of measurement results with highest robustness and zero maintenance. The beginnings of the iBelt project with PPC date back to mid-2015 when indurad was first contacted by PPC Lignite Centre of West Macedonia on behalf of a solution to accurately monitor the volume stream output originally on an excavator in the South Field lignite mine. Previous approaches had all ended unsatisfactorily, and after several meetings it became clear that the specific robustness of indurad radar technology could actually answer the special requirements in the either cold or hot North of Greece around Ptolemaida. Please see below for some impressions of the machine itself:



Figure 1. The PPC South Field lignite BWE (left) and detail shot of the conveyor belt (right)

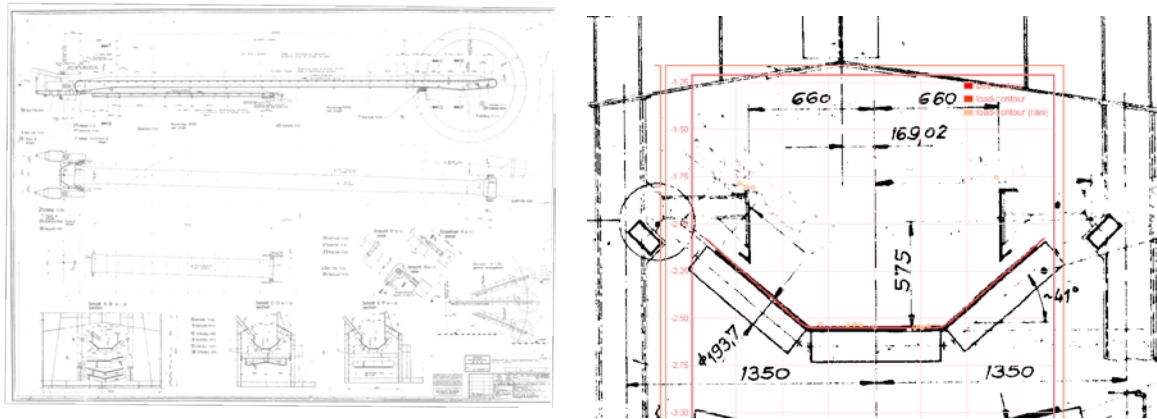


Figure 2. Original plans used during this project, showing the PPC excavator and the belt dimensions

The main challenge in the PPC project was almost a textbook definition of a typical iBelt project: Competing technologies, such as mechanical weighing solutions, are installed in PPC South Field Mine and they suffer in extreme environmental conditions with high dust concentrations, winter rains, low temperatures, fog and dirt everywhere. Bulk material and other dirt particles also easily enter the mechanics of belt scales and make regular maintenance, cleaning and even re-calibration a persistent and cost-intensive requirement [1]. In South Field Mine the mechanical belt scales are installed in a conveyor belt more than 3km away from the excavators, because of the following limitations:

- The scale must be located in the area of lowest tension on the conveyor
- The material to be weighed must settle on the belt before it is weighed
- The conveyor inclination should not exceed the angle at which the material will slide backward and be re-weighed
- If the conveyor has a concave curve, the scale must be located at least 12 metres from the point of tangency, to avoid lifting of the belt

Some of the major shortcomings of belt scales can be seen in the illustration below:

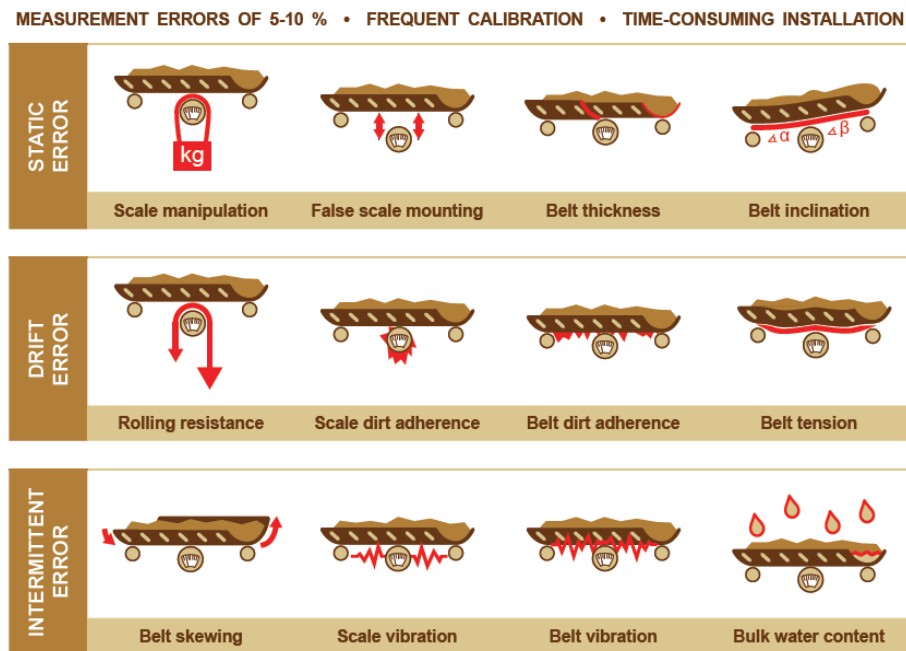


Figure 2. Illustration with major error sources of belt scales

The request of the PPC engineers was the , reliable, real time measurements of the bulk material excavated 24 hours a day, to be visualized in the Operators cabin of the BWE, with minimum maintenance and downtime.

The radar-based iBelt solution, however, was designed and to work specifically under such conditions and has proven the test of time with installations from Chile’s Atacama desert to Russia’s far East near Vladivostok. Thus, temperature range -20 to 40° C in Northern Greece’s weren’t going to be a problem, nor the dust and dirt in the South Field lignite field.

After getting clear on technical potential of the iBelt solution, PPC did the math of the commercial part, approaching it with a long-term perspective and an eye on sustainability: Although the primary investment CAPEX for equipment like belt scales is comparably lower than for iBelt, the accumulating OPEX costs make the total costs of ownership much higher over time. Consequently, the decision for iBelt in the case of PPC was clearly born out of the desire to have stable and reliable conveyor belt volume measurements in a critical process point but without the need to assign special staff to keep the system running. The key to almost every decision for iBelt is long-term process thinking instead of short term investment aspects. Following to that, indurad received the PO in spring of 2016 and immediately began customizing PPC’s own iBelt.

2. IBELT FOR PPC: SOLUTION LAYOUT

Any iBelt starts with our standard layout: one iDRR (indurad DualRangeRadar) sensor is installed above the conveyor belt with a distance of (ideally) 1.5 times the belt width. Typically, one iDVR (indurad DopplerVelocity Radar) is installed in the same mount or casing to measure the material speed to arrive at volumetric measurements. Alternatively, fixed belt speeds can be integrated, in rare cases third-party equipment such as encoders can be used. However, indurad generally recommends using the iDVR sensor for speed measurements to avoid substantial measurement errors by travelling rolls, slippage and other error sources.

Irrespective of the type of conveyor belt, the accurate belt speed is required in order to calculate mass flow over time. iBelt either uses a fixed belt speed parameter, which can be entered via the iWEB interface or input signal by Modbus TCP/IP. Both belt speed (m/s) and cross section (m²) are multiplied for volume flow (m³/s). The volume flow is given in t/hr.

In the case of PPC, the steel beam structure of the BWE’s boom proved to be at an ideal distance for both the iDRR and the iDVR measurements. All plans and mounts were therefore customized to this environment as the ultimate goal was to determine the volume stream on the reclaimer itself. Please see below for some impressions:

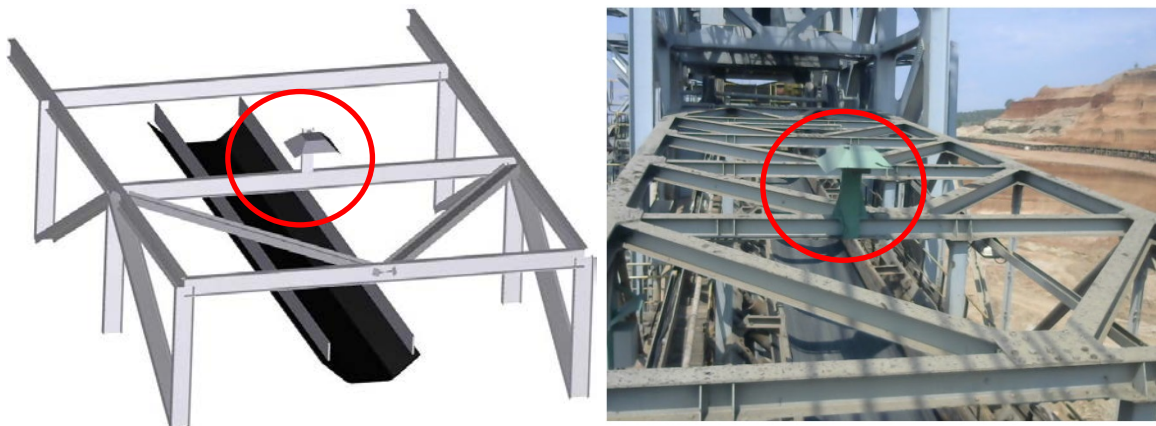


Figure 4. Final installation plans (left) with similar perspective in actual installation (right)

In the PPC project and in any typical iBelt installation, the iDRR is installed with orthogonal orientation towards the conveyor belt, while iDVR speed sensor is ideally installed with an

orientation of in between 30-35° deg to the material stream for optimum material speed measurements. Please see below, iDRR radar measurements in red, iDVR sensor in blue.

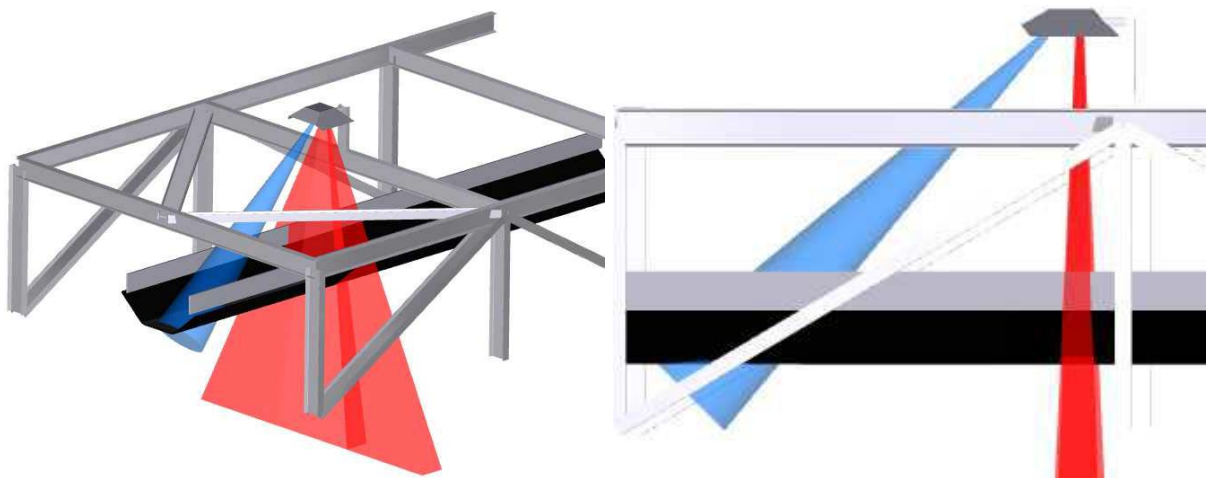


Figure 5. Excerpts from the original PPC iBelt plans 3D visualizations with iDRR (red) and iDVR (blue)



This standardized installation principle has two main advantages: First, the iDRR sensor can be installed on any conveyor belt, irrespective of inclination. Second, the iDVR sensor measures the material speed, not the conveyor belt speed. Slippage-induced errors in the speed measurement are therefore avoided. All plans were based on exact conveyor belt drawings provided by PPC.



Figure 6. Installation of with iDRR and iDVR

3. IBELT FOR PPC: HARDWARE FACTS

A complete iBelt solution installs on any type of conveyor belt (no width restrictions) and contains sensors for volumetric measurements and belt speed measurement. Further sensors for belt misalignment and belt wear measurement are available that were not installed in the PPC context. Please find more information below for the sensors used in the PPC iBelt.

	<p>iDRR iRPU embedded Unit</p> <p>This 7kg embedded unit has a size of 303x132x126 and contains both iDRR and iRPU in one single full metal body casing. IP 66. Also contains a second chamber for cramp connections. Optionally an integrated camera (iCAM), WLAN/3G is available. This sensor has been specifically developed for the mining industry and requires no maintenance.</p>
	<p>indurad Doppler Velocity Radar iDVR-M</p> <p>indurad Doppler Velocity Radar iDVR-M is optimized for belt speed measurement with a speed range between 1m/s and 10m/s. All data is processed and sent via CAN to the iRPU. The iDVR is always the last device in the CAN Bus chain as it is internally terminated. No maintenance required.</p>

4. IBELT FOR PPC – INSTALLATION, COMMISSIONING AND SOFTWARE

The installation work of the iBelt mounts and sensors was entirely conducted by PPC’s South Field Engineers, during the summer months of 2016. At the same time PPC Engineers installed a new HMI visualization with PLC automation on the Bucket Wheel Excavator (BWE). Indurad provided mechanical drawings for mounts. In early September 2016, the commissioning of iBelt could commence, followed by the standard indurad routine of remote commissioning by iRemote connection. This way the indurad Engineer could parameterize the solution based on the customer requirements without causing travel cost and local safety introduction.

The solution was finally installed and commissioned little later on the E3 bucket wheel excavator in November 2016. Production with the system online started almost immediately after the final commissioning and produced reliable and precise measurements from day one on. In early 2017, PPC could issue the letter of final acceptance.

WEB INTERFACE AS SCADA The actual value of iBelt lies in the process data created for PPC. All of these data were made available to PPC via the indurad iWEB HMI (Human Machine Interface) and per PLC integration in the BWE main control cabin. iWEB also allows to monitor the retrospective development of the volume flow to analyze the process over time. This data analysis function contains:

- Dynamical zoom
- Dynamical resolution settings
- Drag & Draw selection of time intervals
- Explicit setting of time interval.

A webserver runs on the radar processing unit, combining setup and maintenance modules with operator interfaces on one platform. Access is as easy as opening a webpage. Usually, cost intensive SCADA integration can be avoided, no additional software installation or maintenance of the same is

required. The iWEB interface visualizes all important process data like current volume flow is and a scalable timeline of volume flow.

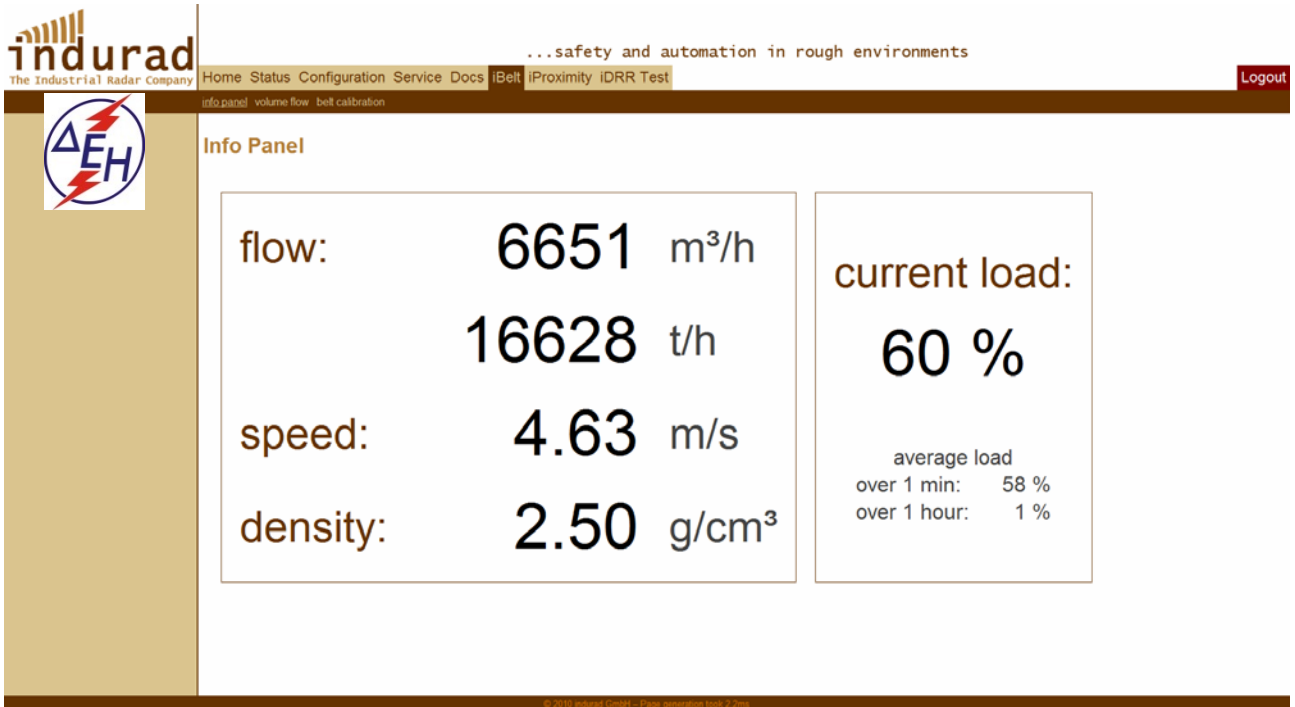


Figure 7. iBelt Volume Flow Overview with iWEB. All relevant production data available at one glance.

Belt Volume Flow

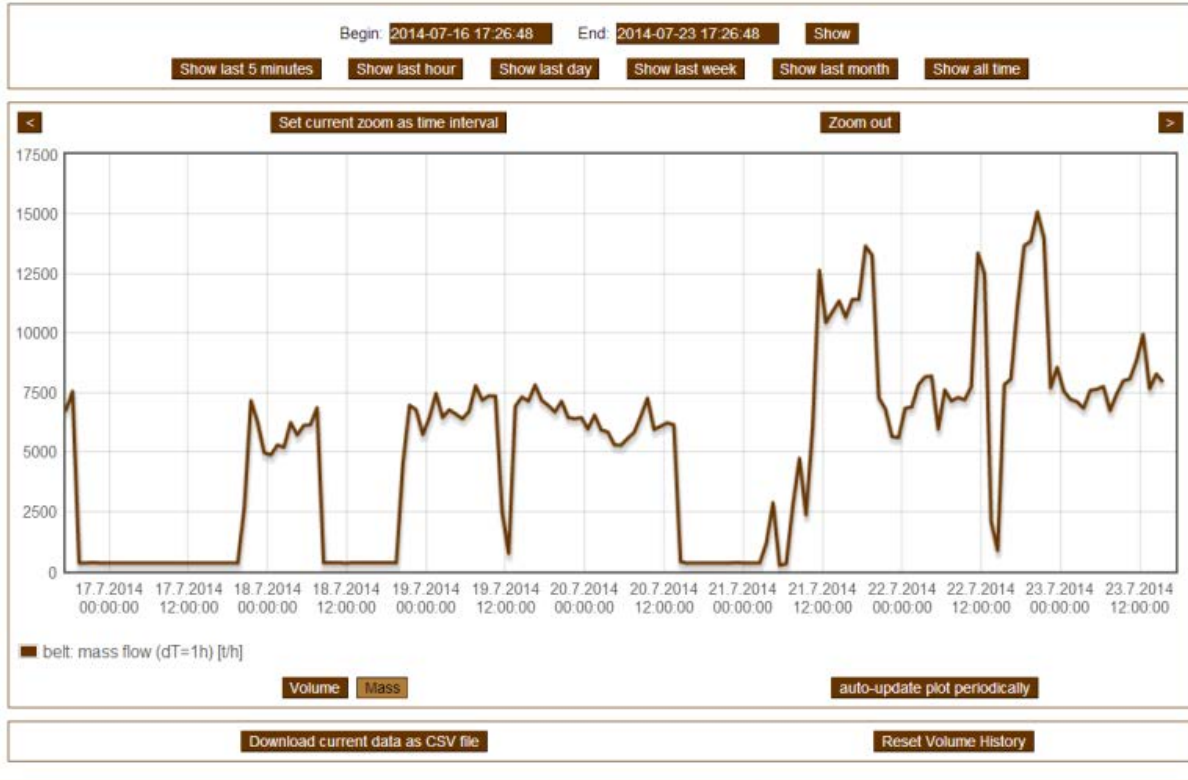
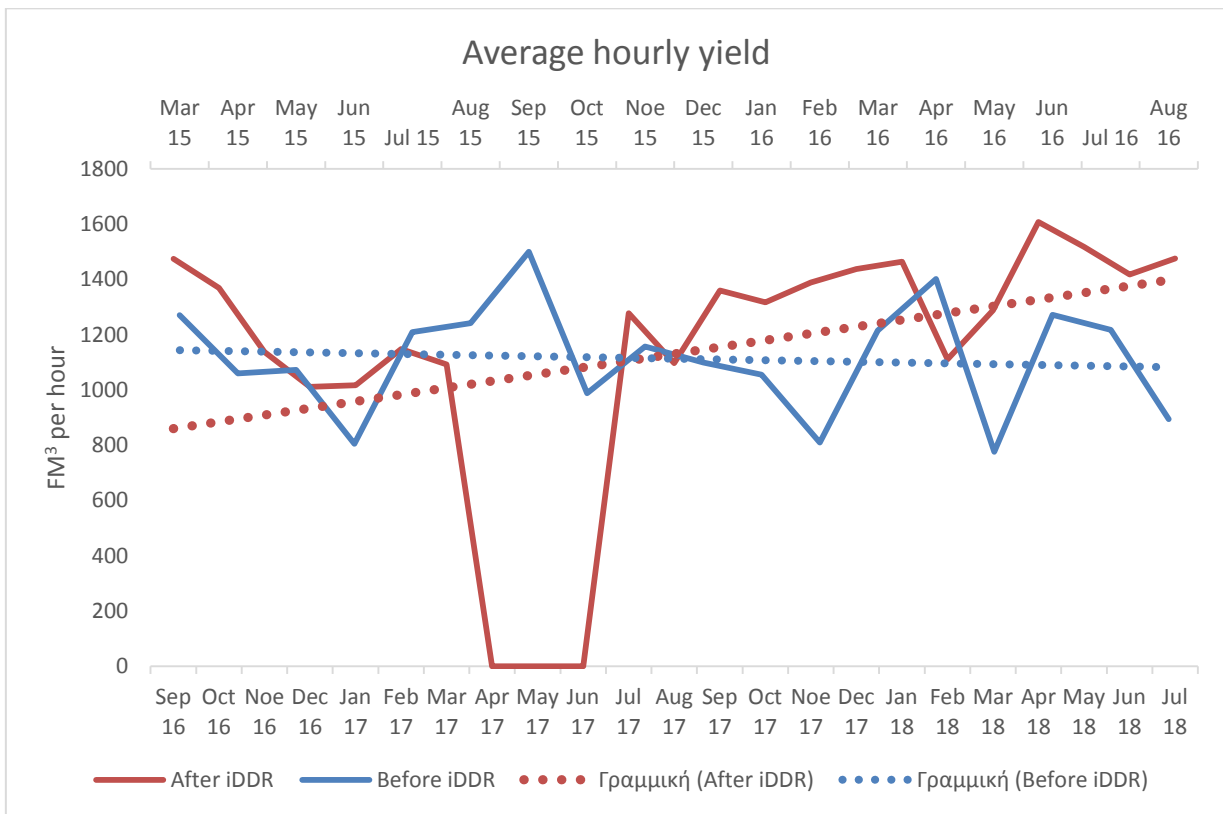


Figure 8. iBelt Volume Flow also allows for defining data period (last month, last day, last minute from... to...) to view production details over time (= x axis)

All PPC production data is stored on the internal memory in differing resolutions, depending on the age of data: The newer the data, the greater the expectable depth of information. All information can be downloaded for further analysis (e.g. with excel or for long term backup) by a simple mouse click. iBelt has contributed to making the local PPC process more efficient by the following results, features and benefits:

- iBelt for PPC helps avoid conveyor belts from running empty, as it reliably detects both belt load and belt movement. Belt running empty can easily be identified, turned off, power can be saved in significant quantities.
- iBelt for PPC does not require frequent re-calibration, saving on money and manpower while still providing reliable information
- With no re-calibration and literally zero maintenance in operation, drives to the installations positions almost equal zero, saving fuel and manpower for other tasks
- iBelt for PPC delivers volumetric data rather than mass data – this allows for planning the consecutive phases of transporting bulk material much more precisely than before and allows to mitigate the negative effects of over- and underfilling in the process chain
- iBelt is a robust industrial grade solution with an extremely long expectable lifetime.



5. CONCLUSION – 10% MORE IN AVERAGE HOURLY PRODUCTION

“The iBelt system is installed on E3Bucket Wheel Excavator boom conveyor belt in South Field coal mine. The material volume excavated is measured and displayed in the operators cabin HMI. Furthermore the iDDR is connected to the Ethernet network of the excavator and so to the industrial

network of the mine. The engineers from a remote engineer station have the ability to control the productivity of the excavator, through the iWEB HMI. The Operator of the BWE knowing the volume of excavated material in Real Time, adjusts the excavators operation to achieve an optimized performance. The result in conjunction with the new HMI automation in the Operators Cabin was a 16% increase in average hourly yield of the excavator. With further optimization and improved utilization of the iBelt system capabilities, the benefits for PPC could be maximized.”

REFERENCES

- [1] Montiea, Bruce (2015). Installation and maintenance of conveyor belts require technical awareness, Mining Weekly (10).

Gearless Drives for Medium Power Belt Conveyors

Ulf Richter

ABB Automation GmbH, Hänchener Str. 14, 03048 Cottbus, Germany

ABSTRACT

Producers who handle ores, rock, coal and the like are heavily dependent on high-capacity conveyor belt systems that are reliable, efficient and very robust. The hourly cost of a conveyor breakdown can be substantial, so uptime is a parameter of primary importance. ABB has long supplied conveyor systems that meet the stringent demands of producers in a wide range of industries (Fig. 1).

ABB's new permanent magnet (PM) motors for medium-power gearless conveyor drives (GCD) reduce production costs and increase competitiveness. A PM motor, combined with gearless technology, also fulfills eco-design requirements, saves energy, reduces failure rates and lowers maintenance overheads.

GEARBOXES

ABB classifies conveyor systems by power band (Fig. 2). Low-power belts are found in almost every material-handling plant; medium-power belts are used extensively for shifting rock and coal; and high-power belts are for more dense commodities, like copper or iron ore that are transported over long distances or steep ascents.



Figure 1. Typical conveyor drive with gearbox.

In the high-power regime, conventional conveyor drives face challenges, mostly associated with the gearbox. Building a gearbox that can handle powers above 3.5 MW is a non-trivial task and even when built they are maintenance-intensive when in operation. Further, their lifetime is relatively short. Other challenges are posed by the vast array of drive constructions - ranging from mobile

units, where motors are housed within the drive station’s steel enclosure, to stationary structures where the motor is foot-mounted on concrete foundations.

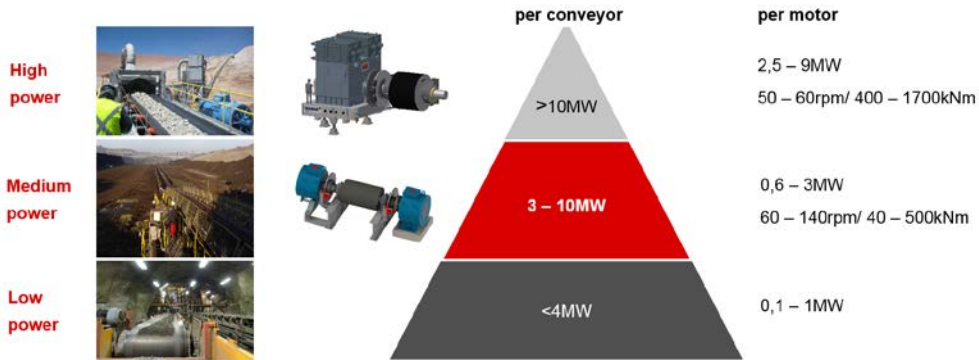


Figure 2. Conveyor classification according to installed power.

Such problems can be avoided by using a gearless drive. A GCD uses a low-speed synchronous electric motor mounted on a pulley shaft that is designed to handle the high torque produced by such motors. The motor is controlled by a variable-speed drive (VSD) to produce a shaft rotational speed of typically 50 to 90 rpm. There are usually several drive modules in a drive station and there can be multiple drive stations on the conveyor. The power of existing GCDs goes from around 2.5 to 6 MW, with a total connected power in the range of 5 to 20 MW.

A GCD is of lean construction and, because it has relatively few parts, it is long-lasting and maintenance-light.

A GCD is of lean construction and, because it has relatively few parts, it is long-lasting and maintenance-light. Indeed, drives delivered to the Prosper Haniel coal conveyor in Germany in 1985 are still running today. GCDs are also attractive from an energy-saving point of view: The gain of 6 to 8 percent they bring to the efficiency of medium-power systems represents significant cumulative savings in electrical costs over the lifetime of the installation (Fig. 3).

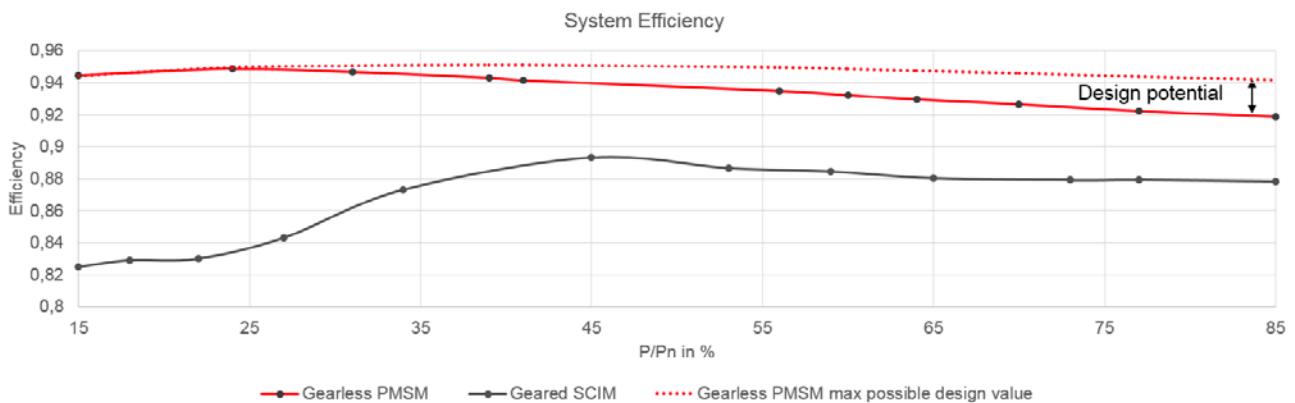


Figure 3. 200 kW direct-drive (Gearless PMSM) and geared drive (Geared SCIM) efficiency comparison, including converter, motor, transformer and gearbox losses.

However, a major disadvantage of current GCD technology is that its capital cost is high, which makes it competitive with conventional designs only in the higher power bracket and where a

long operating life is foreseen. As well as cost considerations, if GCDs are to be commercially feasible in the medium-power segment, lower weight, more efficient cooling and a more compact size are required. In other words, a new approach is needed if customers with medium-power applications are to benefit from GCDs.

ABB has used its long experience to develop a series of PM motors specifically for ABB GCD for medium power.

New GCDs using low- or medium-voltage permanent magnet motors

Permanent magnet motors have been around for decades – in ship propulsion, pumps, fans, blowers, wind power generators, automotive, etc. Now ABB has used its long experience in this field to develop a series of PM motors specifically for ABB GCD.

With a torque range of up to 500 kNm, these new ABB GCDs are ideal for a large number of applications – both newbuild and retrofit – and their costs are comparable with equivalent conventional geared systems.

This pioneering GCD concept is lightweight, compact and can be air or liquid cooled. The motors can be foot-mounted or shaft-mounted, whereby the latter is quicker to install, easier to align and requires less concrete foundation work (Fig. 4). The heavy-duty design is robust enough to deal with the shocks and vibrations associated with handling cement, rock, coal and other common mined materials. An IP66 rating means the motor is completely protected from dust and water contamination. An added benefit is that the GCD has lower operational noise levels.



Figure 4. Foot-mounted (right) and shaft-mounted (left). The motor mounted to and suspended by the pulley shaft has favourable characteristics, such as quick installation or swap-out. However, the foot-mounted version is the easiest to design and dimension, especially as the motor weight has no influence on the dimensioning of the pulley shaft. The choice depends on customer preference.

A GCD has significant operational advantages over geared equivalents:

- Fewer components, so it has a higher reliability (about 50 percent lower failure rate) and less maintenance is required
- Higher energy efficiency with lower energy consumption (up to 8% saving)
- Lower noise emission
- Operational cost savings (OPEX)
- No monitoring and testing of gearboxes
- No oil (reduced fire risk)

- Extended life cycle (expected motor lifetime of 25 years is 10 years longer than with the gearbox-equipped equivalent)

Gearless drives are especially beneficial in installations where:

- The planned life cycle is longer than 10 years
- Gearboxes are a source of trouble
- High availability is required, or no redundant production lines exist
- Material buffers are small or non-existent
- Maintenance work is hard to perform (high altitude, high or low temperatures)
- Maintenance personnel is difficult or expensive to source
- Ambient conditions are harsh

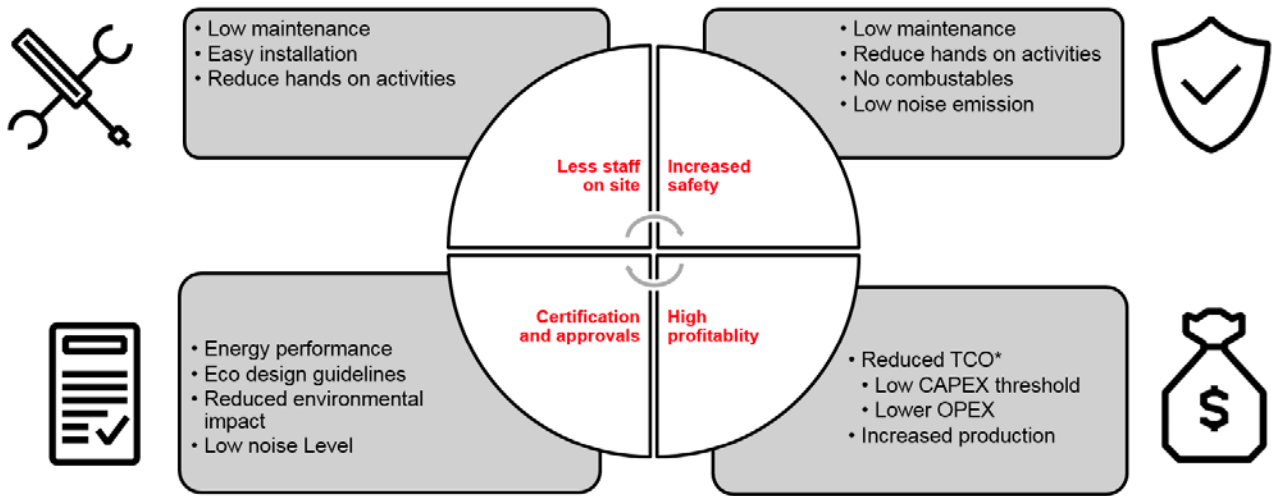


Figure 5. GCD: Customer Values

GCD cost/benefit analysis - a practical example

The following example demonstrates how the new GCD can reduce operational costs for a mining conveyor system. It is based on the following conveyor system design:

- Conveyor line: 10 flights
- Drives: 40 in total
- Power: 1,350 kW
- Tonnage: 12,000 t/hr
- Energy cost: \$60/MWh
- Annual operation time: 6,348 hours

The results are presented in Fig. 6 which shows the cumulative cost savings (including investment) of a conveyor system equipped with the GCD compared to the same system with geared drives.

The considered cost factors are energy (electricity), system maintenance, repair, loss of production and overhaul. Overhaul considers the cost for replacing gearboxes reaching the end of their life after 15 years. The five pillars show the saved cost for each time frame. It is obvious that savings in electricity and overhaul are most significant for this example. After 15 years, a mine would have saved about \$25 million by using the GCD for medium power.

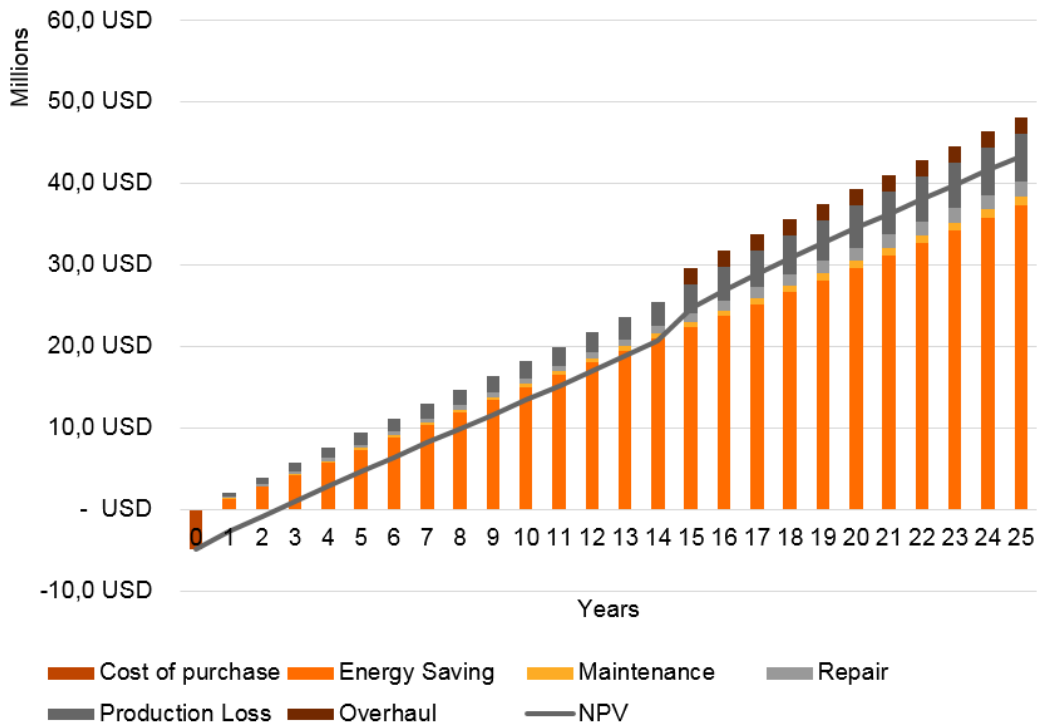


Figure 6. Cumulative cost savings of GCD versus geared WRIM drives for a mining conveyor system. Conveyor length: 40 drives of 1,300 kW, 80 rpm; no buffer capacity.

Pilot project: retrofit of a 200 kW conveyor drive

In July 2017, after one year of planning, ABB started a pilot project with the title “gearless conveyor drive with PM motor” in an open-pit lignite mine close to Cottbus in Germany.

The new medium-power gearless drive runs in parallel to the existing geared drive on the 2.5 m wide discharge belt of a bucket chain excavator, located at the end of the discharge boom. The belt has a capacity of 15,400 tons/hour and moves sand - with inclusions of large rocks (ice-age foundlings) that give rise to mechanical shock and vibration. The ambient temperatures faced by the equipment are extreme: -25 to +40 °C.

The GCD package consists of a PM motor, frequency converter and a transformer (Figs 7-8). Both drives, geared and gearless, are connected to the same pulley shaft. This setup allows exact benchmarking.



Figure 7. The GCD package at the pilot project

The GCD package consists of a PM motor, frequency converter and a transformer.

The two drives are sized according to customer specifications and allow 100 percent production with each drive independently. The time taken for dismantling, installing and commissioning was only two weeks.



Figure 8. Pilot gearless drive.

The pilot project has established the feasibility of installing gearless conveyor drives on mobile mining machines and shows the suitability of PM torque motors to drive conveyors. The GCD so far has performed very well under the challenging conditions.

GCD delivers an efficient, long-lasting and reliable solution that helps operators to increase production and annual revenue, and decrease costs.

The potential for energy savings, reduction of failure rate and maintenance, etc. have also been demonstrated. Also, the pilot project proves that it is possible to install gearless drives as an alternative to conventional geared drives and at the same time fulfill eco-design requirements according to ISO 50001 (energy efficiency) so that the environmental certifications held by mining companies is maintained.

Conclusion

GCDs based on PM motor technology deliver an efficient, long-lasting and reliable solution that helps mining and other industries to increase production and annual revenue, and decrease costs. GCD drastically reduces the effort for maintenance, repair and asset management. While the upfront investment is typically higher when compared to a conventional drive (for a 1.5 MW GCD, the investment for the drive is about 10 to 30 percent higher; the combined cost of the mechanical and electrical equipment of the whole conveyor will be less than 5 percent higher), the savings in maintenance, energy cost and downtime lead quickly to a return on investment of typically less than one or two years. When analyzing the total cost model for a GCD acquisition, it should be borne in mind that the conveyor system usually occupies a critical path in the mining or production facility - should the conveyor malfunction, the work rates of excavators, crushers and other processing equipment will be adversely affected too.

The introduction of a GCD for medium-power conveyor drives based on a PM synchronous motor offers exciting possibilities for mining applications. This new concept allows implementation of a gearless motor into an existing or new medium-power conveyor – an exercise that has been practically difficult and technically infeasible using conventional synchronous motors up to this point.

Mining 4.0 - Our Digital Journey

Thomas Neumann

ContiTech Transportbandsysteme GmbH, Breslauer Straße 14, 37154 Northeim

ABSTRACT

Up to 60% of OPEX result in the transportation cost within a mine.[1] There is a trend to use continuous conveying technology as a cost-effective transport method. Increased application of long as well as steep incline systems can be observed in the markets. The demand for a predictive maintenance is rising. Therefore, solutions for a stationary as well as mobile monitoring of conveyor belts is necessary. Data management and analysis are important conditions on the journey for an innovative service provision. Cloud technology represents an interface for data exchange. Digitalization is the basis for new business models.

1. INTRODUCTION

Transportation cost represent the largest cost factor in the operation of a surface mine and also for underground mine. Therefore, taken measures for cost reduction in this area have a great impact.

So far, innovations in continuous material handling provided technologies which had limited possibilities for mining. Vertical conveyors offer new options - 1500 tons of ore can be conveyed from 1000 m depth. Moreover, MegaPipes can convey up to 10.000 m³ of hard rock per hour parallel to the mine slope. Belt strengths up to 10.000 N/mm open the option for long and high inclined conveyor systems at the same time.

In addition, potential customer can expect an intensive monitoring of operating parameters, a high system availability as well as an effective service provision. Hence, in this area our offers meet the market participants' challenges and herewith form the vision of Mining 4.0.

2. CONTINUOUS CONVEYING TECHNOLOGY IS THE MOST EFFECTIVE TRANSPORT METHOD

For transporting large volume flows continuous conveying technology is the most effective method. This statement is not new. Previous constraints regarding incline and conveying height became less due to innovations in these fields. As a result, application possibilities in continuous conveying technology underwent an expansion.

Basis of the current service offer of ContiTech in the field of conveyor belts are mobile and permanently installed monitoring systems. These systems monitor the condition of the conveyor belts and result in an excellent precondition for an effective predictive system maintenance. Visualized protocols include the status description of the conveyor belt and recommendation for action in an easy understandable way for system operator and service partner.

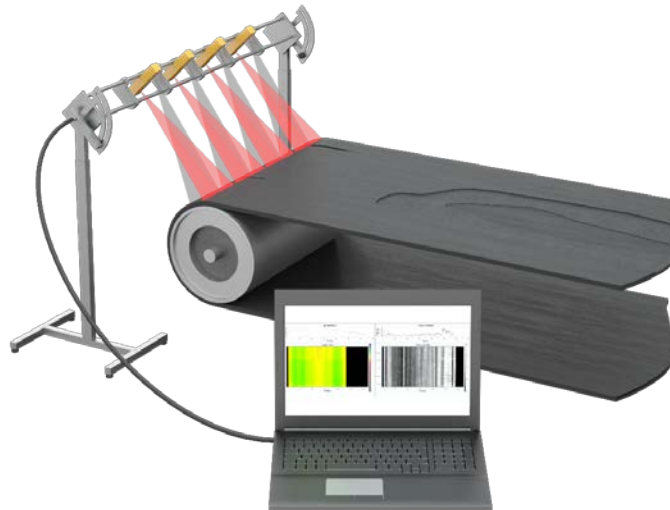


Figure 121. Surface Scanner for monitoring belt usage and surface.

3. CONTI+ - DATA MANAGEMENT AND EFFECTIVE INSTRUMENT FOR MONITORING CONVEYOR BELT CONDITIONS

This software tool is in use already for many hundred times and facilitates monitoring of conveyor belts and conveyor systems. Besides storage of essential systems parameters, pictures, movies, and protocols, this tool determines the dynamic remaining term of conveyor belts. All information and data are provided in a transparent way as well as online on various possible devices. As a result, responsible persons from small to large enterprises utilize this tool for their decision making processes which are herewith based on a realistic fundament. Interesting new possibilities for an effective management of conveyor systems are enabled.



Figure 2. User Interface of CONTI+ - App.

4. MINING 4.0 – OUR DIGITAL JOURNEY

In the centre of vision Mining 4.0 are methods for efficient cost improvements and reduction of unexpected downtime. We are aware that new business model can only be realized if the effects convince the customer and a quantifiable added value arises.

With a fundament of high quality conveyor belts and automated monitoring of relevant parameter ContiTech is currently developing new service concepts. Therefore, products are cross-linked via CONTINETAL.cloud with available information. Customer-specific as well as system-specific evaluations will further contribute to optimize service packages. To point out, key is and will be the value added for our customer.

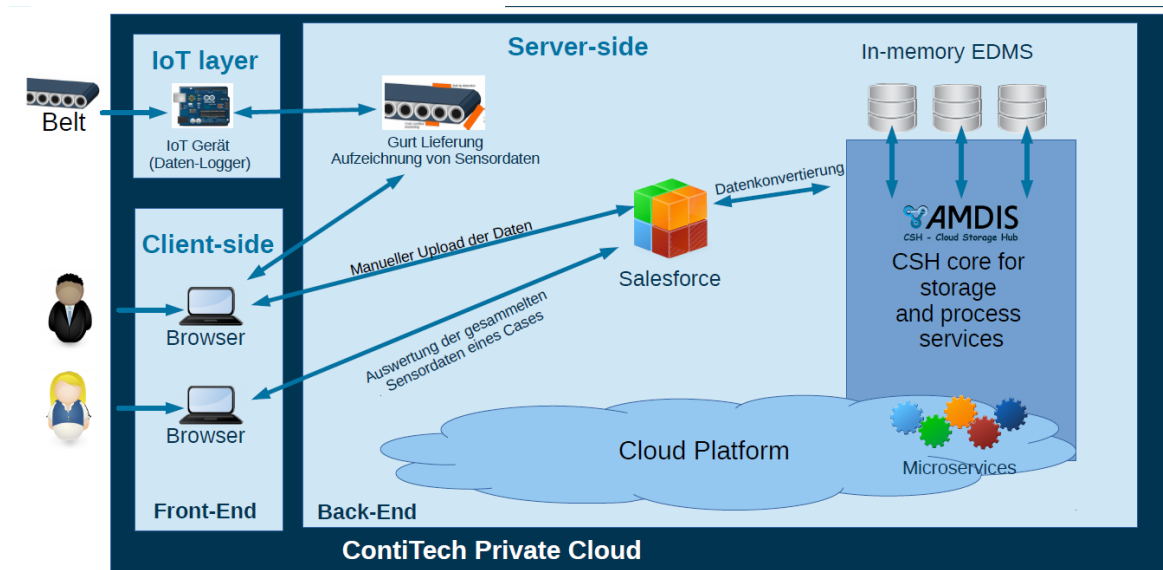


Figure 3. Online data management of conveyor belts.

5. CONCLUSION

Continuous conveyor technologies are the most efficient transport method for large flow volumes. Innovations in conveyor belt technologies significantly expand fields of applications.

Reliable monitoring systems as well as consequent utilization of digital technologies open up completely new business models. As a result, long-term as well as transparent cost overview and minimal ownership costs are ensured plus unexpected downtime is avoided.

REFERENCES

[1] Prof. Dr.-Ing. H. Goergen: Festgesteinstagebau; Trans Tech Publ., 1987.

Session 5: Health & Safety, Environment

Control of Social and Environmental Risks During Opencast Lignite Mining

Natalija Pavlovic¹, Dragan Ignjatovic² and Vladimir Pavlovic¹

¹Opencast Mining Centre, K. Marije 25, Belgrade, Serbia

²Faculty of Mining and Geology, University of Belgrade, Djusina 7, Belgrade, Serbia

ABSTRACT

The opening and development of large opencast lignite mines with complex continuous mining systems is subject to a large number of environmental and social risks. The impact of the mines is constantly increasing, therefore monitoring and adjusting to changes are becoming a priority for the managers of mining companies.

The process of controlling social and environmental risks, which could temporarily or completely stop lignite mining production on opencast mines, is based on the analysis and determination of the probability of occurrence, the operation reliability of the opencast mine, the necessary safety reserves of lignite and the required costs for minimizing the impact of the risk to a minimum.

Social risks are related to sustainable development, harmonization with the local community and government legislation. Environmental risks can be controlled, when it comes to sustainable mining, and partially uncontrolled, in relation to natural disasters. Together they represent a serial stochastic process with probabilities which define the reliability of the opencast mine production as a whole.

The set methodological approach allows for practical interactive control of the social and environmental risks during opencast lignite mining in real space and time, and is the basis for optimizing the process of sustainable mining.

1. INTRODUCTION

The reliability of an opencast mine as a business system implies adapting and complying with real risks. Given that there is no *zero risk*, it is necessary to conduct good quality identification, analysis and valorization of risks in all areas of business, and then identify measures to reduce risk or bring risk to an acceptable state.

Modern business systems, such as opencast mines, are conditioned and accompanied by a very wide range of potential hazards and threats, which very often and completely negatively affect the company's business and performance. There is a variety of external factors (social changes, uncertain economic situations, inadequate and heavily burdensome legislations, narrow selection of competent workforce etc.) which often can't be influenced. Also, numerous internal threats for the business system safety could arise from the business domain (in terms of organization and business processes), and domains of and sociological influences and ecology.

Opencast mines have a considerable number of environmental and social aspects (Figure 1) with high risk intensities during their whole lifespan, starting with the sensitive process of transforming resources into coal reserves, the process of obtaining permits for mining, to the process of development and closure (Figure 2) [4]. The impact of these aspects is constantly increasing, so tracking and alignment with changes is almost a priority for managers of mining companies. Especially when it comes to the increasingly complex risks, which are related to the need for obtaining a series of approvals related to the environment and the local community, urban planning, displacement, water, landfills and hazardous waste disposal, emissions, as well as the development

of the community and employment. Other natural unpredictable risk factors, such as earthquakes, floods and large landslides, which threaten infrastructure facilities and mining equipment, as well as increased risks associated with inevitable global climate change, should be added to this.



Figure 1. Business, environmental and sociological aspects with high intensity of internal risks for the sustainable operation of the opencast mine

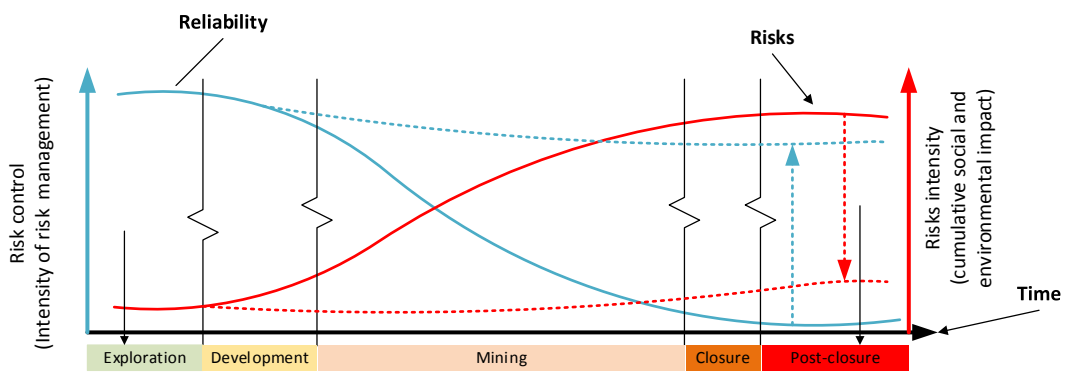


Figure 2. Changes in reliability and risk in the life cycle of an opencast mine

Since mining companies work in conditions of uncertainty and turbulent environments, whether it's business, technological or natural uncertainty, it is essential that they continuously and proactively affect the internal and external risks to which they are exposed. This is especially important considering the long lifespan of large opencast lignite mines which consists of discrete stochastic activities (Figure 1) and relatively frequent changes in the environment, especially when it comes to uncontrolled natural disasters. In all phases of making the Environmental and Social Impact Assessment (ESIA), it's almost impossible to predict a range of social and environmental risks in the most important and longest part of the mining process, related to opencast mine development.

This approach to dealing with uncertainty of operations is a controlled risk management process aimed at sustainable opencast mining, which implies harmonization of economic growth and development with the interest of environmental protection and social development. In this way, economic sustainability represents a necessary, but not sufficient, requirement for realization. The approach, i.e. the methodological framework for risk management, is also very important when it comes to opencast mining. In accordance with the classic definition, risk is defined as the product of the probability of occurrence and the consequences of risks. In this sense, the risk of system failure is the product of failure probability and costs incurred after it. However, such an approach does not show the risks of losses that exceed the acceptable limit. In this regard, the approach to the analysis of social and environmental risks based on the principle of potential losses was developed, which includes determining the probability and time of failure. These risks are presented in a serial link of elements whose individual reliability should minimize total capital and operating costs and losses due to failure, among other things, through the net present value cash-flow model. In this way, the complex management of social and environmental risks is objectified.

2. ANALYSIS OF SOCIAL AND ENVIRONMENTAL RISKS ON LIGNITE OPENCAST MINES

As a rule, all phases of the opencast mine life cycle seen as a discrete random process are followed by a large number of geological, technological, technical, economic, ecological (environmental), social and financial risks. It is not possible to precisely and with certainty determine the importance any of the mentioned risks might have on the realization of lignite mining and what might be the realization reliability of particular activities (Figure 1). The management of risks on opencast mines is especially important considering that the overall risks and losses in mining are due to failure and simultaneous unknowns that determine the stability and costs of lignite production.

Opencast mining and a significant part of the necessary accompanying activities bear a number of direct, indirect, permanent and temporary complex spatial changes and certain adverse environmental impacts, which from the aspect of the impact analysis and controlled risks as a whole make it an extremely complex problem (Table 1). Negative impacts of opencast mining, which can be controlled in the short and long term, most often appear as:

- spatial (change of the terrain morphology, destruction of the land, resettlement and displacement of settlements, relocation of infrastructure, construction of specific infrastructure, construction of specific communications),
- technical-technological (landslides, ground subsidence due to drainage, noise and vibrations),
- physical-chemical (physical destruction, water pollution, air pollution, chemical oxidation, biological activity, microclimate changes, seismic influences).

Negative spatial environmental effects are characteristic, with lower and higher intensity, in almost all stages of opencast mining, from exploration and preparatory work, the period of mine opening, the period of full production, to the period of closure and post closure. The technical-technological and physical-chemical effects of opencast mining are intensive during the period of preparatory work, opening, achieving full production and closure of the opencast mine.

On the other hand, uncontrolled environmental impacts also have a major impact on the operation of opencast mines, and cause serious crisis situations that need to be defined in more detail. These are, above all, natural disasters, most of which are getting more frequent due to climate change. The emergence of a crisis situation in relation to an opencast mine can be due to very different causes, such as earthquakes, landslides, floods, infrastructure destruction, social unrest and even epidemic diseases.

Special attention is increasingly required for social and environmental risks in relation to costs (Figure 2). Risks can be divided into controlled risks, which are predictable and could have short-term planned control in the opencast mine area, and uncontrolled risks, which are related to external influences whose occurrence cannot be predicted short term and as a rule relate to the contour of the mine. Uncontrolled risks, which are particularly related to ecological hazards, may have catastrophic consequences on mining and lead to a prolonged temporary suspension of work, as well as the complete closure of the opencast mine with great losses. From a sociological point of view, uncontrolled risks most often relate to the intermingling of settlements and expropriation in the function of mining.

Proper crisis management is usually addressed in three phases: the preparation of a tactic if a crisis cannot be prevented, the preparation of planning documents and crisis resolution if it appears, and forming a post-crisis conclusion in order to continuously improve management. The establishment of such an approach requires time and careful preparation.

Except in the context of risk as failure, management in opencast mining increasingly needs to pay attention to social and environmental risks from the aspect of the lignite production cost, (Figure 3).



Figure 3. Social and Environmental sustainability in the function of Costs

Table 1 shows important controlled and uncontrolled environmental and socio-economic lignite mining impacts in relation to opening and development activities.

Table 1. Opencast lignite mining Controlled and Uncontrolled Environmental and Socio-Economic impacts

	Activities	Controlled Environmental Impacts	Uncontrolled Environmental Impacts	Socio-economic Impacts
Mine Development and Operation	Infrastructure Development, Overburden Removal, Lignite mining.	Land disturbance, Geomechanical stability, Mining output stability, Vegetation disturbance, Noise, Dust, Aesthetics, Water and Energy consumption, Surface and underground water discharge, disruption and pollution, Air emissions, Biodiversity protection, Resource efficiency.	Earthquakes, Floods, Landslides ...	Worker H&S, Community H&S, Capacity building, Skills development, Land and asset acquisition - displacement, Politics, Enhanced community services, Jobs, Royalties, Taxes, Capital investment.
Lignite Handling	Lignite transport to TPP, Storage.	Land disturbance, Vegetation disturbance, Noise, Dust, Water and Energy consumption.	Earthquakes, Floods, Landslides ...	Worker H&S, Community H&S, Jobs, Investments.
Overburden and Waste Disposal	Overburden and mine waste to inside or outside dumps.	Land surface disturbance, Water contamination, Aesthetics.	Earthquakes, Floods, Landslides ...	Worker H&S, Community H&S, Investments.

Social and environmental risks are generally defined as a *possibility of unwanted consequences caused by future hazardous events*. The effectiveness of risk management depends on risk cause identification and on the measures that are being implemented to reduce possible failures and negative consequences. Reducing the probability of failure is a more effective way of managing risks than analyzing and subsequently removing the consequences of unwanted events. Risk is essentially an unreliability, and its value is the probability of complementing the reliability up till value one. Same as any process, the risk management process has a measure of efficiency that depends on the quality of the implementation of process analysis and the risk management plan (Figure 4), where the measures are implemented to reduce the unreliability and its negative consequences. Also, effective

risk management involves a range of activities for overcoming the potential risks (failures), that must be continuously carried out over the lifetime of the opencast mine, in order to maintain its reliability at an acceptable level.

The most commonly used methodology in risk assessment, also known as semi-quantitative risk analysis, is based on the interaction between the likelihood that the risk will arise and the consequences that a social or environmental risk might cause to a business activity, process or to the company as a whole. The product of the scores expressing the probability of failure and the consequence from failure gives the each individual risk score. This traditional approach based on risk matrix is suitable for situations where the opencast mines system failure is caused by single failure events [7]. However, in most cases, failure is due to various factors whose overall risk is difficult to express in this way. Therefore it is necessary to calculate total risk for the mutually exclusive individual events of social and environmental failures and the risks associated with them, with respect to risk acceptability criteria.

In general, a risk can be acceptable or unacceptable.

An acceptable risk, which includes insignificant, minor and moderate risk, implies exposure to a risk which is tolerated without taking any measures. The risk is also acceptable in situations where the cost of taking measures is disproportionate to the potential benefits, but it can be controlled with measures or plans to reduce or mitigate the consequences of risks.

An unacceptable risk is usually passed on to a third party or being avoided by abandoning activities which carry such a risk. Transferring risk to a third party or sharing a risk with a third party is practically the best response to significant and unacceptable risks. In those events where extremely dangerous consequences can occur, it is necessary to further verify the probability of such an event, in order to define the required level of risk mitigation activities. The non-acceptance of a high and extreme risk by avoiding most often causes the abandonment of an activity which carries such a risk.

In Figure 4, a general model of social and environmental risks analysis process and risk management process is presented. The results of the risk analysis are used as a basis for risk management. The risk analysis process is iterative.

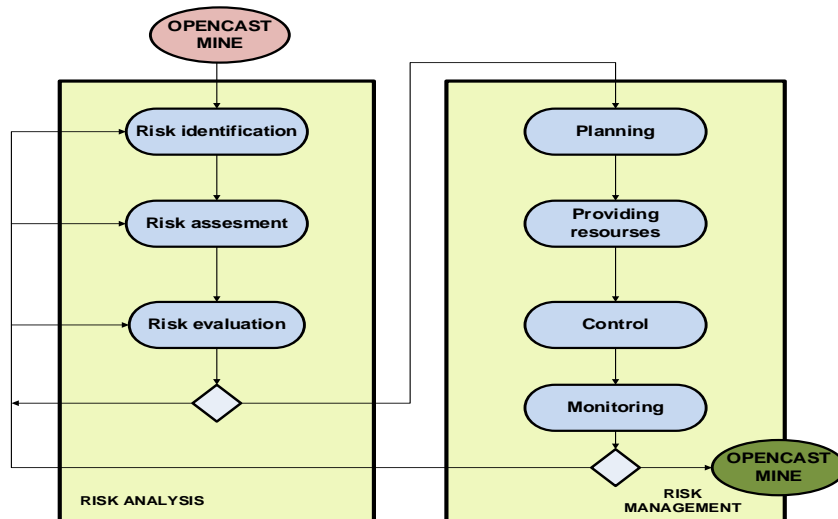


Figure 4. A general model of the risk analysis process and risk management process

The first cycle through the risk analysis process identifies the perceived risks, which become more or less important when the cycle is completely repeated. In order to understand the importance of the risk to the opencast mine, it is necessary to assess the probability of its occurrence and its consequences. This assessment may be limited to a qualitative or semi-quantitative description, which suffices in many cases, when it comes to individual causes of risk. The probability and

consequences of summarized risks can then be quantified and unified, and thus serve for a more detailed and more realistic analysis.

The process of analyzing social and environmental risks or unreliability includes the following common process activities [9]:

- *Risks identification* - forming a list of all potential risks for the operation of the opencast mine.
- *Assessment of individual risks* - determining the importance of risk based on the assessment of the probability of occurrence and the consequences of risks for the operation of the opencast mine.
- *Evaluating individual risks* - deciding whether the degree of each risk is (not) acceptable.
- *Risk summarization* - a summarized evaluation of several risks serially connected, with the establishment of eligibility criteria. In case of risk unacceptability, it is necessary to determine the measures that make the risk more acceptable.

Social and environmental risk management includes the following basic activities: planning, resource provision, control and monitoring (Figure 4). Considering that the process of elimination or reduction of risk is carried out simultaneously with other business activities, risk management practically starts at the exploration phase for the opencast mine, along with the process planning. Those risks are identified and evaluated, plans for their partial elimination are set, and this process continues throughout the life cycle of the opencast mine (Figure 2). The probabilities of occurrence and the impact of identified risks are assessed, taking into account the previous experience and data, paying attention to the methods and criteria, and considering the increasingly more frequent and complex changes in the environment.

Quantitative and qualitative methods or some of their variations are used for the risk analysis, as part of the risk management process [1, 9]. The mining industry commonly uses qualitative risk analysis methods to analyze hazards and business risks, including many classified as catastrophic risks [11]. Despite the widespread use, qualitative methods suffer from a number of limitations. For instance, the use of language to describe hazards and risks creates inherent subjectiveness. The resultant uncertainty combined with the natural or statistical variability within the often scarce information that is available further complicate scenario predictions and comparisons, particularly around catastrophic failure events that society so often associates with mining. Peoples' inexperience, perceptions and assumptions particularly in times of skill shortage and high employee turnover, are also part of the dilemma.

Today, quantitative methods for risk assessment are increasingly being used in the world, as they also give more objective risk assessments on the basis of better decision making in the domain of managing business, environmental and sociological risks.

3. PROBABILITY ASSESSMENT AND SOCIAL AND ENVIRONMENTAL RISKS MANAGEMENT

An analysis of social and environmental risks is necessary in order to support the correct management decisions on lignite opencast mines. Risk analysis helps with identifying a number of alternatives for the reliable realization of the expected production, in accordance with a set of certain criteria and limitations that influence the risk assessment.

For mutually exclusive individual events of social and environmental failures, the appropriate risks should be assessed and accumulated to the total risk (of an exceedance event) [8, 12]. Total risks are divided into social, environmental, which can be easily controlled by project design, operational measures and investments, and uncontrollable environmental risks associated with ecological disasters (earthquakes, floods, enormous landslides, etc.) (Figure 5). The total estimated risk is then verified by comparing the eligibility criteria for the elements of the socio-ecological

subsystem, such as the minimum permissible values of reliability, risk of failure and present value of losses.



Figure 5. Enormous landslides (2.8 km²) on opencast coal mine Collolar in Turkey which sadly killed ten employees (2011)

The process of assessing the total risk of scenarios with mutually independent social and environmental failures involves (Figure 6):

- Identifying all potential hazards and failure scenarios.
- Estimating the probability of occurrence of each failure scenario.
- Estimating the consequences (losses) for each scenario in regard to its occurrence.
- Estimating the risk associated with each failure scenario.
- Estimating the total risk by accumulating the risks associated with the separate failure scenarios.
- Comparing the total estimated risk with the criteria of risk admissibility.

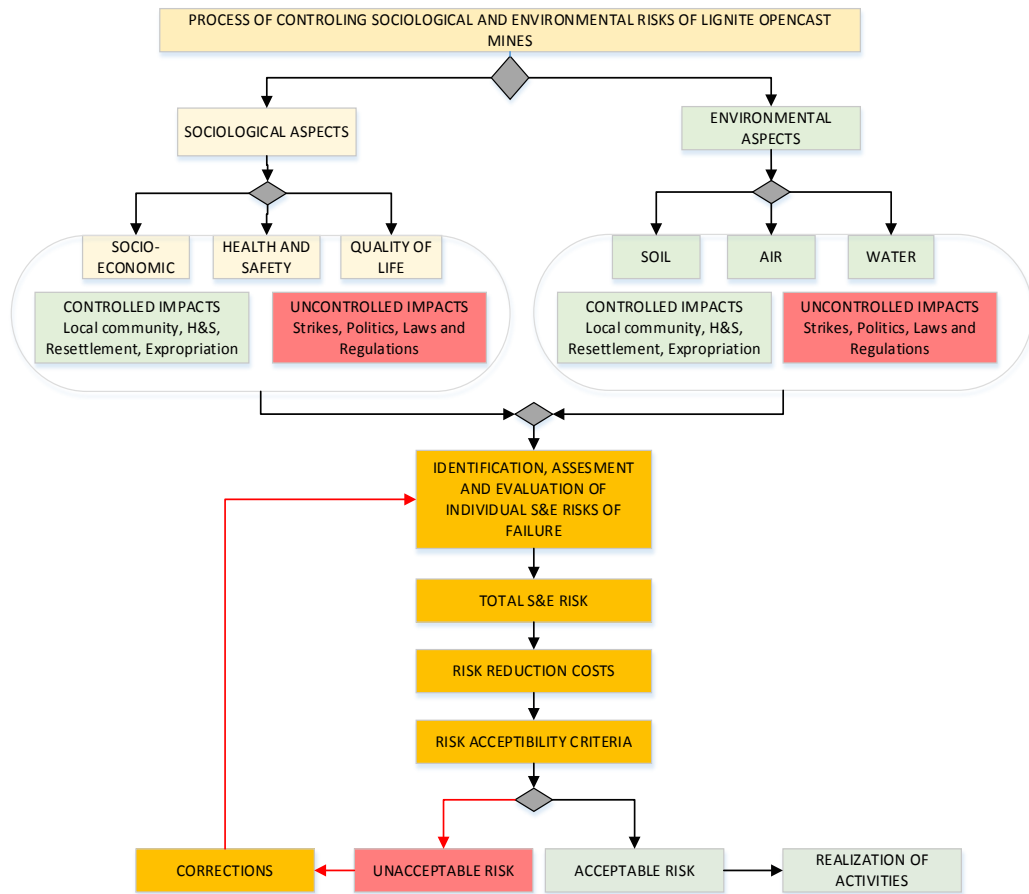


Figure 6. The process of assessment and management of social and environmental risks of failure

According to the classic definition, the risk of social and environmental failure is practically the possibility of occurrence of a situation or event that can have negative consequences on the function and operation of the opencast mine, and it's defined as:

$$R = P_f \cdot C \tag{1}$$

Where: P_f - probability of social and environmental failure (exceedance probability)
 C - losses caused by failure

The basic losses from failures due to social and environmental causes can be classified in several main categories:

- *Loss of life or damage to health.*
- *Losses associated with damage to the environment, contours and infrastructure of the opencast mine.*
- *Financial losses including loss of production, cost of intervention and repair, losses due to change of laws, environmental disasters, social unrest, cost overruns, inflation, capital costs changes, exchange rate changes, etc.*
- *Loss of reputation, including mistrust in production stability and management, change of contract, impact of the share value, social changes, etc.*

Depending on the category, losses can be expressed in monetary units, the number of deaths, loss of time, the amount of lost production, the amount of pollutants released into the environment, etc. Total failure losses in opencast mines are usually expressed in monetary units.

For i mutually independent failures, the total risk of failure is:

$$R_t = P_{f1} \cdot C_1 + \dots + P_{fn} \cdot C_i \tag{2}$$

Where: R_t - total risk of social and environmental failure

P_{fi} - probability of failure of the i -th element ($i = 1, \dots, n$)

C_i - expected losses due to the failure of the i -th element

Any individual risk of failure $R_i = P_{fi} \cdot C_i$ could be acceptable, while the overall (aggregate) risk might be unacceptable. The total risk of failure in the serial systems which consist of social and environmental elements might be unacceptable because it may cause a high risk of system failure as a whole, even though the risk of failure of every individual element is permitted.

The maximum allowed risk tolerance level (R_{max}) or the maximum acceptable probability of failure (P_{fmax}) is:

$$P_{fmax} = R_{max} / C \quad (3)$$

The limit of the risk of failure R being less than R_{max} corresponds to the limit probability of failure P_f being less than the acceptable level of P_{fmax} ($P_f \leq P_{fmax}$): $P_f \leq P_{fmax} = R_{max} / C$. When this condition is met, the risk of failure R is less than R_{max} ($R \leq R_{max}$) and practically represents the *maximum acceptable failure loss*.

If the minimum reliability or operational probability of the element $P_{omin} = 1 - P_{fmax} = 1 - (R_{max}/C)$ is at least equal to the maximum allowed risk of failure (R_{max}) in order to keep the risk of failure at a certain level, then the maximum risk of failure for the given minimum system reliability is:

$$R_{max} = (1 - P_{omin}) \cdot C \quad (4)$$

This equation encompasses the states of social and environmental systems in which the risk of failure is below the maximum allowed level of R_{max} , where the failure element which entails significant losses must be more reliable than the failure element that entails less losses. Elements which generate massive failure losses must be planned with a higher level of reliability.

Operation probability until the failure of social, controlled and uncontrolled environmental elements within a serial connection as a subsystem of a complex opencast mining system (Figure 7), can be described by different laws of distribution, depending on the characteristics of the system and its elements, operating conditions, failure characteristics, and so on [6, 13]. The simplest, in practice of system stationary probabilities, verified and the most used is the exponential distribution with the following stationary distribution function of system elements (i) operating time:

$$R_{oi}(t) = \exp(-a_i \cdot t), i = 1, \dots, n \quad (5)$$

Where: t - set operating time, a_i - distribution parameter (failure intensity).

The mean operating time to failure of system elements is:

$$T_{oi} = \int P_{oi}(t) dt = \int \exp(-a_i \cdot t) dt = 1/a_i \quad (6)$$

On the other hand, risk or the renewal probability after a failure by the time t at an exponential law of time distribution for restoring of system elements with the parameter b_i (renewal intensity) in time from 0 to t is:

$$P_{fi}(t) = \exp(-b_i \cdot t) \quad (7)$$

The mean renewal time of the system elements is:

$$T_{ri} = \int P_o(t)dt = \int \exp(-b_i \cdot t) dt = 1/b_i \tag{8}$$

The structural schemas that represent the graphical display of elements in the system can define unambiguously operation or failure of the system [3]. System elements are connected in series. If the system consists of (n) elements connected in series, the system probability operation $P_{so}(t)$, for the probability of each element operation $P_{oi}(t)$, is:

$$P_{so}(t) = P_{o1}(t) \cdot P_{o2}(t) \cdot \dots \cdot P_{on}(t) = \prod_{i=1}^n P_{oi}(t) \tag{9}$$

Probability of the system operation is:

$$P_{soi}(t) = \exp(-a_1 \cdot t) \exp(-a_2 \cdot t) \dots \exp(-a_n \cdot t) = \exp(-t \sum_{i=1}^n a_i) \tag{10}$$

Probability of the system failure is:

$$P_{sf} = 1 - P_{so}(t) \tag{11}$$

Mean time of the system operation is:

$$T_{so} = 1 / \sum_{i=1}^n a_i \tag{12}$$

Mean losses of the serial social and environmental elements from failure (C_i) by time t is:

$$L(t) = t \cdot \sum_{i=1}^n a_i \cdot C_i \tag{13}$$

When $t \rightarrow \infty$, limited stationary operation elements probabilities (P_{oi}) and the renewal elements probabilities elements after failure (P_{fi}) of the serial social and environmental mining subsystem are:

$$P_{oi} = b_i / (a_i + b_i), P_{fi} = a_i / (a_i + b_i) \tag{14}$$

The graph of process state and probabilities of social (P_{o1}, P_{f1}), controlled (P_{o2}, P_{f2}) and uncontrolled (P_{o3}, P_{f3}) environmental elements in a serial system connection is shown on Figure 6.

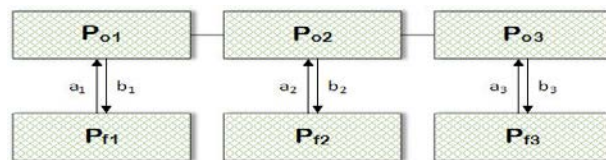


Figure 7. Probabilities of social (P_{o1}, P_{f1}), controlled (P_{o2}, P_{f2}) and uncontrolled (P_{o3}, P_{f3}) environmental elements in a serial system connection

Opencast mine production systems, as a rule, have extremely high losses due to failures of elements, including elements related to social and environmental risks. It is customary to estimate losses due to failure through the availability (the ratio of realized and maximum possible production) [2]. However, bearing in mind that the failures occur at different times, the financial impact on production losses and the cost of regenerating system elements are important, so it's useful to use the

present value of total losses at a given time t in risk assessments, through the known equation $PV_i = C_i/(1+r)^t$, where r is the discount rate.

Often, in opencast mining, the cost of recovery is greater than the loss of production, so accepting only the capacitive utilization does not indicate the real losses due to cancellation.

Ecological risks that cannot be controlled, like catastrophic events such as disaster, floods and earthquakes, and increasingly frequent storms generally caused by global warming, can cause high costs for the opencast mines in terms of cost recovery and consequential losses due to production interruption. It is customary for the reliability analysis in these cases to use geometric distribution with a parameter related to the return period (T_r) of catastrophic events with a probability p , where $p = 1/T_r$, with the function $f(t) = p(1-p)^t$. The return period is an unconditional time until the occurrence of a catastrophic event without the assumption of such an event in the first year [5, 10].

The probability that a catastrophic event will not occur during the analyzed period of the project of n years is:

$$P_o = (1-p)^n \quad (15)$$

The risk, that is, the probability that the event will happen at least once during the analyzed period of the project is:

$$P_f = 1-(1-p)^n \quad (16)$$

4. SOCIAL AND ENVIRONMENTAL RISKS ANALYSIS ON OPENCAST MINE TAMNAVA-WEST FIELD

Opencast mine Tamnava-West Field, with an annual output of 15 Mt of lignite, is the most important supplier for the Thermal Power Plants (TPP) Nikola Tesla of Electric Power of Serbia. Social and environmental risks significantly affect the stability and costs of the production of this opencast mine. Analysis has shown that, due to social problems (land acquisition, migration, strikes, etc.), production halts for a month every biennial year, and the costs due to production losses and additional fees add up to around 5 M euros. Controlled environmental impacts (emissions of harmful gases and materials, local landslides, climatic seasonal effects, etc.) occur annually and terminate the operation for two months with costs related to losses in production, rehabilitation and fees of about 10 M euros. Uncontrolled environmental impacts seriously jeopardized the work of the surface mine.

As a result of extreme rainfall in April 2014, the surface of Tamnava-West Field was almost completely flooded (Figure 8). The repair of the opencast mine and submerged equipment, which lasted ten months, cost about 100 M euros, while the losses in the production of lignite, which was interrupted for five months, resulted in a loss of a 15 M euros profit. For a more precise definition of uncontrolled catastrophic risks such as floods, it is important to determine the time of the planned period of occurrence n , provided that the catastrophic event will not occur with a given permissible probability $P_{o \text{ min}}$ equal to or greater than 90% for the realization of the maximum tolerable risk of failure of R_{max} (4). On the other hand, the legally anticipated return period is 100 years, so $p = 0.01$. From here it is clear that $n = 10$ years since (15): $P_{o \text{ min}} = (1 - 0.01)^{10} = 0.9$. The risk or probability that the event will occur in this period is 10%.



Figure 8. Flooded opencast mine Tamnava-West Field (April 2014)

The assessment of social and environmental risks has been done in two variants. In Variant 1 (V1) the analysis was performed with the indicated conditions, with failure and renewal intensities, probabilities, losses given in Table 2. Significant changes were made in Variant 2 (V2). In order to increase the reliability of mining from the aspect of social and environmental risks, it was determined that an additional retention embankment should be created, with a price of about 6 M euros, which reduces the renewal time of uncontrolled environmental impacts to two months. It was also planned to increase the volume of the lignite stockyard (Figure 9) with costs of about 60 M euros, which provides additional 15 days of supply reserves for the TPP. That also conditionally reduces the renewal time of social and environmental elements of the system. Failure and renewal intensities, probabilities, losses and risks for Variant 2 are given in Table 3.

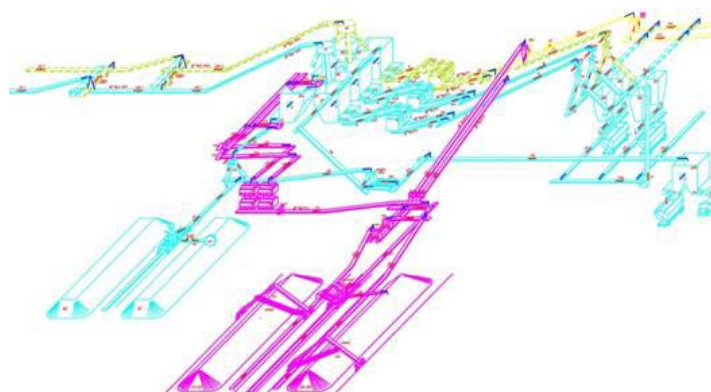


Figure 9. Expansion of lignite storage area Tamnava-West Field, marked with purple

Table 2. Parameters and analysis of social and environmental risks in Variant 1

Parameter	Social	Environmental Controlled	Environmental Uncontrolled
Failure intensity (year ⁻¹) (6)	0.1	1	0.1
Renewal intensity (year ⁻¹) (8)	12	6	1.2
Nonexceedance probability (15)	0.96	0.86	0.92
Exceedance probability (16)	0.04	0.14	0.08
Losses (M euros)	5	10	115
Risk (1)	0.2	1.4	9.2

According to Variant 1, the total serial nonexceedance probability (9) is 0.76, the exceedance probability (11) is 0.24, and the total losses are $C_{V1} = 135$ M euros. Total risk of failure amounts to (2):

$$R_{tV1} = 0.04 \cdot 5 + 0.14 \cdot 10 + 0.08 \cdot 115 = 10.8$$

The present value of total losses at a planned time of exceedance $t = 10$ years in risk assessments, where r is the discount rate equaling $r = 8\%$ is:

$$PV_{V1} = C_{V1} / (1 + r)^{tV1} = 135 / 1.08^{10} = 62.5$$

Table 3. Parameters and analysis of social and environmental risks in Variant 2

Parameter	Social	Environmental Controlled	Environmental Uncontrolled
Failure intensity (year ⁻¹)	0.1	1	0.1
Renewal intensity (year ⁻¹)	24	8	6
Nonexceedance probability (12)	0.98	0.89	0.98
Exceedance probability (12)	0.02	0.11	0.02
Losses (M Euro)	3	68.5	14
Risk (1)	0.06	7.54	7.9

According to Variant 2, the total serial nonexceedance probability (9) is 0.85, the exceedance probability (11) is 0.15, and the total losses are $C_{V2} = 85.5$ M euros. Total risk of failure amounts to (2):

$$R_{tV2} = 0.02 \cdot 3 + 0.11 \cdot 68.5 + 0.02 \cdot 14 = 7.9$$

The present value of total losses at a given time of construction of the retention embankment and extension of the lignite storage area in $t = 5$ years, where r is the same discount rate $r = 8\%$ equals:

$$PV_{V2} = C_{V2} / (1 + r)^{tV2} = 85.5 / 1.08^5 = 58.2$$

A comparative analysis of the variants shows that the social-environmental system in Variant 2 is more reliable by 12%, that the risk of failure is reduced by 37% and that the present value of losses is reduced by 7%. Of course, the shortening of the deadline for the expansion of the coal stockyard area in V2 leads to a larger current value of losses in relation to V1. In any case, the increase in the volume of the opencast mine lignite storage area leads to an increase in reliability and other operational and technological elements of the mining system. Considering that the lifetime of the opencast mine will be over 20 years and that the probability of the number of exceedances is significantly increasing, the implementation of V2 is fully justified and the facilities for increasing reliability and risk reduction are in the realization phase.

5. CONCLUSIONS

Opencast coal mining is a costly and hazardous endeavor when it comes to environmental and social risks during mining. Responsible and sustainable mining demands compliance of social, environmental and economic components.

It's definitely necessary to do a basic and the most common semi-quantitative risk analysis, which is based on the interaction between the probability that the risk will arise and the negative cost consequences for every individual social and environmental risk. However, when it comes to complex, mutually exclusive individual events of social and environmental failures and the risks associated with them in opencast coal mining, it is necessary to use quantitative Risk Assessment Based on Assessing Individual Risks proceeding from risk acceptability criteria.

After the identification of all potential socio-ecological risks, the probability of their occurrence and corresponding losses are calculated, the total risks with the criteria of risk admissibility using the present value of total losses at a given time are finally determined.

Generally, in addition to social risks, in a series of probability calculations, controlled and uncontrolled environmental risks are included. The probability of uncontrolled hazard risks is calculated on the basis of the return period during mining.

Tamnava-West Field opencast coal mine has been used as an example of socio-ecological risk analysis, with concrete data on hazardous events. It was established that enhanced defense measures for the protection of the opencast mine from uncontrolled flood risks and the triple increase in the volume of coal stockyard are in function of timely reserves for the opencast coal mining system. The adopted Variant 2 provides the required total serial nonexceedance probability of 0.85, the exceedance probability of 0.15, and the total loss of 85.5 M euros. Total risk of failure amounts to 7.9. Work on the realization of additional retention embankment and rehabilitation of existing channels and retentions have been completed, while the commissioning of new additional stockyards is expected in 2019.

The set methodological approach for control and assessment of socio-ecological risks opens new possibilities for optimizing management and overall risks of opencast mining systems and subsystems using the reliability theory.

REFERENCES

- [1] Anderson R. D., Sweeney J. D., Williams A. T. (2003). *Management Science*. Tomson, Ohio, 567-577.
- [2] Barlow R. E. (1998). *Engineering Reliability*. ASA-SIAM Series on Statistics and Applied Probability, Philadelphia, 137-148.
- [3] Cox D. R. & Miller H. D. (1998). *The Theory of Stochastic Processes*. Chapman and Hall, London, 171-177.
- [4] Korakianiti M. & Pavlovic N. (2015). Environmental problems and environmental aspects related to the surface coal. 7th International Conference COAL2015, Zlatibor.
- [5] Ozga-Zielinski B., Adamowski J. and Ciupak M. (2018). Applying the Theory of Reliability to the Assessment of Hazard, Risk and Safety in Hydrologic System: A Case Study in the Upper Sola River Catchment. *Water*, 2018, 10 (723).
- [6] Pavlovic V. (1998). *Continuous Mining Reliability*. Ellis Horwood Limited, Chichester, 16-22.
- [7] Pavlovic. V., Ignjatovic D., Subaranovic T. (2016). Implementation of the rehabilitation operational strategy for the flooded opencast coal mine Tamnava-West Field. IMWA2016, Leipzig.
- [8] Pavlović V., Ignjatović D., Šubaranović T. (2017). Reliability and risks of mining projects realization. 8th International Conference COAL2017, Zlatibor.
- [9] Pavlovic V., Pavlovic V., Jovicic V. (2006). *Managing of Ecological Processes in Surface Mining*. ISCSM2006, Aachen.

- [10] Read K. L. & Vogel M. R. (2015). Reliability, return periods, and risk under nonstationarity. American Geophysical Union, AGU Publications.
- [11] Raschel T. & Knights P. (2012). The Case for Quantitative Risk Analysis in the Mining Industry, Queensland Mining Industry Health and Safety Conference.
- [12] Todinov M. T. (2006). Risk-Based Reliability Analysis and Generic Principles for Risk Reduction. Elsevier Science & Technology Books, 59-71.
- [13] Wolstenholme L. C. (1999). Reliability Modelling. Chapman and Hall, London, 149-160.

A Review of the Effectiveness of Health & Safety Management Systems according to OHSAS 18001 Standard at PPC's Lignite Mines

Th. Vlachos

Assistant Director - Central Support of Mines Dept., Public Power Corporation S.A, Athens- Greece

ABSTRACT

PPC's Mining Business Unit in seeking to achieve free from injury and disease lignite mines' workplaces, in collaboration with PPC's Department of Health & Safety at Work, works to lead and coordinate efforts to prevent workplace death, injury and disease. For the Public Power Corporation S.A respect for the society and the environment, it's not just a legal obligation but a fundamental corporate goal, a key part of the broader business policy and a cornerstone of corporate social responsibility. Mining Business Unit has integrated the planning, management and performance evaluation of health & safety issues through the development of a Health & Safety Management System according to international standard OHSAS 18001 at its workplaces (mines and support units). The objective of this paper is to review the effectiveness of this system in Lignite Centers' operation and to show the gains and the simplicity of development and implementation, the lessons learned and the opportunities of further development and continual improvement. Occupational health & safety system performance is not easily measured. The complexity of occupational health & safety is such that simple quantified measures are often inadequate and does not represent the overall performance of the System or its impact on organisation's safety culture. Increased attention has been given to positive performance indicators and audit tools as measures of some aspects of health & safety management system performance.

1. INTRODUCTION

During the last decade , the approach of the development and implementation of Occupational Health & Safety Management Systems (OHSMS) for the management of health & safety issues, has become popular and has been introduced in large and medium-sized companies. Experience shows that OHSMS is a logical and useful tool for the promotion of continual improvement of Occupational Health & Safety (OHS) performance at the organisation's level. OHS is a discipline dealing with the prevention of work-related injuries and diseases as well as the protection and promotion of the health of employees.

Public Power Corporation SA (PPC) is the leading producer and supplier of electricity in Greece, with approximately 7.5 million customers. Its infrastructure extends from lignite mines to power stations and renewable energy. PPC's Mining Business Unit consists of the Department of Central Support of Mines which is located in Athens and the Lignite Centre of Western Macedonia (LCWM) in Northern Greece – Macedonia. The former Lignite Centre of Megalopolis (former LCM) in Southern Greece – Peloponnese is now part of PPC's subsidiary under the name Lignitiki Megalopolis S.A. Five open-cast mines are located at PPC's Lignite Centres (West Macedonia and Megalopolis) with an annual lignite production of about 35Mt (2017).

Within the framework of continuous improvement in Health & Safety issues, Public Power Corporation/Mining Business Unit (MBU) redefining its strategy through:

- Management Commitment
- Employee involvement and continuous consultation
- Continuous evaluation and review of Health & Safety initiatives

- Management of OH&S on the basis of carrying out risk assessment and ongoing review
- Encouraging effective 'bottom-up' communication
- OH&S performance measurement and monitoring

Although the evaluation of the level of OHS according to published statistics, classifies PPC's mines among the safest mines sites across Europe, PPC's MBU has decided to integrate its planning, management and performance evaluation of OHS issues through the development and implementation of an OHSMS according to international standard OHSAS 18001 requirements. Within the last 4 years, three out of five lignite mines have already certified by independent Certification Bodies according to OHSAS 18001 requirements. The other two mines as well as Support Units are under certification. This paper assess the effectiveness of certified OHSMS in improving OHS conditions at PPC's open-cast lignite mines.

2. RATIONALE FOR THE IMPLEMENTATION OF CERTIFIED OHSMS

Precursors of undesired OHS outcomes lie in areas relating to [1]:

- people (including leadership, behavior and degree of ownership)
- organisations (including culture)
- systems (across all business areas)
- processes (especially technical, but also administrative)
- physical plant and processing (technical and technological)

The health and safety management system comprises three levels of control [2]:

Level 3 - effective workplace precautions provided and maintained to prevent harm to people at the point of risk.

Level 2 - risk control systems (RCSs): the basis for ensuring that adequate workplace precautions are provided and maintained.

Level 1 - the key elements of the health and safety management system: the management arrangements (including plans and objectives) necessary to organise, plan, control and monitor the design and implementation of RCSs.

A certified OHSMS takes a systems approach. This is based on the "Plan, Do, Check, Act" cycle, which is composed of items such as policy, objectives, procedures and roles as Figure 1 depicts [3].

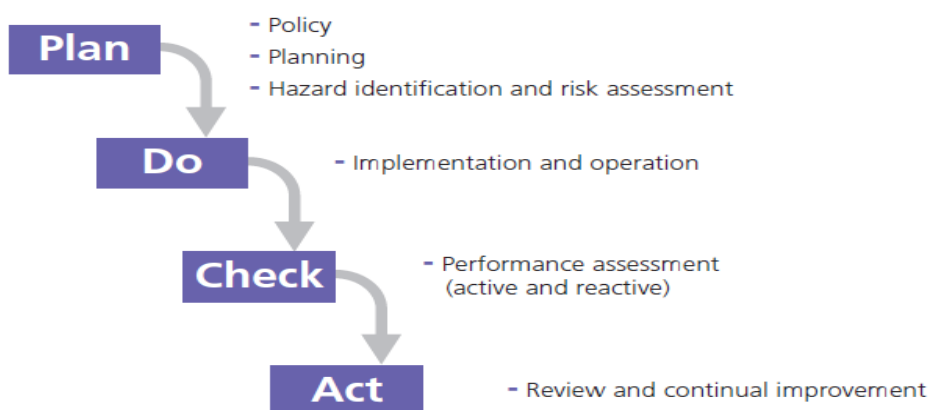


Figure 1 : Plan-Do-Check-Act diagram

Therefore, the core elements of a management system, as OHSAS 18001, are policy, planning, operation, monitoring and review which comprises the aforementioned three levels of control. Several studies shows that the use of OHSMS play a fundamental role in tackling OHS challenges, improving worker safety, reducing workplace risks and creates better and safer working conditions [4]. The results of several studies revealed that the safety performance of OHSAS 18001-certified

companies is better than that of non-certified companies as well as the effectiveness of OHSMS in improving OHS outcomes [4], [5], [6]. Findings of studies shows that certified companies are most likely to enforce OHS rules and procedures which has an important role in improving OHS performance. Their enforcement can improve the safety behavior of employees, which may in turn, prevent accidents [4].

Several researchers have demonstrated that OHSAS 18001-certified companies have an adequate and functioning safety management system in order to control occupational hazards and have a stronger management commitment, better organized safety training, higher workers' involvement in safety, more efficient safety communication and feedback, explicit safety rules and procedures, fairer safety behavior and reasoned safety promotion policies [7]. Implementation of OHSAS 18001 will not automatically ensure high safety activities in a company. However, it creates a basis for a systematic work in the area of OHS documented policies and procedures, detailed working instructions, audits at planned intervals, management reviews, targeted training, explicit roles and responsibilities, preventive and corrective actions and measuring and monitoring of results.

The implementation of certified OHSMS drives mining company from the Reactive stage to the Generative stage according to the evolutionary model of Safety Culture [8] (Fig.2).

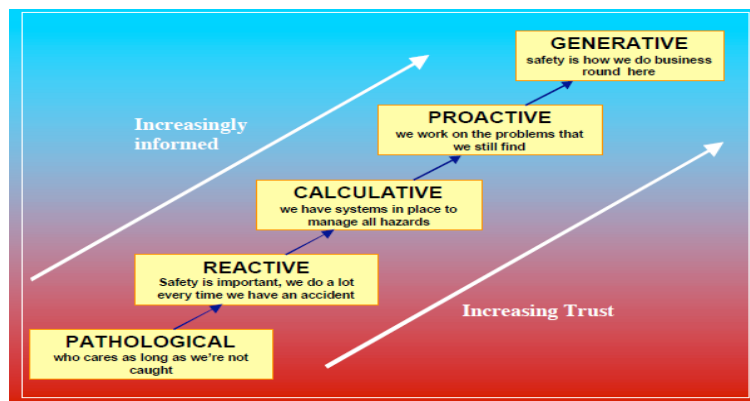


Figure 2. The evolutionary model of Safety Culture

The evolutionary model of Safety Culture, is an evolutionary ladder consisting of five levels. The model assumes that the safety culture of a company has reached a certain level of maturity. The model distinguishes between five culture levels. Each culture level reflects the development phase of the company in terms of safety.

3. OHS PERFORMANCE MEASUREMENT

OHS performance can be described as a measure of the level of effectiveness of those business activities aimed at the prevention of injury and disease to persons in the workplace. The most important reason for measuring OHS performance is to monitor the level of success of activities aimed at preventing workplace injury and disease and to identify OHS areas for improvement [9] as well as to provide information on the progress and current status of the strategies, processes and activities used by an organization to control risks to health and safety. Measurement information sustains the operation and development of the health and safety management system, and so the control of risk, by:

- providing information on how the system operates in practice;
- identifying areas where remedial action is required;
- providing a basis for continual improvement; and
- providing feedback and motivation

In order to assess the effectiveness of an OHSMS a company should measure the degree of conformance with the management system requirements, namely OHSAS 18001 and the outcomes of OHS initiatives.

The effectiveness of implementing OHSMS could be measured through [10]:

- Prevention of accidents
- Improving safety consciousness of management and workers
- Legal compliance
- Effective on-site safety and health management
- Improving quality and productivity

a set of indicators should be used across all of these areas.

4. LAGGING AND LEADING INDICATORS

Indicators have been used for many years in mining and other high-reliability and high-risk industries. Indicators are useful in determining progress in the implementation of management systems, and whether business objectives and targets have been met. The many indicators that health & safety professionals use can be divided into two categories: lagging and leading indicators.

Lagging indicators (also referred to as re-active or outcome indicators) measure the end result of OHS processes, policies and procedures. They are a record of things that have already happened. Since they record things after the fact, they inform a reactive health and safety culture. They measure negative or unwanted outcomes such as injuries, illnesses or deaths [11]. They also referred as outcomes indicators as they measure the final outcomes.

Leading indicators (also referred to as pro-active, positive or predictive indicators) focus on future health and safety performance with the intent of continuous improvement. They are indicators that can give advance warning about what might be going wrong. They can be used to measure activities undertaken to positively impact on outcome performance at the workplace, and to identify problem areas where additional preventative action is required.

Using leading indicators, mining companies can identify whether proactive risk-lowering decisions and actions are being effective, and why a desired result has or has not been achieved (as measured by a lagging indicator). In this way, leading and lagging indicators together trace cause and effect pathways [9]. Although, the sensitivity of the outcomes (as measured through lagging indicators) to the various leading indicators can be difficult to determine, there is a strong relationship between leading and lagging indicators and OHS performance as Figure 3 shows [11].

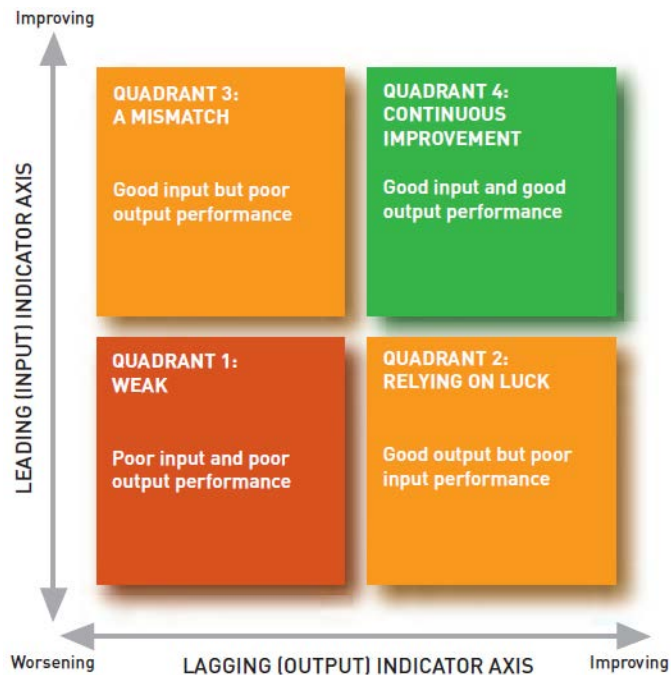


Figure 3: Relationship between leading and lagging indicators, and performance

Lagging indicators demonstrate output performance while leading indicators demonstrate input performance. Quadrant 1 indicates poor results and poor proactive measures. Quadrant 2 indicates good results (relying on luck) and poor measures. Quadrant 3 indicates good measures do not match the results, possibly due to inappropriate measures or due to the time lag between measures and results. Quadrant 4 is where an organization can be reassured that they are on a continuous improvement. This diagram also gives an indication of the effectiveness of a certified OHSMS. An effective certified OHSMS place an organization at Quadrant 4.

5. ASSESSMENT OF THE EFFECTIVENESS OF CERTIFIED OHSMS AT PPC'S MINES

5.1 Quantitative Results

As it is already mentioned, PPC's Mining Business Unit has developed and implemented a certified OHSMS according to international standard OHSAS 18001, in addition to OHS procedures and initiatives which are implemented centrally by PPC's Department of Health & Safety at Work. In order to assess the effectiveness of certified OHSMS at PPC's mines, we will take into consideration OHS leading and lagging indicators of the former Lignite Centre of Megalopolis, which has been certified according to OHSAS 18001 requirements since the mid of 2014.

Various researchers in quality management systems have shown that measuring direct effects of certified management systems at outcomes is difficult. As the OHSMS is certified according to OHSAS 18001 since the mid of 2014 (2013 was the development and implementation year), eight years measurements are taken into consideration (2010-2017), namely four years before the certification (2010-2013) and for years after the certification (2014-2017).

Within that framework, leading indicators such as:

- Safety training
- Number of safety audits contacted
- Number of near misses reported
- Number of employees that are periodically under medical supervision
- Hazard assessments contacted
- Meetings of employees safety committee and number of recommendations made

• Full scale drills of Emergency Preparedness are considered more representatives to assess the effect of the certified OHSMS on them. Table 1 shows leading indicators measurements before and after the certification according to OHSAS 18001.

Table 1: OHS Leading indicators of Lignite Centre of Megalopolis

	2010	2011	2012	2013*	2014	2015	2016	2017
Number of hours in Health & Safety training per employee	N/A	N/A	8,3	10,8	8,3	9,7	9,6	11
Number of safety audits	14	12	8	20	32	42	55	69
Number of near misses reported	0	0	0	4	2	4	4	3
Number of employees that are periodically under medical supervision	77	44	105	52	154	364	537	424
Hazard assessments	Assessment studies since 2000				New assessment studies		Revised assessment studies	
Meetings of employees safety committee (yearly)	0	0	0	0	2	3	3	3
Full scale drills of Emergency Preparedness	0	0	0	0	1	1	1	1
	Before certification				After certification			

(*Implementation year)

As it concerns Megalopolis’ Lignite Mine lagging indicators:

- Accident Frequency Indicator
- Accident Seriousness Indicator
- Number of accidents

are considered more representatives to assess the effectiveness of the certified OHSMS on OHS outcomes. Table 2 shows lagging indicators measurements before and after the certification according to OHSAS 18001.

Table 2: OHS Lagging indicators of Megalopolis’ Lignite Mine

	2010	2011	2012	2013	2014	2015	2016	2017
Accident Frequency Indicator	4,94	4,46	7,89	4,85	4,66	2,19	5,65	1,88
Accident Seriousness Indicator	101	91	184	97	92	58	77	46
Number of accidents	9	8	13	8	8	4	10	3
	Before certification				After certification			

Overall, statistical comparison of leading and lagging indicators between two periods (four years each), before and after the certification is as follows.

Table 3: Statistical comparison of OHS indicators

Leading indicators	
Safety training (hrs/employee)	same level
Number of safety audits	267% increase
Number of near misses reported	225% increase
Number of employees that are periodically under medical supervisison	432% increase
Hazard assessments	<ul style="list-style-type: none"> ➤ Assessment studies since 2000 (2010-2013) ➤ New assessment studies and biannual review (2014-2017)
Meetings of employees safety committee	From none (2010-2013) to 11 (2014-2017)
Full scale drills of Emergency Preparedness	From none (2010-2013) to 4 (2014-2017)
Lagging indicators	
Accident Frequency Indicator	34% reduction
Accident Seriousness Indicator	42% reduction
Number of accidents	34% reduction

The average annual accident rates during the period after the certification are lowered by 34%-42% than that of the period before the certification. These results are in line with other studies who noted that accident rates decrease when a company is OHSMS certified [4], [6], [10],[12].

It is also worth noted that leading indicators are dramatically improved the period after the certification compared to the period before the certification, which indicates the effect of certified OHSMS on safety climate and safety culture. These results are also in line with studies which noted the positive consequences of certification on values, logics and discourses [12] as well as the higher levels of safety management practices and safety behavior of certified companies compared to non-certified [6]. The lack of difference in safety training, before and after the certification, contributed to a significant safety training program which has started before. The difference on this criterion is that after the certification, training is more focused on specific issues according to hazard assessments findings which are now revised periodically.

5.2 Qualitative Results

Certified management systems must be evaluated not only on a scale estimating the extent in which they make work environment better or worse, but also in terms of how they may qualitatively influence the scope, intentions and contents of OHSMS [12].

Except from quantitative leading indicators, there are also some salient qualitative non measured factors that management consider the key features of the system as follows:

- Internalization of values (tidiness and order)
- Responsible line managers
- Employee involvement through roles, accountabilities and communication about safety issues
- Use of Personal Protective Equipment (PPE)

which are under close monitoring after the implementation and certification of OHSMS.

More employees are involved in OHS issues either as internal auditors of OHSMS or trainers in specific OHS subjects (especially foremens and engineers at shift level) or members of emergency teams.

6. CONCLUSION

A certified OHSMS per se is not effective in terms of preventing and reducing the number of accidents at work, if management commitment, safety climate and safety culture are absent. However, the development and implementation of an OHSMS can blow a wind of change in the organization and mobilize management and employees to the direction of bringing health and safety to the frontline together with productivity and other business objectives. Through the use of a set of leading and lagging indicators, the effectiveness of a certified OHSMS in an organization could be determined as a preventative and corrective mechanism.

Accident rates were found to be significantly reduced after the development-implementation-certification of an Occupational Health & Safety Management System according to OHSAS 18001 international standard requirements at PPC's lignite mines.

From the above analysis it is obvious that four years after the development and implementation of certified OHSMS, Megalopolis' Lignite Mine is at Quadrant 4 of Figure 3 (Continuous Improvement) and with Accident Frequency Indicator at 1.88 for 2017, ranked among the safest mines worldwide.

The development-implementation and certification of OHSMS have formulated a safety climate which reflected at the OHS outcomes. It can be said that, OHSAS 18001 certification gave at PPC's lignite mines health and safety culture gains, strength and momentum from within.

The sensitivity of the outcomes (as measured through lagging indicators) to the various leading indicators can be investigated thorough research among many mining companies with proper data collection and it warrants further studies in the future.

REFERENCES

- [1] International Council of Mining & Metals. Report (2012). Overview of leading indicators for occupational health and safety in mining. [Online]. Available: <https://www.icmm.com/website/publications/pdfs/health-and-safety/4800.pdf>
- [2] HSE Health & Safety Executive (2001). A guide to measuring health & safety performance.
- [3] Institution of Occupational Safety and Health, UK (2015). Systems in focus. Guidance on Occupational safety and health management systems. [Online]. Available: www.iosh.co.uk/systems
- [4] Iraj Mohammadfam, Mojtaba Kamalinia, Mansour Momeni, Rostam Golmohammadi, Yadollah Hamidi, Alireza Soltanian (2016). Evaluation of the Quality of Occupational Health and Safety Management Systems Based on Key Performance Indicators in Certified Organizations, Occupational Safety and Health Research Institute. Published by Elsevier.
- [5] Hafez Alavi and Jennie Oxley (2013). A Snapshot Review Influence of OHS certification and non-certified systems: Monash University Accident Research Centre. [Online]. Available: www.worksafe.vic.gov.au/data/assets/pdf_file/0020/158033/Safety-Certification-Evidence-Review.pdf
- [6] M.N.Vinodkumar, M.Bhasi (2011). A study on the impact of management system certification on safety management. *Safety Science* 49, 498-507
- [7] O. Paas, K. Reinhold and P. Tint (2015). Estimation of safety performance by MISHA method and the benefits of OHSAS 18001 implementation in Estonian manufacturing industry. *Agronomy Research* 13(3), 792–809

[8] Hudson P.T.W. (2001), Safety Management and Safety Culture: The Long, Hard and Winding Road. In: Pearse W., Callagher C., Bluff L. (Eds.) Occupational Health and Safety Management Systems, Melbourne, Australia: Crowncontent. 03-32.

[9] Australian Government. Department of Employment and Workplace Relations (2005). Guidance on the use of Positive Performance Indicators. [Online]. Available: https://www.safeworkaustralia.gov.au/system/.../guidanceonuseofppis_2005_pdf.pdf

[10] Seok J.Yoon, Hsing K. Lin, Gang Chen, Shinjea Yi, Jeawook Choi, Zhenhua Rui (2013). Effect of Occupational Health and Safety Management System on Work-Related Accident Rate and Differences of Occupational Health and Safety Management System Awareness between Managers in South Korea's Construction Industry, Occupational Safety and Health Research Institute. Published by Elsevier.

[11] Alberta Government (2015). Leading Indicators for Workplace Health and Safety: a user Guide. [Online]. Available: <http://work.alberta.ca/documents/ohs-best-practices- BP019.pdf>

[12] Pernille Hohnen, Peter Hasle (2011). Making work environment auditable-A “critical case” study of certified occupational health and safety management systems in Denmark. Safety Science 49, 1022-1029

Innovative Approaches to Coal Surface Mine Sites Rehabilitation: A Case Study of Megalopolis Lignite Fields

Ariadni Sokratidou¹, Eleni Gkouvatso², Christos Roumpos¹, Angeliki Perdiou², Giorgos Tsagkarakis² and Stella Kaimaki²

¹Public Power Corporation, Athens, Greece

²ADENS SA, Athens, Greece

ABSTRACT

Coal surface mining can have significant effects on environment, related to both physical disruption of land morphology, habitats and ecosystems. It can also affect substrate factors such as ground/surface water quality. More significantly however, coal mine sites could leave behind a legacy of secondary detrimental effects due to permanent land form alterations. Traditionally, mine site rehabilitation should return sites to safe and geotechnical and geochemical stable conditions where, land forms, soils, hydrology, habitats and flora and fauna are self-sustaining and compatible with surrounding land uses. To this end coal mine sites are usually returned to their pre-mine uses, which, for the majority of mines is agriculture, wildlife habitat or forestry.

However, new ethos in mine closure plans is the repurposing of mine sites i.e the identification of a creative, successful and economically sustainable future use taking advantage of the existing infrastructure and being the result of a successful collaboration of mining companies, regulators, land-use planners, investors, and citizens to identify the most beneficial use.

This paper examines some rehabilitation practices, leading to repurposing of mine sites on some mostly typical lignite and coal mines worldwide. Some good national examples are also used to point out how mine closure plans can be drafted before mine activity closure, leading to the creative and successful re-use of decommissioned mines.

The case study presents a rehabilitation plan of Megalopolis lignite fields, where continuous surface mining has been applied.

Keywords: Coal, Surface Mines, Rehabilitation, Lignite Fields, Closure, Sustainable

1. INTRODUCTION

Coal mining contributes towards the economic development of a country, while some of the beneficial impacts of mining projects include employment and income opportunities, infrastructural and community development.

However, mining activity, has also a great impact upon environment. One of the critical parameters which affect the viability of the surface mining projects in the new competitive market refers to the stringent environmental conditions in relation to the continuously varying mining conditions [1]

Surface mining activity removes the soil and rock above coal deposits, or seams. This form of extraction changes the landscape and has impacts on local flora and fauna, particularly where diversion of forest land for mining takes place. Surface mining and associated activities can significantly modify the landscape at the site and hence have a major impact on land use options and human activities, from recreational or aesthetic perspectives. Further modifications to landscape can occur if it is necessary to divert surface waters in proximity to the mine. The overall effect on the landscape will depend ultimately on the size of the mining operations and to some extent on the

geometric configuration of the deposit. The effect of mining on water and soil quality is also of great concern. Acid mine drainage and metal leaching from mine waste dumps are naturally occurring processes which are accelerated by intensification of mining operations [2], [3]. Inadequately closed mines may continue to degrade surrounding land, water bodies and air [4]. In this framework, effective life-of-mine strategic planning of surface lignite mining projects incorporating sustainability concepts, with emphasis on mine closure phase, is essential for an integrated approach [5].

Post-mining land use is generally determined by economic, social and technical factors as well as mine site properties. Factors identified as important in the selection process include land resources (e.g. physical, biological and cultural characteristics), ownership, type of mining activity, legal requirements, location, needs of the community, economic, environmental, technical and social factors. The suitability of former mining sites for different activities depends, for example, on current land use surrounding the site, infrastructure and facilities, and the extent of any environmental impacts, such as soil and water contamination [6], [4].

Possible alternative for post-mining land-uses are presented in Table 1. The most common post-mining land use purposes include agriculture, forestry, recreation, construction, conservation and lakes. Post-mining landscapes can harbour unique natural, cultural and economic potential. Examples of these are pastures, aquaculture, wildlife habitats, educational, sport and leisure facilities and industrial uses [4].

Table 23. Possible alternative for post-mining land-uses [7]

Land-use Types	Exercised Post-mining Land Uses
Agriculture	Arable farmland, garden, pasture or hay-land, nursery
Forestry	Lumber production, woodland, shrubs and native forestation
Lake or Pool	Aquaculture, sailing, swimming, water sports etc., water supply
Intensive Recreation	Sport field, sailing, swimming, fishing pond, hunting
Non-intensive Recreation	Park and open green space, museum or exhibition of mining activity
Construction	Residential, commercial (e.g. shopping centre), industrial (e.g. factory), educational (e.g. university), sustainable community.
Conservation	Wildlife habitat, water supply (surface and groundwater)
Pit Backfilling	Possibility of landfill (as last resort)

Post-mining conditions should provide ecosystem services and produce lands capable of supporting societal needs in the future. Successful mine rehabilitation, as needed to satisfy today's society demands, requires engineering, design, and purposeful reconstruction of the full mining disturbance, not just its surface, and control of waters leaving the mine site [8].

In general, there will always be differences in pre-mining and post-mining ecosystems and landscapes. Reclaimed mining land, often has significantly lower levels of biodiversity and ecosystem services than land that has not been mined [9].

This paper presents mine closure paradigms leading to repurposing of mine sites worldwide. Past and future rehabilitation works in Megalopolis Lignite Centre, Greece, are also presented that are aligned with the emerging new ethos in mine closure plans.

2. MINE CLOSURE PLANS

Nowadays, mining companies following national legislation or in the framework of their Corporate Environmental Responsibility view closure and rehabilitation planning as an integral part

of the operating plan. Numerous guidelines on mine closure and mine closure planning have been drafted by international organizations (the World Bank, the International Council on Mining and Metals, The United Nations Development Programme, etc). Closure guidelines exist at national scale (e.g., the Finish Mine Closure Handbook, Guidelines for Preparing Mine Closure Plans in Western Australia, Swedish Guidelines, US, Canadian, etc) and industry sector guidelines [10], [11].

In the European Union, the mining wastes, materials that must be removed to gain access to the mineral resource, are regulated by the 2006/21/EC Mining Waste Directive (MWD). The MWD has specific provisions for closure and after-closure procedures for waste facilities. The 1st Best Available Techniques Reference document for Management of Tailings and Waste-Rock in Mining Activities that was developed in 2009 is currently under review.

The terms restoration/ rehabilitation/remediation/ reclamation/ regeneration are often used interchangeably in literature [11]. However, there are different formal definitions of each which apply in different circumstances. Pearman, G. (2009) summarised these different meanings of these words in a mine closure perspective to provide an explanation for each term [12]:

Reclamation is the process of converting derelict land to usable land and may include engineering as well as ecological solutions. In other words, reclamation is about to restore the land surface to some sort of productive use.

Restoration, in an ecological sense, seeks to artificially accelerate the processes of natural succession by putting back the original ecosystem's function and form. In an archaeological sense, the term implies the repair of old man-made structures to something approaching the original style, often using traditional materials and methods. Thus, restoration is reclamation that is guided by ecological principles and promotes the recovery of ecological integrity; reinstatement of the original (pre-mining) ecosystem in all its structural and functional aspects

Rehabilitation is progression towards the reinstatement of the original ecosystem and an aspect of reclamation. Some ecosystems may have been changed so dramatically that a return to the original landscape is no longer possible and rehabilitation - a partial return to a previous state - could be the only option. It noted though that under MWD rehabilitation means the treatment of the land affected (by a waste facility) in such a way as to restore the land to a satisfactory state, with particular regard to soil quality, wild life, natural habitats, freshwater systems, landscape and appropriate beneficial uses.

Remediation generally applies to the environmental clean-up of land and water contaminated by organic, inorganic or biological substances. It involves treatment to reduce harm to humans and environment.

Regeneration: Increasingly, society is demanding more from post-mining landscapes so that they can return economic as well as ecological benefits to offset negative closure impacts. Regeneration implies that a broad socio-economic (and environmental) perspective is being taken, including the mine site but also the environment and communities beyond the mine site itself.

A study conducted in the framework of the revision of the 1st Reference Document for Management of Tailings and Waste-Rock in Mining Activities, based on the experience from completed and on-going remedial programmes for closed and abandoned mines concluded that [11]:

- There is a need for proper closure and remediation of closed and abandoned mine sites
- A systematic long-term approach is necessary to address the issues
- Remedial programmes can be performed on many scales (national, regional, river basin, etc.)
- Financing the remedial programme is always an issue and resources are always limited
- Limited resources make it necessary to prioritise between sites (facilities) and to rank the sites in order of priority
- Rehabilitation works beyond those necessary to ensure safety and eliminate health hazards should not be attempted if funds are not sufficient to ensure lasting environmental improvements

- Any decision to perform remediation at a site should be based on solid information and go through a stakeholder consultation process
- The end result of any rehabilitation programme should be self-sustaining sites, compatible with the surroundings and requiring minimal on-going maintenance
- Follow-up and feedback is important in order to improve the remedial programme, the implemented remedial measures, to develop the regulatory framework for operating and future mining operations, promote stakeholder involvement, etc.

Likewise, the recent Guidelines for Preparing Mine Closure Plans, published by the Government of Western Australia [13] point out that the rehabilitation objectives must be established through defining the post-mining land use(s) and site-specific closure objectives consistent with those land use(s). These Guidelines define rehabilitation as the return of disturbed land to a safe, stable, non-polluting/noncontaminating landform in an ecologically sustainable manner that is productive and/or self-sustaining and consistent with the agreed post-mining land use. Rehabilitation outcomes may include revegetation, which is defined as the establishment of self-sustaining vegetation cover after earthworks have been completed.

Rehabilitation normally comprises the following:

- developing designs for appropriate landforms for the mine site;
- creating landforms that will behave and evolve in a predictable manner; according to the design principles established; and
- establishing appropriate sustainable ecosystems.

Principles of mine closure planning are for rehabilitated mines to be (physically) safe to humans and animals, (geo-technically) stable, (geo-chemically) non-polluting/non-contaminating, and capable of sustaining an agreed post-mining land use.

The following key principles and approaches should be considered when preparing a Mine Closure Plan [14]:

- Planning for mine closure should be fully integrated in the life of mine planning and should start as early as possible and continue through to final closure and relinquishment.
- Mine Closure Plans must be site-specific.
- Closure planning should be risk-based, taking into account results of materials characterisation, data on the local environmental and climatic conditions, and consideration of potential impacts through contaminant pathways (including but not limited to site activities or infrastructure) and environmental receptors.
- Consultation should take place between proponents and stakeholders which should include acknowledging and responding to stakeholders' concerns. Information from consultation is central to closure planning and risk management. The closure objectives and completion criteria of the mine should be developed in consultation with key stakeholders
- Post-mining land uses should be identified and agreed upon through consultation before approval of new projects. This should take into account the operational life span of the project and should include consideration of opportunities to improve management outcomes of the wider environmental setting and landscape, and possibilities for multiple land uses. For existing mining projects, post-mining land uses should be agreed as soon as practicable.
- Materials characterisation needs to be carried out prior to project approval to a sufficient level of detail to develop a workable closure plan.
- Closure planning should be based on adaptive management. Closure plans should identify relevant experience from other mine sites and research, and how lessons learned from these are to be applied.
- Closure plans should demonstrate that appropriate systems for closure performance monitoring and maintenance and for record keeping and management are in place

3. POST-MINING LAND-USE OPPORTUNITIES

3.1. Repurposing

As mentioned above, options for post-mining land use are varied. Recent mine closure projects have proved that they can return economic as well as ecological benefits both at local but also at regional scale.

The Eden Project was built in a 160-year-old exhausted china clay quarry in Cornwall, UK. Two huge enclosures consisting of adjoining domes are housing plant species and emulating natural biomes, a rainforest environment and a Mediterranean environment. The site has also an outside botanical garden which is home to many plants and wildlife native to Cornwall and the UK. The project, that attracts thousands of visitors each year, aims to educate them about the importance of a sustainable environment through the study and education of plants [15].

One of the biggest projects of integrated of coal mining closure focussing in giving mined lands a new and constructive future use is currently executed by the Lausitzer und Mitteldeutsche Bergbau-Verwaltungsgesellschaft mbH (LMBV) in Germany. LMBV, that is owned by the Federal Republic of Germany, represented by the German Federal Ministry of Finance, was assigned the responsibility for phasing out and restructuring the lignite mining regions of Central Germany and Lusatia [16].

LMBV has concentrated its activities on remediation of former lignite mining areas: i.e., in conversion of these regions to new and constructive future use. LMBV administered more than 30,000 hectares of real estate in Lusatia and Central Germany. This real estate includes forest areas being re-cultivated, areas for agricultural use, former industrial facilities, bodies of water and their shorelines, as well as former open-cast mines that still in remediation. Many of these surface areas are now usable or will become usable in the near future. The remaining real estate has been in the process of preparation, in the form of remediation measures, for specific future use in accordance with the stipulations of state and regional planning policy. With ongoing progress in remediation, the offering of marketable real estate accordingly increases. This offering primarily includes newly created areas suitable for industrial and commercial parks; wind and solar parks; residential building; streets, paths, and highways; agriculture and forests; leisure and rehabilitation projects; and nature preserves [17].

Examples of projects of the LMBV in the Lusatian and Central – German lignite regions and similar repurposing projects from other countries, focussed on coal mines, are given in the following paragraphs.

3.2. Green energy infrastructure

Many mined lands have been given a second productive life as have been used to accommodate green energy infrastructure.

Photovoltaic systems are operated at abandoned mines around the world. Germany's largest photovoltaic power station, the **Meuro solar park**, that is a **166 MW** photovoltaic power station located in the Lusatian lignite region, is built on a former lignite mine. In the Lusatian region in a former open pit area is also located the **Finsterwalde solar park (80 MW)**.



Meuro solar park [18]



Finsterwalde solar park

Figure 122. Solar parks in the Lusatian and Central – German lignite regions

In **Kidston gold mine**, Australia, the mining operations left behind an open-cut mine with craters up to 300 meters deep. A project is under way to turn the mine into a massive renewable energy hub. The first phase is the construction of a 50MW Solar Project on top of the tailings of the gold mine. The second phase is a hybrid solar and hydro project. It will comprise of a 250MW pumped hydroelectricity storage facility and a 270MW solar PV power plant. The project will turn the craters into a pumped hydroelectric energy storage system [19].

The **Woodlawn** zinc and copper mine, Australia, located approximately 250 km southwest of Sydney, left a large pit where a bioreactor was placed in 2004. The Woodlawn Bioreactor currently manages around 20% of Sydney's putrescible waste and capturing its emissions to generate clean energy for up to 30,000 homes. Since opening, over 4.1 Mt of waste has been processed at the facility, most of which has been used to generate green electricity. The project also includes a windfarm that harnesses 48.3 megawatts per year and a solar farm utilising increased sun exposure from cleared land to produce 2.5 megawatts of energy per year [20].

3.3. Recreation opportunities in new water bodies

Flooding, as a part of an extensive regeneration programme, several decommissioned lignite opencast mines in the Lusatian and Central – German lignite regions, created two Lake Districts in Germany. The **Lusatian Lake District**, the largest artificial network of watercourses in Europe is among the most spectacular LMBV projects. The **Central German Lake District** likewise represents an aquatic sports facility of large scale. In this Lake District, the lakes are not only connected to each other: they are also linked to existing rivers – such as the Pleisse and the White Elster – to form one large watercourse network.

The **Central German Lake District** offers numerous perspectives for new uses. As a tourist destination, it includes 12 large pit lakes. Sites for recreation, tourism and water sports have emerged, such as the Cospudener, Markkleeberger and Störmthaler lakes, south of Leipzig, the Schladitzer lake north of Leipzig, and the Grosser Goitzschensee lake at Bitterfeld. Sea promenades, beaches, restaurants and numerous water sports have already turned these lakes into popular national attractions.



Artificial lakes south of Leipzig



A holiday resort at the Störmthaler lake

Figure 123. Artificial lakes in the Central – German lignite region

Leipzig New Lakeland is currently undergoing a transformation with almost 70 km² of lakes and waterways. A series of tourism trails allowing the area to be explored by boat is especially prominent. Waterways connect the city of Leipzig with the new lakes of the mined landscape. Around 200 km of navigable waterways are to be created.

The Geiseltal lake with a water surface of 18.4 km², a depth of up to 80 meters and more than 40 km of shoreline offers the best conditions for recreation, tourism and water sports. North of the lake stretches the heap of Klobikau, on whose western part vineyards have been successfully cultivated for some years. The Marina Mücheln on the southwestern shore of the Geiseltal lake is a central point of contact for locals and guests. The marina itself is designed as an ensemble with boathouses, a holiday home and a harbour.

The Lusatian Lake District is a key element of the redevelopment. A large number of new lakes with a total water surface of 140 km² have being created. The flooding of the lakes takes place from the rivers Spree, Schwarze Elster and Neisse. The Lusatian Lake District as a tourist destination includes 23 lakes. Of these, 9 lakes with the existing Senftenberger lake are connected by navigable channels. The planning includes the expansion of maritime connections so that they can also be used by sailboats and passenger ships.



Artificial lakes in the Lusatian Lake District



Canal between Geierswalder and Partwitzer lakes

Figure 124. Artificial lakes in the Lusatian lignite region

Water activities are already possible at Gräbendorfer, Partwitzer, Geierswalder, Sedlitzer and Bärwalder lakes in geotechnically safe areas. Rehabilitation is not yet complete in the Lusatian Lake District. There may be temporary restrictions on the use of farm roads and other areas as a result of ground fissures on tipping areas and the associated additional testing of geotechnical safety.

The activity opportunities include sailing, surfing and paddling, swimming and diving, water skiing and boating. Many lakes have surfing and Sailing schools established. In some lakes there are marinas. The Lusatian Lake District also offers habitat to many passing, resting and breeding water birds. The low-nutrient soils of the mining landscape are habitat for rare animals and plants.

The major use of the lakes is recreation. Many lakes also became part of protected areas for nature conservation (e.g. Lake Rassnitz, Lake Paupitzsch, Lake Gremmin). A few lakes are used for fish breeding (e.g. the Muldereservoir). In the majority of the pit lakes, however, fishery is done only on the basis of the natural development of the fish community after an initial stocking. A few lakes are used for purposes of water management, mainly flood protection (e.g. Lake Borna, Lake Zwenkau after reaching planned water level). The function as geochemical sink is most impressive in the Mulde reservoir due to the permanent through-flow of the complete River Mulde. It acts as a sink for heavy metals originating from abandoned ore mines in the Ore Mountains at the Czech-German border. In this way, the River Elbe is protected from strong contamination [21].

Weaver's opencast coal mine, in the Waikato New Zealand, was closed in 1993. The opencast pit was allowed to fill with water, forming a small lake, and the surrounding area has been smoothed out and planted in grass and shrubs to form a recreation area. The pit is now called Lake Puketirini and is used by a diving school due to its depth, to train divers for under water engineering projects. Lake Puketirini is available for activities such as kayaking, boating, and water-skiing. Walking and cycling around the lake are also popular recreational activities [22].

3.4. Heritage preservation and recreation

The Ruhr Valley in western Germany was once the country's industrial heartland. Coal mines and iron and steel mills changed drastically the landscape. After the decline of the industries, the industrial landscape was transformed through a special framework of projects named IBA Emscher Park. Dealing primarily with ecological issues, IBA projects aimed at reversing the ecological, aesthetic, and social abuse of the landscape, including a special treatment for slag heaps.

The **Emscher Landscape Park** combines industrial heritage and landscape art with a lot of nature. The park in the northern Ruhr region consists of gardens and parks, foot and cycle paths and numerous tips with unique landmarks.

Underground mines left behind waste tips and subsidence lakes. The stone dumps and slack heaps are typical elements of the landscape in the Ruhr area and part of the industrial heritage. Within the framework of Emscher Landscape Park several heaps were designed by artists and landscape architects. Now dumps and heaps are important points of identification for the inhabitants and landmarks in the Region, visible from far away [23].

On the tipped cone tip of the former Schleswig mine in Dortmund-Asseln a **mountain biking** area has been designed. On the Prosper tip in Bottrop operates Alpicenter, **the longest indoor skiing hall in the world**. Other tips are sites of arts and parts of the route of landmark art. Before a tip can be used for new purposes the danger of fire must be excluded as fractions of coal remaining in the tip material can inflame under pressure and can smolder in the inner body of the tip for a long time.

The Zollverein industrial complex in Land Nordrhein-Westfalen consists of the complete infrastructure of a historical coal-mining site, with some 20th-century buildings of outstanding architectural merit. It has been inscribed into the **UNESCO** list of World Heritage Sites since 2002 and is one of the anchor points of the European Route of Industrial Heritage [24].

The grounds of the former Zeche Nordstern coal mine have been turned into an example of an industrial landscape park. In 1997, the disused industrial site was turned into the Nordstern Park, a public recreation area with a variety of leisure facilities. The 160-ha site is covered with a network of paths and viewing axes, lined with gardens, open areas of meadow and a large number of playgrounds and quiet zones. In the park there is an amphitheatre for audiences of up to 6,000 in the summer.

3.5. Other infrastructure

The LMBV has created seven industrial parks in Lusatia and Central Germany lignite regions. These sites were selected in close cooperation with the state, the regions and the municipalities for industrial and commercial use and were re-developed into modern high-performance industrial areas on the basis of development plans. The industrial areas were integrated into a liveable post-mining landscape with a wide range of residential, recreational and recreational opportunities.

Sites of former coal mines located within easy reach of roads and railroad networks often make optimal facilities for logistics service providers. One such site is located in a former coal mine of an area of approximately 1 km² northwest of Dortmund, Germany.

4. THE MEGALOPOLIS CASE

4.1. The Megalopolis Lignite Centre

The Megalopolis Lignite Centre (MLC) is located in central Peloponnese and until recently was owned and operated by the Public Power Corporation (PPC) of Greece SA. Under the new law 4533/2018 the exploration and exploitation rights at the MLC are passed to the subsidiary company “LIGNITIKI MEGALOPOLIS SA”.

Mining and deposition of waste rock are carried out in three open-cast mines: the Choremi mine, the Marathousa mine and the Kyparissia mine. Mining activity began in 1970 from the Thoknia mine, which has already been depleted since 1994. The continuous surface mining systems, employing bucket wheel excavators, belt conveyors, stackers and spreaders, are used in the exploitation, in combination with non-continuous mining equipment. Alfios and Elisson rivers flow between the mines. In Alfios River several diversions of its riverbed were made, for the protection and proper operation of the mines. Both rivers will be diverted in the future for the development of the mine.

Lignite production on an annual basis is about 9 million tons. In order to achieve this production, it is necessary to transport about 40 million m³ of materials (lignite and waste rock). Annual production is expected to decline from 2028 to 5 million tons. The horizon of exploitation of the mining activity is 2040, parallel to the operation of the thermal power plants, which it supplies with lignite. The environmental rehabilitation of the mines will be completed by 2045 [25].

4.2. Rehabilitation Approach

In MLC, lignite mine wastes have been used so far for backfilling of excavation voids or deposited in heaps according to the waste management plan that includes the proposed plan for closure, including rehabilitation, after-closure procedures and monitoring required by both MWD and Environmental Impact Assessment (EIA) Directives.

The environmental terms of the mining activity in the MLC incorporate appropriate measures aiming to prevent the potential impacts during the operation of the activity and measures to be taken during closure and environmental rehabilitation of the intervention area. The measures aim to address the environmental impacts, by the following hierarchical order:

- Prevention - avoidance
- Decrease in intensity and extent
- Restoration

Closure design and rehabilitation of the intervention area of the MLC take into account both the existing environmental situation and the one that will occur after the end of the production period. The closure and environmental rehabilitation activities for the MLC apply to the following main categories:

- surface areas of the final excavations and internal deposits,
- surface areas of external deposits, and

- premises of ancillary facilities.

The long-term goals of the closure and rehabilitation design are focused on establishing stable and safe environmental conditions that will require minimum maintenance and monitoring. To this end, the relevant actions will be carried out in accordance with the following five basic criteria, applicable to the mining industry.

Table 24. Key criteria for closure and environmental rehabilitation of MLC [25]

Criteria	Description
<i>protection of public health and safety</i>	Creation of conditions that will not pose a risk to the safety and health of people, fauna, flora and generally to the safety of the man-made and natural environment
<i>geotechnical stability</i>	All remaining structures, including those made in the natural relief of the project area, should exhibit geotechnical stability in order to ensure public health, safety and protection of the immediate environment.
<i>geochemical stability</i>	All remaining materials should be geochemically stable and should not pose a potential risk to future users of the area, public health or the immediate environment, especially soil, water resources, flora, fauna, etc.
<i>biological stability</i>	Rehabilitation works should lead towards a self-sustaining ecosystem typical of the area. The restoration program should respond to the future land uses of the area and aim at restoring safe and stable conditions that will encourage the natural regeneration and the biodiversity development in the project area.
<i>landscape adaptation</i>	Rehabilitation of the environment should lead to the landscaping of the area of intervention in a way that is harmoniously connected and integrated into its natural features.

The general environmental protection measures implemented by PPC SA include the following:

- Unconditional compliance with the Approved Environmental Terms for the Operation of Mines and the implementation of the Environmental Restoration Program.
- Design aiming to prevent the potential environmental impacts through the adoption of best methods and techniques to avoid the occupation of new areas and to reduce the disturbances caused by the mining activity (internal disposals instead of external disposals at uninterrupted areas).
- Maximum utilization of waste rock for backfilling of excavation voids and the rehabilitation of depleted mines.
- Reduction of volume of mining waste produced.
- Gradual systematic environmental rehabilitation of the intervention areas of the Project, to reduce the nuisance and gradual, smooth harmonization of the restored areas with the natural environment of the wider region.
- Implementation of rehabilitation methods adapted to the particular environmental conditions of the area (e.g. private plants nursery etc.) and the use of alternative planting materials and methods (e.g. endemic species, test plantings, etc.).
- Conservation and enhancement of biodiversity and landscape physiognomy.
- Measures for fire protection of vegetation.
- Extensive collaboration with Researchers, Universities and other social partners to protect the natural environment in the immediate and wider area of intervention, and to enhance the performance of environmental rehabilitation.

4.3. Rehabilitation works

Between 2004-2012, more than 6.5 km² of the external deposits of the Choremi and Thoknia mines have been rehabilitated. Main planted species include *Robinia pseudoacacia*, *Cupressus arizonica*, *Pinus pinea*, *Eucalyptus* sp, that are fast-growing and resistant with limited maintenance requirements. Other species that have been used are *Pinus halepensis*, *Spartium junceum*, *Olea europaea*, *Castanea sativa*, *Juglans regia*, *Ficus carica*, *Cedrus* sp. and *Catalpa* sp.



Figure 125. Rehabilitation in external deposits of Megalopoli mines

After the deposition of waste rock for the filling of Thoknia open pit mine remnant void and the formation of geological barrier, by-products of the desulfurization plants of the Power Stations are deposited.

Ponds have been created in the remnant Kiparissia field and at the pumping sites in Marathousa and Choremi mines [26]. Recent studies have concluded that the mine operation has no remarkable influence on the quality of the surface and groundwaters in the area [26], [27].



Figure 126. Planting and maintenance works in external deposits of Choremi mine

Tree plantings for timber production and for the optimization of the rehabilitation of the deposits by the end 2045 will cover a total area of 6.24 km². By the end of rehabilitation works a total area of 7.8 km² will be available for agricultural use. Another future plan of the area includes the creation of lakes. In the pit of Choremi mine a lake of a total surface area of 11.5km² will be created. In Kiparissia pit a small lake a total surface area of 0.25 m² will also be created.

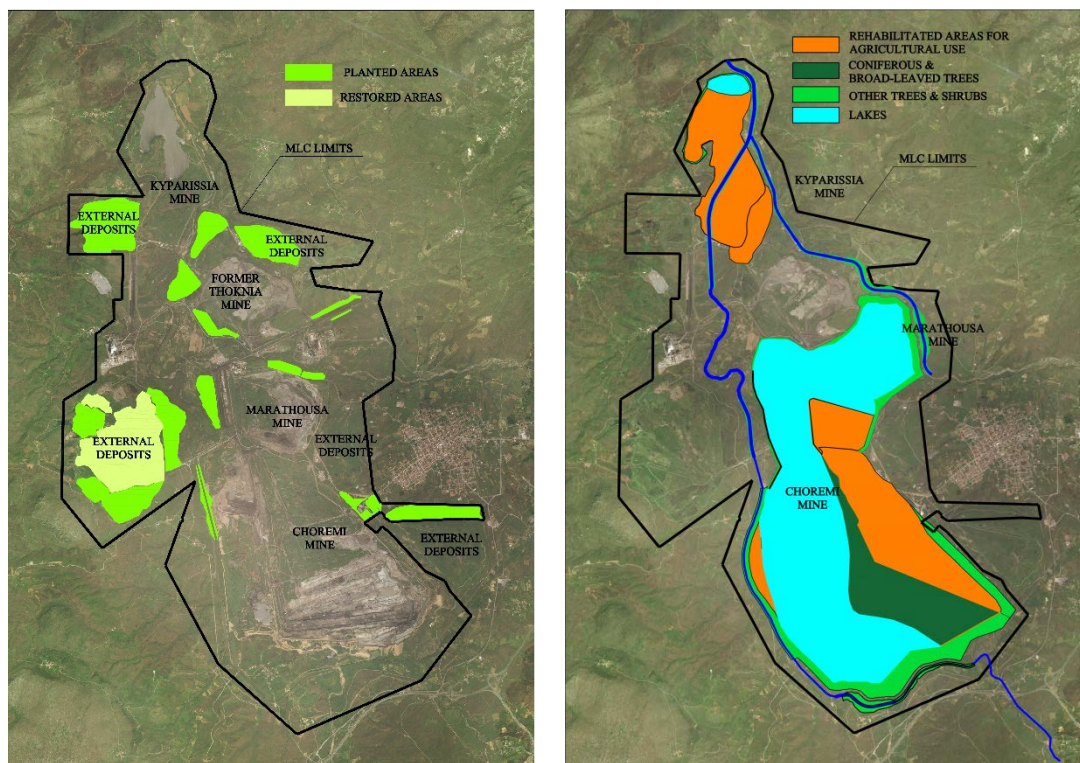


Figure 127. Current rehabilitated areas (left) and rehabilitated areas in 2045 (right)

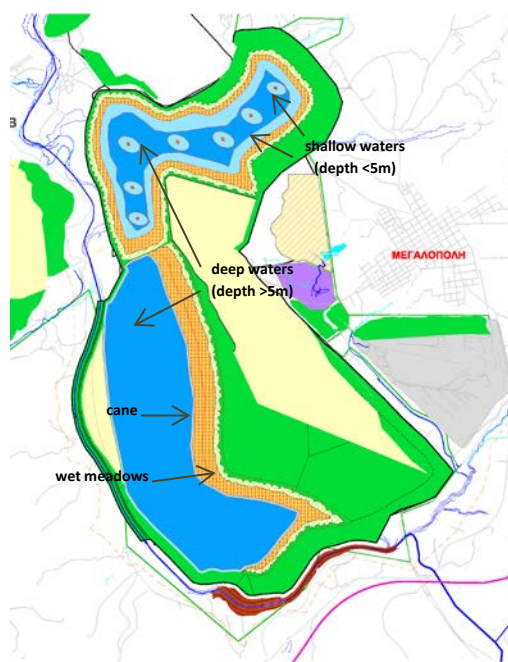


Figure 128. Planned wetlands in Choremí and Marathoussa mines, according to PPC EIA Study [25]

Other current or future projects in the framework of the MLC closure plan are presented in the following paragraphs.

In the area of external deposits of Choremí mine PCC SA has completed a study in order to promote the agricultural and livestock production and also to boost the development of agritourism in the whole region. The study area has a size of 2.5 km². Within this area 10 plots of land will be formulated along with the supporting technical infrastructure (roads and 6 irrigation reservoirs). The

reservoirs will provide irrigation water and in combination with plantation of water-bearing trees will create opportunities for observation and recreation. The project also aims to create hedgerows with selected species that are resistant to weather conditions, vary in size, arbours, flowering, fruit and colours that will serve as windbreaks but also will formulate an attractive environment and improve the biodiversity.

The PPC Renewables SA has licenced the construction of a 50 MW photovoltaic power station in an area of deposited heaps of the MLC. The project also incorporates tree plantings and the construction of 2 ponds serving as wetlands.

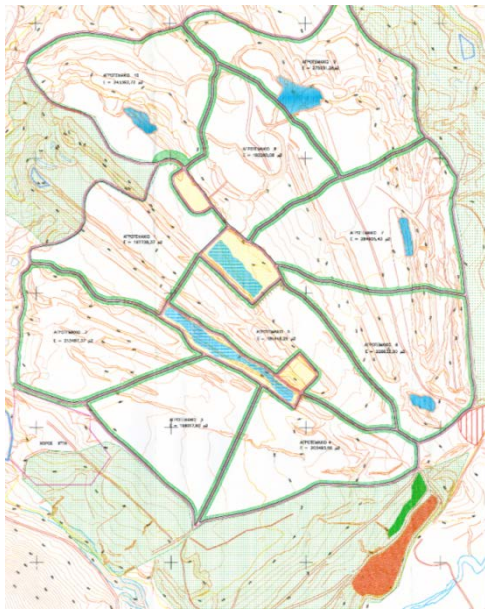


Figure 129. Proposed farmland plots in Choremi (left) and planned photovoltaic power station (right)

In the MLC’s reclaimed areas, the Megalopolis motocross track operates, that hosts Greek and international tournaments. This project has been referenced as an example of successful case study of Mine Closure in a recent EU funded project [28].



Figure 130. Megalopolis motocross track

As already mentioned part of the void of Thoknia exhausted mine is used for the deposition of by-products of the desulfurization plants of the Power Stations. Another part is reserved for landfilling of hazardous waste, mainly asbestos wastes that will be produced from the future decommissioning of the units of the thermal plants of the PPC or from other public buildings such as schools, hospitals etc. in the Peloponnese Region.

At the external deposits of Marathousa mine an area has been granted for the construction of an industrial park.

Finally, the PPC has signed a Memorandum of Cooperation and Understanding with the Ministry of Culture for the protection, preservation and enhancement of the archaeological sites of the MLC area.



Figure 131. The archaeological site of Kyparissia mine

5. CONCLUSION

Modern rehabilitation plans consider a number of different factors which may influence decisions in selecting a rehabilitation strategy that have environmental, economic and social dimensions. These include:

- The conservation value of the proposed environmental outcome
- The economic productivity of the proposed future land capability
- The consistency of the proposed land use with local and regional plans and other infrastructure
- The importance to local communities and land owners of the proposed scheme

Current practices adopted by PPC SA advocate measures that re-construct disturbed areas within MLC to comply with regulatory requirements and to satisfy the needs of multiple land users as well as needs of the public sector. So far, rehabilitation works are aligned with international good practices and the restrictions resulting from the mine operation.

However now, more than 10 years before mine closure, there is an opportunity to integrate the mitigative approaches that have been used into a holistic rehabilitation plan.

A multi-disciplinary approach should be adopted in order to develop a new vision for the area, taking into account a thorough assessment of constraints and opportunities.

Whether the vision for the area would be the development of museums or education centres and archaeological sites, visitor attractions, scientific centres, recreational areas, gardens or parks, forestry or agriculture, green or other infrastructure, this should be developed as soon as possible. Emergent technologies and Best Management Practices focusing on holistic approaches should be used for creating solutions to restore the complex MLC site.

The local knowledge available through PPC SA staff, land users, government officers and practitioners can be integrated with technical know-how for successful reclamation outcomes.

The active participation of Local and Central Authorities, land owners, local communities, regulatory authorities, mining proponents and other affected parties in the final decision of the reclamation is very important to the effectiveness of the plan. While achieving consensus is desirable, it is realized that this may not be possible in all cases. It is important that at a minimum, all views and opinions of the parties involved are clearly and accurately documented and considered in the decision-making process.

The concept of economic sustainability should be central to these plans requiring the collaboration of PPC SA, regulators, land-use planners, investors, and citizens to identify the most beneficial use of, leading to the creative and successful re-use of the area. Repurposing of MLC can take advantage of existing infrastructure and reclamation projects already completed and contribute to the local economy after the final closure of the area.

REFERENCES

- [1] Roumpos C., Pavlidakis F., Kouridou O. (2016). Managing Surface Lignite Mining Projects in a Competitive Environment. IX International Brown Coal Mining Congress "Brown coal as a safeguard of energy security", Bełchatów, Poland; 04/2016.
- [2] Banerjee, D. (2014). Acid drainage potential from coal mine wastes: Environmental assessment through static and kinetic tests. *International Journal of Environmental Science and Technology*. 11: 1365.
- [3] Heikkinen PM (Ed.), Noras P (Ed.), Salminen R (Ed.), Mroueh U-M, Vahanne P, Wahlström M, Kaartinen T, Juvankoski M, Vestola E, Mäkelä E, Leino T, Kosonen M, Hatakka T, Jarva J, Kauppila T, Leveinen J, Lintinen P, Suomela P, Pöyry H, Vallius P, Nevalainen J, Tolla P, Komppa V (2008). *Mine Closure Handbook*, Geological Survey of Finland, Special Publications, Espoo, 169 p
- [4] Kivinen, S. (2017). Sustainable Post-Mining Land Use: Are Closed Metal Mines Abandoned or Re-Used Space? *Sustainability*, 9, 1705
- [5] Roumpos, C., Papacosta E., (2013). Strategic mine planning of surface mining projects incorporating sustainability concepts, *Proceedings, 6th International Conference on Sustainable Development in the Minerals Industry (SDIMI 2013)*, 30 June – 3 July 2013, Milos Island, Greece: 645–651.
- [6] Mborah, Ch., Bansah, K. and Boateng, M. (2016). Evaluating Alternate Post-Mining Land-Uses: A Review. *Environment and Pollution*. 5. 10.5539/ep.v5n1p14.
- [7] Narrei, S., and Osanloo, M. (2011). Post-mining land-use methods optimum ranking, using multi attribute decision techniques with regard to sustainable resources management. *OIDA International Journal of Sustainable Development*, 2(11), 66-76.
- [8] Skousen, J. and Zipper, C. (2014). Post-mining policies and practices in the Eastern USA coal region. *International Journal of Coal Science and Technology* 1 (2):135-151.
- [9] Fritsche, U., Berndes, G., Cowie, A., Johnson, F., Dale, V., Langeveld, H., Sharma, N., Watson, H., Woods, J. (2017). *Energy and Land Use - Global Land Outlook Working Paper*. 10.13140/RG.2.2.24905.44648.
- [10] Garcia, D. (2008). "Overview of international mine closure guidelines", in Meeting of the American Institute of Professional Geologists, Arizona Hydrological Society, and 3rd International Professional Geology Conference, American Institute of Professional Geologists, pp. 1–9.
- [11] European Commission, DG Environment. (2012). Establishment of guidelines for the inspection of mining waste facilities, inventory and rehabilitation of abandoned facilities and review of the BREF document. No. 070307/2010/576108/ETU/C2. Annex 3 Supporting document on closure methodologies for closed and abandoned mining waste facilities. April 2012.
- [12] Pearman, G. (2009). 101 Things to do with the hole in the ground. Post Mining Alliance, Eden Project.
- [13] Western Australia Government. (2015). Department of Mines and Petroleum. Environmental Protection Authority. Guidelines for Preparing Mine Closure Plans, May 2015.
- [14] Australian Government. (2016). Mine Closure. Leading Practice Sustainable Development Program for the Mining Industry
- [15] Blewitt, J. (2004). The Eden Project – making a connection. *Museum and society*, University of Leicester. 2 (3) 175-189

[16] Lausitzer und Mitteldeutsche Bergbau-Verwaltungsgesellschaft mbH. Einblicke. Sanierung, Sicherung und Rekultivierung von Bergwerken und Tagebauen. Views Redevelopment and recultivation of mining landscapes.

[17] <https://www.lmbv.de>

[18] <http://www.gemeinde-schipkau.de>

[19] <https://arena.gov.au>

[20] <https://www.veolia.com>

[21] Schultze, M. Pokrandt, K.-H., Hille, W. (2010). Pit lakes of the Central German lignite mining district: Creation, morphometry and water quality aspects. *Limnologica - Ecology and Management of Inland Waters*. 40. 148-155.

[22] Waikato District Council, New Zealand. (2009). Puketirini. Management Plan

[23] Andreas Keil und Burkhard Wetterau: Metropolis Ruhr. A Regional Study of the New Ruhr. First edition 2013. Essen: Regionalverband Ruhr, 2013. ISBN: 978-3-939234-05-0

[24] Regionalverband Ruhr. Emscher Landscape Park. Visitor's Guide

[25] PPC SA (2016). Environmental Impact Assessment Study for PPC Megalopolis Mines

[26] Louloudis, G. (2017). The worth of hydro geochemical data factor analysis (PCA) in interpretation of underground water origin. Megalopolis lignite bearing fields mine water and regional waters relations case study. 15th International Conference on Environmental Science and Technology. Rhodes, Greece, 31 August to 2 September 2017.

[27] Dimitrakopoulos, D., Vassiliou, E., Tsangaratos, P., & Ilia, I. (2010). Environmental management of mine water, considering European Water Legislation. Case study of Megalopolis mines. *Bulletin of the Geological Society of Greece*, 43(4), 1688-1696.

[28] MIN-GUIDE. Innovative Waste Management and Mine Closure. D5.2: Report on innovation evaluation criteria and best-case practices in waste management and mine closure. Final, July 2017.

Impact of Environmental Policies on Lignite Plants Generation In the Greek Wholesale Electricity Market

Iraklis Skoteinos¹, Asimina Vlachou², Giorgos Panagakis³ and Giorgos Orfanos⁴

¹ Independent Power Transmission Operator S.A., 89 Dyrachiou str., 10443, Athens, Greece

^{2,4} Public Power Corporation, 30 Chalkokondyli str., 10432, Athens, Greece

³ Volton S.A., 14 Skouze str., 18536, Pireas, Greece

ABSTRACT

Lignite is a significant and essential part of the Greek electricity generation mix. Historical data demonstrate the critical contribution of lignite plants throughout the years. EU energy policies are currently focusing, among other targets, to the decarbonization of European electricity market. Greece, as an EU member state follows the EU trend by adopting all relevant regulation at national level. Scope of this paper is to investigate the impact of environmental EU and national policies into the generation output of lignite plants in Greece. The measures of the EU Emissions Trading System (EU ETS) and the Transitional National Emission Reduction Plan (TNERP) are presented and their impact on lignite plants generation in the Greek Wholesale Market between 2013 and mid 2018 is discussed.

1. INTRODUCTION

By overviewing the European energy regulatory framework the past decade, it is clear that the goal of achieving a decarbonized economy is a solid and stable choice for the EU and this is very unlikely to change in future years. The Greek Electricity System used to be highly dependent during the past decades on lignite plants in order to meet its growing demand needs. However, Greece, as a member of the EU, has to align with the various European energy Directives and Guidelines regarding energy policies. Scope of this paper is to present two key European environmental policies which greatly affect lignite plants generation and to investigate, through a statistical analysis, their impact on lignite plants output in the Greek wholesale electricity market.

2. THE EU PATH TO DECARBONIZATION

In 1997, the Kyoto Protocol [1] set for the first time legally-binding emissions reduction targets, for 37 industrialized countries, leading to the need for policy instruments in order to meet the Protocol targets. In 2000, the European Commission presented a Green Paper [2], a draft of first ideas on the design of a greenhouse gas emissions trading scheme within the European Union, which served as a basis for creating the European Union Emissions Trading System (EU ETS). The EU ETS Directive [3] was adopted in 2003 and the system was launched in 2005, when the Kyoto Protocol entered into force.

In December 2009, The Treaty of Lisbon [4], set goals for the decarbonization of European energy markets, specifically stating that “*in the context of the establishment and functioning of the internal market and with regard for the need to preserve and improve the environment, Union policy on energy shall aim ... to promote energy efficiency and energy saving and the development of new and renewable forms of energy*”. Under this context, the Directive 2009/28/EC [5] set mandatory national targets for Renewable Energy Sources (RES) share in the generation mix until 2020 for all EU countries. In February 2015, the European Commission announced an Energy Union Package

[6], aiming to ensure affordable, secure and sustainable energy for Europe and its citizens, with specific measures covering five key areas including energy efficiency and decarbonization of the energy sector. This Energy Union Package is a policies framework regarding climate and energy with timeframe until 2020 and it combines various Union policy sectors into a single, coherent strategy. In order to achieve the ambitious EU commitment of an at least 40% domestic reduction in greenhouse gas emissions compared to 1990 by 2030, the package defines that “*the cornerstone of Europe’s climate policy is a well-functioning EU Emissions Trading System*”.

In 2015 the European Commission published another Energy Union Package, The Paris Protocol, a blueprint for tackling global climate change beyond 2020 [7]. This European Commission communication set the European expectations and goals regarding the new global agreement on climate change during the 2015 United Nations Climate Change Conference (also known as COP 21 or CMP11) [8] and it also set the next EU steps before the Conference by focusing on the 40% reduction in greenhouse gas emissions target. COP 21 negotiated the Paris Agreement [9], a global agreement on the reduction of climate change, dealing with greenhouse-gas-emissions mitigation, adaptation, and finance, starting in the year 2020, with the long-term goals to keep the increase in global average temperature to well below 2 °C above pre-industrial levels; and to limit the increase to 1.5 °C. In 2016, EU signed the Paris Agreement, among 55 other countries and the Agreement was set into force in November 2016.

By the end of 2016, the European Commission presented a new package of measures with the goal of providing the stable legislative framework needed to facilitate the clean energy transition, the so called “Winter Package”, or “Clean Energy Package” [10]. One of the fundamental goals of the package is decarbonization of the economy, driven by efficient integration of RES, dispersed generation, storage technologies, electric vehicles and demand response into energy markets. Currently, the European Commission proposals for renewable energy and energy efficiency are under Committee approval, while the amendments on Electricity Regulation and the Electricity Directive are being drafted.

2.1. The EU Emissions Trading System

The EU ETS aims to be the key tool for reducing greenhouse gas emissions cost-effectively in the European region by delivering a meaningful price on carbon emissions, thus stimulating cost-efficient greenhouse gas emission reductions. Furthermore, the European Commission wants the EU ETS to fully play its role as a technology neutral, cost-effective and EU-wide driver for low-carbon investments [6].

The EU ETS is based on the 'cap and trade' principle [11]. A cap is set on the total amount of certain greenhouse gases that can be emitted by installations covered by the System. Within the cap, companies receive or buy emission allowances which they can subsequently trade with one another according to their needs. The cap is being reduced over time in order for total emissions fall. After each year, a company must surrender enough allowances to cover all its emissions, otherwise heavy penalties are imposed. The system covers the various sectors and gases emissions that can be measured, reported and verified with a high level of accuracy, including carbon dioxide (CO₂) emissions in the power generation sector.

The EU ETS has undergone various changes since 2005 and it is currently on phase 3 (2013-2020), which focuses on a single, EU-wide cap and on auctioning as the default method for allocating allowances within the EU ETS. Auctioning takes place in two auction platforms, the European Energy Exchange (EEX) [12] and the ICE Futures Europe (ICE) [13]. The legislative framework of the EU ETS for phase 4 trading period was revised in 2018 [14] to enable it to achieve the EU's 2030 emission reduction targets in line with the 2030 climate and energy framework [15]. The revision focuses on increasing the pace of annual reductions in allowances by 2,2% per year and

on helping industry and the power sector to meet the innovation and investment challenges of the low-carbon transition via several low-carbon funding mechanisms.

According to last year’s report prepared by the European Environmental Agency (EEA) regarding Trends and projections in the EU ETS [16], the EU ETS has clearly resulted in reduction of emissions since 2005, as shown in Figure 1, however, projected scenarios reported by the EU Member States in 2017 do not align with the 2030 targets. The report indicates that until 2016, halfway of the third trading period, power generation continues to drive emission reductions in the EU ETS. According to the report, CO₂ emissions prices remained low during the examined period, however, during 2018 a sharp increase on prices was preserved [12], as shown in Figure 2, which may lead to significant changes in the verified emissions output of 2018, compared to previous years.

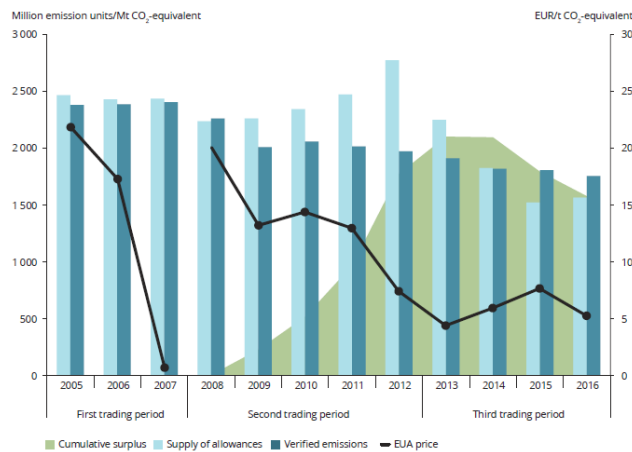


Figure 132. Emissions, allowances, surplus and prices in the EU ETS 2005-2016, source: [16]

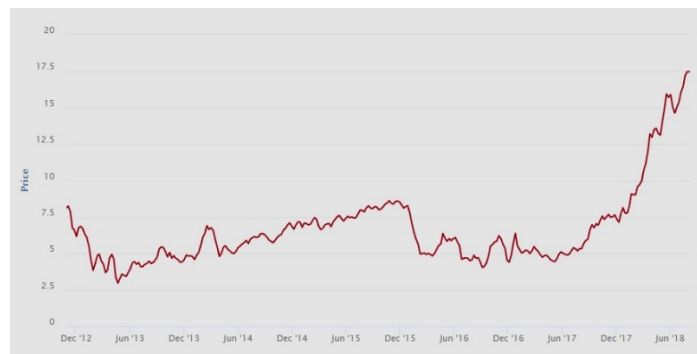


Figure 133. EU Futures CO₂ Emissions Allowances for 2013-2020 in the EEX Secondary Market, source: [12]

2.2. The Transitional National Emission Reduction Plan

In order to further control industrial emissions, the European Commission has developed a general framework based on integrated permitting, meaning that permits must take account of a plant’s complete environmental performance to avoid pollution being shifted from one medium - such as air, water and land - to another. Priority be given to preventing pollution by intervening at source and ensuring prudent use and management of natural resources. In Article 32 of the Directive 2010/75/EU [17], it is stated that “during the period from 1 January 2016 to 30 June 2020, Member States may draw up and implement a transitional national plan covering combustion plants which were granted the first permit before 27 November 2002 or the operators of which had submitted a complete application for a permit before that date, provided that the plant was put into operation no later than 27 November 2003”. The plan must cover emissions by one or more of the following

pollutants: nitrogen oxides, sulphur dioxide and dust. Article 33 of the same Directive states that “during the period from 1 January 2016 to 31 December 2023, combustion plants may be exempted from compliance ... and from their inclusion in the transitional national plan referred to in Article 32”, provided a set of conditions are fulfilled.

In this context, the Greek state drafted and submitted for approval to the European Commission its Transitional National Emission Reduction Plan (TNERP), concerning the following lignite units: Agios Dimitrios I-V, Kardias III-IV, Megalopoli III-IV and Meliti I. The TNERP was approved in 2013 and in November of the same year an amended plan was submitted to the European Commission, after request by the lignite units owner company, excluding Kardias III-IV units. The amended TNERP was approved by the European Commission with Decision C (2014) 4533/final [18] and it was implemented into national Law the next year. In addition, the lignite units’ owner company, which was until May 2018 the sole owner of all lignite units in the Greek electricity System, submitted for approval to the European Commission a request for exemption from compliance for units Amyndeo I-II and Kardias I-IV, according to Article 33 of the Directive 2010/75/EU [17], declaring that those units will not operate for more than 17.500 operating hours between 2016 and 2023. This approach was chosen by the company since those units also provide district heating services for six months per year (October – March). Finally, the company has also decided to perform all necessary environmental upgrades on units Agios Dimitrios I-V in order to comply with the TNERP targets. Application of the aforementioned requirements will lead to a 2.451 MW decrease of lignite units’ total net installed capacity by 2030, which is currently 3.904 MW.

3. LIGNITE UNITS IN THE GREEK WHOLESALE MARKET

3.1. The Greek Wholesale Electricity Market Model

The Greek wholesale day-ahead electricity market is currently organized as a centralized mandatory pool [19, 20]. According to this market model, each generating unit submits energy and reserves offers in addition to declarations of techno-economic data and availabilities. The Market Operator solves a short-term unit commitment problem on a daily basis, the Day-Ahead Scheduling (DAS), where a 24-hour co-optimization of energy and reserve offers is performed under a set of unit and system constraints (i.e. minimum-up/down time constraints, min/max power output restrictions, ramp up/down rate limits, system reserves requirements, transmission limits, etc.). The DAS objective is the maximization of the social welfare, or equivalently the minimization of the total production cost minus the load utility, within the 24-hour period of the next day [21]. In the mandatory pool model all energy offers and bids are required to pass through the Day-Ahead market, while no physical delivery bilateral energy transactions are allowed. The Greek electricity wholesale market is organized by this market model since 2012 and it is governed by the Market and System Operator Codes [22, 23], which were approved by the Regulatory Authority for Energy (RAE) the same year [24, 25].

The aforementioned optimization of offers and bids under the various technical system and units constraints within the 24-hour period of the day leads to a market model that actually co-optimizes both energy and reserves within this time frame by providing a market solution which is also operational from the system view. However, this approach, due to mainly the system reserves requirements, the minimum-up/down time constraints of generating units and the startup cost of generating units which has been modeled in the market algorithm as a shutdown cost in order to disincentivize frequent generating units shut down, leads to market solutions in which units may be chosen by the algorithm to be online, even for the entire 24-hour period, at their technical minimum, regardless of the System Marginal Price (SMP) being lower than the unit submitted offer. This approach leads to technically feasible market solutions, where however, the above unit state is very common, as it is shown in the past market solutions [26],

Another important element in the current Greek wholesale day-ahead electricity market are generating units' offers limitations. In the Market Operator Code it is specified that all generating units must submit offers to the Day-Ahead Market above a certain threshold in €/MWh, which is their calculated minimum average variable cost. This requirement was set by the Regulator in order to mitigate exercise of market power by the generators, especially since the market share of the incumbent remains high as shown in the Market Operator and the System Operator reports [27, 28].

3.2. Lignite Units In The Greek Electricity System

According to the latest Transmission System Operator yearly adequacy report [29] available, the total installed net capacity of lignite units in the Greek Electricity System is 3.904 MW, as shown in Table 1. Until 2030 it is expected the decommissioning of lignite units of total installed net capacity of 2.451 MW and the construction of a new lignite unit in Ptolemaida of 660 MW installed capacity, while it is yet unknown if the permit of Meliti II specified in the TNERP will lead to an actual investment.

Table 25. Lignite Installed Net Capacity in the Greek Electricity System

Unit Name	Installed Net Capacity (MW)
Agios Dimitrios I	274
Agios Dimitrios II	274
Agios Dimitrios III	283
Agios Dimitrios IV	283
Agios Dimitrios V	342
Amyndeo I	273
Amyndeo II	273
Kardia I	271
Kardia II	271
Kardia III	280
Kardia IV	280
Megalopoli III	255
Megalopoli IV	256
Meliti I	289
Total	3.904

An important characteristic of all lignite units in the Greek electricity system is that their technical minimum is quite high compared to their net capacity, with this ratio being usually above 55%. Furthermore, most of the units are quite old, resulting in rather lower efficiency, while the lignite quality is poor, with a lower heating value below 1.400 kcal/kg. All the above factors lead to a specific emission factor for Greek lignite units between 1 ton CO₂/MWh for newer and more efficient plants to 1,5 ton CO₂/MWh for older plants, which is approximately three times higher than a typical natural gas unit, which has a specific emission factor of 0,44 ton CO₂/MWh [30, 31]. This has great impact on the lignite unit variable cost which is formed by three components; a fuel cost, an operation and maintenance cost and an emissions cost component. Lastly, Greek lignite units have generally high Equivalent Forced Outage Rate demand (EFOR_D), resulting in lower overall average unit availability, compared to a typical Greek System natural gas-fired unit [29].

4. ANALYSIS

4.1. Methodology Overview

The impact of the EU ETS and the TNERP policies on lignite plants generation in the wholesale market is being examined for the period from January 1st 2013 until June 30th 2018. During those years, the Greek wholesale electricity market model had minor changes affecting production units dispatch, while this period covers the entire phase 3 application of the EU ETS until

now. Furthermore, it includes the period beyond 2016 when TNERP was applied. Therefore, it covers the entire period of the application of a stable and mature environmental market mechanism, but also a discontinuity caused by the application of a mechanism that directly affects lignite units generation.

The analysis approach is based on statistical analysis of various key parameters that are assumed to have impact on lignite generation. Therefore, the dependent variable of the statistical analysis is lignite generation (MWh), while the control variables decided are a) lignite units' availability (MW) b) lignite units' net capacity (MW) c) emission rights price (€/tn) d) System load (MWh) and e) SMP (€/MWh).

Regarding variables a) to c) which are related to the units, considering high EFOR_D of lignite units, it was assumed that average availability should be taken into account on the statistical analysis. Regarding total net capacity, it is obvious that it is related to the production output of lignite units, regardless of the fact that no new lignite unit was commissioned during the examined period. Emission rights price is also a key variable related to the EU ETS mechanism, which directly affects lignite units' minimum average variable cost, which is, as discussed above, the lower bidding cap for all generating units; furthermore it affects one of the three variable cost elements of production units. Regarding variables d) and e), the total System load has a direct impact on thermal units generation, while the SMP price is another potential market indicator. Additionally, it should be noted that SMP is related to the emission rights price, which is a cost component affecting all thermal units.

Regarding data sampling, hourly data could have been used for four out of five variables, however, the emission rights price does not change throughout a month's period. The producer owning the Greek System lignite units, purchases carbon emission rights which are being allocated to generating units at the end of each month for the next month's period, therefore thermal units emission variable cost remains constant throughout each month. For this reason, monthly values were chosen for the performed analysis; a total of 66 (months) x 6 (variables) values. Regarding lignite generation and system load, total monthly values in MWh were used; for availability and net capacity average monthly values summed for all units in MW were calculated; while for the emission rights price and the SMP, the monthly average price in €/MWh was used.

Statistical analysis follows three steps. Initially, graphical analysis is performed in order to identify possible correlation of each variable with the dependent variable. On the next step, Analysis Of Variance (ANOVA) is performed, as a means for exploratory data analysis regarding yearly and monthly lignite units production [32]. Lastly, based on the ANOVA results, a regression model is presented, serving as a basis for performing stepwise regression and forward selection. The later method involves starting with no variables in the model, testing the addition of each variable using a chosen model fit criterion, adding the variable whose inclusion gives the most statistically significant improvement of the fit and repeating this process until none improves the model to a statistically significant extent. All statistical analysis was performed with IBM SPSS 24 [33, 34].

4.2. Graphical Analysis

Figures 3 and 4 show that there is no clear correlation between lignite units' production and CO₂ price. Some outliers are distinctively shown on the bottom right of Figure 3. Figure 4 however shows that that the outlier data belong in year 2018, during which, a CO₂ emissions rights price rally was observed. A more clear correlation could be identified if values referred to daily or weekly data, or if more 2018 high CO₂ emissions rights price data were available.

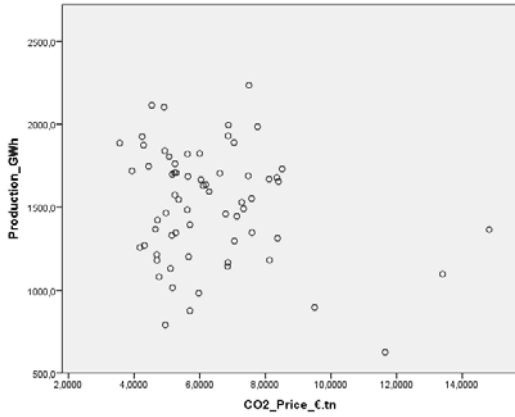


Figure 134. Lignite production and CO₂ prices plot

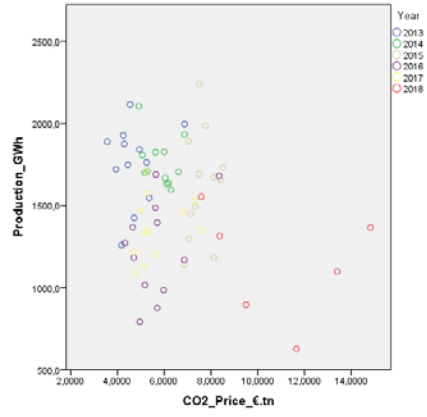


Figure 135. Lignite production and CO₂ prices plot, years indication

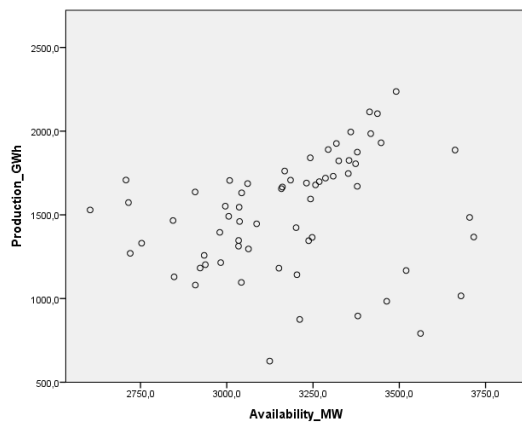


Figure 136. Lignite production and average monthly availability

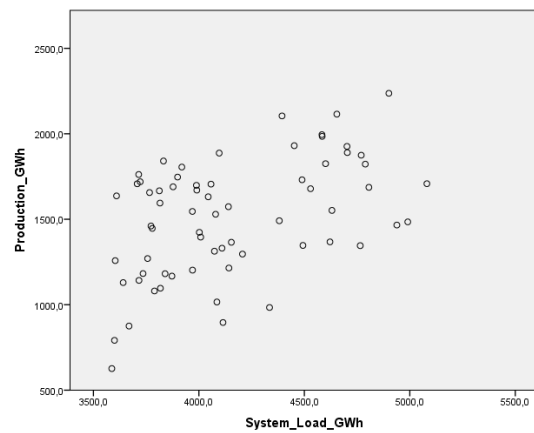


Figure 137. Lignite production and System Load

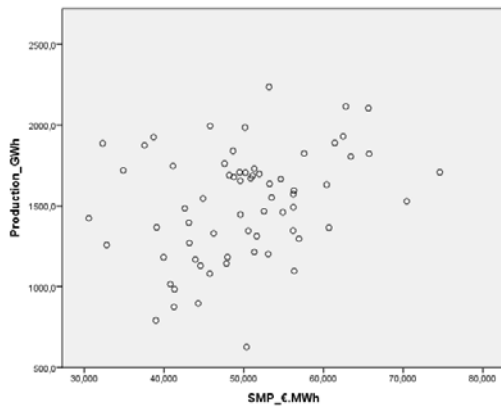


Figure 138. Lignite production and SMP

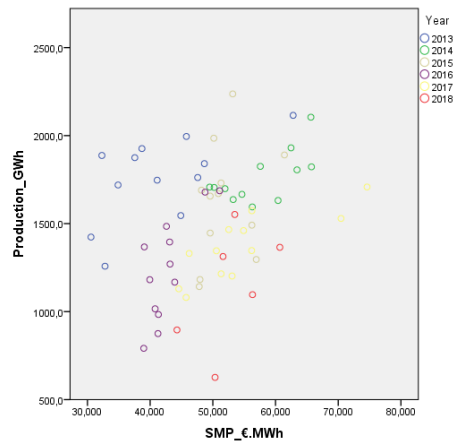


Figure 139. Lignite production and SMP, years indication

Figure 5 shows light correlation between lignite units' production and average monthly availability, which however faints as availability reaches higher values. Figures 6-8 show a similar, light correlation between lignite units' production and system load (Figure 6) and the SMP (Figures 7-8). Figure 8 shows however a distinct values group for 2018 regarding the SMP.

4.3. Statistical Analysis

Table 2 shows the results of the ANOVA [35] tests when comparing mean yearly lignite production per year. The mean difference of the test is statistically significant at a 0,05 level according to the Least Significant Difference (LSD [36]) test. A significant result means that at least one of the groups tested differs from the other groups. By analyzing the results, mean production values for years 2013, 2014 and 2015 but also for years 2016, 2017 and 2018 are statistically equal and marked on the ANOVA table with yellow color, while Figure 9 means plot shows the same grouping.

Table 26. ANOVA test, LSD, multiple comparisons, dependent variable: Production_GWh

(I) Year	(J) Year	Mean Difference (I-J)	Std. Error	Sig.	95% Confidence Interval	
					Lower Bound	Upper Bound
2013	2014	-2,8500	105,3374	,979	-213,556	207,856
	2015	139,7000	105,3374	,190	-71,006	350,406
	2016	516,3167*	105,3374	,000	305,611	727,023
	2017	392,2917*	105,3374	,000	181,586	602,998
	2018	616,3750*	129,0114	,000	358,314	874,436
2014	2013	2,8500	105,3374	,979	-207,856	213,556
	2015	142,5500	105,3374	,181	-68,156	353,256
	2016	519,1667*	105,3374	,000	308,461	729,873
	2017	395,1417*	105,3374	,000	184,436	605,848
	2018	619,2250*	129,0114	,000	361,164	877,286
2015	2013	-139,7000	105,3374	,190	-350,406	71,006
	2014	-142,5500	105,3374	,181	-353,256	68,156
	2016	376,6167*	105,3374	,001	165,911	587,323
	2017	252,5917*	105,3374	,020	41,886	463,298
	2018	476,6750*	129,0114	,000	218,614	734,736
2016	2013	-516,3167*	105,3374	,000	-727,023	-305,611
	2014	-519,1667*	105,3374	,000	-729,873	-308,461
	2015	-376,6167*	105,3374	,001	-587,323	-165,911
	2017	-124,0250	105,3374	,244	-334,731	86,681
	2018	100,0583	129,0114	,441	-158,003	358,120
2017	2013	-392,2917*	105,3374	,000	-602,998	-181,586
	2014	-395,1417*	105,3374	,000	-605,848	-184,436
	2015	-252,5917*	105,3374	,020	-463,298	-41,886
	2016	124,0250	105,3374	,244	-86,681	334,731
	2018	224,0833	129,0114	,088	-33,978	482,145
2018	2013	-616,3750*	129,0114	,000	-874,436	-358,314
	2014	-619,2250*	129,0114	,000	-877,286	-361,164
	2015	-476,6750*	129,0114	,000	-734,736	-218,614
	2016	-100,0583	129,0114	,441	-358,120	158,003
	2017	-224,0833	129,0114	,088	-482,145	33,978

*. The mean difference is significant at the 0.05 level.

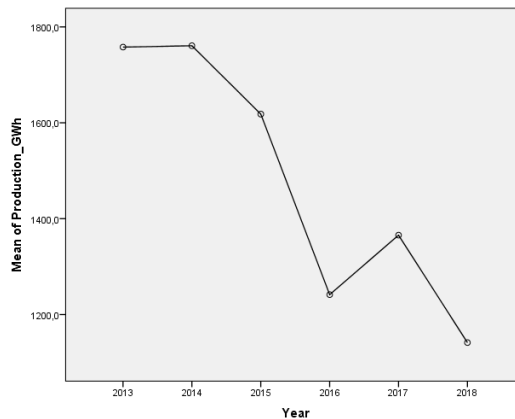


Figure 140. Means plot of yearly lignite production

In Table 3, Tukey's range test (Tukey's HSD [37]) results are presented, where the grouping identified for years 2013-2015 and 2016-2018 is also clearly shown, indicated by yellow and red color, while a third group for years 2015 and 2017 is also identified.

Table 27. Tukey's HSD for mean yearly lignite production

Tukey HSD ^{a,b}	Year	N	Subset for alpha = 0.05		
			1	2	3
	2018	6	1141,483		
	2016	12	1241,542		
	2017	12	1365,567	1365,567	
	2015	12		1618,158	1618,158
	2014	12			1757,858
	2013	12			1760,708
	Sig.		,372	,244	,809

Means for groups in homogeneous subsets are displayed.
 a. Uses Harmonic Mean Sample Size = 10,286.
 b. The group sizes are unequal. The harmonic mean of the group sizes is used.

Table 4 shows the results of the ANOVA tests when monthly production is considered. The test compares all mean production values per pair of months, regardless of year, showing that most months have statistically equal mean values.

Table 28. Tukey HSD, multiple comparisons, dependent variable: Production_GWh

(I) Month	(J) Month	Mean Difference (I-J)	Std. Error	Sig.	95% Confidence Interval	
					Lower Bound	Upper Bound
1	2	371,1667	167,9649	,550	-202,437	944,770
	3	510,9167	167,9649	,125	-62,687	1084,520
	4	723,9833*	167,9649	,004	150,380	1297,587
	5	500,5000	167,9649	,143	-73,104	1074,104
	6	348,2000	167,9649	,643	-225,404	921,804
	7	44,4433	176,1631	1,000	-557,157	646,044
	8	131,4433	176,1631	1,000	-470,157	733,044
	9	342,3033	176,1631	,728	-259,297	943,904
	10	353,1833	176,1631	,688	-248,417	954,784
	11	210,7833	176,1631	,987	-390,817	812,384
	12	59,4033	176,1631	1,000	-542,197	661,004
	2	1	-371,1667	167,9649	,550	-944,770
3		139,7500	167,9649	,999	-433,854	713,354
4		352,8167	167,9649	,625	-220,787	926,420
5		129,3333	167,9649	1,000	-444,270	702,937
6		-22,9667	167,9649	1,000	-596,570	550,637
7		-326,7233	176,1631	,781	-928,324	274,877
8		-239,7233	176,1631	,966	-841,324	361,877
9		-28,8633	176,1631	1,000	-630,464	572,737
10		-17,9833	176,1631	1,000	-619,584	583,617
11		-160,3833	176,1631	,999	-761,984	441,217
12		-311,7633	176,1631	,827	-913,364	289,837
3		1	-510,9167	167,9649	,125	-1084,520
	2	-139,7500	167,9649	,999	-713,354	433,854
	4	213,0667	167,9649	,980	-360,537	786,670
	5	-10,4167	167,9649	1,000	-584,020	563,187
	6	-162,7167	167,9649	,998	-736,320	410,887
	7	-466,4733	176,1631	,280	-1068,074	135,127
	8	-379,4733	176,1631	,588	-981,074	222,127
	9	-168,6133	176,1631	,998	-770,214	432,987
	10	-157,7333	176,1631	,999	-759,334	443,867
	11	-300,1333	176,1631	,859	-901,734	301,467
	12	-451,5133	176,1631	,326	-1053,114	150,087
	4	1	-723,9833*	167,9649	,004	-1297,587
2		-352,8167	167,9649	,625	-926,420	220,787
3		-213,0667	167,9649	,980	-786,670	360,537

	5	-223,4833	167,9649	,971	-797,087	350,120
	6	-375,7833	167,9649	,531	-949,387	197,820
	7	-679,5400*	176,1631	,015	-1281,141	-77,939
	8	-592,5400	176,1631	,057	-1194,141	9,061
	9	-381,6800	176,1631	,580	-983,281	219,921
	10	-370,8000	176,1631	,622	-972,401	230,801
	11	-513,2000	176,1631	,165	-1114,801	88,401
	12	-664,5800*	176,1631	,019	-1266,181	-62,979
5	1	-500,5000	167,9649	,143	-1074,104	73,104
	2	-129,3333	167,9649	1,000	-702,937	444,270
	3	10,4167	167,9649	1,000	-563,187	584,020
	4	223,4833	167,9649	,971	-350,120	797,087
	6	-152,3000	167,9649	,999	-725,904	421,304
	7	-456,0567	176,1631	,311	-1057,657	145,544
	8	-369,0567	176,1631	,628	-970,657	232,544
	9	-158,1967	176,1631	,999	-759,797	443,404
	10	-147,3167	176,1631	,999	-748,917	454,284
	11	-289,7167	176,1631	,884	-891,317	311,884
	12	-441,0967	176,1631	,360	-1042,697	160,504
6	1	-348,2000	167,9649	,643	-921,804	225,404
	2	22,9667	167,9649	1,000	-550,637	596,570
	3	162,7167	167,9649	,998	-410,887	736,320
	4	375,7833	167,9649	,531	-197,820	949,387
	5	152,3000	167,9649	,999	-421,304	725,904
	7	-303,7567	176,1631	,849	-905,357	297,844
	8	-216,7567	176,1631	,984	-818,357	384,844
	9	-5,8967	176,1631	1,000	-607,497	595,704
	10	4,9833	176,1631	1,000	-596,617	606,584
	11	-137,4167	176,1631	1,000	-739,017	464,184
	12	-288,7967	176,1631	,886	-890,397	312,804
7	1	-44,4433	176,1631	1,000	-646,044	557,157
	2	326,7233	176,1631	,781	-274,877	928,324
	3	466,4733	176,1631	,280	-135,127	1068,074
	4	679,5400*	176,1631	,015	77,939	1281,141
	5	456,0567	176,1631	,311	-145,544	1057,657
	6	303,7567	176,1631	,849	-297,844	905,357
	8	87,0000	183,9963	1,000	-541,351	715,351
	9	297,8600	183,9963	,894	-330,491	926,211
	10	308,7400	183,9963	,870	-319,611	937,091
	11	166,3400	183,9963	,999	-462,011	794,691
	12	14,9600	183,9963	1,000	-613,391	643,311
8	1	-131,4433	176,1631	1,000	-733,044	470,157
	2	239,7233	176,1631	,966	-361,877	841,324
	3	379,4733	176,1631	,588	-222,127	981,074
	4	592,5400	176,1631	,057	-9,061	1194,141
	5	369,0567	176,1631	,628	-232,544	970,657
	6	216,7567	176,1631	,984	-384,844	818,357
	7	-87,0000	183,9963	1,000	-715,351	541,351
	9	210,8600	183,9963	,991	-417,491	839,211
	10	221,7400	183,9963	,986	-406,611	850,091
	11	79,3400	183,9963	1,000	-549,011	707,691
	12	-72,0400	183,9963	1,000	-700,391	556,311
9	1	-342,3033	176,1631	,728	-943,904	259,297
	2	28,8633	176,1631	1,000	-572,737	630,464
	3	168,6133	176,1631	,998	-432,987	770,214
	4	381,6800	176,1631	,580	-219,921	983,281
	5	158,1967	176,1631	,999	-443,404	759,797
	6	5,8967	176,1631	1,000	-595,704	607,497
	7	-297,8600	183,9963	,894	-926,211	330,491
	8	-210,8600	183,9963	,991	-839,211	417,491
	10	10,8800	183,9963	1,000	-617,471	639,231
	11	-131,5200	183,9963	1,000	-759,871	496,831
	12	-282,9000	183,9963	,923	-911,251	345,451
10	1	-353,1833	176,1631	,688	-954,784	248,417
	2	17,9833	176,1631	1,000	-583,617	619,584
	3	157,7333	176,1631	,999	-443,867	759,334
	4	370,8000	176,1631	,622	-230,801	972,401
	5	147,3167	176,1631	,999	-454,284	748,917

	6	-4,9833	176,1631	1,000	-606,584	596,617
	7	-308,7400	183,9963	,870	-937,091	319,611
	8	-221,7400	183,9963	,986	-850,091	406,611
	9	-10,8800	183,9963	1,000	-639,231	617,471
	11	-142,4000	183,9963	1,000	-770,751	485,951
	12	-293,7800	183,9963	,903	-922,131	334,571
11	1	-210,7833	176,1631	,987	-812,384	390,817
	2	160,3833	176,1631	,999	-441,217	761,984
	3	300,1333	176,1631	,859	-301,467	901,734
	4	513,2000	176,1631	,165	-88,401	1114,801
	5	289,7167	176,1631	,884	-311,884	891,317
	6	137,4167	176,1631	1,000	-464,184	739,017
	7	-166,3400	183,9963	,999	-794,691	462,011
	8	-79,3400	183,9963	1,000	-707,691	549,011
	9	131,5200	183,9963	1,000	-496,831	759,871
	10	142,4000	183,9963	1,000	-485,951	770,751
	12	-151,3800	183,9963	1,000	-779,731	476,971
12	1	-59,4033	176,1631	1,000	-661,004	542,197
	2	311,7633	176,1631	,827	-289,837	913,364
	3	451,5133	176,1631	,326	-150,087	1053,114
	4	664,5800*	176,1631	,019	62,979	1266,181
	5	441,0967	176,1631	,360	-160,504	1042,697
	6	288,7967	176,1631	,886	-312,804	890,397
	7	-14,9600	183,9963	1,000	-643,311	613,391
	8	72,0400	183,9963	1,000	-556,311	700,391
	9	282,9000	183,9963	,923	-345,451	911,251
	10	293,7800	183,9963	,903	-334,571	922,131
	11	151,3800	183,9963	1,000	-476,971	779,731

*. The mean difference is significant at the 0.05 level.

Table 5 displays a better grouping of data, where statistically equal means for monthly production are clustered. Mean production values form homogenous groups for months July, December and January, while the rest of the months is grouped together. Also, April forms a different group according to production means. This information is indicating that dummy variables should be used during the modeling process. This observation is also clearly shown in the monthly production means plot in Figure 10.

Table 29. Data grouping according to statistically equal means for monthly production

Production_GWh			
Tukey HSD ^{a,b}			
Month	N	Subset for alpha = 0.05	
		1	2
4	6	1097,400	
3	6	1310,467	1310,467
5	6	1320,883	1320,883
2	6	1450,217	1450,217
10	5	1468,200	1468,200
6	6	1473,183	1473,183
9	5	1479,080	1479,080
11	5	1610,600	1610,600
8	5	1689,940	1689,940
12	5		1761,980
7	5		1776,940
1	6		1821,383
Sig.		,057	,170

Means for groups in homogeneous subsets are displayed.

a. Uses Harmonic Mean Sample Size = 5,455.

b. The group sizes are unequal. The harmonic mean of the group sizes is used

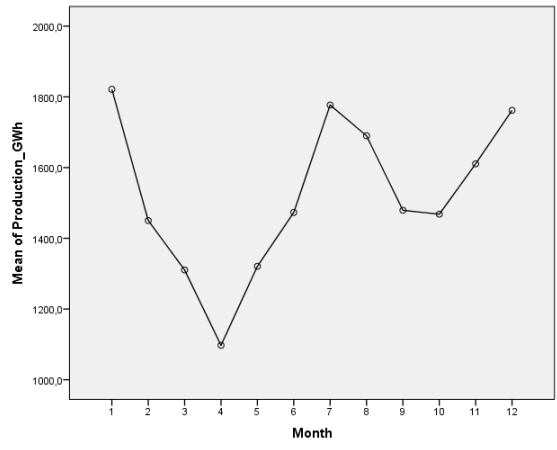


Figure 141. Monthly production means plot

If more data were available, it would be interesting to investigate the interaction between years and months, however, those tests are not performed due to the small data set available, requiring a bigger number of degrees of freedom in order to estimate possible interactions.

4.4. Modelling

Purpose of the modelling process is to investigate correlation between lignite units production with the rest of the variables. From the ANOVA analysis above, it is shown that lignite production means for years 2013-2015 and 2016-2018 do not differ statistically. Furthermore, a clear reduction trend is obvious, as shown in Figure 10. The same figure also shows seasonality, which is however less obvious for years 2014 and 2017.

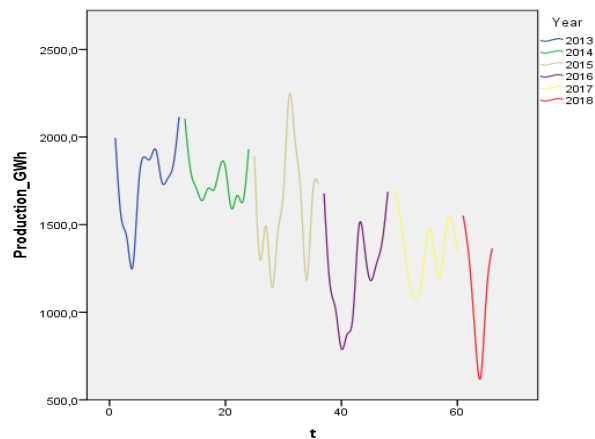


Figure 142. Lignite Production means trend

The total data available is limited, therefore it is not possible to perform time series modelling, where at least 5.000 values would be needed in order to draw clear conclusions for this set of variables [38]; therefore, regression modelling is performed [39]. In order to import seasonality into the model, dummy variables are created, taking the value “1”, if the value refers to a specific year or month and taking the value “0” elsewhere. This means that 5 dummy variables should be used for the 6 years examined, standing for 6 years minus 1 for the reference year and 11 dummy variables should be used for the 12 months examined, again standing for 12 months minus 1 for the reference

month. The reference year and month are arbitrarily chosen. However, according to the variance analysis for mean yearly production in Table 3, only one dummy variable can be used for the modeling process, taking the value “0” for reference years 2013-2015 and 1 for the rest of the years. In the same way, according to Table 5 only two dummy variables could be used, where the first takes the value “1” for months 7, 12, 1 and “0” elsewhere, while the second takes the value “1” for months 2,3,5,6,8,9,10,11 and “0” elsewhere, with the reference month being month April.

The rest of the variables X are the one initially chosen, presented in 4.1; a) lignite units’ availability (MW) b) lignite units’ net capacity (MW) c) emission rights price (€/tn) d) System load (MWh) and e) SMP (€/MWh). The results of regression modeling are presented in Table 6.

Table 30. Regression model summary

Model Summary ^b										
Model	R	R Square	Adjusted R Square	Std. Error of the Estimate	Change Statistics					Durbin-Watson
					R Square Change	F Change	df1	df2	Sig. F Change	
1	,874 ^a	,765	,736	175,1525	,765	26,900	7	58	,000	1,340

a. Predictors: (Constant), D_Month_not_1_7_12, Dummy_year, CO2_Price_€/tn, Availability_MW, System_Load_GWh, SMP_€/MWh, D_Month1_7_12

b. Dependent Variable: Production_GWh

The model R² change is 76,5%, which is satisfactory but not high enough in order for the model to be used for predictions. This value means that approximately 76,5% of unexplained dispersion of variable Y, that is lignite production, can be explained by the independent variables X and it implies that either a variable is missing from the model or X variables transformation is necessary. Durbin Watson value [40] is near the rejection area, therefore, the existence of positive correlation is marginally not rejected, which is nevertheless something common for time series data. However, as already stated, the model cannot be used for predictions, therefore, its performance is satisfactory.

Table 7 displays the coefficients of the model, where it is shown that availability is statistically unimportant to a great degree. System load is also marginally statistically unimportant, while all other variables are statistically important. All diagnostics of the model (homoscedasticity, normality, multicollinearity etc.) have no negative indications, therefore we assume that model conclusions are statistically correct.

Table 31. Regression model coefficients

Coefficients ^a						
Model		Unstandardized Coefficients		Standardized Coefficients	t	Sig.
		B	Std. Error	Beta		
1	(Constant)	597,288	453,034		1,318	,193
	CO2_Price_€/tn	-26,992	11,863	-,162	-2,275	,027
	System_Load_GWh	,172	,091	,209	1,887	,064
	SMP_€/MWh	6,481	3,127	,171	2,073	,043
	Availability_MW	-,008	,103	-,006	-,080	,936
	Dummy_year	-420,880	47,506	-,619	-8,859	,000
	D_Month1_7_12	408,437	128,601	,517	3,176	,002
	D_Month_not_1_7_12	251,016	84,750	,350	2,962	,004

a. Dependent Variable: Production_GWh

In order to address the fact that some of the variables of the regression model are statistically unimportant, stepwise regression and forward selection is performed, since those methods are used in

order to select only the statistical important variables on our model, by excluding variables that contribute the least. Regression modeling identified an unimportant variable, unit availability. By performing stepwise regression, month dummy variables which were previously statistically important are excluded from the model, indicating that more month dummy variables could be used, making however the model more complex. Month dummy variables express seasonality, therefore it was decided to keep them in the final model presented in Table 8.

Table 32. Final stepwise regression and forward selection model

Model		Coefficients ^a					Collinearity Statistics	
		Unstandardized Coefficients		Standardized Coefficients	t	Sig.	Tolerance	VIF
		B	Std. Error	Beta				
1	(Constant)	-1105,979	583,356		-1,896	,063		
	Dummy_year	2260,151	633,725	3,326	3,566	,001	,004	256,370
	D_Month1_7_12	319,398	118,910	,405	2,686	,009	,150	6,686
	D_Month_not_1_7_12	201,923	78,432	,281	2,574	,013	,284	3,520
	Availability_MW	,533	,171	,395	3,115	,003	,211	4,739
	System_Load_GWh	,212	,081	,258	2,604	,012	,345	2,896
	Inter_Year_Avail	-,847	,197	-3,917	-4,297	,000	,004	244,982

a. Dependent Variable: Production_GWh

This model has improved R^2 of 80%, compared to the initial regression model and it takes into account system load, availability, months and years as described above, but also the interaction between availability and year, showing that availability had different impact on lignite production during years 2013-2015 compared to years 2016-2018. However, an alternative model was also examined, as shown in Table 9, which takes into account CO₂ prices, the SMP, months and years, as described above, without considering any interactions of the two variables with months or years.

Table 33. Alternative stepwise regression and forward selection model

Model		Coefficients ^a					Collinearity Statistics	
		Unstandardized Coefficients		Standardized Coefficients	t	Sig.	Tolerance	VIF
		B	Std. Error	Beta				
1	(Constant)	1182,919	142,588		8,296	,000		
	Dummy_year	-406,851	44,702	-,599	-9,101	,000	,965	1,036
	D_Month1_7_12	586,353	90,428	,743	6,484	,000	,318	3,140
	D_Month_not_1_7_12	317,743	78,307	,443	4,058	,000	,351	2,849
	CO2_Price_€tn	-29,928	11,703	-,180	-2,557	,013	,846	1,182
	SMP_€MWh	6,993	2,818	,185	2,481	,016	,753	1,328

a. Dependent Variable: Production_GWh

This model has lower R^2 than the model presented in Table 8, of 74,9%. If all variables and all interactions are inputted in a stepwise regression and forward selection model, the final model after the elimination process is the one presented Table 8, as it shows that CO₂ prices and the SMP do not contribute statistically to the model. However, the model presented in Table 9 is worth mentioning, since it shows that CO₂ prices and the SMP alone can explain lignite production.

5. CONCLUSIONS

As shown in the graphical analysis, there is no clear correlation between lignite production and CO₂ prices for years 2013-2017. However, the 2018 outlier data indicate that once CO₂ prices start to

rise sharply, a clear correlated pattern appears. This could mean that relatively low CO₂ emission rights prices during the first years of the EU ETS mechanism, typically between 5 and 8 €/ton CO₂, did not have a direct impact on lignite units production, an observation which is in line with the EEA 2017 report [16]. Graphical analysis also shows that average availability, system load and the SMP are more correlated to lignite production. Reduced CO₂ prices correlation to lignite production can also be an impact of the current market model, which, as described, promotes keeping lignite units online, regardless of their market offers, due to system or unit technical constraints [21]. Finally, it should be noted that lignite units are considered as base units and this is reflected in the producer bidding strategy in the Day-Ahead market. Therefore, it seems that the EU ETS mechanism, even though it directly affects lignite offers, even in a greater degree than competitive gas technology units [30], due to a) relative low emissions allowances prices present for most of the examined period, b) the pool market model and possibly c) producer's bidding strategy, had limited impact on lignite units production, at least compared to the other parameters examined.

The ANOVA tests and the Tukey's range test when examining mean yearly production, show that two distinct groups of data exist; one for the period 2013-2015 and one for the period 2016-2018. This is a clear indication that the TNERP, applied in 2016 [17, 18], had a direct impact on lignite generation. According to the scheme, some lignite units had to comply with the restriction for 17.500 operating hours between 2016 and 2023, thus remaining online only for a few months each year past 2016. Furthermore, in order to comply with the scheme requirements, some lignite units had to reduce generation levels, in order to not exceed a certain level of SO_x and NO_x emissions, while some other units have to remain offline in order to perform all necessary environmental upgrades to meet emissions requirements set by the TNERP. It should be also noted that application of TNERP in 2016 was followed by a considerable decrease in natural gas prices [41], which resulted in a change of the merit order list of Greek thermal units. When examining mean monthly lignite units productions according to ANOVA and Tukey's range tests, three distinct groups are identified, one for months July, December and January, one for month April and one for the rest of the months. The first set of months consists of the peak load months [29], therefore it is expected all thermal plants production to be high during this period, while April is typically the lowest demand month in Greece, usually including the hour of minimum demand during the year, on Sunday Easter. However, regardless of seasonality, lignite units with an operating hours limitation were chosen to be online during peak months by the producer, in order to meet yearly peaking demand. Regarding the rest of the months, further grouping could be performed, for example months were lignite units provide heating services (October – March period), resulting in two more subgroups, one for months October, November, February and March and one for May, June, August and September. Further tests were however not performed, due to the small data set available, requiring a bigger number of degrees of freedom in order to estimate possible interactions; and due to the fact that this would lead to a complex model, when dummy variables during the modelling phase had to be used. This approach is reserved for future research after phase three of the EU ETS has been concluded.

Observations of the graphical analysis and the statistical tests were used in order to create a statistical model in order to investigate correlation between lignite units production with the rest of the examined variables. Due to lack of sufficient data in order to perform time-series modeling, regression modeling was performed. The model was enhanced by dummy variables in order to include the years and months data clustering reflecting seasonality but the resulting R² of 76,5% makes it not suitable for forecasting purposes. Model fit also indicates that either a variable is missing from the model or some X variables transformation is necessary. As already discussed, further months grouping could provide better results, while, regarding the missing variable, the natural gas price could be a possible option. However, an interesting observation concluded by the model coefficients is that average lignite availability is statistically insignificant. This could be explained by the fact that in the Greek System for the examined period there is sufficient lignite capacity, therefore, the outages rate of lignite units does not affect greatly lignite units' production.

The regression model also shows that system load is statistically unimportant, but it should be taken into account that month dummy variables already reflect load seasonality.

Stepwise regression and forward selection was performed in order to improve the initial regression model, a method which eliminates statistically unimportant variables. The analysis also took into account interactions between dependent variables, resulting in two improved models. The first model, with an R^2 of 80%, describes lignite production by taking into account system load, availability, months and years, but also the interaction between availability and year, showing that availability had different impact on lignite production during years 2013-2015 compared to years 2016-2018. This observation validates once more the impact of TNERP application on lignite production in 2016, while this model totally ignores CO₂ emissions allowances prices, showing that EU ETS has insignificant impact on lignite production. From the policy maker point of view, this shows that an environmental mechanism that sets clear emission and operation restrictions has immediate impact on high polluting units production. However, the second model, with an R^2 of 74.9%, takes into account CO₂ prices, the SMP, months and years, without considering any interactions between those two variables and months or years, showing that CO₂ prices and the SMP alone can explain lignite production. The model presented in Table 9 shows that lignite production increases as SMP increases, which is expected since after 2016 natural gas prices decrease lignite units are more expensive than gas-fired units, therefore acting also as peak units along with hydro units and interconnections [26], while lignite production decreases as CO₂ emissions price rises. This shows that the market alone can provide the right incentives towards production reduction of high polluting technologies, provided the right price signal is given by market emissions reduction mechanisms, such as the EU ETS.

Concluding the analysis, it is shown that both the TNERP and the EU ETS mechanisms do have an impact on lignite units production in the Greek System. However the degree of observed results depends on structural parameters such as the market model or the cap of emission allowances traded, but also on other factors such as competing technologies production cost and units availability. The findings presented in this paper can be of use to either policy makers when designing environmental policies or to market participants when considering lignite units market participation and estimation of future lignite exploitation.

REFERENCES

- [1] KYOTO PROTOCOL TO THE UNITED NATIONS FRAMEWORK CONVENTION ON CLIMATE CHANGE, United Nations, 1998
- [2] European Commission: Green Paper on greenhouse gas emissions trading within the European Union, COM/2000/0087 final
- [3] DIRECTIVE 2003/87/EC OF THE EUROPEAN PARLIAMENT AND OF THE COUNCIL of 13 October 2003 establishing a scheme for greenhouse gas emission allowance trading within the Community and amending Council Directive 96/61/EC, Official Journal of the European Union
- [4] Consolidated versions of the Treaty on European Union and the Treaty on the Functioning of the European Union - Consolidated version of the Treaty on the Functioning of the European Union - Protocols - Annexes - Declarations annexed to the Final Act of the Intergovernmental Conference which adopted the Treaty of Lisbon, signed on 13 December 2007 - Tables of equivalences, Official Journal of the European Union, 2012/C 326/01
- [5] DIRECTIVE 2009/28/EC OF THE EUROPEAN PARLIAMENT AND OF THE COUNCIL of 23 April 2009 on the promotion of the use of energy from renewable sources and amending and subsequently repealing Directives 2001/77/EC and 2003/30/EC, Official Journal of the European Union

- [6] ENERGY UNION PACKAGE: COMMUNICATION FROM THE COMMISSION TO THE EUROPEAN PARLIAMENT, THE COUNCIL, THE EUROPEAN ECONOMIC AND SOCIAL COMMITTEE, THE COMMITTEE OF THE REGIONS AND THE EUROPEAN INVESTMENT BANK: A Framework Strategy for a Resilient Energy Union with a Forward-Looking Climate Change Policy, COM(2015) 80 final
- [7] ENERGY UNION PACKAGE: COMMUNICATION FROM THE COMMISSION TO THE EUROPEAN PARLIAMENT AND THE COUNCIL The Paris Protocol – A blueprint for tackling global climate change beyond 2020 {SWD(2015) 17 final}, COM(2015) 81 final
- [8] United Nations Climate Change Conference, <http://www.cop21paris.org/> (accessed August 10, 2018)
- [9] United Nations Treaty Collection, CHAPTER XXVII, ENVIRONMENT, 7. d Paris Agreement, Paris, 12 December 2015
- [10] COMMUNICATION FROM THE COMMISSION TO THE EUROPEAN PARLIAMENT, THE COUNCIL, THE EUROPEAN ECONOMIC AND SOCIAL COMMITTEE, THE COMMITTEE OF THE REGIONS AND THE EUROPEAN INVESTMENT BANK: Clean Energy For All Europeans, COM(2016) 860 final
- [11] Robert N. Stavins, Experience with Market-Based Environmental Policy Instruments, Discussion Paper 01–58, November 2001, Resources for the Future
- [12] European Energy Exchange, EEX, <https://www.eex.com/en/products/environmental-markets>, (accessed August 10, 2018)
- [13] Intercontinental Exchange Futures Europe, ICE, <https://www.theice.com/emissions/auctions> (accessed August 10, 2018)
- [14] DIRECTIVE (EU) 2018/410 OF THE EUROPEAN PARLIAMENT AND OF THE COUNCIL of 14 March 2018 amending Directive 2003/87/EC to enhance cost-effective emission reductions and low-carbon investments, and Decision (EU) 2015/1814, Official Journal of the European Union
- [15] Council of the European Union, Communication from the Commission to the European Parliament, the Council, the European Economic and Social Committee and the Committee of the Regions: A policy framework for climate and energy in the period from 2020 to 2030, COM(2014) 15 final/2
- [16] Trends and projections in the EU ETS in 2017: The EU Emissions Trading System in numbers, ISSN 1977-8449, European Environment Agency, November 2017
- [17] DIRECTIVE 2010/75/EU OF THE EUROPEAN PARLIAMENT AND OF THE COUNCIL of 24 November 2010 on industrial emissions (integrated pollution prevention and control), Official Journal of the European Union
- [18] Decision C(2014) 4533/final on the notification by the Hellenic Republic of a modified transitional national plan referred to in Article 32 of Directive 2010/75/EU on industrial emissions, Official Journal of the European Union
- [19] Chao, Hung-po & Wilson, Robert, Design of wholesale electricity markets, 2018
- [20] Stoft, S., 2002. Power Systems Economics: Designing Markets for Electricity, IEEE Press, John Wiley and Sons
- [21] C. K. Simoglou, P.N. Biskas, S. I. Vagropoulos, A. G. Bakirtzis, Electricity Market Models and RES Integration: The Greek Case, Energy Policy, Volume 67, April 2014, Pages 531-542
- [22] Market Operator, Codes and Regulation, <http://www.lagie.gr/rythmistiko-plaisio/kodikis-kanonismoi/doccat/list/Document/650/>

- [23] Transmission System Operator, Codes and Regulation, <http://www.admie.gr/en/regulatory-framework/codes/>
- [24] RAE Decision 56/2012,
http://www.rae.gr/site/file/categories_new/about_rae/actions/decision/2012_A0056?p=files&i=0
- [25] RAE Decision 57/2012,
http://www.rae.gr/site/file/categories_new/about_rae/actions/decision/2012_A0057?p=files&i=0
- [26] Market Operator, Market Solutions, <http://www.lagie.gr/agora/proimerisia-agora/apotelesmata/>
- [27] Market Operator, Monthly Market Report, <http://www.lagie.gr/agora/analysisi-agoras/miniaia-deltia-iep/>
- [28] Transmission System Operator, Monthly Energy Report, <http://www.admie.gr/deltia-agoras/miniaia-deltia-energeias/>
- [29] Transmission System Operator, Greek Electricity System Adequacy Report, http://www.admie.gr/fileadmin/groups/EDAS_DSS/AnaptixiSistimatos/Meleti_eparkeias_2017_2027.pdf
- [30] Kavouridis K., Roumpos C., Galetakis, M., (2007). The effect of power plant efficiency, lignite quality and inorganic matter on CO₂ emissions and competitiveness of Greek lignite, *Górnictwo i Geoinzynieria*, Rok 31, Zeszyt 2: 355-369.)
- [31] Roumpos C., Paraskevis N., Galetakis M., Michalakopoulos T. (2014). Mineable lignite reserves estimation in continuous surface mining, 12th International Symposium Continuous Surface Mining (ISCSM), Aachen, Germany, 21-23 September: In book: Proceedings of the 12th International Symposium Continuous Surface Mining - Aachen 2014, Edition: Lecture Notes in Production Engineering 2015, Publisher: Springer International Publishing, Editors: Christian Niemann-Delius, pp.177-194.
- [32] Diez, David M; Barr, Christopher D; Cetinkaya-Rundel, Mine (2017). *OpenIntro Statistics* (3rd ed.). OpenIntro. Retrieved 11 November 2017
- [33] Tabachnick, B. G. & Fidell, L. S., *Using multivariate statistics* (4th ed.). Boston, MA: Allyn and Bacon, 2001
- [34] IBM, *IBM SPSS Regression* 24, 2016
- [35] Montgomery, Douglas (2013). *Design and analysis of experiments* (8th ed.). Hoboken, NJ: John Wiley & Sons, Inc.
- [36] Lynne J. Williams, Herve Abdi, *Fisher's Least Significant Difference (LSD) Test*, *Encyclopedia of Research Design*, Thousand Oaks, CA: Sage, 2010
- [37] Lowry, Richard. "One Way ANOVA – Independent Samples". Vassar.edu.
- [38] John E. Hanke, Dean Wichern, *Business Forecasting* 9th Edition, Pearson, 2009
- [39] Draper, N. and Smith, H. (1981) *Applied Regression Analysis*, 2d Edition, New York: John Wiley & Sons, Inc.
- [40] Durbin, J.; Watson, G. S., "Testing for serial correlation in least squares regression III", *Biometrika* 58, 1971
- [41] Y charts, European Union Natural Gas Import Price Chart, https://ycharts.com/indicators/europe_natural_gas_price, (accessed August 10, 2018)

Alkali Activating of Low-Alumina Mine Tailings for more Sustainable Raw Material Supply

Mahroo Falah¹, Robert Obenaus-Emler² and Mirja Illikainen¹

¹University of Oulu, Fiber and particle engineering research unit, 90014 University of Oulu, Finland

²Montanuniversitaet Leoben, Chair of Ceramics, 8700 Leoben, Austria

ABSTRACT

Each year, the mining industry generates a significant amount of mine tailings. Disposal of mine tailings (MT) has environmental impacts such as air pollution from dust emissions and release of heavy metals to surface and underground water. The EU funded project 'Integrated mineral technologies for more sustainable raw material supply (ITERAMS)' as a part of its aims is trying to develop an alkali activated materials from low-Aluminium mine tailings from the Kevitsa mine in northern Finland using different alkali activator solutions investigated firstly the compressive strength of the final products. Based on the final strength of the prepared samples, the selected activator (sodium silicate here) was subsequently used for the further experiments. The alkali activated mine tailings (AAMT) were prepared by mixing different concentrations of sodium silicate solution, water and the MT powder. The MT contains X-ray amorphous material in addition to Quartz, Tremolite, Dolomite, Forsterite and Enstatite. Using a curing temperature of 40 °C led to strengthened and dense materials. The structure and morphology of the alkali activated products was determined by Scanning Electron Microscopy (SEM) which also confirmed the presence of phases leading to an increase in the compressive strength. It should be noted that the alkali activation of MT constitute new and novel materials with potential environmental protection applications such as low permeability covers for surface deposits of tailings to seal the surface tailings disposal area. Alkali activation involves the manipulation of materials within the tailings to change the properties of the resulting material. The water penetration and the permeability of oxygen are crucial factors for proper functionality of the installed covering layer.

1. INTRODUCTION

The mining industry has been subjected to increase the environmental principles in recent years. Disposal of mine tailings in impoundments can cause environmental and safety problems including serious water pollution arising from contamination of surface water, groundwater and soils due to the leaching of heavy metals, mill reagents, and sulphur compounds. Mine tailings are waste materials generated by mining operations and generally contain process water, gangue minerals, heavy metals, and any toxic substances used in the dressing of the ores [1]. Developing cost-effective and environmentally acceptable strategies for the disposal of such waste has thus become critical for the productivity of mining operations.

There are different approaches to reduce the potential environmental hazards imposed by mine tailings: (i) isolation of MT, (ii) chemical stabilization of MT, and (iii) a combination of these two methods [5]. For the isolation techniques the tailings impoundment surface are capped [2]. The chemical stabilization includes addition of chemicals or cementitious materials to immobilize the heavy metals in MT through chemical reactions. For the simultaneous use of isolation and stabilization techniques the tailings surface can be treated by binders such as organic polymers, water glass and Ordinary Portland cement (OPC) to improve surface erosion resistance and reduce water

infiltration, which isolates the underlying tailings from the surrounding environment [3]. Although OPC has its benefits in stabilization of certain mine tailings, it has several drawbacks such as low acid resistance, high cost, and high energy consumption and CO₂ emissions related to the production of OPC.

In recent years, the utilisation of mine tailings has been getting much attention globally; this phenomenon can help reduce the emission of greenhouse gases by stabilization or isolation of tailings and providing cheaper alternative materials for building and construction, and for natural resource conservation. Different applications proposed for mine tailings include road construction [4], ceramics [5], construction materials [6], light-weight aggregates [7], mine backfilling [8], and utilizing tailings as a source of metals and chemicals [9].

A promising method, namely alkali-activation or geopolymerization of tailings, has been suggested to immobilize tailings as a raw material for construction. By alkali-activation, different mineral raw materials can be turned to valuable cementitious-like materials with low environmental impact. Recently, alkali-activated cements (AAC) produced from various industrial by-products such as slag and fly ash at low cost have been reported to have superior strength and stability performance in concrete applications even under aggressive environmental conditions [10–14]. Alkali activation of mine tailing can represent one of these low cost treatments to generate matrices for the encapsulation of hazardous elements [15–18]. However, the effect of activator concentration can lead to brittleness problems or decrease in strength in low and high concentrations of the alkaline activator respectively [14]. For MT not containing a high amount of aluminium the addition of an external source of Aluminium has to be considered.

To our knowledge, no previous practical studies have been conducted using just alkali activator solution, water and mine tailings for the production of AAMT. The use of a sodium silicate solution alone could reduce the cost of alkali activator in the production of the final AAMT.

This study attempts to emphasis on this path by using sodium silicate solution for the production of environmentally friendly AAMT. Obenaus-Emler *et al.* (2017) have previously reported a target applications for the ITERAMS concepts and technologies regarding tailings which validated by industrial and research partners at partners' mine sites. The impact of ITERAMS will promote new mining practices and the development of novel technologies to store and utilize mine tailings and solid waste [19]. In this study low alumina mine tailings were activated using different alkali activators. Based on the initial results of the compressive strength of the final product the activator was selected. Sodium silicate showed to be an acceptable activator and further experiments were performed using it at different concentrations (10-30 wt. %). The strength of AAMT products were examined in the period of 7, 14 and 28 days. Furthermore a detailed microstructural characterization of the final products was conducted to help understand the origin of the properties of the resulting products.

2. EXPERIMENTAL

2.1. Sample Synthesis

Mine tailings were supplied from Kevitsa Mining Oy in Northern Finland in the Lapland province. Sodium silicate solution from VWR chemicals with a modulus ($M_s = \text{SiO}_2/\text{Na}_2\text{O}$) of 3.5 was selected as an alkali activator. Potassium silicate solution was selected as another alkali activator. The solution was prepared by mixing a commercial potassium silicate solution (Kasil 2135; PQ Europe) with potassium hydroxide to obtain $\text{K}_2\text{O}/\text{SiO}_2 = 0.8$ (65 wt. % of H₂O). Sodium hydroxide with a purity >99% was achieved from Merck (Germany) and nitric acid (64-66%) from Sigma-Aldrich.

The alkali activated materials (AAMs) were prepared by blending the tailings with combinations of activators (sodium silicate, potassium silicate, sodium hydroxide, potassium

hydroxide). The molarity of each activator solution was 6 and additional water was added to the mixture in order to achieve a required slurry concentration. The mixing was continued for a further 5 min, then the slurry transferred to prismatic beam moulds (20×20×80 mm) and vibrated for 60 s on a vibrating table. The samples were sealed and cured at 40 °C for 7 days before determining the compressive strength. Regarding their hardening behaviour and resulting compressive strength the mixture containing sodium silicate solution, water and tailing powder indicated the highest compressive strength of 4 MPa after curing for 7 days.

According to the results of the initial experiments sodium silicate solution was selected as the activator for the further experiments. Different percentage of the sodium silicate solution (10, 15, 20, 25 and 30 wt. %) were added to the tailings and mixed for 5 min. Finally, water was added to the mixture in order to adjust the liquid-to-solid mass ratio of 0.23. The slurry was stirred for another 5 minutes, transferred to prismatic beam moulds (20×20×80 mm) and vibrated for 60 s on a vibrating table. Again, the samples were sealed and cured at 40 °C for 7, 14 and 28 days. The following properties were determined after curing: solubility in water, chemical analysis and morphology structure, water absorption and compressive strength. The recipes of the tested mixtures are given in table 1.

Table 1. Composition of the samples (Mass %)

Label	Mine Tailing	Sodium Silicate	Water	Water / Binder
IT-NSi-10%	73.20	10	16.80	0.23
IT-NSi-15%	71.07	15	13.93	0.23
IT-NSi-20%	68.93	20	11.07	0.23
IT-NSi-25%	66.93	25	8.07	0.23
IT-NSi-30%	63.75	30	6.25	0.23

3. CHARACTERIZATION

3.1. X-Ray Fluorescence

The milling of the material was prepared using a vibratory disc mill (Retsch RS 200) for 1-5 min to get the desired particle size. Particle size analysis of the powdered material was performed with a LS 13320 laser diffraction particle size analyser from Beckman Coulter, using air as a dispersion medium. The chemical composition results of the mine tailing was determined by X-ray fluorescence (XRF, PANalytical AxiosmAX) equipped with a rhodium tube with a maximum power rating of 4 kW. The result of XRF analysis of the selected tailing sample is given in Table 2. The tailings have considerably low amount of Al₂O₃.

Table 2. Composition of the tailings as determined by XRF

Na ₂ O	MgO	Al ₂ O ₃	SiO ₂	SO ₃	K ₂ O	CaO	TiO ₂	MnO	Fe ₂ O ₃	LOI
0.58	21.82	3.99	47.96	0.15	0.23	11.28	0.37	0.17	12.06	1.6

3.2. Solubility Test

The solubility tests have been done on 13 tailing samples in order to select the most reactive sample with high solubility in silica and alumina. Although the alumina content in the samples are low a high alumina solubility is more favourable for alkali activation. The solubility experiments were carried out using samples initially milled in a Retsch disk mill to a particle size between 1 µm and 10 µm. The dissolution experiments were conducted in polypropylene bottles with 6 M NaOH

solution, at a solid/liquid ratio of 40 w/w. The samples were stirred on a horizontal shaking table for 24 h at 23 ± 0.5 °C, filtered afterwards through a 0.4 μm filter paper and finally acidified with 6M HNO_3 to pH lower than 2. The final solutions were analysed with ICP-OES.

The solubility in 6 M NaOH solution after 24 hours is shown in Fig. 1. The results show that about 10 wt.% of the overall silica and a round 2-8 wt.% of the overall alumina content is soluble in the solvent. The amount of calcium in the solution is very low which might be caused by the formation of Ca-containing precipitates while leaching this will be further assessed by mineralogical investigations.

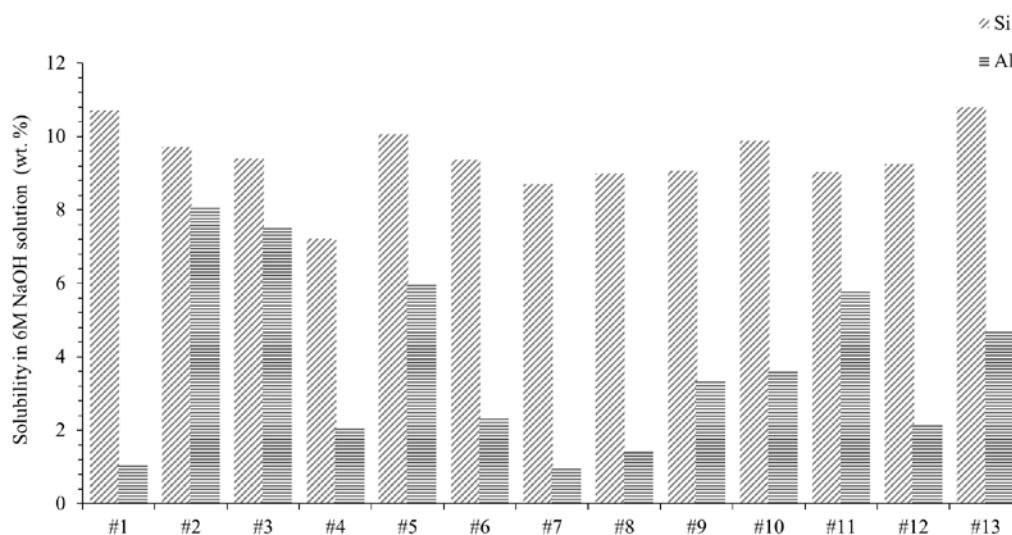


Fig. 1. Alkaline solubility of silicon and aluminium. Results are expressed as soluble weight percentage based on the amount in the original material.

3.3. Microstructural analysis

The original mine tailing and the synthesised AAMT were characterised with field emission scanning electron microscope (FE-SEM) using a Zeiss Ultra Plus microscope fitted with an electron dispersive (EDS) detector an energy dispersive x-ray spectroscopy (EDX). An accelerating voltage of 15 keV was used to analyse the structural and chemical texture of the samples. The samples were carbon coated with a 7–9 nm carbon layer.

3.3.1. SEM–EDX analysis of the hardened AAMT

The microstructure of the MT and MT containing 30 wt. % of sodium silicate after 28 days curing are presented in Fig. 2 (a, b). The figure shows a SEM micrograph of a representative location of each sample. The morphology of AAMT samples changed with addition of alkali activator. The change in nature of reaction product is evident in SEM and EDX. Generally, the micrographs show a homogeneous, compact and uniform microstructure. Modification of the MT was observed with formation of larger aggregates compared to unreacted MT. Treatment of MT with a higher amount of sodium silicate resulted in an improvement in the compressive strength.

The microstructure of MT with a 30% sodium silicate content (Fig. 2b) reveal a morphology consisting of a random array of sheet-like unaggregated particles. The structure appeared to be more homogenous and denser with continuous gel matrix which is due to the high dissolution of amorphous silica, magnesia and calcium present in the raw materials. The flat areas in the structure become more obvious and the degree of the reticulation appears to decrease. This may be a reason

that the combination with sodium silicate can improve the final strength. The compressive strength was higher compared to the other mixes containing different activator contents.

EDS elemental analysis confirms the presence of all the expected elements in MT treated with sodium silicate (Si, Al, Na, Mg, Fe and Ca) (Fig. 2 c), with the additional presence of C from the carbon coating. The presence of sodium silicate can control the microstructural properties of the final product.

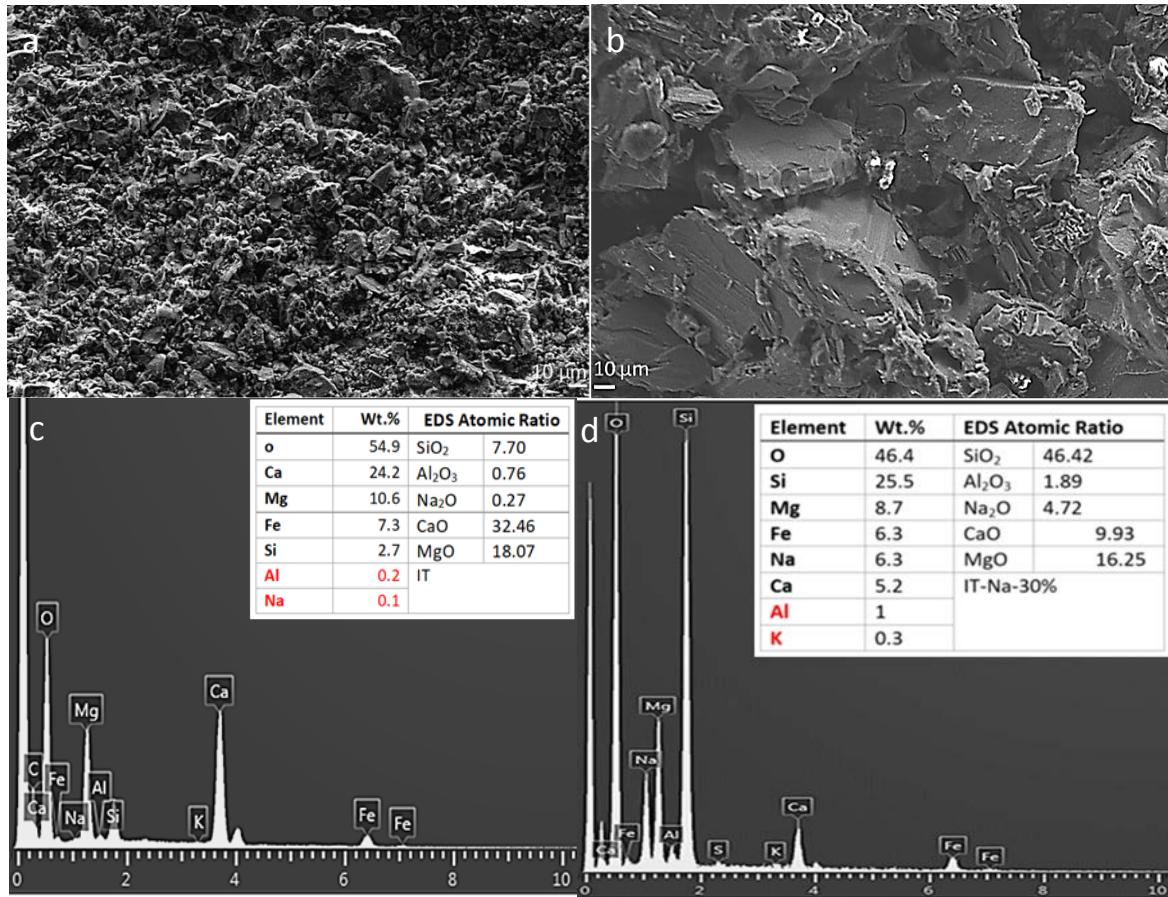


Fig. 2. Representative SEM micrographs of (a, b) original MT, and IT-NA-30%, (c, d) Backscattered SEM micrographs of MT, and IT-NA-30%.

3.4. Soaking Test

The effect of water absorption on AAMT was investigated in accordance with BS EN ISO 62:1999 [18]. Overall 15 prismatic beams (20×20×80 mm) were prepared and cured for 28 days using the procedure mentioned above. First all the specimens were dried in an oven at 105 °C and then allowed to cool to room temperature before weighing. This process was repeated until a constant mass of the specimens was reached. Water absorption tests were conducted by submerging the specimens in a water bath at 23°C for 24 hrs. After immersion for 24 h, the specimens were taken out from the water and the surface water was removed by wiping with a clean dry cloth. The specimens were reweighed within 1 min after removing them from the water. The water absorption capacity was determined using the following equation:

$$W_a(\%) = \frac{W_f - W_i}{W_i} \times 100$$

where, W_a is water absorption (d.b. %), W_f is weight of specimen after immersion (g) and W_i is weight of specimen before immersion (g).

3.4.1. Water Absorption results

The plot of water absorption and compressive strength for different sodium silicate additions (Fig.3.) shows a trend of increasing compressive strength with decreasing water absorption. The water absorption of the specimens decreased with the higher sodium silicate concentration, which indicates a denser structure (less porosity) [20, 21] resulting in a higher compressive strength. The lowest values of water absorption (10.2 %) of the 28-day cured specimen at 40°C from AAMT with 30 wt. % sodium silicate indicated higher degree of reaction for this sodium silicate addition compared with other specimens, and result in the highest compressive strength (15.84 MPa). When the MT activated with high amount of sodium silicate solution the resulting material develops a very dense structure with the lowest apparent porosity. In fact good correlation is observed, mostly between compressive strength and the water absorption in AAMT.

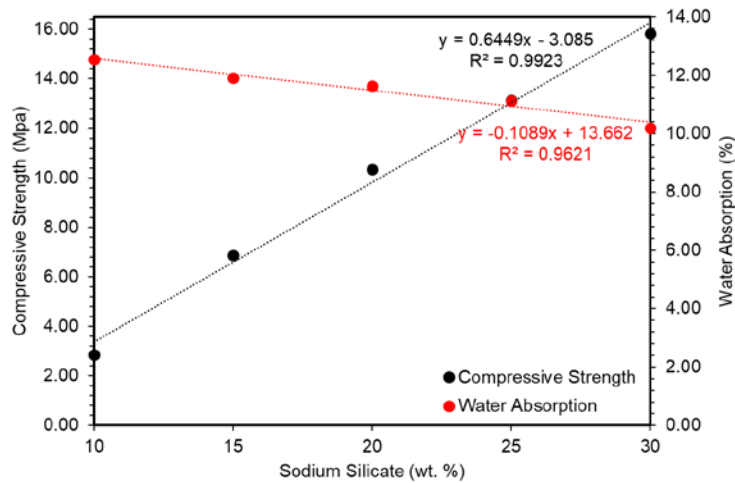


Fig 3. The effect of the amount of sodium silicate solution on water absorption and compressive strength of AAMT

When the amount of sodium silicate solution is increased the amount of soluble silica in the mixture is increased as well. Hence the polymerization processes is accelerated to some extent. The best-fit curves were obtained using the least squares method and the fitting quality was analysed by the coefficient of determination (R^2), for which the correlation coefficients R^2 are all >0.90 .

3.5. Compressive test

The compressive strength of the specimens was measured using portions of prismatic beams broken by flexural testing according to the ASTM C116-90 recommendation 50. All the broken prismatic beams were measured under a compressive load with a constant displacement rate of 2mm/min. The compressive load was measured with a Zwick Z100 Roell testing machine with a maximum load capacity of 100 kN. The results were obtained from the average of six tested replicates.

3.5.1. Compressive Strength

The compressive strength of the treated MT samples with different activators after curing at 40 °C for 7 days is presented in Fig. 4. The maximum compressive strength is obtained for the mixture containing sodium silicate solution (4 MPa). In addition, the sodium silicate solution causing an increase in the solubility of the silica solution in the mixture.

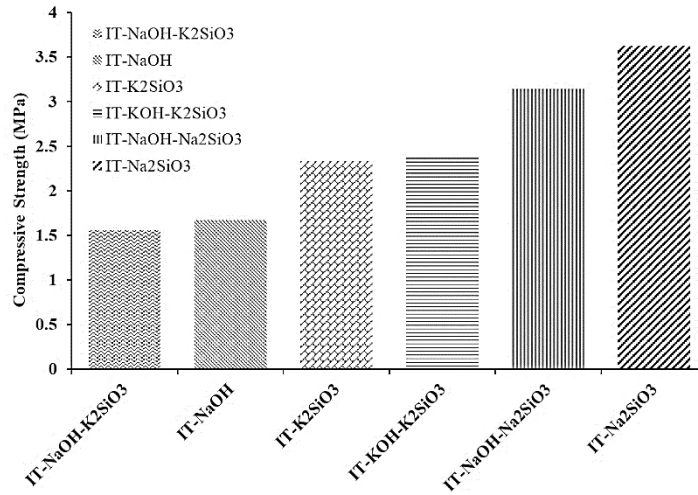


Fig. 4. Compressive strength of the final products after 7 days of curing at 40 °C.

According to initial compressive results, and the economic point of view, the sodium silicate solution has been selected for the subsequent experiments. The compressive strength of the treated MT samples with increasing amount of sodium silicate solution after curing for 7, 14 and 28 days at 40 °C is summarized in Fig. 5. The addition of sodium silicate causes an increase in compressive strength of the treated samples. The presence of silicon could result in the formation of several polymeric or simple structures. Furthermore the strength and compressibility of the MT treated sodium silicate solution is related to the structure as confirmed with microstructure analysis (Fig. 2.). It should be noted that the curing time has a considerable impact on mechanical strength development.

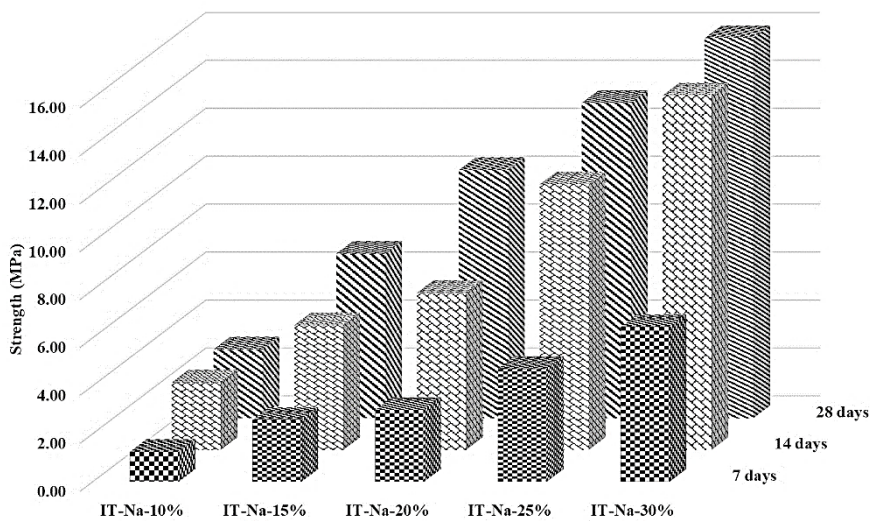


Fig. 5. Compressive strength of the final products after 7, 14 and 28 days of curing at 40 °C.

Compressive strength was observed to rise with alkali content which is related to the amount of the soluble silica. It can be noted that increasing the activator solution content from 10 to 30 wt. % gradually increases the strength of the final product. Generally speaking the highest strength of all mixes was attained with the addition of 30 wt. % of sodium silicate solution. The compressive strength of the IT-NA-30% after 28 days is 15.84 MPa showing an increase by 18 % in comparison to the IT-NA-10%.

4. CONCLUSION

Stabilization of mine tailings using optimized alkali-activation solutions transforms such waste into a matrix with adequate strength. The laboratory studies were aiming to determine the efficient proportion of activator solution for stabilizing the tailings under consideration. Five alkali-activated mine tailing mixtures were produced adding varying amount of sodium silicate solution in order to improve the final strength. Test specimens were cured at 40 °C and the chemical composition of the resulting matrix was determined by SEM/EDX. Furthermore the water absorption and compressive strength was investigated. The addition of sodium silicate to MT results in higher compressive strength and lower water absorption. The amount of sodium silicate solution and the curing time are two major factors affecting the behaviour of AAMT. The SEM investigations show the formation of more compact microstructure when increasing the sodium silicate content of the mixture.

A possible explanation is as follows: Higher sodium silicate addition contributes to the dissolution of silica and subsequent formation of a higher amount of alkali-activated gels resulting in a higher compressive strength. The AAMT reach their ultimate strength within approximately 28 days.

Adding a sodium silicate solution up to 30 wt. % resulted in a compressive strength of the final product of up to 16 MPa after 28 day of curing at 40 °C. The compressive strength increased with the increase of alkaline solution from 10 to 30 wt. %. Among the mixtures of this study, the mixtures having 30 wt. % sodium silicate can be considered as the optimum mixture for reasonable compressive strength under the curing condition studied here.

ACKNOWLEDGMENT

This project has received funding from the European Union's Horizon 2020 research and innovation programme under grant agreement No 730480 (ITERAMS).

REFERENCES

- [1] L. Zhang, S. Ahmari, J. Zhang, Synthesis and characterization of fly ash modified mine tailings-based geopolymers, *Constr. Build. Mater.* 25 (2011) 3773–3781. doi:10.1016/J.CONBUILDMAT.2011.04.005.
- [2] G.M. Smith, Evolution of Disposal Cell Cover Design Used for Uranium Mill Tailings Long-Term Containment, (1999). <http://www.wmsym.org/archives/1999/51/51-3.pdf> (accessed April 12, 2018).
- [3] S. Ahmari, L. Zhang, Durability and leaching behavior of mine tailings-based geopolymer bricks, *Constr. Build. Mater.* 44 (2013) 743–750. doi:10.1016/j.conbuildmat.2013.03.075.
- [4] S. Ahmari, R. Chen, L. Zhang, Utilization of mine tailings as road base material, in: 2012: pp. 3654–3661. doi:10.1061/9780784412121.374.

- [5] Kinnunen, Ismailov, Solismaa, Sreenivasan, Räisänen, Levänen, Illikainen, Mine tailings as a raw material for chemically bonded ceramics (CBC) – a review, 2016 (2016).
- [6] S. Ahmari, L. Zhang, Production of eco-friendly bricks from copper mine tailings through geopolymerization, *Constr. Build. Mater.* 29 (2012) 323–331. doi:10.1016/j.conbuildmat.2011.10.048.
- [7] Yliniemi, Paiva, Ferreira, Tiainen, Illikainen, Development and incorporation of lightweight waste-based geopolymer aggregates in mortar and concrete, *Constr. Build. Mater.* 131 (2017) 784–792. doi:10.1016/j.conbuildmat.2016.11.017.
- [8] Q. Chen, Q. Zhang, A. Fourie, C. Xin, Utilization of phosphogypsum and phosphate tailings for cemented paste backfill, *J. Environ. Manage.* 201 (2017) 19–27. doi:10.1016/j.jenvman.2017.06.027.
- [9] C. Falagán, B.M. Grail, D.B. Johnson, New approaches for extracting and recovering metals from mine tailings, *Miner. Eng.* 106 (2017) 71–78. doi:10.1016/j.mineng.2016.10.008.
- [10] F. Pacheco-Torgal, Z. Abdollahnejad, A.F. Camões, M. Jamshidi, Y. Ding, Durability of alkali-activated binders: A clear advantage over Portland cement or an unproven issue?, *Constr. Build. Mater.* 30 (2012) 400–405. doi:10.1016/J.CONBUILDMAT.2011.12.017.
- [11] T. Bakharev, J.G. Sanjayan, Y.-B. Cheng, Sulfate attack on alkali-activated slag concrete, *Cem. Concr. Res.* 32 (2002) 211–216. doi:10.1016/S0008-8846(01)00659-7.
- [12] T. Bakharev, J. Sanjayan, Y.-B. Cheng, Resistance of alkali-activated slag concrete to acid attack, *Cem. Concr. Res.* 33 (2003) 1607–1611. doi:10.1016/S0008-8846(03)00125-X.
- [13] T. Bakharev, Resistance of geopolymer materials to acid attack, *Cem. Concr. Res.* 35 (2005) 658–670. doi:10.1016/J.CEMCONRES.2004.06.005.
- [14] F. Cihangir, B. Ercikdi, A. Kesimal, H. Deveci, F. Erdemir, Paste backfill of high-sulphide mill tailings using alkali-activated blast furnace slag: Effect of activator nature, concentration and slag properties, *Miner. Eng.* 83 (2015) 117–127. doi:10.1016/J.MINENG.2015.08.022.
- [15] I. Lancellotti, E. Kamseu, M. Michelazzi, L. Barbieri, A. Corradi, C. Leonelli, Chemical stability of geopolymers containing municipal solid waste incinerator fly ash, *Waste Manag.* 30 (2010) 673–679. doi:10.1016/j.wasman.2009.09.032.
- [16] L. Zheng, W. Wang, X. Gao, Solidification and immobilization of MSWI fly ash through aluminate geopolymerization: Based on partial charge model analysis, *Waste Manag.* 58 (2016) 270–279. doi:10.1016/J.WASMAN.2016.08.019.
- [17] E. Ivan Diaz-Loya, E.N. Allouche, S. Eklund, A.R. Joshi, K. Kupwade-Patil, Toxicity mitigation and solidification of municipal solid waste incinerator fly ash using alkaline activated coal ash, *Waste Manag.* 32 (2012) 1521–1527. doi:10.1016/J.WASMAN.2012.03.030.
- [18] J. Kiventerä, I. Lancellotti, M. Catauro, F.D. Poggetto, C. Leonelli, M. Illikainen, Alkali activation as new option for gold mine tailings inertization, *J. Clean. Prod.* 187 (2018) 76–84. doi:10.1016/j.jclepro.2018.03.182.
- [19] R.O.Emler, M. Illikainen, M.Falah, P.Kinnunen, K.Heiskanen, Geopolymers from mining tailings for more sustainable raw material supply, *MATEC Web Conf.* 2017.
- [20] M.P. Lorenzo, S. Goñi, A. Guerrero, Activation of Pozzolanic Reaction of Hydrated Portland Cement Fly Ash Pastes in Sulfate Solution, *J. Am. Ceram. Soc.* 85 (2004) 3071–3075. doi:10.1111/j.1151-2916.2002.tb00581.x.
- [21] S.-S. Park, H.-Y. Kang, Strength and microscopic characteristics of alkali-activated fly ash-cement, *Korean J. Chem. Eng.* 23 (2006) 367–373. doi:10.1007/BF02706736.

Occupational Accidents in Turkish Energy Sector

Sotirios Nik. Longinos and Mahmut Parlaktuna

Department of Petroleum and Natural Gas Engineering, Middle East technical University, Ankara, Turkey

ABSTRACT

In a developing world, the spreading and progress of industry, agriculture and social service is a necessity. Such a progress is often associated with an increase of occupational accidents. Unfortunately, occupational accidents are destined to reiterate itself and the reasons are in very case the same (human mistake, poor regulatory enforcement, etc.). There are 2.78 million deaths per year and 374 million non-fatal work related injuries and illnesses each year. The human rate of this daily adversity is high and the economic onus of not enough occupational safety and health practices is assessed at 3.94 per cent of global Gross Domestic Product each year. Work accidents occur in Energy sector as other sectors with the difference that happens more often. Petroleum and Natural Gas sector play the most crucial role in the world in power generation. Many accidents happen in Petroleum and Natural Gas fields and the negative outcomes affect the surroundings. In this attempt, the official statistics on Turkish crude petroleum and natural gas sector are analyzed for the period between 2011 – 2016. All studied data are taken from Social Security Institution of Turkey (SGK), which includes the fatalities, serious injuries, minor injuries and working population for Turkish Petroleum Industry for the period 2011-2016. Fatal Accident Rate (FAR), Serious Injuries Rate (SIR) and Individual Risk (IR) are calculated together with F-N curve analysis. Moreover, OSHA incident rate (based on lost workdays) is also calculated. Furthermore, some recommendations are made in order to take the necessary preventative measures to decrease all the necessary rates related with occupational accidents. It should be mentioned that his method of analysis could be applied to chemical-petrochemical activities and surface mining activities (continuous and non-continuous) for the exploitation of coal deposits.

Keywords: Energy Sector, Occupational Accidents, Turkey

1. INTRODUCTION

In a developing world, the spreading and progress of industry has incredible benefits but regrettably such an industrial expansion brings with it some menaces. It has presented that market systems in many countries have the weakest capabilities to devise and implement a monitoring structure that protects both the workers and consumers [1,2]. The risks of globalization can often be realized by observing the number of occupational accidents, which has continuously exhibited an increasing trend. Unfortunately, occupational accidents are destined to take place consistently and the reasons are very akin in most occasions (human mistake, poor regulatory enforcement, etc.) [3][4]. Work accidents may happen suddenly, but their causes last for years. Work accidents can be considered as one of the most crucial problems of the worldwide business because of the undesirable effects they pose [5]. Problems related with work place safety threaten not only worker's life and health, but also the labor productivity and endanger companies. Subsequently healthier and safer work environment is the main premise to a more productive work [6,7]. It has an sublime importance to diminish the fatalities, serious injuries and physical disabilities ensuing from work accidents by

confening the unsafe conducts of the employees and creating a stable and safe working environment which is significant for the function of human resource management [8,9].

2. OBJECTIVES AND METHODOLOGY

In this study ‘work accident statistics’ which took place in Turkish Petroleum and Natural Gas industry were examined methodically between 2011 and 2016. During this analysis, the statistical yearbooks regularly published by Social Security Institution (SGK) have been used as a data source. This division of oil and gas industry is defined by NACE [10] and contains the production of crude petroleum, the mining and extraction of oil from oil shale and oil sands and the production of natural gas and recovery of hydrocarbon liquids. The most concessive data related to occupational accidents is collected and published by SGK which is a public institution. According to data collected from these statistical yearbooks [11,12,13,14,15,16], the number of Fatal Accident Rate (FAR), the number of Serious Injuries Rate (SIR), Individual Risk (IR) and F-N Curve are calculated between 2011 and 2016 for Petroleum and Natural Gas industry which are mostly used by British Chemical Industry. Furthermore, as a second approach OSHA incident rate (based on lost workdays) is also calculated. Changes in trends with the years are analyzed, estimated and interpreted [17].

3. RESULTS AND DISCUSSIONS

The word safety has two explanations; first describes a position in which a person feels secure while the second explanation implies that the possibility of conversion from safe to unsafe state must be sufficiently low. On the other hand, an accident sequence is shown below:

$$\text{Hazard} \rightarrow \text{Accident/Failure Event} \rightarrow \text{Undesired Consequences} \quad (1)$$

The word ‘Hazard’ in the sequence refers to an item that can inflict harm or pose danger to human life, property or environment. The failure event indicates the presence of a flaw in the functioning of a part of the system [18,19].

One of the complications in understanding the field of risk management is the limited understanding of the word ‘risk’ itself. The product of the probability of a failure event and the resulting consequence of the failure event constitute the risk [20].

$$\text{Risk} = \text{Probability of the failure event occurring} \times \text{Undesired consequences} \quad (2)$$

The first measure to quantify the ‘Risk’ is the term Fatal Accident Rate (FAR). FAR is a measure of the risk present from hazards that have experienced actual failure events in at least one fatality. The FAR is usually quoted as the number of fatalities that occur in a defined group of people per 10^8 hours of exposure to the total number of hours worked.

$$FAR = \frac{10^8 \times \sum_{i=1}^m N(w_i)}{D \times H \times \sum_{i=1}^m w_i} \quad (3)$$

Where N is number of fatalities in year i, m total year of statistic, w_i the workers per year i, D the number of days per year i and H the number of hours per day.

The form of the above equation means it is possible to compare the FAR for individual years, or sum the results from a number of years to gain the FAR for a longer time period - both approaches are valid. Due to the fact that FAR is measured in Petroleum Industry (onshore and offshore fields)

the schedule in Turkey is 3 weeks work and 2 weeks off where its shift is 12 hours and since one year has 52 weeks, the working days for a person is 224 (32 weeks* 7 days).

The following term is Serious Injuries Rate (SIR). SIR is a measure of the risk present from hazards that have experienced actual failure events and the undesired human consequences in the form of serious injuries. The SIR is also quoted as a function of 1×10^8 exposure hours, and is calculated in a very similar manner to the FAR:

$$SIR = \frac{10^8 \times \sum_{i=1}^m S(w_i)}{D \times H \times \sum_{i=1}^m w_i} \tag{4}$$

Where S is number of serious injuries in year i and m total year of statistic, D is the number of days per year i, H the number of hours per day and w_i the workers per year i.

The Individual Risk (IR) is the probability of death in a calendar year for an individual member of a specified group.

$$IR = \frac{\sum_{i=1}^m N(w_i)}{\sum_{i=1}^m w_i} \tag{5}$$

Where N is the number of fatalities in year i across the population w_i .

Furthermore, one way of representing the frequency of ‘N-or-more’ fatalities is through the use of an F-N curve. Two concepts are involved in an F-N curve. The ‘F’ is the annual frequency with which a particular type of fatal event occurs. The ‘N’ is the number of fatalities caused by a particular failure event. The F-N curve plots annual event frequency against N or more fatalities in the event [21,22].

The OSHA formula that is used from American Industry for Incident Rate (based on lost workdays) are presented below

$$\text{IncidentRate}(\text{based on lostwork days}) = \frac{\sum_{i=1}^m L(w_i)}{D \times H \times (\sum_{i=1}^m w_i)} \times 200.000 \tag{6}$$

Where L is the number of lost work days in year i and m total year of statistic, D is the number of days per year i, H the number of hours per day and w_i the workers per year i.

The term Incident Rate is defined as the number of occupational injuries and/or illnesses or lost workdays per 100 full-time employees while the term lost workdays is defined as the number of days (consecutive or not) after but not including the day of injury or illness during which the employee would have worked but could not do so, that is, during which the employee could not perform all or any part of his or her normal assignment during all or any part of the workday or shift because of the occupational injury or illness.

Table 1 presents Social Security Institution (SGK), the number of fatalities, serious injuries and (Minor) Injuries In this context minor injuries are defined as the number of workers having work injuries by 1, 2 , 3 and 4 incapacity days while serious injuries are considered as the number of workers having work injuries 5 or more incapacity days.

Table 1. Number of fatalities, serious juries and minor injuries in Petroleum & Natural Gas sector from 2011-2016 [11, 12, 13, 14, 15,16]

Year	2011	2012	2013	2014	2015	2016
Total Number of Workers	3451	3403	3387	3356	3118	3038
Total Number of Minor Injuries	106	88	74	117	53	49
Total Number of Serious	54	50	44	48	31	30

Injuries						
Total Number of Injuries	160	138	118	165	84	79
Total Number of Deaths	1	0	3	1	0	0

When the data is examined in Figure 1, it is obvious that there is a reduction in the number of workers each year which is the expected outcome of reduction in oil price since 2012. Nevertheless, the important drop in oil prices started in 2014 (Figure 2) as well as the reduction in drilling operations. The total number of employees diminished by 12 % in 6 years period.

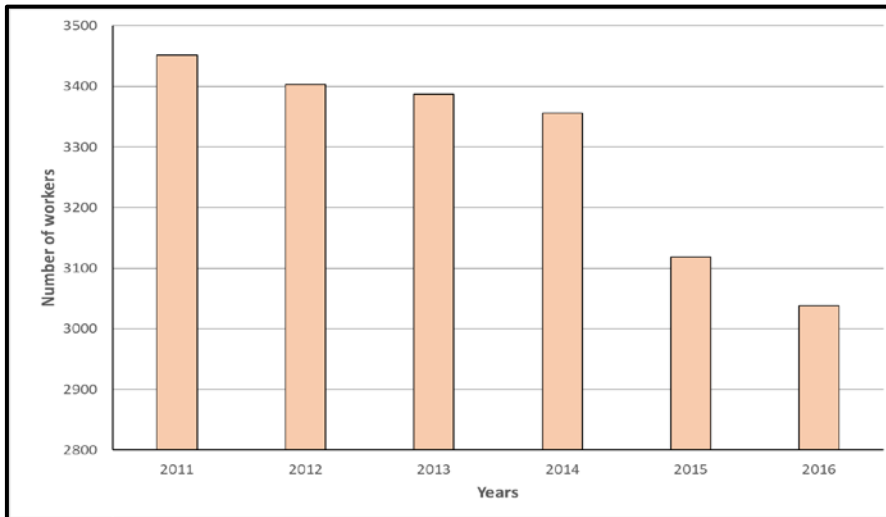


Figure 1. Number of workers in extraction of crude petroleum and natural gas sector between 2011-2016

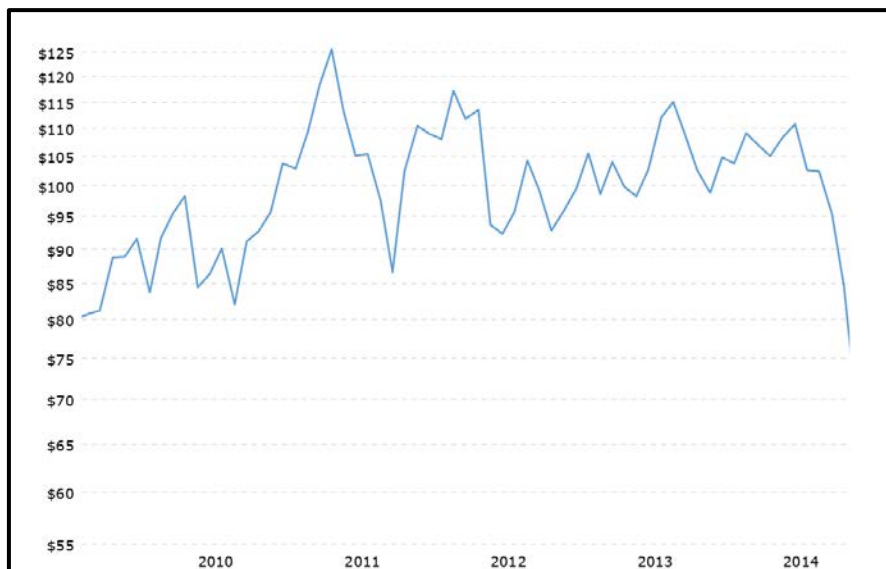


Figure 2. Oil prices from 2010 to 2014

Figure 3 nominates that there is a reduction in both minor and serious injuries if the data for 2014 is excluded (red arrows). If it is assumed that any worker is injured in a given year only once, the percent of injured workers is calculated from Table 1 and presented in Figure 3. The percent of injured employee reduced from 4.64 % to 2.60 in 6 years with the exception of 2014. It is seen that every 5 worker out of 100 injured in 2014 and this exceptional difference can be attributed to the augmented drilling operations in 2014 (Figure 5 and Figure 6). There were two leading driving

reasons for augmented drilling operation, higher oil prices in the period of 2010 – 2014 (Figure 7) and increased exploration activities on geothermal growth. The fatalities (Figure 7), on the other hand, are few and in some years does not exist.

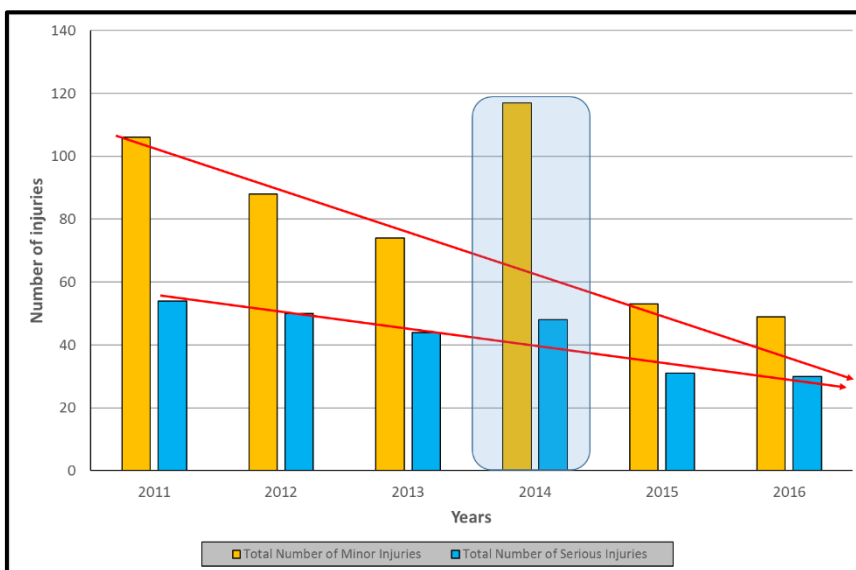


Figure 3. Presentation of Minor Injuries and Serious Injuries between 2011-2016

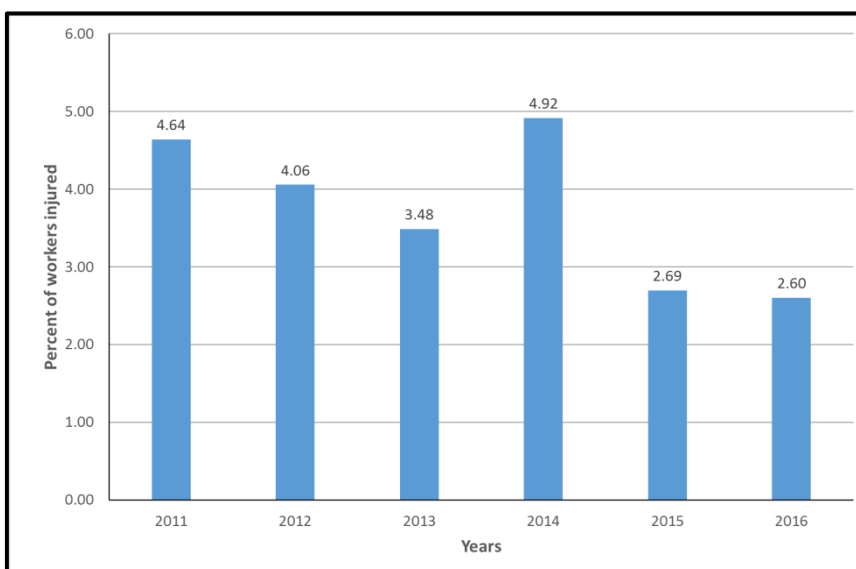


Figure 4. Percent of workers injured between 2011-2016

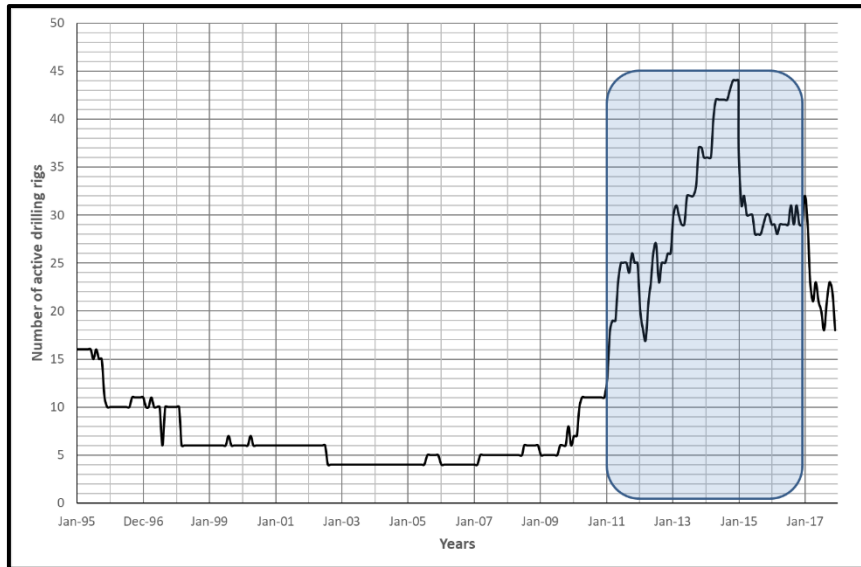


Figure 5. Percent of workers injured between 2011-2016

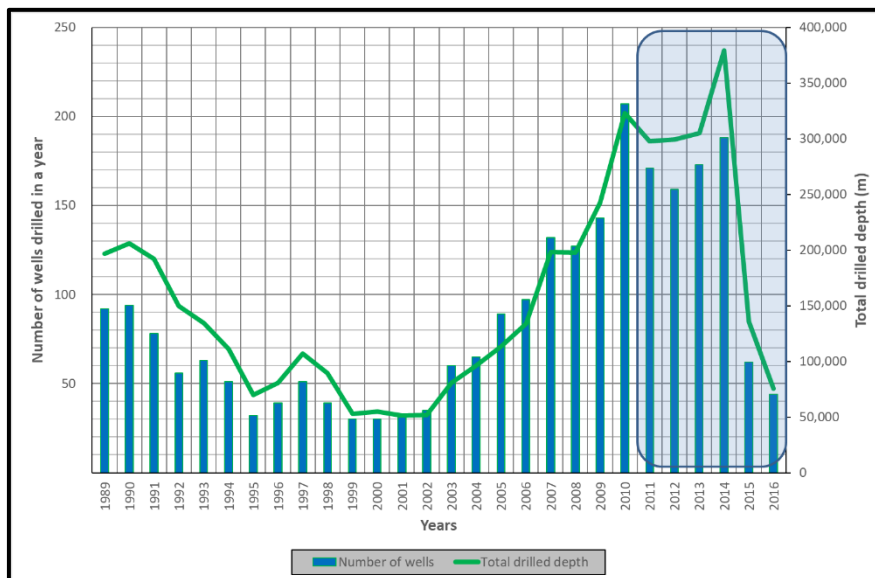


Figure 6. Percent of workers injured between 2011-2016

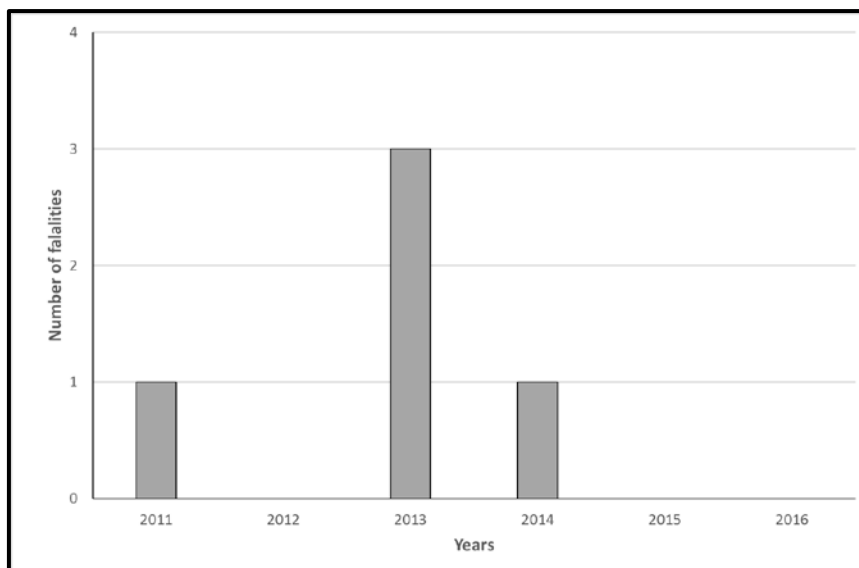


Figure 7. Number of fatalities between 2011-2016

From Table 1 and by the use of Equations 3, 4 and 5 Fatal Accident Rate (FAR), Serious Injuries Rate (SIR) and Individual Risk (IR) are calculated. The outcomes are presented in Table 2.

Table 2. Calculations for the terms FAR, SIR and IR from 2011-2016 per 10⁸ exposed hours

	2011	2012	2013	2014	2015	2016
FAR	10.41	5.24	14.03	13.21	10.74	9.09
SIR	562.06	545.03	519.10	517.78	487.81	467.34
IR	0.00029	0.00015	0.00039	0.00037	0.00030	0.00025

Table 2 shows that Fatal Accident Rate is low. It starts with 10.41 fatalities per 10⁸ exposure hours and then follows a decrease with 5.24 fatalities per exposure 10⁸ hours (2012). In period 2012 to 2013 there is the only increase and then from 2013 until 2016 there is a downward trend which reaches 9.09 fatalities per 10⁸ exposure hours. In the Serious Injuries Rate is observed that from 2011 to 2016 there is a respectful decrease. In 2011 SIR starts with a value of 562.10 per exposure 10⁸ hours and until 2016 reaches the value of 467.34 per exposure 10⁸ hours where this entails a reduction of 16.85%. The Individual Risk is also low due to the fact the deaths are few and fluctuates the three first years. Individual Risk from 2013 to 2016 follows a reduction equal to 35.89%. Figure 8 shows the FAR and SIR per 10⁸ exposure hours.

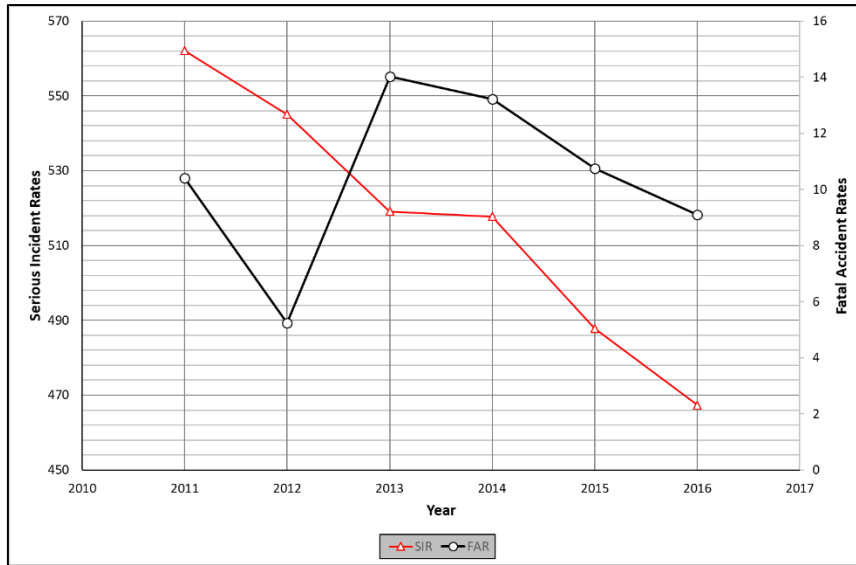


Figure 8. Fatal Accident Rate (FAR) & Serious Accident Rate (SIR) per 10⁸ exposure hours from 2011-2016

As far as it concerns the F-N Curves, it should be mentioned that is a useful way of comparing industries. Similar curves have been developed for several industries and activities and examples are contained in Evans [23] book. This is the legal requirement in the United Kingdom (U.K) as stipulated in the Health and Safety at Work Act in 1974 and it is also called criterion lines [24]. This use of *F-N* curves has been challenged by some authors [25,26] as it does not conform to decision theory, which has demonstrated that it is the expectation (or average) fatalities per accident that should be used to determine the optimum investment in control measures [27].

The calculations for F-N Curve for Turkish Petroleum Industry are presented in the Table 3.
 2011:1 event with 1 fatality
 2013: 2 events with 3 fatalities
 2014: 1 event with 1 fatality

Figure 9 showss the F-N Curve graph for the data set of fatal accident events across the Turkish Petroleum industry for the period between 2011 and 2016. It is obvious from the graph that the accidents per year with N or more fatalities are reduced due to the fact that there are only few events (3) with one fatality, one event with two fatalities and no events with more than two fatalities.

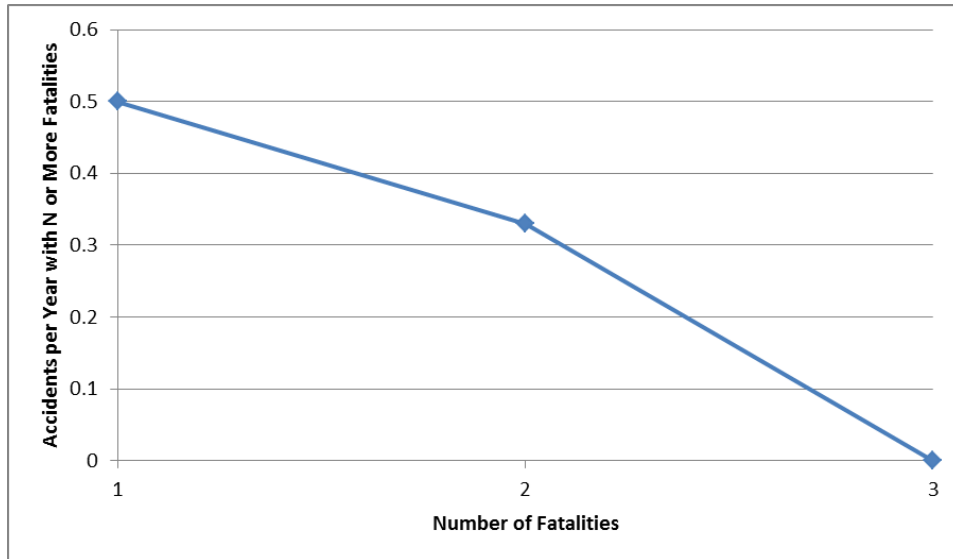


Figure 9. F-Curve for Petroleum Industry between 2011 and 2016

SGK statistics presents Table 4 which includes the total lost work day and days of temporary incapacity for both outpatient and Inpatient occasions from 2011 to 2016

Table 4 Number of total work lost days, days of temporary incapacity both (outpatient) and (inpatient) for Turkish Petroleum sector from 2011 to 2016

	2011	2012	2013	2014	2015	2016
Days of temporary incapacity (Outpatient)	1226	1254	1283	934	809	686
Days of temporary incapacity (Inpatient)	23	82	44	3	28	21
Total work lost days	1249	1336	1327	937	837	707

The Figure 10 presents the days of temporary incapacity (outpatient), days of temporary incapacity (inpatient) and the total work lost days from 2011 to 2016. The days of temporary incapacity (outpatient) have a small augmentation for one year and then there is a gradually reduction, where in 2016 almost reaches half of the days from 2011. On the other hand, the temporary days of incapacity (outpatient) fluctuate with the highest value to be in 2012, 82 days spending in hospital for the employees for a whole year and the smallest value of spending the employees in hospital for a whole year to be in 2014 only 3 days.

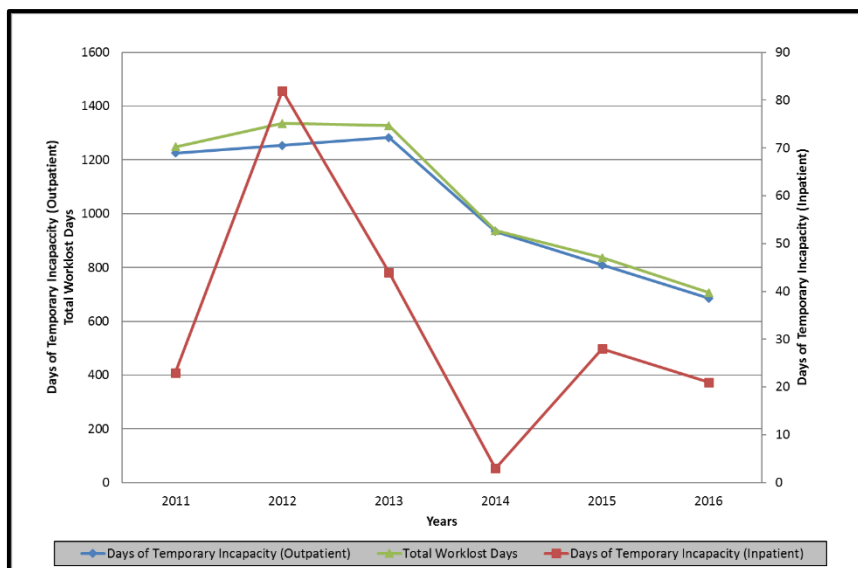


Figure 10 Total work lost days-Days of Temporary Incapacity (Outpatient)-Days of Temporary (Inpatient) from 2011 to 2016

According to equation (6) the Table 5 shows the outcomes for Incident Rate (based on lost work days)

Table 5 Outcomes for Incident Rate (based on lost work days) according to OSHA from 2011 to 2016

	2011	2012	2013	2014	2015	2016
Incident Rate (based on lost work days)	26.00	27.09	27.44	25.62	24.44	23.25

Incident Rate of lost work days follows a small augmentation in the starting years of our research due to both increase in outpatient and inpatient lost work days. From 2013 to 2016 there is a gradually reduction especially to outpatient lost work days. The minimum value of Incident Rate based on lost work days takes place the last year of our research in 2016. Apart from Petroleum Industry all these calculations can be implemented in chemical-petrochemical activities and surface mining activities (continuous and non-continuous) for the exploitation of coal deposits [28].

4. CONCLUSION

The current review highlights the fatal accidents, serious accidents, minor accidents and the number of total work lost days both outpatient and inpatient between 2011 and 2016 for Turkish Petroleum and Natural Gas sector but it can also be implemented in chemical, petrochemical and surface mining (continuous and non-continuous) for the exploitation of coal deposits .

- As far as it concerns the fatalities, with annual average of death 0.67 (per year) show that the results are good with the note that Turkish Petroleum industry is small compared to other ones.
- Minor and serious Accidents have a decreasing trend between 2011 and 2016 with the exception of 2014 due to increase in drilling activities.
- Total work lost days also follow downward trend with from 1249 (2011) to 707 (2016) which corresponds to a change of 57%. This is a sign of improvement in safety practices within oil industry.

REFERENCES

- [1] Lucchini R.G, London L, “Global Occupational Health: Current Challenges and the Need for Urgent Action”, *Annals of Global Health* 2014; 80: 251-256
- [2] London L, Kisting S, “Ethical concerns in international occupational health and safety”, *Occup Med* 2002; 17: 587e600
- [3] Mihailidou K.E, Antoniadis K.D, Assael M.J, “The 319 Major Industrial Accidents Since 1917”, *International Review of Chemical Engineering (I.RE.CH.E.)* 2012; Vol. 4, N. 6, pp.529-539
- [4] Melamed S, Yekutieli D, Fromm P, Kristal-Boneh E, Ribak J, “Adverse work and environmental conditions predict occupational injuries. The Israeli cardiovascular occupational risk factors determination in Israel (CORDIS) study”, *Am J Epidemiol* 1999; 150:18–26
- [5] Unsar A. and S,Sut A.* “Occupational Accidents in the Energy Sector: Analysis of Occupational Accidents That Occurred In Thermal and Hydroelectric Centrals between 2002 And 2010 In Turkey”, *Social and Behavioral Sciences* 181 (2015) 388-397
- [6] Ceylan H., A new approach to occupational accidents: “Technique of deviation from means”, *Energy Educational Science and Technology Part B: Social and Educational Studies* 2013 Volume: 5(2): 819-830
- [7] Ahiskali A “Energy use in transportation and the effects on road accidents of improvement in the highway safety systems. *Energy Educational Science Tech-A* 2012; 1:643-648
- [8] Cavide U.,Adal Z.,A., Cevat Ataay I.,Acar A.C.,Ozdelik O., Dundar G., Sadullah O, Tuzuner L.,(2009). *Insan Kaynaklari Yonetimi, Beta Basim Yanim Dagitim A.S., 4.Baski, Istanbul*
- [9] Longinos S.N, Qadri Y.M, Parlaktuna M, “Health and Safety Conditions in Four Major Industrial Sectors of Pakistan from 2010 to 2015”, *International Journal of Petroleum and Petrochemical Engineering (IJPPE)* 2017; 3(4), pp.102-110
- [10] NACE Rev. 2, (2008) *Statistical Classification of Economic Activities in the European Community*, ISSN 1977-0375
- [11] SGK (Social Security Institution), “2011 Statistical Yearbooks”, SGK Yayini, Ankara, 2011
- [12] SGK (Social Security Institution), “2012 Statistical Yearbooks”, SGK Yayini, Ankara, 2012
- [13] SGK (Social Security Institution), “2013 Statistical Yearbooks”, SGK Yayini, Ankara, 2013
- [14] SGK (Social Security Institution), “2014 Statistical Yearbooks”, SGK Yayini, Ankara, 2014
- [15] SGK (Social Security Institution), “2015 Statistical Yearbooks”, SGK Yayini, Ankara, 2015
- [16] SGK (Social Security Institution), “2016 Statistical Yearbooks”, SGK Yayini, Ankara, 2016
- [17] Renton N.C, Baker M.J and Tan H. “Fundamental Safety engineering and Risk Management Concepts”, 2012/2013, Aberdeen Lecture Notes, Scotland
- [18] Renton N.C, Baker M.J and Tan H. “Fundamental Safety engineering and Risk Management Concepts”, 2012/2013, Aberdeen Lecture Notes, Scotland
- [19] Hughes P. and Ferrett E., *Introduction to Health and Safety at Work*, 3rd edition, 2007
- [20] BS 4778-3.1:1991. *Quality vocabulary. Availability, reliability and maintainability terms. Guide to concepts and related definitions.* British Standards Institute, 1991
- [21] Hagon D.O. Use of frequency-consequence curves to examine the conclusions of published risk analysis and to define broad criteria for major hazard installations, *Chemical Engineering Research and Design*, 62(6):381–386, 1984

- [22] Romer H., Haastrup P., and H. J. Styhr Petersen. Accidents during marine transport of dangerous goods. Distribution of fatalities, *Journal of Loss Prevention in the Process Industries*, 8(1):29–34, 1995
- [23] Evans A.W. RR073-Transport fatal accidents and FN-curves: 1967-2001. Health and Safety Executive. 2003. URL www.hse.gov.uk/research/rrpdf/rr073.pdf.
- [24] Health and Safety Executive. The tolerability of risk from nuclear power stations. HMSO, 1992.
- [25] Evans A.W and Verlander N.Q. What is wrong with criterion FN-lines for judging the tolerability of risk? *Risk Analysis*, 17(2):157–168, 1997.
- [26] Hirst I.L. Risk assessment. a note on f-n curves, expected numbers of fatalities, and weighted indicators of risk. *Journal of Hazardous Materials*, 57(1-3):169–175, 1998
- [27] Lindley D.V. *Making Decisions*. 1985
- [28] Ceylan H., Analysis of Occupational Accidents According to the Sectors in Turkey, *Gazi University Journal of Science*, 25(4):909-918, 2012

Adaptation of Fruit Crops in Rehabilitated Old Mines Soils in West Macedonia Lignite Centre

I. Papadopoulos¹, M. Tentsoglidou², C. Papadopoulos², B. Taralidis² and F. Papadopoulou¹

¹Technological Education Institute of West Macedonia, 53100 Florina, Greece

²Public Power Corporation, West Macedonia Lignite Centre, P.O.Box 21, 50200 Ptolemaida, Greece

ABSTRACT

The primary purpose of rehabilitation in post mine area in West Macedonia Lignite Centre, Northern Greece is the recovery of the nature and ecosystem, and the creation of a self-sustaining land surface. However, the effective utilization of post mine area for the productive uses such as agricultural crops and other potential economic have been taken into consideration in recent years. About 1,000 ha of these land are already covered annually with cereal crops, but require specific treatment if they are to be rehabilitated for fruit land production. A 5ha orchard and a vineyard were established by the Public Power Corporation SA in an old mine to evaluate the adaptability of 12 fruit trees species in this specific environment. In 2001 were planted 15 apple, 9 pear, 10 cherry, 3 walnut, 9 peach, 1 nectarine, 1 plum, 4 grapevine, 1 quince, 1 jujube, 1 raspberry, 1 gooseberry and 2 persimmon varieties. After 15 years of cultivation several problems recorded regarding adaptation on soil or climatic conditions. Success of crop adaptation was judged on the basis of yield, blossom set, incidence of disease and survival rates in comparison to adjacent control orchards. Grapevine, cherry, walnut, apple and jujube trees responded quite well while persimmon, plum, peach, raspberries pear and quince trees revealed severe adaptation problems. Fruit yield in rehabilitated soils did not exceed 60% of control orchards yield while tests for heavy metal did not show significant differences compared with local market fruits.

1. INTRODUCTION

The lignite production activities carried out for more than five decades in Ptolemais lignite-bearing basin, in the Region of West Macedonia, Northern Greece, have caused significant modifications in numerous environmental constituents of the greater area mainly due to their size and the applied surface mining method [1,2].

The primary purpose of rehabilitation in post mine area is the recovery of the nature and ecosystem, and the creation of a self-sustaining land surface. However, the effective utilizations of post mine area for the productive uses such as agricultural crops and other potential economic use options have been taken into consideration in recent years [3]. In case that the selected land use is 'agricultural land' the type of crops or tree species could be planted are relevant to the suitability of soil for supporting growth of plants since the soil of a mine site might be in extreme conditions with a heavy lack of nutrients and a high level of toxicity [4]. Climatic conditions as well as determine the adaptation of species in a region. In this research, evaluated the adaptation of tender-fruit trees in a post mine area [5].

2. METHODOLOGY

The study area was located on a waste dump, in rehabilitated land cultivated for more than a decade with cereal crops. A 5ha orchard and a vineyard were established by the Public Power Corporation SA to evaluate the adaptability of 12 fruit trees species in this specific environment

(Figures 1 and 2). Slopes varied from nearly level to gentle, making farm management easier as well as permitting cold air drainage and surface water drainage. According to the results of lab analyses the soil was characterized by an alkaline pH and normal electrical values. The particle size distribution varied from moderately coarse to fine low clay percentages, a typical feature of recently formed soils. The organic matter content varied from medium to high due to lignite of low calorific value been dumped. Reduction of organic matter content with depth, which is typical in normal agricultural soils, was not observed. There was a high CaCO₃ content since mine spoils were formed by marls. Cation exchange capacity (CEC) was high, mainly due to high concentrations of Fe in assimilable form. Sufficient concentrations of the exchangeable cations K⁺ Ca²⁺ and Mg²⁺ were determined while the Phosphorus concentrations were below the accepted availability level of 20mg/kg. Regarding the availability of micronutrients, only Zn exhibited deficiency, while the Fe and Mn concentrations were too high. Moreover Co and Ni concentrations were below the level of toxicity and the probability to trace them in the food chain was very low, taking into consideration the high soil pH values, which does not favour the mobility of metals and, consequently, the increase of their availability to plants [6].

In 2001 were planted 15 apple, 9 pear, 10 cherry, 3 walnut, 9 peach, 1 nectarine, 1 plum, 4 grapevine, 1 quince, 1 jujube, 1 raspberry, 1 gooseberry and 2 persimmon varieties. Plant care program on the advice of horticulturists of West Macedonia Technological Institute, included fertilization according to soil test or leaf tissue analyses, appropriate staking of new trees, pruning and pesticide applications.

3. RESULTS AND DISCUSSION

During 2010-2014 growing periods detailed notes concerning health of the fruit trees, relative amount of blossom, relative yields, soil characteristics, farm management and special problems in rehabilitation success were taken (Table 1).

Grapevine, cherry, walnut, apple (except Gala and Scarlet varieties) and jujube trees responded quite well yielding up to 60% of control orchards yield while tests for heavy metal didn't show significant differences compared with local market fruits. Peach and Persimmon were the most sensitive fruit crops, damaged by late spring frosts. Raspberries failed probably due to the high soil pH values. Pear and Quince withstand low spring temperatures but suffered from severe fire blight infection (except Nashi and Harrow sweet varieties) resulting in destruction of all trees 10 years after planting.

It seems that in order for fruit tree crops on the rehabilitated soils not to be restricted due to soil infertility, rates of fertiliser to be applied should exceed normal agricultural dressings. Further investigation on the use of soil amendments such as bio solids, mulch and compost for improvement of crop growth and yield, is necessary [7].



Figure 1. The 5ha orchard of West Macedonia Lignite Centre



Figure 2. Aerial photograph of Ptolemais lignite-bearing basin (a) and the 5ha orchard located in the reclaimed waste heap of Main Field Mine

Table 1. Adaptation, response and problems recorded of fruit tree species planted on rehabilitated soils in West Macedonia Lignite Centre.

Tree species	Variety / rootstock	Adaptation	Problems
Apple	Red chief / MM106	<input type="checkbox"/> <input type="checkbox"/> <input type="checkbox"/>	
	Golden delicious / M26	<input type="checkbox"/> <input type="checkbox"/> <input type="checkbox"/>	
	Golden smooth / M26	<input type="checkbox"/> <input type="checkbox"/> <input type="checkbox"/>	
	Scarlet / M106	<input type="checkbox"/>	
	Jona gored / M26	<input type="checkbox"/> <input type="checkbox"/> <input type="checkbox"/>	
	Jona gold / M26	<input type="checkbox"/> <input type="checkbox"/> <input type="checkbox"/>	
	Gala / M26	<input type="checkbox"/>	
	Pink kiss / M26	<input type="checkbox"/> <input type="checkbox"/> <input type="checkbox"/>	
	Pink kiss / M9	<input type="checkbox"/> <input type="checkbox"/>	
	Fuji / M26	<input type="checkbox"/> <input type="checkbox"/> <input type="checkbox"/>	
	Guerin / M26	<input type="checkbox"/> <input type="checkbox"/>	
	Firiki / M26	<input type="checkbox"/> <input type="checkbox"/> <input type="checkbox"/>	
	Red chief spur / M26	<input type="checkbox"/> <input type="checkbox"/> <input type="checkbox"/>	
	Fuji kiku 8 / M9	<input type="checkbox"/> <input type="checkbox"/>	
	Red chief sandige / M26	<input type="checkbox"/> <input type="checkbox"/>	
Pears	Kristali / OHF333	<input type="checkbox"/> <input type="checkbox"/>	Fire blight
	Toska / OHF333	<input type="checkbox"/> <input type="checkbox"/>	Fire blight
	Kontoula / OHF333	<input type="checkbox"/> <input type="checkbox"/>	Fire blight
	Nashi	<input type="checkbox"/>	
	Abate fetell	<input type="checkbox"/> <input type="checkbox"/>	Fire blight
	Williams / OHF333	<input type="checkbox"/> <input type="checkbox"/>	Fire blight
	Highland / OHF333	<input type="checkbox"/> <input type="checkbox"/>	Fire blight
	Harrow sweet / OHF333	<input type="checkbox"/> <input type="checkbox"/>	
General Leclerc / OHF333	<input type="checkbox"/>	Fire blight	
Cherries	Grace star / Gi	<input type="checkbox"/> <input type="checkbox"/> <input type="checkbox"/>	
	UFO	<input type="checkbox"/> <input type="checkbox"/> <input type="checkbox"/>	
	Black star / Gi	<input type="checkbox"/> <input type="checkbox"/> <input type="checkbox"/>	
	Kordia / Gi 6	<input type="checkbox"/> <input type="checkbox"/> <input type="checkbox"/>	
	Ferrovio / Gi 5	<input type="checkbox"/> <input type="checkbox"/> <input type="checkbox"/>	
	Regina / PIKU 1	<input type="checkbox"/> <input type="checkbox"/> <input type="checkbox"/>	
	Lapen / Gi 5	<input type="checkbox"/> <input type="checkbox"/>	
	Tragana / CAB	<input type="checkbox"/> <input type="checkbox"/> <input type="checkbox"/>	
	Bakirtzi / CAB	<input type="checkbox"/> <input type="checkbox"/> <input type="checkbox"/>	
	Harond giant / CAB	<input type="checkbox"/> <input type="checkbox"/>	
Walnuts	Franquette	<input type="checkbox"/> <input type="checkbox"/> <input type="checkbox"/>	
	Pentro	<input type="checkbox"/> <input type="checkbox"/>	
	Melanez	<input type="checkbox"/> <input type="checkbox"/>	
Peaches	Andros / GF677	<input type="checkbox"/>	
	Fayette	<input type="checkbox"/>	
Nectarine	Red gold / CF677	<input type="checkbox"/> <input type="checkbox"/>	
Grapevines	Xinomavro / 41B	<input type="checkbox"/> <input type="checkbox"/> <input type="checkbox"/>	
	Shiraz / 41B	<input type="checkbox"/> <input type="checkbox"/>	
	Chardone / 110R	<input type="checkbox"/> <input type="checkbox"/>	
	Cabarnet / 41B	<input type="checkbox"/> <input type="checkbox"/> <input type="checkbox"/>	
Persimmon	Vanilla	<input type="checkbox"/>	
	Hana fugiou	<input type="checkbox"/>	
Quince	Giant	<input type="checkbox"/>	Fire blight
Jujube	Lag	<input type="checkbox"/> <input type="checkbox"/>	
Raspberry		<input type="checkbox"/>	
Gooseberry		<input type="checkbox"/> <input type="checkbox"/>	

- Well adapted, good growth, 50-60% of control orchards yield
 Well adapted medium growth, 30-50% % of control orchards yield
 Poor adaptation, limited growth and yield

4. CONCLUSIONS

The lignite mining activities carried out since 1950's in West Macedonia Lignite Centre, Northern Greece, have caused significant modifications in numerous environmental constituents of the greater area mainly due to their size and the applied surface mining method. To this extent, the primary purpose of rehabilitation in a post mine area of about 16,000 ha is the recovery of the nature and ecosystem, and the creation of a self-sustaining land surface.

However, all decisions related to the reclamation of mine land should take into account the need of developing new economic activities, which will compensate, even partly, the loss of thousands of jobs related directly or indirectly with mining and electricity generation activities. For this reason, the effective utilization of post mine area for productive uses, such as agricultural crops, has been investigated in recent years. About 1,000 ha of mine land that has already been reclaimed is covered annually with cereal crops, but require specific treatment if they are to be rehabilitated for fruit land production.

The 5 ha orchard, which was established in 2001 in the reclaimed waste heap of Main Field mine, was the ideal place to evaluate the adaptability of 12 fruit trees species in this specific environment. After 15 years of cultivation several problems recorded regarding adaptation on soil or climatic conditions. Success of crop adaptation was judged on the basis of yield, blossom set, incidence of disease, and survival rates in comparison to adjacent control orchards. Grapevine, cherry, walnut, apple and jujube trees responded quite well while persimmon, plum, peach, raspberries pear and quince trees revealed severe adaptation problems.

REFERENCES

- [1] Pavloudakis F., C. Roumpos (2004). Evaluation of land reclamation and environmental protection strategies in open-pit lignite mines, Intl. Conf. on Advances in Mineral Resources Management and Environmental Geotechnology, Hania, Greece, 9-11 June 2004, pp. 473-480.
- [2] Pavloudakis F., M. Galetakis and C. Roumpos (2009). A spatial decision support system for the optimal environmental reclamation of open-pit coal mines in Greece. *International Journal of Mining, Reclamation and Environment*. 291-303. 10.1080/17480930902731935.
- [3] Hargraves, A. J., C.H. Martin & Australasian Institute of Mining and Metallurgy (1993). *Australasian coal mining practice* (2nd ed). Australasian Institute of Mining and Metallurgy, Parkville, Vic.
- [4] Subodh K. M., A. Kumar and J. Ahirwal (2015). Bioaccumulation of metals in timber and edible fruit trees growing on reclaimed coal mine overburden dumps, *International Journal of Mining, Reclamation and Environment*, 30:3, 231-244, DOI: 10.1080/17480930.2015.1038864.
- [5] Dagar C., G. Singh & N. T. Singh (2010). Evaluation of Forest and Fruit Trees Used for Rehabilitation of Semiarid Alkali-Sodic Soils in India, *Arid Land Research and Management*, 15:2,115-133, DOI:10.1080/15324980151062742
- [6] Papadopoulou C., C. Geka, F. Pavloudakis, C. Roumpos and S. Andreadou (2015). Evaluation of the Soil Quality on the Reclaimed Lignite Mine Land in West Macedonia, Greece. *Procedia Earth and Planetary Science*. 15. 928-932.
- [7] Neldner, VJ, Ngugi, MR (2014). 'Application of the BioCondition assessment framework to mine vegetation rehabilitation', *Ecological Management & Restoration*, 15(2):158-161.

Evaluation of Honey Producing Potential of Robinia Pseudacacia in Reforested Old Lignite Mines in West Macedonia

F. Papadopoulou¹, M. Tentsoglidou², F. Pavloudakis², N. Papadimopoulos² and I. Papadopoulos¹

¹Technological Education Institute of West Macedonia, 53100 Florina, Greece

²Public Power Corporation, West Macedonia Lignite Centre, P.O.Box 21, 50200 Ptolemaida, Greece

ABSTRACT

Opencast mining is important for local and global economy, but this operation mostly and inevitably leads to substantial environmental damage. Potential future use of the post-mining lands basically depends on the nature of the land, soil conditions, and communal structure of nearby surrounding to be rehabilitated by technical, biological, agricultural means or forestry applications. Vegetation cover has significant functions on post-mining landscapes so, in order to reduce the probability of negative impacts, selection of suitable plant material, which may be preferably native but also introduced plant species, is critical. In West Macedonia Lignite Centre, about 1,500 ha of these land have already reforested by the Public Power Corporation S.A., with Robinia pseudacacia L., one of the most criticized non-native tree species in Europe, because its rootstocks spread into neighbouring areas, repressing native species. The tree is an excellent species for revegetating poor or damaged soils and its fast-growing nature, makes it popular for former lignite mine reclamation, reforestation and erosion control. Robinia forests represent a valuable nectar and pollen source in late spring for many insects, especially Hymenoptera, such as *Apis mellifera*. That has increased dramatically the regional honey producing potential. In this study, the annual potential honey production of 1,500ha black locust forests established in reforested old mines land, was estimated from 50,000 to 70,000 kg honey, depending on the year, which is sufficient for up to 1,000 bee hives to survive for one year. For the efficient utilization of this valuable honey producing source by the beekeepers, a plan should be developed, to facilitate accessibility to the region and proper beehives dispersion.

1. INTRODUCTION

Coal mining forms an important industry branch, which covers a large segment of energy demand in Greece. While coal mining entails infrastructure and jobs for West Macedonia region, have caused significant modifications in numerous environmental constituents of the greater area mainly due to their size and the applied surface mining method. Potential future use of the post-mining lands basically depends on the nature of the land, soil conditions, and communal structure of nearby surrounding to be rehabilitated by technical, biological, agricultural means or forestry applications. In West Macedonia Lignite Centre, about 1,500 ha of old lignite mines land have already reforested by the Public Power Corporation S.A., with Robinia pseudacacia L., one of the most criticized non-native tree species in Europe, because its rootstocks spread into neighbouring areas, repressing native species [1]. Known as the black locust in the USA and as false acacia in Europe, Robinia pseudoacacia L. belong to the Fabaceae family and has been imported all over Europe since the beginning of the eighteenth century thanks to its ability to adapt to different environmental conditions. The tree has nodules of nitrogen-fixing bacteria on its roots which make it an excellent species for revegetating poor or damaged soils and its fast-growing, sun-light loving and unpretentious nature makes it popular for former brown-coal mine reclamation, reforestation and

erosion control (Figure 1). In addition, black locust starts flowering early, often at an age of six years [2] and the flowers are highly valued for their source of nectar and pollen for many insects, especially Hymenoptera, such as *Apis mellifera* (Figure 2). Black locust honey is often sold as acacia honey [3] and the production of this type of honey is very common and economically important [2]. The research objectives of this study is to evaluate the honey producing potential of the largest black locust forest can be found in Greece, created by PPC plantations in West Macedonia Lignite Centre, by estimation of the number of flowers and nectar production of *R. pseudoacacia*.

2. METHODOLOGY

The study area was previously used for brown-coal mining and has now been recultivated with different tree species. The black locust plantations started 30 years ago and continued up to 2016 covering more than 1,500ha with average density 2,000 trees per ha. Plantations were classified in four categories depending on the tree age, planting density, and canopy diameter (Table 1).

For each category three 100m² plots selected randomly and all trees harvested at May 2015 flowering period and flowers weighted. Furthermore, a sample of 100 inflorescences of each plot were selected randomly, weighted and the total number of flowers was counted.

The total flower number for each plot is calculated:

$$n \text{ plot flowers} = \text{total weight of flowers} / (\text{weight} / \text{number of sample flowers}).$$

The mean flower number per hectare for each category is calculated by multiplying the mean flower number of the 3 plots by 100.

Nectar estimation is based on literature information [4, 5, 6]. *R. pseudoacacia* blossoms flower for 5.5 days and produce 1.6–3.7 mg nectar per flower over 24 h. Robinias nectar has a sugar concentration of 34–67%, so the sugar mass per flower over 24 h is 0.8–2 mg.



Figure 1. *Robinia pseudoacacia* L. plantations used for slope stabilisation and erosion control in Amynteon mine, West Macedonia Lignite Centre, Greece.

Table 34. Area of *Robinia* forest categories according to the age and canopy cover percentage and estimated nectar production

	Robinia forest category	Area (ha)	Mean Number flowers/ha (millions)	Nectar/ha* (kg)	Nectar production (kg)
A	10 years old, canopy cover > 90%	874.5	10.24	112.6	98,500

B	10 years old, canopy cover 70-90%	321.7	11.41	125.5	40,400
C	10 years old, canopy cover 50-70%	17.8	9.75	107.3	1,900
D	6-10 years old, canopy cover 70-90%	247.3	8.83	97.1	24,000
E	6-10 years old, canopy cover 50-70%	36.0	7.89	86.8	3,100
Total		1,497.3			167,900

*Assuming 2mg nectar yield/flower/day, and average flowering period of 5,5 days

3. RESULTS AND DISCUSSION

Based on aerial photographs (Figure 4) the total Robinia forests area classified in five categories depending on the canopy cover percentage (Table 1).

Mean number of flowers/ha and corresponding nectar production/ha were higher in plantations with an age >10 years than younger plantations. Farkas and Zajacks reported, nectar and honey yield of black locust in Hungary, increases from year 6 to year 15 [6]. Within the same age plantations those with lower canopy cover produced more flowers/ha compared to those with greater canopy cover. In *Eucalyptus nitens* as tree density decreased, the production of flowers and capsules increased on both a per-tree and per-hectare basis [7].

Robinia flowers attract the honey bee as well as other bee species. Papilionate flowers, such as those of *Robinia pseudoacacia* L., show tripping mechanisms that prevent pollen release: only those bees which apply the right force on petals induce pollen to be deposited on their bodies. *Apis mellifera* is considered a poor visitor of such flowers, since individuals are usually too weak to trip the mechanism.

This deficiency has been acknowledged as the reason why honey bees usually avoid flowering Fabaceae [8], visit already tripped flowers [9] or turn to alternative strategies, such as robbery, to collect nectar on them [10, 11].



Figure 2. (a) The flowers of *Robinia pseudoacacia* L. (b) Bee hives located at the foot of the reclaimed waste heap of Amynteon mine.



Figure 3. Aerial photograph of *Robinia pseudoacacia* L. plantations (dark green colour) in the waste heap of Amynteon mine, West Macedonia Lignite Centre, Greece.

In the first day of anthesis we recorded many visits of *Xylocopa* sp. And *Bombus* sp. on *Robinia* flowers but none of *Apis mellifera* honeybees. In

fact *Apis mellifera* cannot access nectar in *Robinia* flowers at the beginning of anthesis with petals perfectly distended and fresh, therefore the main collection starts when flowers show the first evidence of ageing. Ageing flowers may differ in the arrangement [12] and turgescence of their petals due to water loss during flowering or due to previous visits of other pollinators. We estimate 70-90% of the total nectar secretion of *Robinia* flowers can be utilized by *A. mellifera* colonies . That means 50-70 t of honey/year are obtainable in *Robinia* forests of Lignite Center in West Macedonia which is sufficient for up to 1,000 bee hives to survive for one year. Nectar flows vary from year to year as are very dependent on local weather conditions. Good forage activity cannot be expected under 20°C. Heavy rains, which is often the case at the flowering of the black locust enhance the aging and destruction of flowers and thus can cause severe losses exceeding 50% of the expected nectar flow.

Robinia honey, is the latest crystallizing among honeys, has a mild flavour, has an important role on the international honey market, considering both quantity and quality. Among European countries producing significant amount of *Robinia* honey are Hungary, Romania, Italy, France and Slovakia. Since a prerequisite of producing *Robinia* honey is the effective positioning of beehives in order to the colonies be maximally able to collect the nectar, a plan should be developed, to facilitate accessibility to the Lignite Centre of West Macedonia *R. pseudoacacia* plantations and proper beehives dispersion.

4. CONCLUSION

Opencast mining is important for global economy and regional development. However, this operation threaten quality of environmental in numerous ways. Particularly in cases of large-scale coal and lignite mines, the disturbance of land is an unavoidable impact that affects both nature and society. Therefore, the development of a site-specific land reclamation programme is essential for minimising the adverse environmental impacts. To this extent, the establishment of a vegetation cover has significant functions on post-mining landscapes. This is also the case of West Macedonia Lignite Centre, where about of 1,500 ha of waste heaps final surfaces have already reforested with *Robinia pseudacacia* L.. This is one of the most criticized non-native tree species in Europe, because its rootstocks spread into neighbouring areas, repressing native species. Nevertheless, this tree is an excellent species for revegetating poor or damaged soils and its fast-growing nature, makes it popular for former lignite mine reclamation, reforestation and erosion control.

Robinia forests represent a valuable nectar and pollen source in late spring for many insects, especially Hymenoptera, such as *Apis mellifera*. That has increased dramatically the regional honey producing potential. In this study, the annual potential honey production of 1,500ha black locust forests established in reforested old mines land, was estimated from 50,000 to 70,000 kg honey, depending on the year, which is sufficient for up to 1,000 bee hives to survive for one year.

Taking into consideration the above facts, the efficient utilization of this valuable honey producing source must be taken into account in decision-making and planning procedures related to the selection of the optimum mix of land uses for the reclaimed mine land.

REFERENCES

- [1] Basnou C., (2006). European Commission under the Sixth Framework Programme through the DAISIE Project. Delivering Alien Invasive Species Inventories for Europe—Species Factsheet *Robinia Pseudoacacia*. Available online: <http://www.europe-alien.org/speciesFactsheet.do?speciesId=11942>.
- [2] Ridei, K. (2013). Black Locust (*Robinia pseudoacacia* L.) Growing in Hungary; Hungarian Forest Research Institute: Sarvar, Hungary, 2013; pp. 72–73.
- [3] Aronne G, Buonanno M, De Micco V., (2008). Improving honey production and marketing. S. B. R, Naples. ISBN 88-901941-3-8.
- [4] Maurizio, A., Graf1, I., (1982). Das Trachtpflanzenbuch. Nektar und Pollen — die wichtigsten Nahrungsquellen der Honigbiene. Munich, German Federal Republic: Ehrenwirth Verlag. 368 pages. 3rd ed.
- [5] Cran E. and P. Walker. (1985). Some nectar characteristics of certain important World honey sources, *Pszczel. Zesz. nauk.* 29: 29-45
- [6] Farkas A. and Zajacz E. (2007). Nectar production for the Hungarian honey industry. *The European Journal of Plant Science and Biotechnology* 1(2): 125-151.
- [7] Dean R. W., B. M. Potts, W. A. Neilsen & K. R. Joyce, (2013). The effect of tree spacing on the production of flowers in *Eucalyptus nitens*, *Australian Forestry*, 69:4, 299-304, DOI: 10.1080/00049158.2006.10676250.
- [8] Cordoba S.A, Cocucci A.A, (2011). Flower power: its association with bee power and floral functional morphology in papilionate legumes. *Ann Bot* 108:919–931. doi:10.1093/aob/mcr196.
- [9] Parker I.M, Engel A, Haubensak K.A, Goodell K, (2002). Pollination of *Cytisus scoparius* (Fabaceae) and *Genista monspessulana* (Fabaceae), two invasive shrubs in California. *Madrono* 49(1):25–32.

[10] Etcheverry A.V, Aleman M.M, Figueroa Fleming T, (2008). Flower morphology, pollination biology and mating system of the complex flower of *Vigna caracalla* (Fabaceae: Papilionoideae). *Ann Bot* 102:305–316. doi:10.1093/aob/mcn106.

[11] Aronne G, Giovanetti M, De Micco V, (2012). Traits and pollination mechanisms of *Coronilla emerus* L. flowers (Fabaceae). *Scientific World Journal* 2012, Article ID 381575. doi:10.1100/2012/381575.

[12] Willmer P, Stanley D.A, Steijven K, Matthews I.M, Nuttman C.V, (2009). Bidirectional flower color and shape changes allow a second opportunity for pollination. *Curr Biol* 19:919–923.

Sustainable Development Analysis of Lignite Mining, by Coupling Environmental, Economic and Social Indicators

Nikolaos Paraskevis, Daphne Sideri, Nikolaos Stathopoulos, Christos Roumpos and Francis Pavloudakis

Public Power Corporation of Greece, Mines Division, 29 Chalkokondili Str., Athens, Greece

ABSTRACT

Energy sufficiency is a primary target for all countries worldwide. Fossil fuels lie at the top of the list of resources that must be exploited to accomplish this target. Continuous surface mining occupies a high proportion of the category of coal/lignite production, thus holding a leading role both in the energy and financial markets. In addition, these large-scale operations extend to more areas of human life with various environmental, social and economic impacts. All the above, constitute the evaluation and assessment of a lignite deposit, in terms of sustainable exploitation, a particularly complex process. This paper attempts to contribute on this field by presenting an indicator for sustainable development called “TOSDIMA” (TOTAL Sustainable Development Indicator for Mining Activity) and by implementing it in a lignite deposit in Greece. TOSDIMA is synthesized by three Environmental, four Economic and two Social sub-indicators which are directly linked with the sustainable development assessment. The proposed method includes the analysis and quantification of the sub-indicators and their synthesis for estimating the TOSDIMA value for the lignite deposit. The proposed framework can constitute a useful tool for planning exploitation strategies, managing mining activities, supporting and validating research and operational objectives, by always taking into consideration sustainability standards and viable development perspectives.

Key words: TOSDIMA, Lignite Deposits, Mining Management & Planning

1. INTRODUCTION

Mining industry is a key factor of national economies and energy sufficiency worldwide. In the 21st century, the exploitation of natural resources is considered to be an extremely sensitive and important topic, as it implicates environmental, social and economic aspects with significant impacts on the financial markets, the societies, the human life and the global ecosystem. In these terms, sustainable exploitation and development is considered to be crucial in all activities of the mining sector. All the above, constitute the evaluation and assessment of natural resources, and especially lignite deposits, in terms of sustainable exploitation, a very composite and complex attempt.

In this light, many researchers have worked on aspects of sustainable development in surface mining. Many countries depend on coal mining in order to ensure their energy adequacy, constituting the matter of sustainability, on this field, a primary research topic. In China, Yu [1] and Song et al. [2] discussed the matter of environmental and sustainable development in coal mining. Chikkatur et al. [3] examined the sustainable development of the Indian coal sector and Crayon et al. [4] used a GIS-based methodology to identify sustainability conflict areas in mine design for a surface coal mine in the USA. As it can be clearly understood by the above research works, sustainability in coal mining is a matter of global interest.

In a more applied and operational aspect, several research works have been made on the development of various indicators and criteria suitable to research, estimate and assess sustainable mining. In 2003, Hilson and Basu [5] described the critical background issues when devising

Sustainable Development Indicators (SDIs). Moreover, Chen's et al. [6] applied a multicriteria analysis in order to evaluate and measure SDIs, within economic categories under uncertainty, for the mining industry of China. According to the research works which are mentioned above, it can be clearly seen that the development and proper use of SDIs is not an easy process and demands a detailed analysis. Furthermore, Roumpos et al. [7] published a comparative analysis and evaluation of the application of specific SDIs that represent economic, environmental, and social performance of the mining companies.

As can be seen from the above, the matter of sustainable development research in the mining sector, with the form of analysis via indicators, is also a topic of global interest, which is applied in various types of mining. In Niger, for example, Chamaret et al. [8], proposed a top-down/bottom-up approach for developing SDIs and applied the method to the Arlit uranium mines. From a different point of view, Putzhuber and Hasenauer [9] used statistical models to assess and apply sustainability impact indicators at the Eisenwurzen region in Austria, an old and famous mining area within the Alps, creating thus a diagnostic tool able to provide insights for assessing SDIs.

Furthermore, Dong et al. [10] covered a different type of mining, in specific phosphorus mines, by selecting and applying 31 evaluation indices covering aspects like general management, environmental protection, mining techniques, mining economy, waste management, providing thus an important guidance for the sustainable development of phosphorous mines. Finally, a very interesting research work is the one of Marnika et al. [11], who formulated and proposed 36 SDI's for mining sites in protected areas (NATURA 2000, etc.), which were categorized in 7 groups and each one's importance value was determined on the scale of 0 – 5. They also developed a decision support tool, based on these indicators, and assessed 12 different mining scenarios.

The trend to analyse and design mining activities via SDI's kept rising through the years and many researchers attempted to propose new ways and techniques, either for developing new indicators or for working properly with them. Azapagic [12] developed a framework for SDI's as a tool for performance assessment and improvements in the mining and minerals industry. His footsteps were followed, the following year, by Roumpos et al. [13], who developed a decision making model based on indicators, which formed a final index, for the evaluation of the exploitation strategy for lignite deposits. From another prospect Worrall et al. [14] created a sustainability criteria and indicators framework for suiting the needs of legacy mine land. Their resulting framework consisted of 14 criteria and 72 indicators. Finally, an interesting view on mining sustainability was also the work of Poveda [15] concerning a methodology for pre-selecting SDIs and its application to surface mining operations.

Moreover, most researchers attempted to assess different aspects of the mining activities with SDIs. From an economic point of view, Rodriguez [16], proposed a productivity index for measuring the economic sustainability of the Spanish mining industry. Focusing on social analysis, Horsley et al. [17] published their framework for sustainable livelihoods and indicators for regional development in mining economies, and on the same page Suopajarvi et al. [18] published their study on social sustainability in northern mining communities, focusing on European North and Northwest Russia. From an environmental perspective, Wozniak & Pactwa [19] discussed the environmental activity of Poland's mining industry by analyzing the value of SDIs and their use in this field.

In conclusion, SDIs occupy a key role in contemporary mining development covering many environmental, social and economic aspects. They are used to evaluate alternatives in mine planning [20], to classify the exploitation of various natural resources [21], to evaluate the sustainability performance of mining companies [22] and in many other applications. Finally, sustainable development is also important in other types of exploitation, like Deep-Sea Mining, taking under consideration economic, technical, technological and Environmental aspects [23].

Considering the development of continuous surface mining projects for the exploitation of multiple-seam lignite deposits, in relation to their large-scale operations and the current economic, social and environmental conditions, a further investigation for the sustainability of these projects is

essential. In this framework, an integrated TOtal Sustainable Development Indicator for Mining Activity (TOSDIMA) is developed in this paper and it is applied in a lignite deposit in Greece.

2. THEORETICAL ANALYSIS

The application of sustainable development indicators in a lignite deposit is an attempt to evaluate the future mining works which are not active at the time of the assessment. In the case of a mine in operation, most of the parameters associated with indicators are directly measurable. On the contrary, in the case of a lignite deposit, the available information is based on the drilling data and the technical studies regarding its future development. Therefore, the number of the available indicators, which reflects the viability of the mining activity, is limited.

Based on a previous work [30], a quantitative model for the evaluation of a lignite deposit in combination of a power plant operation, is based on the parameters of Table 1.

Table 1: Parameters of a lignite deposit evaluation model [30]

Parameter	Symbol	Unit
Lignite reserves	R	t
Low calorific value	H	kcal/kg
Capacity of power plant	P	MW
Efficiency of power plant	n	%
Hours of power plant operation (annually)	T	h/y
Annual lignite production of the mine	L	t
Project life time	N	y
Time of negative cash flow for power plant construction and mine opening phase	k	y
Mining capital expenditure	I_1	€
Depreciation time period for mining equipment	μ	y
Power plant capital expenditure	I_2	€
Depreciation time period for power plant equipment	ν	y
Mining operating cost	c_m	€/t
Power plant operating cost	c_p	€/kWh
Environmental cost	c_{env}	€/t
Electricity selling price	p	€/kWh
Discount rate	ε	%
Tax rate	t	%

Based on the model parameters, the analytical form of Net Present Value of project cash flow is the following:

$$Z = f(\kappa, \varepsilon) \cdot [10^3 \cdot g(N(P), \varepsilon) \cdot P \cdot T \cdot (1-t) \cdot (p - c_p - \frac{0,86 \cdot c_m}{H \cdot n}) + g(\mu, \varepsilon) \cdot t \cdot \frac{I_1(P)}{\mu} + g(\nu, \varepsilon) \cdot t \cdot \frac{I_2(P)}{\nu}] - [I_1(P) + I_2(P)] \quad (1)$$

where: $f(k, \varepsilon) = \frac{1}{(1+\varepsilon)^k}$ and $g(N, \varepsilon) = \frac{(1+\varepsilon)^N - 1}{(1+\varepsilon)^N \cdot \varepsilon}$ are the discount factors of a single amount and uniform series amount, respectively.

The above model is based on quantitative parameters. However, other criteria should be taken into account for the evaluation of the lignite deposits under current environmental, economic and social conditions. A first approach in the evaluation of a lignite deposit, including quantitative criteria of these three main categories of indicators, could be based on the environmental cost (ξ_1), the fixed cost (ξ_2) and the variable cost (ξ_3) according to the following equations:

$$\xi_1 = f(\kappa, \varepsilon) \cdot g(N, \varepsilon) \cdot \frac{860 \cdot P \cdot T}{10^6 \cdot H \cdot n} \cdot c_{env} \cdot 10^6 (1-t) \quad (2)$$

$$\xi_2 = I_1 + I_2 + f(\kappa, \varepsilon) \cdot g(N, \varepsilon) \cdot [(1 - \delta_1) \cdot \frac{P \cdot T}{1000} \cdot c_p + (1 - \delta_2) \cdot \frac{860 \cdot P \cdot T}{10^6 \cdot H \cdot n} \cdot c_m] \cdot 10^6 (1-t) \quad (3)$$

$$\xi_3 = f(\kappa, \varepsilon) \cdot g(N, \varepsilon) \cdot [\delta_1 \cdot \frac{P \cdot T}{10000} \cdot c_p + \delta_2 \cdot \frac{860 \cdot P \cdot T}{10^6 \cdot H \cdot n} \cdot c_m] \cdot 10^6 (1-t) \quad (4)$$

where,

δ_1 : the percentage of the operating cost that corresponds to the fixed cost of power plant (~60%)

δ_2 : the percentage of the operating cost that corresponds to the fixed cost of mining operations (~70 %)

In a further analysis based on the multi-criteria decision making approach, the choice of the indicators should be carefully made in order to propose a framework which will be effective and will contribute to safe conclusions. In this context, environmental, economic and social indicators could be applied to cover the environmental, economic and social characteristics of the lignite mining project. The corresponding sub-indicators form the framework for the sustainability's evaluation through the total indicator (TOSDIMA).

The TOSDIMA model is based on the following steps:

- (a) Definition of surface mining sub-indicators
- (b) Determination of SDI values according to the definition
- (c) Synthesis of TOSDIMA

The values of the indicators range from 0.1 to 0.9, assuming that 0 and 1 value correspond to unrealistic lignite mining conditions [28]. Initially, the environmental, economic and social indicators are derived by a balanced participation of the individual indicators by category and then

the TOSDIMA is averaged. Below, the nine (9) indicators, which form the TOSDIMA, are briefly presented.

Firstly, the three sub-indicators that form the total environmental indicator can be described as: the “Distance from Natura 2000”, the “Land Rehabilitation” and the “Lignite quality”. The “Distance from Natura 2000” sub-indicator defines whether the Natura 2000 area is affected by the exploitation. Natura 2000 is a network of core breeding and resting sites for rare and threatened species, and some rare natural habitat types, which are protected in their own right [29]. The criterion of quantification for this sub-indicator is the distance of the lignite mining activity from the Natura area. The “Land Rehabilitation” sub-indicator defines how the reclamation proceeds in relation to the excavation. The criterion of quantification for this sub-indicator is the ratio between the restored and the non-restored land. The “Lignite quality” sub-indicator is defined by the value of the extracted lignite’s Low Calorific Value comparing to specific limits.

The four sub-indicators that form the total economic indicator can be defined as: the “Reserve”, the “Stripping ratio”, the “Inside – Outside dumping area” and the “Distance from Power Plant”. The “Reserve” sub-indicator defines whether the deposit can fully supply a Power Plant. The “Stripping ratio” sub-indicator is defined by the ratio of the waste material volume which is required to be excavated in order to extract tonnage of lignite. The “Inside-Outside dumping area” sub-indicator is defined by the ratio between the inside and the outside dumping volume. The “Distance from Power Plant” sub-indicator is defined by the distance between the mine and the supplied Power Plant.

The two sub-indicators that form the total social indicator are the “Employment” and the “Expropriation of Villages” indicators. The “Employment” sub-indicator is defined by the number of employees coming from the wider area in relation to the total number of employees. The “Expropriation of Villages” sub-indicator is defined by the time that the expropriation will take place from the start of mining activity.

The calculation of the quantitative data of sub-indicators is based on the parameters of the above mentioned model.

3. THE STUDY AREA

The exploitation of lignite mines, mainly by Public Power Corporation of Greece, in the areas of Ptolemais – Amyntaio (Western Macedonia, Greece) and Megalopoli (Southern Greece) has historically played a key role in the Greek electricity generation system, and in the overall development of the country. Lignite remains a significant domestic fossil fuel resource, accounting for almost a third of the total electricity generation in Greece [24]. Greece holds the fourth largest lignite production capacity in the European Union [25]. Based on the total remaining reserves and assuming that the current consumption rate will remain the same in the future, it is estimated that the available lignite in the mines under exploitation are sufficient to cover the production needs for the next 35 years [26]. Until now, a total of 2 billion tons of lignite had been mined, while the remaining exploitable reserves are estimated to about 3 billion tons.

The extracted lignite quantities till the end of 2017 correspond to about 40% of the total known mineable reserves. In the year 2017, a total of 37.5 million tons of lignite were extracted in Greece [24].

The current study was carried out in the lignite deposit of Komnina – Mesovouno (Greece), which is located within the concession area of PPC SA in Western Macedonia, 8 to 15 kilometers northeast of the city of Ptolemais. The lignite deposit of Komnina – Mesovouno is surrounded by the villages Anatoliko, Pelargos and Mesovouno (Fig. 2).

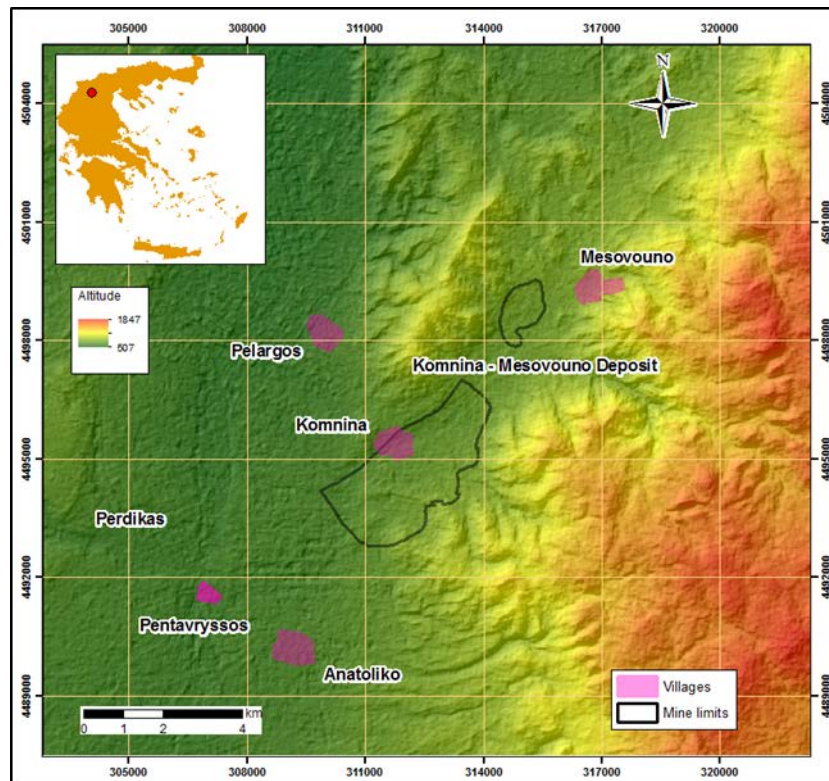


Figure 2. Komnina – Mesovouno deposit and mine limits.

The lignite field belongs to the broader Florina-Vegoritiss-Ptolemais lignite basin (north-western Macedonia, Greece). According to the tectonic zones of Greece, the study area belongs to the Pelagonian zone. Geomorphologically, this principal lignite basin is subdivided by ridges and hills into several sub-basins trending NE-SW, almost perpendicular to the main direction of the large basin [27].

The Komnina lignite deposit and the adjacent Mesovouno lignite deposit are located in a valley within a long and relative narrow lignite field. Between the two deposits there is available a ridge showing no lignite appearance. The area of the two lignite fields covers approximately 10 km².

4. APPLICATION OF TOSDIMA IN KOMNINA – MESOVOUNO DEPOSIT

4.1. Environmental indicators

The minimum distance of the mining activities from the nearest Natura area is set at 5 km, as shown in Fig. 3. There will be no interaction between exploitation and Natura area. The value of the environmental indicator “Distance from Natura 2000” for the Komnina – Mesovouno lignite deposit is 0.9.

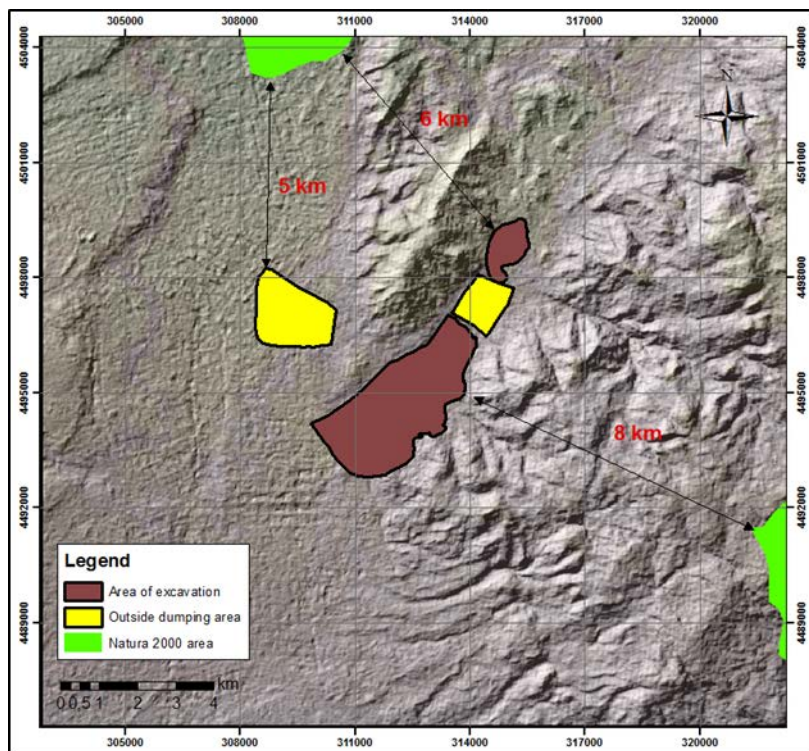


Figure 3. Mining activities distance from Natura 2000 area

In Fig. 4 the reclamation after the mine closure is presented. Table 2 shows the land cover before the start of mining activities and after the completion of the restoration.

After the mine closure, the area where the mining activities were developed will have been restored. The value of the environmental indicator “Land Rehabilitation” for the Komnina – Mesovouno lignite deposit is 0.9.

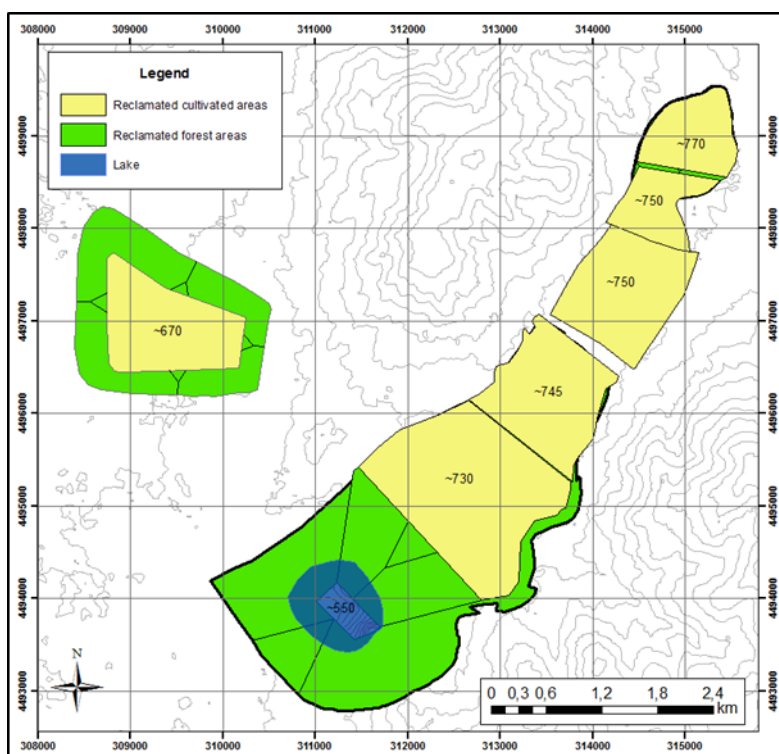


Figure 4. Map of reclamation after the mine closure**Table 2.** Land cover before the start of mining activities and after the completion of the restoration

Land cover	Before the start of mining activities (m ²)	After the completion of the restoration (m ²)
Urban fabric	427,064	
Agricultural land	13,567,239	8,086,432
Forest land	356,590	5,524,631
Lake		739,830
Total	14,350,893	14,350,893

The “Lignite quality Indicator” is estimated by the Low Calorific Value (LCV) of the lignite and it is defined as 0.1, when the value of the LCV is less than or equal to the minimum observed (851 kcal/kg, Kyparissia lignite mine), and as 0.9, when the value of LCV is equal to or more than the maximum observed (2,100 kcal/kg, Vevi deposit). Then, the “Lignite quality Indicator” is calculated by linear interpolation. The value of the “Lignite quality Indicator” for the Komnina – Mesovouno deposit (1,693 kcal/kg) is 0.639.

4.2. Economic indicators

The “Reserve Indicator” is estimated by the number of years that the deposit can entirely supply a Thermal Power Plant (TPP), given that the average operation time of TPP is 30 years and the minimum acceptable supply time from a mine is 10 years.

According to the above model, the annual required lignite production (L), in order to cover the supply needs of TPP, is calculated by the following equation:

$$L = \frac{860 \cdot P \cdot T}{\theta \cdot n} \quad (5)$$

For P = 450 MW, T = 7,446 h (365 days × 24h/day × 0.85), $\theta = 1,692$ kcal/kg and n = 0.4, the required annual lignite production for the supply of a 450 MW TPP is about 4.26×10^6 t/year. Based on the above, the Komnina – Mesovouno deposit, with reserve of 102.5×10^6 t of lignite, can support the supply of a 450 MW TPP for about 24 years (102.5×10^6 t / 4.26×10^6 t/year = 24.06 years).

The “Reserve Indicator” is defined as 0.1, when the supply capability of a deposit is less than or equal to 10 years, and as 0.9, when the supply capability is equal to or more than 30 years. Then, the “Reserve Indicator” is calculated by linear interpolation. The value of the “Reserve Indicator” for the Komnina – Mesovouno deposit is 0.660.

The “Stripping ratio” sub-indicator is defined by the ratio of the volume of the waste material which is required to be excavated in order to extract tonnage of lignite. The “Stripping ratio indicator” is defined as 0.1, when the value of the stripping ratio is more than or equal to the maximum calculated (11.2 m³/t for Lofi – Meliti deposit), and as 0.9, when the stripping ratio is equal to or less than the minimum calculated (4.23 m³/t for Domeniko deposit). Then, the “Stripping Ratio Indicator” is calculated by linear interpolation. The value of the “Stripping Ratio Indicator” for the Komnina – Mesovouno deposit (7.15 m³/t) is 0.603.

The “Inside – Outside Dumping Area Indicator” is estimated according to the volumes of waste materials in the inside and the outside dumping area.

In Fig. 5 the inside – outside dumping areas of Komnina – Mesovouno mine is presented.

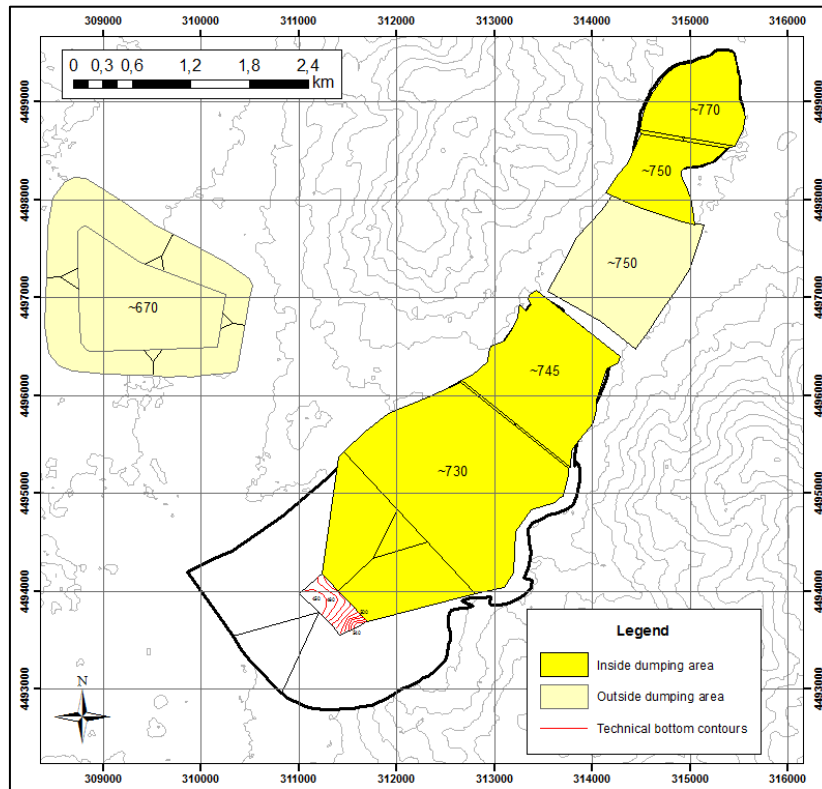


Figure 5. Map of the inside – outside dumping areas of Komnina – Mesovouno mine.

The total amount of the waste materials is $714 \times 10^6 \text{ m}^3$, $132 \times 10^6 \text{ m}^3$ of which will be deposited in the two outside dumping areas, while the rest ($582 \times 10^6 \text{ m}^3$) will be deposited in the inside dumping area.

The “Inside – Outside Dumping Area Indicator” is defined as 0.1, when the total amount of waste materials is deposited in the outside dumping area, and as 0.9, when the total amount of waste materials is deposited in the inside dumping area. Then, the “Inside – Outside Dumping Area Indicator” is calculated by linear interpolation. The value of the “Inside – Outside Dumping Area Indicator” for the Komnina – Mesovouno deposit is 0.752.

The “Distance from Power Plant Indicator” is estimated by the length of lignite transport route. The Komnina – Mesovouno mine will supply a unit, located in Amyntaio TPP. In Fig. 6 an indicative lignite transport route is presented. The length of this route is about 15 km. Taking into account the average transport distance from the lignite excavation area to the mine crest, which is approximately 1.6 km, the length of indicative lignite transport route is calculated about 17 km.

The “Distance from Power Plant Indicator” is defined as 0.1, when the length of the lignite transport route is more than or equal to the maximum observed (40 km, supply of Meliti – Florina TPP from Amyntaio mine), and as 0.9, when the lignite transport route is equal to or less than the minimum observed (supply of Kardia TPP from Kardia mine). Then, the “Distance from Power Plant Indicator” is calculated by linear interpolation. The value of the “Distance from Power Plant Indicator” for the Komnina – Mesovouno deposit is 0.560.

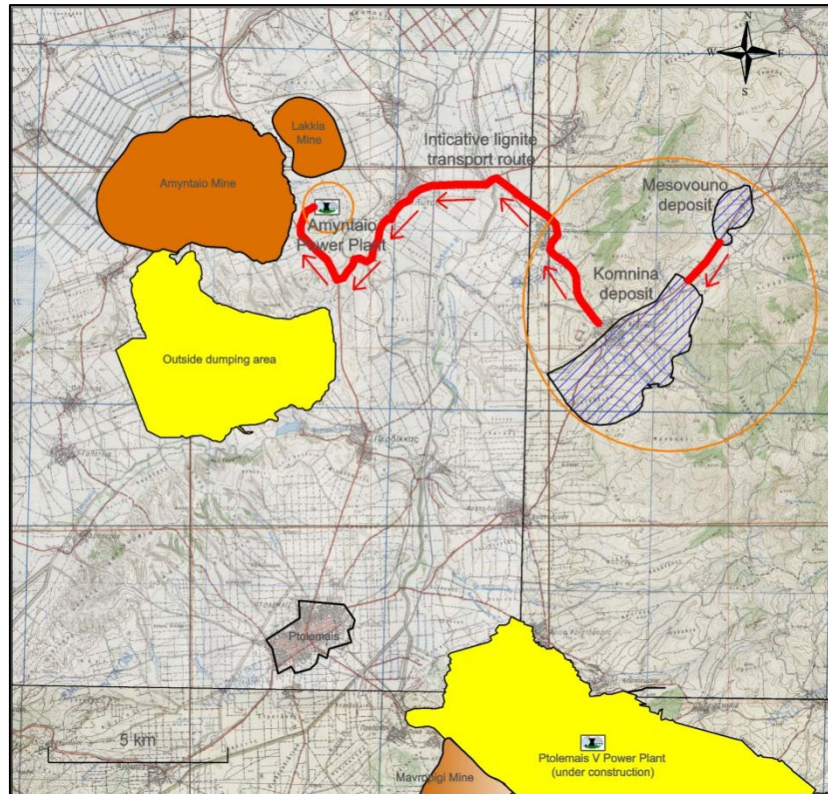


Figure 6. Map of indicative lignite transport route

4.3. Social indicators

The “Employment Indicator” is estimated by the number of employees who are residents of the wider area in relation to the total number of employees.

The “Employment Indicator” is defined as 0.1, when no employees are residents of the wider area, and as 0.9, if all the employees are residents of the wider area. Then, the “Employment Indicator” is calculated by linear interpolation. The value of the “Employment Indicator” for the Komnina – Mesovouno deposit is estimated at 0.9.

The “Expropriation of Villages Indicator” is based on the time the expropriation takes place, in relation to the start and also the duration of the mining activity. Fig. 7 shows the minimum distance of mining activities from the nearest villages.

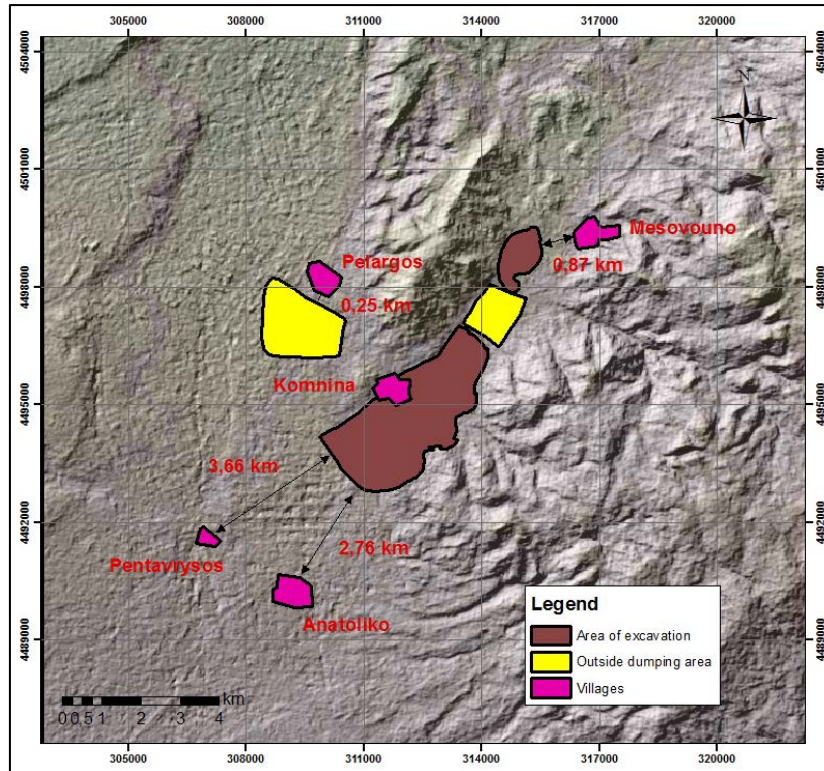


Figure 7. Distance of mining activities from the nearest villages

According to the 85th article of the Regulation on Mining and Quarrying Activities [31], mining activities are not allowed to approach villages of more than 250 m. Figure 7 shows that the corresponding restriction is observed for the nearest villages, except the Komnina village, which is located within the boundary of the mine. The expropriation of this village is necessary and will carry out at the end of ninth operation year of mine, when the mining activities will approach the village at 250 m, while the operation of the mine is expected to last about 28 years [32].

The “Expropriation of Villages Indicator” is defined as 0.1, in case of the immediate necessity of the expropriation for the needs of the exploitation, and as 0.9, when an expropriation is not required. Then, the “Expropriation of Villages Indicator” is calculated by linear interpolation. The value of the “Expropriation of Villages Indicator” for the Komnina – Mesovouno deposit is 0.357.

4.4. Analysis of the results

A simplistic expression for Total Sustainable Development Indicator (TOSDIMA), based on the weights of the indicators is the following weighted value Z:

$$Z = \sum X_i W_i \tag{6}$$

where X_i is the value of indicator i and W_i the corresponding weight. Another expression, based on the ideal point approach, is the following:

$$Z = \{ \sum W_i^2 (1 - X_i)^2 \}^{1/2} \tag{7}$$

The Sustainable Development Indicators by category, as well as the overall indicator (TOSDIMA), as it results from the balanced participation of the individual indicators, are presented in Table 2.

Table 2. Valuation of indicators

Indicator		Value	
Env	Distance from Natura 2000	0.900	0.813
	Land Rehabilitation	0.900	
	Lignite Quality	0.639	
Eco	Reserve	0.660	0.644
	Stripping Ratio	0.603	
	Inside-Outside Dumping Area	0.752	
	Distance from Power Plant	0.560	
Soc	Employment	0.900	0.629
	Expropriation of Village	0.357	
Total Sustainable Development Indicator		0.697	0.695

Based on the average values of sub-indicators, the value of the Total Environmental Indicator (0.813) is quite high because Komnina – Mesovouno deposit is located at a satisfactory distance from Natura 2000 area, the environmental reclamation of land after mining operations will be complete and the quality of extracted lignite is among the highest in Greece.

The corresponding value of the Total Economic Indicator (0.644) is quite satisfactory. The reserve of the deposit is sufficient for the 24-year supply of a 450 MW power plant, the stripping ratio is good compared to the lignite deposits in Greece, while the dumping schedule ensures the minimum possible waste material volume for outside dumping. The distance of the deposit from the power plant is not an impediment for the exploitation.

The Total Social indicator (0.629) has the lowest value of the three indicators. The expropriation of the Komnina village will be needed the ninth year of the exploitation. All employees are expected to come from the local community.

Taking into account the values of the three Total indicators, the average value indicating the total Sustainable Development Indicator for Mining Activity in Komnina – Mesovouno deposit is 0.695. This value could be used as a basis for comparing this lignite deposit with other deposits in a decision making process for a surface mine development. For a further analysis, the weighted indicators according to the equations (6) and (7) should be applied. In addition, more advanced expressions of TOSDIMA could incorporate a stochastic evaluation of the deposit. For a hierarchical ranking of candidate lignite fields for mine development, a combination of the quantitative optimization model (eq. (1)) and a multi-criteria approach (eq. (2-4) and TOSDIMA) can be implemented to the optimal choice of a lignite field for mine development.

5. CONCLUSION

The exploitation of the lignite deposits in Greece ensures the country's energy sufficiency. The exploitation of lignite deposits should be carried out according to sustainable development terms. Sustainable development, under the mining activities, aims at optimizing the environmental, social and economic performance of mining operations.

In this work, the evaluation of the sustainability of a lignite deposit is attempted, through a new total indicator, by combining equally environmental, economic and social sub-indicators. Through this total indicator an original stable framework could be created. Within this framework, the deposits in Greece will be ranked, via the comparative analysis of their TOSDIMA values, where the one with the highest value gathers the most favourable (in terms of sustainable development) conditions for exploitation.

The proposed framework can constitute a useful tool for planning exploitation strategies, managing mining activities, supporting and validating research and operational objectives.

REFERENCES

- [1] Yu, X. (2017). Coal mining and environmental development in southwest China. *Environmental Development*, 21, 77-86.
- [2] Song, M., Wang, L. J., & Li, W. B. (2009). Efficiency assessment of coal industry sustainable development by improved data envelopment analysis. In *Management Science and Engineering, 2009. ICMSE 2009. International Conference on* (pp. 1830-1835). IEEE.
- [3] Chikkatur, A. P., Sagar, A. D., Sankar, T. L. (2009). Sustainable development of the Indian coal sector. *Energy*, 34(8), 942-953.
- [4] Craynon, J. R., Sarver, E. A., Ripepi, N. S., Karmis, M. E. (2015). A GIS-based methodology for identifying sustainability conflict areas in mine design—a case study from a surface coal mine in the USA. *International Journal of Mining, Reclamation and Environment*, 30(3), 197-208.
- [5] Hilson, G., Basu, A. J. (2003). Devising indicators of sustainable development for the mining and minerals industry: An analysis of critical background issues. *The International Journal of Sustainable Development & World Ecology*, 10(4), 319-331.
- [6] Chen, R. H., Lin, Y., Tseng, M. L. (2015). Multicriteria analysis of sustainable development indicators in the construction minerals industry in China. *Resources Policy*, 46, 123-133.
- [7] Roumpos, C., Pavloudakis, F., Galetakis, M. (2007). Benchmarking and sustainability indicators for surface mining operations. In *Proceedings of the 3rd International Conference on Sustainable Development Indicators in the Mineral Industries (SDIMI 2007): 17-20 June 2007, Milos Islands, Greece* (p. 295), Heliotopos Conferences.
- [8] Chamaret, A., O'Connor, M., Récoché, G. (2007). Top-down/bottom-up approach for developing sustainable development indicators for mining: application to the Arlit uranium mines (Niger). *International Journal of Sustainable Development*, 10(1-2), 161-174.
- [9] Putzhuber, F., Hasenauer, H. (2010). Deriving sustainability measures using statistical data: a case study from the Eisenwurzen, Austria. *Ecological Indicators*, 10(1), 32-38.
- [10] Dong, L., Shu, W., Li, X., Zhang, J. (2018). Quantitative evaluation and case studies of cleaner mining with multiple indexes considering uncertainty factors for phosphorus mines. *Journal of Cleaner Production*, 183, 319-334.
- [11] Marnika, E., Christodoulou, E., Xenidis, A. (2015). Sustainable development indicators for mining sites in protected areas: tool development, ranking and scoring of potential environmental impacts and assessment of management scenarios. *Journal of Cleaner Production*, 101, 59-70.
- [12] Azapagic, A. (2004). Developing a framework for sustainable development indicators for the mining and minerals industry. *Journal of cleaner production*, 12(6), 639-662.
- [13] Roumpos, C., Pavloudakis, F., Galetakis, M. (2005). Modelling and evaluation of open-pit lignite mines exploitation strategy. In *2nd Int. Conference on Sustainable Development Indicators in the Minerals Industry (SDIMI 2005)* (pp. 1127-1139).
- [14] Worrall, R., Neil, D., Breerton, D., Mulligan, D. (2009). Towards a sustainability criteria and indicators framework for legacy mine land. *Journal of cleaner production*, 17(16), 1426-1434.
- [15] Poveda, C. A. (2014). A methodology for pre-selecting sustainable development indicators (SDIs) with application to surface mining operations. *WIT Transactions on Ecology and the Environment*, 181, 519-530.
- [16] Rodríguez, X. A. (2010). A new productivity index to measure economic sustainability of the mining industry. *Dyna*, 77(161), 11-20.

- [17] Horsley, J., Prout, S., Tonts, M., Ali, S. H. (2015). Sustainable livelihoods and indicators for regional development in mining economies. *The Extractive Industries and Society*, 2(2), 368-380.
- [18] Suopajarvi, L., Poelzer, G. A., Ejdemo, T., Klyuchnikova, E., Korchak, E., Nygaard, V. (2016). Social sustainability in northern mining communities: A study of the European North and Northwest Russia. *Resources policy*, 47, 61-68.
- [19] Woźniak, J., Pactwa, K. (2017). Environmental activity of mining industry leaders in Poland in Line with the principles of sustainable development. *Sustainability*, 9(11), 1903.
- [20] Yaylacı, E. D., Düzgün, H. Ş. (2017). Evaluating the mine plan alternatives with respect to bottom-up and top-down sustainability criteria. *Journal of Cleaner Production*, 167, 837-849.
- [21] Shaheen, M., Shahbaz, M., Guergachi, A., Rehman, Z. (2011). Mining sustainability indicators to classify hydrocarbon development. *Knowledge-Based Systems*, 24(8), 1159-1168.
- [22] Wibowo, S. (2013). A new sustainability index for evaluating the sustainability performance of mining companies. In *Computational Intelligence and Design (ISCID), 2013 Sixth International Symposium on* (Vol. 1, pp. 185-188). IEEE.
- [23] Sharma, R. (2011). Deep-sea mining: Economic, technical, technological, and environmental considerations for sustainable development. *Marine Technology Society Journal*, 45(5), 28-41.
- [24] Public Power Corporation (2018). Lignite production review in 2017. Unpublished report.
- [25] European Association for Coal and Lignite (2016). Annual Report, 24 p.
- [26] Public Power Corporation (2011). Environmental Impact Assessment of Ptolemais Lignite Mines. Unpublished report.
- [27] Pavlides, S., Mountrakis, D. (1987). Extensional tectonics of north-western Macedonia, Greece, since the late Miocene. *J. Struct. Geol.* 9, 385–392.
- [28] Batzias, F.A., Roumpos, C. (2000). Multicriteria choice of a lignite field for mine development and power plant construction. *Proc. 9th International Symposium on Mine Planning and Equipment Selection*, Athens: 783-788.
- [29] http://ec.europa.eu/environment/nature/natura2000/index_en.htm.
- [30] Roumpos, C.P. (2005). Optimisation of the combined project of a lignite mine exploitation and power plant operation. *Mining–Metallurgical Annals*, Vol. 1, 45–64
- [31] Greek Mining Enterprises Association (2011). Regulation on Mining and Quarrying Activities.
- [32] Pagonis, G., Roumpos, C. (2007). Development of Komnina - Mesovouno Mine. Power Public Corporation. Unpublished mining study.

Technological and environmental upgrading of lignite from Amynteon and Ahlada deposits, in Northern Greece, via selective grinding

Despina Vamvuka, Aggeliki Kreona, Aikaterini Mantza, Michael Galetakis and Anthoula Vasileiou

School of Mineral Resources Engineering, Technical University of Crete, Greece

ABSTRACT

Lignite plays a dominant role for energy production in Greece, covering over 50% of the demand for electricity generation. Energy crisis requires, additionally to alternative energy sources, an increase in energy supply from both old and new deposits. Due to the low quality of mined lignite, methods of upgrading in terms of power plants' efficiency and environmental performance need to be applied. In this work, the technique of Selective Size Reduction (SSR) was adopted for two deposits in North Greece, Amynteon and Ahlada, in order to improve lignite quality through reduction of its mineral matter content. The variation of the qualitative characteristics of the grain fractions produced by SSR provided useful information on both the suitability of these fractions for combustion in the power plants of the area, as well as on the emissions of greenhouse gases. The results have shown that fractions, which were produced from the first stage of crushing, with a recovery between 83% and 95%, had lower ash by 18-27% than the raw material and were of acceptable quality for combustion in the power plants of the area. Beneficiated fractions could give energy efficiency between 34 and 36%, while a reduction in CO₂ emissions up to 29%.

1. INTRODUCTION

Greek brown coals constitute the major energy resource in Greece, accounting about 30% of the primary energy consumption and over 50% of power generation. Mineable coal deposits amount to 4.6 billion tons and are exploited by the Public Power Corporation of Greece. Over the last five years, lignite production is almost constant at the level of ~50Mt per annum. This output ranks Greece as the second largest lignite producer in the European Union and the fifth in the world. Almost all of the output is burned in power stations, which are all, more or less, mine mouth plants, whereas approximately 1% is used to produce dry lignite and briquettes. The total electric generating capacity is 5289MWe. Consumer prices are significantly below those of European Union and cheaper than those of oil or gas [1-6].

The quality of the run of mine lignite is not constant and/or uniform, but exhibits inhomogeneity and large fluctuations. The alteration of intercalated and lignite layers during the excavating process results in mixing of the thin layers of waste with lignite, worsening the already poor quality of the product, by increasing its ash content and consequently decreasing its calorific value. This variability in quality causes problems in the lignite handling and ash removal facilities, as well as detrimental effects on industrial processes such as slagging and fouling, increasing maintenance costs. As a result, the efficiency of the power plants decreases, with significant negative impact on the CO₂ emissions and the cost of electricity produced [6-8].

The competitiveness of the lignite sector in Greece will greatly depend on its ability to keep a constant fuel quality and power plant efficiency, meeting at the same time CO₂ emission limits, as specified by the Kyoto Protocol. The application of the Emission Trading Scheme has greatly affected the power generation sector, by increasing the operating cost of current units, as well as the investment cost for new units [6, 8].

Present study aimed at investigating the effect of a simple and cheap quality control technique, Selective Size Reduction (SSR), in improving lignite quality from two deposits in Northern Greece, through reduction of its mineral matter content. The qualitative characteristics of the grain fractions produced by SSR were determined, in order to provide information on the suitability of these fractions for combustion in the power plants of the area, the energy efficiency, as well as CO₂ emissions.

2. EXPERIMENTAL

The samples which were used in this study were delivered from Amynteon and Ahlada mines of Western Macedonia in Greece. Representative samples, after air drying, homogenization and riffing, were ground by a jaw crusher and a ball mill to a particle size of -250 μ m and subjected to qualitative analysis. Proximate and ultimate analyses were carried out according to the ASTM standards (D5142, D5373, D4239) using programmable laboratory furnaces and a CHNS Flash 2000 type analyzer. Gross calorific value (Q_g) was determined by a Leco AC-300 type calorimeter (D5865), while the chemical analysis of ashes by an X-ray fluorescence spectrometer (XRF), type SRS-303 of Siemens (D4326). Carbon dioxide emitted from carbonate minerals during combustion was determined by an asbestometer type Dietrich-Fruhling.

The methodology of SSR was applied as follows: Raw samples were initially crushed with a jaw crusher and classified by sieving to particle sizes between -100mm and -0.1mm (1st stage). Consequently, the coarser fraction was crushed and sieved to same particle sizes as before and a new size distribution was obtained (2nd stage). The procedure was repeated up to the 4th stage of crushing.

Representative samples from all fractions of all stages of crushing were analyzed using the above techniques, aiming to determine the optimum cut size of the screening, in terms of recovery, ash content, net calorific value (Q_n), CO₂ emissions and energy efficiency. The latter was calculated as [9]:

$$n=(0.0066xQ_n) + 25.1 \quad (1)$$

where,

$$Q_n=[[(Q_g-5.85x9x(100-A_d)x0.05]x(100-M)]/100 - (5.85xM) \text{ (kcal/kg)} \quad (2)$$

A_d : ash content (% dry)

M : moisture content (%)

3. RESULTS AND DISCUSSION

The proximate and ultimate analyses results of raw fuels are represented in Table 1. As can be seen, Ahlada lignite had much higher ash content than Amynteon lignite, 45% and a lower carbon content, resulting in a reduced calorific value. The concentrations of nitrogen and sulphur were low for both fuels, implying low toxic emissions of SO₂ and NO_x during combustion. From the chemical analysis of ashes in Figure 1 it can be observed that Amynteon ash was very rich in CaO, while

Table 1. Proximate Analysis, Ultimate Analysis and Calorific Values of the Fuels (% dry)

Sample	Volatile matter	Fixed carbon	Ash	C	H	N	O	S	Q_g^1
Amynteon lignite	46.5	31.5	22.0	38.7	3.4	1.7	33.2	1.3	3073.7
Ahlada lignite	36.4	18.6	45.0	27.3	2.1	0.6	24.2	1.1	2124.8

¹Gross calorific value (kcal/kg)

Ahlada ash in SiO₂ and to a lesser extent in CaO. Amynteon ash was also abundant in SiO₂, whereas both ashes contained significant amounts of Fe₂O₃ and Al₂O₃.

Basic criteria, for the successful applicability of the SSR technique as a simple and cheap upgrading method of lignite, were considered the yield of improved samples, the content of ash, the calorific value and the percentage of CO₂ emitted from inorganic substances during combustion (moisture content as received, although an important parameter too, could not be measured accurately, because the samples were air dried). Best separation between organic and inorganic part of the samples occurred during the first stage of crushing for both lignites. The results are presented in Table 2 and Figures 2 and 3.

The fractions which were characterized as upgraded, in comparison to the raw fuels, were grouped together. The cumulative qualitative characteristics were then determined for each beneficiated material, in order to investigate whether the methodology produced fractions of specific quality, acceptable for use in the power plants of the area of Western Macedonia. Table 2 shows that the increasing distribution of ash from the coarser towards the finer fractions was raised up to 40% for Amynteon lignite and up to 120% for Ahlada lignite and was most probably related to the more brittle lignite partings. The highest degree of liberation of organic material from minerals occurred for particle sizes of -25+16mm in case of Amynteon lignite, while -100+50mm in case of Ahlada lignite. For Amynteon lignite, as upgraded fraction was selected the -100+2mm, which was recovered by 95%, had 18% ash on a dry basis and a Q_n of 1673kcal/kg (Figure 2a and Figure 3a). The reduction of ash with respect to the initial sample was 18%, whereas the increase in lower heating value was ~1%. On the other hand, for Ahlada lignite, as upgraded fraction was selected the -100+2mm, with a recovery of 83%, ash content on a dry basis 33% and Q_n of 1336kcal/kg (Figure 2b and Figure 3b). For this fuel, the reduction of ash with respect to the raw sample was much greater 27%, while the increase in lower heating value was 2.8%.

Table 2. Qualitative Characteristics of Lignite Fractions produced by Selective Size Reduction

Particle size (mm)	Cumulative weight (%)		Cumulative ash (%)		Cumulative Q _n (kcal/kg)	
	Amynteon lignite	Ahlada lignite	Amynteon lignite	Ahlada lignite	Amynteon lignite	Ahlada lignite
+100	8.1	2.2	19.4	18.2	1622.2	1645.0
-100+50	23.2	5.2	19.2	19.6	1625.3	1617.3
-50+25	57.5	18.4	15.7	20.2	1668.9	1605.7
-25+16	72.6	27.0	15.4	26.3	1676.3	1476.6
-16+8	88.7	50.9	17.5	30.0	1674.0	1400.3
-8+4	92.6	70.3	17.9	32.3	1673.5	1359.2
-4+2	94.5	82.5	18.0	33.0	1673.0	1336.0
-2+1	95.8	89.3	18.6	34.5	1670.4	1325.0
-1+0.5	96.7	94.1	19.4	36.2	1668.1	1318.7
-0.5+0.3	97.5	96.5	20.2	38.7	1665.7	1309.8
-0.3+0.1	98.8	99.3	20.9	40.3	1664.2	1306.8
-0.1	100	100	21.6	42.9	1661.0	1302.3

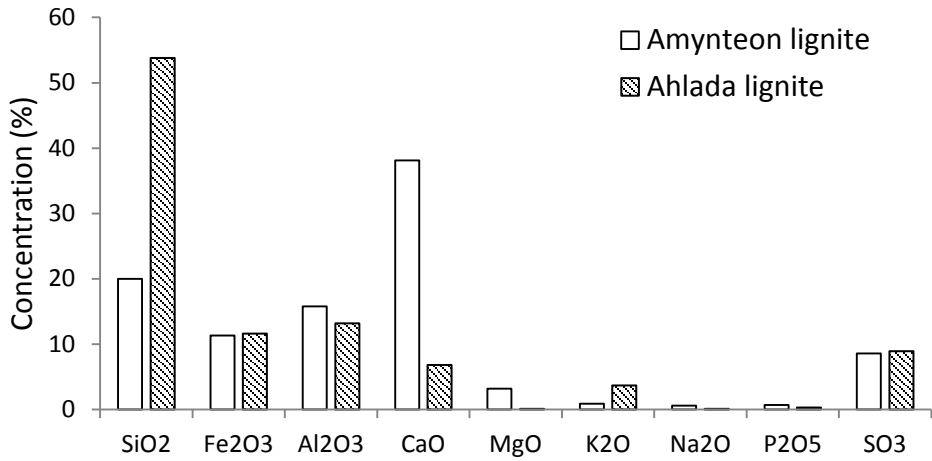


Figure 1. Chemical analysis of lignite ashes in major oxides

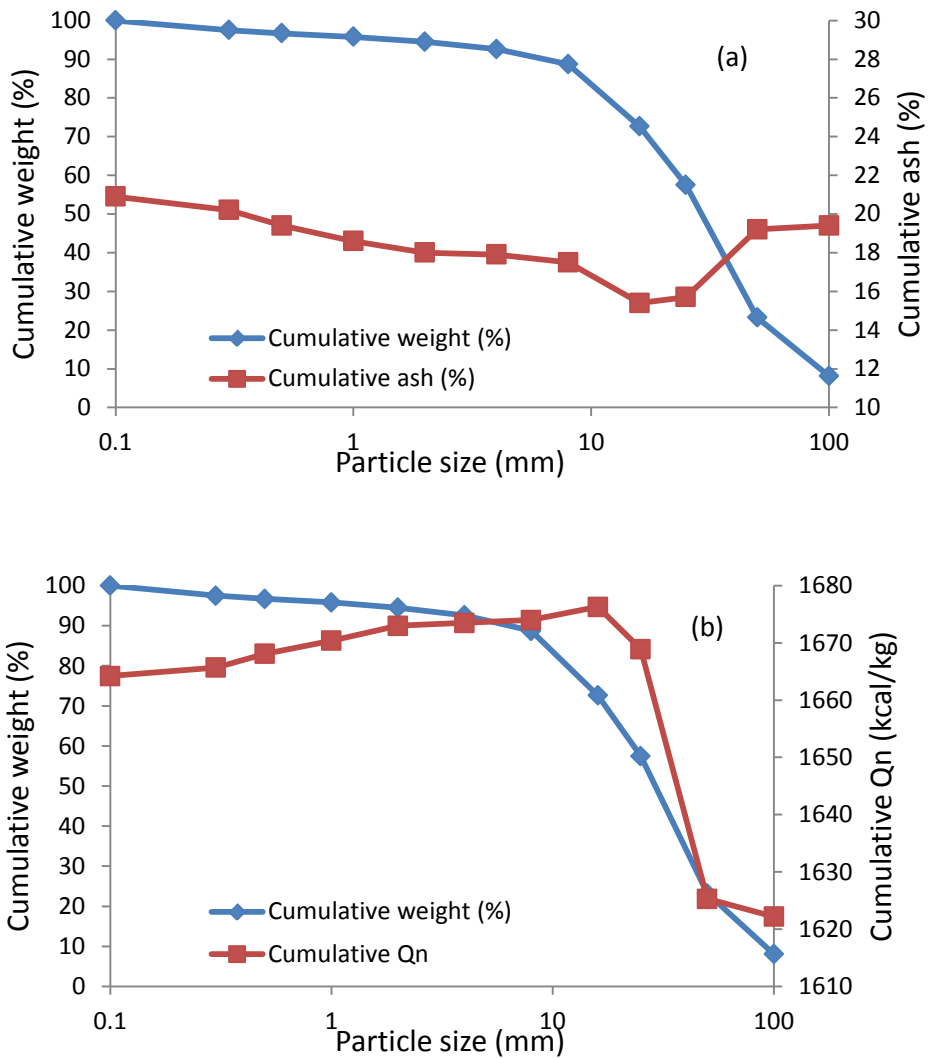


Figure 2. Variation of cumulative weight and cumulative ash (a), cumulative weight and cumulative Q_n (b), as a function of particle size for Amynteon lignite

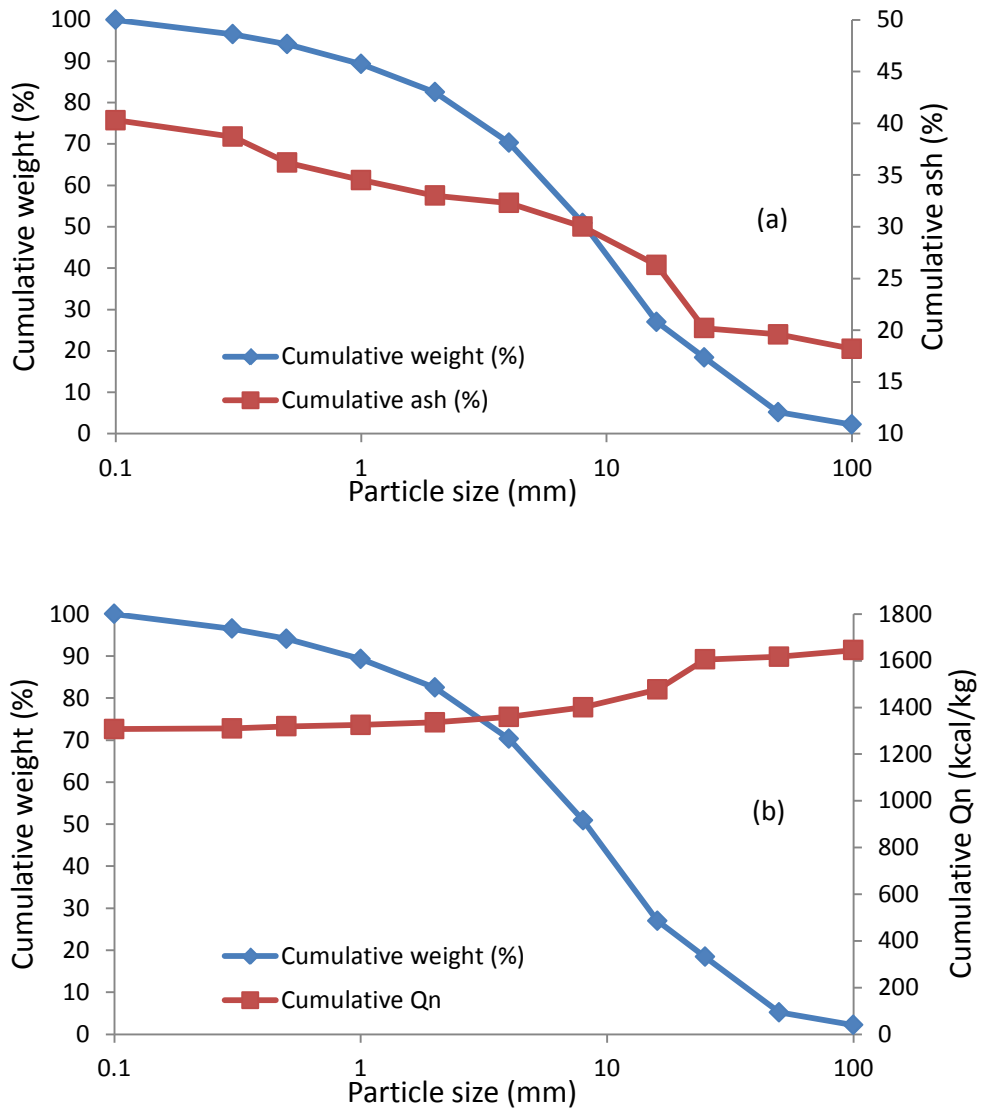


Figure 3. Variation of cumulative weight and cumulative ash (a), cumulative weight and cumulative Q_n (b), as a function of particle size for Ahlada lignite

The considerable improvement of ash content and Q_n of the samples obtained from the SSR method is important for industrial units, as ash can cause operational problems (slagging/fouling, corrosion) and environmental pollution (SO₂, toxic heavy metals), while the lower heating value determines the degree of loading of the units, for which a specified power can be achieved. Both these parameters define the efficiency and availability of the facilities and thereby the power cost. The results of Table 2 show that the selected upgraded fractions meet the fuel specifications for the power plants of the area, i.e. ash content 13-55% on a dry basis and lower heating value 1300-2030kcal/kg.

A comparison between the qualitative characteristics of the beneficiated materials and those of the raw fuels is made in Table 3 and Figure 4. As can be seen, for Amynteon lignite the reduction of CO₂ produced from carbonate minerals of the selected fraction was 19.7% and the energy efficiency 36.1%, remaining practically unchanged. For the upgraded fraction of Ahlada lignite, CO₂ emissions can be lowered by 29%, while the energy efficiency increased by ~1%, reaching a value of 34%. Concerning the refuse (fractions <2mm), which constitutes approximately 5% and 17% of the initial sample of Amynteon and Ahlada lignites, respectively, with an ash content of 40-42%, it could be

worth to investigate its use as an additive of raw materials of the cement industry, or alternatively its blending with other waste materials for use in soil amendment and amelioration.

Table 3. Qualitative Characteristics of Lignite Upgraded Fractions

Sample	Particle size (mm)	Cumulative ash (%)	Cumulative Q _n (kcal/kg)	Lignite CO ₂ (%)	Energy efficiency (%)
Amynteon lignite (raw)	+100-0.1	22.0	1660.0	6.6	36.0
Amynteon lignite (upgraded)	+100+2	18.0	1673.0	5.3	36.1
Ahlada lignite (raw)	+100-0.1	45.0	1300.3	2.4	33.6
Ahlada lignite (upgraded)	+100+2	33.0	1336.0	1.7	33.9

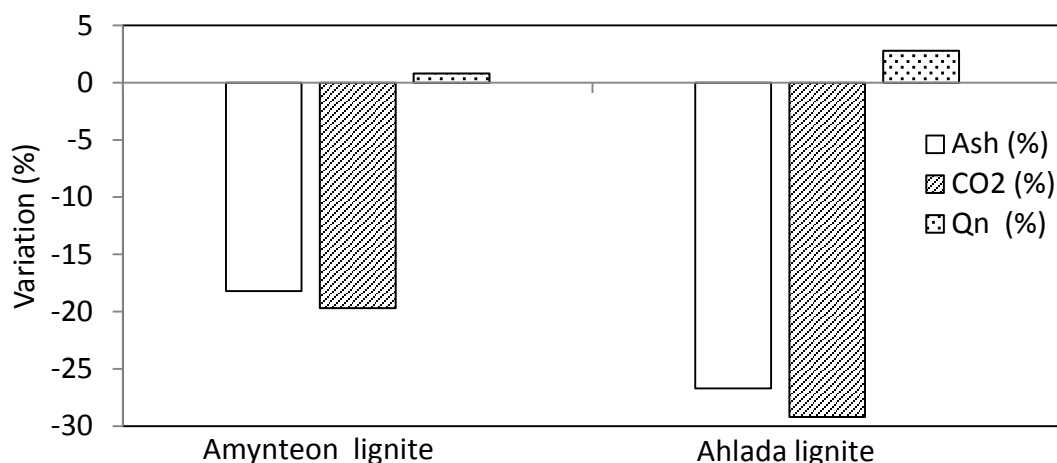


Figure 4. Variation of qualitative characteristics of upgraded samples, as a function of those of raw fuels.

4. CONCLUSION

The application of SSR, a simple method with no use of chemical additives, to low quality lignites, proved to be successful for the beneficiation of the samples, without any optimization of the process what so ever. Upgraded materials produced from the first stage of crushing presented improved combustion characteristics with respect to raw fuels and were of acceptable quality for combustion in the power plants of Western Macedonia. Ash reduction varied between 18% and 27%, revealing decreasing deposition problems in boilers and less environmental pollution. CO₂ emissions from minerals were lowered up to 29%, whereas the lower heating value of beneficiated samples was improved up to 3%.

REFERENCES

- [1] World Energy Statistics 2010. World Coal Institute, 2010 (<http://www.wci-coal.com>).
- [2] Public Power Corporation of Greece, 2016 (<http://www.dei.gr>).

- [3] Kavouridis, K. (2008). Lignite industry in Greece within a world context : Mining, energy supply and environment. *Energy Policy*, 36, 1257-1272.
- [4] Galetakis, M., Alevizos, G., Pavloudakis, F., Roumpos, C., & Kavouridis, C. (2009). Prediction of the performance of on-line ash analyzers used in the quality control process of a coal mining system. *Energy Sources, Part A*, 3, 1127-1142.
- [5] Galetakis, M., & Vamvuka, D. (2009). Lignite quality uncertainty estimation for the assessment of CO₂ emissions. *Energy and Fuels*, 23, 2103-2110.
- [6] Vamvuka, D., & Galetakis, M. (2010). Carbon dioxide emissions from coal-fired power plants in Greece in relation to mined lignite quality. *Energy and Fuels*, 24, 1396-1401.
- [7] Vamvuka, D. (2009). *Biomass, bioenergy and the environment*. Tziolas publications, Salonica.
- [8] Vamvuka, D., Galetakis, M., & Roumpos, C. (2013). Coal quality control techniques and selective grinding as means to reduce CO₂ emissions. 6th Int.Conference on Sustainable Development in the Minerals Industry, Milos, Greece.
- [9] Vamvuka, D. (1996). Study on the possibility of recovering lignites from refused innerburden. *Energy Exploration and Exploitation*, 14(5), 439-447.

Session 6: Land reclamation

Moving from Energy Depletion to Energy Crops in Exhausted Continuous Surface Mines

Vasileios G. Iliadis¹ Spyridon M. Kastanakis² and Aikaterini V. Iliadi³

¹ Dipl. Fuel & Energy Engineer BEng MSc, MBA, / Iliadis Energy, Athens, Greece

² Dipl. Chem. Engineer, University of Patras, Greece

³ Environment and Natural Resources Management, Student University of Patra, Greece

ABSTRACT

Agriculture is a sector that can provide considerable quantities of biomass to be used in regional biomass power facilities. Agricultural residues represent an attractive alternative source to fossil fuels in Greece and the considered available quantities have been evaluated up to over 4.5×10^6 dt/yr (dry tones/year, dt=tn) [1]. In this study, an analysis and cost evaluation for the development of an agricultural biomass supply chain is conducted regarding energy crops. It concerns the tillage, collection, processing and storage of perennial herbaceous biomass, to be cultivated in the depleted Continuous Surface Mines in Ptolemaida (PCSM) area, that belongs to the Public Power Corporation (PPC), and is scheduled to be restored and rehabilitated after mine's exhaustion. This is for the full compliance with the environmental terms set by the Ministry of Environment that allocate 37% (5.471 hectares), of the total restoration area for cultivation. The residues that are produced from the cultivation of *Cynara Cardunculus* L (Cardoon), have been investigated and analyzed in terms of quantities, energy potential and spatial distribution, in an attempt to identify and determine the ability of this particular feed stock to support district heating or electricity production either by itself or by co-firing with lignite in the neighboring PPC's Power Generation plants. Moreover the economic viability of this particular feedstock, from the investor's point of view is also examined, by comparing the costs of the different harvesting, transporting and storing methods in conjunction with proprietary or hired equipment. The results revealed that, the most cost-effective harvesting method is in bulk; the machinery equipment used for harvesting and transporting the crop are proprietary; the personnel employed in harvesting transport and storage are in an employment relationship with the collector, and that storage is more economical when it is bulk windrows in open space with cover to protect against weather conditions. Moreover the thermal content of the biomass itself can easily support district heating or power generation up to a certain extent.

1. INTRODUCTION

According to the Environmental Impact Assessment (EIA), elaborated by the Public Power Corporation (PPC) [1], for the evaluation of the consequences resulting from the closure of the PCSM, there is a series of proposed environmental rehabilitation interventions aiming to rectify the adverse effects, caused by the mining activity, on the geomorphological and landscape features of the area over the past years. According to this assessment, by the end of the 2050s, after the completion of the mining and restoration works, 81.7% of the total area of PCSM to be licensed will be covered with forest land, cultivated land and lakes, compared with the 20.8% of the current status. A representative depiction of the final plan after restoration is shown in figure 1.



Figure 1. Final restoration map [1]

Considering that the wider area of Ptolemais constitutes the energy centre of Greece and in combination with the set Environmental Impact Terms, that allocate a large percentage of the PCSM land for agricultural purposes (37%), the restoration of the area offers a unique investment opportunity for introducing a Renewable Energy Source (RES), in the Greek state's overall energy balance by cultivating energy crops. The outcome serves two purposes: On one hand it will contribute to the fulfilment of the commitments endorsed by the European council [2] for an increase of the proportion of RES, in the EU's final energy consumption to at least 20%, and on the other hand it will provide a profitable investment not only in terms of the direct revenue gained by selling the biomass, but also, in terms of the CO₂ emissions reduction that constitutes an indirect source of revenue.

The aim of this present work is to assess for all the components that constitute the cost of the cultivation of *Cynara Cardunculus* L-Cardoon as energy crop within the PCSM land, based on the energy potential output that the allocated area of 5.470 ha can provide.

There are four main components that constitute the total biomass investment cost, namely the cost of land, the cultivation cost, the processing cost and the safe storage cost. The evaluation of each particular component requires a different approach that is being assessed and discussed.

In the first part the characteristics of the Cardoon as an energy crop are presented [3], and its adaptability to the particular climatic conditions of the PCSM area is assessed. Moreover the biomass and energy yield of the crop is determined. In the second part, an analysis and evaluation of the different parameters composing the total investment cost are performed. Moreover, for the estimation of the harvest, transportation and safe storage costs, an analysis of the currently available technologies is accounted for and a comparison between proprietary and hired equipment is demonstrated in order to highlight the most viable and economical solution for the overall operation of the supply chain.

2. CROP CHARACTERISTICS - REQUIREMENTS AND YIELD

Cynara Cardunculus L - Cardoon is a perennial herbaceous plant species that is native to the Mediterranean region and highly adaptable to the local climate conditions that are characterized by moist and mild cold winters and hot summers.

Although the lifespan of a single plant and therefore the number of possible development cycles remains unknown, experiments have shown that the crop duration lasts for at least 15 years [3]. The plant itself has a vertical deep-root system able to penetrate several soil meters in depth. It grows over the winter /spring period, when it attains stem height of up to 2-2.5m and a width of 1.5-2m, and presents no serious disease problems. In the summer period its over ground part is drying up, while the root and the buds at its base are kept alive. After the harvest that takes place between June and August, the new cycle begins with the start of rains by the sprouting of the underground buds. The plant rises from the stump very quickly developing rosettes and provided that the plant density is adequate, 15.000 plants/ha, the whole cultivation territory is covered in a few days. The crop grows well in neutral soils, it is moderately tolerant to salinity and requires deep soils, moderate limy, with light texture, preferably loamy with capacity of retaining water along with the soil profile (1-5 m). The plants will be harvested in the second year of growing, since at this time the plant have completed its development, i.e, formation of stalks, flowers and seeds [3].

The expected biomass yield of cardoon ranges from 10 - 15 dt ha⁻¹ yr⁻¹ without irrigation (500 mm rainfall), when the crop is well established. However, if the crop receives 2–3 irrigation applications from mid-April to late May, dry biomass yields in excess of 20-25 dt ha⁻¹ may be easily attainable. This is in agreement with data obtained in the Mediterranean basin [4,5].

The gross heating value of the dry biomass is measured at 16.5 GJ/tn (seed excluded), to 18.5 GJ/dt (seed included) [4,7]. Such yields correspond to 5.7 – 7.5 oil equivalents (TOE) ha⁻¹ for the rain fed and greater than 11.0 toe ha⁻¹ for the irrigated crops respectively.

3. CROP CHARACTERISTICS - REQUIREMENTS AND YIELD

Within the framework of PPC's environmental strategy for the exploitation of lignite deposits, the primary objective is the restoration of the areas of the depleted mining sites converting them into cultivation and reforestation land as well as artificial lakes.

The total area dedicated to cultivation after completion of the Ptolemaida Mining Restoration Project is estimated to be 5,471 ha, (1 ha=10.000m²), or 37.0% of the total area, and is considered to be a medium scale cultivation. For the selection of the most appropriate crops and the investigation of their environmental impact, an experimental cultivation program commenced in 1986 and was implemented on the land that has resulted from the PCSM deposits of PPC. The species used were similar to the ones grown in the neighboring areas (like hard and soft wheat), aiming to identify the evolution of the fertility and explore the adaptability of energy crops in the soils of the new territories to be created. The assessment of the results of all past years indicated that the productivity of the soils developed in the restored deposits of raw materials in mining, ranges to the same level as that of the wider region and in some cases it is further improved [1]. Moreover, the cereal crops produced from the reclaimed soils of exhausted PCSM mines appear to contain almost identical nutrients and trace elements to those grown in the cultivated soils produced in the wider area [1] upstream of the lignite PCSM.

For the evaluation of the cardoon biomass and energy yield of the area under discussion the following assumptions have been made:

A plant density of 15.000 plants/ha is considered

The soil used is almost neutral (pH 6.5-7.5)

The cultivation available area is 5.470 ha

Harvesting takes place in late July-October when the moisture content of cardoon ranges within 7-10%

Gross heating value (GHV) of 18 GJ/dt (seed included).

The dry biomass yield is 20 dt ha⁻¹ (irrigated twice within the April-May period)

The duration of the cultivation is 10 years

Total Biomass yield = 5.471 ha x 20 dt/ha = 109,420 dt

Total Energy yield = 109.420 dt x 18 GJ/dt = 1,969.56 TJ

4. INVESTMENT COST EVALUATION

There is an extensive amount of literature regarding the estimation of the biomass cost [13, 14, 15]. The calculation of biomass cost of feeding the biomass into the energy unit incorporates a series of different components being expressed in the following general relation:

Biomass cost = Production Cost + Harvest Cost + Transport Cost + Storage Cost

In this present work the cost of biomass has been determined regarding the output quantities to be gained under the assumptions made before.

4.1. Production cost

The production cost of the energy crop is expressed in terms of the economic compensation that a farmer needs to get in order to grow that energy crop. Three main components of the production cost are accounted for:

Production Cost = Cost of land + Cost of cultivation + Cost of risk

Cost of land

The land of the PCSM under discussion is a property of PPC and has been gained through expropriations over a series of years. It comprises dry and irrigable fields. The land can either be used by the owner or to be rent to farmers. In any case there is a cost of exploitation incorporated in the calculation. For the scope of this work the cost of land taken into account refers to the current potential land rental rate of 100 €/ha to be paid by the farmer for a yield of 20 tn/ha. This results to a land cost of 5 €/tn.

Cost of cultivation

The Cardoon cultivation under discussion is considered to be a medium scale cultivation the cost of which includes all expenditures, (machinery and labour included), associated with the planting and growing the energy crop. The main costs are those of sowing, fertilization, irrigation, weed control, brokerage, overheads and wind-up, (when terminating cultivation), and they include both labour and machinery costs. Brokerage, overheads and wind-up are not included since they mainly refer to contractors' costs and are beyond the scope of this assessment. Cultivation costs are analysed for two periods: The initial sowing year, when the yield is estimated at 10 dt/ha, and the rest 9 year period when the plants have attained their full size and the yield is estimated at 20 t/ha. The cost breakdown for a plant density of 15.000 plants/ha, ($\approx 115,000$ seeds ha⁻¹ or 2 kg ha⁻¹ of seeds) [6, 7, 9], is presented in Tables 1 and 2. The prices indicated are current market prices and the machinery used is farmer owned.

Table 1. Cost Analysis (1st year of cultivation)

	Required Quantity		Unit Cost		Total Cost	Total Area Cost
	(Kg/ha)	(m ³ /ha)	(€/kg)	(€/m ³)	(€/ha)	(€5.471 ha)
Plowing (labour & machinery)					100	547,100
Seed	2		50		100	547,100
Compound Fertilizer	700		0.23		161	880,831
Herbicides/insecticides	5		38		190	1,039,490
Irrigation		2,500		0.08	200	1,094,200
Total					751	4,108,721

The final results also include land-use and transportation costs, which are excluded since these are estimated separately. One of the parameters determining production costs is the length of time in which the farmer will recover his fixed initial costs of establishing the cardoon. A ten year period is used in the analysis, which is consistent with the duration of cultivation. In order to calculate the costs for the differing lengths of time, Khanna et al method [10] is used. Costs in the first year, (751 €/ha), are amortized over the entire period whereas costs in the second year, (480 €/ha) are amortized over one fewer years. The discount rate used is 4%, Using these parameters, and by dividing the cost/ha by the yield/ha the cultivation cost (CC) in €/tn of cardoon is obtained according to equation (1):

$$CC = 751\text{€/ha} \times \frac{0.04}{1-1.04^{-t}} + 480 \text{ €/ha} \times \frac{0.04}{1-1.04^{-(t-1)}} \times \frac{1}{y \text{ tn/ha}} = 7.88 \text{ €/tn} \quad (1)$$

Where, t = No of years over which costs are spread (amortized), y = yield in tn/ha.
This does not include land rent costs.

Table 2. Annual Cost Analysis (9 years of cultivation)

	Required Quantity		Unit Cost		Total Cost	Total Area Cost
	(Kg/ha)	(m ³ /ha)	(€/kg)	(€/m ³)	(€/ha)	(€5.471 ha)
Compound Fertilizer	500		0.18		90	492,390
Herbicides/Insecticides	5		38		190	1,039,490
Irrigation		2,500		0.08	200	1,094,200
Total					480	2,626,080

Cost of Risk

The cost of risk describes the compensation - risk premium that the farmer requires in order to shift production from a cereal to an energy crop and is associated with an additional real or perceived risk undertaken by this change [11]. Its size varies between farmers and depends on the type of the crop. A higher risk premium is generally ascribed to perennial energy crops due to the limited knowledge and experience of growing these crops and the low flexibility in land use i.e. the ability to choose a crop based on current prices on the market. The price of cereals has a considerable impact on the relative viability of cereals and energy crops. An increase in wheat prices is likely to increase the price of certain inputs in the short term. In addition to the effect on the cost of land, higher cereal

prices are also likely to increase the risk premium ascribed to the growing of perennial energy crops since the farmer risks missing out on future high economic returns from cereal crop production. Its evaluation [12], is best described in terms of the Net Present Value (NPV). The NPV for cropping system j over a period of T years is defined by equation (2).

$$NPV_{ij} = \sum_{t=1}^T \delta^t G_{ijt} \quad (2)$$

where δ is the discount factor, and G_{ijt} denotes the gross margin (cash flow), of crop j cultivated in year t under state of nature i . Although an accurate evaluation of the cost of risk is beyond the scope of the current paper, an average percentage value of 15% has been accounted for in the evaluation of the cultivation cost in order to compensate for the risk.

4.2. Harvest cost

Harvesting the cardoon crop is the first step in the supply chain that takes place on farmland and as most agricultural works today it is fully mechanized. Making use of the breakdown of the harvest cost presented in table 3, evaluation for the two different harvest methods, bales and bulk, is performed. Moreover, the cost of proprietary or leased harvesting equipment, (silage combine harvesters and balers), is distinguished. The results are presented in table 4.

Table 3. Cardoon Harvest cost breakdown

	Parameter	Value	Unit
AREA – PERSONEL			
1	Annual Cardoon Biomass Yield	109,420	dt (tn)
2	Harvesting Period	120	days
3	Cultivated area	5,471	ha
4	Area Yield per tn	0.05	ha/tn
5	Dry Biomass yield	20	tn/ha
6	Bale weight	0.3	tn
7	Number of bales per tn	3.33	bales/tn
8	Annual yield Potential	109,420	tn
9	Daily collection capacity (area)	46	ha/day
10	Daily collection capacity (weight)	911.83	tn/day
11	Hourly collection capacity (8 hrs)	113.98	tn/hr
12	Maximum Transport load	15	tn
13	Cost of bunding material	3.49	€tn
14	Labor cost (employees)	0.48	€tn
15	Labor cost (contractors)	0.69	€tn
16	Labor cost (drivers)	0.37	€tn
MACHINERY			
17	Average combined harvester capacity	2.7	ha/hr
18	Hourly harvester capacity	54	tn/hr
19	Combine Harvester operational cost	3.5	€tn
20	Combine Harvester maintenance cost	0.15	€tn
21	Baler operational cost	*	€tn
22	Tractor operation/maintenance cost	2	€tn

23	Baler maintenance cost	0.05	€tn
24	Average Silager capacity	2.7	ha/hr
25	Hourly Silager capacity	54	tn/hr
26	Silager operational cost	3.5	€tn
27	Silager maintenance cost	0.15	€tn
28	Diesel cost	1.4	€lt

Table 4. Harvest Cost

Leased (€tn)		Owned (€tn)	
Bales	Bulk	Bales	Bulk
40	*	19.29	12.61

It should be noted that regardless of whether the potential investor owns or rents the land or the equipment, there must be a certain minimum harvesting area for which the cost of harvest is the same as the cost of rent. This is the Break Even Point (BEP), beyond which the investment is becoming profitable. The area resulting is 2.873 ha, and is evaluated by equation (4):

$$\text{Breakeven Point} = \frac{\text{TCO}}{\text{Leasing cost} - \text{operating cost}} \quad (4)$$

TCO is the annual Total Cost of Ownership that results for a ten year period of operation. The parameters involved in the calculation include the costs of purchase, depreciation, interest, tax, insurance, fuel, maintenance and repairs.

4.3. Transportation cost

The transport of biomass is usually limited by the energy density of the bulk material. Knowing the calorific value of Q_{net} (MJ/kg) and the bulk density ρ_{bulk} for a particular type of biomass, the bulk density Q_{vol} is calculated by equation (5):

$$Q_{\text{vol}} = Q_{\text{net}} \times \rho_{\text{bulk}} \text{ MJ/m}^3 \quad (5)$$

The lower the energy density, the lower the total amount of energy that can be loaded and transported resulting to increased transport costs.

This section examines the cost of transporting the harvested chopped biomass from the field to the storage point that is located at a central point on the field so as to minimize transport distances, after harvesting. Two modes are examined. Transport in bales and in bulk. For the purpose of this work we consider that crops are transported to an average distance of 10 km to the storage area. The evaluation accounts for the cost components assembling the total transport expenditure. Parameters such as, annually covered distance, trucks (annual fuel consumption, ownership, maintenance), personnel (hourly compensation, overtimes, standby costs), have all been accounted for. Moreover, a comparison between leased and privately owned vehicles is performed. The results are presented in table 5.

Table 5. Transportation Cost (10 km)

Leased (€tn)		Owned (€tn)	
Bales	Bulk	Bales	Bulk
3.7	1.35	3.17	1.17

4.4. Storage cost

The storage mode affects the quality and the cost of the fuel. The aim is to keep the fuel quality at a high level by preventing the mass loss on one hand and the increase of its humidity on the other. The biomass storage warehouse is assumed to be located at a central point of the harvested area in order to keep the transportation distance and cost to a minimum (10 km). The above storage methods are referring to biomass harvested either in bales (round and rectangular), or in bulk form. Round and rectangular modes of storage are depicted in figure 1. The size estimation of the storage area is based on the annual cardoon biomass yield accumulated within a 120 - day harvest period.

The modes examined and presented in this work are:

Outdoor storage with burlap cover, method with the highest loss of mass, (1-1.5% / month).

Storage in a sheltered space, without drying infrastructure (0.5% / month loss of mass)

Storage in a closed space with the possibility of drying, avoiding its degradation while simultaneously improving its energy content (zero dry mass loss).

For a bale size of $\Phi 1.67\text{ m} \times 1.5$, and a stack up in 3 rows (4m height), the required area for the harvested quantity (109,420 dt \approx 400,000 bales), is estimated at 50 ha. For rectangular bales 2.4m (L) x 1.3m (W) x 1.2m (H), stacked up in 4 rows (4.8m height), the required area for the harvested quantity (109,420 dt \approx 110.000 bales), is estimated at 8.5 ha.

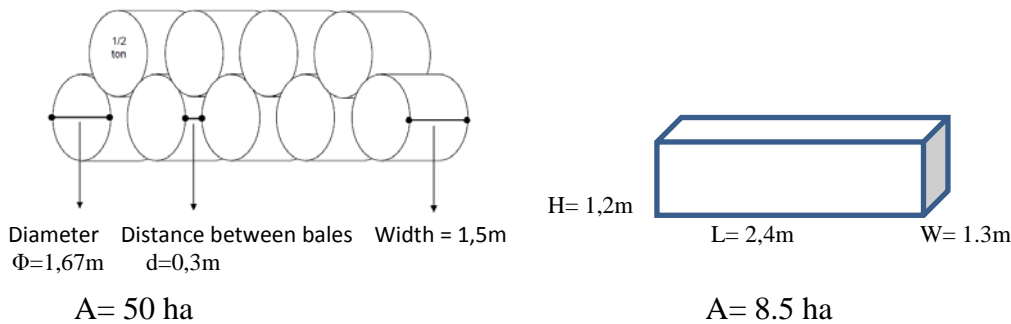


Figure 2. Bale stacking modes

4.5. Bulk Storage

The storage surface area is directly dependent on the accumulation method. A simple circular stack maximizes the mass that can be stored per surface unit. However, the constraints associated with the management of the available equipment for biomass accumulation and ventilation, lead to a rejection of this particular mode and to a selection of a different distribution in the heap and more extended storage space as shown in the table 6 below. For Biomass bulk density = 273 kg/m^3 at an angle of repose = 36° , the resulting required area is 10.9 ha.

Table 6. Windrow Piles characteristics

Pile Width (m)	Pile Length (m)	Angle of repose ($^\circ$)	Pile Height (m)	Pile Volume (m^3)	Cardoon Biomass stored (tn)	Area Covered (m^2)	Storage Capacity (tn/m^2)	No of piles needed	Area required (ha)
18	502	36	6.6	30,004	9,092	9,036	1	12	10.9

The parameters considered for the evaluation of the storage cost for each different mode are:

For the free storage: floor preparation, cost of land rental, burlap for pile coverage

For the Open storage: cost of land, shedding, construction cost

For Closed Storage: cost of land, building cost

For the determination of the cost on a per-ton delivered basis, the following equation (6) has been used where the factor 10% represents the annual cost of ownership.

$$\text{Storage Cost (SC)} = \frac{(\text{building/rental cost})/\text{€} \times 10\% \frac{\text{yr}}{\text{yr}} + \text{cost of land}/\text{€}}{\text{stored quantity} \left(\frac{\text{tn}}{\text{yr}} \right)} \quad (6)$$

The results for each mode are presented in Table 7.

Table 7. Storage Cost

Free Storage (€tn)		Open Storage (€tn)		Closed Storage (€tn)	
Bales	Bulk	Bales	Bulk	Bales	Bulk
Round	Rectangular	Rectangular		Rectangular	
5,43	3,72	2,61	12	6	30
					15

5. DISCUSSION

The results have revealed that the optimal method for handling the cardoon biomass cultivated in the PCSM area is harvesting and transporting it by proprietary equipment and free storing it in windrow piles. The cost for the whole logistics chain is evaluated at 30.45 €/tn, and its percentage composition is shown in figure 3. The current market price for the biomass from energy crops with a moisture content of 8-10% and a GHV of 18 GJdt⁻¹, lies between 65 - 75 €/tn with a tendency to increase. This price does not include any form of allowances. Following modest scenarios for a retail price of 70 €/tn, there is a remarkable annual gross margin profit of approximately 40 €/tn or 800 €/ha resulting, making it an uncontroversial stimulus for a potential investor wishing to invest on the cultivation of Cardoon in the PCSM area. In the contrary, the gross profit margin for hard wheat cultivation is estimated at 31 €/tn or 620 €/ha (82 €/tn selling price including allowances – 51 €/tn cost of production) [7]. The comparison favors the energy crop cultivation. The benefit will be by far greater if one considers the rights of CO₂ emission acquired the current rate of which is 17.5€/tn, with a prospect to reach 25 €/tn by 2025 or 55 €/tn by 2030 if the European Commission decides to align the permitted pollutant levels with the objectives of the Paris climate agreement. Of course this profit can also be split between producer and consumer. Further to the gross profit made, additional issues that are considered, regard the accumulated thermal capacity of 1,969.56 TJ. (≈470 Tcal). This thermal capacity is adequate for the annual supply of a 30-35 MWe biomass power generation plant or, feed partially the new 75 MWe biomass power plant being built by PPC Renewables in the nearby area. Moreover, a thermal plant with a combustion yield of 80%, supplied with this thermal load operating on a 24 hour basis for 200 days (October –April), yields 547 GWh_{th} a thermal capacity that exceeds Ptolemaida needs for district heating. An alternative proposal is to use the biomass for co-firing with lignite at a proportion of (5%) in one of the PPCs' existing power plants.

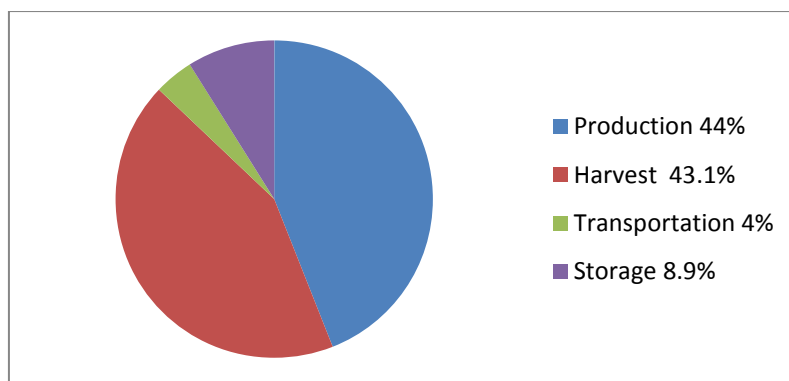


Figure 3. Biomass cost composition (%)

6. CONCLUSIONS

Analyzing and processing the parameters that constitute the cost of cultivating, harvesting, transporting and storing biomass and comparing the results produced, some general conclusions about the optimal supply chain management method are emerging. Cultivation of Cardoon - *Cynara Cardunculus* L in the PSCM is viable providing a yield of 20 dt ha⁻¹. The most cost-effective biomass logistics chain is the one in which: proprietary machinery is used, the personnel employed is in an employment relationship with the collector. Storage is more economical when it is bulk in open space windrow lines with cover to protect against weather conditions. The yields obtained, by implementing the most economical modes result to a total cost for biomass cultivation in the PCSM area of 30.45 €/tn. The thermal capacity of the harvested biomass can either be used for district heating, or, back up one of the PPC's nearby power plants by 5%, or support a biomass combustion power plant of 30-35MW.

REFERENCES

- [1] ECHMES Ltd . May 2010. PPC Environmental Impact Assessment of Ptolemaida mines N. Kozanis.
- [2] Council of the European Union. Brussels European Council 8/9 March 2007 - Presidency conclusions. Brussels, 7224/1/07 REV 1, 2007.
- [3] J. Fernandez, M.D. Curt. State of the art of *Cynara Cardunculus* L as an energy crop, , Dept of Plant Production: Botany and Plant Protection, Polytechnic University of Madrid,2006
- [4] Panagiotis Grammelis, Anastasia Malliopoulou, Panagiotis Basinas, and Nicholas G. Danalatos, Cultivation and Characterization of *Cynara Cardunculus* for Solid Biofuels Production in the Mediterranean Region * Int J Mol Sci. 2008 Jun; 9(7): 1241–1258.
- [5] Gonzales J, Perez F, Fernandez J, Lezaun JA, Rodriguez D, Perea F, Romero C, Ochoa MJ, Garcia M. Study of *Cynara cardunculus* L. lignocellulosic biomass production in dry conditions. Acta Hortic. 2004;660:221–227.
- [6] Jorge Gominho, Ana Lourenço, Maria Dolores Curtb, Jesus Fernández, Helena Pereira. 2014. *Cynara Cardunculus* in Large Scale Cultivation. A Case Study in Portugal. chemical engineering transactions vol. 37.
- [7] George Manelis. July 2012. Technological Study of Energy Crops for the Production and Exploitation of Biomass, NTUA Thesis.

- [8] Panagiota Kazai. June 2008. Plants for the production of solid biofuels in Europe. Institutional Repository - Library & Information Centre - University of Thessaly Thesis
- [9] Giannoulis K.D., Danalatos N.G. and M. Sakellariou. 2018. Switchgrass, Cardoon and Miscanthus Perennial Crops as alternatives for solid bio-fuel production in Central Greece.
- [10] Madhu Khanna Basanta Dhungana John Clifton-Brown. , June 2008. Costs of producing miscanthus and switchgrass for bioenergy in Illinois. Biomass and Bioenergy Volume 32, Issue 6, Pages 482-493.
- [11] Karin Ericsson¹, Håkan Rosenqvist and Lars J. Nilsson. 2009. Energy crop production costs in the EU. Environmental and Energy Systems Studies, Lund University. Published in Biomass and Bioenergy Vol 33 (11) 1577-1586.
- [12] Theodoros Skevas , Scott M. Swinton , Sophia Tanner, Gregg Sanford and Kurt D. Thelen. (2016). Investment risk in bioenergy crops. GCB Bioenergy 8, 1162–1177.
- [13] Ch. Papapostolou, M. Minoyiannis, E. Kondili. Biomass Supply Chain Development in Greece with Special Focus on the Utilization of Biomass Residues Dept of Mech.Eng. Technological Education Institution of Piraeus, 1st Olympus International Conference on Supply Chains, 1-2 October, Katerini.
- [14] Duffy, Mike, “Estimated Costs for Production, Storage and Transportation of Switchgrass,” Ames, Iowa: Iowa State University, University Extension, February 2008.
- [15] Giovanni Mauromicale, Orazio Sortino, Gaetano Roberto, Pesce Michele, Agnello Rosario, Paolo Mauro. June 2014 Suitability of cultivated and wild cardoon as a sustainable bioenergy crop for low input cultivation in low quality Mediterranean soils. Industrial Crops and Products Volume 57, Pages 82-89

Towards a New Deal for the Lignite Industry in Western Macedonia

Dimitrios Sotiropoulos¹, Evangelos Karlopoulos¹, Dionysios Giannakopoulos¹ and Dimitrios Mavromatidis¹

¹ Technical Chamber of Greece/Department of Western Macedonia, Bousiou & Estias 3, Kozani, Greece

ABSTRACT

Having reached its peak in 2004, the production of lignite and lignite power accordingly have been steadily declining in Western Macedonia, coming to a mere 50% of its corresponding production in 2004. Estimates for the next 15 years indicate that this decline will continue towards the end of this period, resulting in lignite production in the region dropping to 1/3 compared to that of 2004. In this paper, there is documentation by quantitative indicators of the heavy negative impact that will be brought on the Western Macedonia economy by the escalation of the decommissioning of lignite units, both in terms of Gross Added Value and in terms of income generation for the wider region, unless simultaneous large-scale development actions and substantial employment support are promptly implemented. In addition, the paper presents the basic parameters of a New Deal for the lignite utilization as a raw material in the production of high added value products, along with its use in power generation, creating a secure and viable bridge for the transition of Western Macedonia to the post- lignite era.

1. INTRODUCTION

Dating back to the mid-1950s, the lignite industry grew in the energy axis of Western Macedonia at rates never before experienced in Greece. The security of national energy supply, the predictable availability cost as well as the reliability enhancement of long-term energy planning rendered domestic lignite as the dominant fuel on a national level. Lignite activity in Western Macedonia includes open-cast mines over a total area of 160 square kilometres, while from the onset of lignite exploitation, 6 Thermal Power Plants (TPP) amounting to a total installed power capacity of 4,4 GW were erected, thereby covering 70% of the electric power needs in Greece for decades. On the other hand, the size as well as the operational needs of the lignite industry, in effect those of the Public Power Corporation (PPC), triggered mobility of the local workforce on a large scale. Traditional professional skills were substantially confined. Conditions of one-dimensional development with all the traits of pathogenesis were established. A high negative environmental impact ensued, putting heavy pressure both on human and natural environment. During the last 15 years, the penetration of natural gas in power generation, the rapid development of renewable energy, the liberalization of the electricity market, the implementation of stricter environmental emission limits and the introduction of the carbon dioxide (CO₂) emissions pricing in the electricity market pricing, have exerted strong pressure on the competitiveness of domestic lignite. All of the above characteristics illustrates that Western Macedonia has entered the post-lignite era.

The significantly negative impact to the Western Macedonia economy by the escalation of decommissioning of lignite units, is documented by quantitative indicators while the basic parameters of a New Deal for the lignite utilization as a raw material in the production of high added value products, creating a secure bridge for the transition of Western Macedonia to the post- lignite era are also presented.

2. THE PERSPECTIVES OF LIGNITE IN WESTERN MACEDONIA IN A CONVENTIONAL EXPLOITATION CONDITIONS

Both current and future conditions that outline the prospects of the lignite industry in Western Macedonia are now completely different from the past, i.e. regarding the development of lignite activity and, above all, irreversible:

- Strict environmental constraints that put pressure on existing lignite plants and almost prohibitive for installation of new, conventional units
- Expensive allowances for carbon dioxide (CO₂)
- Excessive lignite units with low flexibility of cooperation with stochastic Renewable Energy Sources (RES)
- Large penetration of RES
- Introduction of imported, competitive fuels with significantly higher operational flexibility and comparatively better environmental performance
- Lower electricity prices in neighbouring markets, putting pressure on the Greek market

On the basis of the above, it is clear that lignite, as a primary source of electricity generation, will be under escalating pressure and with constantly decreasing competitiveness, with a very high probability that in the next decade it will cover only 15% of the national electricity generation. Such an evolution certainly will have negative effects on the productive and social network of Western Macedonia.

2.1. The price of decarbonisation for the economy of Western Macedonia

The European Union energy and climate policy architecture has at its core target to deliver decarbonisation. On the basis of a long-term vision of reducing greenhouse-gas emissions by 80-95 per cent by 2050 compared to 1990, the EU has set a binding 40 per cent emissions reduction target to be achieved by 2030 compared to 1990 [1].

On the Western Macedonia regional level, the Technical Chamber of Greece/Department of Western Macedonia has estimated the consequences of the decarbonisation process in quantitative terms:

- The lignite mining and power generation sectors provide a 2.6 income multiplier, in the local labour market, according to the most recent available data of 2013 [3].
- Based on 2009 data, decommissioning of 300 MW lignite installed capacity would deprive the local economy of 83 million EUR on an annual basis. If 2,400 MW are decommissioned, without any supporting actions taking place, the figures may prove nightmarish and irreversible for the productive and social network of Western Macedonia [2].

Moreover, according to the Consultation document for the National Strategy for Adaptation Measures to Climate Change, Ministry of Energy (2015), where the vulnerability of each region was examined in terms of economic activity sectors, it was estimated that the negative impact on Western Macedonia could potentially be four times that of other Greek regions, with the economic losses mainly deriving from the reduction of mining activity, practically of the lignite industry. And all the above will be taking place in a Region where the unemployment rate is approximately 30% with that among young people at the highest European Union level.

3. THE NEED FOR A NEW AGREEMENT ON DOMESTIC LIGNITES

In order to investigate the possible future options of Western Macedonia evolution in relation to domestic lignite, three scenarios were examined as follows:

3.1. Scenario A: Escalated decommissioning of lignite firing Units – Business as usual

For Western Macedonia, the implications of this scenario are predetermined: heavy deindustrialisation, loss of the energy character of the area, risk of destabilization of the productive network, difficulty in rebuilding the local economy [3].

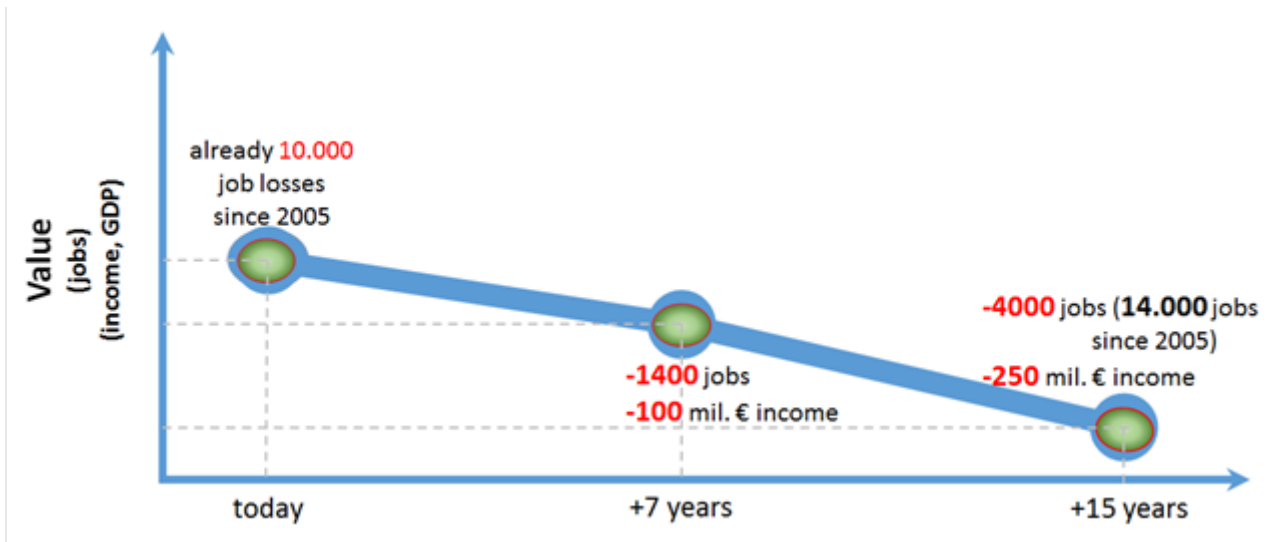


Figure 1. Escalated decommissioning of lignite fired Units in Western Macedonia – Business as usual.

As illustrated in Figure 1, the escalation of the lignite withdrawal, without large-scale development actions and a strong indicator of employment support, will have a heavy negative impact on the economy of Western Macedonia. Over the next seven years, 1400 direct, indirect and induced jobs will be lost. Within fifteen years, the value of Western Macedonia will be reduced both by 250 million euros in terms of Gross Added Value and income generation, and by 4000 jobs.

3.2. Scenario B: Conventional actions on local scale

This scenario involves action and interventions of a conventional nature such as combined combustion of lignite and natural gas, extensive upgrading of lignite units, use of biomass fuels and utilization of dry lignite.

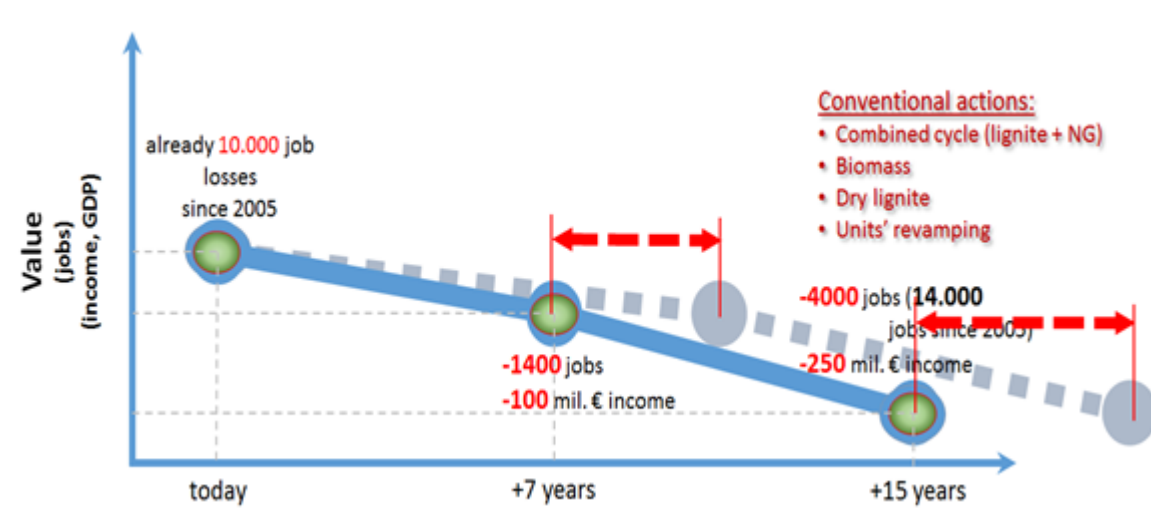


Figure 2. Conventional actions on local scale.

As outlined in Figure 2, the up-taking of conventional actions and interventions has the potential to cumulatively prolong energy activity in Western Macedonia without, however, preventing productive shrinkage. The positive effect of this scenario is that through these interventions, the necessary time for differentiation of the region's productive model could be given.

3.3. Scenario C: Long-term actions - New Deal

This scenario, through a New Deal for Greek lignite, requires the use of lignite, in addition to conventional power generation, to be converted to products of high added value. It requires long-term actions, excellent planning, consistency in implementation and long-term acceptance from regional and local authorities. It requires significant investment in research and technological development, strong extroversion, international alliances and, above all, consistent support from the Greek government.

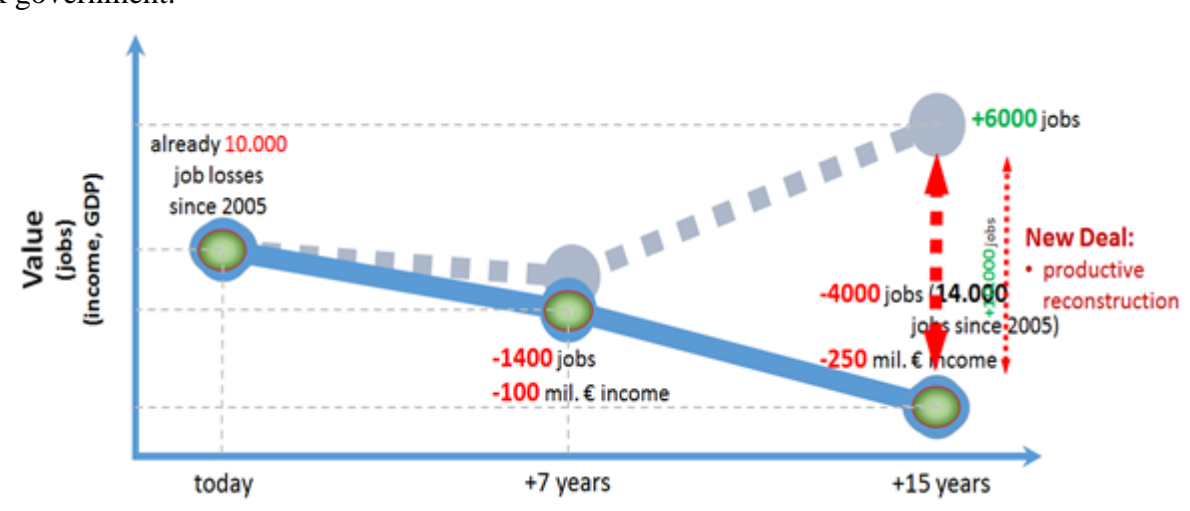


Figure 3. Long-term actions (productive reconstruction) - New Deal.

The aim of the New Deal is to capitalize on existing know-how and infrastructure through interventions that radically change the conventional energy character of Western Macedonia, thus creating a safe and viable means of transition of the region into the post lignite era [4,5,6].

4. OUTLINE OF THE NEW DEAL EFFECT ON DOMESTIC LIGNITES

The exploitation of lignite in Western Macedonia has taken place in an utterly conventional way, namely extraction of lignite, combustion and ash management. In practice, there is no utilization of lignite in non-electrical uses. However, lignite can be used as raw material in the production of a range of products and energy carriers with a very high added value. According to the first intermediate results of the Technical Chamber of Greece /Department of Western Macedonia Working Group, which is dealing with the New Deal's prospects for Greek lignite, 5 million tonnes of Greek lignite can alternatively be converted into 1 million tonnes of Methanol, 2 million tons of Urea, 2.5 million tonnes Coke, or 1bn m3 Synthetic Natural Gas [4,5,6].

The use of lignite in the production of these commodities-energy carriers, offers the possibility of a generalized productive reconstruction of Western Macedonia, creating many and differentiating business opportunities with a substantial positive impact on local employment.

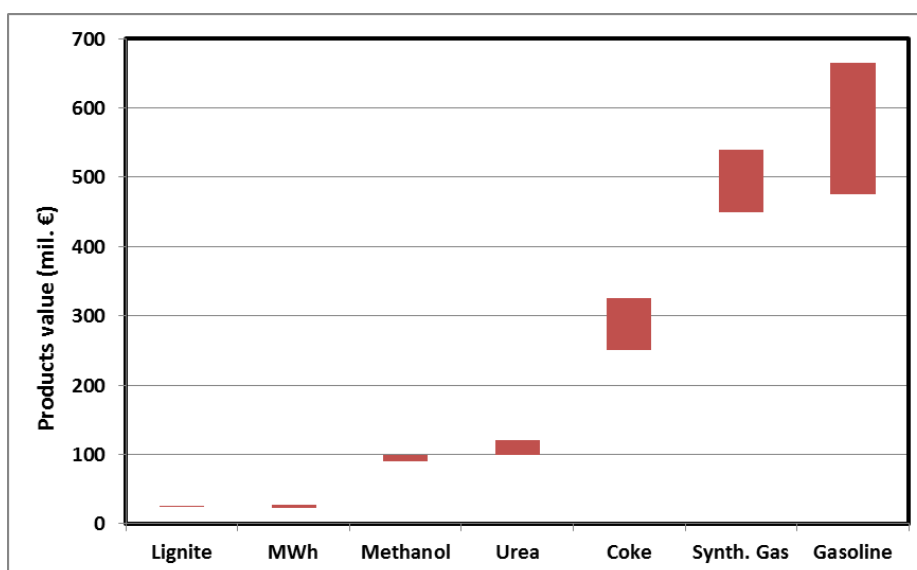


Figure 4. Value of different products produce from Greek lignite (for each million tonnes of lignite raw material)

As shown in Figure 4, the commercial value of one tonne of Greek lignite is approximately 25 euros. Through the combustion of lignite in the conventional lignite units of Western Macedonia, its value is 45-55 euros, as is the value of the MWh produced. In comparison, with the same amount of lignite, methanol can be produced with a commercial value of around 100 euros, or synthetic gasoline with a commercial value ranging from 450 to 650 euros.

Similarly, the impact on employment is shown in Figure 5. While conversion of 1 million tonnes of lignite into electricity maintains about 150 direct, indirect and induced jobs, the production of added value products significantly increases the employment rate. In the case of synthetic gasoline production, the employment rate is increasing by an order of magnitude, creating multi-faceted satellite entrepreneurship and new high-skilled jobs.

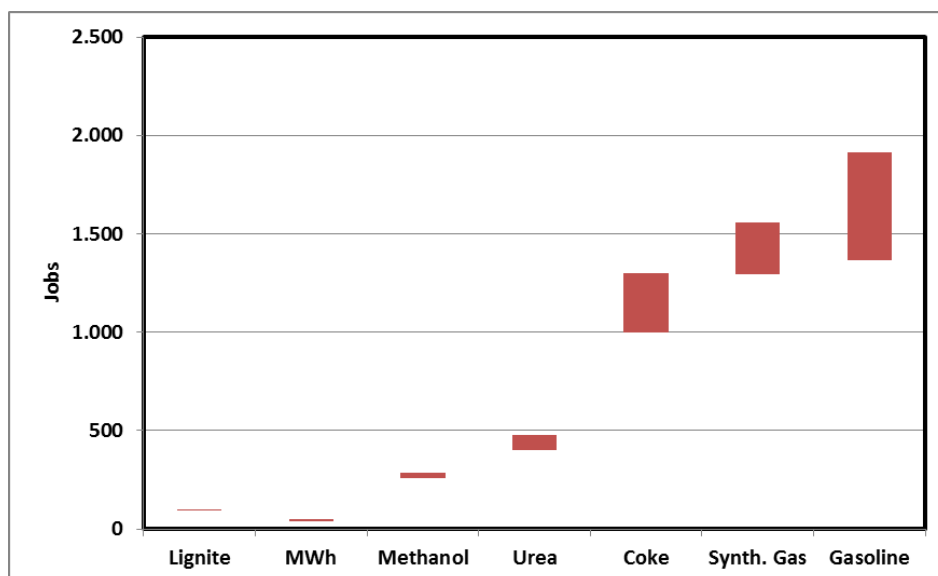


Figure 5. Job creation of different products based on Greek lignite (for each million tonnes of lignite raw material)

In any case, most of the available technologies are commercially mature and obviously require capital-intensive investments. However, with oil prices exceeding \$ 80-85 per barrel, the use of lignite in high added value products will become increasingly attractive in the future [6]. For Western Macedonia, the necessary steps towards a New Lignite Agreement are briefly summarized as follows:

- Analysis of the economic, environmental, technical and social parameters of the new coal utilization technologies
- Evaluation, ranking and prioritization of technologies and requirements of a Technological Foresight through multi-criteria analysis
- Integration of the most promising technologies into a future-proof business model for Western Macedonia
- Detailed design and implement the New Deal

An approach that takes into account technological developments, environmental constraints, national and European energy policies, the geostrategic of Energy and, of course, the real potential and competitive advantages of Western Macedonia is needed.

5. CONCLUSION

The escalation of environmental constraints, the entry of new fuels and renewable energy technologies into power generation and the tendency for decentralized energy systems lead to a drastic reduction in lignite production in Western Macedonia. This will increase the pressure on the productive and social network of the region, particularly in terms of jobs. Following the business as usual scenario, 1800 jobs will have been lost over the next 15 years, while with the conventional scenario, there will be simply a postponement of the negative impact by about five years. An active response to the problem is the use of lignite as a raw material in the production of a range of products and energy carriers with a very high added value through a development platform, a New Deal for local lignite. The aim of the New Deal is to capitalize on existing know-how and infrastructure through interventions that will radically change the conventional energy nature of Western Macedonia, creating a safe and viable means of transition of the region towards the post lignite era.

REFERENCES

- [1] COM (2011) 112 - A Roadmap for moving to a competitive low carbon economy in 2050.
- [2] Technical Chamber of Greece (2012). Estimation of the transition cost to a low lignite production economy for the Region of Western Macedonia, Department of Western Macedonia, Kozani.
- [3] Technical Chamber of Greece (2018). Determination of the contribution of various economic sectors to the production model of Western Macedonia Region with emphasis in the lignite industry, Department of Western Macedonia, Kozani.
- [4] Technical Chamber of Greece (2018). A New Deal for the Greek lignite, Department of Western Macedonia, Kozani. (Ongoing study).
- [5] UPDATED MANUFACTURING MULTIPLIERS FROM 2010/11 DATA, BERL Economics, BERL House, NZ, 2012.
- [6] isw-Gesellschaft für wissenschaftliche Beratung und Dienstleistung mbH. Regionalwirtschaftliche Effekte der Nutzung von Braunkohle unter Berücksichtigung als Chemierohstoff. Studie-stand 27/02/2015.

Backfilling and Securing of abandoned Small Scale Coal Mines in Mongolia with Coal Combustion By-Products (CCB's) - the BASMIC Project

Martin Knippertz¹ and Peter Vossen²

¹RWTH Aachen / Lehrstuhl für Physische Geographie und Geoökologie, Templergraben 55 52056 Aachen, Germany

²German-Mongolian Institute for Resources and Technology / GMIT Campus, 2nd Khoroo, Ulaanbaatar, Mongolia

ABSTRACT

In Mongolia more than 500.000 t of “Coal Combustion By-products” (CCB's: Fly Ash, Bottom Ash, Boiler Slag) are generated by 5 Power Plants. Most of these CCB's are usually disposed to special designed ponds without any environmental or social benefits. Particularly the pozzolanic material behaviors qualify CCBs as stable construction material, e.g. for backfilling operations in underground mines.

In Nalaikh - 30 km southeast of Ulaanbaatar - hundreds of small scale miners are digging for coal, leaving behind a multitude of unsecured surface openings and unclear branches towards the subsurface (Fig.1). During the peak season in winter up to 2.000 Nina-miners work in around 200 mine shafts. Nalaikh's coal counts to about 70% of the 1 Mio. t coal burned every year in UB's ger district.

The abandoned small scale mines, over time, often pose a permanent threat to humans in the neighborhood. Stabilization of these mine sites is a crucial part of a rehabilitation concept that has been developed at GMIT for the Nalaikh mining area. The aspect of rehabilitation in mining areas is becoming more and more important in society. For the bigger mine sites in Mongolia rehabilitation concepts are available. For the smaller mine sites and especially for the Ninja-mines of Nalaikh such concepts are not yet available, even if the necessity is given and commonly accepted.

Currently the “German Mongolian Institute for Resources and Technology” (GMIT) is starting a project “Backfilling and Securing of abandoned Small Scale Coal Mines with Coal Combustion By-Products (CCB's) generated at Power Plant Sites and with Domestic Coal Combustion By-Products generated at Ger District Sites” (BASMIC) to improve both, the sustainable usage of CCB's and the stability of abandoned small scale mines.

BASMIC analyses CCB's and CCB's in combination with other materials to determine their suitability as backfill material for abandoned mining sites. The abandoned small scale coal mines should be backfilled with CCB's, to ensure ground support and regional stability.



Fig.1: Mining Licence Area of Nalaikh. Photo: Knippertz, 2017

1. COAL COMBUSTION IN MONGOLIAN POWER PLANTS

During the year-round incineration of coal in the power plants of Ulaanbaatar as well as in the surrounding area, different fractions of residues remain as so-called “coal combustion by-products” (CCB’s). More than 500.000 t CCBs are generated by the Central Energy System of Mongolia, consisting of 5 Power Plants with an electrical capacity of 796 MW.

Due to the mandatory electrostatic separators for collecting fly ash in industrial countries CCB’s can be divided in the fractions with the following mass distribution

1. Fly Ash (ca. 74 mass %),
2. Bottom Ash (ca. 20 mass %)
3. Boiler Slag (ca. 6 mass %)

In Mongolia only the TPS4 power plant collects fly ash with an electrostatic separator. Other (thermal) power plants generate much higher mass-% of bottom ash and boiler slag.

2. DISPOSAL AND RECOVERY OF CCB’S

CCB’s generally hold high recovery and recycling characteristics. Particularly the pozzolanic material behaviors qualify CCB’s as stable but flexible construction material.

Although CCB’s in Mongolia are used for recovery purposes due to the huge amounts of generated CCB and a lack of recovery opportunities most of the CCB masses are usually disposed to special designed ponds without any environmental or social benefits. Moreover due to land shortages in Ulaanbaatar the construction of new ash ponds is desired neither from a social nor from an environmental view.

The recycling properties of CCBs for stabilizing ground and underground applications are proven. In particular, due to the pozzolanic properties, ash is a popular material for backfilling operations in underground mines, especially in industrialized countries like Germany. Backfilling of CCBs in German underground mines has improved the stability both in the subsurface and on the surface during the last decades without any doubt.

In industrial states opportunities are created to recover up to 40% of the CCBs as an additive in a variety of applications such as a cement substitute in concrete and a filler for asphalt. Coal ash is also used in construction projects to level out uneven terrain. The remaining 60% is disposed in ponds and landfills. In developing countries the disposed part of CCBs is significant higher while CCBs can serve as material substitutes, e.g. for cement and therefor prevention of energy dissipation for cement production. Many actual publications regarding the characteristics of CCBs. Hence the recovery of CCBs do not allow other conclusions: Recovery and recycling of CCBs is a task of high relevance for the Mongolian society for environmental and social reasons.

3. SMALL SCALE COAL MINING IN NALAIKH

In Mongolia small scale mining activities at the surface and in the underground take place in many places. These are in most cases unauthorized mines operated by only one or a few workers. Special characteristics of these activities are e.g. low qualification of the miners, primitive technical equipment (often only with shovel and hoe), the work in the pits take place under considerable danger (every year people die due to sudden slides and caves to the surface).

Hundreds of small scale miners are digging for coal in the southern part of Nalaikh, leaving behind a multitude of unsecured surface openings and unclear ramifications towards the subsurface. These abandoned small scale mines, over time, often pose a permanent threat to other neighboring miners as well as to every human and animal staying at the site.

Small scale mining activities cause environmental, health and social problems. It seems of fundamental interest to the Mongolian Government that legal, technical, socially and environmentally compatible solutions are being developed for non-legal small-scale mining activities. Alone 2 out of 17 articles of the "Policy to ensure sustainable economic development" of 2016 were launched, in order to liberate the nationwide small-scale mining from the shadows of the illegality. The Mongolian Ministry of Environment estimates that an area of approximately 4,000 ha of unregulated abandoned mining has been left in 566 places of 15 aimags.

Some small scale mining activities in Mongolia have left a noticeable burden to the surrounding area. Innovative processes for the environmental improvement are necessary at such sites. In particular there are many approaches for interdisciplinary research such as the reuse of CCBs.

In and around Nalaikh the environmental impacts of mining (related) activities has been investigated within a GMTI-project. Samples of soil, water and air were taken and analyzed. Besides these ecological components also the socio-economic conditions are of importance for the derivation of recommendations for a better understanding and management of Nalaikh's environment (rehabilitation concept).

The above mentioned socio-economic results are based on interviews with 17 people from different residential areas of Nalaikh (Fig.2).

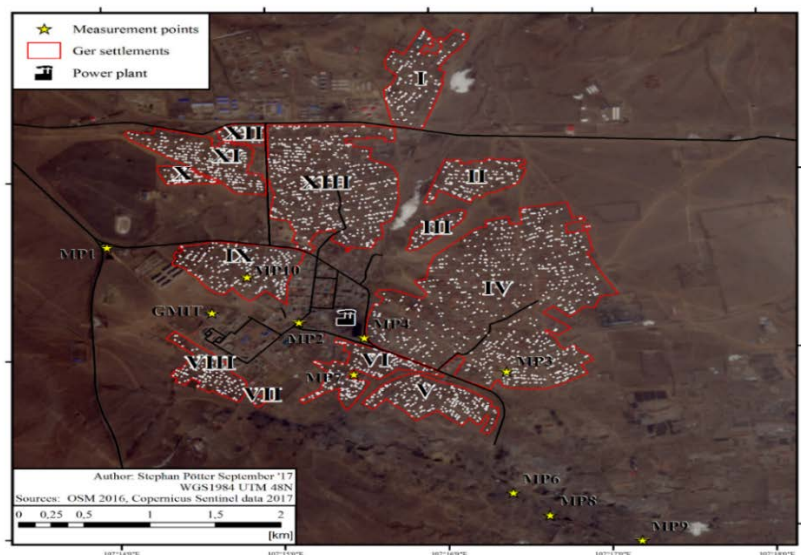


Fig.2: Residential areas in Nalaikh, with the “Normal settlement” in the center, the “Ger settlements” (red lines, I-XIII) and the “Mining Area” in the south. Pötter, 2017

An interesting finding of the socio-economic research was, that the people living outside the mining area blame the mining activities for a variety of environmental damages (which in this case is not true).

Soil analysis in the project area focuses on heavy metal contents, additional soil features were analyzed. In general the soil features are good, heavy metal concentrations are within the guidelines, except for Arsenic (As). The Geoaccumulation index (Igeo)

$$I_{geo} = \ln(C) \text{ (with } C = \text{measured value/ (reference value (= 8,6 ppm As) * 1,5))}$$

indicates no major influence of mining activities on the As content in the soils (Fig.3). The maximum Igeo along two transects (black dotted lines in Fig.3) is 0,13. Point Y-06 (red colour) with the absolute maximum of all samples (2,13) represents the ash basin next to the power plant.

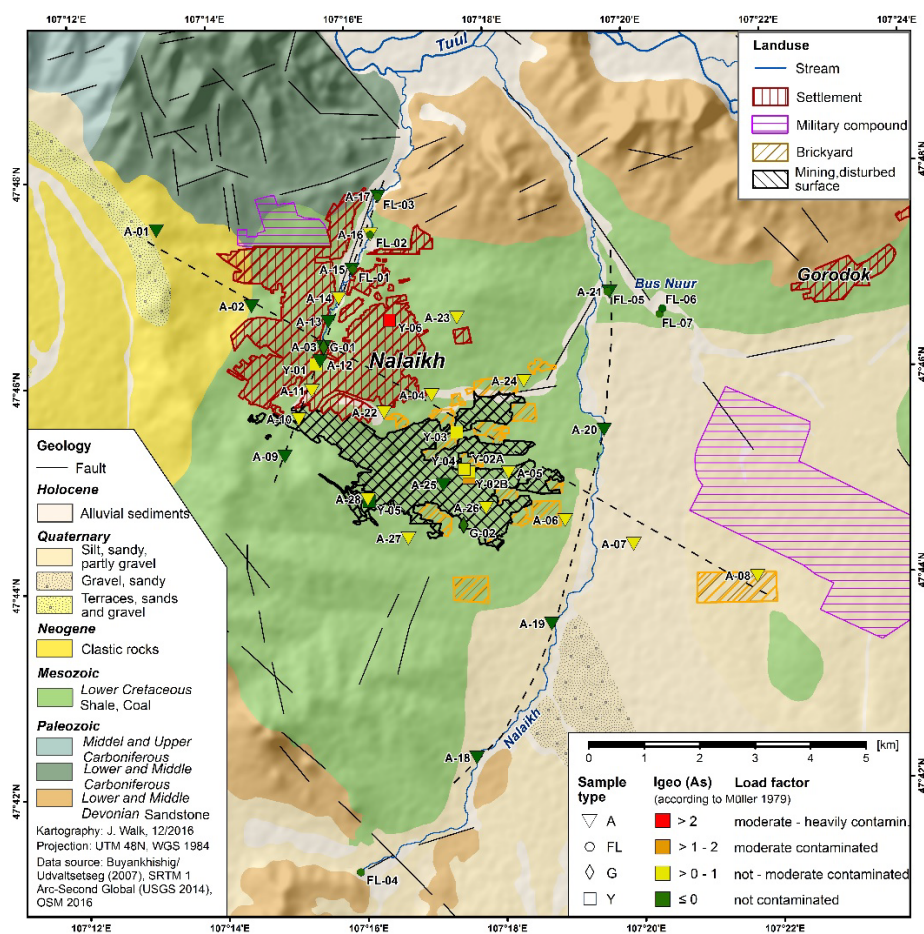


Fig.3: Geoaccumulation index in the research area. Walk, 2017.

A-topsoil, FL-fluvial sediment, G-geogenic substrate, Y-anthropogenic substrate

Water analysis in the wells as well as in adjacent streams is mainly concentrating on As. Contamination of (ground) water with As is well known for major parts of Mongolia and also for coal mining areas and poses a health risk to the affected people. The highest measured As-concentrations were found in surface waters around Nalaikh, with > 100µg/l in Bus Nuur (WHO-guideline is 10 µg/l) (Fig.4). The drinking water quality in Nalaikh is within the guidelines.

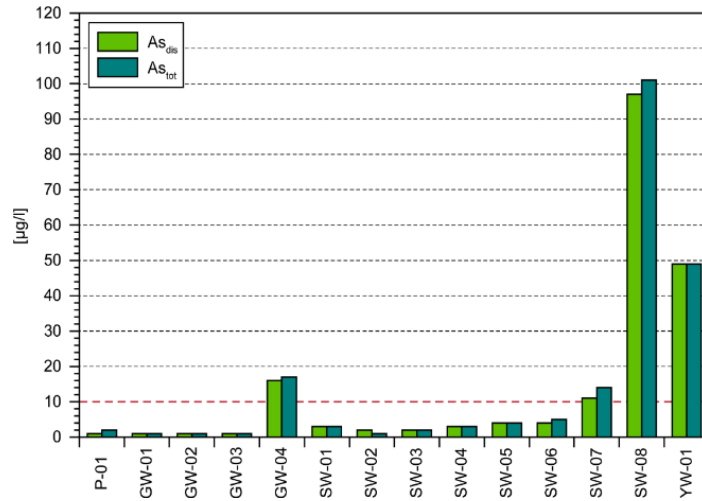


Fig.4: Dissolved (As_{dis}) and total Arsenic (As_{tot}) in selected water samples in the Nalaikh region. Walk, 2017.

P-precipitation water, GW-ground water, SW-surface water, YW-anthropogenic water body (ash basin), SW-08=Bus Nuur.

Mining combined with general human activities in Nalaikh is also subject to high particulate matter (PM) pollution in the air. PM and black carbon were measured. During winter the average PM 2.5 concentration in Nalaikh is 200 µg/m³ (WHO-guideline is 25 µg/m³) (Fig.5). The main source for air pollution are Nalaikh's ger settlements.

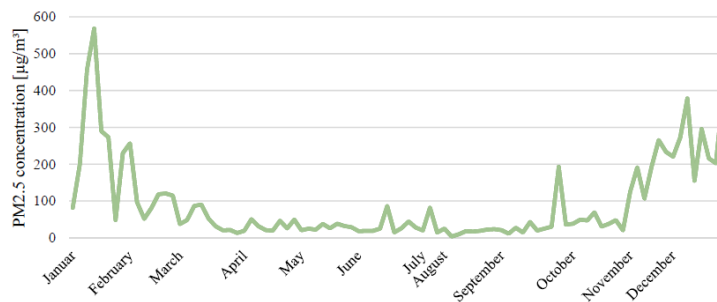


Fig.5: Annual course for PM2.5 concentration for Nalaikh (2016). Pötter, 2017

In general it can be stated, that there is little ecological impact of the mining activities on the environment. Anyway, ecological recommendations were given to Nalaikh's authorities. Further geotechnical measures (like backfilling) are necessary in the mining area to ensure a long-term stability of the environment.

4. GOALS OF THE BASMIC-PROJECT

The BASMIC projects purpose is to investigate on a theoretical basis whether there are opportunities to use CCB's from the power plants for backfilling and securing abandoned small scale mining sites in Nalaikh beginning with a laboratory investigation on the CCB's to show, whether their properties hold the demanded characteristics to propose an improvement in ground and underground stability.

The technical suitability of the CCBs generated in Mongolian power plants as backfill material should also be demonstrated in combination with other materials for abandoned mining sites on a laboratory scale.

In the long winter time in Mongolia CCB's are also generated in another manner than described. Significant amounts of ashes are generated by coal combustion in the Ger districts. While the fly ash is usually completely emitted unfiltered into the air, a significant amount of rust ash is produced, which is disposed uncontrollably by the individual dwelling-house or -yurt owners in most cases. These procedures are usually associated with damages to the environment.

Furthermore a part of BASMIC is to examine how it can succeed in the Ger districts to bring people together to collect their ash as well in order to use these for backfilling the abandoned small scale mines. A more detailed sociological study should bring out how to change the environmental awareness of the people living in the Ger districts with regard to the handling of the ashes generated by the household combustion adapted to the prevailing conditions, taking into account the socio-cultural characteristics of the Mongolian residents.

5. IMPLEMENTATION OF BASMIC AND FOLLOW-UP PROJECT

The first task of BASMIC is to demonstrate the characteristics of Mongolian CCBs in combination with other materials for abandoned mining sites on a laboratory scale. CCB samples should be collected after incineration at different power plant sites in water-resistant containers and subsequently mechanical and chemical processed at GMIT's Labs.

The second task is to investigate a change in environmental awareness of the people living in the Ger districts with regard to the handling of the ashes generated by the household combustion. For this purpose, methods should to be investigated which were already successfully used in other sociological investigations with the same aim.

Of course, the output of the BASMIC-project should be operated into practice in a subsequent project. For this purpose, first an industrial partner should be found, ideally a coal-fired power plant. In this subsequent project, it would be desirable if an abandoned small scale mining site could be backfilled with known and manageable measurements as described in the pre-recorded project.

Another aspect to be explored in an advanced project would be to discuss the economics that transport CCBs to the abandoned mining sites would entail. In this comparison, the benefits to the environment would have to be included, also in view of the fact that the power plants in the future would have to operate less (financial) effort to acquire valuable space for their ponds.

The study of the benefits of CCBs with regard to the safety of handling primary raw materials such as coal is undoubtedly one of Mongolia's future tasks and has already been recognized as such by the government. GMIT should therefore make targeted input of its scientific capabilities to bring benefits to Mongolian society.

REFERENCES

- [1] Vossen, P., Asenbaum, P. Die Verwertung von mineralischen Abfällen in Tagebauen (eine Bestandsaufnahme im Focus der EU Abfallrechtsnormen), 10th ISCSM, Sept. 2010, TU Bergakademie Freiberg, S. 429-451; ISBN 978-3-86012-406-2. (in German)
- [2] Kumar, V., Matsuda M., Miyake M. Resource recovery from coal fly ash waste; (2008), Journal of the ceramic society of Japan, 116, 165-175.
- [3] Minjigmaa A., Zolzaya Ts., Davaabal B., Bayarzul U., Temuujin J. Preliminary results on characterization of various coal combustion products from Mongolian thermal power stations and their application for preparation of geopolymers; (2012) Mongolian Journal of Chemistry, 13(19), 78-81.

- [4] Hadbaatar, A., Mashkin, A.N., Stenina, N.G. Study of Ash-Slag Wastes of Electric Power Plants of Mongolia Applied to their Utilization in Road Construction; International Conference on Industrial Engineering, ICIE 2016.
- [5] N.N. Investing in research and development of greener construction products and practices in Mongolia; Switch Asia Impact Sheet, Greener Construction; 2017.
- [6] Ahmaruzzaman M. A review on the utilization of fly ash (2010), Progress in Energy and Combustion Science, 36, 327-363.
- [7] N.N. Anforderungen des Länderausschusses Bergbau an die stoffliche Verwertung von Abfällen im Bergbau über Tage [LAB-Regeln 1998]. (in German)
- [8] Backes, H.-P., Brandenburger, D., Meissner, M. Modernes Baustoffmanagement am Beispiel von Steinkohlenflugasche; VGB PowerTech 12/2005. (in German)
- [9] Knippertz, M. (2005). Analysis of rehabilitation potentials in copper mining areas of Zambia and Mongolia. Aachener Geographische Arbeiten 40. Aachen. (in German)
- [10] Pötter, S. (2017). Air pollution in small-scale mining areas – a multi-methodological case study in the Nalaikh district, Ulaanbaatar, Mongolia. Master Thesis, RWTH Aachen. (unpublished)
- [11] Walk, J. (2017). Geoecological research on Arsenic in the small-scale mining area of Nalaikh (Mongolia). Master Thesis, RWTH Aachen. (in German, unpublished)

Environmental Reclamation Planning of Continuous Surface Lignite Mines in Closure Phase: A Risk-Based Investigation

Christos Roumpos¹, Philip-Mark Spanidis² and Francis Pavloudakis¹

¹Public Power Corporation of Greece, *Mines Business Unit*

²ASPROFOS Engineering, *Division of Project Management, Greece*

ABSTRACT

The exploitation of a continuous surface lignite mine is a complex framework that requires high capital and operational expenditures, resources and intensive use of continuous excavating, transporting and dumping equipment for several decades. When the lignite mine enters the closure phase, the environmental reclamation of the wider exploitation area constitutes a multidisciplinary intervention of high impact for the lignite and energy producers as well as local societies.

This paper investigates the critical technical, geological, socio-economic, environmental and permitting questions and associated operational risks involved with the environmental reclamation of a lignite field into mine closure phase, based on empirical evidence and managerial practices followed in relevant projects. The selection of a low risk reclamation technology is analysed as a critical decision-making problem for lignite mining organizations and environmental stakeholders to achieve cost effective and environmentally acceptable reclamation solutions.

Recommendations and proposals for development of a risk-based multi-criteria methodology advised, perceived as a tool for efficient control of risks in managing projects of lignite mines environmental reclamation.

1. INTRODUCTION

Continuous surface mining projects are very complicated because of the uncertainties associated with their dynamic situation. Project risk may relate to geological, technical, environmental, social, economic or other factors. Especially the environmental parameters play a significant role in mining operations. Direct factors, such as the cost of the necessary measures for the protection of environment and the financial liabilities of the legislation, as well as indirect factors, namely the reaction of local society, create crucial uncertainties at all stages of the projects life cycle and an increase of the corresponding risk.

In the case of exploitation of lignite deposits, the new competitive environment of the lignite mining and corresponding power plants operations, which affects their competitiveness, mainly refers to (a) the economic conditions in relation to electricity market, (b) the stringent environmental legislation, (c) the more complicated and continuously varying mining conditions and (d) the technological advances of new high-efficiency and low-emission power plants [1].

Regarding in particular mining conditions, the geometrical characteristics of multi-seam lignite deposits as well as the spatial variability of the quantitative and qualitative deposit characteristics have a strong effect on the economic viability and the environmental sustainability of the corresponding surface mining projects. The environmental impacts of the related projects arise almost inevitably and may include: land use, modification of morphology, air emissions, visual impacts or other disturbances (noise, vibrations, etc). They are connected to the landscape – topography patterns and other ecological processes. Suitable strategic planning aims at the restriction of the possible environmental impacts from mine operation in minimum.

The environmental protection and land reclamation programmes applied in surface mines aim at the minimisation of the long-term impacts in relation to the project viability, which in turn is closely connected with mine planning, production scheduling and project management procedures. The selection and implementation of measures for the elimination of adverse environmental impacts and proper restoration of the post-mining land are based on certain terms and conditions determined by the following documents:

- The Regulation of Mining and Quarrying Operations.
- The National and European laws and directives.
- The environmental permits.

The main issues introduced by the environmental permits include (a) development and implementation of a land reclamation programme, according to specific guidelines (b) management of various waste streams (c) monitoring of the environmental quality. Environmental permits refer also to the costs of implementing the above-mentioned terms and conditions for the permitting period and until mine closure / rehabilitation. This cost includes all the activities required for environmental management during mining operations and land reclamation according to the plans that have been approved by the authorities [2].

When the lignite mine enters the closure phase, the environmental reclamation of the wider exploitation area constitutes a multidisciplinary intervention of high impact for the lignite and energy producers as well as local societies. Taking into consideration the observation of balance between ecology, economy and production, the main objective of mine land reclamation should be the continuous upgrade of the environment. Based on the rules of aesthetics as well as of landscape architecture, the reclaimed areas should be perfectly integrated to the landscape [3].

A holistic approach model for the mine planning of surface mining projects should be based on an integrated approach to the long-term strategic mining planning and development, taking into account the latest technical, environmental, economic and social data with regards to the operation of surface mines (Figure 1). In this framework, in order to identify the process with the largest environmental impact, all stages of the system's life-cycle must be examined with a detailed coverage of the mining activities (i.e. excavation, material handling, and dumping) [4].

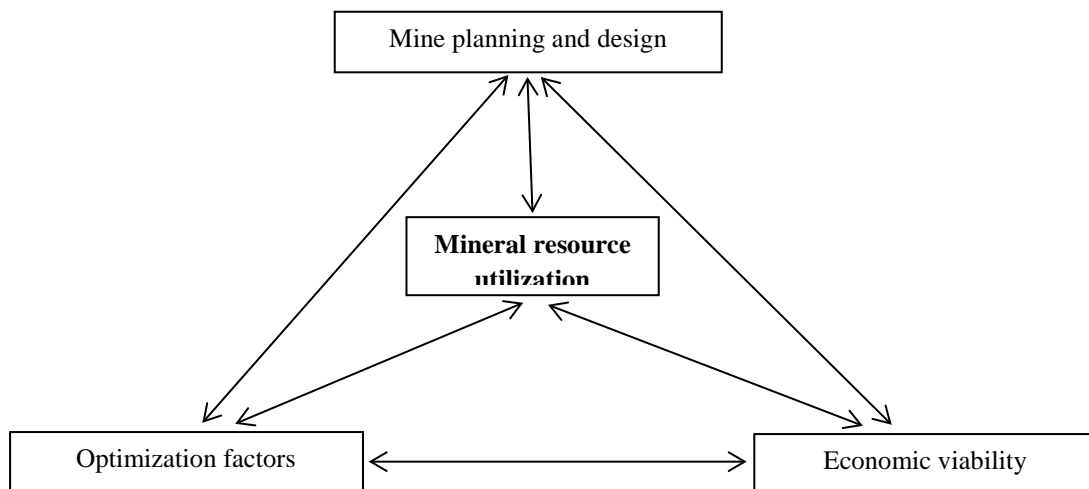


Figure 1. Mineral resource utilization in relation to corresponding factors

This paper investigates the critical technical, geological, socio-economic, environmental and permitting questions and associated operational risks involved with the environmental reclamation of a lignite field into mine closure phase, based on empirical evidence and managerial practices followed in relevant projects. The selection of a low risk reclamation technology is analysed as a critical decision-making problem for lignite mining organizations and environmental stakeholders to achieve cost effective and environmentally acceptable reclamation solutions.

2. STAGES OF MINE DEVELOPMENT AND THE CRITICAL CLOSURE PHASE

For large-scale projects and activities, like the exploitation of a lignite field for electricity production, it would be appropriate to consider the anticipated impacts in terms of their implications for sustainable development. Emphasis should be placed development of infrastructure viable in the after-lignite time period to ensure long-term sustainability. The environmental planning and design regarding the closure phase should be applied in all mine development stages (Figure 2).

In the optimization process sustainability parameters should be incorporated in all phases of the mining project, throughout the whole mine life cycle, from the first exploratory stages to the post mining period [5].

The duration of lignite exploitation projects usually lasts several decades, with an increasing trend in larger and deeper excavations, corresponding towards fewer, larger and deeper operations. Although each project is unique, because of differences in geological and technical characteristics, for the analysis of the environmental impacts during the mine development/operation period, all surface mining projects can be divided into the following phases (Figure 3) [6], [7]:

- a. **The exploration phase.** The mine activities of this phase include: exploration, road construction, rock core drilling, geochemical analysis (principal mine planning action). The relevant environmental impacts are considered as minor. However, depending upon prevailing legislation, environmental planning can commence. This may require the preparation of a brief environmental impact assessment and management plan, based on the exploration permit that provides the measures for mitigating impacts caused mostly by the construction of access roads and core drilling.
Furthermore, in this phase the relationship between the community and mining company is set up and depending on how it is managed, can result in either positive or negative perceptions of the company for a long time, including the later stages of mine development and operation..
- b. **The development phase.** It is the period from the beginning of mining activities until the full installation of the equipment in the last mine bench. Although a relatively shorter period comparing to the total mine life, through the development of infrastructure, this phase is probably of greatest impact in the short term and has long-term implications. The waste material (overburden and interburden) is dumped outside the mine and the reclamation has not started. The principal mine planning actions that are related to environmental effects include: access and haul road development, site clearing and grubbing, earth moving and surface water management, mine dewatering, utilities installation, building and infrastructure construction. The corresponding principal environmental management actions include: installation of pollution control facilities, general environmental management (air, water, land), as well as construction phase reclamation and closure.
- c. **The maturity / full production phase.** In this phase high levels of production are achieved and the operating costs are low. Referring to the local community and the environment, this is the longest period of impacts. Approximately in the middle of this phase, all waste is dumped inside mine and, at the same time land reclamation begins from outside dumps. In that phase, the principal environmental management actions include: General environmental management, performance assessment / audit, monitoring, concurrent reclamation, final closure design, partial closure and partial bond release.

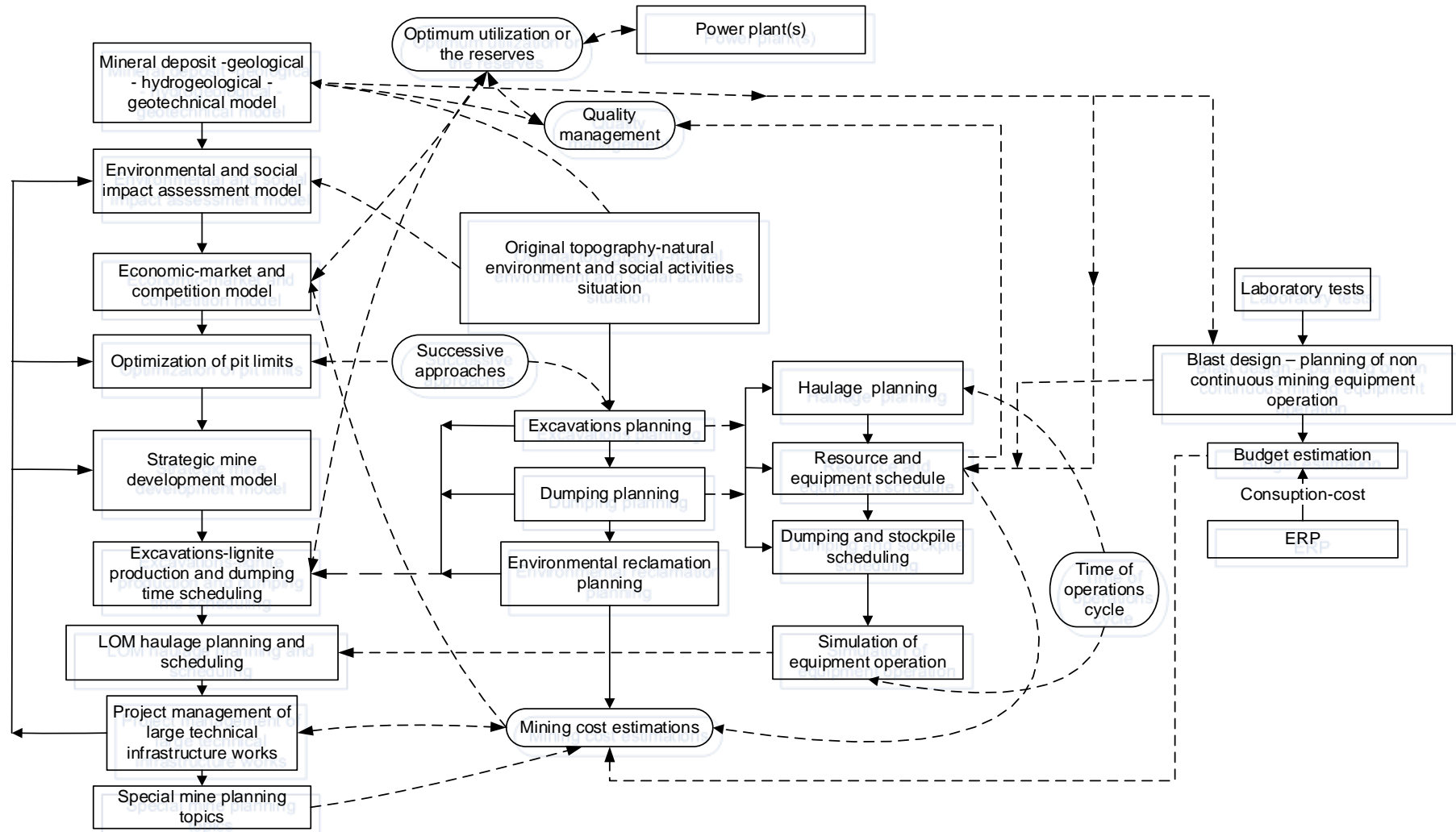


Figure 2. Stages of mine planning and scheduling of continuous surface mines

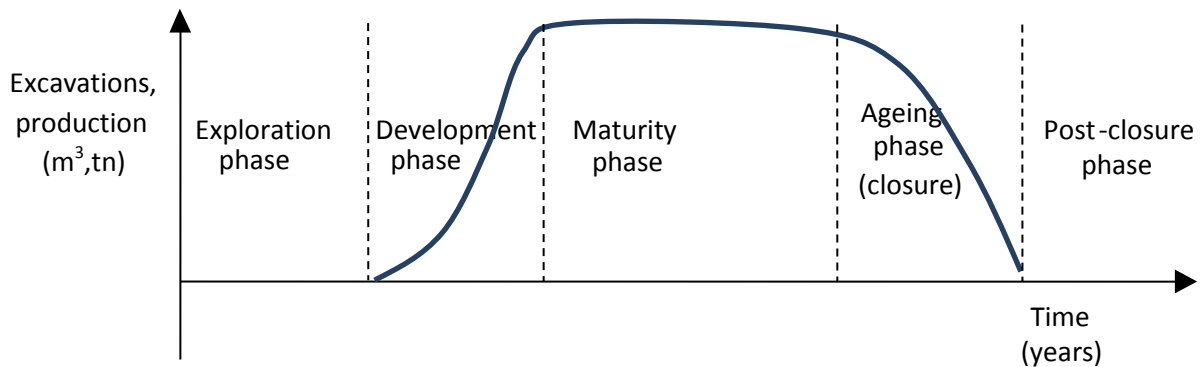


Figure 3. Life cycle phases of an open-pit lignite mine

- d. **The mine closure or aging phase.** This is the last phase of the mine life cycle, when the production is declining till the exhaustion of the mine. The impact of this phase depends largely on the degree of forward planning and the available means to sustain benefits, such as institutional capacity and financial resources. In this phase, principal mine planning actions include: elaboration of the final impact assessment study, implementation of closure plan, facilities decommissioning, dismantling, decontamination, burial, removal, asset recovery and recycling, final reclamation, including post closure planning for recultivation of mine sites, rehabilitation and use, mine water management, innovative uses of final pit voids, subsidence management, administrative structures, socio-economic studies, investigation of the contribution of land forest reclamation to the environmental protection and to mitigating climate change, optimal exploitation of reclaimed mine areas or preservation of cultural heritage.
- It is worth noticing that in this phase the rapid drop of lignite production and the consequent loss of incomes for the mining company may result to a very limited budget to finance environmental management and land reclamation activities. This fact increases risks related directly to the deterioration of environmental quality, with secondary impacts on human health and life standards, unless an effective bonding system is applied.
- e. **The post closure phase.** It is the post-mining phase, after the exhaustion of mine. In this phase the environmental management is related to treatment, maintenance, monitoring, and final bond release.

A characteristic example of mines in mature/full production phase, including also mining areas in the post closure phase, is the case of Ptolemais mines in north Greece (Fig. 4).

Based on these steps, five main risk factors categories, with sub-factors of each category, associated with mine closure of continuous surface mining projects are defined and classified.

The planned environmental reclamation of these mines according to the strategic mining planning is shown in Fig. 5.

Examples of specific mining areas for the investigations of risk factors are also shown in Figure 5 [14-16]:

A: Subsidence investigation. Area of new railway line and road construction

B, C: Slope stability analysis. Outside waste dumping area.

D: Technical-Geotechnical – environmental investigation. Area of a new power plant under construction.

E, F: Pit lakes stability analysis - hydrogeological management. Remaining pit voids.

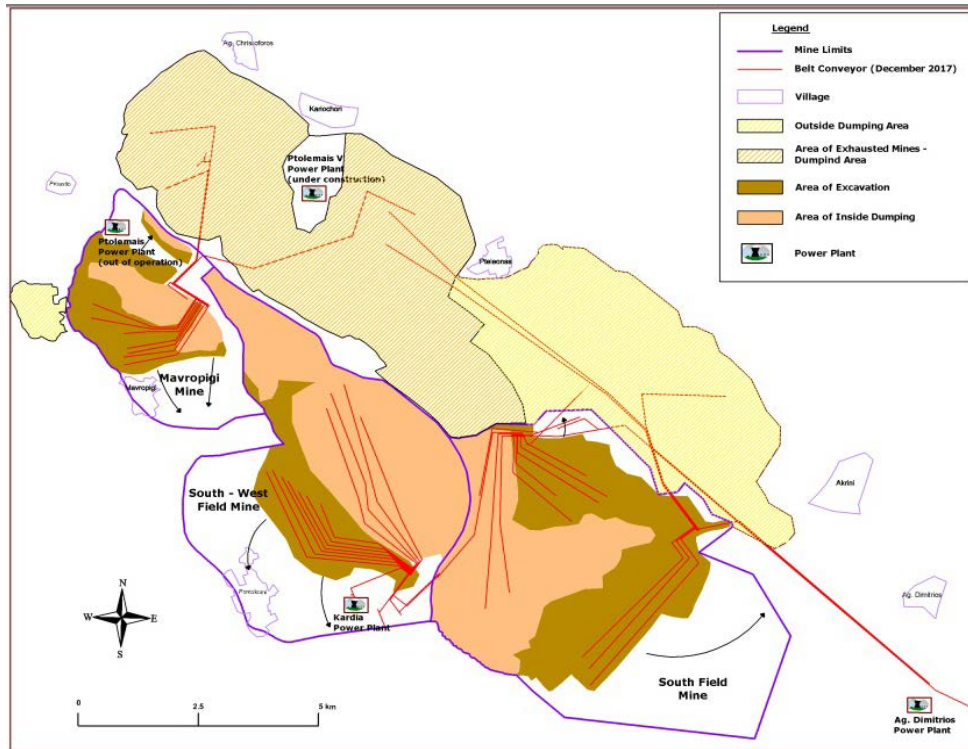


Figure 4. General overview of the Ptolemais mines, north Greece (December 2017)

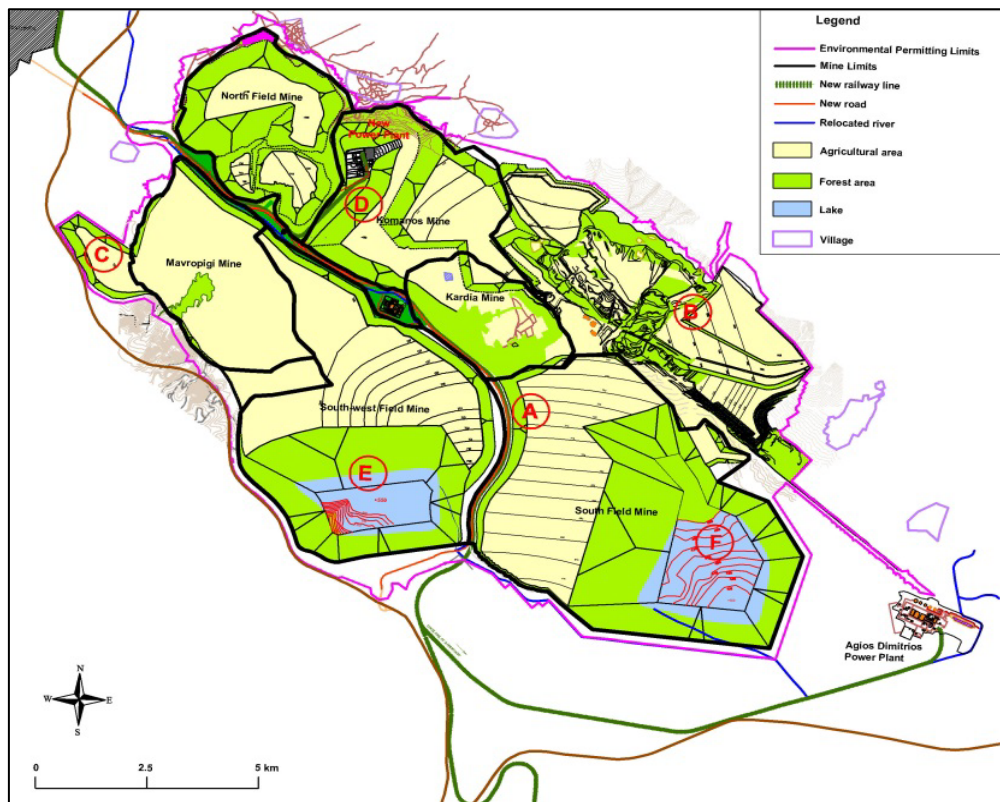


Figure 5. Land reclamation plan of the Ptolemais mines according to a strategic mine plan

Considering the above described steps of a surface mine development, it is obvious that the reclamation is an integral part of mining activities. Knabe [8] provided one of the earliest descriptions for methods and results of strip-mining reclamation in Germany. According to his analysis, the most important component of reclamation in German opencast mines was the separate disposal of topsoil or fertile layers like loess, in order to cover the spoil banks after grading and to provide a basis for good crops. In this framework, he concluded that the investigation of the agricultural value of the different layers before mining is very important.

3. RISK FACTORS IN MINE CLOSURE PHASE

Effective planning and management of continuous surface mining projects require identification of risk sources, as well as the quantification and incorporation of risk into the decision-making process. The related risk models define risk according to the objectives of the system under consideration and the nature and risk tolerance of the various stakeholders involved. For a comprehensive and systematic way of identifying and analyzing risks, a risk management approach can be adopted within a project management context, according to the mining project objectives. The risk management framework could be more efficient by combining qualitative and quantitative risk analysis.

Dey [9] suggested a project management model to identify risk factors of a project, to analyse their effect on various activities, and to derive responses in line with project objectives, the organization's policy, and business opportunities. The model combined identification of risk factors and analysis of their effects, while allowing responses through desired actions and controlling these responses in an interactive way by involving all project stakeholders.

The risk-based decision-making with a main input the results of risk assessment could be applied in the environmental reclamation planning of continuous surface lignite mines in closure phase.

Formally, risk is defined the product of the probability of occurrence and the consequence of an incident/event that could be happen in real life ([10-11]). This mathematical expression constitutes a fundamental element of the risk management and it has been mostly applied in risk analyses developed in recent decades to support needs of decision making under uncertain conditions. The accurate identification of risk probability of occurrence and consequence, however, is not always feasible due to unavailability of reliable data and/or lack of official statistical evidence. In such cases, the risk is identified and quantified upon experts' judgment and disciplinary knowledge aggregation. This approach has been currently adopted in the investigation of restoration/reclamation risks on the basis of scientific interpretation of mining practices and empirical evidence as well.

The methodology followed in this paper for risk factors and sub-factors identification, with the descriptions of tasks and decision nodes as a sequence of steps is illustrated in the flowchart in Figure 6. The process describes the involvement of a team of experts aiming at analysing and defining the suitable restoration methods and technologies. They were given all available data and details concerning the strategic planning and design in mines closure phase in relation to mines reclamation. The data were based on literature reviews, best practices and empirical evidence. The main questions include the following:

- (i) Are the available data appropriate/sufficient?
- (ii) Is the restoration project properly defined?
- (iii) Is the risk based analysis satisfactory?
- (iv) Is the risk identification satisfactory?

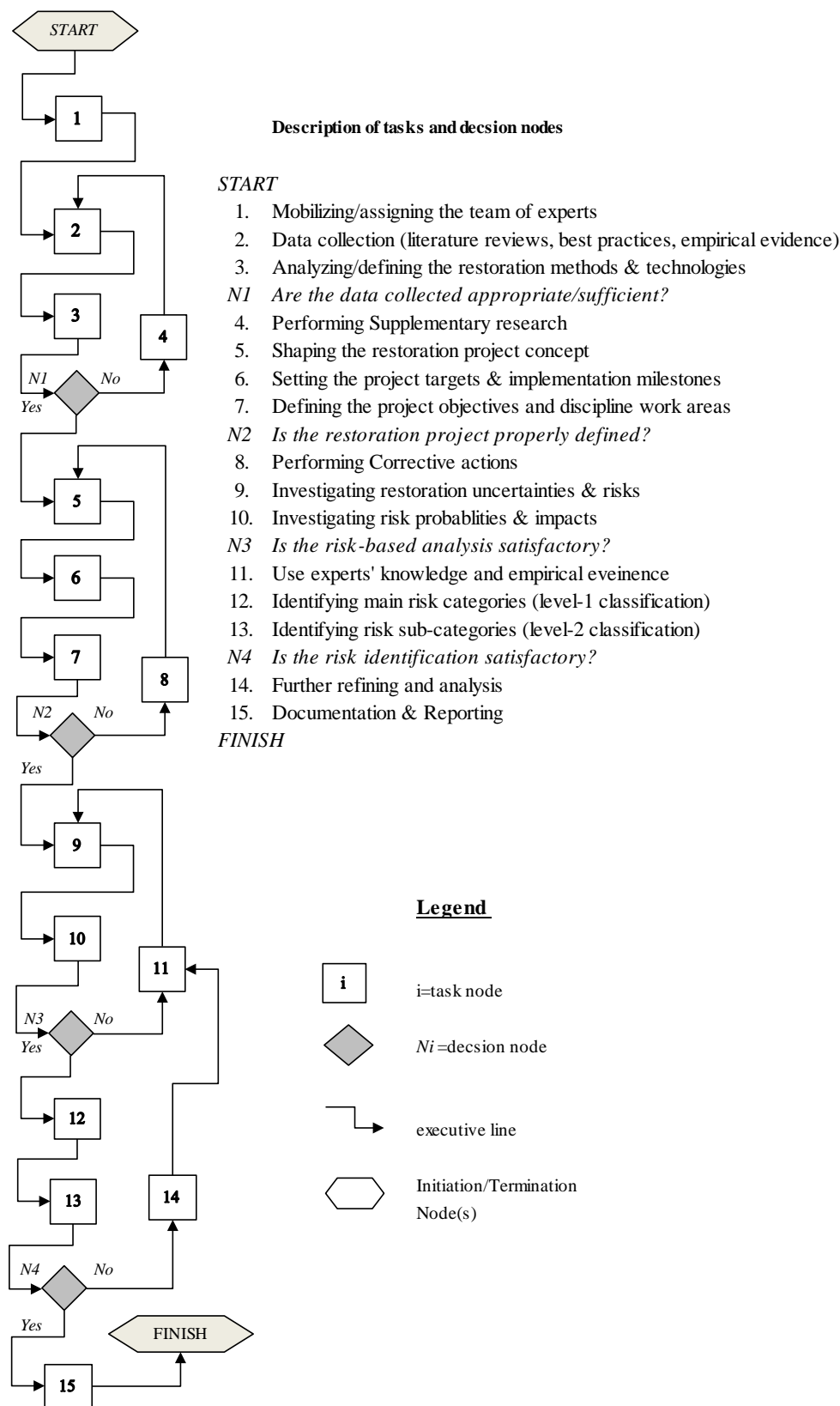


Figure 6. Methodology for Risks Investigation (Process Flow Diagram)

3.1. Technical risks

Several technical parameters must be examined in order to avoid risks related either to the deterioration of the environmental quality due to inadequate waste management (e.g. during the decommissioning phase) or to the preparatory actions during mine operation, which affect the effectiveness of the land reclamation plan.

- Landscape formation incompatible with existing infrastructures (roads, railways, buildings, photovoltaic park, etc)
- Re-handling of disposed waste material.
- Restrictions due to remaining/exploitable mineral resources
- Mine closure requirements before the exhaustion of the reserves
- Failures of excavation machinery
- Inappropriate mine decommissioning plan (for large facilities, plants and equipment)

3.2. Geological - Geotechnical risks

This category of risks refers to technical failures that are related to some of the most severe environmental damages in the recent history of surface mining. In these cases, time is a critical factor that complicates further risk management, since some types of failures, such as landslides and ground water contamination phenomena may occur or may last, respectively, many years after the mine closure.

- Landslides, slope instabilities and soil deformations
- Pit lakes stability problems
- Subsidence phenomena
- Hydrogeological management problems
- Inappropriate reinstatement of the terrain relief and topography
- Seismicity and tectonics

3.3. Socio-economic risks

Every mining project must contribute to the national, regional and local development and welfare. In this context, project proponents and supervising authorities must be able to communicate and collaborate effectively with public interest groups and all stakeholders in order to avoid political damage. This is a critical step for the minimisation of risks that may lead to financial losses or even cancellation of a mining project. Public involvement in environmental management of surface mining projects must be seriously considered as an alternative for successfully addressing various environmental and socioeconomic issues, including the prediction of the budget that is required for financing environmental protection and land reclamation works throughout the entire life of a mine, as well as the associated risks. In several cases, uncertainties were minimised when mining companies, supervising authorities and the public are committed by a 'contract-based' agreement [12].

- High capital expenditures of reclamation works
- High maintenance cost of reclaimed lands
- High cost of environmental monitoring and control measures
- Requirements for land acquisition
- Utilization of low quality and productivity soil
- Protests of local communities against the reclamation plans

- Low returns to local and regional economy
- Low priority of reclamation plan, according to a strategic mine closure plan
- Visual amenity and aesthetic impacts
- Lack of technical and economic capabilities for beneficial modification of the post mining area
- Low value of reclaimed land

3.4. Environmental risks

Environmental protection and land reclamation are widely recognised as key-elements for the development of every mining activity. Although the legal framework regulates most of the issues related to environmental impacts, some problems still exist. The development of an environmental management strategy, which will be based on both remedial and preventive actions, starting from the early stages of mine development, is possible to improve the overall environmental performance of a mine and reduce the relevant risks. This strategy should incorporate the main principles of sustainability, allowing assessment of all environmental threats associated with the mine operation throughout its life cycle. Also, it should allow the development of processes that support the monitoring and periodic evaluation of the environmental management strategy and the decision making as far as the optimal mine development strategy is concerned [11].

According to Glossary of Risk Assessment Terms [13], environmental risks include risks to natural ecosystems or to the aesthetics, sustainability or amenity of the natural world.

- Requirements for re-exploitation of already restored mines area
- Effects on groundwater, surface water, noise and air quality
- Loss and/or alteration of biodiversity and biotopes
- Post-mining natural hazards
- Post-mining drainage problems
- Effects to flora, fauna and vegetation
- Effects to surrounding habitats
- Legal requirements for the management of mining by-products (ash, sludge)
- Incompatibility with the surrounding environment and landscape.
- Low soil fertility
- Remaining pit voids
- Unavailability of topsoil material
- Misalignment of the rehabilitation plan from the objectives of sustainable development

3.5. Permitting risks

According to a study prepared for the US National Mining Association [10], unexpected and often unnecessary delays in obtaining environmental permits affect the development of mining projects in numerous ways. Mining companies, particularly these operating in Europe or other developed countries, accept that there will always be some delays and will build appropriate contingency and mitigation measures into their business plan. However, delays for unforeseen reasons, or the delays to the expected process, are a real problem for the industry, and by extension, the economy as a whole. The key findings of this study are the following: (a) Unexpected delays in the permitting process alone reduce a typical mining project's value by more than one-third, (b) the higher costs and increased risk that often arise from a prolonged permitting process can cut the expected value of a mine in half before production even begins, (c) The combined impact of unexpected, and open-ended, delays and higher costs and risks can lead to mining projects becoming financially unviable.

- Delays of the permission process
- Deviations of the reclamation plan from development plans approved by authorities
- Conditions, technologies and activities of high cost and complexity requested by Environmental authorities
- Constraints due to claims and requests addressed by the stakeholders

4. CONCLUSION

The exploitation of a continuous surface lignite mine is a long-lasting project that requires high capital and operational expenditures. When the lignite mine enters the closure phase, the environmental reclamation constitutes a multidisciplinary intervention of high impact for the mining company and local societies. Nevertheless, the success of every action plan of mine land reclamation depends on a series of preventive and mitigation measures that must be implemented from the beginning of the deposit exploration to the aging phase of the mine life-cycle.

For every lignite mining project, the risks related to technical, geological, socio-economic, environmental and permitting factors can be identified based on empirical evidence and managerial practices. Furthermore, the minimisation of these risks can be considered as a critical decision-making problem for the mining companies and all the involved stakeholders aiming at the optimisation – balancing of costs and environmental acceptance of reclamation solutions.

REFERENCES

- [1] Roumpos C., F. Pavloudakis, O. Kouridou (2016). Managing Surface Lignite Mining Projects in a Competitive Environment. IX International Brown Coal Mining Congress "Brown coal as a safeguard of energy security", Bełchatów, Poland; 04/2016
- [2] Pavloudakis, F. F., Agioutantis, Z. (2008). Using environmental permits for boosting the environmental performance of large-scale lignite surface mining activities in Greece. Proceedings American Society of Mining and Reclamation, 785-806.
- [3] Roumpos C., Pavloudakis F., Galetakis M. (2005). Modelling and evaluation of open-pit lignite mines exploitation strategy, 2nd Int. Conference on Sustainable Development Indicators in the Minerals Industry (SDIMI 2005), May 18th - 20th, 2005, Aachen, Germany: 1127-1139.
- [4] Papavasiliou A., C. Roumpos, A. Voulgarakis, T. Michalakopoulos (2016). Life cycle analysis of a lignite-fired electricity generation system, 13th ISCSM 2016, Belgrade; 09/2016.
- [5] Roumpos C., Papacosta E (2013). Strategic mine planning of surface mining projects incorporating sustainability concepts, Proceedings, 6th International Conference on Sustainable Development in the Minerals Industry (SDIMI 2013), 30 June – 3 July 2013, Milos Island, Greece: 645–651.
- [6] Roumpos C., Spanidis F., (2003). A project management approach to open - pit lignite mine planning and exploitation [open-pit project management]. World Coal (April issue): 55-61.
- [7] Roumpos C., Pavloudakis F., (2006). Environmental management of surface mining projects: A comparative analysis 8th International Symposium Continuous Surface Mining (ISCSM), Aachen, Germany, 24-27 September: 495-502.
- [8] Knabe W. (1964). Methods and results of Strip-Mining reclamation in Germany. The Ohio Journal of Science, 64, 75-105.
- [9] Dey P. K. (2002). Project risk management: a combined analytic hierarchy process and decision tree approach, Cost Engineering, Vol. 44, , no. 3, pp. 13-27.

- [10] Farooki M., Hinde C., Fellows M., Borssen A., Lof O. (2015). Permitting, Economic Value and Mining in the United States. Report Prepared for the National Mining Association published by SNL Metals & Mining.
- [11] Pavloudakis F., Environmental and socioeconomic impacts of surface mining operations: A review of the Greek experience
- [12] Pavloudakis F., Roumpos C., Galetakis M. (2012). Public acceptance of surface mining projects and the determination of the marginal environmental cost. *International Journal of Mining, Reclamation and Environment*, 26:4, 292-308
- [13] ISSMGE TC32 - Technical Committee on Risk Assessment and Management (2004). Glossary of Risk Assessment Terms – Version 1, July 2004
- [14] Roumpos C., K. Liakoura, N. Paraskevis (2011). A model for management of large technical projects in surface lignite mines, *MINERAL WEALTH* 159/2011, 9-22.
- [15] Pavloudakis F., Galetakis M., Roumpos C., (2009). A spatial decision support system for the optimal environmental reclamation of open-pit coal mines in Greece. *International Journal of Mining, Reclamation and Environment*, Vol. 23, No. 4, December 2009, 291–303.
- [16] Pavloudakis F., Roumpos C., Sachanidis C. (2011). Planning Land Reclamation and Uses at Ptolemais Lignite Surface Mines Complex, V International Conference Coal Zlatibor, Serbia, 19-22 October: 263-276.

A Multi-Criteria Methodology for Low-Risk Evaluation of Mine Closure Restoration in Continuous Surface Lignite Mining Projects

Philip-Mark Spanidis¹, Christos Roumpos² and Francis Pavloudakis²

¹ASPROFOS Engineering, *Division of Project Management, Greece*

²Public Power Corporation of Greece, *Mines Business Unit*

ABSTRACT

The restoration of continuous surface lignite mines that fuel mine-mouth located thermal power plants is a complex, long-term and multidisciplinary initiation, particularly in the case of mines that have been operating for many decades and now enter the closure phase. Various environmental, technical, economic, social and engineering factors have to be early considered during the assessment and evaluation of alternative restoration technologies of which reclamation is the most critical. This context inserts critical decision-making risks, since projects of this nature have considerable environmental and social impacts. Therefore, the project decision makers have to select the most appropriate and lower risk solution among a set of several restoration/reclamation alternatives. The paper identifies the decision-making problem and suggests a multi-criteria methodology combining the AHP (Analytical Hierarchy Process) and TOPSIS (Technique for Order of Preference by Similarity to Ideal Solution) techniques with a case study for ranking of the lower risk restoration/reclamation alternative in a closing lignite mine. The methodology is suggested as a low cost and easy development tool for lignite mining operators, reclamation project managers and environmental stakeholders.

1. INTRODUCTION

The continuous surface lignite mines are large-scale excavation sites of high importance for the production of primary energy as the lignite exploited from these mines fuels high capacity thermal power plants. Usually, the operation life of a lignite mine lasts for many decades. However, after an intensive exploitation period the material of lignite basin is depleted. Then, the mine enters to closure phase where regulatory and other requirements necessitate restoration of the sites and upgrading of the post-mining land uses with beneficial effects to environment and society.

Literature reports various restoration methods. Some are technical dealing with engineering solutions for remodeling of post-mining landscape by taking, mainly, measures for environmental upgrading ([1], [2]). Other, refer to the potential of natural restoration known as '*spontaneous succession*' [1], while other suggest hybrid or '*near natural*' solutions ([3], [4]). Most of the methods cited, however, consider the *reclamation* as a fundamental restoration activity consisted of extended earthworks for removal of the excavated soils and reuse of this material for resurfacing of pits and voids shaped during the exploitation period [27].

Reclamation is an activity of extended human-made intervention, where numerous restoration factors of high importance are considered. These factors are socioeconomic status, landscape, topography, geology, slope stability, water and air quality, biodiversity, reforestation, soil productivity, seismicity, permitting, land use and infrastructures. All these factors are co-evaluated during the elaboration of relevant restoration plans in which reclamation constitutes the most critical activity ([2], [5], [6]).

Reclamation planning is a complex and multidisciplinary task requiring synergy between mining managers, engineers, environmentalists and experts from various fields of science and technology in order to outline a set of techno-economically feasible and environmentally sustainable restoration/reclamation alternatives, from which the most advantageous has to be selected. However, any restoration/reclamation project plan contains its own uncertainties and risks. The early identification of these risks and the consequences of their impacts enables decision makers to have a substantial basis of understanding of the advantages and disadvantages of each alternative and select, on reasonable basis, the one that concentrates the lower risks.

The objective of this paper is to demonstrate the decision-making problem related to the selection of an appropriate post-mining restoration/reclamation method and suggest a Multi-Criteria Decision Making (MCDM) methodology as a decision-making support tool for implementation in similar project contexts. The paper is structured as follows: second section refers to the concept of restoration planning and the related to risks and third section presents practical decision-making problems and questions. The fourth section describes a hybrid MCDM methodology outlined as a combination of AHP (Analytical Hierarchy Process) ([7], [8], [9], [10]) and TOPSIS (Technique for Order of Preference by Similarity to Ideal Solution) implemented in a case study for selection of the lower risk restoration/reclamation method ([10], [11], [12], [13]). The fifth, section presents the results of the methodology implementation, while the last section discusses essential views of the proposed methodology and highlights areas for further research.

2. RESTORATION RISKS

In many countries, like Germany [1], Czech Republic [2], India [5], UK [14], US [15] and Greece [26], the restoration of mining sites and industrial deposits constitutes a regulatory requirement. For the continuous surface lignite mines, restoration represents a multidisciplinary and properly planned effort of returning the mined-out lands to a form of acceptable environmental condition and productivity [5] with beneficial returns to society, economy and sustainable development. Nevertheless, mining practice and history show that there is a multitude of restoration philosophies and methods. This is because restoration does not follow a standard type of development, since mines differ significantly from one to another. The exploitation models are very different and depend on the specific to each mine exploitation targets, post exploitation geo-environmental content and the regulatory and legislative constraints. Empirical evidence and literature refer three generic restoration types: (a) *technical restoration* focused on high escalation engineering solutions and integrated developmental interventions ([2], [16]), (b) *natural restoration* driven by interactions between bio-ecological factors [1] and (c) *combined restoration* solutions produced in terms of synergies between human intervention and natural restoration processes ([2], [4], [6]).

The basis for a techno-economically effective and environmentally friendly restoration plan is the successful *reclamation* of the mine-out lands. The term reclamation refers to large scaled earthworks for removing of excavated soils from the mine disposal areas and using the removed material for extended resurfacing of open pits, benches and voids inappropriately shaped during the exploitation period ([2], [5]). In principle, reclamation constitutes a landscape reinstatement framework aiming the mine-out site to return to its original state in terms of land-use, ecology and productivity. Thus, reclamation enables the landscape remodeling and aligned with other human-made interventions and natural processes, contributes to the recovery of area(s) affected during, and because of, the mining processes.

From the project management point of view, reclamation may be seen a sub-project in a wider restoration project or a standing alone restoration project maintaining its own customization mode in terms of planning, organization, human resources, budget, schedule and equipment. Once a restoration/reclamation project initiates, managers, engineers and restoration experts are working in

synergy to produce a multidisciplinary assessment analyzing the geo-environmental situations of the post-mining surface and the techno-economic analysis of the restoration/reclamation framework. In this analysis, critical factors are taken into consideration, such as, quality of disposed soil, watercourses (lakes and rivers), air pollution, quality of topsoil and fertility, infrastructures (roads, railways and welfare facilities), abandoned mining machinery, toxicity of discarded wastes, reforestation, recreation, post mining geo-hazards, land use reforming, etc. The data required for the restoration analysis are collected through field investigations across the mined-out sites, laboratory analysis of water and soil, satellite imagery and cartographic products ([2], [17]), reviews of statistical records, scientific literature and technical documents retrieved from the files of mine facility. Further to post-mining conditions analysis, the restoration plan recommends several alternative methods of restoration/reclamation, as technically appropriate and suggests the most advantageous one as appropriate for implementation. The, the plan is delivered to the involved parties (environmental agencies, investors, municipalities, steering committees, etc.) for evaluation and decision making.

On the other hand, the mine restoration/reclamation projects, being long-term interventions (restoration lasts from few years to decades and depend on the size of restoration area, landscape and topographical heterogeneity, near mine infrastructures, watercourse networks, land use complexity, eco-biological features, regulatory constraints, etc.) of high complexity incorporate, unavoidably, various types of inherent risks. According to the conventional risk management practices, these risks have to be, as early as possible, identified with an analysis of the probability of occurrence and the impacts that any specific risk relates. This work is critical for the examination of every single reclamation/restoration alternative, in order the lower risk and most beneficial one to be properly documented and, at final stage, selected by the decision makers.

The reclamation/restoration risks are thoroughly investigated in relevant work addressed by Roumpos *et al.* [18]. Thus, further elaboration on this topic falls out of the scope of this paper. The identified risks are grouped in five main categories, while each category is entirely divided in sub-categories. The main risk categories encountered are: (a) *Technical Risks*, (b) *Geological and Geotechnical Risks*, (c) *Permitting Risks*, (d) *Socio-Economic Risks* and (e) *Environmental Risks*. Hereunder, these risks and their impacts are analyzing in a case study presenting the decision-making purposes of a certain restoration/reclamation project.

3. DECISION MAKING: PROBLEMS AND QUESTIONS

The restoration of continuous surface lignite mines are projects of high technical, environmental and socioeconomic complexity. The success of these projects depends on reasonable decisions taken in the pre-investment phase. An unsuccessful decision should promote an ambiguous or controversial restoration/reclamation project or, conversely, to advise as non-feasible or non-sustainable a project that has the appropriate evidence and substantial basis for implementation. The decision-making required to select the most advantageous restoration/reclamation method is very critical, since its consequence should be a project to be successfully performed, suspended or failed. Therefore, the pre-investment decisions are crucial and demonstrate if a restoration/reclamation project has the appropriate level of maturity for implementation, or not.

The reclamation/restoration projects present significant differences from each other. This fact introduces various technical and managerial problems. That means that for some of the primary factors considered for the situation of the mine-out area may be conflicting. For example, a large scale, but low cost, resurfacing framework in a mining site polluted by toxic discarding materials is very possible to generate environmental impacts of higher severity and hazardousness to those it comes to mitigate. This kind of activity can be also charged by other constraints, so that the restored

land is proven inappropriate for reforestation, replantation or re-cultivation, therefore, it might be subject to rejection by environmentalists, permitting authorities and/or socioeconomic analysts.

In project management contexts, various decision making practices are reported which depend on the project size and type, the collective knowledge and performance of experts and managers, the environmental restoration policies, the budgetary and resource constraints and other geo-environmental factors as well. Some of these practices are very formal and tend to move within the requirements of the administrative and legal protocols. Other are more empirical and based on experts' technical judgement of making comparisons with previous projects of similar scale, type and techno-economic profile. Other practices are seen to be combinations of empirical evidence and analysis of the geo-environmental and ecological situation of the under restoration mining plants or focus on pure socio-economic aspects of the restoration/reclamation plan. In any case, project managers and restoration experts, in order to execute and operate a restoration/reclamation project of high performance and progress, are usually obliged to solve various problems and answer to managerial questions of high criticality, such as:

- Which method is most beneficial to society and environmental friendly?
- Which alternative method is most cost-effective against others?
- Which alternative method should be appropriate for getting quickly the required permits?
- Which alternative requires minimum reconstructions/modifications/deviations of existing infrastructures?
- Which alternative enables best remodeling of landscape and visual amenity?
- Does the restoration/reclamation project budgeted well?
- Are the environmental, ecological and biodiversity requirements completely met?
- Are the alternative methods in line with the requirements of sustainable development?
- Do alternative methods satisfy the needs for new businesses opportunities, reduction of unemployment and ensuring the livelihood of local communities?
- Are the alternatives appropriate for the recovery of biodiversity, reforestation, replantation and re-cultivation?
- Are the water management proposals appropriate for development of recreational facilities?
- Are the post-mining geo-hazards and soil stabilization measures well defined?
- Does seismicity, at the wider mine region, allow erection of building facilities at the reclaimed lands?
- Are the toxic wastes management activities adequate to ensure people's safety and sanity?
- Are the available mechanical means and resources for the reclamation works execution?
- Are there any possibilities for resumption of the mining activities in future?
- Should the occupational health and safety precautions during the field reclamation works execution be properly keeping?

From the above it is obvious that decisions embody significant and multilateral uncertainties generating various managerial and operational risks. Since the main objective of the decision making is the selection of the lower risk alternative, it is worthwhile these risks not to be embodied in a restoration/reclamation plan as an empirically costed contingency element. Instead, the scientifically substantial manner is risks to be classified in groups of content specific entities, interpreted in terms of criteria for evaluation of the risk of each restoration/reclamation alternative method and properly quantified in form of numerical data. Therefore, all restoration/reclamation methods can be evaluated with respect to their significance over each risk specific criterion enabling definition of a total 'score' for each alternative, so that the alternative with the lower total risk score to be demonstrated and suggested to the interested parties as appropriate for implementation.

4. SUGGESTED DECISION MAKING METHODOLOGY

The methodology suggested by the authors focuses on MCDM techniques and aims to be demonstrated as a tool of supporting reasonable decision making for evaluation of post-mining restoration/reclamation projects. The objectives of the suggested methodology are:

- (a) To interpret the reclamation/restoration risks [18] in terms of project evaluation criteria and to show how the relative weight of every single criterion and sub-criterion can be expressed in numerical form;
- (b) To show how any alternative restoration/reclamation method can be decomposed in a risk-based classification matrix according to pattern for classification of risk impacts as entities of *low, medium or high* severity;
- (c) To present how the relative weights of the criteria identified can be used for the numerical expression of each alternative over every single risk (and sub-risk) to produce the overall risk of each alternative enabling the final ranking of all alternatives;
- (d) To prove the applicability of the methodology in an experimental research referred to a restoration/reclamation project presenting technical and geo-environmental characteristics similar to an under decommissioning continuous surface lignite mine in Greece.

The methodology is consisted of two main techniques: AHP applied for the quantitative expression of risk-based criteria and TOPSIS for the calculation of the overall risk of each alternative.

AHP is a groupware technique where experts use their experience and knowledge to break down the decision making problem into hierarchy and solve it following an evaluation process based on quantified selection criteria. In AHP, the decision makers perform pairwise comparisons according to the 1-9 evaluation scale advised by Saaty ([7], [8], [9], [19]) to evaluate the impacts of all criteria on each other and to structure and normalize a reciprocal pairwise comparison matrix. Then, a control follows to check the mathematical consistency of the computational process. TOPSIS is based on the assumption that the most advantageous solution (alternative) should have the shortest distance from the ideal solution and the farthest distance from the negative ideal solution (the distance of measuring is meant to be Euclidean entity). Thus, each alternative maintains a certain distance from the ideal and a certain distance from the negative solution respectively that can be expressed in a numerical form enabling the final ranking ([10], [11], [13]). Figure-1 depicts the methodology, as an algorithmic process model, including the AHP and TOPSIS techniques (see nodes from No.9 to No.15), the interim tasks and the decision nodes (see *N1, N2, N3* and *N4* nodes).

5. IMPLEMENTATION

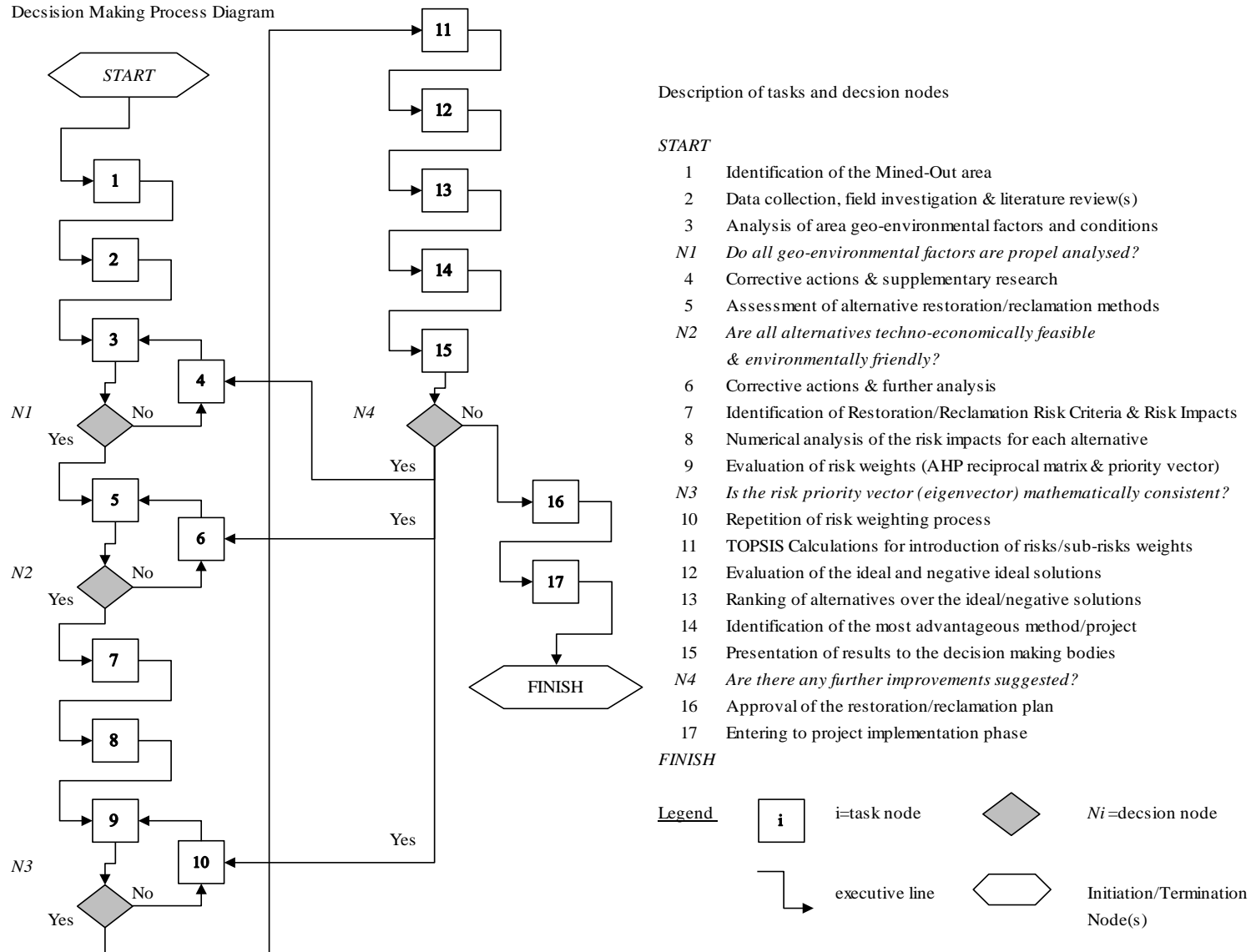
This section reports the implementation of the suggested methodology through a case study referring to a (hypothetical) project of restoration/reclamation of a surface mine with continuous operations.

5.1. Case Study

The case study regards refers to a project of restoration of a surface mine with continuous operations equipped with bucket wheel excavators, conveyors and spreaders that is in operation for 20 years and its remaining mine life is approximately 10 years. The mine contributes in meeting the lignite demand of a power plant located 12 [km] Westerly from the mine. The area of planned mining activity covers approximately 9.0 [km²]. The mining area is hilly with surface altitudes ranging between (+) 700 [m] and (+) 900 [m] above the mean sea level. The lignite basin has a

channel form and it is progressively broadened from NE to SW direction along with increases of surface altitudes. The deposit is of multiple-layered form and lignite seams are almost horizontally bedded. However, a series of normal faults results in a progressive and systematic deepening of the beds and in a corresponding increase

Figure-1: Suggested Decision Making Methodology



of the thickness of overburden material towards the East-South rim of the basin. The main deposit's characteristic is the occurrence of conglomerate hard material in the overburden formations.

At a distance of 2.0 [km] NE to the mine, there is a village with 100 inhabitants. A river with NE-SW direction is located along the mine. This river was relocated for needs of the exploitation development. Prior to the beginning of the mining activity, the land use was mainly agricultural and forestry. The outside waste dumping area is located 1.5 [km] NW from the mine, while dumping activities are not any more performed. Nowadays, the waste material of the exploitation is transported to the inside dumping area. Following the mine closure, a lake has planned to fill the existing area voids.

Due to confidentiality, the project identity is not disclosed. The purpose of the case study is to demonstrate the effectiveness and applicability of the suggested methodology in contexts of multi-criteria evaluation and selection of restoration/reclamation projects.

5.2. Description of Alternatives

In the restoration/reclamation plan, three (3) restoration/reclamation alternatives advised as techno-economically feasible and environmentally friendly solutions. These alternatives are as follows (comparative cost data sourced from [22], [23], [24], [25]):

- (A1) Technical Restoration/Reclamation: the alternative refers to an extended project with high capital expenditures (3.500-5.000 €/ha) and 3-4 years estimated period of implementation. The project targets are: (a) large-scale reclamations for recovering of the affected landscape, (b) treatment of contaminated, polluted or toxic soils and waters, (c) measures and infrastructures enabling development of recreation activities, (c) upgrading of biodiversity at post-mining ecosystem(s). The measures and main infrastructures suggested for implementation are: excavation and backfilling of removed earth material; soil and slope stabilization; land compaction and levelling; complete redesign and reconstruction of existing roads; erection of buildings for accommodation of 300 visitors; erection of recreation and cultural facilities (sport camps and a museum for the mining history); reforestation/replantation to the 35-40% of project area; regeneration of the near lake settlement; installation of fire protection system; utilities for irrigation, sewing, water supply, power and communication; removal of polluted, contaminated and toxic wastes and water bodies; replacement of removed/selected topsoil; measures ensuring good land fertility; measures for recovery of sensitive habitats and biota; measures for increase of employment;
- (A2) Restoration focused on Natural Processes: the alternative refers to a project with low capital expenditures (less than 500 €/ha) and 10 years minimum estimated period of implementation. The project targets are: (a) medium to low scale reclamations for recovering the affected landscape, (b) treatment of contaminated, polluted or toxic soils and waters, (c) protection of biodiversity at post-mining ecosystem(s). The measures and main infrastructures suggested for implementation are: selective backfilling at the most adversely excavated lignite layers and seams; soil and stabilization at locations with the highest possibility of post-mining erosion effects; removal of polluted, contaminated and toxic soil, mining wastes and water bodies; installation of fire protection system; irrigation and water management measures; measures for recovery of sensitive habitats and biota; replacement of removed/selected topsoil at locations with physical re-cultivation capability and good fertility; implementation of a long-term environmental monitoring and physical restoration plan (also known as '*spontaneous succession*' [2]) plan;
- (A3) Combined Solution: the alternative refers to a project with moderate capital expenditures (800-1500 €/ha) and 5-7 years estimated period of implementation. The project targets are: (a) large-scale reclamations for recovering the affected landscape, (b) treatment of contaminated,

polluted and toxic soils and waters, (c) measures and infrastructures enabling mainly the development of agroforestral activities, (c) upgrading of the biodiversity at post-mining ecosystem(s). The measures and main infrastructures suggested for implementation are: excavation and backfilling of removed earth material; soil and slope stabilization; compaction and levelling; local modifications of existing traffic network; erection of low scale recreation and cultural facilities (sport camps and a museum for the mining history); reforestation/replantation of the 25-35% of the project area; installation of fire protection system; removal of polluted, contaminated and toxic soil, mining wastes and water bodies; replacement of removed/selected topsoil at the 40-50% of the project area; measures for recovery of sensitive habitats and biota; implementation of a long-term environmental monitoring and physical restoration plan.

5.3. Risk Based Analysis

Formally, risk is defined the product of the probability of occurrence and the consequence of an incident/event that could be happen in real life ([20], [21]). This mathematical expression constitutes a fundamental element of the risk management and it has been mostly applied in risk analyses developed in recent decades to support needs of decision making under uncertain conditions. The accurate identification of risk probability of occurrence and consequence, however, is not always feasible due to unavailability of reliable data and/or lack of official statistical evidence. In such cases, the risk is identified and quantified upon experts' judgment and disciplinary knowledge aggregation. This approach has been adopted in the research of Roumpos *et al.* [18] where the investigation of restoration risks has been performed based on scientific interpretation of mining practices and empirical evidence as well. Upon this research, a table of risk severity impacts has been formulated (Table-1) reflecting the classification of risks and the units/parameters by which the risk severity can be measured on practical basis. In turn, the risk severity is classified in three (3) main categories as *low*, *medium* and *high*, followed by the numerical values of risk severity impact. These values are in compliance with PMI [20] practices in a view the risk severity escalation not to follow necessarily linear order, but could be in accordance, in a more conservative approach, with the sequential relation $a(n)=2^n$, $n \in \mathbb{N}_0$. Thus, $2^0=1$ refers to low impact, $2^1=2$ to medium impact and $2^2=4$ to high impact [21]. Table-2 presents the results of the performed risk-based analysis.

5.4. Definition of Risk Weights: application of AHP

The definition of the relative weight of each criterion has been performed by applying the AHP technique ([8], [9], [10], [19]) and in accordance with the following steps:

- Step-1: establishment of a pairwise comparison matrix for weighting the main risks; the experts compose a square matrix consisted of two triangular sub-matrices by making pairwise comparisons of each criterion with each one of the other criteria using the Saaty scale of comparison (Table-3a). Calculation mode: if $a(i, j)$ is an element of this matrix (k: column and l: row) the lower diagonal element is produced using the formula $a(k, l)*a(l, k)=1$ (Table-3b);
- Step-2: normalization of the pairwise comparison matrix and extracting the relative weight of each criterion, $WR_i \mid i=1, 2, \dots, n, n \in \mathbb{N}$; n is the number of criteria; $WR(i)$ represents the priority, or eigenvalue, vector (Table-3c). Mathematical conditions: $0 < WR_i < 1$ and $\sum_{i=1}^n WR_i = 1$;
- Step-3: performing of consistency control to validate the consistency of priority vector; the control aims to check, if the consistency ratio, CR, of priority vector, is less than 0.10; if so, the data of priority vector is appropriate for further utilization as inputs in TOPSIS calculations. Otherwise, the risk weighting process is repeated;

- Step-4: the same steps are followed to produce the priority vectors $WR(i, j)$ of each group of sub-criteria.

5.5. Ranking of Alternatives: application of TOPSIS

The TOPSIS application aims to define the score of each alternative and the final ranking of the alternatives and, hence, to demonstrate the lower risk, or ‘best’, alternative restoration/reclamation method. The steps developed for TOPSIS technique application are the following:

- Step-1: calculation of $S = \{ \sum_{i=1, j=1}^{i=m, j=m} Rv(i, j) \}^{1/2}$, where, i =number of criteria/sub-criteria, j =number of alternatives and $Rv(i, j)$ the risk severity value of each alternative j over the criterion i (data extracted from Table-2) and division of each $Rv(i, j)$ element by S to get the $R(i, j)$ vector;
- Step-2: multiplication of each $R(i, j)$ element by $WR(i)$ to get the vector $V(i, j)$;
- Step-3: determination of the *ideal solution* A^* by forming vector $V^*(j)$ that contains the minimum value elements of vector $V(i, j)$ (the lower risk element of each criterion);
- Step-4: determination of the *negative ideal solution* A' by forming vector $V'(j)$ that contains the maximum value elements of vector $V(i, j)$ (the higher risk element of each criterion);
- Step-5: calculation of the separation from the ideal solution (Euclidean distance) by forming the vector $Si^* = \{ \sum_{j=1}^{j=m} [V(j)^* - V(i, j)]^2 \}^{1/2}$;
- Step-6: calculation of the separation from the negative ideal solution (Euclidean distance) by forming the vector $Si' = \{ \sum_{j=1}^{j=m} [V(j)' - V(i, j)]^2 \}^{1/2}$;
- Step-7: calculation of the relative closeness to the ideal solution $Cj^* = Sj^* / (Sj^* + Sj')$; the elements of Cj^* vector represent the score of each alternative; the optimum or ‘best’ alternative is the one with the highest total score: $\max [Cj^*] = \max [C_1^*, C_2^*, \dots, C_j^*]$.

5.6. Results

The results of final ranking are shown in Table-4: $C_3^* = 0,8189 < C_2^* = 0,5150 < C_1^* = 0,4469$. The *lower (total) risk alternative* is A3 that relates to the combined restoration/reclamation method as appropriate; second best is alternative A2 and last, the higher risk alternative, is A1 (see Table-4).

6. DISCUSSION AND CONCLUDING REMARKS

The MCDM methods should be implemented in projects of open surface lignite mines restoration. The selection of the lower risk restoration/reclamation method is very critical for ensuring the reclamation/restoration project is completed within budget and schedule and it is also socially acceptable, environmentally friendly, and according to the objectives of sustainable development. In mining project management, the target of MCDM methods is to identify and suggest to decision makers the lower risk restoration/reclamation method from a set of available alternatives.

Table-1 Classification of Risk Severity Impacts

Risk-ID	Units & Parameters of Risk Evaluation	Low (L)	Medium (M)	High (H)	Impact L - M - H
R1 Technical Risks					
R1.1	length of interfered infrastructures [km]	none	one (1)	more than one (1)	1-2-4
R1.2	1 million [m ³]	less than 1 mil [m ³]	between 1 & 2 mil [m ³]	more than 2 mil	1-2-4
R1.3	[%] of the proven mine reserves [m ³]	less than 10%	between 10% & 20%	more than 20%	1-2-4
R1.4	[%] of the proven mine reserves [m ³]	less than 10%	between 10% & 20%	more than 20%	1-2-4
R1.5	incidents per month	none	one (1)	more than one (1)	1-2-4
R1.6	[%] delay of total time plan in months	less than 10%	between 10% & 20%	more than 20%	1-2-4
R2 Geological and Geotechnical Risks					
R2.1	cases of instability / [km ²]	up to 2 per [km ²]	between 2 & 5 / [km ²]	more than 5 / [km ²]	1-2-4
R2.2	cases of subsidences / [km ²]	up to 2 per [km ²]	between 2 & 5 / [km ²]	more than 5 / [km ²]	1-2-4
R2.3	average terrain slopes [inclination %]	slopes $\leq 10\%$	10% < slopes $\leq 25\%$	slopes >25%	1-2-4
R2.4	area [%] of watercourses / [km ²]	up to 2%	between 2 & 5 %	more than 5%	1-2-4
R2.5	[%] of the reclamation area [km ²]	up to 5%	between 5 & 10 %	more than 10%	1-2-4
R2.6	Seismic Zone (*)	Zone-I	Zone-II	Zone-III	1-2-4
R3 Permitting Risks					
R3.1	approval time in months	less than 6 months	between 6-12 months	more than 12 months	1-2-4
R3.2	number of discrepancies [%]	less than 5	between 5 & 10	more than 10%	1-2-4
R3.3	[%] increase of reclamation budget [€]	less than 5%	between 5 & 10 %	more than 10%	1-2-4
R3.4	impact of stakeholders claims	low intensive	moderately intensive	highly intensive	1-2-4
R4 Socio-Economic Risks					
R4.1	CAPEX of the reclamation project [€/ha]	less than 1000 €/ha	bet. 1000-3000 €/ha	more than 3000 €/ha	1-2-4
R4.2	[%] of reclamation CAPEX [€]	less than 5%	between 5 & 10 %	more than 10%	1-2-4
R4.3	[%] of reclamation CAPEX [€]	less than 5%	between 5 & 10 %	more than 10%	1-2-4
R4.4	[%] of the reclamation area [km ²]	less than 2%	between 2 & 5 %	more than 5%	1-2-4
R4.5	[%] of the reclamation area [km ²]	less than 2%	between 2 & 5 %	more than 5%	1-2-4
R4.6	months of delays	less than 6 months	between 6-12 months	more than 12 months	1-2-4
R4.7	[%] of reclamation CAPEX [€]	less than 5%	between 5 & 10 %	more than 10%	1-2-4
R4.8	transition period [months]	less than 4 months	between 4-10 months	more than 10 months	1-2-4
R4.9	[%] of the reclamation area [km ²]	less than 5%	between 5 & 10 %	more than 10%	1-2-4
R4.10	Missing resources in [%] of CAPEX [€]	less than 5%	between 5 & 10 %	more than 10%	1-2-4
R4.11	[%] increase of land value [€]	less than 5%	between 5 & 10 %	more than 10%	1-2-4
R5 Environmental Risks					
R5.1	Probability of reexploitation	less than 0.15	between 0.15 & 0.30	more than 0.30	1-2-4
R5.2	Increase of pollution potential [%]	less than 1%	between 1 & 5 %	more than 5%	1-2-4
R5.3	[%] changes of the biotic content	less than 1%	between 1 & 5 %	more than 5%	1-2-4
R5.4	Probability of post-mining hazards	less than 0.05	between 0.05 & 0.10	more than 0.10	1-2-4
R5.5	[%] of the reclamation area [km ²]	less than 5%	between 5 & 10 %	more than 10%	1-2-4
R5.6	[%] of the reclamation area [km ²]	less than 10%	between 10 & 20 %	more than 20%	1-2-4
R5.7	[%] of the reclamation area [km ²]	less than 10%	between 10 & 20 %	more than 20%	1-2-4
R5.8	[%] of mining by-product volume	less than 10%	between 10 & 20 %	more than 20%	1-2-4
R5.9	[%] of the reclamation area [km ²]	less than 20%	between 20 & 40 %	more than 40%	1-2-4
R5.10	[%] of reclaimed soil volumes	more than 70%	between 70% & 35 %	less than 35%	1-2-4
R5.11	[%] of the reclamation area [km ²]	less than 35%	between 70% & 35 %	more than 70%	1-2-4
R5.12	[%] of the required topsoil volume [m ³]	more than 70%	between 70% & 35 %	less than 35%	1-2-4
R5.13	criticality of non-sustainable deviations	low criticality	medium criticality	high criticality	1-2-4

(*) According to the New Anti-Seismic Regulation of Greece (NEAK) 73

Table-2: Risk Based Analysis

Risk-ID	Units & Parameters of Risk Evaluation	Alternative A1 - Rv(1, j)	Alternative A2 - Rv(2, j)	Alternative A3 - Rv(3, j)
R1	Technical Risks			
R1.1	length of interfered infrastructures [km]	4	1	2
R1.2	1 million [m ³]	4	1	2
R1.3	[%] of the proven mine reserves [m ³]	2	1	2
R1.4	[%] of the proven mine reserves [m ³]	2	2	2
R1.5	incidents per month	4	1	2
R1.6	[%] delay of total time plan in months	4	2	2
R2	Geological and Geotechnical Risks			
R2.1	cases of instability / [km ²]	2	4	2
R2.2	cases of subsidences / [km ²]	2	4	2
R2.3	average terrain slopes [inclination %]	2	4	2
R2.4	area [%] of watercourses / [km ²]	4	2	2
R2.5	[%] of the reclamation area [km ²]	1	4	2
R2.6	Seismic Zone (*)	2	1	1
R3	Permitting Risks			
R3.1	approval time in months	4	2	1
R3.2	number of discrepancies [%]	4	2	1
R3.3	[%] increase of reclamation budget [€]	4	2	1
R3.4	impact of stakeholders claims	2	4	2
R4	Socio-Economic Risks			
R4.1	CAPEX of the reclamation project [€ha]	4	1	1
R4.2	[%] of reclamation CAPEX [€]	4	2	1
R4.3	[%] of reclamation CAPEX [€]	1	4	2
R4.4	[%] of the reclamation area [km ²]	4	1	2
R4.5	[%] of the reclamation area [km ²]	1	4	2
R4.6	months of delays	2	4	2
R4.7	[%] of reclamation CAPEX [€]	1	4	2
R4.8	transition period [months]	4	1	2
R4.9	[%] of the reclamation area [km ²]	1	4	2
R4.10	Missing resources in [%] of CAPEX [€]	2	1	2
R4.11	[%] increase of land value [€]	2	1	1
R5	Environmental Risks			
R5.1	Probability of reexploitation	2	2	2
R5.2	Increase of pollution potential [%]	1	4	2
R5.3	[%] changes of the biotic content	1	2	1
R5.4	Probability of post-mining hazards	1	2	1
R5.5	[%] of the reclamation area [km ²]	1	4	2
R5.6	[%] of the reclamation area [km ²]	2	4	2
R5.7	[%] of the reclamation area [km ²]	2	4	2
R5.8	[%] of mining by-product volume	1	4	1
R5.9	[%] of the reclamation area [km ²]	2	4	1
R5.10	[%] of reclaimed soil volumes	2	4	2
R5.11	[%] of the reclamation area [km ²]	1	2	1
R5.12	[%] of the required topsoil volume [m ³]	2	2	2
R5.13	criticality of non-sustainable deviations	1	4	1

Table-3a: Scale of Criteria comparison (Saaty and Vargas, 1991)

1	Equal importance
3	Moderate importance of one criterion over another
5	Strong or essential importance
7	Very strong importance
9	Extreme importance
2, 4, 6, 8	Values for inverse comparison

Table-3b: AHP Reciprocal Matrix

Main Risks		<i>R1</i>	<i>R2</i>	<i>R3</i>	<i>R4</i>	<i>R5</i>
Technical	<i>R1</i>	1,00	2/3	2/3	3/5	1/2
Geological/Geotechnical	<i>R2</i>	3/2	1,00	1/2	1/3	1/2
Permitting	<i>R3</i>	3/2	2,00	1,00	1/2	1/3
Socio-Economic	<i>R4</i>	5/3	3,00	2,00	1,00	3,00
Environmental	<i>R5</i>	2,00	2,00	3,00	1/3	1,00

Table-3c: Normalized Matrix and Priority Vector, WR_i (Risk Weights)

Main Risks		<i>R1</i>	<i>R2</i>	<i>R3</i>	<i>R4</i>	<i>R5</i>	WR_i
Technical	WR_1	0,13	0,08	0,09	0,22	0,09	0,110
Geological/Geotechnical	WR_2	0,20	0,12	0,07	0,12	0,09	0,120
Permitting	WR_3	0,20	0,23	0,14	0,18	0,06	0,161
Socio-Economic	WR_4	0,22	0,35	0,28	0,36	0,56	0,349
Environmental	WR_5	0,26	0,23	0,42	0,12	0,19	0,260
		1,00	1,00	1,00	1,00	1,00	1,000

Consistency Control:

CI =	0,086	RI =	1,12	CR =	0,041	< 0,10
------	-------	------	------	------	-------	--------

The methodology suggested demonstrates the combination of AHP and TOPSIS techniques in projects related to the closure phase of open surface lignite mines. The AHP allows the analysis and quantification of project risks. All identified risks are interpreted in form of selection criteria/sub-criteria, where every single risk is characterized by its own relative weight (numerical value) that is produced by pairwise comparisons, normalization and consistency calculations. In turn, TOPSIS uses, as an input, the relative weights of the criteria identified by the AHP for definition of the numerical analysis and definition of the ideal and the negative ideal solutions and, thereof, for the final ranking of all restoration/reclamation alternatives. Literature suggests that both techniques are being extendedly used in projects of industry and technology, engineering and manufacturing systems, logistics, business and marketing, scientific research, etc. ([9], [10]). AHP is suggested as a simple, easy to use and programmable group technique. The data required for the AHP application are collected through properly prepared questionnaires delivered to experts for aggregating, in explicit form, their knowledge at every specific risk or alternative. The use of questionnaires ensures the confidentiality of the technique. On the other hand, TOPSIS is suggested as an easily understood analysis of each alternative over each selection criterion, while the computational context of the technique seems to be quite simple and not dealing with complex calculations.

The case study presented in the paper proves that the combination of AHP and TOPSIS constitute an efficient tool enabling incorporation of project risks for the evaluation and selection of the lower risk, or 'best', restoration/reclamation alternative through an easily controlled and low cost procedure. The quantitative results of the multi-criteria evaluation process can be presented, in a simplified and communicable manner to decision making bodies/agents, in order for them to discuss, criticize and adopt the 'best' alternative based on an efficiently quantified, objective, mathematically consisted and techno-economically reasonable outcome.

Concluding, some perspectives for further research could be advised. One relates to investigation of project risks in more advanced mode. For example, the crisp values 1, 2 and 4 corresponding to risk impacts classification as low, medium and high, should be further analyzed in five levels by defining interim numerical values between low and medium and between medium and high level of severity. Thus, the risk impact classification and analysis can be formulated in more reasonable basis allowing better analysis of risks and risk impacts. Another perspective is the crisp values to be substituted by means of fuzzy variables to express the uncertainty of each specific risk in more physical manner by using appropriate linguistic expressions. From the previous, it seems that there is room for further improvement of the methodology incorporating the uncertainty in a more advanced form, but complicated also, as the calculations of fuzzy AHP techniques are more complex. Finally, researchers can investigate, also, other equivalent MCDM techniques, such as PROMETHEE series, ELECTRE series, Bayesian networks, neuro-fuzzy algorithms or other hybrid techniques [10].

REFERENCES

- [1] F. Schulz, G. Wiegleb (2000). Development Options of natural habitats in a post-mining landscape, *Land Degradation and Development*, vol.(11), pp. 99-110
- [2] T. Chuman, (2015) Restoration Practices used on Post mining Sites and Industrial Deposits in the Czech republic with an Example of Natural Restoration of Granodiorite Quarries and Spoil Heaps, *Journal of Landscape Ecology*, vol.(8), No.2, pp. 29-46
- [3] K. Prach, R. J. Hobbs, (2008). Spontaneous succession versus technical reclamation in the restoration of disturbed sites, *Restoration Ecology*, vol.(16) pp. 363-366
- [4] S. Tischew, A. Krimer, A. Lorenz, (2009). Alternative Restoration Strategies in Former Lignite Mining Areas of Eastern Germany, *BIODIVERSITY: STRUCTURE AND FUNCTION*, vol.(II), EOLSS Publishers Co Ltd, Oxford, UK.

- [5] Sinha, S. (2015). Overview on Reclamation and rehabilitation of Mines, Overview: Indian Mineral Sector, *Indian Bureau of Mines* (available in the web)
- [6] C. Imboden, N. Moczek, (2015). Risks and opportunities in the biodiversity management and related stakeholder involvement of the RWE Hambach Lignite Mine, *International Union for Conservation of Nature*, www.iucn.org/publications
- [7] T. L. Saaty, (1980). *The Analytic Hierarchy Process*, N.Y. McGraw Hill International
- [8] K. A. Al-Harbi (2001). Application of the AHP in project management, *International Journal of Project Management*, vol.(19), pp. 19-27
- [8] T. L. Saaty, (2008). Decision making with the Analytic Hierarchy Process, *International Journal of Services and Sciences*, vol.(1) No.1, pp. 83-98
- [9] M. Velasquez, P. T. Hester, (2013). An Analysis of Multi-Criteria Decision Making Methods, *International Journal of Operations Research*, vol.(10), No.2, pp. 56-66
- [10] R. A. Krohling, T. T.M. de Souza, (2011). Two Examples of Application of TOPSIS to Decision Making Problems, *Revista de Sistemas de Informacao*, No.8, pp. 31-35
- [11] M. R. Ghanbarpour, K. W. Hipel, (2011). Multi-Criteria Planning Approach for Ranking of Land Management Alternatives at Different Scales, *Research Journal of Environmental and earth Sciences*, vol.(2), No.2, pp.167-176
- [12] P. K. Parida, S. K. Sahoo, (2013). Multiple Attributes Decision Making Approach by TOPSIS Technique, *International Journal of Engineering Research and Technology*, vol.(2), No.11, pp. 907-912
- [13] A. Bradshaw, (1997). Restoration of mined lands using natural processes, *Ecological Engineering*, vol.(8), pp. 255-269
- [14] LUMINANT, (2015). An Overview of Lignite Mine Reforestation at Luminant's Martin Lake Mines in Eastern Texas
- [15] Z. Kasztelewicz, (2014). Approaches to post-mining land reclamation in Polish open-cast lignite mining, *Civil and Environmental Engineering Reports*, vol.(12), No.1, pp. 55-67
- [16] A. Erener, (2011). Remote sensing of vegetation health for reclaimed areas of Seyitomer open cast coal mine, *International Journal of Coal Geology*, vol.(86), pp.20-26
- [17] C. Roumpos, P-M. Spanidis, F. Pavloudakis (2018). Land reclamation planning of continuous surface lignite mines in closure phase: A risk-based investigation, *Proceedings of the 14th International Symposium of Continuous Surface Mining, ISCSM2018*
- [18] T. L. Saaty, L. G. Vargas (1991). *Prediction, Projection and Forecasting*, Kluwer Academic Publishers, Dordrecht, pp. 251
- [19] PMI (2000). *A Guide to Project Management Body of Knowledge*, USA
- [20] K. Kirytopoulos (2010). *Manual for Projects' Risk Management*, Klidarithmos Publications, Greece
- [21] L. Sloss, (2013). Coal mine site reclamation, CCC/216, ISBN 978-92-9029-536-5, IEA Clean Coal Centre (available in the web)
- [22] K. Leathers, (1980). Costs of Strip Mine Reclamation in the West, *US Department of Agriculture*, Rural Development Research Report No.19 (available in the web)

[23] A. Rovolis, P. Kalimeris (2016). Roadmap for the Transition of the Western Macedonia Region to a Post-Lignite Era, WWF, Economic and Technical Assessment www.wwf.gr/images/pdfs/Rmap_Study.pdf

[24] W. Knabe, (1964). Methods and Results of Trip-Mine Reclamation in Germany, *Ohio Journal of Science*, vol.(64), No.2, pp.74-105

[25] Regulation on Mining and Quarrying Activities (2011). Greek Mining Enterprises Association

[26] C. Roumpos, P. – M. Spanidis (2003). Open Pit Project Management, *World Coal*, pp.55-61.

Session 7: Water management - Environmental monitoring

Planning of Mavropigi and Kardias Mines Depressurization Systems by Three Dimensional Groundwater Flow Numerical Modeling

George Louloudis

Public Power Corporation of Greece, Mines Central Support Department,
29 Chalkokondili str., 10432 Athens, Greece

ABSTRACT

Mavropigi and Kardias lignite mines, located on western margins of South lignite bearing Ptolemais basin (NW Macedonia, Greece), have an annual lignite production of $15 \cdot 10^6$ tones available, to provide it as partial contribution to the 3000 MW Power Plants' Electric System.

The confined loose water bearing formations under lignite seams, in fact can be extremely dangerous as water may enter the excavation area, after piping or heaving the mine bottom and benches.

In present paper there is an effort to simulate in three dimensions the underneath lignite seams aquifer's groundwater flow into the loose Neogene sediment's porous media, only to confront heaving and piping effects. The model has developed in order to implement a depressurization water well's system of appropriate magnitude and other dewatering of mine measures or acts to be dimensioned.

The studied part of this aquifer was simulated in two layers of 1086 nodes each one, which lie in a square grid with a distance of 300 m between them. The simulation was performed on FREEWAT MODFLOW-2005 application in cooperation with Q-GIS open source that held all geological and hydrological information. The results of 3 stress periods model running revealed that is feasible the decompression of the aquifer under approximately $1500 \text{ m}^3/\text{h}$ average pumping rate in both mines. The afterwards decompression, dewatering of free aquifer is not included to present investigation, because the appropriate ground water lowering to ensure slope stability is not geotechnical investigated yet.

The possibility of an artificial recharge on the decompressed aquifer is prospected to be simulated in future by the same numerical model. Thus it will be a further future investigation, going to the right direction of regional water resources rational management.

1. INTRODUCTION

In the region of South lignite bearing basin of Ptolemais (Macedonia, NW Greece) (Fig. 1), Public Power Corporation of Greece has developed a great mining activity in order to provide adequate lignite quantities to 3000 MW Power Plants.

Mavropigi and Kardias (Southwest field) mines (Fig. 2.) are two of the exploitation fields in which Ptolemais lignite bearing basin has been divided. The known lignite deposits of both fields rises up to $360 \cdot 10^6$ tn lignite with $15 \cdot 10^6$ tones average annual production.

Water inflow in the mining area creates slope stability problems, makes it difficult to operate and can even jeopardize the safety of the work [1, 2]. The loose water bearing formations under lignite seams, in fact can be extremely dangerous as they are likely to be under pressure (confined) and thus water may enter the excavation area after piping (groundwater vertical upwards flow through veins or faults filled with permeable porous material etc.) or heaving the mine bottom and benches.

Mavropigi and Kardia open pits are located on western margins of South lignite bearing Ptolemais basin, on Askion mountain's foothills. The up till now review of hydrogeological studies on the mine's area existing aquifers, clusters 3 group of aquifers. In this modeling case study the simulation was oriented only in the under lignite aquiferous system that was confirmed in area of Mavropigi mine [3] and in area of Kardia Southwestern Ptolemais Mine Field [4]. These under lignite aquifers are very significant for Mavropigi and Kardia mines' operations integrity causing potential piping and heaving intrushes' problems.

The under pressure aquifer of Mavropigi-Kardia (Northwestern Greece) strip mine projects is located on western margins of South lignite bearing Ptolemais basin next to Askion Mountain.

This aquatic system is under pressure, cause upon its roof is covered by impermeable formations consisting by lignite and clay marl seams (Figure 3). It is extended almost in whole Komanos horst region from Askion foothill till Vermion foothills, covering 92,5 km² with average thickness of 260 m, and keeping reserves of water exceeding $1,6 \cdot 10^9 \text{ m}^3$ [3].



Figure 1. Region of research. South lignite bearing basin of Ptolemais (Macedonia, NW Greece)

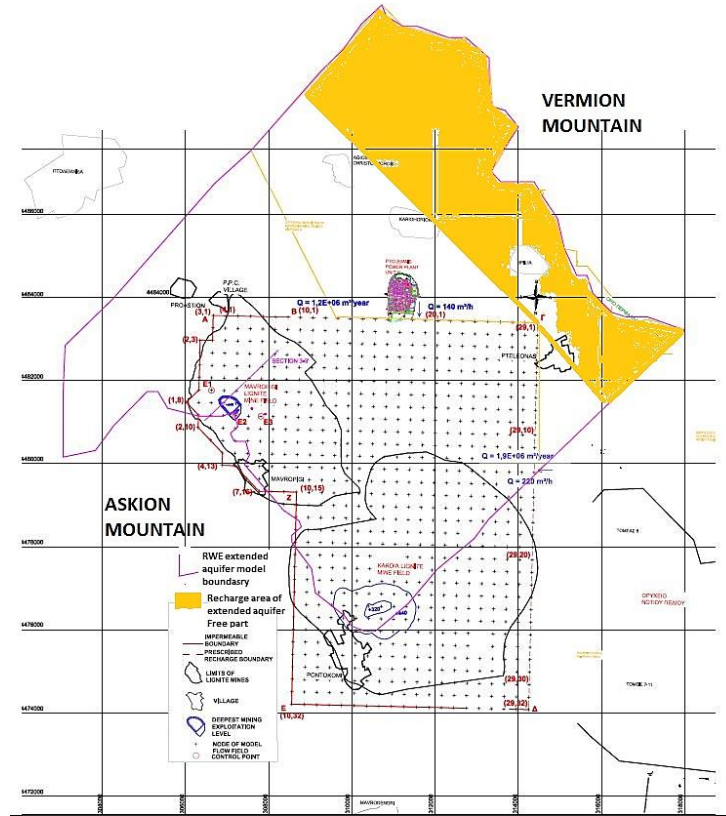


Figure 2. Mavropigi and Kardia mines layout. Water wells location map. Boundary conditions of model's layers I, II

The piezo metric groundwater levels in the part aquifer's sector that include Mavropigi Kardia mines, ranges from 600 m a.s.l. in Mavropigi region till 570 m in Soulou river let region east of Kardia mine (Figure 4.). The main direction of flow in the region of Mavropigi – Kardia mines is North Northeast to South Southwest, revealing a mean gradient 2,5% in Southwest part of Mavropigi mine, 0,25% in Northeast part of Mavropigi mine and 1% in the region of Kardia mine [4] (Fig. 4.). The recharge of this narrow area under simulation is realized by lateral inflows of the large regional Komanos horst aquifer towards the model area (Fig.4).

A general review of the results deduced by analysis and interpretation of 28 wells pumping tests performance's data acquisition indicates a range of transmissivities between 10^{-4} and 10^{-2} m²/sec [4].

2. METHODOLOGY

Main subject of a dewatering study is the determination of basic elements needed to plan depressurizing systems. The solution of such a problem requires the knowledge of hydrological, hydrogeological conditions, the hydraulic properties of aquifer that appear in the region of mine estimation, in combination with future mine's exploitation plans scheduled.

To be specific the engineers in cooperation with geologists have to determine the number, location and technical prescriptions of drainage wells in order to avoid under the lignite aquifer inrush risk on Mavropigi and Kardia mines. The solution is based usually on mathematical model simulation of groundwater flow results [4,5,6].

In these under pressure sub lignite horizons the water level in Mavropigi and Kardia mines central part is recorded approximately at 600 a.s.l., that means 160 m higher than the prescheduled deepest stand of Mavropigi exploitation bottom's elevation of +440 m a.s.l. [7] (Fig. 8., Fig. 11.) It also means that piezometry is 280 m higher than the prescheduled deepest stand of Kardia exploitation bottom's elevation of +320 m a.s.l [8] (Fig. 8., Fig. 11.).

It's absolute necessity of depressurizing the aquifer at least at a water level of 490 a.s.l. [6], in order to secure the deeper sector of Mavropigi mine against heaving and piping under seepage hazard. This sector will be exploited into the next decade [7].

There is also a need of 160 m lowering of pressure in the region of Kardia mine. The piezometry must be reached below the +440 a.s.l. at 1.1.2032, in order to secure Kardia mine's exploitation against heaving and piping under seepage hazard, into the period 2023-2042.

Additional to these withdraws must operate a dewatering well point system for the lowering of water table after decompression complete, in order to secure the mines from classical slope stability. These quantities are expected to be significant but didn't take into account in the present simulation .

In order to design the dewatering process we used as basic tool a mathematical model, based on the solution of differential equation that describes the time variant water flow in porous media all over field, expressed as follows:

$$\frac{\partial(kx*\frac{\partial h}{\partial x})}{\partial x} + \frac{\partial(ky*\frac{\partial h}{\partial y})}{\partial y} + \frac{\partial(kz*\frac{\partial h}{\partial z})}{\partial z} = S*\frac{\partial h}{\partial t} + Q \quad (1)$$

where: kx is the permeability in X direction
 ky is the permeability in Y direction
 kz is the permeability in Y direction ,
 h is the piezo metric head or pressure in node
 S is coefficient of storage,
 Q is the inflow or outflow per unit area.

This is Boussinesq continuity equation, which governs groundwater flow and naturally satisfies the preservation of mass [9]. This equation was also incorporated by McDonald et al to the first 3D MODFLOW models [10]. The system of partial derivative equations, that governs non-permanent three dimensional water flow in non - homogeneous and non-isotropic aquifer has been solved with finite difference method of slice successive over relaxation technique.

The studied part of this aquifer was simulated in two confined layers in early stages that in late stages become unconfined convertible layers [5, 14] with 1086 nodes each one. The layer I consists mainly by green fine to medium sandy with clay. The layer II consists mainly by gravel layers with sand. The nodes lie in a square grid with a distance of 300 m between them. FREEWAT Mudflow's application undertook the solution of equations' system in cooperation with Q-GIS open source [15, 16, 5], that held all geological and hydrological information.

The FREEWAT platform is based on open source solutions to perform an integrated coupling between the QGIS desktop software, surface and subsurface model engines, mostly based on fully distributed and numerically-based codes developed by the USGS [6,13], and other software applications, and the SpatiaLite spatial database[13].

When the process of evaluating and predicting groundwater flow was started, these data were transformed into files that the core program of MODFLOW2005 could read [6,14].

Simulating Mavropigi mine aquifer part three types of boundaries conditions are settled (Fig. 4, Fig. 5):

- Impermeable boundaries
- Prescribed recharge boundary
- Prescribed heads boundary

Impermeable boundary type is considered in nodes where no flux passes through this boundary.

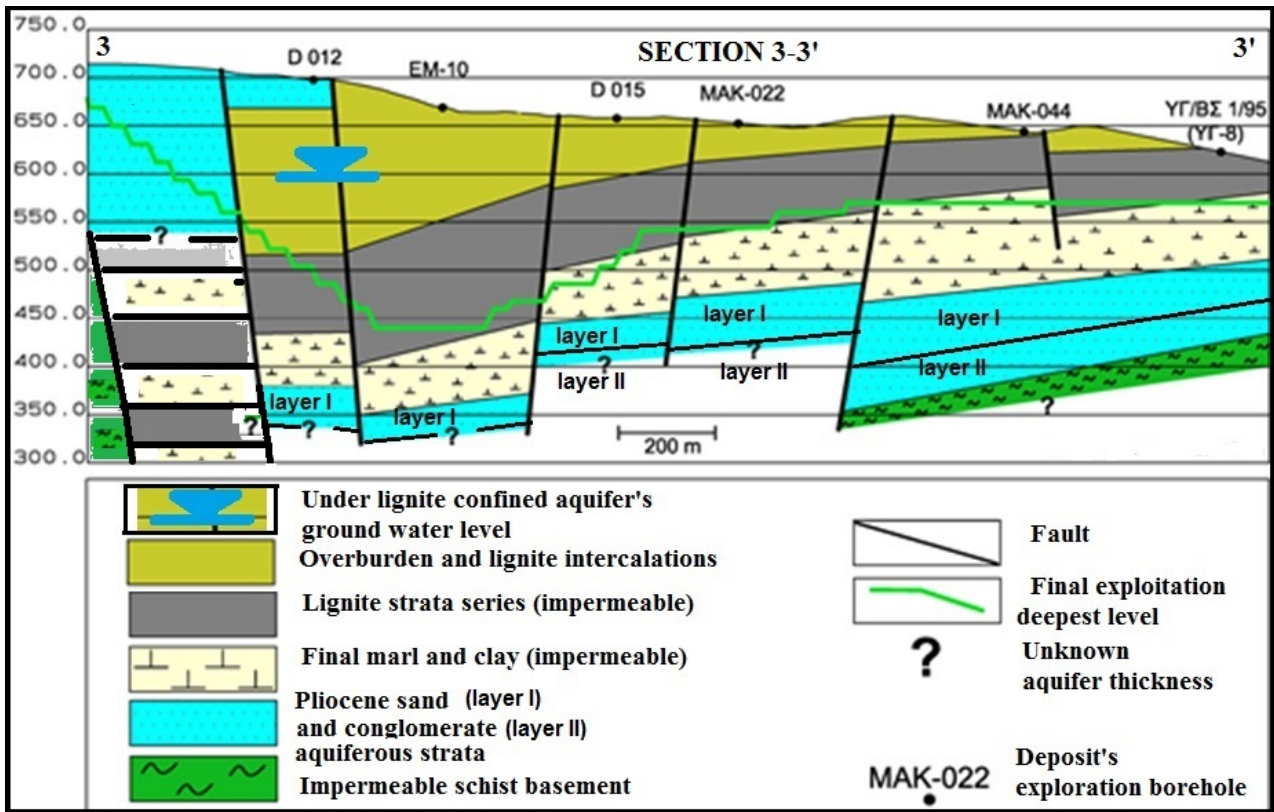


Figure 3. Two layers groundwater model

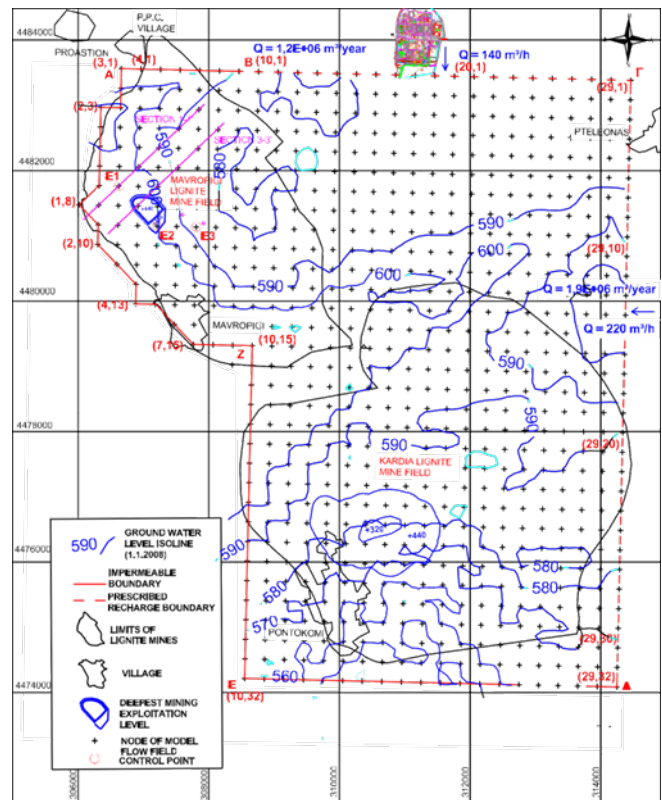


Figure 4. Groundwater flow pattern (1.1.2008). Piezo metric equipotential lines in 1.1.2008

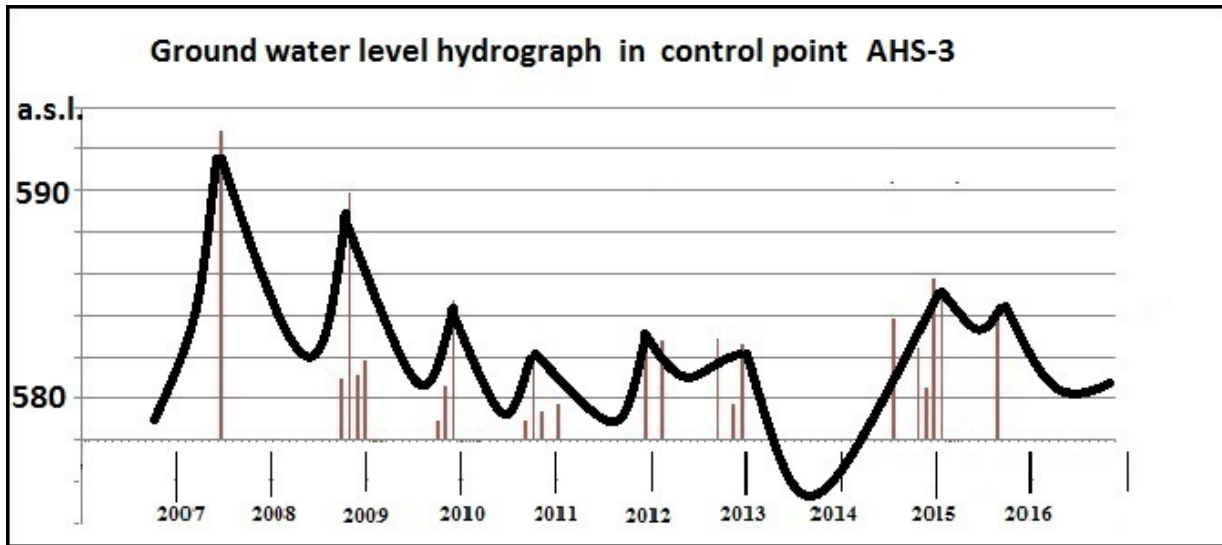


Figure 5. Prescribed head boundary fluctuation

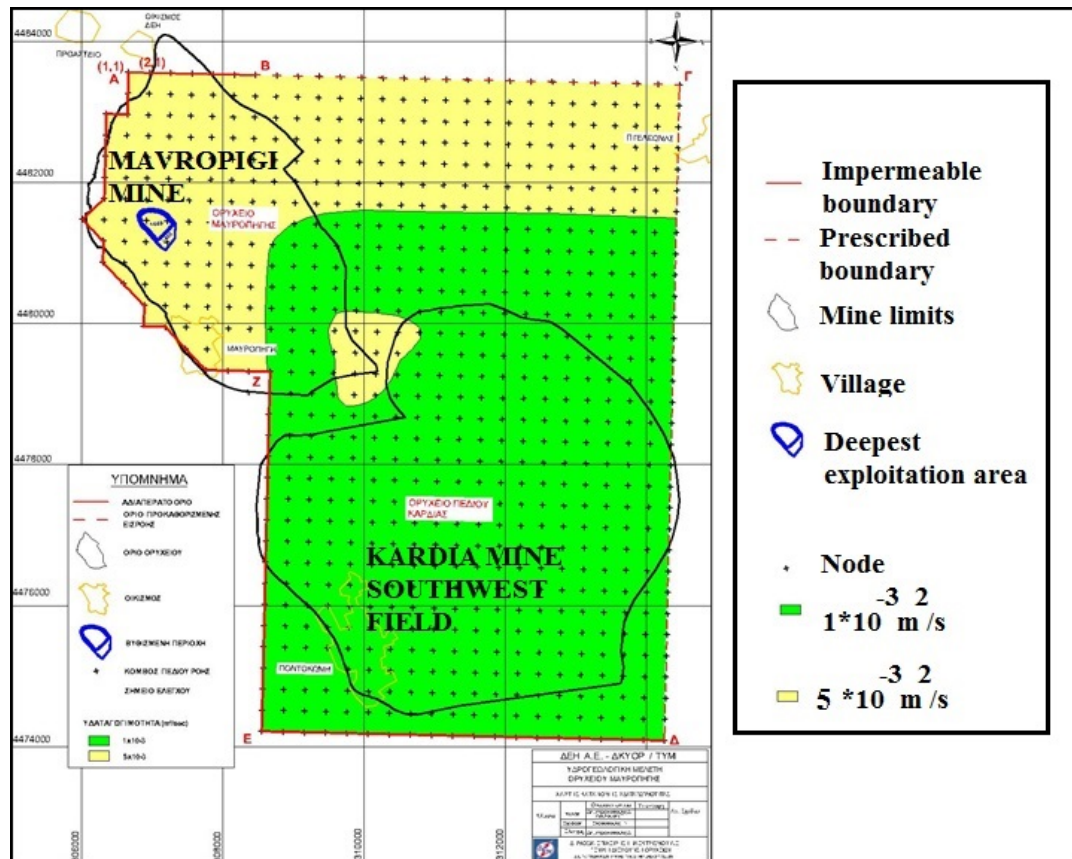


Figure 6. Transmissivity values distribution map. SVD determination.

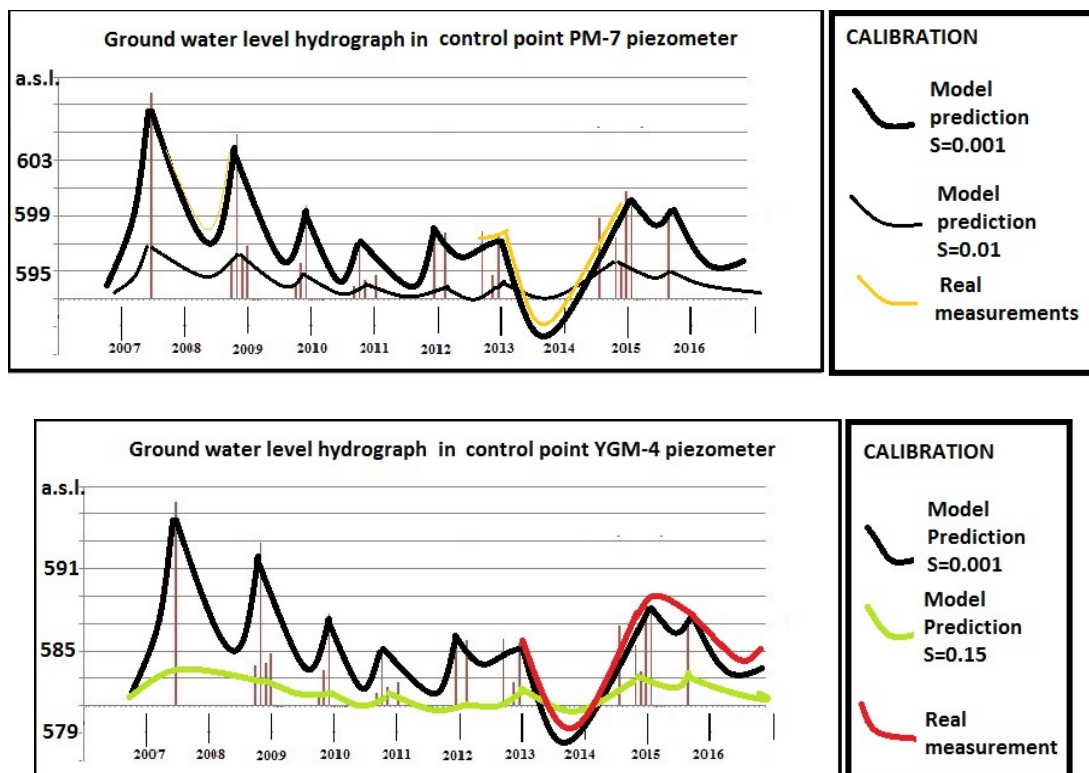


Figure 7. Storage coefficient inverse modelling determination

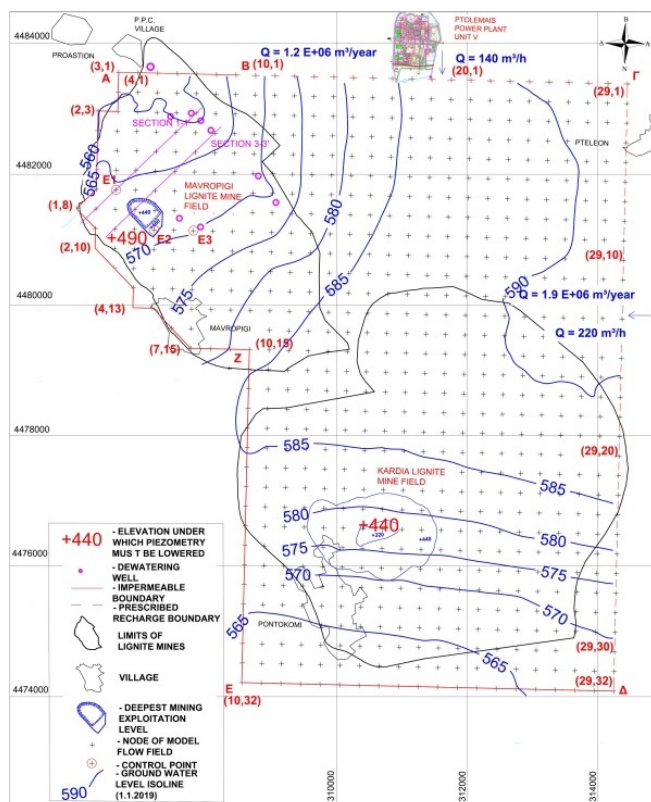


Figure 8. Prediction of groundwater flow pattern 1.1.2019. Piezo metric equipotential lines in 1.1.2019

The boundary conditions of the model were selected according to geological and hydro geological conditions of the Mavropigi mine area.

The borders between consolidated sediments schists of Askion and unconsolidated sediments of South lignite bearing Ptolemais basin were treated in West side of model net as impermeable boundary. Such a type of boundary was installed at a small part of Southeast to Northwest direction fault that separates Komanos horst from internal Ptolemais basin. In South end of model net a part of fault that separates Kardia mine from South lignite bearing Ptolemais basin is considered as impermeable.

During calibration by inverse modeling the prescribed constant head fluctuation (Fig. 5) in line BF was introduced. This fluctuation is the outcome of unsaturated zone water balance in the north east unconfined part (Fig. 6) of the hole aquifer.

By inverse modeling subroutine UCODE 2014 runs, the spatial transmissivity distribution that is depicted on figure 6 was defined and then the transmissivities were introduced (expressed as permeability's input data) to the mathematical model MODFLOW. The inverse modeling involved Singular Value Decomposition SVD technique.

As far as it concerns a storage coefficient the value of approximately 0.001 fitted the real groundwater level fluctuation with model results, after sensitivity analysis and calibration procedure. The compliance between ground water level fluctuation and appropriate storage coefficient (Fig. 7) involved weighted linear regression [20].

In late stages, while layers become unconfined a value of S equal to 0.07 is set to layer I and S equal to 0.10 is set to layer II.

The initial conditions at 1.1.2019 (Fig. 8.) of the groundwater simulation were settled as the results of a 10 year stress period (2008-2019) mean values [11,13] of recharges and out charges simulation near the date of the drainage initialization period (1.1.2019).

This simulation was carried out on an annual basis for a period of 25 years (until 2032) and aims at estimating the water inflows into the mining site during the study period, as well as planning the best possible drainage measures to be implemented, in order for the exploitation's works to continue without problems inside the mine.

For this purpose, several alternative drainage scenarios (with different pumping rates, different number of wells drilled, etc.) were investigated and simulated and the optimum one is selected. In particular, the number, location and technical characteristics of the drainage boreholes to be constructed, in order to prevent the risk of groundwater inflow from the lignite deposit's subjacent aquifer into Mavropigi mine, are specified for each scenario.

The selected scenario has three stress periods (Fig. 12.). First stress period corresponds the up till 1.1.2023 (Fig. 5.) need of depressurization the deepest part of Mavropigi. Second stress period (2023-1.1.2032) is starting depressurization of Kardia in addition with Mavropigi. In third stress period (2032-2042) Mavropigi decompression terminates and begins water level recovery in the region. Kardia's decompression is continuing in third stress period.

3. RESULTS

The model results, in the worst case scenario, estimate inflows of 950 m³/h in Mavropigi mine, while the best dewatering design scenario (among the tested ones) that can confront most effectively these inflows in a realistic and operationally applicable way, is based on 600 m³/h of initial pumping peripheral the exploitation and an increase of 200 m³/h to the mine internal area corresponding to 10-20 additional wells to be drilled, equipped by pumps and operate for the next 4 years (2019-2023) into mine Mavropigi.

The groundwater flow pattern prediction for 1.1.2023 (Fig. 9.), that ensures geotechnical safety in Mavropigi, indicates inverse groundwater flow direction from South to North and duplication of hydraulic gradient. Despite the zero pumping rates in Kardia region during first stress period there is a worthwhile drawdown of 40 m in Southwest lignite Ptolemais Field, but not sufficient for geotechnical safety in Kardia.

After that first stress period (Fig. 12.), that involves no dewatering to Kardia mine, the next stress period (second period) continues for 10 more years following the same pumping rates mentioned in first stress period for Mavropigi mine. Additional to these the second stress period, that ensures at his end geotechnical safety for both mines, involves 1100 m³/h pumping rates into Kardia mine (2023-2032) coming from 10-20 additional wells in Southwest lignite of Ptolemais Field.

The groundwater flow pattern prediction for 1.1.2032 (Fig. 10.) indicates rein verse groundwater flow direction from North to South and duplication of hydraulic gradient in Kardia.

The third stress period (2032-2042) years, involves decompression pumping only in Kardia region, while in Mavropigi region is finally attenuate to no pumping (Fig. 12.). The zero pumping in Mavropigi results in a partial recovery of groundwater level in Mavropigi mine neighborhood as it reveals in groundwater flow pattern prediction for 1.1.2042 (Fig. 11.).

4. DISCUSSION

The results of the method are reliable and are confirmed by the current drainage practice applied in the Mavropigi mine. This methodology is a particularly effective and an operationally useful practice for drainage planning of lignite deposits that will be or are under exploitation.

The model results on the selected scenario are reliable, confirmed by the up till now following dewatering process and subjected in calibration and future revision of the dewatering process modeling.

By incorporating the vertical component of flow 3D FREEWAT platform's application MODFLOW model, gave us the capability of simulating two layers and two possible conditions (free and under pressure state transition) that can appeared in first layer. Thus the 3D solution can be considered more accurate in comparison with the two dimensional finite difference application [4].

There is a difference between the FREEWAT application and RE finite element model. In comparison with the results of the RE finite element model [1] that overestimated the dewatering measures involving the need of more than 60 wells in order to achieve the level of +440 m.

In its conceptual model RE uses unnecessary wells patterns that cover all region of exploitation, in contradiction with our model, that installs wells only aligned along lines that would remain stable for a long time, providing a sustainable well's operational life. Indeed, as open cast mine's operations due to strip mining's excavations creates a continuously modified in topography environment that threads damages to dewatering water wells or destroys them. In contrary with partial recovery of wells technique, it is more convenient and friendly to rest mining activities the depressurizing wells group to be aligned along lines that would remain stable for a long time, providing a sustainable well's operational life.

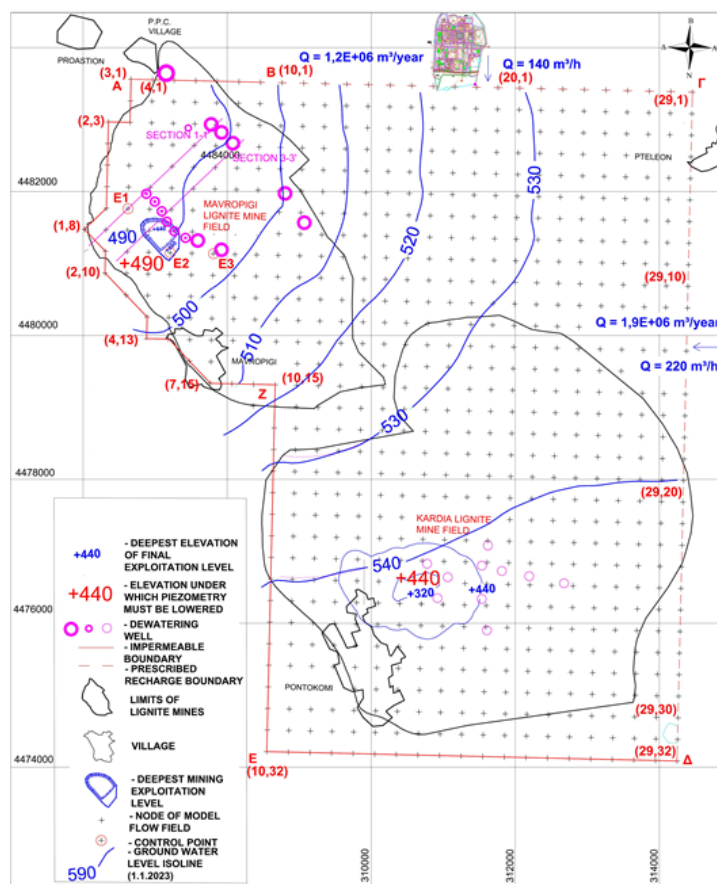


Figure 9. Prediction of groundwater flow pattern in 1.1.2023. Piezo metric equipotential lines in 1.1.2023

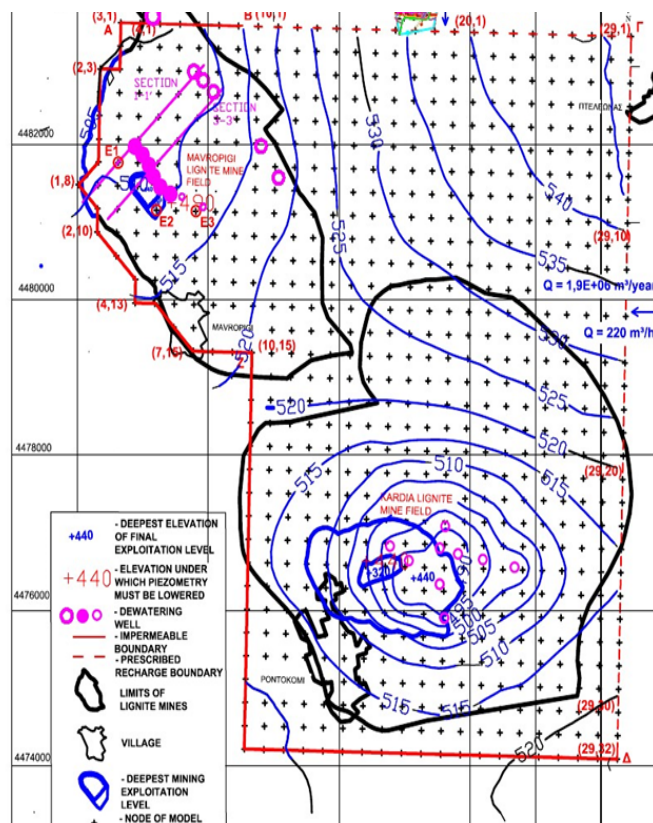


Figure 10. Prediction of groundwater flow pattern 1.1.2032. Piezo metric equipotential lines in 1.1.2032

In addition to this in the RE's flow conceptual model incorporate both decompression stage and dewatering of the remain free water table till dry, meaning lowering of aquifer till level +440 a.s.l. In the present conceptual model a geotechnical study of heaving and piping risk (according to US standards of safety [19]), that precede the groundwater flow model. This geotechnical study, concludes that the safety maximum decompression ground water level in Kardia is +440 and in Mavropigi +490, meaning 50m higher than lower bottom excavations' levels.

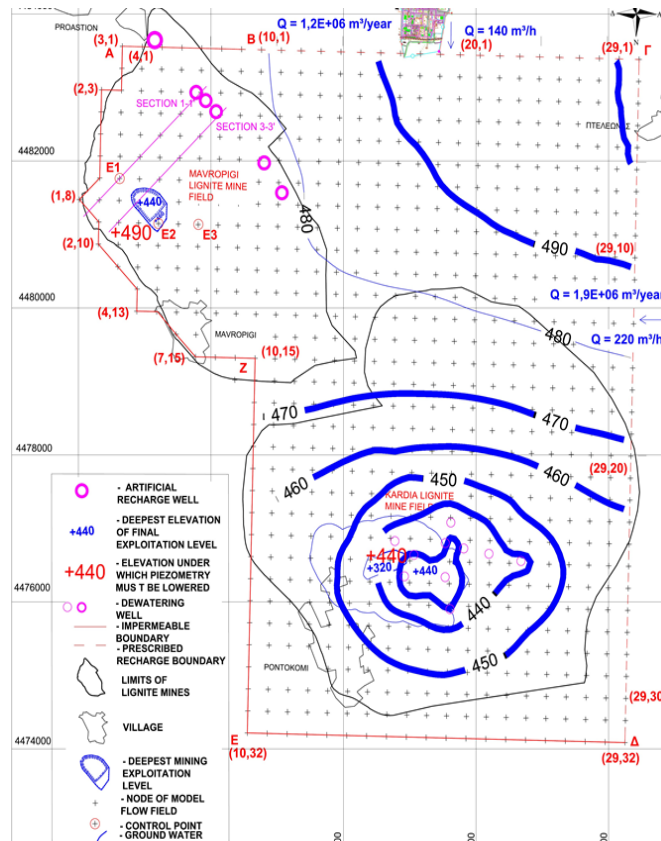
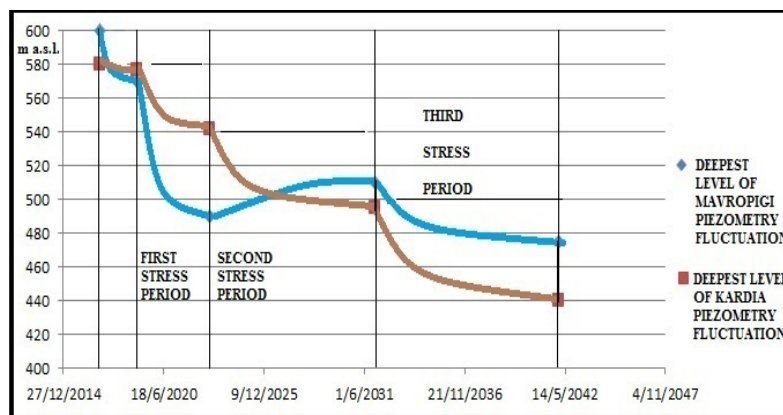


Figure 11. Prediction of groundwater flow pattern 1.1.2042. Piezo metric equipotential lines in 1.1.2042.



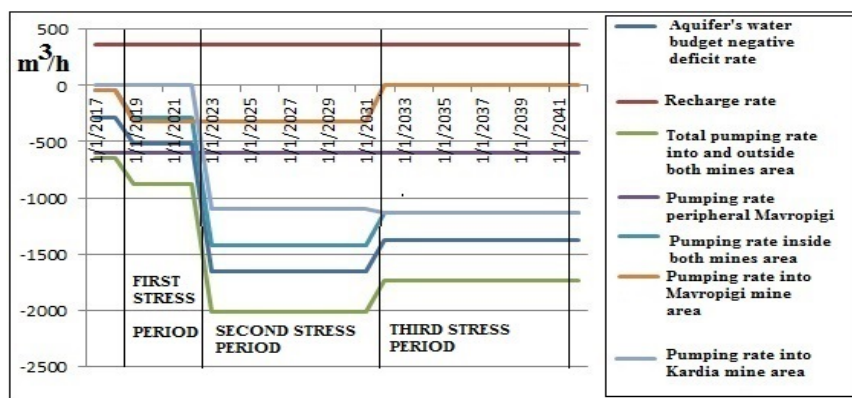


Figure 12. Subsurface hydrologic unit future water budget. Recharge and drainage withdraws rate. Ground water level piezometry prediction in deepest exploitation level of each mine

5. CONCLUSION

The results of 3 stress periods model running revealed that is feasible the decompression of the aquifer under approximately 1500 m³/h average pumping rate in both mines. These results of MODFLOW can refeed Q-GIS data base [16] in a total holistic management of ground and surface waters of the area, that takes account also the demands of city, agriculture and industry in water.

After evaluated, by geotechnical slope stability investigation, the after decompression necessary a.s.l. of groundwater horizon, the future model's runs are called to calculate the appropriate well points discharge rates to reach this safety lowering water level.

It is suggested to proceed in investigation by modeling how likely is the implementation of artificial recharge of groundwater horizon in the region of peripheral Mavropigi dewatering wells feasible, during the third stress period, in order to compensate the environmental impacts of dewatering as far as possible.

REFERENCES

- [1] Dimitrakopoulos D., Louloudis G., Koumantakis J. (1991). Environmental Impacts in Relation to the Ground Water in Open Lignite Mines of P.P.C., Greece, 4th International Mine Water Association Congress, Ljubljana-Portschach.
- [2] Louloudis G. (1991). Hydrogeological conditions of South lignite bearing Ptolemais Field – Groundwater problems confrontation during exploitation, PhD Thesis, NTUA, Athens, Greece.
- [3] Voigt J. and Schwarzenberg T. (2004). Groundwater model for Mavropigi Mine, Final report to Public Power Corporation of Greece, Mines Engineering and Development Department, RWE Power International, Germany.
- [4] Louloudis G., Stathopoulos N. and Dimitrakopoulos D. (2017). Groundwater flow simulation via mathematical modeling and drainage planning of Mavropigi mining site, 11th International Hydro geological Congress of Greece, Conference Proceedings, Athens.
- [5] Filippis G., Borsi I., Foglia L., Cannata M., Velasco Mansilla V., Vasquez-Suñe E., Ghetta M. and Rossetto R. (2017). Software tools for sustainable water resources management: the GIS-integrated FREEWAT platform, *Rend. Online Soc. Geol. It.*, Vol. 42 (2017), pp. 59-61, 3 figs. (doi:10.3301/ROL.2017.14) © Società Geologica Italiana, Roma.
- [6] Harbaugh A.W. (2005). MODFLOW-2005, The U.S. Geological Survey Modular Ground-Water Model - the Ground-Water Flow Process. U.S. Geological Survey, Techniques and Methods 6-A16, 253 pp.

- [7] Pagonis G., Roumpos C., Liakoura K. and Paraskevis N. (2009). Revised mining study of Mavropigi mine, Mines Engineering and Development Department, Public Power Corporation of Greece, Athens.
- [8] Papageorgiou C. and Kolovos C. (2010). Revision of South West Lignite Mine Field Mining Plan under condition of Pontokomi Municipality settlement relocation, General Mine Administration PPC.
- [9] Walton W.C. (1970). Groundwater Research Evaluation, Mc Graw Hill, New York.
- [10] McDonald M. G. and Harbaugh A. W. (1988). A modular three-dimensional finite-difference ground-water flow model: Techniques of Water-Resources Investigations of the United States Geological Survey, Book 6, Chapter A1, 586 p.[11] K.R. Rushton,. Groundwater Hydrology: Conceptual and Computational Models, Wiley, USA,2003.
- [12] Smith W. H. F. and Wessel P. (1990). Gridding with continuous curvature splines in tension., Geophysics, Vol. 55, No3, p. 293-305.
- [13] Harbaugh A. W., Banta E. R., Hill M. C. and McDonald M. G. (2000). MODFLOW 2000 - User Guide to Modularization Concepts and the Groundwater Flow Process, U.S. GEOLOGICAL SURVEY, Virginia, 30-33 pp.
- [14] Shiqin Wang, Jingli Shao, Xianfang Song, Yongbo Zhang, Zhibin Huo, Xiaoyuan Zhou (2008). Geology Application of MODFLOW and geographic information system to groundwater flow simulation in North China Plain, China, Environ 55:1449–1462, DOI 10.1007/s00254-007-1095-x.
- [15] Lin Y. F. and Anderson M. P. (2003). A Digital Procedure for Ground Water Recharge and Discharge Pattern Recognition and Rate Estimation, Ground Water 41(3), p. 306-315.
- [16] Q-GIS User Guide (2017). Release 2.18.
- [17] Childs E.C., Bybordi M. (1969). The vertical movement water in stratified porous material: 1.Infiltration. Water Resources Research, an agu journal, Wiley, USA.
- [18] Rushton K. R. (1971). L.A. Wedderburn, . Starting conditions for aquifer simulations, Ground Water, Vol 9, No5.
- [19] Flood Damage Reduction Feasibility Study (1998). Engineering Appendix to the Interim Feasibility Report, GEOTECHNICAL ANALYSIS NORTH KANSAS CITY - LOWER (HARLEM AREA), Section 216 – Review of Completed Civil Works Projects, Kansas City, Missouri and Kansas.
- [20] Poeter E. P., Hill M. C., Dan Lu, Tiedeman C. R. and Mehl S. (2014). UCODE with New Capabilities to Define Parameters Unique to Predictions, Calculate Weights using Simulated Values, Estimate Parameters with SVD, Evaluate Uncertainty with MCMC, and More UCODE_2014, with New Capabilities to Define Parameters Unique to Predictions, Calculate Weights using Simulated Values, Estimate Parameters with SVD, Evaluate Uncertainty with MCMC, and More, International Groundwater Modeling Center, IGWMC report GWMI 2014/02, 2014.

Improvement Methods of Pumping Station Function in Coal Mines of Western Macedonia Lignite Centre

N. Koukouzas¹, R. Karametou¹, V. Gemeni¹, C. Roumpos², C. Sachanidis² and F. Pavloudakis²

¹Centre for Research and Technology Hellas, Chemical Process and Energy Resources Institute, 50200, 40 km Ptolemais-Mpodosakeio, Greece

²Public Power Corporation of Greece-Mines Division, 104 42 Athens, Greece

ABSTRACT

Lignite mines dewatering efficiency in Western Macedonia Lignite Centre is based on a complex pumping system with appropriate capacities. This paper discusses the results of two series of water and sludge samplings from pumping stations of mines in Western Macedonia Lignite Centre. These samples were analysed in order to identify the water quality of mine pumping stations. Particularly, physicochemical parameters and the concentration of suspended particulates solids were tested. The results showed that the pumped water quality of Western Macedonia Lignite Centre mines is within the limits set by the local authorities for the protection of the aquatic receiver of mine water discharges. Many samples meet even the EU standards for the suitability of drinking water. Consequently, the pumping system of these mines is characterized sufficient enough. Moreover, sludge samples were tested via X-ray powder diffraction (XRD) analytical technique. The analyses results showed that the mineralogical composition of sludge samples is similar to the geoenvironmental profile of the greater mining area. The paper concludes by outlining some methods for the mine pumping station upgrade.

1. INTRODUCTION

Extensive groundwater quantities are being pumped from the Western Macedonia Lignite Centre in order to dewater the open pit lignite mines and secure their operation. This paper discusses the results of two series of water and sludge sampling from pumping stations of mines in Western Macedonia Lignite Centre. Particularly, the concentration of suspended solid particles in the water of the pumping stations was measured. Generally, suspended solid particles are dispersed in water either through suspension or dissolution. They may be consisted of inorganic or organic particles or immiscible liquids. Inorganic solids such as clay, sludge and other soil components are often found in surface water. Organic materials such as plant fibres and organic solids (bacteria, etc.) are also common components of surface water [1].

The separation of suspended solid particles is typically done by means of gravity forces with the use of settling techniques. The particles are considered precipitated and removed from the fluid when they reach the bottom of the settling zone and enter and remain in the sludge area. The sedimentation time of the suspended particulates solids differs and it depends on their type and their size [2].

Table 35. Sedimentation time of suspended particulates solids

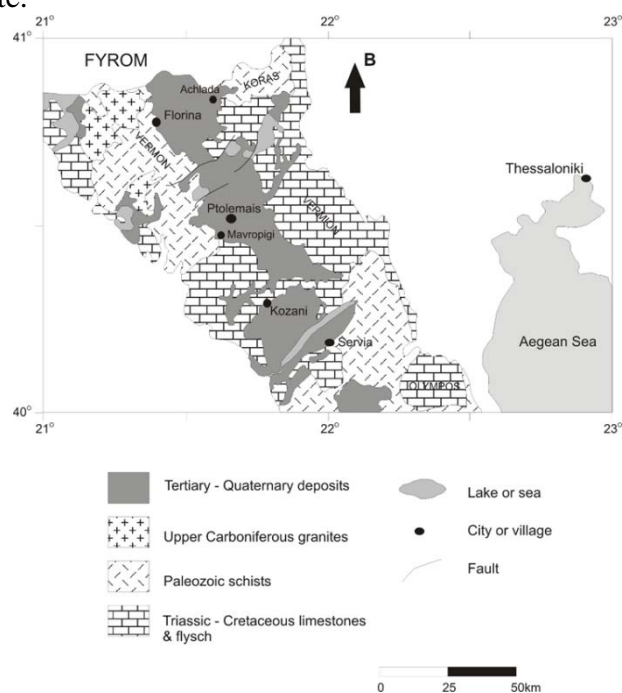
Material	Size (μm)	Sedimentation time
Sand	10.000/1.000/100	1 sec/10 sec/125 sec
Slurry	10	108min
Bacteria	1	180hrs
Colloids	0.1	Many days

1.1. Geological background

The study area is part of a tectonic graben, over 250km in length that extends from northern Greece into the Former Yugoslav Republic of Macedonia. The basin is divided into two elongated grabens (Fig 1.) that are characterized by different stratigraphic evolution and different subsurface morphology. The basin formation occurred at the end of the Tertiary era and its creation is considered to be a consequence of subsidence in large NW–SE fault zones.

The different sedimentation rates of the basin resulted in frequent intercalation between the lignite layers and the sterile which consist, mainly, of marls and subsequently from clay and sand. The end of the genesis of the lignite coincides with the change in the climatic conditions and the beginning of the ice age.

The basement underlying the basin includes Paleozoic schists, ophiolites and granites. Above the basement, lays the Pelagonian Structural Zone, which consists from Mesozoic dolomitic limestones, interlaying with volcanic sediments with ophiotic blocks, and flysch. The basin itself is filled with Tertiary and Quaternary sediments up to 1000 m thick. The upper part of the basin fill includes Miocene to Pleiocene sand, sandy clay, lignite and marl, mainly of fluvial to lacustrine origin. More specifically, in the surface lay the Quaternary sediments, then the Pleio-Pleistocen unit that has a thickness of 20-100m and consists of sand and clay which intercalate with marls and conglomerates. Below this sequence lay the Pleio-Miocene deposits consisting of layers of lignite and sand. These sediments are rich in CaCO_3 since it can be found in all the sediments of the sequence, including the lignite.

**Figure 143.** Synthetic geological map [3], [4].

1.2. Mine pumping station description

The examined pumping stations are located in Amyntaio Mine, Kardias Mine, South Field and Mavropigi Mine of Western Macedonia Lignite Centre. Their characteristics are presented in the following Table 2.

Table 2. Pumping stations characteristics

Mine pumping station	Storage capacity(m ³)	Pumped water quantity for 2015 yr(m ³)
Amyntaio Mine	410.000	8.378.951
Kardias Mine	120.000	6.509.460
South Field Mine - N.Komvos	300.000	2.891.000
South Field Mine – E7	250.000	3.944.000
South Field Mine – E6	600.000	9.546.000
South Field Mine – E4	20.000	2.394.600
Mavropigi Mine	17.000	2.735.520



Figure 2. Amyntaio and South Field Mine E6 pumping stations.

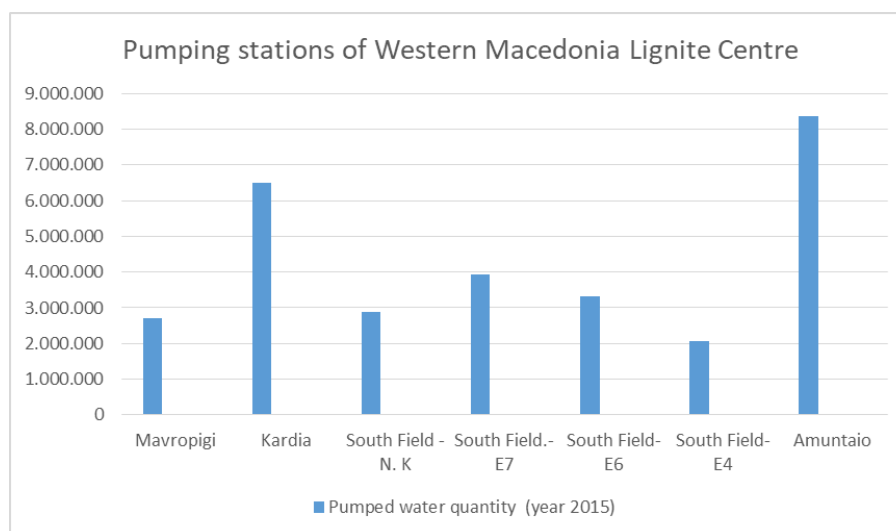


Figure 3. Total pumped water quantity of Western Macedonia Lignite Centre for 2015.

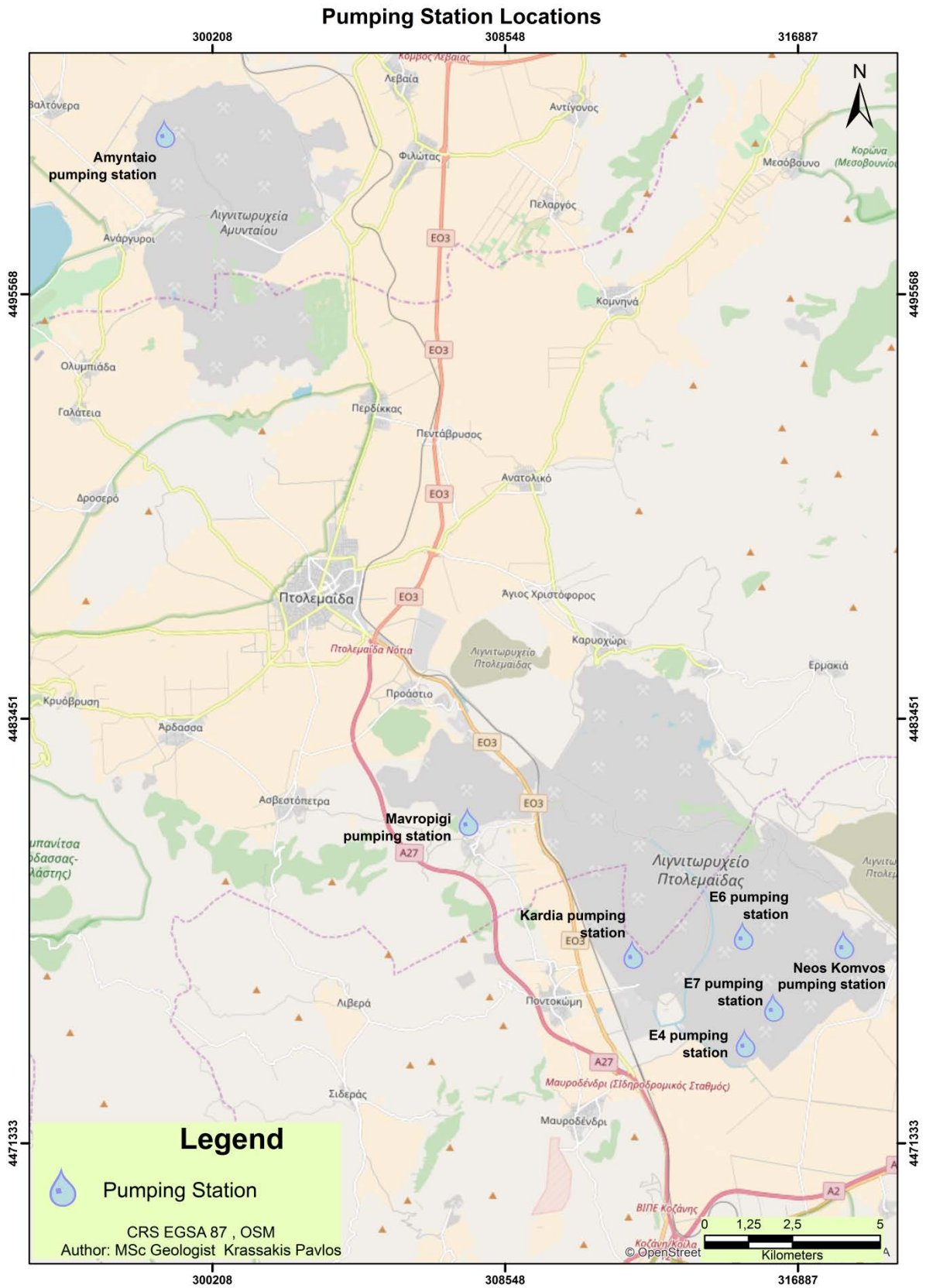


Figure 4. Pumping station of Western Macedonia Lignite Centre location.

1.3. Methodology - Results

During 2016, two series of water and sludge sampling took place in Western Macedonia Lignite Centre Mines in order to examine their quality. The first sampling campaign took place on 23/05/2016. Water and sludge samples were taken from the input and the output of each pumping station. It must be mentioned that on the previous day, on 22/05/2016, in the Prefecture of Kozani there was a heavy rainfall. The second series of sampling was held on 14-16/11/2016. The in situ measurements were made using portable laboratory equipment and included: pH, T ($^{\circ}$ C), conductivity (μ S / cm) and dissolved oxygen O₂ (mg /lit).

For the suspended particulates solids measurement, a filter with pore size of 0.45 μ m was used. The filter, after the filtration, was dried and weighed again. The difference in filter weight before and after filtration was the suspended solids in mg per litre of filtered sample. The measurement process was simple and lasted about 3-4 hours for each sample. The suspended particulates solids values for the two series samplings, were within the limits set by the local authorities for the protection of the aquatic receiver of mine water discharges (35mg/lit). The metal analyzes of the pumping water were done with the use of atomic absorption spectrophotometer.

Water analyses results

With respect to the quality of the pumping water, in both samplings, the values of both physicochemical parameters and particulate matter were within the limits set by the European Union. Based on the water analyses, the efficiency of pumping stations (Table 3) could be characterized very good. However, the results of the two series of analyses are not the same and the efficiency of pumping stations is differentiated. Regarding all the results of the second series of sampling, there is a decrease in pumping station efficiency, except for Kardia and Neos Komvos pumping stations. It should be mentioned that in E4 pumping station, the efficiency was changed from 87% in the first sampling to 7% in the second one. This is related to a problem revealed related to the dimensioning of the pumping station and its difficulty to assimilate large water quantities, as it happens in consecutive days of heavy rainfall.

Concerning total dissolved solids (TDS), as it is shown by the results of the field analyzes, during the second sampling, they are increased in the output compared to the input in Kardia, Mavropigi, Neos Komvos and E6 pumping stations. On the other hand, during the first sampling, the variations of the TDS input and output measurements are much smaller. In addition, some values of the total dissolved solids were up to the limits. These excesses were due to the presence of carbonate salts and are related to the alumino-manganic precipitates which are accumulated in the pumping stations [5].

Table 3. Sampling – Pump station efficiency.

Sampling	Sampling– Efficiency %															
	SS		TDS		Cd		Cr		Cu		Ni		Pb		Zn	
	1 st	2 nd	1 st	2 nd	1 st	2 nd	1 st	2 nd	1 st	2 nd	1 st	2 nd	1 st	2 nd	1 st	2 nd
Kardia	50	75	43	-33	15	97	61	126	31	13	55	2	-19	550	-4	36
E6	83	66	-7	8	10	20	35	-15	20	38	30	17	35	603	14	14
Neos Komvos	89	96	2	-12	29	78	26	48	33	75	5	6	35	55	15	42
E7	61	18	0	-45	9	89	60	8	3	16	32	63	20	-41	-10	-54
E4	87	7	-64	0	9	99	43	3	-36	2	-49	-52	24	51	-9	30
Mavropigi			3	-1	-14	67	44	13	34	25	-2	20	-10	44	-22	35
Amyntaio	62	72	-13	47	4	0	91	2	23	-90	63	-45	52	2	7	-59
Average	72	26			9	64	51	9	15	11	19	2	20			6

Regarding the other measured metals, pumping stations' efficiency for Cd and Cr is quite good. For the other metals, no differentiation is observed in neither of the two sampling series. At this point, it should be mentioned that the concentration of the metals in both series of samplings for all the pumping stations, are within the limits, set by the EU regarding drinking water quality. Moreover, all the results are analogous to the geology of the area and are consistent with similar studies carried out by Sachanidis et al (2015).

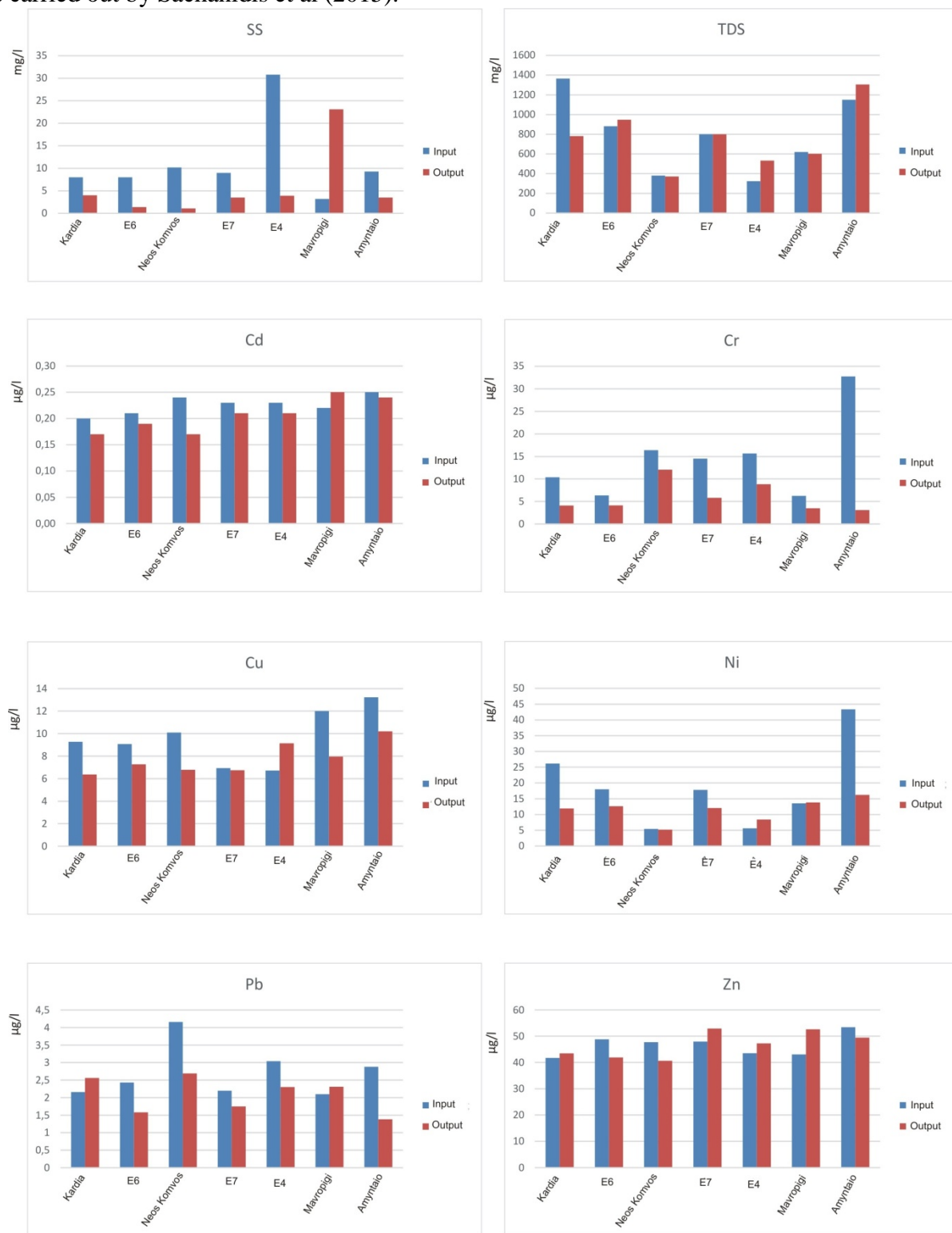


Figure 5. Chemical analyses results of first series of water samplings.

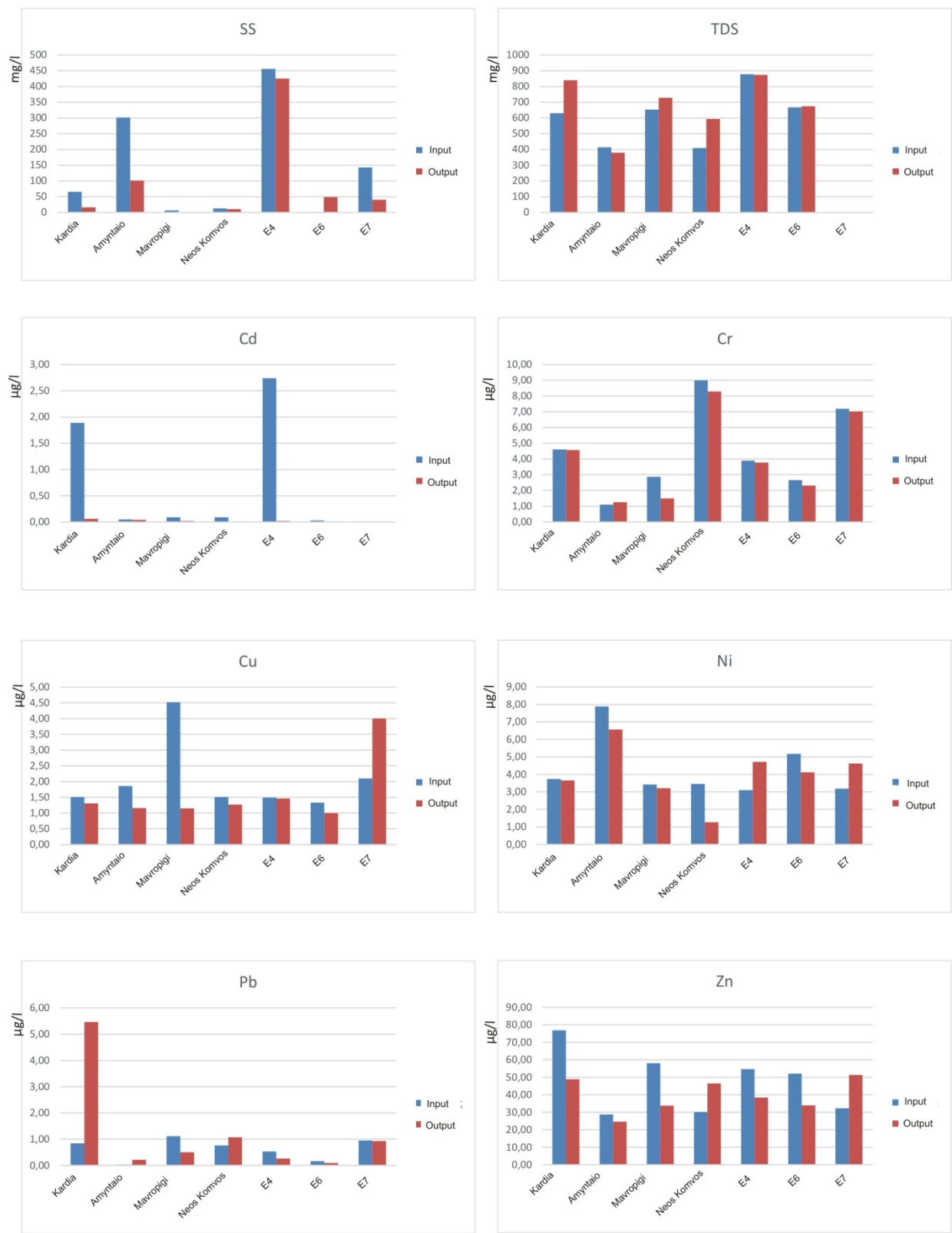


Figure 6. Chemical analyses results of second series of water samplings.

Sludge analyses results

For the sludge samples analyses, X-ray powder diffraction (XRD) analytical technique was used. The total number of samples was 28, where respectively 14 samples from each sampling phase

were studied. Based on the XRD results, an estimate of their mineralogical composition was made, as well as an estimate of the percentage of participation of the mineral phases in each sample.

Quartz and carbonate minerals (calcite, Mg-rich calcite, dolomite, ankerite) were found as the main mineral phases in almost all samples and specifically they were 40-80% of the mineral phases. In this point, it should be mentioned that in Amyntaio mine a relatively smaller proportion of carbonate minerals and higher of quartz and feldspars was found.

The content of feldspars (plagioclase and alkali feldspars) in most of the samples ranges from 5 to 15%. Most of the sludge samples also contain clinopyroxene and graphite but they usually did not exceed the 10%. The content of mica (biotite, muscovite), secondary and metamorphic (chlorite, epidote, garnet, staurolite) and clay minerals was found to be less than 10%.

Fe-Ti-Cr-Al-Cu-Zn-Ni-Mn-Mg oxides and hydroxides were identified at relatively low levels as non-essential phases (~ 1-5%). However, the sludge samples from E6, E7 and Mavropigi pumping stations, contain more than 5% minerals that contain Cu. Finally, the samples from E4 and Amyntaio pumping station contain minerals from the spinel group and Fe-Ti oxides about 10%.

1.4. Upgrade mine pumping station methods

Taking into account both the data and the corresponding requirements of the pumping stations of Western Macedonia Lignite Centre, the existing pumping stations could be characterized as sufficient. They are considered to be able to cope with the present mine conditions. It is proposed, however, to optimize the existing pumping stations operation in order to achieve better pumping systems function and reduce the degradation, operating and maintenance costs. In particular, the actions that are proposed are the following: a) Inverters installation in order to control engine operation at the desired speed level so as to achieve less power consumption and b) Soft starters installation as to protect the pump assemblies both in electrically and hydraulically way. This will bring the lowest power consumption during starting and stopping procedure.

Moreover, some maintenance work, which is considered to be necessary for each pumping station, must be carried out at regular basis. Specifically, the maintenance work includes: repair of coatings, paints, insulation, equipment leaks and overhead pipelines, regular inspection and cleaning, lubrication of moving pumping parts, usual pump oil control and electrical circuits fuses control.

In addition, another intervention that is proposed is the removal of suspended solid particles of pumping stations. The proposed method is addition of specific coagulant in order to have chemical precipitation. Two kinds of flocculants can be used in order to remove the suspended solid particles. They are calcium oxide ($\text{Ca}(\text{OH})_2$) and ferric chloride sulfate (FeClSO_4). These flocculants can achieve binding and removal of suspended solid particles and phosphates and the effective control of the floating sludge phenomenon in mine pumping stations.

2. CONCLUSION

Lignite mines dewatering efficiency in Western Macedonia Lignite Centre is based on a complex pumping system with specific capacities. In order to evaluate the pumping system operation of Western Macedonia Lignite Centre mines, chemical and mineralogical analyses of two series of water and sludge samplings were conducted. The physicochemical parameters and the concentration of suspended particulates solids were within the limits set by local authorities for the protection of the aquatic receiver of mine water discharges. Moreover, all the water results are analogous to the geology of the area. Quartz and carbonate minerals were found as the main mineral phases in almost all samples followed by feldspars with percentage ranging from 5 to 15%. Consequently, the existing pumping stations could be characterized sufficient and suitable to the present mine conditions. In order to achieve the optimization of mine pumping system regular maintenance work and total

removal of suspended solid particles of pumping stations with the use of specific flocculants is suggested.

REFERENCES

- [1] Darakas, E. (2000). Environmental Engineering, Section 5: Sedimentation - Sedimentation Tanks, Open Academic Courses, Department of Civil Engineering, Aristotle University of Thessaloniki.
- [2] Ioakeimidis, I. (2015). Study of transgenic processes within the reservoirs of the oil basin of Prinos - Kavala, Specialization Dissertation, Postgraduate Studies, Specialization Branch: Mineral Resources and Environment, Aristotle University of Thessaloniki.
- [3] Steenbrinck, J., Hilgen, F.J., Krijgsman, W., Wijbrans, J.R., Meulenkamp, J.E. (2006). Late Miocene to Early Pliocenedepositional history of the intramontane Florina-Ptolemais-Servia Basin, NW Greece: Interplate between orbital and forcing tectonics. In: Paleogeography, Paleoclimatology, Paleoecology, Elsevier, 238 (2006), 151-178.
- [4] Koukouzas, N., Colin, R., Zhongsheng, L. (2010). Mineralogy of lignites and associated strata in the Mavropigi field of the Ptolemais Basin, northern Greece, International Journal of Coal Geology, Volume 81, Issue 3.
- [5] Sachanidis, C.G., Sachanidis, C., Pavloudakis, F., Andreadou, S., Triveli, A., Roubos, C., Kofidou, S. (2015). Environmental quality monitoring in surface lignite mines of Ptolemais basin (in Greek), 2nd Environmental Conference of Thessaly, Skiathos, 26-28 September 2015.

Alfeios River Sectional Diversion for the Expansion of the Continuous Surface Mining Operations of Megalopolis Mines in the Peloponnese Peninsula, Greece

Anthimos Spyridis¹, Christos Roumpos², Vasiliki Koutalou¹, Aikaterini Liakoura² and Nikolas Arampelos¹

¹"HYETOS S.A.", Ippodromiou sq. 7 Thessaloniki, 54621, Greece

² Mining Engineering Department, Public Power Corporation, Greece

ABSTRACT

Strategic planning and operation of continuous surface mining projects are in many ways influenced by the Geological, Geotechnical, Hydrogeological and Hydrological conditions of the mineral deposit and the mining field. The Hydrological conditions prevailing in lignite deposits with extensive horizontal spatial distribution often relate to streams or rivers which are mainly associated with the formation of the deposits. They have a significant effect on: (a) the long term planning and mining sequence from the initial cut to the depletion of the mine, (b) the boundaries of the mining field which may change during planning and operations processes, (c) the slope stability of the excavations, (d) the mine closure and land reclamation.

This paper investigates the hydrological conditions related to the development of Megalopolis continuous surface mines, in the Peloponnese Peninsula, Greece. The analysis is focused on the successive diversions of Alfeios River for the expansion of the lignite mining activities and the corresponding risk factors. Alfeios is the longest river in the Peloponnese. The river is about 110.00 km long, flowing through the regional units of Arcadia and Elis. Its origin is located close to the village of Dorizas, about halfway between Tripolis and Megalopolis, in the highlands of Arcadia.

Emphasis is placed on the considerations, the methodology and the final design for the planned sectional diversion of Alfeios River, for the extension of the boundaries of the Choremi mine. In order for the mining activity to expand towards the south-most part of the Megalopolis Mine Complex (Choremi mine), it is necessary for a section of approximately 2.70 km of the Alfeios River channel to be relocated further to the south. The study for the abovementioned diversion takes into consideration the Hydraulic, Geotechnical and Structural aspects of the complete project.

Particularly, as far as the Hydraulic design is concerned, a detailed hydrological analysis was conducted for the calculation of the flood runoff, using the Soil Conservation Service (SCS) unit hydrograph method. The design flow values were estimated for design periods T of fifty (50) years and one hundred (100) years. The flow of Alfeios River was simulated using one-dimensional, step by step, steady flow analysis for open channels.

Furthermore, for the verification of the overall design, all the necessary Geotechnical considerations were addressed. Detailed, long-term, steady state seepage models were constructed, both for non-ruptured and ruptured lining, in order to determine the maximum possible level of the water table due to the hydraulic load in the channel. In addition, extended stability analyses were performed for the diverged channel slopes, the embankments and the southern mine slopes, taking into account the pore water pressure conditions dictated by the aforementioned steady state seepage analysis. The performance of the clay lining was estimated and special erosion control measures were prescribed considering the flow conditions in the channel.

Finally, the energy dissipation works at the confluence of Alfeios River and two significant secondary streams in the area (Kserilas Stream and Ag. Giannis Stream), were designed and verified by specific structural analysis, according to Greek and European Codes.

1. INTRODUCTION

Lignite (brown coal) exploitation is of primary interest in Greece as lignite currently contributes in the production of more than 30% of domestic electricity demand [1]. Continuous surface mining operations are dynamic complex systems, with a long-term horizon. They are related to many technical, environmental and other uncertainties connected with the dynamic situation that they present. The required investments for the corresponding mining operations are characterized by high risk. In this framework, the determination of the mine limits before the beginning of the exploitation is a very interesting and challenging problem. Furthermore, the mining operations are in many ways influenced by the geological, geotechnical, hydrogeological and hydrological conditions of the mineral deposit and the mining field. Thus, geotechnical and hydrogeological investigations are a critical issue of the mine planning process in relation to the sustainability of surface mining projects [2]. The spatial distribution of the mineral deposit characteristics, especially in the boundaries of the mining area, is very important for defining the final mine limits.

Strategic planning and design of such projects, referring to the sequence of mine exploitation, that begins with the opening phase of the mine) and continues through all exploitation life, require an integrated approach conditions [3]. The changing technical, environmental, economic and social conditions affect the economic performance of the projects. The optimal sequence of mine operations in continuous surface mines in relation to the location of basic mining infrastructure is a very interesting optimization problem. Simulation techniques and optimization algorithms could be applied as an integral part of mine planning and design process [4].

The hydrological conditions prevailing in lignite deposits with extensive horizontal spatial distribution often relate to streams or rivers which are mainly associated with the formation of the deposits. They have a significant effect on: (a) the long term planning and mining sequence from the initial cut to the depletion of the mine, (b) the boundaries of the mining field which may change during planning and operations processes, (c) the slope stability of the excavations, (d) the mine closure and land reclamation.

This paper investigates the hydrological conditions related to the development of Megalopolis continuous surface mines, in the Peloponnese Peninsula, Greece. The analysis is focused on the successive diversions of Alfeios River for the expansion of the lignite mining activities and the corresponding risk factors. Alfeios is the longest river in the Peloponnese. The river is about 110.00 km long, flowing through the regional units of Arcadia and Elis. Its origin is located close to the village of Dorizas, about halfway between Tripolis and Megalopolis, in the highlands of Arcadia.

In Fig. 1 the mine limits of the initial mining study (1978) as well as their extensions are presented in relation to the hydrographic network. The final diversions of the rivers are required in order to recover the currently exploitable reserves.

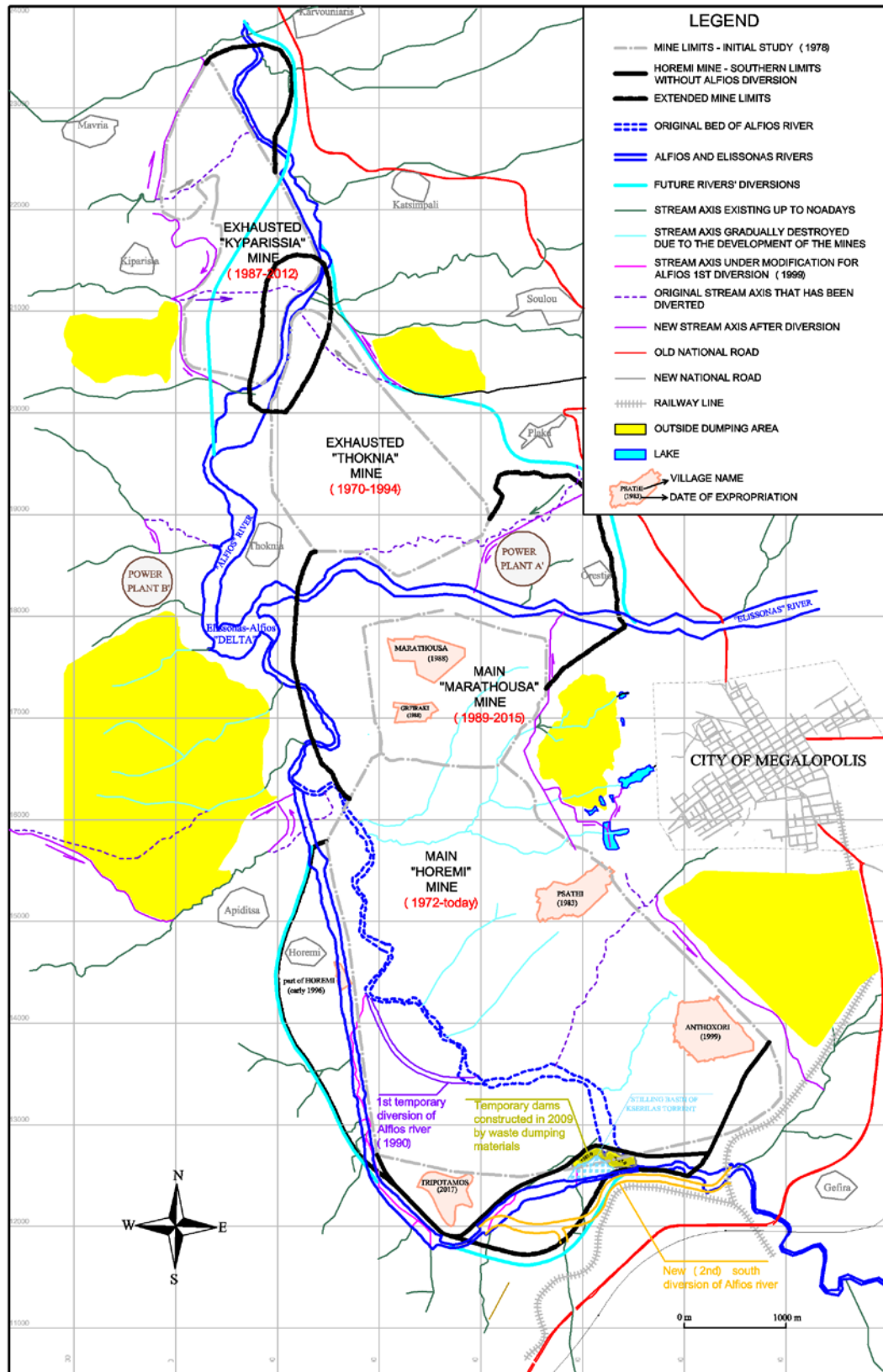


Figure 144. General map of Megalopolis mines and hydrographic network

2. PRESENT CONDITIONS

At present, the southern boundaries of the Choremi mine are adjacent to the existing channel of Alfeios River. For the expansion for the mining activity to expand towards the south-most part of the Megalopolis Mine Complex (Choremi mine), it is necessary for a section of approximately 2.70 km of the Alfeios River channel to be relocated further to the south (Fig. 2).

Moreover, the junction of the two secondary streams in the area, Kserilas Stream and Ag. Giannis Stream and the existing Alfeios River channel, is formed naturally, without adequate scour and erosion protection and lacking specific hydraulic design considerations.

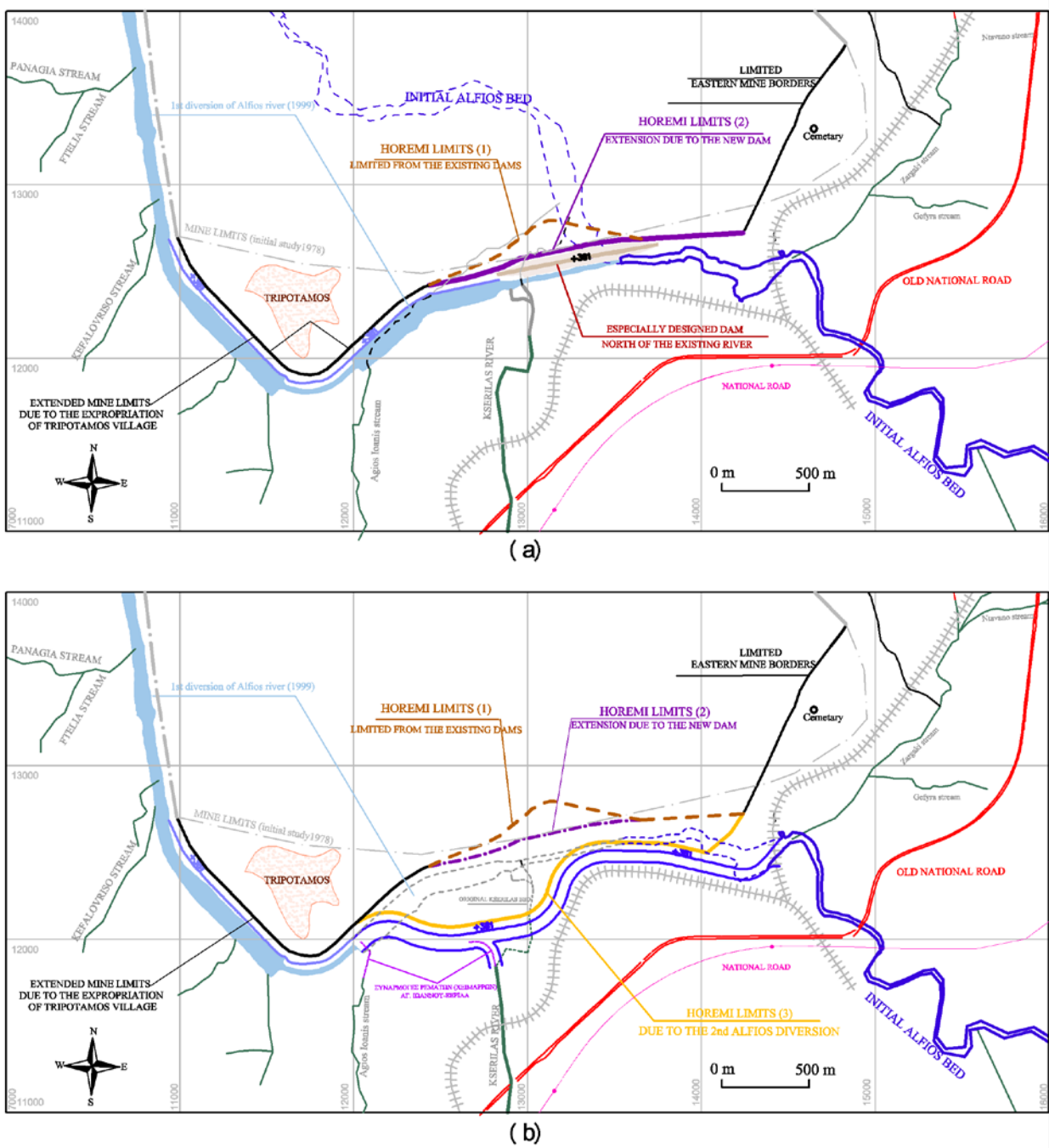


Figure 145. (a) Especially constructed new dam in Alfeios borders and (b) new (2nd) south diversion of Alfeios river.

3. PROPOSED DIVERSION WORKS

The relocation of Alfeios River is divided into two main sections along its axis, separated by the junction with the Kserilas Stream (Figs 3 & 4). The origin of the new trench is located approximately 1,200 m downstream to the existing relocation projects. The first 1,500 m of the new trench axis is parallel to a railway line found to the south of the mine, with a general northwest direction. It continues to the southwest until it is joined by Kserilas Stream to flow towards the west into the entrance of an existing triple box culvert. Prior to the entrance of the culvert, the Ag. Giannis Stream intersects from the South.



Figure 146. Layout of the south-most part of the Megalopolis Mine Complex. The red line designates the existing Alfeios channel. The blue line to the south corresponds to the axis of the sectional diversion project.

For the first section, prior to the intersection with the Kserilas Stream, the hydraulic cross-section is trapezoidal, with a bottom width of 10 m and a slope inclination of 3:1 (base : height). For the second section of the relocation, the trench cross-section is of similar design with an increased bottom width of 25 m.

The total length of the relocated trench is about 2,664 m and the channel's bottom inclination is set at 0.15%, with a starting bottom level of +373 m and a bottom level of +369.45 m at the entrance of the existing triple box culvert.

For the first section of the relocation project, the freeboard is set at 1.75 m, while the corresponding freeboard for the second section (wider bottom trench), is set at 1.89 m. The corresponding maximum trench depth at various locations of the project ranges from 8.36 m to 11.38 m. At the crest of the trapezoidal trench, an 11.40 m wide berm is designed, in order to provide access for maintenance purposes along the axis of the project.

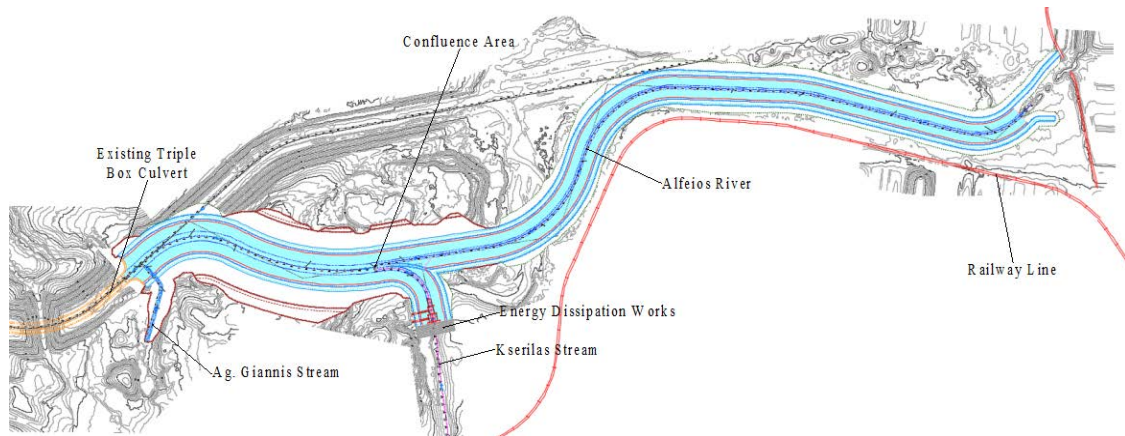


Figure 147. Plan view of the sectional diversion works.

The cross-section profile of the project is generally formed with 3:1 inclination benches of 15 m height separated by 8 m width berms (Fig. 5).

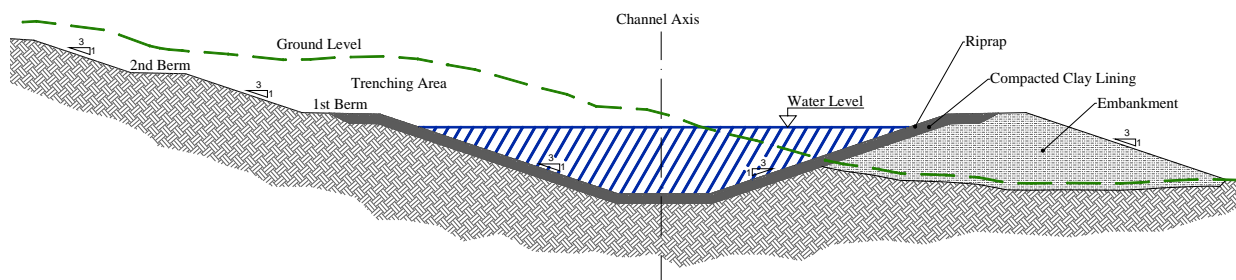


Figure 148. Indicative cross-section profile of the new channel of Alfeios River.

Throughout the project, where the proposed cross-section profile is not occurring solely through excavation works, the construction of suitable embankments is proposed, consisting of heavily compacted excavation materials from the A-6 or A-7 classes of the AASHTO soil classification system [5]. As far as the construction and the foundation of the embankments is concerned, all the necessary actions prescribed in the national technical specifications are going to be met.

The hydraulic insulation of the proposed new trench consists of compacted clay lining (CCL) with a thickness of 1.10 m and hydraulic conductivity $k \leq 10^{-9}$ m/s. The clay material will be provided from excavation products with the appropriate on-site treatment. The lining layer resides on geotextile fabric sheets. The thickness and specifications of the lining material were specifically chosen in order to achieve acceptable underground hydraulic conditions, regarding total stability and minimization of water flow towards the Choremi mine pit, related to the hydraulic load of the new river trench.

For the purpose of scour and erosion protection, a 0.30 m thick layer of suitable grading rock riprap was prescribed.

The insulation layer and the scour and erosion protection layer are separated by non woven, needle punched geotextile fabric sheets, which are anchored at the crest of the trench.

Similarly, at the Kserilas - Alfeios confluence area, the trench is insulated with compacted clay lining and protected by means of rock filled Reno type mattresses, instead of plain rock riprap. The

confluence area is specifically designed in order to facilitate the gradual join of the energy grade lines of the two streams.

Finally, the energy dissipation works at the confluence of Alfeios River and the two significant secondary streams in the area, Kserilas Stream and Ag. Giannis Stream, were designed and verified. Specifically for the Kserilas Stream, a reinforced concrete step by step layout combined with material-retaining basins was designed, as well as slope and bottom protection works. The design facilitates the necessary access for maintenance purposes. Similarly, for Ag. Giannis Stream, a step by step energy dissipation system formed by rock filled gabions and Reno type mattresses was prescribed.

4. HYDRAULIC ANALYSIS

4.1. Design Flow

For the calculation of the flood runoff, detailed hydrological analysis was conducted. The area of interest is situated in the Megalopolis region, in the highlands of Arcadia. Two main catchment basins of great significance to the hydrological model are found. The first basin ($\Lambda 1$ 194.77 km²) drains off into Alfeios River while the second ($\Lambda 2$ 142.70 km²) drains off into Kserilas Stream. In order to calculate the flood runoff, both in the upstream and downstream to the confluence sections, the Soil Conservation Service (SCS) unit hydrograph method was used. The hydrograph was calculated for each of the abovementioned basins. The flood runoff downstream to the confluence section was estimated using the synthesis of the two individual hydrographs of the respective basins ($\Lambda 1$ & $\Lambda 2$). Finally, the flood runoff of the Ag. Giannis Stream ($\Lambda 3.1$ 1.03 km²) was calculated using the rational method, due to its insignificant basin area.

The design flow values were estimated for design periods T equal to fifty (50) years and one hundred (100) years respectively and sediment transport flow was also taken into account. The estimation of the maximum sediment transport flow for a design period equal to that of the hydrological investigation was conducted using the Stiny-Herheulidze method [6]. The design flow values for the relative basins for design periods T of 50 and 100 years are shown in the Tables 1 & 2.

Table 1. Design flow values for T=50 years

Location	Flood Runoff (m ³ /s)	Sediment Transport Flow (m ³ /s)	Design Flow Values (m ³ /s)
Alfeios River Upstream ($\Lambda 1$)	314.73	37.47	352.20
Kserilas Stream ($\Lambda 2$)	231.86	27.60	259.46
Alfeios River Downstream ($\Lambda 1+\Lambda 2$)	514.04	61.20	575.24
Ag. Giannis Stream ($\Lambda 3.1$)	4.58	0.55	5.13

Table 2. Design flow values for T=100 years

Location	Flood Runoff (m³/s)	Sediment Transport Flow (m³/s)	Design Flow Values (m³/s)
Alfeios River Upstream ($\Lambda 1$)	383.86	45.70	429.56
Kserilas Stream ($\Lambda 2$)	290.09	34.53	324.62
Alfeios River Downstream ($\Lambda 1+\Lambda 2$)	633.93	75.47	709.40
Ag. Giannis Stream ($\Lambda 3.1$)	5.17	0.61	5.78

4.2. Freeboard Calculation

The calculation of the freeboard level in the diversion channel is in accordance with the "Design Standards No.3 Canals and Related Structure, United States - Department of the Interior, Bureau of Reclamation, 1967" [7].

4.3. Roughness Coefficients Calculation

The estimation of the Manning's n coefficient was performed using the Blodgett, 1986a formula, as suggested by the issue of the "Federal Highway Administration", entitled "Hydraulic Engineering Circular No. 15, Third Edition - Design of Roadside Channels with Flexible Linings" [8]. In this formula, the n coefficient is dependant of the water level and the D₅₀ granule size of the protective layer (Table 3).

Table 3. Roughness Coefficients

Location	Lining Type	Manning's n
First section	Rock riprap D ₅₀ = 0.10	0.041
Second section	Rock riprap D ₅₀ = 0.15	0.037
Kserilas Stream step by step (bottom)	Reinforced Concrete	0.016
Kserilas Stream (slopes)	Reno type mattresses	0.025
Confluence area	Reno type mattresses	0.025
Ag. Giannis stream	Gabions	0.025

4.4. HEC-RAS Hydraulic Simulation

In order to estimate the hydraulic capacity of the proposed cross-section, a hydraulic simulation was performed using the step by step method for steady state conditions. The method was applied using the HEC-RAS software of the U.S. Army Corps of Engineers [9].

The total simulated length of Alfeios River and Kserilas Stream is approximately 3,343 m and 377 m respectively. Furthermore, fifty seven (57) individual cross-sections were used for the simulation of Alfeios River and twelve (12) for the Kserilas Stream. The distance between each cross-section is chosen to be less than fifty (50) meters according to national specifications. In

addition, suitable boundary conditions were used in the simulation model as far as channel inclination, flow depth and junction points are concerned.

The use of the uniform hydraulic model allowed the determination of the flow profile and the maximum water level for each cross-section, using the flood design flow values for both T=50 and T=100 years design periods.

Especially regarding the Kserilas Stream confluence works, two simulations were deemed necessary. For the first simulation, simultaneous flow from both Alfeios River and Kserilas Stream has been included in the hydraulic model (Fig. 6). In this uniform hydraulic model, water level elevation is formed because of losses due to the entry in the existing triple box culvert, while the flow in Alfeios is subcritical, resulting in flow velocity reduction along with significant flow depth increase.

The second simulation was performed considering dry conditions in the Alfeios River, in order for the flow velocity and water level in Kserilas Stream to remain unaffected. Thus, maximum velocity and flow profile in the step by step energy dissipation area are successfully calculated. This type of data was also of great significance to the formation of realistic scenarios used for the stability and structural analysis of the energy dissipation works.

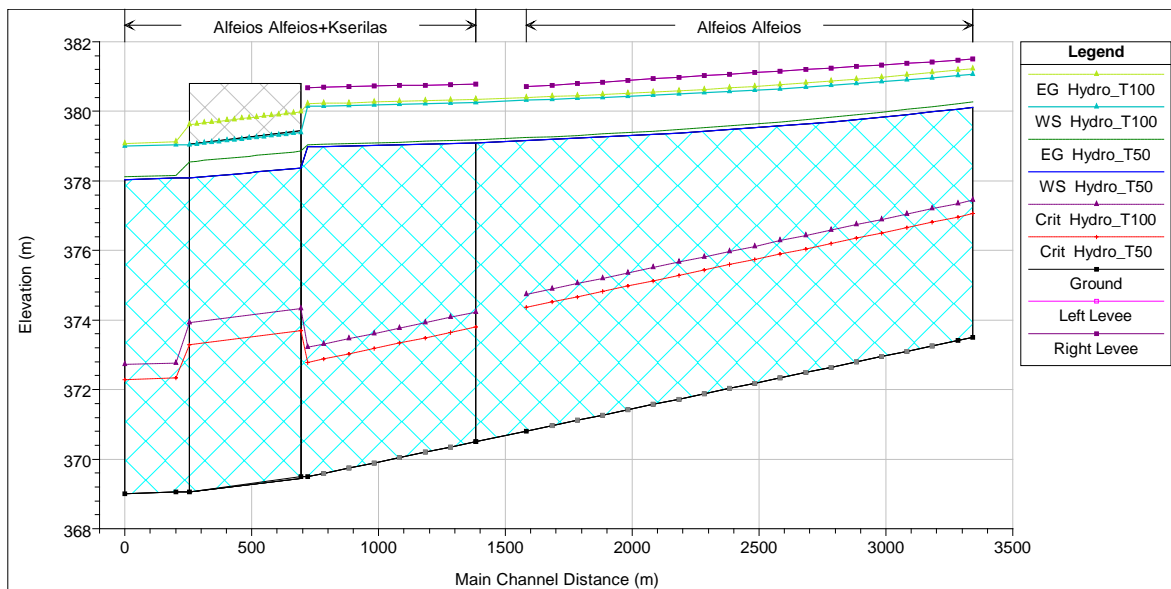


Figure 149. Hydraulic profile of the diverted section of Alfeios River (Scenario 1- Simultaneous flood flow in Alfeios River and Kserilas Stream).

5. GEOLOGY & GEOTECHNICAL CONSIDERATIONS

The geotechnical aspect of the project concerns the complete and safe design of all the technical parameters and structural details for the new sectional diversion of Alfeios River trench. In particular, the specific definition of the proposed materials and all the necessary works throughout the project are addressed, as well as the stability and strength analysis for all of the retaining and reinforcement elements of the project.

Detailed, long-term, steady state seepage models were created, both for non-ruptured and ruptured lining, in order to determine the maximum possible level of the underground water table, due to the hydraulic load in the channel.

In addition, extended stability analyses were performed for the diverged channel slopes, the embankments and the southern mine slopes, taking into account the pore water pressure conditions dictated by the aforementioned steady state seepage analysis.

The overall geotechnical design, addresses the definition of the technical parameters for the insulation, scour and erosion protection works, taking into account the mechanical and permeability characteristics of the subsoil materials and the flow conditions in the channel. Moreover, the performance of the clay lining was estimated and found to be adequate.

5.1. Geological - Geotectonic Data

According to data collected from the geological map sheet “MEGALOPOLIS” (1:50.000 scale) of the Institute of Geology & Mineral Exploration [10], the terrain of the broader area of interest consists of alluvial deposits, more specifically, unbound aluminum-silicate materials, gravel, crockers and variations of marigolds, clays, humus clays and lignite with sand and conglomerates.

The area of interest belongs to the wider geotectonic areas of Pindos and Gavrovo - Tripoli (Domestic Greek). Tectonically, Pindos zone is lying on the Gavrovo - Tripoli zone. The general axes of the faults is of NW - SE direction which are directly related to the majority of carbonaceous sources. The tectonic of the region is particularly active until today and has played a key role in shaping the geomorphological profile, the development of the hydrographic element and the formation of hydrogeological conditions. It is worth noting that the area is characterized by rugged and uneven terrain, which is due to the intense tectonism, and also because of the quite coherent geological formations that prevail in the area and create slopes with great inclination.

5.2. Earthquake Data

The diversion of Alfeios River project takes place in the Megalopolis area, in Arcadia region. According to the Greek Antiseismic Regulation [11], the project's area corresponds to the Second (II) Seismic Zone depending on the local hazard resulting in reference peak ground acceleration (PGA) equal to 0.24 g (Fig. 7). Finally, the subsoil is generally of "Γ" to "Δ" type, consisting mainly of medium to high plasticity clay, sands and scarce pockets of gravel.

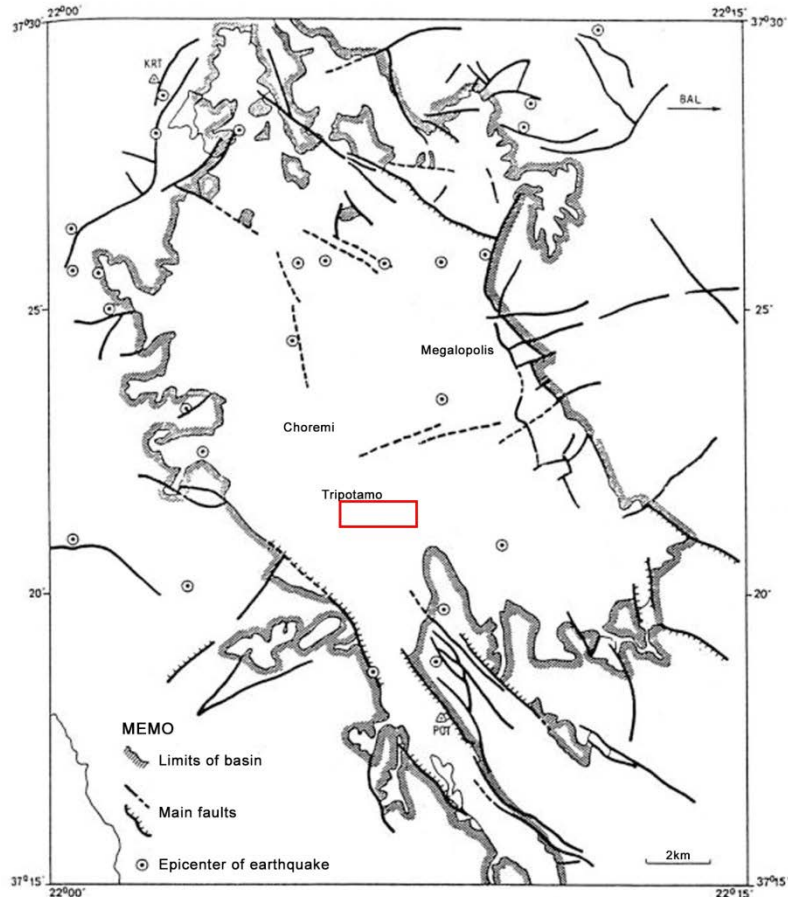


Figure 150. Map of the main faults and epicenters of seismic activity from February - August 1980 period. The project area is marked in the red rectangle.

Furthermore, taking into consideration the distance of the project area to potentially active faults, further increase in the design seismic action is deemed unnecessary.

5.3. Steady State Seepage and Stability Analysis Modeling

Detailed, two dimensional, long-term, steady state seepage models were constructed, both for non-ruptured and ruptured lining, in order to determine the maximum possible underground water table level due to the hydraulic load in the channel (Figs 8 & 9). In total, four (4) finite element analysis models were constructed, corresponding to four (4) cross-sections along the axis of the project in order to cope with potentially varying conditions as far as geometry, subsoil stromatography and underground water are concerned. Of particular importance are the cross-sections that refer to the highest embankment and deepest trench locations.

The results of the steady state seepage models acted as initial conditions for corresponding overall stability models for the trench slopes, the embankment slopes and the southern Choremi mine slope profile.

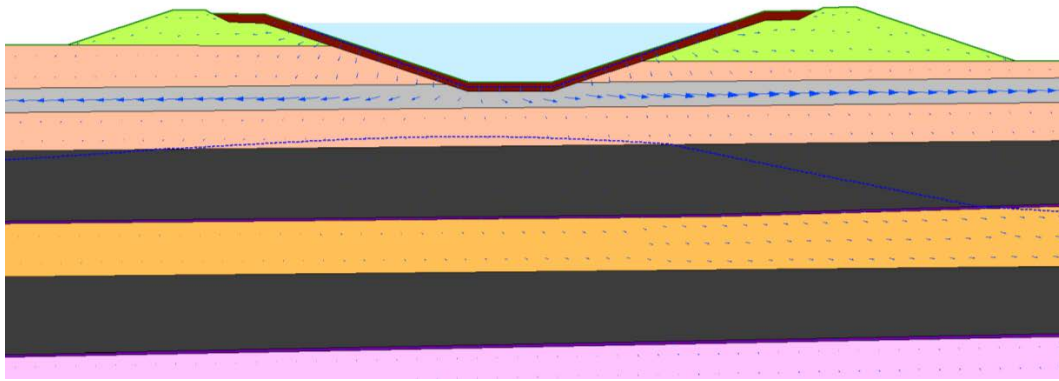


Figure 151. Cross-sectional profile results of the steady state seepage analysis (Intact CCL).

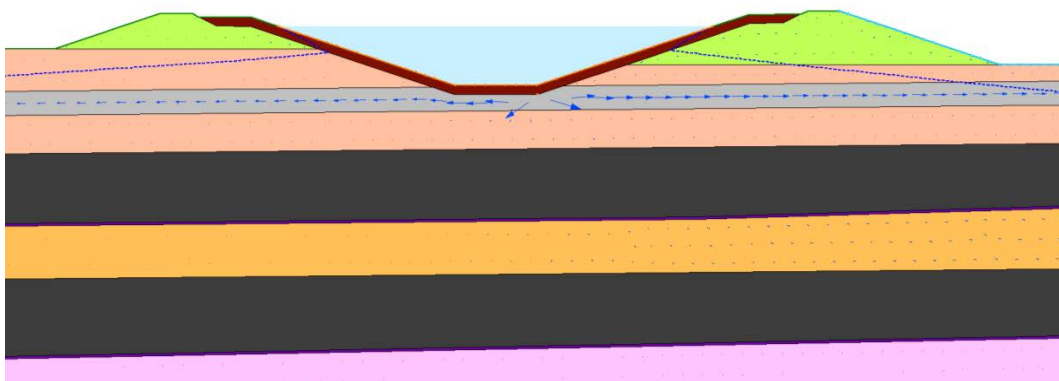


Figure 152. Cross-sectional profile results of the steady state seepage analysis (Ruptured CCL).

The subsoil mechanical parameters of the seepage and stability models were deduced from specific geotechnical investigation [12] and in accordance with Ore Deposit Drilling Results [13] and the work of prof. Kavvadas which concerned the stability of the final slopes of the Megalopolis Lignite Center in the regions of the villages of Choremi, Tripotamos and Thoknia [14] and the report for the landslide at the Megalopolis Lignite Center [15]. Of great importance to the stability analysis modeling, is the thin clay layer of poor mechanical properties found below and sometimes above the lignite deposit layers, that is believed to be mainly responsible for the landslide events of the 14th of September of 2013 [16].

As far as the underground water table is concerned, data from the environmental impact assessment study for the drainage of the Megalopolis mines [17], clearly show that the south part of megalopolis mine is lacking of a definite phreatic line. Instead, there are isolated, localized pockets of saturated sandy-clay materials that should not pose as major stability threats provided that suitable measures are taken at the time of excavation. Thus, the results of the steady state seepage analysis models were chosen to be fed as very unfavorable initial conditions to the stability models, considering that they are produced by a constant, steady hydraulic load, corresponding to a flood flow with design period T of 50 years.

A different approach would dictate the use of transient analysis with a time dependant hydraulic load produced from flow hydrographs, that would perhaps lead to lower level water table and more favorable initial condition scenarios than the ones produced from the steady state seepage analysis. Driven by the need to achieve the safest possible design for the sectional diversion project of Alfeios River, the results from the steady state seepage models were chosen to be integrated in the stability analysis models. It is worth mentioning that steady state seepage analysis was conducted for both intact and ruptured lining condition. The latter naturally led to even higher and more unfavorable underground water level table, though it is important to keep in mind that as the seepage

model is two dimensional, the crack in the liner is considered to extend in the out of plane dimension along with the length of the trench. This, of course, is highly unlikely to occur in reality, especially taking into account the self-healing nature of CCL.

Furthermore, by implementing analytical finite element seepage models, the evaluation of performance of the insulating layer was possible. The simulated results clearly reveal great improvement in the expected conditions in the mine pit compared to existing pumping log data.

Moreover, extended stability analyses according to the Greek Guidelines for the design of Highway Projects [18] were performed for the diverged channel slopes, the embankments and the southern mine slopes, taking into account the pore water pressure conditions dictated by the aforementioned steady state seepage analyses.

As far as seismic loading is concerned, pseudo-static analysis is used in accordance with the Greek Antiseismic Regulation [11].

Additional regulatory traffic loads are used on the crest of all of the embankments in accordance with the Greek Guidelines for the design of Highway Projects [18].

According to the extensive stability analysis for the diverged channel slopes (Fig. 10), the embankments and the southern mine slopes, all the regulatory factors of safety for static, dynamic and rare hydraulically unfavorable conditions were met. Some needed, localized modifications, of minor importance were revealed concerning the final design of the uppermost part of the Choremi mine slope, but these are in no way related to the diversion project itself. The above seems to be a product of particularly unfavorable considered mechanical characteristics for the relevant soil layers, along with exaggerated seismic action (return period of 475 years) and hydraulic conditions, but nevertheless it must be considered as advisable action during the expansion of the mining operation.

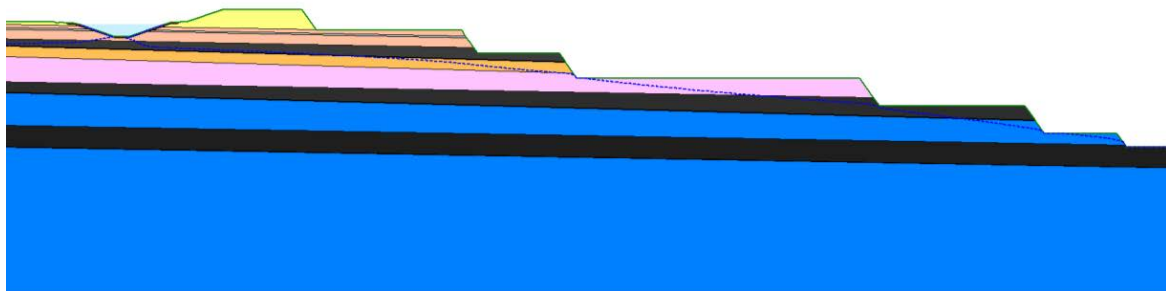


Figure 153. Cross-sectional profile for the stability analysis of the diverged channel slopes, the embankments and the southern mine slopes.

As far as the stability of the scour and erosion protection measures is concerned, FHWA HYDRAULIC TOOLBOX software was used in order to determine the relevant factor of safety between the maximum shear stress and the permissible shear stress in the channel. The general methodology used, is described in the FHWA-NHI-05-114/2005 "Design of Roadside Channels with Flexible Linings" [19] manual. Based on the results of the hydraulic analysis, throughout the diversion project, the overall design of the scour and erosion protection lining is proven to be successful as far as stability is concerned.

6. KSERILAS STREAM ENERGY DISSIPATION WORKS

The energy dissipation works at the confluence of Alfeios River and Kserilas Stream are of great significance and were designed and verified by specific stability and structural analysis, according to Greek and European Codes. The need for such works is dictated by the significant bottom level difference of over 4 m between the two channels. Two alternative solutions were examined from a technical and economical aspect.

The first solution consists of a typical USBR type IV stilling basin layout [20] (Fig. 11). While, this solution seemed adequate in the initial stages of design, it quickly became apparent that it led to bulky and costly structures that were not suitable for the non permanent nature of the relocation project.

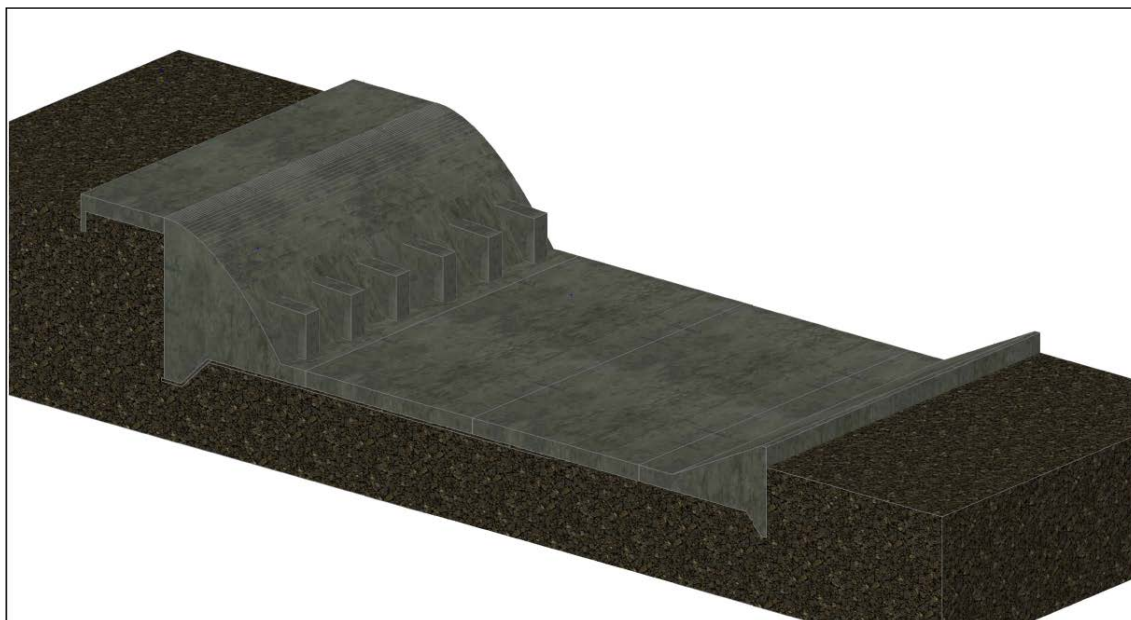


Figure 154. Three-dimensional representation of the typical USBR type IV stilling basin layout of the first alternative solution.

The second alternative solution, which is the solution of choice for this particular project consists of a combination of light reinforced concrete structures and embankments with scour and erosion protection layering (Fig. 12).

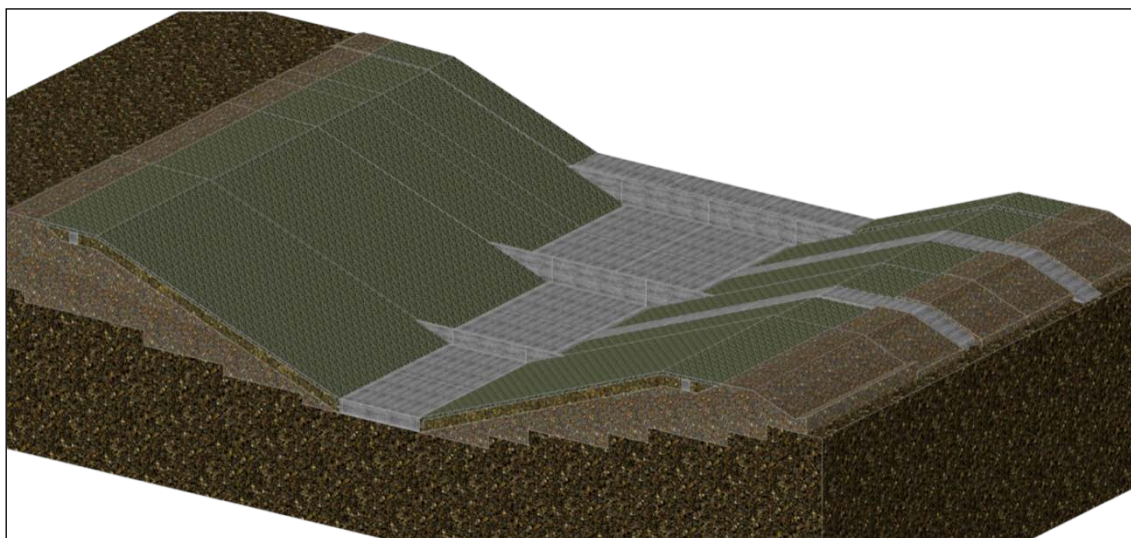


Figure 155. Three-dimensional representation of the prescribed energy dissipation works in Kserilas Stream.

The total length of the prescribed energy dissipation structures is equal to 65.00 m, with an elevation difference between the entry point and the exit point equal to 4.15 m.

Specifically, the abovementioned layout consists of three (3) consecutive steps, configured by three different types of reinforced concrete retaining walls, with a total height of 3.50 m each, measured from the foundation to the crest. Beneath each wall, transversal cut-off curtains were

designed, in order to further contribute to the overall stability while minimizing failure hazard due to piping phenomena. Between each step, reinforced concrete stilling and sediment basins of adequate dimensions and capacity are designed.

The layout is laterally bound by embankments of similar design characteristics to the rest of the project. The crest width is equal to 11.40m and slope inclination is set to 3:1 (base : height). The utilization of materials from structural excavation is deemed suitable for the construction of the embankments, being from the A-6 or A-7 classes of the AASHTO soil classification system. As far as the construction and the foundation of the embankments is concerned, all the necessary actions prescribed in the national technical specifications are going to be met. For the slope scour and erosion protection, rock filled Reno type mattresses are prescribed to be layered above well compacted clay liner.

Regarding the maintenance of the stilling and sediment basins, two reinforced concrete access roads of 4.00m width each are designed on the eastern embankment.

The concrete strength for the entire project is selected to meet the C40/50 class, based on the strict regulatory demands of the Greek Concrete Technology Regulation published in 2016 [21]. Emphasis is given on durability requirements, which relate to the environmental conditions that the structure is exposed to. In particular, the selected exposure classes best describing this particular project are XC2, XC4, XF1, XF3, XA1 and XM2. The structures will be reinforced with steel rebar of the B500c strength class.

The energy dissipation works were designed as to meet several hydraulic, structural and geotechnical criteria. Specifically, the whole structure is a product of detailed hydraulic design and is verified against overall stability, overturning, sliding, foundation soil overstressing, piping, scour and erosion hazard and structural failure. All of the above verifications concern four specifically chosen state scenarios.

The first scenario represents the transitional stage from dry conditions to a fully flooded state in Kserilas Stream. In this scenario, Alfeios River is considered to be dry and the energy dissipation works are working at full capacity.

The second and third scenarios represent conditions of normal flow in Kserilas Stream. In these scenarios, Alfeios River is considered to be dry and the energy dissipation works are working in their normal state. The two distinct scenarios concern either dry or saturated subsoil conditions.

The fourth and final scenario represents fully flooded steady state conditions both in Kserilas Stream and Alfeios River.

The above scenarios were verified for both static and dynamic conditions where it was deemed necessary.

7. CONCLUSION

All of the described Hydraulic, Geotechnical and Structural considerations, as well as the methodologies implemented for the final design of the planned sectional diversion of Alfeios River, clearly reveal the complexity of such an endeavor. However, the holistic scientific approach that was undertaken, will surely lead to a successful implementation of the final design and an overall safe and complete project so that the mining activity will expand towards the south-most part of the Megalopolis Mine Complex.

LICENSING

The diversion project, as described, is included in the following Environmental Permit, according to the M.D. of Ministry of Environment & Energy: 8684/27-04-2018 [22].

REFERENCES

- [1] Roumpos C., Pavloudakis F., Liakoura A., Nalmpanti D., Arampatzis K. (2018). Utilisation of lignite resources within the context of a changing electricity generation mix, 10th Jubilee International Brown Coal Mining Congress" Belchatów ", Belchatów, Poland; 04/2018, 355-365
- [2] Roumpos C., Papacosta E (2013). Strategic mine planning of surface mining projects incorporating sustainability concepts, Proceedings, 6th International Conference on Sustainable Development in the Minerals Industry (SDIMI 2013), 30 June – 3 July 2013, Milos Island, Greece: 645–651.
- [3] Roumpos C., Pavloudakis F., Galetakis M. (2005). Modelling and evaluation of open-pit lignite mines exploitation strategy, 2nd Int. Conference on Sustainable Development Indicators in the Minerals Industry (SDIMI 2005), May 18th - 20th, 2005, Aachen, Germany: 1127-1139.
- [4] Roumpos, C., Partsinevelos P., Agioutantis, Z., Makantasis, K., Vlachou, A. (2014). The optimal location of the distribution point of the belt conveyor system in continuous surface mining operations, Simulation Modelling Practice and Theory, Volume 47, 19-27.
- [5] Hogentogler, C.A., Terzaghi, K. (1929). "Interrelationship of load, road and subgrade". Public Roads: 37–64.
- [6] Kotoulas, D. (2001). Mountain Hydrominics Vol. I.
- [7] Department of the Interior Bureau – United States (1967). Design Standards No.3 Canals and Related Structure.
- [8] Federal Highway Administration, Blodgett Formula (1986). Hydraulic Engineering Circular No. 15, Third Edition – Design of Roadside Channels with Flexible Linings.
- [9] U.S. Army Corps of Engineers (1995). HEC-RAS modeling software.
- [10] Institute of Geology & Mineral Exploration (1996). Geological Map Sheet “MEGALOPOLIS”.
- [11] Greek Antiseismic Regulation (EAK).
- [12] GEOT.ER. Didaskalou S.P. (2017). Geotechnical Research in the area of Southern Choremi of the Megalopolis Lignite Center.
- [13] Public Power Company (1960, 1975, 1981, 1982). Ore Deposit Drilling Results.
- [14] Kavvadas, M. (2006). Stability analyses of the final slopes of the Megalopolis Lignite Center in the regions of the villages of Choremi, Tripotamos and Thoknia.
- [15] Investigation Committee (2015). Report on the landslide at the Megalopolis Lignite Center.
- [16] Kavvadas, M. (2013). Reformed Slope Stability Analyses on the Southern Front of the Choremi Mine (with a minimum excavation floor of about +300,00) due to the landslide of the 14th of September, 2013.
- [17] Chatzisavvas, K. (2014). Course of drainage activities in Megalopolis mine complex, 2013 - Environmental impact assessment.
- [18] Guidelines for the design of highway projects (O.M.O.E. – 11).
- [19] FHWA (2005). Design of Roadside Channels with Flexible Linings.
- [20] United States Department of the Interior, Bureau of Reclamation (1960). “Design of Small Dams”.
- [21] Greek Concrete Technology Regulation (2016).

[22] Ministry of Environment & Energy (2018). Joint Ministerial Decision for Approving Environmental Terms (March 2018): 8684/27-04-2018.

Surface Mining in Western Macedonia, Greece: PM10 Emissions and Dispersion

Triantafyllou A.^{1,4}, Andreadou M.², Moussiopoulos N.³, Garas S.¹, Kapageridis I.^{1,4}, Tsegas G.³, Diamantopoulos Ch.¹, Saxanidis Ch.² and Skordas J.¹

¹LAPEP – Laboratory of Atmospheric Pollution and Environmental Physics, TEI of Western Macedonia, 50100 Kozani, Greece, e-mail: atria@teiw.m.gr

²PPC, Western Macedonia Lignite Center, Greece

³LHTEE-Laboratory of Heat Transfer and Environmental Engineering, Aristotle University of Thessaloniki, 54124 THESSALONIKI

⁴TRC – Technological Research Center, 50100 Kozani, Greece

ABSTRACT

The operation of large open-pit lignite mines represents a significant source of fugitive dust emissions connected to energy production. In the process of extracting and handling excavation materials (overburden, lignite, waste material), a series of fugitive dust emission sources are recorded. The quantification of the emissions of each individual source and the investigation of atmospheric dispersion are subjects of great interest, because of the specificity of diffuse emission sources and the wide range of the particular characteristics of the excavation and handling materials. They constitute the foundation for the development and implementation of the environmental management and decision-making system that aims to avoid exceedance of air quality limits in the neighbouring residential areas. In this study, the contribution of the surface mining on the air environment of Western Macedonia, an industrial area in NW Greece, is investigated. Four open lignite mines (South field, Kardias, Mavropigi, Amyntaio) feed the lignite power plants operating in this area, contributing to the atmospheric pollution of the region. This study is referred to the PM10 emissions, emitted from the newer of the above mines (Mavropigi). Specifically, the percentage of the contribution of each individual activity – emission of fugitive dust over the period of one year is calculated. Furthermore, the dispersion of PM10 emitted from the whole mines operating in the area is simulated. For this purpose, emission factors were used that were calculated specifically for the mines of the Western Macedonia region in the context of the THEOPHRASTOS project, funded by the Lignite Centre of West Macedonia / Public Power Corporation SA. Specifically, the contribution of the individual PM10 emission sources recorded in the continuous and non-continuous extraction method was quantified and particularly by the following activities - PM emission of the Mavropigi mine: shovel excavation and loading, hauling and dumping, moving vehicles on unpaved haul road, bucket-wheel excavators, excavator's head, stacker head, multiple cross point. At the same time, there was an effort to investigate the dispersion of air pollutants emitted from each individual mine (South field, Kardias, Mavropigi, Amyntaio) and source activity and assess the contribution of the mining activities to the air quality of the surrounding areas, by using a three-dimensional, nestable, prognostic meteorological, and air pollution model. The results can contribute to the implementation of measures and scenarios for the air quality management in the area.

1. INTRODUCTION

Particulate Matter (PM) is a major pollutant in air environment of open cast lignite mines. Ambient air quality depends on emission sources and meteorological conditions. In an open-pit mine there co-exist fixed (e.g., power plants), mobile (e.g., trucks, bulldozers, etc.), and fugitive (e.g.

loading and unloading of material) sources of emissions. It has been found that particulate matter from non-combustion sources is by far the main pollutant generated in an open-pit mine [1,2,3]. Its dispersion has been found to be a major concern in air quality modeling of open cast mines.

The basic step in looking at potential solutions to the air pollution problem is to quantify the mass of PM that are being emitted into the atmosphere and especially the investigation of the contribution into the whole PM emissions of each separately activity, such as topsoil and overburden removal, lignite extraction, transportation on haul road etc. On the other hand, the reliable quantification of the total pollutants emissions from the fugitive sources, is an obligation of the mining enterprises according to the 166/2006 Regulation [4], with a special emphasis on the contribution of each mining activity (excavation – transportation – deposition for barren, lignite and ash) to the total dust emissions and represents the first step in applying corresponding countermeasures.

The usual practice to quantify the mass of particulate material emitted into the atmosphere by activities inherent to open-pit mining is to estimate such emissions based on the emission factors recommended by the USEPA for this purpose [5,6]. However, there is a disagreement over the specific emission factors that must be used for each activity and the applicability of such factors to cases quite different to the ones under which they were obtained [7]. The quantification of dust emissions from open pits is strongly related to the exploitation method applied, the equipment used, the dust and other transported materials characteristics (e.g. silt content) as well as to the meteorological characteristic of the area. As a result, real data covering the area under study are necessary for a reliable calculation of dust emissions. The quantity of PM emitted from Mavropigi mine is calculated by using emission factors which have been developed for the specific mines of the area, in the frame of THEOPHRASTOS project [8]. This project was supported by Lignite Centre of Western Macedonia of Public Power Corporation of Greece and focused on the PM10 emission factors development of each mining activity (excavation, transportation, deposition for barren, lignite and ash). In summary, regarding the methodology applied, field measurements were conducted for all the main fugitive dust sources in the four open lignite mines in Western Macedonia, in “upwind-downwind” configuration. The data collected were used as input in Reverse Dispersion Modelling [9]. More details can be found in [10,11].

Finally, the dispersion of PM10 emitted from each individual source activity of the four mines in the area (South field, Kardias, Mavropigi, Amyntaio) and the contribution of the mining activities to the air quality of the surrounding areas are investigated, by using a three-dimensional, nestable, prognostic meteorological, and air pollution model.

2. MATERIALS AND METHOD

2.1. General Description of the Area

Lignite is an important energy source for Greece, contributing more than 50% (53.15%) of the country's production in 2011, the reference year of this study. The most important lignite resources are in West Macedonia where four mines are in operation, constituting the Lignite Centre of Western Macedonia (LCWM) – the South Field, the Kardias Field, the Main Field (Mavropigi), and the Amyntaio mine (Fig.1). These are surface mines and operate using the German continuous mining method, i.e. with large electrical bucketwheel excavators, as the main extraction mean, conveyor belts for moving overburden, midburden and lignite, and stackers. There is also a large number of diesel powered equipment supporting the main installed electrical units. The annual production is around 50 million tonnes of lignite (2012). The remaining lignite reserves in West Macedonia are estimated to be 1.4 billion tonnes. Using current data, this is projected to lead to a potential closure of lignite mining at the West Macedonia PPC mines in 2050. Surface mining includes excavation,

hauling, dumping of waste and piling of lignite. The mining, hauling and dumping processes are significant sources of fugitive dust emission.

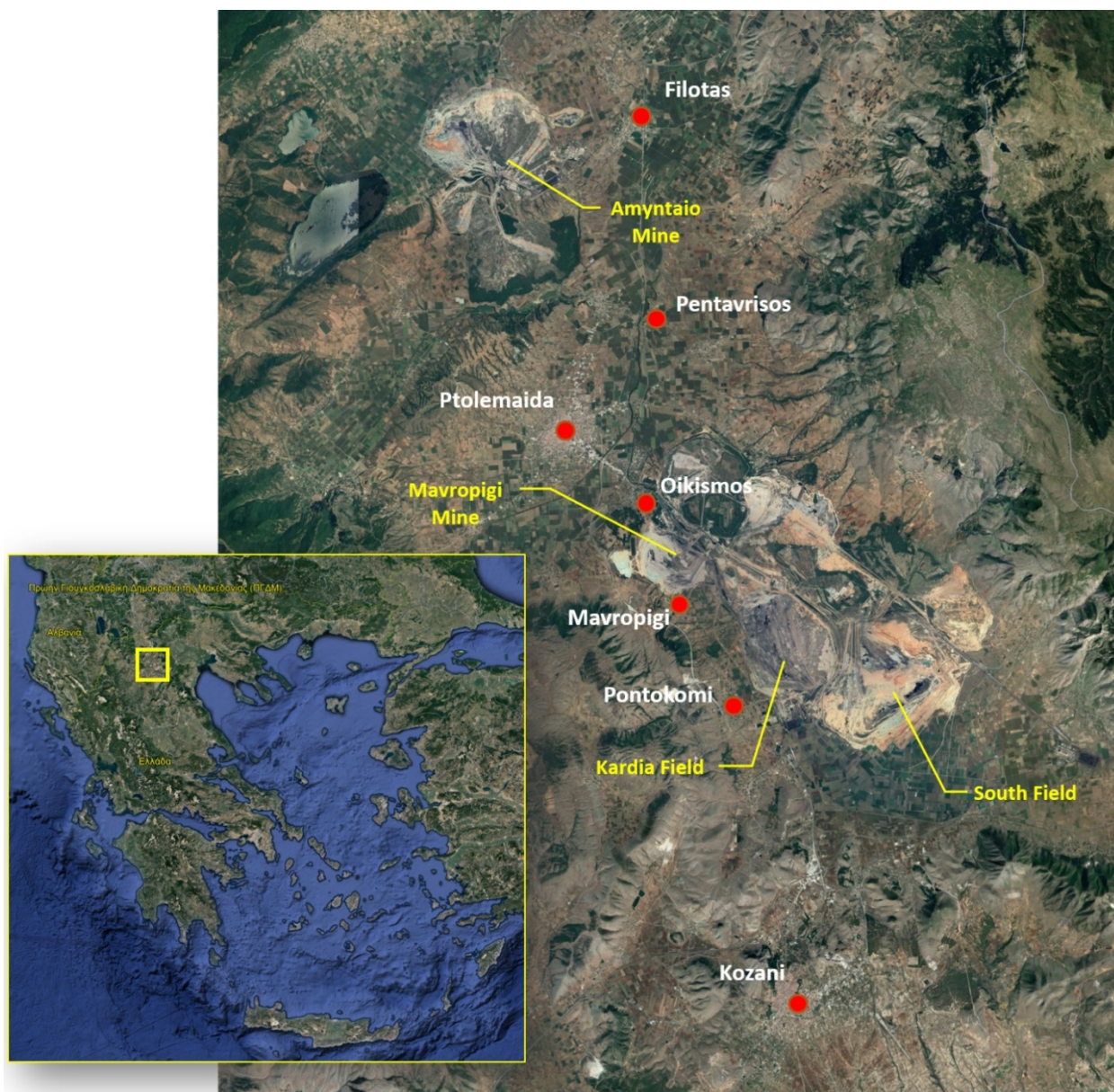


Figure 1. Map showing the opencast lignite mines of Western Macedonia, Greece. Kozani and Ptolemaida, the main towns in the area are also shown, as well as the locations of the receptors Pentavrisos, Oiksmos, Mavropigi, Pontokomi, where PM10 concentration measurements were taken.

2.2 Main PM Sources in the Mavropigi Mine

Two mining methods are used in the Mavropigi mine - the continuous (German) method, using bucketwheel excavators for mining, conveyor belts for hauling and stackers for dumping, and the truck and shovel method using large dumpers and trucks for hauling and dumping of material. These processes include the following sources of PM10 emission:

- Bucketwheel excavator mining (BE)
- Bucketwheel excavator head
- Stacker
- Stacker head

- Shovel excavation and truck loading
- Truck travel on gravel and dirt road
- Truck dumping
- Bunker
- Ash handling
- Complex

The individual source contribution to the total emissions was estimated for a period of one calendar year (2012).

2.3. Model Configuration, Data and Field Observations

The Air Pollution Model (TAPM) was used in this study. TAPM is a nestable, prognostic meteorological and air pollution model that solves fundamental fluid dynamics and scalar transport equations to predict meteorology and pollutant concentration for a range of pollutants important for air quality assessment. For computational efficiency, it includes a nested approach for meteorology and air pollution, with the pollution grids optionally being able to be configured for a sub-region and/or at finer grid spacing than the meteorological grid, which allows a user to zoom-in to a local region of interest quite rapidly. More information can be found in [12,13,14,15]

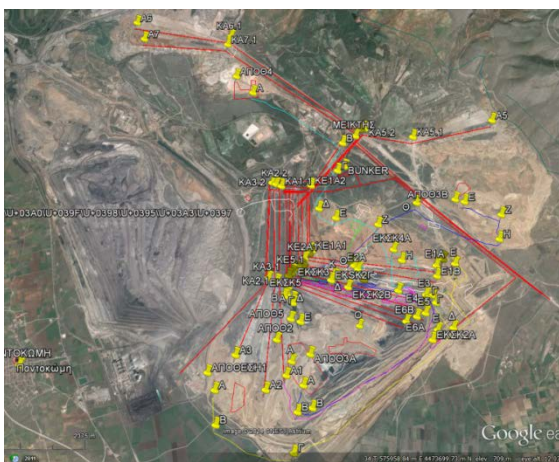
The model was applied for two periods of one month each, representing the cold and warm periods, respectively respectively, using 25 vertical model levels ranging from 10 m up to 8000 m, and four horizontally nested domains incorporating 37×37 horizontal grid points with a 30-, 10-, 3- and 1-km spacing for the meteorology, and 3-, 1-, 0.3- and 0.1-km spacing for the dispersion model, respectively (Fig. 2). NCEP synoptic analysis data were used to define the outer grid boundary conditions [12, 13].



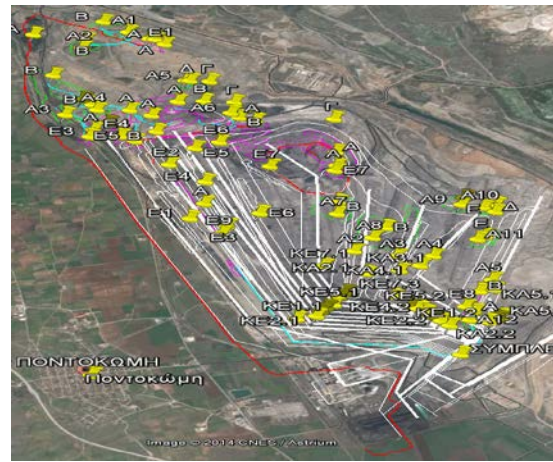
Figure 2. The four nested grids used for the simulation of meteorology.

The various PM10 emitting sources such as excavators, conveyor belts, excavator heads, complex, stackers, bunker, mining, hauling and dumping contractors, and equipment movement on dirt roads, were considered as linear, surface or volume sources for the simulation of mining, hauling and dumping sources of PM10 emission (Fig.3). As already mentioned, for each one of the above sources, emission factors have been used as they were calculated under the framework of project THEOFRASTOS of the LCWM [10]. This calculation was performed in conjunction with concentration measurements “upwind – downwind” of each source and reverse dispersion modelling [9].

In the following, we assume a 24-hour operation of the continuous mining equipment and 10-hour operation of the activities-sources of non-continuous mining, as a worst-case scenario. Once the activity parameters were defined, the topography of the area in high resolution (90m, STRM3) was imported to the model. TAPM evaluation was performed by producing PM10 concentrations forecasts in six selected sites-receptors located in Pentavrisos, Ptolemaida, Oikismos DEH (PPC), Mavropigi, Pontokomi, and Kozani.



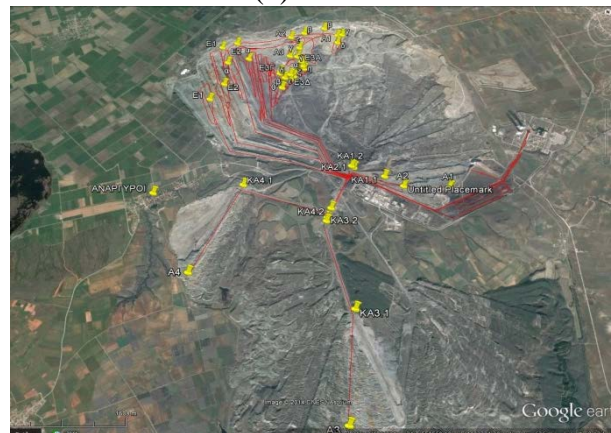
(a)



(b)



(c)



(d)

Figure 3. Locations of PM10, linear, surface and volume sources (excavators, conveyor belts, excavator heads, complex, stackers, bunker, mining, hauling and dumping contractors, equipment movement) digitised for the simulation of (a) South Field, (b) Kardia Field, (c) Main Field (Mavropigi Mine), (d) Amyntio Mine.

For the dispersion simulation, the month of the hot period with the highest average monthly concentration was chosen. Figure 4 shows the average monthly concentration of PM10 at the Western Macedonia basin in 2012, from measurements of PPC and TEIWM. It is evident that July is the month with the highest average monthly concentration.

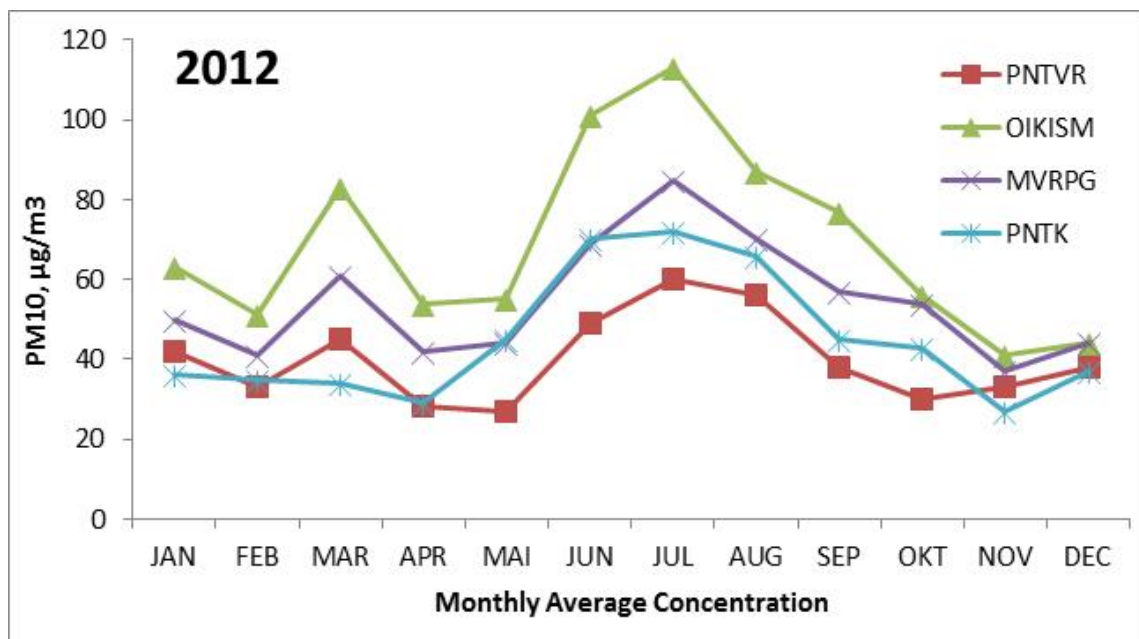


Figure 4. Average monthly PM10 concentration at the receptors near the Mavropigi mine in 2012 (PPC measurements).

A month of the cold period, January 2013, was chosen respectively. Figure 5 shows wind rose diagrams at the Pontokomi receptor, approximately 5.5 km SE of the Mavropigi mine limits, for each of the simulation months.

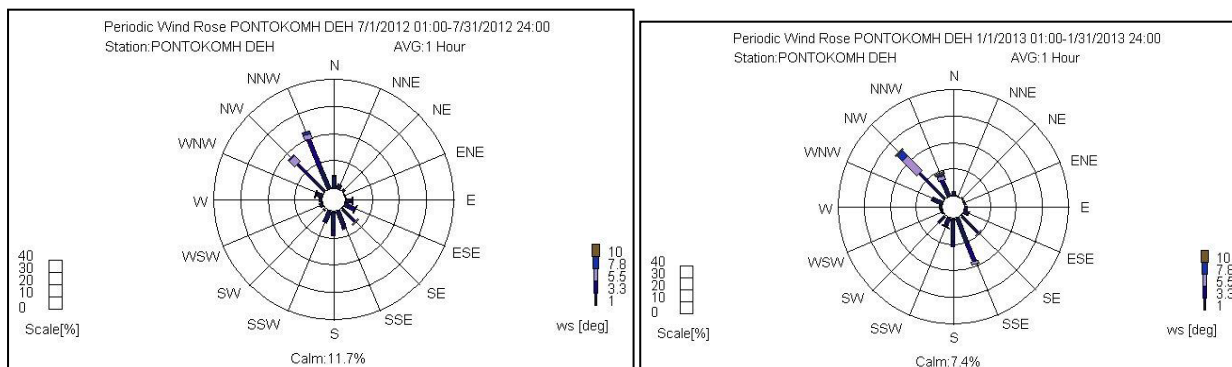


Figure 5. Wind rose diagrams from the Pontokomi receptor for the simulation months, i.e. June 2012 (left) and January 2013 (right).

The wind direction in both months is from the NW being strongest in January. The highest percentages of calms were found in July.

3. RESULTS AND DISCUSSION

3.1. Emissions Calculation

The following mining activity parameters were used, provided by LCWM.

Table 36. Mavropigi mine operational parameters for the period 01/2012 – 12/2012.

Parameter	Quantity	Units
Waste removal	84952667	t
Lignite mining	5888469	t
Ash quantities moved	988085	t
Strip ratio	7.4	m ³ /t
Waste specific gravity	1.95	t/m ³
Ash specific gravity	0.85	t/m ³
Lignite specific gravity	1.23	t/m ³
Truck capacity for compact material	14	m ³
Waste quantity hauled with trucks	38466979	T
Lignite quantity hauled with trucks on asphalt road	3226647	T
Ash handler operation hours	3364	T
Lignite quantity hauled on dirt road	3226647	T
Lignite conveyor belt travel length	3.7	Km
Waste conveyor belt travel length	2.46	Km
Stackers operation hours for mixed material	12799	h
Stacker heads number	8	
Excavator operation hours for lignite	2352	h
Excavator operation hours for waste	24861	h
Lignite excavator heads number	16	

Figure 6 presents in pie chart format the percentages of contribution for each activity to the total emission of escaping dust from the Mavropigi mine for 2012.

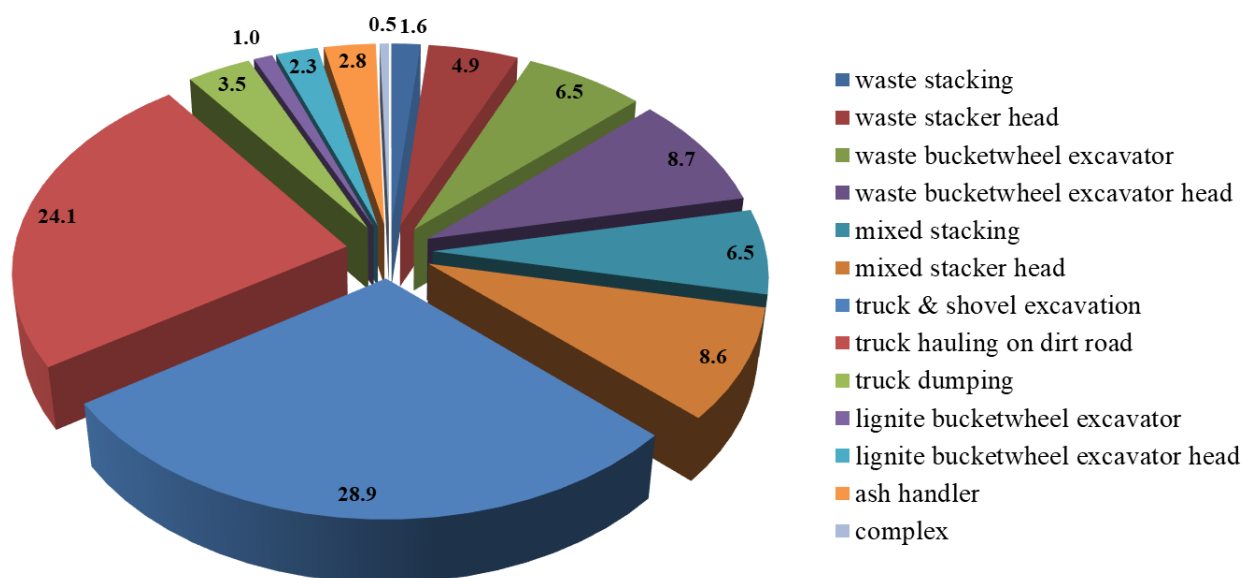


Figure 6. Contribution of each activity at the Mavropigi mine to the total escaping dust emissions of the mine during the period 01/2012 – 12/2012.

The total emissions are distributed to the individual activities as follows:

- Shovel excavation and truck loading (28.87%),
- Truck hauling on dirt road (24.11%),
- Bucketwheel excavator head – waste mining (8.69%),
- Stacker head – mixed (8.59%),
- Bucketwheel excavator – waste mining (6.54%),
- Stacking – mixed (6.54%),
- Stacker head – waste (4.92%),
- Truck dumping (3.50%),
- Bucketwheel excavator head – lignite (2.30%),
- Ash handling (2.82%),
- Stacking – waste (1.58%),
- Bucketwheel excavator – lignite mining (1.04%),
- Complex (0.49%) and
- bunker (0.01%).

The maximum PM10 contribution to the total mine emissions are from the activities related to truck & shovel excavation and loading, and truck hauling on dirt roads.

3.2. Dispersion

Figures 7a and 7b show PM10 pollution contours for per month as derived through simulations. They present the average monthly levels of PM10 concentrations produced by the emissions of the three mines (South, Kardias and Mavropigi) for the studied worst-case scenario.

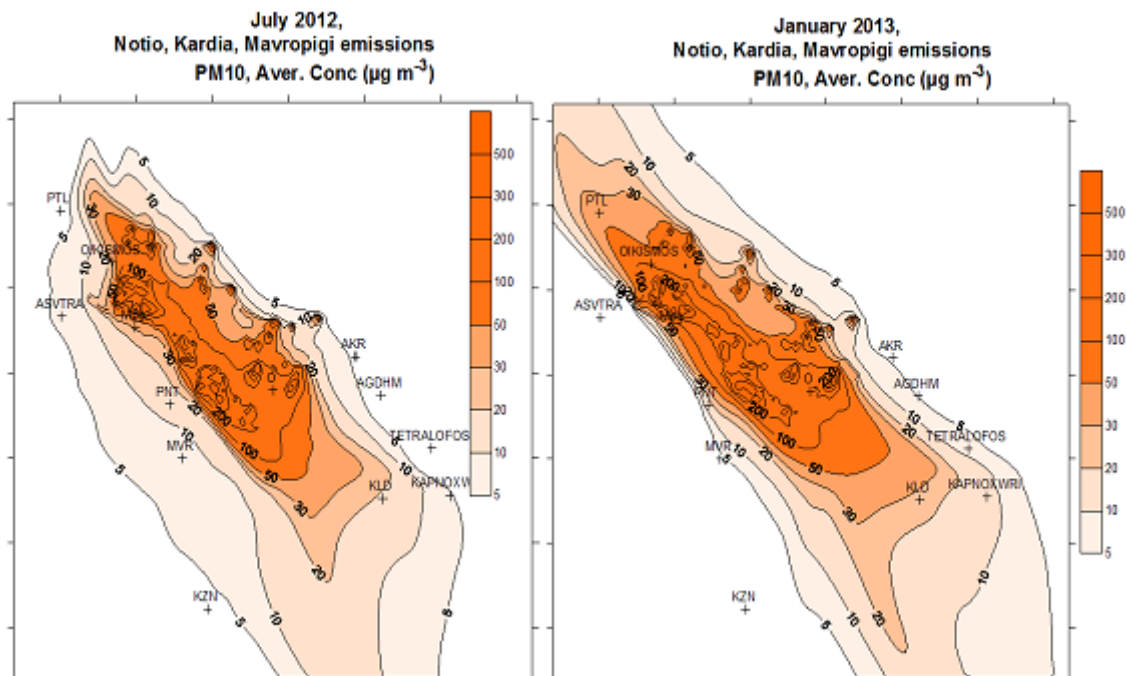


Figure 7. PM10 pollution contours due to emissions from the Mavropigi, Kardias and South Field mines in July 2012 (left) and January 2013 (right).

The higher dispersion and transport of PM10 at greater distances during the cold period is characteristic of the prevailing conditions of that period, namely stronger winds and a more shallow mixing layer.

In Table 2, second row (Measured Average - MA), the average PM10 concentrations of the simulation period, as measured at the stations are given. Row three shows the corresponding values obtained from the simulations (Simulation Average - SA), i.e. the PM10 concentration contribution at the respective receptor attributed to the mines' (Amyntaio, Mavropigi, Kardias and South Field) emissions, according to the studied worst-case scenario. Row four shows the PM10 concentration contributed by the mines for the operation data considered in the simulation, as a percentage of the measured concentration at the same period and receptor (Overestimated Mine Contribution %, OMC%).

It is noted that the concentrations at the receptors due to mine emissions, and thus the mines contribution percentage (row four in the table) refer to the scenario of mines operation considered, while the measured values correspond to the actual mines operation. For a more accurate estimation of the mines contribution, we define some indicators of mines influence in the range of 0 to 10. By setting the value of 10 to the Oikismos area receptor, where the highest concentrations were measured ($73 \mu\text{g}/\text{m}^3$), as well as the highest mines influence ($70 \mu\text{g}/\text{m}^3$), we define three indicators:

1. The **Relative Indicator of Measured PM10 concentrations (RIMPM10)** from all sources. It rescales the measured PM10 concentrations at each receptor to a standard scale of 0-10 with reference to the concentrations measured at Oikismos.
2. The **Relative Indicator of Calculated PM10 concentrations (RIMP10C)** for the contribution due to the mines emissions. It rescales the calculated PM10 concentrations at each receptor to a scale of 0-10, relative to the concentrations calculated for Oikismos.
3. The **Overestimated Relative Indicator of Mines Influence (ORIMI)**. It rescales the relative influence of the mines from their operation as a percentage of the measured concentrations to a standard scale of 0–10, with the highest value assigned for Oikismos (10).

This way all three indicators can be presented in a scale of 0 to 10, where the value of 10 was set at Oikismos. In rows 5, 6 and 7 of Table 2, the indicator values for Pentavrisos, Ptolemaida, Oikismos, Mavropigi, Pontokomi and Kozani are presented.

Table 2. Observed, predicted PM10 concentrations and contribution indicators of surface mining PM10 emissions

1	Receptor	Pentavrisos	Ptolemaida	Oikismos	Mavropigi	Pontokomi	Kozani
2	MA ($\mu\text{g}/\text{m}^3$)	45	58	73	57	38	29
3	SA ($\mu\text{g}/\text{m}^3$)	12	32	70	48	14	3
4	OMC%	27	55	96	84	38	10
5	RIMPM10	6.2	7.9	10.0	7.8	5.2	3.7
6	RIMP10C	1.7	4.6	10.0	6.9	2.0	0.4
7	ORIMI	2.8	5.7	10.0	8.7	3.9	1.0

The above values are shown graphically in Fig. 8. It is evident that Ptolemaida has equal or slightly higher PM10 concentration indicator value than Mavropigi, but the later has much higher mining contribution indicator value.

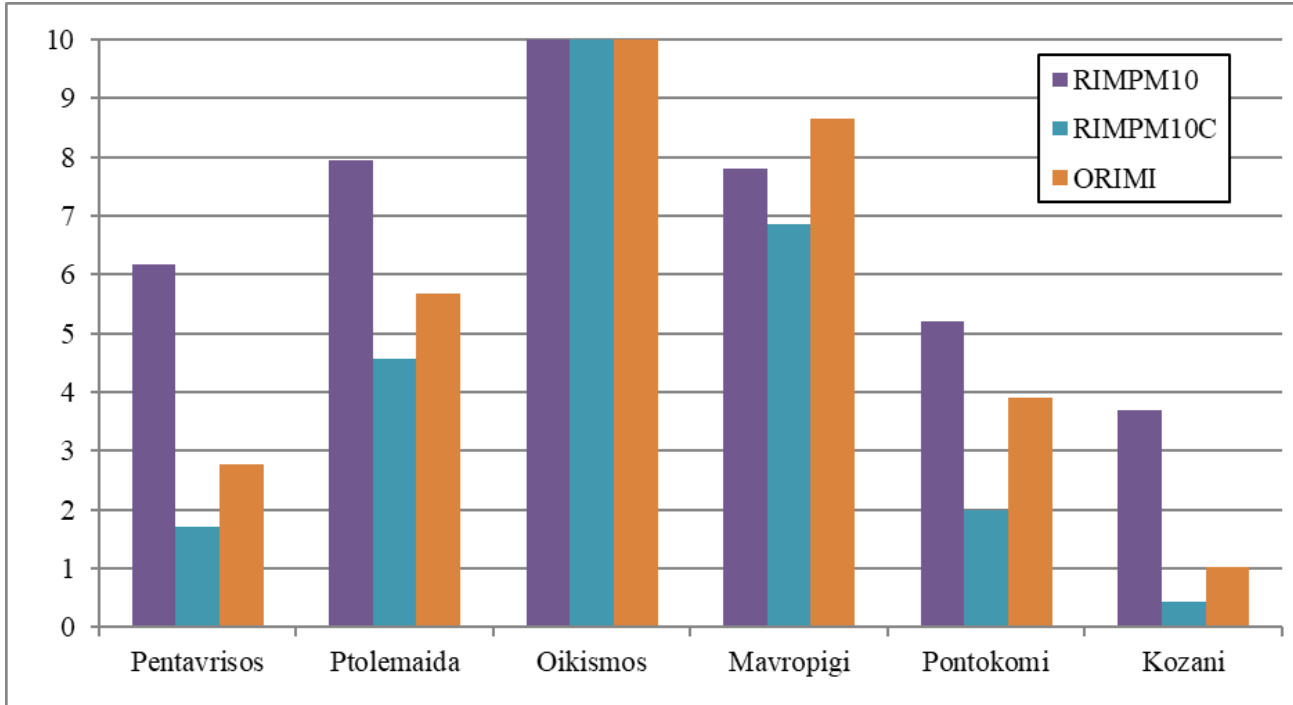


Figure 8. Surface mining contribution indicators on atmospheric pollution of specific receptors, computed by using observed and predicted (worst case scenario) PM10 concentration.

The above analysis refers to two-month average values, one in the hot period and one in the cold. One should note the very wide range of average daily concentrations at the receptors, particularly those closer to the PM emitting activities.

4. CONCLUSIONS

More than 50% of the total annual PM10 emitted mass from a specific surface lignite mine (Mavropigi) in Western Macedonia was produced by activities related to non-continuous mining and specifically from truck & shovel excavation and loading, and truck hauling on dirt roads. The relative indicator of PM10 concentration measurements, as they were taken at receptors and were caused by all PM10 emission sources in the area, the relative indicator of measured PM10 calculated concentrations as they were calculated from simulations and are caused only by the mines' (South field, Kardia, Mavropigi, Amyntaio) dust emissions, and the overestimated relative indicator of mines' influence, are useful tools for the assessment of the relative contribution of the fugitive dust emissions on the PM10 concentrations measured at the selected receptors in the area. Finally, it is possible to design and implement an integrated system for the management of the various mining activities, incorporating an operational module for the forecasting of their contribution to the PM10 concentration levels at selected receptors, aiming at the improvement of air quality in the area affected by the operation of the surface mines.

REFERENCES

- [1] Ghose MK, Majee SR (2000) Assessment of dust generation due to opencast coal mining—an Indian case study. *Environ Monit Assess* 67:255–256
- [2] Ghose MK, Majee SR (2001) Air pollution caused by opencast mining and its abatement measures in India. *J Environ Manage* 63 (2):193–202
- [3] José I. Huertas, María E. Huertas, Sebastián Izquierdo, Enrique D. González (2012). Air quality impact assessment of multiple open pit coal mines in northern Colombia. *Journal of Environmental Management* 93 (2012) 121e129
- [4] Regulation (EC) No 166/2006 of the European Parliament and of the Council of 18 January 2006 concerning the establishment of a European Pollutant Release and Transfer Register and amending Council Directives 91/689/EEC and 96/61/EC
- [5] USEPA (2008) Revision of emission factors for AP-42. Chapter 11: mineral products industry. Section 11.9: Western Surface Coal Mining. <http://www.epa.gov/ttn/chief/ap42/index.html>. Accessed 1 April 2009 *Environ Sci Pollut Res*
- [6] USEPA (2009) Emission factors & AP 42. <http://www.epa.gov/ttnchie1/ap42/>. Accessed 13 July 2009
- [7] Jose I. Huertas & Dumar A. Camacho & Maria E. Huertas (2012). Standardized emissions inventory methodology for open-pit mining areas *Environ Sci Pollut Res* DOI 10.1007/s11356-012-0778-3
- [8] Triantafyllou AG., Garas S., Crestou A., Diamantopoulos Ch., Skordas I., Leivaditou E., Matthaios V., Proiou D., Coutsochristos A., Tzhkalios A., Tsakouras V., Koios K., Clossas G., Partalidou X., Christou M., Zapsis S., (2015). Quantification of the opencast lignite mines of the Lignite Centre of Western Macedonia due to present and future activities in the sources and receptors. Technical report for LCWM/Public Power Corporation, GREECE.
- [9] BS EN 15445:2008, “Fugitive and diffuse emissions of common concern to industry sectors. Qualification of fugitive dust sources by reverse dispersion modeling”, September 2008.
- [10] Triantafyllou A., Moussiopoulos N., , Garas S., Krestou A., Douros I., Diantopoulos Ch., Skordas J., Matthaios V., Leivaditou H., Tsegas G., Fragkou E., Pavloudakis F., Andreadou M., and Kouridou O., 2015, “THEOPHRASTOS: PMX Emissions factors – dispersion from fugitive dust sources in lignite mines of western Macedonia, Greece”, Proceedings of the 14th International Conference on Environmental Science and Technology Rhodes, Greece, 3-5 September 2015, CEST2015_00264
- [11] Triantafyllou A., Moussiopoulos N., Krestou A., Tsegas G., Barmpas F., Garas S., and Andreadou M. (2017) "Application of inverse dispersion modelling for the determination of PM emission factors from fugitive dust sources in open – pit lignite mines", *Int. J. Environment and Pollution*, Vol. 62 Nos. 2/3/4, pp.274-290.

- [12] Hurley P (1997) An evaluation of several turbulence schemes for the prediction of mean and turbulent fields in complex terrain. *Bound-Layer Meteorol* 83:43–73
- [13] Hurley P (2000) Verification of TAPM meteorological prediction in the Melbourne region for a winter and summer month. *Aust Meteorol Mag* 49:97–107
- [14] Hurley P, Blockley A, Rayner K (2001) Verification of a prognostic meteorological and air pollution model for year-long predictions in the Kwinana region of Western Australia. *Atm Environ* 35(10): 1871–1880. [https://doi.org/10.1016/S1352-2310\(00\)00486-6](https://doi.org/10.1016/S1352-2310(00)00486-6)
- [15] Triantafyllou A., Krestou A., Hurley P. and Thatcher M., 2011: An operational high resolution local – scale meteorological and air quality forecasting system for western Macedonia, Greece Q Some first results. *Proceedings of the 12th International Conference on Environmental Science and Technology (CEST 2011)*, 8-10 September 2011, Rhodes –Greece, 1904-1911.

Statistical Analysis and Spatial Distribution of Trace Elements Contained in Clays Excavated in Western Macedonia Continuous Surface Mining Complex

Francis Pavloudakis, Christos Roumpos and Christos Sachanidis

Public Power Corporation SA, General Division of Mines, 32, Chalkokondili str., 104 32 Athens, Greece

ABSTRACT

Twenty one clay samples of Pliocene – Pleistocene age were collected from five active and three inactive mines of Western Macedonia Lignite Centre and were tested by the INAA and ICP-OES methods to determine the concentrations of 10 major and 39 trace elements. The content of clay samples in carbon and sulphur and the loss of ignition were also determined.

According to the results of a statistical processing that was conducted, the comparison of trace elements concentrations of clay samples collected from the entire lignite-bearing Neogene basin of Ptolemais as well as the comparison of the same concentrations with the mean values of the Earth's crust (MVEC), preliminary conclusions have been drawn concerning the spatial (horizontal and vertical) distribution of trace elements concentrations in the clays contained in overburden and intercalate waste of the lignite deposit. Furthermore, useful information has been gathered about the behaviour of trace elements contained in clay layers during lignite combustion - utilisation processes.

The average concentrations of all the analysed major elements are similar to the MVEC. Regarding trace elements, Co, Cs, Hf, Rb, Sc, Th, U, La, Ce, Nd, Sm, Eu, Tb, Yb, Lu, Cu, Pb, Zn, Ni, Cd, Ba, Sr, Y, Sn, Zr, Be and V exhibit enrichment factors that vary from 0.5 to 3.0 among the different mines of the examined area, while the highest enrichment factors exhibit the elements Sb (3.5 ppm), Ag (4.1 ppm) and Cr (4.6 ppm) (average values in the entire Ptolemais – Amynteon basin). Nevertheless, the elements of greatest environmental concern (As, Se, B, Cd, Hg, Mo, Pb) are present in clays in low concentrations.

Taking into consideration the alkaline pH values of the surface water, groundwater and soils of Ptolemais basin, the probability to occur severe pollution incidents due to toxicity caused by the trace elements contained in the clays of the lignite deposit is negligible.

1. INTRODUCTION

The greater lignite-bearing basin of Ptolemais-Florina is the largest and most important in Greece including 65-70% of the total lignite reserves of the country (Figure 1). The certain lignite reserves exceed 4 billion tones [1, 2].

Lignite extraction and combustion can adversely impact the environment in many ways. In the particular case that is investigated in the present study, a probable increase in trace or major elements concentrations contained in clay layers that are included either in the lignite deposit, though they are less in number and thinner than the layers of marls, or in the overburden strata are considered as a potential threat for the quality of waters and soils.

During the lignite combustion the inorganic components undergo a series of physical and chemical processes, which are possible to lead to increased concentrations of major and trace elements in the fly and bottom ash. The same but to a lesser extent (it depends on the co-excavation of lignite and clay layers due to the so-called zebra-type structure of the deposit) also occurs with

the elements of the intermediate clayey and marly layers of the lignite deposit located in Ptolemais basin [3, 4].

Trace elements are defined the elements with concentration in a lignite layer less than 0.02% wt or <200ppm [5]. For the purpose of this study the term trace element refers to those elements typically present in coal at concentrations <0.1 wt% [6]. Trace elements concentrations in coal basins depends on many factors, such as their occurrence during the plants growth, enrichment during decomposition of organic matter, burial, sedimentation, diagenesis and carbonization as well as mineralization [6, 7]. Furthermore, the horizontal and vertical distribution of trace elements in a coal deposit is determined by geological parameters, such as the nature and geochemical characteristics of rocks, the climate, hydrological pattern and leaching processes taking place above, below and at the margins of the coal bearing formation [5, 6, 8, 9, 10].

The objective of the present work is the determination of the concentrations of 12 major and 39 trace elements in 21 samples of clays contained in the overburden strata and in the lignite deposit of eight surface mines located in Ptolemais basin, West Macedonia, Greece. The spatial variation of these concentrations is also examined. Finally, the trace elements concentrations are compared with the average concentrations of Earth's crust and the relevant enrichment factors are estimated as a preliminary assessment of the potential threats for the environment. It should be noticed that the number of clay samples that have been analysed is limited compared with the horizontal expansion of the lignite deposit. So, the present study is based on the assumption of a homogenous and isotropous deposit, at least within the borders of each one of the mines under investigation.

2. MATERIALS AND METHODOLOGY

Twenty one clay samples of the Pliocene - Pleistocene age were collected from four active surface mines: South Field (S), Sector 6 (TE), Mavropigi (MA) and Amynteon Field (AM), and from three inactive mines: Kardia (KR), North Field (N) and Anargiri Field (AP) of Western Macedonia Lignite Centre, Ptolemais, Greece (Figure 1). The samples were collected from the open bench slopes following the time-stratigraphy and litho-stratigraphy of each formation according to specifications and trying to avoid pollution due to mixing with material coming from other seams. Each sample weighed 10kg and was collected from a vertical trench in order to be representative of the composition of the entire lignite seam [11].

Chemical analyses for the determination of trace elements concentrations were carried out using Instrumental Neutron Activation Analysis (INNA) and Inductively Coupled Plasma - Optical Emission Spectrometry (ICP-OES) methods. More analytically, ICP OES method was used for chalkofiles elements: Cu, Pb, Zn, Ag, Ni, Cd, Bi. Preparation for the analysis of these elements included total digestion with hydrochloric acid (HCl). The elements Ba, Sr, Y, Sc, Zr, Be, V were prepared with fiction, using metaboric or tetraboric acid $\text{LiB}_4\text{O}_7/\text{LiBO}_2$. INAA was used for determining the concentrations of the following elements: Au, As, Br, Co, Cs, Hf, Ir, Mo, Rb, Sb, Sc, Se, Te, Th, U, W, La, Ce, Nd, Sm, Eu, Tb, Yb, Lu. Sulphur and carbon contents were determined using a LECO device. Loss of ignition was also determined.

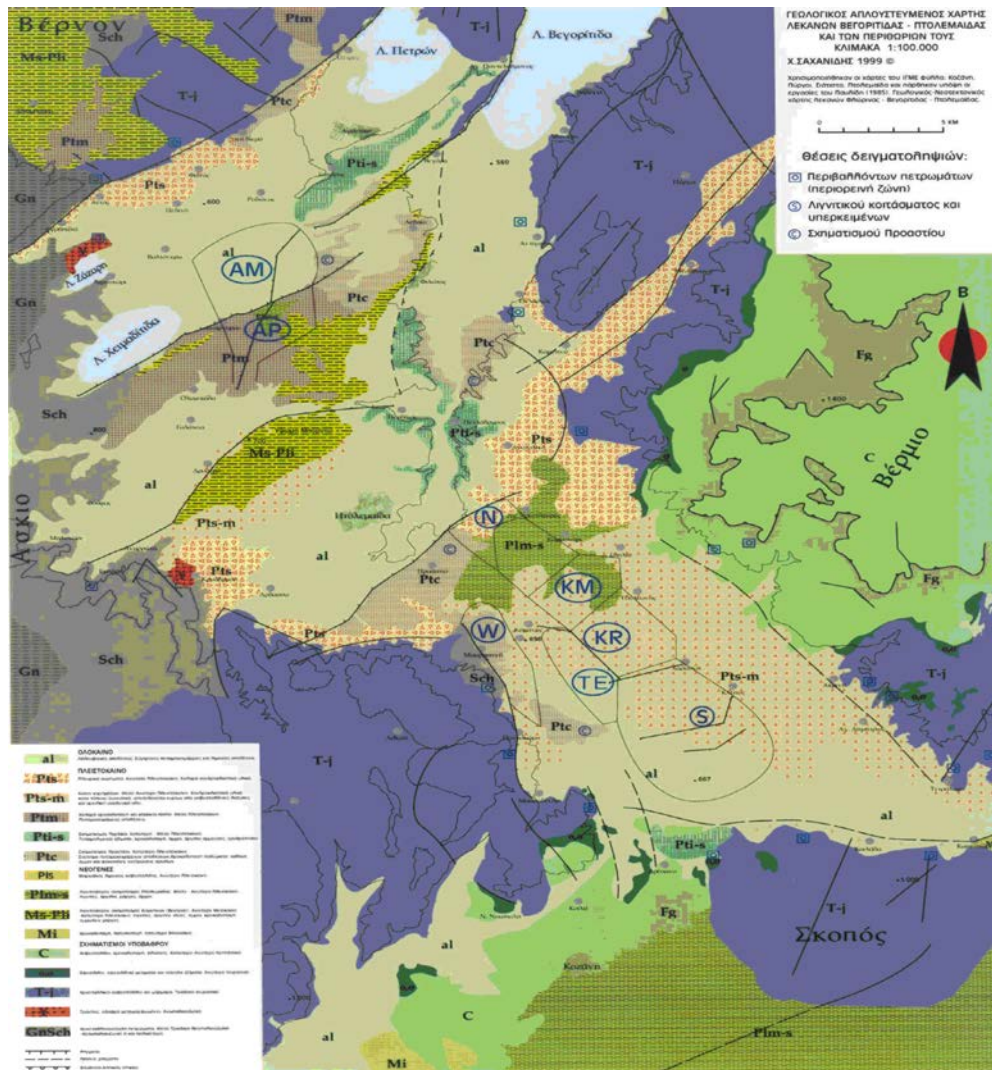


Figure 1. Simplified geological map of the Ptolemais-Amynteon basin (IGME)

3. RESULTS AND DISCUSSION

According to the lab analyses results presented in Table 1, the trace and major elements contained in the clay layers of Ptolemais and Amynteon lignite deposits exhibit low concentrations compared with the mean values of main rocks of the Earth's crust [11, 12, 13, 14].

From the 39 trace elements that were examined in the present study, Au, Ir, Mo, Se, W, Ag and Bi exhibit concentrations below the detection limits of the analytical instruments.

The enrichment factor (EF), which is the quotient of the average concentration of a certain group of clay layers divided by the mean values of main rocks of the Earth's crust, is less than 1 in all the examined mines for the elements Br, Sc, Ta, Lu, Cu, Ba, Sr, Y, Sn, Be and V and less than 2 for the elements Co, Rb, Th, U, La, Ce, Nd, Sm, Eu, Tb, Yb, Zn and Zr. The elements Cs, Hf and Cd exhibit EF less than 3, with the maximum EF values to have been determined in the mines of Kardia, Sector 6 and West Field, respectively. The EF of Pb is less than 4 and the maximum EF value has been determined in Sector 6 mine, while the EF of Ni and Sb are less than 5 and the maximum values have been determined in Amynteon and Kardia mines, respectively. Only As and Cr exhibit systematically high EF. The range of variation of EF is from 2 to 8 for As and from 3 to 10 for Cr, with the minimum and maximum values to correspond for As to the mines of Amynteon and Kardia and for Cr to the mines of Kardia and West Field.

Table 1. Trace and major elements concentrations in the clay layers of Ptolemais – Amynteon lignite deposit

Samples	Au ppm	As ppm	Br ppm	Co ppm	Cr ppm	Cs ppm	Hf ppm	Ir ppm	Mo ppm	Rb ppm	Sb ppm	Sc ppm	Se ppm	Ta ppm	Th ppm	U ppm	W ppm
Det.limits.*	5,0	2,0	1,0	1,0	1,0	0,5	0,5	5,0	5,0	20,0	0,2	0,1	3,0	1,00	0,50	0,50	3,00
M.C.A.**	0,004	1,8	2,5	25	100	3	3	0,001	1,5	90	0,2	22	0,05	2,0	7,2	1,8	1,5
S.AL1	8,0	10,0	<1	24	472	6,4	5,8	<5	<5	75	0,9	11,3	<3	<1	11,4	2,8	<3
S.AL3	7,0	<2	<1	34	401	6,5	4,2	<5	<5	139	0,9	18,3	<3	<1	12,7	3,0	<3
S.AL18	<5	4,0	<1	15	321	3,2	4,0	<5	<5	53	0,7	7,1	<3	<1	6,4	3,5	<3
Average	6,7	5,3	<1	24,3	519,3	5,4	4,7	<5	<5	89,0	0,8	12,2	<3	<1	10,2	3,1	<3
E.F.		3,0	0,4	1,0	5,2	1,8	1,6		<3,3	1,0	4,2	0,6		<1	1,4	1,7	2,0
TE.AL1	<5	9,0	<1	25	522	6,0	6,3	<5	<5	90	0,9	10,8	<3	<1	11,9	2,2	<3
TE.AL3	<5	<2	<1	38	345	6,4	3,5	<5	<5	135	0,9	18,8	<3	2	12,1	2,7	<3
TE.AL16	<5	6,0	2,0	25	425	7,4	9,6	<5	<5	75	0,4	12,8	<3	<1	12,8	4,1	<3
Average	<5	5,7	1,3	29,3	528,0	6,6	6,5	<5	<5	100,0	0,7	14,1	<3	1,3	12,3	3,0	<3
E.F.		3,1	0,5	1,2	5,3	2,2	2,2		<3,3	1,1	3,7	0,6		0,7	1,7	1,7	2,0
KR.AL1	<5	24,0	<1	43	482	11,2	4,8	<5	<5	171	1,8	17,7	<3	<1	18,9	3,5	<3
KR.AL2	<5	4,0	2,0	5	94	2,2	0,8	<5	<5	29	<0,2	2,6	<3	<1	3,0	0,9	<3
Average	<5	14,0	1,5	24,0	364,5	6,7	2,8	<5	<5	100,0	1,0	10,2	<3	<1	11,0	2,2	<3
E.F.		7,8	0,6	1,0	3,6	2,2	0,9		<3,3	1,1	5,0	0,5		<1	1,5	1,2	2,0
N.AL1	<5	5,0	<1	27	593	4,7	7,0	<5	<5	88	0,7	12,4	<3	<1	10,9	2,8	<3
W.AL1	<5	7,0	<1	27	548	5,7	5,5	<5	<5	78	0,8	14,3	<3	<1	11,8	2,5	<3
W.ALS2	<5	<2	<1	33	559	2,0	5,0	<5	<5	48	0,5	10,9	<3	<1	4,9	1,3	<3
W.ALM3	<5	3,0	<1	32	754	5,9	4,0	<5	<5	109	0,7	14,9	<3	<1	9,4	2,3	5,0
Average	<5	4,0	<1	30,7	933,0	4,5	4,8	<5	<5	78,3	0,7	13,4	<3	<1	8,7	2,0	<3,7
E.F.		2,2	0,4	1,2	9,3	1,5	1,6		<3,3	0,9	3,3	0,6		<1	1,2	1,1	2,4
AM.AL1	<5	3,0	<1	13	782	1,9	4,4	<5	<5	55	<0,2	8,1	<3	<1	5,1	1,6	<3
AM.AL3	<5	2,0	<1	34	272	3,9	6,2	<5	<5	89	0,4	22,5	<3	<1	9,4	2,8	<3
AM.AL14	<5	5,0	<1	46	616	6,9	4,1	<5	<5	52	0,7	23,8	<3	<1	12,4	3,8	<3
AM.AL16	<5	3,0	<1	42	501	5,9	5,2	<5	<5	62	0,6	20,7	<3	3	11,6	4,0	<3
AM.AL17	<5	<2	<1	43	492	5,2	5,0	<5	<5	77	0,5	20,7	<3	<1	11,4	4,1	<3
AM.AL18	<5	6,0	<1	47	598	8,0	4,0	<5	<5	66	0,8	23,8	<3	2	13,1	3,7	<3
Average	<5	3,5	<1	37,5	673,8	5,3	4,8	<5	<5	66,8	0,5	19,9	<3	1,5	10,5	3,3	<3
E.F.		1,9	0,4	1,5	6,7	1,8	1,6		<3,3	0,7	2,7	0,9		0,8	1,5	1,9	2,0
AP.AL1	<5	4,0	3,0	19	251	4,5	5,4	<5	<5	71	0,7	15,3	<3	<1	9,7	2,4	<3
AP.ALS2	<5	5,0	<1	15	502	1,9	4,9	<5	<5	50	0,3	8,6	<3	<1	5,0	0,8	<3
AP.ALM3	6,0	<2	<1	23	129	3,5	6,5	5,0	<5	92	0,4	20,9	<3	<1	9,3	2,2	<3
Average	5,3	3,7	1,7	19,0	392,3	3,3	5,6	<5	<5	71,0	0,5	14,9	<3	<1	8,0	1,8	<3
E.F.		2,0	0,7	0,8	3,9	1,1	1,9		<3,3	0,8	2,3	0,7		<1	1,1	1,0	2,0

* Det. limits: Detection limits, in ppm,

**M.C.A.: Average composition of Earth's crust, in ppm (Mason and Moore, 1982)

***Average: Mean arithmetic value

****E.F.: Enrichement factor

Table 1. (continue) Trace and major elements concentrations in the clay layers of Ptolemais – Amynteon lignite deposit

Samples	La ppm	Ce ppm	Nd ppm	Sm ppm	Eu ppm	Tb ppm	Yb ppm	Lu ppm	Cu ppm	Pb ppm	Zn ppm	Ag ppm	Ni ppm	Cd ppm	Bi ppm	Ba ppm	Sr ppm	Y ppm	Sn ppm	Zr ppm	Be ppm	V ppm
Det.limits.*	0,50	3,00	5,00	0,10	0,10	0,50	0,10	0,05	1,00	5,00	1,00	0,50	1,00	0,50	10,00	1,00	1,00	1,00	1,00	1,00	1,00	5,00
M.C.A.**	30	60	28	6	1,2	0,9	3,4	0,5	55	13	70	0,07	75	0,2	0,2	425	375	33	22	165	2,8	135
S.AL1	37,9	61	31	5,4	1,1	<0,5	2,7	0,41	20	39	80	<0,5	164	<0,5	<10	329	121	24	10	192	2	85
S.AL3	34,6	62	27	5,8	1,4	<0,5	2,9	0,42	33	47	117	<0,5	310	<0,5	<10	359	166	27	17	130	2	116
S.AL18	24,4	45	20	3,9	0,9	<0,5	2,0	0,31	16	8	69	<0,5	137	<0,5	<10	162	136	18	7	142	1	42
Average	32,3	56,0	26,0	5,0	1,1	<0,5	2,5	0,38	23,0	31,3	88,7	<0,5	203,7	<0,5	<10	283,3	141,0	23,0	11,3	154,7	1,7	81,0
E.F.	1,1	0,9	0,9	0,8	0,9	0,6	0,7	0,76	0,4	2,4	1,3		2,7	<2,5		0,7	0,4	0,7	0,5	0,9	0,6	0,6
TE.AL1	36,4	61	25	5,3	1,1	<0,5	2,5	0,37	19	37	80	<0,5	159	<0,5	<10	333	117	25	11	204	2	76
TE.AL3	33,0	66	29	5,8	1,5	<0,5	3,1	0,47	32	81	77	<0,5	39	<0,5	<10	371	156	29	18	118	2	119
TE.AL16	41,0	78	32	7,0	1,4	1,2	4,9	0,68	26	28	111	<0,5	232	0,7	<10	265	68	39	12	297	2	64
Average	36,8	68,3	28,7	6,0	1,3	0,7	3,5	0,51	25,7	48,7	89,3	<0,5	143,3	0,6	<10	323,0	113,7	31,0	13,7	206,3	2,0	86,3
E.F.	1,2	1,1	1,0	1,0	1,1	0,8	1,0	1,01	0,5	3,7	1,3		1,9	<2,8		0,8	0,3	0,9	0,6	1,3	0,7	0,6
KR.AL1	37,3	74	24	5,0	0,9	<0,5	2,5	0,35	45	28	107	<0,5	453	<0,5	<10	491	91	23	18	162	3	139
KR.AL2	10,1	15	9	1,5	0,3	<0,5	0,6	0,09	6	5	49	<0,5	50	<0,5	<10	89	100	8	3	33	1	32
Average	24	44,5	16,5	3,3	0,6	<0,5	1,6	0,2	25,5	16,5	78,0	<0,5	251,5	<0,5	<10	290,0	95,5	15,5	10,5	97,5	2,0	85,5
E.F.	1	0,7	0,6	0,5	0,5	0,6	0,5	0,4	0,5	1,3	1,1		3,4	<2,5		0,7	0,3	0,5	0,5	0,6	0,7	0,6
N.AL1	32,1	62	25	5,7	1,2	<0,5	3,0	0,46	21	12	72	<0,5	161	<0,5	<10	355	112	26	13	239	2	98
W.AL1	34,2	63	22	5,2	1,2	0,8	2,1	0,31	27	12	87	<0,5	232	<0,5	<10	371	120	26	15	217	2	94
W.ALS2	18,6	33	13	3,3	0,9	<0,5	1,7	0,25	17	5	59	<0,5	314	<0,5	<10	221	121	18	11	174	1	60
W.ALM3	28,3	50	22	4,6	1,0	<0,5	1,9	0,28	24	28	88	<0,5	311	0,7	<10	305	148	24	15	149	2	91
Average	27,0	48,7	19,0	4,4	1,0	0,6	1,9	0,28	22,7	15,0	78,0	<0,5	285,7	0,6	<10	299,0	129,7	22,7	13,7	180,0	1,7	81,7
E.F.	0,9	0,8	0,7	0,7	0,9	0,7	0,6	0,56	0,4	1,2	1,1		3,8	<2,8		0,7	0,3	0,7	0,6	1,1	0,6	0,6
AM.AL1	18,3	36	13	3,4	0,8	<0,5	1,9	0,28	10	6	33	<0,5	66	<0,5	<10	339	127	15	8	141	1	50
AM.AL3	37,4	72	34	7,1	1,6	0,9	3,7	0,56	39	14	98	<0,5	169	<0,5	<10	389	215	36	23	213	2	128
AM.AL14	39,6	74	32	6,8	1,4	0,7	3,1	0,45	73	20	151	<0,5	453	<0,5	<10	334	72	36	24	137	2	148
AM.AL16	37,6	68	28	6,5	1,5	<0,5	2,6	0,39	45	14	105	<0,5	382	<0,5	<10	345	123	31	21	192	2	121
AM.AL17	38,1	73	30	6,6	1,5	0,5	2,8	0,42	47	14	100	<0,5	375	<0,5	<10	349	117	31	21	178	2	120
AM.AL18	39,5	74	30	6,8	1,5	1,1	3,2	0,47	73	19	151	<0,5	461	<0,5	<10	339	73	37	24	144	3	148
Average	35,1	66,2	27,8	6,2	1,4	0,7	2,9	0,43	47,8	14,5	106,3	<0,5	317,7	<0,5	<10	349,2	121,2	31,0	20,2	167,5	2,0	119,2
E.F.	1,2	1,1	1,0	1,0	1,2	0,8	0,8	0,86	0,9	1,1	1,5		4,2	<2,5		0,8	0,3	0,9	0,9	1,0	0,7	0,9
AP.AL1	33,3	62	24	5,7	1,2	1,3	2,6	0,37	26	54	77	<0,5	94	0,6	<10	383	210	29	16	192	2	102
AP.ALS2	19,3	37	16	3,4	0,9	<0,5	1,7	0,25	11	5	46	<0,5	104	<0,5	<10	295	170	17	9	176	1	47
AP.ALM3	37,7	68	28	6,9	1,8	1,0	2,7	0,42	35	13	88	<0,5	58	<0,5	<10	442	249	35	22	252	2	128
Average	30,1	55,7	22,7	5,3	1,3	0,9	2,3	0,35	24,0	24,0	70,3	<0,5	85,3	0,5	<10	373,3	209,7	27,0	15,7	206,7	1,7	92,3
E.F.	1,0	0,9	0,8	0,9	1,1	1,0	0,7	0,69	0,4	1,8	1,0		1,1	<2,7		0,9	0,6	0,8	0,7	1,3	0,6	0,7

Table 1. (continue) Trace and major elements concentrations in the clay layers of Ptolemais – Amynteon lignite deposit

Samples	SiO ₂ %	Al ₂ O ₃ %	Fe ₂ O ₃ %	MnO %	MgO %	CaO %	Na ₂ O %	K ₂ O %	TiO ₂ %	P ₂ O ₅ %	C %	S %	LOI*** (%)
Det.limits.*													
M.C.A.**	59,30	15,36	7,14	0,12	3,46	5,07	3,81	3,11	0,73	0,24	0,02	0,03	
S.AL1	50,14	9,63	4,35	0,10	1,54	14,78	0,56	1,30	0,52	0,05	2,55	0,02	17,73
S.AL3	47,17	13,68	7,60	0,12	3,76	8,54	0,85	1,98	0,67	0,14	2,42	0,02	15,89
S.AL18	33,18	6,62	1,86	0,02	6,34	17,10	0,51	0,70	0,35	0,08	11,15	0,13	32,19
Average	43,50	9,98	4,60	0,08	3,88	13,47	0,64	1,33	0,51	0,09	5,37	0,06	21,94
E.F.	0,73	0,65	0,64	0,67	1,12	2,66	0,17	0,43	0,70	0,38	268,67	2,18	
TE.AL1	50,63	10,23	4,61	0,11	1,60	13,19	0,56	1,20	0,54	0,05	2,72	0,01	18,08
TE.AL3	45,68	13,89	7,56	0,11	4,30	8,18	0,50	2,00	0,67	0,12	2,09	0,01	16,20
TE.AL16	51,54	11,49	2,65	0,03	3,87	6,07	0,56	1,52	0,60	0,08	5,40	0,11	20,22
Average	49,28	11,87	4,94	0,08	3,26	9,15	0,54	1,57	0,60	0,08	3,40	0,04	18,17
E.F.	0,83	0,77	0,69	0,69	0,94	1,80	0,14	0,51	0,82	0,35	170,17	1,67	
KR.AL1	49,68	16,05	8,30	0,16	3,21	4,29	0,33	2,34	0,67	0,09	0,75	0,01	15,72
KR.AL2	7,92	2,39	1,27	0,03	0,90	46,75	0,06	0,32	0,10	0,06	9,05	0,01	38,91
Average	28,80	9,22	4,79	0,10	2,06	25,52	0,20	1,33	0,38	0,08	4,90	0,01	27,32
E.F.	0,49	0,60	0,67	0,79	0,59	5,03	0,05	0,43	0,52	0,31	245,00	0,38	
N.AL1	62,26	12,04	5,18	0,10	1,55	4,80	1,44	1,64	0,67	0,06	0,89	0,01	11,24
W.AL1	55,26	12,87	6,01	0,11	2,55	6,42	1,18	1,52	0,65	0,07	1,08	0,01	14,00
W.ALS2	58,42	8,52	4,32	0,08	3,93	8,86	1,49	1,23	0,47	0,06	1,75	0,01	11,49
W.ALM3	52,81	11,55	6,13	0,10	3,75	8,63	1,11	1,73	0,57	0,11	2,20	0,03	14,24
Average	55,50	10,98	5,49	0,10	3,41	7,97	1,26	1,49	0,56	0,08	1,68	0,02	13,24
E.F.	0,94	0,71	0,77	0,81	0,99	1,57	0,33	0,48	0,77	0,33	83,83	0,64	
AM.AL1	81,56	7,56	2,84	0,06	0,90	1,51	1,49	1,43	0,51	0,04	0,05	0,01	2,14
AM.AL3	56,63	14,91	7,17	0,10	3,76	4,98	2,16	1,61	0,80	0,15	0,41	0,14	6,70
AM.AL14	47,80	17,95	7,33	0,04	6,05	1,49	0,44	1,02	0,86	0,07	2,12	0,04	15,96
AM.AL16	57,31	15,23	6,53	0,06	5,14	1,89	1,29	1,42	0,80	0,07	0,90	0,04	9,17
AM.AL17	56,08	15,97	6,60	0,05	5,11	1,81	1,23	1,43	0,81	0,07	1,01	0,03	9,70
AM.AL18	48,35	18,22	7,91	0,04	6,03	1,49	0,45	1,10	0,86	0,09	2,14	0,03	15,96
Average	57,96	14,97	6,40	0,06	4,50	2,20	1,18	1,34	0,77	0,08	1,11	0,05	9,94
E.F.	0,98	0,97	0,90	0,49	1,30	0,43	0,31	0,43	1,06	0,34	55,25	1,86	
AP.AL1	56,45	12,68	5,69	0,10	2,23	6,94	1,48	1,43	0,71	0,07	1,12	0,02	11,41
AP.ALS2	66,95	8,72	2,92	0,07	1,48	7,50	2,17	1,27	0,45	0,06	1,24	0,01	7,52
AP.ALM3	61,78	14,46	6,84	0,10	2,95	3,83	2,45	1,80	0,90	0,12	0,12	0,08	3,58
Average	61,73	11,95	5,15	0,09	2,22	6,09	2,03	1,50	0,68	0,08	0,83	0,04	7,50
E.F.	1,04	0,78	0,72	0,75	0,64	1,20	0,53	0,48	0,93	0,35	41,33	1,41	

It should be noted that similar concentrations in the trace elements As, Cd, Co, Cr_{tot}, Cu, Ni, Pb, Zn, Mo and V as well as the major elements Ca, Mg and Mn have been determined by the recent study of NTUA regarding the south part of Ptolemais basin [15].

Horizontal variations of trace elements concentrations

Horizontal variations in trace elements concentrations of clay layers are evident both within the lignite bearing strata and the overburden. In the mines of South Field, Kardina and Sector 6 (i.e. in the south part of Ptolemais basin) the minimum values of the average per mine concentrations are observed for the elements Cr, Hf, Sc, Ag, Cd, Sr, Y, Sn, Zr, V and all the rare earth elements that were examined (La, Ce, Nd, Sm, Eu, Tb, Yb, Lu). The maximum concentrations are usually observed in the mines of Amynteon, Anargiri and Sector 6: La, Ce, Nd and Sm in Amynteon mine, Cs, Hf, Rb, Sb, Sc and Tb in Anargiri mine, Yb, Lu, U and almost all the rare earth elements in Sector 6 mine, Cr in Mavropigi mine, while the siderophile elements Ni and Sn, the chalkophiles Pb,

Cd, Zn, Ag and the lithophiles Cs, Ba, Sr, Y, Zr and V exhibit considerably higher concentrations in the north part of the basin, in the mines of Amynteon and Anargiri.

In the south-central area of Ptolemais deposit, between the sampling points of Sector 6 and Kardia mines, which are located at a distance of less than 2km, significant variations of trace elements concentrations are observed. Only As, Br, Sb and Ni exhibit higher average concentrations in Kardia mine, while Co, Cr, Hf, Sc, Ta, Th, U Pb, Zn, Ba, Y, Sr, Zr and all the 8 rare earth elements that were examined exhibit higher concentrations in Sector 6 mine, with the EF to differ more than 100% in the cases of As, Pb and Zr. Similarly, spatial differences have been determined in the trace elements concentrations of the neighbouring mines of Amynteon and Anargiri (north part of the lignite deposit), where Pb and Sr exhibit significantly higher concentrations in Anargiri mine and Co, Cr, U, Zn and Ni in Amynteon mine.

In Figure 2 are shown the variations of the concentrations of 7 trace elements among six mines of the Ptolemais – Amynteon basin, for the upper and the deeper clay layer of each mine. It is obvious that, as far as the deeper layers are of concern, Kardia mine exhibits the lowest concentrations. It is also evident that the pick concentrations of the upper and deeper layer for each element are not detected in the same mine.

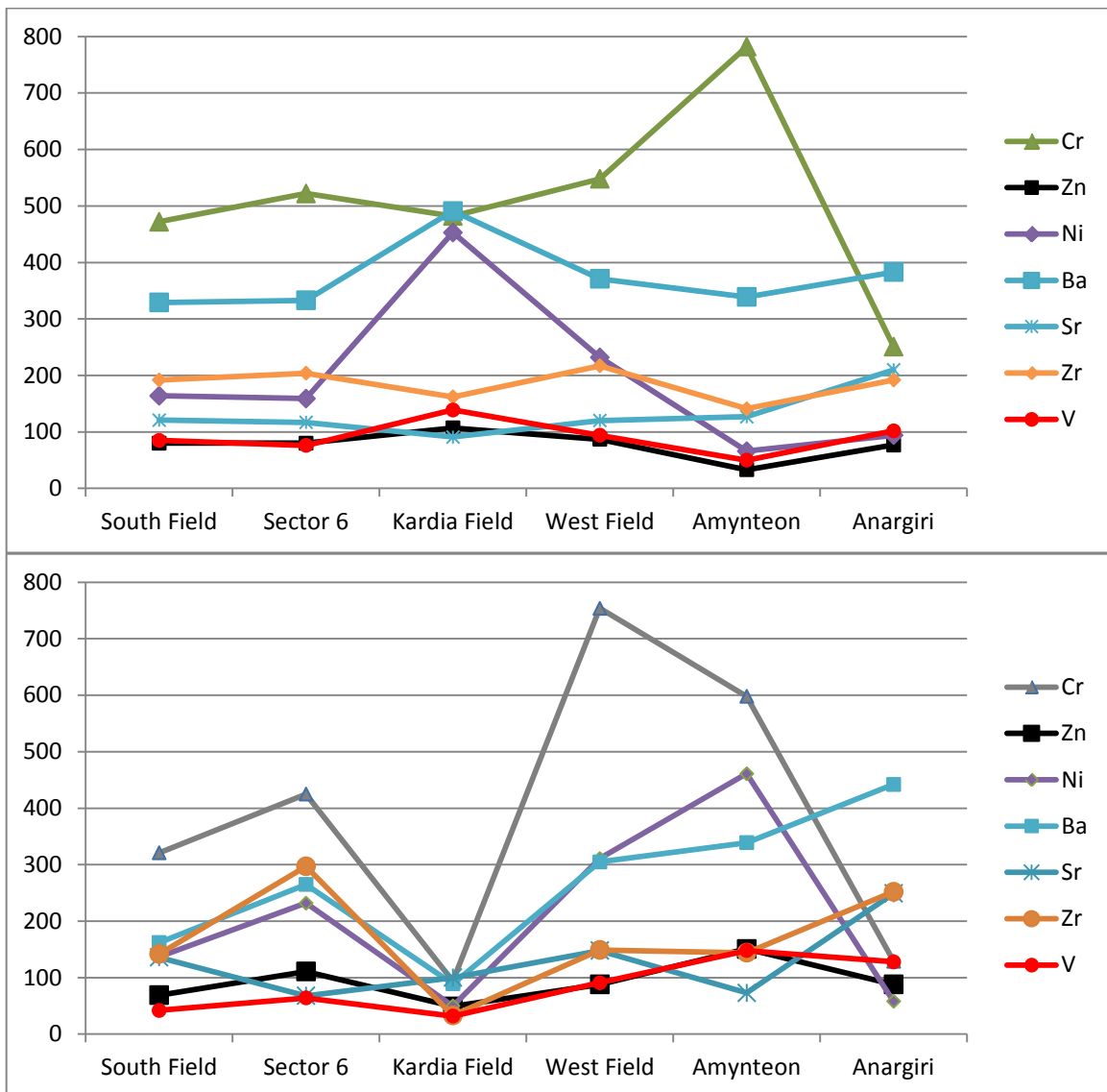


Figure 2. Variations of the concentrations (in ppm) of 7 trace elements among six mines of the Ptolemais – Amynteon basin, for the upper and the deeper clay layer of each mine

Regarding major elements, almost all (SiO₂, Al₂O₃, Fe₂O₃, MnO, Na₂O, K₂O, TiO₂, P₂O₅, CaO and MgO) exhibit minimum concentrations in the south part of the basin, apart from CaO and MgO, which have been observed in low concentrations in the mine of Amynteon and Anargiri. All the other major elements, mainly SiO₂, Fe₂O₃ and MgO, exhibit maximum concentrations in these two mines, probably because of the presence of the metamorphic schists and gneiss-schists of the Upper Palaeozoic.

In general, from the above-presented results it is obvious that, in the central part of Ptolemais basin, the concentrations of the majority of trace elements in the clay layers are varying when moving in the same time-stratigraphic horizons from one mine to another. These variations, which concern both the trace and major elements, can be explained by the local palaeogeographic conditions and, particularly, the hydrographic network of the Pliocene lake, which was fed with large quantities of clastic, fine, carbonaceous materials (Kardia mine) and clayey and sandy materials coming from the west margins of the basin (Amynteon and Anargiri mines). Moreover, the observed variations of the trace elements concentrations in certain stratigraphic horizons of the lignite-bearing formation are directly connected with the changes of their lithologic composition (gradual transition of lateral contacts of clays to sandy clays or marly clays).

Vertical variations of trace elements concentrations

Because of the limited number of the clay layers of the lignite-bearing formation, it is difficult to come to safe conclusions regarding the vertical distribution of the trace elements. However, for some elements, it is clear that their concentrations vary in relation to the depth. The element As exhibits minimum concentrations in the lower clay layer in the mines of South Field, Sector 6, West Field, Amynteon and Anargiri. Cs and Hf exhibit minimum concentrations in the upper clay layer of the overburden strata of Amynteon and Anargiri mines, respectively.

Maximum concentrations in the upper layers exhibit As, in the south part of the deposit (10ppm in South Field mine and 24 ppm in Kardia mine) and Sb (1.8 ppm in Kardia mine). For the other trace elements, Rb, Th, U, rare earth elements (La, Ce, Nd, Sm, Eu, Tb, Yb, Lu), Cu, Pb, Zn, Ni, Ba, Sr, Y, Sn, Zr, Be and V there is not clear tendency of increased or decreased concentrations in relation to the stratigraphy of the lignite deposit and the overburden strata.

In the mines of Kardia and Anargiri, Cr exhibits minimum (94ppm) concentrations in the lower clay layers of the deposit, while its maximum (616ppm) concentrations are observed in the lower layers of Amynteon mine. The increase of Cr concentrations in Amynteon mine is directly related to the palaeogeographic conditions and the sediments of Pleiocene - Pleistocene that were formed with the transport of ultrabasic material from streams and rivers that flew from the south part of Ptolemais basin to Amynteon basin [16, 4].

For the trace elements As, Hf, Cs, Sb, Th, U, the most of rare earth elements (La, Ce, Nd, Yb, Lu), Ni, Ba and Y, the concentrations peaks are observed in the first clay layer of Kardia mine and the deepest clay layer of Sector 6 mine.

In Figure 3 is shown the variation of the concentrations of selected trace elements (Co, Cs, Th, Cu, Pb) in the clay, sandy-clay and marly-clay layers of six mines of Western Macedonia Lignite Centre. In the mine of Anargiri, the lower concentrations are observed in a sandy-clay layer. In the neighbouring mine of Amynteon, the maximum concentrations are systematically exhibited by the third and the deeper clay layer, while minimum concentrations for all the presented trace elements are exhibited by the upper clay layer. In the mines of Kardia and South Field the deeper clay layers have always lower concentrations than the upper ones. Finally, in the mine of Sector 6, the concentrations of Th and Cs remain practically constant in the three clay layers that were sampled, while the middle layer exhibits higher concentrations for the elements Pb, Co and Cu.

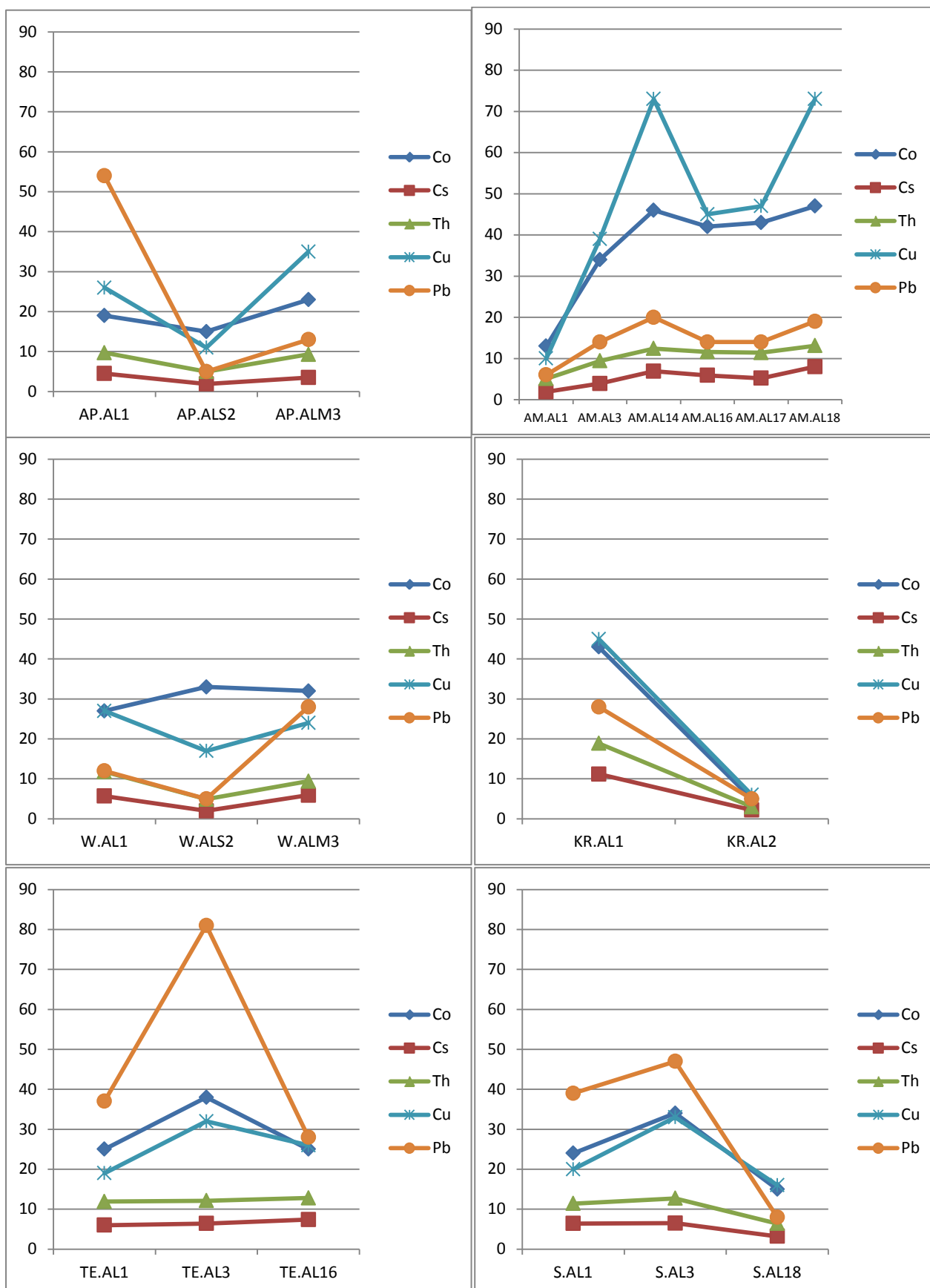


Figure 3. Variation of the concentrations (in ppm) of selected trace elements in the clay (AL), sandy-clay (ALS) and marly-clay (ALM) layers of Anargiri (AP), Amynteon (AM), West Field (W), Kardia (KR), Sector 6 (TE) and South Field (S) mines

The deeper clay layers of the overburden in the mine of Anargiri and the upper clay layers in the mine of Amynteon are separated by a Quaternary fault of maximum vertical displacement of 120m. For many trace elements, the average concentrations determined in the samples of Anargiri mine are considerably less than those of the samples collected in Amynteon mine (e.g. Cr 392.3ppm vs. 673.8ppm, Pb 24.0ppm vs. 47.8ppm, Ni 85.3ppm vs. 317.7ppm). The wide variations of the concentrations within a such close distance is explained by the presence of fine, sandy clay and marly clay material originated from the metamorphic rocks of the mountains that form the west margins of Amynteon basin.

In the south-central part of Ptolemais basin (Kardia and Sector 6 mines) there is clear difference of the concentrations of most trace and major elements between the overburden and lignite-bearing strata. In the north part of the basin this difference are not so clear. In Kardia mine, the strong relation between trace elements concentrations and time-stratigraphic characteristics of the deposit is attributed to the lithology of the overburden and the presence of coarse and fine clastic sediments, more or less carbonated and/or sandy.

General remarks

The relatively higher concentrations in the north part and the south-central part (Kardia and Sector 6 mines) of the lignite-bearing basin are attributed to the local palaeogeographic conditions and, particularly, to the hydrographic network. The lakes of Pliocene were fed with large amounts of clay and coarse sediments from the surrounding mountains and from numerous palaeochannels of the lower Pleistocene rivers, which transported materials of different lithological-petrographic composition. This is the case of deposition of ultramafic strains in several areas distributed from the south margins of Ptolemais basin to Amynteon basin [16]. More analytically, the maximum concentrations of the trace elements are connected with spatial variations (horizontal and vertical) that are attributed to the existence of clay minerals, argillaceous sediments, sandstones, partly to weathering of limestones and dolomites, to the transfer from mafic and ultramafic rocks (dunites, peridotites, pyroxenites) for the elements Th, U, Y and Ni, and metamorphic rocks, mainly clay shales. The occurrence of Ba is linked with alkali feldspar and biotite [17, 14, 8].

From an environmental point of view, it is worth noticing that the trace elements As, Cd, Hg, Mo, and Se, which are considered as trace elements of greatest environmental concern, have low concentrations in relation to the average concentrations of the main rocks of the Earth's crust. The trace elements of moderate environmental concern (Cu, Ni, V, Zn), the trace elements of minor concern (Ba, Co, Mn, Sb, Sr), the radioactive elements (Th, U) [7] and the elements of environmental concern that are usually present in very low concentrations (Be, Sn, Te) exhibit also low to very low concentrations.

Cr exhibits higher concentrations in relation to the mean values of the main rocks of the Earth's crust. The higher enrichment of this lithophile element, in relation to the rest of the examined elements, can be explained from its geochemical affinity with oxides and oxygen compounds in the silicate rocks of the sedimentary basin and mainly from the disintegration of the chromium minerals of the serpentinised peridotites of the mountains that surround the lignite-bearing basin [12, 16, 15].

4. CONCLUSIONS

The trace and major elements contained in the clay layers of Pliocene - Pleistocene epochs of the Ptolemais and Amynteon lignite deposits exhibit low to very low concentrations. For 11 out of 39 trace elements that were investigated in this study the determined EF are less than 1, while for another 13 trace elements the EF are less than 2. The trace elements Hf, Cd, Pb, Ni and Sb exhibit enrichment factors that vary, among the different mines, from 0.5 to 5.0. Only As and Cr exhibit

systematically higher EF than the other elements, with their maximum EF values per mine varying from 2 to 10.

The average concentrations of all the analysed major elements are similar to the MVEC. Regarding trace elements, Co, Cs, Hf, Rb, Sc, Th, U, La, Ce, Nd, Sm, Eu, Tb, Yb, Lu, Cu, Pb, Zn, Ni, Cd, Ba, Sr, Y, Sn, Zr, Be and V exhibit enrichment factors that vary from 0.5 to 3.0 among the different mines of the examined area, while the highest enrichment factors exhibit the elements Sb (3.5 ppm), Ag (4.1 ppm) and Cr (4.6 ppm) (average values in the entire Ptolemais – Amynteon basin). Nevertheless, the elements of greatest environmental concern (As, Se, B, Cd, Hg, Mo, Pb) are present in clays in low concentrations.

In combination with the low alkaline pH values prevailing in the surface water, groundwater and soils of Ptolemais basin, the probability to detect toxic conditions due to the presence of trace elements and other residues in the waters and soils of Ptolemais area is negligible.

REFERENCES

- [1] Koukouzas C. & Koukouzas N. (2000). Classifications of the Greek lignite deposits according to the United Nations International Framework classification for reserves/resources. *Mineral Wealth*, 4/2000, 117, pp.17-36.
- [2] Varvarousis G., Metaxas, A., Kotis, Th., Ploumidis, M. (2000). The Neogene deposits of Kozani-Servia basin, Westwern Macedonia, Greece. *Geological society of Greece, Special Publications*, No 9, 227-233. *Proceedings interim Colloquium RCMNS*, Patras, Greece, may 1998.
- [3] Kassoli-Fournaraki A., Georgakopoulos A., Michailidis K., Filippidis A. (1993). Morphology, mineralogy and chemistry of the respirable size (<5 μ) fly ash fraction from the main and Northern lignite fields in Ptolemais, Macedonia, Greece. In: *Current research in geology Applied to Ore Deposits*, F. Hach-Ali, J. torres-Ruiz & F. Gervilla, Eds., La Guioconda, Granada, 727-730.
- [4] Sachanidis C., Georgakopoulos A., Filippidis A., Kassoli-Fournaraki A. (2001). Trace elements concentrations in marly seams of Ptolemais Amyntaion lignite bearing formations, West Macedonia. *Bulletin of the Geological Society of Greece*. VolXXXIV/3. 1115-1122, 2001 *Proceedings of the 9th International Congress*. Athens, September 2001.
- [5] Finkelman R.B. (1993). Trace and Minor elements in coal. In: *Organic Geochemistry*, Engel, M.H., Macko S.A. (Ed.), 593-607 (Plenum Press, New York).
- [6] Swaine D.J. & Goodarzi, F. (1995). *Environmental aspects of trace elements in coal*, 312 pp. (Kluwer Academic Publishers, the Netherlands).
- [7] Clarke L.B. and Sloss, L. (1992). *Trace elements Emissions from coal combustion and gasification*. IEACR/49, London.
- [8] Filippidis A. & Georgakopoulos A. (1992). Mineralogical and chemical investigation of fly ash from the Main and Northern lignite fields in Ptolemais, Greece. *Fuel*, Vol. 1. No. 4, April 1992, Butterworth-Heinemann.
- [9] Filippidis A., Georgagopoulos A, Kasoli-Fournaraki A, Misaelides P, Yiakkoupis P, Brossoulis J. (1996). Trace elements content in composite samples of three lignite seams from the central part of Drama lignite deposit, Macedonia, Greece. *Intl. J. Coal Geol.* (29), pp.219-234.
- [10] Christanis et al. (1998). Geological factors influencing the concentration of the trace elements in the Philippi peatland, eastern Macedonia, Greece. *Int. J. Coal.* 36, 295-313.
- [11] Swaine D.J. (1990). *Trace elements in coal*. Butterworths publications.

- [12] Mason B. & Moore C.B. (1982). Principles of geochemistry, 344 pp. (John Wiley and Sons, New York).
- [13] Faure G. (1991). Principles and Applications of inorganic Geochemistry, (MacMillan, New York).
- [14] Krauskopf K.B. & Bird D.K. (1995). Introduction to geochemistry, 647 pp. (MacGraw-Hill, New York).
- [15] National Technical University of Athens (2016). Mineralogic-minerals and ores-petrologic and geochemical correlation in geological formations (ultramafic rocks, lignite and the combustion products of lignite (fly ash) with the surface and underground quality water of the Sarigiol lignite fields. FINAL REPPORT. In Greek. National Technical University of Athens, September 2016. pp 802.
- [16] Faugeres L. (1978). Recherches geomorphologiques en Grece septentrionale. Macedoine Centrale et Occidentale. Tome I et II. PARIS 1978.
- [17] Kabata-Pendias A. & Pendias H. (1992). Trace elements in Soils and Plants. 2nd ed. CRC Press. Boca Raton, Ann Arbor, London.
- [18] Skoulikidis N.T. (2001). Levels and possible sources of the Heavy metals in surficial sediments of lake Vegoritis. Bulletin of the Geological Society of Greece. VolXXXIV/3. 1123-1130,2001 Proceedings of the 9th International Congress. Athens, September 2001 (in Greek).

Session 8: Geological exploration, quality control, homogenization

Structural Geology of the Lignite Mines in the Ptolemais Basin, NW Greece

E. Delogkos^{1,2}, V. Papanikolaou¹, T. Manzocchi^{1,2}, C. Childs^{1,2}, V. Roche¹, G. Camanni¹, M. P. J. Schöpfer³, J. J. Walsh^{1,2}, S. Pavlides⁴, A. Chatzipetros⁴, C. Sachanidis⁵ and T. Barbas⁵

¹Fault Analysis Group, UCD School of Earth Sciences, University College Dublin, Belfield, Dublin 4, Ireland

²Irish Centre for Research in Applied Geosciences, UCD School of Earth Sciences, University College Dublin, Belfield, Dublin 4, Ireland

³Department for Geodynamics and Sedimentology, University of Vienna, Althanstrasse 14, A-1090 Vienna, Austria

⁴Department of Geology, Aristotle University of Thessaloniki, Thessaloniki, Greece

⁵Public Power Corporation of Greece, Western Macedonian Lignite Centre, Ptolemais, Greece

ABSTRACT

The active, opencast, lignite mines in the Ptolemais Basin, NW Greece, provide world-class outcrops for characterising and understanding normal fault systems from km- down to mm-scale. We have visited and mapped these mines 26 times at ca. 3 month intervals since October 2009. The data collected during each fieldwork campaign were structural measurements, interpretations, various resolutions of photographs and GPS locations for all exposed faults and related structures observed in each mine. Part of this unique dataset has been imported within a fully georeferenced 3D structural interpretation package and has been used for fault and horizon interpretations. Our motivation for this work is to advance our generic understanding of the structure and development of normal faults, but in this contribution, we focus on some of our findings that might be of more general interest to mine planners and designers.

1. INTRODUCTION

The Ptolemais Basin is an elongated intramontane lacustrine basin and is part of Florina-Ptolemais-Servia Basin which is a NNW-SSE trending graben system that extends over a distance of 120 km from Bitola in the Former Yugoslavian Republic of Macedonia (F.Y.R.O.M.) to the village of Servia, south-east of Ptolemais, NW Greece [1]. The basin is filled with a 500-600 m (in a few areas up to about 1000 m) thick succession of sediments which are divided into the Upper Miocene to Lower Pliocene Lower Formation, the Pliocene Ptolemais Formation and the Quaternary Upper Formation. The Ptolemais Formation contains the upper and lower lignite seams which alternate with clays, marls, sandy marls and sands [1, 2].

The basin is bounded by two fault systems which can be related to two extensional episodes [3, 4]. The first, Late Miocene episode resulted in the origin of the Florina-Ptolemais-Servia Basin in response to NE-SW extension, which was subsequently subjected to NW-SE extension during the Quaternary, resulting in the NE-SW-striking faults which currently bound a number of sub-basins, including the basins of Florina, Ptolemais and Servia [3] (Fig. 1).

There is little surface evidence of the Late Miocene NW-SE-striking faults that control the basin margins, although their presence is confirmed from boreholes [3] and from some recent exposures along the western margin of the Ptolemais Basin in the vicinity of Mavropigi lignite mine (Fig. 1). The surface geology is dominated by the Quaternary faults, which have orientations ranging from the expected NE-SW strikes to the north of the region, to NNE-SSW orientations to the north

of the Mavropigi Mine, and through to approximately east–west strikes in the vicinity of the Kardia and Notio mines (Fig. 1).

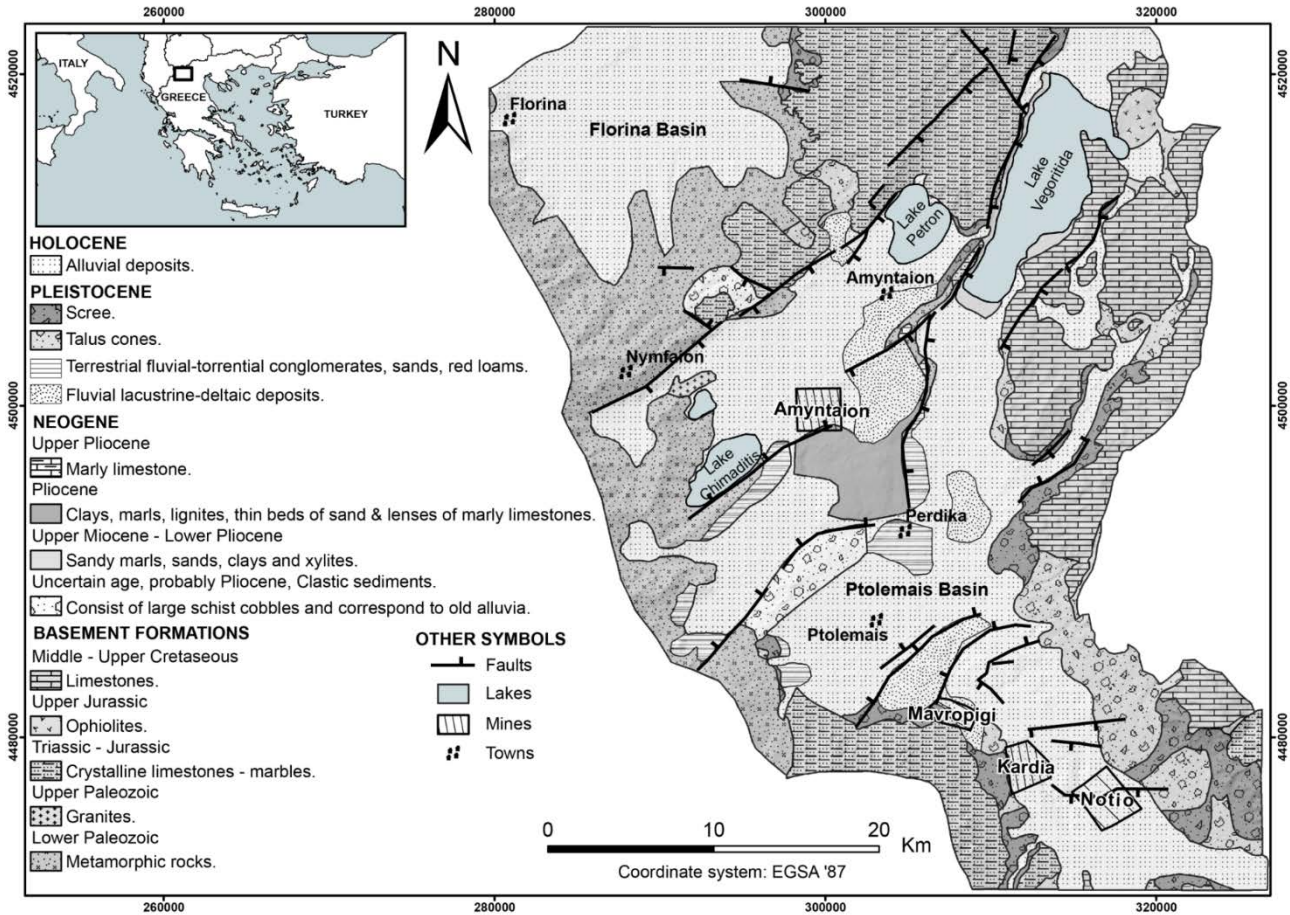


Figure 156. Geological map of the Ptolemais Basin showing the major fault structures and the locations of the four active, open-pit lignite mines (modified after [1]).

In this paper we present (1) the general characteristics of the normal faults observed within the lignite mines in Ptolemais Basin, (2) the structures associated with the contemporaneous bed-parallel slip and normal faulting observed in Kardia Mine and (3) our interpretation of the compressional structures observed in Notio Mine.

2. GENERAL CHARACTERISTICS OF THE NORMAL FAULTS

The exposed lignite-marl sequence is displaced by numerous normal faults with maximum displacement up to 65 m (e.g. Fig. 2). The faults form soft-linked systems [5], characterised by a prevalence of fault tips as opposed to branch-points, with ductile bed rotations between faults accommodating transfers of strain between adjacent faults. Quantitative analysis of the faults indicates that these systems are extremely soft and that for a given throw, these faults are both shorter and more segmented than many other fault systems [6, 7]. Furthermore, these faults have anomalously high fault displacement to fault rock thickness ratios compared to normal faults in other areas. Wide zones of fault rock (e.g. breccias, cataclasites) are not developed in these faults. Small-scale lenses and splays that, with increasing displacement, would be pulverized and converted into fault rock in other lithologies, are preserved in these rocks, allowing their detailed structure to be examined at high strains.

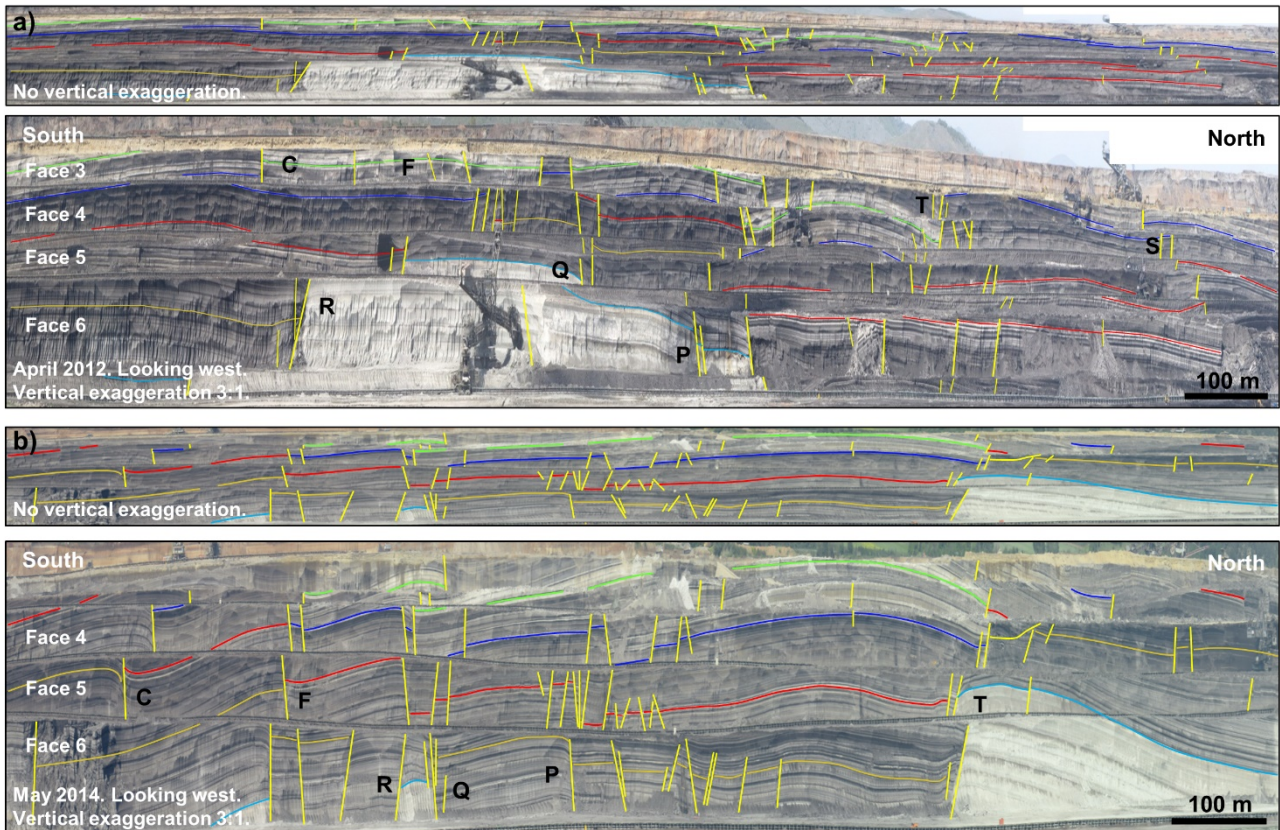


Figure 2. True scale and $\times 3$ vertically exaggerated panoramic view of the active, open-cast, Kardia Mine in (a) April 2012 and (b) May 2014. Faults are drawn as yellow lines and a selection of horizons is highlighted. The letters (C, F, R, Q, P, T and S) are the names of the interpreted fault zones. After [8].

Vertically exaggerated field photographs (e.g. Fig. 2) clearly show folds present in these mines. The folds are spatially related to the faults and show normal and reverse drag geometries, which indicates that they are part of the same geological deformation event. Reverse drag refers to folding within the volume surrounding a fault, resulting in layers that are concave towards the slip direction [9], with the development of hanging wall rollover and footwall uplift. Reverse drag is a much larger scale feature than normal drag and defines the displacement field associated with the faults. Often it is difficult to identify reverse drag in the field, especially in areas of high fault density. We expect greater expression of reverse drag on the hanging wall rather than on the footwall of the normal faults in the Ptolemais Basin, as it has been estimated that the footwall uplift/hanging-wall subsidence ratio is 1:2 for these faults [10]. The vertically exaggerated panoramic view of the Kardia Mine (Fig. 2) clearly shows reverse drag structures on the hanging wall of fault zones R and T. Figure 2a also shows the product of opposing reverse drag zones, in the form of an anticline, between the two opposite-dipping large fault zones, P and T. Normal and reverse drag can often occur on the same fault (e.g. Fig. 2b, fault zone T at face 6), with the reverse drag occurring over a much larger distance, but with relatively lower bed rotations.

Another form of folding related to the faults in Ptolemais are monoclines in which a geometrical offset is observed over a localized volume of rock, but where no discrete faults are formed. A partly faulted monocline structure exists in fault zone Q in Kardia mine, overlying an array of soft-linked fault segments. Monoclines are also observed at the tips of individual fault segments.

3. BED-PARALLEL SLIP AND NORMAL FAULTING (KARDIA MINE)

The normal faults exposed in Kardia lignite mine formed at the same time as bed-parallel slip-surfaces, so that while the normal faults grew they were intermittently offset by bed-parallel slip [11, 12]. Bed-parallel slip has a persistent top-to-the-north slip direction, ranging from a few centimetres up to 4.5 m, and is attributed to reverse-drag folding (i.e. rollover) in the hangingwall of a north-dipping basement normal fault south of the Kardia Mine. Following offset by a bed-parallel slip-surface, further fault growth is accommodated by reactivation on one or both of the offset fault segments. Where one fault was reactivated the site of bed-parallel slip is a bypassed asperity. Where both faults are reactivated, they propagate past each other to form a volume between overlapping fault segments. These structures contain either a repeated (e.g. Fig. 3) or a missing section of stratigraphy which has a thickness equal to the throw of the fault at the time of the bed-parallel slip event, and the displacement profiles along the relay-bounding fault segments have discrete steps at their intersections with bed-parallel slip-surfaces (e.g. Fig. 3). With further increase in displacement, the overlapping fault segments connect to form a fault-bound lens. Geometrical restoration of cross-sections through selected faults shows that repeated bed-parallel slip events during fault growth can lead to complex internal fault zone structure that masks its origin.

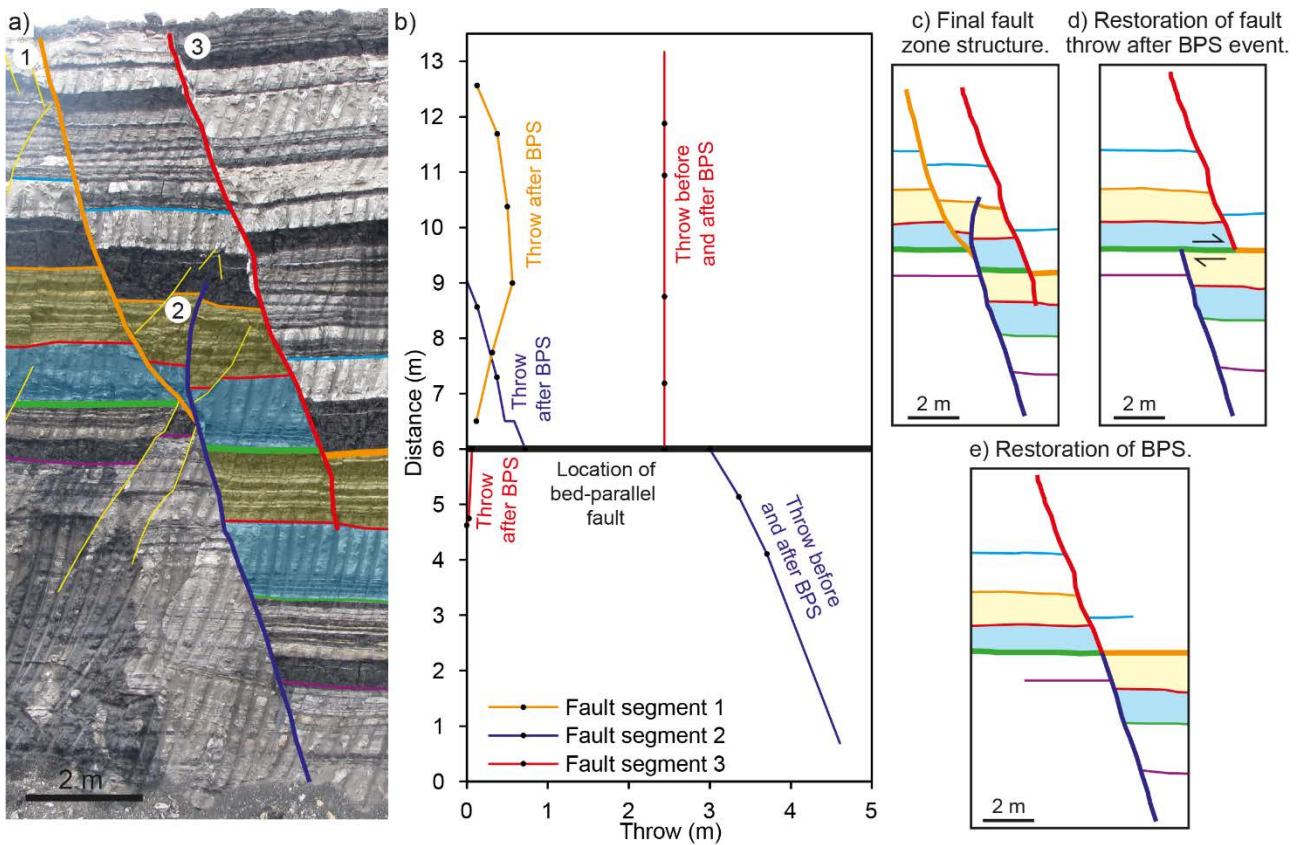


Figure 3. a) Outcrop photograph of a ca. 4 m throw normal fault zone which is displaced by bed-parallel slip during its growth. The colour filled part of the sequence is repeated within the fault zone. b) Displacement profiles along the main fault segments showing displacement gradient singularities where they cross the bed-parallel slip-surface that marks the transition from the pre-existing fault segments to the post bed-parallel slip segments. c) Simplified sketch of the final fault zone structure. d) Restoration of the fault throw accommodated after the bed-parallel slip event. e) Restoration of the bed-parallel slip. The bold lines on all figures indicate the bed-parallel slip-surface; these lines change in colour as the slip-surface moves from one horizon to another. After [11].

4. SYNSEDIMENTARY SUBAQUEOUS LANDSLIDE (NOTIO MINE)

One of the mines, Notio Mine, contains thrusts that predate Quaternary faults but have identical strikes (Figs. 4 and 5). It has been suggested [13] that the normal faults and thrusts are

associated with extension above, and compression below, a neutral surface associated with folds developed in an active transpressional zone.

Detailed mapping, however, shows that the thrusts are constrained within a well-defined approximately 30 m-thick stratigraphic interval [6] (Fig. 4). The base of the interval is a decollement about five meters below the Ptolemais Formation from which the individual thrusts rise. The top of the interval is an unconformity associated with a prominent marl couplet within the Ptolemais Formation. We have not seen any thrusts above this unconformity (where there is extensive outcrop) or below the decollement (where outcrop is sparser) [6].

We interpret this interval to represent a synsedimentary subaqueous landslide, with the presence of geometries similar to, but on a larger scale than, those contained in soft sediments in the Dead Sea described by [14]. Therefore, the thrusts are not associated with tectonic compression, but instead are of very early, synsedimentary gravity-driven origin. The thrusts are consistently cross-cut by the normal faults and occasionally reactivated as normal faults, providing further evidence for the early timing of the thrusts. Our interpretation of synsedimentary slumping followed by normal faulting and fault-related folding is significantly different to the model for these structures suggested by [13], which requires a transtensional-dominated regime.

Apart from the fact that a portion of the sequence being faulted is thrust, we see little difference in character of the large normal fault zones in the Notio Mine and elsewhere. However, there are cases where the normal faults steepen from a thrust dip (ca. 30°) above the unconformity and into the underlying marl and therefore the normal offsets are demonstrably later than the thrusts (which do not exist above the unconformity or below the decollement) but we have also observed many examples of smaller thrusts reactivated as normal faults within the thrust interval [6]. The development of this unusual type of reactivation arises from the fact that the thrusts are in the ideal orientation for exploitation by the normal faults (Fig. 5).

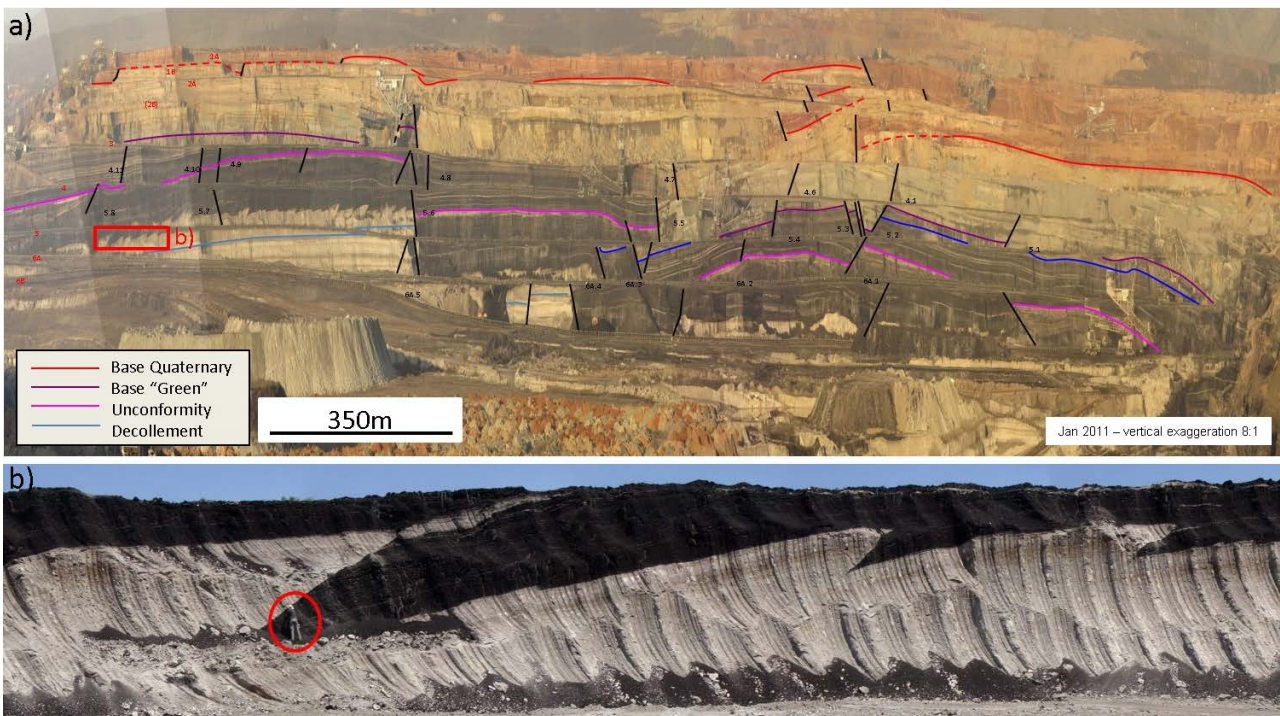


Figure 4. a) Photomontage of the Notio Mine. b) Close up view of the area indicated in (a). After [6].

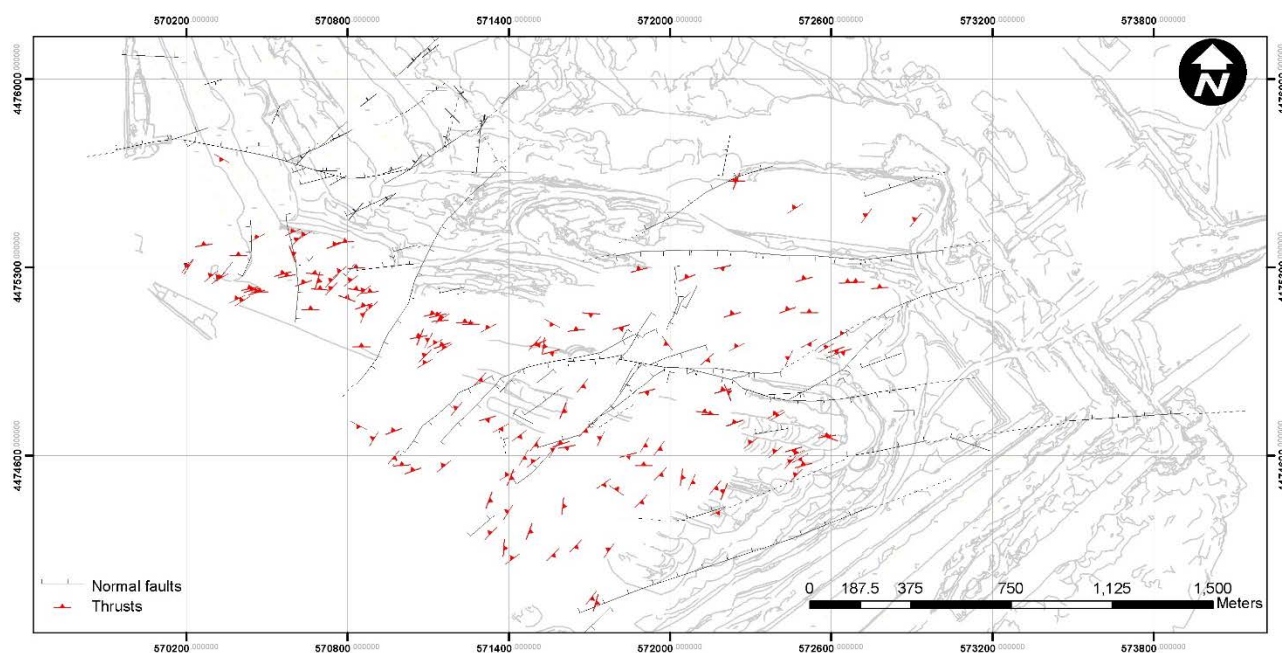


Figure 5. Fault map of the Notio Mine.

5. CONCLUSION

The exposed lignite-marl sequence of the Ptolemais Basin is displaced by numerous normal faults with maximum displacement up to 55 m. The displacement along each fault surface decreases from a maximum value at the centre of the fault surface towards zero-displacement fault tips. A notable characteristic of these faults is that they have higher displacement gradients (i.e. the ratio between maximum displacement and length) than normal faults in other areas, and are also more segmented at a range of scales. A characteristic of the mines is the presence of gentle folds which often become more pronounced close to the normal faults. These folds are not formed by tectonic compression, but are the result of normal and reverse drag geometries developed during the growth of the extensional normal fault system. Furthermore, in Kardia Mine, normal faulting was associated with contemporaneous bed-parallel slip resulting in further segmentation of the normal faults and in the development of structures that can contain either a repeated or a missing section of stratigraphy. Finally, Notio Mine contains thrusts within a well-defined stratigraphic interval towards the lower part of the Ptolemais Formation. These thrusts have a syn-sedimentary rather than tectonic origin, and are contained within a mass transport complex extending over the width of the mine, and containing an irregular stratigraphy. The thrusts are sometimes reactivated in extension during the later faulting event.

REFERENCES

- [1] Pavlides, S. (1985) 'Neotectonic evolution of the Florina-Vegoritits-Ptolemais basins'. PhD thesis. University of Thessaloniki Greece, 256 pp.
- [2] Koufos, G., Pavlides, S. (1988) 'Correlation between the continental deposits of the lower Axios valley and Ptolemais basin'. *Bull Geol. Soc. Greece* 1988; 20:9–19.
- [3] Pavlides, S.B., Mountrakis, D.M. (1987) 'Extensional tectonics of northwestern Macedonia, Greece, since the late Miocene'. *J. Struct. Geol.* 9 (4), 385–392.
- [4] Mercier, J.L., Sorel, D., Vergely, P. (1989) 'Extensional tectonic regimes in the Aegean basins during the Cenozoic'. *Basin Res.* 2, 49–71.

- [5] Walsh, J. J., Watterson, J. (1991) 'Geometric and kinematic coherence and scale effects in normal fault systems'. In: *Geometry of Normal Faults* (edited by Roberts, A., Yielding, G. & Freeman, B.). *Spec. Pub. geol. Soc. Lond.* 56, 193-203.
- [6] Fault Analysis Group, UCD. (2011) 'Structural geological observations in the Ptolemais lignite mines – a preliminary report'. Unpublished.
- [7] Delogkos, E. (2011) 'Quantitative analysis of geometric evolution of fault zones of Mavropigi' lignite field in Ptolemais Basin (W. Macedonia, Greece)'. Master thesis. Aristotle University of Thessaloniki, Greece, 98 pp.
- [8] Delogkos, E., Manzocchi, T., Childs, C., Sachanidis, C., Barmpas, T., Schöpfer, M., Chatzipetros, A., Pavlides, S., Walsh, J.J. (2016) Throw partitioning across normal fault zones in the Ptolemais Basin, Greece. In: Childs, C., Holdsworth, R. E., Jackson, C. A.-L., Manzocchi, T., Walsh, J. J. & Yielding, G (eds). *The Geometry and Growth of Normal Faults*. Geological Society of London: Special Pub. 439. doi:10.1144/SP439.19
- [9] Barnett, J.A.M., Mortimer, J., Rippon, J.H., Walsh, J.J. & Watterson, J. 1987. Displacement geometry in the volume containing a single normal fault. *American Association of Petroleum Geologists Bulletin*.
- [10] Doutsos, T. and Koukouvelas, I. 1998. Fractal analysis of normal faults in northwestern Aegean area, Greece. *Journal of Geodynamics*, 26, 197–216, doi: 10.1016/S0264-3707(97)00052-5.
- [11] Delogkos, E., Childs, C., Manzocchi, T., Walsh, J.J., Pavlides, S. (2017) The role of bed-parallel slip in the development of complex normal fault zones. *Journal of Structural Geology*. doi: 10.1016/j.jsg.2017.02.014.
- [12] Delogkos, E., Childs, C., Manzocchi, T., Walsh, J.J. (2018) The nature and origin of bed-parallel slip in Kardias Mine, Ptolemais Basin, Greece. *Journal of Structural Geology*. doi: 10.1016/j.jsg.2018.05.015.
- [13] Diamantopoulos, A., Krohe, A. & Dimitrakopoulos, D. 2013. Deformation partitioning in a transtension-dominated tectonic environment: the illustrative kinematic patterns of the Neogene–Quaternary Ptolemais Basin (northern Greece). *Journal of the Geological Society, London*, doi: 10.1144/jgs2012-138.
- [14] Alsop, G.I. and Marco, S. 2013. Seismogenic slump folds formed by gravity-driven tectonics down a negligible subaqueous slope. *Tectonophysics*, 605, 48–69, doi: 10.1016/j.tecto.2013.04.004.

Structural Analysis of Greek and Bulgarian Coals by Solid-State ¹³C Nuclear Magnetic Resonance (NMR) Spectroscopy

Christina Apostolidou and Andreas Georgakopoulos

Laboratory of Economic Geology,
Department of Mineralogy – Petrology – Economic Geology, School of Geology, Aristotle
University of Thessaloniki, 54124 Thessaloniki, Greece

ABSTRACT

In the present study, lignites and sub-bituminous coal samples from Greece and Bulgaria are characterized through high-resolution, solid-state ¹³C Nuclear Magnetic Resonance Spectroscopy (NMR). Solid state ¹³C Nuclear Magnetic Resonance (NMR) spectroscopy is a very powerful tool for determining the chemical structure of complex organic substrates such as coals of various ranks and the effects of this structure on conventional pulverized coal combustion. Additionally, from an environmental point a view, ¹³C-NMR spectroscopy technique is widely used to investigate the possible link between Balkan Endemic Nephropathy (BEN) – a form of interstitial nephritis which can cause irreversible kidney failure, affecting rural people in Croatia, Bosnia and Herzegovina, Serbia, Romania, and Bulgaria but not in Greece – and the leaching of toxic organic compounds from Pliocene lignites in the Balkans by groundwater. Hence, the intention to shed light on the relationship between BEN disease and the organic functionality of coals by means of the solid-state ¹³C Nuclear Magnetic Resonance (NMR) spectroscopy is also embedded in this research work.

1. INTRODUCTION

The initial step in most solid-state magic angle spinning (MAS)-NMR pulse sequences depends on the transfer of magnetization from abundant ¹H spins to dilute rare spins such as ¹³C (abundance 1.1 % of all naturally occurring carbon) or ¹⁵N by means of cross polarization (CP). The gain in sensitivity afforded by CP usually outweighs the drawbacks associated with the technique. However, there are cases where the CP spectra exhibit problems related to interference such as spinning sidebands (SSB) in the spectra, the presence of para- and/or ferromagnetic centers in the sample, and low or remote protonation of the aromatic carbons.

In coal geology, it is important to understand the transformation process that affects organic molecules during coalification, as well as the chemistry of the several organic fractions the coal is consisted of. Comparison of these fractions from different coals gives information about the different conditions under which the coalification took place, the rank of each coal and the included toxic organic compounds in their structure. In this procedure, solid state ¹³C CP/MAS NMR analysis is a very powerful tool for determining the chemical structure of complex organic substrates such as lignins, humic substances, and coals of various ranks and simultaneously it differentiates coals from areas which are geographically close in proximity. Determination of the coal constituents offers valuable knowledge about the chemical and thermal behavior of coal during the exploitation process. ¹³C CP/MAS NMR has been used to investigate coals of variable ranks, in order to examine their structural and dynamic heterogeneity [1]. The results from this method have been used to indicate that the higher rank coals are indeed highly aromatic substances and the cross-polarization ¹³C NMR could be used with confidence to determine the carbon aromaticity [2].

The ¹³C CP/MAS NMR spectroscopy can help industry develop cleaner and more efficient uses for coals of different rank but can also be used to go deeper into other issues of interest such as

human health and environmental protection. As an example, several authors [3-6] have studied the organic functions of Pliocene lignites from known endemic areas in Serbia, Montenegro and Bosnia, in an effort to identify the possible link between Balkan endemic nephropathy (BEN) and the leaching of toxic compounds of these lignites by groundwater. Chemical analyses using ¹³C nuclear magnetic resonance spectroscopy indicated a high degree of organic functionality in the Pliocene lignites from the Balkans and suggested that groundwater can readily leach organic matter from the coal beds [7]. The present work is concerned with Greek and Bulgarian coals of various ranks. The evolution of the major organic structural units in the samples was identified by using high-resolution, solid-state ¹³C nuclear magnetic resonance spectroscopy (NMR), using a spectrometer with cross-polarization and magic-angle spinning.

2. MATERIALS

For the purposes of the present study, twenty-two samples from well-studied coal basins in Greece and Bulgaria were selected. The samples were obtained from outcrops, mine excavations, and drill holes and represent xylite-rich and matrix lignites, as well as sub-bituminous coals. Sample location, rank and lithotype are presented in Figure 1 and in Table 1.

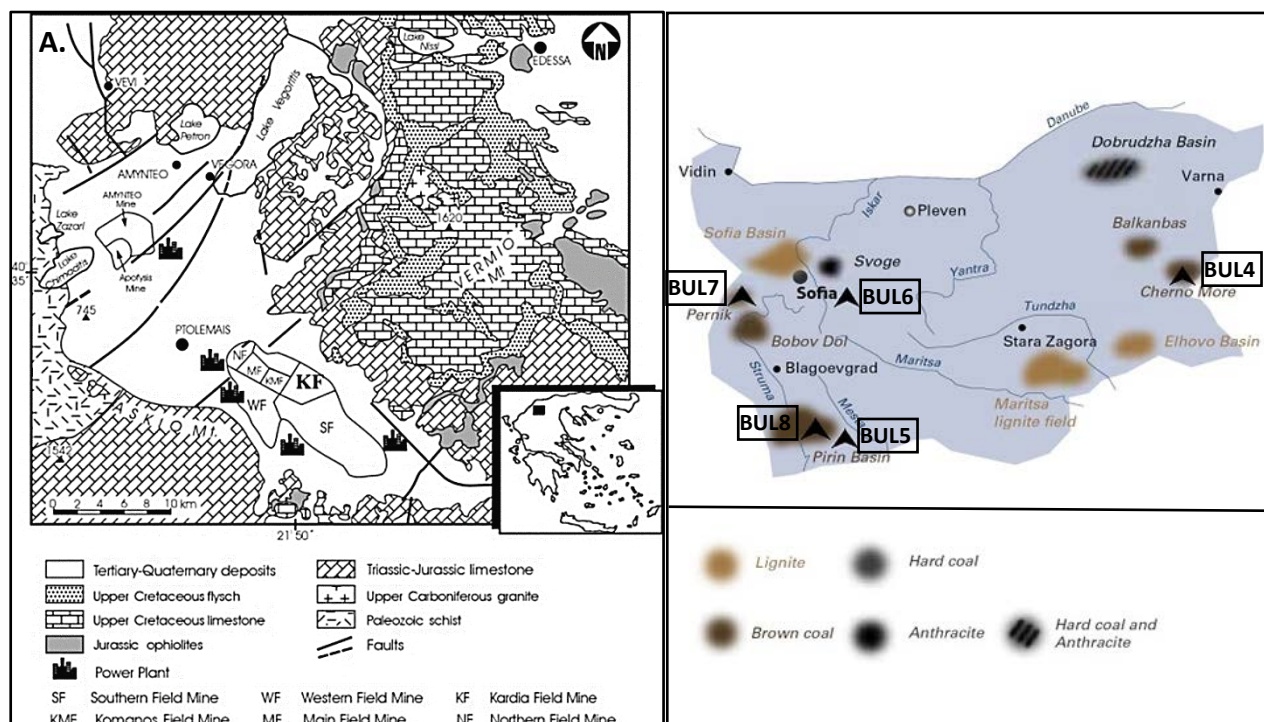


Table 37. Samples of the present study

Sample	Location	Lithotype
1. ACH1	Achlada mine, Greece	Xylite
2. ACH2	Achlada mine, Greece	Xylite
3. ACH3	Achlada mine, Greece	Xylitic lignite
4. BGR1	Vegora deposit, Greece	Xylite
5. VEV1	Vevi mine, Greece	Xylite
6. VEV2	Vevi mine, Greece	Xylite
7. AMX22	Amyntaio mine, Greece	Xylite
8. SL14	Southern field mine, Greece	Lignite
9. SL21	Southern field mine, Greece	Lignite
10. NL17	Northern field mine, Greece	Lignite
11. KRL17	Kardia mine, Greece	Lignite
12. TEL20	Sector six mine, Greece	Lignite
13. KML18	Komanos mine, Greece	Lignite
14. SRVX1	Servia deposit, Greece	Xylite
15. SRVL2	Servia deposit, Greece	Lignite
16. XOR	Horemi mine, Greece	Lignite
17. KYP	Kyparissia mine, Greece	Lignite
18. BUL4	Burgas basin, Bulgaria	Lignite
19. BUL5	Goltse area, Bulgaria	Lignite
20. BUL6	Tchukurovo basin, Bulgaria	Xylite
21. BUL7	Pernik basin, Bulgaria	Sub-bituminous coal
22. BUL8	Pirin basin, Bulgaria	Sub-bituminous coal

3. METHODS

For the coal samples under study solid-state ^{13}C CP/MAS NMR analysis was carried out with a Bruker AMX300 spectrometer operating at 75.48 MHz on the ^{14}C and ^1H resonance frequency of 300.136 MHz. Cross-polarization with magic angle spinning (CPMAS) was applied at 5 kHz. A contact time of 1ms, with a pulse delay of 1s, was chosen. The samples were ground to pass through the 60-mesh sieve and were packed into a 7-mm diameter cylindrical zirconia rotor with Kel-F end-caps which was allowed to spin before each experiment in order to stabilize the sample packing and improve the field homogenization. Chemical shifts, given in parts per million (ppm), were referred to the resonance signal of tetramethylsilane (TMS). More than 6000 scans were needed to obtain acceptable S/N (signal/noise) ratios for these coal samples. The spectrometer was calibrated before and during the NMR spectra acquisition with glycine ($\text{H}_2\text{NCH}_2\text{COOH}$, Merck standard). A line broadening (LB) of 100 Hz was applied to transform all the free induction decays (FIDs). Usually, in a typical NMR study, the spectra of the analyzed samples are integrated by the available spectrometer software for resonance intervals 220–190 ppm (ketones, quinones, and aldehydes), 190–162 ppm (carboxyls), 162–145 ppm (phenolic carbons), 145–120ppm (quaternary aromatic carbons), 120–108 ppm (protonated aromatic carbons), 108–96 ppm (anomeric carbons), 96–60 ppm (oxidized carbons), 65–50 ppm (nitrogenated carbons), 50–35 ppm (complex aliphatic carbons), 35–25 ppm (methylene carbons), and 25–0 ppm (methyl carbons). Although by applying the CP/MAS method a relatively rapid acquisition of spectra with high signal-to-noise ratio is achieved, the quantification of carbon moieties is not always feasible due to effects from paramagnetic species and from free organic radicals, which cause the occurrence of spinning sidebands (SSB) [10,11]. To investigate a possible influence of paramagnetic species on the CPMAS-NMR spectra of the coals examined in the present study, EPR (Electron Paramagnetic Resonance) studies were performed. EPR studies provide significant information on the nature and dispersion of mineral matter in coal, identification of organic matter and of interactions between mineral and organic matter. A Bruker

ESP 300E apparatus was used. Typical operating parameters were as follows: microwave frequency of 9.63 GHz, microwave power 2.6 mW, modulation frequency 100 kHz, and sweep time 42s. The sweep width was of 5000G, while the value of the centerfield was 3444G. The EPR spectrum of the glass holder was subtracted from the EPR spectra of the coal samples in order the noise provoked by the resonance of the glass to be avoided.

4. RESULTS AND DISCUSSION

4.1. NMR Spectra

NMR technique is a powerful tool for the study of coals. It provides valuable information concerning the coal structure and organic compounds. Detailed determination of coal organic constituents such as lignin, cellulose, humic substances and aromatic carbons is often associated with mining, combustion and post-combustion properties of coal. For example, investigation of organic functions of coal and especially polycyclic aromatic carbon content is necessary for the improvement of new combustion techniques, such as Fluidized Bed Combustion (FDC) [12-14]. In this direction, a considerable number of studies have been published concerning NMR spectroscopy applications in coals or soil substances [15-29].

The spectra of coals are divided into two regions, aliphatic (0-90 ppm) and aromatic (90-220 ppm). Table 2 represents NMR spectra peaks for the coals under study. Major peaks are observed at aliphatic carbons (0-50 ppm interval), with a significant peak at 32 ppm (methylene carbons), methoxyl carbons (50-60 ppm interval) with a peak at ~56 ppm, oxidized carbons (60-96 ppm region) with a peak at ~73 ppm (carbohydrates), aromatic carbons (110-150 ppm region) with peaks at ~115 ppm and 127 ppm, phenolic carbons (145-162 ppm region), with significant peak at 147 ppm and carboxyl/carbonyl carbons (162-220 ppm region) with a carboxyl peak at 176 ppm and a carbonyl peak at ~202 ppm. It should be mentioned that the 190-220 ppm interval designates broad spinning sideband (SSB) of the aromatic peak in all samples.

The CPMAS spectra of the samples under study are shown in Figures 2-6. In general, similarities are observed between spectra of coal samples of similar rank. Spectra of all the xylite and matrix lignite samples display peaks in the low field region beyond 147 ppm, which were assigned to oxygenated carbon atoms, and indicated that polar groups such as hydroxyl, methoxyl, carboxyl, and carbonyl groups were abundantly present in these low-rank coals. The presence of methoxyl, phenolic, and residual polysaccharides in the spectrum indicate that this coal is relatively unaltered [7]. It has been observed that carboxyl and carbonyl groups decrease significantly with coal rank, suggesting that they were easily eliminated during coalification.

The lowest rank samples were classified into three different groups depending on NMR spectra peaks. In group A samples ACH1, ACH2 and VEV2 (Fig. 2) show sharp peaks at aliphatic moieties (0-50 ppm), methoxyl carbons (55-56 ppm) and phenolic carbons (147 ppm). Broad peaks appear at oxidized carbons, specifically with a peak at 72-74 ppm polysaccharides and a presence of aromatic carbons in 105-140 area. Carbonyl and carboxyl groups appear with slightly recognizable peaks at 176 and 200 ppm. These three xylites have almost identical spectra, which reveal similar coalification stage. The only differences were noticed at the intensity of specific peaks such as 72-74 ppm, where xylite from Vevi mine seems to be slightly richer in polysaccharides. In this stage of coalification, oxygenated aliphatic carbons decrease with the simultaneous increase of methoxyl and protonated carbons.

The second group of xylite samples (Fig. 3) consists of ACH3, VEV1, BGR1, and BUL6, which provide the same peaks with similar intensity at 56, 72-74, 105, 115, 147, 176 and 200 ppm. Samples ACH3 and VEV1 show an extra peak at the aliphatic area (32 ppm). ACH3 and BGR1 appear to have a small extra peak at 85 ppm, showing their increased carbohydrates presence. ACH3

also seems to have a slightly smaller peak at phenolic carbons (147 ppm) compared to the other three samples of group B. The Bulgarian xylite also falls in this group. Although sample BUL6 is not geographically connected with the Greek xylite basins, it shows an extreme similarity with the Greek xylites, whereas it is completely different from the rest of Bulgarian samples, consisting of lignites and sub-bituminous coals.

Table 38. Chemical shifts and assignment of resonances in ¹³C CP/MAS NMR spectra of the samples under study

Sample	Lithotype	Major Peaks (ppm)								
		30-33	55-56	72-75	104-106	114-116	120-130	147	176	190-220
1.ACH1	Xylite	x	x	x			x	x	x	x
2.ACH2	Xylite	x	x	x			x	x	x	x
3.ACH3	Xylitic lignite	x	x	x	x	x	x	x		x
4.BGR1	Xylite	x	x	x	x	x	x	x	x	x
5.VEV1	Xylite	x	x	x	x	x	x	x	x	x
6.VEV2	Xylite	x	x	x	x	x	x	x	x	x
7.AMX22	Xylite	x	x	x	x	x	x	x	x	x
8.SL14	Lignite	x	x	x			x	x	x	x
9.SL21	Lignite	x	x	x		x	x	x	x	x
10.NL17	Lignite	x	x	x			x	x	x	x
11.KRL17	Lignite	x	x	x		x	x	x	x	x
12.TEL20	Lignite	x	x	x			x	x	x	x
13.KML18	Lignite	x	x	x			x		x	x
14.SRVX1	Xylite	x	x	x	x	x	x	x	x	x
15.SRVL2	Lignite	x	x	x	x	x	x	x	x	x
16.XOR	Lignite	x	x	x		x	x	x	x	x
17.KYP	Lignite	x	x	x	x	x	x	x	x	x
18.BUL4	Lignite	x				x	x			x
19.BUL5	Lignite	x	x				x		x	x
20.BUL6	Xylite	x	x	x	x		x	x		x
21.BUL7	Sub-bituminous coal	x					x		x	x
22.BUL8	Sub-bituminous coal	x					x			x

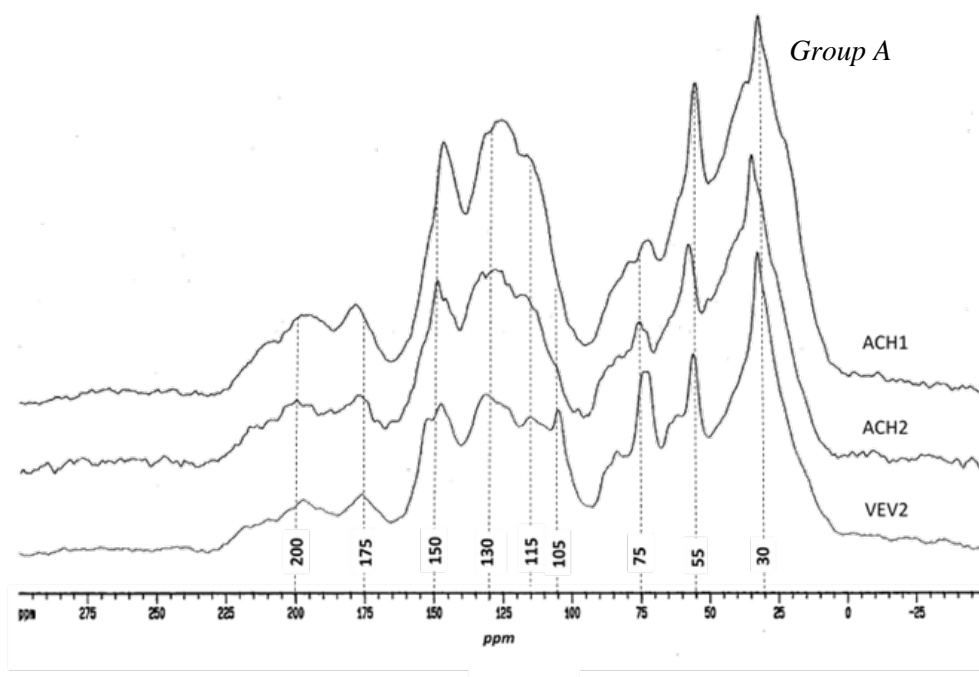


Figure 158. ^{13}C CPMAS NMR spectra of group A xylite samples.

AMX22 and SRVX1 samples are placed in the third group (Fig. 3) and present intense sharp peaks at 32, 56, 65, 72, 74, 104 and 147 ppm. They also show small peaks at the aromatic area (115 ppm) and carbonyl/carboxyl area (176, 200 ppm). Differences are also identified between these samples. Intensity at 105 ppm peak in SRVX1 is smaller, showing a lower amount of aromatic carbons in Serbia Xylite. AMX22 shows an intense double peak assigned to carbohydrates (72-74 ppm interval), whereas SRVX1 has a slightly recognizable double point in this area.

As previous studies have highlighted, heat, pressure and time are essential parameters in the coalification process, that allow for several reactions [7,23,31]. The influence of these parameters appears to be accompanied by changes in spectra between the samples. For instance, it is observed that as coalification proceeds there is a loss of methoxyl at first, followed by the loss of phenolic carbons. At the same time, aromatic content increases being an evidence of higher rank coal.

Group A shows a higher aromatic carbon content with more intense peaks at 105-150 ppm interval. ACH1, ACH2, and VEV2 xylites show aromaticity because lignin is aromatic.

Group B and group C show an important loss at methoxyl carbons, but there is a significant presence of oxidized carbons in 72-74 ppm area. The peak at 72 ppm indicates that most of the cellulose and other carbohydrates in the original plant material have not been biodegraded and have not been lost during coalification [22, 30]. Moreover, an extra peak at 65 ppm in group C enhances this inference.

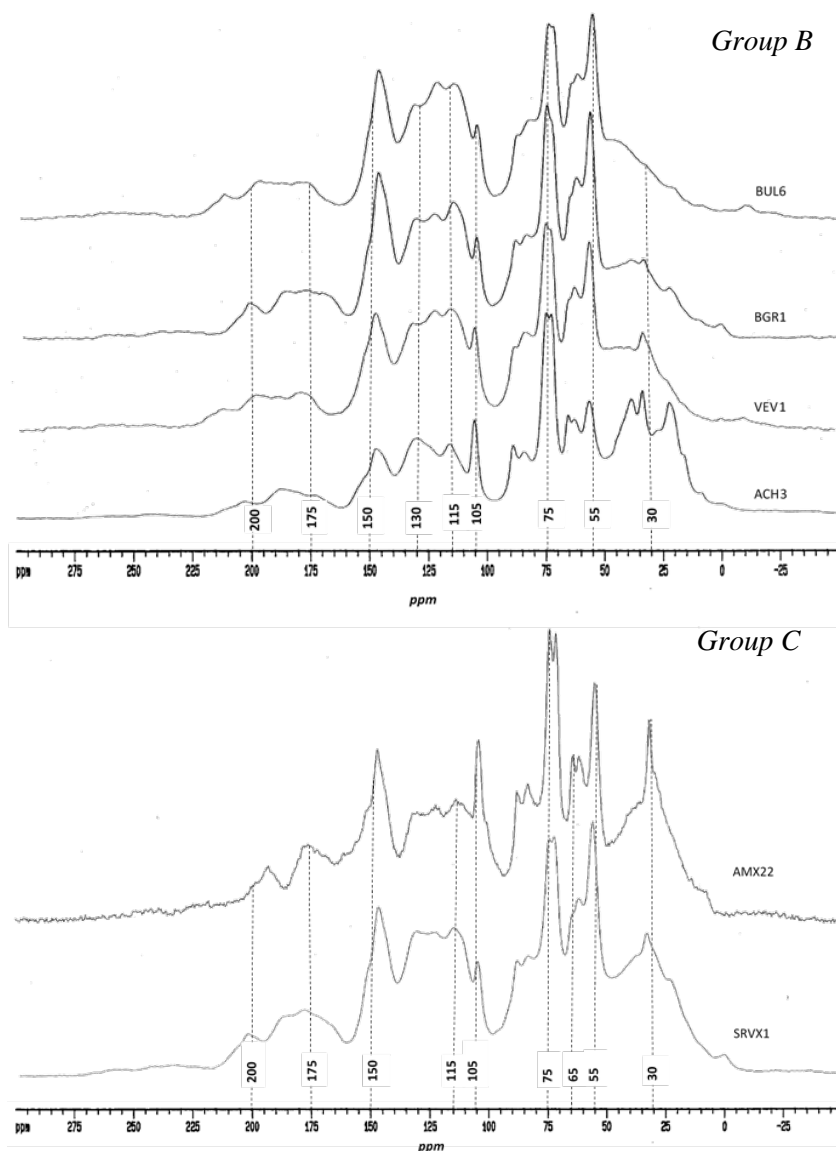


Figure 159. ^{13}C CPMAS NMR spectra of group B and C xylite samples.

Lignite samples were divided into two groups according to their location. Group D (Fig. 4) refers to lignites from Florina-Ptolemais-Kozani basin in Western Macedonia. Samples are named KML18, SRVL2, TEL20, NL17, SL21, SL14, and KRL14. The main picture of the spectra reveals no significant differences among the samples. They present a strong sharp peak at methylene carbons (32 ppm) and broader peaks at 55, 72, 127, 156, 176, and 200 ppm. Group E (Fig.5) consists of lignites from Peloponnesse area, named XOR and KYP. The spectra of these samples show sharp intense peaks at 32 and 55-56 ppm area and broader peaks at 72, 116, 129, 155, 180, 200 ppm. In general, there were almost no differences observed among the Peloponnese lignites. The spectra interpretation reveals low oxidized carbon content and a remarkable presence of aromatic carbon, compared with the other lignite samples. According to NMR spectra, as they were compared to all lignite samples, a low carbonyl and carboxyl content, low oxidized carbons content and a low aromaticity in group D compared with group E is observed, while an intense aliphatic carbons presence in both groups is noticed. These aliphatic carbons likely represent refractory cuticular waxes from vascular plants, microbial lipids, long chain hydrocarbons and fatty acids [7].

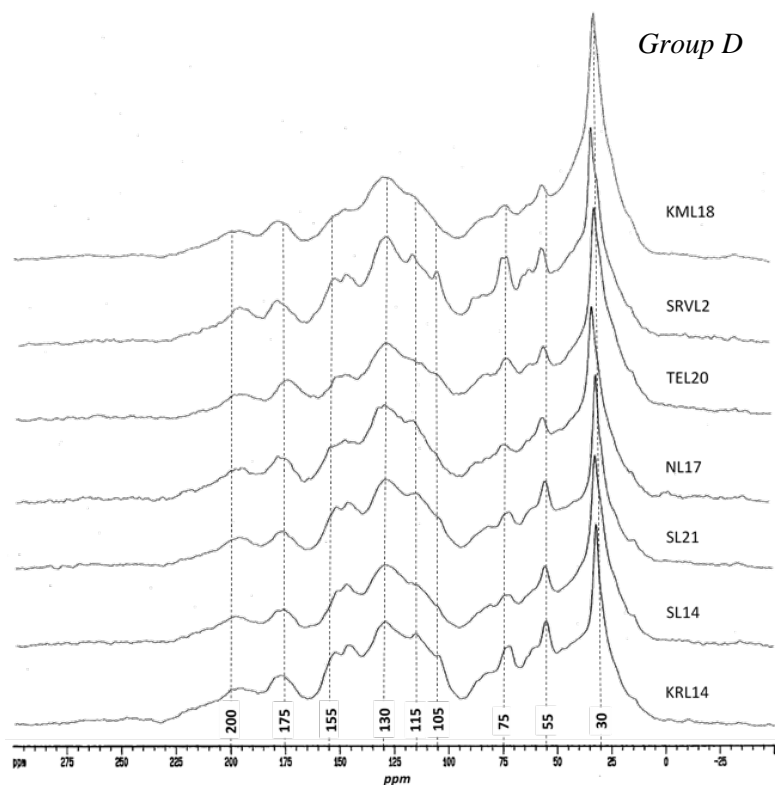


Figure 160. ^{13}C CPMAS NMR spectra of group D lignite samples from Florina-Ptolemais-Kozani basin.

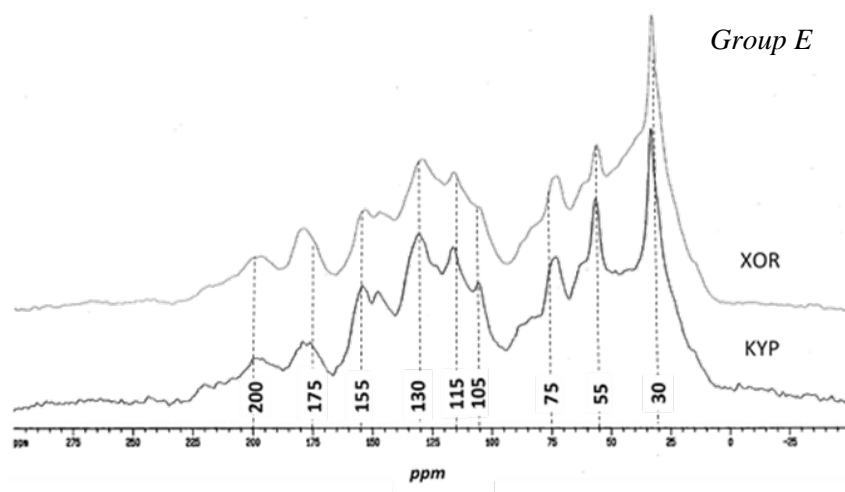


Figure 161. ^{13}C CPMAS NMR spectra of group E lignite samples from Peloponnese area.

Figure 6 presents NMR spectra of Bulgarian coals, which consist of two lignite (BUL4, BUL5) and two sub-bituminous (BUL7, BUL8) coal samples. Spectra analysis found a significant peak in 32 ppm which originates from methylene carbons in aliphatic chains. Both lignite samples display a small peak at 55 ppm, which is missing from sub-bituminous coals. The presence of methoxyl peaks in lignite samples shows that these samples are not highly altered from the peat stage [22]. The lack of peaks in oxidized carbon area indicates that all Bulgarian samples have lost most of their oxygen functionality during the coalification process. Moreover, the sub-bituminous samples show a decrease in the phenolic carbon interval (145-162 ppm). The diminished intensity of phenolic carbon spectra indicates a rapid loss of O-containing functional groups substituted to aromatic carbon [21] and is one of the main alterations in the coalification path from lignite to sub-bituminous coal [32].

Once the O-containing functional groups were replaced by hydrogen or a carbon-substituent, the relative percentage of protonated and/or carbon-substituted carbon increased [21]. This is identified in the spectra from Bulgarian samples with intense peaks at 127- 130 ppm protonated aromatic carbons area.

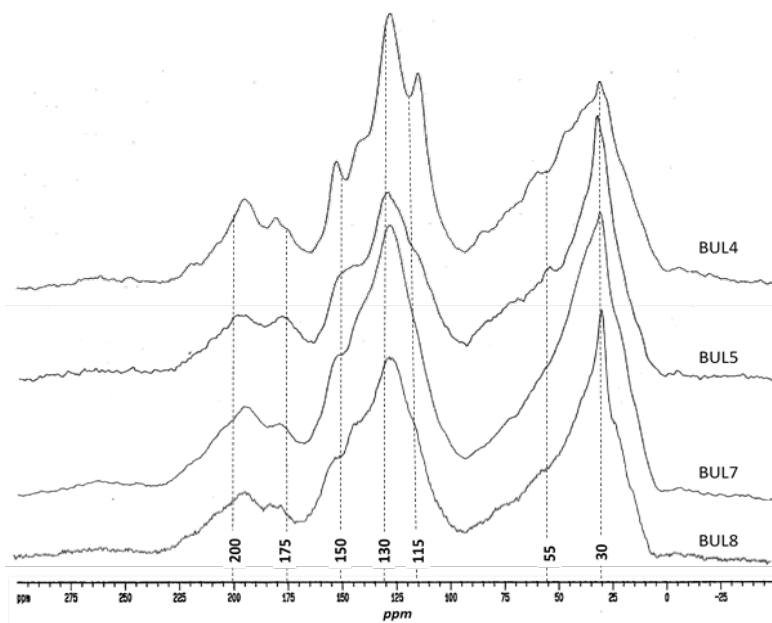


Figure 162. ¹³C CPMAS NMR spectra of Bulgarian lignites and sub-bituminous coals.

The similarity of lignite and sub-bituminous spectra in combination with the distinctive differences between Greek and Bulgarian lignites leads to the inference that Bulgarian lignites are of higher rank compared to the Greek ones. Following the interpretation of the NMR spectra the Bulgarian lignite samples should be classified as Lignite A while the Greek lignite samples should be classified as Lignite type B, in accordance with ASTM D388 – 12 [Standard Classification of Coals by Rank]. Among the Bulgarian samples there is a notable difference of the Bulgarian xylite (Fig. 3, BUL6 sample), which is attributed to the entirely different lithotype and rank of BUL6 sample emerged from the lower degree of thermal alteration it had undergone.

As previously mentioned, NMR spectroscopy has been used in many ways in order to determine the organic character of various organic substances mostly from an industrial or environmental point of view. More specifically, several authors have used NMR spectroscopy to study Balkan Endemic Nephropathy (BEN). BEN is a fatal kidney failure disease geographically restricted to several countries of the Balkan peninsula, mostly Serbia, Montenegro, Bosnia and Herzegovina, Romania and Bulgaria, whereas Greece does not belong to the endemic areas. Previous studies attended to investigate the organic functions of different coal samples among the Balkan areas and have revealed an apparent close association between BEN endemic areas and the presence of Pliocene lignite coal deposits in the former Yugoslavia and Romania [3,22,33], while other studies deal with the leachability and mobility of the toxic organic compounds [4-7]. Pliocene lignites from the endemic areas seem to have a particular geochemical composition, with many potentially nephrotoxic/carcinogenic aromatic and nonaromatic molecules, leachable into organic solvents as well as into water [3]. Chemical analysis of Pliocene lignites from the endemic areas using ¹³C NMR spectroscopy showed the coals to be of very low rank, highly unaltered, with a high degree of organic functionality (e.g., methoxyl, phenolic, and O-bonded aliphatic hydrocarbon groups) [7]. Natural water analyses from water wells from endemic areas contained a greater number of different compounds and in greater abundance than water from nonendemic areas [34]. It was also found to be enriched in polycyclic aromatic hydrocarbons suggesting a possible coal source. The present study

corroborates previous results [7] stating that Greek Pliocene lignites have undergone a greater degree of alteration than the Pliocene lignite samples from endemic areas of the former Yugoslavia. This is indicated in the ¹³C NRM results by the significantly intense resonances for methoxyl, phenolic and polysaccharides moieties in the spectrum of Greek lignites (Figs. 4, 5). In opposition, the spectrum of Bulgarian lignites is quite different from the Pliocene lignite samples from Greece, with only two major peaks at aliphatic and aromatic carbons regions (Fig. 6).

4.2. EPR spectra

Quantification of NMR spectra may often be problematic regarding the paramagnetic compounds occurrence in the samples, which may cause broadening or displacement of the chemical shift. It should be mentioned that there is restricted literature referring to paramagnetic centers investigation in coal samples [25, 35-38]. Paramagnetic centers are formed by cleavage of covalent bonds between elements of condensed structures and are stabilized by hydrogen atom transfer, mainly from the aliphatic part of the sample [32]. Figure 7 presents EPR results of four representative samples, since all of the 22 samples appeared to be similar.

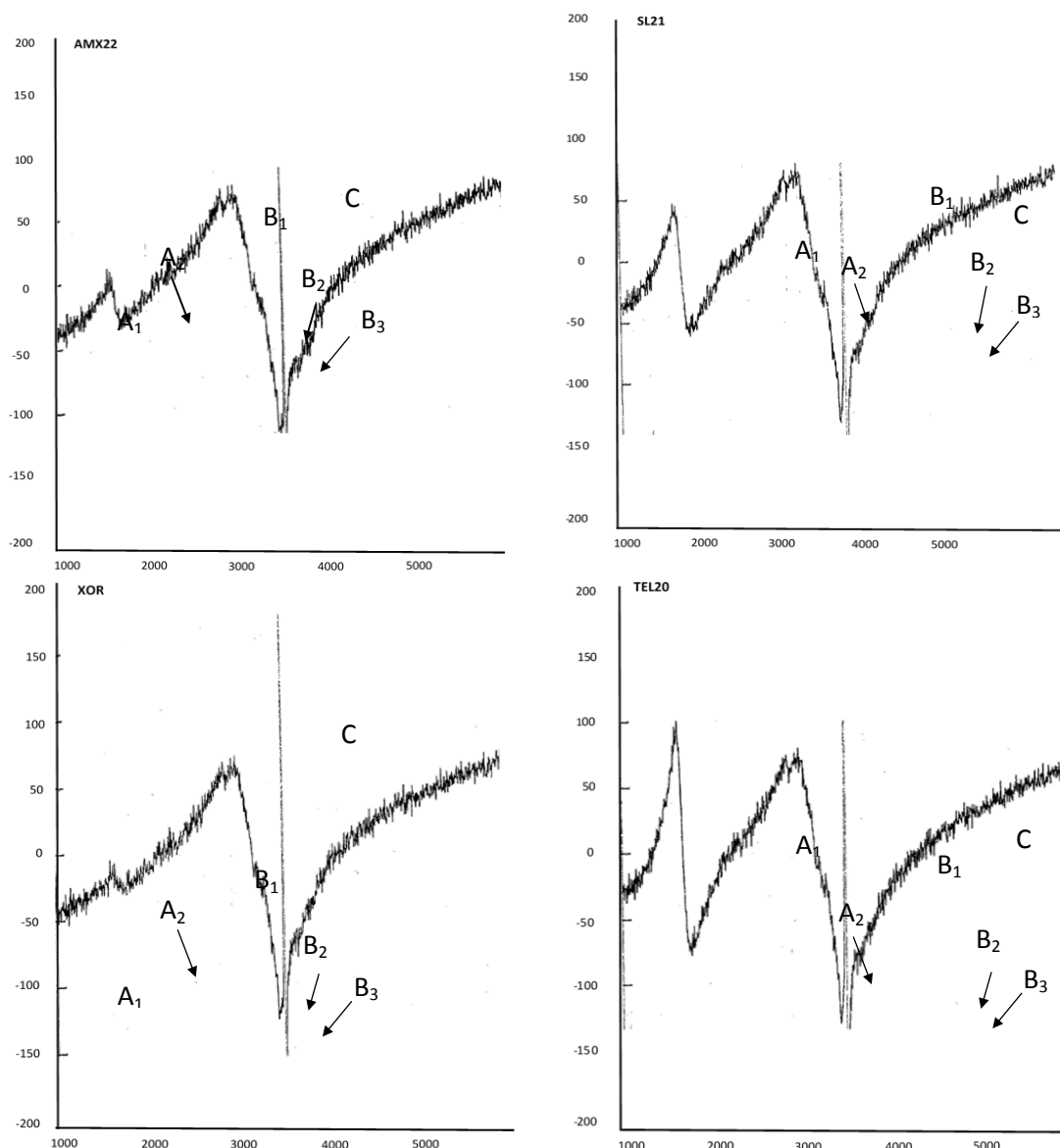


Figure 163. EPR spectra of four representative samples.

A₁-A₂ represent peaks of Fe⁺³ ions, B₁ - B₂ - B₃ represent peaks of Mn⁺² ions and C refers to free organic radicals.

The association of paramagnetic spectra with the aromatic carbons causes peak broadening in the aromatic area and can lead to underestimation of their concentration in the samples. EPR spectroscopy identifies the chemical species with unpaired electrons present in organic compounds. Calculation of paramagnetic and ferromagnetic spectra content carried out with Electron Paramagnetic Resonance (EPR). Low concentration of paramagnetic and ferromagnetic compounds (free organic radicals, Fe⁺³, Mn⁺², Cu⁺², Co⁺² etc.) can provide at least semi-quantitative results. Taking into consideration that several authors have reported obstacles in the quantification of NMR spectra due to paramagnetic centers, all twenty-two samples were examined with EPR technique, which revealed that signal loss and broadening were not so severe in the samples under study. This is probably due to a C: Fe ratio > 1. Moreover, paramagnetic centers affect mostly the aromaticity measurements in coals [33]. The samples of the present study have low aromatic carbon content; therefore paramagnetic compounds caused no severe problems. As shown in Figure 7 all EPR diagrams present an important sharp peak at 3450G, which is associated with the free organic radicals. Organic radicals are abundant in all organic compounds and they are released with the condensation of polycyclic aromatic systems of coals during coalification [32]. Peaks A₁ and A₂ are

caused by the presence of Fe⁺³ ions, while peaks B₁₋₃ are assigned to Mn⁺² ions. All samples present the same peaks, with only small and insignificant differences in the intensity.

5. CONCLUSIONS

Twenty-two samples from coal basins in Greece and Bulgaria, representing xylite-rich and matrix lignites, as well as sub-bituminous coals, were studied by solid state ¹³C CP/MAS NMR, which is a very powerful technique to determine the gross chemical structure of the organic materials. Determination of the coal organic constituents offers valuable knowledge about the chemical and thermal behavior of coal associated with mining, combustion and post-combustion properties. Investigation of organic functions of coal and especially polycyclic aromatic carbon content is necessary for the improvement of new combustion techniques, such as Fluidized Bed Combustion.

The NMR spectra of the coals of the present study are divided into two main regions, aliphatic (0-90 ppm) and aromatic (90-220 ppm). Similarities are observed between spectra of coal samples of similar rank. Spectra of all the xylite and matrix lignite samples display peaks in the low field region beyond 147 ppm, which were assigned to oxygenated carbon atoms, and indicated that polar groups such as hydroxyl, methoxyl, carboxyl, and carbonyl groups were abundantly present in these *low-rank coals*. The presence of methoxyl, phenolic, and residual polysaccharides in the spectrum indicate that this coal is relatively unaltered. It has been observed that carboxyl and carbonyl groups decrease significantly with coal rank, suggesting that they were easily eliminated during coalification.

Coal samples were classified into six different groups depending on NMR spectra peaks. In group A samples ACH1, ACH2 and VEV2 show sharp peaks at aliphatic moieties (0-50 ppm), methoxyl carbons (55-56 ppm) and phenolic carbons (147 ppm). These three xylites have almost identical spectra, which reveal similar coalification stage.

Group B includes xylite samples which provide the same peaks with similar intensity at 56, 72-74, 105, 115, 147, 176 and 200 ppm. Although sample BUL6 is not geographically connected with the Greek xylite basins, it shows an extreme similarity with the Greek xylites, whereas it is completely different from the rest of the Bulgarian samples, consisting of lignites and sub-bituminous coals.

Lignite samples were divided into two groups according to their location. Group D refers to lignites from Florina-Ptolemais-Kozani basin in Western Macedonia. The main picture of the spectra reveals no significant differences among the samples. Group E consists of lignites from Peloponnesse area. There were almost no differences observed among the Peloponnesse lignites. The spectra interpretation reveals low oxidized carbon content and a remarkable presence of aromatic carbon, compared with the other lignite samples. According to NMR spectra, as they were compared to all lignite samples, a low carbonyl and carboxyl content, low oxidized carbons content and a low aromaticity in group D compared with group E is observed, while an intense aliphatic carbons presence in both groups is noticed. These aliphatic carbons likely represent refractory cuticular waxes from vascular plants, microbial lipids, long chain hydrocarbons and fatty acids.

Bulgarian coals consist of two lignite (BUL4, BUL5) and two sub-bituminous (BUL7, BUL8) coal samples. The presence of methoxyl peaks in lignite samples demonstrates that these samples are not highly altered from the peat stage. The lack of peaks in oxidized carbon area indicates that all Bulgarian samples have lost most of their oxygen functionality during the coalification process. The diminished intensity of phenolic carbon spectra indicates a rapid loss of O-containing functional groups substituted to aromatic carbon and is one of the main alterations in the coalification path from lignite to sub-bituminous coal. Once the O-containing functional groups were replaced by hydrogen or a carbon-substituent, the relative percentage of protonated and/or carbon-substituted carbon

increased. This is identified in the spectra from Bulgarian samples with intense peaks at 127- 130 ppm protonated aromatic carbons area. The similarity of lignite and sub-bituminous spectra in combination with the distinctive differences between Greek and Bulgarian lignites leads to the inference that Bulgarian lignites are of higher rank compared to the Greek ones. Following the interpretation of the NMR spectra the Bulgarian lignite samples should be classified as Lignite A while the Greek lignite samples should be classified as Lignite type B, in accordance with ASTM D388 – 12.

The ¹³C CP/MAS NMR spectroscopy can help industry develop cleaner and more efficient uses for coals of different rank but can also be used to go deeper into other issues of interest such as human health and environmental protection. In this direction NMR spectroscopy is used to study Balkan Endemic Nephropathy (BEN), a fatal kidney failure disease geographically restricted to several countries of the Balkan peninsula, *whereas Greece does not belong to the endemic areas*. Previous researches have revealed an apparent close association between BEN endemic areas and the presence of Pliocene lignite coal deposits in countries of the Balkan peninsula, while other studies deal with the leachability and mobility of the toxic organic compounds. The results of the present study corroborate previous findings stating that Greek Pliocene lignites are completely different in their chemical composition and have undergone a greater degree of alteration than the Pliocene lignite samples from endemic areas.

ACKNOWLEDGMENTS

The authors are immensely grateful to Ass. Professor Stavros Kalaitzidis, Department of Geology, University of Patras, for his valuable comments and suggestions on an earlier version of the manuscript.

REFERENCES

- [1] Tekely, P., Nicole, D. & Delpuech, J.J. (1990). Advanced methodologies in coal characterization. *Coal Science and Technology*, 15, 135.
- [2] Speight, J.G. (1994). Application of spectroscopic techniques to the structural analysis of coal. *Applied Spectroscopy Reviews*, 29(2), 117-169.
- [3] Orem, W.H., Tatu, C.A., Feder, G.L., Finkelman, R.B., Lerch, H.E., Maharaj, S.V.M., Szilagyi, D., Dumitrascu, V., Paunescu, V. & Margineanu, F. (2002). Environment, geochemistry and the etiology of Balkan endemic nephropathy: lessons from Romania. *Medicine and Biology*, 9(1), 39-48.
- [4] Maharaj, S.V.M., Orem, W.H., Tatu, C.A., Lerch, H.E. & Szilagyi, D.N. (2014). Organic compounds in water extracts of coal: links to Balkan endemic nephropathy. *Environmental Geochemistry Health*, 36(1), 1-17.
- [5] Maharaj, S.V.M. (2014). Limitations and plausibility of the Pliocene lignite hypothesis in explaining the etiology of Balkan endemic nephropathy. *International Journal of Occupational and Environmental Health*, 20(1), 77-91.
- [6] Voice, T.C., McElmurry, S.P., Long, D.T., Dimitrov, P., Ganev, V.S. & Petropoulos, E. (2006). Evaluation of the hypothesis that Balkan endemic nephropathy is caused by drinking water exposure to contaminants leaching from Pliocene coal deposits. *Journal of Exposure Science and Environmental Epidemiology*, 16(6), 515-524.

- [7] Orem, W.H., Feder, G.L. & Finkelman, R.B. (1999). A possible link between Balkan endemic nephropathy and the leaching of toxic organic compounds from Pliocene lignite by groundwater: preliminary investigation. *International Journal of Coal Geology*, 40(2-3), 237-252.
- [8] Iordanidis, A. & Georgakopoulos, A. (2003). Pliocene lignites from Apofysis mine, Amynteo basin, Northwestern Greece: petrographical characteristics and depositional environment. *International Journal of Coal Geology*, 54(1-2), 57-68.
- [9] European Association of Coal (2017). Coal Industry across Europe. Available at: <https://www.braunkohle.de/files/euracoal-coal-industry-across-europe-6th.pdf>
- [10] Snape, C.E., Axelson, D.E., Botto, R.E., Delpuech, J J., Telely, P., Gerstein, B.C., Pruski, M., Maciel, G.E. & Wilson, M.A. (1989). Quantitative reliability of aromaticity and related measurements on coals by ¹³C N.M.R. A debate. *Fuel*, 68(5), 547-548.
- [11] Kawashima, H. & Yamada, O. (1999). A modified solid-state ¹³C CP/MAS NMR for the study of coal. *Fuel Processing Technology*, 61(3), 279-287.
- [12] Valentim, B., Lemos de Sousa, M.J., Abelha, P., Boavida, D. & Gulyurtlu, I. (2006). Combustion studies in a fluidised bed - The link between temperature, NO_x and N₂O formation, char morphology and coal type. *International Journal of Coal Geology*, 67(3), 191-201.
- [13] Wang, R., Liu, G., Sun, R., Yousaf, B., Wang J., Liu, R. & Zhang, H. (2018). Emission characteristics for gaseous-and size-segregated particulate PAHs in coal combustion flue gas from circulating fluidized bed (CFB) boiler. *Environmental Pollution*, 238, 581-589.
- [14] Solimene, R., Cammarota, A., Chirone, R., Leoni, P., Rossi, N. & Salatino, P. (2017). Combustion of lignin-rich residues with coal in a pilot-scale bubbling fluidized bed reactor. *Powder Technology*, 316, 718-724.
- [15] Kanca, A., Dodd, M., Reimer, J.A. & Uner, D. (2016). Following the structure and reactivity of Tuncbilek lignite during pyrolysis and hydrogenation. *Fuel Processing Technology*, 152, 266-273.
- [16] Al-Faiyz, Y.S.S. (2013). CPMAS ¹³C NMR characterization of humic acids from composted agricultural Saudi waste. *Arabian Journal of Chemistry*, 10, S839-S853.
- [17] Conte, P. & Bernes, A.E. (2008). Dynamics of Cross Polarization in Solid State Nuclear Magnetic Resonance Experiments of Amorphous and Heterogeneous Natural Organic Substances. *Analytical sciences*, 24(9), 1183-1188.
- [18] Monda, H., Cozzolino, V., Vinci, G., Spaccini, R. & Piccolo, A. (2017). Molecular characteristics of water-extractable organic matter from different composted biomasses and their effects on seed germination and early growth of maize. *Science of the Total Environment*, 590, 40-49.
- [19] Clouard, M., Criquet, S., Borschneck, D., Ziarelli, F., Marzaioli, F., Balesdent, J. & Keller, C. (2014). Impact of lignite on pedogenetic processes and microbial functions in Mediterranean soils. *Geoderma*, 232, 257-269.
- [20] Gentzis, T., Goodarzi, F. & McFarlane, R.A. (1992). Molecular structure of reactive coals during oxidation, carbonization and hydrogenation an infrared photoacoustic spectroscopic and optical microscopic study. *Organic Geochemistry*, 18(3), 249-258.

- [21] Erdenetsogt, B.O., Lee, I., Lee S.K., Ko, Y.J. & Bat-Erdene, D. (2010). Solid-state C-13 CP/MAS NMR study of Baganuur coal, Mongolia: Oxygen-loss during coalification from lignite to subbituminous rank. *International Journal of Coal Geology*, 82(1-2), 37-44.
- [22] Georgakopoulos, A. (2003). Aspects of solid-state ¹³C CPMAS NMR spectroscopy in coals from the Balkan peninsula. *J. Serb. Chem. Soc.*, 68 (8-9), 599-605.
- [23] Hackley, P.C., Warwick, P.D., Hook, R.W., Alimi, H., Mastalerz, M. & Swanson, S.M. (2017). Organic geochemistry and petrology of subsurface Paleocene–Eocene Wilcox and Claiborne Group coal beds, Zavala County, Maverick Basin, Texas, USA. *Organic Geochemistry*, 46, 137-153.
- [23] Bardet, M. & Pournou, A. (2017). NMR Studies of Fossilized Wood. In: *Annual Reports on NMR Spectroscopy*, Vol. 90, pp. 41-83, Academic Press.
- [24] Hatcher, P.G, Lerch, H.E., Bates, A.E. & Verheyen, T.E. (1989). Solid-state ¹³C nuclear magnetic resonance studies of coalified gymnosperm xylem tissue from Australian brown coals. *Organic Geochemistry*, 14(2), 145-155.
- [25] Wilson, M.A. (1987). *NMR Techniques and Applications in Geochemistry & Soil Chemistry*. 1st Edition, Pergamon Press, London.
- [26] Wei, Q. & Tang, Y. (2018). 13C-NMR Study on Structure Evolution Characteristics of High-Organic-Sulfur Coals from Typical Chinese Areas. *Minerals*, 8(2), 49.
- [27] Yoshida, T. & Maekawa, Y. (1987). Characterization of coal structure by CP/MAS carbon-13 NMR spectrometry. *Fuel Processing Technology*, 15, 385-395.
- [28] Vamvuka, D. Kastanaki, E. Lasithiotakis, M. & Papanicolaou, C. (2004). Combustion behavior of xylite/lignite mixtures. *Carbon*, 42(2), 351-359.
- [29] Kalaitzidis, S., Georgakopoulos, A., Christanis, K., & Iordanidis, A. (2006). Early coalification features as approached by solid state 13C CP/MAS NMR spectroscopy. *Geochimica et Cosmochimica Acta*, 70(4), 947-959.
- [30] Erdenetsogt, B.O., Lee, I. & Ko, Y.J. (2017). Carbon isotope analysis and a solid-state ¹³C NMR study of Mongolian lignite: Changes in stable carbon isotopic composition during diagenesis. *Organic Geochemistry*, 113, 293-302.
- [31] Hatcher, P.G. (1988). Dipolar-dephasing ¹³C NMR studies of decomposed wood and coalified xylem tissue: evidence for chemical structural changes associated with defunctionalization of lignin structural units during coalification. *Energy and Fuels*, 2(1), 48-58.
- [32] Hatcher, P.G., & Clifford, D.J. (1997). The organic geochemistry of coal: from plant materials to coal. *Organic Geochemistry*, 27(5-6), 251-274.
- [33] Orem, W., Tatu, C., Pavlovic, N., Bunnell, J., Lerch, H., Paunescu, V., Ordodi, V., Flores, D., Corum, M. & Bates, A. (2007). Health Effects of Toxic Organic Substances from Coal: Toward “Panendemic” Nephropathy. *A Journal of the Human Environment*, 36(1), 98-102.
- [34] Finkelmana, B., Orem, W., Castranova, V., Tatu C.A., Belkina, H.E., Zheng, B., Lerch, H.E., Maharaj, S.V. & Bates A.L. (2002). Health impacts of coal and coal use: possible solutions. *International Journal of Coal Geology*, 50(1-4), 425-443.

- [35] Pilawa, B., Wieckowski, A.B., Lewadowski, M. & Dzierzega-Leczna A. (1997). EPR studies of interactions between paramagnetic centers of exinite, vitrinite and inertinite during thermal decomposition. *Fuel*, 76(1), 79-83.
- [36] Solum, M.S., Pugmire, R.J. & Grant, D.M. (1989). ¹³C Solid-State NMR of Argonne Premium Coals. *Energy and Fuels*, 3(2), 187-193.
- [37] Snape, C.E., Axelson, D.E., Botto, R.E., Delpuech, J.J, Tekely, P., Gersteint, B.C., Pruskit, M., Maciel, G.E. & Wilson, M.A. (1989). Quantitative reliability of aromaticity and related measurements on coals by ¹³C N.M.R. A debate. *Fuel*, 68(5), 547-548.
- [38] Sarypov, V.I., Kuznetsov, B.N, Baryshnikov, S.V., Beregovtsova, N.G., Selyutin G.E., Chumakov, V.G. & Kamianov, V.F. (1999). Some features of chemical composition, structure and reactive ability of Kansk-Achinsk lignite modified by ozone treatment. *Fuel*, 78(6), 663-666.

Energy Efficiency by Ecological Coal Quality Management in EPS and Its Benefits

Nadica Drljevic¹ and Miodrag Andric²

¹EPS/Branch “Open cast mines Kolubara”, Lazarevac, Serbia

²EPS/ Main office for overburden and coal production, Belgrade, Serbia

ABSTRACT

Production of electric power in a power plant from the coal excavated in Kolubara mines lasts more than 50 years.

Besides the significant resources that are still available within the Kolubara basin, and continuance in the coal exploitation, it is necessary to fulfil the following: very strict requirements for environmental protection and preservation, demands from power plants regarding quality of coal, required sustainability in coal production, demands for securing stable and reliable existence for inhabitants from local communities etc.

Among others, afore mentioned are the reasons for implementing Coal Quality Management System (CQMS), and through its development and implementation the rational use of coal deposit and excavation of all parts with changeable and lower quality will result in constant quality.

Particular and specific solutions in CQMS project are reflected, not only in the definition of work during coal exploitation, but in the immediate benefits as well.

Those benefits will be seen in the coal mine production-as a supplier and power plant-as a consumer, during the production of energy.

Key words: coal exploitation, quality, homogenization, control, rationalization

1. INTRODUCTION

Coal, as one of the main raw material, is significant for electric production and that need is more and more expressed. In total energy reserves in Serbia coal participates with 84%. For that, it is important to invest investments funds for development of mining sector and procurement of new equipment to secure stable supply for power plants and to respect legislation and regulative in the area of environment protection.

Long-time period of use in lignite mines and deposit's exploitation led to the occurrence that the best parts were already finished, and the work on coal digging, in time, goes toward parts with more expressed complex conditions. These complexity refers toward increase of depth for coal mines and changes in quality.

To valorise all useful parts of coal deposit it is necessary to implement system for coal quality control and management. This system will be able to equalize required value of the observed parameter (eg. coal calorific value) during excavation on mine's site, transportation on the belt conveyors and before loading into the train for power plant. This will provide economical use of boilers without expressed oscillation during their work.

Coal Quality Management System, which will be introduced, is part of “Project for environmental improvement in Mining Basin Kolubara”, financed by means from EBRD, KfW and EPS, with three parts:

Project A - procurement and erection of ECS system for Field “C”,

Project B - procurement of spreader for interburden at open cast mine “Tamnava-West Field”,

Project C - procurement of hardware and software for the coal quality management in the western part of Kolubara coal basin.

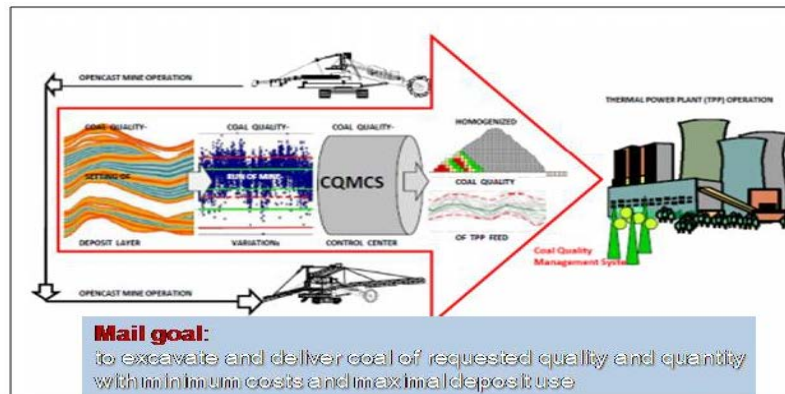


Figure 164. Graphical scheme of system for coal quality management

2. COAL QUALITY MANAGEMENT - EUROPEAN EXPERIENCES

Lignite reserves and the coal used in power plants for production of electric energy all over the world has no comparison with other organic fuels or some other sources cannot provide equal mass production of energy. Because of that fact, all parts of coal deposits need to be exploited, and demanded quality can be obtained by using specially developed systems which can provide fulfillment of wide spectrum of requirements coming from users.

The biggest mining companies in Europe, over the time, developed their own concepts for coal quality management according to their specifics and requirements of consumers.

2.1. Germany - solution for coal quality management

For many years Germany is a leader in lignite production, along with production of mechanization for the work at open cast mines. Currently, within Germany's lignite basins production is more than 200 mill. tons of coal, and around 26% of total electric energy is produced from it [1]. For this large production Germany was the first country which started development of system and implementation of processes which enables procedure for excavation of coal with different quality, regarding observed parameters, and mixing in order to achieve required demand.

Each coal basin and defined open cast mines within them have their specifics, and for that independent systems were developed enabling fulfillment of all demands for the quality required from final consumers. Joint thing to all of these systems is approach to the problem, development of activities according to the demands and making of integrated model for coal quality management, which, essentially, is reflected in:

- planning of production at different levels,
- determination of necessary quality and quantity for coal,
- development of appropriated models (geological, technological, model of the stockyard)
- schedule and engagement of the excavators,
- operational monitoring of coal excavation, transportation and usage on the stockyard,
- management of the mechanisation on stockyard according to plan,
- the use of additional equipment for the work control,
- output control of coal's quality and quantity.

This is a way how the system for coal quality management will guarantee compliance of contractual obligations and ecological parameters along with significant decrease of costs for electric

production. Additional meaning in implementation of system lies in increase of technological discipline of all employees.

2.2. Greece - solution for coal quality management

Coal is basic energy resource in Greece and production of energy from coal combustion fulfils 70-75% of country needs. Within two coal basins (Ptolemaida and Megalopolis) different and uneven characteristic of coal led to development of system for coal quality management [1].

Demanded coal quality, on both basins, has been achieved with homogenisation at stockyard. Previous to that, it is necessary to make good exploration of coal deposit, production planning and tracking of excavated coal through the planning of works according to geological model, plans of customer's consumption, preparation of operational working plan for the mechanization, and coal transportation to the stockyard. With corresponding method of coal disposal (mixing/deposition) at stockyard, the harmonisation of coal's required quality is obtained.

From the stockyard, coal is taken and transported toward customers, with previous control via online analysers before and after mixing.

2.3. Bulgaria - solution for coal quality management

The largest Bulgarian lignite basin with biggest reserves is Marica East. There, from three open cast mines: Trojanovo 1, Trojanovo north and Trojanovo 3, comes annual production of 25 mill.t. [1].

Changeability in coal's characteristics led to introduction of system for coal quality management. Basic activities of concept are reflected in:

- geological exploration works and development of geological model of quality,
- development of technological model for mechanisation's work according to predicted quality and capacity,
- control, comparison and processing of realized and planned data,
- use of online measurement instruments and scales for tracking information at the excavators,
- use of devices for measurement of ash and moisture content in coal, and devices for weight measurement at the belt conveyers for control of quality and capacity.

To equalize the coal quality it is necessary to excavate benches by digging the sub-benches with different content of observed parameter, and to limit capacity for the excavator during work in coal with different characteristics. After that, a mass flow of coal with corresponding quality and capacities is controlled on conveyers, and during loading into wagons, too.

2.4. Summary of foreign experiences

All implemented systems for coal quality, management and control are based on:

- integrated models of coal quality management (model of deposit, technological model, stockyard model),
- additional exploration and quality analyses for updating of deposit's model (in situ) ,
- existence of professional and efficient service for production planning,
- at all open cast mines there are significant reserves in excavator's capacity for the purposes of stabile supply with coal toward power plants,
- online analysers are just control - they are not used for planning and running of processes,
- system of coal quality management integrates several mines and more power plants,
- high technological responsibility of all participants through this system is essential.

3. DEVELOPED CONCEPT OF COAL QUALITY MANAGEMENT IN EPS

3.1. Preconditions and causes for the system’s implementation

The most important energetic potential in Serbia is coal and in structure of total energy reserves it participates with over 84%. For that, the main goal in exploitation of coal at open cast mines is to procure sufficient amount of fuel for combustion in power plants, with appropriate quality and minimal costs [2].

During more than half of the century of lignite production in Kolubara coal basin, easy reachable and quality equalised parts of deposit are already finished. The rest of the coal’s reserves, on active and further open cast mines, are with very changeable quality and, on average level, with lower heating value.

In order to satisfy demands for realisation of planned balance for coal’s excavation and demands for minimum requested quality for power plant “Nikola Tesla”, it is necessary to implement system which will allow rational use of mining resources, increase reliability of thermo capacities and optimal use of power plants, improve environment’s demands and reduce negative impacts on it and provide production of cheaper electricity [3].

3.2. Adopted concept of coal quality management system

The main objective of system’s implementation is excavation and distribution of coal for power plant “Nikola Tesla with sufficient amounts, required quality with minimum excavation expenses and maximum usage of deposit. The aspect of planning is the first and leading step to determine, according to the level of plans, distribution of total tonnage and quality parameters.

To achieve all of this, integrated conceptual design of coal quality management was developed and its consists of:

- CQMS mining planning software
- SYMS system software for control and management of processes

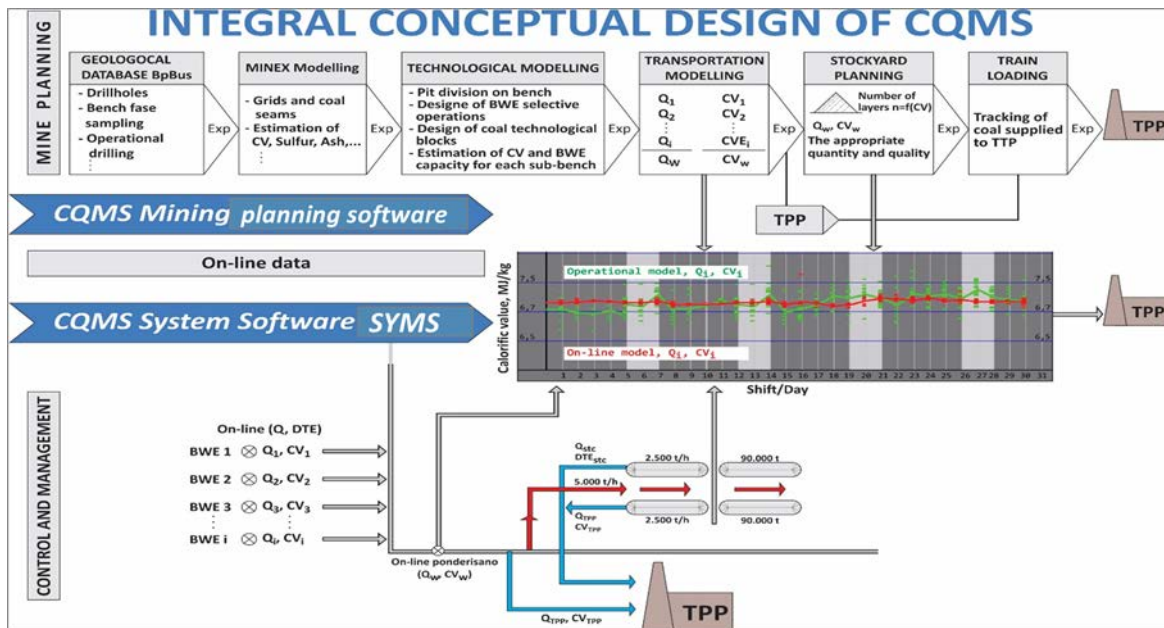


Figure 2. Adopted solution for coal quality management system

Each of these software contains different and interconnected activities, which must be carry out in defined order so that all necessary data are processed, transferred and observed during processes of coal excavation, transport and distribution on stock yard or loading into trains.

CQMS mining planning software contains several models and connected actions from geological modelling, bench modelling, technological modelling, transportation modelling, stockyard planning and train loading [4].

From detail mine exploration, sampling and laboratory analyses, the basis for a further work was made by creation of geological model in software package MINEX. Geological blocks, defined in model, contain all necessary informations regarding volume, quality etc. in assigned net 20x20m.

After that, in technological modelling bench model will be developed, also in MINEX, with clear vertical division of coal deposit regarding height for each coal system. Next step is modelling of technological blocks where, based on the planned balance for coal excavation, technical characteristics of equipment and geological conditions inside the geological blocks for every coal bench, technological blocks anticipated for excavation will be created for each coal system and belonging excavators, with defined selective work, the number of sub-benches and quality and capacity for each of them along with appropriate working capacity for excavators (bucket wheel and chain excavators). After starting of model for material transport, next activity in planning is simulation of excavators work and analysis for created technological blocks on all benches along with conveying of material to destination (loading into wagons or stockyard).

As for the stockyard planning, depending on the destination for excavated coal from the mine, it can be used for disposal of coal (Strata method which will enable homogenisation of coal until required average quality), or taking of coal with two reclaimers. Also, for the old stockyard and the combined machine working there, coal can be disposed or taken as well.

Final step of planning is train loading directly from open cast mine, combined loading from mine and from stockyard(s), or direct loading from the stockyard.

SYMS - system software for monitoring, control and management of processes integrates necessary data from planning software, and according to additional measurement devices positioned throughout whole production system (GPS, online analyzers and belt scales) provides all necessary informations, audio and visual, about fulfilment of requested goal in system for coal quality management.

4. EFFECTS OF COAL QUALITY MANAGEMENT SYSTEM IMPLEMENTATION

The essence of implementation for Coal Quality Management System is to, during coal excavation as primary energy source, optimizes quality in open cast mine and to achieve higher energy efficiency comparing to the existing condition while combustion in boilers of power plant Nikola Tesla.

A great number of aspects, under the influence of both sides in energy production process, additionally give complex cause-effect relationships and clear display of benefits or disadvantages of particular parts of processes and activities with or without implementation of Coal Quality Management System.

4.1. Advantages and profit for the open cast mines

At open cast mines main benefit reflects in maximum use of deposit. Considering decrease of high-calorie parts with introduction of Coal Quality Management System use of low-calorie parts within deposit, currently around 18%, will be achievable. With percent participation of 20% of high-

calorie parts (above 8000 kJ/kg) around 40% of total coal will be optimized, and at the same time the working life of mine will be extended.

Next benefit, which can be economically expected after implementation, will be due to conditions of paying for coal with different values from the power plant. Overview of incomes is shown in table.

Table 39. Amount of coal outside limited value

Exploitable coal (t.)	
< 5.500 – 3.500 kJ/kg	> 8.000 kJ/kg
20.000.000	85.000.000
Average: 800.000 tons/year	Average: 2.800.000 tons/year

Total annual profit based to coal homogenisation will be:

$$800.000 \text{ tons} \times 6100 \text{ kJ/kg} \times 1,67 \text{ €GJ} = 8.148.000 \text{ €} [5].$$

Beside these benefits, there are uneconomical calculations reflected in decrease of transport and disposal of low-caloric coal, treated as overburden, meaning creation of additional usable space for proper work of overburden systems on disposing side.

Also, disposed low-caloric coal have a tendency for self-ignition, so implemented Coal Quality Management System reduces negative impacts on environment due to emission of combustion gasses into the atmosphere.

4.2. Advantages and profit for the power plant “Nikola Tesla”

After the implementation of Coal Quality Management System, the biggest economic effects are on the power plant “Nikola Tesla”, considering the influence of achieving optimal quality of coal for all phases in technological process of energy production.

They are reflected in:

- maintenance of nominal blocks power during combustion of coal with required quality,
- stabile combustion process in burners without additional use of fuel oil.

Between 2010-2016 inadequate coal quality caused large fuel oil consumption for combustion support in power plant Nikola Tesla.

In 2016, the expense was: 17.500 t. × 360 €/t = 6.300.000 €_{god}

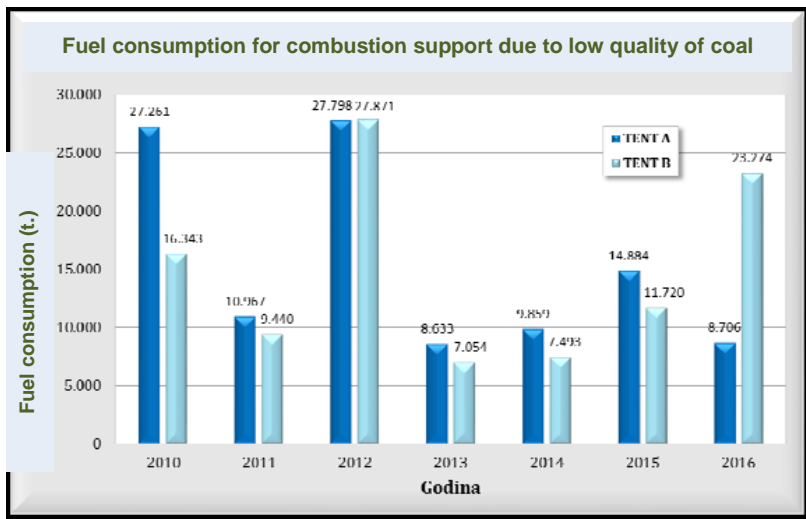


Figure 3. Consumption of fuel oil in Power Plant Nikola Tesla

- increase of utility degree for boilers facility for 12% ,
- reliable coal preparation for combustion without additionally activated mills in power plant “Nikola Tesla”, and without extra burdens for the rest of equipment in system, until combustion (bunkers, dozers, feeders, conveyors, etc.),
- optimization and automatics in business of bloc’s running and work,
- decrease of own electricity spending for 10%, meaning around 0,7-10% more energy will be delivered into electro-energy system (50×10^6 kWh/year).
- stabile work of system for delivery and fuel preparation, boilers bed and other heating surfaces, removal system for ash and slag and ventilators of smoke gasses.
- reduce of coal dust speed and other products of combustion
- less erosion and wear along whole boiler’s tract,
- lowering of total ash and slag amount due to stabile work of boilers,
- less load for the entire system for ash and slag removing,
- significant reduce of pollution of environment due to lowering of combustion products for the same degree of cleaning’s system efficiency and increase of dedusting for electro filters. According to all mentioned effects after implementation of Coal Quality Management System from the side of power plant “Nikola Tesla”, it is estimated that saving might be:

$$268 \text{ GWh} \times 0.0417 \text{ €/kWh} = 11.176.000 \text{ €god. [5].}$$

5. CONCLUSION

Characteristics of lignite in Kolubara coal basin, which is available for excavation, is express stratification inside the deposit and significance variations in quality. In order to provide continuity for power plant supply, it is important to implement a system which will enable detailed planning and coal exploitation with control of quality, and at the same time a techno-economy effect will rise during utilisation of low quality parts of deposit.

Mentioned system is based on planning, control and management of all parts during exploitation, transport, disposal and loading of coal. At the same time, system enables monitoring and provides possible solutions as well as opportunity for employees in system to react accordingly to the potential problems during work. System requires that each participant in process have concrete, clear and unequivocal tasks to establish complete technological discipline and work organisation. This is provided with the use of highest technical achievements which connect natural conditions in deposit and possibilities of mining’s and thermo-energetic equipment.

Coal Quality Management System has multiple benefits. Open cast mines would work rationally without uncontrolled spreading from natural recourse and with possibility of expansion for coal production as raw material. In such system it is possible to valorise maximum from total coal reserves, even there where the value of the observed parameter for quality is less than required. For this, the mine will sell its goods with the requested characteristics per defined price!

In power plant “Nikola Tesla” this system provides and creates regular conditions for coal combustion with appropriate quality thereby producing cheaper electric energy. It also enable higher utilisation of facility and increase of energy-efficiency throughout production of electricity.

Furthermore, undoubtable macroeconomic effects are reachable through generally less dependence on imports (fuel oil, spare parts, etc), lower influence on environment and eco system and providing of better social-economy conditions for municipalities influenced by the whole process.

Each of the parties during production of electricity must respond to the all requirements of Coal Quality Management System in order to accomplish power balance in Republic of Serbia.

REFERENCES

- [1] D.Ignjatovic, D.Knezevic, B.Kolonja, N.Lilic, R.Stankovic (2009). Coal quality management, Monograph, Mining-Geology Faculty Belgrade, 2007, pp 9-26, pp 27-34, pp 35-42
- [2] Faculty of Mining and Geology, Belgrade (2009). Conceptual program with feasibility study for introduction of system for operational management and coal quality control at Tamnava mines, pp 1-3
- [3] Faculty of Mining and Geology, Belgrade (2004-2005). Managing the process for coal homogenization in order of increasing utilization of coal with low value and oil savings in power plants, pp 12-15
- [4] N.Drljevic: Development of technological model of excavator's work for operational planning and coal quality management at Tamnava mines, Master thesis, Belgrade (2010), pp 36-45
- [5] Faculty of Mining and Geology, Belgrade (2017). Feasibility study for introduction of system for operational management and control of coal quality at eastern part of Kolubara coal basin - Excerpt from Study, pp 65- 67

Morphology, Mineralogy, and Chemistry of Fly Ash from the Ptolemais Power Stations, Northern Greece, and its potential as partial Portland cement substitute

Apostolidou Ch. and Georgakopoulos A.

Department of Mineralogy – Petrology – Economic Geology, School of Geology, Aristotle University of Thessaloniki, 54124 Thessaloniki, Greece.

ABSTRACT

Morphological, mineralogical, and chemical properties of three composite Fly Ash samples from Agios Dimitrios, Amyntaio and Kardias lignite-fired Power Stations, Northern Greece, were studied applying Scanning Electron Microscopy (SEM), X-ray Diffraction (XRD) and X-ray Fluorescence (XRF) methods. The $-45\ \mu\text{m}$ fraction of each sample was also analyzed. Morphologically, fly ash consists mostly of silica coated plerospheres, cenospheres, and calcic-sulphuric agglomerations. Fiber shaped silica phases were found in the fly ash sample from Amyntaio Power Plant. The fly ash samples are mainly composed of anhydrite, lime, calcite, gehlenite, and quartz. Differences in the mineral and the chemical composition between the bulk sample and the $-45\ \mu\text{m}$ fraction were noticed. Fly ash samples picked up from Agios Dimitrios and Kardias are mainly calcareous while in Amyntaio Fly ash silica oxides prevail. The potential of the fly ash samples as a pozzolanic additive to Portland cement was examined on the basis of the ASTM C311 standards.

1. INTRODUCTION

Greece is the fourth largest producer of lignite within the European Union [1] producing around 30 Mt annually. Despite the fact that only 30% of Greece's electricity needs are covered by lignite, the latter plays a significant role in the Greek economy, since it is an indigenous and low-cost mined energy resource. There are two lignite centers in Greece, one in Peloponnese, Southern Greece and one in Western Macedonia, Northern Greece. In Western Macedonia lignite is excavated from four big mines, with the biggest one being the Southern Field Mine, from which 12 Mt lignite are produced annually. Southern Field's production feeds the Agios Dimitrios Power Plant, the biggest one in Greece, with 1584 MW total installed capacity.

Fly ash, along bottom ash, is the inorganic solid residue after coal combustion. Greek lignite yields, on average, around 30% inorganic content (fly and bottom ash) [2], which constitutes a major problem due to the enormous amounts produced from lignite combustion. Concretely, over a year, Public Power Corporation of Greece produces and stores 12 Mt of fly ash in the entire Western Macedonia Region [3]. Mineral and chemical composition of fly ash, as well as its physicochemical properties, change over time depending on both the chemical composition of the lignite deposit and the combustion properties [2,4,5,6]. Fly ash from Agios Dimitrios, Kardias and Ptolemais Power Plants is enriched in CaO, whereas fly ash from Amyntaio and Meliti Power Plants is enriched in SiO₂ [7]. Due to increased specific surface of its particles, fly ash is capable of restraining elements and participating in chemical reactions. This ability is caused by microporous minerals, such as clays and micas [8]. Moreover, SiO₂ presence in fly ash is the main carrier of pozzolanic properties making it useful in cement as an additive. The above facts reveal the necessity of studying the mineral and chemical compositions of Greek fly ash, in order to examine potential applications. Within this framework, the current study aims to contribute enlightening the fly ash potential for several applications.

2. MATERIALS AND METHODS

One 30-day composite fly ash sample obtained from each of the Agios Dimitrios (AD), Amyntaio (AM) and Kardias (KA) lignite-fired Power Plants (PP) in Ptolemais Basin, was studied in order to investigate the behavior and properties of fly ash. The analytical characterization included: Grain Size analysis, Mineralogical composition, Morphological determination, Chemical composition and Swelling tests.

2.1. Grain Size Analysis

Grain size analysis was performed in the Laboratory of Sedimentology, Department of Physical and Environmental Geography, Aristotle University of Thessaloniki, where approximately 100g from each sample were dried in an oven at 90°C. After cooling down to ambient temperature (20°C), the samples were re-weighed. The fact that fly ash is a combustion product leads to almost zero moisture, especially when the amount of hygroscopic materials is low. Afterward, each sample was placed in a sieve of 2mm diameter to separate the gravel size particles. The -2mm fraction was placed in a column of eight sieves with different mesh size (Table 1).

Table 40. Sieves used for fraction separation of the AD, AM, and KA fly ash samples

Sieves	Mesh ϕ	Opening diameter (in μm)
1	1	500
2	1.5	350
3	2	250
4	2.5	175
5	3	125
6	3.5	95
7	4	63
8	4.5	45

After 30 min of dry-sieving, nine fractions of fly ash, also including the $-45\mu\text{m}$ fraction, have been separated, for each one of the three initial samples.

2.2. Powder X-Ray Diffraction

Powder X-Ray Diffraction (PXRD) was performed on six samples, the three original (AD, AM, KA) and their $-45\mu\text{m}$ fraction sub-samples (ADDDB, AMDB, KADB). A Philips (PW1710) diffractometer with Ni-filtered Cu K_{α} radiation was used. The samples were scanned over the 3–53° 2θ interval at a scanning speed of 1.2°/min. Semi-quantitative estimates of the abundance of the mineral phases were derived from the PXRD data, using the intensity of a certain reflection, the density and the mass absorption coefficient for Cu K_{α} radiation for the minerals contained. In the PXRD patterns, the amorphous material was clear as a broad background hump between 10 and 20° 2θ . The semi-

quantitative estimation of the total amorphous material content was achieved by comparing the area of each broad background hump with the analogous area of standard mixtures of minerals with different contents of natural amorphous material [9] scanned under the same conditions.

2.3. Chemical composition

The bulk composition was determined in the six fly ash samples (AD, AM, KA, ADDB, AMDB, KADB), using a Bruker S4-Pioneer XRF wavelength dispersive spectrometer. The spectrometer was fitted with an Rh tube, five analyzing crystals, namely: LIF200, LIF220, LIF420, XS-55 and PET, and the detectors were a gas-flow proportional counter, a scintillation detector or a combination of the two. Samples were analyzed at 60 kV and 45mA tube-operating conditions.

2.4. Scanning Electron Microscopy

Morphology and elemental composition of the three bulk samples (AD, AM, KA) and the -45 μ m fraction sub-samples (ADDB, AMDB, KADB), were studied using a JEOL JSM-840 scanning electron microscope JEOL JSM-840 type, equipped with an INCA 300 energy-dispersive X-ray spectrometer (EDS) with 20 kV accelerating voltage and 0.4 mA probe current. The samples were carbon coated to acquire conductance.

2.5. Swelling tests

Swelling tests were performed in the AD, AM, KA fly ash samples according to the *Le Chatelier* method for a mixture of 30% Fly ash and 70% Cement with thickening time of about 2 hours for a Cement/fly ash 75/25 mixture. The samples were prepared and adjusted according to ASTM C311-07 standard [10] and the swelling tests followed the procedure of ASTM C 157/C 157M [11].

3. RESULTS AND DISCUSSION

Fly ash morphology, mineralogy and chemistry depend on the mineral matter contained in the coal, the combustion process and the post-combustion cooling conditions [12, 13, 14, 15, 16, 17, 18]. Our multi-method approach of fly ash examination revealed significant differences among the ash samples from the Greek thermal stations and between the coarser and finer fraction of each sample as well. In addition, considerable limitations were revealed concerning the uses of Greek fly ash, due to its chemical and morphological characteristics, also mentioned in previous studies [19, 20].

3.1. Particle size distribution

Figure 1 presents a grain size distribution among the studied fly ash samples. Agios Dimitrios and Amyntaio ashes show an inverse proportional relation between grain size and its mass percent distribution, revealed with an increase of particle percentage participation with size decrease in both samples. Agios Dimitrios ash has a higher amount of 63-45 μ m particles compared with Amyntaio fly ash, whereas Amyntaio fly ash appears to have a slightly higher amount of 250-125 μ m particles among all samples. Fly ash from Kardias thermal station follows the same distribution of particle size in coarser particles (500-250 μ m), but it shows a higher amount of 95-45 μ m particles, compared with the other samples and a significantly lower amount of -45 μ m fraction. Particle size distribution is strongly connected to combustion conditions. A greater weight loss of finer particles with increased combustion temperature has been observed, mainly caused by thermal disruption of carbonate salts of Ca, abundant in finer particles [18]. Considering that the three fly ash samples are

obtained from different thermal stations and have been produced under different combustion conditions, it is believed that the dissimilar distribution of Kardia ash particles was created by changes of combustion temperatures.

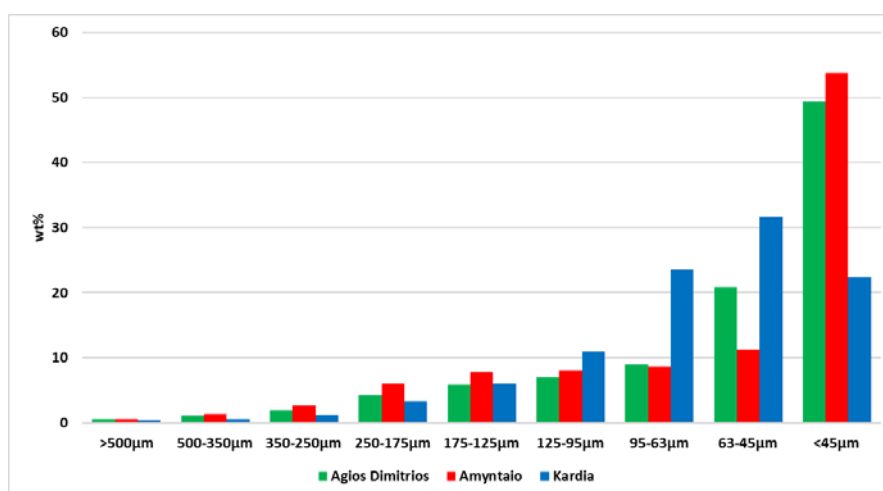


Figure 165. Particle size distribution of the three fly ash composite samples.

3.2. Morphology

The samples examined under the Scanning Electron Microscope proved to consist of plerospheres, cenospheres (hollow spheres) and agglomerates, resulted from lignite combustion properties. Plerosphere is a cenosphere which may encapsulate a mass of microspheres (1 μm or less in diameter) [4] and is generally silica coated (Fig. 2c, 3d). In some cases, plerospheres are caught releasing their enclosure, which consists of spheres or gases and volatiles emitted during lignite combustion process (Fig. 2a, 2b). During this gas release, the larger fly ash particles produce a considerable number of micron-sized particles, which reinforces particle size distribution [22]. Small particles, often sub-micron sized, are found adhering to larger particles (Fig. 2c) and there are clumps or agglomerates of small particles [4]. Table 2 shows the elemental analysis carried out applying SEM-EDS during the examination of ash morphology. It provided us with information about specific areas of the samples. Through this analysis, the alumino-silicate composition of the spheres was confirmed (Table 2, columns 1, 2 & 7) [23]. The relative content of aluminum and silicon varied from sphere to sphere and among the samples as well.

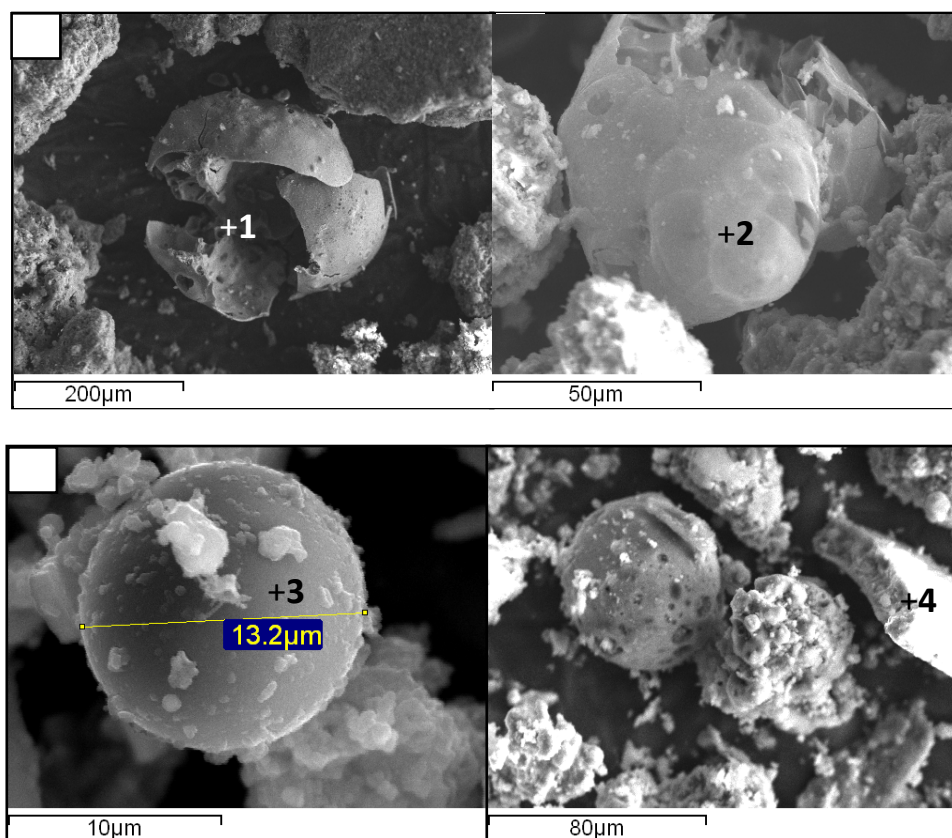


Figure 166. Fly ash particles from Agios Dimitrios Power Plant: a, b) Cenospheres after releasing their gases, c) Silica-coated perfect sphere with smaller particles on its surface, d) Agios Dimitrios ash with calcium-rich mineral phases. (1,2,3,4: at these points, microanalysis was performed, see Table 2).

Table 41. Elemental analysis using SEM-EDS microanalysis in specific areas of the samples

Oxides	Agios Dimitrios				Amyntaio		Kardia	
	1	2	3	4	5	6	7	8
Na ₂ O	bdl	1.75	0.13	bdl	0.42	17.79	0.4	bdl
MgO	14.1	0.31	2.97	0.73	bdl	9.96	1.52	0.21
Al ₂ O ₃	17.38	12.56	13.27	4.01	0.17	6.45	3.09	9.67
SiO ₂	43.29	74.46	38.31	5.09	99.87	16.3	69.73	8.43
P ₂ O ₅	bdl	0.01	0.09	0.23	bdl	2.15	0.52	1.25
SO ₃	0.94	0.67	0.03	15.68	0.01	4.25	6.99	46.32
K ₂ O	2.8	5.75	1.34	0.22	0.63	1.25	0.49	2.1
CaO	1.42	2.5	25.79	72.97	0.54	38.49	13.75	27.72
TiO ₂	1.31	0.35	0.17	0.31	0.07	0.15	0.19	1.35
MnO	0.42	0.06	bdl	bdl	bdl	1.04	0.06	bdl
FeO	18.5	1.57	17.94	1.14	bdl	2.18	3.26	3.85

It was noticed that the morphology of fly ashes depends on silica dioxide content. For instance, in Amyntaio fly ash silica oxides appear to prevail, leading to the distinctive characteristic of fiber-shaped silica phases (Fig. 3a, 3b). These fiber phases present up to 99% of SiO₂ (Table 2) and appear exclusively in Amyntaio fly ash. The length varies being by far longer than 10 μm, which is a crucial environmental limit for air particles. Furthermore, there are impressive fossil structures in Amyntaio ash (Fig. 3c). In all samples, there was a significant amount of unburnt lignite particles mostly in the 500-350 μm fraction. The unburnt lignite was more intense in Kardia fly ash (Fig. 3e) being rich in carbon and sulfur. Unburnt carbon in fly ash indicates inefficiency in combustion and may be an impediment to the beneficial use of fly ash or ash products in a variety of applications; particularly when contained in significant proportions it limits or precludes the use of fly ash as a substitute for Portland cement in concrete [21].

Major factors affecting the presence of unburnt carbon in fly ash may be the coal rank and type and the behavior of different macerals during the combustion process.

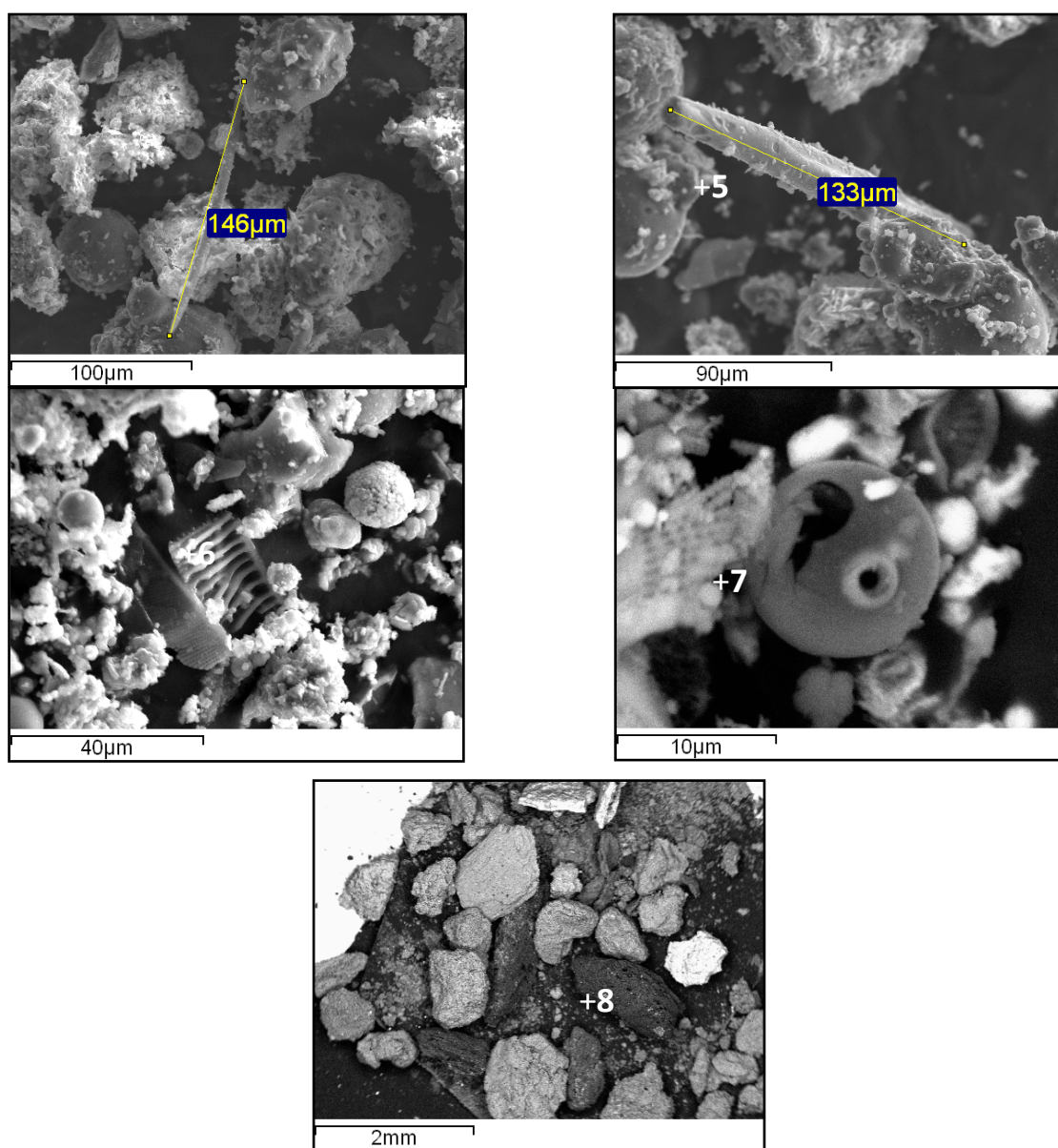


Figure 167. Fly ash particles from Amyntaio Power Plant: a, b) Fiber shaped silica mineral phases, c) Fossil structures within fly ash particles, d) Silica-coated cenosphere, e) Backscattered image of Fly ash from Kardia Power Plant plenty of unburnt lignite particles (black and dark grey). (5,6,7,8: at these points, microanalysis was performed, see Table 2).

3.3. Mineralogical Composition

From mineralogical viewpoint fly ash consists mainly of three types of components: crystalline minerals, unburnt lignite, and alumino-silicate amorphous material. The results of the mineralogical analysis of three composite samples and their -45 μm fraction are shown in Table 1, while Powder X-ray diffraction patterns are shown in Figure 4. The ash from Agios Dimitrios PP consists mainly of anhydrite, lime, calcite, small amounts of gehlenite, hematite and quartz and very low amounts of plagioclase, micas and clay minerals. As being noticed, the -45 μm fraction is enriched in calcite compared with the initial sample. The Amyntaio ash sample consists of anhydrite and lime, while gehlenite, quartz, plagioclase, hematite, and calcite are included in smaller amounts. Hematite is contained at a severe percentage (7%) in the initial sample, while it was not traced in the -45 μm fraction. The main constituents of Kardia PP ash are also lime, anhydrite, calcite, gehlenite and in lower amounts quartz, plagioclase and hematite. Micas appear in traces in the -45 μm fraction. Quartz, feldspars, calcite, micas, and clays were constituents of the mined lignite, while anhydrite, lime, and gehlenite were formed during lignite combustion [6,7,25,26]. Most of the calcic minerals such as calcite (CaCO_3), anhydrite (CaSO_4) and gehlenite ($\text{Ca}_2\text{Al}[\text{AlSiO}_7]$), were enriched in the -45 μm fraction, whereas quartz, lime, and hematite were decreased in the same fraction. Particularly, calcite was enriched three times in Agios Dimitrios finest fraction (from 6 to 18wt%) and 2.1 times (from 7 to 15wt%) in Kardia finest fraction. A slight enrichment of 1.6 times was observed for anhydrite (from 20 to 31wt%) in Amyntaio and of 1.8 times (from 12 to 22wt%) in Kardia finest fraction. Similar enrichment of 1.8 was also determined for gehlenite (from 8 to 14wt%) for Kardia. On the contrary, quantities of quartz, lime, and hematite were not determined in the -45 μm fraction, while the rest of the mineral phases did not reveal changes in their quantity. The above mineralogical differences are imprinted on the PXRD patterns (Fig. 4), with changes of peaks position or intensity.

Table 42. Mineral composition (in %) of fly ash samples. AD: Total sample from Agios Dimitrios Power Plant, ADDB: -45 μm fraction of fly ash from Agios Dimitrios Power Plant. AM: Total sample from Amyntaio Power Plant, AMDB: -45 μm fraction of fly ash from Amyntaio Power Plant, KA: Total sample from Kardia Power Plant, KADB: -45 μm fraction of fly ash from Kardia Power Plant.

Power Plant	Agios Dimitrios		Amyntaio		Kardia	
	AD	ADDB	AM	AMDB	KA	KADB
Quartz	10	5	6	6	10	6
Anhydrite	17	19	20	31	12	22
Lime	35	21	30	24	34	25
Plagioclase	4	2	4	3	4	3
Calcite	6	18	5	6	7	15
Gehlenite	9	10	13	13	8	14
Hematite	6	5	7	-	4	-
Mica	1	1	-	1	-	1
Clay Minerals	1	1	-	-	-	-
Amorphous	11	18	15	16	21	14

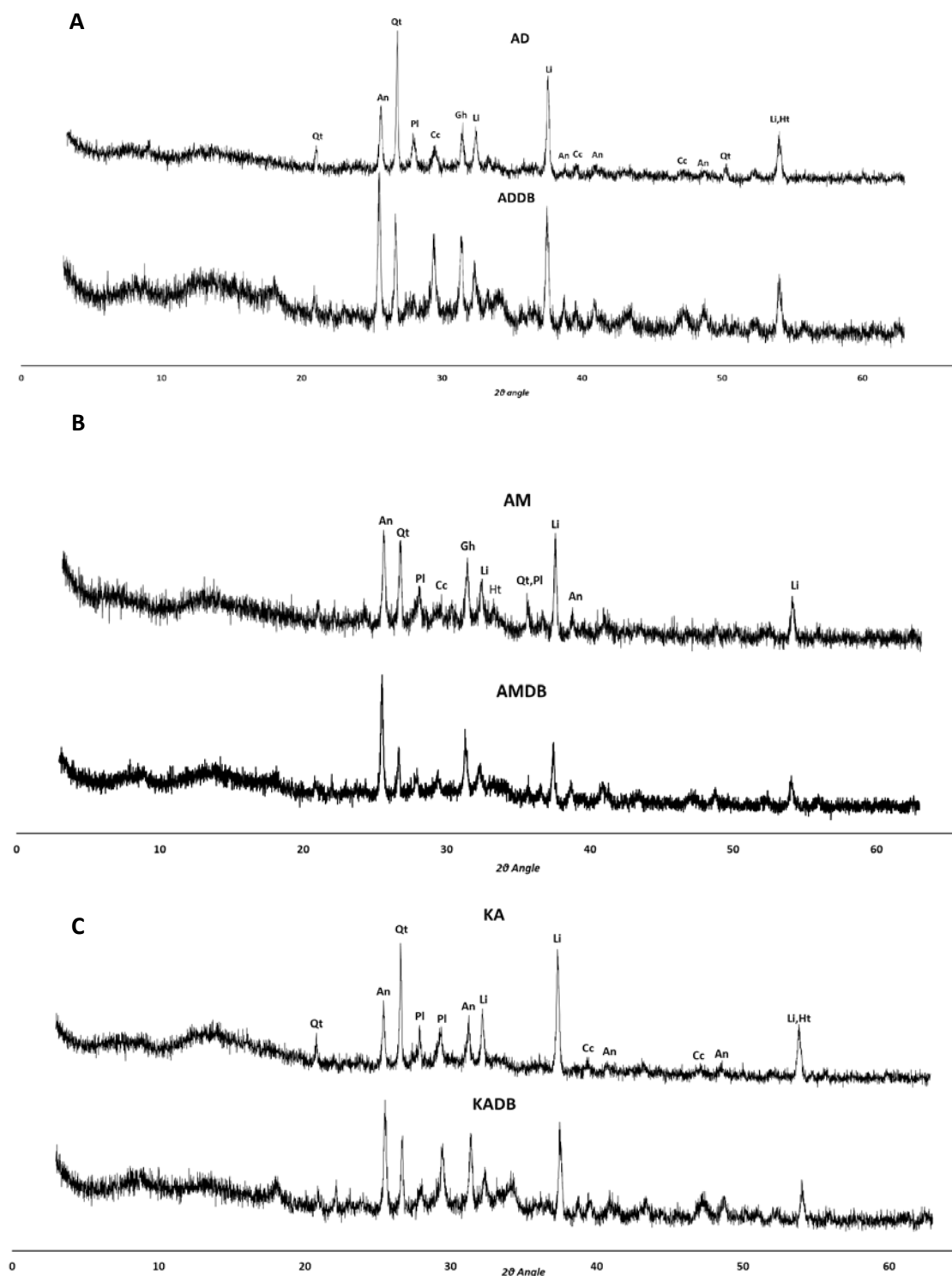


Figure 168. PXRD patterns of the six fly ash samples from the PPs of Agios Dimitrios (A), Amyntaio (B), Kardia Power (C). An: Anhydrite, Qt: Quartz, Pl: Plagioclase, Cc: Calcite, Gh: Gehlenite, Li: Lime, Ht: Hematite.

Specifically, ADDB showed more intense anhydrite, calcite, and gehlenite peaks, whereas AD bulk sample has greater quartz peaks. Total ash of Amyntaio (AM) reveals higher peaks for lime compared with AMDB sample. Finally, KA sample shows greater peaks for quartz compared with KADB samples, which has more intense peaks for anhydrite and calcite.

3.4. Chemical Composition

Chemical studies on fly ashes have been conducted from an environmental [4,27,28,29,30] or utilization [17,31,32,33] viewpoint by several authors. Table 4 presents the chemical composition of the fly ash samples under study. Based on the results the fly ashes from Agios Dimitrios and Kardias PPs have a relatively high CaO content, while Amyntaio fly ash shows a lower concentration in CaO. The SiO₂ content also shows a significant difference between Amyntaio fly ash (rich in silica) and Agios Dimitrios and Kardias fly ashes, which have a lower SiO₂ content. However, according to mineralogical analysis, Amyntaio contains a lower amount of quartz, which supports the opinion that most of the fly ash spheres consist of amorphous aluminosilicate material [23]. A variation also appears in Fe₂O₃ concentration, where Amyntaio and Kardias ashes show a slightly higher Fe₂O₃ content compared to this of Agios Dimitrios. The Al₂O₃ and the other oxides concentrations are low in all fly ash samples. It is worth mentioning that SO₃ shows no difference among all ashes. Trace elements were also determined (Table 4) but proved without any distinctive variation among the samples. It is obvious that chemical composition varies between the silica-rich ashes (Amyntaio) and the calcic ashes (Kardias, Agios Dimitrios).

Table 43. Chemical composition (in %) of the fly ashes under study (bdl: below detection limit)

Samples	Agios Dimitrios		Amyntaio		Kardia	
	AD	ADDB	AM	AMDB	KAR	KADB
Oxides						
CaO	54.59	57.54	42.77	46.00	52.66	54.58
SiO ₂	16.05	14.22	25.88	22.73	16.96	16.17
Fe ₂ O ₃	9.43	8.44	11.65	10.99	11.11	10.49
Al ₂ O ₃	5.83	5.16	5.96	5.06	6.18	5.66
S+A+F*	31.31	27.82	43.49	38.78	34.25	32.32
SO ₃	9.90	10.98	9.47	11.4	8.68	9.11
K ₂ O	1.25	1.08	1.60	1.37	1.46	1.31
MgO	0.58	0.63	0.49	0.90	0.55	0.58
TiO ₂	1.10	1.07	0.89	0.87	1.07	1.00
Cr ₂ O ₃	0.24	0.18	0.16	0.16	0.23	0.25
P ₂ O ₅	0.30	0.28	0.25	0.24	0.19	0.20
MnO	0.07	0.07	0.13	0.12	0.11	0.11
SrO	0.10	0.09	0.08	0.07	0.07	0.07
NiO	0.07	0.06	0.03	0.02	0.07	0.06
Na ₂ O	bdl	bdl	0.04	0.04	bdl	bdl
ZrO ₂	0.03	0.02	0.02	0.02	0.03	0.02
CuO	0.02	0.02	0.03	0.02	0.03	0.02
ZnO	0.02	0.02	0.02	0.02	0.02	0.02
Rb ₂ O	0.01	bdl	0.01	0.01	0.01	0.01

*S+A+F: The total silica, aluminum and iron oxides content of each sample.

The presence of silica dioxide in calcium-rich fly ashes is important even in small amounts. It has been demonstrated [34] that when incorporating high-calcium fly ashes in cementitious systems, the soluble silica present in the ash significantly affects their hydration. Although ash rich in active silica is generally more preferable, this does not exclude the possibility of achieving higher reaction rates and superior performance when utilizing different ashes [33].

According to ASTM standards, fly ash is classified based on the content of its major elements (ASTM 618 C), to Class F and Class C. Class F comprises ashes produced from high-rank coals with at least 70% SiO₂+Al₂O₃+Fe₂O₃, while Class C comprises ashes produced from low-rank coals with more than 50% but less than 70% SiO₂+Al₂O₃+Fe₂O₃. All of the samples under study present

$\text{SiO}_2 + \text{Al}_2\text{O}_3 + \text{Fe}_2\text{O}_3$ less than 70% as it is required for Class C classification (Table 4). $\text{SiO}_2 + \text{Al}_2\text{O}_3 + \text{Fe}_2\text{O}_3$ content also has to be $>50\%$, which is not the case in Greek fly ash due to its high CaO content. However, several authors [3,4,15,19] classify Greek fly ash in Class C, taking in consideration the significant high CaO concentration. A major problem concerning fly ash utilization is the heterogeneity of its chemical composition derived from the chemical composition of feed lignite, the combustion conditions and the amount of co-excavated inorganic strata led to combustion. The variability of these factors excludes a constant chemical composition of fly ash for further utilization.

As far as mineralogical and chemical compositions are concerned, an inverse proportional relation between Ca and particle size distribution is revealed, where CaO content (Table 4) and calcic minerals (Table 3) are increased with decreased particle size. Ramasubramania (2002) distinguished the elements contained in the fly ash into two groups based on their dependence upon particle size, namely those with no enrichment in the finest particle size and those which are enriched [35]. Ramasubramania (2002) also observed that the Ca content reaches a maximum concentration in a particle size of 5 μm and then decreases with increase in particle size. Our results confirm the inference of the enrichment of specific elements in fine particles, with a dominant example being the Ca behavior. Fine fly ash particles have a relatively greater surface area which leads to the higher absorption of volatile elements. It has been observed in several trace and major elements such as Ca that volatility increases from a larger to a smaller particle size, which establishes an inverse relationship of volatility and particle size. The intense presence of CaO in the fine-grained fractions (along with their high specific surface area) leads to their high desulphurization capacity and consequently the high concentration of SO_3 in these particles [21]. The enrichment of the finer fraction in anhydrite mineral phase, as presented in Table 3, enhances this inference. On the other hand, SiO_2 displays a lower content in the fine particle-size fraction assuming silica enrichment at coarser particle size. This observation has been also highlighted by other authors [21,37] and was related to the increased pozzolanic reactivity of the coarser fly ash fraction. It has been noticed that the lack of the -50 μm fly ash fraction in the cement production process effectively reduces the concentration of the non-desired chemical compounds: SO_3 and CaO [21] also providing a higher amount of active silica and alumina phases, which are the main carriers of the pozzolanic reactions.

3.5. Swelling

Figure 5 presents the results of swelling tests performed on the three bulk samples of fly ash. The results revealed the major problem of Greek fly ash when added to cement which is the swelling behavior caused by the high concentration of free CaO. Free CaO is directly related to the chemical composition of the feed lignite [14,15,37,38,39,40]. Feed lignite in Northern Greece always carries inorganic matter that causes many of the technological and environmental problems attributed to coal use. Moreover, coal deposits are made up of sedimentary sequences of coal seams interlayered with inorganic layers, primarily marly limestone and carbonaceous marl and secondarily clay and sand. The geological framework of coal deposits makes the co-excavation of coal with the intercalating wastes unavoidable, increasing substantially the inorganic matter content contained naturally in coal. The co-excavation of lignite and intercalating layers increases the calcite content of lignite, raising the ash yield, and decreasing the calorific value of the mined lignite. The CaO (free) content of the fly ash, according to the Hellenic Legislation for fly ash uses, must be kept below the 3% limit.

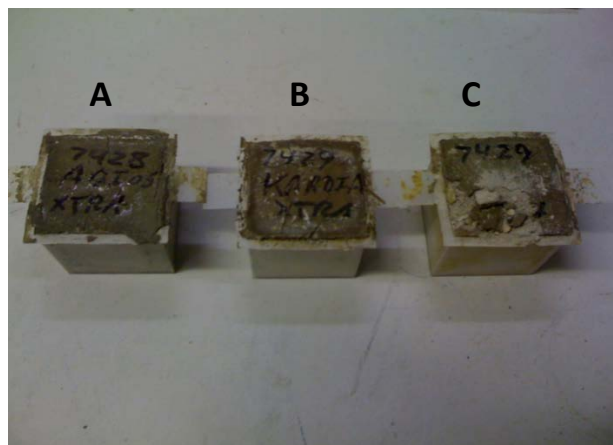


Figure 169. Swelling test results, showing the swelled fly ash-cement mixture. Mixture A: Agios Dimitrios fly ash added, Mixture B: Kardia fly ash added. Mixture C: Amyntaio fly ash added.

4. CONCLUSION

Fly ash samples from different thermal stations present significant differences. Fly ash from Kardia PP presents an irregular particle distribution with lower mass fraction participation of $-45\ \mu\text{m}$. The higher the unburnt lignite content compared with the other ashes results from different combustion conditions in Kardia PP. Amyntaio and Agios Dimitrios ashes presented $>50\ \text{wt}\%$ participation of the $-45\ \mu\text{m}$ fraction in the bulk samples. On the other hand, a relation between chemical composition and morphology was traced, especially in Amyntaio fly ash, where the alumino-silicate chemical compounds affect morphology creating fiber shaped silica phases. The fiber phases were observed exclusively in Amyntaio ash. From the mineralogical point of view, all ash samples contained anhydrite, lime, gehlenite, quartz, calcite, hematite, while micas and clay minerals were included in traces. High amounts of anhydrite and lime were observed, which explains the 40-50% CaO content of all samples. Amyntaio ash contained the lowest CaO and the highest SiO₂ content among the samples. However, this was not expressed with high quartz content, due to amorphous alumino-silicate spheres of fly ash. The chemical composition varies between the silica-rich (Amyntaio) and the calcic ash samples (Kardia, Agios Dimitrios). Differences were also noticed between the bulk samples and their $-45\ \mu\text{m}$ fraction. Ca-rich minerals are enriched in finer particles; this leads to the inference that finer particles are the main carrier of CaO being responsible for swelling behavior of the ash when added in cement. However, silica content thought to be enriched in coarser particles and a further study of coarser fly ash particles is suggested to examine the possibility of pozzolanic properties in the coarser fly ash fraction. Nevertheless, chemical composition, heterogeneity, unburnt lignite particles and high CaO and SO₃ content prevent an extended use of Greek fly ash as a cement additive.

ACKNOWLEDGMENTS

The authors are immensely grateful to Professor Kimon Christanis, University of Patras, for his comments on an earlier version of the manuscript.

REFERENCES

- [1] European Association of Coal (2017). Coal Industry across Europe. Available at: <https://www.braunkohle.de/files/euracoal-coal-industry-across-europe-6th.pdf> [Greece pp. 31-32].
- [2] Kolovos, N. & Georgakopoulos, A. (2005). Contribution on lignite recovery from multi-seam deposits. *Energy Sources*, 27, 975-986.
- [3] Public Power Corporation of Greece (2018). Available at: <https://www.dei.gr/en>
- [4] Georgakopoulos, A. (2003). Chemistry and morphology of fly ash samples from the main lignite power stations of Northern Greece. 8th International Conference of Environmental Science and Technology, 256-163.
- [5] Georgakopoulos, A., Filippidis, A., Kassoli-Fournaraki, A. & Iordanidis, A. (2002). Environmentally important elements in fly ashes and their leachates of the Power Stations of Greece. *Energy Sources*, 24, 83-91.
- [6] Georgakopoulos, A. & Filippidis, A. (1992). Mineralogical and chemical investigation of fly ash from the Main and Northern lignite fields in Ptolemais, Greece. *Fuel*, 71(4), 373-376.
- [7] Kostakis, G. (2009). Characterization of the fly ashes from the lignite burning power plants of northern Greece based on their quantitative mineralogical composition. *Journal of Hazardous Materials*, 166, 972-977.
- [8] Kantiranis, N., Filippidis, A. & Georgakopoulos, A. (2005). Investigation of the uptake ability of fly ashes produced after lignite combustion. *Journal of Environmental Management*, 76, 119-123.
- [9] Kantiranis, N., Stergiou, A., Filippidis, A., & Drakoulis, A. (2004). Calculation of the percentage of amorphous material using PXRD patterns. *Bulletin of the Geological Society of Greece*, 36, 446-453.
- [10] ASTM C 157/C 157M-08. Standard Test Method for Length Change of Hardened Hydraulic-Cement Mortar and Concrete.
- [11] ASTM C 311-07. Standard Test Methods for Sampling and Testing Fly Ash or Natural Pozzolans for Use in Portland-Cement Concrete.
- [12] Swaine, D.J. (1995). The contents and some related aspects of trace elements in coals. In: *Environmental aspects of trace elements in coal* (pp. 5-23). Springer, Dordrecht.
- [13] Fernández-Turiel, J.L., Georgakopoulos, A., Gimeno, D., Papastergios, G. & Kolovos, N. (2004). Ash Deposition in a Pulverized Coal-Fired Power Plant after High-Calcium Lignite Combustion. *Energy & Fuels*, 18, 1512-1518.
- [14] Adamidou, K., Kassoli-Fournaraki, A., Filippidis, A., Christanis, K., Amanatidou, E., Tsikritzis, L. & Patrikaki, O. (2007). Chemical investigation of lignite samples and their ashing products from Kardias lignite field of Ptolemais, Northern Greece. *Fuel*, 86, 2502-2508.
- [15] Koukouzas, N., Ward, C.R., & Li, Z. (2010). Mineralogy of lignites and associated strata in the Mavropigi field of the Ptolemais Basin, northern Greece. *International Journal of Coal Geology*, 81, 182-190.

- [16] Li, F.H., Ma, X.W., Guo, Q.Q., Fan, H.L., Xu, M.L., Liu, Q.H., & Fang, Y.T. (2016). Investigation on the ash adhesion and deposition behaviors of low-rank coal. *Fuel Processing Technology*, 152, 124-131.
- [17] Valentim, B., Flores, D., Guedes, A., Shreya, N., Paul, B. & Ward, C.R. (2016). Notes on the occurrence of char plerospheres in fly ashes derived from Bokaro and Jharia coals (Jharkhand, India) and the influence of the combustion conditions on their genesis. *International Journal of Coal Geology*, 158, 29-43.
- [18] Fuller, A., Maier, J., Karampinis, E., Kalivodova, J., Grammelis, P., Kakaras, E. & Scheffknecht, G. (2018). Fly Ash Formation and Characteristics from (co-) Combustion of an Herbaceous Biomass and a Greek Lignite (Low-Rank Coal) in a Pulverized Fuel Pilot-Scale Test Facility. *Energies*, 11, 1-38.
- [19] Chousidis, A., Rakanta, E., Ioannou, I. & Batis, G. (2015). Mechanical properties and durability performance of reinforced concrete containing fly ash. *Construction and Building Materials*, 101, 810-817.
- [20] Skodras, G., Karangelos, D., Anagnostakis, M., Hinis, E., Grammelis, P. & Kakaras, E. (2005). Coal fly ash utilization in Greece. In: *Int. Ash Utilization Symposia and the World F Coal Ash Conference*. April 11-15, Lexington, Kentucky, USA.
- [21] Itskos, G.S., Itskos, S. & Koukouzas, N. (2009). The effect of the particle size differentiation of lignite fly ash on cement industry applications. In: *World of Coal Ash Conference (WOCA) Proceedings*.
- [22] Smith, R.D. (1980). The trace element chemistry of coal during combustion and the emissions from coal-fired plants. *Progress in Energy and Combustion Science*, 6 (1), 53-119.
- [23] Kutchko, B.C & Kim, A.G. (2006) Fly ash characterization by SEM-EDS. *Fuel*, 85, 2537-2544.
- [24] Hower, J.C., Groppo, J.C., Graham, U.M., Ward, C.R., Kostova, I.J., Maroto-Valerd, M.M. & Dai, S. (2017). Coal-derived unburned carbons in fly ash: A review. *International Journal of Coal Geology*, 179, 11-27.
- [25] Filippidis, A., Georgakopoulos, A., & Kassoli-Fournaraki, A. (1996). Mineralogical components of some thermally decomposed lignite and lignite ash from the Ptolemais basin, Greece. *International Journal of Coal Geology*, 30, 303-314.
- [26] Megalovasilis, P., Papastergios, G. & Filippidis, A. (2016). Mineralogy, geochemistry, and leachability of ashes produced after lignite combustion in Amyntaio Power Station, northern Greece. *Energy Sources, Part A: Recovery, Utilization and Environmental Effects*, 30(10), 1385-1392.
- [27] Georgakopoulos, A., Filippidis, A. & Kassoli-Fournaraki, A. (2002). Leachability of major and trace elements of fly ash from Ptolemais Power Station, Northern Greece. *Energy Sources*, 24, 103-113
- [28] Georgakopoulos, A., Filippidis, A. & Kassoli-Fournaraki, A. (1994). Morphology and trace element contents of the fly ash from main and Northern lignite fields, Ptolemais, Greece. *Fuel*, 73(11), 1802-1804.

- [29] Filippidis, A., Georgakopoulos, A., Kassoli-Fournaraki, A., Misaelides, P., Yiakkoupis, P. & Broussoulis, J. (1996). Trace element contents in composited samples of three lignite seams from the central part of the Drama lignite deposit, Macedonia, Greece. *International Journal of Coal Geology*, 29, 219-234.
- [30] Megalovasilis, P., Papastergios, G. & Filippidis, A. (2013). Behavior study of trace elements in pulverized lignite, bottom ash, and fly ash of Amyntaio power station, Greece. *Environmental Monitoring and Assessment*, 185(7), 6071-6076.
- [31] Zeng, Q. & Li, K. (2015). Reaction and microstructure of cement – fly – ash system. *Materials and Structures*, 48(6), 1703-1716.
- [32] Zunino, F., Bentz, D.P. & Castro, J. (2018). Reducing setting time of blended cement paste containing high-SO₃ fly ash (HSFA) using chemical/physical accelerators and by fly ash prewashing. *Cement and Concrete Composites*, 90, 14-26.
- [33] Antiohos, S.K., Maganari, K. & Tsimas, S. (2005). Evaluation of blends of high and low calcium fly ashes for use as supplementary cementing materials. *Cement & Concrete Composites*, 27(3), 349-356.
- [34] Antiohos, S.K., Maganari, K. & Tsimas, S. (2005). Investigating the role of reactive silica in the hydration mechanisms of high-calcium fly ash/cement systems. *Cement & Concrete Composites*, 27(2), 171-181.
- [35] Ramasubramania, I. (2002). The surface chemistry of leaching coal fly ash. *Journal of Hazardous Materials*, 93, 321–329.
- [36] Antiohos, S.K. & Tsimas, S. (2006). A novel way to upgrade the coarse part of a high calcium fly ash for reuse into cement systems. *Waste Management*, 27(5), 675-683.
- [37] Iordanidis, A. & Georgakopoulos, A. (2003). Pliocene lignites from Apofysis mine, Amynteo basin, Northwestern Greece: petrographical characteristics and depositional environment. *International Journal of Coal Geology*, 54, 57-68.
- [38] Kolovos, N. (2002). The effects on the mined lignite quality characteristics by the intercalated thin layers of carbonates in Ptolemais mines, Northern Greece. *Energy Sources*, 24, 761-772.
- [39] Kolovos, N., Georgakopoulos, A., Filippidis, A. & Kavouridis, C. (2002). Utilization of lignite reserves and simultaneous improvement of dust emissions and operation efficiency of a power plant by controlling the calcium (total and free) content of the fed lignite. Application on the Agios Dimitrios Power Plant, Ptolemais, Greece. *Energy & Fuels*, 16, 1516-1522.
- [40] Konidaris, D.N. (2012). Natural desulfurization in coal-fired units using Greek Lignite. *Journal of the Air & Waste Management Association*, 60(10), 1269-1273.

Open Pit Mine 3D Geological face mapping perspectives obtained by a fully automated, terrain following, rotary-wing UAVs mission

Ioannis Karnaris and Nestor Kolovos

Public Power Corporation S.A, Western Macedonian Lignite Center, Greece

ABSTRACT

Geological face mapping is perhaps the most significant method of mining benches imaging, as it maps out the stratigraphy, the existing geological structures and helps understand the geology of the mine in order to efficiently plan the exploitation of the deposits. This paper presents how new perspectives are being created in open pit mining with the use of a small commercial rotary-wing UAV performing geological face mapping in a fully automated terrain following mission.

Keywords: open pit mine; UAV; geological face mapping; rotary-wing; automated terrain following mission.

1. INTRODUCTION

Greece is the fifth largest lignite producer within the European Community. The exploitable lignite reserves in the Florina–Ptolemais-Kozani tectonic basin come up to 1,7 billion tons, representing 2/3 of the total lignite reserves of Greece. Western Macedonian Lignite Center produces today about 30 million tons of lignite annually to feed 4 thermal power plants, with 17 lignite thermal units and with a total installed capacity of 3775 MW. This intensive exploitation of lignite requires the excavation of about 150 million m³ (bank material) of overburden and interbedded sediments per year. Lignite is produced in 4 big mines, with the Southern Field Mine being the biggest lignite mine in the Balkan peninsula, feeding the Agios Dimitrios Power Plant since 1983. Its annual lignite production ranges between 14-21 million tons and total excavations ranging between 80x10⁶ - 90x10⁶ m³ (bulk).

The Kozani-Ptolemais basin has been formed by NW-SE and NE-SW tectonic forces by the end of Mesozoic. It belongs to a larger basin located at the Northwestern part of Greece. The sediments of the Ptolemais basin overlay both Paleozoic metamorphic rocks and Mesozoic crystalline limestones (Figure 1).

The Neogene-Quaternary sediments of the basin are divided into 3 lithostratigraphic formations. The lowest (Upper Miocene to Lower Pliocene) consists of basal conglomerates, passing upward to marly sand, clay, and lignite (partly xylitic) layers. The Pliocene middle formation contains intensively exploited lignite beds alternating with clays, marls, and sands. The Quaternary upper formation consists of terrestrial and fluvio-terrestrial conglomerates, lateral fans, and alluvial deposits. In the opencast Southern Field Mine, the lignite deposit is characterized as a "zebra" type or multiseam lignite deposit. The mean thickness of the overburden is 80 m, while the thickness of the total coal strata is also 80m

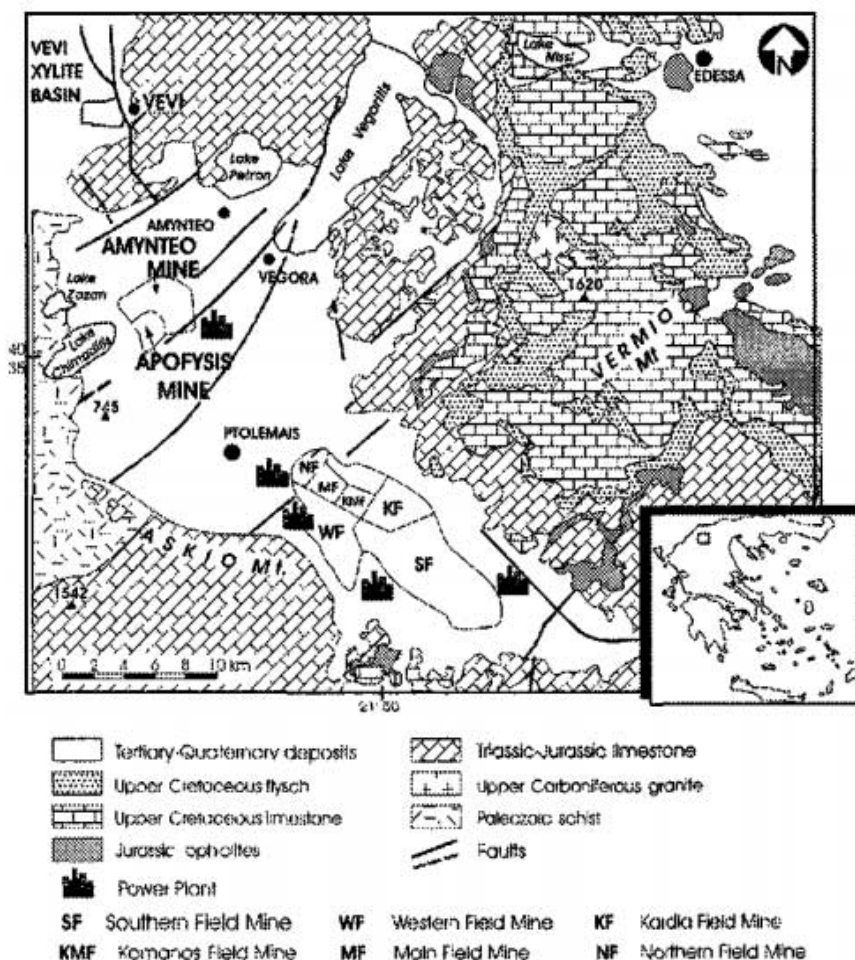


Figure 1. Simplified geological map of the Ptolemais basin, showing the Southern Field lignite mine.

Multiple interchanges of lignite and thin intercalated sterile layers of marly limestones, carbonaceous marls, clays, and sands characterize the Southern Field lignite deposit. The mean thickness of the overburden is 80 m, while the thickness of the total coal strata is also 80m. Multiple interchanges of lignite and thin intercalated sterile layers of marly limestones, carbonaceous marls, clays, and sands characterize the Southern Field lignite deposit. This form of deposit requires selective excavation of both lignite and thin sterile layers in separate blocks. The net calorific value of the lignite ranges between $1100 \text{ kcal kg}^{-1}$ and $1800 \text{ kcal kg}^{-1}$ having a mean value of $1465 \text{ kcal kg}^{-1}$. In “zebra” type deposits, the knowledge of the geometry and the quality characteristics of both the lignite and the sterile intercalated layers are of the utmost importance in designing the optimum lignite recovery of lignite reserves.

The application of selective excavation requires the determination of recoverable lignite layers or lignite blocks fulfilling specific technical and quality criteria. [1] For lignite quality optimization and helping the bucket wheel operators overcome lignite recovery difficulties, traditional geological face mapping has been used, paying special attention to the stratigraphy and the geological structure of the lignite deposit. In addition to the stratigraphy, areas of hard formations are also indicated as well as the way of their excavation, blasting, ripping, shoveling or bucket wheel excavating. In lignite face mapping attention is given to the naming and numbering of lignite layers, the quality of the lignite layers, the geometrical characteristics and the area where lignite is to be delivered after its excavation, either the mine bunker or the power plant yard. Areas of particular interest, such as faulting zones, water appearance and areas of potential instability are also indicated.

The face mapping plans are delivered to the relevant mine staff such as the field engineers, the foremen, the mine control room and the operators of the bucket wheel excavators. (Figures 2, 3 and 4).

However, traditional face mapping is –firstly- not accurate, while cost defective and time consuming. Due to the big heights of the benches -which vary between 22–28m in height- and the steep slopes, traditional face mapping contains a high degree of inaccuracies and danger due to accessibility problems.

Digital photography face mapping (Figure 4) is less costly because it's less time consuming. Still it covers only a small area on the mine bench, in each photo, of about 60m and has no coordinates so there is no real accuracy over the excavated areas. Besides, frequently, a photo only manages to capture part of the bench due to random stockpiles in front of it. The procedure is simple; in 60m length segments of the conveyor belt, from beginning to the end, a photo is taken and a photo leaflet is made -and distributed- for each lignite bench which forms the excavation guide of the next 3 months to come. It cannot give the entire picture of the bench, but a puzzle of it. However, it helped to improve the excavated lignite quality and the communication between mines' technicians and engineers.

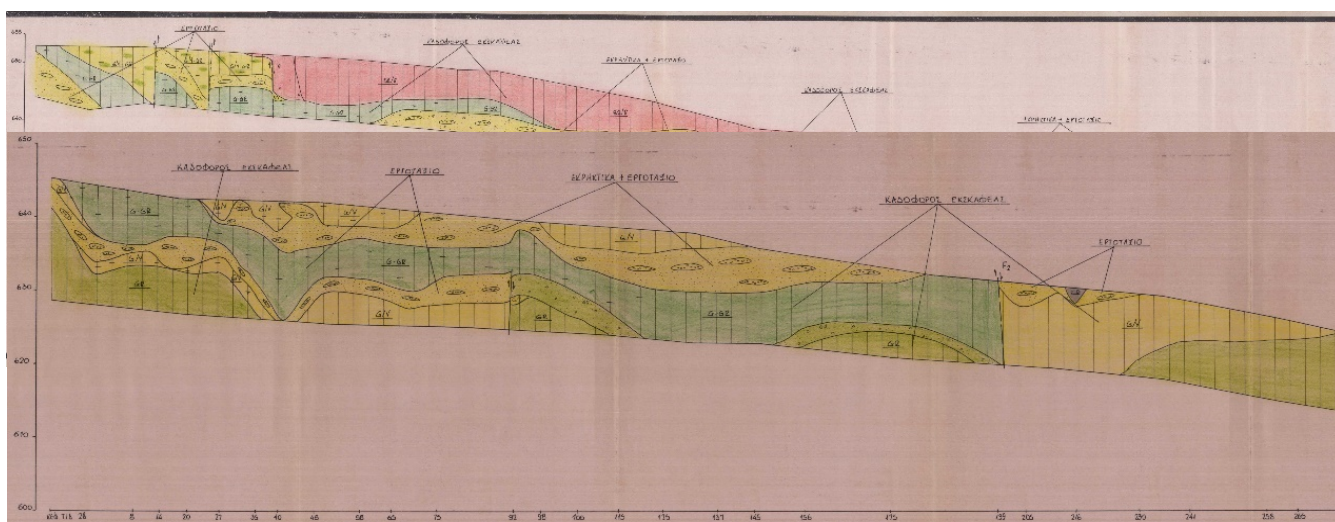


Figure 2. Traditional face mapping of overburden benches

A 3D model could improve the overall face mapping, offering more advantages to the face mapping, mine works and mine results. In order to eliminate the aforementioned problems, moving forward can be achieved by using modern photogrammetry techniques. Civil Unmanned Aerial Vehicle (UAV) technology has become commercially available at a very reasonable price for a number of diverse applications [Asgan Riza Nasrullah, 2016].

UAVs have a variety of features suitable for face mapping in the field such as maneuverability, stability, user-friendliness and customization, small size and weight, high -performance camera. They can be autonomously programmed to complete repetitive yet precise missions, and also have the capability to enter unsafe environments while not constrained by a pilot's physical limits [Asgan Riza Nasrullah, 2016]. This paper presents how through a small commercial rotary wing UAVs' fully automated and terrain following mission a 3D geological mapping of the slopes of mines can be obtained. At the same time, it presents new perspectives in geology that are being created in open pit mining and each one will be further analyzed in upcoming papers

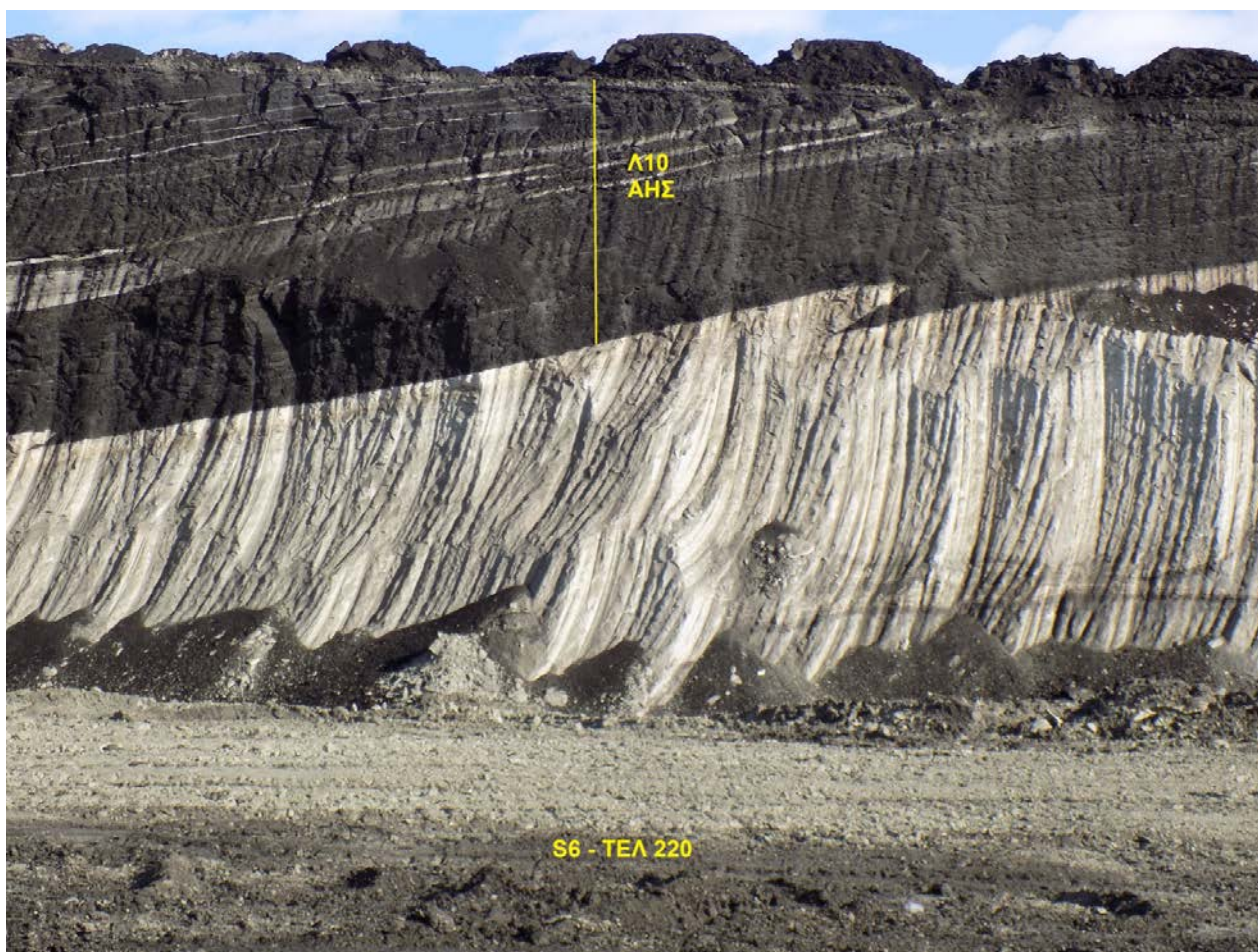
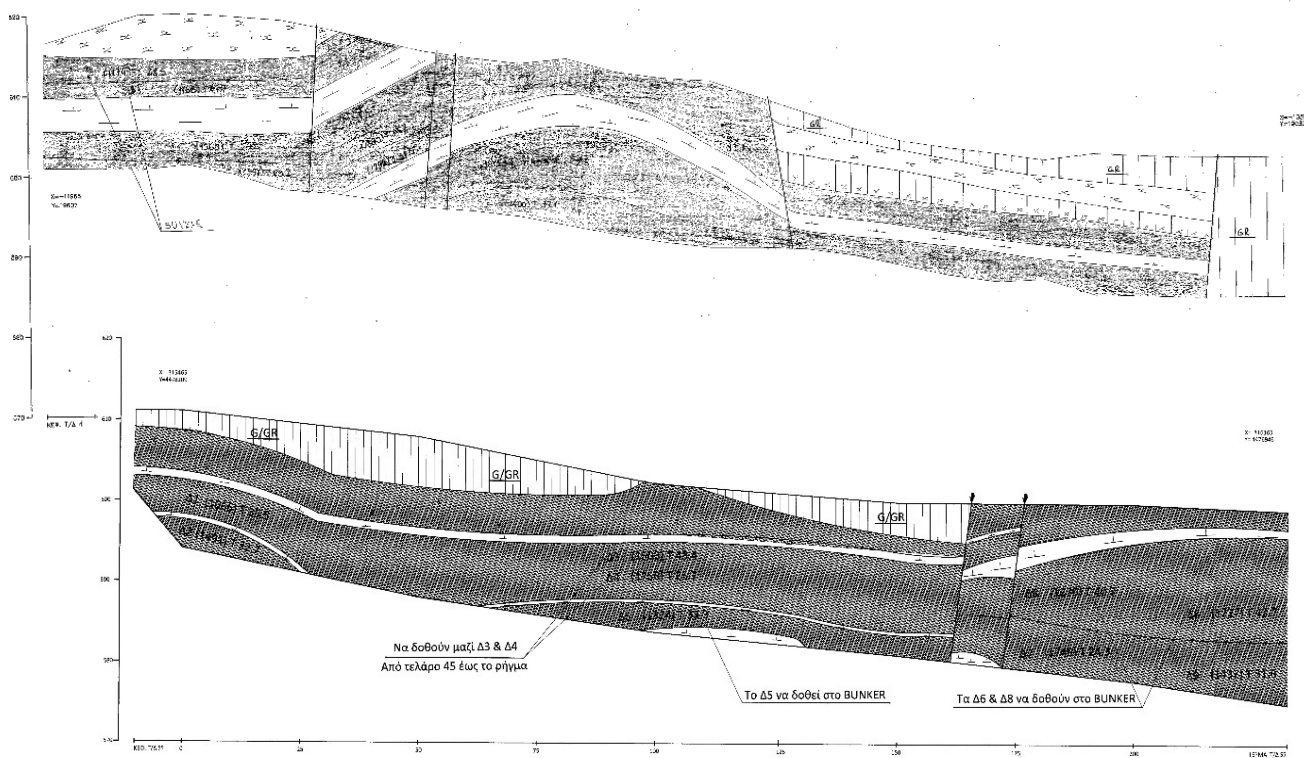


Figure 4. Today's face mapping of lignite benches using digital photography

2. MATERIALS AND METHODS

2.1. Defining parameters and prerequisites of the new methodology

At the end of each calendar month, the earthworks conducted within the mines' site are being surveyed mostly for;

- Calculation of the overall productivity of the mine and
- Updating of the mines studies

For the past two years, PPCs' [2] Western Macedonia Lignite Centre (WMLC) surveying teams have been using fixed wing RTK UAVs for surveying and mapping of the mines replacing traditional surveying equipment such as RTK GNSS receivers and total stations. A typical monthly flight of a mine consists of a two hour preflight preparation & flight mission and up to 5 hours of processing time depending on the PC(s) used. The end product is a point cloud followed by its Orthomosaic and Digital Surface Model (DSM) [3] with an accuracy achieved - horizontally and vertically- of 10-30cm.

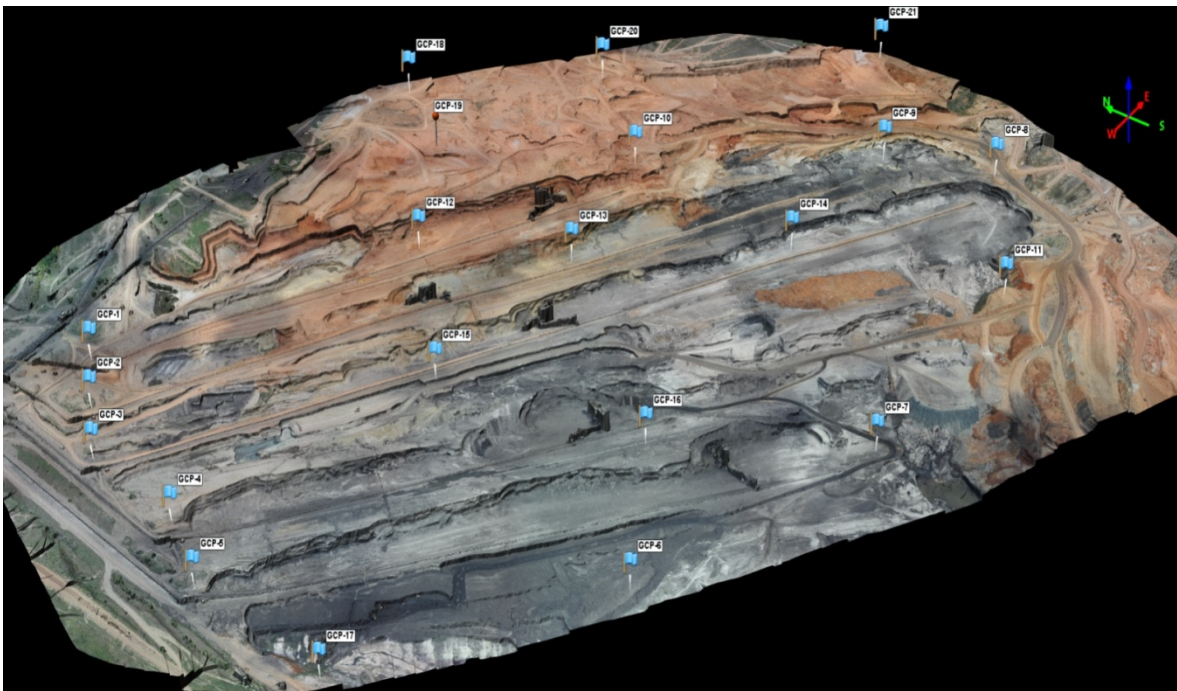


Figure 5. Typical WMLC open pit mine Orthomosaic and Digital Surface Model with verification points (blue flags) created by a fixed wing RTK UAV flight

A rotary wing UAV was chosen, a DJI Phantom 4 Pro [4] for the 3D geological face mapping because;

- fixed wing UAVs only take nadir photos so point clouds would have big blank spots.
- due to the mines' topography, it is impossible to fly below a certain height so as to capture the faces of the benches in nadir photos and even if achievable it would require lots of flight hours (one flight per mine bench). Regarding maintenance costs, an hour of a commercial quad-copter is cheaper than that of a fixed wing.
- laser scanner couldn't be the solution because it would be time consuming and cost defective; the existence of stockpiles or regional landslides in front of many mines toes, would block the scanning view so it would require too many different stations in order to complete one mines' scanning. Also, dust and haze are often an issue.
- The takeoff and landing of the quad-copter is fully automated.

2.2. Workflow basic steps

The basic steps of the workflow are;

- *Creating Crest / Toe 3D Breaklines of the mines' benches*

By using the derivatives of the monthly UAV RTK flight, the Crest / Toe 3D Breaklines of an entire mine can be automatically created with the appropriate software (i.e. Virtual Surveyor®[5], 3DReshaper®[6]) within a few minutes

- *Creating the flight path*

With the desideratum being capturing at all time the entire bench (crest to toe) with the lowest possible Ground Sample Distance [7] (GSD, the distance -in a digital photo of the ground from air- between 2 consecutive pixel centres measured on the ground) in a constant elevation difference above ground without crashing the UAV to the Bucket Wheel Excavator (BWE)[8], appropriate

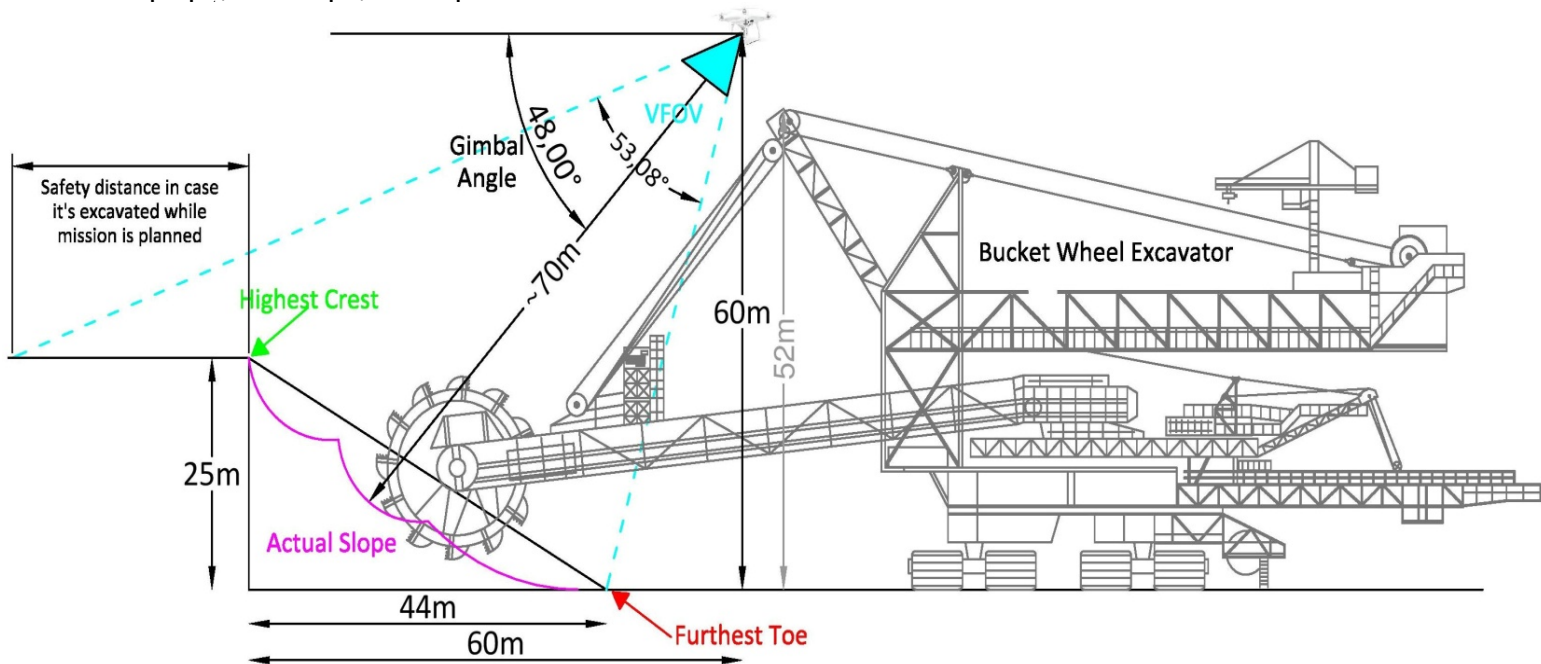


Figure 6. Flight Height, Mines Bench, P4P & Bucket Wheel Excavator

- *Litchi [9]App Workflow*

Deciding Overlap and calculating cruising speed and time intervals between 2 captures; in the methodology used, with a flight speed of 3.5m/sec and a 90% side overlap (given the fact that P4P will be moving sideways so as to capture the benches) the drone can capture an average PPCs mine bench of 2.5km length within one P4P battery's capacity.

- *Fieldwork*

Prior to flight, DJI P4Ps camera must be adjusted with the appropriate Focus, ISO, Aperture, Shutter Speed, and White Balance Settings. Notably, a high aperture f-stop number and a fast shutter speed will generally contribute in the photogrammetry software algorithm performing more efficiently, during the matching of the photos.

- *Officework - Point Cloud and Orthomosaic / DSM generation*

The GSD achieved is **1.79cm/pix** which according to literature an error of 1-3 times the pixel size for a correctly reconstructed model, both horizontally and vertically is expected_[10]. This means that the achievable relative accuracy is within of 2 - 5.4cm. The absolute accuracy of a survey is

absolutely dependent of the accuracy of the Ground Control Points (GCP) measurement and cannot be higher than the GCPs' accuracy.



Figure 7. Dense cloud and images captured by P4P in Agisoft Photoscan Pro® [11]

2.3. 3D Geological face mapping perspectives

From a geological and mining point of view, 3D face mapping is of great assistance since it offers many advantages as:

- ✓ Full detailed 3D view of the sites' benches and a detailed view of the entire mine when combined with an fixed wing UAV mission
- ✓ High accuracy of the flight derivatives and in consequence of any measurement, within few centimeters both horizontally and vertically
- ✓ A high level of safety is achieved given that the entire flight is fully automated
- ✓ Better communication within the mines' staff and management
- ✓ Time, labour and cost savings

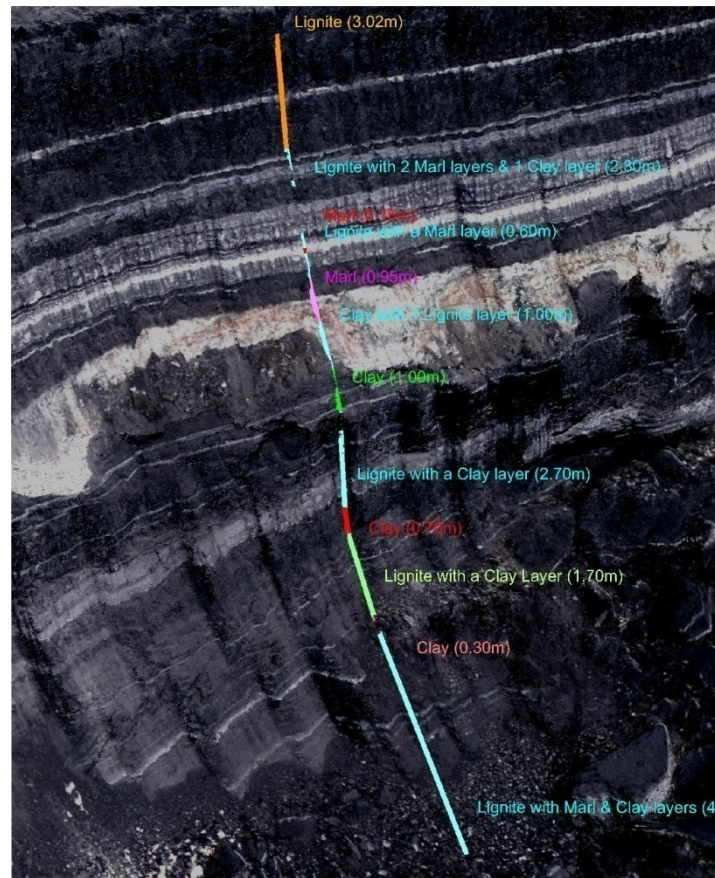


Figure 8. Comparison of the original drillholes stratigraphy translated into vectors and the actual bench

Furthermore, new perspectives have emerged regarding 3D face mapping:

➤ **Re-evaluate drillhole data.**

Many drillholes were conducted decades ago with lesser technology. It is now feasible to re-evaluate them and compare –and correct if needed- the drilling data evaluation. In Figure 8, a 30 year old drillholes' data (N^o 142-288) were translated into vectors and can now be compared with the actual visible stratigraphy of the bench S6 of the WMLC South Field Mine. The specific original drillhole was 2m away horizontally from the benches current crest so it is safe to compare the past data recorded in the drillhole and the benches stratigraphy. For example, it is clear that the first layer of 3.02m pure lignite recorded in the drillhole, omitted a 20cm marl layer in its original evaluation.

➤ **Correlate drilling data with open slope face layers and recalculate the mining model.**

The existing drillhole network of WMLC consists of drillholes that have a distance of about 200m between them. Apart from re-evaluating the drilling data, it is possible to create drilling data from the benches faces in order to densify the drillhole network. Along with sending the different layers for chemical analysis in order to be precise in the evaluation, the geological model can be dynamically rebuilt with enhanced precision by using the appropriate software (i.e. Carlson®^[12], Vulcan®^[13], Surpak®^[14], Surfer®^[15] etc)

➤ **Apply Machine Controlling software in the Bucket Wheel Excavators' operation.**

The WMLC has zebra type deposits so it was, until now, almost impossible to predict what lies ahead within a few meters. However, along with the correlation of the existing drilling data / benches 3D face mapping stratigraphy and the new geological block model that will be continuously built, machine controlling implementation will be possible due to the constant flow of data coming from the excavations correlated with the existing drillholes. The BWE operator won't have to decide what to excavate but simply follow the fill / cut indication on the controller which will result in better lignite quality and level ground surfaces.

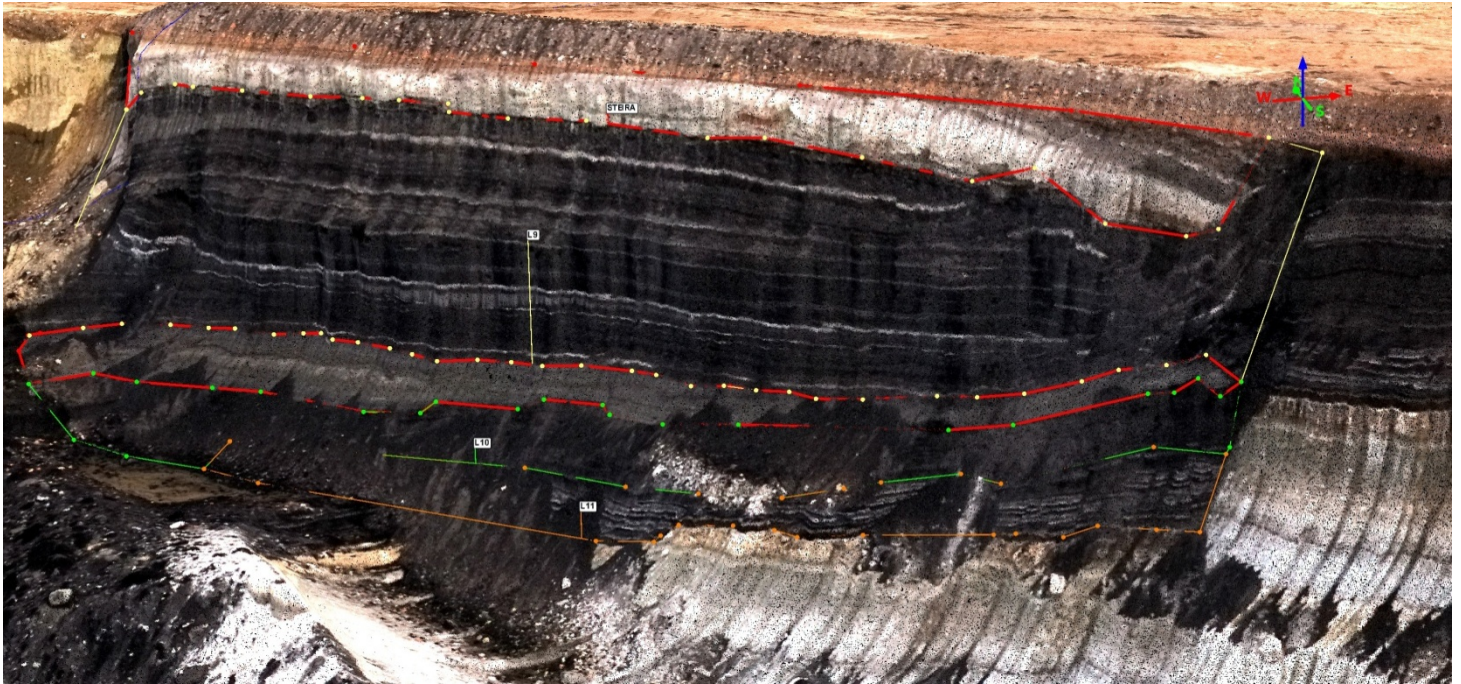


Figure 9. 3D Polygons of categorized geologic layers, ready to be excavated and transported appropriately. With Machine Controlling Software, there can be cm high precision in excavating

- **Watch, design and map water works as passages, channels, pit ponds and pump stations.**

3D face mapping can help in decision making even for water passages and channels, since all data can be combined and visualized within one software. In Figures 10 & 11, it is shown how a wrong spatial selection for the water passage can accelerate a regional landslide, especially when there's a fault in the area (Figure 11, red line)

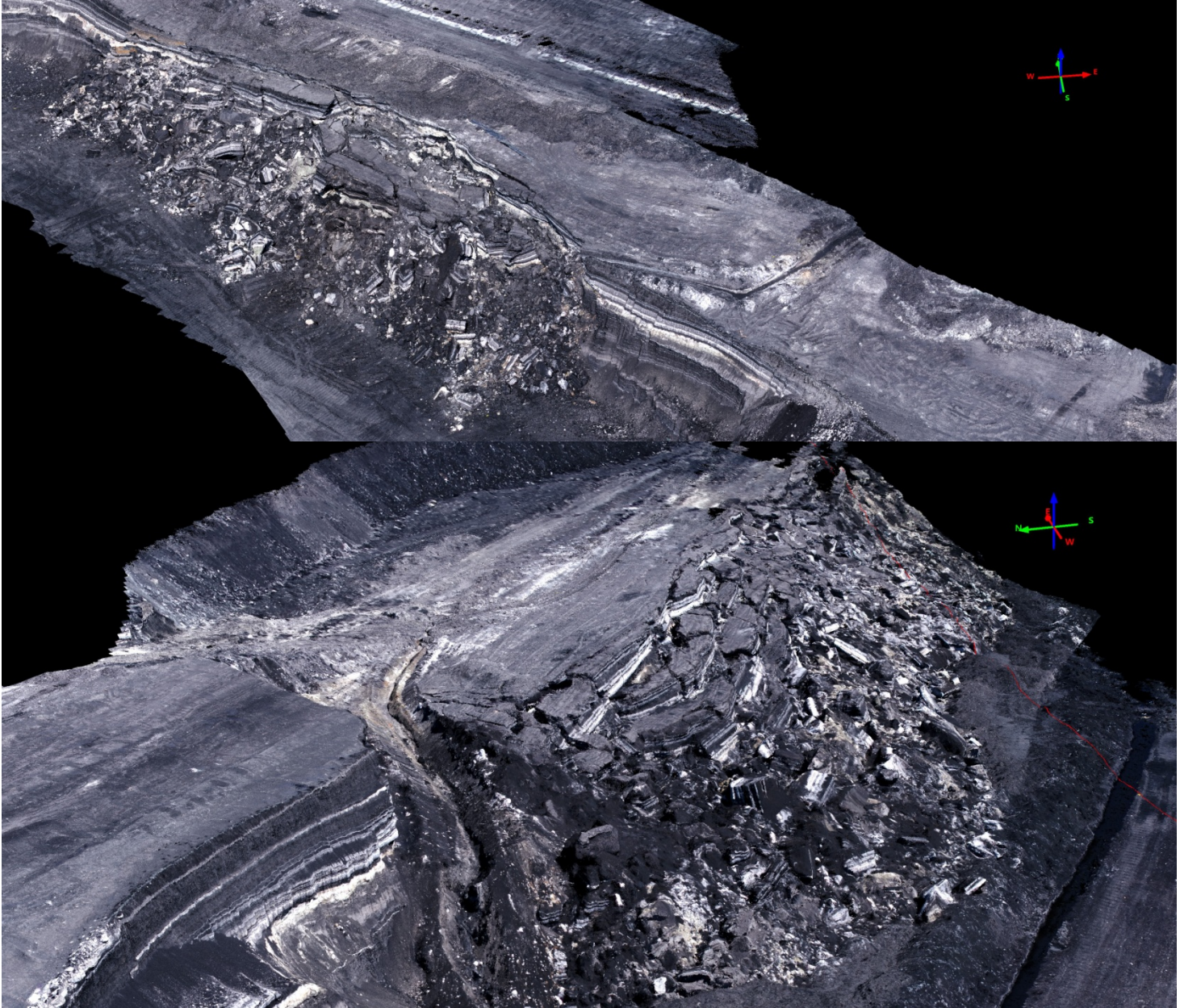


Figure 10 & 11. Regional landslides accelerated by water passages, presented in point clouds

- **Watch and map earth movements as deformations, displacements and local or overall slope failures.**

It is a lot easier, safer and more efficient to search for imminent slope failures by having a 3D bench in its entirety. In Figure 12, it is obvious that a small regional landslide will result in a bigger one according to the multiple cracks near the benches crest and the water pond created in the benches toe.

- **Determine, understand and map hard rock materials as conglomerates, sandstones and silts, which need drilling and blasting for loosening and breaking, and diesel machinery as dozers, rippers, shovels and trucks to be loaded and transported to the dump site.**

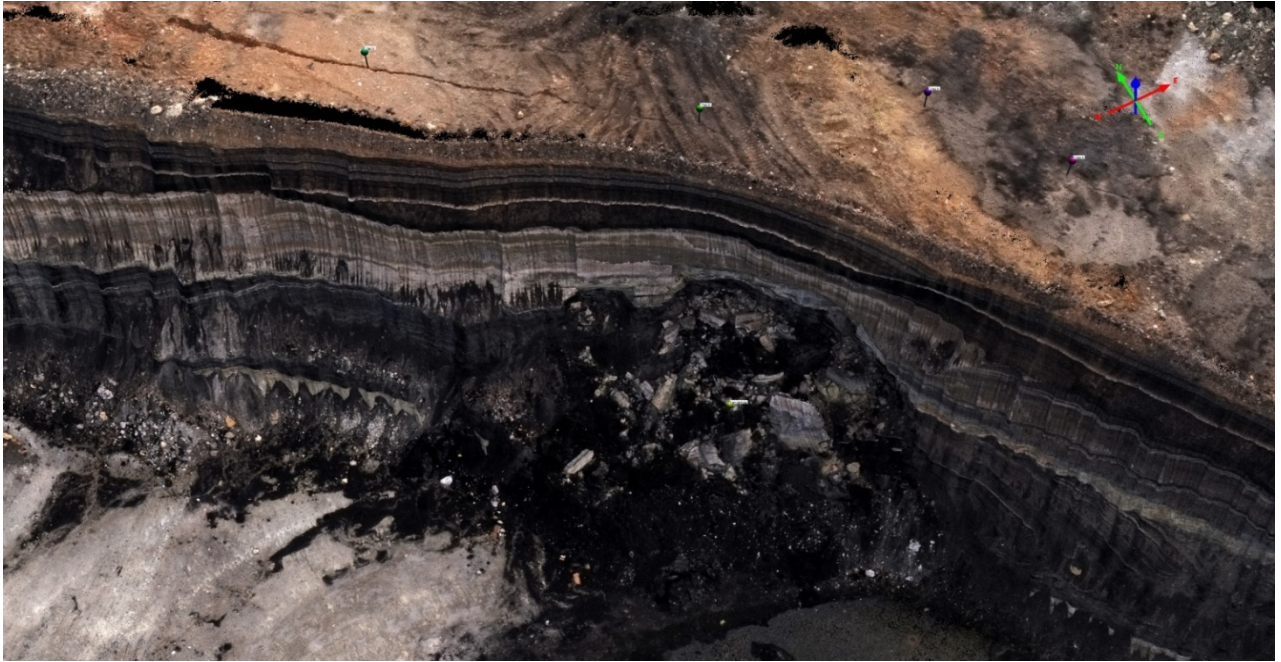


Figure 12. Regional landslide, shown in a point cloud in Quick Terrain Modeller®[16], which will result in a bigger one according to the cracks near the benches crest and the water pond on the benches toe

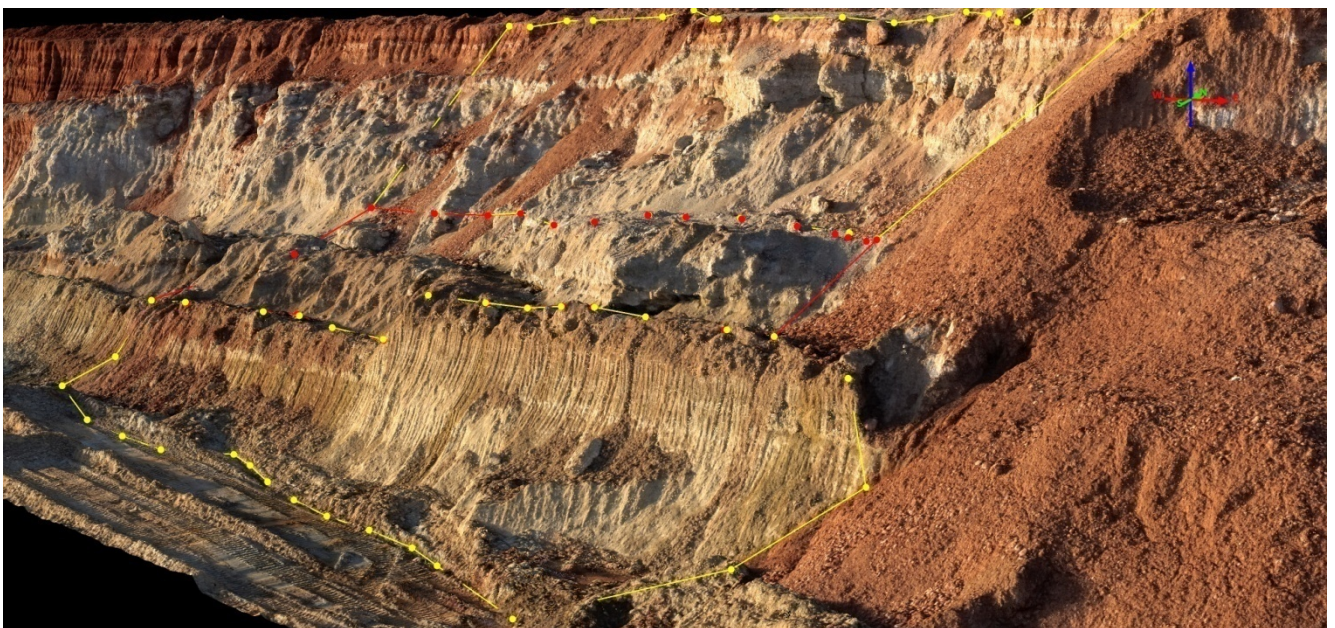


Figure 13. Hard and soft formations separation in Point Clouds; Soft for the Bucket Wheel Excavator and Hard for the diesel machinery of the mine after they have been drilled and blasted

➤ **Compare the excavating packages from the study with the executed ones.**

Often, there is a deviation from the theoretical excavating lignite packages that derived from the study, due to the different asking calorific value from the collaborating Power Plant. In Figure 14, in the final lignite layer, according to the evaluation of Drillhole N° 130-296, a 1m long layer of combined lignite with marl was added in order to obtain the wanted calorific value.

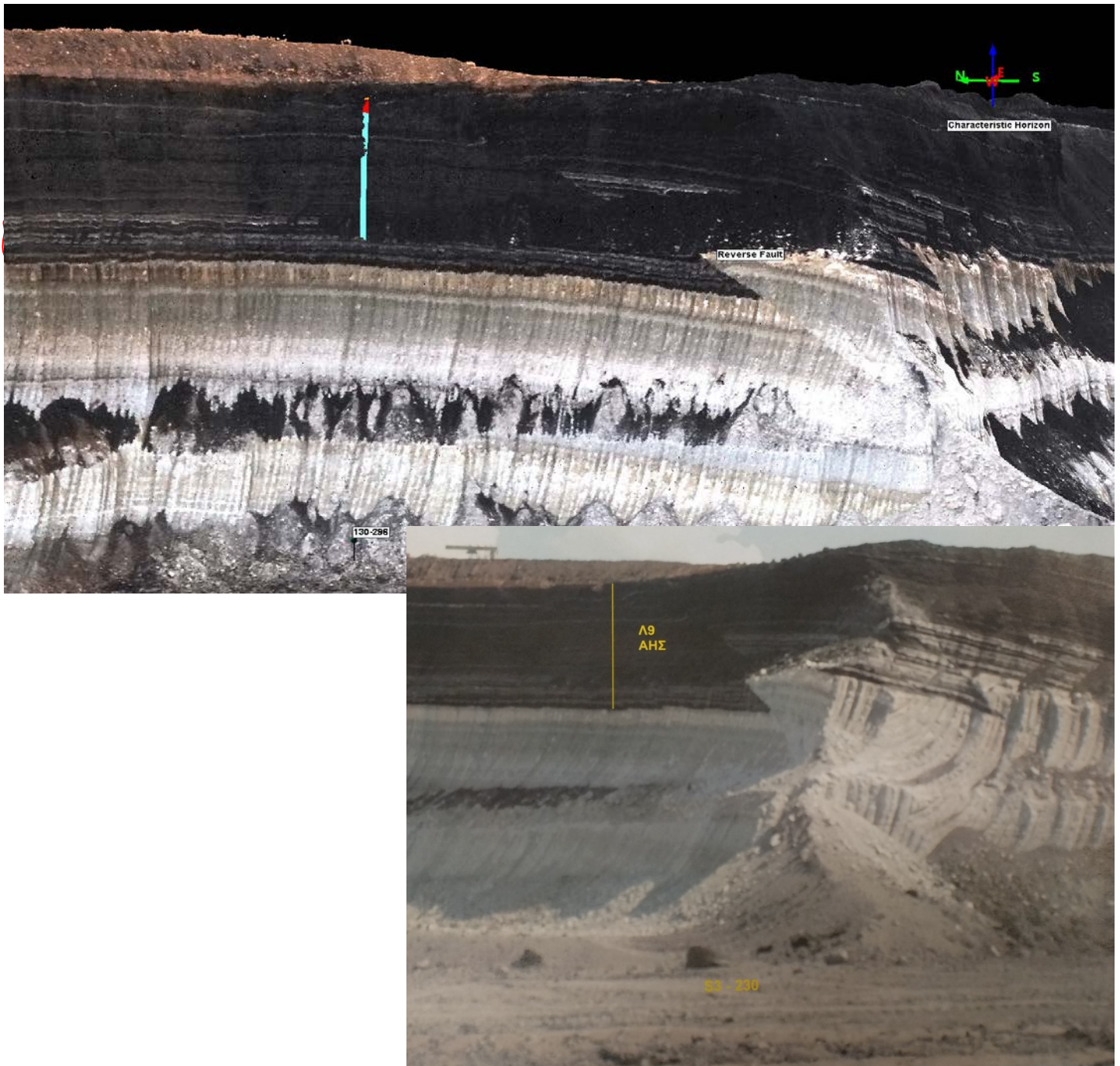


Figure 14. In the final lignite layer according to the study, a 1m long layer of combined lignite with marl was added in order to obtain the wanted calorific value from the Power Plant.

3. RESULTS AND DISCUSSION

In regards to the quad-copter UAV planning;

- The project, presented in this paper was actually the worst case scenario; Mission took place at a cloudy 07:30am morning, after rain showers and with the highest BWE as the base for the calculations. The flight height will drop at least 10m and GSD to 1.5cm/pix on the rest benches, raising the accuracy.
- A flight of all the mines' benches, even in high altitude must be preceded either with a fixed wing UAV or a rotary wing one, in order to obtain the crest and toe breaklines and the

planning of the mission to be feasible. This flight can be the monthly mine site one and the entire procedure for both (monthly fixed wing RTK flight and benches flights with their corresponding planning and GCPs placement and surveying) will take no more than 3 days. It could be possible -and yet to be researched- to use free Satellite Imagery i.e. EUs' Copernicus^[18] (Sentinel, 10m/pixel) as the source of the mines' crest and toes and in feasible and accurate, the RTK UAV flight will no longer be necessary. Currently, face mapping is conducted every 3 months which could now become once a month at no actual additional cost.

- Given the Vertical Field Of View ^[17] of the P4P, the benches flights can be postponed for some days due to bad weather, without any loss in the sought out data.
- By using an average PC, the point cloud created can be imported in a free *.las format viewing software (e.g Applied Imagery's Quick Terrain Reader), replacing digital photos in face mapping derived from geologists work. Head Managers, Mining Engineers, Technicians and -perhaps- most importantly BWE operators are few clicks away from any area of the mines site.
- The workflow can be improved, as some of the stages of the planning procedure can be automated with Python programming.

In regards to open pit mine geological 3D face mapping, it can;

- make the correlation of drilling data with open slope face layers and rebuild the mining model, possible and usable through machine controlling software leading in better lignite quality
- eliminate accessibility problems due to the big height and steepness of slope faces
- eliminate accessibility problems due to the flooding of mining floors and due to the presence of water channels crossing the mining roads
- lessen or even eliminate mine site hazards for surveying teams and geologists
- provide accurate 3D info of the entire mines stratigraphy and the various geologic layers as well as the mines' slopes and their geometrical characteristics (Figure 15)

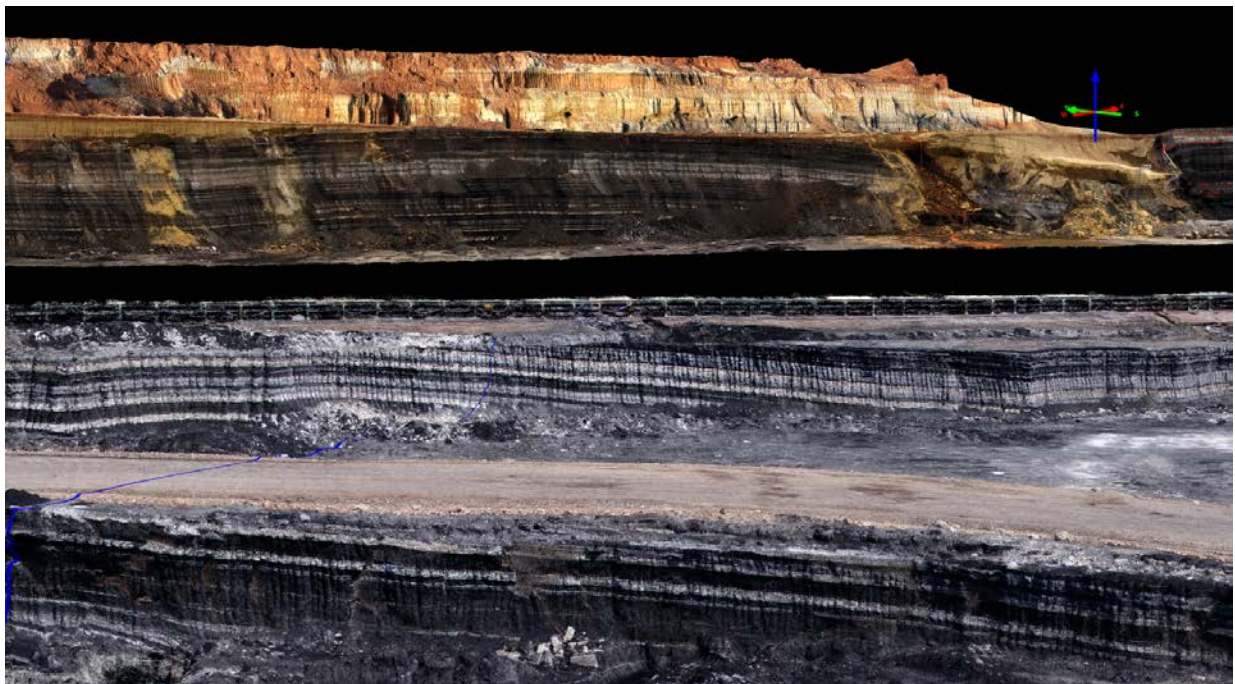


Figure 15. Point Cloud of the slopes S2, S3 & S4 (top to bottom) of WMLC South Field Mine. The blue line depicts a fault of the mine

- help mining staff understand, design, watch and map the water aquifers and the water flow on slopes as well as water works as passages, channels, pit ponds and pump stations.
- help mining staff understand the geological boundaries, i.e. top soil, overburden, soft layers, hard layers, ore deposit, underburden, ore deposit roof, ore deposit bottom, characteristic horizons and intermediate steriles
- help in determining, understanding and mapping of earth movements as deformations, displacements, local or overall slope failures as well as structural elements as folds, faults and discontinuities with their characteristics.
- provide -a few cm high accurate- 3D information about soft materials as clays, sands, gravels, marls and lignite which can be excavated by bucket wheel excavators, transported by conveyor belts and dumped by stackers as well as hard rock materials as conglomerates, sandstones and silts, which need drilling and blasting for loosening and breaking, and diesel equipment as dozers, rippers, shovels and trucks to be loaded and transported to the dump site

4. CONCLUSIONS

Given the fact that face mapping of lignite mine benches still remains the most valuable tool for optimum lignite excavation, a fully automated terrain following rotary wing UAV flight can really level up the data acquired at no additional cost. Many scientific fields regarding open pit 3D face mapping with rotary wing automated flights are yet to be further researched such as the use of Copernicus Satellite Imagery instead of a RTK UAV flight, the correlation of the existing drilling data with data derived from the faces of the slopes, machine control implementation in regards to lignite deposit 3D polygons, Python programming implementation in the mission planning procedure etc.

Potential Conflicts of Interest

The authors declare no conflict of interest.

Acknowledgments

The authors thank the anonymous reviewers for their advices and suggestions.

REFERENCES

Journals;

KolovosN., A. Georgakopoulos, A. Filippidis, C. Kavouridis, 2002a. Environmental effects of lignite and intermediate steriles co-excavation in the Southern Field Mine of Ptolemais, Northern Greece. *Energy Sources*, 24 (6) 561-573.

KolovosN., A. Georgakopoulos, A. Filippidis, C. Kavouridis, 2002b. The effects of the mined lignite quality characteristics by the intercalated thin layers of carbonates in Ptolemais mines, Northern Greece. *Energy Sources*, 24 (8) 347-352.

Kolovos N., D. Sotiropoulos, A. Georgakopoulos 2003. Evaluating the loss of “geological” lignite in “zebra” type deposits. *Proceedings, 18th International Mining Congress & Exhibition of Turkey, IMCET 2003, June 10-13, 2003, Antalya, 49-54.*

Asgan Riza Nasrullah, (2016), Systematic Analysis of Unmanned Aerial Vehicle (UAV) Derived Product Quality, MSc Thesis, Faculty of Geo-Information Science and Earth Observation, Twente

University Product Quality, MSc Thesis, Faculty of Geo-Information Science and Earth Observation, Twente University

Webpages;

- [1] http://greeklignite.blogspot.gr/2014/04/blog-post_16.html. To dispel two myths that are called against the lignite (last access 06/2018)
- [2] <https://www.dei.gr> (last access 06/2018)
- [3] <https://gisgeography.com/dem-dsm-dtm-differences> (last access 05/2018)
- [4] <https://www.dji.com/phantom-4-pro/info#specs> (last access 05/2018)
- [5] <https://www.virtual-surveyor.com/productivity> (last access 05/2018)
- [6] <https://www.3dreshaper.com> (last access 07/2018)
- [7] https://en.wikipedia.org/wiki/Ground_sample_distance (last access 06/2018)
- [8] https://en.wikipedia.org/wiki/Bucket-wheel_excavator (last access 05/2018)
- [9] <https://flylitchi.com> (last access 06/2018)
- [10] <http://geoawesomeness.com/accurate-drone-survey-everything-need-know> (last access 05/2018)
- [11] <http://www.agisoft.com> (last access 08/2018)
- [12] <http://www.carlsonsw.com> (last access 06/2018)
- [13] <http://www.maptek.com> (last access 07/2018)
- [14] <http://www.3ds.com> (last access 07/2018)
- [15] <http://www.goldensoftware.com> (last access 07/2018)
- [16] <http://appliedimagery.com> (last access 08/2018)
- [17] <http://therandomlab.blogspot.com/2013/03/logitech-c920-and-c910-fields-of-view.html> (last access 05/2018)
- [18] <https://www.copernicus.eu> (last access 08/2018)

Investments in Geological Exploration and Affection on Mining Operating Cash Costs at Lignite Open Pits Kolubara (Lazarevac), Serbia

Bogoljub Vuckovic¹ and Bojan Dimitrijevic²

¹EPS, Kolubara Coal Mines, Division Project, Kolubarski trg 8, 11050 Lazarevac, Serbia

²Mining and Geology Faculty; Mining Dept., Belgrade University, Djusina 7, 11000 Belgrade, Serbia

ABSTRACT

This paper presents a brief overview of the spent funds on geological explorations in the past few decades of the Kolubara mining basin ^[1-9]. The results of the performed surveys are extremely important. They reflected in the following: 1.1B t lignite mined out. On four active surface mines, at the exploitation stage is more than 1B t of lignite. The next 1B t is in the phase of final geological exploration, design and investment in future mining technological processes. The last 1B t of useful mineral raw materials is still in the form of mineral resources. In addition, several hundred million tons of quartz sands of Pliocene and Quaternary gravel within the lignite deposits, for now, are still only in the form of mineral resources, and represent additional opportunities to increase total profits of open pits. This paper presents a summary of costs, natural and combined factors and indicators of realized geological exploration on selected lignite deposits in the Kolubara coal basin.

By the end of 2017, the total geology research costs barely reach 1.2 euros cent / tonne of lignite, which is extremely low and does not burden the costs of investments, expropriation, excavation-exploitation, processing and transshipment of coal. The commercial sales price of coal to thermal power plants is 1.74 €/ GJ (reference selling price) ^[12-14].

Key Words: geology, mining, exploration, exploitation, investment, operating cash cost

1. REGIONAL SETTINGS OF KOLUBARA COAL BASIN

Kolubara Coal Mines (KCM) is part of Kolubara Coal Basin. It seat in western Serbia, 50 km southwest of Belgrade with 600-km² area. Kolubara Coal Basin represents a complex metamorphic, magmatic and sedimentary litho logical suite of Palaeozoic (Pz), Mesozoic (Mz) and Kenozoic (K) age (Figures 1, 2).

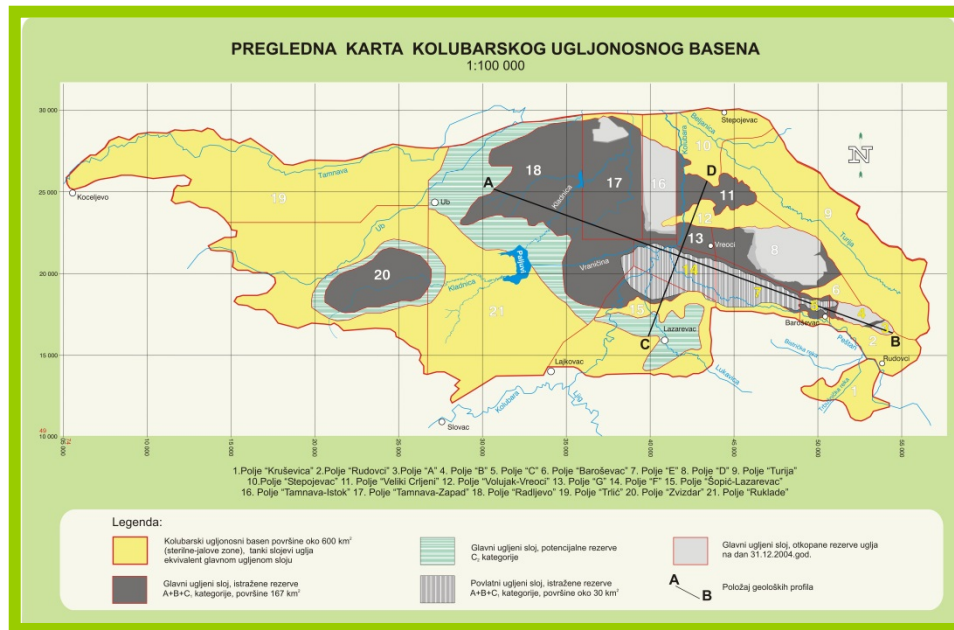


Figure 1. KCM Schematic draw with most productive and well explored ore fields; grey and black colour represent the most important deposits and open pits (after Stojakovic at all 2004; after Vuckovic 2008)

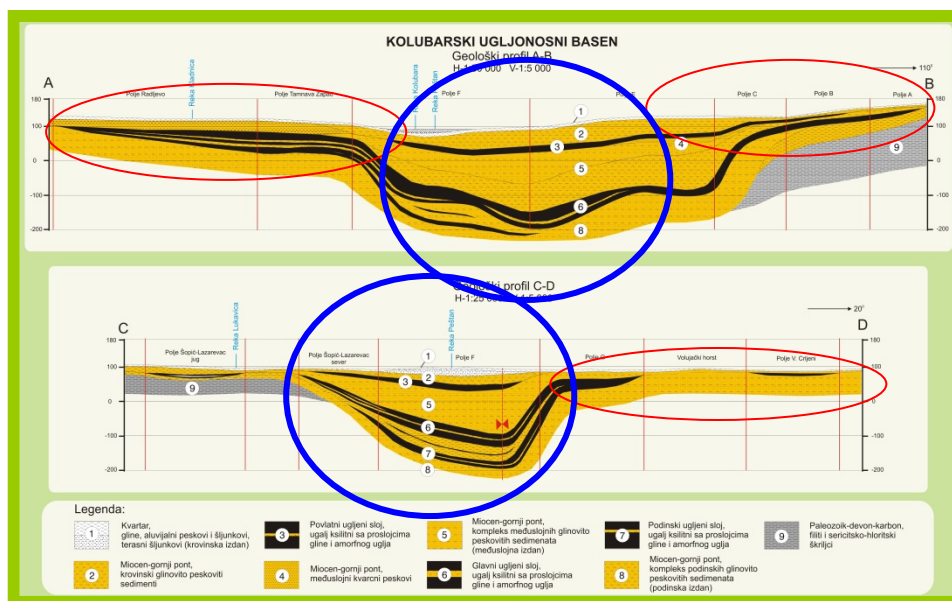


Figure 2. KCM vertical cross sections AB and CD; Legend : 9. Gray - Palaeozoic suite; 8, 5, 4, 2. Yellow – Miocene/Pliocene sedimentary sands, clays, gravels; 3.Black – Roof coal bed; 6, 7. Black – Floor (deep-seated, in economic view main) coal beds; 1. Light grey - Quaternary sands, gravels, clays; Red ellipsoid – pass mining exploitation; Blue circles – mining operations in next 50 years; (after Stojakovic at all, 2004; after Vuckovic 2008)

2. KOLUBARA COAL MINES GEOLOGY SURVEY

At last 60 (and few more) years at KCM were performed a suite of representative modern geological explorations with economic geology works as principle [1-9]. Mentioned explorations were conducting by the KCM Geology Survey, which seat on active open pits and in enterprise headquarter in Lazarevac. By the way, as summary, we can talk of about 4B tons of lignite in numerous exploration/exploitation coalfields, with additional non-metallic resources. Three of important deposits were under open pit running and all of them reach its dead end. Deposits “ore

field A” at early 60^s and “Tamnava-East Field” at 2004 are examples. In addition, open pits “Veliki Crljeni” and “ore field B” mined out partially at 2015 [12-14]. All of four mentioned possess its own geological exploration data’s, but according to its dead-end, they are not a topic of this paper. The other deposits (better to say ore fields) are widespread all over Kolubara sedimentary basin with its own level of geological exploration stage. We have deposits that are under early phases of geological exploration, and from the other side well explored deposits that are under mining operations. The last ones define economy of the company [12-14]. The exploration results could report in a few aspects of view, in naturally and semi-economic parameters.

3. PRINCIPLE GEOLOGY DATA’S

3.1. Naturally Parameters of Geological Explorations [1-9]

Such as number of drill-holes, total meters of drilling, number of laboratory assays, the ore reserve stadium, ore reserve amounts, quality of ore and so on ... all of them will be briefly report in next few statements, diagrams and tables. As a first spot, it is the ore reserve quantities and exploration stadium. The parameters of selected deposits are show on diagrams 1-4. At least 75,000 m of additional core drilling had to perform in next few years.

For example, on these ten-selected coalfields, there are 3.700 drill holes with 330.000 m of core drilling. In addition, it was taken 17.000 samples for coal quality assaying and 10.000 additional for geotechnical and hydro geological surveys. Even 1,1B t is mined out, there still seat 3 billion tons of coal, or 1 m of drilling define 8,800 t of coal.

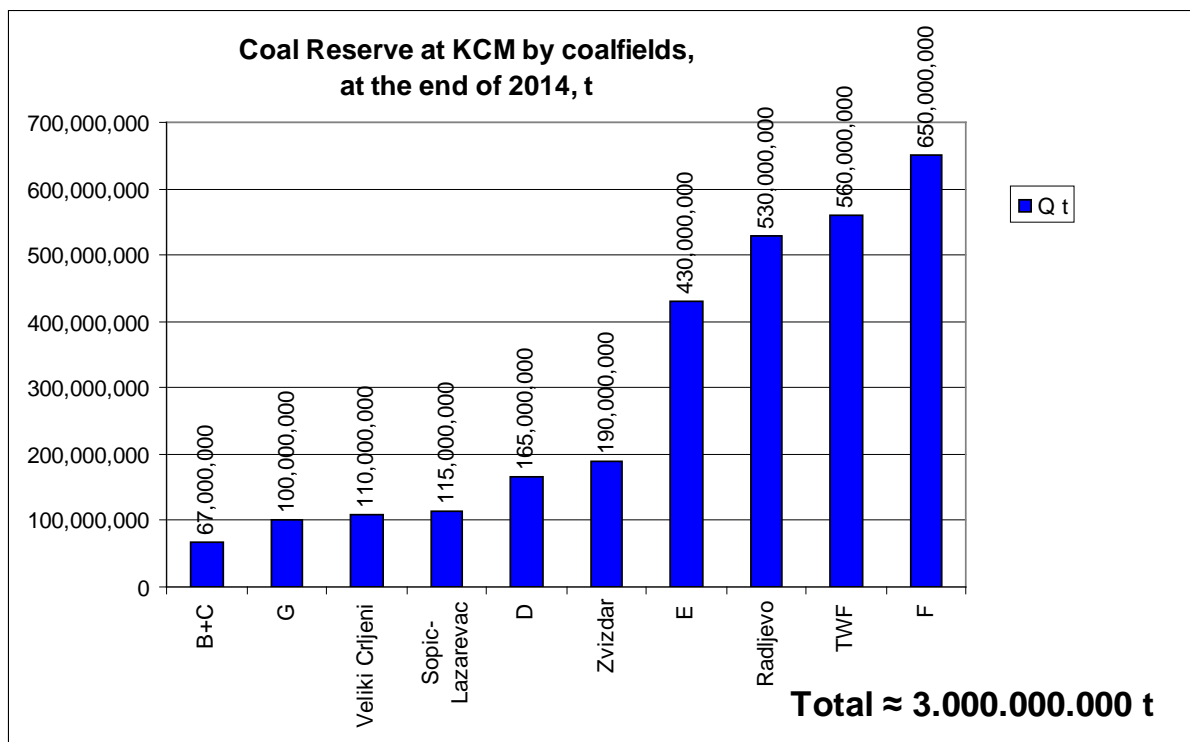


Diagram 1. Coal Reserve Quantities in Selected Ore Fields of KCM, (in metric tons); Note: green – under exploration phase, magenta – under open pit running; light blue – partially mined out (modified Vuckovic, Dimitrijevic at all, 2018)

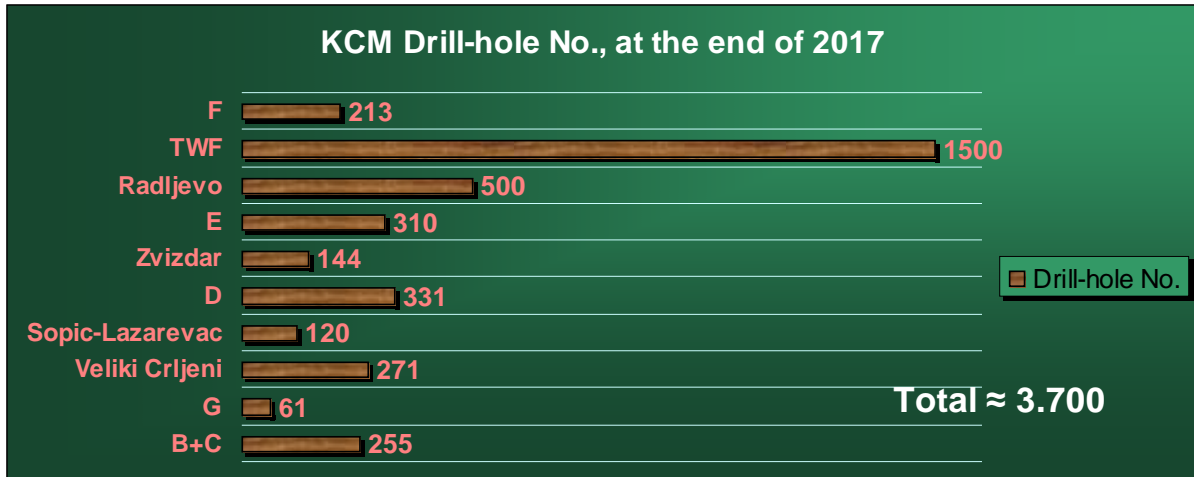


Diagram 2. Number of core drilling-holes on selected deposits in KCM; Note: blue – under open pit running (modified Vuckovic, Dimitrijevic at all, 2018)

3.2. Geology Exploration Costs ^[1-9]

At geological exploration it is spent 36M € or better to say that coal exploration cash costs seat between 0.004 €/t up to 0.030 €/t, average 0.012 €/t. It means that it is 1.2 € cents spent for exploration of 1t of coal. From the other hand it means that one € spent on geological explorations define 81 t of coal in all kind of deposits/coalfields. All said are in next few diagrams.

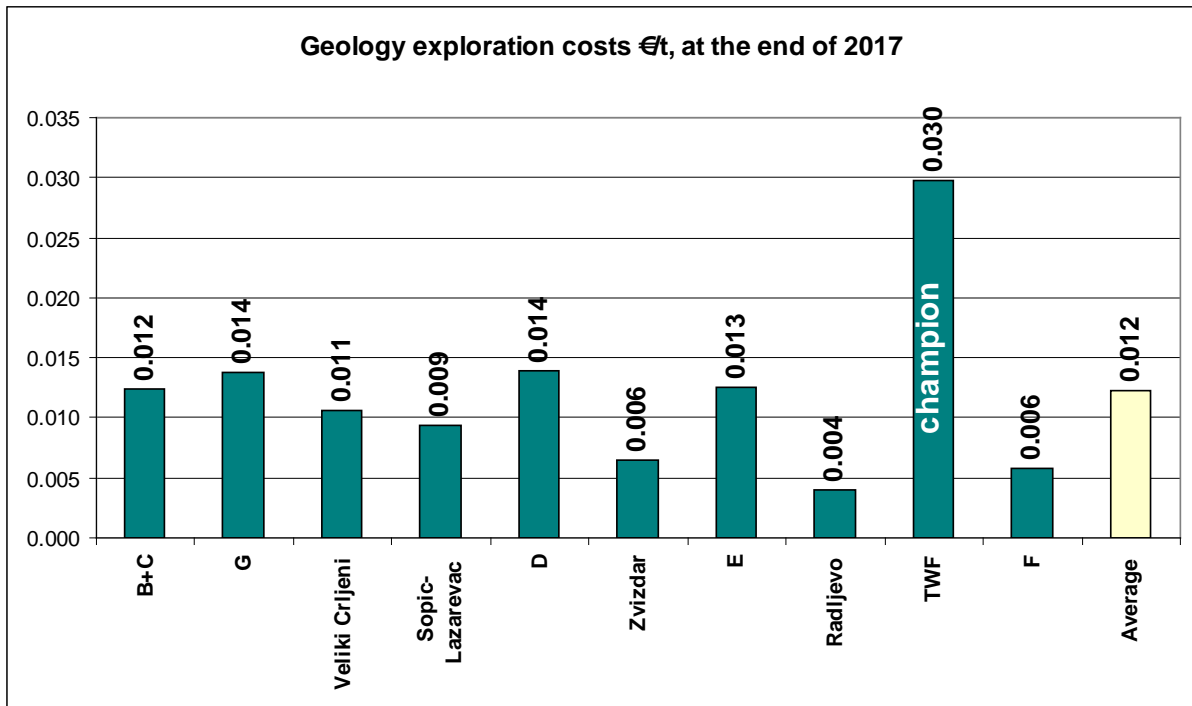


Diagram 3. Geology Exploration Costs €1 t of Coal; on Selected Deposits in KCM; Note: champion is Tamnava West Field (TWF) with 3 €cents/t; minor are coalfields Radljevo and Zvizdar with 0,4-0,6 €cent/t because of its poor geology explorations and huge ore reserves, (Vuckovic, Dimitrijevic at all, 2018)

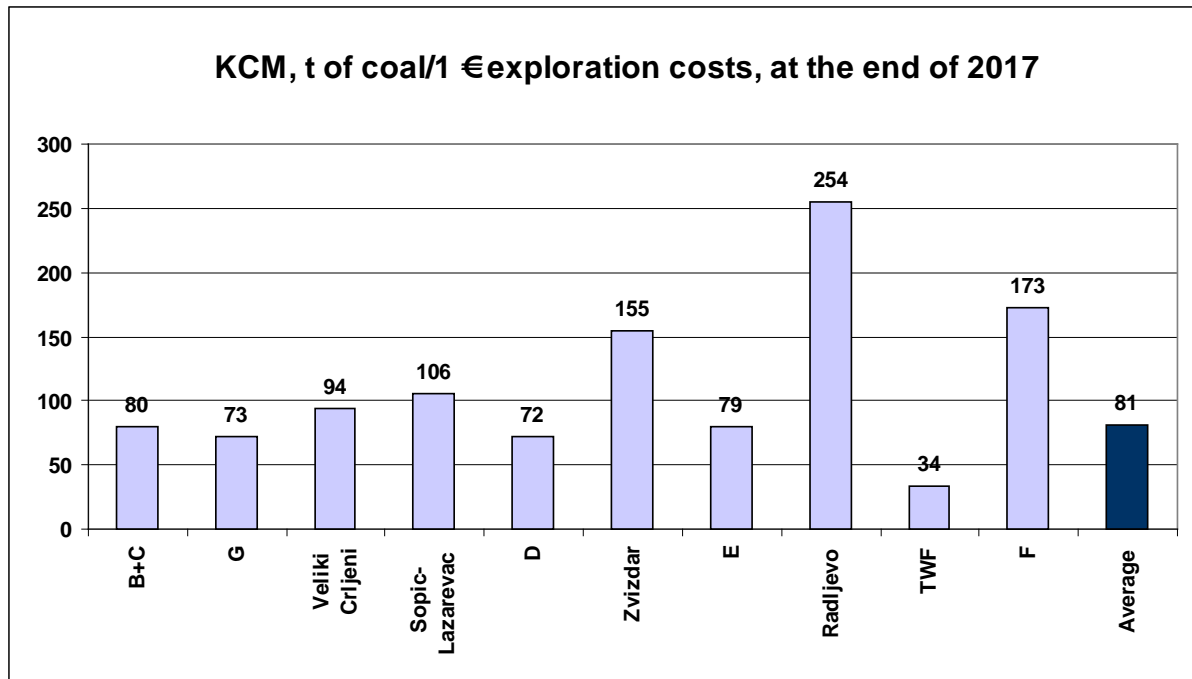


Diagram 4. Tons of explored coal for 1 € spent on Geology Exploration; on Selected Deposits in KCM (Vuckovic, Dimitrijevic at all, 2018)

As we saw, the KCM Geology Survey spent 36M € for geology exploration in last 60 years, which result in 3 billion metric tons of lignite in ten selected and reviewed deposits. In this “bill” calculation we did not calculate spent money on two deposits (open pits) which finished their lives. We did not calculate the geology exploration costs on last 50 years most important deposit – ore field D in 75% of deposit area, which is exhausted; in this paper we are talking only of a rest of coal masses on the D deposit. Remain coal masses on this deposit are more the 165M t of coal.

With average lower heating value of 7.5 GJ/t the energetic capacities seated in those ten calculated deposits reach at least 22,000,000,000 GJ; and with average 1,74 €/GJ selling price (at the moment), total worth of energy seat in coal masses reach 38B €

Therefore, we geologists found something worth 38B and spent 36M €, what is 0.1% of KCM deposit value. All of the mined out coal shipped directly to thermo energetic plants for electricity production. Comparing with electricity selling price generated from this coal, we can say that it is 4 times higher than raw coal price.

4. MINING OPERATIONS ^[12-14]

4.1. Short History

First mining operations in this area start at the end of XIX century, by underground mining. Those kinds of works in four underground fields last up to the late 60's of XX century. Few millions tons of coal was mined out.

First one open pit operations start at the end of 50's in XX century, on coalfield "A". It was the first one, based on USSR mining equipment. Later, in the early 60's, few additional open pits run – open pit "B" and open pit "D". They were the major mine producers until early 80's, when open pit "Tamnava East Field" (TEF) start to run. Open pits "A" and TEF are closed long time ago, new open pits run now. Meanwhile, in 2014 open pit "B" also pass, but it is continuing in open pit "C", so it is the same coal bad in the same geology and mining conditions. In short period of 5 years, one third of "Veliki Crljeni" deposit was open pit under running; infrastructure problems delay further mining

activities, it is on "standby" arrangement. In this open pit era, it mined out 1.1 billion tons of coal and more than 2.5 billion m³ of overburden.

4.2. These Mining Days

Now there are four open pits under running, hits 30M tons of coal annually. In addition, 70M m³ of overburden scored annually. Those production results last for 10 years from nowadays, and seem to be continuing in next period.

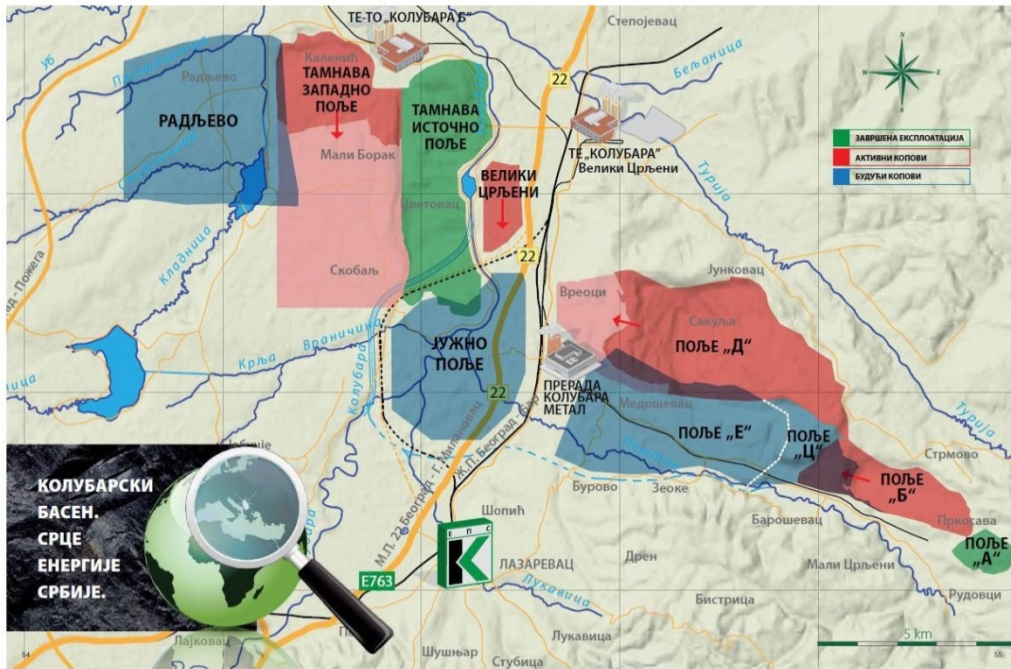


Figure 3. Overview map of mining activities in Kolubara Coal Basin; Note : green –reach dead end, partially recultivated; red – under running; light blue – under consideration for opening. (www. RB Kolubara, official site)

Many infrastructure problems see on figure 3, (relocation of roads, railways, rivers, pipes, settlements ...), expropriation of land, graveyards, industrial objects and others, burdens current production of coal and increase the cost of production.

Also, the bad geology settings (figure 3) e.g. morphology and depth of coal beds, poor quality of coal, dewatering and geotechnical problems, abundance of waste seams in coal, higher coal processing needs and so, affect on final production cash costs.

4.3. KCM Open Pits Operating Cash Costs

Official KCM company annual business and production report for 2017 year [12-14], show the individual operating cash costs on active open pits and last year KCM achieve average production cash cost (including processing the coal) of 1,152 din/t, or 9.6 €/t. From this price, the open pit production cash costs is 9.27 €/t and processing cash cost seat at 0.33 €/t. In next few diagrams, 5-9, is show annual production of overburden and coal, costs, benefits and so on...

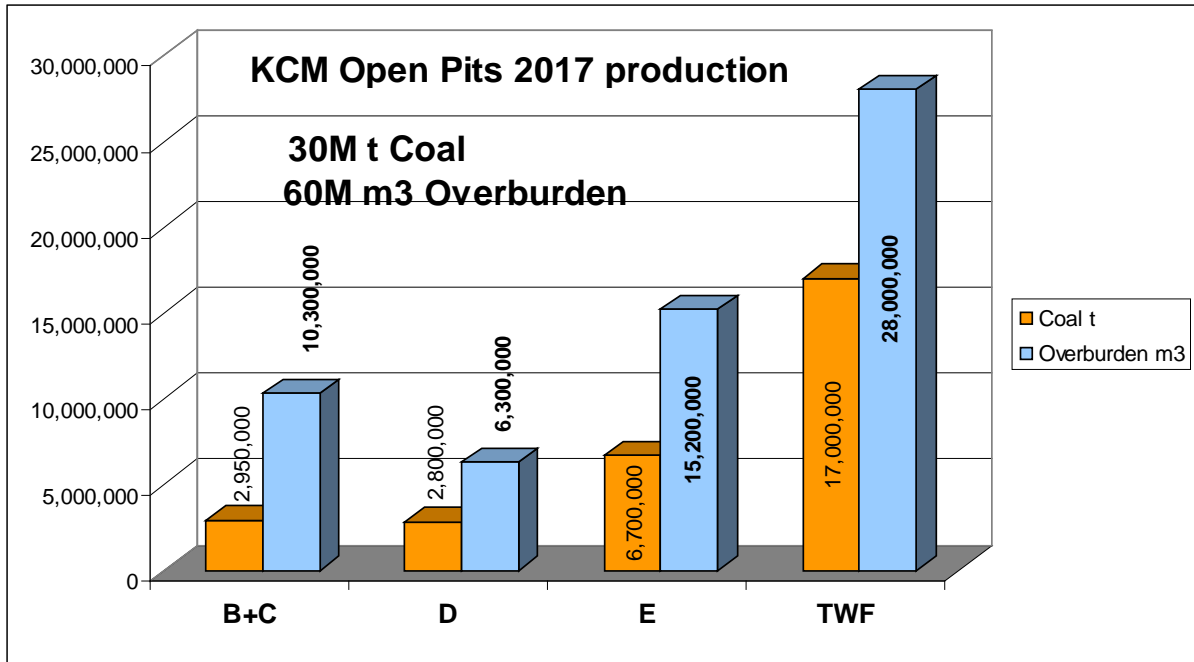


Diagram 5. KCM 2017 production results; official company report for 2017, (Vuckovic, Dimitrijevic at all, 2018)

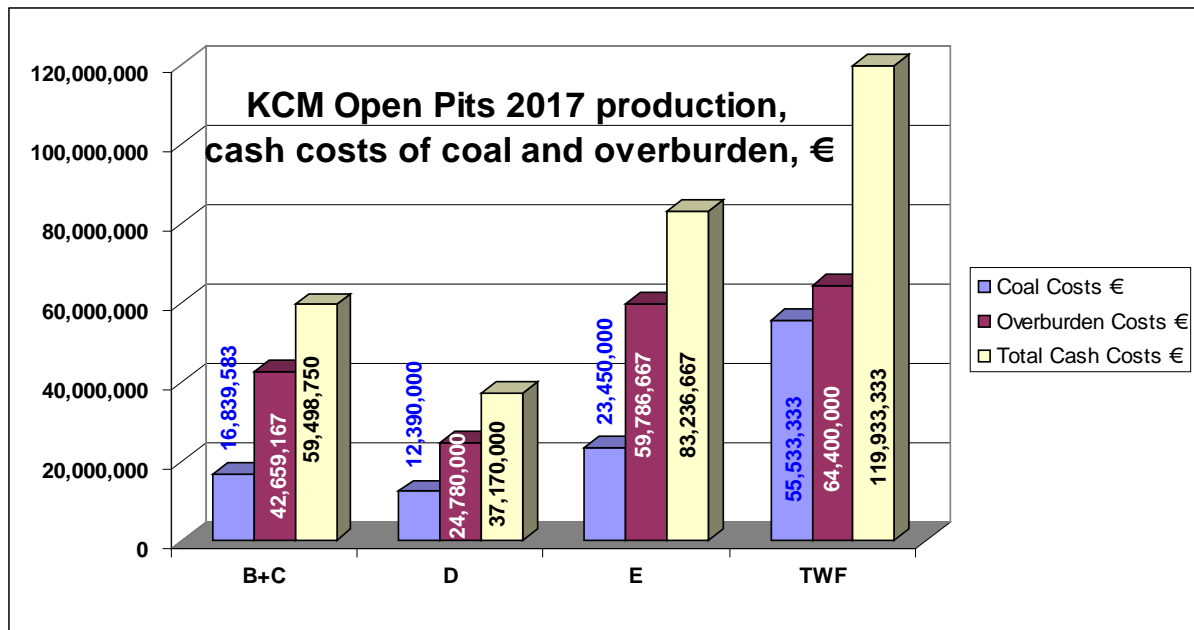


Diagram 6. KCM 2017 production; cash costs of coal and overburden, (Vuckovic, Dimitrijevic at all, 2018)

Individual production cash costs for one t of mined out coal, including processing the coal, on open pits separately in 2017-year look like this

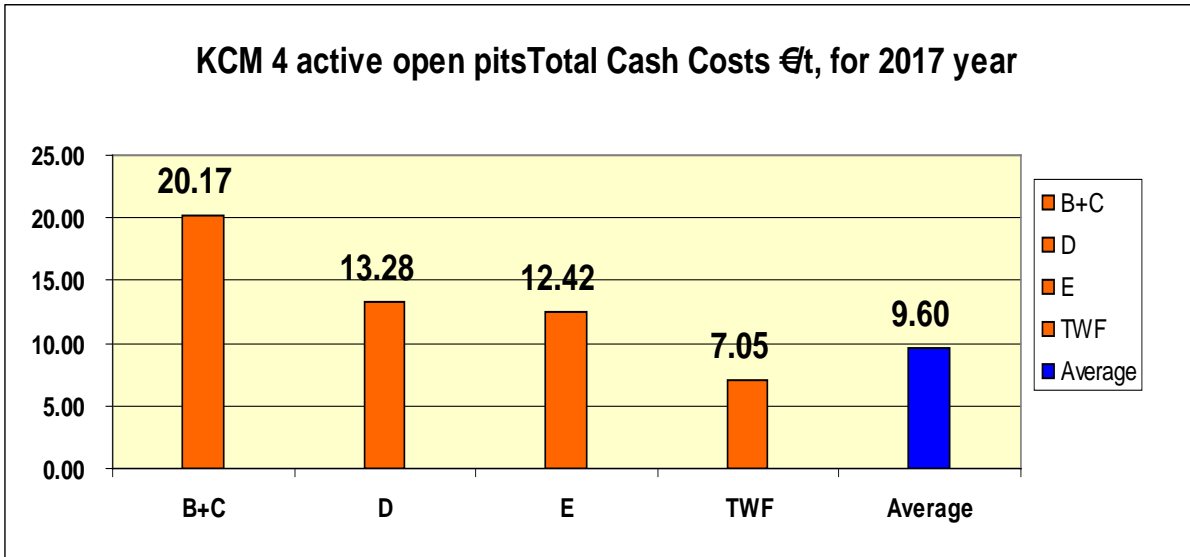


Diagram 7. KCM, four active open pits total cash costs in 2017; cash costs of coal and overburden production, (Vuckovic, Dimitrijevic at all, 2018)

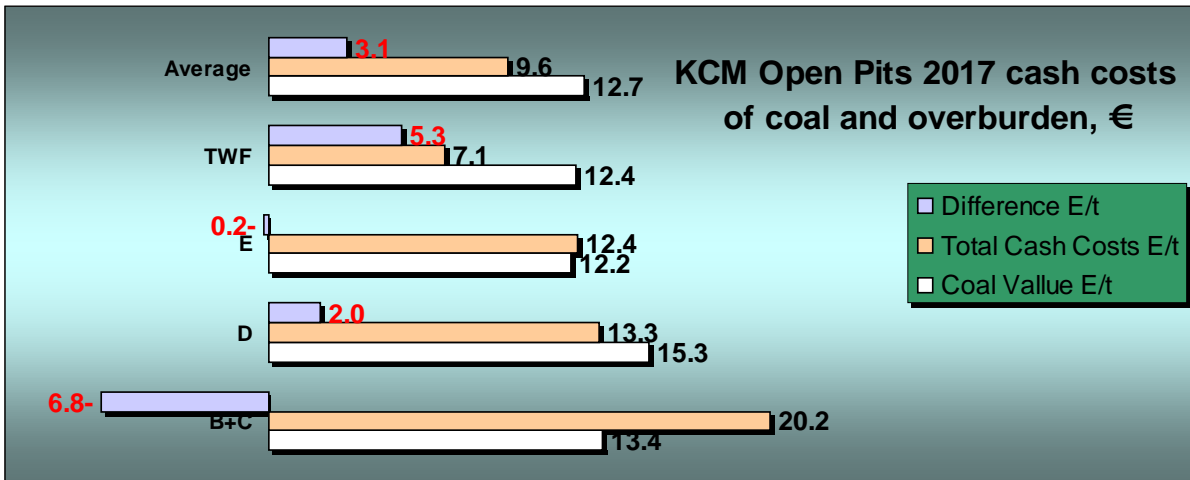


Diagram 8. KCM, four active open pits total cash costs in 2017; difference between production and selling price and benefits; Note : white bars – coal value at 1.74 €/GJ selling price/1 t; light brown bars – Total cash costs; light violet bars - benefit (Vuckovic, Dimitrijevic at all, 2018)

At 1.74 €/GJ transferred selling price to the thermo energetic facilities, total worth of shipped energy reach 375M €

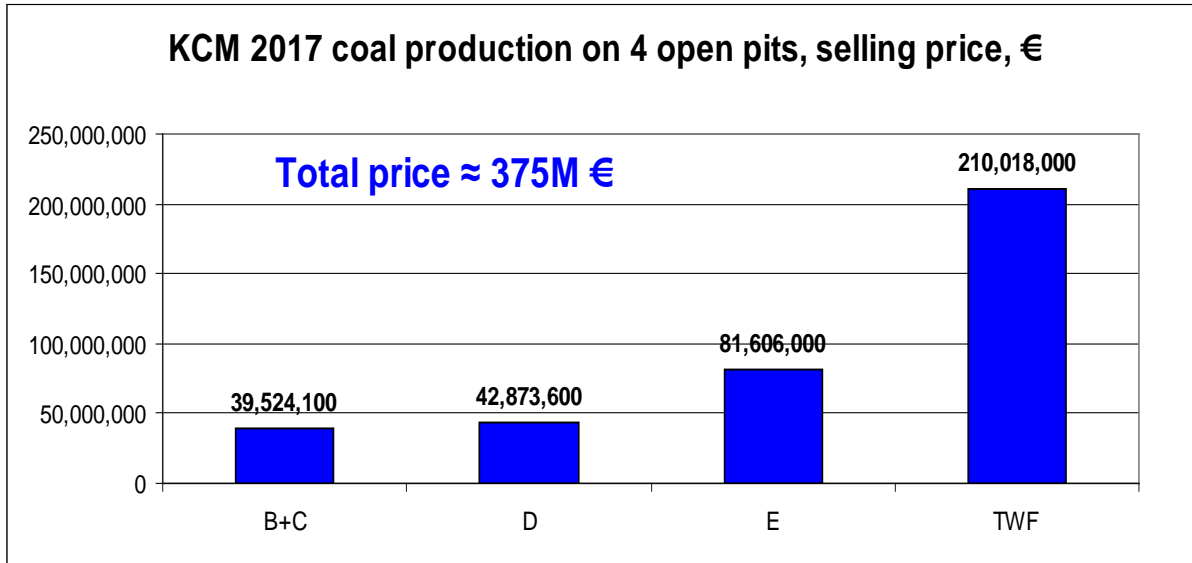


Diagram 9. KCM 2017 selling price; official company report for 2017, (modified Vuckovic, Dimitrijevic at all, 2018)

5. GEOLOGY VS MINING OPERATIONS

As it was explained above, this paper is divide in two parts geology and mining, elaborated in details, so it is possible to compare geology and mining data's and to see does the geology exploration costs significantly affect on mining production costs. With average 0.012 €/t coal of geology exploration costs and average 9.6 €/t of mining production total cash costs, we geologists hit the mining operations with 0.125% of total costs. Even, the best-explored deposit, as TWF is, with its 0.03 does not devaluate too much mining operations. In diagram10, it is show.

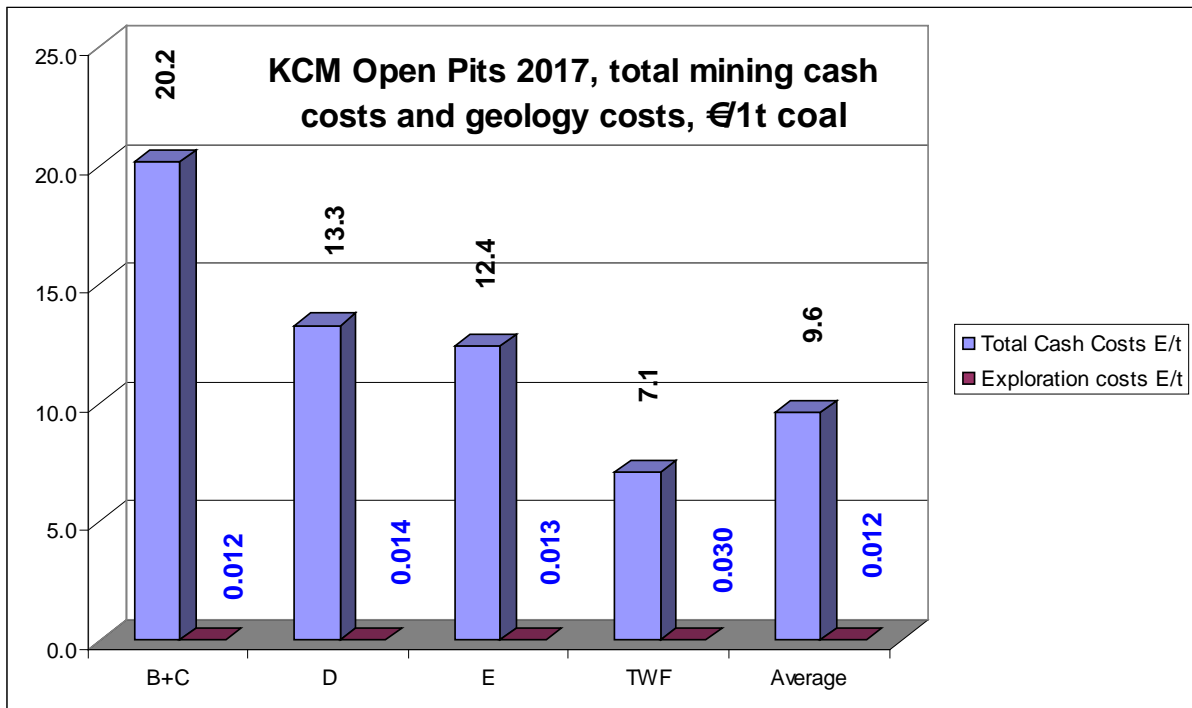


Diagram10 KCM Open Pits 2017, total mining cash costs and geology costs, (after Vuckovic, Dimitrijevic at all, 2018)

As we see, on diagram 10, the geology burden is flat and it is in line with base of diagram. Is there some conclusion?

6. CONCLUSION

Based on all of above-mentioned, related to the official company data's, and expert calculations and modifications, it is obvious that the geology exploration cost of barely 0,012 /t coal does not burden anyway and anyhow the mining operations at KCM.

As a base year, it was taken 2017, but anyway, every past or year ahead should have the very similar features like this one. So, if geology burden mining activities with only 0,125% of total cost of coal production, it is reasonable to announce that the geology still have enough room for development and realisation, even in a complex mining and other conditions.

REFERENCES:

- [1] Vuckovic B., Nesic D., Bogdanovic V., Ilic Z. (2011) - Sustainable Development in Kolubara Coal Mines, Serbia – Non Metallic Resources as a Significant Additional Coal Open Pit's Income (Possible \$ Scenario) – VII International Brown Coal Mining Congress, 13-17 April, Belchatow, Poland, 2011., p. 727-734
- [2] Vuckovic B., Nesic D. (2011) - Beyond 2010, Sustainable Development in Kolubara Coal Mines, Serbia - SGEM 11th International Multidisciplinary Scientific GeoConference, 20-25 June, Albena, Bulgaria, 2011, p. 727-734
- [3] Vuckovic B., Nesic D., Andjelkovic N., Radovanovic B., Rankovic A. (2012) - Analysis of the geological exploration of the ore fields of the Kolubara Coal Basin, Serbia – 3rd Symposium with International Participation "Mining 2012", 07-10. May 2012, Zlatibor Mt, p. 99-107.
- [4] Vuckovic B., Nesic D., Andjelkovic N. (2012) - Geological Exploration Investments, what does it worth? (Review of Kolubara Coal Mines, Serbia) - SGEM 12th International Multidisciplinary Scientific GeoConference, 17-23 June, Albena, Bulgaria, 2012., p. 593-602.
- [5] Vuckovic B. (2014) - Geological exploration of coal in the field "G", Kolubara Coal Basin - previous and planned, with a special focus on sulfur - X Conference with international participation, Environmental protection and sustainable development "Energy and Mining 2014", 11-13. March 2014, Tara Mt, Srbija, p. 403-415.
- [6] Vuckovic B., Radosavljevic S., Ignjatovic M., Bakic V. (2015) - Investments in Geology Explorations – Results (Review of the Kolubara Coal Mines, Serbia) - 47th IOC, International October Conference on Mining and Metallurgy, 04-06 October, Bor Lake, Bor, Serbia, 2015., p. 41-44.
- [7] Vuckovic B., Simic Zh., Stevanovic-Petrovic N., Radovanovic B. (2015) - Geological and Exploitation reserves of coal deposit Veliki Crljeni, Kolubara Coal Basin - a view of exploitation in the period of exploitation - VI International Conference "COAL 2015", 14-17. October 2015. Zlatibor Mt, Srbija, p. 459-466.
- [8] Vuckovic B., Stojkovic H., Ignjatovic M., Subaranovic T., Rakijas M. (2016) - Comparison of kolubara lignite value (with selected natural and artificial materials), natural indicators – 13th International Symposium Continuous Surface Mining "ISCSM 2016", 11-14. Sept. 2016, Belgrade, Serbia, p. 657-673. ISBN: 978-86-83497-23-2.

[9] Vuckovic B., Bacanac V., Bakic V. (2016) - Operating costs of geological surveys in selected deposits of lignite - Mining basin Kolubara, Serbia - I International Symposium "Investments, New Technologies in Mining and Sustainable Development 2016", 24-25. November 2016, Sabac, Srbija, p. 79-87, ISBN: 978-86-80464-04-6.

[10] Ilic S. Subaranovic T., Dimitrijevic B. (2016) - Selective dumping possibility analysis on opencast mines in eastern part of Kolubara Coal Basin, EPS - 13th International Symposium Continuous Surface Mining "ISCSM 2016", 11-14. Sept. 2016, Belgrade, Serbia, p. 125-130. ISBN: 978-86-83497-23-2.

[11] Polomcic D., Zdravkovic J., Vojnic M., Dimitrijevic B. (2016) - Recalibration of the hydrodynamic model for lignite deposit Drmno in the period of 2015 - 13th International Symposium Continuous Surface Mining "ISCSM 2016", 11-14. Sept. 2016, Belgrade, Serbia, p. 341-350. ISBN: 978-86-83497-23-2

JOURNAL, WWW, DOCUMENTATION CENTRE:

[12] EPS, Kolubara Coal Mines, Technicien & Design Documents

[13] EPS, Designing Division "Project", Technical & Designing Documents

[14] Www. EPS.co.rs

Do Coal Combustion Products Affect the Groundwater Quality Around Power Plants Area of the Lignite Ptolemais Basin?

Vasileiou E.¹, Dimitrakopoulos D.², Papazotos P.¹, Oikonomopoulos I.¹, Stathopoulos N.¹, Skliros V.¹ and Perraki M.¹

¹National Technical University of Athens, School of Mining and Metallurgical Engineering, Department of Geo-Sciences, Heroon Polytechniou 9, GR 15773, Zografou Campus, Greece.

²Public Power Corporation of Greece (PPC), Direction of Studies and Development of Mines, Department of Hydrogeological Studies, 29 Chalkokondyli st., GR - 104 32, Athens, Greece.

ABSTRACT

The West Macedonia Lignite Center (WMLC) is located in Ptolemais basin and constitutes the largest coal-mining district in Greece. The power plants (PPs) in Kardias and Ag. Dimitrios are in operation today, whereas the Ptolemais PP has ceased operations since 2014. This paper examines the influence of the lignite combustion products (fly-ash) on groundwater quality near PPs, by evaluating data from: a) wells' lithological sections, b) water table measurements, c) pumping tests and soil permeability tests, d) soil and fly-ash chemical analyses, e) Soulou stream water and groundwater, chemical analyses and f) land uses.

The hydrogeological conditions between the three areas are different. The presence of ultra-mafic rocks of Vermion Mt. influences groundwater recharge and quality at Ag. Dimitrios region. Groundwater depth varies from 7.5 m in Ptolemais PP up to 102 m in Ag. Dimitrios. Permeability of the sediments of the basin (k) ranges between 1.55×10^{-3} and 7×10^{-6} m/sec. Soil permeability (k) of the vadose zone varies between 1.2×10^{-5} - 4.7×10^{-7} m/sec. The geochemical environment (alkaline) is not conducive to mobilize metals in groundwater. Heavy metals and trace elements (As, B, Ba, Cd, Co, Cu, Mn, Ni, Pb, Se, Sb, Sr, V, Zn) are recorded in low concentrations, under the limits of WHO (2011), in most of the groundwater and surface water samples. Elevated values of Cr_{tot} (up to 137.89 $\mu\text{g/l}$) in groundwater were measured only near Ag. Dimitrios PP, although Kardias and Ag. Dimitrios fly-ashes have similar composition and similar deposition conditions. In the wider area of Ag. Dimitrios PP, soils are highly enriched in serpentine, comparing to the soils of the other two PPs, due to the occurrence of ultra-mafic rocks in Vermion Mt. Agricultural activities are extensive (fertilizers, pesticides, etc.) in Ag. Dimitrios area, as indicated by NO_3^- concentrations (up to 139 mg/l) in groundwater. The geological environment influences significantly the quality of the groundwater of the basin, with agricultural activities and the use of fertilizers playing locally an important role as well. The contribution of fly-ash to groundwater quality is of minor significance.

1. INTRODUCTION

For more than a century, coal combustion has been the main source of power generation. Fly ashes are solid residues and are the most common coal combustion by-products. Fly ash contains several main elements including Al, Ca, Fe, K, Na, and Si as the predominant elements [1,2], Cd, As, B, Se, Pb, Ni, Cu, Cr, Co, Mo, Be, Se in trace amounts may also occur in lower but still significant concentrations [1,3,4,5].

Globally, less than 25% of the produced fly ash is utilized [6]. Since there is no effective utilization, the disposal of fly ash becomes a significant environmental problem [7,8]. The disposal of fly ash is possible to affect the soil-water system; therefore sufficient environmental management of fly ash is necessary. The most crucial factors which control the mobilization and leachability of

heavy metal(oid)s are the properties of the fly ash, which depend on the physical and chemical properties of the coal source, the pH, the sorption reactions and the hydrogeological/hydrochemical conditions [1,9,10,11,12].

In Greece four mines ie Main field, South field, Kardias field and Amyndeon-Florina constitute the Lignite Center of West Macedonia (WMLC) with an annual production of 25–30 Mt. In this paper the following three power plants in the Ptolemais-Sarigkiol basin, supplied by lignite from WMLC, are studied:

- ✓ Agios Dimitrios with a total capacity of 1.595 MW, completed between 1984 and 1997.
- ✓ Kardias PP with a total capacity of 1.250 MW, completed between 1975 and 1987.
- ✓ Ptolemais PP which had five units of 620 MW, completed between 1959 and 1973. PP terminated its operation in 2014.

The acceptable disposal practice of fly ash in the afore-mentioned PPs, is co-deposition with the waste material of the excavation of the lignite mines, in the dumping sites usually in the voids remaining after mine exploitation. Fly ash is transported mainly by a system of belt conveyors. A small site in the vicinity of the PPs is used for the temporary dumping of fly ash, in the case of serious damage or malfunction of the belt conveyor system. A plant for the grinding of fly ash which was used for the construction of a dam, was in operation in Ptolemais PP.

This paper focuses on the influence of the lignite combustion products (fly-ash) on groundwater quality near PPs, evaluating data from: a) wells' lithological sections, b) water table measurements, c) soil permeability tests and pumping tests, d) soil and fly-ash analyses, e) groundwater and Soulou stream water analyses and f) land uses. The significant roles of the hydrogeological environment and the land uses are highlighted as determinant factors, concerning the water quality near PPs.

2. MATERIAL AND METHODS

2.1. Geological- Hydrogeological setting

The Sarigkiol basin is part of the Ptolemais-Kozani basin in West Macedonia and lies between the latitudes 21 46'00 and 22 40'00'N and the longitudes 40 20'00 and 40 28'00'E. It is surrounded by Vermion Mt in the NE, Skopos Mt in the S and Askion Mt in the W. The dominant geological formations of the mountains are carbonate rocks (Triassic and Cretaceous limestones), Jurassic ultramafic rocks (serpentinites and peridotites), Maastrichtian flysch. The basin fill consists of Neogene-Quaternary sediments, which have a thickness up to 1000 m [13]. The quaternary sediments (sands, clays, gravels, talus cones, breccias and limnic deposits) overly the Neogene formations (lignite series and alternating layers of sandy or clay marls, clays, silts, sands and conglomerates) in a large part of the study area.

The main aquifer systems in the area are [14, 15]:

- The aquifer in the sandy sediments of the green and yellow series of the overburden of lignite series
- The aquifer in the sandy sediments of the underburden of lignite series
- The deep karstic aquifer in the limestones of the basement
- The overhanging relatively small karstic aquifers in the Cretaceous limestones

Soulou stream is the main surficial water body receiving the surface runoff of the basin. It flows in the vicinity of the aforementioned PPs, receiving any surface runoff from them, from the dewatering of the mines and from the temporary dumping sites of fly ash (fig. 1).

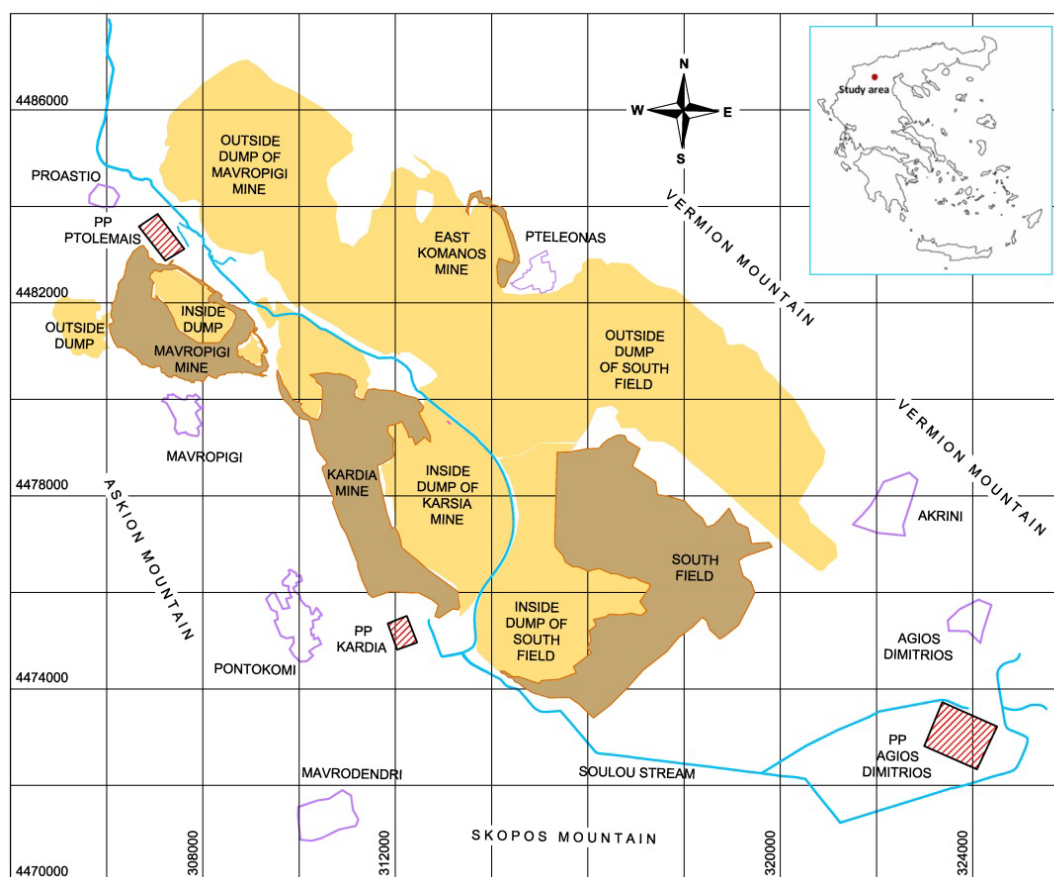


Figure 1. The location of the three Power Plants in Ptolemais basin.

In the area of Ag. Dimitrios PP, geological structure consist of clays, sand gravels, conglomerates with red clay, scree with alterations of brownish sandy clay etc (Fig. 3). The thickness of the unsaturated zone in the well K is 57 m. According to pumping tests performed in the surrounding area of PP, the transmissivity is $T=10^{-5}$ - 10^{-6} m²/s and the permeability $k= 10^{-7}$ m/s (medium to low). The depth of groundwater level in the area around Ag. Dimitrios PP, varies from 50 up to 102 m. The main aquifer systems are developed in conglomerates and screes of the Quaternary deposits (Fig. 2). The main recharge is from the precipitation and the lateral recharge from Vermion Mt, where ultra-mafic and carbonate rocks occur.

In the area of Kardias PP, the regional hydrogeological setting differs compared to the one of the Ag. Dimitrios PP. Considering the lithological section of YNP113, which is representative, the geological structure consists of: a) brownish clay up to 2.5 m, b) loose conglomerates and sand - gravel with clays (conglomerate of Proastion). The thickness of the unsaturated zone of the well is 22 m. Alterations of conglomerates and sand gravel with clays is observed up to the depth of 84 m. According to pumping tests the conglomerates of Proastion have a high transmissivity (T) = 10^{-3} - 10^{-4} m²/sec, $k= 10^{-4}$ - 10^{-6} m/sec and a storage coefficient ~ 8 -12%. The depth of the groundwater level in the area ranges from 7 up to 40 m (Fig.3).

Ptolemais PP is located on Quaternary deposits and Neogene sediments. The area of PP and the adjacent Mavropigi mine has many faults (fig. 2). There are two main aquifers; one phreatic in the conglomerates of Proastion and one confined in the underburden of the lignite series. The aquifer of underburden in local areas is able to communicate with both the surface flowing water and the aquifer of conglomerates of Proastion, because of the numerous faults and the more than 30 water wells in the vicinity of PP, which facilitate the leak or the inflow of water into the confined aquifer and vice versa. Recent measurement in the mine verified the above suggestion. In the lithological

section of water well Ptol2, the sequence of the geological formations is described (Fig. 3). The water depth is 7.50 m.

In waste dump areas of South field, Kardia field, Mavropigi field, where fly ash has been co-deposited with waste, numerous pumping tests and permeability tests (Maag, Lefranc tests) have been performed,. According to these, permeability *k* is in the order of 10⁻⁷-10⁻⁹ m/s. It has been observed that permeability decreases with depth (table 1) and time. This is due to the compaction of the waste caused by the weight of the material deposited on top and to the pozzolanic properties of fly ash which are activated when it is hydrated.

Table 1. Values of permeability (*k*) of dumping sites.

Borehole	Location	Coordinates		(2 m)	(5 m)	(10 m)	(20 m)	Method
		X	Y					
M3	Mavropigi	306.504	4.482.763	-	1.9 x10 ⁻⁶	8,4 x10 ⁻⁷	-	Maag
M6	Mavropigi	308.126	4.481.451	-	3.4 x10 ⁻⁶	6.6 x10 ⁻⁷	-	Maag
M9	Mavropigi	307.164	4.481.481	-	3.7 x10 ⁻⁶	4.1 x10 ⁻⁶	-	Maag
M10	Mavropigi	307.142	4.481.712	-	1.2 x10 ⁻⁵	5.8 x10 ⁻⁶	-	Maag
E1	S. Field	314.716	4.479.953	2.64x10 ⁻⁵	1.0 x10 ⁻⁵	4.9x10 ⁻⁶	1.77x10 ⁻⁷	Maag
G3 DEI	S. Field	313421	4482306	7.8x10 ⁻⁷	-	1x10 ⁻⁸	6.1x10 ⁻⁹	Maag -Lefranc
Y5	Kardia	313.294	4.481.866	1.45 x10 ⁻⁷				Cooper-Jacob

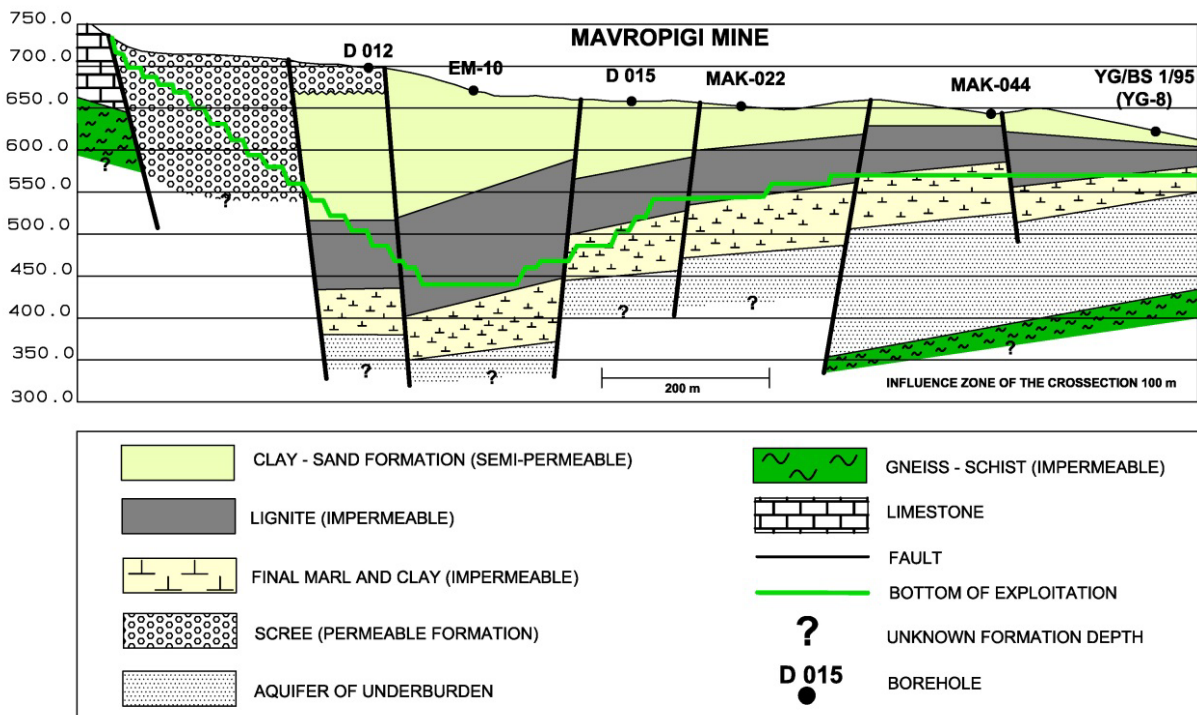


Figure 2. Simplified geological section in Mavropigi Mine – Ptolemais PP area.

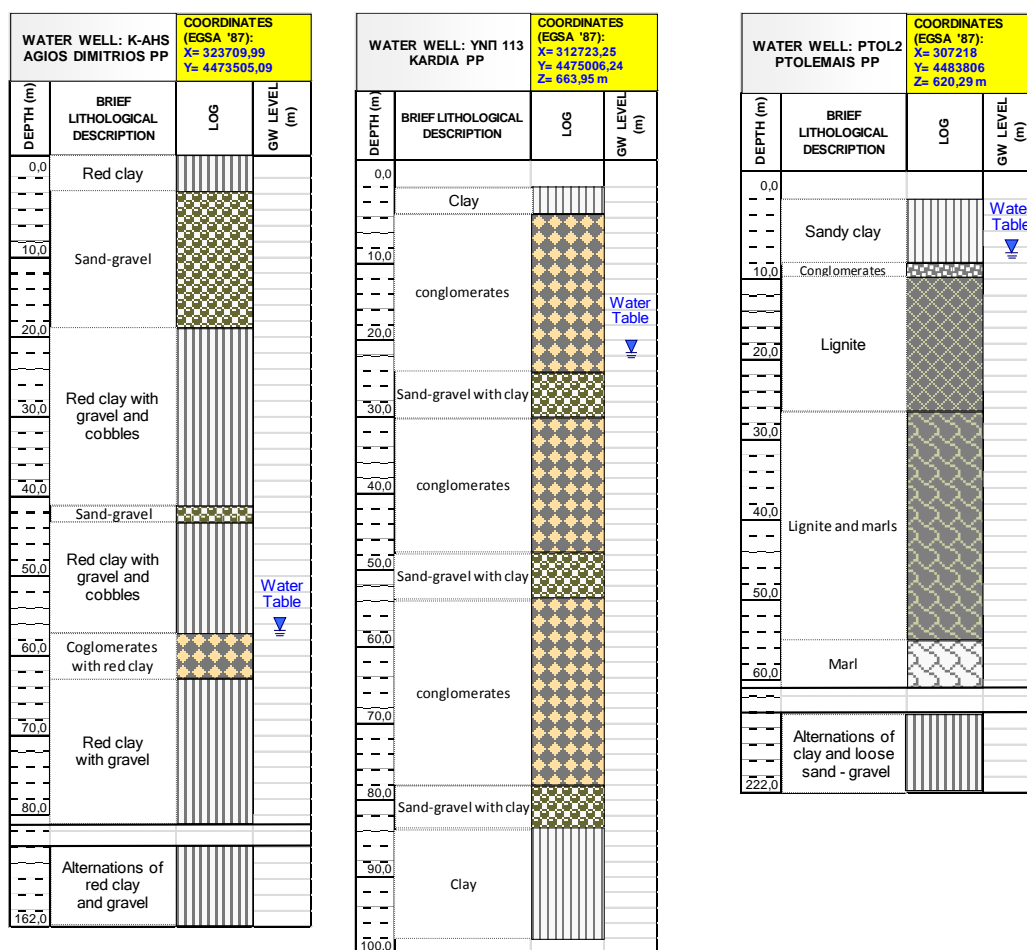


Figure 3. Lithological sections from water-wells in the area of the three Power Plants.

2.2. Sampling and Analytical methods

A total of thirty seven (37) representative surface- and ground-water samples were collected from irrigational wells and dewatering wells (34), Soulou stream (3) and wells for the uses of PPs, the sampling took place during the wet and dry periods from 3/2014 to 10/2017. Temperature (T), pH, redox (Eh), dissolved oxygen (DO) and electrical conductivity (EC) were measured in situ. For chemical analyses, three samples were stored in 0.5 L, 0.1 L and 0.05 L polyethylene bottles and transported in a refrigerator. The first subsample was stored in a bottle of 0.5 L without further treatment, for the analyses of the major ions (Ca^{2+} , Mg^{2+} , Na^+ , K^+ , NO_3^- , SO_4^{2-} , NO_2^- , NH_4^+ , Cl^- , HCO_3^- , PO_4^{3-}). The second subsample was filtered in situ through a 0.2 μm membrane of a disposable syringe, subsequently acidified to $\text{pH} < 2$ with about 1 ml ultra-pure HNO_3 and finally stored in a bottle of 0.1 L, for the analyses of minor and trace elements (Ag, Al, As, B, Cd, Co, Cr_{tot} , Cu, Fe, Mo, Mn, Ni, P, Pb, Rb, Sb, Se, Si, Sn, Zn). The third subsample was filtered through a 0.2 μm membrane, conserved by NaOH 1M for $\text{pH} > 10$, and stored in 0.05 L bottle, for the analysis of Cr^{6+} . Analyses were performed at ACME Analytical Laboratories Ltd., Canada, by means of inductively coupled plasma mass spectrometry (ICP-MS). The ionic chromatographic method was applied for the determination of Cr^{6+} . The charge-balance error for major ionic species, calculated using Microsoft Excel and the software package AQUACHEM 5.0, did not exceed 10%. All analyses were performed according to EL0T EN ISO/IEC -17025 Standard.

The time series of water table measurements were collected from PPC and new measurements were done, in order to determine the water depth level (2015-1017).

3. RESULTS AND DISCUSSION

3.1. Influence of hydrogeological conditions

The hydrogeological setting in the surrounding areas of the three PPs presents some differences.

Unsaturated zone operates as a physical filter and can retain the pollutants before infiltrating in the saturated zone (aquifer). Shallow aquifers are more vulnerable against pollution in comparison to the deeper ones [16]. The water depth in the area of Ag. Dimitrios ranges from 50 up to 100 m, in the area of Kardia PP from 15 up to 30 m and in Ptolemais area from 7 up to 40 m.

The composition of the unsaturated zone is also a significant factor that can control the infiltration of pollutants. The presence of clays in the unsaturated zone makes more difficult the infiltration of the pollutants in deeper aquifers. Clay minerals assist many natural processes in the unsaturated zone, such as ion exchange, adsorption, absorption and dissolution, which could influence the infiltration of pollutants (heavy metals and trace elements) [17]. Ag. Dimitrios area has significant thickness of clay layers above the saturated zone, so the infiltration and diffusion of pollutants must be considered as limited. In Kardia PP the unsaturated zone mainly consists of conglomerates, sand and gravels, which favor the infiltration of possible pollutants in deeper zones.

Permeability (k) in the area of Ag. Dimitrios PP ranges between 10^{-5} - 10^{-7} m/sec, characterized as medium permeability. In Kardia PP, $k=10^{-4}$ - 10^{-7} m/sec, and in Ptolemais PP, $k=10^{-3}$ - 10^{-6} m/sec. In Ptolemais PP the existence of many faults and many water wells permit the hydraulic communication of the aquifers locally. Concerning k values, is clear that the areas of Kardia and Ptolemais PPs present higher values and this creates favorable conditions for the infiltration of any pollutant (table 2).

Table 2. Values of hydraulic conductivity according pumping tests.

WELL ID	LOCATION	Q (m ³ /h)	T (m ² /sec)	k (m/sec)
YNII-113/97	KARDIA	12	1.02×10^{-4}	3.39×10^{-6}
YNII-116/97	KARDIA	10	2.21×10^{-5}	6.31×10^{-7}
YNII-117/97	KARDIA	15	3.47×10^{-5}	9.90×10^{-7}
YNII-164/01	KARDIA	30	6.10×10^{-5}	2.03×10^{-6}
YNII-165/01	KARDIA	30	1.57×10^{-4}	5.24×10^{-6}
YNII-165A/03	KARDIA	35	5.26×10^{-5}	1.75×10^{-6}
YNII-222/05	KARDIA	30	6.30×10^{-5}	2.10×10^{-6}
YNII-155/01	AG.DIMITRIOS	2	6.78×10^{-6}	2.26×10^{-7}
YNII-No2/92 (323 ΚΛΕΙΤΟΣ)	AG.DIMITRIOS	4	9.24×10^{-6}	2.64×10^{-7}
YNII-311/12	AG.DIMITRIOS	15	2.31×10^{-5}	6.80×10^{-7}
AHS PTOL 2	PTOLEMAIS	40	1.70×10^{-4}	5.67×10^{-6}
AHS PTOL 3	PTOLEMAIS	60	4.40×10^{-3}	1.47×10^{-4}
YG/BS 1/95	PTOLEMAIS	150	7.00×10^{-3}	2.33×10^{-4}

3.2. Fly Ash

Fly ashes are characterized by their composition in relation to major elements. The fly ash of Ptolemais belongs to class F and modic type (rich in Si and Al) and fly ashes from Kardia and Ag. Dimitrios belong to class C and calcic type (rich in Ca) [18,19]. In strong alkaline and high calcite fly ashes the mobility of the elements is $B > V > Cr > Ca > Mo > As$. Boron is the most mobile trace element [20]. The mobility of most elements of fly ash is strongly correlated with the pH range of the water-fly ash system [20]. The leachates of fly ash depend on the pH range. It has been recorded that As is released in pH=6-10, Cr in pH=7-11, Mo in pH=6-11, Ni in pH>10, Sb in pH=6-10, Se in pH=6-11, V in pH=6-11 [21]. Dissolved Si decreases its leaching in pH range of 8-10. Mo and Se are

the basic elements and good indicators of leaching potential of fly ash, in order to evaluate groundwater pollution [21]. According to Georgakopoulos [22], in Sarigkiol basin, Se is the most enriched element (273 times) compared to the earth's crust elements; enrichment is also observed in As, Ag, B, Cd, Mo, Ni, Sb and U. Comparing the chemical composition of fly ashes from the three PPs (Table 2) the main remarks are:

- Ptolemais fly ash is the most enriched in As, Ba, Co, Cr, Cu, Mo, Pb, Sb, Se, Zn compared to the fly ashes from Kardia and Ag. Dimitrios PPs.
- Fly ash from Ag. Dimitrios is highly enriched in B, Cd, Hg, Ni, Rb.
- Fly ash of Kardia is enriched in Sr.

The alkaline environment generally favors the mobilization of As, Cr⁶⁺, Mo, Se in groundwater. On the contrary, elements such as Cd, Co, Cu, Fe, Mn, Ni, Pb, Sn, Zn achieve the minimum solubility in alkaline conditions since they are mobilized in acid conditions [23]. Considering all the above, the main elements that could be potentially leached from alkaline and calcite fly ashes in groundwater of Ptolemais basin are: As, B, Ba, Ca, Cd, Cr, Mo, Rb, Sb, Se, Sr, V.

One of the most important properties of the fly ash is its pozzolanicity, where the system fly ash-water interacts and fly ash is cemented and becomes impermeable. Permeability tests have been performed in many sites in waste -fly ash co-deposition areas in order to determine the permeability of them (Table 1, [24]). Low permeability was measured in a range of 10^{-6} - 10^{-9} m/sec. These values of permeability prevent the percolation of rain water in the mass of the waste dump areas and consequently the leaching of fly ash, in deeper layers up to the saturated zone.

Table 3. Fly ash composition of the three PPs.

Element	Agios Dimitrios		Kardia		Ptolemais	
	FA1-MAR	FA1-OCT	FA2-MAR	FA2-OCT	FA3-MAR	FA3-OCT
As	22.08	27.22	31.64	29.89	29.48	31.02
B	117.34	26.77	8.50	28.35	33.48	59.19
Ba	389.90	381.52	350.41	391.00	435.66	408.12
Cd	1.43	1.72	0.90	1.12	1.42	1.18
Co	30.08	30.77	17.98	22.69	32.21	31.99
Cr	459.69	441.80	290.07	270.07	485.17	461.65
Cu	58.77	57.92	39.13	47.80	66.03	64.25
Hg	1.62	0.15	0.90	0.36	0.51	0.07
Mo	5.61	5.58	7.55	6.81	7.09	8.41
Ni	438.93	457.63	264.97	321.36	434.26	439.05
Pb	36.90	34.13	26.21	26.04	38.92	42.53
Rb	77.05	75.76	46.51	54.28	74.36	75.78
Sb	1.26	0.79	1.47	0.88	1.30	2.27
Se	6.21	8.54	7.73	10.60	8.26	13.29
Sn	1.68	0.88	1.73	0.64	2.05	1.43
Sr	498.19	446.33	455.64	512.18	395.51	393.66
Zn	319.83	269.30	176.33	198.77	364.47	339.47

In the three PPs the operations and the management of fly ash are similar. In Kardia (Figure 4c) and Ag. Dimitrios PPs (Figure 4a,b) there are sites for the temporary deposition of fly ash, which is then transported to the waste dump areas where the final deposition takes place. In Ptolemais there was also an open temporary disposal site, with similar operation as in the other two PPs (Fig. 4).



Figure 4. The temporal deposition sites of fly ashes in three PPs: a) A9 in Ag. Dimitrios 2015, b) A9 in 2018, c) Kardia d) Ptolemais.

3.3. Water quality

The chemistry of groundwater in wells from the three PPs and Soulou stream were statistically analyzed and the results were summarized by minimum, maximum, mean in Table 4. Physical and chemical parameters were compared with the acceptable limits of World Health Organization (2011), as there is no legislation concerning the mine water quality, or industrial zones in Greece.

All pH values are within the acceptable limit of 6.5 – 8.5 (except one in Ptolemais), for drinking water according to WHO guidelines 2011. Waters are characterized as slightly to strongly alkaline. The alkaline environment creates favorable conditions for the mobilization of As, Cr, Mo, Se, Sb, V [23]. Eh values are higher in Kardia and Ag. Dimitrios areas than in Ptolemais. The oxidative conditions in Kardia and Ag. Dimitrios PPs, facilitate the oxidation of some metals, such as Cr^{3+} to Cr^{6+} [26].

In Ptolemais basin elevated values of NO_3^- (up to 139 mg/l) were recorded which exceed the acceptable limit of 50 mg/l, for drinking water according to WHO guidelines (2011). The nitrate pollution in the area is extended due to the improvident use of fertilizers [27,28]. The role of nitrates is suggested as crucial, concerning the oxidation of Cr^{3+} to Cr^{6+} [29,30]. SO_4^{2-} concentrations present significant fluctuations in groundwater of Ptolemais basin up to 490 mg/l. According to WHO (2011), 4 samples exceed the acceptable limit of 250 mg/l for drinking water. The increased values could be attributed to fertilizers as they were recorded near to cultivated areas.

The concentrations of the enriched components of fly ash were recorded within the acceptable limits of WHO (2011), Ba (700 $\mu\text{g/l}$), B(1000 $\mu\text{g/l}$), As(10 $\mu\text{g/l}$), Se(10 $\mu\text{g/l}$) respectively. Additionally Rb, Sb, V were measured in very low concentrations in groundwater of Ptolemais basin.

B is considered as the most mobile element of fly ash components, although in the Ptolemais basin its values are low [21]. The mobilization of As is a complex process, the favorable alkaline

conditions were not sufficient for its release from fly ash [31]. The alkaline conditions didn't also mobilize Se, Sb, Mo, V, showing that the effect of fly ash on groundwater is of minor importance. All values of Mo were low and below the acceptable limits of 70 µg/l for drinking water, according to WHO guidelines (2011). In one site, Mo was measured 77 µg/l, this well is located at the waste dump area of fly ash deposition, in an area that a landslide took place; it is below the acceptable limit of the New Dutch list (300 µg/l). This water well is used only for the dewatering of the mine and for industrial use.

Sr concentrations in groundwater are relatively low. There is not upper limit for Sr in surface- and ground- waters. Considering the enrichment in Sr of fly ash (336 ppm-512 ppm), the potential leaching of fly ash in Sr must be regarded as minor. Additionally ultra-mafic rocks and the carbonate formations could be the geogenic sources for the occurrence of Sr in groundwater [32]. In low concentrations the presence of Sr and V could be also attributed to anthropogenic sources as fertilizers [33].

Cr_{tot} concentrations in groundwater of Ptolemais PP vary from 5.60 up to 10 µg/l (average value 7.80 µg/l), in Kardias PP range from 1.30 up to 11.50 µg/l (average values 4.58 µg/l), in Ag. Dimitrios PP fluctuate from 0.70 µg/l up to 134.70 µg/l (average value 63.94 µg/l) and in Soulou stream vary from 2.10 to 6.70 µg/l (average 4.83 µg/l), respectively.

Cr_{tot} presents significant variations in groundwater, mostly in the area of Ag. Dimitrios PP, where 14 water samples exceed the upper acceptable limit of 50 µg/l, according to the WHO guidelines (2011). In the surrounding areas of the other PPs, Cr_{tot} in groundwater does not exceed the limit of 50 µg/l, although the operational and management conditions are similar. In the Soulou stream very low concentrations of chromium were measured. This finding is very significant considering that the surface drainage body of the area, which receives the water that is pumped out for the protection of the mine (from wells, PP of Ag. Dimitrios or directly from the mining sumps) present no deterioration regarding heavy metals and trace elements. The distribution of Cr_{tot} in the groundwater of the three areas is recorded in Fig. 5. As it is shown in the distribution map, the highest values of Cr_{tot} are observed in the eastern part of the Sarigkiol basin and more specifically in the irrigational wells. All the extreme values of Cr_{tot} were measured in water wells, which are exclusively used for covering irrigational purposes.

Another crucial factor concerning the quality of water wells at the eastern part of the area (Ag. Dimitrios PP) is the occurrence of ultramafic rocks in Vermio Mt and the natural recharge from it. The geochemical signature in the Sarigkiol basin has been strongly affected by the presence of ultramafic and carbonates rocks surrounding the basin; additionally the soils are rich in material of the weathered ultra-mafic formations. Ultramafic rocks are rich in Si, Mg enriched As, Co, Cr, Ni etc [34].

Considering the chemical characteristics of groundwater and Soulou stream, it is noticeable that the only element that presents elevated values is Cr_{tot}. No other element, which is directly linked with fly ash, presents elevated values. This fact indicates that the leaching potential of fly ash is minor. Cr_{tot} is primarily related with the ultramafic rocks [34]. The occurrence of Cr_{tot} has also been associated with the fly ash and the fertilizers [22, 35, 36, 37, 30].

The elevated concentrations of Cr must be investigated considering various anthropogenic sources. The potential leaching of fly ash is not imprinted in groundwater of Ptolemais basin. Elements such As, B, Ba, Mo, Se, Sb, Sr, V were not released in groundwater, indicating the leaching from the fly ash is minor. Although, this seems to be inconsistent with laboratorial leaching tests [21,38] in nature the prevailing conditions such as high pH values, high calcite content, low permeability, co-depositing fly ash with mine waste and fly ash hydration resulting in the formation of stable pozolanic phases, prevent metal dissolution [38].

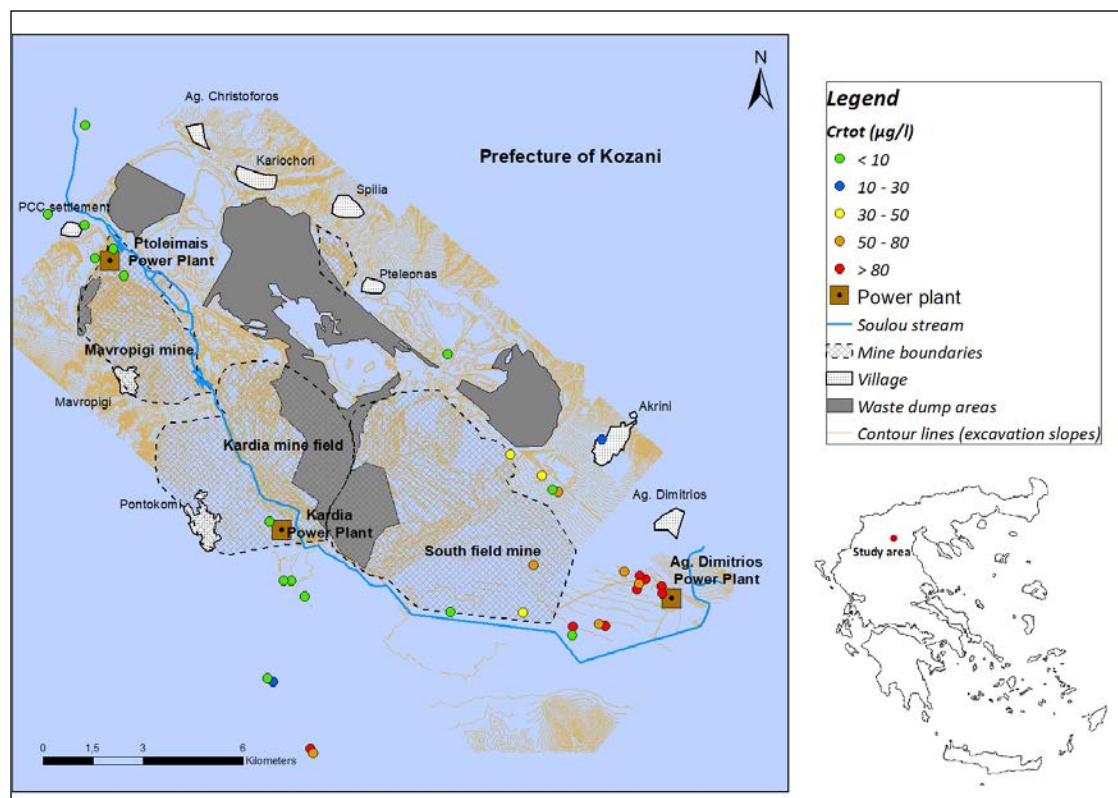


Figure 5. Distribution map of Cr_{tot} at the neighboring areas of three PPs.

The main differences between the three PPs, are the occurrence of ultramafic rocks in the area of Ag.Dimitrios, the hydrogeological conditions and the land uses. Although in Kardias PPs the hydrogeological conditions are favorable, no groundwater deterioration is observed concerning Cr_{tot} . In the areas of Ptolemais and Kardias PPs, there are not increased values in groundwater concerning the mobile elements of fly ash in alkaline environment (As, B, Cr, Mo, Sb, Se, etc). In Ag. Dimitrios PP, they were recorded increased values only for Cr in groundwater, all the other heavy metals and trace elements which are associated with fly ash were measured in very low values. The natural waters in the eastern part of the Sarigkiol basin show different physico-chemical characteristics than those of leachates of fly ash. Ph in natural waters ranges between 7.5 and 8.5, although in fly ash leachates pH was measured up to 13. The natural environment is oxidative, instead of the reducing one that fly ash creates. EC values are significant low (257-907 $\mu\text{S}/\text{cm}$), although in fly ash leachates EC values are up to 10.000 $\mu\text{S}/\text{cm}$ [21, 38].

Table 4. Statistical analyses of surface and ground waters chemical analyses.

Sampling sites	Ag.Dimitrios			Kardia			Ptolemais			Soulou stream		
	Average	Max	Min	Average	Max	Min	Average	Max	Min	Average	Max	Min
pH	8,06	8,50	7,52	8,03	8,26	7,73	8,04	9,70	7,46	8,04	8,06	8,02
Temp	14,65	32,30	8,90	10,65	13,40	8,60	12,72	13,90	10,40	12,13	14,80	8,10
D.O. (mg/l)	8,89	11,28	6,75	9,47	12,09	7,64	6,17	7,75	1,90	8,30	9,50	6,30
E.C. (µS/cm)	447,05	1156,00	257,00	566,33	907,00	325,00	671,92	921,00	144,50	988,33	1071,00	844,00
Eh (mV)	306,13	399,00	217,30	312,37	396,00	240,40	115,35	220,60	27,00	277,23	348,00	218,00
Ca ²⁺ (mg/l)	56,64	199,00	22,70	96,99	115,00	75,50	62,03	87,90	7,27	67,02	82,96	54,30
Mg ²⁺ (mg/l)	24,11	52,90	8,89	35,27	59,30	4,92	48,93	95,50	5,59	33,53	45,70	23,49
Na ⁺ (mg/l)	8,91	50,70	0,00	5,57	7,60	2,60	8,57	10,30	4,48	84,46	114,41	66,20
K ⁺ (mg/l)	1,80	14,80	0,60	1,19	3,80	0,30	5,12	16,00	1,29	3,25	4,06	1,70
NO ₃ ⁻ (mg/l)	28,38	132,00	0,00	50,85	73,70	10,20	24,95	32,50	11,30	5,13	5,60	4,30
Cl ⁻ (mg/l)	17,36	121,00	0,00	33,67	44,00	0,00	29,80	63,00	9,00	48,00	69,00	15,00
SO ₄ ²⁻ (mg/l)	41,45	490,00	0,00	76,67	121,00	0,00	128,14	368,00	11,40	212,33	392,00	24,00
HCO ₃ ⁻ (mg/l)	195,86	333,00	142,00	268,83	355,00	196,00	250,88	326,00	68,30	171,67	324,00	79,00
Al (µg/l)	20,55	253,00	1,00	11,17	40,00	1,00	5,00	13,00	3,00	49,00	96,00	22,00
As (µg/l)	1,36	3,70	0,50	2,16	4,40	0,50	0,95	1,10	0,80	1,30	1,60	1,10
B (µg/l)	17,55	59,00	6,00	29,67	76,00	15,00	21,17	33,00	11,00	110,33	117,00	101,00
Ba (µg/l)	29,71	63,23	4,71	41,83	55,40	21,03	39,56	67,58	7,23	24,30	30,54	18,76
Cd (µg/l)	0,14	0,30	0,05	0,21	0,26	0,16	<D.L.	<D.L.	<D.L.	0,06	0,07	<D.L.
Co (µg/l)	0,25	1,40	0,02	0,41	0,75	0,06	0,18	0,32	0,02	0,07	0,14	<D.L.
Cr _{tot} (µg/l)	63,94	134,70	0,70	4,58	11,50	1,30	7,80	10,00	5,60	4,83	6,70	2,10
Cr ⁶⁺ (µg/l)	52,24	89,80	0,50	3,68	11,10	0,10	1,97	5,60	0,35	4,30	6,50	1,20
Cu (µg/l)	2,21	19,30	0,40	1,98	3,10	1,10	1,52	3,10	0,70	4,07	4,50	3,30
Mn (µg/l)	54,40	848,80	0,28	11,83	65,93	0,78	39,74	111,06	1,30	5,10	7,35	3,23
Mo (µg/l)	6,07	77,70	0,10	0,44	1,10	<D.L.	0,42	1,40	<D.L.	6,77	8,90	5,10
Ni (µg/l)	3,13	10,90	0,20	2,88	6,40	1,10	1,16	2,70	0,50	1,80	2,80	0,20
Pb (µg/l)	0,83	2,60	0,10	0,54	1,90	0,10	0,40	0,70	0,10	0,70	1,60	<D.L.
Rb (µg/l)	0,63	1,57	0,20	0,66	0,99	0,34	2,13	9,80	0,42	3,65	4,25	2,79
Sb (µg/l)	0,34	2,80	0,06	1,05	4,09	0,15	0,15	0,32	0,06	0,60	0,74	0,34
Se (µg/l)	1,96	7,20	0,60	0,80	1,00	0,60	0,85	1,00	0,70	0,50	0,50	<D.L.
Si (µg/l)	11605,55	27651,00	4780,00	13167,17	18979,00	8324,00	11554,67	18055,00	165,00	3238,33	4271,00	1807,00
Sn (µg/l)	0,27	1,09	0,05	0,07	0,07	0,07	0,11	0,14	0,08	<D.L.	<D.L.	<D.L.
Sr (µg/l)	160,45	527,08	29,95	180,55	243,34	144,68	185,47	270,15	12,30	184,36	220,92	165,52
V (µg/l)	3,51	8,30	0,70	3,15	8,20	0,70	1,40	5,30	0,20	8,23	9,20	7,00
Zn (µg/l)	73,37	796,50	3,80	244,93	1083,00	12,10	23,20	77,40	7,40	80,53	205,90	14,60

3.4. Land Cover

The total extent of the Ptolemais basin amounts to 1953 km², the land cover is shown in table 5, according to Corine 2012 [39]. The main crops in the basin are hard wheat, soft wheat, barley, sugar beet, maize, potatoes, oat and pastures (According to National Statistics Service of Greece). As it seems in the satellite image of July 2018 (LANDSAT-8 OLI/TIRS LEVEL-1 15/7/2018, time 18:50:32"), the main crops are expanded at the eastern and central part of Sarigkiol basin, specifically in the surrounding area of PPs of Ag. Dimitrios. In the other two PPs, there are not significant cultivated lands (Fig. 6).

Table 5. Land cover (Corine 2012).

Land cover	(%)
Discontinuous urban fabric	0.68
Industrial or commercial units	0.52
Road and rail networks and associated land	0.62
Mineral extraction sites	4.49
Non-irrigated arable land	64.82
Permanently irrigated land	1.11
Pastures	0.23
Complex cultivation patterns	0.11
Land principally occupied by agriculture, with significant areas of natural vegetation	1.55
Broad-leaved forest	0.75
Mixed forest	0.68
Natural grasslands	8.68
Sclerophyllous vegetation	0.36
Transitional woodland-shrub	0.62
Sparsely vegetated areas	14.80
	100.00

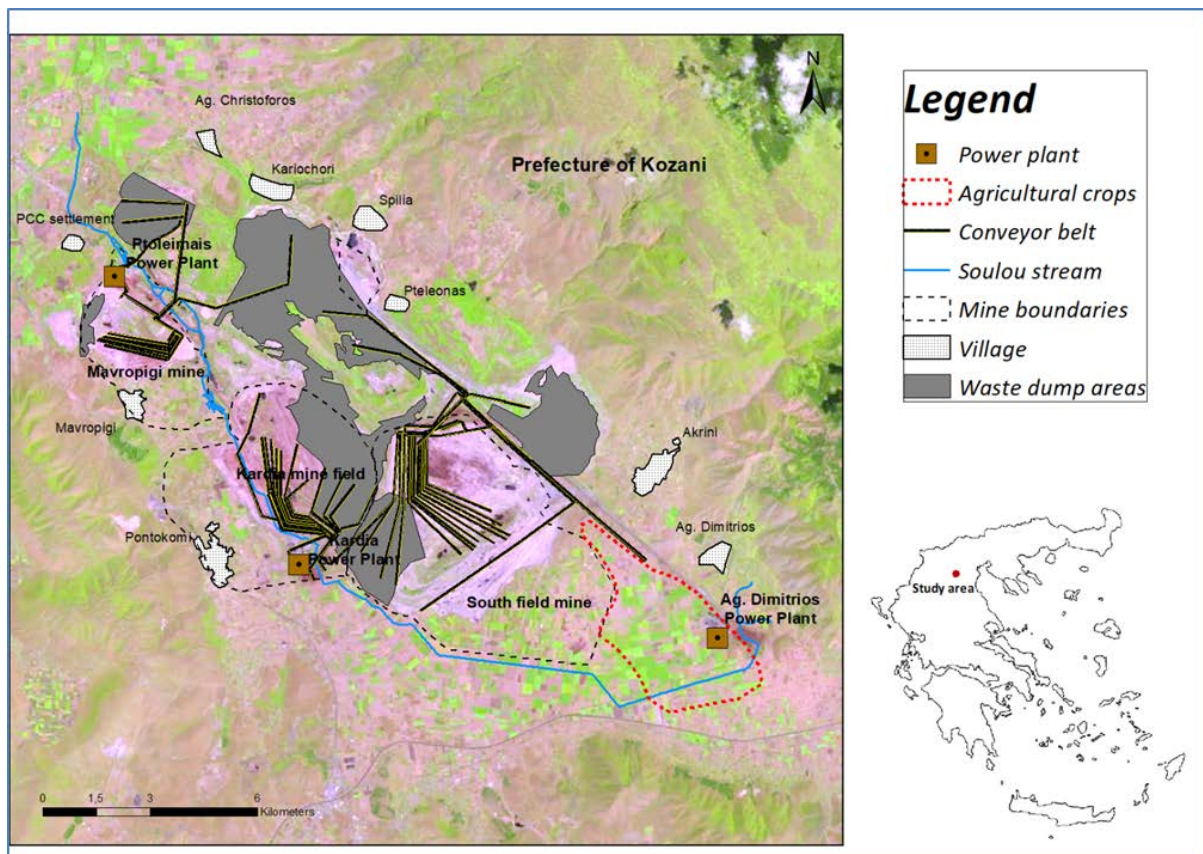




Figure 6. Satellite image of Ptolemais basin (above), showing the agricultural crops (July 2018) and images from google earth (below).

4. CONCLUSIONS

The main conclusions are:

- Ptolemais, Kardia and Ag.Dimitrios PPs operate under similar conditions (lignite combustion, fly-ash production, transportation, and disposal).
- As, B, Ba, Mo, Rb, Sb, Se, Sr and V exhibit low concentrations in surface- and ground-water of the Ptolemais basin. Cr presents elevated concentrations only in the area of the Ag. Dimitrios PP.
- The significant fingerprint of the ultramafic rocks on soils and groundwater quality is recorded in the broader area of the Ag. Dimitrios PP.
- A main difference of the land uses between the three PPs, is the extended agricultural activities in the surrounding area of the Ag. Dimitrios PP whereas mining excavations prevail in the Kardia and Ptolemais PP.
- Soulou, which is the surficial receiving water body of the basin, exhibits no deterioration of the water quality with regards to heavy metals/loids and trace elements, indicating no influence from the mining activities and PPs on water resources.

Considering all the above, the coal combustion products of the PPs in WMLC have minor effect on groundwater quality. The hydrogeological conditions (high values of k, shallow aquifer in Kardia, alkaline environment), despite the fact that they favor the mobility of heavy metals/loids and trace elements (As, B, Ba, Mo, Sb, Se, Sr,V), were not sufficient for their release in groundwater. The geological environment and the land uses constitute the significant controlling factors on groundwater quality. The role of agricultural activities (agrochemical products), needs further investigation, as an important anthropogenic source of Cr in groundwater.

REFERENCES

- [1] Adriano, D. C., Page, A. L., Elseewi, A. A., Chang, A. C. and Straughan, I.: 1980, 'Utilization and disposal of flyash and other coal residues in terrestrial ecosystems: A review', *J. Environ. Qual.* 9, 333–344.
- [2] Mattigod, S. V., Rai, D., Eary, L. E. and Ainsworth, C. C.: 1990, 'Geochemical factors controlling the mobilization of inorganic constituents from fossil fuel combustion residues: 1. Review of the major elements', *J. Environ. Qual.* 19, 188–201.
- [3] Page, A.L., Elseewi, A.A., Straughan, I., 1979. Physical and chemical properties of flyash from coal fired plants with reference to environmental impacts. *Residue Rev.* 71, 83–120.
- [4] Aitken, R. L. & Bell, L. C. (1985). Plant uptake and phytotoxicity of boron in Australian fly ashes. *Plant and Soil*, 84, 245-57.
- [5] Jankowski, J., Ward, C.R., French, D. & Groves, S. 2006, "Mobility of trace elements from selected Australian fly ashes and its potential impact on aquatic ecosystems", *Fuel*, vol. 85, no. 2, pp. 243-256.
- [6] Lyer RS, Scott JA. Power station fly ash – a review of value-added utilization outside of the construction industry. *Resour Conserv Recycl* 2001;31:217–28.
- [7] Fulekar, M.H.; Dave, J.M. Disposal of fly ash - An environmental problem. *Inter. J. Environ. Studies* 26: 191-215; 1986.
- [8] Ahmaruzzaman. M. (2010). A review on the utilization of fly ash. *Progress in Energy and Combustion Science* 36, 327-363 (2010).
- [9] Carlson C, Adriano D.C., Environmental impacts of coal combustion residues, *J. Environ. Qual.* 22 (1993) 227 – 247.
- [10] Bayat, B. (2002a). "Comparative study of adsorption properties of Turkish fly ashes. I: The case of nickel (II), copper (II) and zinc (II)." *J. Hazard. Mater.*, B95(3), 251–273.
- [11] Kim AG, Kazonich G., Dahlberg M. (2003) Relative solubility of cations in class F fly ash. *Environ Sci Technol* 37(19):4507–4511.
- [12] Sivapullaiah, P. V., and Moghal, A. A. B. (2010). "Leachability of trace elements from two stabilized low lime Indian fly ashes." *Environ. Earth Sci.*, 61(8), 1735–1744.
- [13] Anastopoulos C. and Koukouzas N (1972). Geological and ore deposit survey in North part of Lignite Field in Ptolemais. Institute of Geology and Mineral Exploration, Athens (in Greek).
- [14] Louloudis G., 1991. Hydrogeological conditions of South lignite bearing field of Ptolemais region. Confrontation of groundwater problems during the exploitation. Phd thesis, National Technical University of Athens.
- [15] Stamos A. (2010), "Chemical analyses of groundwater in Sarigkiol basin-Recording and evaluating the groundwater and aquifer systems of Greece", IGME, Athens.
- [16] Samake M., Z. Tang, W. Hlaing, N. Innocent, K. Kasereka, W.O. Balogun (2011). Groundwater Vulnerability Assessment in Shallow Aquifer in Linfen Basin, Shanxi Province, China Using DRASTIC Model. *Journal of Sustainable Development*, 4 (2011), p. 53

- [17] Chen Yueh-Min, Gao Jin-bo, Yuana Yong-Qiang, Jun Maa, Shen Yua 2016. Relationship between heavy metal contents and clay mineral properties in surface sediments: Implications for metal pollution assessment. *Continental Shelf Research*, Volume 124, 1 August 2016, Pages 125-133.
- [18] Suloway, J.J., W.R. Roy, T.M. Skelly, T.R. Dickerson, R.M. Schuller and R.A. Grif □n.1983. Chemical and toxicological properties of coal fly ash. *Environ. Geol. Notes* 105:1–70.
- [19] Georgakopoulos, A. 2003. Chemistry and morphology of fly ash samples from the main lignite power stations of Northern Greece. *Proc. of 8th International Conference on Environmental Science and Technology*, 256-263.
- [20] Izquierdo, M., Koukouzas, N., Toulidou, S., Panopoulos, K.D., Querol, X., Itskos, G. 2011. Geochemical controls on leaching of lignite-fired combustion by-products from Greece. *Applied Geochemistry*, 26, 1599-1606.
- [21] Izquierdo M., Querol X., 2012 “Leaching behaviour of elements from coal combustion fly ash: An overview” *International Journal of Coal Geology* 94. DOI: 10.1016/j.coal.2011.10.006.
- [22] Georgakopoulos, A., Filippidis, A., Kassoli-Fournaraki, A., Iordanidis, A., Fernandez-Turiel, J.L., Llorens, J.F., Gimeno, D., 2002a. Environmentally important elements in fly ashes and their leachates of the power stations of Greece. *Energy Sources*, 24, 83-91.
- [23] Hermann R, P. Neumann-Mahlkau, 1985. The mobility of zinc, cadmium, copper, lead, iron and arsenic in ground water as a function of redox potential and pH. *Sci Tot Environ*.
- [24] Kavvadas, M. 2010. Research project – Study for the influence of mixing fly ash of Power Plants in the intersectional strength of mine waste deposits in Lignite Center of West Macedonia. Final Report, Financed by PPC.
- [25] World Health Organization guideline 2011.
- [26] Rai, D., Sass, B.M. & Moore, D.A. 1987, "Chromium(III) Hydrolysis Constants and Solubility of Chromium(III) Hydroxide", *Inorganic chemistry*, vol. 26, no. 3, pp. 345-349.
- [27] Voudouris, K.S., 2009. Assessing groundwater pollution risk in Sarigkiol basin, NW Greece. *River Pollution. Research Project*.
- [28] Aschonitis, V., et al. (2012) Assessment of the intrinsic vulnerability of agricultural land to water and nitrogen losses, via deterministic approach and regression analysis. *Water Air Soil Poll.* 223(4), 1605–1614.
- [29] Mills, C.T., Morrison, J.M., Goldhaber, M.B. & Ellefsen, K.J. 2011, "Chromium(VI) generation in vadose zone soils and alluvial sediments of the southwestern Sacramento Valley, California: A potential source of geogenic Cr(VI) to groundwater", *Applied Geochemistry*, vol. 26, no. 8, pp. 1488-1501.
- [30] Hausladen D., Ozinskas A., McClain C., Fendorf Sc., 2018, "Hexavalent Chromium Sources and Distribution in California Groundwater" *Environ. Sci. Technol.*, Article ASAP DOI: 10.1021/acs.est.7b06627 Copyright © 2018 American Chemical Society.
- [31] Guo, H.M., Wen, D.G., Liu, Z.Y., Guo, Q., 2014. A review of high arsenic groundwater in Mainland and Taiwan, China: distribution, characteristics and hydrogeochemical processes. *Appl. Geochem.* 41 (1), 196–217.

- [32] Brand, U., Azmy, K., Tazawa, J., Sano, H., Buhl, D. 2010. Hydrothermal diagenesis of paleozoic seamount carbonate components. *Chemical Geology*, 173-185
- [33] Kabata-Pendias, A. 1992. Behavioural properties of trace metals in soils. *Applied Geochemistry*, 3-9.
- [34] Oze, C., Bird, D., Fendorf, S. 2007. Genesis of hexavalent chromium from natural sources in soil and groundwater. *Proc. of the National Academy of Sciences*, 104, 6544-6549.
- [35] Mortvedt J. J. Heavy metal contaminants in inorganic and organic fertilizers *Fertilizer Research* 43: 55-61, 1996. Kluwer Academic Publishers. Printed in the Netherlands.
- [36] Remoundaki, E., Vasileiou, E., Philippou, A., Perraki, M., Kousi, P., Hatzikioseyan, A., Stamatis, G. 2016. Groundwater deterioration: The simultaneous effects of intense agricultural activity and heavy metals in soil. *Journal Proceedia Engineering*.
- [37] Krüger, O., Fiedler, F., Adam, C., Vogel, C. & Senz, R. 2017, "Determination of chromium (VI) in primary and secondary fertilizer and their respective precursors", *Chemosphere*, vol. 182, pp. 48-53.
- [38] NTUA Research Project, 2016. Mineralogical, petrological and geochemical study of heavy minerals with emphasis on chromium in the geological formations (ultrabasic rocks, lignite, clay formations) and the coal-fired products (fly ash) and the quality of surficial and underground aquifers of the Sarigkiol basin (NW Greece). Scientific Responsible Perraki Maria, Assistant Professor, Final Report, pp 826.
- [39] Corine Land Cover 2012. Copernicus Europe's eyes on earth. <https://land.copernicus.eu/pan-european/corine-land-cover/clc-2012/view>.